IMPERIAL INSTITUTE
OF
AGRICULTURAL RESEARCH, PUSA

PROCEEDINGS

OF THE

ROYAL SOCIETY OF LONDON

SERIES A

CONTAINING PAPERS OF A MATHEMATICAL AND
PHYSICAL CHARACTER.

VOL. CXXIII.

LONDON:
PRINTED FOR THE ROYAL SOCIETY AND SOLD BY
HARRISON AND SONS, LTD., ST. MARTIN'S LANE,
PRINTERS IN ORDINARY TO HIS MAJESTY.

APRIL, 1929.

LONDON:
HARRISON AND SONS, LTD., PRINTERS IN ORDINARY TO HIS MAJESTY,
ST. MARTIN'S LANE.

CONTENTS.

SERIES A. VOL. CXXIII.

No. 791—March 6, 1929.

PAGE

The Reflexion and Transmission of Electric Waves at the Interface between Two Transparent Media. By H. M. Macdonald, F.R.S. 1

On the Variability of the Quiet-Day Diurnal Magnetic Variation at Eskdalemuir and Greenwich. By S. Chapman, F.R.S., and J. M. Stagg 27

The Spectrum of H_2. The Bands analogous to the Parhelium Line Spectrum.—Part I. By O. W. Richardson, F.R.S., and P. M. Davidson 54

Patterns and Paschen-Back Analogue in the Stark-effect for Neon. By J. S. Foster and W. Rowles. (Plates 1 and 2.) Communicated by A. S. Eve, F.R.S. 80

Stark-effect in a Violet Region of the Secondary Spectrum of Hydrogen. By J. K. L. MacDonald. (Plate 3.) Communicated by A. S. Eve, F.R.S. 103

Relative Intensities of Stark Components in Hydrogen. By J. S. Foster and L. Chalk. (Plates 4 and 5.) Communicated by A. S. Eve, F.R.S. 108

The Relativity Theory of Divergent Waves. By O. R. Baldwin. Communicated by G. B. Jeffery, F.R.S. 119

The Thermal Conductivity of Gas Mixtures. By T. L. Ibbs and A. A. Hirst. Communicated by S. W. J. Smith, F.R.S. 134

The Behaviour of a Single Crystal of Zinc subjected to Alternating Torsional Stresses. By H. J. Gough and H. L. Cox. (Plates 6–11.) Communicated by Sir Thomas Stanton, F.R.S. 143

Infra-red Radiations of Active Nitrogen. By P. K. Kichlu and D. P. Acharya. (Plate 12.) Communicated by M. N. Saha, F.R.S. 168

The Penetration of Hydrogen into Metal Cathodes and its effect upon the Tensile Properties of Metals and their Resistance to Repeated Stresses; with a note on the Effect of Non-Electrolytic Baths and Nickel Plating on these Properties. By F. C. Lea. (Plates 13 and 14.) Communicated by Sir Robert Hadfield, F.R.S. 171

The Electrical Conductivity of Thin Oil Films. Part I.—General Nature of the Phenomenon. By H. E. Watson and A. S. Menon. Communicated by Sir William Hardy, F.R.S. 185

PAGE

An Investigation of the Combustion of Platinum. By E. K. Rideal and O. H. Wansbrough-Jones. Communicated by T. M. Lowry, F.R.S. 202

The Forces on a Solid Body Moving through Viscous Fluid. By S. Goldstein. Communicated by H. Jeffreys, F.R.S. 216

The Steady Flow of Viscous Fluid past a Fixed Spherical Obstacle at Small Reynolds Numbers. By S. Goldstein. Communicated by H. Jeffreys, F.R.S. 225

Equilibrium in the System Methyl Alcohol-Hydrogen-Carbonic Oxide. By D. M. Newitt, B. J. Byrne and H. W. Strong. Communicated by W. A. Bone, F.R.S. 236

On the Chemical Interaction of Ions and the "Clean Up" of Gases at Glass Surfaces under the Influence of the Electrical Discharge. By J. Taylor. Communicated by Sir Joseph J. Thomson, F.R.S. 252

Some Experiments on Vacuum Distillation. By C. R. Burch. Communicated by Sir Ernest Rutherford, P.R.S. 271

Further Experiments on the Combustion of Well-dried Carbon Monoxide and Oxygen Mixtures. Part III.—By W. A. Bone, F.R.S., F. R. Weston and D. A. Winter. (Plates 15 and 16.) 285

The Change of Electrical Conductivity in Strong Magnetic Fields. Part I.—Experimental Results. By P. Kapitza. (Plate 17.) Communicated by Sir Ernest Rutherford, P.R.S. 292

The Change of Electrical Conductivity in Strong Magnetic Fields. Part II.—The Analysis and the Interpretation of the Experimental Results. By P. Kapitza. Communicated by Sir Ernest Rutherford, P.R.S. 342

No. 792—April 6, 1929.

Discussion on the Structure of Atomic Nuclei. Opened by Sir Ernest Rutherford, P.R.S. 373

The Total Reflexion of Electric Waves at the Interface between Two Media. By H. M. Macdonald, F.R.S. 391

The Measurement of Flame Temperatures. By E. Griffiths, F.R.S., and J. H. Awbery 401

The Arc Spectrum of Silicon. By A. Fowler, F.R.S. (Plate 18.) 422

On the Vortex Theory of Screw Propellers. By S. Goldstein. Communicated by L. Prandtl, For. Mem. R.S. 440

The Spectrum of H_2. The Bands analogous to the Parhelium Line Spectrum.—Part II. By O. W. Richardson, F.R.S., and P. M. Davidson 466

The Wave Equation in Five Dimensions. By J. W. Fisher. Communicated by O. W. Richardson, F.R.S. 489

The Structure of the Benzene Ring in $C_6(CH_3)_6$. By K. Lonsdale. Communicated by R. Whiddington, F.R.S. 494

PAGE
The Ionisation of Potassium Vapour. By R. W. Ditchburn and F. L. Arnot. Communicated by Sir Joseph Thomson, F.R.S. 516

The Determination of Parameters in Crystal Structures by means of Fourier Series. By W. L. Bragg, F.R.S. 537

A New Band System of Carbon Monoxide ($3\,{}^1S \rightarrow 2\,{}^1P$), with remarks on the Ångström Band System. By R. C. Johnson and R. K. Asundi. Communicated by O. W. Richardson, F.R.S. 560

A New Integrating Photometer for X-Ray Crystal Reflections, etc. By W. T. Astbury. (Plate 19.) Communicated by Sir William Bragg, F.R.S. 575

The Adsorption of Hydrogen on the Surface of an Electrodeless Discharge Tube. By M. C. Johnson. Communicated by S. W. J. Smith, F.R.S. 603

On the Design and Use of a Double Camera for Photographing Artificial Disintegrations. By P. M. S. Blackett. (Plates 20 and 21.) Communicated by Sir Ernest Rutherford, P.R.S. 613

The Absorption Band Spectrum of Chlorine. By A. Elliott. (Plate 22.) Communicated by T. H. Havelock, F.R.S. 629

Streamline Flow through Curved Pipes. By C. M. White. Communicated by E. V. Appleton, F.R.S. 645

On the Measurement of the Dielectric Constants of Liquids, with a Determination of the Dielectric Constant of Benzene. By L. Hartshorn and D. A. Oliver. Communicated by D. W. Dye, F.R.S. 664

The Molecular Dimensions of Organic Compounds. Part I.—General Considerations. By T. M. Lowry, F.R.S., and A. G. Nasini 686

The Molecular Dimensions of Organic Compounds. Part II.—The Viscosity of Vapours: Benzene, Toluene and Cyclohexane. By A. G. Nasini. Communicated by T. M. Lowry, F.R.S. 692

The Molecular Dimensions of Organic Compounds. Part III.—The Viscosity of Vapours: Thiophen and α-Methylthiophen, Pyridine and Thiazole. By A. G. Nasini. Communicated by T. M. Lowry, F.R.S. 704

Quantum Mechanics of Many-Electron Systems. By P. A. M. Dirac. Communicated by R. H. Fowler, F.R.S. 714

Index 734

Minutes of Meetings of January 31; February 7, 21, 28; March 7, 14, 1929.

PROCEEDINGS OF
THE ROYAL SOCIETY.

SECTION A.—MATHEMATICAL AND PHYSICAL SCIENCES.

The Reflexion and Transmission of Electric Waves at the Interface between Two Transparent Media.

By H. M. MACDONALD, F.R.S.

(Received September 25, 1928.)

The effect of a transparent sphere on a train of plane waves has been fully investigated by Lorentz* in an important paper. The object of the present communication is to obtain approximate expressions for the electric and magnetic forces in the transmitted and in the reflected waves, where electric waves are incident on the interface between two media, the surface of separation being any surface. In a former paper† the writer investigated in particular the case of a perfectly conducting obstacle, and the method adopted for that purpose will be applied in the present case. The assumption is that the most important parts of the electric and magnetic forces in the transmitted and reflected waves are due to the magnetic and electric distributions at any point on the separating surface which would produce the electric and magnetic forces in the immediate neighbourhood of the point if the surface were a plane surface. The equations which express the magnetic and electric forces at a point in terms of the magnetic and electric current distributions are:—

$$\frac{\partial \alpha}{\partial t} = \mu \frac{\partial}{\partial t} \iiint \left\{ \frac{\partial}{\partial y} \frac{i_\zeta}{r} - \frac{\partial}{\partial z} \frac{i_\eta}{r} \right\} d\xi\, d\eta\, d\zeta$$

$$- \iiint \left\{ \frac{\partial^2}{\partial x^2} \frac{m_\xi}{r} + \frac{\partial^2}{\partial x\, \partial y} \frac{m_\eta}{r} + \frac{\partial^2}{\partial x\, \partial z} \frac{m_\zeta}{r} - \mathrm{K}\mu \frac{\partial^2}{\partial t^2} \frac{m_\xi}{r} \right\} d\xi\, d\eta\, d\zeta.$$

$$\frac{\partial \beta}{\partial t} = \mu \frac{\partial}{\partial t} \iiint \left\{ \frac{\partial}{\partial z} \frac{i_\xi}{r} - \frac{\partial}{\partial x} \frac{i_\zeta}{r} \right\} d\xi\, d\eta\, d\zeta$$

$$- \iiint \left\{ \frac{\partial^2}{\partial x\, \partial y} \frac{m_\xi}{r} + \frac{\partial^2}{\partial y^2} \frac{m_\eta}{r} + \frac{\partial^2}{\partial y\, \partial z} \frac{m_\zeta}{r} - \mathrm{K}\mu \frac{\partial^2}{\partial t^2} \frac{m_\eta}{r} \right\} d\xi\, d\eta\, d\zeta,$$

---

* 'Œuvres Scientifiques,' t. 1.

† 'Phil. Trans.,' A, vol. 212, p. 299 (1912).

$$\frac{\partial \gamma}{\partial t} = \mu \frac{\partial}{\partial t} \iiint \left\{ \frac{\partial}{\partial x} \frac{i_\eta}{r} - \frac{\partial}{\partial y} \frac{i_\xi}{r} \right\} d\xi \, d\eta \, d\zeta$$

$$- \iiint \left\{ \frac{\partial^2}{\partial x \, \partial z} \frac{m_\xi}{r} + \frac{\partial^2}{\partial y \, \partial z} \frac{m_\eta}{r} + \frac{\partial^2}{\partial z^2} \frac{m_\zeta}{r} - \mathrm{K}\mu \frac{\partial^2}{\partial t^2} \frac{m_\zeta}{r} \right\} d\xi \, d\eta \, d\zeta,$$

$$\frac{\partial \mathrm{X}}{\partial t} = \frac{1}{\mathrm{K}} \iiint \left\{ \frac{\partial^2}{\partial x^2} \frac{i_\xi}{r} + \frac{\partial^2}{\partial x \, \partial y} \frac{i_\eta}{r} + \frac{\partial^2}{\partial x \, \partial z} \frac{i_\zeta}{r} - \mathrm{K}\mu \frac{\partial^2}{\partial t^2} \frac{i_\xi}{r} \right\} d\xi \, d\eta \, d\zeta$$

$$+ \frac{\partial}{\partial t} \iiint \left\{ \frac{\partial}{\partial y} \frac{m_\zeta}{r} - \frac{\partial}{\partial z} \frac{m_\eta}{r} \right\} d\xi \, d\eta \, d\zeta,$$

$$\frac{\partial \mathrm{Y}}{\partial t} = \frac{1}{\mathrm{K}} \iiint \left\{ \frac{\partial^2}{\partial x \, \partial y} \frac{i_\xi}{r} + \frac{\partial^2}{\partial y^2} \frac{i_\eta}{r} + \frac{\partial^2}{\partial y \, \partial z} \frac{i_\zeta}{r} - \mathrm{K}\mu \frac{\partial^2}{\partial t^2} \frac{i_\eta}{r} \right\} d\xi \, d\eta \, d\zeta$$

$$+ \frac{\partial}{\partial t} \iiint \left\{ \frac{\partial}{\partial z} \frac{m_\xi}{r} - \frac{\partial}{\partial \xi} \frac{m_\zeta}{r} \right\} d\xi \, d\eta \, d\zeta,$$

$$\frac{\partial \mathrm{Z}}{\partial t} = \frac{1}{\mathrm{K}} \iiint \left\{ \frac{\partial^2}{\partial x \, \partial z} \frac{i_\xi}{r} + \frac{\partial^2}{\partial y \, \partial z} \frac{i_\eta}{r} + \frac{\partial^2}{\partial z^2} \frac{i_\zeta}{r} - \mathrm{K}\mu \frac{\partial^2}{\partial t^2} \frac{i_\zeta}{r} \right\} d\xi \, d\eta \, d\zeta$$

$$+ \iiint \left\{ \frac{\partial}{\partial x} \frac{m_\eta}{r} - \frac{\partial}{\partial y} \frac{m_\xi}{r} \right\} d\xi \, d\eta \, d\zeta,$$

where K, μ are the constants of the medium,* and, when the magnetic, and electric current distribution on the interface determined on the assumption stated above are substituted in these equations, the components of the electric and magnetic forces due to this distribution at any point are obtained. In this way the most important parts of the electric and magnetic forces in the transmitted and in the reflected waves are obtained both at an ordinary point and at a point on or near to a caustic, the order of approximation being the same as in the case of a perfectly conducting obstacle. Limits are obtained for the rate of transfer of energy into the second medium when there is a simple oscillator in the first medium, and the separating surface is convex. The results are also applied to the case where the separating surface is a sphere.

It is sufficient to investigate the effect of a simple oscillator situated at a point O, and emitting waves of wave-length $2\pi/\kappa$. Taking the point O as origin of co-ordinates and the axis of z along the axis of the oscillator, the components of the magnetic force, H_ξ, H_η, H_ζ† at the point Q (ξ, η, ζ) due to the oscillator are given by

$$\mathrm{H}_\xi = \frac{\kappa}{\mathrm{V}} \frac{\partial}{\partial \eta} \frac{e^{\iota\kappa(\mathrm{V}t - r_1)}}{r_1}, \quad \mathrm{H}_\eta = -\frac{\kappa}{\mathrm{V}} \frac{\partial}{\partial \xi} \frac{e^{\iota\kappa(\mathrm{V}t - r_1)}}{r_1}, \quad \mathrm{H}_\zeta = 0,$$

---

* ‘Roy. Soc. Proc.,’ A, vol. 113, p. 237 (1926).

† The components of the electric magnetic forces are denoted throughout the present communication by E_x, E_y, E_z, H_x, H_y, H_z instead of X, Y, Z, α, β, γ, the older notation.

where $r_1^2 = \xi^2 + \eta^2 + \zeta^2$, and V is the velocity of radiation in the medium in which the oscillator is situated. When r_1 is great compared with the wavelength, these expressions can be replaced by

$$H_\xi = \frac{-i\kappa^2\eta}{Vr_1^2} e^{\iota\kappa(Vt-r_1)}, \quad H_\eta = \frac{\iota\kappa^2\xi}{Vr_1^2} e^{\iota\kappa(Vt-r_1)}, \quad H_\zeta = 0,$$

and, to the same order, the expressions for the components of the electric force are

$$E_\xi = \frac{\iota\mu\kappa^2\zeta\xi}{r_1^3} e^{\iota\kappa(Vt-r_1)}, \quad E_\eta = \frac{\iota\mu\kappa^2\eta\zeta}{r_1^3} e^{\iota\kappa(Vt-r_1)}, \quad E_\zeta = \frac{-\iota\mu\kappa^2(\xi^2+\eta^2)}{r_1^3} e^{\iota\kappa(Vt-r_1)},$$

where μ is the magnetic permeability of the medium, and, to this order of approximation, the wave front is perpendicular to the straight line OQ. Hence, if l, m, n are the direction cosines of the normal to the surface of separation of the two media at the point Q on it, and, if l_1, m_1, n_1, are the direction cosines of the line of intersection of the wave front and the tangent plane to the surface at Q,

$$l_1/(m\zeta - n\eta) = m_1/(n\xi - l\zeta) = n_1/(l\eta - m\xi) = 1/r_1 \sin\theta,$$

where θ is the angle between OQ and the normal at Q. Further, if l_2, m_2, n_2 are the direction cosines of the straight line in the tangent plane at Q perpendicular to l_1, m_1, n_1,

$$l_2/(\xi - lr_1\cos\theta) = m_2/(\eta - mr_1\cos\theta) = n_2/(\zeta - nr_1\cos\theta) = 1/r_1\sin\theta.$$

Therefore the tangential components of the magnetic force due to the oscillator in the plane of incidence and perpendicular to the plane of incidence respectively are $l_1H_\xi + m_1H_\eta$, $l_2H_\zeta + m_2H_\eta$, that is

$$\iota\kappa^2 e^{\iota\kappa(Vt-r_1)}(-l_1\eta + m_1\xi)/Vr_1^2, \quad \iota\kappa^2 e^{\iota\kappa(Vt-r_1)}(-l_2\eta + m_2\xi)/Vr_1^2,$$

or

$$\iota\kappa^2 e^{\iota\kappa(Vt-r_1)}\{n(\xi^2+\eta^2+\zeta^2) - \zeta(l\xi + m\eta + n\zeta)\}/Vr_1^3\sin\theta,$$
$$i\kappa^2 e^{\iota\kappa(Vt-r_1)}\{-\eta(\xi - lr_1\cos\theta) + \xi(\eta - mr_1\cos\theta)\}/Vr_1^3\sin\theta,$$

that is

$$\iota\kappa^2 e^{\iota\kappa(Vt-r_1)}(nr_1 - \zeta\cos\theta)/Vr_1^2\sin\theta, \quad \iota\kappa^2 e^{\iota\kappa(Vt-r_1)} n_1\cos\theta/Vr_1.$$

Similarly, the tangential components of the electric force due to the oscillator in the plane of incidence, and perpendicular to the plane of incidence respectively are

$$l_1E_\xi + m_1E_\eta + n_1E_\zeta, \quad l_2E_\xi + m_2E_\eta + n_2E_\zeta,$$

that is

$$\iota\mu\kappa^2 e^{\iota\kappa(Vt-r_1)}\{l_1\zeta\xi + m_1\eta\zeta - n_1(\xi^2+\eta^2)\}/r_1^3,$$

$$\iota\mu\kappa^2 e^{\iota\kappa(Vt-r_1)}\{l_2\zeta\xi + m_2\eta\zeta - n_2(\xi^2+\eta^2)\}/r_1^3,$$

or

$$\iota\mu\kappa^2 e^{\iota\kappa(Vt-r_1)}\{\zeta\xi(m\zeta - n\eta) + \eta\zeta(n\xi - l\zeta) - (\xi^2+\eta^2)(l\eta - m\xi)\}/r_1^4 \sin\theta,$$

$$\iota\mu\kappa^2 e^{\iota\kappa(Vt-r_1)}\{\zeta\xi(\xi - lr_1\cos\theta) + \eta\zeta(\eta - mr_1\cos\theta) - (\xi^2+\eta^2)(\zeta - nr_1\cos\theta)\}/r_1^4 \sin\theta;$$

that is

$$\iota\mu\kappa^2 e^{\iota\kappa(Vt-r_1)}(m\xi - l\eta)/r_1^2 \sin\theta,$$

$$\iota\mu\kappa^2 e^{\iota\kappa(Vt-r_1)}\{nr_1^2 - \zeta(l\xi + m\eta + \eta\zeta)\}\cos\theta/r_1^3 \sin\theta,$$

or

$$-\iota\mu\kappa^2 n_1 e^{\iota\kappa(Vt-r_1)}/r_1, \quad \iota\mu\kappa^2 e^{\iota\kappa(Vt-r_1)}(nr_1 - \zeta\cos\theta)\cos\theta/r_1^2 \sin\theta.$$

If the surface at the point Q were a plane, the tangential components of the electric and magnetic forces at the point Q would be

$$E_t = -\iota\mu\kappa^2 e^{\iota\kappa(Vt-r_1)}\, 2n_1\sigma\cos\theta/(\sigma\cos\theta + \sigma'\cos\theta')r_1,$$

$$E_p = \iota\mu\kappa^2 e^{\iota\kappa(Vt-r_1)}\, 2\sigma\cos\theta\cos\theta'(n\sin\theta - n_2\cos\theta)/(\sigma'\cos\theta + \sigma\cos\theta')r_1,$$

$$H_t = \iota\kappa^2 e^{\iota\kappa(Vt-r_1)}\, 2\sigma'\cos\theta(n\sin\theta - n_2\cos\theta)/(\sigma'\cos\theta + \sigma\cos\theta')Vr_1,$$

$$H_p = i\kappa^2 e^{\iota\kappa(Vt-r_1)}\, 2n_1\sigma'\cos\theta\cos\theta'/(\sigma\cos\theta + \sigma'\cos\theta')Vr_1,$$

for

$$nr_1 - \zeta\cos\theta = r_1(n\sin\theta - n_2\cos\theta)\sin\theta;$$

where, if K and μ are the constants of the first medium, K′, μ' of the second medium, $V' = (K'\mu')^{-\frac{1}{2}}$ the velocity of radiation in the second medium,

$$\sin\theta/V = \sin\theta'/V', \quad \sigma = (K/\mu)^{\frac{1}{2}}, \quad \sigma' = (K'/\mu')^{\frac{1}{2}}.$$

Now the components of the electric and magnetic current distributions on the surface at Q which would produce these magnetic and electric forces tangential to the surface at Q are

$$l_1H_p - l_2H_t, \quad m_1H_p - m_2H_t, \quad n_1H_p - n_2H_t;$$

$$l_1E_p - l_2E_t, \quad m_1E_p - m_2E_t, \quad n_1E_p - n_2E_t,$$

and the components of the magnetic force at the point P (x, y, z) in the second medium due to this distribution are given by

$$4\pi\dot{\mathrm{H}}_x = \frac{\partial}{\partial t}\iint\left[\frac{\partial}{\partial y}\left\{\frac{n_1\mathrm{H}_p' - n_2\mathrm{H}_i'}{r}\right\} - \frac{\partial}{\partial z}\left\{\frac{m_1\mathrm{H}_p' - m_2\mathrm{H}_i'}{r}\right\}\right] d\mathrm{S}$$

$$- \frac{1}{\mu'}\iint\left[\frac{\partial^2}{\partial x^2}\left\{\frac{l_1\mathrm{E}_p' - l_2\mathrm{E}_i'}{r}\right\} + \frac{\partial^2}{\partial x\,\partial y}\left\{\frac{m_1\mathrm{E}_p' - m_2\mathrm{E}_i'}{r}\right\}\right.$$

$$\left. + \frac{\partial^2}{\partial x\,\partial z}\left\{\frac{n_1\mathrm{E}_p' - n_2\mathrm{E}_i'}{r}\right\} - \mathrm{K}'\mu'\frac{\partial^2}{\partial t^2}\left\{\frac{l_1\mathrm{E}_p' - l_2\mathrm{E}_i'}{r}\right\}\right] d\mathrm{S},$$

$$4\pi\dot{\mathrm{H}}_y = \frac{\partial}{\partial t}\iint\left[\frac{\partial}{\partial z}\left\{\frac{l_1\mathrm{H}_p' - l_2\mathrm{H}_i'}{r}\right\} - \frac{\partial}{\partial x}\left\{\frac{n_1\mathrm{H}_p' - n_2\mathrm{H}_i'}{r}\right\}\right] d\mathrm{S}'$$

$$- \frac{1}{\mu'}\iint\left[\frac{\partial^2}{\partial x\,\partial y}\left\{\frac{l_1\mathrm{E}_p' - l_2\mathrm{E}_i'}{r}\right\} + \frac{\partial^2}{\partial y^2}\left\{\frac{m_1\mathrm{E}_p' - m_2\mathrm{E}_i'}{r}\right\}\right.$$

$$\left. + \frac{\partial^2}{\partial y\,\partial z}\left\{\frac{n_1\mathrm{E}_p' - n_2\mathrm{E}_i'}{r}\right\} - \mathrm{K}'\mu'\frac{\partial^2}{\partial t^2}\left\{\frac{m_1\mathrm{E}_p' - m_2\mathrm{E}_i'}{r}\right\}\right] d\mathrm{S},$$

$$4\pi\dot{\mathrm{H}}_z = \frac{\partial}{\partial t}\iint\left[\frac{\partial}{\partial x}\left\{\frac{m_1\mathrm{H}_p' - m_2\mathrm{H}_i'}{r}\right\} - \frac{\partial}{\partial y}\left\{\frac{l_1\mathrm{H}_p' - l_2\mathrm{H}_i'}{r}\right\}\right] d\mathrm{S}$$

$$- \frac{1}{\mu'}\iint\left[\frac{\partial^2}{\partial x\,\partial z}\left\{\frac{l_1\mathrm{E}_p' - l_2\mathrm{E}_i'}{r}\right\} + \frac{\partial^2}{\partial y\,\partial z}\left\{\frac{m_1\mathrm{E}_p' - m_2\mathrm{E}_i'}{r}\right\}\right.$$

$$\left. + \frac{\partial^2}{\partial z^2}\left\{\frac{n_1\mathrm{E}_p' - n_2\mathrm{E}_i'}{r}\right\} - \mathrm{K}'\mu'\frac{\partial^2}{\partial t^2}\left\{\frac{n_1\mathrm{E}_p' - n_2\mathrm{E}_i'}{r}\right\}\right] d\mathrm{S},$$

where

$$r^2 = (x - \xi)^2 + (y - \eta)^2 + (z - \zeta)^2,$$

and H_p', etc., denote the values of H_p, etc., where $t - r/\mathrm{V}'$ is written for t.

The principal parts of the integrals in these expressions are contributed by the portion of the surface which is in the neighbourhood of the point or points where $\kappa r_1 + \kappa' r$ is stationary, for each integral contains the factor $e^{-\iota\kappa r_1 - \iota\kappa' r}$, where $\kappa'\mathrm{V}' = \kappa\mathrm{V}$. If P_1 is a point on the surface where $\kappa r_1 + \kappa' r$ is stationary, then taking P_1 as origin, the normal to the surface at P_1 as the axis of z', the axes of x' and y' can be chosen so that the co-ordinates of O are x_1, 0, z_1, the equation to the surface can be written

$$z' = \tfrac{1}{2}(\mathrm{A}x'^2 + 2\mathrm{H}x'y' + \mathrm{B}y'^2) + \ldots,$$

further

$$r_1^2 = (x_1 - x')^2 + y'^2 + (z_1 - z')^2, \quad r^2 = (x - x')^2 + (y - y')^2 + (z - z')^2,$$

and the conditions that $\kappa r_1 + \kappa' r$ is stationary at the origin are

$$\kappa x_1/r_1 + \kappa' x/r = 0, \qquad y = 0.$$

Again, if the distance OP_1 is R_1, and the distance PP_1 is R, and the angle of incidence of the waves at P_1 is θ,

$$x_1 = -\mathrm{R}_1 \sin\theta \qquad z_1 = -\mathrm{R}_1 \cos\theta,$$

therefore $x = \mathrm{R}\sin\theta'$, where $\kappa\sin\theta = \kappa'\sin\theta'$, that is, where θ' is the angle of refraction, and it follows that $z = \mathrm{R}\cos\theta'$. Hence

$$r_1^2 = \mathrm{R}_1^2 + 2\mathrm{R}_1 x'\sin\theta + 2\mathrm{R}_1 z'\cos\theta + x'^2 + y'^2 \dots,$$

$$r^2 = \mathrm{R}^2 - 2\mathrm{R}x'\sin\theta' - 2\mathrm{R}z'\cos\theta' + x'^2 + y'^2 \dots;$$

that is

$$r_1 = \mathrm{R}_1 + x'\sin\theta + z'\cos\theta + (x'^2\cos^2\theta + y'^2)/2\mathrm{R}_1 + \dots,$$

$$r = \mathrm{R} - x'\sin\theta' - z'\cos\theta' + (x'^2\cos^2\theta' + y'^2)/2\mathrm{R} + \dots,$$

and therefore

$$\kappa r_1 + \kappa' r = \kappa\mathrm{R}_1 + \kappa'\mathrm{R} + \tfrac{1}{2}(\kappa\cos\theta - \kappa'\cos\theta')(\mathrm{A}x'^2 + 2\mathrm{H}x'y' + \mathrm{B}y'^2)$$
$$+ \kappa(x'^2\cos^2\theta + y'^2)/2\mathrm{R}_1 + \kappa'(x'^2\cos^2\theta' + y'^2)/2\mathrm{R} + \dots,$$

that is

$$\kappa r_1 + \kappa' r = \kappa\mathrm{R}_1 + \kappa'\mathrm{R} + \tfrac{1}{2}(\mathrm{A}'x'^2 + 2\mathrm{H}'x'y' + \mathrm{B}'y'^2) + \dots,$$

where

$$\mathrm{A}' = (\kappa\cos\theta - \kappa'\cos\theta')\mathrm{A} + \kappa\cos^2\theta/\mathrm{R}_1 + \kappa'\cos^2\theta'/\mathrm{R},$$

$$\mathrm{B}' = (\kappa\cos\theta - \kappa'\cos\theta')\mathrm{B} + \kappa/\mathrm{R}_1 + \kappa'/\mathrm{R},$$

$$\mathrm{H}' = (\kappa\cos\theta - \kappa'\cos\theta')\mathrm{H};$$

and writing

$$\mathrm{A}(\kappa\cos\theta - \kappa'\cos\theta') + \kappa\cos^2\theta/\mathrm{R}_1 + \kappa'\cos^2\theta'\mathrm{A}_1 = 0,$$

$$\mathrm{B}(\kappa\cos\theta - \kappa'\cos\theta') + \kappa/\mathrm{R}_1 + \kappa'\mathrm{B}_1 = 0,$$

$$\mathrm{H}(\kappa\cos\theta - \kappa'\cos\theta') = \kappa'\cos\theta'\mathrm{H}_1,$$

it follows that

$$\mathrm{A}'\mathrm{B}' - \mathrm{H}'^2 = \kappa'^2\cos^2\theta'\{(\mathrm{R}^{-1} - \mathrm{A}_1)(\mathrm{R}^{-1} - \mathrm{B}_1) - \mathrm{H}_1^2\}$$
$$= \kappa'^2\cos^2\theta'\{\mathrm{R}^{-2} - (\mathrm{A}_1 + \mathrm{B}_1)\mathrm{R}^{-1} + \mathrm{A}_1\mathrm{B}_1 - \mathrm{H}_1^2\};$$

whence, writing

$$\mathrm{A}_1 + \mathrm{B}_1 = f_1^{-1} + f_2^{-1}, \quad \mathrm{A}_1\mathrm{B}_1 - \mathrm{H}_1^2 = f_1^{-1}f_2^{-1},$$

$$\mathrm{A}'\mathrm{B}' - \mathrm{H}'^2 = \kappa'^2\cos^2\theta'(\mathrm{R}^{-1} - f_1^{-1})(\mathrm{R}^{-1} - f_2^{-1}),$$

and

$$(\mathrm{B}_1 - \mathrm{A}_1)^2 + 4\mathrm{H}_1^2 = (f_1^{-1} - f_2^{-1})^2,$$

therefore, if

$$\mathrm{B}_1 - \mathrm{A}_1 = (f_1^{-1} - f_2^{-1})\cos 2\psi, \quad 2\mathrm{H}_1 = (f_1^{-1} - f_2^{-1})\sin 2\psi,$$

$$\mathrm{A}_1 = f_1^{-1}\sin^2\psi + f_2^{-1}\cos^2\psi, \quad \mathrm{B}_1 = f_1^{-1}\cos^2\psi + f_2^{-1}\sin^2\psi$$

$$2\mathrm{H}' = (f_1^{-1} - f_2^{-1})\kappa'\cos\theta'\sin 2\psi.$$

Turning the axes of x' and y' through an angle ϕ so that

$$\mathrm{A}'x'^2 + 2\mathrm{H}'x'y' + \mathrm{B}'y'^2 \quad \text{becomes} \quad \mathrm{A}''\xi'^2 + \mathrm{B}''\eta'^2,$$

$$\tan 2\phi = 2\mathrm{H}'/(\mathrm{A}' - \mathrm{B}'),$$

and the position of the focal line corresponding to $R = f_1$ is given by $\tan\phi = \tan\psi\sec\theta'$, while the position of the focal line corresponding to $R = f_2$ is given by $\tan\phi = \tan\psi\cos\theta'$.

The components of the magnetic force at the point P are given by

$$\begin{aligned}
4\pi\mu' H_x = {} & [\mu'\kappa'^2 V' [\{n_1(y-\eta) - m_1(z-\zeta)\} H_p' R^{-2} \\
& - \{n_2(y-\eta) - m_2(z-\zeta)\} H_i' R^{-2}] + \\
& \kappa'^2 [\{(x-\xi)(l_1(x-\xi) + m_1(y-\eta) + n_1(z-\zeta)) - l_1 R^2\} E_p' R^{-3} \\
& - \{(x-\xi)(l_2(x-\xi) + m_2(y-\eta) + n_2(z-\zeta)) - l_2 R^2\} E_i' R^{-3}]\, I, \\
4\pi\mu' H_y = {} & [\mu'\kappa'^2 V' [\{l_1(z-\zeta) - n_1(x-\xi)\} H_p' R^{-2} \\
& - \{l_2(z-\zeta) - n_2(x-\xi)\} H_i' R^{-2}] \\
& + \kappa'^2 [\{(y-\eta)(l_1(x-\xi) + m_1(y-\eta) + n_1(z-\zeta)) - m_1 R^2\} E_p' R^{-3} \\
& - \{(y-\eta)(l_2(x-\xi) + m_2(y-\eta) + n_2(z-\zeta)) \\
& \qquad\qquad - m_2 R^2\} E_i' R^{-3}]\, I, \\
4\pi\mu' H_z = {} & [\mu'\kappa'^2 V' [\{m_1(x-\xi) - l_1(y-\eta)\} H_p' R^{-2} \\
& - \{m_2(x-\xi) - l_2(y-\eta)\} H_i' \,.\, R^{-2}] \\
& + \kappa'^2 [\{(z-\zeta)(l_1(x-\xi) + m_1(y-\eta) + n_1(z-\zeta)) - n_1 R^2\} E_p' R^{-3} \\
& - \{(z-\zeta)(l_2(x-\xi) + m_2(y-\eta) + n_2(z-\zeta)) - n_2 R^2\} E_i' R^{-3}]\, I,
\end{aligned}$$

where

$$I = \iint e^{-\iota\kappa(r_1 - R_1) - \iota\kappa'(r - R)}\, dS,$$

and, for the order of approximation adopted, the parts of the expressions on the right-hand side outside the sign of integration have the values which belong to the point P_1.

Now, since in these expressions ξ, η, ζ denote the co-ordinates of the point P_1,

$$x - \xi = R(l_2\sin\theta' + l\cos\theta'), \quad y - \eta = R(m_2\sin\theta' + m\cos\theta'),$$
$$z - \zeta = R(n_2\sin\theta' + n\cos\theta');$$

hence

$$\begin{aligned}
n_1(y-\eta)/R - m_1(z-\zeta)/R &= (n_1 m_2 - n_2 m_1)\sin\theta' + (mn_1 - m_1 n)\cos\theta' \\
&= l\sin\theta' - l_2\cos\theta', \\
n_2(y-\eta)/R - m_2(z-\zeta)/R &= (n_2 m - m_2 n)\cos\theta' = l_1\cos\theta', \\
l_1(z-\zeta)/R - n_1(x-\xi)/R &= (l_1 n_2 - l_2 n_1)\sin\theta' + (nl_1 - n_1 l)\cos\theta' \\
&= m\sin\theta' - m_2\cos\theta', \\
l_2(z-\zeta)/R - n_2(x-\xi)/R &= (l_2 n - n_2 l)\cos\theta' = m_1\cos\theta',
\end{aligned}$$

$$m_1(x-\xi)/R - l_1(y-\eta)/R = (m_1 l_2 - m_2 l_1)\sin\theta' + (lm_1 - l_1 m)\cos\theta'$$
$$= n\sin\theta' - n_2\cos\theta',$$

$$m_2(x-\xi)/R - l_2(y-\eta)/R = (m_2 l - l_2 m)\cos\theta' = n_1\cos\theta',$$

$$l_1(x-\xi)/R + m_1(y-\eta)/R + n_1(z-\zeta)/R = (l_1 l_2 + m_1 m_2 + n_1 n_2)\sin\theta'$$
$$+ (l_1 l + m_1 m + n_1 n)\cos\theta' = 0,$$

$$l_2(x-\xi)/R + m_2(y-\eta)/R + n_2(z-\zeta)/R = (l_2^2 + m_2^2 + n_2^2)\sin\theta'$$
$$+ (ll_2 + mm_2 + nn_2)\cos\theta' = \sin\theta',$$

and

$$\{(x-\xi)/R\}\{l_2(x-\xi)/R + m_2(y-\eta)/R + n_2(z-\zeta)/R\} - l_2$$
$$= \sin\theta'(l_2\sin\theta' + l\cos\theta') - l_2 = \cos\theta'(l\sin\theta' - l_2\cos\theta'),$$

$$\{(y-\eta)/R\}\{l_2(x-\xi)/R + m_2(y-\eta)/R + n_2(z-\zeta)/R\} - m_2$$
$$= \cos\theta'(m\sin\theta' - m_2\cos\theta'),$$

$$\{(z-\zeta)/R\}\{l_2(x-\xi)/R + m_2(y-\eta)/R + n_2(z-\zeta)/R\} - n_2$$
$$= \cos\theta'(n\sin\theta' - n_2\cos\theta').$$

Therefore

$$4\pi\mu'\dot{H}_x = [\mu'\kappa'^2 V'\{(l\sin\theta' - l_2\cos\theta'\}H_p'/R - l_1\cos\theta' H_i'/R\}$$
$$+ \kappa'^2\{-l_1 E_p'/R - \cos\theta'(l\sin\theta' - l_2\cos\theta')E_i'/R\}]\,I,$$

$$4\pi\mu'\dot{H}_y = [\mu'\kappa'^2 V'\{(m\sin\theta' - m_2\cos\theta'\}H_p'/R - m_1\cos\theta' H_i'/R\}$$
$$+ \kappa'^2\{-m_1 E_p'/R - \cos\theta'(m\sin\theta' - m_2\cos\theta')E_i'/R\}]\,I,$$

$$4\pi\mu'\dot{H}_z = [\mu'\kappa'^2 V'\{n\sin\theta' - n_2\cos\theta')H_p'/R - n_1\cos\theta'/H_i'/R\}$$
$$+ \kappa'^2\{-n_1 E_p'/R - \cos\theta'(n\sin\theta' - n_2\cos\theta')E_i'/R\}]\,I,$$

where

$$I = \iint e^{-\iota\kappa(r_1 - R_1) - \iota\kappa'(r-R)}\,dS;$$

that is

$$4\pi\mu'\dot{H}_x = \kappa'^2[(l\sin\theta' - l_2\cos\theta')(\mu' V' H_p'/R - E_i'\cos\theta'/R)$$
$$- l_1(\mu' V' H_i'\cos\theta'/R + E_p'/R)]\,I,$$

$$4\pi\mu'\dot{H}_y = \kappa'^2[(m\sin\theta' - m_2\cos\theta')(\mu' V' H_p'/R - E_i'\cos\theta'/R)$$
$$- m_1(\mu' V' H_i'\cos\theta'/R + E_p'/R)]\,I,$$

$$4\pi\mu'\dot{H}_z = \kappa'^2[(n\sin\theta' - n_2\cos\theta')(\mu' V' H_p'/R - E_i'\cos\theta'/R)$$
$$- n_1(\mu' V' H_i'\cos\theta'/R + E_p'/R)]\,I.$$

Now

$$\mu'V'H_p' - E_t' \cos\theta' = \iota\kappa^2 e^{\iota\kappa Vt - \iota\kappa R_1 - \iota\kappa' R}$$

$$\{2\mu'V'n_1\sigma' \cos\theta \cos\theta'/V + 2\mu n_1\sigma \cos\theta \cos\theta'\}/(\sigma\cos\theta + \sigma'\cos\theta')\,R_1$$

$$= 4\iota\kappa^2 n_1 \cos\theta \cos\theta' e^{\iota\kappa Vt - \iota\kappa R_1 - \iota\kappa' R}/(\sigma\cos\theta + \sigma'\cos\theta')\,R_1 V,$$

for $\mu'\sigma'V' = \mu\sigma V = 1$.

Similarly,

$$\mu'V'H_t' \cos\theta' + E_p'$$

$$= 4\iota\kappa^2 \cos\theta \cos\theta' (n \sin\theta - n_2 \cos\theta)\, e^{\iota\kappa Vt - \iota\kappa R_1 - \iota\kappa' R}/(\sigma\cos\theta' + \sigma'\cos\theta)\,VR_1.$$

therefore

$$H_x = \kappa'\kappa^2\sigma' I \cos\theta \cos\theta'$$

$$\{n_1 (l \sin\theta' - l_2 \cos\theta')/(\sigma\cos\theta + \sigma'\cos\theta')$$

$$- l_1 (n \sin\theta - n_2 \cos\theta)/(\sigma\cos\theta' + \sigma'\cos\theta)\}\, e^{\iota\kappa Vt - \iota\kappa R_1 - \iota\kappa' R}/\pi VR_1 R,$$

$$H_y = \kappa'\kappa^2\sigma' I \cos\theta \cos\theta'$$

$$\{n_1 (m \sin\theta' - m_2 \cos\theta')/(\sigma\cos\theta + \sigma'\cos\theta')$$

$$- m_1 (n \sin\theta - n_2 \cos\theta)/(\sigma\cos\theta' + \sigma'\cos\theta)\}\, e^{\iota\kappa Vt - \iota\kappa R_1 - \iota\kappa' R}/\pi VRR_1,$$

$$H_z = \kappa'\kappa^2\sigma' I \cos\theta \cos\theta'$$

$$\{n_1 (n \sin\theta' - n_2 \cos\theta')/(\sigma\cos\theta + \sigma'\cos\theta')$$

$$- n_1 (n \sin\theta - n_2 \cos\theta)/(\sigma\cos\theta' + \sigma'\cos\theta)\}\, e^{\iota\kappa Vt - \iota\kappa R_1 - \iota\kappa' R}/\pi VRR_1.$$

Again

$$I = \iint e^{\iota\kappa (r_1 - R_1) - \iota\kappa' (r - R)}\, dS,$$

and, unless $R - f_1$ or $R - f_2$ is a small quantity, that is unless the point P is on or near a caustic, this becomes

$$I = \int_{-\infty}^{\infty}\int_{-\infty}^{\infty} e^{-\iota (A'x'^2 + 2H'x'y' + B'y'^2)/2}\, dx'\, dy'.$$

that is

$$I = 2\pi/\iota\,(A'B' - H'^2)^{\frac{1}{2}} = 2\pi/\iota\kappa' \cos\theta'\,(R^{-1} - f_1^{-1})^{\frac{1}{2}}\,(R^{-1} - f_2^{-1})^{\frac{1}{2}};$$

and, therefore,

$$\begin{aligned}H_x = 2\iota\kappa^2\sigma' \cos\theta\, e^{\iota\kappa Vt - \iota\kappa R_1 - \iota\kappa' R} \{ & l_1 (n \sin\theta - n_2 \cos\theta)/(\sigma \cos\theta' + \sigma' \cos\theta) \\ & - n_1 (l \sin\theta' - l_2 \cos\theta')/(\sigma \cos\theta + \sigma' \cos\theta')\} \\ & \times (R^{-1} - f_1^{-1})^{-\frac{1}{2}} (R^{-1} - f_2^{-1})^{-\frac{1}{2}} R^{-1} R_1^{-1} V^{-1},\end{aligned}$$

$$\begin{aligned}H_y = 2\iota\kappa^2\sigma' \cos\theta\, e^{\iota\kappa Vt - \iota\kappa R_1 - \iota\kappa' R} \{ & m_1 (n \sin\theta - n_2 \cos\theta)/(\sigma \cos\theta' + \sigma' \cos\theta) \\ & - n_1 (m \sin\theta' - m_2 \cos\theta')/(\sigma \cos\theta + \sigma' \cos\theta')\} \\ & \times (R^{-1} - f_1^{-1})^{-\frac{1}{2}} (R^{-1} - f_2^{-1})^{-\frac{1}{2}} R^{-1} R_1^{-1} V^{-1},\end{aligned}$$

$$\begin{aligned}H_z = 2\iota\kappa^2\sigma' \cos\theta\, e^{\iota\kappa Vt - \iota\kappa R_1 - \iota\kappa' R} \{ & n_1 (n \sin\theta - n_2 \cos\theta)/(\sigma \cos\theta' + \sigma' \cos\theta) \\ & - n_1 (n \sin\theta' - n_2 \cos\theta')/(\sigma \cos\theta + \sigma' \cos\theta')\} \\ & \times (R^{-1} - f_1^{-1})^{-\frac{1}{2}} (R^{-1} - f_2^{-1})^{-\frac{1}{2}} R_1^{-1} R^{-1} V^{-1}.\end{aligned}$$

Further, since

$$K' \frac{\partial E_x}{\partial t} = \frac{\partial H_z}{\partial y} - \frac{\partial H_y}{\partial z}, \text{ etc.,}$$

$$K'E_x = H_y (z - \zeta)/V'R - H_z (y - \eta)/V'R, \text{ etc.,}$$

to the same order of approximation, that is

$$\begin{aligned}K'E_x = {} & \kappa'\kappa^2\sigma' I \cos\theta \cos\theta'\, e^{\iota\kappa Vt - \iota\kappa R_1 - \iota\kappa' R} \\ & [n_1 \{(m \sin\theta' - m_2 \cos\theta')(z - \zeta)/R - (n \sin\theta' - n_2 \cos\theta')(y - \eta)/R\} \\ & /(\sigma \cos\theta + \sigma' \cos\theta') - (n \sin\theta - n_2 \cos\theta) \\ & \{m_1 (z - \zeta)/R - n_1 (y - \eta)/R\} \\ & /(\sigma \cos\theta' + \sigma' \cos\theta](\pi V V' R R_1)^{-1}, \text{ etc.,}\end{aligned}$$

or

$$\begin{aligned}K'E_x = \kappa'\kappa^2\sigma' I \cos\theta \cos\theta'\, e^{\iota\kappa Vt - \iota\kappa R_1 - \iota\kappa' R} [& n_1 l_1/(\sigma \cos\theta + \sigma' \cos\theta') \\ & + (n \sin\theta - n_2 \cos\theta) \\ & \times (l \sin\theta' - l_2 \cos\theta')/(\sigma \cos\theta' + \sigma' \cos\theta)] (\pi V V' R R_1)^{-1}, \text{ etc.,}\end{aligned}$$

hence, since

$$\kappa'\kappa^2\sigma'/K'VV' = \kappa'\kappa^2\sigma\mu,$$

$$\begin{aligned}E_x = \pi^{-1}\kappa'\kappa^2\sigma\mu I \cos\theta \cos\theta'\, e^{\iota\kappa Vt - \iota\kappa R_1 - \iota\kappa' R} [& n_1 l_1/(\sigma \cos\theta + \sigma' \cos\theta') \\ & + (n \sin\theta - n_2 \cos\theta) \\ & \times (l \sin\theta' - l_2 \cos\theta')/(\sigma \cos\theta' + \sigma' \cos\theta)] (R R_1)^{-1}, \text{ etc.,}\end{aligned}$$

and, therefore, unless $R - f_1$ or $R - f_2$ is a small quantity,

$$\begin{aligned} E_x = &- 2\iota\kappa^2\sigma\mu \cos\theta\, e^{\iota\kappa Vt - \iota\kappa R_1 - \iota\kappa' R}[n_1 l_1/(\sigma\cos\theta + \sigma'\cos\theta') \\ &+ (n\sin\theta - n_2\cos\theta)(l\sin\theta' - l_2\cos\theta')/(\sigma\cos\theta' + \sigma'\cos\theta)] \\ &\times (R^{-1} - f_1^{-1})^{-\frac{1}{2}}(R^{-1} - f_2^{-1})^{-\frac{1}{2}}(RR_1)^{-1}, \end{aligned}$$

$$\begin{aligned} E_y = &- 2\iota\kappa^2\sigma\mu \cos\theta\, e^{\iota\kappa Vt - \iota\kappa R_1 - \iota\kappa' R}[n_1 m_1/(\sigma\cos\theta + \sigma'\cos\theta') \\ &+ (n\sin\theta - n_2\cos\theta)(m\sin\theta' - m_2\cos\theta')/(\sigma\cos\theta' + \sigma'\cos\theta)] \\ &\times (R^{-1} - f_1^{-1})^{-\frac{1}{2}}(R^{-1} - f_2^{-1})^{-\frac{1}{2}}(RR_1)^{-1}, \end{aligned}$$

$$\begin{aligned} E_z = &- 2\iota\kappa^2\sigma\mu \cos\theta\, e^{\iota\kappa Vt - \iota\kappa R_1 - \iota\kappa' R}[n_1^2/(\sigma\cos\theta + \sigma'\cos\theta') \\ &+ (n\sin\theta - n_2\cos\theta)(n\sin\theta' - n_2\cos\theta')/(\sigma\cos\theta' + \sigma'\cos\theta)] \\ &\times (R^{-1} - f_1^{-1})^{-\frac{1}{2}}(R^{-1} - f_2^{-1})^{-\frac{1}{2}}(RR_1)^{-1}. \end{aligned}$$

and it may be verified that these values of the components of the magnetic and electric forces satisfy the surface conditions.

The rate of transfer of energy in the second medium across an element of surface, whose normal has l', m', n' as direction cosines, is

$$\begin{aligned} \frac{dS}{8\pi}[&M_x(m'\dot{H}_z - n'\dot{H}_y) + M_y(n'\dot{H}_x - l'\dot{H}_z) + M_z(l'\dot{H}_y - m'\dot{H}_x) \\ &- \dot{M}_x(m'H_z - n'H_y) - \dot{M}_y(n'H_x - l'H_z) - \dot{M}_z(l'H_y - m'H_x)], \end{aligned}$$

where M_x, M_y, M_z are the components of momentum. In the direction of the ray

$$\begin{aligned} l' = (x - \xi)/R = l_2\sin\theta' + l\cos\theta', \quad m' &= (y - \eta)/R = m_2\sin\theta' + m\cos\theta', \\ n' &= (z - \zeta)/R = n_2\sin\theta' + n\cos\theta', \end{aligned}$$

whence, writing $I = -\iota I_1$, and taking the real parts of the expressions for the components of the magnetic and electric forces

$$\begin{aligned} m'H_z - n'H_y = \frac{\kappa'\kappa^2\sigma' I_1\cos\theta\cos\theta'}{\pi VRR_1}\sin(\kappa Vt - \kappa R_1 - \kappa' R)\Big[&(m_2\sin\theta' + m\cos\theta') \\ \left\{\frac{n_1(n\sin\theta' - n_2\cos\theta')}{\sigma\cos\theta + \sigma'\cos\theta'} - \frac{n_1(n\sin\theta - n_2\cos\theta)}{\sigma\cos\theta' + \sigma'\cos\theta}\right\} &- (n_2\sin\theta' + n\cos\theta') \\ &\left\{\frac{n_1(m\sin\theta' - m_2\cos\theta')}{\sigma\cos\theta + \sigma'\cos\theta'} - \frac{m_1(n\sin\theta - n_2\cos\theta)}{\sigma\cos\theta' + \sigma'\cos\theta}\right\}\Big], \end{aligned}$$

that is

$$m'\mathrm{H}_z - n'\mathrm{H}_y = -\frac{\kappa'\kappa^2\sigma'\mathrm{I}_1\cos\theta\cos\theta'}{\pi\mathrm{VRR}_1}\sin(\kappa\mathrm{V}t - \kappa\mathrm{R}_1 - \kappa'\mathrm{R})$$

$$\left[\frac{n_1 l_1}{\sigma\cos\theta + \sigma'\cos\theta'} + \frac{(n\sin\theta - n_2\cos\theta)(l\sin\theta' - l_2\cos\theta')}{\sigma\cos\theta' + \sigma'\cos\theta}\right],$$

and the rate of transfer of energy along the ray is

$$\frac{\kappa'^2\kappa^4\sigma\sigma'\mu\mathrm{I}_1{}^2\cos^2\theta\cos^2\theta'}{8\pi^3\mathrm{VR}^2\mathrm{R}_1{}^2}\left[\left\{\frac{n_1 l_1}{\sigma\cos\theta + \sigma'\cos\theta'}\right.\right.$$

$$\left.\left. + \frac{(n\sin\theta - n_2\cos\theta)(l\sin\theta' - l_2\cos\theta')}{\sigma\cos\theta' + \sigma'\cos\theta}\right\}^2 + \ldots + \ldots\right],$$

or

$$\frac{\kappa'^2\kappa^4\sigma'\mathrm{I}_1{}^2\cos^2\theta\cos^2\theta'}{8\pi^3\mathrm{V}^2\mathrm{R}^2\mathrm{R}_1{}^2}\left[\frac{n_1{}^2}{(\sigma\cos\theta + \sigma'\cos\theta')^2} + \frac{(n\sin\theta - n_2\cos\theta)^2}{(\sigma\cos\theta' + \sigma'\cos\theta)^2}\right],$$

that is $\sigma'\mathrm{A}'^2/8\pi$, where A′ is the amplitude of the electric force in the second medium. Similarly it may be shown that the rate of transfer of energy in the direction l, m, n is

$$\frac{\kappa'^2\kappa^4\sigma'\mathrm{I}_1{}^2\cos^2\theta\cos^3\theta'}{8\pi^3\mathrm{V}^2\mathrm{R}^2\mathrm{R}_1{}^2}\left[\frac{n_1{}^2}{(\sigma\cos\theta + \sigma'\cos\theta')^2} + \frac{(n\sin\theta - n_2\cos\theta)^2}{(\sigma\cos\theta' + \sigma'\cos\theta)^2}\right].$$

and at the surface, substituting the value of I_1, this becomes

$$\frac{\kappa^4\sigma'\cos^2\theta\cos\theta'}{2\pi\mathrm{V}^2\mathrm{R}_1{}^2}\left[\frac{n_1{}^2}{(\sigma\cos\theta + \sigma'\cos\theta')^2} + \frac{(n\sin\theta - n_2\cos\theta)^2}{(\sigma\cos\theta' + \sigma'\cos\theta)^2}\right].$$

hence the total rate of transfer across a portion of the surface separating the two media, if total reflexion does not take place at any point on it, is

$$\mathrm{W} = \frac{\kappa^4\sigma'}{2\pi\mathrm{V}^2}\iint\frac{\cos^2\theta\cos\theta'}{\mathrm{R}_1{}^2}\left[\frac{n_1{}^2}{(\sigma\cos\theta + \sigma'\cos\theta')^2} + \frac{(n\sin\theta - n_2\cos\theta)^2}{(\sigma'\cos\theta + \sigma\cos\theta')^2}\right]d\mathrm{S}.$$

Further, if $\sigma > \sigma'$

$$\frac{\kappa^4}{2\pi\mathrm{V}^2\sigma'}\iint\frac{\cos^3\theta\cos\theta'}{\mathrm{R}_1{}^2(\cos\theta + \cos\theta')^2}\{n_1{}^2 + (n\sin\theta - n_2\cos\theta)^2\}d\mathrm{S}$$

$$> \mathrm{W} > \frac{\kappa^4\sigma'}{2\pi\mathrm{V}^2\sigma^2}\iint\frac{\cos^2\theta\cos\theta'}{(\cos\theta + \cos\theta')^n}\{n_1{}^2 + (n\sin\theta - n_2\cos\theta)^2\}\,d\mathrm{S},$$

now it may be shown that

$$n_1{}^2 + (n\sin\theta - n_2\cos\theta)^2 = (\xi^2 + \eta^2)/\mathrm{R}_1{}^2.$$

therefore

$$\frac{\kappa^4}{2\pi\mathrm{V}^2\sigma'}\iint\frac{\cos^2\theta\cos\theta'(\xi^2 + \eta^2)}{\mathrm{R}_1{}^4(\cos\theta + \cos\theta')^2}d\mathrm{S} > \mathrm{W} > \frac{\kappa^4\sigma'}{2\pi\mathrm{V}^2\sigma^2}\iint\frac{\cos^2\theta\cos\theta'(\xi^2 + \eta^2)}{\mathrm{R}_1{}^4(\cos\theta + \cos\theta')^2}d\mathrm{S}.$$

Again, if W_0 is the rate of transfer of energy across the surface when the two media are the same

$$W_0 = \frac{\kappa^4}{8\pi V^2\sigma}\iint \frac{\xi^2 + \eta^2}{R_1{}^4} \cos\theta \, dS,$$

hence

$$\frac{\sigma}{\sigma'} W_0 > W,$$

and, if the source is at a distance from the surface such that

$$(\cos\theta - \cos\theta')^2/(\cos\theta + \cos\theta')^2$$

is negligible, that is such that $(\nu^2 - 1)^2 \tan^4\theta$ is negligible for all points on the surface, then to the order of approximation adopted

$$\sigma W_0/\sigma' > W > \sigma' W_0/\sigma.^*$$

If either of the quantities $R - f_1$ or $R - f_2$ is very small the terms of the third order in the equation of the surface in the neighbourhood of the point P_1 must be retained, and the equation of the surface with P_1 as origin of co-ordinates and the same axes of reference as above is now

$$z' = \tfrac{1}{2}(Ax'^2 + 2Hx'y' + By'^2) + \tfrac{1}{6}(Cx'^3 + 3Lx'^2y' + 3Mx'y'^2 + Dy'^3).$$

The value of $\kappa r_1 + \kappa' r$ is now given by

$$\kappa r_1 + \kappa' r = \kappa R_1 + \kappa' R + \tfrac{1}{2}(A'x'^2 + 2H'x'y' + B'y'^2)$$
$$+ \tfrac{1}{6}(C'x'^3 + 3L'x'^2y' + 3M'x'y'^2 + D'y'^3),$$

where

$$C' = (\kappa\cos\theta - \kappa'\cos\theta')C - 3A(\kappa\sin\theta\cos\theta/R_1 + \kappa'\sin\theta'\cos\theta'/R)$$
$$- 3\kappa\sin\theta\cos^2\theta/R_1{}^2 + 3\kappa'\sin\theta'\cos^2\theta'/R^2,$$

$$L' = (\kappa\cos\theta - \kappa'\cos\theta')L - 2H(\kappa\sin\theta\cos\theta/R_1 + \kappa'\sin\theta'\cos\theta'/R),$$

$$M' = (\kappa\cos\theta - \kappa'\cos\theta')M - B(\kappa\sin\theta\cos\theta/R_1 + \kappa'\sin\theta'\cos\theta'/R)$$
$$- \kappa\sin\theta/R_1{}^2 + \kappa'\sin\theta'/R^2,$$

$$D' = (\kappa\cos\theta - \kappa'\cos\theta')D.$$

Turning the axes of x' and y' through the angle ϕ so that

$$A'x'^2 + 2H'x'y' + B'y'^2 \quad \text{becomes} \quad A''\xi'^2 + B''\eta'^2,$$

$$A'' = \tfrac{1}{2}(A' + B') + \tfrac{1}{2}\sqrt{\{(A' - B')^2 + 4H'^2\}},$$

$$B'' = \tfrac{1}{2}(A' + B') - \tfrac{1}{2}\sqrt{\{(A' - B')^2 + 4H'^2\}},$$

---

* *Cf.*, 'Roy. Soc. Proc.,' A, vol. 114, p. 375.

hence, taking the case where $R - f_1 = \epsilon$,

$$A' + B' = \kappa' (f_1^{-1} - f_2^{-1}) (\cos^2 \theta' \cos^2 \psi + \sin^2 \psi) - \kappa' \epsilon f_1^{-2} (1 + \cos^2 \theta'),$$
$$A'B' - H'^2 = - \kappa'^2 \epsilon f_1^{-2} (f_1^{-1} - f_2^{-1}) \cos^2 \theta',$$

whence

$$\sqrt{\{(A' - B')^2 + 4H'^2\}} = \kappa' (f_1^{-1} - f_2^{-1}) (\cos^2 \theta' \cos^2 \psi + \sin^2 \psi)$$
$$- \kappa' \epsilon f_1^{-2} (1 + \cos^2 \theta') + 2\kappa' \epsilon f_1^{-2} \cos^2 \theta' / (\cos^2 \theta' \cos^2 \psi + \sin^2 \psi),$$

and therefore, retaining only the principal parts,

$$A'' = \kappa' (f_1^{-1} - f_2^{-1}) (\cos^2 \theta' \cos^2 \psi + \sin^2 \psi),$$
$$B'' = - \kappa' \epsilon f_1^{-2} \cos^2 \theta' / (\cos^2 \theta' \cos^2 \psi + \sin^2 \psi),$$

or

$$B'' = - \kappa' \epsilon f_1^{-2} \cos^2 \phi_0 / \cos^2 \psi,$$

where ϕ_0 is the value of ϕ which corresponds to $R = f_1$. Again,

$$C'x'^3 + 3L'x'^2y' + 3M'x'y'^2 + D'y'^3$$

becomes

$$C''\xi'^3 + 3L''\xi'^2\eta' + 3M''\xi'\eta'^2 + D''\eta'^3,$$

where

$$D'' = - C' \sin^3 \phi_0 + 3L' \sin^2 \phi_0 \cos \phi_0 - 3M' \sin \phi_0 \cos^2 \phi_0 + D' \cos^3 \phi_0, \text{ etc.},$$

and the value of I is given by

$$I = \int_{-\infty}^{\infty} \int_{-\infty}^{\infty} e^{-\frac{1}{2}\iota (A''\xi'^2 + B''\eta'^2) - \frac{1}{6}\iota D''\eta'^3} \, d\xi' \, d\eta',$$

that is

$$I = 2e^{-\frac{\pi\iota}{4}} (2\pi/A'')^{\frac{1}{2}} (-6/D'')^{\frac{1}{3}} \, 3^{-\frac{1}{2}} \, \iota \, m e^{2m^3\iota} \, K_{\frac{1}{3}} (2\, m^3 \iota)$$

where

$$m = - 6^{-\frac{1}{3}} B'' \, D''^{-\frac{2}{3}}$$

When the point $P(x, y, z)$ is in the first medium, the components of the magnetic force due to the distribution on the surface which is in the opposite sense to the distribution on the other side of the surface, that is, the components of the magnetic force in the reflected wave, are given by

$$- 4\pi \dot{H}_x = \frac{\partial}{\partial t} \iint \left[\frac{\partial}{\partial y} \left\{ \frac{n_1 H_p' - n_2 H_i'}{r} \right\} - \frac{\partial}{\partial z} \left\{ \frac{m_1 H_p' - m_2 H_i'}{r} \right\} \right] dS$$
$$- \frac{1}{\mu} \iint \left[\frac{\partial^2}{\partial x^2} \left\{ \frac{l_1 E_p' - l_2 E_i'}{r} \right\} + \frac{\partial^2}{\partial x \, \partial y} \left\{ \frac{m_1 E_p' - m_2 E_i'}{r} \right\} \right.$$
$$\left. + \frac{\partial^2}{\partial x \, \partial z} \left\{ \frac{n_1 E_p' - n_2 E_i'}{r} \right\} - K\mu \frac{\partial^2}{\partial t^2} \left\{ \frac{l_1 E_p' - l_2 E_i'}{r} \right\} \right] dS,$$

$$-4\pi\dot{H}_y = \frac{\partial}{\partial t}\iint\left[\frac{\partial}{\partial z}\left\{\frac{l_1H_p' - l_2H_i'}{r}\right\} - \frac{\partial}{\partial x}\left\{\frac{n_1H_p' - n_2H_i'}{r}\right\}\right]dS'$$

$$-\frac{1}{\mu}\iint\left[\frac{\partial^2}{\partial x\,\partial y}\left\{\frac{l_1E_p' - l_2E_i'}{r}\right\} + \frac{\partial^2}{\partial y^2}\left\{\frac{m_1E_p' - m_2E_i'}{r}\right\}\right.$$

$$\left. + \frac{\partial^2}{\partial y\,\partial z}\left\{\frac{n_1E_p' - n_2E_i'}{r}\right\} - K\mu\frac{\partial^2}{\partial t^2}\left\{\frac{m_1E_p' - m_2E_i'}{r}\right\}\right]dS,$$

$$-4\pi\dot{H}_z = \frac{\partial}{\partial t}\iint\left[\frac{\partial}{\partial x}\left\{\frac{m_1H_p' - m_2H_i'}{r}\right\} - \frac{\partial}{\partial y}\left\{\frac{l_1H_p' - l_2H_i'}{r}\right\}\right]dS$$

$$-\frac{1}{\mu}\iint\left[\frac{\partial^2}{\partial x\,\partial z}\left\{\frac{l_1E_p' - l_2E_i'}{r}\right\} + \frac{\partial^2}{\partial y\,\partial z}\left\{\frac{m_1E_p' - m_2E_i'}{r}\right\}\right.$$

$$\left. + \frac{\partial^2}{\partial z^2}\left\{\frac{n_1E_p' - n_2E_i'}{r}\right\} - K\mu\frac{\partial^2}{\partial t^2}\left\{\frac{n_1E_p' - n_2E_i'}{r}\right\}\right]dS,$$

where H_p', etc., now denote the values of H_p, etc., when $t - r/V$ is written for t. The principal parts of the integrals in these expressions are contributed by the portion of the surface which is in the neighbourhood of the point or points on the surface where $\kappa r_1 + \kappa r$ which is stationary, for each integral contains the factor $e^{-\iota\kappa r_1 - \iota\kappa r}$. If P_2 is a point on the surface where $\kappa r_1 + \kappa r$ is stationary, then, taking P_2 as origin, the normal to the surface at P_2 as axis of z', the axes of x' and y' can be chosen so that the co-ordinates of O are x_2, 0, z_2, and the equation of the surface can be written

$$z' = \tfrac{1}{2}(Ax'^2 + 2Hx'y' + By'^2) + \dots;$$

further

$$r_1^2 = (x_2 - x')^2 + y'^2 + (z_2 - z')^2, \quad r^2 = (x - x')^2 + (y - y')^2 + (z - z')^2,$$

and the conditions that $\kappa r_1 + \kappa r$ is stationary at the origin are

$$x_2/r_1 + x/r = 0, \qquad y = 0.$$

Again, if the distance OP_2 is R_2, and the distance PP_2 is R,

$$x_2 = -R_2 \sin\theta, \quad z_2 = -R_2\cos\theta,$$

where θ is the angle of incidence of the waves at P_2, therefore

$$x = R\sin\theta, \quad z = -R\cos\theta.$$

Hence

$$r_1^2 = R_2^2 + 2R_2(x'\sin\theta + z'\cos\theta) + x'^2 + y'^2 + z'^2,$$

$$r^2 = R^2 - 2R(x'\sin\theta - z'\cos\theta) + x'^2 + y'^2 + z'^2,$$

and, to the second order of small quantities x', y',

$$r_1 + r = R_2 + R + \tfrac{1}{2}(A'x'^2 + 2H'x'y' + B'y'^2),$$

where

$$A' = 2A\cos\theta + (R^{-1} + R_2^{-1})\cos^2\theta, \quad B' = 2B\cos\theta + R^{-1} + R_2^{-1}.$$
$$H' = 2H\cos\theta,$$

and, as before, writing

$$2A\cos\theta + R_2^{-1}\cos^2\theta + A_1\cos^2\theta = 0, \quad 2B\cos\theta + R_2^{-1} + B_1 = 0,$$
$$2H\cos\theta = H_1\cos\theta,$$
$$A'B' - H'^2 = \cos^2\theta\,[(R^{-1} - A_1)(R^{-1} - B_1) - H_1^2]$$
$$= (R^{-1} - f_1^{-1})(R^{-1} - f_2^{-1})\cos^2\theta,$$

where

$$A_1 + B_1 = f_1^{-1} + f_2^{-1}, \quad A_1B_1 - H_1^2 = f_1^{-1}f_2^{-1},$$

whence, writing

$$2H_1 = (f_1^{-1} - f_2^{-1})\sin 2\psi,$$
$$A_1 = f_1^{-1}\sin^2\psi + f_2^{-1}\cos^2\psi, \quad B_1 = f_1^{-1}\cos^2\psi + f_2^{-1}\sin^2\psi,$$
$$2H' = (f_1^{-1} - f_2^{-1})\sin 2\psi\cos\theta.$$

The components of the magnetic force in the reflected wave at P are given by

$$\begin{aligned}
-4\pi\mu\dot{H}_x = [\mu\kappa^2 V\,[\,&\{n_1(y-\eta) - m_1(z-\zeta)\}\,H_p'R^{-2}\\
&- \{n_2(y-\eta) - m_2(z-\zeta)\}\,H_i'R^{-2}]\\
&+ \kappa^2[\{(x-\xi)(l_1(x-\xi) + m_1(y-\eta) + n_1(z-\zeta)) - l_1R^2\}\,E_p'R^{-3}\\
&- \{(x-\xi)(l_2(x-\xi) + m_2(y-\eta) + n_2(z-\zeta)) - l_2R^2\}\,E_i'R^{-3}]\,]\,I.
\end{aligned}$$

$$\begin{aligned}
-4\pi\mu\dot{H}_y = [\mu\kappa^2 V\,[\,&\{l_1(z-\zeta) - n_1(x-\xi)\}\,H_p'R^{-2}\\
&- \{l_2(z-\zeta) - n_2(x-\xi)\}\,H_i'R^{-2}]\\
&+ \kappa^2[\{(y-\eta)(l_1(x-\xi) + m_1(y-\eta) + n_1(z-\zeta)) - m_1R^2\}\,E_p'R^{-3}\\
&- \{(y-\eta)(l_2(x-\xi) + m_2(y-\eta) + n_2(z-\zeta)) - m_2R^2\}\,E_i'R^{-3}]\,]\,I,
\end{aligned}$$

$$\begin{aligned}
-4\pi\mu\dot{H}_z = [\mu\kappa^2 V\,[\,&(m_1(x-\xi) - l_1(y-\eta))\}\,H_p'R^{-2}\\
&- \{m_2(x-\xi) - l_2(y-\eta))\}\,H_i'R^{-2}]\\
&+ \kappa^2[\{(z-\zeta)(l_1(x-\xi) + m_1(y-\eta) + n_1(z-\zeta)) - n_1R^2\}\,E_p'R^{-3}\\
&- \{(z-\zeta)(l_2(x-\xi) + m_2(y-\eta) + n_2(z-\zeta) - n_2R^2\}\,E_i'R^{-3}]\,]\,I,
\end{aligned}$$

where

$$I = \iint e^{-\iota\kappa(r_1 - R_2) - \iota\kappa(r - R)}\,dS,$$

and, to the order of approximation adopted, the parts of the expressions on the right-hand side outside the sign of integration have the values which belong to the point P_2. Now, since in these expressions ξ, η, ζ denote the co-ordinates of the point P_2,

$$x - \xi = R\,(l_2 \sin\theta - l\cos\theta), \qquad y - \eta = R\,(m_2 \sin\theta - m\cos\theta),$$
$$z - \zeta = R\,(n_2 \sin\theta - n\cos\theta),$$

hence

$$n_1\,(y-\eta)/R - m_1\,(z-\zeta)/R = l\sin\theta + l_2\cos\theta,$$
$$n_2\,(y-\eta)/R - m_2\,(z-\zeta)/R = -\,l_1\cos\theta,$$

$$l_1\,(z-\zeta)/R - n_1\,(x-\xi)/R = m\sin\theta + m_2\cos\theta,$$
$$l_2\,(z-\zeta)/R - n_2\,(x-\xi)/R = -\,m_1\cos\theta,$$

$$m_1\,(x-\xi)/R - l_1\,(y-\eta)/R = n\sin\theta + n_2\cos\theta,$$
$$m_2\,(x-\xi)/R - l_2\,(y-\eta)/R = -\,n_1\cos\theta,$$

$$l_1\,(x-\xi)/R + m_1\,(y-\eta)/R + n_1\,(z-\zeta)/R = 0,$$

$$l_2\,(x-\xi)/R + m_2\,(y-\eta)/R + n_2\,(z-\zeta)/R = \sin\theta,$$

and

$$\{(x-\xi)/R\}\,\{l_2\,(x-\xi)/R + m_2\,(y-\eta)/R + n_2\,(z-\zeta)/R\} - l_2$$
$$= -\cos\theta\,(l\sin\theta + l_2\cos\theta),$$

$$\{(y-\eta)/R\}\,\{l_2\,(x-\xi)/R + m_2\,(y-\eta)/R + n_2\,(z-\zeta)/R\} - m_2$$
$$= -\cos\theta\,(m\sin\theta + m_2\cos\theta),$$

$$\{(z-\zeta)/R\}\,\{l_2\,(x-\xi)/R + m_2\,(y-\eta)/R + n_2\,(z-\zeta)/R\} - n_2$$
$$= -\cos\theta\,(n\sin\theta + n_2\cos\theta).$$

Therefore

$$-\,4\pi\mu\dot{H}_x = [\mu\kappa^2 V\,\{(l\sin\theta + l_2\cos\theta)\,H_p'/R + l_1\cos\theta\,H_i'/R\}$$
$$+\,\kappa^2\,\{-\,l_1 E_p'/R + \cos\theta\,(l\sin\theta + l_2\cos\theta)\,E_i'/R\}]\,I,$$

$$-\,4\pi\mu\dot{H}_y = [\mu\kappa^2 V\,\{(m\sin\theta + m_2\cos\theta)\,H_p'/R + m_1\cos\theta\,H_i'/R\}$$
$$+\,\kappa^2\{-\,m_1 E_p'/R + \cos\theta\,(m\sin\theta + m_2\cos\theta)\,E_i'/R\}]\,I,$$

$$-\,4\pi\mu\dot{H}_z = [\mu\kappa^2 V\,\{(n\sin\theta + n_2\cos\theta)\,H_p'/R + n_1\cos\theta/H_i'/R\}$$
$$+\,\kappa^2\,\{-\,n_1 E_p'/R + \cos\theta\,(n\sin\theta + n_2\cos\theta)\,E_i'/R\}]\,I\,;$$

that is

$$4\pi\mu\dot{\mathrm{H}}_x = -\kappa^2[(l\sin\theta + l_2\cos\theta)(\mu\mathrm{VH}_p'/\mathrm{R} + \mathrm{E}_i'\cos\theta/\mathrm{R}) \\ + l_1(\mu\mathrm{VH}_i'\cos\theta/\mathrm{R} - \mathrm{E}_p'/\mathrm{R})]\,\mathrm{I},$$

$$4\pi\mu\dot{\mathrm{H}}_y = -\kappa^2[(m\sin\theta + m_2\cos\theta)(\mu\mathrm{VH}_p'/\mathrm{R} + \mathrm{E}_i'\cos\theta/\mathrm{R}) \\ + m_1(\mu\mathrm{VH}_i'\cos\theta/\mathrm{R} - \mathrm{E}_p'/\mathrm{R})]\,\mathrm{I},$$

$$4\pi\mu\dot{\mathrm{H}}_z = -\kappa^2[(n\sin\theta + n_2\cos\theta)(\mu\mathrm{VH}_p'/\mathrm{R} + \mathrm{E}_i'\cos\theta/\mathrm{R}) \\ + n_1(\mu\mathrm{VH}_i'\cos\theta/\mathrm{R} - \mathrm{E}_p'/\mathrm{R}]\,\mathrm{I}.$$

Now

$$\mu\mathrm{VH}_p' + \mathrm{E}_i'\cos\theta = i\kappa^2 e^{\iota\kappa(\mathrm{V}t-\mathrm{R}-\mathrm{R}_2)} \\ \{2\mu n_1\sigma'\cos\theta\cos\theta' - 2\mu n_1\sigma\cos^2\theta\}/(\sigma\cos\theta + \sigma'\cos\theta')\,\mathrm{R}_2,$$

$$\mu\mathrm{VH}_i'\cos\theta - \mathrm{E}_p' = i\kappa^2 e^{\iota\kappa(\mathrm{V}t-\mathrm{R}-\mathrm{R}_2)} \\ \{2\mu\sigma'\cos^2\theta - 2\mu\sigma\cos\theta\cos\theta'\}(n\sin\theta - n_2\cos\theta)/(\sigma\cos\theta' + \sigma'\cos\theta)\,\mathrm{R}_2,$$

Therefore

$$\mathrm{H}_x = -\kappa^3 e^{\iota\kappa(\mathrm{V}t-\mathrm{R}-\mathrm{R}_2)}[n_1(l\sin\theta + l_2\cos\theta)(\sigma'\cos\theta' - \sigma\cos\theta)/(\sigma'\cos\theta' \\ + \sigma\cos\theta) + l_1(n\sin\theta - n_2\cos\theta)(\sigma'\cos\theta - \sigma\cos\theta')/(\sigma'\cos\theta \\ + \sigma\cos\theta')]\,\mathrm{I}\cos\theta/2\pi\mathrm{VRR}_2,$$

$$\mathrm{H}_y = -\kappa^3 e^{\iota\kappa(\mathrm{V}t-\mathrm{R}-\mathrm{R}_2)}[n_1(m\sin\theta + m_2\cos\theta)(\sigma'\cos\theta' - \sigma\cos\theta)/(\sigma'\cos\theta' \\ + \sigma\cos\theta) + m_1(n\sin\theta - n_2\cos\theta)(\sigma'\cos\theta - \sigma\cos\theta')/(\sigma'\cos\theta \\ + \sigma\cos\theta')]\,\mathrm{I}\cos\theta/2\pi\mathrm{VRR}_2,$$

$$\mathrm{H}_z = -\kappa^3 e^{\iota\kappa(\mathrm{V}t-\mathrm{R}-\mathrm{R}_2)}[n_1(n\sin\theta + n_2\cos\theta)(\sigma'\cos\theta' - \sigma\cos\theta)/(\sigma'\cos\theta' \\ + \sigma\cos\theta) + n_1(n\sin\theta - n_2\cos\theta)(\sigma'\cos\theta - \sigma\cos\theta')/(\sigma'\cos\theta \\ + \sigma\cos\theta')]\,\mathrm{I}\cos\theta/2\pi\mathrm{VRR}_2.$$

Now, unless $\mathrm{R} - f_1$ or $\mathrm{R} - f_2$ is a small quantity, that is, unless the point P is on or near a caustic the value of I is

$$\int_{-\infty}^{\infty}\int_{-\infty}^{\infty} e^{-\frac{\iota\kappa}{2}(\mathrm{A}'x'^2 + 2\mathrm{H}'x'y' + \mathrm{B}'y'^2)}\,dx'\,dy',$$

that is

$$2\pi/\iota\kappa\,(\mathrm{A}'\mathrm{B}' - \mathrm{H}'^2)^{\frac{1}{2}} = 2\pi/\iota\kappa\cos\theta\,(\mathrm{R}^{-1} - f_1^{-1})^{\frac{1}{2}}(\mathrm{R}^{-1} - f_2^{-1})^{\frac{1}{2}},$$

and therefore the values of the principal parts of the components of the magnetic force in the reflected wave are given by

$$\begin{aligned} \mathrm{H}_x = \iota\kappa^2 e^{\iota\kappa(\mathrm{V}t-\mathrm{R}-\mathrm{R}_2)} & [n_1 (l \sin\theta + l_2 \cos\theta)(\sigma' \cos\theta' - \sigma\cos\theta)/(\sigma'\cos\theta' + \sigma\cos\theta) \\ & + l_1 (n \sin\theta - n_2 \cos\theta)(\sigma'\cos\theta - \sigma\cos\theta')/(\sigma'\cos\theta + \sigma\cos\theta')] \\ & (\mathrm{R}^{-1} - f_1^{-1})^{-\frac{1}{2}} (\mathrm{R}^{-1} - f_2^{-1})^{-\frac{1}{2}} (\mathrm{VRR}_2)^{-1}, \end{aligned}$$

$$\begin{aligned} \mathrm{H}_y = \iota\kappa^2 e^{\iota\kappa(\mathrm{V}t-\mathrm{R}-\mathrm{R}_2)} & [n_1 (m \sin\theta + m_2 \cos\theta) \\ & (\sigma'\cos\theta' - \sigma\cos\theta)/(\sigma'\cos\theta' + \sigma\cos\theta) + m_1 (n \sin\theta - n_2 \cos\theta) \\ & (\sigma'\cos\theta - \sigma\cos\theta')/(\sigma'\cos\theta + \sigma\cos\theta')] \\ & (\mathrm{R}^{-1} - f_1^{-1})^{-\frac{1}{2}} (\mathrm{R}^{-1} - f_2^{-1})^{-\frac{1}{2}} (\mathrm{VRR}_2)^{-1}, \end{aligned}$$

$$\begin{aligned} \mathrm{H}_z = \iota\kappa^2 e^{\iota\kappa(\mathrm{V}t-\mathrm{R}-\mathrm{R}_2)} & [n_1 (n \sin\theta + n_2 \cos\theta)(\sigma'\cos\theta' - \sigma\cos\theta)/(\sigma'\cos\theta' + \sigma\cos\theta) \\ & + n_1 (n \sin\theta - n_2 \cos\theta)(\sigma'\cos\theta - \sigma\cos\theta')/(\sigma'\cos\theta + \sigma\cos\theta')] \\ & (\mathrm{R}^{-1} - f_1^{-1})^{-\frac{1}{2}} (\mathrm{R}^{-1} - f_2^{-1})^{-\frac{1}{2}} (\mathrm{VRR}_2)^{-1}, \end{aligned}$$

and it may be deduced that the values of the components of the electric force in the reflected wave are, to the same order of approximation,

$$\begin{aligned} \mathrm{E}_x = i\mu\kappa^2 e^{\iota\kappa(\mathrm{V}t-\mathrm{R}-\mathrm{R}_2)} & [n_1 l_1 (\sigma'\cos\theta' - \sigma\cos\theta)/(\sigma'\cos\theta' + \sigma\cos\theta) \\ & - (l \sin\theta + l_2 \cos\theta)(n \sin\theta - n_2 \cos\theta) \\ & (\sigma'\cos\theta - \sigma\cos\theta')/(\sigma'\cos\theta + \sigma\cos\theta')] \\ & (\mathrm{R}^{-1} - f_1^{-1})^{-\frac{1}{2}} (\mathrm{R}^{-1} - f_2^{-1})^{-\frac{1}{2}} (\mathrm{RR}_2)^{-1}, \end{aligned}$$

$$\begin{aligned} \mathrm{E}_y = i\mu\kappa^2 e^{\iota\kappa(\mathrm{V}t-\mathrm{R}-\mathrm{R}_2)} & [n_1 m_1 (\sigma'\cos\theta' - \sigma\cos\theta)/(\sigma'\cos\theta' + \sigma\cos\theta) \\ & - (m \sin\theta + m_2 \cos\theta)(n \sin\theta - n_2 \cos\theta) \\ & (\sigma'\cos\theta - \sigma\cos\theta')/(\sigma'\cos\theta + \sigma\cos\theta')] \\ & (\mathrm{R}^{-1} - f_1^{-1})^{-\frac{1}{2}} (\mathrm{R}^{-1} - f_2^{-1})^{-\frac{1}{2}} (\mathrm{RR}_2)^{-1}, \end{aligned}$$

$$\begin{aligned} \mathrm{E}_z = i\mu\kappa^2 e^{\iota\kappa(\mathrm{V}t-\mathrm{R}-\mathrm{R}_2)} & [n_1^2 (\sigma'\cos\theta' - \sigma\cos\theta)/(\sigma'\cos\theta' + \sigma\cos\theta) \\ & - (n \sin\theta + n_2 \cos\theta)(n \sin\theta - n_2 \cos\theta) \\ & (\sigma'\cos\theta - \sigma\cos\theta')/(\sigma'\cos\theta + \sigma\cos\theta')] \\ & (\mathrm{R}^{-1} - f_1^{-1})^{-\frac{1}{2}} (\mathrm{R}^{-1} - f_2^{-1})^{-\frac{1}{2}} (\mathrm{RR}_2)^{-1}. \end{aligned}$$

It may be verified that these values of the components of the electric and magnetic forces in the reflected wave, along with the components of the electric and magnetic forces due to the source, satisfy the boundary conditions.

As above, if either of the quantities $\mathrm{R} - f_1$ or $\mathrm{R} - f_2$ is very small, the terms of the third order in the equation of the surface in the neighbourhood of P_2 must be retained, and the equation of the surface is now

$$z' = \tfrac{1}{2}(Ax'^2 + 2Hx'y' + By'^2) + \tfrac{1}{6}(Cx'^3 + 3Lx'^2y' + 3Mx'y'^2 + Dy'^3),$$

and the value of $r + r_1$ is given by

$$\begin{aligned} r + r_1 = R + R_2 &+ \tfrac{1}{2}(A'x'^2 + 2H'x'y' + B'y'^2) \\ &+ \tfrac{1}{6}(C'x'^3 + 3L'x'^2y' + 3M'x'y'^2 + D'y'^3), \end{aligned}$$

where A′, B′, H′ have the values given above, and

$$\begin{aligned} C' &= 2C\cos\theta - 3A\sin\theta\cos\theta\,(R_2^{-1} - R^{-1}) + 3\sin^3\theta\,(R_2^{-2} - R^{-2}), \\ L' &= 2L\cos\theta - 2H\sin\theta\cos\theta\,(R_2^{-1} - R^{-1}), \\ M' &= 2M\cos\theta - B\sin\theta\,(R_2^{-1} - R^{-1}), \qquad D' = 2D\cos\theta. \end{aligned}$$

Turning the axes of x', y' through an angle ϕ so that $A'x'^2 + 2H'x'y' + B'y'^2$ becomes $A''\xi'^2 + B''\eta'^2$, it may be shown that

$$\begin{aligned} A'' = (R^{-1} - f_1^{-1})&(\cos\phi\cos\theta\sin\psi - \sin\phi\cos\psi)^2 \\ &+ (R^{-1} - f_2^{-1})(\cos\phi\cos\theta\cos\psi + \sin\phi\sin\psi)^2, \\ B'' = (R^{-1} - f_1^{-1})&(\sin\phi\cos\theta\sin\psi + \cos\phi\cos\psi)^2 \\ &+ (R^{-1} - f_2^{-1})(\sin\phi\cos\theta\cos\psi - \cos\phi\sin\psi)^2, \end{aligned}$$

and therefore, if ϕ_1 is the value of ϕ corresponding to $R = f_1$,

$$A'' = (f_1^{-1} - f_2^{-1})\cos^2\psi\cos^2\theta/\cos^2\phi_1, \quad B'' = -\varepsilon_1 f_1^{-2}\cos^2\phi_1/\cos^2\psi,$$

when $R = f_1 + \varepsilon_1$, and, if ϕ_2 is the value of ϕ when $R = f_2$,

$$A'' = -\varepsilon_2 f_2^{-2}\cos^2\phi_2\cos^2\theta/\cos^2\psi, \quad B'' = (f_2^{-1} - f_1^{-1})\cos^2\psi/\cos^2\phi_2,$$

when $R = f_2 + \varepsilon_2$. The expression for $r + r_1$ when $R = f_1 + \varepsilon_1$ is therefore

$$R + R_2 + \tfrac{1}{2}(A''\xi'^2 + B''\eta'^2) + \tfrac{1}{6}(C''\xi'^3 + 3L''\xi'^2\eta' + 3M''\xi'\eta'^2 + D''\eta'^3),$$

where

$$D'' = -C'\sin^3\phi_1 + 3L'\sin^2\phi_1\cos\phi_1 - 3M'\sin\phi_1\cos^2\phi_1 + D'\cos^3\phi_1,$$

when $R = f_1 + \varepsilon_1$, and the value of C″ is

$$C'' = C'\cos^3\phi_2 + 3L'\cos^2\phi_2\sin\phi_2 + 3M'\cos\phi_2\sin^2\phi_2 + D'\sin^3\phi_2,$$

when $R = f_2 + \varepsilon_2$, to the order of approximation required. Hence when $R = f_1 + \varepsilon_1$ the value of I is given by

$$\int_{-\infty}^{\infty}\int_{-\infty}^{\infty} e^{-\frac{1}{2}\iota\kappa(A''\xi'^2+B''\eta'^2)-\frac{1}{6}\iota\kappa D''\eta'^3}\,d\xi'\,d\eta',$$

that is

$$I = 2e^{-\frac{\pi\iota}{4}}(2\pi/\kappa A'')^{\frac{1}{2}}(-6/\kappa D'')^{\frac{1}{3}}\,3^{-\frac{1}{2}}\,\iota m e^{2m^3\iota}\,K_{\frac{1}{3}}(2m^3\iota)$$

where

$$m = -6^{-\frac{1}{3}}\kappa^{\frac{1}{3}}B''D''^{-\frac{2}{3}}$$

Similarly, when $R = f_2 + \varepsilon_2$,

$$I = 2e^{-\frac{\pi\iota}{4}}(2\pi/\kappa B'')^{\frac{1}{2}}(-6/\kappa C'')^{\frac{1}{3}}\,3^{-\frac{1}{2}}\,\iota m e^{2m^3\iota}\,K_{\frac{1}{3}}(2m^3\iota)$$

where

$$m = -6^{-\frac{1}{3}}\kappa^{\frac{1}{3}}A''C''^{-\frac{2}{3}}$$

In the above it has been assumed that the coefficients of the terms of the third degree in the expression for $r + r_1$ are finite; when this condition is not satisfied, as in a case to be treated later, the terms of the fourth order must be retained; it has been assumed also that there is only one point on the surface where $r + r_1$ is stationary, when there is more than one such point, each point can be treated separately and the results added.

When $K'\mu'/K\mu < 1$ and $\sin\theta > (K'\mu'/K\mu)^{\frac{1}{2}}$, there is total reflexion at the surface separating the media, and writing $\sin\theta_0 = (K'\mu'/K\mu)^{\frac{1}{2}}$, the tangential components of the electric and magnetic forces at a point on the surface at a distance r_1 from the oscillator, if the surface were a plane surface, are

$$\begin{aligned}
E_t &= -i\mu\kappa^2 n_1(1-e^{-\iota\chi})\,e^{\iota\kappa(Vt-r_1)}/r_1,\\
E_p &= i\mu\kappa^2(n\sin\theta - n_2\cos\theta)\cos\theta\,(1+e^{-\iota\chi'})\,e^{\iota\kappa(Vt-r_1)}/r_1,\\
H_t &= i\kappa^2(n\sin\theta - n_2\cos\theta)(1-e^{-\iota\chi'})\,e^{\iota\kappa(Vt-r_1)}/Vr_1,\\
H_p &= i\kappa^2 n_1\cos\theta\,(1+e^{-\iota\chi})\,e^{\iota\kappa(Vt-r_1)}/Vr_1,
\end{aligned}$$

where

$$\tan\tfrac{1}{2}\chi = \sigma\cos\theta/\rho,\quad \tan\tfrac{1}{2}\chi' = \cos\theta/\rho'\sigma,\quad \rho = \nu/\kappa\mu'V,\quad \rho' = \nu/\kappa K'V,$$
$$\nu^2 = \kappa^2(\sin^2\theta - \sin^2\theta_0),^{*}$$

and therefore in the expressions for the components of the electric and magnetic forces in the reflected waves

$$\mu VH_p' + E_t'\cos\theta = 2i\mu\kappa^2 n_1\cos\theta\,e^{\iota\kappa(Vt-R-R_2)-\iota\chi}/R_2,$$
$$\mu VH_t'\cos\theta - E_p' = -2i\mu\kappa^2(n\sin\theta - n_2\cos\theta)\cos\theta\,e^{\iota\kappa(Vt-R-R_2)-\iota\chi'}/R_2,$$

---

[*] 'Roy. Soc. Proc.,' A, vol. 119, p. 523.

Hence, when there is total reflexion, the components of the magnetic force in the reflected wave are given by

$$H_x = -\kappa^3 e^{\iota\kappa(Vt-R-R_2)}[n_1(l\sin\theta + l_2\cos\theta)e^{-\iota\chi} - l_1(n\sin\theta - n_2\cos\theta)e^{-\iota\chi'}]\,I\cos\theta/2\pi VRR_2,$$

$$H_y = -\kappa^3 e^{\iota\kappa(Vt-R-R_2)}[n_1(m\sin\theta + m_2\cos\theta)e^{-\iota\chi} - m_1(n\sin\theta - n_2\cos\theta)e^{-\iota\chi'}]\,I\cos\theta/2\pi VRR_2,$$

$$H_z = -\kappa^3 e^{\iota\kappa(Vt-R-R_2)}[n_1(n\sin\theta + n_2\cos\theta)e^{-\iota\chi} - n_1(n\sin\theta - n_2\cos\theta)e^{-\iota\chi'}]\,I\cos\theta/2\pi VRR_2,$$

and I has the value given above.*

When the surface separating the two media is a sphere of radius a, or the portion of the surface in the neighbourhood of the point P_2 is a sphere of radius a, and the oscillator is at a distance b from the centre of the sphere with its axis along the radius through the point,

$$\xi = a\sin\chi\cos\phi, \qquad \eta = a\sin\chi\sin\phi, \qquad \zeta = a\cos\chi - b,$$
$$l = \sin\chi\cos\phi, \qquad m = \sin\chi\sin\phi, \qquad n = \cos\chi,$$

where χ, ϕ are the polar co-ordinates of a point on the sphere, the radius through the oscillator being the axis of the co-ordinates, then

$$l_1/-\sin\phi = m_1/\cos\phi = n_1/0 = 1,$$
$$l_2/\cos\phi\cos\chi = m_2/\sin\phi\cos\chi = n_2/-\sin\chi = 1,$$

and

$$n\sin\theta - n_2\cos\theta = \sin(\theta+\chi) = a\sin\chi/R_2.$$

Hence, when $R - f_1$ and $R - f_2$ are both finite

$$(H_x, H_y, H_z) = (l_1, m_1, 0)\,i\kappa^2 e^{\iota\kappa(Vt-R-R_2)}(a\sin\chi/VRR_2^2)$$
$$\{(\sigma'\cos\theta - \sigma\cos\theta')/(\sigma'\cos\theta + \sigma\cos\theta')\}\cdot(R^{-1} - f_1^{-1})^{-\frac{1}{2}}(R^{-1} - f_2^{-1})^{-\frac{1}{2}}.$$

Now, in this case,

$$\cos\theta(1/R_2 + 1/f_2) = 2/a, \qquad 1/R_2 + 1/f_1 = 2\cos\theta/a,$$

therefore

$$(H_x, H_y, H_z) = (l_1, m_1, 0)\,i\kappa^2 e^{\iota\kappa(Vt-R-R_2)}(a\sin\chi/VRR_2^2)$$
$$\times\{(\sigma'\cos\theta - \sigma\cos\theta')/(\sigma'\cos\theta + \sigma\cos\theta')\}$$
$$\times(R^{-1} + R_2^{-1} - 2a^{-1}\cos\theta)^{-\frac{1}{2}}\{R^{-1} + R_2^{-1} - 2(a\cos\theta)^{-1}\}^{-\frac{1}{2}},$$

---

* It may be observed that in the region of the second medium beyond the portion of the separating surface where there is total reflexion there is a shadow, as there is no point P_1 on this portion of the separating surface where $\kappa r_1 + \kappa' r$ is stationary.

and when $R = R_2$, this becomes

$$(H_x, H_y, H_z) = (l_1, m_1, 0)\ \iota\kappa^2 e^{\iota\kappa(Vt-2R_2)}$$
$$\{(\sigma' \cos\theta - \sigma\cos\theta')/(\sigma'\cos\theta + \sigma\cos\theta')\}\, a^2 \sin\chi\, (\cos\theta)^{\frac{1}{2}}$$
$$/2VR_2^2 (a - R_2\cos\theta)^{\frac{1}{2}}\,(a\cos\theta - R_2)^{\frac{1}{2}}.$$

Now

$$a - R_2\cos\theta = b\cos\chi, \qquad a\cos\theta - R_2 = b\,(a\cos\chi - b)/R_2,$$

whence

$$a^2\sin\chi\,(\cos\theta)^{\frac{1}{2}}/R_2^2 (a - R_2\cos\theta)^{\frac{1}{2}}\,(a\cos\theta - R_2)^{\frac{1}{2}}$$
$$= \{a^2\sin\chi/bR_2^2\cos^{\frac{1}{2}}\chi\}\,\{(a - b\cos\chi)/(a\cos\chi - b)\}^{\frac{1}{2}},$$

and therefore

$$(H_x, H_y, H_z) = (l_1, m_1, 0)\ i\kappa^2 e^{\iota\kappa(Vt-2R_2)}$$
$$\{(\sigma'\cos\theta - \sigma\cos\theta')/(\sigma'\cos\theta + \sigma\cos\theta')\}\,\{a^2\sin\chi/2VbR_2^2(\cos\chi)^{\frac{1}{2}}\}$$
$$\times\{(a - b\cos\chi)/(a\cos\chi - b)\}^{\frac{1}{2}},$$

and, if ψ denotes the magnetic force at the point multiplied by the distance of the point from the axis of the oscillator,

$$\psi = \iota\kappa^2 V^{-1} e^{\iota\kappa(Vt-2R_2)}\,(a/R_2)^2\sin^2\chi\,(\cos\chi)^{\frac{1}{2}}$$
$$\{(a - b\cos\chi)/(a\cos\chi - b)\}^{\frac{1}{2}}\,\{(\sigma'\cos\theta - \sigma\cos\theta')/(\sigma'\cos\theta + \sigma\cos\theta')\}.$$

Again, if $\bar{\psi}$ denotes the value of ψ when the medium is the same throughout,

$$\bar{\psi} = \iota\kappa^2 V^{-1} e^{\iota\kappa(Vt-2b\sin\chi)}\cos^2\chi,$$

and therefore the ratio of the amplitudes of ψ and $\bar{\psi}$ is

$$(a/R_2)^2\sin^2\chi\,(\cos\chi)^{-\frac{3}{2}}\{(a - b\cos\chi)/(a\cos\chi - b)\}^{\frac{1}{2}}$$
$$\times\{(\sigma'\cos\theta - \sigma\cos\theta')/(\sigma'\cos\theta + \sigma\cos\theta')\}.$$

When there is total internal reflexion at the surface of the sphere, the values of H_x, H_y, H_z are given by

$$(H_x, H_y, H_z) = (l_1, m_1, 0) \times -\iota\kappa^2 e^{\iota\kappa(Vt-R-R_2)-\iota\chi'}\,(a\sin\chi/VRR_2^2)$$
$$\times\{R^{-1} + R_2^{-1} - 2\cos\theta/a\}^{-\frac{1}{2}}\{R^{-1} + R_2^{-1} - 2/(a\cos\theta)\}^{-\frac{1}{2}},$$

the point not being near to nor on a caustic, and when $R = R_2$ this becomes

$$(H_x, H_y, H_z) = (l_1, m_1, 0) \times -\iota\kappa^2 e^{\iota\kappa(Vt-2R_2)-\iota\chi'}\,\{a^2\sin\chi/2VbR_2^2(\cos\chi)^{\frac{1}{2}}\}$$
$$\times\{(a - b\cos\chi)/(a\cos\chi - b)\}^{\frac{1}{2}},$$

where

$$\tan\tfrac{1}{2}\chi' = \kappa K'V\cos\theta/v\sigma.$$

The value of ψ is given by

$$\psi = -\iota\kappa^2 V^{-1} e^{\iota\kappa(Vt-2R_2)-\iota\chi'} (a/R_2)^2 \sin^2\chi\,(\cos\chi)^{\frac{1}{2}}\{(a-b\cos\chi)/(a\cos\chi-b)\}^{\frac{1}{2}},$$

and therefore the ratio of the amplitudes of ψ and $\overline{\psi}$ in this case is

$$(a/R_2)^2 \sin^2\chi\,(\cos\chi)^{-\frac{3}{2}}\{(a-b\cos\chi)/(a\cos\chi-b)\}^{\frac{1}{2}}.{}^{*}$$

When there is a simple oscillator at the surface of a perfectly conducting sphere of radius b, the axis of the oscillator being normal to the surface of the sphere, and there is a discontinuity in the constants of the surrounding medium at the surface of the concentric sphere radius a, the components of the electric and magnetic forces at any point P can be deduced immediately from the above. In particular the value of the magnetic force at a point P on the surface of the sphere of radius b is four times that given above, there being complete reflexion at the oscillator and also at the point P, and therefore the value of the ratio $\psi/\overline{\psi}$ in this case is four times that given above, agreeing with a former result.[†]

When the point P is on or near to a caustic, that is when R differs from $2/(a\cos\theta) - 1/R_2$ or from $2\cos\theta\,(a - 1/R_2)$ by a small quantity or takes either of these values, small quantities of higher order must be retained in the above investigation. The equation to the surface of the sphere is

$$z' = -(x'^2+y'^2+z'^2)/2a,$$

and therefore

$$r_1^2 = R_2^2 + 2R_2x'\sin\theta + (x'^2+y'^2+z'^2)(1-R_2\cos\theta/a),$$
$$r^2 = R^2 - 2Rx'\sin\theta + (x'^2+y'^2+z'^2)(1-R\cos\theta/a),$$

whence

$$\begin{aligned} r_1 = {} & R_2 + x'\sin\theta + (x'^2+y'^2+z'^2)(1-R_2\cos\theta/a)/2R_2 - x'^2\sin^2\theta/2R_2 \\ & - x'\sin\theta\,(x'^2+y'^2+z'^2)(1-R_2\cos\theta/a)/2R_2^2 \\ & - (x'^2+y'^2+z'^2)^2(1-R_2\cos\theta/a)^2/8R_2^3 \\ & + x'^3\sin^3\theta/2R_2^2 + 3x'^2\sin^2\theta\,(x'^2+y'^2+z'^2)(1-R_2\cos\theta/a)/4R_2^3 \\ & - 5x'^4\sin^4\theta/8R_2^3, \end{aligned}$$

with a similar expression for r. Therefore to the fourth order of small quantities

$$\begin{aligned} r_1 + r = R_2 + R + \tfrac{1}{2}(A_1x'^2 + B_1y'^2) & \\ + \tfrac{1}{6}(C_1x'^3 + 3L_1x'^2y' + 3M_1x'y'^2 + D_1y'^3) & \\ + \tfrac{1}{24}[E_1x'^4 + 6G_1x'^2y'^2 + F_1y'^4], & \end{aligned}$$

---

[*] There is a second reflected wave at P from another point Q′ on the great circle through P and the oscillator.

[†] 'Roy. Soc. Proc.,' A, vol. 108, p. 65 (1925).

where

$$A_1 = \cos^2\theta\,[1/R_2 + 1/R - 2/(a\cos\theta)], \quad B_1 = 1/R_2 + 1/R - 2\cos\theta/a,$$

$$C_1 = -3\sin\theta\cos^2\theta\,(1/R_2 - 1/R)(1/R_2 + 1/R - 1/a\cos\theta),$$

$$L_1 = 0, \quad M_1 = -\sin\theta\,(1/R_2 - 1/R)(1/R_2 + 1/R - \cos\theta/a), \quad D_1 = 0,$$

$$\begin{aligned} E_1 = {} & 3\,(1/R_2 + 1/R - 2\cos\theta/a)/a^2 - 3\,[(1 - R_2\cos\theta/a)^2/R_2^3 \\ & + (1 - R\cos\theta/a)^2/R^3] \\ & + 18\sin^2\theta\,[(1 - R_2\cos\theta/a)/R_2^3 + (1 - R\cos\theta/a)/R^3] \\ & - 15\sin^4\theta\,[1/R_2^3 + 1/R^3], \end{aligned}$$

$$\begin{aligned} G_1 = {} & (1/R_2 + 1/R - 2\cos\theta/a)/a^2 - [(1 - R_2\cos\theta/a)^2/R_2^3 \\ & + (1 - R\cos\theta/a)^2/R^3] + 3\sin^2\theta\,[(1 - R_2\cos\theta/a)/R_2^3 \\ & + (1 - R\cos\theta/a)/R^3], \end{aligned}$$

$$\begin{aligned} F_1 = {} & 3\,(1/R_2 + 1/R - 2\cos\theta/a)/a^2 - 3\,[(1 - R_2\cos\theta/a)^2/R_2^3 \\ & + (1 - R\cos\theta/a)^2/R^3]. \end{aligned}$$

When B_1 vanishes P is on the axis of the oscillator, and there are reflected waves arriving at P from every point on the small circle of the sphere through Q perpendicular to the axis of the oscillator, and the integral has to be taken over a belt of the sphere instead of an area surrounding Q. When A_1 vanishes

$$R^{-1} = 2/(a\cos\theta) - R_2^{-1}$$

and writing R_0 for this value of R when A_1 is small

$$R = R_0 - \varepsilon,$$

and

$$A_1 = \varepsilon R_0^{-2}\cos^2\theta.$$

Also, neglecting small quantities

$$B_1 = R_2^{-1} + R_0^{-1} - 2\cos\theta/a = 2\sin^2\theta/a\cos\theta,$$

$$\begin{aligned} C_1 & = 6\sin\theta\,(R_2^{-1} - (a\cos\theta)^{-1})(2/a\cos\theta - \cos\theta/a) \\ & = 6\sin\theta\,(a\cos\theta - R_2)(1 + \sin^2\theta)/a^2 R_2\cos^2\theta. \end{aligned}$$

The value of I in this case is as above

$$I = 2\,e^{-\frac{1}{4}\pi\iota}\,(2\pi/\kappa B_1)^{\frac{1}{2}}\,(-6/\kappa C_1)^{\frac{1}{3}}\,3^{-\frac{1}{2}}\iota\,m e^{2m^3\iota}K_{\frac{1}{3}}\,(2m^3\iota),$$

where B_1, C_1 have the values given above, and

$$m = -6^{-\frac{1}{3}}\,\kappa^{\frac{2}{3}}\,A_1 C_1^{-\frac{2}{3}}.$$

It follows that the components of the magnetic force at the point P are given by

$$(\mathrm{H}_x, \mathrm{H}_y, \mathrm{H}_z) = (l_1, m_1, 0) \times -\kappa^3 e^{\iota\kappa(\mathrm{V}t-\mathrm{R}-\mathrm{R}_2)} (a \sin\chi/\mathrm{VRR}_2{}^2)$$
$$\times (\sigma' \cos\theta - \sigma\cos\theta')/(\sigma'\cos\theta + \sigma\cos\theta') (\mathrm{I}\cos\theta/2\pi).$$

when $\mathrm{R} = \mathrm{R}_2$, the coefficients C_1 and M_1 vanish, and the terms of the fourth order must be retained. Writing $\mathrm{R} = \mathrm{R}_2 = a\cos\theta - \varepsilon$, where ε is small the values of the coefficients, retaining the most important parts only, are

$$\mathrm{A}_1 = 2\varepsilon/a^2, \quad \mathrm{B}_1 = 2\sin^2\theta/a\cos\theta, \quad \mathrm{C}_1 = 0, \quad \mathrm{E}_1 = 6\sin^2\theta/a^3\cos\theta,$$

and the value of I is given by

$$\mathrm{I} = \int_{-\infty}^{\infty}\int_{-\infty}^{\infty} e^{-\frac12\iota\kappa(\mathrm{A}_1x'^2+\mathrm{B}_1y'^2)-\frac{1}{24}\iota\kappa\mathrm{E}_1x'^4}\,dx'\,dy',$$

that is

$$\mathrm{I} = e^{-\frac14\pi\iota}(2\pi/\kappa\mathrm{B}_1)^{\frac12}\int_{-\infty}^{\infty} e^{-\frac12\iota\kappa\mathrm{A}_1x'^2-\frac{1}{24}\iota\kappa\mathrm{E}_1x'^4}\,dx',$$

or

$$\mathrm{I} = 2\,e^{-\frac14\pi\iota}(2\pi/\kappa\mathrm{B}_1)^{\frac12}(24/\kappa\mathrm{E}_1)^{\frac14}\int_0^{\infty} e^{-\iota(\zeta^4+m\zeta^2)}\,d\zeta,$$

where

$$m = \tfrac12\kappa\mathrm{A}_1(24/\kappa\mathrm{E}_1)^{\frac12} = 2\kappa^{\frac12}\varepsilon(\cos\theta)^{\frac12}/a^{\frac12}\sin\theta,$$

and, substituting the values of B_1 and E_1,

$$\mathrm{I} = \{(2\pi)^{\frac12}e^{-\frac14\pi\iota}a^{\frac54}(\cos\theta)^{\frac34}/\kappa^{\frac34}(\sin\theta)^{\frac32}\}\int_0^{\infty} e^{-\iota(\zeta^4+m\zeta^2)}\,d\zeta.$$

Therefore

$$\psi = -2^{\frac32}\pi^{-\frac12}\kappa^{\frac94}\mathrm{V}^{-1}e^{\iota\kappa(\mathrm{V}t-2\mathrm{R})-\frac14\pi\iota}a^{\frac14}\mathrm{W}_1(\sin\theta)^{\frac12}(\cos\theta)^{\frac34}$$
$$(\sigma'\cos\theta - \sigma\cos\theta')/(\sigma'\cos\theta + \sigma\cos\theta'),$$

where

$$\mathrm{W}_1 = \int_0^{\infty} e^{-\iota(\zeta^4+m\zeta^2)}\,d\zeta;$$

as ϵ increases W_1 tends towards the value

$$2^{-1}1^{\frac12}\pi^{\frac12}e^{-\frac14\pi\iota}a^{\frac14}\kappa^{-\frac14}(2\varepsilon)^{-\frac12}(\sin\theta)^{\frac12}(\cos\theta)^{-\frac14},$$

whence ψ tends towards the value

$$\iota\kappa^2e^{\iota\kappa(\mathrm{V}t-2\mathrm{R})}\mathrm{V}^{-1}a^{\frac12}\varepsilon^{-\frac12}\sin\theta(\cos\theta)^{\frac12}(\sigma'\cos\theta - \sigma\cos\theta')/(\sigma'\cos\theta + \sigma\cos\theta'),$$

which is the value the former expression for ψ tends towards, when $a\cos\theta - \mathrm{R}$ becomes small.* The ratio of the amplitudes of ψ and $\bar{\psi}$ is

$$2^{\frac12}\pi^{-\frac12}(\kappa a)^{\frac14}\mathrm{W}_1(\sin\theta)^{-\frac12}(\cos\theta)^{\frac34}(\sigma'\cos\theta - \sigma\cos\theta')/(\sigma'\cos\theta + \sigma\cos\theta'),$$

which is of a higher order than the ratio when $a\cos\theta - \mathrm{R}$ is not small.

---

* For the case where there is total reflexion at the surface of the sphere of radius a, the results are modified in the same way as above.

When there is a perfectly conducting sphere of radius b concentric with the sphere of radius a the value of the ratio $\psi/\bar{\psi}$ cannot be deduced at a point on the surface of the sphere of radius b which is on or near to a caustic as there is a diffraction effect due to the conducting sphere which is not negligible at such a point, but it can be inferred that the value of the ratio lies between four times the above value and the above value.

On the Variability of the Quiet-Day Diurnal Magnetic Variation at Eskdalemuir and Greenwich.

By S. Chapman, F.R.S., and J. M. Stagg, M.A., B.Sc.

(Received December 6, 1928.)

Introduction.

§ 1. The solar diurnal magnetic variation on quiet days (conveniently denoted by S_q) undergoes more or less *regular* changes of two kinds: one, affecting both type and amplitude, in the course of each year—an annual variation; the other, affecting chiefly the amplitude, in the course of the sunspot cycle—this will be termed the solar-cyclic change. In addition, it undergoes irregular or fortuitous changes from day to day. These have scarcely been studied as yet, and there is no precise systematic information available concerning them. They are of considerable interest owing to their probable connection with day-to-day changes in the sun's ultra-violet radiation. We therefore propose to examine them systematically, especially with reference to their similarity at different stations. In this paper we confine ourselves to the records for Eskdalemuir and Greenwich, the respective geographical co-ordinates being :—

	Latitude.	Longitude.
	° ′	° ′
Eskdalemuir	55 19 N	3 12 W
Greenwich	51 28 N	0 0

The material used consists of the daily ranges, in all three magnetic elements, on 819 very quiet days. It is shown that the ranges suffice for the comparison of different days, since (§ 15) the irregular changes in S_q, at any particular season and solar epoch, affect almost solely the amplitude of the daily variation, while the type, that is, the form of the curves representing the diurnal inequalities, remains constant.

The fortuitous percentage departures of the daily ranges from their normal value at any season and solar epoch are found to be considerable, often amounting to ± 25 per cent., while much larger departures are not uncommon (§ 14).

On the average the departures from the normal ranges are of the same sign, on any day, for all three elements at both observatories, though there are many individual exceptions to this rule. The correlation between the departures for the same element at the two observatories is much closer than that between the departures of different elements at the same observatory (§§ 16, 17).

Besides these main results, some interesting and unexpected correlations have been discovered between the fortuitous variations of S_q and of the non-cyclic changes in north and vertical force, and also between these and the departures of the daily mean values of the magnetic elements from their monthly means.

Symbols of Abbreviation.

§ 2. The discussion is facilitated by the use of the following symbols :--

E = Eskdalemuir. G = Greenwich.

w = winter (November-February).

s = summer (May-August).

e = the remaining " equinoctial " months.

y = year.

N = north component of magnetic force.

Z = downward vertical component.

H = horizontal component.

W = west component, at E, or west declination, at G, the changes in the latter case being measured in force units.

⊓ = sunspot maximum.

⊔ = sunspot minimum.

R = the range, on any day, in the diurnal inequality of a magnetic element, as expressed by hourly means or hourly values ; the distinction is unimportant in the case of the really quiet days here considered.

$\overline{R}$ = the mean value of R for any assigned interval or group of days.

R_n = the adopted normal value of R at any particular date (*cf.* § 12).

ΔR = the percentage departure of the actual value of R on any day from the normal value for that date (*cf.* § 13).

α = the non-cyclic variation in any element on any day, *i.e.*, the (positive or negative) excess of its value at the end of the day (24^h) over its initial value (at 0^h).

D = the (positive or negative) excess of the daily mean value of any element over the mean value for the same calendar month.

The notations $\bar{\alpha}$, α_n, $\Delta\alpha$, $\bar{D}$, D_n, ΔD will be used in the same sense relative to α and D as for R.

Unit of Force.

§ 3. The unit of force used throughout the paper is 1γ, or 10^{-5} gauss.

Period and Grouping of the Years considered.

§ 4. The data used relate to the well-developed sunspot-cycle 1913–23. The mean sunspot number for each year is given in Table I, row 2. Sunspot maximum occurred in 1917, and sunspot minima in 1913 and 1923.

In parts of our work we have divided the whole set of 11 years into the two following groups of years of greater and less sunspottedness. Data referring to these groups will be distinguished by the symbols ∩, ∪.

Group ∩; 5 years; 1915–19; mean sunspot number, 70·5.

Group ∪; 6 years; 1913, 1914, 1920–23; mean sunspot number, 15·8.

The Choice of Quiet Days.

§ 5. The choice of quiet days was based on the international magnetic character figures, which give an indication of the degree of disturbance existing on each Greenwich day from midnight to midnight. The figures range from 0·0, representing extreme quiet, to a maximum value 2·0. In investigations relating to quiet days it is customary to use the five quiet days per month chosen under the international scheme, but in some months these may include days that are not quite quiet. In order to ensure that the days we used should be as quiet as possible, we confined ourselves to those having character figures 0·0 or 0·1, however many or however few there might be in any particular month.

In some parts of our work we have separately considered the two classes of day, 0·0 and 0·1, but the results show that there is very little systematic difference between them as regards S_q-variability. Hence in general we have used the two sets of days in combination without distinction.

The total number of quiet days used was 819, one-third being of character figure 0·0 and two-thirds 0·1. The average number per month was 2·05 of character 0·0, and 4·15 of character 0·1. The average total number of quiet days used per month, 6·2, exceeds the monthly number of international quiet days (5), but this excess proceeds from the minimum solar years (∪), when an average of 6·76 days of character 0·0 and 0·1 were available; in the maximum solar years (∩) the average number of days used per month was 5·53. It is not improbable that the days here considered are slightly quieter than the international days, or, at least, include fewer that are slightly disturbed.

Tables I and II show the distribution of the 0·0 and 0·1 days between the different years, and between the calendar months and seasons; in the latter case the distribution of 0·0 and 0·1 days combined is given for the ∩ and ∪ years separately.

Description of the Original Data.

§ 6. The ranges in the hourly inequalities of the three magnetic elements at E and G for the selected quiet days were abstracted from the published annual records of the magnetic observations at these stations.

The elements registered at E throughout the 11 years covered by the investigation were N, W and Z, while at G they were west declination (D), Z and N, except that in 1913 and 1914 data for H instead of N were given. With a mean declination of just over 15° for 1913 and 1914 the disparity between the daily ranges of horizontal force on quiet days measured along the geographical and magnetic meridians was considered sufficiently small to allow the H ranges to be treated as those from a north force instrument.

The individual declination ranges in minutes of arc were converted into force units by means of the relation

$$\Delta\mathrm{D}\ (\gamma) = \Delta\mathrm{D}\ (\text{mins. of arc}) \times \mathrm{H} \times \text{arc } 1',$$

using mean values of H for each of the 11 years. The secular change in H at G resulted in a decrease from 18530 γ in 1913 to 18432 in 1923, so that the equivalent of 1′ change in D fell from 5·39 γ in the former to 5·36 γ in the latter year. The ranges of west D (so converted) were treated as ranges of west force.

At E the published hourly values are means for hourly intervals centred at the exact hours of Greenwich mean time; at G during 1913 and 1914 small irregularities in the magnetograms were first smoothed out, and then instantaneous hourly values at each exact hour tabulated. Subsequent to 1914, mean values for the intervals between successive exact hours of Greenwich mean time have been published.

Examination of the actual E magnetograms for a number of quiet days for which the tabulated ranges appeared to be in some way irregular, showed that though complete absence of small perturbations was rare, the use of hourly means would in all but a few cases give values which smoothed out the effects of these perturbations. The preliminary pencil smoothing of the curves for the G data of 1913–14 would have a similar effect.

Temperature corrections for the records from N (or H) and W variometers are accurately determinable, and D requires no temperature correction, but the method of registration of Z is such that the necessary correction may be both large and inaccurate. At both E and G the corrections for the vertical force variometers are large, 26 γ for 1° C. throughout the period after June, 1913, at E (no Z data are published for the earlier months of that year), and 17 γ up to February, 1917, at G. After February, 1917, a new variometer, subsequently compensated for temperature changes as an additional safeguard, was run at G in a room whose temperature was controlled by a thermostat.

Since the amplitude of the diurnal inequality is least in the winter months, accidental inaccuracies arising from faulty temperature correction are proportionally greater than in the other seasons (see § 14).

The 11-*year Mean Values of* R.

§ 7. In Table I the mean ranges are given for each year (all months), and in Table II for each calendar month and season (all years), for the 0·0 and 0·1 days combined. The results are illustrated in figs. 1 and 2 (*a*); in every case there is a considerable annual and solar-cyclic variation (§§ 8, 9). In forming

Table I.—Mean Annual Sunspot Number, Number of Quiet Days used, and Mean Range, for each Year, 1913–23.

——	1913.	1914.	1915.	1916.	1917.	1918.	1919.	1920.	1921.	1922.	1923.	Mean.
Sunspot number	1·4	9·6	47·4	57·1	103·9	80·6	63·6	37·6	26·1	14·2	5·8	40·7
Number of 0·0 days	36	36	34	20	22	18	19	20	16	23	27	25
Number of 0·1 days	59	61	58	39	44	41	37	56	45	37	71	50
All days	95	97	92	59	66	59	56	76	61	60	98	74
$\bar{R}$ (EN)	29·7	33·4	36·5	42·7	48·3	44·9	43·5	41·7	36·5	33·4	29·7	38·2
$\bar{R}$ (GN)	28·3	31·1	30·7	36·9	40·9	38·4	36·0	36·7	31·5	29·9	26·2	33·3
$\bar{R}$ (EW)	33·5	34·8	38·4	48·2	50·1	45·6	43·1	42·9	41·0	36·4	32·5	40·6
$\bar{R}$ (GW)	34·8	35·2	41·8	50·8	55·0	50·0	47·4	45·8	41·9	37·2	34·6	43·1
$\bar{R}$ (EZ)........................	12·5	13·8	14·9	15·5	17·5	17·4	17·4	16·2	14·4	14·5	13·2	15·2
$\bar{R}$ (GZ)........................	23·0	19·9	20·1	20·1	25·4	20·0	21·3	20·0	17·6	18·1	17·7	20·3

these means equal weight has been given to the mean range for each individual calendar month, irrespective of the number of 0·0 and 0·1 days included in it. Had this not been done, the ∪ years, which contribute a larger proportion of the days than the ∩ years, would have had undue weight, and the means would have been too small.

The ranges in N and W are of the same order of magnitude, the 11-year means, for E and G combined, being 35·8 and 41·9; the corresponding value for Z, 17·8, is much smaller.

The 11-year mean values are less at E than at G, in Z and W, and greater in N. The differences E − G, expressed as percentages of the mean $\frac{1}{2}$(E + G), are as follows:—

Values of $100\,\{R(E) - R(G)\}/\frac{1}{2}\,\{R(E) + R(G)\}$

N.	W.	Z.
13·7	−6·0	−28·7

The percentage difference is notably greater for Z than for N and W, and the sign of the difference in Z is of special interest. On disturbed days the ranges are greater at E than at G in all elements, but especially in Z; whereas we here see that on quiet days R (Z E) is *less* than R (Z G), and by an amount proportionally much greater than for N and W.

S_q in Z and W changes sign at or near the equator, and R (Z), R (W) are there small, and increase polewards. At the poles R (Z) must be zero, at least in so far as S_q there depends on local time; hence R (Z) should have a maximum between the equator and the pole. It appears from the above that this maximum occurs south of E.

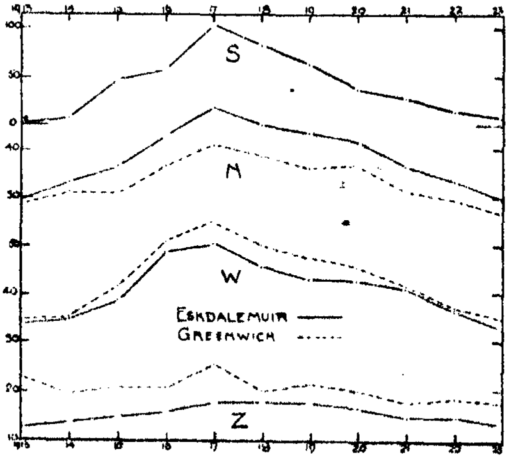

Fig. 1.—Mean Annual Sunspot Numbers (S) and Inequality Ranges, 1913-23.

There is no such limitation of N and W at the poles, but Table I suggests that R (W) also has a maximum south of E.

S_q in N changes sign in latitude 30° or 35°, and R (N) increases from this latitude towards both the equator and the pole. The poleward increase would appear to extend at least as far north as E.

The Solar-cyclic Variation.

§ 8. From Table I and fig. 1 it appears that the solar-cyclic variation is most regular in N and W, being an unbroken ascent to and descent from sunspot maximum, except for a slight irregularity in R (N, G) in 1919. In Z the variation of R is regular at E, but the progression in the Greenwich values of R (Z) is anomalous.

The increase from sunspot minimum (the mean of 1913 and 1923) to sunspot maximum (1917), expressed as a percentage of the 11-year mean R, is as follows :—

Values of $100\{R(\cap) - R(\cup)\}/\bar{R}$.

R (N, E)	R (N, G)	R (W, E)	R (W, G)	R (Z, E)	R (Z, G)	**Mean**
48·7	41·0	42·1	47·1	30·6	24·9	39·1

The Annual Variation.

§ 9. Table II and fig. 2 show that the annual variation in the S_q range is, on the whole, a regular rise and fall between a sharp winter minimum and a broad summer maximum, or series of maxima. The curves show some slight irregularities in this progression, the chief being a dip in R (N) and R (W) in May ; this seems to be real, since it appears in almost every subdivision of the data. The maximum in R (Z) occurs earlier than in R (N) and R (W), by about a month.

Figs. 2 (*c*), 2 (*d*), for the ∩ and ∪ groups of years, suggest that there is no significant change in the type of the annual variation from sunspot maximum to minimum. The amplitude of the annual variation is greater for the ∩ group, but the changes expressed as percentages of the annual mean value for the group of years considered are about the same in the two cases. This is illustrated by the following table, which gives these percentages, corresponding to the difference between the mean ranges for summer (§ 2) and the mean range for the month of minimum (December in all cases save for R (Z, G, ∩), when it was January) ; the mean for the four summer months was chosen instead of that for the actual month of maximum range, because of the somewhat irregular progression of $\bar{R}$ during this season.

Table II.—Number of Quiet Days (character 0·0 and 0·1) used in each Calendar Month and Season, and Mean Values of R for 0·0 and 0·1 Days combined.

Group of years.	Type of day.	Jan.	Feb.	Mar.	Apr.	May.	June.	July.	Aug.	Sept.	Oct.	Nov.	Dec.	Summer.	Equinox.	Winter.	Year.	Average for month.
All	0·0	23	16	14	20	27	28	29	19	22	22	22	29	103	78	90	271	2·05
	0·1	43	54	42	51	42	47	52	37	34	38	60	48	178	165	205	548	4·15
	0·0+0·1	66	70	56	71	69	75	81	56	56	60	82	77	281	243	295	819	6·20
⌓	0·0+0·1	32	28	23	27	20	39	33	24	27	27	27	25	116	104	112	332	5·53
◡	0·0+0·1	34	42	33	44	49	36	48	32	29	33	55	52	165	139	183	487	6·76
Element	Station.	$\bar{R}$ on 0·0 and 0·1 days combined (all years).															Year.	
N	E	20·1	24·4	37·9	49·6	48·3	52·5	49·8	49·8	47·2	37·4	23·5	16·5	50·1	43·0	21·1	38·1	
N	G	22·6	23·9	33·5	40·1	37·4	42·9	40·8	42·9	39·6	34·9	23·2	17·9	41·0	37·0	21·9	33·3	
W	E	21·3	25·5	40·4	50·3	52·1	57·5	57·8	52·2	45·3	38·3	26·3	18·2	54·9	43·6	22·8	40·4	
W	G	23·8	28·0	44·8	55·6	56·1	58·4	58·1	55·0	48·6	42·3	29·0	19·2	56·7	47·8	25·0	43·2	
Z	E	7·7	10·3	15·7	19·9	23·2	21·4	22·8	20·0	15·7	11·6	7·9	7·1	21·8	15·7	8·3	15·3	
Z	G	11·4	14·9	21·0	27·8	29·2	26·8	26·1	23·4	20·4	16·2	13·0	11·0	26·4	21·3	12·6	20·1	

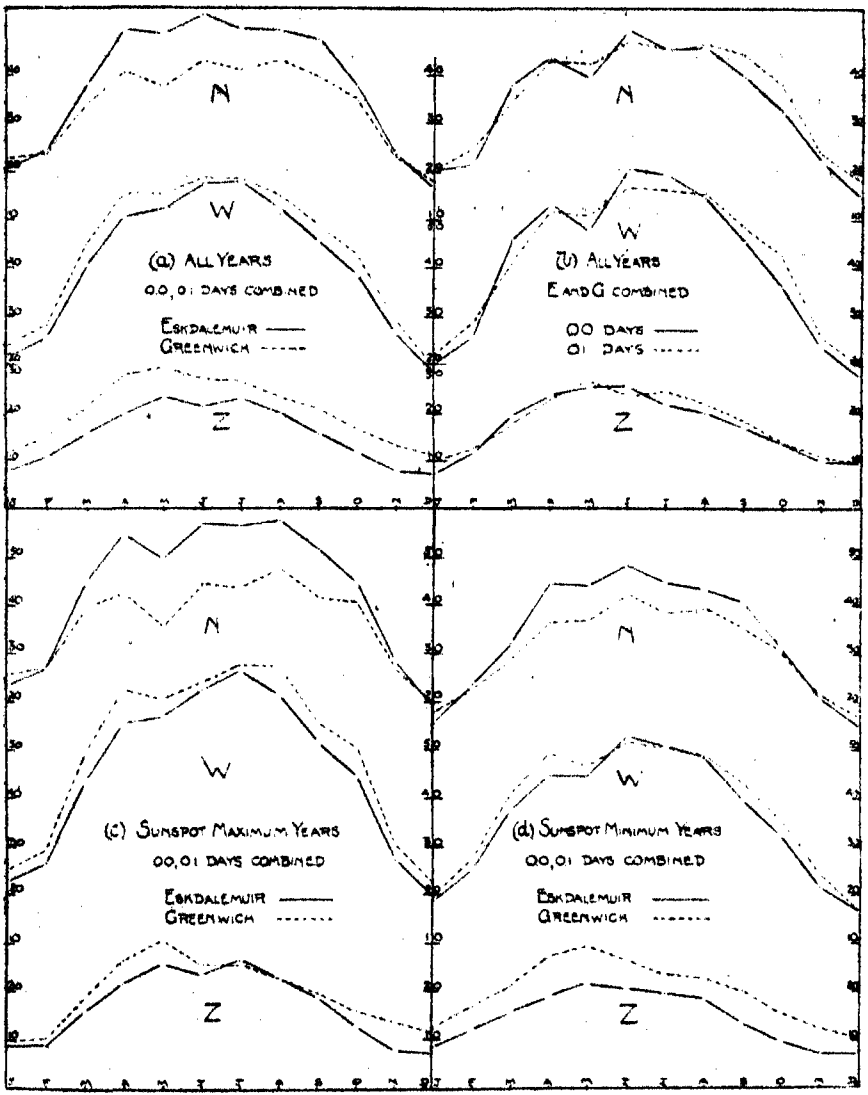

FIG. 2.—ANNUAL VARIATION OF INEQUALITY RANGES AT ESKDALEMUIR AND GREENWICH

Percentage increase of range from winter to summer :—

	R (NE)	R (NG)	R (WE)	R (WG)	R (ZE)	R (ZG)	Mean
∩	84	65	93	86	107	84	86
∪	91	74	89	85	89	76	83

It appears from this table that the percentage annual variation is about twice as great as the percentage solar-cyclic variation, the excess being most notable in the case of Z.

Comparison between 0·0 and 0·1 Days.

§ 10. An examination of the mean ranges for the 0·0 and 0·1 days separately shows that the systematic differences between them are small. The difference R (0·1) — R (0·0), expressed as a percentage of the mean range for the combined set of days, is given for each season and for the year in the following table; the differences for the year are given separately for the ∩ and ∪ groups.

—	Summer.	Equinox.	Winter.	Year.	
				∩	∪
R (NE)	2	5	11	6	7
R (NG)	−1	3	8	6	2
R (WE)	−1	2	10	1	6
R (WG)	−2	0	7	1	3
R (ZE)	7	2	18	5	10
R (ZG)	1	−3	4	−1	0
Mean	1·0	1·5	9·7	3·0	4·7

While the most important feature of the table is the smallness of the percentage difference in nearly all cases, the effect of the slight amount of disturbance which distinguishes the 0·1 days from the 0·0 days is apparent in the table, particularly in winter; though disturbance is most frequent at the equinoxes, the winter values of R are so small that even a slight amount of disturbance produces an appreciable percentage change in R. Similarly, though disturbance is more common in ∩ than in ∪ years, the smaller values of R in the latter years renders $\{R(0\cdot1) - R(0\cdot0)\}/\bar{R}$ greater in ∪ years. The greater degree of disturbance experienced at Eskdalemuir than at Greenwich is also manifested in the table, particularly as regards the vertical force Z (*cf.* § 7).

The annual variations for the 0·0 and 0·1 days separately, for all years and for E and G combined, are shown in fig. 2 (*b*), which again illustrates how small are the differences between the two sets of days. An unexpected feature shown by the curves is that the above excess of R (0·1) over R (0·0) for the equinoctial season is due to September and October, the difference being actually reversed for the two vernal equinoctial months.

The differences between R (0·1) and R (0·0) are on the whole so small that in general no distinction is made between the two sets of days in the further discussion.

Examples of Fortuitous Variations.

§ 11. As stated in § 1, there are irregular variations of S_q in addition to the regular annual and solar-cyclic changes. These fortuitous variations can be illustrated most effectively by quoting a number of cases where R in one or more elements undergoes a marked change on *successive* 0·0 days, for here there can be no possibility of ascribing the change to the regular variation of S_q.

Table III.

—	Eskdalemuir.			Greenwich.		
	R (N).	R (W).	R (Z).	R (N).	R (W).	R (Z).
1919. February 10	42	27	8	39	65	13
1919. February 11	23	24	6	21	50	5
1922. May 29	63	44	14	53	87	26
1922. May 30	44	52	19	39	96	25
1920. July 28	44	52	16	38	98	24
1920. July 29	61	58	22	54	115	29
1923. September 21	29	31	12	24	54	15
1923. September 22	43	46	14	43	95	15
1913. October 2	37	47	10	35	94	26
1913. October 3	29	36	8	37	66	33
1913. November 14	20	22	4	14	43	18
1913. November 15	10	19	5	9	48	18
1913. November 16	21	23	4	15	49	16

Many other examples might be given, but these suffice to demonstrate the existence of irregular changes; they also show that the three elements do not always vary in parallel at the same observatory, nor does the same element always vary alike at the two observatories.

The magnetograms for Eskdalemuir were examined to see whether slight irregularities in the curves could account for the occasional instances of opposite variations in R (N) and R (W) on successive 0·0 and 0·1 days. A few such cases were found, particularly on 0·1 days, but on the whole the examination showed that the ranges on these quiet days are seldom affected by disturbance, which, being slight, can alter the range only if it occurs near the turning points on the curve.

The Normal Range on any Date.

§ 12. In order to investigate the fortuitous changes in S_q it is necessary to allow for the regular annual and solar-cyclic variations. The annual variation is the more important of the two, and produces considerable percentage changes in R even in the course of a single month, especially near the equinoxes.

It was decided to construct graphs which should give the supposed normal or standard value of R on each individual date throughout the 11 years; this was done in the following way. It was assumed that the annual variation of R (for any element at E or G) in any year was proportional to the 11-year mean annual variation given in Table II and illustrated in fig. 2 (*a*); the constant of proportionality was taken to be the ratio of the mean R for that year to the 11-year mean, as given in Table I. For example, the annual variation of R (NE) in 1913 was taken to be that given for R (NE) in Table II, multiplied by 29·7/38·2 or 0·78; the factors used, based in this way on Table I, are given in the following Table IV.

Table IV.—Ratios of $\bar{R}$ for each Year to the corresponding 11-year Mean of R.

	—	1913.	1914.	1915.	1916.	1917.	1918.	1919.	1920.	1921,	1922.	1923.
Eskdalemuir..........	N	0·78	0·87	0·96	1·12	1·26	1·18	1·14	1·09	0·96	0·87	0·78
	W	0·83	0·86	0·95	1·19	1·23	1·12	1·06	1·06	1·01	0·90	0·80
	Z	0·82	0·91	0·98	1·02	1·15	1·14	1·14	1·07	0·95	0·95	0·87
Greenwich..............	N	0·85	0·93	0·92	1·11	1·23	1·15	1·08	1·10	0·95	0·90	0·79
	W	0·81	0·82	0·97	1·18	1·28	1·16	1·10	1·06	0·97	0·86	0·80
	Z	1·13	0·98	0·99	0·99	1·25	0·99	1·05	0·99	0·86	0·89	0·87

The monthly mean values of R thus derived for each calendar month of any year were taken to refer to the middle of that month, and a graph was constructed for each element and each year, having R as ordinates and daily epoch in the year as abscissæ, by joining the ends of the ordinates for the middle points of successive months by straight lines. That is, R was supposed to vary uniformly from the middle of one month to the middle of the next. The ordinate on any date was taken as defining the normal value of R on that date; this can only be an approximation to the truth, but the method at least gives a value of R which takes into account much the greater part both of the annual and solar-cyclic variation of R.

The Percentage Departures of R.

§ 13. As described in § 12, the normal value (R_n) of R was determined for each of the elements at E and G, on each of the 819 quiet days used. In general R_n for any day differed from the actual value of R for the day. The difference $R - R_n$ was expressed as a percentage departure (ΔR), in terms of the mean value ($\bar{R}$) of R for the corresponding month: the precise definition of ΔR is therefore

$$\Delta R = 100\,(R - R_n)/\bar{R}.$$

Tables of ΔR, thus determined, formed the basis of the discussion of the fortuitous changes of S_q.

The Distribution of the Percentage Departures ΔR.

§ 14. In order to examine how the percentage departures ΔR were distributed, a table was constructed showing, for each set of values of ΔR, how many occurred in each of a series of intervals 5 units wide, spaced consecutively on either side of a middle interval centred at $\Delta R = 0$; any such interval can be specified by its central value of ΔR, which is always an integral multiple of 5.

The number of occurrences of ΔR in each interval was then divided by the total number (n) of values in the set under consideration; the result, multiplied by 1000, is termed the *frequency* f of occurrence of ΔR for that interval. The sum of the frequencies for all the intervals is therefore 1000.

The values of f are given, to the nearest unit, in Table V; the three main sections refer to N, W, Z; in each of these are given first the E and then the G values for the year and the three seasons, from 0·0 to 0·1 days combined; the remaining rows refer to the E and G data combined, for the whole year, and give the frequencies for the ∩ and ∪ years separately, and for the 0·0 and 0·1 days separately. The table extends from the interval centred at $\Delta R = -75$ per cent. (corresponding to $R = \frac{1}{4}R_n$) to $\Delta R = +100$ per cent. (corresponding to $R = 2R_n$). Negative departures numerically greater than 100 per cent. (or, more strictly, $100R_n/\bar{R}$) are impossible by virtue of the definition of ΔR; actually the extreme negative departures are those given in the column $\Delta R = -75$. The positive departures are not subject to any such limit, and actually there were 13 days, all of character 0·1, for which, in one or other element, $\Delta R > 100$; these are not included in Table V. None of these refers to N, so that the first section of Table V is complete. One case refers to W, namely, ΔR (WE) = 120 on January 23, 1922; but this anomalous W range arises because a disturbance began during the last hour (24) of the day (the following day was of character 1·8); if this last hourly value were ignored, ΔR (WE) for this day would be reduced to 63, the day being really one of large range in WE, though not so abnormal as the uncorrected value of ΔR (WE) would suggest. The other 12 cases relate to Z, 10 at E and 2 at G; of these 9 (7 E, 2 G) occur in winter, 2 (E) in *e*, and 1 (E) in *s*; 9 are in ∪ years, and 3 in ∩; they are probably partly due to small perturbations, which affect ΔR specially in winter and ∪ years, when R is small.

The frequency distributions in Table V are illustrated in fig. 3. Inspection

Table V.—Frequency Distribution of ΔR (§ 14).

Component and observatory.	Group.	No. of days.	Negative values of ΔR.															0	Positive values of ΔR.																			
			75	70	65	60	55	50	45	0	35	30	25	20	15	10	5		5	10	15	20	25	30	35	40	45	50	55	60	65	70	75	80	85	90	95	100
NE	y	810		1	2	6	6	12	9	16	16	40	42	36	84	96	95	93	99	74	68	65	47	26	16	7	10	9	7	4	1	4	4	3	1		1	
	s	280									7	29	50	29	111	107	121	125	93	79	75	61	43	32	14	7	11	3						3				
	e	241								8	9	21	37	38	83	104	83	112	112	91	83	95	62	21	9	4		12	12	4								
	w	289		3	7	17	17	35	24	38	31	66	38	42	59	90	80	45	93	56	48	45	38	24	24	11	17	10	10	7	4	10	10	4	4		3	
NG	y	809		1	1	4	6	12	20	20	21	52	52	63	64	83	93	64	74	78	63	53	45	30	25	24	9	4	10	6	6	7	6	2	1	1		
	s	277						7	11	7	18	36	61	43	98	87	101	72	69	115	83	43	36	25	18	18	7	11	11	4	11	4		4				
	e	241						8	12	13	4	33	58	62	54	83	108	87	96	62	95	88	42	21	21	17	13		4	4	4	4	12					
	w	291		3	8	10	17	21	34	38	38	83	38	83	41	79	72	38	62	55	17	38	55	41	35	34	7		14	10	3	14	7	4	3	3		
E + G......	∩	653				3	5	8	9	12	20	49	35	50	81	92	95	92	99	86	60	51	60	24	18	12	6		11	3	5	3	5	5		1		
	∪	966		2	3	6	7	16	18	22	18	43	55	49	69	88	93	70	78	69	69	65	36	30	22	18	12	10	7	6	3	7	5	1	2		1	
	0·0	536			5	6	9	17	19	15	19	73	50	56	91	76	95	75	80	60	58	54	47	32	19	11	7	7	6	2	2	4	3	2				
	0·1	1083		2		5	5	10	12	19	18	32	45	46	66	96	93	80	90	84	69	€2	45	26	21	18	10	6	10	6	6	6	6	3	2	1	1	
WE	y	807	2		1	6	4	1	11	11	22	35	56	72	67	93	98	110	82	73	61	53	32	31	22	24	4	11	5	3	4	3		1	1			
	s	278								7	4	25	36	72	72	90	130	130	93	97	87	50	25	36	26	11		7	8									
	e	240								4	4	21	50	79	37	113	96	125	88	79	75	71	42	50	21	29	0	8	0	4	4							
	w	289	7		4	17	10	4	31	21	55	55	80	66	87	80	69	80	66	45	24	41	31	10	21	31	10	17	10	4	7	7		4	3			
WG	y	812		1	2	1	4	6	14	11	11	36	49	62	81	85	97	108	92	85	65	51	49	25	27	9	12	5	3	4	1	1			3			
	s	278									4	43	32	75	83	90	83	180	112	111	68	65	61	7	14	11	4	4	3									
	e	243			4						8	4	45	41	78	78	78	157	115	95	66	66	58	50	33	8	12			4								
	w	291		3	3	4	10	17	38	31	21	55	69	65	82	86	127	48	55	52	62	24	31	21	34	7	21	10	4	7	3	3			7			
E + G......	∩	656				3	2	3	11	15	23	30	56	56	85	98	92	104	84	76	67	59	49	27	24	9	9	5	5	2	3	2			1			
	∪	963	2	1	3	4	6	4	14	8	13	38	50	74	67	83	102	113	89	81	60	47	35	28	25	21	7	10	3	4	2	2		1	2			1
	0·0	535	4	2	4	6	9	4	15	6	15	41	54	52	71	97	92	129	118	62	62	35	43	32	21	11	7	6	2						2			
	0·1	1084			1	3	1	4	11	14	17	32	51	74	76	85	100	99	72	87	64	60	40	26	27	18	8	9	5	5	4	3		1	2			
ZE	y	771	1	3	3	10	18	18	38	25	31	60	40	49	84	69	52	99	51	47	62	27	32	43	26	22	21	8	17	4	5	8	6	1	3	3	3	
	s	265					7	4	11	23	30	45	41	49	113	94	79	64	68	64	57	38	38	45	34	30	19	8	19			8	4				4	
	e	232		4		9	13	13	13	22	9	52	43	47	77	90	82	99	90	43	56	89	26	39	22	17	26	17	5	4	13		9	4		9		
	w	274	4	4	7	22	33	36	84	29	51	80	36	51	62	26	0	131	0	33	73	7	33	44	22	18	18	0	25	7	4	14	7		7		4	
ZG	y	788	3		3	5	3	8	25	28	27	53	46	70	55	80	72	85	61	63	46	68	46	27	33	23	15	13	10	8	5	4	1	4		1	2	1
	s	272					7	7	19	26	33	29	44	52	48	77	110	88	63	92	74	44	44	29	29	18	18	15	7		11	4		4		4	4	
	e	231	4			4		5	17	17	22	56	30	74	61	69	87	69	104	56	39	82	69	30	28	36	9	9	5	18		4		4				
	w	285	3		7	10		10	39	39	25	74	60	84	56	91	25	95	25	42	32	81	35	21	42	18	18	14	18	10	4	4	3	3			3	3
E + G......	∩	644	3	2	3	12	11	25	25	26	33	43	45	59	59	76	71	100	50	50	47	51	48	26	28	22	23	12	14	6	3	5			3		3	3
	∪	915	1	1	2	4	10	4	36	26	26	66	42	60	77	73	56	80	60	59	61	46	35	40	31	28	14	9	13	6	7	7	7	4		3	2	
	0·0	515			4	13	16	12	38	37	27	60	52	47	66	83	70	100	47	60	56	47	35	41	25	23	10	8	2		6	2	4	2	2	2		
	0·1	1044	3	2	2	5	8	13	30	21	30	55	38	66	71	70	58	83	60	53	54	49	43	32	31	22	22	11	19	9	5	6	4	3	1	2	4	1

of the table and figure shows the following main features: (*a*) the positive departures extend to more extreme values (including some, over 100, not shown in fig. 3) than the negative, and this difference has to be balanced by an excess of moderate negative departures; but the considerable degree of symmetry in the distribution of positive and negative departures is more remarkable than the slight asymmetry; (*b*) the distribution of ΔR in each element is approximately the same at G as at E, hence in fig. 3 only the *y* curves are given for the two stations separately; (*c*) the spread of ΔR is least in summer and greatest in winter; since, however, ΔR is a percentage of the mean range, which is much less in winter than in summer, the spread of the actual departures, R − R_n, from the normal values, is least in winter*; (*d*)

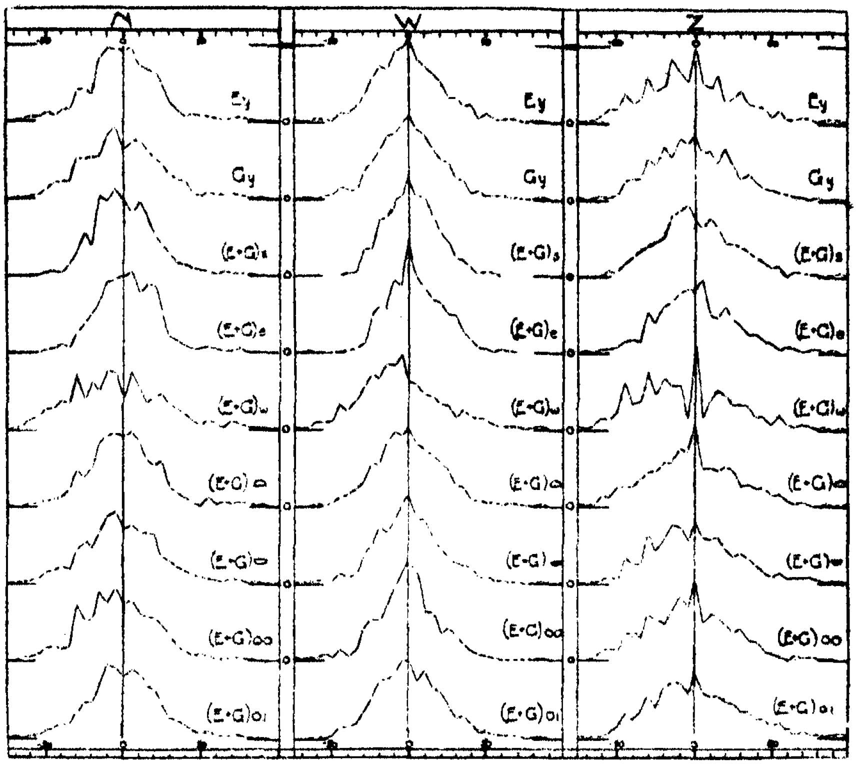

FIG. 3.—FREQUENCY CURVES FOR ΔR. The Vertical Interval between the base lines of successive curves represents 100 units.

---

* The jagged appearance of the curves for Z in fig. 3, especially for *w*, arises because R is measured only to 1γ, and a change of R by 1 γ may alter the value of ΔR by 10 per cent., since the mean range in Z is of the order 10 to 14 γ in *w*. Since Table V relates to 5 per cent. intervals of ΔR, the frequencies alter rather abruptly in successive columns; they and the corresponding curves should be smoothed by taking overlapping means, to get a fair representation of the distribution of ΔR.

there is but little systematic difference between the percentage departures ΔR in ∩ and ∪ years ; (e) the spread of ΔR on 0·0 and 0·1 days is nearly the same, though large positive values are more common for 0·1 than for 0·0 days.

These conclusions are more precisely illustrated by the mean values of the positive and negative departures separately, denoted by $| \Delta_+R$, $| \Delta_-R |$, and by the mean departure $| \Delta R |$ having no regard to sign ; these are given in Table VI. The mean values $| \Delta R |$ are smaller than the means of $| \Delta_+R |$ and $| \Delta_-R |$, because there were days of zero ΔR.

Table VI.—Mean Positive, Negative and Arithmetical Departures of Ranges from their Standard Ranges.

Observatory Station.	Year, season or day.	N.			W.			Z.		
		$\|\Delta_+R.\|$	$\|\Delta_-R.\|$	$\|\Delta R.\|$	$\|\Delta_+R.\|$	$\|\Delta_-R.\|$	$\|\Delta R.\|$	$\|\Delta_+R.\|$	$\|\Delta_-R.\|$	$\|\Delta R.\|$
E	*y*	19·1	18·2	17·7	19·3	17·7	17·4	30·9	25·4	25·1
	s	16·4	12·6	13·5	15·0	12·9	13·6	25·5	18·9	20·6
	e	16·4	14·0	14·6	17·9	13·8	15·1	27·8	21·1	21·9
	w	24·9	26·0	24·4	27·0	23·9	23·0	40·8	34·6	32·2
G	*y*	22·5	20·2	20·3	17·7	16·9	16·5	25·9	22·0	21·8
	s	20·0	16·9	17·6	14·2	13·6	13·6	23·8	19·6	19·7
	e	19·9	16·9	17·2	16·9	12·9	14·2	22·3	20·0	19·7
	w	27·9	25·0	25·4	23·6	21·4	21·2	31·9	25·3	25·6
E + G	∩	19·3	17·2	17·3	17·7	16·6	16·5	27·4	24·2	22·8
	∪	21·9	20·5	20·2	19·0	17·8	17·3	28·8	23·4	23·9
	0·0	19·9	20·7	19·4	16·1	18·2	16·1	23·7	24·3	21·4
	0·1	21·2	18·3	18·8	19·6	16·9	17·4	30·1	23·4	24·5

Examination of the Type of S_q on Days of Widely Different Range.

§ 15. In order to determine whether the type of S_q at any epoch varied with the range, it was judged sufficient to consider the hourly inequalities for three groups of days of different range at one station (E) and one season only. Actually the examination was confined to the 156 quiet days of June and July, when S_q has its largest amplitude. For each element these days were divided into three nearly equal groups according to their values of ΔR for that element ; the mean diurnal hourly inequality was then formed for each group. The number of days, and the mean range, for each such group are shown in Table VII, which also gives the average hourly numerical departure of the element from its mean value, derived from the inequality for the group.

Table VII.

Element.	Group of days.	No. of days.	Mean R.	Average departure.	Mean R ÷ average departure.
N	Large Δ_-R	51	38·6	10·0	3·9
	Small ΔR	50	45·1	11·8	3·8
	Large Δ_+R	53	53·3	13·5	3·9
W	Large Δ_-R	51	42·8	11·0	3·9
	Small ΔR	48	54·4	13·5	4·0
	Large Δ_+R	53	64·9	14·8	4·4
Z	Large Δ_-R	47	13·2	3·1	4·3
	Small ΔR	47	18·9	4·2	4·5
	Large Δ_+R	46	26·1	6·0	4·4

The inequalities or daily variations are plotted in fig. 4, for each element; the curves show that the considerable differences of amplitude in the diurnal inequalities for the three groups are unaccompanied by any appreciable change of type; this is more clearly brought out by the lowest curves, which represent the difference between the curves for the groups of largest and smallest range. These curves are almost exactly of the same type as the others, showing that the curves of largest amplitude are merely magnified versions of the curves of smaller amplitude. The same fact is illustrated in another way by the similarity of the ratios of the mean ranges to the average departures for the inequalities

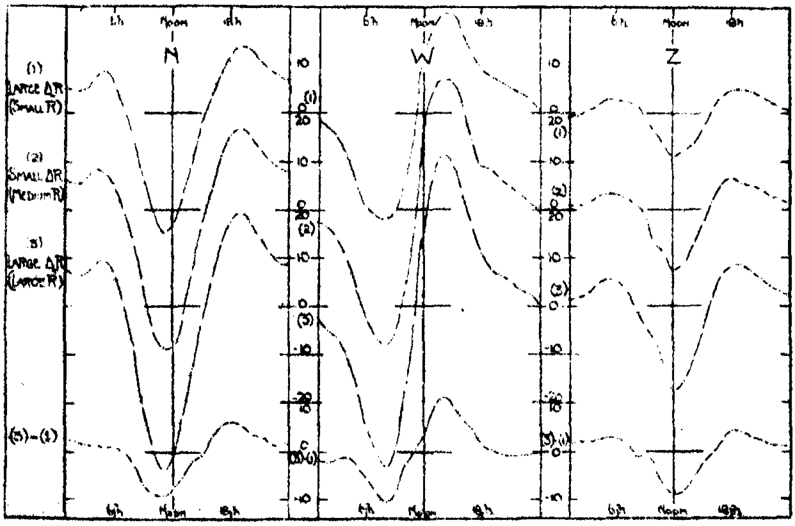

FIG. 4.—DIURNAL VARIATIONS ON QUIET DAYS, GROUPED ACCORDING TO THEIR ΔR. (Eskdalemuir, June–July, 1913–23.)

for the three groups of days for each element, as indicated in the last column of Table VII. The evidence here afforded is taken to be sufficient proof of the adequacy of R as an index of the S_q variation at any epoch.

The Relation between Corresponding Values of ΔR *for the same Element at the Two Observatories.*

§ 16. It has been seen that the distribution of the fortuitous changes in R is much the same for all three elements and at the two observatories. It is important to ascertain how far the percentage departures of any element at one observatory are paralleled by those of the same element at the other observatory.

To examine this point, the mean values of ΔR (NE) and ΔR (NG) were formed for the mean values of the groups of days for which ΔR (NE), at any season or for the whole year, lay within the successive intervals 5 units wide considered in Table V: the value of ΔR (NG) on any day did not always lie in the same interval as ΔR (NE) for that day. Sets of pairs of corresponding mean values of ΔR (NE) and ΔR (NG) were thus obtained, for the three seasons and the whole year; these pairs of values were taken as co-ordinates of points on four curves, which are reproduced in fig. 5 (*a*), as curves (1)–(4), in the order *s*, *e*, *w* and *y*. Alongside each point is given the number of days from which the corresponding mean values of ΔR were derived; points based on less than 5 days are not included in the diagram.

Curves (5)–(8) and (9)–(12) were constructed, similarly, from the values of ΔR (W) and ΔR (Z) at E and G, for groups of days at which ΔR (WE) or ΔR (ZE) fell within the 5-unit intervals of Table V.

If each element always changed in the same proportion at the two observatories, the curves in fig. 5 (*a*) would all be straight lines inclined at 45° to the axes, corresponding to ΔR (E) = ΔR (G). The figure shows that for N and W the curves approximate to such straight lines, though with accidental irregularities; that is, these elements do vary nearly proportionately at the two stations. The agreement is closest in summer. On the other hand, for Z the curves depart somewhat widely from the form ΔR (E) = ΔR(G), and are much more irregular than for N and W.

These facts are summed up in a brief and quantitative manner by the following correlation coefficients between ΔR(E) and ΔR(G); these coefficients have been calculated directly from the whole set of individual values of ΔR.

Table VIII.—Correlation Coefficients.

——	ΔR (NE), ΔR (NG).	ΔR (WE), ΔR (WG).	ΔR (ZE), ΔR (ZG).
Summer	0·798	0·871	0·642
Equinox	0·761	0·847	0·504
Winter	0·761	0·801	0·253
Year	0·773	0·840	0·466

The table shows that W is the element in which the departures from the normal range are most clearly correlated at the two observatories, while in Z the relation is least close, though even for Z the correlation in summer reaches a high value. These high correlations incidentally testify to the accuracy of the data afforded, quite independently, by the two observatories; if the data were affected by much accidental error, such high correlations could hardly be manifested.

The Relation between Corresponding Values of ΔR *for Different Elements at the same Observatory.*

§ 17. The correlation between the proportionate departures of the different elements from their normal values at the same observatory was next examined, on lines similar to those of § 16. In this section of the discussion the E and G data were combined without distinction. In considering the relations between N and W, and N and Z, the mean values of ΔR were determined for the groups of days on which ΔR (N) lay within the 5-unit intervals of Table V; in considering the relation between W and Z, the groups of days used were those for which ΔR (W) lay within such intervals. The results, in the form of graphs in which the co-ordinates are ΔR (N), ΔR (W), or ΔR (N), ΔR (Z), or ΔR (W), ΔR (Z), are plotted in fig. 5 (*b*), in three sets each of four curves, for the seasons *s*, *e*, *w* and for the year. If the fortuitous variations of S_q affected the three elements proportionately, all these curves would be straight lines inclined at 45° to the axes, but actually they depart from this ideal far more than do the curves in fig. 5 (*a*). The relation between N and W seems to be the least affected by accidental irregularities, while that between N and Z seems most affected.

The following correlation coefficients illustrate the same facts in a more definite but less detailed way. The E and G data have here been separately considered, and also those for the ∩ and ∪ groups of years. In the determination of each coefficient neither element involved has been treated as primary, in the sense that N (or W) was taken as primary in forming the graphs of fig. 5 (*b*).

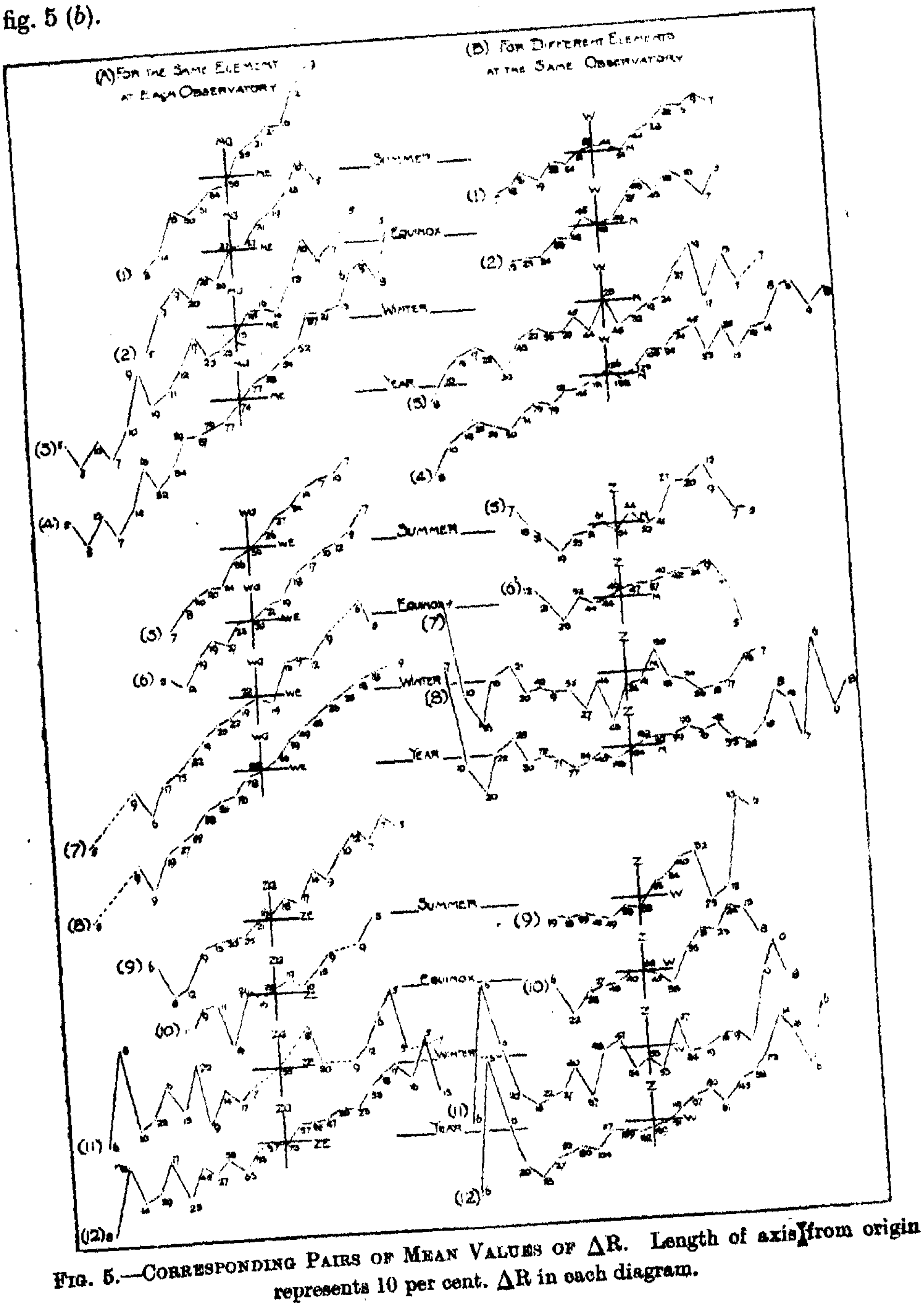

Fig. 5.—Corresponding Pairs of Mean Values of ΔR. Length of axis from origin represents 10 per cent. ΔR in each diagram.

Table IX.—Correlation Coefficients.

——	ΔR (NE), ΔR (WE).	ΔR (NE), ΔR (ZE).	ΔR (WE), ΔR (ZE).	ΔR (NG), ΔR (WG).	ΔR (NG), ΔR (ZG).	ΔR (WG), ΔR (ZG).
Summer	0·340	0·249	0·304	0·405	0·183	0·240
Equinox	0·466	0·125	0·333	0·424	0·050	0·290
Winter	0·329	0·156	0·339	0·414	−0·014	0·169
Year	0·378	0·177	0·325	0·414	0·073	0·233
⌓	0·399	0·233	0·379	0·438	0·052	0·264
◡	0·370	0·115	0·306	0·420	0·052	0·147

The most striking feature of the above table is the much smaller correlations throughout, as compared with those shown by Table VIII. Another curious feature is that the N-Z and W-Z coefficients are smaller for G than for E, although for N-W the relationship is closer at G than at E. Summer is no longer the season in which all the relationships are closest, as was the case in Table VIII. The correlations appear somewhat closer in ⌓ than in ◡ years.

Interpretation of the S_q *Variability.*

§ 18. Though it is not possible, as yet, to interpret the results of §§ 11–17 in any detail, it may be of interest to consider briefly their significance in relation to the overhead electric current system which is the main cause of S_q. This current-system is of simple form, consisting of four families of oval curves, two north and two south of the equator, and separated approximately by the sunrise and sunset meridians; the current-intensity is much greater over the day than over the night hemisphere. The current system is stationary in form relative to the meridian plane through the sun; the rotation of the earth carries any station round a circle of latitude drawn in this spherical current-system, and hence S_q depends on local time, being repeated at corresponding local times at different stations in the same latitude.

The S_q variations in N and W are determined mainly by the (intensity and direction of the) currents within a not very large distance of each station, at each time of day; the Z variation depends rather on the rate of space-variation of the overhead currents. An increase in the amplitude of S_q betokens a general intensification of the current-system; the constancy of the type of S_q in any element, throughout the changes of range (§ 15), indicates that the general form of the current-system, and especially the great difference between the day and night hemispheres, is preserved while the current intensity changes. The fact that the S_q ranges for the different elements at the same station do not always change in the same proportion indicates, however, that the current-system does not remain absolutely constant in form; the direction of the current-flow undergoes changes, thus altering the ratio of R (N) and R (W), while the space-variation of the currents is also modified, affecting R (Z). But the current system is so extensive and so simple in form that any such changes in it affect large areas in a similar manner; hence we see that the changes in any one element at E and G are closely correlated.

§ 19. The preceding section completes the main part of this paper. Having shown the existence, amount, and principal properties of the irregular changes of S_q at two stations not very far apart, the next step must be to determine how far the variations are worldwide, that is, what degree of correlation is shown between the values of ΔR for more distant stations. If the correlation is found to be considerable, it is hoped to develop a practical plan for the assignment to each Greenwich day of an index of the intensity of S_q on that day, whether, as on quiet days, S_q appears in its pure form, or whether, as during periods of magnetic activity, S_q is overlaid by irregular magnetic changes. Such daily indices should be of value in the investigation of solar and terrestrial relationships, since they relate to a feature of the magnetic variations quite different from that to which the daily magnetic character figures refer. It is intended to compare these S_q indices with various solar and geophysical data, such as the ozone content of the atmosphere, the sun's ultra-violet radiation, and radio data.*

At the present stage it is premature to assign daily indices even for the quiet days here used. But some interesting and unexpected correlations of a local kind, which may, however, have a wider significance, have been found, between ΔR and α and D (§ 2). This part of the work has been confined to the E data in view of the close correlation found between the E and G results; similar results may be expected to hold good for the G data also.

§ 20. The values of ΔR for each element (and for each season) were divided into three nearly equal groups corresponding to days of large negative departures, small departures, and large positive departures from the normal ranges. The values of α and D for these groups of days were tabulated and their means determined. In the case of N a rather more elaborate process was adopted: "normal" values of α (N) and D (N) were determined by a procedure similar to that used in the case of R_n, and the tabulations gave $\alpha - \alpha_n$, $D - D_n$ instead of the simple values of α and D, as for the other elements.

The results are given in the following Tables X, XI, and XII. The three seasons and the year were separately treated, and the ∩ and ∪ groups of years were also considered separately and together.

---

* *Cf.* Chapman, 'Nature,' vol. 121, p. 989 (1928).

Table X.—Mean Values of $\alpha - \alpha_n$, $D - D_n$ for NE for sets of Days grouped according to their values of ΔR (NE).

	Days of large negative ΔR.				Days of small ΔR.				Days of large positive ΔR.				Means.	
	Number of days.	Mean ΔR.	Mean $a-a_n$.	Mean $D-D_n$.	Number of days.	Mean ΔR.	Mean $a-a_n$.	Mean $D-D_n$.	Number of days.	Mean ΔR.	Mean $a-a_n$.	Mean $D-D_n$.	a.	D.
All years	264	−23·0	−0·64	0·95	272	−1·6	0·08	−0·10	270	24·0	0·23	−0·86	2·40	2·37
⌓	102	−21·6	−0·91	1·01	114	−0·5	0·59	0·03	109	22·4	−0·28	−0·91	3·46	3·20
◡	162	−23·9	−0·48	0·91	158	−2·5	−0·28	−0·19	161	25·1	0·57	−0·83	1·68	1·81
s	93	−16·4	−0·70	0·76	92	−1·0	−0·03	−0·15	94	19·8	0·17	−0·51	2·56	0·90
s ⌓	39	−16·7	−1·13	1·36	39	−0·9	0·87	−0·03	37	16·8	−1·68	0·00	3·39	1·51
s ◡	54	−16·1	−0·39	0·33	53	−1·0	−0·70	−0·25	57	21·7	1·37	−0·84	1·98	0·48
e	76	−16·5	−0·68	0·97	83	+2·0	−0·36	0·20	81	22·5	0·49	−1·10	2·65	3·18
e ⌓	29	−15·1	−1·14	0·03	35	+3·0	−0·26	−0·46	38	21·0	1·34	−1·55	4·11	3·52
e ◡	47	−17·4	−0·40	1·55	48	+1·3	−0·44	0·69	43	23·8	−0·26	−0·70	1·57	2·93
w	95	−34·8	−0·56	1·11	97	−5·4	0·57	−0·31	95	29·5	0·06	−1·00	2·03	3·12
w ⌓	34	−32·8	−0·47	1·44	40	−3·2	1·05	0·50	34	30·1	−0·56	−1·18	2·94	4·69
w ◡	61	−35·9	−0·61	0·92	57	−7·0	0·23	−0·88	61	29·2	0·41	−0·90	1·48	2·17

Table XI.—Mean Values of α (WE) and D (WE) for sets of Days grouped according to their Values of ΔR (WE).

	Days of large negative ΔR.				Days of small ΔR.				Days of large positive ΔR.				Mean.	
	Number of days.	Mean ΔR.	Mean a.	Mean D.	Number of days.	Mean ΔR.	Mean a.	Mean D.	Number of days.	Mean ΔR.	Mean a.	Mean D.	a.	D.
All years	275	−22·2	1·72	0·76	267	−1·8	1·19	0·89	264	23·7	0·98	0·93	1·30	0·86
◠	109	−21·7	2·38	1·15	108	−1·7	1·18	1·47	108	23·5	1·16	1·40	1·57	1·34
◡	166	−22·6	1·28	0·50	159	−1·8	1·19	0·50	156	23·9	0·87	0·60	1·12	0·53
s	94	−16·2	1·07	0·13	93	0·7	1·11	0·42	91	19·7	0·86	0·28	1·01	0·28
s ◠	33	−16·3	1·15	0·70	39	2·0	1·13	0·85	42	20·1	0·71	0·48	0·98	0·67
s ◡	61	−16·1	1·04	−0·18	54	−0·4	1·09	0·11	49	19·4	0·98	0·10	1·04	0·01
e	82	−16·3	2·94	1·02	77	2·2	0·79	1·47	80	24·0	0·69	2·03	1·49	1·50
e ◠	34	−14·6	3·41	1·50	32	1·7	0·25	1·56	36	23·5	1·39	2·56	1·71	1·89
e ◡	48	−17·5	2·60	0·69	45	2·8	1·18	1·40	44	24·5	0·11	1·59	1·34	1·21
w	99	−32·9	1·31	1·13	97	−7·3	1·58	0·89	93	27·4	1·37	0·62	1·42	0·88
w ◠	42	−31·7	2·50	1·21	37	−8·6	2·03	2·05	30	28·2	1·50	1·30	2·06	1·52
w ◡	57	−33·8	0·44	1·07	60	−6·5	1·30	0·17	63	27·0	1·30	0·30	1·03	0·50

Table XII.—Mean Values of α (ZE) and D (ZE) for sets of Days grouped according to their values of ΔR (ZE).

	Days of large negative ΔR.				Days of small ΔR.				Days of large positive ΔR.				Mean.	
	Number of days.	Mean ΔR.	Mean a.	Mean D.	Number of days.	Mean ΔR.	Mean a.	Mean D.	Number of days.	Mean ΔR.	Mean a.	Mean D.	a.	D.
All years	252	−31·3	−1·07	0·40	259	−5·1	−0·69	−0·13	257	34·9	0·33	0·58	−0·48	0·28
◠	104	−32·9	−1·35	0·52	119	−5·5	−0·88	0·30	106	33·7	0·25	1·59	−0·66	0·79
◡	148	−30·2	−0·88	0·31	140	−4·7	−0·54	−0·49	151	35·7	0·38	−0·13	−0·34	−0·10
s	90	−23·6	−0·50	0·91	88	−1·1	0·02	1·40	87	30·9	0·86	0·28	0·12	0·86
s ◠	32	−22·3	−0·78	0·72	38	−1·8	−0·08	2·39	46	31·0	1·28	0·98	0·27	1·37
s ◡	58	−24·3	−0·34	1·02	50	−0·5	0·10	0·64	41	30·8	0·39	−0·51	0·01	0·47
e	72	−27·2	−0·96	0·26	78	−2·2	−0·50	−1·12	79	32·6	0·09	1·57	−0·44	0·24
e ◠	26	−30·0	−0·73	−0·04	43	−2·5	−0·91	−0·84	33	34·6	−0·91	3·18	−0·85	0·67
e ◡	46	−25·6	−1·09	0·43	35	−1·9	0·00	−1·46	46	31·1	0·80	0·41	−0·10	−0·09
w	90	−42·3	−1·73	−0·01	93	−11·2	−1·54	−0·74	91	40·6	0·02	0·01	−1·08	−0·25
w ◠	46	−42·0	−2·09	0·70	38	−12·4	−1·66	−0·50	27	37·4	−0·07	0·70	−1·45	0·29
w ◡	44	−42·6	−1·36	−0·75	55	−10·4	−1·45	−0·91	64	42·0	0·06	−0·28	−0·83	−0·62

Discussion of Tables X, XI, XII.

§ 21. The foregoing tables show that the mean values of α and D in N and W are positive, while in Z they are smaller, and perhaps change sign in the course of the year, the mean values being negative for α and positive for D. In all three elements, but especially in Z, the mean values are small, of the order $1\,\gamma$, so that they are liable to a proportionately larger accidental error than R.

The positive mean values of α and D for N and W correspond to the known fact that since disturbance reduces the mean value of H, on quiet days the mean value is above the mean H for all days, and H is on the whole increasing, by way of recovery from the disturbance depression. Since H at E and G has N and W components, both positive, α and D for N and W are positive.

Disturbance tends to raise the mean value of Z, but only very slightly; a similar argument would imply that α and D for Z should be negative; this is true for α, in the mean of the year, while D appears to be positive, but so small that its sign is perhaps doubtful.

The novel feature of Tables X to XII, however, is the evaluation of α and D for quiet days of different S_q range; the principal results which appear are:—

(*a*) There is a considerable and systematic decrease of D (N) as R (N) increases.
(*b*) There is a distinct and fairly regular increase of α (N) with R (N).
(*c*) There is no marked regular change of α and D with R in W.
(*d*) There is no marked regular change of D (Z) with R (Z).
(*e*) There is a considerable and systematic (algebraic) increase in α (Z) with R (Z).

The relations (*a*), (*b*) point to an inverse correlation between α (N) and D (N) on quiet days; this appears not to have been noticed hitherto. Such a relation is to be expected on the days (whether quiet or not) following a large magnetic disturbance, for then D is negative and numerically decreasing, but algebraically increasing, while α, the rate of recovery towards normal, decreases as the normal is approached. If the normal or undisturbed value of H is not attained, even after many days, this relation should be maintained even when D is positive, the real correlation, however, being that between α and the departure from the undisturbed (not the mean) value. But this explanation gives no account of the correlation of α and D with the S_q range R. This correlation is an unexpected one precisely because α and the changes in D are usually thought of as connected with magnetic disturbance, whereas it has seemed doubtful whether there is any systematic connection between disturbance and the S_q range. No explanation of the relationships (*a*)–(*e*) is offered, but they seem likely to have an interesting significance, and to be worthy of further study in the records of other observatories.

Summary.

§ 22. The regular changes of the solar diurnal magnetic variation on really quiet days at Eskdalemuir and Greenwich, in the course of the year and the sunspot cycle, are investigated, and used to define a "normal" range R_n of the daily variation on each such quiet day in the period 1913–23. The actual ranges R are found to differ from the normal ones R_n, and their percentage departures (ΔR) from the normals are investigated. The average numerical departures ΔR for different elements and seasons range from about 20 to 30 per cent.; the distribution is fairly symmetrical about the mean, and similar in different elements and for the two observatories. It is found that corresponding daily values of ΔR for the same element at the two observatories are closely correlated, whereas there is much less correlation between corresponding values of ΔR for different elements at the same observatory. It is shown that R or ΔR sufficiently characterises the daily variation at any season, because the variation is the same, except in scale, on days of large as on days of small range. Finally, some distinct and unexpected relationships are found between the values of ΔR, the non-cyclic variation, and the departure of the daily mean from the monthly mean values of the horizontal and vertical magnetic force.

The Spectrum of H_2. The Bands analogous to the Parhelium Line Spectrum.—Part I.

By O. W. Richardson, F.R.S., Yarrow Research Professor of the Royal Society, and P. M. Davidson, B.A., King's College, London.

(Received January 4, 1929.)

Synopsis.

§ 1. Previous history and general statement. § 2. Properties of the system $3\ {}^1B \rightarrow 2\ {}^1S$, here called the strong Q band system. § 3. Properties of the $2\ {}^1S$ state and comparison with the B state of the ultra-violet bands. § 4. Properties of the system $3\ {}^1C \rightarrow 2\ {}^1S$, here called the system with R very strong, P weak. § 5. Comparison of $3\ {}^1B \rightarrow 2\ {}^1S$ and $3\ {}^1C \rightarrow 2\ {}^1S$. The energy levels and the combination rules.

Note.—In these papers we keep to the formulæ of the old quantum mechanics, except where it is necessary for special purposes to translate them into the formulæ of the wave mechanics. Such special cases are clearly indicated.

§ 1. *Introduction.*

This investigation originated in a paper[*] entitled "The Hydrogen Band Spectrum: New Band Systems in the Violet," which described the discovery of a number of progressions extending from the green to the ultra-violet part of the spectrum and included a preliminary attempt to arrange some of the strongest of them. The extensive nature of these bands and the way they are interwoven made their further investigation very difficult and uncertain in its results and the conclusion was reached that little progress was likely to be made until the whole spectrum had been remeasured with greater resolution and dispersion than that which had been used in constructing the then existing tables. At this stage it was arranged by one of us (O.W.R.) in collaboration with Mr. Wilfred Hall, of Tynemouth, to take and measure a series of plates on his 21-foot Rowland grating. Soon after this work was started, however, it transpired that Messrs. Gale, Monk and Lee had almost completed a similar undertaking at Chicago and it was decided to await the results before proceeding with the experimental work. As the tables published by Gale, Monk and Lee[†] are both very accurate and extensive it was deemed unnecessary to do so. The present work may be regarded as the result of a re-examination of the series of band systems referred to above with the help of the new tables. We are much indebted to Prof. Gale for facilitating the work by supplying us with copies and a proof in advance.

---

[*] O. W. Richardson, 'Roy. Soc. Proc.,' A. vol. 115, p. 528 (1927).

[†] 'Astrophysical Journal,' vol. 67, p. 89 (1928).

It soon became evident,* as had been suspected, that the bands already published were but a small fragment of a much larger number of related bands. Instead of 6 progressions with a maximum of 4 members each we now have over 50 progressions, several of them extending to 9 members. These progressions include the strongest lines and indeed most of the strength of the secondary spectrum from $\lambda = 3394$ to λ 8902. In fact when the bands which correspond to the other orthohelium line spectrum† are added to them there are very few lines of any strength left in the spectrum. The irregular doublets previously described have now disappeared, the lines of all bands being single. The origin of this confusion is attributable to the fact that the stronger of the apparent faint components are mostly other lines of the same or related bands, which would account for their apparent physical connection. Since the note to 'Nature' was published we have found in many of the bands two rotational levels lower than the one there given as the lowest.

These bands form the part of the spectrum of the H_2 molecule which is analogous to the parhelium line spectrum and the final states of all these progressions belong to the electronic state $2\,^1S$. There are no combinations between any of the lines of these bands and those of the α, β, γ, etc., bands. On the other hand they do seem to have the same final states as the B states of Dieke and Hopfield and will presumably combine with the lines of the Lyman bands. The justification of some of these statements will be clearer when some of the bands have been described.

§ 2. *The Strong* Q *Band System.*

We shall start with this as it contains the first of any of these bands to be recognised,‡ the old 20 Q (m), and it is the strongest system except one in the whole spectrum. In some ways it has a very simple structure, each band consisting solely of one single Q form branch. The system consists of 4 progressions, the lines of which are given in Table I. In this table and throughout the paper the lines are numbered according to their final rotational levels, the lowest being called $m = 1$. Thus P (m), Q (m) and R (m) each refer to lines which end on the mth level. This system avoids any possibility of confusion as the properties of the final state are thoroughly established. In the table the wave number of each line is preceded by the measured value of the intensity given by Kapuscinski and Eymers* where such measurement exists and followed by the intensity estimate of Gale, Monk and Lee. In a few cases where their tables do not contain the line wave numbers and intensities taken from the tables of Merton and Barratt,† Tanaka,‡ Deodhar,§ and Finkelnburg|| have been inserted. These are indicated by the letters M, D, T and F respectively.

---

* Richardson and Davidson, 'Nature,' June 30, 1928.

† Richardson, 'Roy. Soc. Proc.,' A, vol. 113, p. 368 (1926); Richardson and Das, *ibid*, vol. 122, p. 688 (1929).

‡ Richardson and Tanaka, 'Roy. Soc. Proc.,' A, vol. 107, p. 619 (1925).

All the lines in Table I as well as of all the other bands in the large number of progressions under consideration satisfy the simple numerical rule that for any progression all the lines of a given m (whether P, Q, or R) have the same set of differences when arranged in order of magnitude. This is true to the high accuracy of the data of Gale, Monk and Lee when only lines from their tables are involved, except where the contrary is stated in the text. In the other cases, which have only been put in for completeness and on which no reliance is placed in regard to any important conclusions, the accuracy is that of the relevant measurements. The operation of this principle is due to the fact that all the progressions have the same set of final states and these invariable differences are the final vibrational term differences for a set of rotational states characterised by a given m. This rule appears to be exact and this fact, together with the high accuracy of the tables, enables all doubtful lines to be eliminated with certainty except in a few cases.

In a sense every line in this spectrum is a blend because there are so many interwoven bands that by exciting the higher rotational states a line could be made to appear anywhere. However, under ordinary low temperature excitation such lines would be so weak as to be imperceptible. It is convenient to call a blend of that character trivial. We believe that in spite of the high resolution which has been brought to bear on the spectrum there are still some blends left which are not trivial.

Turning to Table I we are struck at once by the alternation in intensity of

---

* 'Roy. Soc. Proc.,' A, vol. **122**, p. 58 (1929).

† 'Phil Trans.,' A, vol. **222**, p. 369 (1922).

‡ 'Roy. Soc. Proc.,' A, vol. **108**, p. 592 (1925).

§ 'Roy. Soc. Proc., A, vol. **113**, p. 420 (1926).

|| 'Zeits. für Physik,' vol. **52**, p. 27 (1928).

Table I.

n' ↓	n'' → m ↑	0.	1.	2.	3.	4.	5.	6.	7.
0	2	60 21830·56 (5)	20514·19 (2)	6·5 19234·62 (1)	1·8 17989·11 (1)	……………	……………		
	3	286 21827·99 (10)	90·0 20515·48 (8)	25·2 19238·85 (8)	9·1 17996·46 (3)	16787·38 (0)	15610·91 (0)		
	4	76 21837·43 (6)	21·9 20530·48 (4)	8·6 19258·66 (2)	12·1 18020·72 (2h)	……………			
	5	134 21862·78 (8)	20563·05 (3)	19297·49 (7)	5·2 18064·93 (3)	16864·10 (1)			
	6	19·0 21905·79 (3)	7·9 20614·80 (0)	19356·75 (1)	2·9 18130·90 (1c)				
	7	28·2 21967·13 (5)	10·4 20686·21 (5)	6·5 19436·91 (0)	2·8 18218·89 (1)				
	8	22047·14 (1)	20777·30 (1)	19537·49 (0)	18327·61 (00)				
1	2	57·3 23929·78 (5)	7·4 22613·42 (1)	29·0 21333·56 (3)	16·7 20088·33 (3)	5·7 18876·62 (3)	17697·87 (1)		
	3	375 23938·19 (10)	35·4 22620·69 (4)	159 21344·12 (8)	49 20101·74 (8)	26·5 18892·67 (9)	15·4 17716·35 (5)	16572·33 (0)	
	4	88 23944·42 (6)	12·5 22637·48 (2)	38·8 21365·71 (5)	30·7 20127·64 (6)	9·3 18922·37 (3)	17749·72 (1)		
	5	137 23966·56 (10)	10·2 22666·93 (2)	60·9 21401·31 (7)	22·1 20168·72 (5)	14·0 18968·59 (4)	5·1 17800·63 (2)		
	6	16·1 24001·74 (3)	22710·94 (1)F	7·9 21452·78 (1)	10·2 20226·86 (3)	3·2 19033·23 (1)	17870·80 (0)		
	7	28·9 24051·24 (4)	22770·26 (0)	10·2 21520·92 (3)	7·8 20302·96 (3)	19116·21 (0)		(10·1) 16836·04 (1)?	
	8	6·6 24115·47 (2)		21606·01 (1)					
2	2	16·9 25872·14 (1)	60·9 24555·69 (4)		11·9 22030·56 (2)	20818·88 (2a)	8·4 19640·06 (1)	18493·72 (1)	17379·89 (0)
	3	75·2 77·96 (4)	395 65·35 (10)	5·4 23288·85 (1)	61·0 22046·37 (6)	72·2 20837·28 (2)	40·4 60·83 (9)	18516·91 (4)	17404·90 (2)
	4	86·7 89·38 (4)	[24582·41]		12·4 72·46 (2)	17·0 67·24 (2)	9·7 94·55 (1)		
	5	37·1 25908·41 (2)	193 24608·70 (8a)	3·0 23343·15 (0h)	ca. 18 22110·43 (3)	ca. 25 20910·38 (5)	<29·2 19742·22 (6)	9·0 18606·12 (2)	17501·97 (1)
	6	36·44 (1)	14·6 645·40 (2)	87·51 (0,1)F	22161·50 (1b)	3·5 20967·65 (0)	19805·44 (0a)	74·65 (0)	
	7	74·90 (1)	22·5 693·85 (4)	23444·60 (0d)	22226·50 (0)	4·1 21039·79 (2)			
	8	26024·48 (1d)	4·5 754·51 (2)		22304·85 (1)?				
3	2	27644·53	26328·24 (2)	11·4 25048·41 (6)*					
	3	27644·53 (1)	102 31·92 (6)	142 55·40 (0)*	29·3 23812·99 (3)	11·9 22004·07 (1)	44·4 21427·56 (6)	88·0 20283·29 (8) 20283·93 (9)	16·5 19171·51 (6)
	4		25·6 46·75 (1)	30·6 74·95 (0)*	6·8 36·80 (1)	47·0 31·71 (5)	8·5 58·84 (1)	6·3 20318·18 (1)	5·5 19209·46 (1)?
	5		35 68·00 (2)	48·6 25102·42 (1)*	8·7 69·73 (1)	69·78 (00a)	13·6 21501·68 (1)		
	6								
	7								
	8								

* These are the intensities actually given by Gale, Monk and Lee, but they probably should be (2), (8), (3) and (4) respectively, owing to a slip in the tables.

the lines of the bands of this system, the strong lines being those for which m is odd. This property is also possessed by the bands which end on $2\,^3S$ which have been arranged already. It will be seen from the intensity measures, if allowance is made for the temperature effect, that the weight ratio of alternate rotational states is close to 3 : 1. The only intensity data which conflict with this rule are :—(1) 0 → 3″ Q (4) 18020·72 (2h) = 12·1. This is marked h by Gale, Monk and Lee, meaning probably double. (2) 2 → 0″ Q (4) 25889·38 (4) = 86·7. This is too strong. (3) 2 → 1″ Q (4). This should be a strong line and is absent. This seems to be a definite perturbation. (4) 3 → 4″ Q (4) 22631·71 (5) = 47·0. This line is too strong and is probably a blend. (5) 3 → 6″ Q (3). If the lines given are correct the line is too strong and split up. (6) 3 → 7″ Q (3) 19171·51 (6) = 16·5. This is too strong in Gale, Monk and Lee. The only certain irregularity in the table is the absence of 2 → 1″ Q (4) = [24582·41].

An important characteristic of this band system is that the lines do not give the Zeeman effect. The only exceptions are :—(1) 3 → 4″ Q (4) 22631·71 (5) = 47·0. As we have seen this is too strong and may cover up the band line. (2) 3′ → 4″ Q (3) 22604·07 (1) = 11·9. This a weak line in the same band and (3) 3′ → 6″ Q (3) 20283·29 (8) + 20283·93 (9). Whether this affair really belongs to the bands is uncertain but it is curious that all these Z lines should be found in high vibration states where the conditions are very unstable. The intervening 3′ → 4″ Q (3) 21427·56 (6) = 44·4 is given as Z = 0 in Merton and Barratt. There are a good many lines in this system which are definitely marked Z = 0 in Merton and Barratt's tables.

It would take too much space to give the line differences for all the bands. The following are the values for the 0 — 0″, 1 — 0″, 2 — 0″ and 3 — 0″ bands. The data for 3 — 0″ are computed indirectly from lines for stronger bands using the combination intervals.

Table II.

0, 0″	1st diff.	−2·57		+9·44		25·33		43·03		61·34		80·01
	2nd ,,		12·01		15·89		17·70		18·31		18·67	
1, 0″	1st ,,	3·41		11·23		22·22		35·08		49·50		
	2nd ,,		7·82		10·99		12·86		14·42			
2, 0″	1st ,,	5·82		11·42		19·03		28·03		38·46		49·61
	2nd ,,		5·60		7·61		9·00		10·43		11·15	
3, 0″	1st ,,	13·07		9·17		14·00						
	2nd ,,		−3·90		4·83							

Whether the bands of this system consist of Q, P or R branches (as they are single branches and Q form Q is much more likely) successive lines will in any event be given by expressions of the form.

$Q(m) = \nu_0 + F'(\mu) - F''(m)$, $Q(m+1) = \nu_0 + F'(\mu+1) - F''(m+1)$ $Q(m+2) = \nu_0 + F'(\mu+2) - F''(m+2)$ where ν_0 is the result of the energy change not arising from rotation. If they are Q branches $\mu = m$, but for P $\mu = m - 1$ and for R $\mu = m + 1$.

Now the values of $F''(m+2) - F''(m)$ are known unequivocally from the combinations in the other progressions with the same final $2\,^1S$ state (see below); so that we can at once deduce the values of $F'(\mu+2) - F(\mu)$ for the initial state from the differences. This involves no theoretical assumptions. We can, however, go a step further. It happens that the final rotational states are closely represented by the simple anharmonic formula with a fourth power term in m, in fact $F''(m) = B_0(m-\frac{1}{2})^2 - C(m-\frac{1}{2})^4$ where $2''B_0 = 38{\cdot}911$ and $C = 0{\cdot}0152$. This enables the lowest $F''(m)$ (for $m = 1$) to be calculated with precision. From this and the known values of $F''(m+2) - F''(m)$ the values of each $F''(m)$ can be derived and a table of values of $F''(m+1) - F''(m)$ can be set up. From these and the differences of the consecutive lines of the bands we can derive the corresponding values of $F'(\mu+1) - F'(\mu)$. Such rotational properties of the initial states of this band system are given in Table III.

The values of $F(\mu+2) - F(\mu)$ are independent of any assumptions, however well vindicated, as to the theoretical structure of any levels. They can be got from Table III by adding the values of consecutive pairs of values of $F(\mu+1) - F(\mu)$. The $F(\mu+1) - F(\mu)$ terms we are unable to represent satisfactorily by any expression of the type

$$F(\mu) = (B\sqrt{j^2-\sigma^2} - e)^2 + C(\sqrt{j^2-\sigma^2} - e)^4.$$

This expression does not seem to be of the right form. On the face of it the 0′ terms would approximate to what would be given by e slightly $> +\frac{1}{2}$ and $\sigma = 0$ and the $-2'$ terms by $e = 0$ using semi-integral j values. There seems to be a progressive change in the values of these quantities in passing from one upper vibrational level to the next. The differences of $F(\mu+1) - F(\mu)$ are fairly constant at about the fifth level and as the effect of the C term has been allowed for by adding $3{\cdot}6$ to these differences the numbers in the table can probably be taken to represent the values of $2B'$ rather closely. The value $45{\cdot}2$ for $2B'$ at $n' = 3$ is probably a little too low.

Table III.

Initial vibration state.	0′.			1′.			2′.			3′.		
$F_8 - F_7$												
$F_7 - F_6$	282·09	52·10$_5$		270·25	48·11$_5$		259·21	44·22$_5$				
$F_6 - F_5$	229·98$_5$	52·97	−0·86$_5$	222·13$_5$	48·31	−0·19$_5$	214·98$_5$	44·27	−0·045			
$F_5 - F_4$	177·01$_5$	52·51$_5$	0·45$_5$	173·82$_5$	47·53$_5$	0·77$_5$	170·71$_5$	44·23$_5$	0·035	165·68	41·45	
$F_4 - F_3$	124·50	49·77	2·74$_5$	126·29	45·58	1·95$_5$	126·48	43·36	0·87$_5$	124·23	46·93	−5·48
$F_3 - F_2$	74·73			80·71			83·12			77·30		
$2B'$	56·6			52·0			48·0			45·2		
C^1	−0·0154											
$I' \times 10^{40} \approx$	0·98			1·09			1·15			1·23		
$Q(2) - B'\mu_0^2$	21805			23893·8			25828·7			27616		
$\Delta Q(2) - B'\mu_0^2$		2088·8			1934·9			1787				
Next Δ				153·9			148					
Apparent μ_0	·92			1·14			1·38			1·15		

The values of 2B′ so estimated are set out immediately below the $F(\mu+1) - F(\mu)$ values in Table III and the corresponding moments of inertia I′ in the next row but one. Assuming $F(\mu) = B\mu^2$ as a first approximation for small values of μ and taking μ to increase by 1 in passing from the lowest to the next μ the values of the lowest μ got from B′ and $F(3) - F(2)$ are given under "apparent μ_0" in the lowest row. These bear out the apparent changes in ϵ and σ with n' already referred to. As the Q (1) line is quite definitely absent we take the lowest j value to be $j_0 = 3/2$ and the variations in the table to be due to variations in ϵ and σ or to some other matters not yet taken account of. The value of $Q(2) - B'\mu_0{}^2 = n'\omega_0{}'(1 - x'n')$ + electronic constants + constants of the lower level with $n'' = 0$, $m'' = 1\frac{1}{2}$. The second difference of this is $-2\omega_0 x$. The initial vibration differences (of $Q(2) - B'\mu_0{}^2$) are 2088·8, 1934·9 and 1787 with second differences −153·9 and −148. The inconstancy of these suggests that the quadratic formula in n' is inaccurate which is no doubt true, but there are so many uncertainties in the detailed treatment that we shall not pursue this refinement at present but keep to the quadratic formula in n' and take the second difference as 154. If 21830 is the $n' = 0$ series $\omega_0 - \omega_0 x = 2088{\cdot}8$ giving $\omega_0 = 2166$, $\omega_0 x = +77$, and $x = 0{\cdot}036$. The four values of $2B_n{}'$ give the differences 4·6, 4·0 and 2·8 average 3·8, so that $\alpha = 1{\cdot}9$ (in $B_n{}' = B_0{}' - \alpha_n{}'$). The product $I_0\omega_0$ is 2123×10^{-40} which is about the same as the values found in other bands of the H_2 spectrum.

The great strength of the 21830 progression and the fact that it does not fit on to anything in the part of the spectrum further towards the red is sufficient to prove that it must be the $0' \rightarrow n''$ progression. But if further proof were needed the matter is settled beyond the possibility of doubt when the intensity distribution in the band is examined. In fig. 1 are tabulated, by the usual

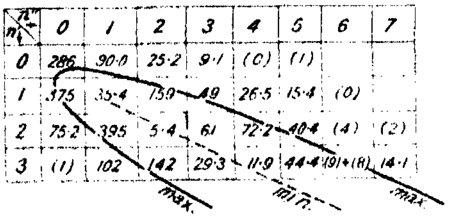

$n'' \rightarrow$ / $n' \downarrow$	0	1	2	3	4	5	6	7
0	286	90·0	25·2	9·1	(0)	(1)		
1	375	35·4	159	49	26·5	15·4	(0)	
2	75·2	395	5·4	61	72·2	40·4	(4)	(2)
3	(1)	102	142	29·3	11·9	44·4	(9)+(8)	14·1

FIG. 1.

double entry method according to the initial and final vibration states, the intensities of the strong Q (3) lines of each band as measured by Kapuscinski and Eymers. Where these measurements are not available, and in one case where they are doubtful, Gale, Monk and Lee's intensity estimates are given in brackets. It will be seen that the maximum intensities all lie along a parabolic curve and that there is an intervening line of minimum intensities following the axis of the parabola.

Similar results are obtained if the intensities of all the lines in each band are added together instead of taking a single strong line, but as there is an element of uncertainty in the addition of eye estimates to measured intensities this method has not been adopted. This type of intensity distribution is a common occurrence in band systems which has been accounted for theoretically by Condon.*

The value of ν_0 the electron jump frequency of this band system can be got from the Q (2) lines of the $0' \rightarrow 0''$ band by the relation

$$Q(2) = \nu_0 + F'(1\tfrac{1}{2}) - F''(1\tfrac{1}{2}).$$

The value of $F''(1\frac{1}{2})$ is 43·71. That of $F'(1\frac{1}{2})$ is uncertain owing to the absence of a satisfactory theoretical formula, but extrapolation from the values of $F'(m+1) - F'(m)$ for the higher m's shows that it must be close to 35. This value gives $\nu_0 = 21839 \cdot 27$, so that we can take ν_0 to be within one or two units of 21839.

The value of C_0' given in Table III is got from the relation

$$C_0' = B_0'(2B_0'/\omega_0)^2.$$

There are not enough data to check this directly from the coefficient of the fourth power term in m. It is practically the same as the value C_0'' for the final state.

The only irregularity in Table III, if it be one, is the large second difference $-5 \cdot 48$ in the $3'$ level. The energy of the molecules when $n' = 3$ is very high (not much below the equivalent of the ionisation potential) and such irregularities are to be expected in the circumstances. In agreement with this we find no evidence in the spectrum of the existence in this system of any initial vibrational levels with $n' > 3$.

§ 3. *The Final Rotation and Vibration States.*

Before proceeding to describe any more band systems perhaps it would be as well to give the rotational and vibrational properties of the final states as these are common to all the progressions under consideration. Fortunately this state is very regular and its properties quite simple compared with those of the initial states. Owing to the large number of progressions and the great strength of many of them the data can be ascertained with a very high degree of precision. The vibrational data are set out in Table IV. In the vertical column under m are given, opposite $n''_x - n''_{x-1}$, the average values of the differences of the R (1) lines (these end on the lowest rotational level) for the $x - 1$th and xth members of the progressions. Similarly in the column under m_2 on the same horizontal row are given the differences of the P (2), Q (2) and R (2) lines and so on. These numbers are extracted from about 40 progressions and as none of the individual values differ from the mean by more than $0 \cdot 10$ they are very accurate. It is probable that in nearly every case the last figure which is not written subscript is reliable to within 1.

---

* 'Phys. Rev.,' vol. 28, p. 1182 (1926).

The numbers which intervene, in the vertical columns, between the foregoing vibration differences, such as $1318 \cdot 34_5$ and $1281 \cdot 47_5$, are differences of successive vibration differences for a given m. Those which intervene in the horizontal rows, such as $1 \cdot 93_5$ between $1318 \cdot 34_5$ and $1316 \cdot 44$, are the differences of the vibrational differences for the same vibrational interval of two successive rotational levels. The numbers immediately below these, and which are neither below the m, nor opposite the $n''_x - n''_{x-1}$ s, are the next differences of these differences. It will be seen that corresponding numbers change in a perfectly uniform way throughout the table so that there are no irregularities in the final states.

The vibrational intervals in Table IV involve a mixture of rotational energy. To take this out we can proceed as follows. For any PQR (m_2) line arising from the transition $n' \rightarrow 0''$, $m_1 \rightarrow m_2$ we have

$$\text{PQR}\ (m_2) = \nu_0 + \text{F}'\ (n) - \text{F}''\ (0) + \text{F}'\ (nm_1) - \text{F}''\ (0_1 m_2)$$

and for the transitions $n' \rightarrow 1''$, $m_1 \rightarrow m_2$

$$\text{PQR}\ (m_2) = \nu_0 + \text{F}'\ (n) - \text{F}''\ (1) + \text{F}'\ (nm_1) - \text{F}''\ (1_1 m_2)$$

where ν_0 is the electronic energy jump, $\text{F}'\ (n)$, $\text{F}''\ (0)$, $\text{F}''\ (1)$ are the purely vibrational terms and $\text{F}'\ (nm_1)$, $\text{F}''\ (0_1 m_2)$, $\text{F}''\ (1_1 m_2)$ are the terms which involve the rotational energy, including the cross terms. Thus the differences such as $1318 \cdot 34_5$ under $n_1'' - n_0''$ in Table IV are equal to $\text{F}''\ (1) - \text{F}''\ (0) + \text{F}''\ (1_1 m_2) - \text{F}''\ (0_1 m_2)$ and their horizontal differences are the values of $\text{F}''\ (1_1 m_2) - \text{F}''\ (0_1 m_2) - \{\text{F}''\ (1_1 m_1) - \text{F}''\ (0_1 m_1)\}$ and so on. Now the behaviour of these states is very like that of the states in Part V where $\text{F}''\ (n_1 m_2)$ is of the form $\text{B}_n m_2^2 + \text{C}_n m_2^4$, C_n/B_n small and $\text{B}_n = \text{B}_0 - \alpha n$. If this applies

Table IV.

	m_1.		m_2.		m_3.		m_4.		m_5.		m_6.		m_7.	m_8.
$n_1'' - n_0''$	$1318\cdot34_6$	$1\cdot93_5$	1316·41	3·86	1312·55	5·61	1306·94	7·26	1299·68	8·69	1290·99	10·05	1280·94	
	36·87	$1\cdot92_5$	36·57	1·75	35·95	1·65	$35\cdot12_5$	1·43	34·09	1·36	32·95		31·62	
$n_2'' - n_1''$	$1281\cdot47_5$	$1\cdot63_5$	1279·84	3·24	1276·60	$4\cdot78_5$	$1271\cdot81_5$	$6\cdot22_5$	1265·59	7·55	1258·04	8·72	1249·32	
	34·76	$1\cdot60_5$	34·59	$1\cdot54_5$	$34\cdot21_5$	1·44	33·69	$1\cdot32_5$	32·98	1·17	32·15		31·30	
$n_3'' - n_2''$	$1246\cdot71_5$	$1\cdot46_5$	1245·25	$2\cdot86_9$	$1242\cdot38_2$	$4\cdot25_7$	$1238\cdot12_5$	$5\cdot51_5$	1232·61	6·72	1225·89	7·86	1218·02	
	33·70	$1\cdot40_8$	33·49	$1\cdot38_9$	33·32	$1\cdot25_8$	$32\cdot95_5$	$1\cdot20_5$	32·51	1·15	32·03		31·27	
$n_4'' - n_3''$	$1213\cdot01_6$	$1\cdot25_5$	1211·76	$2\cdot69_8$	$1209\cdot06_2$	$3\cdot89_2$	1205·17	5·07	1200·10	6·24	1193·86	7·11	1186·75	
	$33\cdot06_5$	$1\cdot44_3$	32·99	$1\cdot19_4$	$32\cdot73_2$	$1\cdot17_6$	32·43	1·17	32·07	0·87	31·61		31·25	
$n_5'' - n_4''$	1179·95	1·18	1178·77	2·44	1176·33	3·59	1172·74	4·71	1168·03	5·78	1162·25	6·75	1155·5	
	32·45	1·26	32·45	1·15	32·33	1·12	32·10	1·07	31·88	0·97	31·48		30·7	
$n_6'' - n_5''$	1147·50	1·18	1146·32	2·32	1144·00	3·36	1140·64	4·49	1136·15	5·38	1130·77	5·97	1124·8	
	32·0	1·14	32·0	1·04	31·96	1·13	31·94	0·89	31·85	0·59				
$n_7'' - n_6''$	1115·5	1·18	1114·32	2·28	1112·04	$3\cdot3_4$	1108·7	4·4	1104·3					
		1·10		1·06	30·75	1·06								
$n_8'' - n_7''$					1081·29									

in the present case and we neglect the C term as a first approximation, the value of $F''(1_1m_2) - F''(0_1m_2) - \{F''(1_1m_1) - F''(0_1m_1)\}$ is $\alpha(m_2^2 - m_1^2)$. Since $m_2 = m_1 + 1$ and so on, the successive differences such as $1\cdot93_5$ in the first row should be $(2m_1 + 1)\,\alpha_1\,(2m_1 + 3)\,\alpha_1\,(2m_1 + 5)\,\alpha$ and so on, and their next differences should be constant and $= 2\alpha$. The successive next differences are seen to be $1\cdot92_5$, $1\cdot75$, $1\cdot65$, $1\cdot43$ and $1\cdot36$. This falling off is due to our neglect of the fourth power term. It will be seen from the table that this behaviour is quite similar for all values of n''. For the lowest values of m its effect will be very small; using the data for these we have $2\alpha = 1\cdot92_5$ and, $\alpha(2m_1 + 1) = 1\cdot93_5$, from which $m_1 = \frac{1}{2}$ and $\alpha = 0\cdot965$. Thus these data lead to the conclusion that the final rotational terms are of the form $B_nm^2 + C_nm^4$ with the lowest $m = \frac{1}{2}$. This conclusion will be established by a direct investigation in a moment. The values of the second differences such as $1\cdot92_5$, $1\cdot60_5$, $1\cdot40_3$, $1\cdot44_3$, $1\cdot26$, $1\cdot14$, $1\cdot10$ in Table IV are now seen to be successive values of 2α. Evidently 2α is not a constant but falls off very markedly as n'' increases.

If we neglect the fourth power term we have $F''(n + 1) - F''(n) = R_n(1) - R_{n+1}(1) + \frac{1}{4}\alpha$. The rotational correction $\frac{1}{4}\alpha$ is quite small, varying from $0\cdot24_1$ to $0\cdot14_2$. When this is made the successive values of $\omega_{n+1} - \omega_n$ are 1318·586, 1281·676, 1246·715, 1213·184, 1180·102, 1147·645 and 1115·642. If we put $\omega_n = n\omega_0(1 + xn + yn^2 + zn^3)$ the direct algebraic evaluation of the first four differences of these numbers gives $\omega_0 = 1337\cdot726$, $x\omega_0 = -19\cdot54$, $y\omega_0 = +0\cdot42$, $z\omega_0 = -0\cdot02$. Direct substitution gives for the last difference 1114·95 as compared with 1115·642. No doubt a better fit could be obtained with some adjustment but this has not been proceeded with as it is easy to show that such a formula up to n^4 is not capable of representing the results to the accuracy of the observational data.

A graphical extrapolation of these vibration intervals by the method described in Part V, p. 415, gave for the heat of dissociation of this final state 27710 wave number $= 3\cdot418$ volt. This is identical with a value 3·41 got by Birge* for the B state from Dieke and Hopfield's ultra-violet data.

The comparison of the vibration differences in Table IV with the vibration differences for Dieke and Hopfield's† B level gives the following results :—

---

* 'Proc. Nat. Acad. Sci.,' vol. 14, p. 15 (1928).

† *Cf.* Dieke and Hopfield, 'Phys. Rev.,' vol. 30, p. 406 (1927).

Table V.

$m \rightarrow$	1.	2.	3.	4.	5.
$B_1-A_4-(B_0-A_4)$	1314	1320	1318	1315	1306
$B_1-A_6-(B_0-A_6)$	1315	1322	1303	1318	1303
$B_1-A_7-(B_0-A_7)$	1313	1312	1319	1314	1301
$B_1-A_9-(B_0-A_9)$	1327	1306		1305	
Average	1317·3	1315·0	1313·3	1313·0	1303·3
$\omega_1-\omega_0$ (Table IV)	1318·34$_5$	1316·41	1312·55	1306·94	1299·68
$B_2-A_4-(B_1-A_4)$	1277	1283	1280	1277	
$B_2-A_8-(B_1-A_8)$	1269	1275	1280	1277	1270
$B_2-A_9-(B_1-A_9)$	1276	1288		1278	
$B_2-A_{10}-(B_1-A_{10})$	1272	1283	1281	1278	1273
Average	1273·5	1282·2	1280·3	1277·5	1271·5
$\omega_2-\omega_1$ (Table IV)	1281·47$_5$	1279·84	1276·60	1271·81$_5$	1265·9

Data for different m's are only available for the B_0, B_1 and B_2 levels but the following data (Table VI) are available for the $m = 2$ lines of two additional levels.

Finally we have the long intervals for the $m = 2$ lines

$$B_4 - A_0 - (B_0 - A_0) = 5045, \quad B_4 - A_6 - (B_0 - A_6) = 5053,$$
$$B_4 - A_9 - (B_4 - A_9) = 5050,$$

average 5049·3 compared with the value 5053·26 for the same interval from Table IV.

Bearing in mind the large number of blends and the uncertainty of identification of some of the lines in the ultra-violet spectrum there is no difference between the vibration intervals of our final level and that of Dieke and Hopfield's B state to the accuracy of the ultra-violet data.

A further test is offered by a comparison of the moments of inertia, or its equivalent the constant B_0, for the two states. This can only be extracted from the material of Table IV by the indirect and inaccurate method which was used in Part V. Among the present data we have, however, a large number of progressions with both P and R branches and from these we can deduce the

Table VI.

			Average.	Table IV.
$B_4 - A_0 - (B_3 - A_0) = 1209$	$B_4 - A_6 - (B_3 - A_6) = 1201$	$B_4 - A_9 - (B_3 - A_9) = 1215$	1208·3	1211·76
$B_3 - A_0 - (B_2 - A_0) = 1247$	$B_3 - A_4 - (B_2 - A_4) = 1250$	$B_3 - A_5 - (B_2 - A_5) = 1248$	1246·5	1245·25
$B_3 - A_8 - (B_2 - A_8) = 1248$	$B_3 - A_9 - (B_2 - A_9) = 1241$	$B_3 - A_{10} - (B_2 - A_{10}) = 1245$		
$B_2 - A_0 - (B_1 - A_0) = 1276$	$B_2 - A_4 - (B_1 - A_4) = 1283$	$B_2 - A_8 - (B_1 - A_8) = 1275$	1280·6	1279·84
$B_2 - A_9 - (B_1 - A_9) = 1288$	$B_2 - A_{10} - (B_1 - A_{10}) = 1281$			
$B_1 - A_0 - (B_0 - A_0) = 1313$	$B_1 - A_4 - (B_0 - A_4) = 1320$	$B_1 - A_6 - (B_0 - A_6) = 1322$	1314·6	1316·41
$B_1 - A_7 - (B_0 - A_7) = 1312$	$B_1 - A_9 - (B_0 - A_9) = 1306$			

rotational constants of the bands directly. Thus for the R (m) and P $(m+2)$ lines of any band we have

$$\text{R}\,(m) = \nu_0 + \text{F}'\,(n'_1\, m+1) - \text{F}''\,(n''_1\, m),$$
$$\text{P}\,(m+2) = \nu_0 + \text{F}'\,(n',\, m+1) - \text{F}''\,(n'',\, m+2),$$

so that R (m) — P $(m+2)$ = F″ $(m+2)$ — F″ (m) for the n'' vibration level. For the bands which end on $n'' = 0$ the averages of the successive values of F″ $(m+2)$ — F″ (m) are 116·15, 192·36, 266·74$_5$, 338·64 and 407·7. These are the averages of a large number of values, none of them differing by more than 0·10 from the mean. We assume that for m small and $n = 0$ $\text{F}''\,(m) = \text{B}_0 m^2 + \text{C}_0 m^4$ and use the first three numbers in the above sequence to determine B_0, C_0 and m_0 (the lowest m). We find $\text{B}_0 = 19{\cdot}455_5$, $\text{C} = -0{\cdot}01520_7$ and $m_0 = 0{\cdot}50013$, and remains very close to $\frac{1}{2}$ throughout the vibration levels. If we recompute the F″ $(m+2)$ — F″ (m) with the help of these numbers we find 116·15, 192·36, 266·74$_5$, 338·57$_5$ and 407·12. The formula thus holds quite well as far as the fourth value and begins to show an error at the fifth. It, therefore, seems justified to use the formula to calculate the first energy interval F″ (m_2) — F″ (m_1). This proves to be 38·85, and without further calculation the F″ $(m+2)$ — F″ (m), which are got directly from observation, give the scheme of energy intervals shown in Table VII.

Table VII.

Energy level intervals.	Differences.	Second difference.
220·7$_5$		
	33·8	
186·95$_5$		1·47
	35·27	
151·68$_5$		1·35$_5$
	36·62$_5$	
115·06		1·13$_5$
	37·76	
77·30		0·69
	38·45	
38·85		

The value $\text{B}_0 = 19{\cdot}455_5$ has been checked in other ways and is believed to be correct to at least 1 part in 2000. C might be wrong by 1 or 2 per cent. and m_1 should probably be $\frac{1}{2}$. This value of B_0 is equivalent to $\text{I}_0 = 1{\cdot}4243_6 \times 10^{-40}$. This constant as determined from the ultra-violet data is very uncertain. Birge* (*loc. cit.*) estimated it to be as high as $1{\cdot}99 \times 10^{-40}$, but it may well be

---

* Since this was written I have been informed by Prof. Birge that as a result of a re-examination of the ultra-violet bands, he and Mr. H. H. Hyman find the value of B_0 for the B level to be 19·46 ± 0·04. This was obtained without any knowledge of our value.—O. W. R.

Table VIII.

j values.	*n* = 0.			*n* = 1.			*n* = 2.			*n* = 3.		
7½												
6½												
5½	220·75			210·7			201·98			194·11		
		33·8			$32\cdot43_5$			$31\cdot26_5$			$30\cdot11_5$	
4½	$186\cdot95_5$		1·47	$178\cdot26_5$		$1\cdot4_6$	$170\cdot71_5$		1·25	$163\cdot95_5$		$1\cdot19_5$
		35·27			33·84			$32\cdot51_5$			31·31	
3½	$151\cdot68_5$		$1\cdot35_5$	$144\cdot42_5$		$1\cdot13_5$	138·20		1·02	$132\cdot68_5$		$0\cdot96_7$
		$36\cdot62_5$			$34\cdot97_5$			$33\cdot53_5$			$32\cdot27_7$	
2½	115·06		$1\cdot13_5$	109·45		$1\cdot03_5$	$104\cdot66_5$		0·93	$100\cdot40_8$		$0\cdot79_9$
		37·76			36·01			$34\cdot46_5$			$33\cdot07_6$	
1½	77·30		0·69	73·44		$0\cdot51_5$	70·20		$0\cdot45_5$	$67\cdot33_2$		$0\cdot44_1$
		38·45			36·52			34·92			$33\cdot51_7$	
½	38·85			$36\cdot91_5$			35·28			$33\cdot81_5$		

j values.	*n* = 4.			*n* = 5.			*n* = 6.			*n* = 7.		
7½												
6½												
5½	187·00			180·25			174·28					
		$29\cdot24_5$			$28\cdot27_5$			$27\cdot68_5$				
4½	$157\cdot75_5$		$0\cdot89_5$	$151\cdot97_5$		$0\cdot79_5$	$146\cdot59_5$		$0\cdot49_5$			
		30·14			29·07			28·18				
3½	$127\cdot61_5$		$0\cdot95_9$	$122\cdot90_5$		$0\cdot90_9$	$118\cdot41_5$		$0\cdot66_9$	$114\cdot01_5$		
		$31\cdot09_9$			$29\cdot97_9$			$28\cdot84_9$			$27\cdot78_9$	
2½	$96\cdot51_5$		$0\cdot78_3$	$92\cdot92_6$		$0\cdot75_3$	$89\cdot56_6$		$0\cdot84_3$	$86\cdot22_6$		$0\cdot84_3$
		$31\cdot88_2$			$30\cdot73_2$			$29\cdot69_2$			$28\cdot63_2$	
1½	$64\cdot63_4$		$0\cdot19_2$	$62\cdot19_4$		$0\cdot08_2$	$59\cdot87_4$		$-0\cdot01_8$	$57\cdot59_4$		$-0\cdot05_8$
		$32\cdot07_4$			$30\cdot81_4$			$29\cdot67_4$			$28\cdot57_4$	
½	32·56			$31\cdot38_0$			30·20			29·02		

much less than this. The value of C_0 given by the theoretical formula $C_0 = B_0(2B_0/\omega_0)^2$ is 0·0165 as compared with the direct value 0·0152. This agreement is satisfactory. In Table VIII are collected rotational energy level data for all the vibrational levels. It should be remembered that the $F''(m+2) - F''(m)$ values, which involve no theoretical assumptions but are directly observed, can be got by adding together any consecutive pair of these.

It is evident from Table VIII that the fourth power term is not operating accurately for the larger values of n. This is shown by the second differences which tend to become negative at the lowest interval, have a big jump at the next interval and then fall off, whereas they should increase uniformly from the lowest upwards. The formula $F(j) = Bj^2 + Cj^4$ does, however, operate satisfactorily up to $n = 3$. If we apply it to this vibrational level taking $j = \frac{1}{2}$, $1\frac{1}{2}$, $2\frac{1}{2}$ and $3\frac{1}{2}$ and applying the formula $C_3(24j + 36)$ to each of these second differences in succession we get the values $-C_3 = 0{\cdot}0092$, $0{\cdot}0111$, $0{\cdot}0101$, $0{\cdot}0099_5$ mean 0·0101 and the accuracy should increase with the higher differences so that this value looks reliable to something close to the last figure. If we now apply the formula $2B_3 + C_3(12j^2 + 24j + 14)$ to the first difference 33·51 using $C_3 = -0{\cdot}0101$ we find $2B = 33{\cdot}81_0$. If α were a constant, this should be equal to $2(B_0 - 3\alpha)$ which would give, with $2B_0 = 38{\cdot}91_1$, $\alpha = 0{\cdot}85_0$. We have seen that α is not really a constant but increases with n so that this is a mean α over the first three intervals. The values of 2α already got for these intervals are $1{\cdot}92_5$, 1·75 and 1·65 and one-sixth of the sum of these is $0{\cdot}88_0$. This check is not unsatisfactory. It will be seen that the first horizontal differences in Table IV are equal to 2α and that this only varies for n small. At the larger values of n it tends to assume the constant value 1·18.

The value of C_n is not constant but varies with n. It can be satisfactorily represented by generalising the usual formula $-C_0 = B_0(2B_0/\omega_0)^2$ into $-C_n = B_n(2B_n/\omega_0)^2$. This is shown by the following figures where under each n is given the sum of the corresponding second differences in Table VIII which sum is proportional $-C_n$ and below the quotient of this sum by $8B_n^3$.

Table VIIIa.

$n \rightarrow$	0.	1.	2.	3.	4.	5.	6.
Σ 2nd diff.	4·65	$4{\cdot}08_5$	$3{\cdot}65_5$	$3{\cdot}40_2$	$2{\cdot}82_9$	$2{\cdot}53_9$	1·99
$\Sigma + 8B_n^3$	1·263	1·232	1·203	1·142	1·223	1·214	1·38

However, the treatment due to Kemble and others* seems to fit the data still better. Putting for the $n = 0$ state

$$F(m) = B_0 m^2 + C_0 m^4 + F_0 m^6 + H_0 m^8 + \dots$$

in which

$$C_0 = -4B_0^3/\omega_0^2, \quad F_0 = (2 - \alpha\omega_0/6B_0^2)\ C_0^2/B_0$$

and

$$H_0 = 3\ F_0 C_0/B_0 - 5C_0^3/B_0^2 + F_0^2/C_0 - 8C_0^2 x/3\omega_0$$

the first four $F(m_0 + 2) - F(m_0)$ S for this vibrational level give

$$m_0 = \tfrac{1}{2}B_0 = 19{\cdot}456, \quad C_0 = -0{\cdot}0157, \quad \text{and } F_0 = 1{\cdot}3 \times 10^{-5}.$$

The calculated F_0 is $1{\cdot}98 \times 10^{-5}$ from $(2 - \alpha\omega_0/6B_0^2)\ C_0^2/B_0$ which would require $C_0 = -0{\cdot}0153$. With these values 2×10^{-5} and $-0{\cdot}0153$ the calculated and experimental values of $F(m_0 + 2) - F(m_0)$ are practically identical up to $F(6\frac{1}{2}) - F(4\frac{1}{2})$ except at the fourth, where there is a deviation of 0·05. This is almost within the range of experimental error.

According to this method $C_n = C_0 + \beta n$ where

$$\beta = (2 - 4H_0 B_0^2/C_0^3 + 9B_0^2 F_0^2/2C_0^4)\ 12B_0^4/\omega_0^3.$$

The experimental data are well covered by $C_n = C_0\ (1 - 0{\cdot}091n)$ so that $\beta = -0{\cdot}091C_0$. The value calculated by the formula is $\beta = -0{\cdot}39C_0$, but it depends on H_0 which is very uncertain. At least it has the right sign.

If we take $F = 2 \times 10^{-5}$ we get $B_0 = 19{\cdot}450$, if we take $F = 1{\cdot}3 \times 10^{-5}$ we get $B_0 = 19{\cdot}462$. If we take $B = 19{\cdot}456$ we think this is certain to more than 1 part in 2000 when all possible errors both of observation and interpretation are taken into account. In neither event does m_0 differ from $\frac{1}{2}$ by more than one-tenth of 1 per cent. It is slightly under in the one case and about equally above in the other.

§ 4. *The System with R very Strong, P Weak.*

This band system is closely related to the strong Q system described in § 2, but it differs from it in one very important particular inasmuch as its lines respond to the Zeeman effect. It is probably the strongest band system in the whole spectrum ; at any rate it contains the strongest individual line 21573·46 = λ 4634·032. The lines and their intensities are set out in Table IX in the same form as those in Table I. Owing to the turning of the R branch of $1' \rightarrow 2''$ the line 21166·94 (10) occupies the position of two lines. It is too strong for

---

* See Pomeroy, 'Phys. Rev.,' vol. 29, p. 59 (1927).

Table IX.

n′ ↓	m ↓	n″ →	0.		1.		2.		3.		4.		5.		6.		7.	
0	1	R	227	21601·63 (10)		20283·29 (8)	14·6	19001·86 (7)	12·8	17755·11 (4)								
		P																
	2	R	160	21585·48 (8)	30·2	20269·03 (7)	9·9	18989·26 (3)	9·7	17743·95 (3a)								
		P		21570·31 (2)		20253·93 (1)		18974·12 (00)		17728·82 (1)								
	3	R	485	21573·46 (10)	92·7	20260·90 (10)	29·2	18984·32 (10)	31·8	17741·92 (8)		16532·87 (0a)						
		P	87	21485·52 (6)	18	20172·92 (6)	3·3	18896·35 (0)	9·2	17654·00 (3)								
	4	R	<146	21570·83 (5)	31·7	20263·88 (4)	10·4	18992·05 (2)	8·5	17753·95 (2)	11·1	16548·90 (3)?						
		P	16·1	21393·11 (3)	6·7	20086·15 (1)	5·3	18814·43 (1)	3·4	17576·22 (1)								
	5	R	233	21583·62 (9)	?	20283·93 (9)	20·8	19018·39 (7)	11·3	17785·83 (5)								
		P	25·1	21306·76 (5)	10·2	20007·03 (3)		18741·52 (6)	12·1	17508·99 (5)		16308·84 (0a)						
	6	R	39·2	21614·14 (5)	10·7	20323·15 (5)	4·9	19065·14 (2)	2·3	17839·31 (1)								
		P	10	21232·31 (2)						17457·57 (00)								
	7	R	17·4	21664·36 (3)			4·0	19134·07 (1)	4·1	17916·30 (1)								
		P	44·1?	21176·05 (1a)	3·8	19895·10 (1)												
	8	R																
		P																
1	1	R	156	23827·38 (6)	8·6	22509·10 (2)	80	21227·60 (10)	35·5	19980·86 (9)	9·2	18767·87 (4)	5·7	17588·00 (5)				
		P																
	2	R	89·0	804·04 (5)		487·68 (1)	47·1	207·81 (6)	25	962·54 (8)	6·0	750·84 (2)	interference					
		P		802·27 (1)			7·3	206·11 (1a)		960·91 (0)	3·4	748·95 (0)		17570·26 (0a)				
	3	R	340	773·97 (9)	15·8	461·50 (5)	105	184·82 (10)	80	942·45 (10)	26	733·29 (5)	25	17557·05 (5)	26·1	16413·37 (7)??		
		P	6·8	711·33 (0)				122·25 (1)	9·9	879·73 (2)				494·35 (1)				
	4	R	90·8	745·57 (5)	6·1	438·69 (1)	127	166·94 (10)	29·1	928·69 (6)	5·4	723·53 (2)	9·9	550·78 (3)		410·14 (0)?		
		P				304·85 (1)?			4·6	794·83 (0)								
	5	R	158	732·21 (10)	26·4	432·61 (1)	127	166·94 (10)	48·5	934·35 (8)	12·5	734·30 (1)	13·3	566·27 (3)		430·10 (0)		
		P							9·8	709·41 (2)				341·26 (1)				
	6	R	13·8	734·82 (1)		443·52 (q) D		185·87 (1)	5·3	959·86 (1)		766·10 (0)	2·3	603·80 (1)				
		P							4·6	632·10 (1)								
	7	R	28·1	750·98 (4)		470·15 (0)	11·2	220·69 (3)	11·0	20002·69 (5)		815·94 (1)	2·8	660·45 (1)				
		P							6·8	19576·38 (1)	2·3	389·66 (0)						

1	5	R																
		P																
2	1	R	29	25828·29 (2)	151	24509·88 (7)	30·4	23228·36 (3)	27·1	21981·71 (5)	31	20768·69 (7)	22·3	19588·70 (4)	8·1	18441·19 (1)		
		P																
	2	R	18·5	805·08 (2)	76·2	488·63 (5)	3·9	208·85 (0)	17·6	963·56 (3)	17·8	751·81 (3)	15·4	573·06 (3)		426·78 (0*a*)		
		P																
	3	R	47·4	769·06 (4)	197	456·42 (9)	11·1	179·90 (2)	35·6	937·52 (4)	52·1	728·46 (8)	44·8	552·06 (7)	12·4	406·15 (3)	12·0	17296·19 (2*h*)
		P						122·87 (0)										
	4	R	9·8	716·94 (1)	24·7	409·98 (3)	2·2	138·13 (00)	4·7	900·12 (0*a*)	8·0	694·84 (0*a*)	8·8	522·09 (1)	10·6	381·39 (3)		
		P												417·96 (00)				
	5	R		646·15 (1)	23·3	346·40 (3)	2·8	080·88 (0)		848·34 (1)	6·2	648·07 (1)	8·8	480·07 (2)	2·7	344·04 (1*h*)	9·9	239·70 (2)
		P						22937·06 (00)					5·9	336·34 (0*a*)	10·8	200·05 (2)		
	6	R																
		P																
	7	R																
		P					2·0	22708·20 (0)										
	8	R																
		P																
3	1	R		27643·95 (1)	72·8	26325·54 (5)	89	25044·09 (5)	31·2	23797·34 (3)	3·3	22584·34 (1)	31·0	21404·31 (4)		20256·79 (3)	13·8	19141·31 (3)
		P																
	2	R			34·7	315·06 (3)	33·3	035·16 (3)	13·6	789·92 (1)			4·7	399·47 (1)	12·0	20253·11 (1*a*)	7·8	138·80 (2)
		P																
	3	R		599·99 (1)	94·5	287·38 (5)	90·5	010·82 (7)	36·0	768·41 (2)		559·44 (1)	34·3	382·99 (4)	26·0	238·91 (4)	23·5	126·96 (6)
		P				215·22 (1)	10·1	24938·63 (2)						310·77 (1)				
	4	R		552·92 (*r*) T	19	246·05 (1)	20·1	24974·33 (2)	7·6	736·04 (1*a*)			7·8	358·18 (1*h*)	13·0	217·55 (2)	6·5	108·90 (1*h*)
		P				132·16 (0)	21·8	860·33 (2)										
	5	R																
		P						768·00 (1)										

additional lines 6·8, 17973·40 (1) = 3′ → 8″ P (3) either. The lines $0' \rightarrow 0''$ P (2) and R (4) are unresolved by Kapuscinski and Eymers. The data of Gale, Monk and Lee suggest that the intensity of P (2) should be about 25 and that of R (4) about 120. The P branches are only well developed in the $0' \rightarrow n''$ progression, in the other horizontal progressions there are only a few of the stronger lines at a few favoured final vibration levels. It will be seen that both P and R branches show the same intensity alternation in successive lines as was noted in the strong Q band system. In fact if allowance is made for the temperature effect the weight ratio of alternate states is seen to be very close to 3 to 1 for all bands. Where this is apparently not the case there is probably some confusion caused by blending or errors in the intensity data, or possibly, but this is not very likely, there may be a few abnormal lines. As in the Q bands the lines which are strong, both in P and R, are those which end on the odd levels and vice versa.

The properties of the upper levels of these bands are set out in Table X in *the same form as those in Table III for the strong Q band system.* The top rotation level difference at $n' = 0$ is uncertain. The R (7) lines in the table give $F(8) - F(7) = 270 \cdot 97$ which joins regularly on to the other values, but these lines are not satisfactory. The failure of the $0' \rightarrow 1''$ R (7) line seems inexplicable. A better set of lines with the correct vibration differences for the R (7)s would be 35·8, 21646·92 (5), 12·5, 20365·97 (5), ... 19116·71 (0), ... 17898·62 (1). The lines have about the intensities to be expected. Thus, on physical grounds, these would appear to be the R (7) lines of this progression. Unfortunately they give the abnormal level value given in Table X. In either alternative we seem to be faced with a perturbation. Either the $1' \rightarrow 0''$ R (7) line is unexpectedly absent or the $m = 8$ rotational level is irregularly placed.

The rotational terms of the $0'$ level show the peculiarities exhibited by the rotational terms of the strong Q system, but in an exaggerated form. The only terms of this type which the authors are familiar with are some recently found by Curtis* in the He_2 spectrum. Since the P (2) lines are present in the $0'$ and $1'$ progressions the lowest j ($j_0 = \frac{1}{2}$) must be present in the upper level, keeping as before to semi-integral j values. The presence of this line also suggests that $\sigma \simeq 0$ for this system. There is no theoretical explanation of the rise of the first differences of $F_{m+1} - F_m$ with m for small values of m but we interpret it as a variation of B with m which is not taken account of in the existing theories. If this is admitted the lowest rotational terms of the $0'$ level are given by $B'(j - e)^2$ where $B' = 15 \cdot 1$ and $e = +1\frac{1}{4}$. Using this

---

* Curtis and Harvey, 'Roy. Soc. Proc.,' A, vol. 121, p. 381 (1928).

Table X.

Initial vibration states. n→	0.			1.			2.			3.		
		1st diff.	2nd diff.		1st diff.	2nd diff.		1st diff.	2nd diff.		1st diff.	2nd diff.
$F_8 - F_7$ ……… or	?270·97 ?253·53	53·52? 36·08?	0·45 −16·99	238·91	47·34$_5$	−3·89$_5$						
$F_7 - F_6$	217·45	53·07	1·17	189·56$_5$	51·24	−0·42$_5$						
$F_6 - F_5$ ………	164·38	51·90	4·66	138·32$_5$	51·66$_5$	12·23$_5$	80·89$_5$	17·99$_5$	−3·57$_5$			
$F_5 - F_4$ ………	112·48	47·24	4·70	86·66	39·43	7·71	62·90	21·57	−4·17	68·05	22·23	2·78
$F_4 - F_3$ ………	65·24	42·54	12·31	47·23	31·72	2·47?	41·33	25·74		45·82	19·45	
$F_3 - F_2$ ………	22·70	30·23		15·51	29·25?		15·59			26·37		
$F_2 - F_1$ ………	−7·53			−13·74?			not known			not known		
2B′ for m large, about………	53 (+3·6)			52 (+3·6)								
2B′ for m small, about ………	30·2			29·2						20		
I′ for m large, about × 10^{40} …	0·98			1·00								
I′ for m small, about × 10^{40} …	1·84			1·90						2·8		
ν_0 ………	21605·54			23832·24			25833·15			27626		
$\Delta\nu_0$ ………			2226·70			2000·91			1793			
Next Δ ………				−225·79			−208					
Value of ϵ for m small ………	1¼			1½			?1½			½		

result we can find the origin ν_0 of this band system from the relation $R(1) = \nu_0 + F'(2) - F''(1)$. $F'(2) = B'(1\frac{1}{2} - 1\frac{1}{4})^2 = 0{\cdot}95$ and $F''(1) = \frac{1}{4}B'' = 4{\cdot}86$, giving $\nu_0 = 21605{\cdot}54$. This should be very close to the correct value. The value of 2B′ for larger m is evidently very nearly the same as that for the $n' = 0$ level of the strong Q system.

Turning to the $n' = 1$ vibrational level the rotational levels are believed to have unique properties, the first differences rising first slowly, then more rapidly and then falling away. There seems to be no very good reason for doubting any of the data for this level but the values depending on the lowest interval have been queried as they depend on the P (2) lines and the P branches are so very weak except in the $n' = 0$ level. The different behaviour of the $n' = 1$ as compared with the $n' = 0$ level is due apparently first to an increase in the constant C of the fourth power term causing an increased rate of diminution of the first differences with increasing m at the higher m's and second to a change in the value of e. This appears to have changed from $1\frac{1}{4}$ to $1\frac{1}{2}$ and is responsible for the peculiar behaviour at the lowest levels. If we represent this level by $F(m) = B'(j - 1\frac{1}{2})^2$ for m small its ν_0 is $23832{\cdot}24$.

At the $n' = 2$ level the C coefficient has increased to such an extent that the first differences are falling away at the lowest levels. This makes the interpretation at small m very dubious, particularly as the P (2) lines of this and of the 3′ level, which should be very weak, have not been found. The ν_0 for this has been calculated by assuming that it behaves like $n' = 1$ and has $\sigma \simeq 0$ and $j \simeq 1\frac{1}{2}$.

At the $n' = 3$ level the first differences are rising again at the lowest levels and the molecule has stabilised itself by adopting an entirely new value of e, viz., $e = \frac{1}{2}$.

It will be seen from the table that the effect of vibration is to increase the moment of inertia as usual, but the effect of rotation is to diminish it. B′ diminishes as n' increase but the data hardly admit of a determination of α. The correction $3{\cdot}6$ to 2B′ for m large is taken from the Q system. As ω_0 is about the same for both systems and these 2B′ values are about the same it is to be expected that the C correction will not be very different.

Assuming the applicability of the formula $n\omega_0(1 - nx)$ to the first two differences of ν_0 we have $\omega_0 = 2339{\cdot}6$ and $\omega_0 x = +112{\cdot}9$. The value of ω_0 is not very far from that for the strong Q system but the value of $\omega_0 x$ is much larger.

The correctness of the numbering of the initial vibration states of this system is verified both by the fact that there is no continuation of it further towards the red and by the intensity diagram shown using R (3) lines in fig. 2. This is essentially the same as fig. 1 for the strong Q system, except that the strength

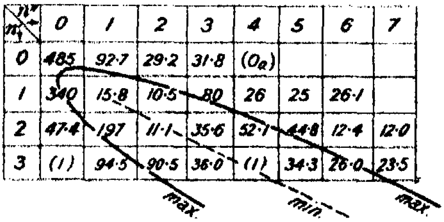

$n'' \rightarrow$ $n' \downarrow$	0	1	2	3	4	5	6	7
0	485	92·7	29·2	31·8	(0_a)			
1	340	15·8	10·5	80	26	25	26·1	
2	47·4	197	11·1	35·6	52·1	44·8	12·4	12·0
3	(1)	94·5	90·5	36·0	(1)	34·3	26·0	23·5

Fig. 2.

is here greater in the 0′ progression and falls off relatively more rapidly as n' increases. The value 34·3 in the bottom row may be too high and would have been less than the next to the right if other lines in this band had been used.

§ 5. *Comparison of the System with R Strong, P Weak, with the Strong Q System.*

These two systems are both very similar and at the same time very different. The similarity consists in the great intensity of both systems which include the individually strongest lines in the secondary spectrum ; they have upper states with practically the same moment of inertia for large m, and the intensity distribution in corresponding bands of the system is very similar. So far one might be tempted to classify them as P to S transitions, the difference between the initial states of the R, P and Q systems respectively being the rotational doubling found with P states. This, however, is believed to be incorrect for a variety of reasons.

The first lies in the differences between the two systems. The values of ω_0 and of $\omega_0 x$ differ appreciably. The electronic jumps differ by 224 which would seem to be very large to be the result of rotational doubling. A still more important difference lies in the magnetic response. No lines of the Q system show the Zeeman effect, whilst every strong line of the strong R, weak P system does show it. Whilst the initial rotational levels of both systems are unusual, those of the Q system are less abnormal than the others.

It is clear from § 3 that the lower states are single with rotational terms given by $Bm^2 - Cm^4$ where m takes the successive values $\frac{1}{2}$, $1\frac{1}{2}$, $2\frac{1}{2}$, $3\frac{1}{2}$, etc.

There are no missing levels ; so that this set of values requires $j_0 = \frac{1}{2}$, $\sigma = 0$ and $e = 0$. These are the properties of $2\,{}^1S$ and as the values of these rotational terms are quite normal there is no reason to doubt that this level is the $2\,^1S$ level. This is confirmed by the ultra-violet data. We have seen that

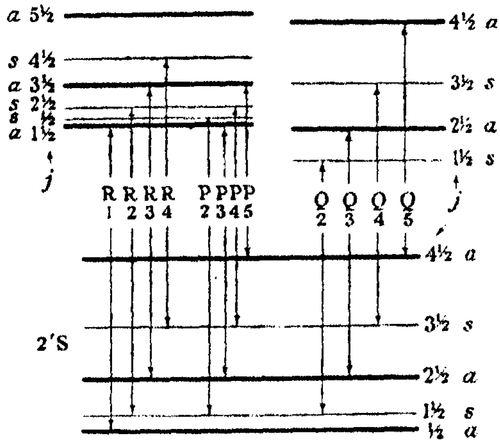

Fig. 3.

the vibrational intervals and also the moment of inertia identify this level with Dieke and Hopfield's B level. The B level has been analysed by Hori,[*] who finds that its transitions to $1\,^1S$ consist of R branches together with another set of branches which, he says, consists of a superposition of identical P and Q lines. Now this analysis is wrong.[†] There is no Q branch, only P and R, and this is precisely what should occur if the transition is $2\,^1S \rightarrow 1\,^1S$. The final levels of the present bands are set out, but not to scale, with their j values at the bottom of fig. 3. In the present bands the strong lines end on the alternate levels marked a, the weak ones on those marked s. Similarly in Hori's arrangement of the Lyman bands the strong lines start from the levels marked a and the alternate weak lines on the levels marked s.

We can now construct a similar scheme for the upper levels. In the Q systems the first line Q (2) is one of the weaker of the alternate pairs of lines and ends on the weak $1\frac{1}{2}$ s level. This line must start from the $1\frac{1}{2}$ level. The possible alternatives would be the $\frac{1}{2}$ or $2\frac{1}{2}$ levels, in which case the branches would be P or R respectively instead of Q. The possibility of such a strong system, containing as it does many of the strongest lines in the whole spectrum, consisting of R without P or P without R branches seems to us so remote that we have dismissed it. Thus the lines of the Q system will come from alternate weak and strong levels as shown on the right-hand side of fig. 3.

---

[*] 'Z. Physik,' vol. 44, p. 834 (1927).

[†] We are indebted to a letter from Prof. Curtis directing our attention to this.

It will be asked how it is that there are no P and R branches in this band containing, for example, lines going from upper $1\frac{1}{2}$ to lower $2\frac{1}{2}$ or $\frac{1}{2}$ respectively. We believe the answer to this to be that *the usual restriction* $\Delta j = 0$ *or* ± 1 *is not the only one which is operative, but that in addition transitions only occur between* $s \rightarrow s$ *or* $a \rightarrow a$ *states.* This principle* operates throughout the bands analogous to the orthohelium lines and so far as we have been able to ascertain is equally applicable in regard to the enormous number of bands which end on $2\,{}^1S$ and form the analogue of the parhelium line spectrum.

If we mark the upper states $1\frac{1}{2}$, $3\frac{1}{2}$, $5\frac{1}{2}$, etc., s, and the states $2\frac{1}{2}$, $4\frac{1}{2}$, $6\frac{1}{2}$, etc., a, this principle in combination with $\Delta j = 0$ or ± 1 will prevent the formation of P and R branches and we shall have Q only. Furthermore, if the a states are strong and the s states weak we shall preserve the alternation in the weight ratio of about 3 to 1, which is such a marked feature of this spectrum. On this scheme the upper level $j = \frac{1}{2}$ is certainly absent because if it were present it should be strong and give rise to strong lines and there are certainly no strong Q (1) lines of this system present in the spectrum.

Turning to the system with R strong, P weak, and applying the same principles the upper levels are as shown in the upper left-hand side of fig. 3. P (2) lines are present, so that the $j = \frac{1}{2}$ level occurs. It lies, however, a little *above* the $j = 1\frac{1}{2}$ level. In contrast to the Q system the s levels are those for which $j = \frac{1}{2}$, $2\frac{1}{2}$, $4\frac{1}{2}$, etc., and the a levels $j = 1\frac{1}{2}$, $3\frac{1}{2}$, $5\frac{1}{2}$, etc. As in the other cases the a levels are strong and the s levels weak. This accounts for the absence of Q branches, for all the lines which are present and for the intensity distribution among the lines.

These new upper levels have electronic quantum number 3, but the discussion of the evidence for that will be deferred for the present. They are neither typical $3\,{}^1S$ nor typical $3\,{}^1P$ levels but have properties which suggest both types of levels. Thus the presence of the $j = \frac{1}{2}$ level in R strong, P weak, suggests an S level, as also does the absence of Q branches, but the response of this system to the magnetic field suggests a P level. The magnetic response cannot be in the final levels since this is an ordinary S level and, anyhow, other systems which end on this level do not show it. The σ, ϵ values are of the same nature, $\sigma = 0$ suggests a ${}^1S$ level but $\epsilon = 1\frac{1}{2}$ does not.

Again, in the upper levels of the Q system, the absence of $j = \frac{1}{2}$ suggests a ${}^1P$ level, but this system shows no Zeeman effect which suggests an upper S level. On the other hand the presence of Q branches would ordinarily be regarded as evidence that the upper level was not S.

---

* Richardson, 'Roy. Soc. Proc.,' A, vol. 116, p. 484 (1927); 'Atti del Congresso Como,' vol. 2, p. 331 (1927); Richardson and Das, 'Roy. Soc. Proc.,' A, vol. 122, p. 688 (1928).

It is interesting to note that the ratio of $\omega_0 x$ for $2\,^1S$, for the upper states of the strong Q system and for the upper states of $R > P$ is very close to $\frac{1}{2} : 2 : 3$. For the upper states these numbers are proportional to $1 \cdot 5 + \varepsilon$. We have evidence that there is at least one other system with an upper state for which $\varepsilon = -\frac{1}{2}$ to which the same rule applies.

An account of the remaining progressions is in course of preparation. They include an RP system with approximately the same $\nu_0 s$ as the strong Q system ; so that it may possibly be the P′R′ branches of that system. Several appear to belong to the transition from the next electronic (4) level higher than the upper levels of the present bands. There are, in addition, a considerable number with P and R branches which are more alike in intensity than those described in this paper.

The relation of these results to the theories of Heisenberg and of Hund will also be deferred for the present.

Patterns and Paschen-Back Analogue in the Stark-effect for Neon.

By J. S. Foster, Ph.D., Assistant Professor of Physics, and W. Rowles, M.Sc., Ph.D., Lecturer in Physics, McGill University.

(Communicated by A. S. Eve, F.R.S.—Received November 2, 1928.)

[Plates 1, 2.]

Introduction.

While the Stark-effect has not been studied so extensively as the Zeeman-effect, either in the experiments or in their interpretations, many of the more prominent features have been observed and have received adequate explanation on the quantum theory. Among these may be mentioned the patterns characteristic of the different series in the singlet system of parhelium.* The variety of observed patterns in the Stark-effect, as contrasted with the normal Zeeman-effect found for all series of this system,† arises from a differential

* Foster, *ibid*, vol. 114, p. 47 (1927).

† Lohmann, 'Physik Z.,' vol. 9, p. 145 (1908).

action of the external electric field on the initial and final states, and a breaking down of the usual selection rule for the azimuthal quantum number. Some simplification is brought about, however, by the fact that only the absolute value of the quantum number m has any meaning in the interpretation of these photographs, since the action of the field is the same for right or left-handed motion of the outer electron in its orbit. This results in asymmetrical patterns for all the lines. The number of components observed in the patterns of individual lines of parhelium is in accord with the theoretical view that the vector j (here equal to l) is resolved along the direction of the applied field to give the integral m values ranging from $-j$ to $+j$, and that the usual selection rule holds for m. The displacements and intensities are in excellent agreement with the theoretical calculations based on the perturbation theory of quantum mechanics.* The spacing of the sub-levels identified by $\pm m$ in the initial state is decidedly irregular in the Stark-effect as compared with the normal Zeeman-effect, where the displacements are proportional to m. The Zeeman order of the levels is usually reversed, in fact, and the spacing is uneven. Displacements in the final state are theoretically very small, and have not been observed with certainty.

In the Stark-effect for orthohelium (triplet system) the same group of patterns was observed. An explanation of these observations, which is slightly less satisfactory than that obtained with parhelium, has been made by similar methods, neglecting the electron spin. Thus the m values were again given ranges determined in each case by the l of the outer electron, and not by the j for the whole atom. Most of the plates failed to reveal any of the fine structure of the normal orthohelium spectrum.

On a few plates, however, the line $2p - 5d$, λ 4026, did appear as a doublet at zero external field, the weakest component of theoretical intensity 1 being well separated from the unresolved pair with intensities 3, 5. This character was also apparent at low fields in the Lo Surdo photographs of the adjacent combination line $2p - 5f$. With increasing external field, this combination line persisted as a doublet, the two members contributing Stark patterns, which gave strong evidence of being identical. If identical, one perpendicular component of the weaker member was not resolved. As a matter of fact it might be expected to be superimposed on a much stronger Stark component of the other member of the observed fine structure. (See Plate 6 (C), 'Roy. Soc. Proc.,' A, vol. 114.)

In the theory of the normal arc spectrum of orthohelium given by Heisenberg, the j values of the final states associated with the fine structure components of intensities 1, 3, 5 are 0, 1, 2 respectively. If now we think of the j as a single vector directly determining the $\pm m$ values in all states, we are led to expect patterns which differ essentially from those observed. In particular, the weak pattern mentioned in the above analysis should, on this basis, be more simple and the stronger more complex. We feel reasonably sure, therefore, that the j does not in this way limit the Stark patterns.

---

* Foster, *ibid*, vol. 117, p. 137 (1927).

Considering the j to be the sum of the vectors l and s, it is clear that the l is far more important than the s in the determination of Stark displacements. This point is mentioned in a brief theoretical treatment of the Stark-effect in alkali spectra by Hund. According to the experiments in helium, there is, indeed, no clear evidence to indicate that the vector s has any effect on the displacements. These are explained with detail sufficient to meet the present observations by a quantum mechanical consideration of the effect of the field on a non-rotating outer electron in the initial states. In this theory, as already mentioned, the vector l of the outer electron is resolved along the field direction to give the m_l values which identify all the observed displacements.

The question as to whether the electron spin can affect the patterns of individual helium lines in the electric field, even though it does not appreciably affect the displacements, is not fully answered by the experiments. It seems most probable that the normal coupling of the vectors l, s in the final state $2p$, is not disturbed by the external field. This view is supported by the uniform spacing of the observed doublet throughout the range of fields represented in the Lo Surdo photographs, and by the (theoretically) small Stark-effects compared with the fine structure separations. It is equally probable that the l, s coupling for the excited electron in initial states is broken down by high fields, and that the l is resolved along the field to give the m_l values which identify the displacements. If we assume that the spins of the two electrons are at the same time resolved in the direction of the field to give $m_s = 0, +1$; and that $m = m_s + m_l$, we arrive at patterns which again differ from those observed. This interpretation is satisfactory so far as the Stark-effect for the weaker fine structure component is concerned; while for the stronger it requires a pattern more complex than the one reported. The increased complexity consists of parallel components identified with $m_l = 2$, and a perpendicular component $m_l = 3$. If present, these would be well separated from other components so as to be easily observable without regard for fine resolutions. They have never been found—even on the plates which are otherwise much over-exposed. There thus appears to be no clear way of including the electron spin so as to get the observed effects, unless the theoretical patterns have, as in hydrogen,* a number of components of zero or very low intensity.

The present extension to the well-known research on neon by Nyquist† was undertaken with a view to obtaining a greater variety in the experimental data on patterns in the Stark-effect for complex spectra. For this purpose neon offers some attractions. The comparatively open structure of the initial states permits observations on the splitting of individual terms, and fairly complete analyses are aided by the high fields which can be established in Lo Surdo tubes containing this gas.

Important observations on the Stark-effect in other complex spectra have already been reported. Chief among these is the work by Hansen, Takamine, and Werner‡ on mercury. Their paper includes, among other things, an interpretation of the new lines appearing in the presence of the electric field, and some interesting new observations on polarisations of $p - p$ combination lines. Since the applied fields were rather low, only one line showed a splitting, and patterns of individual lines were not observed.

In the following report of our experiments with neon, two facts are noteworthy. The observed patterns for the individual arc lines in this spectrum are in no case more complex, and in the majority of cases appear to be identical with those reported in parhelium for lines associated with the same n, l values for the outer electron in initial and final states. Secondly, the displacements for the different members of a complex line are such that the structure tends to fuse and form the normal Stark-effect characteristic of the corresponding singlet line, in a manner analogous to the appearance of the Paschen-Back effect in high magnetic fields. This effect is, of course, not symmetrical with respect to the normal line group. Also it is partial, in the sense that only the initial terms are appreciably affected. The symmetrical patterns which do appear under these conditions are contributed not by one complex line, but by a group of such lines, many of which are brought out by the field itself. These results will be discussed in more detail in later paragraphs.

---

* Schlapp, *ibid.*, vol. 119, p. 313 (1928).

† 'Phys. Rev.,' vol. 10, p. 226 (1917). This paper was published just before the general interpretation of the newly observed combination lines by Bohr, and the complete analysis of the normal spectrum by Paschen. It contains a fairly complete analysis of the Stark-effect for a large number of neon lines, and in only a few cases does there appear to be variations from the results given in the present paper. Possibly these are only apparent, being due to the extreme difficulty of properly assigning new components to lines in a practically unknown and very complex spectrum.

‡ 'Danske Vidensk. Selsk. Math-fys. Medd.,' vol. 5, p. 3 (1924).

Experimental.

In the experiments being reported a direct current at high potential was passed through gases contained in a modified Lo Surdo discharge tube, and the resultant Stark-effect was examined by one of the following three spectrographs: (*a*) an E1 Hilger quartz spectrograph; (*b*) a specially constructed glass prism spectrograph of high dispersion; (*c*) a Rowland grating of 21 feet radius, with stigmatic mounting. In this method the cathode fall automatically supplies an electric field of variable strength within the limits of the Crookes' dark space. The tube was designed to give a maximum field a short distance from the cathode surface. From this point it decreased until at the cathode itself it assumed a value usually a little more than one-half of the maximum strength.

The neon gas was supplied at atmospheric pressure by the Linde Air Products Company, Buffalo, New York, and was transferred to a suitable vacuum system through an adjustable mercury trap. Relatively small portions of helium and hydrogen gases were introduced to make a total pressure of 3 mm. Other gases were removed by a charcoal bulb immersed in liquid air. The vacuum system also included a McLeod gauge and a ballast capacity of 5 litres, the purpose of the latter being to reduce the changes of pressure which occur during exposures. The connection with the discharge tube was made through two ground glass joints with vertical axes 1 metre apart. These joints permitted the adjustments of the tube which were necessary to make the best use of the light emitted by the source.

The discharge tube and high potential apparatus have been fully described in a recent paper. The tube provides a strong source in high fields when required, and avoids the evils of sputtering and excessive cathode pitting. It is excited by a portable electrical apparatus constructed from parts supplied by the General Electric Company, and designed to give a maximum rectified current of 100 mil. amps. at 10,000 volts.

When the tube was properly adjusted, it was relatively hard. The positive column was free from striations and presented the normal salmon-pink colour characteristic of neon. The bluish-gray colour of ionised neon with its accompanying softness is to be avoided. The total gas pressure could be increased far beyond the 3 mm. selected for the best plates without causing any irregularities in the discharge. The maximum fields were then somewhat higher; but the visible light appeared to be weaker.

At 3 mm. pressure, an applied potential of 8500 volts, for example, produced a current of 2 ma. The Crookes' dark space was nearly 1 mm. in length, and the light from this region was much more intense than that from any other section of the tube. After passing through a Wollaston double image prism, the light was focussed on the slit with an F 2·7 Zeiss Tessar lens of 5 cm. focal length. The double image prism was tilted a little about a horizontal axis perpendicular to that of the lens, in order that the two images might focus in the same vertical plane. The magnifications used at the slit were 3, 4, 4 in the quartz, glass, and grating spectrographs respectively.

Normal Spectrum of Neon.

The terms which give rise to the arc spectrum of neon, as analysed by Paschen,* form 4 *s* series, 10 *p* series, and 12 *d* series. In the last group are included the series denoted by $s_1'^{-''''}$; since, as Meissner has pointed out, the Stark-effects observed by Nyquist for these terms are very large. Landé had deduced the *j* values from Zeeman effects investigated by Back. The entire set of terms is commonly considered to be divided into two groups with limits which differ by nearly 780 cm.$^{-1}$. In taking this view it is necessary to neglect appreciable variations from this value which were found by Paschen in the case of a few series. Grotrian has identified the limits with L_{21}, L_{22}; since a reasonable value for the screening constant gives a relativity doublet separation of 780 cm.$^{-1}$ for the neon atom.

The neon terms have been classified by Landé into singlet-triplet and triplet-quintet systems with higher and lower limits respectively. More recently they have been placed in singlet-triplet systems, and partially expressed in Russel-Saunders notation. Uncertainty exists with regard to the latter notation for certain pairs of terms having the same *j* value and the same limit. The following table contains the terms in Paschen and Russel-Saunders notation, together with *f* terms which are arranged with regard to limits according to a scheme given by Hund.† All the members of a triplet do not have the same limit.

---

* 'Ann. d. Physik,' vol. 60, p. 405 (1919).

† 'Linienspektren,' p. 199.

Neon Terms.

	With higher limit.				With lower limit.				
	j values.				values.				
k.	0.	1.	2.	3.	0.	1.	2.	3.	4.
0	s_3 $^3P_0$	s_2 $^3P_1$				s_4 $^1P_1$	s_5 $^3P_2$		
1	p_1 $^3P_1$	p_2, p_5 $^3P_1, {}^3D_1$	p_4 $^3D_2$		p_3 $^1S_0$	p_7, p_{10} $^1P_1, {}^3S_1$	p_6, p_8 $^1D_2, {}^3P_2$	p_9 $^3D_3$	
2		s_1' $^3D_1$	s_1'' s_1'''' $^3D_2, {}^3F_2$	s_1''' $^3F_3$	d_6 $^3P_0$	d_2 d_5 $^1P_1, {}^3P_1$	d_1'' d_3 $^1D_2, {}^3P_2$	d_1' d_4 $^1F_3, {}^3D_3$	d_4' $^3F_4$
3	$^3F_{2,\ 3}$		$^3G_{3,\ 4}$		$^3D_{1,\ 2,\ 3}$, $^3F_4$, $^3G_5$, ($^1D_2$, F_3, G_4)				

We are indebted to Dr. Goudsmit for the suggestion that it may be best not to attempt to classify the neon terms in a scheme suitable for ordinary multiplets. For the higher excited states, with which we are most concerned, it seems most probable that the group of five *p*-electrons has a resultant *j* vector which combines with the individual *j* of the excited sixth electron. Such a coupling may be expected since the inverted doublet $^2P_{\frac{3}{2}}$, $^2P_{\frac{1}{2}}$ energy difference is very large compared with the energy of interaction between the five electrons and the sixth in the excited state. This arrangement leads to terms with the observed *j* values.

Stark-effect in Neon.

A general view of the Stark-effect in this spectrum is given in Plate 1. In the preparation of this plate from the original negative, a magnification of 7·8 diameters was used. Due to the enlarged image at the slit, it will be noted that the length of the Crookes' dark space, as indicated by Stark-effects in the reproduction, is 23·4 times that which existed in the source. The large magnification enables us to leave the burden of innumerable details to the photograph. The Stark components in the upper portion of the figure are plane polarised parallel to the applied field; those in the lower portion are polarised perpendicular to the field.

The lines displaying appreciable Stark-effects are clearly divided into groups which in each case include one or more new combination lines brought out by the field. A few typical groups have been marked with the letters β, γ, δ, ε to emphasise the fact that in high fields they bear a striking resemblance to the group patterns of the Balmer lines H_β, H_γ, H_δ and H_ϵ respectively.

The Paschen series notations, wave-lengths, and intensities for each line are marked in the margin, either above or below the photograph, depending upon the limit of the initial term. If the term has the lower limit, the notation is printed above the photograph. There are separate columns for the sharp series lines, the $2p_j - np_{j'}$ combinations, and the diffuse series; all the remaining observed combination lines are collected in a single additional column. The wave-lengths of certain ionised neon lines are added at the bottom of the plate.

Theoretically, the maximum field, as determined from H_γ, is 137,000 v./cm. The displacements have been measured at 100,000 v./cm. only. Fine lines ruled on parallel and perpendicular images indicate the approximate position of this field in the source. The measurements are given in the second section of Table I. In this table we find many initial terms repeated in the different groups, and thus get more than one observation on them. In the following Table II the terms, with their average displacements, are collected and placed in a form more convenient for reference. Each number in parenthesis is the number of independent measurements of the corresponding displacement.

Table I.—Displacements of Lines, arranged According to Groups.

The field strength is 70,600 v./cm. The displacements are measured from lines, the wave-length of which are roughly indicated, and are expressed in cm.$^{-1}$. In the first column, q and q' represent terms with lower and higher limits respectively. The meaning of the notation (0, 1) and (2) used to identify components is given in the description accompanying fig. 2.

Group.	Initial term.	P-component (0, 1).	S-components.	
			(0, 1).	(2).
$2p_2 - 4q$	$4d_6$	−14·2	−14·6	—
	$4d_5$ (λ 6273)	− 6·9	− 7·5	—
	$4d_3$	28·0	26·5	—
$2p_2 - 4q'$	$4s_1''''$, s_1'' (λ 5965)	− 9·2	− 9·2	− 6·1
	$4s_1'$	− 1·8	− 0·3	—
$2p_3 - 4q$	$4d_5$	−58·4	−59·4	—
	$4d_2$ (λ 6206)	−11·2	−12·4	—
$2p_4 - 4q$	$4d_4$	−20·5	−21·1	—
	$4d_3$	−10·0	−10·6	—
	$4d_1''$, d_1' (λ 6175)	−14·3	−13·8	—

Table I—(continued).

Group.	Initial term.	P-component (0, 1).	S-components.	
			(0, 1).	(2).
$2p_4 - 4q'$	$4s_1'''$ (λ 5902)	−10·8	−11·2	− 6·6
	$4f'$	30·5	30·1	28·0
	$4f'$	14·5	14·5	11·6
	$4f'$ (?)	55·1	54·3	—
$2p_5 - 4q$	$4d_3$	−27·2	−26·7	—
	$4d_2$ (λ 6150)	−11·8	−11·3	—
$2p_5 - 4q'$	$4s_1''''$ (λ 5873)	−10·0	− 9·6	− 4·3
$2p_6 - 4q$	$4d_5$	−80·8	−79·9	—
	$4d_4$	−57·2	−56·7	−52·9
	$4d_3$	−46·1	−45·8	—
	$4d_1'$ (λ 5975)	−13·1	−13·3	—
	$4f$	45·5	43·3	46·0
	$4f$	—	77·6	—
$2p_7 - 4q$	$4d_6$	−65·8	−65·8	—
	$4d_2$ (λ 5914)	−10·6	−11·4	—
	$4d_1''$	− 8·9	− 8·9	—
$2p_8 - 4q$	$4d_4$ (λ 5820)	− 9·1	− 8·5	− 4·6
	$4d_1'', d_1'$	33·2	33·2	—
	$4f$	66·5	66·5	—
	$4f$	86·3	87·8	—
$2p_9 - 4q$	$4d_4'$ (λ 6929)	− 9·2	− 8·8	4·8
	$4d_1'', d_1'$	35·8	34·7	—
	$4f$	67·7	67·7	—
	$4f$	88·0	87·3	—

And in a field of 100,000 v./cm.

Group.	Initial term.	P-component (0, 1).	S-components (0, 1).	S-components (2).
$2p_{10} - 4q$	$4d_5$ (λ 5341)	−13·5	—	—
	$4d_2$	19·5	19·5	—
	$4f$	80·0	—	—
	$4f$	97·4	—	—
$2p_{10} - 4q'$	$4s_1''$ (λ 5116)	−15·1	−15·3	− 7·8
	$4f$	−65·0	−69·0	—
$2p_3 - 5q'$	$5s_1'''', s_1''$ (λ 5193)	−63·0	—	—
	$5g$	91·0*u*	—	—
	$5p_3$	299·5	—	—
$2p_4 - 5q'$	$5s_1'', s_1'''$ (λ 5145)	−66·0	−66·0	−46·0
	$5f$	−14·0	−19·0	—
	$5g$	91·0*u*	100·0	—
	$5p_4$	295·4	—	—
$2p_5 - 5q'$	$5s_1'', s_1''''$ (λ 5122)	−63·6	—	−47·3
	$5p_5$	−307·7	—	—
$2p_6 - 5q$	$5d_1'$ (λ 5204)	—	—	—
	$5d_4$	−87·0	—	−58·9
	$5f$	0·0	3·0	—
	$5f$	6·0	12·0	—
	$5g$	82·0	91·0*u*	—
	$5p_6$	329·2*u*	—	—

Table I.—(continued).

Group.	Initial term.	P-component (0, 1).	S-components. (0. 1).	S-components. (2).
$2p_6 - 5q'$	$5s_1'''$ (λ 5005)	−71·0*u*	—	—
	$5f$	12·0	21·0	—
	$5g$	95·0*u*	—	90·0
$2p_7 - 5q$	$5d_1''$ (λ 5152)	−69·0	—	−58·0*u*
	$5f$	9·0	17·0	—
	$5g$	85·0*u*	—	—
	$5p_7$	321·5	—	—
$2p_7 - 5q'$	$5s_3$	−588·8	−587·0	—
	$5s_1''$ (λ 4957)	−68·2	−68·0	−49·0
	$5f$	12·0	18·0	—
	$5g$	94·0	90·0*u*	—
$2p_8 - 5q$	$5s_5$	−583·0	−581·0	—
	$5s_4$	−540·3	−534·3	—
	$5d_4$ (λ 5080)	−61·0	−61·0	−38·9
	$5d_2$, d_1	−52·0	—	—
	$5f$	17·0	24·0	—
	$5f$	28·0	35·0	—
	$5g$	98·0*u*	114·0	107·0
	$5p_8$	325·0	—	—
$2p_8 - 5q'$	$5s_2$	−555·8	−555·8	—
	$5s_1'''$ (λ 4885)	−68·0	−68·0	−50·0
	$5f$	13·0	19·0	—
$2p_9 - 5q$	$5s_5$	−583·0	−582·0	—
	$5d_4'$ (λ 5038)	−61·0	−64·0	−39·0
	$5d_1'$	−47·0	—	—
	$5f$	17·0	16·7	—
	$5f$	28·0	29·2	—
	$5g$	99·0*u*	111·0	99·0
	$5p_9$	307·0	—	—
$2p_{10} - 5q$	$5s_5$	−588·1	−585·9	—
	$5s_4$	−546·4	−546·8	—
	$5d_3$	−69·0*u*	−64·0*u*	−45·0*u*
	$5d_2$ (λ 4704)	−67·5	−63·0	−45·0
	$5f$	7·0	9·0	—
	$5f$	18·0	19·0	—
	$5g$	89·0	94·0	—
	$5p_{10}$	258·3	—	—
$2p_{10} - 5q'$	$5s_1''''$, s_1'' (λ 4538)	−67·0	−67·0	−48·0
	$5f$	15·0	20·0	—
	$5g$	100·0*u*	100·0*u*	95·0*u*
	$5p_2$	304·0	307·0*u*	—
$2p_4 - 6q'$	$6s_1'''$, s_1'''' (λ 4810)	−133·0*u*	—	—
	$6f$	—	—	−28·0
	$6g$	—	—	55·0
	$6p_4$	223·0	—	—
$2p_5 - 6q'$	$6s_1''$, s_1' (λ 4790)	−130·0	−134·0	−109·0
	$6f$	−43·6	−46·6	−28·8
	$6g$	39·6	—	49·6
	$6p_5$	223·0	—	—

Table I—(continued).

Group.	Initial term.	P-component (0, 1).	S-components.	
			(0, 1).	(2).
$2p_6 - 6q$	$6s_5$	$-346 \cdot 5$	$-347 \cdot 5$	—
	$6s_4$	$-323 \cdot 3$	$-322 \cdot 2$	—
	$6d_3$ (λ 4866)	$-130 \cdot 0u$	$-139 \cdot 0u$	$-96 \cdot 0$
	$6f$	—	$-44 \cdot 0$	—
	$6g$	$41 \cdot 6$	—	—
	$6h$	—	$136 \cdot 0$	$116 \cdot 0$
$2p_7 - 6q$	$6s_4$	$-332 \cdot 8$	$-332 \cdot 8$	—
	$6d_1''$ (λ 4818)	$-144 \cdot 0u$	$-144 \cdot 0$	$-114 \cdot 0$
	$6f$	—	—	$-38 \cdot 0$
	$6g$	—	—	$43 \cdot 0$
	$6p_7$	$224 \cdot 0$	—	—
$2p_7 - 6q'$	$6s_1''$ (λ 4645)	—	$-140 \cdot 0$	$-110 \cdot 0$
	$6f$	—	$-46 \cdot 0$	$-29 \cdot 0$
	$6h$	—	$130 \cdot 0$	—
$2p_8 - 6q$	$6s_5$	$-338 \cdot 2$	$-336 \cdot 0$	—
	$6d_4$ (λ 4753)	$-132 \cdot 0$	$-135 \cdot 0$	$-109 \cdot 0$
	$6f$	$-44 \cdot 0$	$-43 \cdot 0$	$-24 \cdot 0$
	$6g$	$47 \cdot 0$	$50 \cdot 0$	$58 \cdot 0$
	$6h$	—	$142 \cdot 0$	—
$2p_9 - 6q$	$6s_5'$	$-344 \cdot 0$	—	—
	$6d_4'$ (λ 4715)	$-138 \cdot 0$	$-139 \cdot 0$	$-108 \cdot 0$
	$6f$	$-49 \cdot 0$	$-47 \cdot 0$	$-29 \cdot 0$
	$6g$	$42 \cdot 0$	$50 \cdot 0$	—
	$6h$	$133 \cdot 0u$	$146 \cdot 0u$	—
	$6p_9$	$222 \cdot 0$	—	—
$2p_{10} - 6q$	$6s_5$	$-337 \cdot 0$	—	—
	$6s_4$	$-308 \cdot 0$	—	—
	$6d_5, d_6$ (λ 4709)	$-135 \cdot 0$	$-128 \cdot 0$	$-105 \cdot 0$
	$6f$	—	$-49 \cdot 7u$	$-15 \cdot 9$
	$6g$	—	$55 \cdot 0$	—
	$6h$	—	$141 \cdot 0$	—
$2p_{10} - 6q'$	$6s_3$	$-347 \cdot 3$	$-343 \cdot 8$	—
	$6s_2$	$-332 \cdot 5$	$-330 \cdot 5$	—
	$6s_1''''$, s_1' (λ 4276)	$-136 \cdot 2$	$-138 \cdot 2$	—
	$6f'$	$-45 \cdot 9$	$-53 \cdot 1$	$-26 \cdot 1$
	$6g'$	—	—	$50 \cdot 7$
$2p_8 - 7q$	$7d_4$ (λ 4575)	—	$-223 \cdot 0$	$-190 \cdot 0$
	$7f$	Falls on d-line of $2p_8 - 6q'$ group.		
	$7p_8$	$207 \cdot 0u$	—	—
$2p_9 - 7q$	$7d_4'$ (λ 4540)	$-212 \cdot 0$	$-217 \cdot 0$	$-193 \cdot 0$
	$7f$	$-110 \cdot 5$	$-122 \cdot 0$	$-93 \cdot 5$
	$7g$	—	—	$0 \cdot 0$
	$7h$	$110 \cdot 0$	$106 \cdot 0$	—
	$7p_9$	$218 \cdot 0$	$218 \cdot 0$	—
$2p_{10} - 7q$	$7s_5$	$-259 \cdot 6$	$-242 \cdot 0$	—
	$7d_6$ d_5 d_3 (λ 4269)	$-210 \cdot 6$	$-203 \cdot 4$	—
	$7f$	$-114 \cdot 1$	$-116 \cdot 1$	—
	$7g$	$-34 \cdot 1$	$-34 \cdot 1u$	$-20 \cdot 6$

Table I.—(continued).

Group.	Initial term.	P-component. (0, 1).	S-components. (0, 1).	S-components. (2).
With the better resolution of the glass spectrograph we find at 60,000 v./cm.				
$2p_{10} - 5q$	$5d_5$	$-53 \cdot 5$	$-52 \cdot 5$	$-47 \cdot 6$
	$5d_3$ (λ 4704)	$-35 \cdot 3u$	$-34 \cdot 3$	$-31 \cdot 6$
	$5d_6$	$-53 \cdot 5$	$-52 \cdot 5$	—
	$5d_2$	—	$-23 \cdot 0$	—
	$5f$	$9 \cdot 6$	$9 \cdot 6$	$10 \cdot 7$
	$5f$	$18 \cdot 1$	$18 \cdot 1$	—
	$5f$	$21 \cdot 5$	$22 \cdot 3$	—
	$5g$	$63 \cdot 3$	$63 \cdot 1$	$66 \cdot 6$
	$5g$	$71 \cdot 1$	$72 \cdot 2$	—
	$5g$	$74 \cdot 4$	—	—
$2p_9 - 6q$	$6d_4'$ (λ 4715)	$-82 \cdot 8$	$-83 \cdot 0$	$-64 \cdot 0$
	$6f$	$-20 \cdot 2$	$-20 \cdot 7$	$-12 \cdot 0$
	$6g$	$44 \cdot 4$	$45 \cdot 0$	—
	$6g$	$39 \cdot 2$	$39 \cdot 5$	$41 \cdot 1$
	$6h$	$101 \cdot 5$	$101 \cdot 2$	$96 \cdot 1$

The above general view of the Stark-effect in neon has been supplemented by finer analyses partially represented in Plate 2. We notice that appreciable displacements first appear at about 6300 A. The effects increase in magnitude and complexity as we proceed towards the violet until at about 4200 A. the sharp and diffuse series are lost through lack of intensity.

Even before this point is reached, many ionised neon lines appear, and these extend far into the violet and ultra-violet. They are not displaced, but their intensities change rapidly with the field strength. This is due to the greater percentage of ionised atoms in the higher fields.

One might expect a large Stark-effect to appear in the ultra-violet in connection with the principal series and $1 \cdot 5s_i - nq$ (nq') combinations. We have made a very brief search for these without success.

Of the normal lines which are affected by the field, those of the diffuse series show the greatest displacement, and are shifted toward the red. The sharp series lines have much smaller displacements in the same direction, while the members of the principal series which we have photographed are not visibly affected. These are examples of the general fact, first noted by Bohr, that the Stark-effect for a spectral term in theoretically low fields is proportional to the hydrogen difference. The accuracy of this relation is well illustrated in fig. 1 where the displacements of the $4d$ terms are plotted against the corresponding hydrogen differences.

Table II.—Displacement of Terms in a Field of 100 kv./cm., expressed in cm.$^{-1}$.

	$n = 4$.			$n = 5$.			$n = 6$.			$n = 7$.		
	p.	s.		p.	s.		p.	s.		p.	s.	
	$m = 0, 1$.	$m = 0, 1$.	$m = 2$.	$m = 0, 1$.	$m = 0, 1$.	$m = 2$.	$m = 0, 1$.	$m = 0, 1$.	$m = 2$.	$m = 0, 1$.	$m = 0, 1$.	$m = 2$.
s_2				6·3 (1)	6·3 (1)		14·2 (1)	12·2 (1)				
s_3				5·5 (1)	3·7 (1)		16·8 (1)	13·3 (1)				
s_4				5·2 (2)	5·5 (1)		16·8 (3)	16·7 (2)				
s_5				5·3 (3)	3·6 (2)		16·8 (4)	17·3 (1)		58·9 (1)	41·3 (1)	
p_2				10·4 (2)	13·6 (1)							
p_4				9·7 (1)			36·2 (1)					
p_5				11·8 (1)			44·1 (1)					
p_6				12·0 (1)								
p_7				8·0 (1)			38·8 (1)					
p_8				12·6 (1)						91·0 (1)		
p_9				11·3 (1)			48·0 (1)			107·0 (1)	107·0 (1)	
p_{10}				18·7 (1)								
d_1'				72·2 (1)								
d_1''				70·2 (2)								
d_2				72·1 (2)	72·5 (1)	53·5 (1)						
s_1'							133·0 (2)	136·0 (2)	109·0 (1)			
s_1'''				68·5 (4)	67·0 (3)	48·0 (3)	133·0 (1)					
s_1''	15·1 (1)	15·3 (1)	7·8 (1)	65·6 (5)	67·0 (3)	47·8 (4)	130·0 (1)	137·0 (2)	109·0 (1)			
s_1''''				63·3 (2)			134·0 (2)	138·2 (1)				
d_3	13·0 (1)	13·0 (1)		67·5 (1)	63·0 (1)	45·0 (1)	130·0 (1)	139·0 (1)	96·0 (1)			
d_4				61·7 (2)	61·0 (1)	39·0 (2)	132·0 (1)	135·0 (1)	109·0 (1)		223·0 (1)	190·0 (1)
d_4'				64·0 (1)	64·0 (1)	39·0 (1)	138·0 (1)	139·0 (1)	108·0 (1)	212·0 (1)	217·0 (1)	193·0 (1)
d_5	13·5 (1)									210·6 (1)	203·4 (1)	
d_6							135·0 (1)	128·0 (1)	105·0 (1)	210·6 (1)	203·4 (1)	

This is supplemented by the following at 70,600 v./cm.

$4d_1'$	13·0 (2)	13·6 (2)	—
$4d_1''$	13·5 (3)	13·3 (3)	—
$4d_2$	11·5 (3)	11·7 (3)	—
$4s_1'''$	10·8 (1)	11·2 (1)	6·6 (1)
$4s_1''''$	10·0 (1)	9·9 (1)	4·3 (1)
$4d_3$	9·5 (4)	9·8 (4)	—
$4d_4$	9·5 (3)	9·4 (3)	5·0 (2)
$4d_4'$	9·2 (1)	8·8 (1)	4·8 (1)
$4d_5$	7·0 (3)	7·3 (3)	—
$4d_6$	6·5 (2)	6·7 (2)	—

The combination lines $2p_j - nf_j$, $- ng_j$, etc., appear without restriction on Δk and form, with the lines of the normal spectrum, numerous line groups having more or less symmetrical Stark-effects.

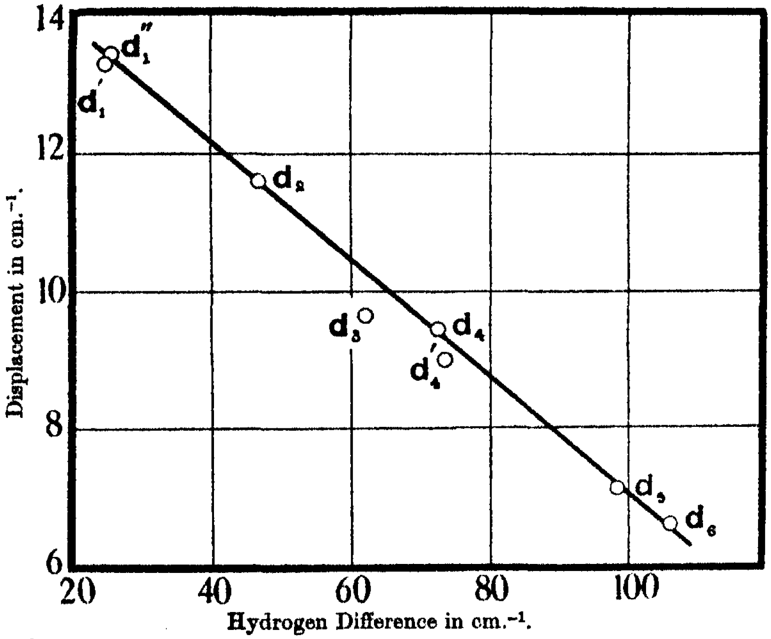

FIG. 1.—Bohr Relation between Hydrogen Differences and Displacements.

The terms which identify the initial states associated with any single group have the same principal quantum number and the same limit. The $2p_j - np_{j'}$ combination lines are found on the violet side of the group, as in parhelium. The remaining combination lines are gradually introduced between the d and p lines, as n increases. The first member of a new series is always next the p line and is shifted toward the violet by the field. The shift becomes less for later members, and is eventually changed from violet to red (see Table III). This effect has been noted in helium and a few other spectra.

Table III.—Displacements of Combination Lines in Electric Field.

n.	$2p_j - nf$.	$2p_j - ng$.	$2p_j - nh$.	$2p_j - ni$.
4	violet ; small	—	—	—
5	red ; very small	violet ; large	—	—
6	red ; large	violet ; small	violet ; large	—
7	red ; very large	red ; large	violet ; large	violet ; very large

The Lo Surdo photographs enable one to obtain measurements or estimates of the values of the f, g, h, ... terms which cannot be found from the visible region of the normal spectrum. The measurements are satisfactory, however, only in the case of the f lines. These lines, $2p_j - nf$, are found in almost zero field, and are sharp enough to permit relatively good readings. The results will be found in Table IV.

Table IV.

Table of f and f' terms obtained by measuring combination lines $2p_j - nf$, $-nf'$ at very nearly zero field. The f' terms have been "reduced" in each case by the required Paschen value.

$4f$.	$4f'$.	$5f$.	$5f'$.	$6f$.	$6f'$.	$7f$.
6863·8	6867·9	4390·3	4394·8	3041·1	3056·7	2240·6
82·2		91·3	95·0	52·3	58·0	
		92·0	95·9	56·2		
		93·5	96·1	56·6		
		95·3	96·1			
		97·4				
		99·8				
		4401·2				
		02·0				

As might be expected, the new terms are obviously complex. In reality we do not see more than three f lines and three g lines in any one group, *e.g.*, group $2p_{10} - 5q$, Plate 2. In each of the "triplets" just cited the two more refrangible members lie close together, and some distance from the third. The h line of group $2p_9 - 6q$ is double. Doubtless the terms are more complex than any single observation indicates. We may assume in fact, that while the ordinary selection rule for j certainly does not hold for transitions between perturbed terms, nevertheless, different groups of type $2p - nq$ will bring to light different members of the complex q, and do so in accord with Pauli's theory of the Stark-effect in complex spectra. The range of observed values for $5f$ and $5f'$ indicates as great complexity as one should expect for these terms.

There are a few interesting features in the intensities of the combination lines. The $2p_j - np_j$ combinations are limited to those where $j = j'$. If, in addition, the terms belong to the same Paschen series, then the early members of the new combination series are found to be almost completely plane polarised. But with increasing n the intensities of parallel and perpendicular components become more nearly equal, and approach the relative intensities found in parhelium. If the terms which combine do not belong to the same series, the perpendicular component is observed to be much the stronger. It may be recalled that Hansen, Takamine and Werner found the polarisation just described for singlet-triplet intercombination lines in mercury.

These shifts in the relative intensities of parallel and perpendicular components of different combination lines are not limited to the $p - p$ series, though they are less pronounced elsewhere. As further examples, we cite the different members of the complex lines, $2p_8 - 5d$, $2p_{10} - 5f$ and $2p_{10} - 5g$, which may be examined on the accompanying plates.

Patterns of Individual Lines.

Let us now briefly consider the patterns of the Stark-effect for individual lines. The members of all sharp series are simply displaced toward the red without separation. The $p - p$ combination lines go toward the violet, are over-exposed, and do not show a fine analysis. Among the members of the diffuse series $2p_j - nd$, $- ns_1{}'^{-''''}$, and the combination series $2p_j - nf$, $- nf'$, etc., the most common pattern is that illustrated in fig. 2. This was first found in parhelium, and in that spectrum the numbers of fig. 2 refer to the m_l values of the initial state. In neon, and in other spectra, components have been found with nearly the same relative displacements. It does not seem unreasonable to assume, in the case of neon, that in high fields and for high quantum number states, the l of the outer electron may be resolved to give the same m_l values characteristic of the observed displacements. It is therefore convenient, and not confusing, to refer to the components of this pattern by the numbers 0, 1, 2. The components (0, 1) appear in both parallel and perpendicular images, and are difficult to resolve in all spectra except hydrogen. The different relative intensities of the members of this complex component, as it appears in the two polarisations, very often assists in the analyses. See, for example, $2p_7 - 5s_1''$, Plate 1. The component (2) is relatively strong, and has been photographed as a perpendicular component only.

We have taken mean values of the complex initial terms for the typical group $2p_9 - 5q$, and have calculated displacements at 100,000 v./cm. by quantum mechanics. At this field the Stark-effects of the fine structure in the diffuse and combination lines have already begun to fuse to such an extent that the very rough theoretical displacements match Plate 1 almost within experimental error. The variations from experiment are, of course, less than the larger separations in the normal fine structure. The theoretical separation of the two components of $2p_9 - 5p_9$ was very small. This explains the lack of fine resolutions in the combination lines of this type.

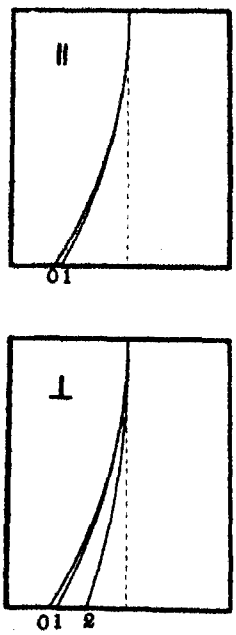

Fig. 2.—Standard Parhelium Pattern in Diffuse and Combination Series.

On the other hand, one may reasonably expect some variations from the parhelium patterns in this very complex spectrum, where some of the relatively large energy differences are presumably due to the spin of the electrons. One might assume that (i) in weak fields the j for the entire atom is retained as a unit, and resolved along the direction of the latter to give the m values; (ii) under moderate external forces, the individual j of the outer electron in initial states determines in a similar way the m values which fix the observable displacements; (iii) in the highest fields the l of the outer electron controls the displacement as in fig. 2, aside from a fine structure which is not observed.

It will give sufficient organisation to the observations to consider them under assumption (i). As will appear in what follows, the scarcity of observed components does not encourage one to make a detailed examination on any obvious basis, such as (ii) and (iii). So long as the j for the entire atom persists as a unit, variations from the standard parhelium pattern characteristic of the diffuse series may be expected in the case of certain lines defined by initial states with $j = 0, 1$, or final states with $j = 0, 2, 3$.

There are fifty or more diffuse and combination lines with $j = 2$ or 3 in final state (p_4, p_6, p_8, p_9). Not one of these gives definite evidence of increased complexity at any field strength. If additional components are present, they

Foster and Rowles. *Roy. Soc. Proc., A, vol.* 123, *Pl.* 1.

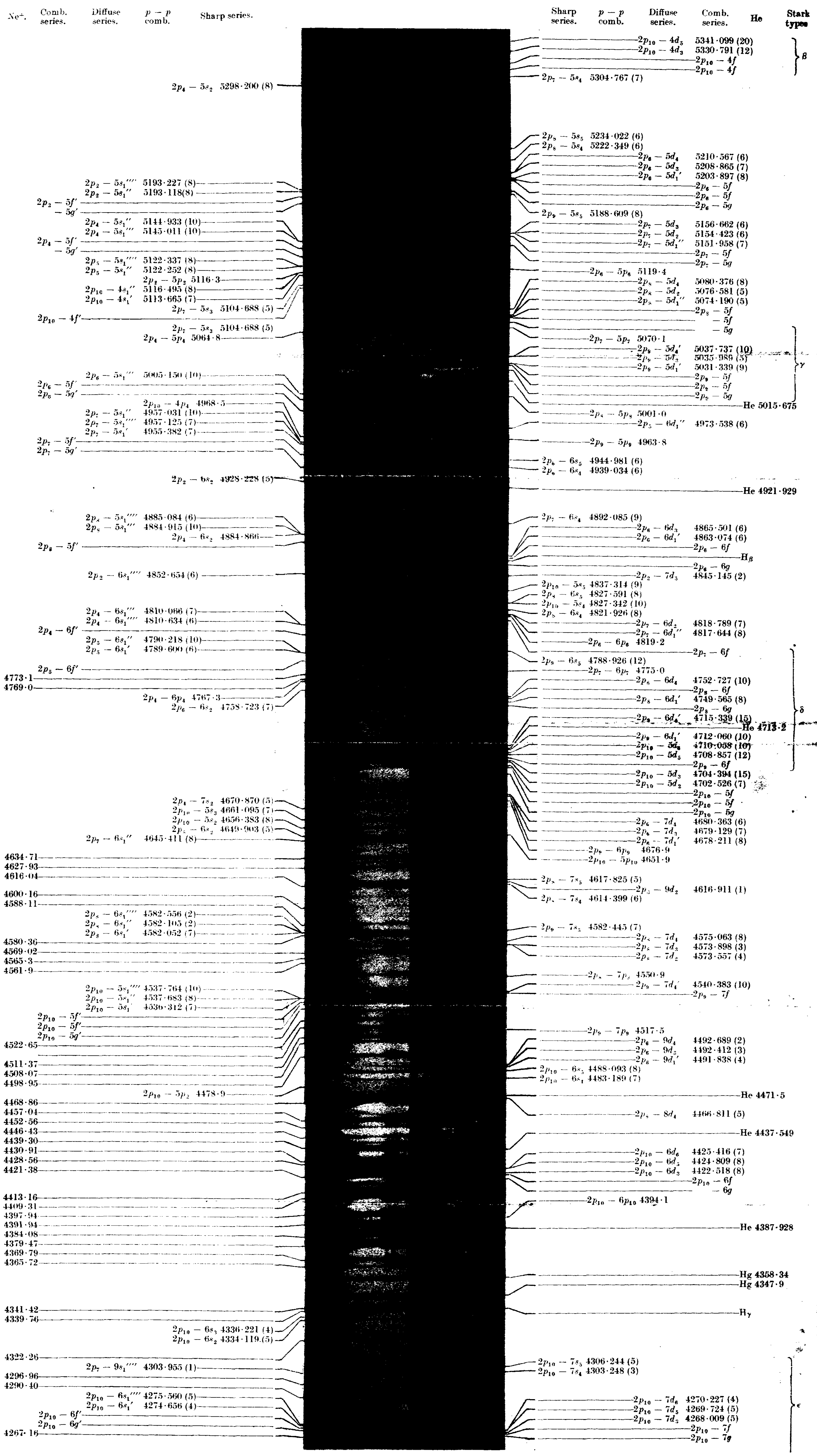

must be limited to very low fields, or be very weak. An outstanding feature, in fact, is a remarkable simplicity in the observed patterns of an appreciable number of the lines in this class. This will be described later.

We have photographed only three diffuse lines with $j = 0$ in final state. Let us first consider $2p_3 - 4s_1'$, λ 5919 (9), since it appears—at least at first sight—to have an unusual pattern. Unfortunately there is, according to Paschen, a weaker companion $2p_7 - 4d_3$ (int. 2) immediately on the red side of this line, the separation being only 0,123 A. These lines are not resolved in the normal spectrum of the present Lo Surdo plates; but in electric fields there are two parallel components and one perpendicular component. If this analysis were to be attributed to the stronger line above, it would constitute a distinct departure from the parhelium patterns, especially in the appearance of a parallel component (2). On the whole we are inclined to think that this is not the case. It seems more probable that the inner parallel component originates in the weaker line $2p_7 - 4d_3$ (Plate 2)—which, according to fig. 1 ought to have the smaller displacement—and that both normal lines contribute to the perpendicular component. There is a slight difficulty in this interpretation; for no other line with intensity so low as $2p_7 - 4d_3$ (2) is found in this section of our plates. It is well known, however, that relative intensities often change greatly with increasing electric fields. Indeed, in this very group of diffuse lines, $2p_7 - 4d_1''$ has been found much stronger than $2p_7 - 4d_2$ even though in the normal spectrum Paschen estimated the intensities to be in the reverse order, viz., 6 : 9. With the above interpretation, there is nothing unusual in the pattern of $2p_3 - 4s_1'$. A similar analysis is found for the remaining lines of this type, viz., $2p_3 - 4d_5$ and $2p_3 - 4d_2$. Thus, while the higher values of j in the final states do not lead to additional components in the patterns; neither does $j = 0$ in these states necessarily restrict the pattern. This last fact—observed also in orthohelium—suggests a breaking down of the coupling which forms the j of the initial state.

Finally, there are ten or more diffuse lines characterised by $j = 0$, or 1 in initial state, which have patterns clearly resolved from those of neighbouring lines. The only member of this group which gives any evidence of possessing a component (2) of the standard parhelium pattern is the one that has been fully discussed in the preceding paragraph. But for this example, one might consider that the low j values had effectively restricted the pattern. This last bit of evidence is of a type not found in orthohelium.

In the above it has been emphasised that no complicated neon patterns are observed; nevertheless, as already intimated, the Stark-effect for many lines has a new character. In most groups we observe diffuse and combination lines with the standard pattern. But in addition to these there are in the same groups, lines of the same types exhibiting a simpler pattern. It consists of but one parallel and one perpendicular component, and the displacement may be as great as that of the standard (0, 1) component. In low fields, especially, the displacements are relatively large. The intensities, however, are somewhat different in that the perpendicular component is much the stronger. This feature would not be unusual if the components (0, 1, 2) were fused. In previously observed cases of the fusion of the components (0, 1, 2) the displacements has been much smaller, *i.e.*, characteristic of the component (2). On these grounds of observed intensities and displacements, therefore, the effect constitutes a variation from the parhelium standard. The above features are illustrated in the following lines of Plate 2: $2p_9 - 5d_1'$; $2p_9 - 5f$ (weak line in low fields); $2p_8 - 6f$ (the weaker line visible over a wide range of field strengths). Plate 1 contains many additional examples, but the details are less evident.

The two types of effects are more easily separated in the groups of diffuse lines shown in the lower photograph of Plate 2. The standard type, perhaps by chance, is contributed by lines for which $\Delta k = \Delta j = -1$. The outstanding intensities of these particular examples cannot be taken as an explanation of a more complete analysis; for the component (2), which appears to be missing in the analyses of the new type, is normally the strongest component in the pattern.

In order to explain the origin of all the components observed for a relatively few lines we must conclude that the coupling which forms the j of the initial state is broken down. At the same time almost any theoretical view gives (on the basis of the m selection rule) more components than have been found for the majority of the lines. It is the latter feature which makes it very difficult to use the observations as a check on any definite coupling of the vectors in the initial states.

As already suggested, one might assume that the individual j_e of the excited electron is resolved to give the m_e values characteristic of the displacements (over a range of moderate fields) and that the displacement of an individual Stark component should depend especially on the component of the outer l in the direction of the external field. For example, one might look for appreciable variations in the displacements of the Stark components (2) contributed by the members of a triplet. We do not see clear evidence of such an effect. The picture is probably faulty, since we already know from

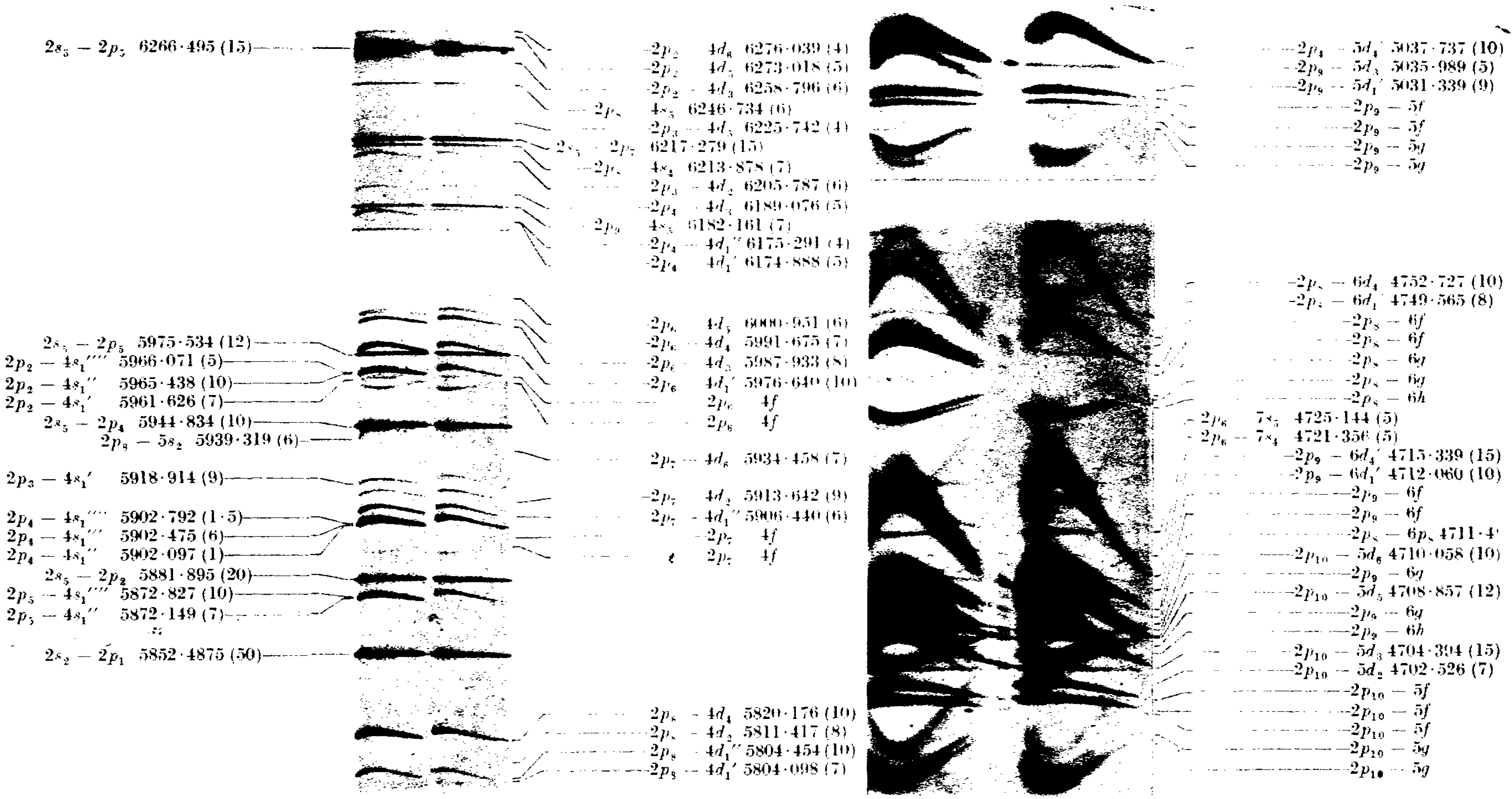
$2s_5 - 2p_5$ 6266·495 (15)
$2s_5 - 2p_5$ 5975·534 (12)
$2p_2 - 4s_1''''$ 5966·071 (5)
$2p_2 - 4s_1''$ 5965·438 (10)
$2p_2 - 4s_1'$ 5961·626 (7)
$2s_5 - 2p_4$ 5944·834 (10)
$2p_9 - 5s_2$ 5939·319 (6)
$2p_3 - 4s_1'$ 5918·914 (9)
$2p_4 - 4s_1''''$ 5902·792 (1·5)
$2p_4 - 4s_1'''$ 5902·475 (6)
$2p_4 - 4s_1''$ 5902·097 (1)
$2s_5 - 2p_2$ 5881·895 (20)
$2p_5 - 4s_1''''$ 5872·827 (10)
$2p_5 - 4s_1''$ 5872·149 (7)
$2s_2 - 2p_1$ 5852·4875 (50)
$2p_2 - 4d_6$ 6276·039 (4)
$2p_2 - 4d_5$ 6273·018 (5)
$2p_2 - 4d_3$ 6258·796 (6)
$2p_8 - 4s_5$ 6246·734 (6)
$2p_3 - 4d_5$ 6225·742 (4)
$2s_5 - 2p_7$ 6217·279 (15)
$2p_8 - 4s_4$ 6213·878 (7)
$2p_3 - 4d_2$ 6205·787 (6)
$2p_4 - 4d_5$ 6189·076 (5)
$2p_9 - 4s_5$ 6182·161 (7)
$2p_4 - 4d_1''$ 6175·291 (4)
$2p_4 - 4d_1'$ 6174·888 (5)
$2p_6 - 4d_5$ 6000·951 (6)
$2p_6 - 4d_4$ 5991·675 (7)
$2p_6 - 4d_3$ 5987·933 (8)
$2p_6 - 4d_1'$ 5976·640 (10)
$2p_6 - 4f$
$2p_6 - 4f$
$2p_7 - 4d_6$ 5934·458 (7)
$2p_7 - 4d_2$ 5913·642 (9)
$2p_7 - 4d_1''$ 5906·440 (6)
$2p_7 - 4f$
$2p_7 - 4f$
$2p_8 - 4d_4$ 5820·176 (10)
$2p_8 - 4d_2$ 5811·417 (8)
$2p_8 - 4d_1''$ 5804·454 (10)
$2p_8 - 4d_1'$ 5804·098 (7)
$2p_9 - 5d_4'$ 5037·737 (10)
$2p_9 - 5d_3$ 5035·989 (5)
$2p_9 - 5d_1'$ 5031·339 (9)
$2p_9 - 5f$
$2p_9 - 5f$
$2p_9 - 5g$
$2p_9 - 5g$
$2p_8 - 6d_4$ 4752·727 (10)
$2p_8 - 6d_1'$ 4749·565 (8)
$2p_8 - 6f$
$2p_8 - 6f$
$2p_8 - 6g$
$2p_8 - 6g$
$2p_8 - 6h$
$2p_6 - 7s_5$ 4725·144 (5)
$2p_6 - 7s_4$ 4721·356 (5)
$2p_9 - 6d_4'$ 4715·339 (15)
$2p_9 - 6d_1'$ 4712·060 (10)
$2p_9 - 6f$
$2p_9 - 6f$
$2p_8 - 6p_8$ 4711·4
$2p_{10} - 5d_6$ 4710·058 (10)
$2p_9 - 6g$
$2p_{10} - 5d_5$ 4708·857 (12)
$2p_9 - 6g$
$2p_9 - 6h$
$2p_{10} - 5d_3$ 4704·394 (15)
$2p_{10} - 5d_2$ 4702·526 (7)
$2p_{10} - 5f$
$2p_{10} - 5f$
$2p_{10} - 5f$
$2p_{10} - 5g$
$2p_{10} - 5g$

(*Facing p.* 98.)

the theory as applied to mercury, hydrogen, and helium, that the effect of an electric field on a particular state cannot be considered apart from the action on other states.

In the region of high quantum numbers and high fields, we feel more confident that the l of the outer electron is resolved in the direction of the field to give the m_l values and the helium-like pattern illustrated in fig. 2.

Normal Lines Resolved by Electric Field.

In the normal neon spectrum there is a diffuse series line, $2p_8 - 5s_1'''$, which accidentally falls on a sharp line $2p_4 - 6s_2$ (λ 4884·903) and the separation is so small that Paschen failed to resolve them. Owing to their very different Stark-effects, however, these lines are separable in electric fields. On Plate 1 the diffuse line (together with $2p_8 - 5s_1''''$) may be seen breaking away from the undisplaced position in fields much lower than that needed to give appreciable displacement to the sharp line. At maximum field, the diffuse and sharp lines have a large separation.

The Paschen-Back Analogue.

There are two main features in what may be called the Paschen-Back analogue in the Stark-effect. (i) The normal fine structure of a complex term fuses in high fields to form a characteristic Stark-effect which lacks symmetry. The observations in complex spectra may be attributed to action (i) in the initial state. (ii) The symmetry, or second feature of the Paschen-Back analogue, comes about in a quite different way. As is well known, the electric field brings out new lines so that groups are formed which represent initial terms of type, s, p, d, f, g, ... Each such term is complex; but in high fields fuses to form a single Stark-effect which usually can be distinguished from those of its neighbours. It is the group pattern, or collection of individual patterns, which possesses symmetry.

These features of the Paschen-Back analogue have received a partial explanation. (i) We have already recalled the Bohr relation between "hydrogen differences" and Stark displacements, and have shown that it holds accurately in low fields provided the hydrogen difference is not too small. So long as the relation is applicable, the members of a complex term must approach one another as the field rises. In addition to this, the present photographs show that all those Stark components of such a complex structure which we have identified by the same m value tend to fuse into a single component.

This action is illustrated in fig. 3, where straight lines connect the initial term values at zero field with the term values corresponding to the Stark components (0, 1) in a field of 137,000 v./cm. (ii) With regard to group symmetry, Pauli* has given a "sum rule" according to which the sum of the displacements of a group of terms identified by n, m will be independent of the applied field.

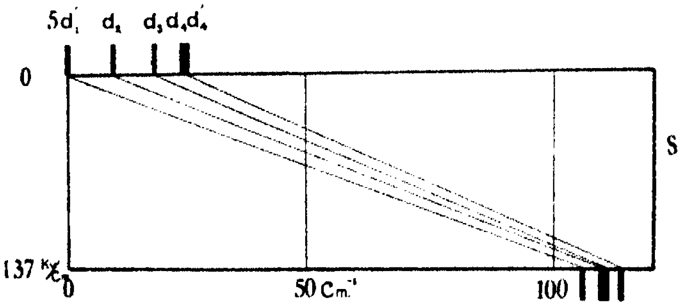

Fig. 3.—Illustration of Paschen-Back Analogue.

Numerous examples of this electric analogue may be found in Plates 1 and 2. Those marked with the Greek letters β, γ, δ and ε are perhaps the best of each type. It will be noticed that the fusion of the complex structure has been carried almost to completion in the groups $2p_i - 6q$.

Comment on other Interpretations of the Stark-effect in Neon.

Two other interpretations of the Stark-effect in neon have recently appeared. These are in some respects similar; yet on a few points differ essentially from the more simple view presented in this paper. A careful consideration of certain details of experimental evidence may perhaps help to bring better harmony among these view-points, and to illustrate the characteristic difficulties one sometimes encounters in the study of Lo Surdo photographs. Incidentally, it may justify the somewhat high magnification of plates which we have adopted at this laboratory as essential to an early decision on just such points as we have now to consider.

The first interpretation is that given by Prof. Stark† in his review of the experimental paper by Nyquist. After assigning many of the simpler analyses to lines in Paschen notation—with only a few errors which will not confuse the careful reader—Stark undertakes the more difficult task of dealing in a similar way with a number of complex analyses. In this latter work we feel he has made a few slips which ought to be corrected; since otherwise a rather strange behaviour is attributed to the lines of the diffuse series. For example, Nyquist reported two components for the line λ 5145 at 29,600 v./cm. with displacements 3·46 A. and 2·24 A. The latter appeared as a perpendicular component only. These are recorded in Table I of the present paper as components (0, 1) and (2) of $2p_4 - 5s_1'''$, λ 5145. Stark, on the other hand, interprets them as components of $2p_4 - 5s_2'''$ and $2p_4 - 5s_1''''$, respectively. He gives fifteen or more examples of this interpretation, wherein the components appearing in both polarisations are attributed to one diffuse line; the additional perpendicular component to a second line of the same character.

---

* 'Handbuch d. Physik' von Geiger und Scheel, vol. 23, p. 146 (1926).

† Wien and Harms, "Handbuch Exp. Physik," vol. 21, p. 471 (1927).

For the higher quantum numbers in initial states it is indeed not possible to resolve many of the diffuse lines of Stark's interpretations with our present spectrographs. Quite apart from such resolutions, however, we note that he has found it convenient to use the term $5s_1''''$ to explain so many components that he has thereby claimed six distinct sub-levels for this term in the electric field. This is so far in excess of any splitting which has been observed for any other term in this spectrum that we hestitate, on this ground, to endorse his interpretation.

For lower quantum numbers it is easier to separate the members of the normal fine structure, and to get direct observations on the individual lines. We note, for example, that the line $2p_8 - 4d_4$ has components (0, 1) appearing in both polarisations and, in addition, the perpendicular component (2). The following member of this series, $2p_8 - 5d_4$, shows exactly the same analysis, and it is important to observe that the splitting occurs before the components of the neighbouring diffuse line $2p_8 - 5d_1''$ blend with those of $2p_8 - 5d_4$ in high fields. No attempt will be made to correct misprints in Stark's interpretation of this particular analysis. Even in the absence of fine resolutions we should prefer, therefore, to assign a similar pattern to the succeeding member of the series, $2p_8 - 6d_4$, rather than to attribute the perpendicular component with the smaller displacement to $2p_8 - 6d_5$, as Stark has done. As a matter of fact, the plates do give detail which will be useful in a later discussion of this line, as well as here. $2p_8 - 6d_5$ does not appear; the line $2p_8 - 6d_1''$, being stronger according to Paschen, does occur and joins with $2p_8 - 6d_4$ in rather low fields. In this case it is not conclusively proven in the photographs that $2p_8 - 6d_4$ is split before this union takes place. If one needs still more direct evidence that the above pattern does persist in diffuse series as the principal quantum number of the initial state increases, it may be found in a nearby group, where $2p_9 - 6d_4'$ is very clearly split before being joined by $2p_9 - 6d_1'$. In addition to the above evidence there is much more of a similar character which any interested reader may find, especially in Plate 2. The conclusion is that the diffuse lines do not have the strange and erratic behaviour in electric fields, which Stark had claimed for them.

The second interpretation to which brief reference will now be made is that given by Ishida in a very recent experimental paper. He has photographed some of the more or less symmetrical group patterns in neon, and these he classifies as type (A) or type (B)—our γ and δ respectively. Ishida feels that his results in some way conflict with the series classification given by Paschen, and mentions, in particular, an apparently strange behaviour in Paschen's diffuse series. In view of the discussion in the immediately preceding paragraphs, we think the analysis of the normal spectrum may still prove satisfactory, and in this connection wish to make a correction to Ishida's report.* In his type (B) (see *e.g.*, $2p_8 - 6q$, Plate 2) he finds the four lines which should appear in a rough analysis. The lines are all complex and some at least are split in the field; but these matters are not essential to the present discussion. We shall consider only the stronger members of the fine structure. The Stark components of two out of the four lines are displaced toward the red. Ishida states that both these lines are present in the normal spectrum, and thus claims very different displacements for two diffuse lines. We believe that only the outer line belongs to the normal spectrum, and that all the others are combination lines. It is a little difficult to observe this; since the new combination *f* line, which is nearest the outer *d* line, makes an almost perfect union with a second and weaker diffuse line at approximately zero field. Our plates make a clear distinction between these lines and, in fact, show the Stark components of the weaker diffuse line as they proceed to join with those of the stronger in high fields. Finally, Ishida reports that the succeeding member of this series of strong diffuse lines, *viz.*, $2p_9 - 7d_4'$, is a " single " line unaccompanied by combination lines in the electric field. As might be expected, however, this line is accompanied by the usual combination lines needed to form the group pattern (ϵ) illustrated in Plate 1.

Summary.

The Stark-effect for 150 lines in the neon spectrum has been examined in high fields.

The observed patterns of the sharp, diffuse, and combination lines are never more complicated, and in most cases are identical with those recently reported in parhelium by one of the authors.

---

* Suppl. 'Sci. Papers,' Tokyo, August, 1928.

An appreciable number of diffuse and combination lines present a more simple pattern, which apparently consists of but one parallel component and one perpendicular component. This pattern is further characterised by relatively large displacements in very low fields.

The displacements in fields above 100,000 v./cm. are in rather good agreement with the results of quantum mechanics obtained by using mean values for the terms in zero field.

A Paschen-Back analogue is observed in (i) the fusion of each complex line into a single asymmetric Stark-effect, together with (ii) the group symmetry presented by the assembly of Stark-effects contributed by each group of normal and combination lines.

A review of the interpretations of the Stark-effect in neon recently given by Stark and by Ishida is added.

Stark-effect in a Violet Region of the Secondary Spectrum of Hydrogen.

By J. K. L. MacDonald, M.Sc., McGill University.

(Communicated by A. S. Eve, F.R.S.—Received November 2, 1928.)

[Plate 3.]

Simultaneously with his examination of the effect of electric fields on the Balmer series in hydrogen, Stark* observed some general characteristics of the secondary spectrum. In the latter he noted the comparatively small displacements, which were proportional to the square of the field; the lack of symmetry in the splitting; and an apparently general irregularity in the effect.

The work was extended by Takamine and Yoshida, Nitta, and Takamine and Kokubu,† whose observations included effects on a total of 54 lines. Kiuti‡ has recently used much higher fields in a far more extensive investigation embracing effects throughout the entire visible spectrum. He found regularities in two groups, each composed of three lines. The members of each group were split in like manner and the original lines were accompanied by "satellites" which were displaced toward the violet without any observed splitting. Within each Fulcher band the displacements were, as a rule, alternately large and small. The bands were further marked by a great increase in intensity for high fields.

---

* "Monograph," p. 76 (1914).

† Takamine and Yoshida, 'Mem. Coll. Sci., Kyoto,' vol. 2, pp. 137, 321 (1917); Nitta, *ibid.*, vol. 2, p. 350 (1917); Takamine and Kokubu, *ibid.*, vol. 3, p. 3 (1919).

‡ 'Jap. J. Phys.,' vol. 1, nos. 3 and 4 (1922), and vol. 4, no. 1 (1925).

These regularities are encouraging despite the fact that most of the observed effects still appear to be of a random character. It is hoped that an extension of the recent, broad theoretical advances by Hund and Kronig* may find practical application in the present problem, since this molecular spectrum is the only one in which appreciable effects are found.

It is well known that the brightest portion of a Lo Surdo tube is within the so-called Crookes' dark space. For this reason many lines of the normal spectrum are photographed only in the region corresponding to high fields. In addition to these there are several which possibly represent transitions permitted only in the presence of the field. It may be recalled, however, that in chromium and in neon many of the "new" lines are due to ionised atoms which occur in appreciable numbers only where the external field is high. Possibly, therefore, some of the apparently "new" lines of the secondary spectrum may originate in ionised molecules.

The present investigation has been confined to a small region in the violet between 3980 and 4080 A. Owing to the relatively low intensity and small Stark-effects very few observations have been made in this part of the spectrum. Takamine and Kokubu have reported on two lines, and Nitta on four, one of which was also observed by Kiuti.

The new plates allow the observations to be extended to include typical Stark-effects on 20 lines. The agreement with previous results is not marked, but the details are reserved for a later paragraph. An interesting feature in the present experiments is the resolution of certain lines which appear to have a complex Stark-effect into two or more lines with simple displacements. In the extension of the present investigation which is now being carried through, it may become clear as to whether or not this effect is very common in the secondary spectrum. It is also of interest to mention that the lines in the violet side of the region investigated are displaced towards the violet; those on the red side towards the red. There is a slight overlapping of the two groups.

The arrangement of apparatus employed in the experiments is illustrated in the figure. The type of vacuum system was suggested by that used by Wood* in his laboratory extension of the Balmer series. Hydrogen gas was generated from an electrolyte formed by adding phosphorus pentoxide to water. This electrolyte had a very low water-vapour pressure, hence the evolved gas was fairly dry. Further purification was effected by the use of a capillary tube T′ through which the hydrogen diffused into the drying chamber of the vacuum system. The apparatus was roasted before the experiments were begun and the impurities thereby driven from the glass walls were absorbed by the charcoal bulb E. Before the spectrograms were made E was sealed off to prevent variations in gas pressure. The capillary permitted continuous flow of gas at constant, low pressure. The flow was maintained by a "Hyvac" pump, which was connected to the system through a second capillary T″. To adjust gas pressure the length of T′ or T″ was changed. A large glass bulb B stabilised the pressure.

---

* 'Z. Physik,' vol. 46, p. 814 (1928).

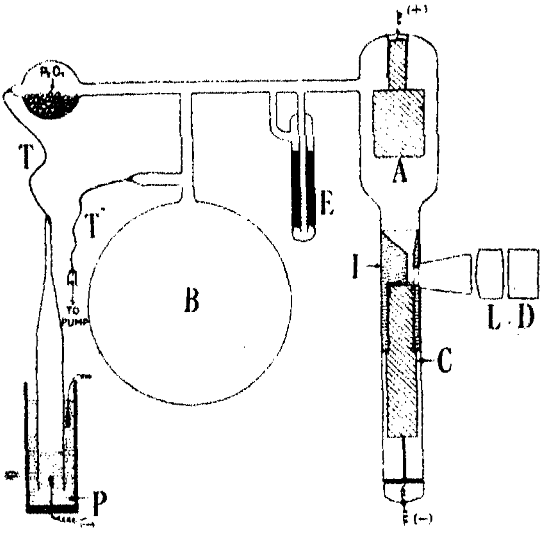

The tubes employed were of the Lo Surdo type, in which the fields are developed by the cathode fall of potential. All seals were made of Pyrex glass to avoid vapour from the grease or wax sometimes used. The electrical discharge took place between a cylindrical anode A and a small cathode C, both constructed of aluminium. Electrical excitation was supplied by a split transformer kenetron rectifier with a maximum output of 100 ma. at 10,000 volts. The source selected for analysis was in a small cylindrical channel cut in a rod of lavite I. Light passed from the source through a lens L and a double-image prism D to a three-prism glass spectrograph. The focal surface of the latter had such curvature as to prohibit the use of glass plates; Agfa portrait films were therefore substituted. The dispersion of the spectrograph was about 4 A./mm. at H_δ, and lines 0·20 A. apart were clearly resolved. The iron arc was used for comparison. This spectrum was superimposed upon the hydrogen lines in the region corresponding to zero field strength. Measurement of the films were made by means of a Hilger travelling micrometer. The wave-lengths were determined from the usual Hartmann formula.

---

* 'Phil. Mag.,' vol. 42, p. 729 (1921).

Experimental Results.—In the following table the first column gives the wave-lengths in International units. In the second column "MB," "T" and "D" refer respectively to the tables of secondary lines given by Merton and Barratt,[*] Tanaka[†] and Deodhar.[‡] To this notation a "—M" is added in the

λ.	Identification table.	Displacements of components at a field strength of 95 k.v./cm.	
		p.	*s*.
A.		A.	A.
4072·98	MB	0·50	0·50
4071·28	MB	0·80; 0	0·80; 0
4067·20	MB–M	0·20	0·20
4066·90	MB	—	—
4066·25	MB–M	0·50	0·50
4062·49	MB	0·45; 0	0·50; 0
4048·45	MB	—	—
4048·05	MB–M	0·20	0·15
4044·49	T, ${}_0\gamma_0Q(5)$	0·60	0·50
4034·12	T	0·60	0·60
4028·35	MB	1·40; 0	1·40; 0
4024·79	MB, ${}_0\gamma_0Q(1)$	−0·40	−0·40
4021·90	T–M	0·75	0·75
4021·62	T	—	—
4009·57	T	0	1·00
4005·96	MB	−0·10	−0·10
4005·54	MB	—	—
4002·59	MB	−0·95	−1·00
3997·65	MB–M	0	0·05 (approx.)
3997·18	MB	—	—
3995·89	D	−0·68	0
3993·92	MB	−0·10	−0·10
3993·27	MB	—	—
3992·45	MB–M	−0·10	−0·10
3991·96	MB	—	—
3991·65	MB–M	−0·20	−0·15
3983·98	MB	0; −0·90	0; −0·95

---

[*] 'Roy. Soc. Proc.,' A, vol. 108, p. 603 (1925).

[†] 'Roy. Soc. Proc.,' A, vol. 113, p. 429 (1926).

[‡] 'Roy. Soc. Proc.,' A, vol. 113, p. 369 (1926).

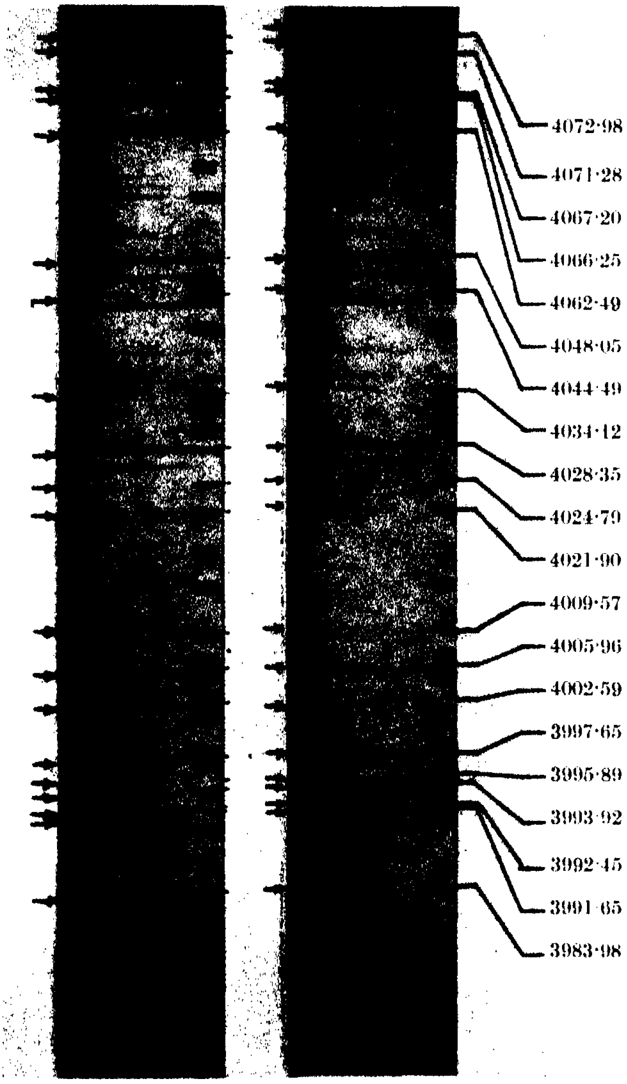
4072·98
4071·28
4067·20
4066·25
4062·49
4048·05
4044·49
4034·12
4028·35
4024·79
4021·90
4009·57
4005·96
4002·59
3997·65
3995·89
3993·92
3992·45
3991·65
3983·98

(*Facing p.* 106.)

cases where a complex structure has been observed by the writer, and the wave-lengths of all members of the structure are bracketed. *Only two of the* following lines are included in Richardson's classification of the secondary spectrum. The origins of these are indicated in his notation. The errors in measurement of displacements should not exceed 0·05 A., and in most cases, 0·02 A.

The observations on the lines 3983·98 A. and 4002·59 A. agree well with the effects reported by Takamine and Kokubu for 3984·5 A. and 4002·6 A. in considerably lower fields, except that in 3983·98 there appear to be definite, undisplaced components not reported by the above workers.

Nitta, using field strengths approximately equal to those employed in the present experiments, reported on the lines 3993·4 A., 4021·9 A. and 4048·6 A. There is practically no agreement between his results and the effects given in the above table. All three lines are accompanied by nearby companions which Nitta possibly mistook for components. Kiuti's observations on 4028·35 A. did not correspond to those by Nitta for his 4028·5 A. The former gives displacements of 4·9 A. and −1·3 A. for *p*—, and 4·9 A. and −1·5 A. for *s*— components at the field strength 206,000 volts per centimetre. In the present investigation the corresponding displacements are 1·4 A. and 0·0 A. for both polarisations. Although the field was about one-half that used by Kiuti, one would have expected some observable indication of the shift toward the violet reported by him, particularly since the displacements of all other components seemed to be proportional to the square of the field strength. The line may be clearly seen in the accompanying photograph (Plate 3).

The author wishes to express his great appreciation for the kind encouragement and useful suggestions given to him by Dr. J. S. Foster under whose direction the work was performed.

Summary.

The Stark-effect is observed for 20 lines in the region 3980–4080 A.

The lines in the violet half of the region investigated are displaced toward the violet; those in the red half, toward the red. There is a slight overlapping of these groups.

Five of the normal lines in this list have a very close structure which has not been reported before.

Comparison is made with previously observed Stark-effects for the six lines which have been examined by other observers.

Relative Intensities of Stark Components in Hydrogen.

By J. STUART FOSTER, Ph.D., Assistant Professor of Physics, and LAURA CHALK, M.Sc., Ph.D., National Research Student, McGill University.

(Communicated by A. S. Eve, F.R.S.—Received November 2, 1928.)

[PLATES 4, 5.]

Introduction.—This quantitative investigation of the intensities of Stark components in hydrogen was started before the advent of the new quantum mechanics. Our original purpose was to obtain a more precise measure of the few serious departures from experimental fact, which one finds in the estimates of these intensities based on the correspondence principle. The somewhat limited measurements in the preliminary report* proved to be in excellent agreement, however, with the new theoretical intensities by Schrödinger,† which had just appeared. These new calculations claimed not only some modifications in the theoretical estimates, but also a few appreciable variations from the original experimental values given by Stark.‡ In extending the work we have, therefore, paid most attention to the relative intensities of those components for which theory and experiment seemed not to agree. Fortunately, this has not required the re-examination of the very weak components, the majority of which have already been studied in a qualitative way at this laboratory. We find that the more reliable quantitative examination of some of the stronger components is sufficient to make the principal corrections needed to bring the experimental intensities into harmony with Schrödinger. Incidentally, it becomes clear that a consideration of the normal fine structure of the Balmer lines is not essential to a quantitative explanation of their observed Stark effects in high fields.

The first satisfactory explanation of Stark displacements in hydrogen was made by Epstein§ through a development of the quantum theory. This did not include a rational basis for the selection rules or a means of estimating intensities. These were supplied by Prof. Bohr‖ through an application of perturbation theory together with his principle of correspondence. Kramers[*] calculated the so-called "characteristic amplitudes" of the motion of the electron in initial and in final orbits, and used these to explain the observed polarisations of Stark components as well as to make estimates of their intensities. The correspondence principle was indefinite, however, in that there were the two amplitudes in each case which should, perhaps, be averaged in some manner not obviously expressed. Kramers used, for convenience, the arithmetical mean. It has been observed that in this particular application it is much better to entirely neglect the amplitudes in the final orbits, since these give rise to all the estimates which can be considered unsatisfactory. This suppression of the above-mentioned final states as important factors in the determination of the intensities is supported by the more recent perturbation theory of quantum mechanics.

---

* Foster and Chalk, 'Nature,' vol. 118, p. 592 (1926).

† 'Ann. Physik.,' vol. 80, p. 437 (1926).

‡ 'Ann. Physik,' vol. 48, p. 193 (1915).

§ 'Ann. Physik,' vol. 50, p. 489 (1916).

‖ 'D .K. D. Vidensk. Selsk. Skr.,' vol. 4, p. 1 (1919).

The first application of quantum mechanics to the Stark effect was made by Pauli.[†] Using special methods in matrix analysis, he calculated the Bohr terms for hydrogen, and outlined a method for determining the first order displacements of the Stark components.

A more comprehensive treatment of the subject is due to Schrödinger. The general wave equation for an electron in a hydrogen atom subjected to a uniform electric field is solved by an application of perturbation theory. To first approximation, the only permissible eigenwerte are those corresponding to term values identified with components which actually appear in the experiments. The relative intensities are given by the square of the Heisenberg co-ordinates. These are found from the normalised eigenfunctions by integration methods developed by Schrödinger.

Epstein[‡] also applied wave mechanics to the calculation of these intensities; but obtained results which differ from the above calculations and from experiment. The more prominent variations are quite apart from those which naturally result from the fact that he has taken the amplitudes themselves as suitable for direct comparison with photographic densities. It therefore seems probable that the work contains numerical errors.

As an application of quantum mechanics, Schlapp[§] has recently considered the effect of a small external field on the fine structure of hydrogen, and also the effect of the fine structure on the Stark components in high fields.

---

[*] 'D.K.D. Vidensk. Selsk. Skr.,' vol. 3, p. 287 (1919).

[†] 'Z. Physik,' vol. 36, p. 336 (1926).

[‡] 'Phys. Rev.,' vol. 28, p. 695 (1926).

[§] 'Roy. Soc. Proc.,' A, vol. 119, p. 313 (1928).

We have not been able to find any positive evidence of the very interesting theoretical modifications thereby obtained.

Experimental.

In these experiments we have used three forms of the general type of two electrode tube first employed by Lo Surdo for the study of the Stark effect. These sources were excited by a specially constructed high potential apparatus, and developed high electric fields in the Crookes dark space. They illustrate the unusual flexibility of this type of discharge tube in meeting the requirements of special investigations. In the preliminary experiments the tube was placed in a horizontal position, and the light to be analysed was taken from a thin layer parallel to the flat cathode surface. This means of selecting a source in a uniform field has already been adopted by Foster* and by Dewey.† Our present modification consisted in the use of a ribbon-like cathode (see fig. 1 (*a*)) to obtain higher fields as well as uniform intensity in the image on the slit of the spectrograph (see Plate 5 (*a*)). Owing to the latter characteristic, it was possible to use a Merton neutral wedge for the direct determination of intensities. Also, since the components were parallel, a Moll photometer could be employed conveniently in the usual way. Balanced against these important advantages, the tube draws a heavy current, and tends to overheat. For this reason it seldom runs long enough to permit analysis of the weaker components. Finally, it does not allow one to detect the presence of foreign lines which may be superimposed on the Stark components. This last disadvantage and the overheating were overcome in a second type of

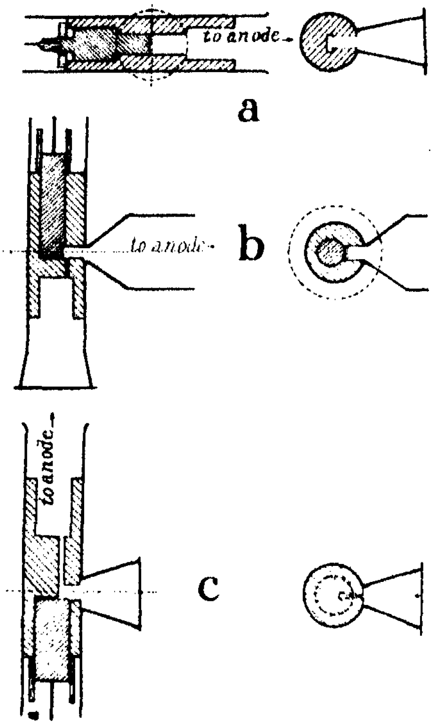

Fig. 1.—Lo Surdo Sources Employed.

---

* 'Phys. Rev.,' vol. 20, p. 214 (1922).

† 'Phys. Rev.,' vol. 28, p. 1108 (1926).

tube illustrated in fig. 1 (*b*). The heavy ½-inch bar of aluminium served to conduct the heat away from the ribbon-like discharge, while its cylindrical surface was of assistance in securing weaker fields at each end of the narrow strip of the source selected for analysis. The components photographed from this tube run almost parallel through their central sections, but have noticeably smaller separation at either end (see Plate 5 (*b*)). This arrangement enables one to use the Moll photometer over the middle portion of the components. At the same time it reveals in the lower fields any secondary or other lines which may be superimposed on the Stark components at the higher field strengths where the measurements are made. The tube requires very careful construction, especially in the spacing of the parts near the cathode, and one can never be certain that the most intense portion of the source has been chosen for analysis.

For the sake of greater light intensity we abandoned this type of tube in our later experiments, and returned to the more simple form shown in fig. 1 (*c*). Slightly greater current density can be maintained in this smaller tube with its discharge of circular cross section. By a suitable gradation of the diameter of the hole through the lavite, especially very near the cathode, and a proper spacing of the cathode surface from the lavite immediately above, the high electric fields which would otherwise develop at the cathode were reduced somewhat, and the components were induced to run nearly parallel for a short distance on the plate. This distance was increased by using a magnification of 4·0 at the slit of the spectrograph.

The high potential apparatus required to operate these tubes has been fully described elsewhere.* The current from a high potential transformer is rectified by two kenotrons, and the pulses are reduced by means of condensers in parallel with the tube and a large inductance and water resistance in series with it.

Hydrogen, helium and neon were the gases used in carrying out these experiments. The hydrogen was never used in a pure state, but was mixed with helium in order to enhance the Balmer lines. Both these gases were kept over water, and were purified by passing over charcoal immersed in liquid air. The neon was admitted to the vacuum system through a mercury trap and was used practically pure, the whole discharge tube being thoroughly roasted and evacuated before admitting the gas. Owing to a remaining trace of hydrogen, H_α always appeared, and was stronger under these conditions than when an appreciable proportion of hydrogen was added.

---

* 'Roy. Soc. Proc.,' A, vol. 114, p. 47 (1927).

The light from the source passed through a Wollaston prism which was tilted at an angle in order to bring the two images more nearly into the same vertical plane at the slit.

The spectrograph is described in a previous paper.* Six prisms were required for the best analyses of H_α and H_β, while two were more suitable for H_γ and H_δ. The dispersions at these points in the spectrum were 15, 6·3, 10 and 7·7 Å. per millimetre, respectively, when the above arrangement of prisms was employed.

Eastman 40 plates were used in the analysis of H_β, H_γ and H_δ; for H_α Eastman panchromatic cinematograph film proved satisfactory.

Intensity Measurements.

A method for the accurate determination of intensities by means of a neutral glass wedge has been developed by Nicholson and Merton† and adopted in a number of subsequent investigations. Our success in obtaining an appropriate source enabled us to use this general method in the present problem.

As is well known, the glass wedge of neutral tint is compensated by a similar wedge of colourless glass with which it forms a plane parallel plate. This plate is placed immediately in front of the slit of the spectrograph. Under these conditions, it follows from the theory of the wedge that the photographic intensities I_1, I_2 of two neighbouring spectral lines of like energy distribution is given with accuracy sufficient for the present purpose by

$$\log_{10} I_1/I_2 = D_\lambda (l_1 - l_2),$$

D_λ is the density of the wedge for the wave-length λ as determined by calibration, and $(l_1 - l_2)$ is the difference in length of wedge penetrated by the two sources.

Since the lines we wish to compare are of nearly the same wave-length, and are equally sharp in character, the photographic intensities will correspond very nearly to the absolute intensities. In the present investigation the photographic intensities only are measured.

The wedge calibration for D_λ was made by using Glann-Thompson prisms to reduce the intensity of the light in a known ratio, and the wedge constant for wave-length λ was then determined from the above formula. In this calibration a Nernst glower served as source, the current being kept constant by the use of a floating battery. From this source a parallel beam of light was

---

* 'Roy. Soc. Proc.,' A, vol. 122, p. 599 (1929).

† 'Phil. Trans.,' A, vol. 216, p. 459 (1916) and vol. 217, p. 237 (1917).

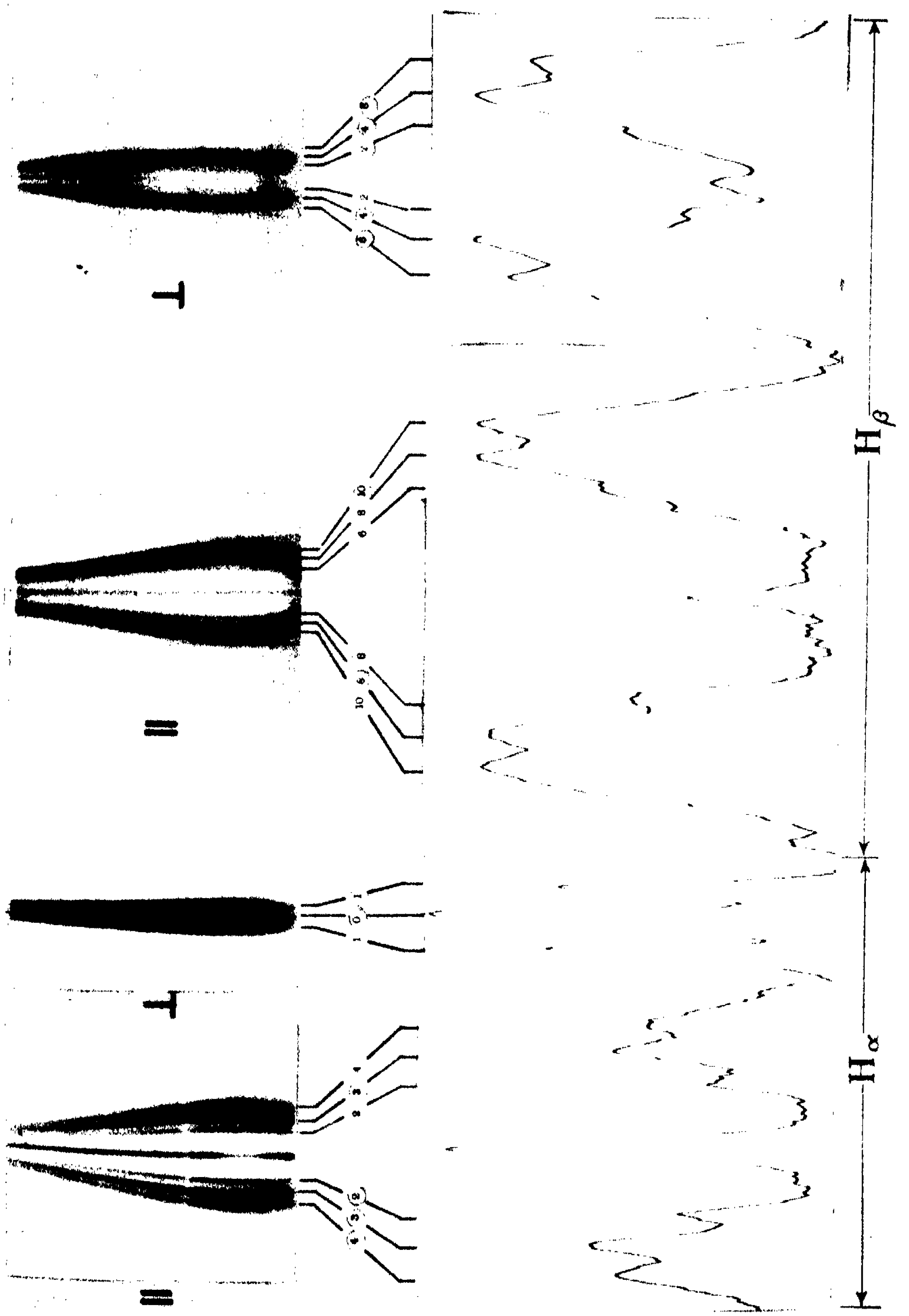
H_β
H_α
2
4
6
8
10
1
3

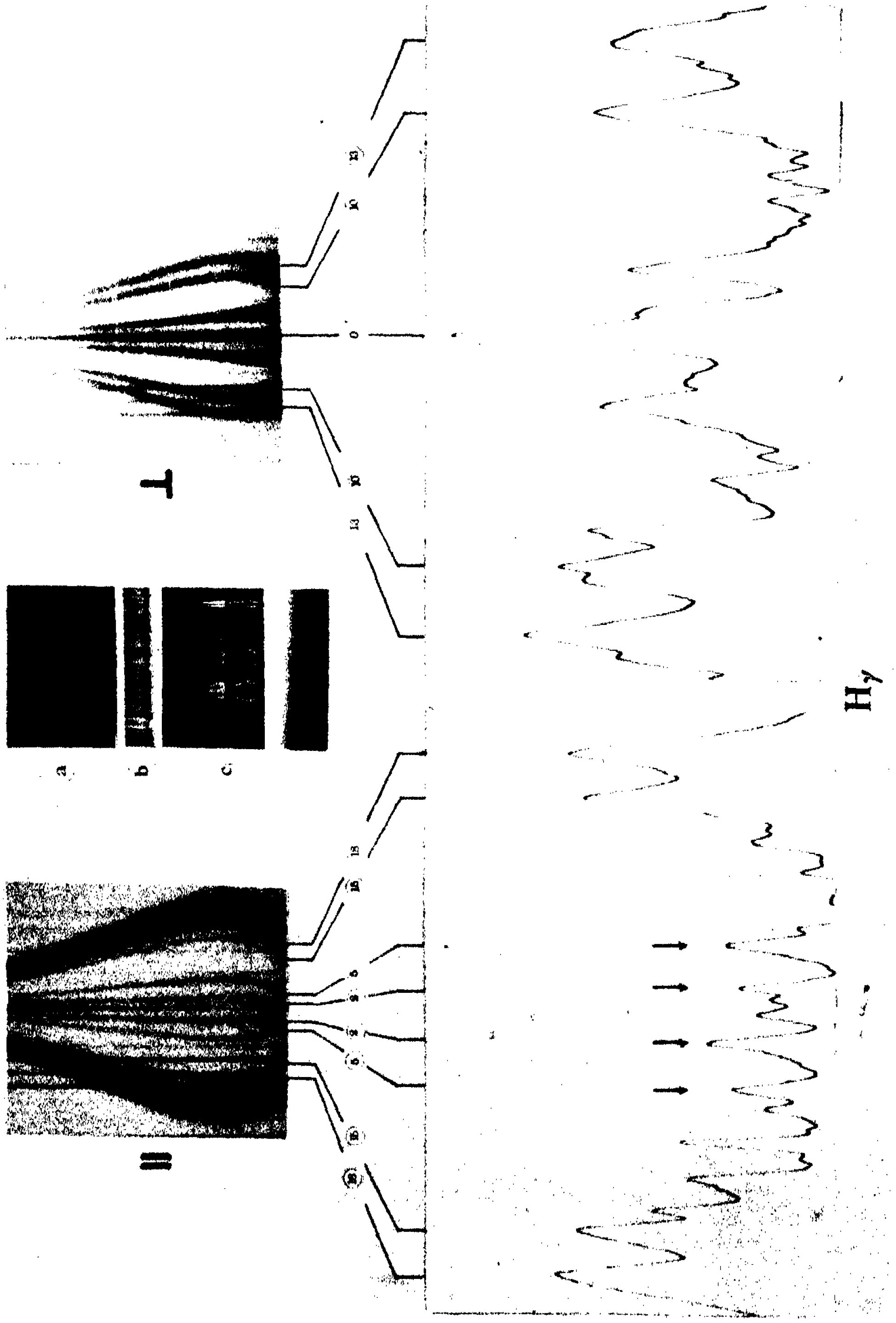
I
13
10
0
10
13
a
b
c
II
18
15
5
2
2
5
15
18
H_γ

passed through a diaphragm, which limited it to a small circular cross section, then through the prisms, and finally was focussed on the wedge at the slit. Exposures of equal periods were then made on the same plate, the intensities being reduced between exposures in the ratio of 10 to 1. Wave-lengths were marked by an iron arc comparison spectrum. With the selected ratio we have

$$D_\lambda = 1/(l_1 - l_2).$$

The blackening of the resulting images was then recorded at the desired wave-lengths by means of a Moll microphotometer. Points of equal blackening were matched in the curves from the two exposures, and, the magnification being known, the distance $(l_1 - l_2)$ could be measured. This quantity was found from a number of plates to eliminate errors which arise principally in the prism setting, and the average value used in the determination of D_λ—

Line	H_α	H_β	H_γ	H_δ
D_λ	0·89	0·309	0·41	0·564

As the figures indicate, the glass is not really neutral, but has a greenish-blue hue.

The relative intensities of the Stark components were determined in two different ways. In the first method tube (*a*) of fig. 1 supplied a source in which the electric field is uniform. A condenser lens gave magnification sufficient to produce images of both parallel and perpendicular components equal in length to the similar neutral wedges placed at the slit of the spectrograph. The resulting plates then indicated the lengths of wedge penetrated by the stronger components of both polarisations. The values of $(l_1 - l_2)$ were taken from a subsequent enlargement of known magnification, and this with D_λ gave the relative intensity of any two components in the small spectral region considered.

The second method was followed in the more recent experiments. Photographs were taken with tubes of general type (*c*) which gave a constant field over only a very limited portion of the source. After each Stark-Lo Surdo exposure was completed, a wedge photograph, with Nernst glower as source, was put on the same plate. In order to determine the intensities in this case, a Moll photometer curve was obtained for the Stark components over the section at maximum field, that is, where the lines ran parallel; and without making any change in the adjustments of the instrument, a second curve was then taken across the wedge photograph in the same region of wave-length.

The maximum densities of the components being compared were matched, by the Moll photometer, with equal densities observed at the same wave-length in the wedge photograph. The points at which these latter densities occur have a separation which corresponds to a definite length on the wedge. This length was obtained from the magnification of the photometer and the focal lengths of the lenses in the spectrograph. Hence the intensities of light, which produced the observed densities, penetrated a known difference in wedge thickness and have a ratio determined by the wedge calibration. We have assumed that this ratio of intensities of light from the Nernst glower is the same as that of the Stark components which produce like photographic effect, and have neglected any small correction due to the difference in time of exposure.

Results.

The results are given in the following table. The numbers in the second column indicate the displacements of the components compared, in terms of the unit which appears in the quantum theory of the Stark effect. The numeral placed in parenthesis after each observation indicates which of the two experimental methods was employed in obtaining the result reported. The calculated values are by Schrödinger.

Line.	Displacements and polarisation of lines compared.	Observed relative intensities.	Mean of observations.	Calculated relative intensities.	Obs./calc.
H_α	$p\ \frac{\pm 3}{\pm 4}$	1·38 (2)	1·38	1·37	1·01
	$p\ \frac{\pm 3}{\pm 2}$	3·32 (2)	3·32	3·16	1·05
	$p\ \frac{\pm 4}{\pm 2}$	2·40 (2)	2·40	2·31	1·04
	$s\ \frac{0}{\pm 1}$	1·40 (2)	1·40	1·42	0·99
H_β	$p\ \frac{\pm 8}{\pm 10}$	1·00 (1) 1·02 (2) 1·11 (2)	1·04	1·06	0·98
	$p\ \frac{\pm 8}{\pm 6}$	4·54 (2) 4·65 (2)	4·59	4·74	0·97
	$p\ \frac{\pm 10}{\pm 6}$	4·45 (2) 4·03 (2)	4·24	4·46	0·95
	$s\ \frac{\pm 4}{\pm 6}$	1·54 (2) 1·59 (1)	1·56	1·56	1·00
	$s\ \frac{\pm 4}{\pm 2}$	6·06 (2) 6·42 (1)	6·23	6·35	0·98
	$s\ \frac{\pm 4}{\pm 2}$	4·00 (2)	4·00	4·07	0·98

Line.	Displacements and polarisation of lines compared.	Observed relative intensities.	Mean of observations.	Calculated relative intensities.	Obs./calc.
H_γ	$p\ \frac{\pm 18}{\pm 15}$	1·18 (2)	1·18	1·14	1·03
	$p\ \frac{\pm 5}{\pm 2}$	1·03 (2)	1·03	1·23	0·84
	$s\ \frac{\pm 10}{\pm 13}$	1·11 (2) 1·05 (2) 1·05 (2)	1·07	1·063	1·01
H_δ	$p\ \frac{\pm 28}{\pm 24}$	1·72 (2)	1·72	1·34	1·28
	$s\ \frac{\pm 6}{\pm 10}$	1·77 (2)	1·77	2·02	0·88

Intensities in H_α were measured from the photographs reproduced in this paper. The plate was exposed for 1 hour to a neon source containing a trace of hydrogen. A potential of 8000 volts produced a steady current of 4 mil. amps. No lines of the secondary spectrum appeared. The measured intensities were strongly supported by numerous visual observations and photometer curves from many other plates. The strong central parallel component which appears in the accompanying photometer curve is due to the overlapping of the perpendicular image on the slit, and does not indicate an undisplaced line in this polarisation.

It may be recalled that the new results as already stated qualitatively in 'Nature,'* differ from those given by Stark mainly in reversal of the relative intensities of the parallel components with displacements ± 3 and ± 4. This is the largest correction to earlier work which is needed to bring the experiments in accord with the theory of Schrödinger. It has recently received qualitative support from experiments by Ishida and Hiyama.† The report by Kiuti‡ on the very weak perpendicular components with displacements ± 5, ± 6 and the doubtful parallel component ± 8 in which he based his estimates on known relative intensities of the original line and grating ghosts, may now be coupled with the present observations to give a very satisfactory experimental verification of the intensities claimed for this line by Schrödinger.

Intensities of H_β were taken from four plates obtained with sources of types

---

* Foster and Chalk, 'Nature,' vol. 121, p. 830 (1928).

† 'Sc. Pap. I.P.C.R., Tokyo,' vol. 9, p. 1 (1928).

‡ 'Jap. Journ. Phys.,' vol. 4, p. 13 (1925).

(*a*) and (*c*). Varying proportions of hydrogen and helium were used in the discharge. Typical photographs from these two sources are reproduced in Plate 5 (*a*) and (*c*).

A few years ago one of the writers made estimates of the intensities of components of H_β. These were based on analyses which varied from the original results by Stark chiefly in the elimination of certain components not claimed by the theory. Only minor changes in the relative intensities of other components were suggested. Later, the present writers reported preliminary quantitative wedge measurements of the stronger components, and these agreed remarkably well with the new calculations based on wave mechanics. In the present extension to these measurements, we find the parallel components ± 8 slightly stronger than the parallel components ± 10, so that these, as well as all other strong components, are in excellent agreement with the theory.

In our measurements of intensities on H_γ we have found it necessary to avoid carefully the numerous secondary lines which frequently appear in the background. They are easily recognised, however, and the measurements have been taken at a section of the plate where they are not superimposed on the components being compared. A second difficulty arose from the large magnification which was used at the slit. Due to an overlapping of the images, the strong inner perpendicular components coincide with the outer parallel components on all the best plates; and for this reason their intensities have not been measured.

The two measured intensity ratios of parallel components $\pm 18/\pm 15$ and $\pm 5/\pm 2$ are not necessarily plotted on the same scale in the intensity diagram, since they were determined independently from two different plates. It was found that the results for H_γ showed a reversal of the $p \pm 2/\pm 5$ intensity ratio as observed by Stark, but otherwise no appreciable variations from his results were obtained in the case of this line.

Measurements on H_δ were still more disturbed by the background, though one plate gave approximate ratios for the strong outer parallel components and the inner perpendicular components.

[*Added December* 5, 1928.—The new results for H_α, H_β, and H_γ are graphically represented by the heavy lines on the left side of fig. 2. The inverted diagrams in thin line represent the values calculated by Schrödinger. At the right are the observations by Stark.

Within the limits of experimental error the new results agree, we believe, with the calculations by Schrödinger. The well-marked agreement in the

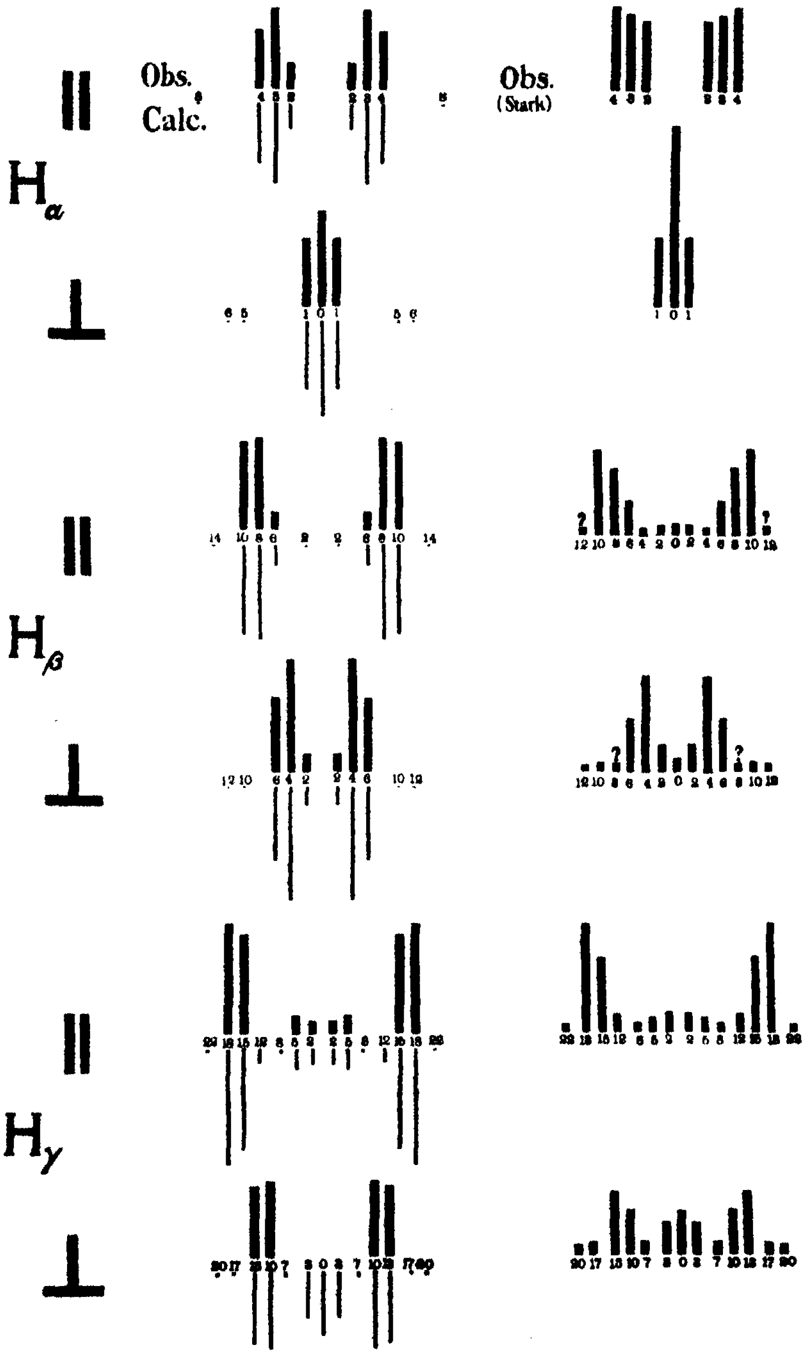

Fig. 2.—Intensities of Stark Components in Hydrogen.

lines H_α and H_β is of especial importance, since it is in the case of low quantum numbers that the new quantum theoretical calculations show the greatest departure from the estimates of the older theory. The results for the components p, $\pm 2/\pm 5$ of H_γ are less satisfactory. It is possible that we have in these components of relatively small displacement an indication of intensities modified by the influence of the fine structure. A study of numerous plates less suitable for photometric measurements make it seem more probable that the variation from Schrödinger is principally an experimental error. The measurements on H_δ are uncertain.]

Prof. Stark* in his recent review does not favour any particular theoretical treatment, and does not supply unretouched reproductions from his original plates. Certain general features in his analyses, nevertheless, suggest that the lack of harmony with recent theory may possibly be attributed mainly to experimental difficulties, and not to any special property of the canal ray source which he employed. From the theoretical point of view, his outer components in each Balmer line are too strong. Possibly this general feature was produced by a slightly unstable field which assumed values higher than normal during a small part of the exposure. There is, however, no obvious, complete explanation of the variation from theory which he observed in the case of H_α.

Thanks are due to the National Research Council of Canada for awards to one of the authors, while this research was in progress.

Summary.

Three modifications of the Lo Surdo source are described which are suited to the study of intensities of Stark components. Their relative merits are discussed.

A neutral wedge is used (i) directly, and (ii) indirectly in quantitative measurements of the intensities of the stronger components of the first four Balmer lines.

Within experimental error, the results agree with the theoretical calculations by Schrödinger.

---

* 'Handbuch Experimentalphysik' (von Wien und Harms), vol. 21, p. 433 (1927).

The Relativity Theory of Divergent Waves.

By O. R. **Baldwin**, University College, London.

(Communicated by G. B. Jeffery, F.R.S.—Received November 13, 1928.)

Einstein investigated the problem of the propagation of gravitational waves in 1916 and 1918.* The special case of plane waves of small amplitude was considered by Weyl,† who showed that such waves may be regarded as the result of superposing waves of three types. Eddington‡ found that of these only one, the transverse-transverse, is real, and identified a particular type of electromagnetic transverse-transverse wave with light. The gravitational potentials in his solution, however, contain an aperiodic term which increases without limit, from which it is inferred that light cannot be propagated indefinitely either in space or time.

We§ considered the case of plane waves of finite amplitude and came to the conclusion that an infinite plane electromagnetic wave cannot be propagated without change of wave-form, and suggested that the relativity theory of light must be approached by way of the study of divergent waves. The present discussion is confined to waves of a purely gravitational nature.

The solution given by Einstein for the general problem involving divergent waves is quoted by Eddington in the second part of his investigation, and the gravitational potentials for waves of small amplitude created by a spinning rod are calculated. In this paper an attempt is made to generalise this result and to discover all the non-spurious waves of the same general character at infinity as Eddington's waves. It is shown that there is only one fundamentally distinct wave of this type, and it seems possible that all waves may be derived from this fundamental type just as ordinary gravitational potentials are derived from $1/r$ by repeated differentiation.

§ 2. *Solutions of the Field Equations.*

Owing to the presence of gravitational waves the potentials $g_{\alpha\beta}$ will differ from their Galilean values $\delta_{\alpha\beta}$, and we suppose that

$$g_{\alpha\beta} = \delta_{\alpha\beta} + h_{\alpha\beta}, \tag{1}$$

---

* 'Berlin Sitzungsberichte,' p. 688 (1916), p. 154 (1918).

† 'Raum, Zeit, Materie,' 4th ed., p. 288, English edition, p. 252.

‡ 'Roy. Soc. Proc.,' A, vol. 102, p. 268 (1922).

§ Baldwin and Jeffery, 'Roy. Soc. Proc.,' A, vol. 111, p. 95 (1926).

where $h_{\alpha\beta}$ is so small that square terms may be neglected. The Christoffel four-index symbols are then given by the formula

$$(2) \qquad (\mu\rho\sigma\nu) = B_{\mu\nu\sigma\rho} = \tfrac{1}{2}\left\{\frac{\partial^2 h_{\mu\nu}}{\partial x_\rho\,\partial x_\sigma} + \frac{\partial^2 h_{\rho\sigma}}{\partial x_\mu\,\partial x_\nu} - \frac{\partial^2 h_{\mu\sigma}}{\partial x_\rho\,\partial x_\nu} - \frac{\partial^2 h_{\rho\nu}}{\partial x_\mu\,\partial x_\sigma}\right\},$$

and the values of the contracted Riemann-Christoffel tensor by

$$(3) \qquad G_{\mu\nu} = \delta^{\rho\sigma}(\mu\rho\sigma\nu).$$

We investigate solutions of the equations $G_{\mu\nu} = 0$ of the form

$$(4) \qquad h_{\alpha\beta} = e^{ip(t-r)}(A_{\alpha\beta}r^{1-n} + B_{\alpha\beta}r^{-n}),$$

in which $A_{\alpha\beta}$ and $B_{\alpha\beta}$ are polynomials in x, y, z $(= x_1, x_2, x_3)$ of degree $(n-2)$, $(n-1)$ respectively, and n is an integer.

As the time co-ordinate t $(= x_4)$ occurs in (4) as an exponential index only, the operation $\partial/\partial x_4$ merely introduces a factor (ip) so it is possible to obtain the expressions for $G_{\mu\nu}$ in two groups by deriving $G_{\mu 4}$ $(\mu = 1, 2, 3, 4)$ from

$$(5) \qquad 2G_{\mu 4} = -ip\frac{\partial}{\partial x_\mu}(h_{11} + h_{22} + h_{33}) + ip\left(\frac{\partial h_{\mu 1}}{\partial x_1} + \frac{\partial h_{\mu 2}}{\partial x_2} + \frac{\partial h_{\mu 3}}{\partial x_3}\right)$$
$$+ \frac{\partial}{\partial x_\mu}\left(\frac{\partial h_{14}}{\partial x_1} + \frac{\partial h_{24}}{\partial x_2} + \frac{\partial h_{34}}{\partial x_3}\right) - \left(\frac{\partial^2}{\partial x_1^2} + \frac{\partial^2}{\partial x_2^2} + \frac{\partial^2}{\partial x_3^2}\right)h_{\mu 4},$$

and the remaining six $(\mu, \nu = 1, 2, 3)$ from

$$(6) \quad 2G_{\mu\nu} = \frac{\partial^2}{\partial x_\mu\,\partial x_\nu}(h_{44} - h_{11} - h_{22} - h_{33}) - \left(\frac{\partial^2}{\partial x_1^2} + \frac{\partial^2}{\partial x_2^2} + \frac{\partial^2}{\partial x_3^2}\right)h_{\mu\nu}$$
$$+ \frac{\partial}{\partial x_\mu}\left(\frac{\partial h_{\nu 1}}{\partial x_1} + \frac{\partial h_{\nu 2}}{\partial x_2} + \frac{\partial h_{\nu 3}}{\partial x_3}\right) + \frac{\partial}{\partial x_\nu}\left(\frac{\partial h_{\mu 1}}{\partial x_1} + \frac{\partial h_{\mu 2}}{\partial x_2} + \frac{\partial h_{\mu 3}}{\partial x_3}\right)$$
$$- ip\left(\frac{\partial h_{\mu 4}}{\partial x_\nu} + \frac{\partial h_{\nu 4}}{\partial x_\mu}\right) - p^2 h_{\mu\nu}.$$

If A^μ denotes $\partial A/\partial x_\mu$; $E_{\alpha\beta} = (n-1)A_{\alpha\beta} + ipB_{\alpha\beta}$; ${}^{\mu\nu}E_{\alpha\beta} = x_\mu E_{\alpha\beta}{}^{\nu} + x_\nu E_{\alpha\beta}{}^{\mu}$;
$F_{\alpha\beta} = (n^2-1)A_{\alpha\beta} + (2n+1)ipB_{\alpha\beta}$; $D_{\alpha\beta} = (2n-1)ipA_{\alpha\beta} - p^2B_{\alpha\beta}$;
for values of μ and ν other than 4 we have

$$(7) \quad \partial h_{\alpha\beta}/\partial x_\mu = e^{ip(t-r)}\left[\begin{array}{l}\{r^{1-n}A_{\alpha\beta}{}^{\mu} - r^{-n-1}x_\mu E_{\alpha\beta}\} \\ \qquad + \{r^{-n}(B_{\alpha\beta}{}^{\mu} - ipA_{\alpha\beta}x_\mu) - nB_{\alpha\beta}x_\mu r^{-n-2}\}\end{array}\right],$$

$$(8) \quad \frac{\partial^2 h_{\alpha\beta}}{\partial x_\mu\,\partial x_\nu} = e^{ip(t-r)}\left[\begin{array}{l}\{r^{1-n}A_{\alpha\beta}{}^{\mu\nu} - r^{-n-1}(p^2A_{\alpha\beta}x_\mu x_\nu + {}^{\mu\nu}E_{\alpha\beta}) + r^{-n-3}F_{\alpha\beta}x_\mu x_\nu\} \\ \qquad + \{r^{-n}(B_{\alpha\beta}{}^{\mu\nu} - ip{}^{\mu\nu}A_{\alpha\beta}) + r^{-n-2}(D_{\alpha\beta}x_\mu x_\nu - n{}^{\mu\nu}B_{\alpha\beta}) \\ \qquad\qquad + n(n+2)x_\mu x_\nu B_{\alpha\beta}r^{-n-4}\}\end{array}\right],$$
$$\mu \neq \nu$$

$$(9) \quad \frac{\partial^2 h_{\alpha\beta}}{\partial x_\mu^2} = e^{ip(t-r)}\left[\begin{array}{l}\{r^{1-n}A_{\alpha\beta}{}^{\mu\mu} - r^{-n-1}(p^2A_{\alpha\beta}x_\mu^2 + {}^{\mu\mu}E_{\alpha\beta} + E_{\alpha\beta}) + r^{-n-3}x_\mu^2F_{\alpha\beta}\} \\ \qquad + \{r^{-n}(B_{\alpha\beta}{}^{\mu\mu} - ip\overline{A_{\alpha\beta} + {}^{\mu\mu}A_{\alpha\beta}}) + r^{-n-2}(x_\mu^2D_{\alpha\beta} - n\overline{B_{\alpha\beta} + {}^{\mu\mu}B_{\alpha\beta}}) \\ \qquad\qquad + n(n+2)x_\mu^2B_{\alpha\beta}r^{-n-4}\}\end{array}\right],$$

The expressions for $G_{\mu\nu}$ obtained by substituting from (7), (8), (9) in (5) and (6) must vanish identically. In each there will be even and odd powers of r, so by separating the rational from the irrational we shall have twenty expressions instead of ten. This is effected by making the separation in (7), (8), (9); in the actual use of (8), for example, only one of the two pairs of curly brackets is employed, not both simultaneously. Each expression contains general polynomials and no further progress can be made until the forms of $A_{\alpha\beta}$ and $B_{\alpha\beta}$ are known, when it is possible to subdivide the twenty polynomials into sets of homogeneous ones. Details of the method will be explained by considering a particular case.

In order to find all solutions in which terms of order r^{-4} are neglected in $(A_{\alpha\beta}r^{1-n} + B_{\alpha\beta}r^{-n})$ when n is 5, the following polynomials are taken for A and B:—

$$\text{(10)} \qquad A_{\alpha\beta} = {}_1A_{\alpha\beta} + {}_2A_{\alpha\beta} + {}_3A_{\alpha\beta}$$

where

$$\begin{aligned} {}_1A_{\alpha\beta} &= ax + by + cz \\ {}_2A_{\alpha\beta} &= dx^2 + ey^2 + fz^2 + gyz + hzx + jxy \\ {}_3A_{\alpha\beta} &= kx^3 + ly^3 + mz^3 + nx^2y + qxy^2 + sy^2z + tyz^2 + uz^2x \\ &\qquad + vzx^2 + wxyz. \end{aligned}$$

$B_{\alpha\beta} = {}_2B_{\alpha\beta} + {}_3B_{\alpha\beta} + {}_4B_{\alpha\beta}$, where ${}_2B$ and ${}_3B$ are the expressions for ${}_2A$ and ${}_3A$ with the coefficients replaced by capital letters and

$$\begin{aligned} {}_4B_{\alpha\beta} = \alpha x^4 + \beta x^3y + \gamma x^2y^2 + \delta xy^3 + \xi y^4 + \eta y^3z + \zeta y^2z^2 + \psi yz^3 \\ + \lambda z^4 + \rho z^3x + \omega z^2x^2 + \sigma zx^3 + \theta x^2yz + \phi xy^2z + \Delta xyz^2. \end{aligned}$$

For this value of n, equations (7), (8), (9) become

$$\text{(11)} \quad e^{ip(r-t)}\,\partial h_{\alpha\beta}/\partial x_\mu = \{r^{-5}(B^\mu - ipAx_\mu) - 5r^{-7}Bx_\mu\} + \{r^{-4}A^\mu - r^{-6}Ex_\mu\},$$

$$\begin{aligned} \text{(12)} \quad e^{ip(r-t)}\frac{\partial^2 h_{\alpha\beta}}{\partial x_\mu\,\partial x_\nu} &= \{r^{-5}(B^{\mu\nu} - ip^{\mu\nu}A) + r^{-7}(Dx_\mu x_\nu - 5\,{}^{\mu\nu}B) + r^{-9}(35x_\mu x_\nu B)\} \\ \mu \neq \nu \qquad & + \{r^{-4}A^{\mu\nu} - r^{-6}({}^{\mu\nu}E + p^2Ax_\mu x_\nu) + r^{-8}Fx_\mu x_\nu\}, \end{aligned}$$

$$\begin{aligned} \text{(13)} \quad e^{ip(r-t)}\frac{\partial^2 h_{\alpha\beta}}{\partial x_\mu\,\partial x_\nu} &= \{r^{-5}(B^{\mu\mu} - ip\overline{A + {}^{\mu\mu}A}) + r^{-7}(Dx_\mu{}^2 - 5\overline{B + {}^{\mu\mu}B}) \\ &\qquad + 35x_\mu{}^2Br^{-9}\} \\ &\quad + \{r^{-4}A^{\mu\mu} - r^{-6}(p^2Ax_\mu{}^2 + E + {}^{\mu\mu}E) + r^{-8}Fx_\mu{}^2\}. \end{aligned}$$

Every expression obtained by substituting (11), (12), (13) in (5) and (6) consists of five homogeneous polynomials; consequently there are 100 polynomials which must vanish identically.

In these the 500 coefficients occurring in (10) fall into two distinct groups. Multiply each set of five homogeneous polynomials by a power of r to remove negative indices, and in the following scheme denote the resulting expression by its degree. The brackets differentiate the two groups, and $\mu, \nu = 1, 2, 3$.

	From odd powers of r^{-1}.					From even powers of r^{-1}.				
G_{44}	6	(5)	4	(3)	2	(5)	4	(3)	2	(1)
$G_{\mu 4}$	(8)	7	(6)	5	(4)	7	(6)	5	(4)	3
$G_{\mu\nu}$	8	(7)	6	(5)	4	(7)	6	(5)	4	(3).

No coefficient appears in both groups. Consider one group. When common factors in r have been removed the degrees of the expressions vary from one to six. In the homogeneous polynomials themselves the coefficients subdivide into four sets, and if the terms x^3, y^2x, z^2x are represented by r^2x, so that r^4xy indicates six and r^6 ten terms, the separation takes place in the various polynomials in the following way:—

$$\begin{array}{llllllll}
r^4(xy) & ; & r^4yz & ; & r^4zx & ; & r^6 \\
r^4(x) & ; & r^4y & ; & r^4z & ; & r^2xyz \\
r^2(xy) & ; & r^2yz & ; & r^2zx & ; & r^4 \\
r^2(x) & ; & r^2y & ; & r^2z & ; & xyz \\
xy & ; & yz & ; & zx & ; & r^2.
\end{array}$$

The group is thus divided into four sections, and three of these are not independent—given one, the other two sets may be written down by a cyclic interchange.

Thus the 500 coefficients may be divided into eight sets, and it is sufficient to work with four. The remaining solutions may be obtained by making a cyclic interchange of x, y, z with a corresponding change in the suffixes of $h_{\alpha\beta}$.

We do not propose to give details of the actual reduction of the sets of conditions. In each case the method consists in expressing as many coefficients as possible (say the dependent) in terms of the others (the independent coefficients). By supposing all the independent coefficients except one to be zero the dependent ones are all expressed in terms of one, and when the corresponding values of A and B in (10) are substituted in (4) a series of values of $h_{\alpha\beta}$ is obtained which constitutes a solution of the equations $G_{\mu\nu} = 0$.

The solutions obtained from one group of coefficients are given in Table I, those from the other group in Tables II and III. The work in connection with the second group requires special consideration. The group consists of

Table I.

$h_{11}e^{ip(r-t)}$	$xyz\mathrm{F}$					$\left(\frac{1}{r^3} - ipx^2\mathrm{F}\right) y$	
$h_{22}e^{ip(r-t)}$			$\left(\frac{2}{p^2r^4} + \frac{3i}{pr^3} + y^2\mathrm{F}\right) y$	$x^2y\mathrm{F}$			$y\mathrm{J}$
$h_{33}e^{ip(r-t)}$							
$h_{44}e^{ip(r-t)}$		$\frac{y}{r^2}$			$\frac{y}{r^3}$		
$h_{12}e^{ip(r-t)}$	$\frac{1}{2}\left(\frac{i}{pr^3} + y^2\mathrm{F}\right) z$		$\frac{1}{2}\left(\frac{2}{p^2r^4} + \frac{i}{pr^3} + y^2\mathrm{F}\right) x$	$\frac{1}{2}\left(\frac{2i}{pr^3} + x^2\mathrm{F}\right) x$		$\frac{1}{2}\left(\frac{1}{r^3} - ipy^2\mathrm{F}\right) x$	$\frac{1}{2}x\mathrm{J}$
$h_{23}e^{ip(r-t)}$			$\frac{1}{2}\left(\frac{2}{p^2r^4} + \frac{i}{pr^3} + y^2\mathrm{F}\right) z$	$\frac{1}{2}x^2z\mathrm{F}$			$\frac{1}{2}z\mathrm{J}$
$h_{13}e^{ip(r-t)}$	$\frac{1}{2}\left(\frac{i}{pr^3} + z^2\mathrm{F}\right) y$					$-\frac{1}{2}ipxyz\mathrm{F}$	
$h_{14}e^{ip(r-t)}$	$-\frac{1}{2}\frac{yz}{r^3}$	$-\frac{1}{2}xy\mathrm{J}$			$-\frac{1}{2}xy\mathrm{F}$	$\frac{1}{2}ip\frac{xy}{r^3}$	
$h_{24}e^{ip(r-t)}$		$-\frac{1}{2}\left(\frac{i}{pr^3} + y^2\mathrm{J}\right)$	$-\frac{1}{2}\left(\frac{i}{pr^3} + \frac{y^2}{r^3}\right)$	$-\frac{1}{2}\frac{x^2}{r^3}$	$-\frac{1}{2}\left(\frac{i}{pr^3} - y^2\mathrm{F}\right)$		$-\frac{1}{2r^2}$
$h_{34}e^{ip(r-t)}$		$-\frac{1}{2}yz\mathrm{J}$			$-\frac{1}{2}yz\mathrm{F}$		

(See § 2. There are six solutions represented by columns 4 and 6 respectively, and three by columns 1, 2, 3, 5, 7.)

$$\mathrm{F} = \frac{1}{r^4} - \frac{3i}{pr^5}, \quad \mathrm{J} = \frac{1}{r^3} - \frac{2i}{pr^4}$$

Table

	X.	Y.	Z.	d_{44}.	α_{11}.	ξ_{22}.
$h_{11}e^{ip(r-t)}$	$-\frac{1}{r}+\frac{i}{pr^2}+x^2J$	$\frac{i}{2pr^2}+\frac{i}{2p}y^2F+z^2N$	$\frac{i}{2pr^2}+\frac{i}{2p}z^2F+y^2N$		$\frac{i}{pr^2}+x^2J$	
$h_{22}e^{ip(r-t)}$	$\frac{i}{2pr^2}+\frac{i}{2p}x^2F+z^2N$	$-\frac{1}{r}+\frac{i}{pr^2}+y^2J$	$\frac{i}{2pr^2}+\frac{i}{2p}z^2F+x^2N$			$\frac{i}{pr^2}+y^2J$
$h_{33}e^{ip(r-t)}$	$\frac{i}{2pr^2}+\frac{i}{2p}x^2F+y^2N$	$\frac{i}{2pr^2}+\frac{i}{2p}y^2F+x^2N$	$-\frac{1}{r}+\frac{i}{pr^2}+z^2J$			
$h_{44}e^{ip(r-t)}$	$-\frac{1}{p^2r^3}+\frac{3x^2}{p}\left(\frac{i}{r^4}+\frac{1}{pr^5}\right)$	$-\frac{1}{p^2r^3}+\frac{3y^2}{p}\left(\frac{i}{r^4}+\frac{1}{pr^5}\right)$	$-\frac{1}{p^2r^3}+\frac{3z^2}{p}\left(\frac{i}{r^4}+\frac{1}{pr^5}\right)$	$\frac{1}{r^2}$		
$h_{12}e^{ip(r-t)}$	$\frac{1}{2}xyN$	$\frac{1}{2}xyN$	$-xyN$		$\frac{1}{2}xyJ$	$\frac{1}{2}xyJ$
$h_{23}e^{ip(r-t)}$	$-yzN$	$\frac{1}{2}yzN$	$\frac{1}{2}yzN$			$\frac{1}{2}yzJ$
$h_{13}e^{ip(r-t)}$	$\frac{1}{2}zxN$	$-zxN$	$\frac{1}{2}zxN$		$\frac{1}{2}zxJ$	
$h_{14}e^{ip(r-t)}$	$(L-\frac{1}{2}x^2F)x$	$(T-\frac{1}{2}y^2F)x$	$(T-\frac{1}{2}z^2F)x$	$-\frac{1}{2}Jx$	$-\frac{x}{2r^2}$	
$h_{24}e^{ip(r-t)}$	$(T-\frac{1}{2}x^2F)y$	$(L-\frac{1}{2}y^2F)y$	$(T-\frac{1}{2}z^2F)y$	$-\frac{1}{2}Jy$		$-\frac{y}{2r^2}$
$h_{34}e^{ip(r-t)}$	$(T-\frac{1}{2}x^2F)z$	$(T-\frac{1}{2}y^2F)z$	$(L-\frac{1}{2}z^2F)z$	$-\frac{1}{2}Jz$		

$$J=\frac{1}{r^3}-\frac{2i}{pr^4}\qquad F=\frac{1}{r^4}-\frac{3i}{pr^5}\qquad N=J-\frac{i}{2p}F=\frac{1}{r^3}-\frac{5i}{2pr^4}-\frac{3}{2p^2r^5}$$

four sets; the coefficients of the independent set are given at the head of the columns in Table II, and this table is given in full. It will be seen that the solutions E_{22} and F_{33} may be obtained from D_{11} by a cyclic interchange corresponding to the interchange of the coefficients of x^2, y^2, and z^2 in (10), and similar relations exist for α_{11}, ξ_{22}, λ_{33}; α_{44}, ξ_{44}, λ_{44}. The solution d_{44} is symmetrical, and transforms into itself as d_{44}, e_{44}, and f_{44} are interchanged. Three coefficients in this table, however, are omitted—those giving rise to the columns X, Y, Z. At one stage in this reduction a choice of independent coefficient was made from d_{44}, e_{44}, f_{44} which occurred among the dependent coefficients in the forms $(d_{44}-e_{44})$, $(e_{44}-f_{44})$, $(f_{44}-d_{44})$. The work was continued in three parallel columns in which d_{44}, e_{44}, and f_{44} were chosen respectively, and in each occurred the final condition

$$\alpha_{33}+\xi_{22}+\lambda_{11}=0.$$

II.

λ_{33}.	D_{11}.	E_{22}.	F_{33}.	a_{44}.	ξ_{44}.	λ_{44}.
	$-\frac{1}{r^3}+ipx^2F$					
		$-\frac{1}{r^3}+ipy^2F$				
$\frac{i}{pr^2}+z^2J$			$-\frac{1}{r^3}+ipz^2F$			
				$\frac{x^2}{r^3}$	$\frac{y^2}{r^3}$	$\frac{z^2}{r^3}$
	$\frac{ip}{2}xyF$	$\frac{ip}{2}xyF$				
$\frac{1}{2}yzJ$		$\frac{ip}{2}yzF$	$\frac{ip}{2}yzF$			
$\frac{1}{2}xzJ$	$\frac{ip}{2}xzF$		$\frac{ip}{2}xzF$			
	$-\frac{ip}{2}\frac{x}{r^3}$			$-\left(\frac{i}{pr^3}+\frac{x^2}{2}F\right)x$	$-\frac{1}{2}y^2xF$	$-\frac{1}{2}z^2xF$
		$-\frac{ip}{2}\frac{y}{r^3}$		$-\frac{1}{2}x^2yF$	$-\left(\frac{i}{pr^3}+\frac{y^2}{2}F\right)y$	$-\frac{1}{2}z^2yF$
$-\frac{z}{2r^2}$			$-\frac{ip}{2}\frac{z}{r^3}$	$-\frac{1}{2}x^2zF$	$-\frac{1}{2}y^2zF$	$-\left(\frac{i}{pr^3}+\frac{z^2}{2}F\right)z$

$$L = \frac{1}{2r^2}-\frac{5i}{2pr^3}-\frac{1}{p^2r^4} \qquad T = -\frac{i}{4pr^3}-\frac{1}{p^2r^4},$$

To complete the reduction one of these had to be retained as a dependent coefficient, the other two yielding solutions. In this way eighteen solutions were found, some of which were those headed X, Y, Z, and the others were linear combinations of one of these and the column d_{44}. If the columns be represented by the coefficients it may be shown that

$$X+Y+Z=d_{44}.$$

Later it will appear that X, Y, and Z denote real waves whilst the d_{44} wave is spurious.

The remaining three sets of this group of coefficients yield fifteen solutions, five of which are given in Table III. The remaining ten are easily obtained by cyclic transformations; for example, there are six solutions of the type α, one of which is β. In a similar way the solutions obtained from the first group may be derived from the typical solutions given in Table I.

Thus the fifty-five sets of values of $h_{\alpha\beta}$ (modified by means of the formula $r^2 = x^2 + y^2 + z^2$, and the omission of arbitrary independent coefficients) which were obtained from the two groups are given in the first three tables.

From these solutions others may be derived. In the first place any linear combination of solutions is also a solution, for the assumption that $h_{\alpha\beta}$ is so small that its square may be neglected reduces the formula for $B_{\mu\nu\sigma\rho}$ to that given in (2) in which product terms are omitted. And, secondly, if we know a series of values $h_{\alpha\beta}$ is a solution, the series obtained by repeated differentiations will also be solutions. If in our particular case we write (4) as $h_{\alpha\beta} = e^{ip(t-r)}\theta_5$, we have

$$\partial h_{\alpha\beta}/\partial x_\mu = e^{ip(t-r)}\theta_7,$$

and successive differentiations will yield terms of the form $e^{ip(t-r)}\theta_{2m+1}$, where

$$\theta_{2m+1} = \sum_{s=m+1}^{2m-1} {}_sA \Big/ r^{2m} + \sum_{s=m}^{2m} {}_sB \Big/ r^{2m+1}.$$

In general, therefore, non-vanishing terms in (2) will remain such, and their combinations will continue to satisfy the condition imposed by (3) and $G_{\mu\nu} = 0$. It is possible to extend any real wave solution in this way, and so the number of solutions may be indefinitely increased.

§ 3. *The Fundamental Type.*

In order to determine whether these waves are physically real or not it is necessary to evaluate the 4-index symbols (2). This is a comparatively easy matter for those waves in which not more than four of the quantities $h_{\mu\nu}$ are non-zero. In every such case all the 4-index symbols vanish and the waves are therefore spurious. This disposes of all waves except X, Y, Z in Table II and X′, Y′, Z′ in Table III.

To facilitate the investigation of the Y wave, it is combined with spurious waves to form the wave Y_2 as follows

$$Y_2 = Y - \xi_{44} - \frac{i}{p} d_{44} + \frac{1}{2p^2}(D_{11} + F_{33}) - \xi_{22},$$

for which four of the quantities $h_{\mu\nu}$ vanish as shown in Table IV. The calculation of the 4-index symbols is thus considerably simplified, and it is found that they do not all vanish. Hence this wave, and therefore the Y wave, is physically real.

In a similar way it may be shown that the X′ wave is physically real, and thus we have the real waves X, Y, Z, X′, Y′, Z′.

Table III.

	X′.	α.	β.	γ.	δ.
$h_{11}e^{ip(r-t)}$	yzf				
$h_{22}e^{ip(r-t)}$			$yz\phi$		yzF
$h_{33}e^{ip(r-t)}$		$yz\phi$		yzF	
$h_{44}e^{ip(r-t)}$	yzf				
$h_{12}e^{ip(r-t)}$	$-\frac{1}{2}xzf$		$\frac{1}{2}xz\phi$		$\frac{1}{2}xzF$
$h_{23}e^{ip(r-t)}$	$\frac{1}{2}\left(\frac{1}{r}-\frac{i}{p}\theta+x^2f\right)$	$\frac{i}{p}\psi+\frac{1}{2}y^2\phi$	$\frac{i}{p}\psi+\frac{1}{2}z^2\phi$	$\frac{1}{2}\left(\frac{i}{pr^3}+y^2F\right)$	$\frac{1}{2}\left(\frac{i}{pr^3}+z^2F\right)$
$h_{13}e^{ip(r-t)}$	$-\frac{1}{2}xyf$	$\frac{1}{2}xy\phi$		$\frac{1}{2}xyF$	
$h_{14}e^{ip(r-t)}$					
$h_{24}e^{ip(r-t)}$	$\frac{1}{2}z\theta$		$-z\psi$		$-\frac{1}{2}\frac{z}{r^3}$
$h_{34}e^{ip(r-t)}$	$\frac{1}{2}y\theta$	$-y\psi$		$-\frac{1}{2}\frac{y}{r^3}$	

(See § 2. The complete table contains 15 solutions.)

$$f=\frac{1}{r^3}-\frac{3i}{pr^4}-\frac{3}{p^2r^5}\,;\quad F=\frac{1}{r^4}-\frac{3i}{pr^5}\,;\quad \psi=\frac{1}{2r^2}+\frac{i}{pr^3}\,;\quad \theta=-\frac{1}{r^2}+\frac{i}{pr^3}\,;\quad \phi=\frac{1}{r^3}+\frac{6}{p^2r^5}.$$

These six physically real types of wave are not, however, fundamentally distinct. Y and Z are obtained from X by cyclic interchange of the axes of co-ordinates, and the other three are similarly related.

Further the X′ wave may be derived from the X type as follows.

Combining the wave Y with the spurious waves ξ_{22}, E_{22} and ξ_{44}, we obtain the wave denoted by

$$Y_1=\tfrac{1}{2}\left(-Y+3\xi_{22}-\frac{3}{2p^2}E_{22}+\xi_{44}\right).$$

The components of this wave are shown in the second column of Table IV. On a cyclic interchange of x, y, z in Y_1 we have another wave which we denote by Z_1 and we combine Y_1 and Z_1 to form the wave denoted by

$$D=Y_1-Z_1$$

Table IV.

	Y_2.	Y_1.	D.	P.	Eddington's solution.
$h_{11}e^{ip(r-t)}$	$-\frac{i}{p}\theta + z^2f$	$-\frac{1}{2}\left\{\frac{i}{2pr^2}+\frac{i}{2p}y^2\mathrm{F}+z^2\mathrm{N}\right\}$	$\frac{1}{2}(y^2-z^2)f$	yzf	$\frac{1}{2}(y-iz)^2f$
$h_{22}e^{ip(r-t)}$	$-\frac{1}{r}$	$\frac{1}{2r}+\frac{i}{pr^2}+\frac{3}{4p^2r^3}+y^2\left(f+\frac{i}{4p}\mathrm{F}\right)$	$\frac{1}{r}+\frac{1}{2}(y^2-z^2)f$	yzf	$\frac{1}{r}+\frac{1}{2}(y-iz)^2f$
$h_{33}e^{ip(r-t)}$	$-\frac{i}{p}\theta + x^2f$	$-\frac{1}{2}\left\{\frac{i}{2pr}+\frac{i}{2p}y^2\mathrm{F}+x^2\mathrm{N}\right\}$	$-\frac{1}{r}+\frac{1}{2}(y^2-z^2)f$	yzf	$-\frac{1}{r}+\frac{1}{2}(y-iz)^2f$
$h_{44}e^{ip(r-t)}$	$\frac{i}{p}\theta - y^2f$	$\frac{1}{2}\left(\frac{1}{p^2r^3}+y^2f\right)$	$\frac{1}{2}(y^2-z^2)f$	yzf	$\frac{1}{2}(y-iz)^2f$
$h_{12}e^{ip(r-t)}$		$\frac{1}{2}xy\mathrm{N}$			
$h_{23}e^{ip(r-t)}$		$\frac{1}{2}yz\mathrm{N}$		$\frac{1}{r}$	$-\frac{i}{r}$
$h_{13}e^{ip(r-t)}$	$-xzf$	$\frac{1}{2}zx\mathrm{N}$			
$h_{14}e^{ip(r-t)}$		$-\frac{1}{2}x\mathrm{T}$			
$h_{24}e^{ip(r-t)}$	$-y\theta$	$\frac{1}{2}\left(-\frac{2}{r^2}+\frac{9i}{4pr^3}+\frac{1}{p^2r^4}\right)y$	$y\theta$	$z\theta$	$(y-iz)\theta$
$h_{34}e^{ip(r-t)}$		$-\frac{1}{2}z\mathrm{T}$	$-z\theta$	$y\theta$	$-i(y-iz)\theta$

whose components are shown in the third column of Table IV. On applying the transformation

$$x = x'; \quad y = (y' + z')/\sqrt{2}; \quad z = (y' - z')/\sqrt{2}; \quad t = t',$$

this wave becomes that denoted by P and is set out in the fourth column of Table IV. Finally

$$\mathrm{P} = \mathrm{X}' + \alpha + \beta - 3i(\gamma + \delta)/p.$$

where the waves denoted by α, β, γ and δ, shown in Table III, are spurious.

Hence the wave X′ may be obtained by combining transformations of the X wave and spurious waves. There is thus only one fundamentally distinct wave.

The relation of this fundamental solution to Eddington's solution is shown in Table IV, where the values of the $h_{\mu\nu}$ in Eddington's wave are seen to be obtained by combining the D and P waves by the relation

$$\mathrm{D} - i\mathrm{P}.$$

It will be noted that in combining D and P in this way no terms disappear. Hence the solution obtained for a spinning rod consists of two parts, each of which represents a real wave solution, and each is a transform of the other.

§ 4. *Degeneracy to Plane Wave Solutions.*

It is interesting to note the form of these waves at a great distance from the source.

Eddington classified transverse-transverse waves by grouping the non-zero values of $h_{\mu\nu}$ as follows

$$h_{23}\,; \quad h_{22}-h_{33}\,; \quad h_{22}+h_{33}.$$

In each type of wave two of these three quantities vanish. At infinity in the direction of the axis of x the surviving term in the solution P is

$$h_{23}=\mathrm{A}e^{ip(t-x)}.$$

and D reduces to

$$h_{22}=-h_{33}=\mathrm{B}e^{ip(t-x)},$$

where A and B are arbitrary constants. Consequently P degenerates into the type h_{23} and D falls into the $h_{22}-h_{33}$ class.

Similarly in the direction of the x axis Y_2 becomes

$$h_{22}=-h_{33}=\mathrm{C}e^{ip(t-x)},$$

and the corresponding reduction for the z axis gives

$$h_{22}=-h_{11}=\mathrm{C}e^{ip(t-z)},$$

C being a constant, so that in both directions the waves are of the second type.

§ 5. *Sources of Gravitational Waves.*

There are three solutions of interest which have been derived from the two real wave solutions X and X′, namely, Y_2, D and P. It seems best to seek first an interpretation of D and P which together constitute the spinning rod solution.

To determine the values of $h_{\mu\nu}$ for waves created by a rod spinning in the yz plane, Eddington* first calculated the values of γ_{22}, γ_{23}, γ_{33} where

$$\gamma_{\mu\nu}=h_{\mu\nu}-\tfrac{1}{2}\delta_{\mu\nu}h, \tag{14}$$

by means of the integrated components of the energy-tensor $\mathrm{T}_{\mu\nu}$ which he denoted by $\{\mathrm{T}_{22}\}$, $\{\mathrm{T}_{23}\}$, $\{\mathrm{T}_{33}\}$. The waves accompanying these simple waves were derived from the equations $\partial\gamma_\mu{}^\alpha/\partial x_\alpha = 0$. Solution D may be obtained by the same method from the values

---

* *Loc. cit.*, p. 277.

$$\{T_{22}\} = -\{T_{33}\} = Ke^{ipt}; \quad \{T_{23}\} = 0;$$

and solution P from

$$\{T_{22}\} = \{T_{33}\} = 0; \quad \{T_{23}\} = Ce^{ipt},$$

where K and C are arbitrary constants.

The stresses required for D occur in the case of two similar rods spinning in opposite directions at the origin, but that cannot be regarded as a simple source. Consider a linear oscillator consisting of two particles each of mass m connected by a spring, of negligible mass, such that the tension in the spring is proportional to its length, *i.e.*, the distance between the particles. Suppose that the particles are situated at the points $y = \pm a \cos \omega t$ so that they oscillate backwards and forwards passing each other at the mean position of their oscillation.

Then

$$\overset{\frown}{yy} = m\ddot{y} = -ma\omega^2 \cos \omega t$$

and

$$\{T^{22}\} = 2ma^2\omega^2 \sin^2 \omega t - 2ma^2\omega^2 \cos^2 \omega t$$
$$= -2ma^2\omega^2 \cos 2\omega t.$$

A possible source for D waves, therefore, is a system consisting of two such doublets lying along the y and z axes respectively, the displacements being given by $y = \pm a \cos \omega t$, $z = \pm a \sin \omega t$.

Now suppose that instead of a linear oscillator we have a rotating system in the yz plane formed by the same two particles connected by the spring. If the inclination of the spring to the y axis at time t be ωt, in this direction $\overset{\frown}{rr} = -ma\omega^2$ so that

$$\overset{\frown}{yy} = -ma\omega^2 \cos^2 \omega t; \quad \overset{\frown}{zz} = -ma\omega^2 \sin^2 \omega t; \text{ and } \overset{\frown}{xy} = -ma\omega^2 \cos \omega t \sin \omega t;$$

and from these

$$\{T^{22}\} = -\{T^{33}\} = -2ma^2\omega^2 \cos 2\omega t; \quad \{T^{23}\} = -ma^2\omega^2 \sin 2\omega t.$$

The stresses required for P are obtained by combining this rotating system with two linear oscillators lying along the y and z axes, defined by $y = \pm a \sin \omega t$, $z = \pm a \cos \omega t$.

It has been shown that the D solution is equivalent to $Y_1 - Z_1$, and that the source for waves of this type consists of two linear oscillators at right angles to each other. The source for the fundamental type of wave must be such that the physical operation corresponding to $Y_1 - Z_1$ gives the D source. The simplest source which would satisfy this condition is a linear oscillator lying along the y axis, for which the integrated stress would be $\{T^{22}\}$ leading to a solution dependent on h_{22}. That the Y solution is of this nature may be seen in the Y_2 column which may be written in the form :—

$$(15)\quad \left\{ \begin{array}{llll} h_{\mu\nu} = -\dfrac{1}{(ip)^2}\dfrac{\partial^2}{\partial z^2}h_{22}, & 0 \quad , & \dfrac{1}{(ip)^2}\dfrac{\partial^2}{\partial z\,\partial x}h_{22}, & 0 \quad , \\ \qquad 0 \quad , & h_{22} \quad , & 0 \quad , & \dfrac{1}{(ip)}\dfrac{\partial}{\partial y}h_{22} \quad , \\ \dfrac{1}{(ip)^2}\dfrac{\partial^2}{\partial z\,\partial x}h_{22}, & 0 \quad , & -\dfrac{1}{(ip)^2}\dfrac{\partial^2}{\partial x^2}h_{22}, & 0 \quad , \\ \qquad 0 \quad , & \dfrac{1}{ip}\dfrac{\partial}{\partial y}h_{22} \quad , & 0 \quad , & \dfrac{1}{(ip)^2}\dfrac{\partial^2}{\partial y^2}h_{22} \; , \end{array} \right.$$

where $h_{22} = \dfrac{e^{ip\,(t-r)}}{r}$.

Consider, therefore, a linear oscillator lying along the y axis. For such a source γ_{22} exists, and it may be assumed that γ_{12}, γ_{23} and also γ_{14}, γ_{34} vanish, consequently the equations $\partial\gamma_\mu{}^a/\partial x_a = 0$ become

$$(16)\quad \left\{ \begin{array}{ll} \dfrac{\partial}{\partial x}\gamma_{11} = -\dfrac{\partial}{\partial z}\gamma_{13}\,; & \dfrac{\partial}{\partial x}\gamma_{13} = -\dfrac{\partial}{\partial z}\gamma_{33}\,; \\ \dfrac{\partial}{\partial y}\gamma_{22} = -\dfrac{\partial}{\partial t}\gamma_{24}\,; & \dfrac{\partial}{\partial y}\gamma_{24} = \dfrac{\partial}{\partial t}\gamma_{44}\,. \end{array} \right.$$

The general solution of these equations is

$$(17)\quad \left\{ \begin{array}{lll} \gamma_{22} = \dfrac{\partial^2\phi}{\partial t^2}\,; & \gamma_{24} = \dfrac{\partial^2\phi}{\partial y\,\partial t}\,; & \gamma_{44} = \dfrac{\partial^2\phi}{\partial y^2}\,; \\ \gamma_{33} = -\dfrac{\partial^2\chi}{\partial x^2}\,; & \gamma_{11} = -\dfrac{\partial^2\chi}{\partial z^2}\,; & \gamma_{13} = \dfrac{\partial^2\chi}{\partial z\,\partial x}\,; \end{array} \right.$$

where ϕ and χ are arbitrary functions. From (14) we have

$$\delta^{\mu\nu}\gamma_{\mu\nu} = \delta^{\mu\nu}h_{\mu\nu} - \tfrac{1}{2}\delta^{\mu\nu}\delta_{\mu\nu}h,$$

therefore

$$(18)\qquad h_{\mu\nu} = \gamma_{\mu\nu} - \tfrac{1}{2}\delta_{\mu\nu}\gamma$$

where

(19)
$$\begin{aligned}\gamma &= -\gamma_{11} - \gamma_{22} - \gamma_{33} + \gamma_{44} \\ &= \left(\frac{\partial^2}{\partial y^2} - \frac{\partial^2}{\partial t^2}\right)\phi + \left(\frac{\partial^2}{\partial z^2} + \frac{\partial^2}{\partial x^2}\right)\chi.\end{aligned}$$

From (18) the components of $h_{\mu\nu}$ are found to be

(20)
$$\left\{\begin{array}{ll} h_{11} = \gamma_{11} + \tfrac{1}{2}\gamma, & h_{13} = \gamma_{13}, \\ h_{22} = \gamma_{22} + \tfrac{1}{2}\gamma, & h_{24} = \gamma_{24}, \\ h_{33} = \gamma_{33} + \tfrac{1}{2}\gamma, & h_{12} = h_{23} = h_{14} = h_{34} = 0. \\ h_{44} = \gamma_{44} - \tfrac{1}{2}\gamma. & \end{array}\right.$$

The formulæ (2) and (3) with these values of $h_{\mu\nu}$ give

(21)
$$\left\{\begin{aligned} 2G_{11} &= \frac{\partial^2}{\partial z^2}\Box\chi - \tfrac{1}{2}\Box\gamma \\ 2G_{22} &= -\frac{\partial^2}{\partial t^2}\Box\phi - \tfrac{1}{2}\Box\gamma \\ 2G_{33} &= \frac{\partial^2}{\partial x^2}\Box\chi - \tfrac{1}{2}\Box\gamma \\ 2G_{44} &= -\frac{\partial^2}{\partial y^2}\Box\phi + \tfrac{1}{2}\Box\gamma \\ 2G_{13} &= -\frac{\partial^2}{\partial x\,\partial z}\Box\chi \\ 2G_{24} &= -\frac{\partial^2}{\partial y\,\partial t}\Box\phi \\ G_{12} &= G_{23} = G_{14} = G_{34} = 0 \\ &\text{where} \\ \Box &\equiv \left(\frac{\partial^2}{\partial x^2} + \frac{\partial^2}{\partial y^2} + \frac{\partial^2}{\partial z^2} - \frac{\partial^2}{\partial t^2}\right). \end{aligned}\right.$$

Thus functions which satisfy the equations $\Box\phi = 0$, $\Box\chi = 0$, will also satisfy the field equations $G_{\mu\nu} = 0$. When ϕ and χ satisfy these conditions the values of the 4-index symbols from (2) are given by :—

$$
(22)\quad \left\{
\begin{aligned}
(1212) &= -(3434) = \tfrac{1}{4}\left(\frac{\partial^4}{\partial y^2\,\partial z^2} - \frac{\partial^4}{\partial x^2\,\partial t^2}\right)(\phi+\chi)\\
(1213) &= (2434) = \tfrac{1}{4}\frac{\partial^2}{\partial y\,\partial z}\left(\frac{\partial^2}{\partial t^2} - \frac{\partial^2}{\partial y^2}\right)(\phi+\chi)\\
(1214) &= (2334) = \tfrac{1}{4}\frac{\partial^2}{\partial y\,\partial t}\left(\frac{\partial^2}{\partial z^2} - \frac{\partial^2}{\partial x^2}\right)(\phi+\chi)\\
(1223) &= -(1434) = \tfrac{1}{4}\frac{\partial^2}{\partial x\,\partial z}\left(\frac{\partial^2}{\partial y^2} + \frac{\partial^2}{\partial t^2}\right)(\phi+\chi)\\
(1224) &= -(1334) = \tfrac{1}{4}\frac{\partial^2}{\partial x\,\partial t}\left(\frac{\partial^2}{\partial t^2} - \frac{\partial^2}{\partial y^2}\right)(\phi+\chi)\\
(1423) &= -(1234) = \tfrac{1}{2}\frac{\partial^4}{\partial x\,\partial y\,\partial z\,\partial t}(\phi+\chi)\\
(1313) &= -(2424) = \tfrac{1}{4}\left(\frac{\partial^2}{\partial x^2} + \frac{\partial^2}{\partial z^2}\right)^2(\phi+\chi)\\
(1314) &= -(2324) = \tfrac{1}{4}\frac{\partial^2}{\partial z\,\partial t}\left(\frac{\partial^2}{\partial x^2} + \frac{\partial^2}{\partial z^2}\right)(\phi+\chi)\\
(1323) &= (1424) = \tfrac{1}{4}\frac{\partial^2}{\partial x\,\partial y}\left(\frac{\partial^2}{\partial x^2} + \frac{\partial^2}{\partial z^2}\right)(\phi+\chi)\\
(1414) &= -(2323) = \tfrac{1}{4}\left(\frac{\partial^4}{\partial t^2\,\partial z^2} - \frac{\partial^4}{\partial x^2\,\partial y^2}\right)(\phi+\chi)\\
(1324) &= 0.
\end{aligned}
\right.
$$

For a linear oscillator we want a solution for which $\gamma_{22} = -e^{ip(t-r)}/r$ to first order, and the other components of $\gamma_{\mu\nu}$ vanish to this order of approximation. We can get this value for γ_{22} by taking

$$\phi = \chi = e^{ip(t-r)}/p^2 r.$$

There is no term in $1/r$ in any of the other components which are :—

$$
(23)\quad \left\{
\begin{aligned}
&\gamma_{24} = \frac{1}{(ip)}\frac{\partial}{\partial y}\gamma_{22}\,; \quad \gamma_{44} = \frac{1}{(ip)^2}\frac{\partial^2}{\partial y^2}\gamma_{22}\,;\\
&\gamma_{33} = \frac{1}{p^2}\frac{\partial^2}{\partial x^2}\gamma_{22}\,; \quad \gamma_{11} = \frac{1}{p^2}\frac{\partial^2}{\partial z^2}\gamma_{22}\,; \quad \gamma_{13} = \frac{1}{(ip)^2}\frac{\partial^2}{\partial x\,\partial z}\gamma_{22}.
\end{aligned}
\right.
$$

The values of $h_{\mu\nu}$ obtained by substituting from (23) in (20) are those given in (15) for the solution Y_2.

A solution satisfying the same conditions could be obtained by taking any other value of χ. The difference between this and the above solution would in general denote a real wave, but its terms of highest order would be of the doublet type. The exact wave of this class to be included must depend on the more minute structure of the oscillator.

The Thermal Conductivity of Gas Mixtures.

By T. L. Ibbs, M.C., Ph.D., and A. A. Hirst, M.Sc., Physics Department, University of Birmingham.

(*Communicated by* S. W. J. Smith, F.R.S.—Received November 28, 1928).

The action of the katharometer* as an instrument for gas analysis depends essentially upon the thermal conductivity of the gas mixture examined. One method of calibration for a given pair of gases is to make a number of mixtures of known composition by volume, and to obtain from them a curve showing how the deflection θ of the galvanometer in the bridge circuit of the instrument depends upon the composition of the mixture which surrounds one of the fine platinum helices. By reference to this curve, any other mixture of the two gases can be analysed when its deflection is known. A typical calibration curve is shown in fig. 1, which is for mixtures of helium and argon. The direction of the galvanometer deflection depends on whether the gas is a better or worse conductor than air. A useful convention is to regard the deflection for gases which are better conductors than air as positive.

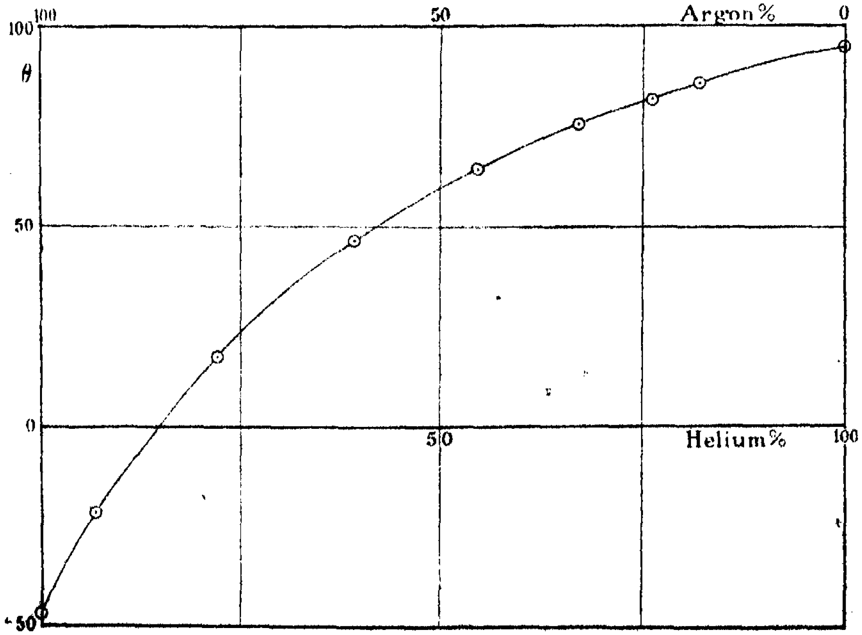

Fig. 1.—Katharometer Calibration Curve for Mixtures of Helium and Argon.

---

* *Cf.* Daynes and Shakespear, 'Roy. Soc. Proc.,' A, vol. 97, p. 237 (1920).

Daynes has examined the nature of the heat losses in the katharometer cell, which are due to (*a*) radiation, (*b*) convection, (*c*) conduction by the gas, (*d*) cooling of the platinum helix by metallic conduction along the copper lead. Even at the highest temperature used in the katharometer, the effect of (*a*) is very small, and will not be influenced directly by the nature of the gas surrounding the wire. Experiments have shown that the effect of (*b*) is also small. The effect of (*c*) on the temperature of the helix is large, and will depend upon the nature of the gas. The effect of (*d*) is also considerable, and will depend upon the temperature of the helix. This effect will consequently vary with the nature of the gas under examination, but the magnitude of the effect in the steady state which is reached depends upon the effect of (*c*) (the small effects of convection and radiation will similarly depend upon the effect of (*c*)). Thus in practice, the thermal conductivity of the gas controls the temperature of the helix, and the instrument will give the same reading for all gases or mixtures having the same thermal conductivity. Owing to the complicated design of the katharometer cell, it is not possible to make a simple calculation of the heat loss due solely to the conductivity of the gas, or to devise a method of converting katharometer readings directly into thermal conductivities. It should be noticed also that the calibration curves for different instruments are not all of quite the same form, owing to small differences in the winding of the helix, or of its position in the cell.

In the course of experiments* on thermal diffusion† for many pairs of gases, a considerable number of calibration curves for one instrument‡ has been obtained. As the readings of the instrument are so closely related to the thermal conductivity of the gas, it appeared to be of interest to try to obtain from these curves information on the conductivity of mixtures by an indirect method.§ This seemed likely to be of value since few observations‖ have been made on gas mixtures, except for air. Weber has made measurements on mixtures of argon and nitrogen, carbon dioxide and hydrogen, and on one mixture of nitrogen and hydrogen. Wassiljewa has worked on mixtures of oxygen and hydrogen, and Wachsmuth has worked on mixtures of argon and helium. The first method that we tried was to construct a curve showing the relation between katharometer deflection and the known thermal conductivity of a number of unmixed gases. By reference to this curve, the deflections for gas mixtures, or for other gases, might be converted into thermal conductivities. A smooth curve was obtained, but the method was not entirely successful. The gases hydrogen, helium and neon gave important points on the curve and any error in the accepted value of their conductivity was found to produce serious differences in its shape. (Gregory and Archer* have pointed out the great inconsistency shown in the results of various observers of the thermal conductivity of gases. For example, the results available for air at 0° C. vary from $4{\cdot}47 \times 10^{-5}$ cal. sec.$^{-1}$ cm.$^{-1}$ deg.$^{-1}$ (Eckerlein) to $5{\cdot}86 \times 10^{-5}$ (Müller). The mean value of 14 observers is $5{\cdot}22 \times 10^{-5}$, the average departure from the mean being about 7 per cent.)

---

* *Cf.* 'Roy. Soc. Proc.,' A, vol. 99, p. 385 (1921), vol. 107, p. 470 (1925), and Proc. Phys. Soc.,' vol. 39, p. 227 (1927).

† *Cf.* papers by Chapman, S., *e.g.*, 'Roy. Soc. Proc.,' A, vol. 93, p. 1 (1916); 'Phil. Trans.,' A, vol. 217, p. 157 (1917); 'Phil. Mag.,' vol. 34, p. 146 (1917), vol. 38, p. 182 (1919), and vol. 48, p. 602 (1924); 'Roy. Soc. Proc.,' A, vol. 119, p. 34 (1928), and vol. 119, p. 55 (1928), etc.

‡ This instrument was lent to us by Dr. G. A. Shakespear, who kindly helped with a number of the earlier calibrations.

§ After this work was begun Dr. Daynes wrote to one of us (T. L. I.) pointing out the possibility of correlating these calibration curves with thermal conductivity, and making a number of useful suggestions.

‖ *Cf.* Landolt and Börnstein's tables, p. 1304.

The next method attempted was to examine one of the pairs of gases for which the thermal conductivity of mixtures had already been measured, and for which we had a calibration curve. By comparing the results of the experiments made by Wachsmuth† on mixtures of helium and argon, with our calibration curve for this pair of gases, we were able to obtain a curve showing the relation between katharometer deflection and thermal conductivity at 0° C. over a wide range of values. Thus from fig. 1 (the calibration curve for the two gases), and fig. 2 (Wachsmuth's results) we were able to obtain fig. 3, showing the required relation between deflection θ and conductivity K_0. The curve can be smoothly extended by adding a point for the conductivity of hydrogen given by Gregory and Archer (*loc. cit.*) and its katharometer deflection. By interpolation from fig. 3 the conductivity corresponding to the galvanometer deflection for any gas or mixture can be obtained. In this way it is possible to draw curves showing the relation between conductivity and the proportions of the gases in a mixture, as shown in figs. 4 and 5. It was convenient to use the results of Wachsmuth for our purpose as the gases used for our calibration of helium and argon had been specially purified.‡ Wachsmuth's measurements are also of special theoretical interest, as they

---

* 'Roy. Soc. Proc.,' A, vol. 110, p. 91 (1926).

† 'Phys. Z.,' vol. 7, p. 235 (1908).

‡ Our thanks are due to Dr. F. W. Aston for valuable advice on the methods of purifying the inert gases.

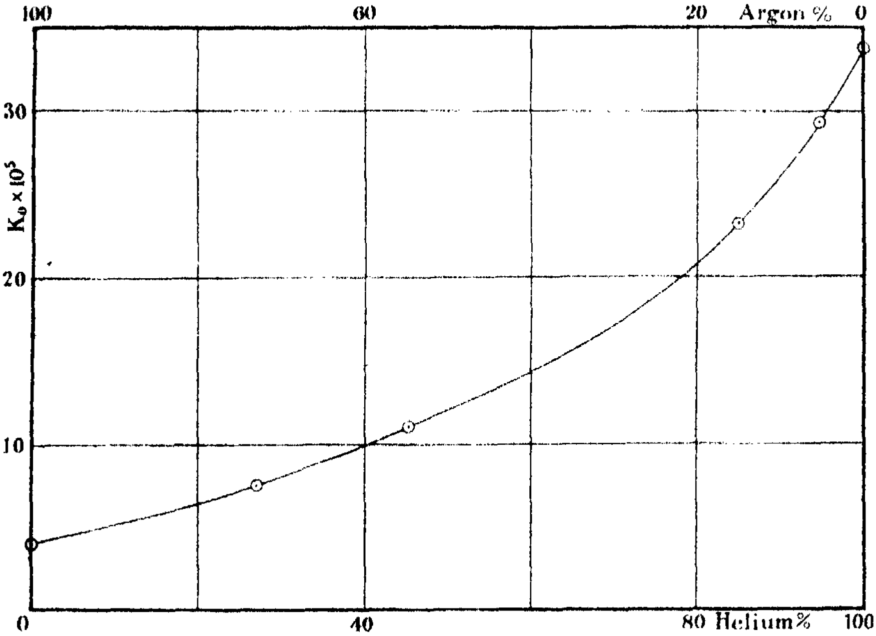

FIG. 2.—Thermal Conductivity of Mixtures of Helium and Argon (Wachsmuth).

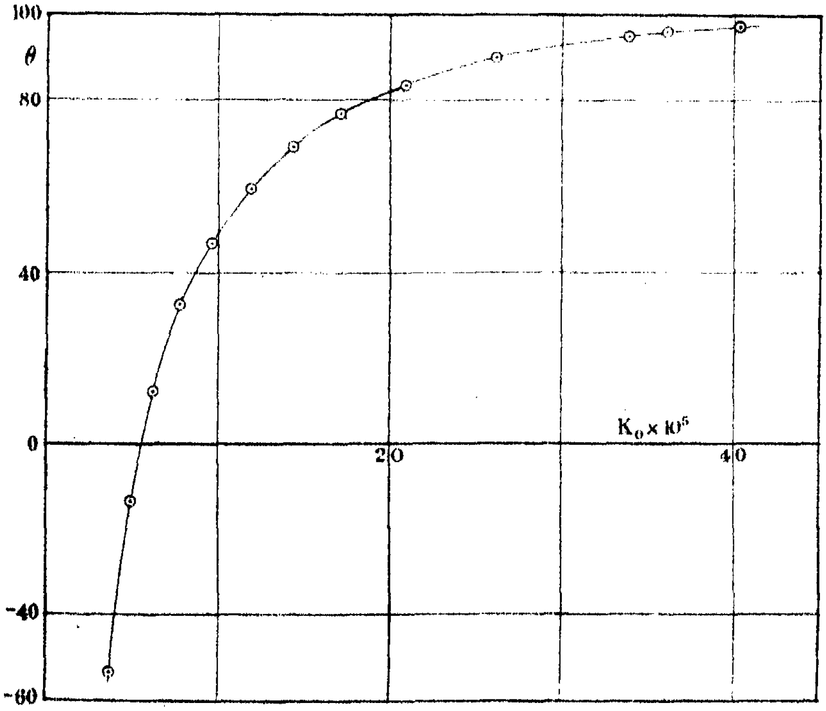

FIG. 3.—Relation between Conductivity and Katharometer Reading.

are in close agreement with Chapman's[*] calculated values of the conductivity of mixtures of these monatomic gases.

The sensitivity of the katharometer as a means of determining small changes of thermal conductivity K_0 is given by the slope of the curve in fig. 3. Thus it will be seen that $d\theta/dK_0$ is greatest when the thermal conductivity of the gas is small, and diminishes as the conductivity increases. This is due to the fact that for gases of low thermal conductivity the exposed platinum helix is at a higher temperature relative to the block, than when surrounded by a gas of greater thermal conductivity. When the temperature of the helix is high, it is more affected by a given change in thermal conductivity of the gas than when it is low. The changes in the resistance of the helix are therefore similarly affected by changes in the thermal conductivity of the gas. In an atmosphere of air the exposed helix has a temperature of about 15° C. above that of the copper block. In an atmosphere of argon the temperature of this helix rises, and in an atmosphere of helium, the temperature falls to little above that of the copper block.

The accuracy of the method depends of course upon the reliability of the absolute determinations on which it is based ; and we can hardly hope to attain by an indirect method a degree of accuracy which might be claimed for absolute determinations. It is found, however, that the values of the thermal conductivity of unmixed gases, derived from their katharometer readings in the way described, generally lie well within the range of published values. For example we obtain :

K_0 for oxygen = $5\cdot 7 \times 10^{-5}$ cal. sec.$^{-1}$ cm.$^{-1}$ deg.$^{-1}$.
,, air = $5\cdot 5 \times 10^{-5}$,, ,, ,,
,, carbon monoxide = $5\cdot 3 \times 10^{-5}$,, ,, ,,
,, carbon dioxide = $3\cdot 6 \times 10^{-5}$,, ,, ,,

The value for the carbon dioxide which was from a cylinder appears rather high, but it differs little from the value recently published by Gregory and Marshall.[†] A further interesting check is given by the results obtained for mixtures of hydrogen and carbon dioxide. These are found to be in satisfactory agreement with Weber's[‡] measurements on mixtures of this pair of gases. This is shown by the curves in fig. 4, where the two sets of values have been plotted. In view of the difficulty of making measurements of the thermal

---

[*] 'Phil. Trans.,' A, vol. 211, p. 467 (1912).

[†] 'Roy. Soc. Proc.,' A, vol. 114, p. 354 (1927).

[‡] 'Ann. Physik,' vol. 54, p. 481 (1917).

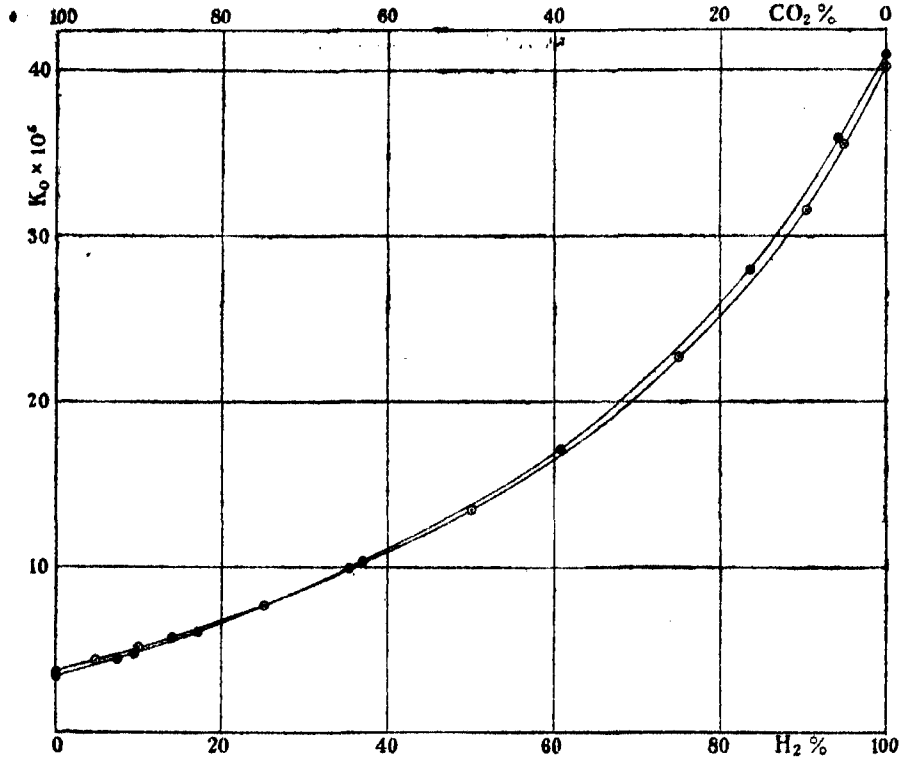

FIG. 4.—Conductivity of Mixtures of Hydrogen and Carbon Dioxide, ⊙ ; Weber's Values, ●.

conductivity of gases, the reasonable agreement in numerical value, and the close similarity in the shape of the curves, can be regarded as giving strong support to our method.

The advantage of the method lies chiefly in the comparative ease and rapidity with which the measurements of conductivity can be obtained. When once the instrument is standardised as described, the value of the thermal conductivity of a gas or mixture can be obtained in a few minutes. The method might be useful in circumstances, if any, where measurements of thermal conductivity are frequently required for practical purposes.* It might also prove to be a convenient way of obtaining the experimental information, which would be required as a starting point, for the development of a general kinetic theory of the conductivity of gas mixtures. For this purpose, where accuracy would be desirable, the gases should be as pure as possible, and the measurements made under steady conditions of temperature. The results shown in Table II generally refer to gases as supplied in cylinders, which were found to be sufficiently pure for our original purpose. The calibrations were made at ordinary room temperature, the fluctuations of which will have a small effect on the readings.* Also in stating the results in terms of K_0, the conductivity at 0° C., we have assumed that the conductivity at room temperature (say 15° C.) is proportional in all cases to the conductivity at 0° C. The small error thus introduced by neglecting the differences in temperature coefficient of conductivity of the various gases, need not be considered at present. The katharometer calibration data, and the derived thermal conductivity for mixtures of five pairs of gases are given in Table II. The results for mixtures of hydrogen and argon, and of hydrogen and nitrogen, are shown graphically in fig. 5. These curves show an interesting difference in shape.

---

* The method would apply to mixtures of two or more constituents.

Table I.—Standardisation Data.

(a) Wachsmuth's values for thermal conductivity of mixtures of helium and argon.		(b) Katharometer calibration data for mixtures of helium and argon.	
Percentage of helium in mixture.	$K_0 \times 10^5$.	Percentage of helium in mixture.	Galvanometer deflection.
0·0	3·894	0·0	−46·9
27·04	7·415	7·0	−22·0
45·37	10·77	22·5	+18·0
84·68	23·20	39·6	46·8
94·61	29·39	54·9	64·3
100·0	33·86	67·5	75·9
		76·4	81·8
		82·2	86·0
		100·0	94·95

---

* *Cf.* Daynes, *loc. cit.*, p. 285.

Table II.—Katharometer Calibration Data, and Deduced Thermal Conductivity for a Number of Gas Mixtures.

Hydrogen and carbon dioxide.

H_2 per cent.	Galvanometer deflection.	$K_0 \times 10^5$.
0·0	−52·8	3·6
4·9	−29·4	4·4
10·0	− 9·6	5·1
14·2	+ 3·2	5·7
25·0	30·4	7·7
35·5	48·9	10·0
50·0	66·5	13·5
75·0	86·2	22·7
90·1	93·8	31·5
95·0	95·7	35·5
100·0	97·8	40·4

Hydrogen and nitrogen.

H_2 per cent.	Galvanometer deflection.	$K_0 \times 10^5$.
0·0	− 0·1	5·5
15·9	+34·4	8·0
39·0	63·2	12·7
65·2	81·5	19·4
79·5	89·0	25·2
80·3	89·4	25·7
100·0	97·8	40·4

Hydrogen and carbon monoxide.

H_2 per cent.	Galvanometer deflection.	$K_0 \times 10^5$.
0·0	− 4·8	5·3
16·3	+34·7	8·0
27·2	51·2	10·3
56·6	79·0	18·0
63·4	83·7	20·9
79·4	90·6	27·0
100·0	97·8	40·4

Hydrogen and nitrous oxide

H_2 per cent.	Galvanometer deflection.	$K_0 \times 10^5$.
0·0	−49·8	3·8
7·5	−14·5	4·8
20·9	+24·2	7·1
38·6	54·1	10·7
59·9	77·2	17·0
81·2	90·9	27·2
100·0	97·8	40·4

Hydrogen and argon.

H_2 per cent.	Galvanometer deflection.	$K_0 \times 10^5$.
0·0	−46·9	3·9
9·0	− 1·2	5·5
18·0	+26·1	7·3
40·0	62·5	12·6
60·0	80·3	18·7
80·2	90·7	27·0
100·0	97·8	40·4

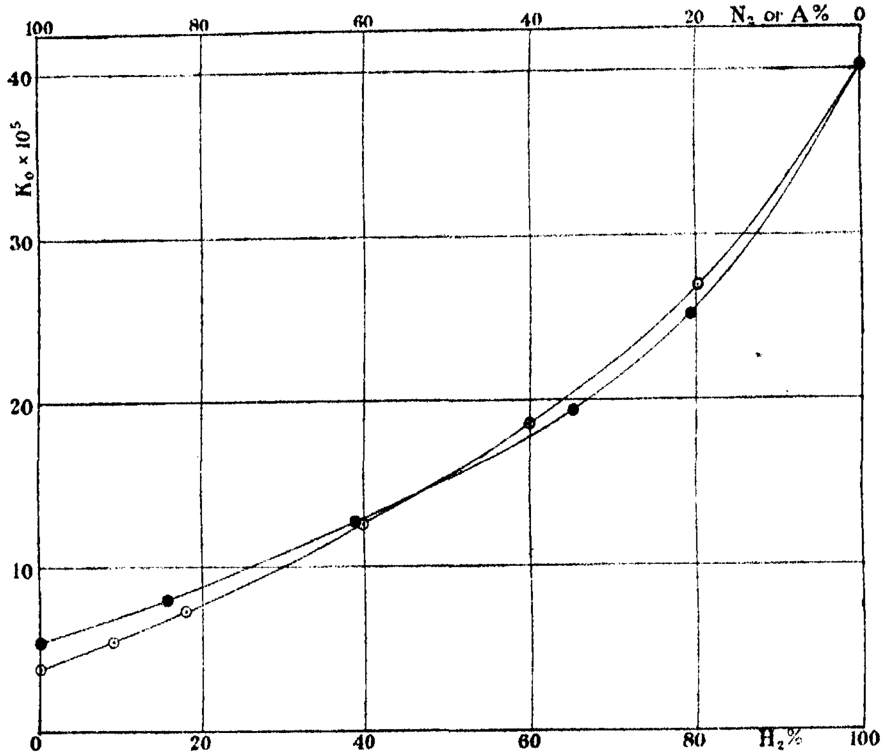

Fig. 5.—Thermal Conductivity of Gas Mixtures. ⊙, Hydrogen and Argon. ●, Hydrogen and Nitrogen.

Values of thermal conductivity might also be obtained in the same way for other pairs of gases which we have examined, where the range of conductivity is more limited, *e.g.*, nitrogen and carbon dioxide. It will be clear, however, that we can take as our starting point the absolute determinations on any other pair of gases, instead of Wachsmuth's values for helium and argon; provided that they cover the range of thermal conductivity required. Thus Weber's results for mixtures of nitrogen and argon might with advantage be employed for dealing with a more limited lower range of conductivities, over which the katharometer is particularly sensitive. Sufficient results have already been given to indicate the possibilities of the method. In the course of further experiments on thermal diffusion now in progress, it is hoped to obtain additional information regarding the conductivity of mixtures.

The Behaviour of a Single Crystal of Zinc subjected to Alternating Torsional Stresses.

By H. J. Gough, M.B.E., D.Sc., Ph.D., and H. L. Cox, B.A., National Physical Laboratory.

(Communicated by Sir Thomas Stanton, F.R.S.—Received December 1, 1928.)

[Plates 6–11.]

The present experiment has been carried out in the course of a general investigation into the causes and characteristics of the failure of metals under repeated cycles of stress which has been in progress for some years past at the National Physical Laboratory. As this research proceeded, one definite and promising line of investigation suggested itself in the study of the behaviour of single metallic crystals under repeated stress systems, and, as a commencement, attention is being directed to typical metals crystallising in the cubic (face-centred, also body-centred), close packed hexagonal, and rhombohedral space lattice systems. The investigation, when completed, should not only give certain fundamental data concerning *fatigue* phenomena, but also, when studied in conjunction with the classical researches of Mark, Polanyi and Schmid, Taylor, Elam, and Farren—who have studied in detail, the characteristics of deformation of single crystals under *static* stressing—afford some contribution towards the discovery of the general laws of deformation of metals subjected to any stress system. Previous reports have described experiments on single crystals of aluminium* † (face-centred cubic) and iron‡ (body-centred cubic). The present paper describes an experiment on a single crystal of zinc, a metal crystallising in the hexagonal (close-packed) lattice.

The deformation of zinc crystals under statical direct stress has received much attention from Mark, Polanyi and Schmid.§ They showed clearly that the principal slip plane is the basal (0001) plane, the direction of slip being that of the most highly stressed (shear stress) primitive direction (normal to the $\bar{1}2\bar{1}0$, $\bar{1}\bar{1}20$, or $2\bar{1}\bar{1}0$ plane) contained by the basal plane. In the last stages of deformation, however, they found that deformation was consistent with slip occurring on planes apparently perpendicular to the basal planes, and they suggested that prismatic planes were also slip planes; they were unable, however, to establish this identity.

---

* 'Phil. Trans.,' A, vol. 226, p. 1 (1926).

† 'J. Inst. Met.,' vol. 36, No. 2 (1926).

‡ 'Roy. Soc. Proc.,' A, vol. 118, p. 498 (1928).

§ 'Z. Physik,' vol. 12, p. 58 (1922).

Mathewson and Phillips* have also studied the deformation of zinc crystals under static loading. They confirmed the identity of the basal plane as the principal slip plane, but found no evidence of slip on prismatic planes. A careful study was also made of the well-known surface markings present in deformed zinc which are usually ascribed to "twin" formation, and excellent evidence was obtained—based on the positions of the edges of these markings—that the twinning plane of zinc was a pyramidal plane of the general type, $01\bar{1}2$. It was shown that twinning about this plane—of the type in which the twinned structure is, in effect, a "mirror-image" of the original structure—would produce a twinned basal plane whose position would make a small angle only, 4°, with prismatic planes of the parent crystal. Hence, it was suggested that the cleavages observed by Mark, Polanyi and Schmid, and associated by them with failure on prismatic planes, might conceivably be due to failure along the twinned basal planes. Romig,† also Wilson and Hoyt,‡ have carried out experiments which in the main confirm the conclusions of Mathewson and Phillips, but contribute little definite evidence on the main questions involved.

Scheme of Present Work.

A study of the previous work on zinc (summarised briefly above) revealed several important points to which attention might usefully be directed. It appeared to be established that the principal slip plane of zinc—under static loading—was the basal (0001) plane, the direction of slip being that of the most highly stressed primitive lattice direction; and, from our previous experience, this law would also be expected to apply under fatigue stressing. Direct evidence was undoubtedly required as to whether prismatic planes would, under suitably chosen conditions, also act as slip planes. By a suitable choice of relative position of the straining and crystallographic axes, the resolved shear stress on prismatic planes could be made, at all parts of the specimen, greater than that on the basal plane; further, by employing alternating torsional stresses, the resolved shear stress on the basal plane, while having a high value at some parts of the specimen, would not exceed a very low value at other parts.

With regard to any possible twinning arising during the test, measurements of the edges of the twins should enable the twinning plane to be identified with certainty and permit of a quantitative study of the relation of the mechanism of formation of the twins to the applied stressing system. Now in the previous work on zinc, the presence of twins was made apparent merely by the difference of colour exhibited by the surface of the material contained within the supposed twin, no indication (beyond some very indefinite X-ray evidence) being obtained of the *structure* within the twin.* By using a very carefully polished crystal surface, however, it should be possible to detect slip bands within the twin, and by means of measurements, to establish the identity of the plane of slip, particularly if, in the course of the experiment, it should emerge conclusively that slip is confined to one particular type of plane only. The choice of alternating torsional stresses was finally determined by the facts that surface phenomena on diametrically opposite portions of the specimens would be precisely similar, although opposite in sign, and that our experience has shown that, with this type of stressing, soft single crystals can be fractured without appreciable distortion of the specimen as a whole.

---

* 'Amer. Inst. Min. Met. Eng.,' Paper No. 1623 E, February, 1927.

† 'Amer. Inst. Min. Met. Eng.,' February, 1927.

‡ 'Amer. Inst. Min. Met. Eng.,' Tech. Pub. No. 25. September, 1927.

Analysis showed that the most suitable specimen for the purpose of the experiment would be a crystal in which the basal planes were approximately parallel to the axis of torsion ($\theta_{0001} \simeq 90°$). The crystals at our disposal were submitted to X-ray analysis and the specimen (Reference Mark Z3A) used in the present experiment was chosen, the value of θ_{0001} being 88°.

Preparation of Specimens, etc.

The single crystal used in the experiment was prepared from the liquid—by the Bridgman method—and was ⅝-inch diameter and 10 inches in length. An X-ray photograph made at this stage revealed clearly defined reflections free from "asterism" effects. The specimen was then machined to a cylindrical form, 0·35-inch diameter and 0·75 inch in length with enlarged ends (joined by transition curves) of diameter 0·5 inch, the total length being 3 inches. Preliminary tests showed that extreme care is necessary in machining these specimens, as the crystals tend to cleave along basal planes; in the final preparation of the specimen used, cuts of 0·001 inch were found to be the maximum permissible. Suitable reference marks were carefully engraved on the enlarged ends of the specimen for purposes of measurement. An X-ray photograph revealed a "powder" (concentric rings) pattern, showing, as was expected, that the effects of machining had produced severe surface distortion and recrystallisation. After etching followed by a metallurgical polishing, a second X-ray photograph showed that the rings were beginning to resolve into spots, but that the effect of the surface deformation was not yet removed. Five such treatments of etching and polishing followed by X-ray analysis were found to be necessary before the crystal was considered to be in a suitable condition to proceed with the experiment. The stereographic diagram of fig. 1 shows the relative orientation of the specimen axis (and reference mark)

---

* [*Added January* 11, 1929.—In a more recent paper by Schmid and Wassermann ('Z. Physik,' vol. 48, p. 377, 1928) an experiment is described in which definite X-ray evidence was obtained that the after-stretching, occurring in the last stages of a static tensile test, is due to a process of slip on twinned basal planes.]

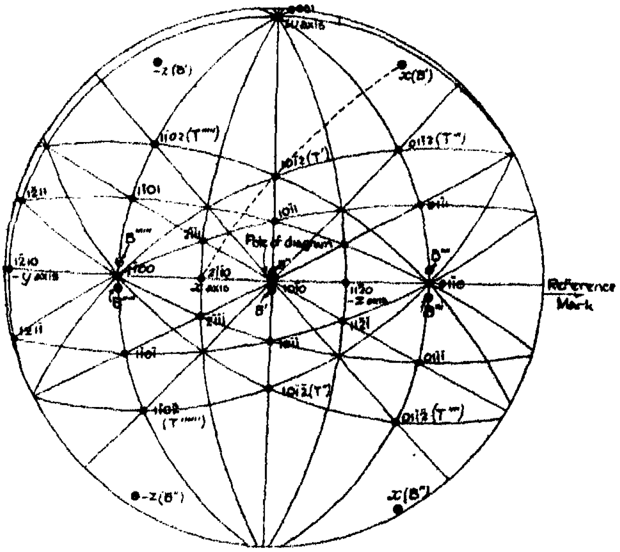

Fig. 1.—Stereographic diagram showing position of principal planes also twinned positions of the basal planes and primitive directions.

Note.—The six possible twinning planes (type $10\bar{1}2$) are denoted by (T'), (T'') ----- (T''''''). The corresponding twinned positions of the basal plane (0001) are shown thus : ⊕ B', ------ ⊕ B''''''.

and the principal crystallographic planes as determined from the corrected X-ray analysis. (The spherical co-ordinates of the planes are listed in Table II.) The diameter of the specimen was found, by projection, to be 0·341 inch.

Record of Experiment.

The specimen was placed in the alternating torsion machine and subjected to one million reversals of a range of torque of ± 8·7 inch lbs. (nominal range of shear stress ± 0·5 tons/inch^2). The entire surface of the specimen was then carefully examined in a metallurgical microscope, using a 4 mm. Apochromat objective (Zeiss). Apart from polishing scratches, the surface was entirely free from markings of any kind, and nothing approaching the appearance of a slip band or twin band was visible. The specimen was replaced in the machine and subjected to one million reversals of a higher range of torque, ± 17·4 inch lbs. ($f_s = \pm 1\cdot0$ tons/inch^2), after which it was removed from the machine. A very searching examination of the surface again failed entirely to reveal any surface markings which could be associated with the straining of the specimen. A series of high magnification photo-micrographs was taken and compared with photographs of the same portions of the surface taken before the test was commenced, and these confirmed the conclusion, drawn from the visual examination, that no visible change had occurred in the surface. Measurement of the relative positions of the reference marks, placed at each end of the specimen, showed that the specimen had not suffered any permanent strain. The specimen was replaced in the testing machine and the applied range of torque adjusted to ± 26·1 inch lbs. ($f_s = \pm 1\cdot5$ tons/inch^2). The automatic cut-out of the machine was adjusted closely so that the machine would be stopped should the range of strain of the specimen increase appreciably. This occurred after a further 768,200 reversals had been endured, and on examination the specimen was found to be cracked. Measurement of the relative positions of the reference marks on the enlarged ends of the specimen showed a total twist of 1·4° only; as this included the movement due to the opening of the crack, the total distortion of the specimen must have been extremely small and may be neglected. Examination of the surface of the specimen, with the unaided eye, revealed the presence of two sets of X markings extending the whole length of the parallel portion of the specimen. Their maximum width and intensity occurred approximately at the positions $\lambda = 0°$ and $\lambda = 180°$ and they were visible within an angle of approximately ± 40° from these positions, the remainder of the specimen being apparently free from these or other markings. Their appearance (dull and lustreless) was typical of the "twin" bands previously reported by many investigators.

A very complete survey was then made of the surface markings on the specimen. The apparatus used for this purpose has been described very fully in a previous paper;* as before, λ represents the angle subtended by the reference plane (containing the reference mark on the enlarged end of the specimen) and the point on the surface referred to.

A number of representative photo-micrographs were taken and some of these are reproduced in Plates 6 to 11. In these photographs, the black vertical line is the reference line—of zero slope—for the slope of the slip bands or twin markings; positive and negative angles are measured, respectively, anticlockwise and clockwise from this datum line.

---

* 'Roy. Soc. Proc.,' A, vol. 118, p. 498 (1928).

Before describing in detail the features exhibited by the microstructure it will be convenient to state the conventions and symbols adopted regarding the crystallographic structure of zinc.

Lattice Structure of Zinc; Conventions and Symbols adopted in the present Research.—Zinc crystallises in the close-packed hexagonal system; the unit atomic spacing on the 0001 (basal) plane being 2·670 Å. while the value of the axial ratio is 1·860.

Fig. 2 is a stereographic diagram showing the positions of the principal crystallographic planes. The primitive lattice directions x, y, z* (normals to the $2\bar{1}\bar{1}0$, $\bar{1}2\bar{1}0$ and $\bar{1}\bar{1}20$ planes, respectively) lie in the plane of the diagram,

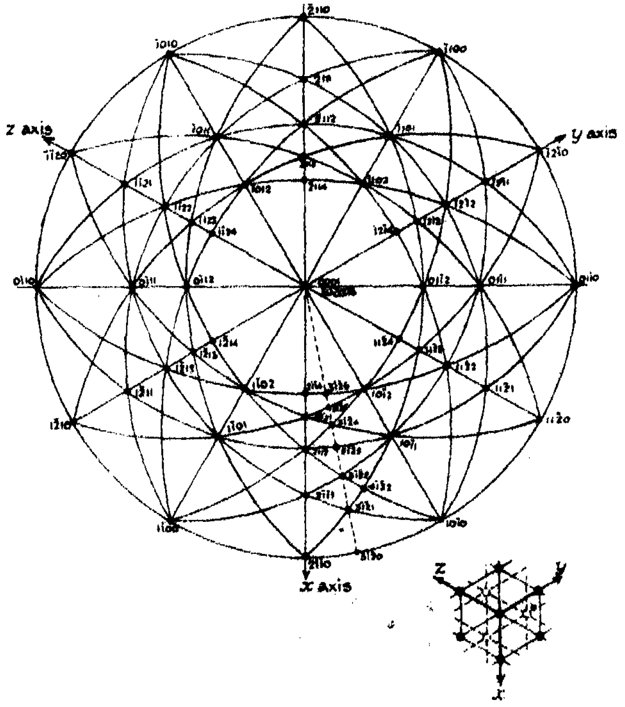

Fig. 2—Stereographic Projection of Hexagonal (close packed) System. Axial Ratio 1·86.

0001	Basal plane.	$11\bar{2}0$	2nd order prismatic.	$10\bar{1}1$	1st order pyramidal.	$11\bar{2}1$	2nd order pyramidal.
$10\bar{1}0$	1st order prismatic.	$\bar{1}210$		$1\bar{1}01$		$\bar{1}211$	
$1\bar{1}00$		$\bar{2}110$		$0\bar{1}11$		$\bar{2}111$	
$01\bar{1}0$				etc.		etc.	

---

* One of these is in effect redundant; two translations being sufficient to include all atoms in the basal plane.

while the remaining primitive direction, w (normal to the 0001 plane) is perpendicular to that plane. The axes x, y, z, are, of course, crystallographically indistinguishable; to avoid confusion, however, the adopted convention has been carefully adhered to throughout this report. The inset diagram in fig. 2 shows the relation of the x, y and z axes with the atoms of adjacent basal planes.

The convention adopted concerning "first" and "second" order planes is as follows:—*First order* prismatic planes each contain one of the primitive directions x, y and z, together with the primitive direction w. Denoting prismatic planes by the letter "P," while an appropriate suffix indicates the primitive direction contained by the plane, the first order prismatic planes—$01\bar{1}0$, $10\bar{1}0$, and $1\bar{1}00$—become P_x, P_y and P_z respectively. The second order prismatic planes—$2\bar{1}\bar{1}0$, $\bar{1}2\bar{1}0$ and $\bar{1}\bar{1}20$—do not contain either x, y or z, but each is equally inclined to two of these directions; they are conveniently denoted, therefore, by the symbols P_{yz}, P_{zx} and P_{xy} respectively.

Pyramidal planes, in general, are denoted by "p." First order pyramidal planes contain one of the primitive directions x, y or z, and are conveniently denoted, in general, by the symbols p_x, p_y or p_z, while p_{yz}, p_{zx} and p_{xy} indicate second order pyramidal planes. But as there exists a single infinity of each type of these planes, some further distinguishing convention is required. Accordingly, first order pyramidal planes of the $01\bar{1}1$ and $01\bar{1}2$ types are termed respectively "first order pyramidal (one)" and "first order pyramidal (two)," and are denoted by the symbols p_x^1 and p_x^2, respectively. Similarly, we obtain the symbols p_{xy}^1, p_{yz}^1 and p_{zx}^1 for the "second order pyramidal (one)" planes. The first and second order pyramidal planes, of any particular type, occur in pairs, *e.g.*, $01\bar{1}1$ and $0\bar{1}11$ being situated on opposite sides of the normal to the 0001 plane and making equal angles with that normal. These pairs are distinguished by plus or minus signs preceding the affix, thus: p_x^1 ($01\bar{1}1$) and p_x^{-1} ($0\bar{1}11$). Table I shows Millerian indices and conventional symbols of the principal crystallographic planes which have been considered in the present research.

Table I.—Spherical Co-ordinates and Stress Equation Constants.

Plane.						Constants in resolved shear stress equations.*			
Millerian indices.	Type.	Relative density.	Symbol.	Spherical co-ordinates.		Symbol.	Resolved Primitive direction.	A.	α°.
				θ°.	ψ°.				
0001 (w axis)	Basal.	1·0	B	88·0	92·1	Bx	$2\bar{1}\bar{1}0$	0·872	3·1
						By	$1\bar{2}10$	0·039	92·0
						Bz	$11\bar{2}0$	0·856	0·9
$01\bar{1}0$	1st order prismatic.	0·47	P_x	60·8	0·9	$P_x x$	$2\bar{1}\bar{1}0$	0·527	88·8
						$P_x w$	0001	0·488	178·5
$10\bar{1}0$			P_y	2·1	289·0	$P_y y$	$1\bar{2}10$	0·999	92·0
						$P_y w$	0001	0·997	2·0
$1\bar{1}00$			P_z	59·3	183·5	$P_z z$	$11\bar{2}0$	0·479	6·8
						$P_z w$	0001	0·527	88·8
$2\bar{1}\bar{1}0$ (x axis)	2nd order prismatic.	0·54	P_{yz}	29·1	186·0	$P_{yz} w$	0001	0·872	3·1
$1\bar{2}10$ ($-y$ axis)			P_{xz}	89·0	182·0	$P_{xz} w$	0001	0·038	2·0
$11\bar{2}0$ ($-z$ axis)			P_{xy}	31·0	358·5	$P_{xy} w$	0001	0·856	0·7
$01\bar{1}1$	1st order pyramidal (one).	0·42	p_x^{1}	62·6	29·2	$p_x^{1}x$	$2\bar{1}\bar{1}0$	0·575	128·4
$01\bar{1}\bar{1}$			p_x^{-1}	64·8	333·3	$p_x^{-1}x$	$2\bar{1}\bar{1}0$	0·625	53·0
$10\bar{1}1$			p_y^{1}	22·9	90·6	$p_y^{1}y$	$1\bar{2}10$	0·921	91·7
$10\bar{1}\bar{1}$			p_y^{-1}	27·1	274·5	$p_y^{-1}y$	$1\bar{2}10$	0·890	92·6
$1\bar{1}01$			p_z^{1}	61·2	155·0	$p_z^{1}z$	$11\bar{2}0$	0·531	54·2
$1\bar{1}0\bar{1}$			p_z^{-1}	63·2	211·9	$p_z^{-1}z$	$11\bar{2}0$	0·581	134·9
$01\bar{1}2$	1st order pyramidal (two).	0·34	$p_x^{2}(T^{3})$	67·5	48·7	$p_x^{2}x$	$2\bar{1}\bar{1}0$	0·682	149·5
$01\bar{1}\bar{2}$			$p^{-2}(T^{4})$	70·9	314·8	$p_x^{-2}x$	$2\bar{1}\bar{1}0$	0·739	35·2
$10\bar{1}2$			$p^{2}(T')$	40·9	91·4	$p_y^{2}y$	$1\bar{2}10$	0·756	91·5
$10\bar{1}\bar{2}$			$p_y^{-2}(T^{2})$	45·1	272·7	$p_y^{-2}y$	$1\bar{2}10$	0·707	93·3
$1\bar{1}02$			$p^{2}(T^{5})$	66·6	135·8	$p_z^{2}z$	$11\bar{2}0$	0·653	33·6
$1\bar{1}0\bar{2}$			$p_z^{-2}(T^{6})$	69·5	230·1	$p_z^{-2}z$	$11\bar{2}0$	0·704	152·2
$11\bar{2}\bar{1}$	2nd order pyramidal (one).	0·26	p_{xy}^{1}	35·1	332·7				
$11\bar{2}1$			p_{xy}^{-1}	33·1	26·8				
$2\bar{1}\bar{1}1$			p_{yz}^{1}	31·8	156·6				
$2\bar{1}\bar{1}\bar{1}$			p_{yz}^{-1}	33·7	213·2				
$1\bar{2}1\bar{1}$			p_{xz}^{1}	89·6	197·3				
$1\bar{2}11$			p_{xz}^{-1}	88·8	167·0				

* $S_{rs} = SA \cos(\lambda - \alpha)$,
where S_{rs} = value of resolved shear stress.
S = nominal maximum shear at surface of specimen.

The convention of symbols explained above is of especial usefulness in denoting resolved shear stresses on a certain crystallographic plane in one of the primitive lattice directions. Thus Bx denotes "value of the shear stress on the basal (0001) plane resolved in x (normal to $2\bar{1}\bar{1}0$ plane) direction."

Table II shows the atomic density on some of the principal crystallographic planes of zinc.

Table II.—Atomic Density on some of the Principal Crystallographic Planes of Zinc.

Plane.	Density.	
	Actual.*	Relative.
0001	1·155	1·00
$2\bar{1}\bar{1}0$	0·621	0·54
$2\bar{1}\bar{1}2$	0·547	$0·47_4$
$01\bar{1}0$	0·538	$0·46_6$
$01\bar{1}1$	0·488	0·42
$01\bar{1}2$	0·393	0·34
$2\bar{1}\bar{1}1$	0·300	0·26

* Atoms per (lattice parameter)^2.

Stress Analysis of Zinc Single Crystal (Z.3A).

Resolved Shear Stress.—The stress equations to the shear stresses on the principal crystallographic planes resolved in the direction of the primitive lattice direction (s) contained by the planes have been evaluated and the equation constants are as stated in Table I. The stress equation* is of the general form

$$S_r/S = A \cos(\lambda - \alpha),$$

where S_r = value of resolved shear stress.

S = maximum shear stress on specimen.

$= \dfrac{2T}{\pi r^3}$ where T is the applied torque and r is the radius of the cross-section of the specimen.

$$A = \{-\tfrac{1}{2}(\cos 2\theta_p + \cos 2\theta_d + 2\cos 2\theta_p \cos 2\theta_d)\}^{\frac{1}{2}}.$$

$$\alpha = \tan^{-1}[(\tan^2\theta_p - 1)\cot(\psi_d - \psi_p)] + \psi_p,$$

and θ_p, ψ_p and θ_d, ψ_d are the spherical co-ordinates of the plane and contained direction, respectively.

In fig. 3 the graphs of these equations have been plotted for the following sets of crystallographic planes :—

Basal plane (B), first order prismatic plane (P),
First order pyramidal—one (p', p^{-1}), and
First order pyramidal—two (p^2, p^{-2}).

---

* See 'J. Inst. Metals,' vol. 36, p. 185 (1926

The diagram shows that the choice of the particular specimen employed—for the purpose of a critical test—was correctly made, as at every point of

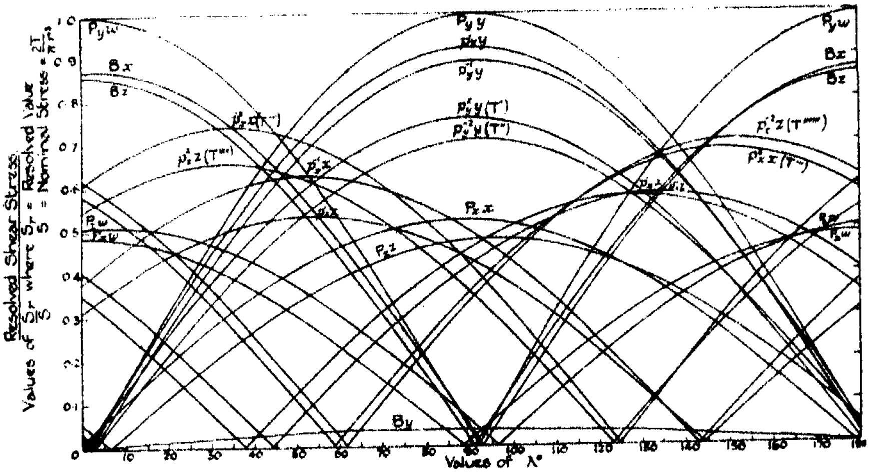

Fig. 3.—Shear Stress Curves on the principal crystallographic planes resolved in the primitive lattice directions.

the circumference, the value of the resolved shear stress on a first order prismatic plane is greatly superior to that on the basal plane, while at the positions denoted by λ = 92° and 272°, the resolved stress on the prismatic plane is a maximum ($S_r/S = 0·999$), while the resolved stress on the basal plane is very low indeed ($S_r/S = 0·039$). The slopes of the traces of the principal crystallographic planes were calculated and expressed graphically, but the reproduction of the diagram here would serve no useful purpose.

Normal Stresses.—Using the equation* $N/S = \sin 2\theta_p \sin (\psi_p - \lambda)$ the value of the normal stresses N on the basal plane, also on the first order pyramidal (two) planes were evaluated and plotted on fig. 7.

Features Exhibited by Microstructure.—The features exhibited by the microstructure were of three distinct types which are conveniently studied separately and in detail. These features were (A) a system of closely spaced slip bands nearly parallel to the axis of the specimen ; (B) a system of two distinct sets of twin bands ; (C) a crack extending over the region λ = 330° to λ = 40°.

Using the measuring apparatus previously described, complete surveys were made of the surface of the specimen at various distances along the axis, and detailed series of measurements taken of the slope of slip bands, edges of twin bands, etc. A very significant fact is that all the features exhibited by the microstructure were reproduced exactly (with, of course, reversal of sign) at diametrically opposite portions of the surface, and this, when studied in conjunction with the applied stress system, shows conclusively that the observed changes in microstructure are due to the applied "stress" effects; this is of especial importance in connection with the observed twinning effects, as it has been stated that metals which crystallise in the close-packed hexagonal lattices, *e.g.*, zinc and cadmium, have no possible twinning planes, and that what is called twinning in these metals is more probably something in the nature of parallel growth.

---

* See 'J. Inst. Metals,' vol. 36, p. 185 (1926).

(A) *Slip Band System.* A closely spaced system of slip, nearly parallel to the axis, extended over the areas $\lambda = 140°$ to $210°$ and $\lambda = 320°$ to $40°$, having maximum intensities in the vicinity of $\lambda = 3°$ and $183°$. Figs. S, T, and U (Plate 10) are typical. On either side of these positions of maximum intensity the extent of the area occupied by the system diminished as the distance from these positions increased. Thus at positions, $\lambda = 30°$, $150°$, $205°$ and $320°$, large areas of the specimen were entirely free from slip bands, although other areas exhibited a closely spaced system. The areas between $\lambda = 40°$ to $140°$, also $\lambda = 210°$ to $320°$ were entirely free from these slip bands with the exception of a little slip in the immediate vicinity of the twins. An illustration of the sudden manner in which these slip bands ceased is brought out by a comparison of figs. P, $\lambda = 310°$ $(130°)$, and Q, $\lambda = 140°$.

The recorded measurement of the slope of the slip bands are indicated by the full circles of the curve marked B of fig. 4*. The actual curve, B, represents the calculated trace of the basal plane, and the agreement of the slip bands with the trace of the basal plane is sufficiently obvious. Referring to fig. 3 and Table I, it is seen that the positions of the maximum values of the resolved shear stresses on the basal plane occur at the points $\lambda = 3\cdot1°$ and $183\cdot1°$ which also correspond to the positions of maximum intensity of the slip bands. Thus it is apparent that the slip plane concerned, in the present experiment, was the basal (B) plane and that the deformation under fatigue stressing resulted according to the law—previously established for other metals—of greatest resolved shear stress in the primitive direction.

It has been mentioned (see fig. 4) that the limits of the areas exhibiting basal plane slip were represented by $\lambda = 40°$, $140°$, $210°$ and $320°$. Fig. 3 shows that at these points the value of the stress factor S_r/S for the basal plane had the values of 0·7, 0·65, 0·77 and 0·65 respectively, corresponding to actual resolved shear stresses, during the third and final fatigue test, of ± 1·05, ± 0·98, ± 1·15 and ± 0·98 tons/inch^2. Thus the resolved shear stress necessary to produce visible slip had a value slightly lower than ± 1 ton per square inch. Now, after the second test, at a *nominal* maximum shear stress of ± 1 ton/inch^2 we were somewhat surprised to find no visible slip bands present. Fig. 3 (and Table I), however, shows that the maximum value of A in the stress equations for the basal plane was 0·872 and the resolved shear stress, at any part of the surface, could not have exceeded 0·872 tons/inch^2. Thus, our observations are entirely consistent and also indicate that this specimen* exhibited a clearly defined "visible slip limit" at a range of stress greater than ± 0·87 and less than ± 0·98 tons/inch^2. Further, if it be assumed (and the asumption is logical) that failure would not have preceded visible slip, the limiting range of resolved shear stress of this particular specimen can be estimated at some value intermediate between ± 1·0 and ± 1·3 tons/inch^2.

---

* *Note.*—The individual readings of the series taken at each value of λ varied by about $\pm 1\cdot5°$ from the values recorded in fig. 4; these small variations have been ignored in preparing the diagram.

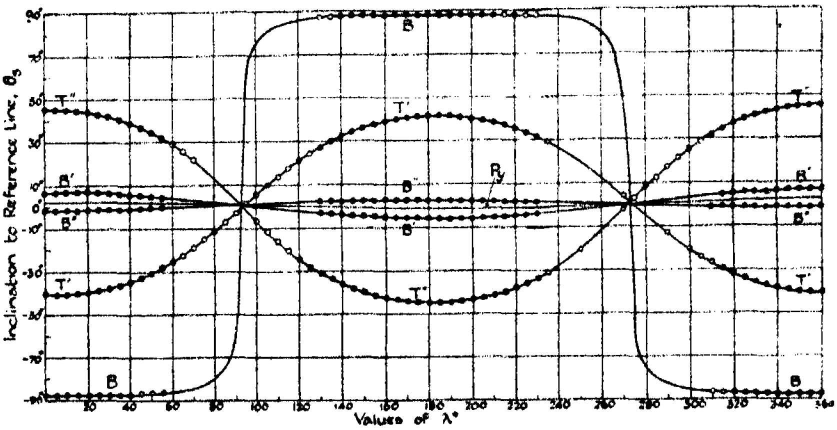

Fig. 4.—Theoretical Slopes of Traces of Twinning Planes, of original basal plane and of the twinned basal planes, together with observed slopes of slip bands and twins.

To return to one of the most important objects of the experiments, *i.e.*, the possibility of prismatic planes as slip planes. The resolved shear stresses on the first order prismatic plane (P_y, see fig. 3 and Table I) attain maximum values at λ = 2°, 92°, 182° and 272°. At the positions λ = 0° and 180°, we have seen that the basal plane was the slip plane, but much more significant is the fact that the surface of the specimen at λ = 90° and 270° (figs. J and K,

---

* Other experiments still in progress have shown that this "slip limit" is partly controlled by the orientation of the slip plane in relation to the straining axis. The restraining influences of the enlarged ends of the specimen are, no doubt, responsible.

Plate 8) was entirely free from any slip band markings. Further, at no portion of the surface were any slip bands observed whose slopes agreed with the calculated traces of prismatic planes. This evidence appears to be conclusive in showing that, even under the critical stress conditions imposed in the present test, slip was confined to the basal plane.

(B) *Twin Markings.*—Two distinct systems of twins were present. In each system, the maximum width of the twin occurred at positions in the neighbourhood of $\lambda = 0°$ and 180°. Figs. R and U (Plate 10) show clearly both sets visible in the same field, while figs. N and O (Plate 9) show two fields—each occupied by one system—taken at equivalent values of λ. (In connection with the photographs it may be mentioned that in an area containing twins distinct differences of level were apparent and the securing of satisfactory photographs was very difficult; the focussing was finally adjusted so as to bring out the maximum amount of *general* detail and thus the photo-micrographs represent a somewhat unsatisfactory compromise. The measurements recorded were obtained using a high-power objective focussed on the particular detail required; hence, the quality of the photographs is necessarily inferior to the accuracy of the measurements; the latter is, however, much more important.) The general characteristics of the twins can be briefly described as follows: within the areas $\lambda = 310°$ to $\lambda = 55°$, also $\lambda = 130°$ to $\lambda = 230°$, the twins were clearly identifiable as such not only by the edge of the twin and the adjacent basal plane slip bands, but also by a system of slip bands clearly visible *within* the twin, the slope of the latter being approximately at right angles to the axis of the specimen; to such cases, we applied the term "resolvable" twins. Figs. A, D, G, Q, R, S, T and U (Plates 6–10) all show clearly the presence of slip bands within the twin. In the regions intermediate between these areas, the twins appeared merely as systems of parallel markings of the varying types shown in figs. J, K, L, M, N and O; we have referred to these as "unresolved twins." With regard to the size and spacing of the twins, the latter were observed to be in the most clearly developed state and in the greatest profusion at the positions $\lambda = 0°$ and $\lambda = 180°$ and diminished both in size and frequency towards $\lambda = 90°$ and $\lambda = 270°$ where very few twins could be observed (see figs. J. and K, Plate 8). Thus at the positions of maximum basal plane slip ($\lambda = 0°$ and 180°), the most fully developed twins occur, while only a very few extremely small twins are found at those positions ($\lambda = 90°$ and 270°) where the resolved shear stress on the basal planes is a minimum; this fact is probably very important.

Referring to fig. 4 the curve, marked B, shows readings—denoted by open circles—in the areas $\lambda = 45°$ to 55°, 130° to 135°, 210° to 230° and 310° to 315°. These record the appearance of patches containing slip bands whose slopes agree with the traces of the basal plane and are probably small areas of the original crystalline structure—in which basal plane slip has occurred—separating twinned regions.

Identification of Twinning Planes.—Careful measurements were made round the entire circumference of the slope of the edge of the twin bands. Except in the case of very large twins, the edges were sharply defined and readings taken at several positions along the specimen at the same value of λ, were in extremely good agreement, the departure from the mean rarely exceeding $\pm 1°$. A few of the largest twins, however, were bounded by very irregular edges. Fig. A shows the most irregular boundary encountered; this irregularity was quite exceptional and was confined to the largest twins; it may, however, illustrate a point on which we desire to lay emphasis, *i.e.*, that the phenomenon of twinning is evidently not one of "slip" along the plane dividing the twinned and untwinned portions. A searching examination of the whole of the surface of the specimen failed to show any signs of slip-bands corresponding to movement on the twinning plane. At each of 72 values of λ equally spaced *round* the specimen five readings were taken (at various positions *along* the specimen) of (*a*) the slope of the edge of the twin, and (*b*) the slope of the slip bands within the twinned portion, where this was resolvable. For convenience, the twins were termed T′ and T″, while the slopes of the corresponding slip bands within these twins were termed B′ and B″. Thus T′ and B′, also T″ and B″ are associated. Although at first sight, the slip (appearing as nearly vertical in the photographs) within both sets of twins had a common slope, detailed examination showed clearly that this was not the case. The recorded measurements are plotted in fig. 4 on the curves marked T′, T″, B′, B″. The full dots on the T′ and T″ curves refer to places where twins were "resolvable" and the slope of the slip bands (B′ and B″) within the twins could be measured. The readings recorded by open dots indicate the slope of the edge of the twin whose appearance was as shown, *e.g.*, in figs. J, K, L and M (Plate 8) where no slip could be seen either within or adjacent to the twin. The planes, whose traces are equivalent to the observed traces, T′ and T″, were calculated and found to correspond to (*a*) $\theta = 41°$, $\psi = 91{\cdot}5°$ (T′), (*b*) $\theta = 45°$, $\psi = 272$ (T″). These planes correspond—within the limits of experimental accuracy—with the particular first order pyramidal (two) planes p_v^{2} and p_v^{-2}, whose spherical co-ordinates (see Table I) as deduced from the corrected X-ray analysis are :—

$$p_v^2,\ \theta = 40^\circ\ 54', \qquad \psi = 91^\circ\ 24'$$
$$p_v^{-2},\ \theta = 45^\circ\ 6', \qquad \psi = 272^\circ\ 42'.$$

The curves drawn through the recorded readings of T′ and T″ on fig. 4 are the calculated traces of the p_v^2 and p_v^{-2} planes, respectively, and the agreement was found to be so exact that it may be regarded as established that the twinning planes operative in the present experiment were planes parallel to this particular pair of first order pyramidal (two) planes. The microstructure at the positions $\lambda = 100^\circ$, also $\lambda = 180^\circ$ is interesting. A few individual twins of both T′ and T″ occur at these points and the recorded angles are as plotted in fig. 4. Fig. L (Plate 8) shows a spot where a twin of apparently wavy form is present. This is really due to the presence of both sets of twins, and the individual slopes of each (T′, $\theta_s = 5^\circ$, T″, $\theta_s = -7^\circ$) are clearly visible together with an intermediate slope due, doubtless, to a close entwinement of twins of each type.

Slip Planes within the Twinned Structure.—The recorded slopes of the slip bands contained by the twins are plotted in fig. 4. These slip bands did not agree with the traces of any of the principal crystallographic planes. The nearest low index plane was the first order prismatic P_v, which occupies an intermediate position between B′ and B″. It is quite certain that the observed slip bands were *not* traces of P_v; in the first place, the difference of slope is much greater than our limits of experimental error but more convincing is the fact that, in many cases, both sets of twins T′ and T″ appeared in close proximity when it was apparent, to the eye, that B′ and B″ could not represent traces of any single plane. As the experiment had shown conclusively that the basal plane is the only slip plane in zinc, the possibility that B′ and B″ were traces of the twinned positions of the original basal plane (about T′ and T″ as twinning planes) was then examined.

To effect this comparison it is necessary to determine the positions and orientations of the twinned positions of the basal planes and this is conveniently done using the stereographic net. Let it be required to determine the twinned position (by reflection) of a line, denoted by θ_s, ψ_s—representing either the normal to a plane, or any line of atoms—about a twinning plane whose normal is denoted by θ_p, ψ_p. Marking these points on the diagram, the stereographic net is placed under the (transparent) diagram in such a position that the poles of the net and diagram coincide, while the normal to the twinning plane, also the original position of the required plane, or line of atoms, both lie on a great circle of the net. The twinned position of the plane or line will then lie on the same great circle on the opposite side of the twinning plane and equidistant from it. The dotted line, in fig. 1, shows the method of finding the twinned position of the primitive direction x with respect to the twinning plane T′. (The geometrical basis of the method will be obvious.)

In this way, the six twinned positions of the original basal plane (B) with respect to the six possible twinning planes of the first order pyramidal (two) type were determined and are denoted, in fig. 1, by the symbol ⊕ followed by the appropriate letter, B′, B″, . . ., B′′′′′′, indicating the particular twinning plane concerned. The twinned positions of the original primitive directions (x, y, z) contained by the original basal plane (B) after twinning about the particular pair of twinning planes (T′ and T″) identified in the present experiment were also determined (see Table IV). The spherical co-ordinates of all the possible twinned positions of the basal plane were as stated in Table III.

Table III.—Data relating to the Twinned Positions of the Basal Plane.

Twinning plane.			Twinned position of basal plane.		
	$\theta°$.	$\psi°$.		$\theta°$.	$\psi°$.
$10\bar{1}2$ (T′)	40·9	91·4	B′	6·5	276·0
$10\bar{1}\bar{2}$ (T″)	45·1	272·7	B″	2·0	79·0
$01\bar{1}2$ (T‴)	67·5	48·7	B‴	60·8	356·5
$01\bar{1}\bar{2}$ (T⁗)	70·9	314·8	B⁗	60·5	5·4
$1\bar{1}02$ (T′′′′′)	66·6	135·8	B′′′′′	59·5	188·4
$1\bar{1}0\bar{2}$ (T′′′′′′)	69·5	230·1	B′′′′′′	59·2	178·8

The traces of these twinned basal planes were plotted and it was found that the traces of B′ and B″ agreed exactly with the observed slip bands in the twinned areas. In fig. 4 the curves drawn through the observed B′ and B″ readings represent the calculated traces of the corresponding twinned basal planes.

Thus the experiment appears to have identified in a conclusive manner the twinning plane of zinc as a first order pyramidal (two) plane and to have shown that the structure within the twin deforms by slip in such a manner as to indicate that the twinned structure is equivalent to a mirror image of the original structure about the twinning plane; assuming merely that slip in the twinned structure is confined to the basal plane as in the original structure.

These facts lead easily to a consideration of one of the most interesting features exhibited by the microstructure (see figs. B, C, F and G). In these fields a large number of twins are present which are not easily seen in the photographs although visual examination under high magnification reveals them clearly and establishes their identity with T′ and/or T″ twins. As the position on the surface—denoted by λ—increases from 0° (or 180°) onwards, the resolved shearing stress on the basal plane falls off rapidly (see fig. 3) and the amount of visible basal plane (B) slip also diminishes, together with the width and number of twins. The microstructure also shows another curious feature, *i.e.*, the *relative* amount of slip on the twinned basal planes (B′ and B″) to that on the basal plane (B) does not fall off but rather increases, so that, although the *total* amount of visible slip is undoubtedly decreasing rapidly (compare fig. A at λ = 0° and fig. C at λ = 30°) yet as λ increases, the slip occurring on the twinned basal planes (B′ and B″) predominates to an increasing extent over the purely basal plane slip. Investigation showed that this can be accounted for satisfactorily from resolved shear stress considerations of the material both within and without the twin. Table IV shows the spherical co-ordinates of the twinned basal planes and of the (twinned) primitive directions contained by these planes, together with the calculated constants for the shear stress equations. (The twinned positions and orientations of the basal planes were determined using the stereographic net and the method previously

Table IV.—Spherical Co-ordinates, also Stress Equation Constants for the Twinned Basal Planes observed on the present specimen (Z.3A).

Basal plane.			Contained primitive direction.*		**Shear stress equation constants.**	
	θ.	*ψ*.	*θ*.	*ψ*.	A.	*a*.
	° ′	° ′	° ′	° ′		° ′
0001 (B) (Original basal plane)	88 0	92 6	*x* 29 6	186 0	0·872	3 8
			y 89 0	182 0	0·039	92 0
			z 31 0	358 30	0·856	0 55
B′ (about the twinning plane = T′)	6 30	276 0	*x*′ 85 6	62 0	0·983	151 39
			y 89 0	182 0	0·994	92 3
			z′ 84 0	122 0	0·977	32 18
B″ (about the twinning plane = T″)	2 0	79 0	*x*″ 88 54	302 0	0·999	32 8
			y 89 0	182 0	0·999	91 56
			z″ 88 0	242 0	0·998	151 55

* *Note.*—The primitive direction "*y*" is common to the original and both "twinned" structures.

described. This method assumes that the twinned structure satisfies the usual definition, namely, that of a "mirror image" about the twinning plane.)

The resolved shear stresses on the original and twinned basal planes, using the constants of Table IV, are plotted in fig. 5 and show that these stresses are equal in intensity at the areas λ ≃ 2° and 182°; as λ increases from these points the resolved shear stresses on the twinned basal planes (both B′ and B″ which are nearly equally stressed) become increasingly greater than on the original basal plane. These stress considerations fit in so completely with the features of the structure exhibited in figs. B, C, F and G (Plates 6-7) as to leave little doubt that their appearance has been satisfactorily accounted for. A further point which clearly emerges is that the twins must have been caused by the applied alternating stress system; for, if twinning had been set up previous to the test, slip bands due to B′ and B″ would be expected to occur in profusion at the positions λ = 90° and 270° where resolved shear stress on the twinned basal planes is a maximum (fig. 5).

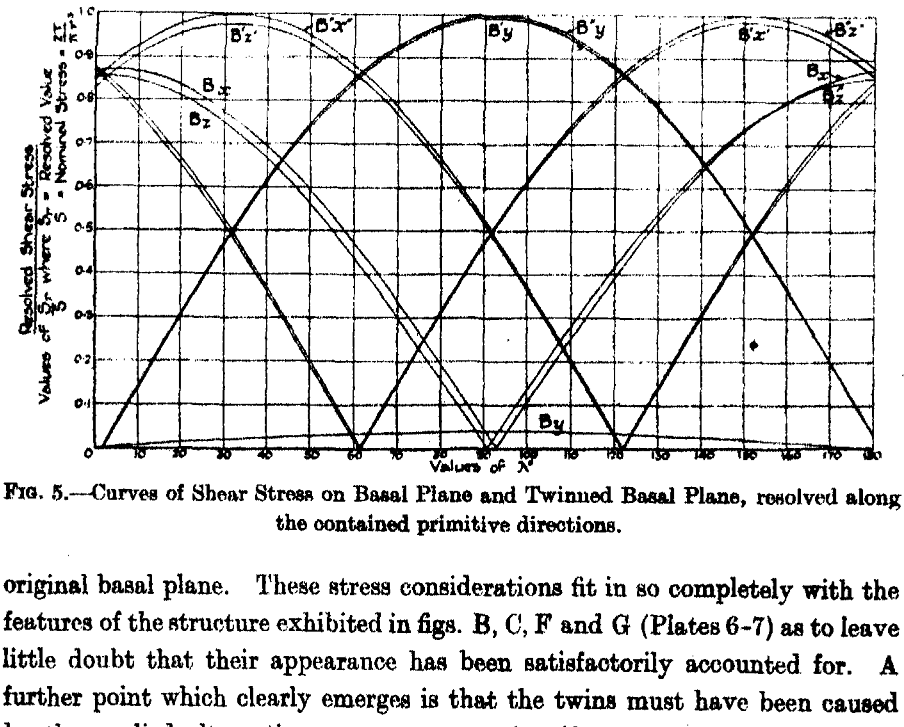

FIG. 5.—Curves of Shear Stress on Basal Plane and Twinned Basal Plane, resolved along the contained primitive directions.

Possible Mechanism of Formation of Twins.—Some of the phenomena of twinning having been established on a quantitative basis and the particular twinning planes concerned in the present experiment having been identified, the exact manner in which twinning in zinc can occur becomes a matter of some interest. In the first place, the previous detailed discussion of the basal plane slip and the occurrence and nature of the observed twins in relation to the resolved shear stress distribution on the basal plane has shown quite clearly

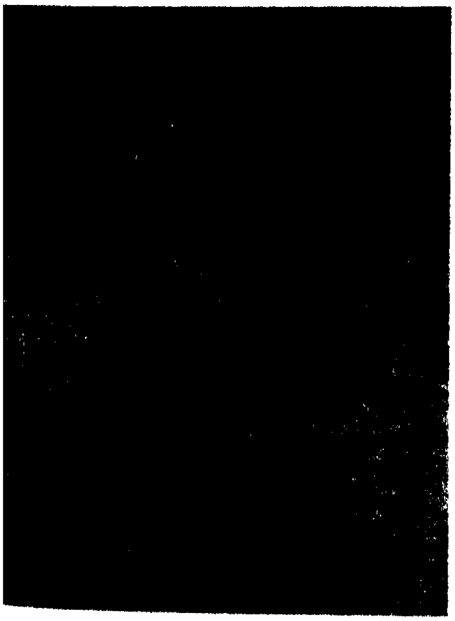

FIG. A. λ = 0. (× 292)

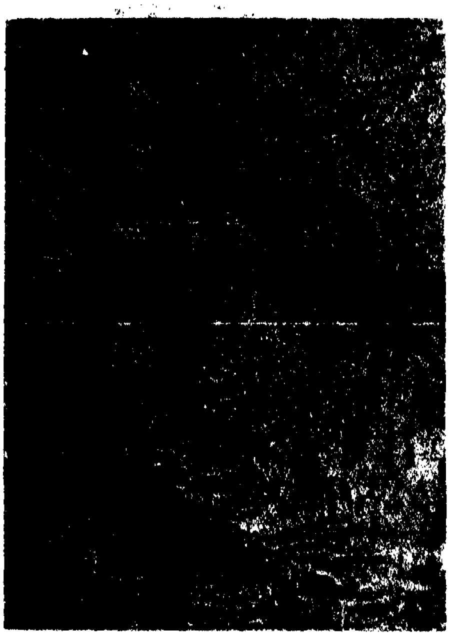

FIG. B. λ = 20°. (× 292)

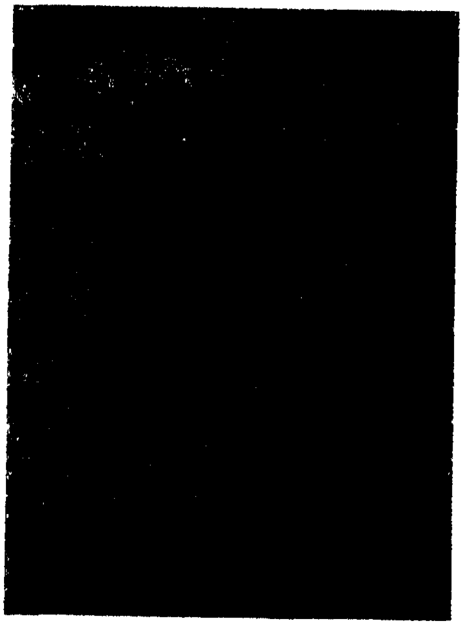

FIG. C. λ = 30°. (× 292)

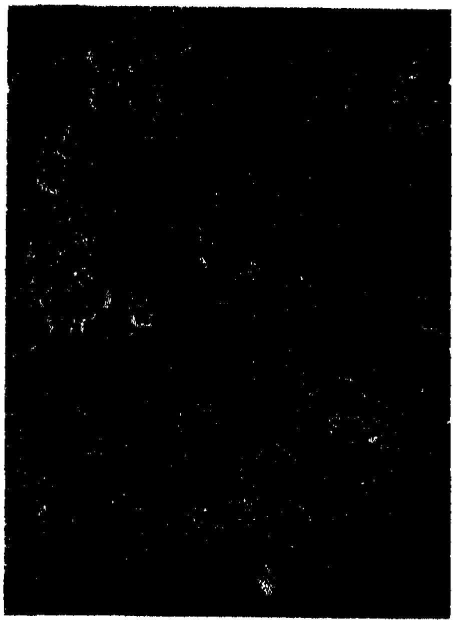

FIG. D. λ = 34°. (× 292)

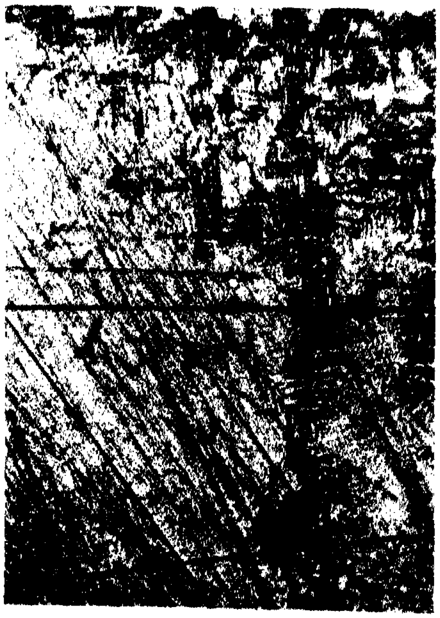

Fig. E. λ = 40°. (× 292)

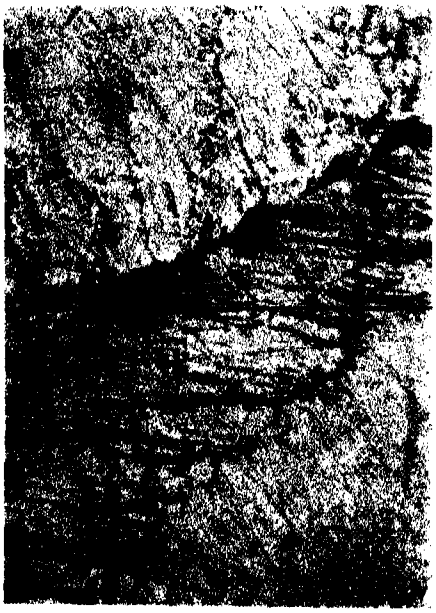

Fig. F. λ = 220°. (× 86)

Fig. G. λ = 50°. (× 292)

Fig. H. λ = 75°. (× 292)

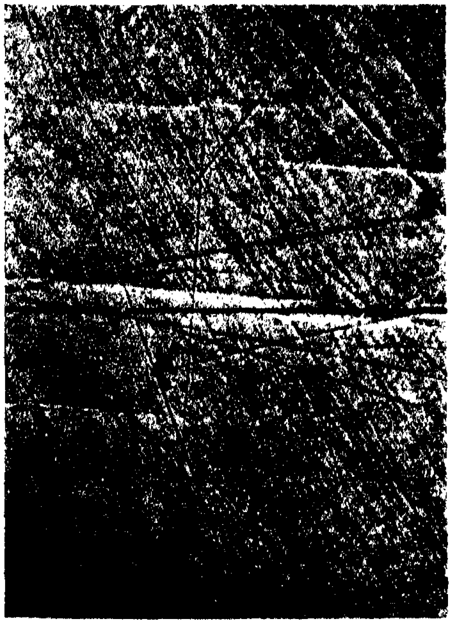

FIG. J. λ = 90°. (× 292)

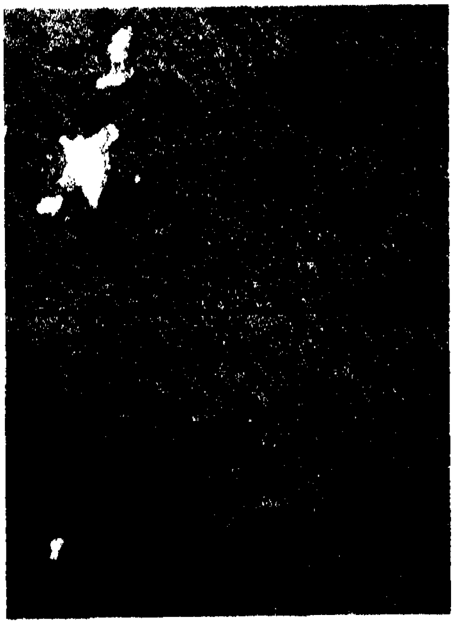

FIG. K. λ = 270 (90°). (× 85)

FIG. L. λ = 100°. (× 292)

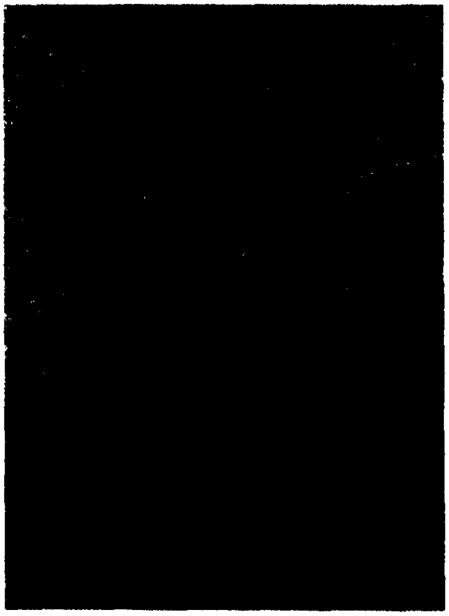

FIG. M. λ = 110°. (× 292)

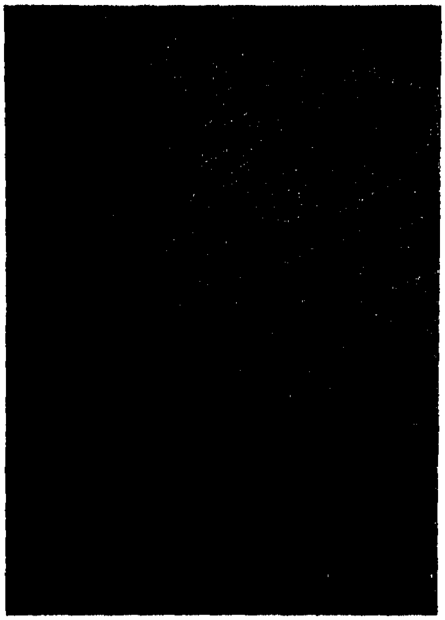

FIG. O. λ = 300° (120°). (× 85)

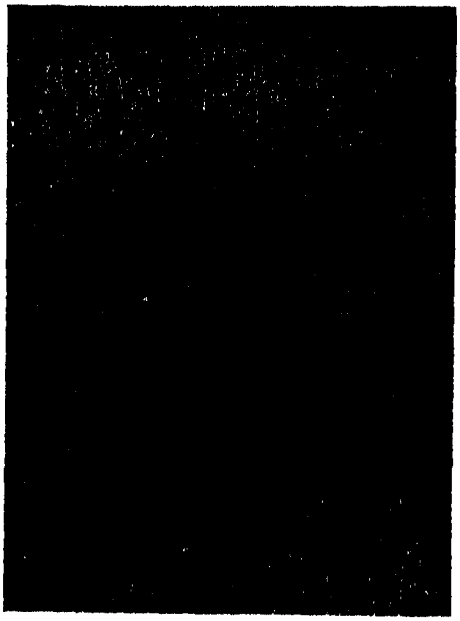

FIG. Q. λ = 140°. (× 85)

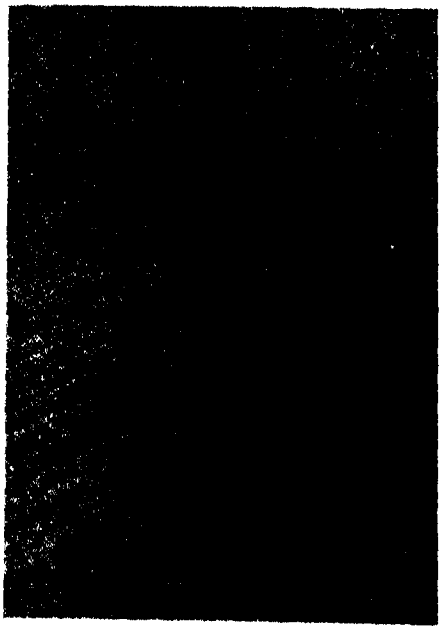

FIG. N. λ = 120°. (× 84)

FIG. P. λ = 310° (130°). (× 85)

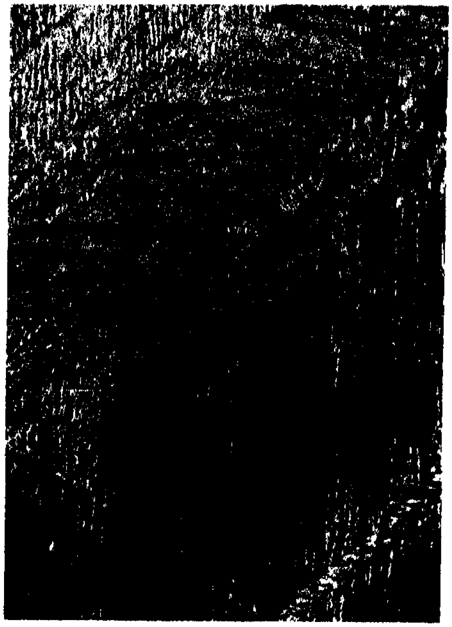

Fig. S. λ = 160°. (× 85)

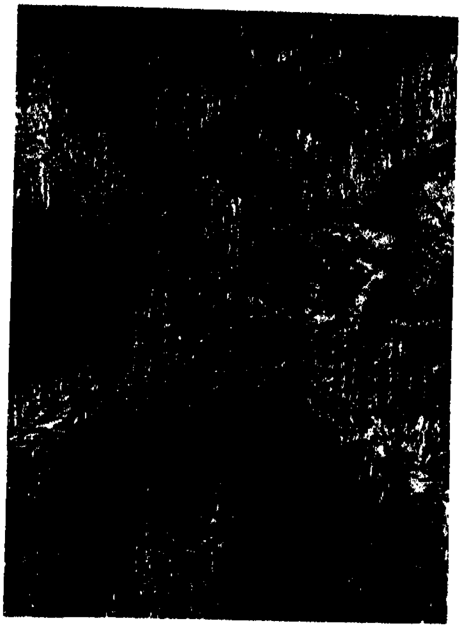

Fig. U. λ = 167°. (× 77)

Fig. R. λ = 320° (140°). (× 85)

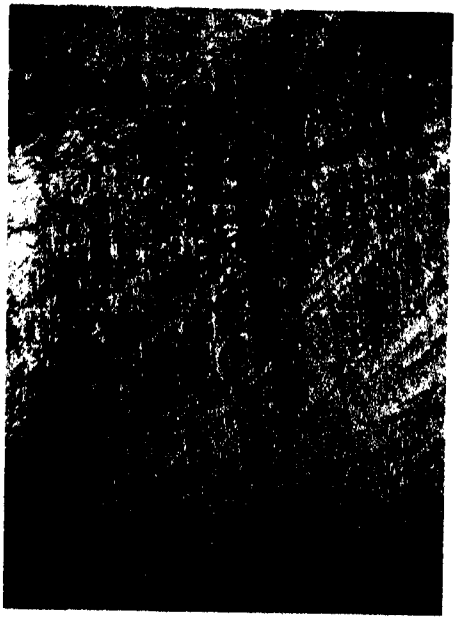

Fig. T. λ = 342° (162°). (× 85)

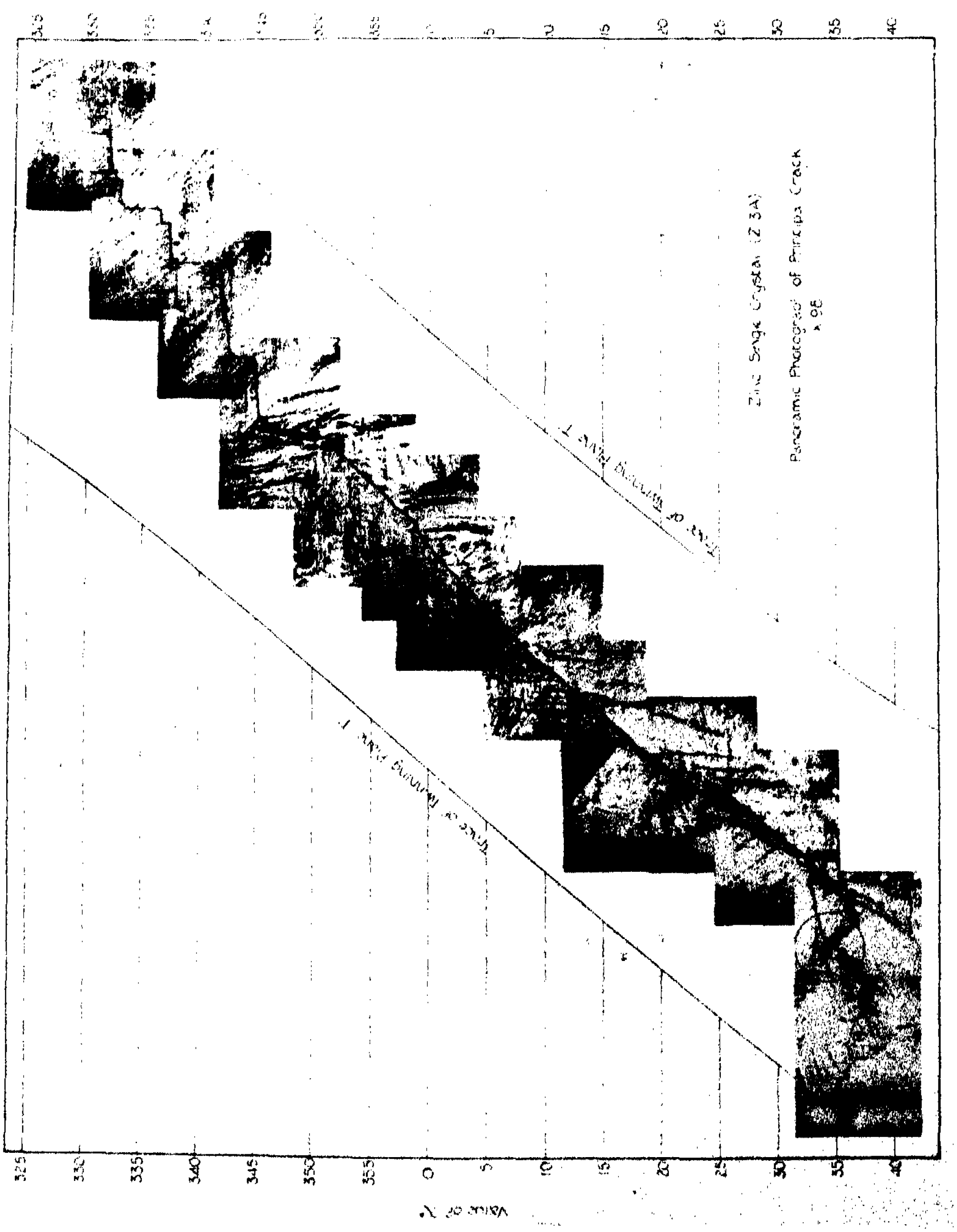
Zinc Single Crystal (Z 3A)
Panoramic Photograph of Principal Crack
× 98
Trace of Twinning Plane T
Trace of Twinning Plane T
Value of χ
325
330
335
340
345
350
355
0
5
10
15
20
25
30
35
40

FIG. V. (× 20).

that the observed twin formation occurs as a *result* of the previous basal plane slip. It is equally certain that it is not due to slip on the twinning plane; this is obvious for two reasons: (*a*) no sign of slip bands corresponding to slip on the twinning plane has been detected at any point of the specimen; (*b*) simple slip on the twinning plane would not produce a twinned structure. Further, twinning cannot occur by differential slip on the twinning plane, but twins can be, and probably are, produced by atomic movements which are in every case less than the movement necessary to produce simple slip on the twinning plane.

Consider fig. 6 representing sections through a conventional lattice-model of the close-packed hexagonal system. Figs. 6 (*a*) and (*b*) are sections parallel

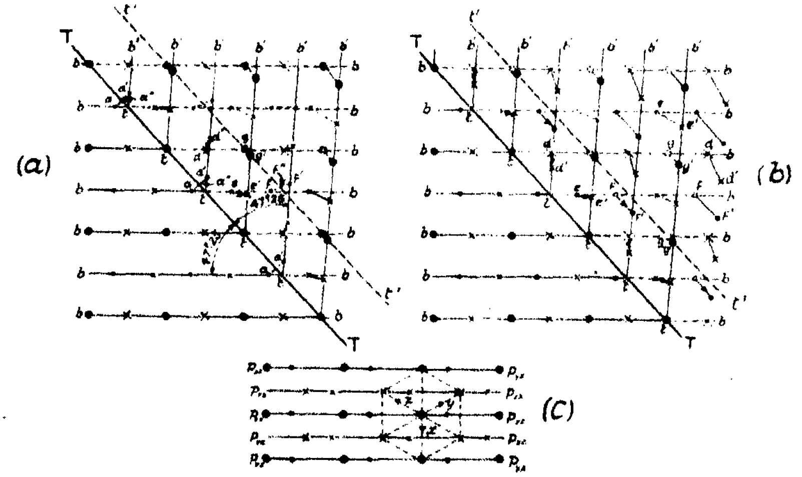

FIG. 6.—Diagrammatic Representation of Possible Mechanisms of Twinning of the Close-packed Hexagonal System about First Order Pyramidal Planes (01$\bar{1}$2). (*a*) Twinned structure as "mirror" image about twinning plane (01$\bar{1}$2). (*b*) Mechanism as suggested by Mathewson and Phillips.

Note.—*btb* = traces of original basal planes (0001) on second order prismatic planes (2$\bar{1}\bar{1}$0).
tb' = traces of twinned basal planes (0001) on second order prismatic planes (2$\bar{1}\bar{1}$0).
$P_{y_1}P_{y_2}$ = traces of second order prismatic planes on original basal planes.

to a second order prismatic plane, while fig. 6 (*c*) is a section parallel to a basal plane, thus representing a plan view of (*a*) and (*b*). The traces of the second order prismatic planes (2$\bar{1}\bar{1}$0) in plan view are denoted by $P_{y_1} \ldots P_{y_5}$, while *b* . . . *b* are the traces of basal planes (0001). T . . . T is the trace of the second order pyramidal (two) plane—denoted by p_x^2—which contains the primitive direction x (normal to the $2\bar{1}\bar{1}0$ plane). The atoms on adjacent *prismatic* planes are distinguished by alternative • and ×, while those on alternate *basal* planes are distinguished by different sizes of the • and ×. Consider fig. 6 (*a*). To the left of the twinning plane T . . . T the positions of the atoms in the original structure are shown, while to the right of T . . . T the *original* positions are indicated by *dotted* ◌ and ×. The structure is then twinned by simple reflection about T . . . T, the new positions of the atoms being shown by full • and × *to the right of* T . . . T. The diagram shows that this re-arrangement could be effected most easily by the three simple translations d to d', e to e', g to g' all confined to the plane of the particular P_{yz} plane concerned. In addition, some slight displacement must occur to every alternate atom along the boundary of the twin, *i.e.*, T — T. To produce a true mirror image about T . . . T, the atoms marked a would be translated to a', but for reasons of symmetry, it would appear more likely that movement would be to a'' or to t. In either case, this movement—and the other movements marked—are small compared with the lattice parameter. The diagram shows that the smallest element in which these translations (and possible rotations due to the shape of the atom) are completed is contained by the trace T . . . T and a parallel trace t' . . . t'. Further, as the distance from T . . . T—measured along the original basal plane—increases, the necessary amount of movement increases up to an amount which cannot be greater than the lattice parameter; when this limit is reached, the process will probably repeat itself. The important point emerges that the twinning action would be expected to spread in directions along and parallel to the twinning plane, thus producing the shape of twin with which experience is so familiar. Returning to fig. 6 (*a*), b' . . . t, b' . . . t, etc., represent traces of the twinned basal plane which make a theoretical angle of 94° 5′ with the original basal plane. In the diagram, T . . . T represents the trace of the twinning plane, $01\bar{1}2$ (p_x^2); the second twinning plane $0\bar{1}12$ (p_x^{-2}) also containing the same primitive direction x, would produce twinned basal planes making an angle of 85° 55′ with the original basal plane. Thus, the traces of the twinned basal planes would be situated symmetrically about the traces of the *first* order prismatic plane P_x and inclined at 4° 5′ only to the latter, with which it might easily be confused. In the specimen used in the present test, the twinning planes operative were p_y^2 and p_y^{-2} and fig. 4 shows the traces of the twinned basal planes situated on opposite sides and in close proximity to the traces of the corresponding first order prismatic plane P_y.

Fig. 6 (*b*) shows the same twinned structure as in fig. 6 (*a*) but the indicated translations are as suggested by Mathewson and Phillips. The present writers suggest that, as the mechanism, in any case, is purely hypothetical, that of fig. 6 (*a*) is perhaps preferable. The conditions of the surface T . . . T in fig. 6 (*a*) are in more complete equilibrium than in fig. 6 (*b*), while the magnitudes of the atomic displacements suggested in fig. 6 (*a*) are smaller than those in fig. 6 (*b*). The point is not really worthy of argument as any direct experimental evidence seems to be at present outside the range of possibility. The important point is that the results of the present experiment and of the work of Mathewson and Phillips are in complete agreement as to the identity of the twinning plane of zinc, and the work has been carried a stage further by the successful resolution of the slip bands within the twinned structure and their identification with the twinned basal planes. The correlation of twinning with applied stress effects *in a quantitative manner* is believed to be the first success in this direction.

Choice of Twinning Planes.—Having established that the twinning plane of zinc is the $01\bar{1}2$ type it is necessary to account for the fact that of the six available planes (p_x^2, p_x^{-2}, p_y^2, p_y^{-2}, p_z^2, p_z^{-2}) twinning occurred on two only of these planes, namely, p_y^2 and p_y^{-2}. During the previous discussion on the variation of basal plane slip and the size, number and nature of the accompanying twin bands, it emerged, fairly conclusively, that the twinning is intimately associated with the basal plane slip and is, probably, a direct result of this slip. The operative twinning planes may therefore be studied with relation to the slip plane and direction of slip. Consider that portion of the specimen extending from $\lambda = 0°$ to $\lambda = 90°$. From fig. 6 we have seen that the atomic translations which are sufficient to account for twinning take place (in the twinned band) in a plane perpendicular to the twinning plane. Further, no signs of slip on the twinning plane were visible. Hence, it may be concluded that shear stress on the twinning plane may be neglected and it is not therefore surprising (see fig. 4) to find that the shear stress on the twinning planes, p_y^2 and p_y^{-2} is very small at the positions where the twins were in their greatest stage of development, *i.e.*, at $\lambda = 0°$. The slip direction on the basal plane (see fig. 3) is x from shear stress considerations. Referring to fig. 6 (which illustrates a twin formed on the p_x^2 plane) it is apparent that the only slip directions (on the basal plane) which have stress components capable of contributing forces to effect the necessary atomic translations are the remaining possible slip directions y and z. Hence it appears reasonable to assume in the general case, that slip occurring on the basal plane along any particular primitive (slip) direction, would, *all other stress considerations being equal,* tend to produce twins on first order pyramidal (two) planes containing one of the *remaining two primitive lattice directions in the basal plane.* According to this reasoning, in the present specimen, the effective basal plane slip direction in the region $\lambda = 0°$ to $90°$ might produce twins formed on the following planes p_y^2, p_y^{-2}, p_z^2 and p_z^{-2} (*i.e.*, T′, T″, T''''' and T''''''). Of these p_y^2 and p_y^{-2} only were visible and a most careful search over the whole of the surface of the specimen failed completely to reveal any signs of any other markings remotely resembling a twin band. One other stress consideration remains, namely, normal stress on the twinning plane which would be expected to facilitate the required atomic translations as the latter are confined to a plane *normal* to the twinning plane. The normal stress curves for the twinning planes were calculated and are plotted in fig. 7, and appear to supply the required evidence. It will be remembered that the limits of visible basal plane slip were the areas $\lambda = 320°$ to $40°$, also $\lambda = 140°$ to $210°$ and fig. 7 shows that in these regions, the normal stresses on p_y^2 and p_y^{-2} planes are greatly superior to those on any of the other possible twinning planes. In the region $\lambda = 47°$ to $110°$, the normal stress on p_z^2 exceeds that on p_y^2 or p_y^{-2}; twins are not formed on this plane, *in this area*, probably because no basal plane slip occurs in this region. (p_x^2 and p_x^{-2} can be neglected, as B_x slip would not, in any case, tend to form twins on these planes.) The fact that the p_y^2 (T′) and p_y^{-2} (T″) twins extend—although greatly diminished in size and number—through the region $\lambda = 40°$ to $140°$, we ascribe to the peculiar manner in which

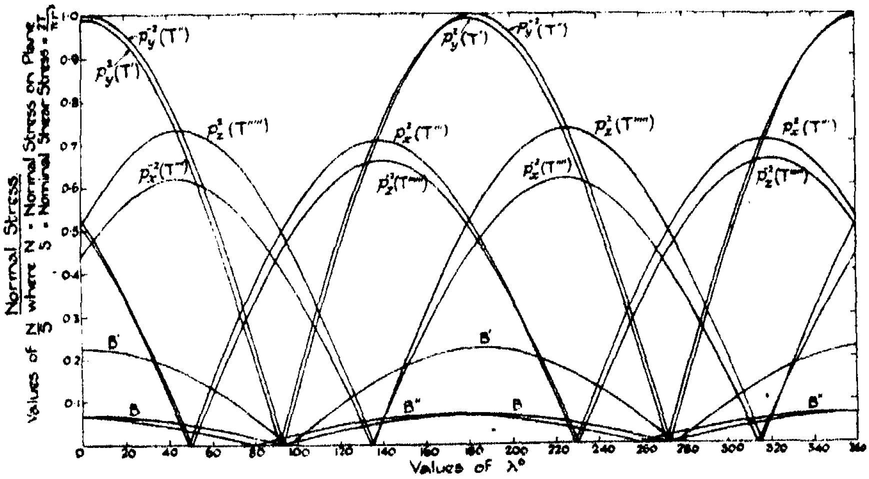

FIG. 7.—Normal Stresses on Twinning Planes (type $10\bar{1}2$).

the twins are doubtless formed, *i.e.*, by a progressive movement *along* the twinning plane; conceivably, the formation process would tend to " over-run " the points at which the basal plane slip responsible for the formation ceases.

It is proposed to test some of the above conclusions by a further critical experiment in which, by a suitable choice of crystal orientation, the direction of slip on the basal plane will change within the area of visible slip. Under these circumstances, it will be interesting to observe if the effective twinning plane(s) also changes, as the mechanism suggested above would indicate.

(C) *Fracture.*—The fracture consisted of one main crack which extended from $\lambda = 330°$ to $\lambda = 38°$. As this crack possesses many interesting features, a sufficient number of photographs (magnification 98) were taken to form a panoramic view, which, in turn, was again photographed to form Plate 11, which thus represents the appearance of a true development of the cracked surface of the specimen. (The final magnification is approximately × 20)

The crack follows three main directions, namely :—

(*a*) Approximately horizontal but agreeing exactly with the traces of the basal plane, thus corresponding to failure along the slip planes.

(*b*) A curved path whose slope varies between the values of $\theta_s = -41°$ at $\lambda = 350°$ and $\theta_s = -38°$ at $\lambda = 30°$. Examination under high power magnification showed that the crack was following the edges of a very large number of T′ twins, its general direction—in spite of small local horizontal and vertical deviations—thus agreeing, in general direction, with the traces of the T′ (p_y^2) twinning planes. To reveal this clearly, two traces of the T′ plane have been added to the photograph. In spite of the loss of resolution due to the double photographing, a number of small T′ twins are visible, in fig. V (Plate 11) their edges being on, or parallel to, the edge of the crack.

(*c*) An approximately vertical path ($\theta_s \simeq 0°$). This is one of the most interesting features of the experiment as it gives direct experimental evidence on the identification of the second cleavage plane of zinc, either as a twinned basal plane or as an original prismatic plane. Although the crack follows the traces of T′ twins, there exist large numbers of T″ twins crossing the crack transversely and some of these are clearly visible even in fig. V. Fig. T is one of the photographs, taken for the panoramic view, at its original magnification (× 98); the position of the field is $\lambda = 342°$. The T″ twins are very evident, and it is apparent that the crack in its vertical deviations, is following the slip bands corresponding to the twinned basal plane (B″) within the T″ twins. Fig. D (Plate 6) corresponds to the spot enclosed by a circle in fig. V and reproduces, in a striking manner, the three main characteristics of the crack; the general direction is seen to follow the edge of a T′ twin, the horizontal direction follows traces of the original basal plane, while the sudden vertical deviation follows the twinned basal plane structure (B″) within the T″ twin. Also, the increasing tendency for the slip on the twinned basal structure (B″) to predominate over that on the basal plane (B) as the position $\lambda = 0°$ is receded from appears to follow the variation in the intensity of resolved shear stress on this plane as shown in fig. 5.

It thus appears to have emerged clearly that the prismatic planes of zinc are neither slip planes nor cleavage planes, and it is probable that what have been interpreted in the past as cleavages on prismatic planes have been fractures along the twinned basal planes.

General Conclusions relating to the Deformation of a Zinc Single Crystal under Alternating Torsional Stresses.—The results of the present experiment may be briefly summarised as follows :—

1. The slip plane of zinc is the basal plane (0001).

2. Three possible slip directions exist, namely, the three primitive directions contained by the basal plane.

3. Deformation, by slip, of a zinc single crystal is controlled purely by resolved shear stress considerations and occurs along the most highly stressed primitive direction contained by the basal plane.

4. The "visible slip limit" (probably of the present specimen only) was clearly defined at a range of resolved shear stress of ± 1 ton/inch^2, while the limiting range (fatigue range) of reversed shear stresses, in the case of the present crystal has a value intermediate between ± 1·0 and ± 1·3 ton/inch^2 in terms of resolved shear stress.

5. The twinning plane of zinc has been identified as first order pyramidal (two)—$10\bar{1}2$ type—producing a twinned basal plane making an angle of 94° 5′ with the original basal plane. The twinned structure has been identified by means of accurate measurements of slip bands on the twinned basal planes. Twinning is probably a secondary result of basal plane slip and the particular twinning planes (of the six available sets) operative appear to be principally determined by the direction of slip on the basal plane and probably by normal stress considerations. Intensity of normal stress on the twinning planes appears reasonably to be an important factor in the process of twinning itself, as it is shown that twinning can be accomplished by small atomic translations confined to a plane normal to the twinning plane. The process of twinning is *not* one of differential slip on the twinning plane.

6. Fracture resulted in three general directions: (*a*) Parallel to the traces of the original basal plane; (*b*) parallel to the traces of the twinned basal plane within the twinned structure; and (c) along the edges of the twins. The latter direction may be due either to the twin boundary being a place of weakness, or to the fact that in the present specimen, these boundaries were exposed to a maximum range of normal stress, or to a combination of these conditions.

7. Prismatic planes are neither slip nor cleavage planes, and it appears very probable that what have previously (by other investigators) been interpreted as cleavages of this type, have been cleavages or fractures along twinned basal planes.

The experiment is an item of the general programme of work performed for the Engineering Research Board of the Department of Scientific and Industrial Research under the general supervision of the Aeronautical Research Committee; the authors' thanks are due to these bodies for the research facilities afforded and for permission to publish the results.

The zinc crystal used was prepared by Mr. V. H. Stott, M.Sc., of the Metallurgical Department of the National Physical Laboratory, and the X-ray analyses were carried out in the Physics Department by Mr. W. Binks, M.Sc.

The authors take this opportunity of expressing their indebtedness to Mr. Stott and Mr. Binks for their invaluable assistance in these directions.

Infra-red Radiations of Active Nitrogen.

By P. K. Kichlu, D.Sc., and D. P. Acharya, M.Sc., Department of Physics,
Science College, Patna, India.

(Communicated by M. N. Saha, F.R.S.—Received November 19th, 1928.)

[Plate 12.]

The spectrum of active nitrogen in the visible and ultra-violet regions was first photographed by Lewis,* with a small quartz spectrograph. Later, Fowler† and Strutt made a more careful study of its spectrum by using instruments of greater dispersion and were able to prove definitely that most of the bands were identical with the first, second and third positive bands of nitrogen. They also observed for the first time in the spectrum of the discharge which produces the after glow, another group of bands about the region λ 2900 to λ 2200 which they called the fourth positive group. The present paper deals with an investigation of the spectrum of active nitrogen in the infra-red.

Apparatus.

The apparatus employed, shown in fig. 1, was very similar to that used by most of the investigators on this subject. The nitrogen is stored in a large bottle A, from which it is drawn through a bottle B of about 2 litres capacity filled with thin sticks of yellow phosphorus. After getting dry by calcium chloride and phosphorus pentoxide contained in C and D respectively, and the supply being partially regulated by the capillary tube X, the nitrogen enters the discharge tube E, and is excited by an oscillatory discharge. The activated

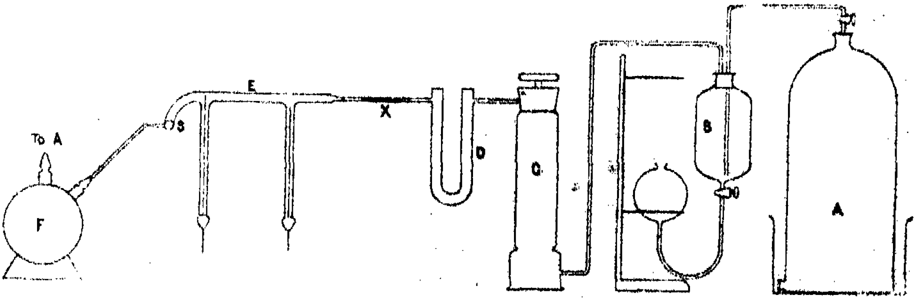

Fig. 1.

---

* 'Astrophys. J.,' vol. 20, p. 49 (1904).

† 'Roy. Soc. Proc.,' vol. 85, p. 377 (1911).

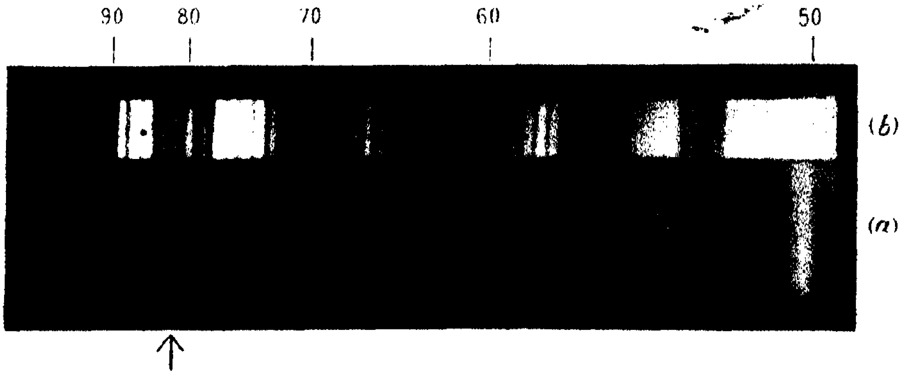

(*a*) Spectrum of active nitrogen. The bands from λ 7500 to λ 8900 are clearly visible. The position of the infra-red lines of atomic nitrogen is indicated with an arrow-head. These are clearly seen in the original negative showing the nitrogen band spectrum, but have not come out well in the reproduction shown in (*b*).

(*b*) Showing the first positive group of nitrogen as obtained from a nitrogen filled tube.

gas then goes to a side tube S, which is not properly seen in the diagram, being perpendicular to the plane of the paper. The observation tube was 30 cms. long with a diameter of about a centimetre, and was bent in such a way that no light from the discharge tube could be seen in the spectroscope. The only light which entered the slit was that of the glow which was observed end on. The nitrogen was sucked by means of a Gaede pump F, and the exhaust gas was pumped back to the reservoir A. The connections for passing the oscillatory discharge into the tube are shown in fig. 2, where the transformer is worked at a capacity of 500 watts, and gave about 10,000 volts in the secondary. The electrode near the observation tube was very carefully earthed. The whole arrangement was automatic, so that very long exposures could be given without much difficulty. The luminosity of active nitrogen, which was yellow in colour when the supply of nitrogen was properly adjusted, was very great indeed.

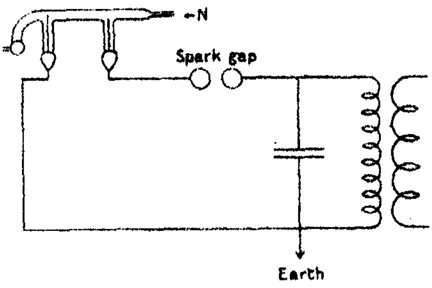

FIG. 2.

The spectrometer employed was a Hilger Constant-Deviation Spectroscope, and neocyanine plates hypersensitised with ammonia were used for photography in the infra-red.

Results.

An exposure of 42 hours brought out the band spectrum extending from λ7500 to λ8900, shown on Plate 12 (*a*). For purposes of comparison this band system as given out by a discharge tube filled with nitrogen, is superposed upon it, and is shown in (*b*). It will be seen that the two are exactly similar with regard to wave-lengths, number and intensity distribution. This point is remarkable, for whereas in the visible and ultra-violet Fowler and Strutt found that only selected bands of nitrogen appeared in active nitrogen, in the infra-red all of them have appeared without distinction. A. H. Poetker* has recently photographed these bands in a nitrogen discharge tube, and shown conclusively that they form part of the first positive group of nitrogen occurring in the yellow, green and red, and investigated before by Deslandres, von der Helm and Birge.† Poetker has extended this band system to λ 10500, but there is no trace of any bands on our plates beyond λ 8900, probably because of the insufficiency of exposure at such long wave-lengths.

---

* 'Phys. Rev.,' vol. 30, p. 812 (1928).

† Deslandres, 'C. R.,' vol. 134, p. 747 (1928); von der Helm, 'Z. Wiss. Phot.,' vol. 8, p. 405 (1910); Birge, 'Astrophys. J.,' vol. 39, p. 50 (1914).

Discussion.

The necessity for the above-mentioned work arose out of a suggestion made in a paper by one of the authors* a few years ago, in order to throw some light on the obscure nature of active nitrogen. An analysis of the band systems of nitrogen by Birge† had shown the presence of a number of electronic levels designated variously as X, A, B, C, and D. Now the strongest bands in active nitrogen correspond to vibration level 11 of electronic level B. H. Sponer‡ from a consideration of the parallel properties of active nitrogen and active hydrogen, assumed that both of them have a similar constitution. Active hydrogen having been proved to be atomic, active nitrogen is also supposed to be atomic in structure. The energy value of the level corresponding to the strongest bands of active nitrogen must then, according to Sponer, be the heat of dissociation of nitrogen. This comes out to be 11·4 volts. It was suggested in the paper by one of us (*loc. cit.*) that if the analogy between active nitrogen and active hydrogen is complete, the former may show the lines of atomic nitrogen, as active hydrogen is known to give out Balmer lines strongly. Now, the lines of atomic nitrogen in the region where the spectrum of active nitrogen had previously been investigated, belong to very subordinate combinations, and may easily have been masked by the strong bands. The analysis of the spectrum of nitrogen by Kiess§ has shown that the resonance lines of nitrogen are to be found at about λ 1700; the next higher group of lines is located in the infra-red at λ 8200. It was with the intention of searching for these latter lines in the infra-red that the experiments described in this paper were undertaken. On our plates there is no trace of these lines and it is certain that they are definitely absent, and could not have been brought out with longer exposures, for in the nitrogen discharge tube these lines come out strongly, and are indicated in the spectrogram of Plate 12, with a mark, and are very much more intense than the band at λ 8187. In the active nitrogen spectrogram this weak band in the vicinity has been photographed but the lines are absent. Of course this result does not disprove the hypothesis of Sponer, but it certainly shows that the analogy of active nitrogen with active hydrogen must not be stretched too far. A conclusive test of Sponer's theory would be obtained if the resonance lines of atomic nitrogen could be photographed in absorption, using active nitrogen. This is being attempted with a vacuum spectrograph.

---

* Kichlu, 'Proc. Ind. Assn. Cult. Sci.' vol. 9, part 4 (1926).

† Birge and Sponer, 'Phys. Rev.,' vol. 28, p. 259 (1926). See also Hopfield, 'Washington Meeting of Am. Phys. Soc.,' abstract 89 (1928).

‡ Sponer, 'Z. Phys.,' vol. 34, p. 622 (1925).

§ 'J. Opt. Soc. Am.,' vol. 11, p. 1 (1924).

It is a pleasure to thank Prof. M. N. Saha, F.R.S., for much helpful advice and criticism in this work. Our sincere thanks are also due to Prof. K. Prosad for providing facilities to carry out these experiments.

Summary.

The spectrum of active nitrogen has been investigated photographically in the infra-red from λ 7500 to λ 8900 and found to consist of an extension of the first positive group of nitrogen seen in the green, yellow and red regions. The most important group of lines of atomic nitrogen at about λ 8200 have been shown to be absent.

The Penetration of Hydrogen into Metal Cathodes and its effect upon the Tensile Properties of Metals and their Resistance to Repeated Stresses; with a note on the Effect of Non Electrolytic Baths and Nickel Plating on these properties.

By Prof. F. C. Lea, D.Sc.

(Communicated by Sir Robert Hadfield, F.R.S.—Received December 13, 1928.)

[Plates 13, 14.]

The attention of a number of workers* has been directed to the effect of occluded hydrogen on the static properties of metals and particularly its effect in producing brittleness. In connection with many industrial processes pickling is resorted to and not infrequently a brittle condition of the metal is produced by the process. The occlusion of hydrogen has been offered as an explanation. Pfeil (*loc. cit.*) has shown that the behaviour of fine grained iron is different from that of a single crystal when tested as a cathode, and that the hydrogen penetrates between boundaries of crystals. Edwards has shown that hydrogen passes through crystals of iron.* Pfeil has also shown that :—

---

* For bibliography see Pfeil, 'Roy. Soc. Proc.,' A, vol. 112, p. 182 (1926).

(1) The tensile strength of a fine grained iron is not affected by the hydrogen penetration but the elongation was very considerably reduced.

(2) That the temperature of the electrolytic bath considerably affects the elongation and that removal of a specimen from the bath allows the hydrogen to escape from the crystal boundaries and the material to return to its normal condition.

The author has elsewhere† shown that the surface condition of a metal is of very considerable importance in relation to its resistance to repeated torsional stresses and it has been shown by MacAdam‡ and others that surface corrosion affects the resistance to repeated stresses very appreciably. It has also been frequently observed that the type of fracture under repeated stresses for brittle materials is different from that of a plastic material and that a small hole drilled at the surface of a plastic material will change the type of fracture under certain types of repeated stresses.

By using metals as cathodes and forcing hydrogen into their crystal boundaries it appeared possible to throw a little more light upon the problem of the failure of metals under repeated stresses. If the hydrogen in any way produced a discontinuity similar to a very fine crack then it might be expected that the range of repeated stress would be very considerably lowered. If it penetrated the material of the crystal boundaries and did not affect the range of repeated stress the experiments might assist in the solution of the problem, not altogether solved, as to whether failure under these stresses occurred by slipping in the crystal or by a crack commencing at the boundary.

Or if the hydrogen produced brittleness similar to that found in quenched and tempered materials then the type of failure of plastic materials when acting as cathodes might be different from the normal fracture when tested in air. Again, it is well known that the fracture of a metal under a single blow depends upon the sharpness of the notch. If hydrogen penetration is the cause of brittleness then it is of interest to ask whether the effect is similar to a crack or a sharp notch ?

Another point of interest that tests of materials as cathodes might throw some light upon is the nature of the film produced by polishing. If polishing should cover the crystal boundaries with a film impervious to hydrogen, then it would appear that in this respect the boundary is dissimilar to the crystal itself. Further, when metals are nickel plated three conditions might arise. Gas might become occluded under the nickel, or stress might be set up in the deposited nickel, or the surface covering might affect the stress distributions. The behaviour of the nickel-plated specimens under static and repeated stresses in comparison with cathode specimens should indicate in some measure which of these conditions is of importance. The experiments described in this paper include static tensile tests, single blow impact tests, repeated stress experiments in torsion and under direct stress, of specimens in acid and alkali baths, both when current was and was not flowing, and also some tests on nickel-plated specimens. The results indicate that hydrogen penetrates the crystal boundaries of mild steel, nickel and alloys rich in nickel and chromium, but the penetration does not influence the tensile strength or the resistance to repeated stresses; it, however, affects the elongation of the mild steel specimen, but does not diminish the resistance of "Izod" mild steel specimens to single blows. They show that nickel-plating does not diminish the tensile strength of mild steel but that it reduces the resistance to repeated stresses very considerably. They also show that polishing mild steel either prevents the hydrogen penetration between the crystals or modifies its action, but acid corrosion affects the surface very considerably and reduces accordingly the resistance to torsional stresses. A caustic soda solution, with or without the presence of hydrogen, protects the specimen and the fatigue range is raised.

---

* 'J. Iron and Steel Inst.,' 1924, ii, p. 42.

† Lea and Heywood, 'Proc. Inst. Mech. Eng.,' 1927.

‡ 'A.S.T.M.,' vol. 26 (1926) and vol. 27 (1927).

Tensile Tests.

Tensile tests were carried out on the following materials as preliminary to the repeated stress tests.

Materials.—Materials used in these tests were :—

(1) 0·14 C steel having the composition :—

C.	Mn.	Si.	S.	P.
0·14	0·68	0·19	0·04	0·045

Nickel-plated specimens of this material were also used.

(2) Commercially pure nickel containing more than 99 per cent. nickel.

(3) Brass, 70 Cu, 30 Zn.

(4) Rustless steel containing about 26 per cent. of nickel and chromium.

The apparatus used is very similar to that used by Pfeil, except that an ebonite tube, instead of a glass tube, was used to hold the electrolyte; the test-piece is the cathode; both acid and alkali electrolytic baths were used.

Table I shows the results of the static tests.

Table I.—Tensile Tests of Various Materials in Air and in Electrolytic Baths.

All specimens had a diameter of about 0·399 inch; area 0·125 square inch and gauge length 2 inches.

Specimen No.	Electrolyte.	Current amps.	Period of flow of current.	Time of loading.	Remarks as to finish of specimens.	Ultimate strength, tons per sq. in.	Elongation per cent.	Reduced in area per cent.		Remarks.
					0·14 C. Steel.					
1	None	—	—	about 5 mins.	Ordinary turned finish	31·48	38	44	Reeled bar as delivered.	Usual "cup and cone" fracture.
2	10 per cent. H_2SO_4	0·25	10 mins.	,,	,, ,,	31·05	25	29		Large number of transverse cracks (see plate 1).
3	,,	0·5	60 mins.	,,	,, ,,	31·1	14	12		Very jagged edges. Very little contraction at fracture.
4	,,	0·25	10 mins.	,,	,, ,,	30·5	41	44		Taken from bath and put in boiling water for 10 mins. before testing in air. Cup and cone fracture. No sign of cracks.
5	None	—	—	,,	,, ,,	28·2	32	67·9	Normalised.	Usual "cup and cone" fracture.
6	10 per cent. NaOH	0·75	10 mins. before test	80 mins.	,, ,,	28·0	25	41		Cracks similar to No. 2.
7	,,	0·75	70 mins.	About 5 mins.	,, ,,	28·0	17·5	51		Large number of transverse cracks; very difficult to measure the reduction in area.
8	,,	0·75	150 mins.	,,	Very carefully polished to remove all scratches. Finished with alumina.	28·0	34·0	68·1		"Cup and cone" fracture.
9	,,	0·75	180 mins.	,,	,, ,,	27·9	33·5	67·0		"Cup and cone" fracture. This test checks No. 8.
10	,,	0·5	7 hrs.	,,	Longitudinal polishing. Scratches made with No. F emery.	28·5	35·0	68·1		"Cup and cone" fracture.
11	,,	0·75	120 mins.	,,	Specially deep circumferential scratches made with rough file.	27·3	†24·0	35·0		Large number of transverse cracks; ragged uneven fracture.
12	—	—	—	,,	Nickel plated coating 0·0015 inch.	*28·8	33·0	67·0		Ragged fracture.

COMMERCIALLY PURE NICKEL.										
13	None	—	—	About 5 mins.	Ordinary turned finish	30·7	47·5	78·8		No circumferential cracks.
14	10 per cent. H_2SO_4	0·25	30 mins.	,,	,, ,,	31·4	‡45·0	78·0		Large number of circumferential cracks.
BRASS.										
15	—	—	—	About 5 mins.	Ordinary turned finish	30·7	30	37		Normal.
16	Tap Water	0·7 0·9	20 mins. 30 mins.	—	,, ,,	30·5	28·5	37		Normal.
Fe.Cr.Ni. RUSTLESS STEEL.										
17	None	—	—	About 5 mins.	Ordinary turned finish	47·32	66	51·7		General extension. No local reduction of area. No visible cracks. Mottled surface.
18	—	—	—	16 mins.	,, ,,	49·8	40	29		Ditto.
19	10 per cent. NaOH	0·5	7 hrs.	About 5 mins.	,, ,,	57·0	29	21·8		Many fine transverse cracks. Several cracks inclined at 10 to 15 degrees to the axis.
20	10 per cent. H_2SO_4	0·5	6 hr. 20 m.	Loaded in steps	,, ,,	60·53	41	28·0		After 30 mins. in bath 30 tons per sq. in. applied for 15 mins, raised to 40 tons per sq. in. for 3 hrs. 30 mins., then to 44 tons per sq in. for 1 hr. 40 mins., then to 46 tons per sq. in. for 15 mins., then to 47 tons per sq. in. for 20 mins., then taken to breaking load. Many transverse cracks.
21	10 per cent. NaOH	0·5	5 hr. 40 m.	5½ mins.	,, ,,	44·2	43	29		Specimens 21 and 22 were cut from adjacent lengths of one bar.
22	None	—	—	16 mins. 1/20-in. per min.	,, ,,	49·8	40	29		—

---

* Measured on total cross sectional area.

† The cracks in this specimen (fig. 3) were wide and the measured elongation is accordingly great.

‡ This included many narrow cracks.

Mild Steel.

Reeled Bar.—The material for the first four tests, Table I, was tested as delivered. It had been cold reeled after hot drawing.

The tests indicate that a current of 0·25 to 0·75 amperes for 10 minutes or longer period diminished the elongation per cent. very markedly when the specimens were finished by a tool in the ordinary way. As will be seen from specimens 1 to 3, Table I, the elongation per cent. was reduced from 38 to 25 and 14 per cent., respectively, while the reduction of area at fracture was changed from 44 per cent. to 12 per cent. The effect on the fracture is illustrated by fig. 1 (Plate 13); No. 1 was tested in air and has a cup and cone fracture; No. 2 was tested as a cathode and has a rough, ragged fracture and many transverse cracks. No. 4 specimen, fig. 2, illustrates the effect of removing the specimen from the bath and boiling in water for 10 minutes. The whole of the brittleness, as indicated by the elongation, appears to be removed and the fracture was quite normal; there were no signs of cracks such as those shown in No. 2 of fig. 1 and on No. 3 of fig. 2. The tensile strength of all the specimens was clearly not affected by the occluded gas.

Normalised Bar.—The steel was normalised at 890° C. and tested in an alkali bath; a current of 0·75 amperes being used for times varying from 10 minutes to 7 hours.

A specimen tested in air No. 5, Table I, gave a tensile strength of 28·2 tons per square inch, and an elongation of 32 per cent. When tested in the bath with a current of 0·75 amperes the elongation was reduced to 17·5 per cent. There were a large number of cracks, the fracture was very ragged and the reduction of area could only be measured with difficulty. Two specimens, Nos. 8 and 9, Table I, were very carefully polished. The results obtained were quite remarkable, as seen by comparing figs. 3 and 4 (Plate 13). The tensile strengths of the specimens were the same as the turned specimen; the elongations per cent. and the reductions of area were almost exactly the same as the specimen tested in air. No. 10 specimen was polished but finished by longitudinal polishing with No. F emery. No. 11 specimen was finished with a file. It broke with ragged fracture and with wide circumferential cracks distributed along the specimen. The measured elongation includes these cracks and the value of 24 per cent. is greater than would otherwise have been obtained. It is worth noting that the reeled bar elongation was reduced more than the normalised bar indicating that even a small amount of cold work may affect the probable penetration.

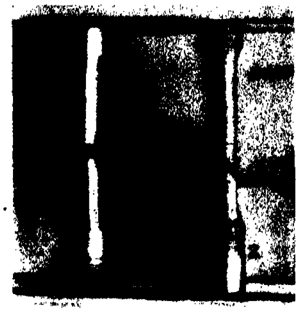

FIG. 1.

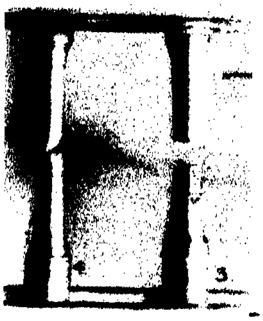

FIG. 2.

0·14 C. steel reeled bar as delivered. No. 1 tested in air, Nos. 2, 3 in 10 per cent. H_2SO_4 electrolytic bath. No. 4 in air after removal from bath and boiling in water.

FIG. 3.—Fracture of a 0·14 C. steel specimen. Rough finished. Normal time test. Hydrogen generated in 10 per cent. caustic soda solution.

FIG. 4.—Fracture of a 0·14 C. steel tensile specimen. Polished longitudinally with No. F emery paper. Hydrogen generated in a 10 per cent. caustic soda solution.

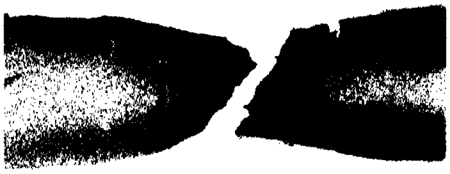

FIG. 5.—Fracture of a pure nickel specimen. Hydrogen generated in acid bath. (× 9/5.)

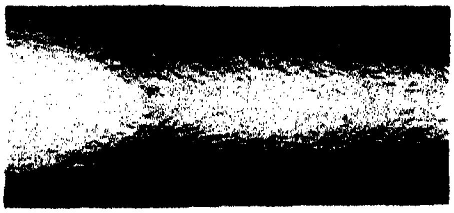

FIG. 6.—Rustless steel tensile specimen. Tested in air. (× 9/5.)

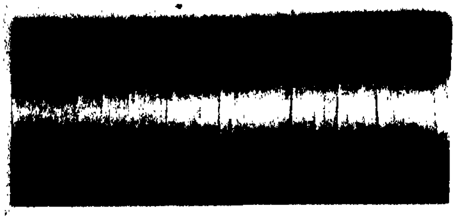

Fig. 7.—Rustless Fe–Cr–Ni alloy tensile specimen. Hydrogen generated in 10 per cent. caustic soda. (× 9/5.)

Fig. 8.—Fracture of a rustless steel specimen. Quick tensile test. Hydrogen generated in acid bath. This material, when fractured in air, has an appearance similar to that of fig. 6.

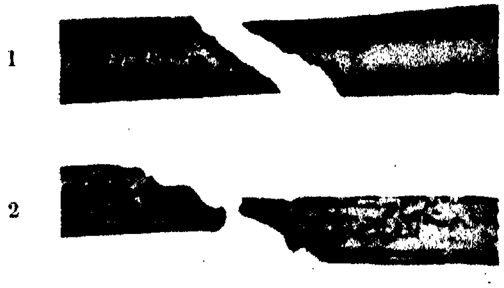

Fig. 11.—0·14 C. steel torsional fatigue specimens. No. 1 cathode in acid bath. No. 2 tested in acid bath, no current flowing.

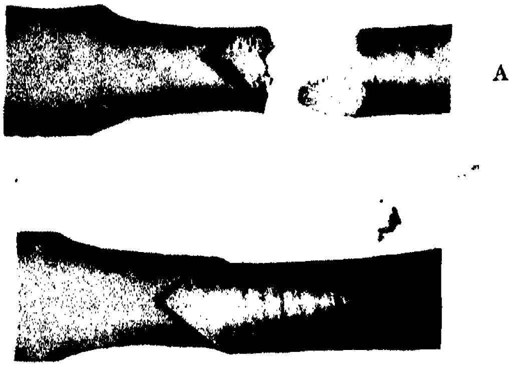

Fig. 12, A and B.—0·14 C. torsion fatigue specimen. Hydrogen generated in alkaline bath. Note the cracks at 45° to the axis.

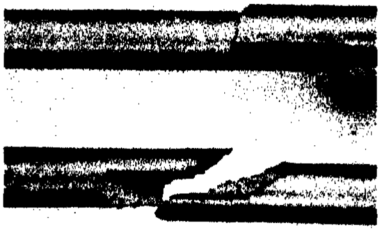

Fig. 13.—0·14 C. steel normalised. Torsional fatigue fractures.

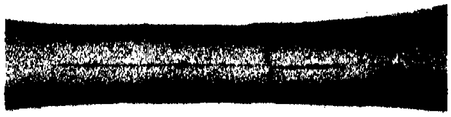

Fig. 15.—0·14 C. steel. Nickel coated. Cracked by repeated stresses. (× 9/5.)

Nickel Plated Specimen.—The effect of nickel-plating deposited on a specimen of mild steel in an acid bath when broken by repeated stresses is shown by specimen No. 16. The strength and other static properties are not seriously affected but as will be seen later the resistance to repeated stresses is very much lowered by nickel-plating.

Nickel Specimens.—The hydrogen developed at the cathode penetrated the specimen without weakening the material. The elongation was slightly lowered. Near the fracture were deep cracks (fig. 5), and away from the fracture were a number of fine cracks similar to those of the high chromium-nickel alloy (fig. 7); the cracks made the total measured elongation correspondingly high.

Rolled Brass.

A preliminary test was made on a 70 per cent. Cu 30 per cent. Zn rolled brass specimen, a water bath being used. The tensile properties were only slightly affected by the current density used and no cracks could be seen. The results obtained were negative but further work may be necessary.

Rustless Steel containing about 26 *per cent. of Nickel and Chromium.*—This is a steel with rather remarkable properties. Its tensile strength and elongation depend very much on the time of loading. When loaded slowly creep and thus cold working takes place. Its primitive limit of proportionality is very low—it may be less than 4 tons per square inch.

Tests were carried out over periods of a few minutes and many hours. Fig. 6 (Plate 13) and fig. 7 (Plate 14) show the appearance of the surface of specimens broken in air and as a cathode in an alkaline bath respectively. Fig. 8 shows the surface when broken in an acid electrolytic bath.

Izod Impact Tests.

Standard izod impact test-pieces were prepared; these were surrounded by a thin rubber disc to which was fixed by rubber solution a piece of rubber tube forming a bath. In this was placed a 10 per cent. solution of sulphuric acid; anodes of iron wire, carbon and platinum were used to complete the electrolytic bath.

The results of the tests of eight specimens are shown in Table II.

The hydrogen which in the case of the last specimen escaped very freely from the cathode, did not affect the impact value. When the current was 0·5 amperes, the temperature of the specimen and bath was about 20° C. In the case of the last specimen the temperature of the bath rose to 29° C., but the specimen temperature could hardly have been raised above 20° C. as it was held in the massive vice of the impact machine. The last column of Table II shows that the mean angle turned through by all specimens was between 50 and 55 degrees.

Table II.—Impact Tests of Izod Specimens of Normalised Mild Steel (0·14 C.).

Specimen No.	Electrolyte.	Current, amperes.	Period of flow of current.	Impact value foot-lbs.	Remarks.	Angle after impact with vertical.
						Degrees
1*a*	None	—	—	81·75	—	—
1*b*	,,	—	—	79·25	—	—
1*c*	,,	—	—	85·00	—	50·5
2	10 per cent. H_2SO_4	0·5	2 hrs.	84·5	An iron wire cathode was used which contained copper. A very thin film of copper was deposited on the specimen.	55·0
3	,,	0·5	25 mins.	81·00	Carbon anode	52·0
4	,,	0·5	2 hrs. 3 mins.	82·20	,,	52·5
5	,,	0·5	1 hr.	84·0	Platinum anode	51·5
6	,,	2·1	10 mins.	81·0	,,	50·0
7	Acid	None	3 hrs. in acid	83·5	—	51·5

Repetition Tests in Tension and Compression Haigh Machine.

The tensile strengths of the materials not having been affected by the hydrogen generated at the surface, although the elongation was diminished, suggested that if the range of repeated direct stress is related, as modern tests indicate, to the ultimate tensile strength more definitely than to other properties, it also ought not to be seriously affected by the hydrogen. In the direct stress machine also the surface condition of the materials is not so important in determining the range of repetition stress, as when the specimen is subjected to bending and torsional stresses.

The apparatus used for the tests was very similar to that used in the former tensile tests, the bath being attached to the lower part of the specimen. The range of repeated stress interpolated from the number of specimens of mild steel tested in air was from 28 to 29 tons per square inch. A specimen 0·2 inch diameter was tested in the acid electrolytic bath with a current of 0·5 amperes, intensity about 0·33 amperes per square inch.

A range of stress of ± 14 tons per square inch was applied to the specimen, which is just below the safe range when tested in air. After 13,000,000 reversals the specimen was unbroken and it was removed from the machine.

As far as could be seen it was quite unharmed but on bending it with the fingers it proved to be brittle and broke very readily. Evidently the effect of the acid bath had been to embrittle the specimen but the strength was not diminished and in the time occupied serious corrosion had not taken place. The specimen was originally well polished. A similar specimen was tested in a 10 per cent. caustic soda bath with a current of 0·5 amperes, at a range of stress ± 15 tons per square inch. Failure occurred after 1,552,300 repetitions, which corresponds to the number of repetitions to be expected when a specimen is tested in air. To test the effect of a solution of NaOH alone, specimens of 0·46 C. steel heat treated so as to give a tensile strength of 40·5 tons per square inch, were tested in air and in a 10 per cent. solution of NaOH with no current flowing. In air the specimen broke at a range of stress of ± 13·5 tons per square inch after 4,669,000 repetitions. In a bath of NaOH without current the specimen withstood 18,000,000 repetitions for the same range of stress without fracture. When taken from the machine the specimen was not corroded and was not brittle when bent by the fingers. Hydrogen penetration does not therefore lower the range of direct repeated stress, although the material becomes brittle in an acid bath. The cause of brittleness is apparently not hydrogen of itself. Further the NaOH solution increases the range of repeated stress rather than lowers it. (See also fig. 10.)

Repeated Torsion Tests on 0·14 *C. Steel.*

Repeated torsion tests have been carried out in the apparatus shown in fig. 9 on 0·14 C. steel specimens. The specimen is subjected to a forced oscillation of 10 degrees amplitude at the right-hand end. The other end is connected to a mass of known moment of inertia and the length of the specimen is chosen so that the oscillating mass has a very small amplitude, or in other words there is a node near to the free end of the specimen. This made it possible to enclose the specimen quite easily in the bath shown in fig. 9. At the right end of the bath there is a packing which keeps in the fluid but offers a very small torsional resistance to the oscillation.

Tests have been carried out as follow :—

(1) In the air.
(2) In H_2SO_4 acid bath with specimen as cathode.
(3) In H_2SO_4 acid bath with specimen, no current flowing.
(4) In NaOH bath with specimen as cathode.
(5) In NaOH bath with specimen, no current flowing.

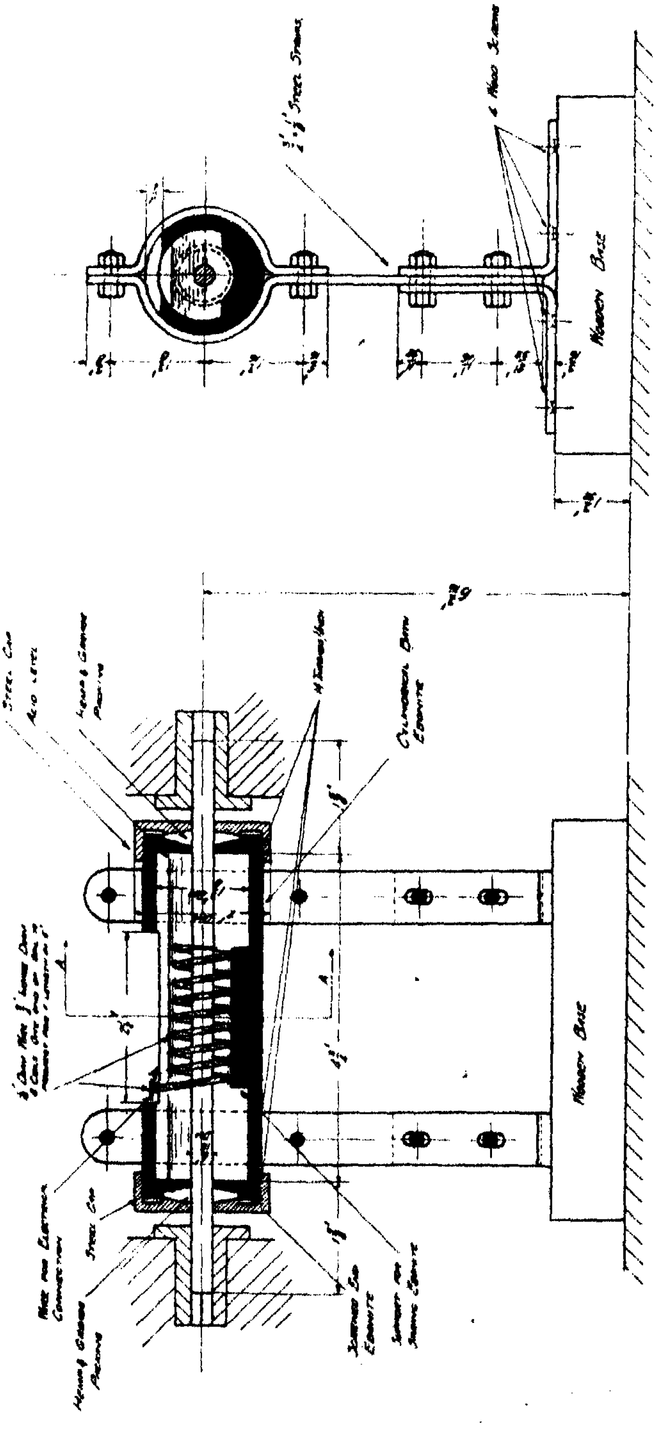

Sectional Elevation.

Section through AA.

Fig. 9.—Electrolytic Bath for Alternating Torsion Machine.

Table III.—Torsional Tests in Air. 0·14 C. Steel Normalised.

Specimen.	Range of stress, tons per square inch.	Repetitions.	Remarks.
1	20·6	920,240	Broken
2	20·6	1,355,000	,,
3	19·8	1,812,400	,,
4	19·2	2,518,400	,,
5	18·9	2,556,800	,,
6	18·3	9,007,680	Unbroken

Table IV.—Torsional Tests in Caustic Soda Bath with Current of 0·4 amperes (about 0·16 amperes per square inch of area). 0·14 C. Steel Normalised.

Specimen.	Range of stress, tons per square inch.	Repetitions.	Remarks.
1	20·8	1,227,360	Broke outside bath near grip.
2	22·6	572,400	Broke in the bath.
3	22·0	1,257,200	,,
4	20·2	5,277,000	Unbroken.
4*a*	20·2	5,000,000	Specimen (4) removed from bath, cleaned in boiling water and retested in the air.
5	18·5	5,114,000	Unbroken.
6	22·0	560,000	Broken in bath without current.

Table V.—Torsional Tests in Acid Bath with Current of 0·4 amperes. (Rate of repetitions 72,000 per hour.) 0·14 C. Steel Normalised.

Specimen.	Range of stress, tons per square inch.	Repetitions.	Remarks.
1	23·3	200,000	Broke in bath.
2	22·8	584,240	,, grip.
3	20·6	964,160	,, bath.
4	18·0	957,840	,, ,,
5	14·6	1,661,560	,, ,,
6	12·0	2,016,720	,, ,,
7	12·0	1,876,000	Tested in acid bath, without current. Corroded very badly and failed in two places.

The results of the repeated stress tests are shown in Tables III, IV, and V, and in fig. 10. The range of repetition stress in air at zero mean stress is seen to be about 18·5 tons per square inch. In the acid bath it is only 12 tons per square inch for 2 million repetitions and it is probable that at much less stresses fracture would have occurred. A specimen was also tested in the acid bath at 12 tons range without current and it will be seen that fracture occurred at 1,876,000 repetitions. This specimen corroded very badly and, as might have been expected, very much worse than when the specimen was a cathode.

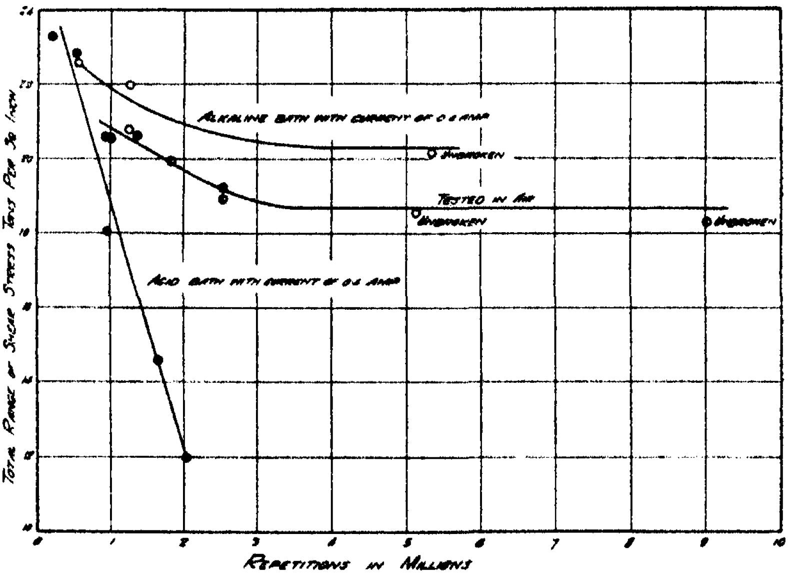

FIG. 10.—Endurance Curves from Torsional Fatigue Tests on 0·14 Steel Specimens as Cathodes under various conditions.

Fig. 11 (Plate 14) shows the two specimens tested at 12 tons range. No. 1 was a cathode; No. 2 was tested with no current flowing. The corrosion in the second case was very serious. The specimens broken in acid, especially at high stress ranges had fractures having the appearance of a rose bit, very similar to those obtained from the same material tested in tension as cathodes. When tested in air the fracture was very clean and at right angles to the axis of the specimen (fig. 13). Tests in the caustic soda bath are particularly interesting.

Tables III and IV show that the range of repetition stress has clearly not been lowered by the alkali bath either when current is flowing or not, but rather raised; the material is apparently hardened by hydrogen or what is more likely the slight surface corrosion that ordinarily takes place is prevented. This point is being further investigated. The fractures (fig. 12) indicate that the material is behaving as a brittle material or as the fracture of a ductile material when a small hole is bored into the surface; whereas the fracture, when no current is flowing, is very similar to that of the specimen fractured in air (fig. 13). The low value of the repetition stresses in the acid bath indicates that corrosion, as distinct from hydrogen, is the most important factor in determining failure. The surface of the metal was deeply pitted, fig. 11, and particularly was this so, as seen in No. 2, when there was no current passing.

Nickel-plated Specimens.

A number of tests have been carried out on nickel-plated specimens, in "Wöhler" and "Haigh" machines, to determine the effect of the surface covering on the range of repetition stress.

Tests under cycles of bending and under cycles of direct stress have been made.

A few of the results obtained are shown in fig. 14 and are compared with results from mild steel and drawn nickel bar. These show that under direct repeated stress the effect of the deposited surface is to lower the fatigue

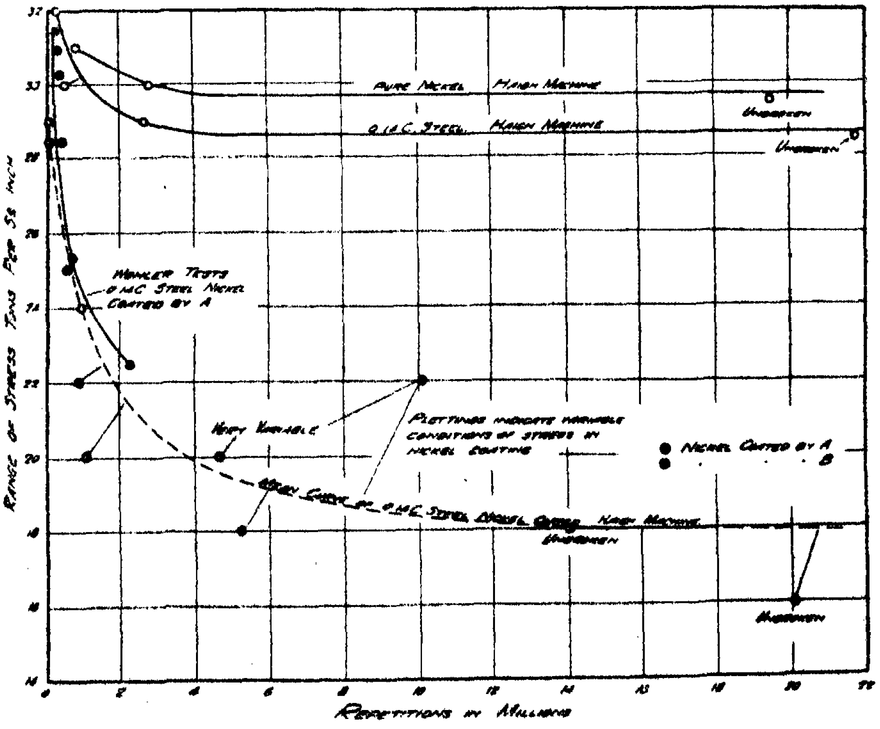

FIG. 14.—Endurance Curves showing Effect of Nickel Coating on 0·14 Steel.

range very appreciably and to make the results erratic. It has also been found by direct experiment that a tool mark having a depth equal to the thickness of the nickel deposit and sharp at the bottom, lowers the fatigue range in bending by the same amount, approximately, as the nickel deposit. The question arises whether the lowering of the stress by the deposit can be attributed to initial stresses in the deposited material, to the surface condition of the specimen or to occluded hydrogen.

It can safely be stated from the results of the tests already detailed that occluded hydrogen does not lower the range, while a sharp tool mark, which certainly concentrates the stress, lowers the repetition stress to a similar amount. It, therefore, seems clear that the nickel is deposited under stress or acts as a discontinuity like the tool mark or a crack is first produced in the deposited nickel.

Fig. 15 (Plate 14) shows a specimen tested in the direct stress machine. The specimen cracked as shown and stopped the machine. The fracture is almost normal to the axis of the specimen and is not very different from a fracture of nickel or of mild steel. The longitudinal crack suggests transverse stress in the deposit.

Conclusions.

1. Nascent hydrogen liberated at a cathode penetrates the crystal boundaries of mild steel, nickel, and "rustless" steel containing about 15 per cent. chromium and 10 per cent. nickel. The penetration does not affect the tensile strength of these materials but it lowers considerably the elongation of specimens of mild steel. The specimens exhibit transverse cracks and indicate that tearing of crystals apart at their boundaries occurs at fractures. The hydrogen clearly interferes with the slip that takes place on certain crystal planes and which, under ordinary conditions, continues apparently across the crystal boundaries.

Hydrogen escapes quickly after the current ceases even at ordinary temperatures, and after heating at 100° C. the properties of the material are restored. Highly polishing the surface of mild steel affects the hydrogen penetrating between the crystal boundaries.

2. Hydrogen in the cathode does not diminish the resistance to impact of mild steel and its effect on repeated stress seems of itself unimportant. The fractures under repeated stresses, however, show that the penetration of hydrogen has an important bearing upon the nature and form of fracture of a plastic material, which under torsional repeated stress, fails in a manner similar to quenched and tempered materials.

It would appear, therefore, that the presence of the hydrogen at the crystal boundaries does not increase the concentration of stress in the repeated stress experiments, nor in the impact tests, but affects the continuity of slip and causes a crack to occur as in the quenched and tempered materials, and suggesting that in all such materials the failure is at the boundaries while the failure of plastic materials occurs by cracking within the crystal.

A cathode specimen of mild steel under repeated direct stress in an acid bath becomes very brittle, but not in a NaOH bath.

3. Nickel plating mild steel lowers the range of repeated stress but this is not apparently due to occluded gases. As drawn nickel bar is as resistant as mild steel under repeated stresses, it would appear that either initial stresses set up by the deposition or the discontinuity between the metals or, more likely, a crack which early forms in the deposited nickel, is the cause of the lowering of the repeated stress range.

A very small groove, perfectly sharp at the bottom, reduces the range of repetition stress to about the same extent as the nickel plating.

The Electrical Conductivity of Thin Oil Films. Part I.—General Nature of the Phenomenon.

By H. E. WATSON, D.Sc., and A. S. MENON, M.Sc.

(Communicated by Sir William Hardy, F.R.S.—Received August 1, 1928.)

It has long been a common practice to cover accumulator terminals with vaseline; Price and others at a discussion at the Physical Society* mentioned that potentiometer contacts were improved by immersion in kerosine oil; Manley† found that the resistance of the plugs in a resistance box was invariably more constant and very nearly always lower when they were lubricated with vaseline than when they were dry; Kraus,‡ and Melsom and Booth§ in investigations upon contact resistances, such as switches for electrical machinery, obtained similar results. Vaseline and heavy paraffin oil are now widely used for application to plugs and sliding contacts on measuring instruments.

---

* 'Proc. Phys. Soc.,' vol. 18, p. 479 (1903).

† 'Phil. Mag.,' vol. 33, p. 211 (1917).

‡ 'Electrotechnik u. Machinenbau,' vol. 30, p. 1 (1920).

§ 'J. Inst. Elec. Eng.,' vol. 60, p. 889 (1922).

In view of the fact that these substances are ordinarily regarded as excellent insulators, their use for the above purpose appears somewhat anomalous, and the object of the present investigation is a detailed examination of the region in which a transition from insulation to conduction appears to take place.

Branly,* in his experiments upon the coherer, found that films of gutta-percha, collodion, mica, celluloid and paraffin wax from 5 to 25 μ in thickness conducted electricity when pressed between optically polished metal discs, and the resistance was reduced by an oscillatory discharge in the vicinity. He did not measure the actual thickness of the dielectrics. Wilson and Daniel† measured the contact resistance of two flat metallic surfaces pressed together and found that a dry resistance of 0·03 ohm increased on immersing the surfaces in mineral oil, continued to increase for about 6 hours and reached a final value of 4·4 ohms, pointing to the gradual building up of an adsorbed film. On application of a very small 1000 cycle alternating E.M.F. the resistance fell rapidly to 0·4 ohm. These results do not appear to be in agreement with those of previous workers since the resistances are much higher. The resistance of the plugs measured by Manley was of the order of 0·002 ohm. The difference may be due to the pressure, which in Wilson and Daniel's experiments was 311 gm./sq. cm. while in the other cases it was probably much greater.

The present paper deals more with the phenomena of breakdown than with the actual values of resistance when "contact" has been established, and is largely an account of the experimental methods used for determining the nature and the thickness of films obtained in different ways. For most of the work a heavy paraffin oil $d^{30^\circ} = 0·886$ and with very slight action on bromine has been used. The breakdown strength kindly measured by Mr. Yoganandam in the Institute high tension testing laboratory was found to be 92,000 volts r.m.s. per centimetre between 2·5 cm. discs 3·8 and 1·2 mm. apart at 60 cycles. Although suffering from the disadvantage of being a mixture of unknown composition, yet, for preliminary work, this is more than counterbalanced by the high insulating properties, large viscosity, low volatility and freedom from action upon metals of the oil, coupled with the fact that it is readily obtainable in large quantities while, since it is actually used for lubrication of contacts, an investigation of its electrical properties is desirable.

It is found that there is a critical thickness of the order 10 μ at which the dielectric strength falls very suddenly and that breakdown takes place in two stages. Measurements have also been made upon the air film which is formed under certain conditions between two plane surfaces.

---

* 'C. R.,' vol. 155, p. 933 (1912).

† 'Ind. Eng. Chem.,' vol. 14, p. 683 (1922).

Experimental.

The experiments were started shortly after the publication of Hardy and Birchumshaw's Bakerian Lecture* on boundary lubrication in which the coefficient of friction was shown to vary with the thickness of the oil film. It was thought that these results might be of value in correlating the thickness of the film with the conductivity, and consequently an apparatus somewhat similar to the one used by these authors was set up and friction measurements were made simultaneously with the others.

The determination of the capacity of the condenser formed by the two metal surfaces and the oil film suggested itself as a possible method of measuring the thickness of the latter and, consequently, arrangements were made to measure this quantity. The whole apparatus is shown diagrammatically in fig. 1.

The slider A weighed 30·3 gm. and consisted of a triangular 6 mm. plate of 35 mm. side with three 6 mm. legs. These were turned down to 3 mm. at the ends, case-hardened and polished. They rested upon a polished steel plate B, half of which was silvered, supported upon a levelling platform C. The whole could be enclosed if required by a glass cover with ground edges under which was a dish of phosphorus pentoxide, but the presence of this drying agent had no marked effect, probably because experiments were not made with perfectly clean surfaces and the laboratory air was very pure and, at the time of the experiments, exceedingly dry. For determining the friction a fine thread

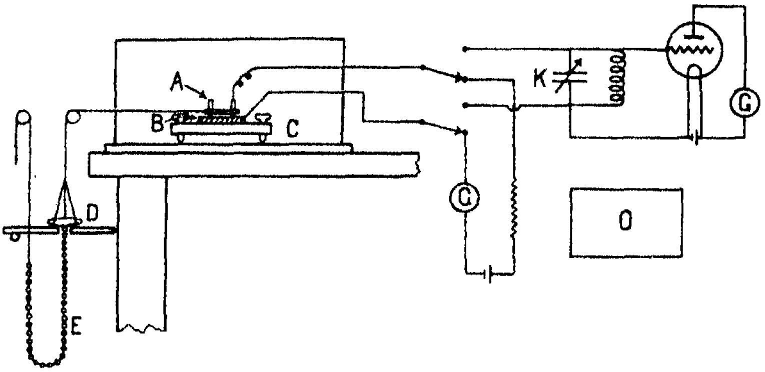

FIG. 1.

---

* 'Roy. Soc. Proc.,' A, vol. 108, p. 1 (1925).

from A passed over a pulley and supported a scale pan D with an adjustable release which would only allow a drop of about 1 mm. Weights nearly sufficient to move A were placed in the pan and the final adjustment to the weight necessary to cause slip was made by means of a fine calibrated chain suspended below D, the principle being that of the chainometric balance. In this way the weight could be increased very smoothly and measurements could be rapidly repeated.

In order to determine if the film was conducting, the slider and plate could be connected in series with a battery, galvanometer and high resistance (about 100,000 ohms) to limit the amount of current passing, connection being made to the slider by a very fine wire to avoid strains. The capacity of the condenser when the film was non-conducting was measured by connecting it in parallel with a calibrated condenser K and an inductance. The circuit could be tuned to resonance with the oscillations from a separate oscillator O, the resonance point being determined by means of the simple valve circuit shown.* Wave-lengths varying from 100 to 300 m. were used. In order to avoid errors due to change in lead capacity, the circuit was first set to resonance with A resting on the oil film, the slider was then raised about 3 mm. by inserting a small ebonite strip between the top and the plate B and measuring the change in K necessary to restore resonance. This change was substantially equal to the capacity of the condensers formed by the three legs of the slider and the plate when separated by the oil film.

Wiped Films.

As soon as the experiments were started it was found impossible to obtain a non-conducting film by placing oil, vaseline, or even a thin film of a solid, on the plate and standing the slider upon it, but if the substance was wiped off until almost invisible, a very stable film was obtained which would frequently withstand the application of 100 volts. The nature of this type of film will be discussed later.

Preliminary experiments were made with myristic acid. A small crystal was melted on the plate, previously thoroughly cleaned by boiling in alcohol and allowed to cool in a vacuum desiccator. The film so formed was wiped, and when the slider was placed on it was non-conducting. A number of measurements of the coefficient of friction were made, the slider being allowed to move about 1 mm. and then replaced in its original position.

---

* *Cf.* Hobbs, 'Wireless World,' vol. 14, p. 77 (1924).

Table I.—Coefficient of Friction, Steel-Silver, Myristic Acid, Non-conducting.

	a.			*b.*	
Weight:	30·3	80·7	130·8	30·3	130·8
Coefficient of friction	0·413 0·390 0·400 0·403	0·283 0·279 0·282 0·284 0·282 0·284	0·253 0·252 0·249 0·237 0·255 0·250	0·374 0·354 0·354 0·337 0·347	0·185 0·184 0·183 0·187
Mean	0·401	0·282	0·249	0·353	0·185

The values (*a*) and (*b*) were obtained with different films, and it will be observed that while sufficiently concordant results with a maximum variation of about 10 per cent. can be obtained in the same part of the same film, much larger variations are found with different films. In the case of a brass plate and the steel slider a mean value of 0·355 was found for a load of 30·3 gm. The area of contact of each leg of the slider was 6·75 sq. mm., so that the actual loads in the three cases were approximately 150, 400 and 650 gm,/sq. cm.

Measurements were next made of the thickness of the films by the dielectric constant method. It was at once found that the film thickness was by no means of molecular dimensions, but large even in comparison with the wavelength of light. Very exact optical polishing of the surfaces was consequently not necessary. The first slider used was slightly convex at the ends of the legs, the flatness over about one-third of the total area being within 1 μ. This was measured by placing a piece of optically worked glass over the legs and observing the positions of the Newton's rings. These were drawn on a larger scale on squared paper and the area corresponding with each thickness computed. The approximate thickness of the film was calculated by means of a curve showing the relation between minimum thickness and capacity.

Table II gives some results for this series of experiments with different films.

A number of experiments with myristic acid showed that widely divergent values could be obtained by placing the slider on different films or on different parts of the same film. The first two figures are the maximum and minimum capacities which were found in this way. The coefficients of friction varied between 0·37 and 0·44, but there appeared to be no relation between the coefficient of friction and the capacity. For determining the variation with pressure, the same part of the same film was used, and it may be seen that the

Table II.—Coefficient of Friction and Minimum Thickness of Non-conducting Wiped Films.

Film.	Weight, gm.	μ.	Capacity, $\mu\mu$ F.	Thickness, mm.$^{-6}$ (ϵ=1).
Myristic acid, silver-steel	30·3	0·43	50·8	1·27
	30·3	0·40	34·2	2·42
	30·3	0·45	36·0	2·24
	80·3	0·31	37·0	2·15
	130·3	0·24	38·9	1·99
	230·3	0·25	39·5	1·93
Paraffin wax, silver-steel	30·3	0·36	29·4	3·10
	80·3	0·175	32·4	2·62
	130·3	0·175	38·0	2·07
	230·3	0·135	44·0	1·63
Paraffin oil, steel-steel	30·3	0·39	22·5	4·55
	80·3	0·19	23·5	4·30
	130·3	0·21	26·4	3·67
	30·3	0·39	45·7	1·52
	80·3	0·32	47·5	1·43
Stearic acid, steel-steel	30·3	0·33	52·0	1·20
	80·3	0·195	57·0	1·03
	130·3	0·155	60·8	0·91
Oleic acid, steel-steel	30·3	0·40	47·5	1·43
	80·3	0·26	48·0	1·41
	30·3	0·36	31·0	2·85
	80·3	0·27	31·0	2·85
Linolenic acid, steel-steel........	30·3	0·44	51·5	1·25
	80·3	0·34	53·5	1·16

coefficient of friction decreases considerably with increase of pressure in agreement with Hardy's results (*loc. cit.*), but the capacity changes very slightly except in the case of paraffin wax. These results are shown in brackets. Where two sets are given for the same substance, the figures refer to different films or the same film after wiping. The various substances used were not specially purified for the preliminary experiments as the object was to ascertain the magnitude of the effect of the material of the film upon the thickness. Actually, the variations with one substance were so great that it was impossible to compare the results for different substances, although it is interesting to note that the thickest films were obtained with paraffin oil and the thinnest with stearic acid. The thicknesses given are the minimum thicknesses, calculated in the manner already described, but, apart from the uncertainty introduced by the curvature of the slider legs, they involve the assumption that the film under each leg is of equal thickness and, consequently, cannot be considered as accurate values. Subsequent experiments after regrinding and polishing the legs until they were almost flat gave very similar results, so that the error is probably not large. In any case the figures for the variation in thickness on weighting are likely to be substantially correct.

The thickness has been calculated with the value 1 for the dielectric constant of the film, whereas the value for all the materials used was not far from 2. The original calculations were made with the latter figure leading to double the film thicknesses given. It was, however, quite obvious that these results were impossible as a film even 1 μ in thickness was quite opaque, while the wiped films were hardly visible. On discussing the matter with Sir William Hardy, he suggested that the films really consisted of air. This would account for the high insulating properties, since it has been shown by Broxon* that air films of the order of 0·5 μ in thickness will withstand a gradient of 640,000 volts per centimetre before breaking down.

Examination under the microscope revealed the rather unexpected fact that the films are not continuous, but consist of a number of minute globules which appear not to wet the surface. Fig. 2 is a microphotograph of a film of paraffin oil on stainless steel in the initial stages of wiping. Fig. 3 is an adjacent portion of the steel plate upon which a steel cylinder had stood overnight in a pool of the oil. Both portions were wiped simultaneously and had stood for 24 hours before being photographed.

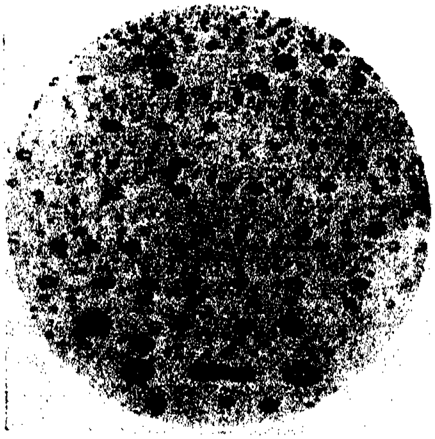

FIG. 2.

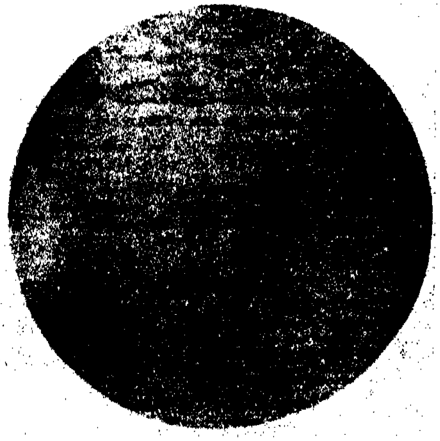

FIG. 3.

The appearance is quite different and it is evident that wetting of some kind has taken place. Melted myristic and oleic acids also formed globules, but nonyl alcohol spread in a continuous thin layer.

---

* 'Phys. Rev.,' vol. 20, p. 476 (1922).

These facts suggest that non-conducting wiped films consist of a number of small oil globules between two adsorbed films of air or water vapour on the metallic surfaces, but their exact nature seems to be one of some complexity, and further discussion will be deferred until the experiments with flooded films have been described.

Flooded Films.

As already mentioned, it was not found possible to obtain a stable non-conducting film when the slider was placed in a pool of lubricant. This was also the case when a steel cylinder of diameter 10·9 mm. and weighing 11·2 gm. was substituted for the slider. It was subsequently found that discs of brass and case-hardened mild steel 18 mm. in diameter and weighing 8·6 and 7·9 gm., respectively, would not only float on the oil but would remain suspended above the plate when the oil was removed.

In order to obtain a film of varying thickness which changed slowly enough for observations to be made with some accuracy, the following device was adopted.

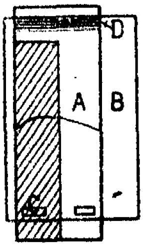

FIG. 4.

A piece of thick plate glass A, fig. 4, with a good optical surface, was silvered or platinised by splashing for half its width, as shown by the shaded area. The silvering was removed for 1 cm. at one end. The glass was placed on a stainless steel mirror or a similar piece of glass with the unsilvered end in contact and the other supported on a small piece of mica C, 32 μ thick, cut into two. The silvering thus formed a wedge with the mirror but was insulated from it. Electrical contact was made at the end of the plate and a drop of liquid was allowed to flow between the two pieces of mica. This gradually extended along the wedge and its progress could be watched through the clear side of the glass. At a certain point the film became conducting and the wedge was then opened and the farthest point to which the liquid had penetrated was observed. From this the thickness could be deduced. The thickness of the mica was measured as accurately as possible with a micrometer. Capacity measurements were not very satisfactory, possibly owing to irregularities in the silvering. The values obtained for the thickness were greater than by direct measurement.

It was found that with very thin layers of oil between two slightly curved plates there was a considerable attraction which was sufficient to bend the plates. In the present series of experiments a few interference bands could be seen at the end of the plate at D, and these did not move appreciably on admitting oil, so that mechanical distortion was absent.

The surfaces were carefully cleaned in boiling ethyl alcohol or by washing with petrol followed by anhydrous methyl alcohol, and paraffin oil or triolein run into the wedge. Some of the individual results for the thickness at which the film became conducting were as follows :—

Paraffin oil—	
Silver-steel	A.C., 8 μ, 15 μ.
Silver-silver	D.C., 6 v.–10 μ ; 110 v.–11 μ.
*Platinum-steel	D.C., 2 v.–11 μ ; 24 v.–11 μ ; 80 v.–13 μ.
Silver-steel	D.C., 2 v.–14 μ.
Triolein—	
Silver-silver	D.C., 6 v.–13, 16 μ ; 110 v.–18 μ.
Silver-steel	D.C., 6 v.–13, 13 μ.

In all cases the point of breakdown was very sharply defined. The thicknesses are not very exact owing to the difficulty of determining the effective thickness of the mica, but the same mica was used throughout so that the values are comparable. In the experiment marked with a star a quartz fibre 27 μ in diameter was used instead of the mica and the diameter of this could be measured with some accuracy. The silver films softened after a few experiments and had to be frequently renewed, but the platinum resisted the oil better.

The most striking feature of these results is that the breakdown thickness appears to be nearly independent of the applied voltage. Exact reproduction of the experimental conditions was a matter of some difficulty, but a good example is seen in the three experiments at 2, 24 and 80 volts with platinised glass. These were made as far as possible under comparable conditions and conduction occurred at very nearly the same thickness in all cases. The possibility of the result being due to a small projecting piece of metal was excluded by the fact that the oil ran rather unevenly, and although at the same distance from the end it was in contact with different parts of the film when breakdown occurred. The figures for triolein appear to be slightly larger than those for paraffin oil. In most of these experiments only the first stage of conduction was obtained; that is to say, the film resistance fell to about 1 megohm.

Although the wedge method was of value for determining the approximate thickness at which conduction took place, its application was limited and it seemed desirable to supplement the results in other ways. For this purpose a more accurate method of measuring capacities was adopted similar to the one used by one of us* for determining dielectric constants. The condenser under observation was placed in parallel with a precision condenser and the capacity determined by the method of beats at a frequency of about 600 k.c. Approximate measurements of the resistance of the condenser could be made simultaneously. With this arrangement a vertical displacement of 0·003 μ could be readily measured, and it was possible to determine if necessary much smaller shifts by means of a vernier condenser. The method possessed the advantage that even rapid movements could be qualitatively followed by ear.

Attempts were first made to determine the thickness at which conduction took place by placing the slider, or the steel cylinder already mentioned, in a pool of oil and noting the maximum capacity reached before oscillation stopped. With paraffin oil, conduction occurred within about 2 seconds and no reliable measurements were possible. With the cylinder, the thinnest film measured was 10 μ in thickness and with the slider and vaseline 8 μ, but these values are probably too large. The magnitude of the alternating E.M.F. applied could not be measured as it varied rapidly, but it was certainly less than 2 volts. The load per square centimetre in the two cases was 144 and 12 gm. When brass and steel discs corresponding to loads of 3·6 and 3·3 gm. per square centimetre were used, they floated in the oil and the films did not conduct. Another system was then tried. A condenser was made by standing the steel cylinder on two quartz or pyrex fibres stretched across a stainless steel mirror. For a very convenient method of drawing the glass fibres we are much indebted to Dr. E. P. Metcalfe, of the Central College, Bangalore. A small bead of glass is melted on an electrically heated platinum wire and the fibre drawn by touching the bead with a very fine platinum wire and pulling out by hand. By regulating the temperature and the rate of pulling, a fibre of approximately correct diameter can be drawn.

Numerous observations have been made with condensers of this type using the method of beats. The results are somewhat irregular, but certain features appear to be fairly definite. The thickness of the air film calculated from the capacity is always slightly greater than the measured thickness of the fibres except in one or two cases in which a fibre may have been displaced while putting down the cylinder. The difference is more noticeable for the thinner fibres. For film thicknesses of the order of 8 μ and under, it was frequently noticed that the cylinder at first assumed a metastable position and could be made to sink by gently tapping the plate or cylinder, but even prolonged tapping would not reduce the thickness to that of the fibres. At the same time attempts to remove a fibre only result in fracture, so that adhesion of some kind is present. The thicker films will stand a D.C. voltage of over 100 without breaking down, the insulation resistance being over 50 megohms and potential gradients of 100,000 v/cm. having been reached. The thinner films break down frequently on application of from 2 to 40 volts and become partially conducting, sometimes the resistance becomes very low. Usually, but not always, a film which has broken down subsequently conducts on application of a lower E.M.F., although it did not do so previously. Tapping restores the insulation. This might possibly be due to a thin bridge of metal, but a calculation of its diameter from the measured resistance in one or two cases assuming the ordinary resistance law to hold, gives a diameter of the order of 3×10^{-7} cm., a rather unlikely quantity. The alternating voltage applied to the film varied from 2·5 to 3 volts r.m.s., but it was not convenient to determine the breakdown point for alternating current with the more sensitive apparatus, as the power factor of the thinner films was appreciable and tended to stop the oscillations before actual conduction occurred. It is noteworthy that all films which would withstand 2 volts D.C. could be measured with the alternating E.M.F. mentioned, a result not to be anticipated from the work of other observers.

---

* 'Roy. Soc. Proc.,' A, vol. 117, p. 43 (1927).

In making these measurements the cylinder was placed on the fibres and the capacity of the system measured. Any change on tapping was noted and oil was then run under the cylinder and the capacity remeasured. The values for the dielectric constant were very close to the correct value and afford a remarkable confirmation of Sir William Hardy and Miss Nottage's observations,* which reached India just after these experiments had been conducted, that a flat steel cylinder does not come into contact with a flat plate when stood upon it, but that a stable air film intervenes and the distance between plate and cylinder is not affected by introducing a lubricant between them. The examples in Table III show, however, that this is not true if the system is in the metastable state already mentioned, since in this case high values are obtained for the dielectric constant indicating that the lubricant pulls the cylinder down to the stable distance. It may be mentioned here that the capacity method has been criticised on the ground that the dielectric coefficient alters for very small thicknesses, but the recent work of Kollmann and Dorch,* who have been unable to detect any variation for several materials down to 1 μ, renders this unlikely, especially when taken in conjunction with the above results obtained by two independent methods.

---

* 'Roy. Soc. Proc.,' A, vol. 118, p. 224 (1928).

Table III gives a few of the results obtained. The value for ε is the ratio of the capacities after and before filling with oil allowing for stray capacities. The thickness of the oil film is calculated on the assumption that $\varepsilon = 2 \cdot 21$, the value obtained by measurement in a larger apparatus. The figures represent mean thicknesses but the minimum thickness is nearly the same (within $0 \cdot 5\ \mu$) as the cylinder and plate were almost flat. Although the absolute values are subject to an error of this magnitude the relative values are much more accurate.

Table III.—Conductivity of Flooded Oil Films of Different Thickness.

Experiment No.	Fibre, μ.	Air film.	Oil film.	ϵ.	Remarks.
1	33 app.	30	30	2·21	Quartz fibre, R very high.
2	2·8	4·5	4·73	2·08	Initial thickness 8·2 μ, value 4·5 after tapping. Oil film 4·15 μ with 50 gm. weight on cylinder. Conductivity irregular.
3	2·8	6·36	6·36	2·21	Initial thickness 15·0 μ, 6·36 after prolonged tapping. Conductivity partial.
4	12	16·8	16·9	2·20	Oil film reduced to 13·7 μ with 50 gm. weight. No conduction 120 v.
5	9	—	9·9	—	Conducted partially.
6	3	11·0	10·9	2·22	Fibres slightly oily; conducted 6 v.
7	3	9·9	10·1	2·17	Thickness before tapping 13·8 μ. Conducted 6 v.
8	9	11·8	11·6	2·24	Partially conducted 24 v.
9	9	10·1	8·3	2·68	Same fibres, one very near edge possibly washed out by oil. Partly conducted 14 v.
10	2·5	4·95	4·9	2·22	Broke down at 66 v.
11	0	2·11	2·10	2·22	No fibres. Initial $\epsilon = 2 \cdot 04$. Partly conducted 2 v.

Experiments 2 and 3 clearly show the metastable floating effect, the thickness of the air film having been reduced to approximately one-half by tapping. Experiment 11 was the only one of many attempts to float the cylinder on the plate without fibres which was successful. It was accomplished by washing the surfaces with anhydrous methyl alcohol, wiping with a clean cloth and

---

[*] 'Z. phys. Chem.,' vol. 126, p. 305 (1927).

immediately placing the two together. Under these conditions it is highly probable that the surfaces were contaminated by an adsorbed layer of alcohol. The cylinder sank slowly (0·04 μ in 10 minutes) just as if it were floating on oil, and was fairly stable to tapping. On introducing oil it rose nearly 0·2 μ, and then sank, at first rapidly, then more slowly, to the original distance, at which point oscillation stopped owing to the high conductivity.

The actual thickness of the air films (4·0 μ) measured by Hardy and Nottage on a contaminated surface is of the same order as those recorded in Table III for very thin fibres. As it has not been possible to obtain a non-conducting layer even with a moderately clean surface, the observation that the film is thicker when the surfaces are clean could not be confirmed. In this connection it may be mentioned that through the courtesy of these authors, we were enabled, while their experiments were in progress, to examine the conductivity of one of their steel plates and cylinders after careful cleaning according to their standard method. The non-conducting state could not be obtained even with the application of only 1·4 volts, but on rubbing the plate with the finger and replacing the cylinder, a very stable non-conducting film, with a resistance of over 10 megohms, was formed and the cylinder could be shaken or moved about on the plate without producing any signs of conduction.

On p. 224 of the paper under reference it is stated "if more accurate methods should confirm the figures, the distance between the cylinder and plate would be the same for a gas as for a liquid and independent of the chemical constitution of the lubricant and of the enclosing solids." If this is true the constancy should hold good not only for any gas but for any gas at any pressure. The present experiments, although limited in scope, indicate that the agreement under suitable conditions may be as close as 1 per cent. for paraffin oil and air at 685 mm. pressure, and, consequently, it was considered of interest to examine the effect of reducing the pressure. The cylinder was floated on an almost invisible "wiped" film of the oil and the whole covered with a bell jar which could be evacuated. The film thickness was 4·0 μ. On reducing the pressure to about 100 mm. a slow steady fall set in, but the distance moved was only 0·01 μ in 9 minutes. On readmitting air the cylinder rose 0·005 μ in 7 minutes and then remained fairly steady. The cylinder was then slightly repolished and floated on a fresh contamination giving a film 3·74 μ in thickness. A similar reduction of pressure caused a fall of 0·027 μ in 3 minutes, the subsequent rise to a steady value being 0·022 μ in 3 minutes. Paraffin oil was then run under the cylinder causing the resistance to fall below 300 ohms, but on vigorous tapping it increased to 50,000 ohms, and then to several megohms, and the film thickness was found to be 3·54 μ, a value sufficiently close to the one with air considering the somewhat rough treatment the cylinder had received.

In another experiment with a larger gap of 12·5 μ, a fall of 0·67 μ, of which half was in the first half minute, was recorded, followed by a rise of 0·38 μ on readmitting air. In this case the cylinder was not fully stabilised by tapping. After three more evacuations to 2 mm. the fall was only 0·07 μ and the rise 0·035 μ. A change in capacity, probably due to the removal of air from the gap and its readmission, could be heard as it was quicker than the movement of the cylinder, but a similar effect would be produced if the cylinder were slightly raised by a release of the pressure on top of it, assuming that the air only issues slowly from the gap. It is not possible to distinguish between the two effects.

These experiments indicate that there is a critical distance between two surfaces at which unexpected phenomena occur. In the case of the cylinder this distance is about 4 μ and for the slider with 3 mm. legs something over 1 μ. The total film thickness depends on the amount of contaminant, as it decreases with wiping or with reduction in size of the glass fibre separators, which appear to act in a similar manner to the oil film, and it might perhaps be expressed as "effective contaminant thickness + a constant." The effect is the same as if each surface were covered with a rigid layer and the contamination forced the two apart, but the formation of these layers appears to be facilitated by the presence of the contamination, since it is very difficult to arrive at the non-conducting state with two clean surfaces. If the quantity of contaminant is excessive, as in the case shown in fig. 2, where the larger droplets are about 50 μ in diameter, when the upper body is placed on them, contact with the oil takes place long before the critical distance is reached, and the effect is the same as when the body is placed in a pool of oil, *i.e.*, conduction occurs if the pressure is sufficient. Non-conducting wiped films can only be obtained when the film is practically invisible.

The rigidity of the composite film is evident from the results in Table II and its stability is so remarkable that it is, on first experiencing it, almost impossible to remove the impression that it is due to dirt between the surfaces, but the reason for the formation of the film is obscure. An electrical repulsion, due to the polarisation of the molecules, appears to be excluded, since the distance remains unchanged when a liquid of different dielectric constant is introduced into the gap, and at present no further explanation is forthcoming. A method has been devised for measuring the thickness of conducting films.

and it is intended to examine outgassed surfaces in the hope that further light may be thrown on the matter.

To return to the figures in Table III; with the exception of experiment 10, which appears to be abnormal, all the films of 11 μ and under in thickness conducted on the application of comparatively low E.M.Fs., but there is no obvious relation between the film thickness and the breakdown E.M.F. This is perhaps to be expected from the results of the wedge experiments. In nearly all cases the first stage of breakdown was to a partially conducting state in which the resistance varied from about 10,000 ohms to a few megohms. The conduction was frequently of an intermittent nature as the galvanometer needle tended to fluctuate some 20 per cent. from the mean, but, occasionally, particularly with heavier currents, it was steady. There appeared to be no polarisation of the electrodes as no current was obtained on shorting the source of E.M.F., whereas a film of octyl alcohol under similar conditions gave an appreciable reverse current for a few minutes changing in direction with a change in the polarity of the initial E.M.F. The resistance of the film invariably decreased with increase of current, and in several cases there appeared to be a tendency for the potential drop across the film to remain constant, some of the results being shown in Table IV where *c* is in microamps. and *e* in volts.

Table IV.—Conductivity of Partially Conducting Oil Films.

a.		*b.*		*c.*		*d.*		*e.*		*f.*		*g.*	
c.	*e.*	*c.*	*e.*	*c.*	*e.*	*c.*	*e.*	*c.*	*e.*	*c.*	*e.*	*c.*	*e.*
1·5	0·44	0·2	1·8	2·1	6	0·5	9	10	9	16	8	75	13
3·2	0·66	1·1	2·9	2·9	7	4·4	10	69	14	46	19	225	18
4·9	1·0	2·5	3·4	9	11	10	10	125	17	108	19	420	18
7·0	1·0	4·2	3·8	16	14	20	10	220	18	208	19	640	17
		6·2	3·8	22	17					475	18	880	12
												1100	12

The figures *a* and *b* refer to the film of experiment No. 3 of Table III with 1 megohm in series. After making the measurements "*a*," the plate was tapped and the resistance increased to over 100 megohms when tested by applying 4 volts. At 6 volts there was partial breakdown and readings "*b*" were taken by applying 2, 4, 6, 8 and 10 volts in succession. On tapping, the resistance again became very high, but the film broke down partially at 4 volts, and with 6 the resistance became very low indeed. This behaviour was typical of the thinner films. The remaining figures all refer to one film, No. 8, of Table III. 11·6 μ in thickness. This film initially broke down with 24 volts. In a preliminary series of readings the resistance fell from 28 to 9 megohms. On repetition it was found to be only 3 megohms and the readings "*c*" were obtained. After standing 24 hours the film became non-conducting with a resistance of over 1000 megohms, but broke down with 62 volts, giving irregular readings. After tapping and allowing to stand for some hours the fairly steady values "*d*" were found at a room temperature of 31°. After standing overnight, 14 volts were required to break down the insulation which had again become high and the values "*e*," "*f*" and "*g*" were obtained in succession at 30°.

With both films the E.M.F. increases with the current for small values of the latter, but Ohm's law is not obeyed; with larger currents the E.M.F. becomes nearly constant and on still further increase it decreases. The behaviour in the later stages resembles the discharge in a gas without a positive column in which the E.M.F. remains constant until the cathode is covered with the glow, followed by arcing under suitable conditions. The steady potential appears to depend upon the thickness of the film, but it may also vary considerably for the same film. Until further experiments have been completed it is not possible to say whether the conductivity is due to impurities in the liquid, to the type of discharge usually associated with dielectric breakdown or to some other effect.

Disc Experiments.

As mentioned above, it was found that discs of brass and steel would float on a layer of oil or of air. The latter effect appeared to be produced very readily if the discs were lightly polished with rouge and water on a pitch polisher and then cleaned with anhydrous methyl alcohol. After immersing in oil and cleaning several times, flotation was more difficult to secure. It seems possible that a trace of contamination from the polisher assists the formation of the film, although it was not sufficient to produce an insulating layer in the case of the slider and the cylinder.

The loads per square centimetre with these discs were 3·6 and 3·3 gm. Ormandy* has given some results for a larger disc in a pool of paraffin oil producing a load of 4·7 gm. per square centimetre. His thicknesses have been miscalculated and should be only one-fourth of those tabulated. The films became conducting after some minutes and a minimum thickness of 2 wavelengths or 1·2 μ was measured, much less than that obtained in the present experiments. In the latter a brass disc placed in a pool of paraffin oil sank in 6 minutes at a temperature of 25° to a distance of 19 μ from the plate, but was still falling slowly. After pressing it sank to 17 μ and remained quite steady. By repeated pressing this was reduced to 12·7 μ, on releasing the pressure (about 500 g.) the disc rose immediately a distance of 0·03 to 0·05 μ.

---

* 'Proc. Inst. Mech. Eng.,' vol. 1, p. 307 (1927).

The same disc floated at a distance of 9 μ from a contamination of myristic acid, while a steel disc initially rested at a distance of 12 μ from a clean plate, sinking very slowly. On tapping it fell to about 4 μ and remained steady. On admitting oil to these air systems in a stable state, values of 2·30, 2·24, 2·24 and 2·33 were obtained for the dielectric constant, showing that the disc was pulled down slightly. On one occasion oil was admitted before tapping and the value found was 2·70, showing a much larger movement. Values for the conductivity analogous to those with the cylinder were obtained, but it was difficult to polish the discs sufficiently flat and, consequently, the figures for the thickness are not very reliable. Further experiments will be made after repolishing.

In conclusion, attention may be drawn to a recent paper by Joffé,* in which he states that exceedingly thin films were found to have a very high dielectric strength. In the absence of experimental details it is difficult to compare these results with those recorded in the present communication.

Summary.

Methods are described for determining non-conducting film thicknesses by means of capacity measurements; with suitable arrangements very minute changes in thickness can be measured.

There is a strong tendency for a film of air of the order 1 to 4 μ in thickness to form between two plane surfaces particularly if one of them is slightly greasy. Hardy's measurements have been confirmed and his hypothesis that the film thickness is unchanged when the air is replaced by oil has been shown to hold good, with certain limitations, to an accuracy of at least 5 per cent. The thickness has also been shown to be nearly independent of the air pressure down to 2 mm.

The coefficient of friction for the air film between contaminated surfaces has been shown to decrease with increase of pressure, although the distance between the surfaces remains nearly constant and there is no relation between the coefficient of friction and the thickness.

Air films have a high insulation resistance and when they break down the

---

* 'Trans. Faraday Soc.,' vol. 24, p. 65 (1928).

resistance usually becomes very low. Flooded films of paraffin oil will stand a high potential gradient (over 100,000 v./cm.) as long as their thickness is more than about 15 μ. At 11 μ there is a tendency to break down with a much smaller potential gradient and the breakdown thickness does not vary greatly with the voltage. The film becomes conducting in two stages; in the first the resistance is of the order of 1 megohm, Ohm's law is not obeyed, but there is a tendency for the E.M.F. across the film to remain constant with variation of currents over a certain range. In the second stage the resistance is very low.

An Investigation of the Combustion of Platinum.

By Eric K. Rideal and O. H. Wansbrough-Jones.

(Communicated by T. M. Lowry, F.R.S.—Received December 24, 1928.)

The attack of metal surfaces by gases at low pressures under conditions such that the products of reaction volatilise too rapidly to affect the reaction velocity is one of the simplest heterogeneous actions and presents many analogies to a simple catalytic action at a surface. Langmuir[*] studied the rate of attack of tungsten by oxygen under these conditions and in this communication the interaction of platinum with oxygen is described. This element was chosen, not only on account of the importance of reactions involving the "clean up" of gases in contact with hot filaments, but also because the electron work functions of both tungsten and platinum are known, so that their relationship to the reaction rate could be studied.

That some connection may exist between the reactivity of a surface and the ease of electron emission has been suggested previously and is to be noted particularly in the investigations of Sir Humphry Davy on the oxidation of zinc and copper, of Langmuir, and of Thompson, Bone, Thomas, and Briner on the surface combustion of gases. From a somewhat different standpoint others, notably Brewer, and Finch and Stimson,[†] suggest that surface reactions take place only after formation of ions on the surface has occurred, the former postulating that ions are formed by molecules entering the intrinsic field of the metal surface and react only after emergence from the field.

---

[*] 'J. Am. Chem. Soc.,' vol. 37, p. 1161 (1915), and 'Trans. Faraday Soc.,' vol. 17, p. 653 (1922).

[†] Davy, Bakerian Lecture, 'Phil. Trans.' (1807); Langmuir, 'J. Am. Chem. Soc.,' vol. 38, p. 2279 (1916); Thompson, 'Phys. Z.,' vol. 14, p. 11 (1913); Bone, 'Brit. Assoc. Reports' (1910); Thomas, 'J. Soc. Chem. Ind.,' vol. 21, p. 62 (1923); Briner, 'Helv. Chim. Acta,' vol. 9, p. 634 (1926); Brewer, 'J. Phys. Chem.,' vol. 32, p. 1006 (1928), and previous papers; Finch and Stimson, 'Roy. Soc. Proc.,' A, vol. 116, p. 379 (1927).

The evidence for a direct reaction between massive platinum and oxygen is conflicting. Deville and Debray[*] stated that "platinum is distinguished from all other metals which accompany it in the mineral by the fact that it does not unite directly with oxygen in whatever condition the two are placed." Moissan[†] also stated that platinum would not burn. Crookes[‡] suggested that the volatility of platinum might be due to the formation and decomposition of an unstable volatile oxide, but he finally discarded this view. Nahrwold, Owen, Stewart and Elster and Geitel[§] noted an increased rate of loss of platinum in the presence of oxygen. De la Rive showed that oxygen liberated at a platinum anode rendered the platinum soluble in hydrochloric acid and that the amount of oxygen retained in the metal bore a simple and constant relation to the amount of platinum dissolved. The anomalous behaviour of the platinum oxygen electrode has likewise been explained by postulating various oxides such as PtO, Pt_2O_3, PtO_2.

Langmuir (*loc. cit.*) concluded that the reaction between oxygen at low pressures and an incandescent platinum wire takes place between platinum vapour and oxygen in the bulk phase, below a certain pressure, which he estimates at 100 to 200 bars, no surface reaction takes place. Later, studying the rate of combination of hydrogen and oxygen at low pressures on a hot platinum filament, he observed deviations from a zero order reaction expression, which he attributed to dissociation of oxygen into atoms which may be frozen out directly or as ozone after combination with molecular oxygen.

EXPERIMENTAL.

The reaction vessel was a cylindrical bulb with a platinum filament some 15 cms. long, tied and welded to stouter platinum leads, sealed through the top. It was exhausted by a metal mercury diffusion pump backed by a "Hyvac" pump, through phosphorus pentoxide drying tubes and cadmium and liquid air traps to exclude mercury vapour. Pure dry oxygen, prepared by heating potassium permanganate, was passed over solid potash, stored over phosphorus pentoxide and admitted through the same traps. Before each experiment the reaction tube was baked for 2 hours at a pressure of 0·05 mm. O_2 and then exhausted to 10^{-5} mm. Hg, all at 400° C. for about 1 hour until no more gas was evolved from walls or filament. It is believed that the tube and oxygen were then free from water and tap grease vapour. Pressure readings were made on a McLeod gauge in the earlier runs, but later a Pirani gauge was used when it was desired to exclude the liquid air trap from the system. The volume of the reaction tube and Pirani gauge was about 200 c.c., they were connected by 1·2 cm. tubing and shut off from the remainder of the system by a specially ground tap which required a minimum of grease. No effect due to tap grease vapour could be detected. Thus after the filament had been glowing for some hours in oxygen, with the reaction vessel surrounded by liquid air, the residual oxygen was pumped off; on removing the liquid air neither a Pirani gauge, which is very sensitive to CO_2 and H_2O, nor a McLeod gauge showed any detectable pressure, and accordingly we believe that no errors were introduced by this tap.

---

[*] 'C. R.,' vol. 57, p. 471 (1878).

[†] 'C. R.,' vol. 142, p. 143 (1906).

[‡] 'Roy. Soc. Proc.,' A, vol. 86, p. 461 (1912).

[§] Nahrwold, 'Wied. Ann.,' vol. 31, p. 126 (1887), and vol. 35, p. 116 (1888); Owen, 'Phil. Mag.,' vol. 6, p. 306 (1903); Stewart, 'Phil. Mag.,' vol. 48, p. 451 (1899); Elster and Geitel, 'Wied. Ann.,' vol. 31, p. 126 (1887).

The Pirani gauge was used in the method recommended by Campbell* in which the voltage required to keep the filament at a constant temperature is measured. If V is this potential and V_0 the potential for the same wire temperature and zero pressure, the function $(V^2 - V_0^2)/V_0^2$ is directly proportional to the pressure over a wide range. Calibration against a McLeod gauge showed no perceptible divergence up to 100 bars. Pressures up to 200 bars were read off from a calibration curve, which was frequently checked but showed little or no variation over a period of months.

With pressures of 100 to 200 bars a heating current of about 25 m.a. was used to bring the wire to 100° C., a suitable temperature. This current was varied as the pressure fell and the potential required to keep the resistance of the filament constant was measured by a potentiometer. Thermal equilibrium was attained in about half a minute but continuous readings were taken in runs extending over about 4 hours without making any corrections for lag, since this correction was too small and uncertain to apply.

The heating current was taken from 220 v. batteries and the filament was inserted in one arm of a Wheatstone bridge. The resistance was kept constant for the low temperature runs where thinning of the wire was very small, but at higher temperatures it was found necessary to alter it slightly as the wire thinned. The change in resistance for constant temperature was calculated beforehand and the heating current altered accordingly.

---

* 'Proc. Phys. Soc.,' vol. 33, p. 287 (1921).

Over the range of temperature used, 1400°–1900° K., it was found that the temperature of the filament could be determined most readily by a direct comparison with a hot filament pyrometer. A temperature-resistance calibration curve was made and after comparison of the pyrometer with a similar filament on which salts of known melting point were examined under a low power microscope, it was found that the zero errors were constant. This correction having been made the temperature was probably known to about 10° and could be kept constant to 5°. As the wire thinned a recalibration was necessary and was made, but as a rule the temperature, as given by a calculation of the amount of thinning from Langmuir's values* for the rate of evaporation of platinum and our own, was sensibly the same. Accordingly the procedure was to calculate the required resistance for a given temperature between each run, and recalibrate directly between every tenth run. Any series in which the two methods did not agree within 10° were discarded. The change in temperature with resistance over the range 1500°–1900° K. over which the temperature coefficient of the thermal reaction was calculated, was found to be given fairly accurately by $R_1 = R_0 (1 + 0{\cdot}0039\,T - 0{\cdot}0000006\,T^2)$ and this expression was used for these calculations.

Despite this, however, the temperature measurements were the least accurate part of the experimental measurements and may have been in error by a larger amount than was believed.

The final runs were made with the Pirani gauge and the reaction vessel surrounded by ice, and with no liquid air on the system. Any run showing a residual pressure of more than 0·5 per cent. of the original pressure was discarded, as showing the presence of water or carbon dioxide. Of some 70 runs, 11 failed by this criterion, a very strict one.

The run was continued until the rate of clean up was too small to be measurable. The initial pressures used varied from 50 to 200 bars—the limit of the Pirani gauge. After running, a brown deposit—later shown to be PtO_2—collected on the walls of the bulb; and eventually became very thick. This deposit was decomposed more or less rapidly on heating to 350° C. with the pumps on; but the platinum obtained thus on the walls was found to be reasonably inactive.

The length of the runs varied between 20 minutes and 6 hours. It was shown that the rates of diffusion even at the lowest pressures between the Pirani gauge and the reaction bulb was large enough to preclude the possibility of any error due to such a cause.

---

* 'Phys. Rev.,' vol. 11, p. 377 (1914).

Experimental Results.

Experiments indicated that the filaments lost weight more rapidly in oxygen than *in vacuo*, and a few runs were made to test this point. The tubes were kept charged to a pressure of about 200–100 bars and the runs extended over some 20 hours. The following table gives details of the results, with Langmuir's values for the rate of evaporation *in vacuo* for comparison. The filaments were weighed before and after the experiments, and a correction was made for the variation in area as the thinning progressed. This change in area had a maximum value of 20 per cent. and the correction was accurate to about 1 per cent. and was much smaller than the effect noticed.

Table I.

Run.	Temperature ° K.	Area of filament.	Pressure range.	Loss in weight.	Apparent loss in gm. weight per cm.^{2} per sec. $\times 10^9$.	Loss found by Langmuir, gm. $\times 10^9$.
		cm.^{2}	bars	gm.		
D2	1750	0·413	200–100	0·0009	30·5	25·4
D3	1750	0·407	0	0·0008	27·3	25·4
D5	1800	0·362	200–100	0·0020	80·1	66·7
D7	1850	0·421	200–100	0·0067	231	168
D8	1850	0·428	0	0·0053	180	168

The runs *in vacuo* were made for comparison and are not as accurate as Langmuir's values. When later it was required to use the rate of evaporation to calculate results, the table given by him was used. The results are, however, sufficiently concordant to show that at high temperatures the loss of weight is appreciably increased on addition of oxygen.

In order to examine the reaction more fully the kinetics were studied as completely as possible. Some 50 runs at various pressures and temperatures were made and the velocity of the reaction examined. It was found that the results were most readily interpreted by postulating a surface reaction whose rate was directly proportional to the pressure, and a zero order bulk phase reaction occurring simultaneously, the combined effect being denoted by an equation of the type

$$-\frac{dp}{dt} = a + bp \quad \text{or} \quad -bt = \log_e \frac{a + bp}{a + bP_0},$$

where P_0 is the initial pressure.

In the following table are given the calculated values of a and b in this equation for a number of runs, the units being bars and seconds. Column "4 'a' calculated" denotes the values obtained from Langmuir's values for the rate of evaporation of platinum *in vacuo*, with the following assumptions :—

(1) That this rate is unchanged by small pressures of oxygen. Langmuir states that this is the case, and further evidence is given by the agreements between the columns 3 and 4.

(2) That the evaporated platinum reacts with oxygen to form PtO_2. The relation between the loss in weight of the filament and the amount of oxygen cleaned up, as shown below, proves this to be the case.

(3) That before the platinum is condensed on the walls of the tube it has all undergone reaction. Langmuir has shown this to be the case above a pressure of 5 bars for tungsten and nitrogen ; and the agreement and constancy of our values above this pressure confirm the view. A consideration of the probability of collision between a platinum atom—assuming the vapour to be monatomic—and an oxygen molecule in a tube of the given dimensions also supports this assumption.

Table II.

Filament.	1. Run.	2. Corrected temperature 0° K.	3. "a" $\times 10^8$.	4. "a" calc. $\times 10^8$.	5. "b" $\times 10^4$.
A Vol. of system = 210 c.c. Length of filament = 14 cm.	3	1710	2·8	2·74	2·22
	4	1710	2·61	2·74	2·03
	5	1600	0·2	0·235	0·44
	6	1840	33·6	32·61	8·13
	7	1850	42·0	40·00	8·76
	9	1900	100·0	94·5	15·40
	10	1900	85·0	92·6	14·60
	12	1725	3·9	3·62	2·48
	14	1770	8·5	8·46	4·18
	15	1830	27·0	26·00	7·25
	16	1710	3·0	2·54	2·20
	17	1880	64·0	61·40	11·60
B Vol. of system = 170 c.c. Length of filament = 9·2 cm.	5	1740	4·0	3·96	2·72
	7	1650	0·40	0·615	0·72
	9	1760	6·1	5·83	3·6
	10	1780	9·0	8·65	4·3
	11	1800	14·6	13·10	4·7
	12	1820	20·1	18·80	4·7
	15	1840	28·0	26·53	7·2
	17	1860	36·0	38·0	9·0
	18	1880	47·0	52·5	10·6
E Vol. of system = 168 c.c. Length of filament = 10·8 cm.	2	1900	85·1	93·1	13·82
	3	1850	40·0	39·0	8·39
	4	1800	16·0	15·6	4·83
	5	1750	7·0	5·82	3·28
	6	1700	1·5	2·05	1·85

A few of the actual experimental runs are shown in the following curves, figs. 1 and 2.

Fig. 1 shows four of the actual experimental curves (selected at random) obtained by plotting the pressure against the time.

Fig. 2 shows the result of plotting the time against the expression log $(a + bp)$. The departures from the straight line at low pressures are due to the mean free path of the platinum atom becoming large enough to allow some to strike the glass walls without reacting with oxygen.

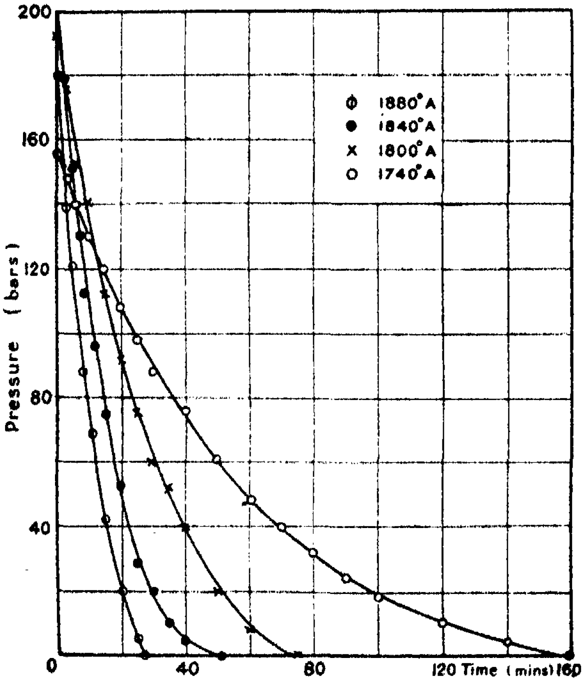

Fig. 1.

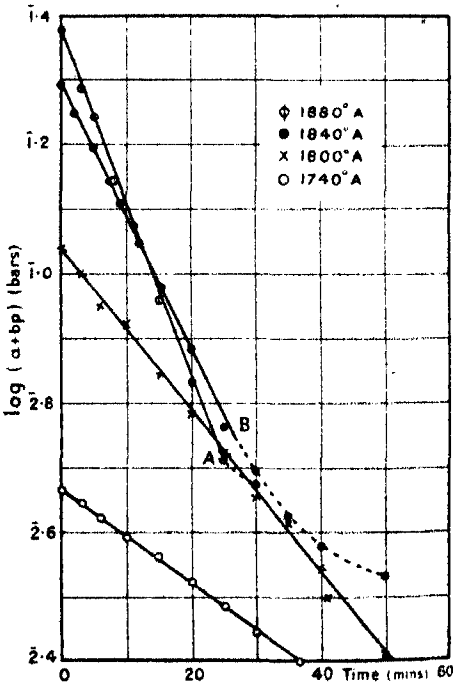

Fig. 2.

The point A is at a pressure of 5 bars, and B is rather higher, 25 bars.

The agreement between the two values of "a" is, in the majority of cases, good; and we have accordingly used this agreement as a further criterion of accuracy. All results showing a discrepancy of more than 10 per cent. have been discarded as showing an error in the temperature measurements. All temperatures have been corrected for the change in resistance due to thinning; and the weight lost by evaporation corrected for the same change. In these runs there were fluctuations in the constancy of b of the order of 10 per cent. but in no one run was there a drift in one direction; and it is considered that the values are correct to 5 per cent.

In order to correlate the *b* values for the three series of runs we have expressed *b* as the fraction ε of the total number of molecules of oxygen striking the filament which react to give PtO_2. This fraction should be independent of bulb size, filament length, and temperature of the gas. (In all cases the length of filament given is the corrected length, allowance having been made for the cooling by the leads.)[*] In the following curve the values of ε are plotted as a function of the temperature.

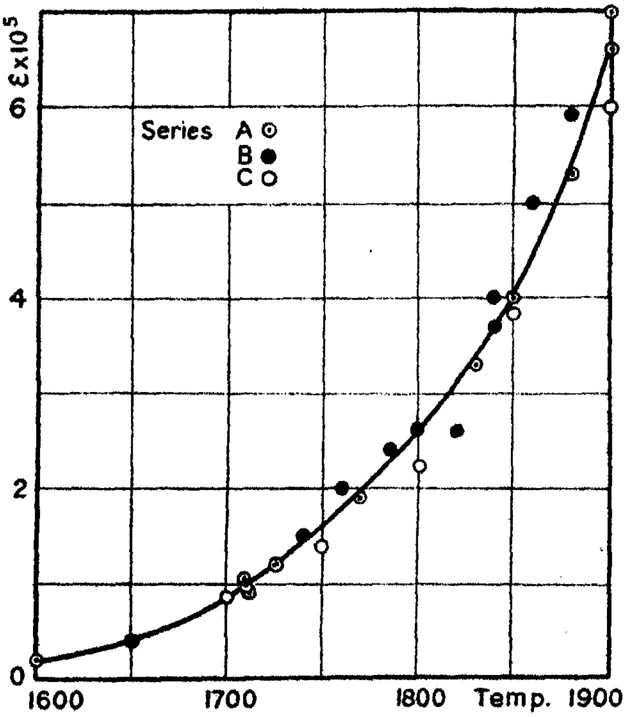

Fig. 3.

It is considered that the variations of the values of ε are, at any one temperature, sufficiently small for us to assume that the reaction is independent of the bulb size. The high temperature coefficient of this reaction, in distinction to Langmuir's values for tungsten and oxygen, is of interest, and we shall return to this point later.

At the end of series E the total loss in weight of the filament was found and a calculation made from the weight of oxygen cleaned up, in order to find the composition of the product.

It was found to give the value Pt : O :: 1 : 1·92. As the exact value of this ratio was of importance, two more runs were made to test this point. As an additional check the platinum oxide was dissolved off the glass and estimated colorimetrically with potassium iodide. The weight of platinum found by the two methods was sensibly the same. The results are summarised below in Table IV.

---

[*] *Cf.* Langmuir, *loc. cit.*, and 'Gen. Elec. Rev.,' vol. 19, p. 210 (1916).

Table IV.

Run	E	1	2
Ratio Oxygen/Platinum	1·92	1·95	1·88

In view of the experimental errors it was assumed that the composition of the oxide was PtO_2. Additional evidence was given by the fact that the deposit on the walls dissolved readily and completely in hydrochloric acid.

From these results it appears that below 1700° K. and even above this temperature for pressures below 50 bars, the bulk reaction between platinum vapour and oxygen predominates; this, together with our own values for the constant "a" of the bulk reaction, is entirely in agreement with Langmuir's observation. To account for the alteration in reaction rate at high pressures and temperatures Langmuir suggested the removal of oxygen by condensation of ozone or oxygen atoms; whereas the direct operation of a surface reaction seems more probable.

In support of this view it may be noted that there is no sensible alteration in reaction rate when the bulk temperature is varied between that of liquid air and the room after correction had been made for the alteration in rate of impact of the oxygen on the filament, although ozone would not be frozen out in the latter condition, and only a small quantity of oxygen atoms could remain condensed; moreover, the rate of clean-up is unaffected by the presence of platinum or platinum oxide on the glass surface, in which circumstances the ozone would be expected to decompose. Finally the constancy of the stoichiometric ratio $Pt : O_2$ under widely varying conditions is indicative of no reaction involving the removal of oxygen *per se*.

Attempts to synthesise ozone by heating the platinum filament to just below the melting point in a bulb with an appendix cooled in liquid air proved abortive. After 3 or 4 hours' running there was no trace of any condensible gas in the appendix (though at higher temperatures one would expect some ozone formation).

Interpretation of Results.

The rates of surface reaction are seen to be quite small even at temperatures as high as 1900° K., being very much less than the corresponding reaction on a tungsten surface. It seems probable that only those molecules having a high energy react, and in accordance with the Maxwell-Boltzmann distribution the number of these molecules on the surface is given by $n = \mathrm{NA}\, e^{-\mathrm{E/RT}}$, where E is the excess energy required, and N the number of molecules on the surface. Since $\varepsilon = n/$Number of molecules striking the wire $= n/\kappa p$, and assuming the validity of the Langmuir absorption isotherm $\mathrm{N} = a'b'p/(1+a'p)$ we obtain

$$\varepsilon = \frac{\kappa}{1 + a'p}\, e^{-\mathrm{E/RT}},$$

since the rate at which oxygen strikes the wire is independent of relatively small changes in the temperature of the wire (Langmuir*).

As $1 + a'p$ is nearly equal to unity we obtain $d \log_e \varepsilon / d\mathrm{T} = \mathrm{E/RT}^2$ from which the energy of activation is calculated in the usual way. To justify this equation it is assumed that the excited molecule reacts instantaneously, or at all events in a shorter time than its mean life on the surface, and its correctness in this case is shown by the constancy of the energy of activation which does not vary between greater limits than 62,000 cals. to 64,000 over the range 1700° K.–1900° K., and also by the accuracy with which the reaction velocity equation is obeyed. If the complete form of the equation be considered and P is not assumed small, we see that the reaction velocity is given by

$$-\frac{dp}{dt} = a + \frac{\kappa' p}{1 + a'p}\, e^{-\mathrm{E/RT}},$$

which will rise to a maximum value. That the simple equation $-dp/dt = a + bp$ could not hold at high pressures is evident since platinum does not burn rapidly in a high oxygen pressure. Exact figures for the constants in this equation are not available; but up to 200 bars the error introduced by assuming the simple equation to hold is negligible.

The energy of activation, 63,000 cals. per gm. mol., is very high, in distinction to Langmuir's values for the oxidation of tungsten, calculated in the same way, which has an energy of activation of about 20,000 cals. per gm. mol. Expressed in equivalent volt electron units $\mathrm{E_{Pt}} = 2\cdot 74$ v. and $\mathrm{E_W} = 0\cdot 87$ v., with a difference $\mathrm{E_{Pt}} - \mathrm{E_W} = 1\cdot 87$ v. Taking the work function of platinum as 6·35 v. (Dubridge)† and of tungsten as 4·48 (mean value, Schottky‡) $\phi_{\mathrm{Pt}} - \phi_{\mathrm{W}} = 1\cdot 87$, a value identical with $\mathrm{E_{Pt}} - \mathrm{E_W}$. This exact numerical agreement is to some extent fortuitous since the values of the work functions are not accurate to more than 0·1 v. and no greater accuracy can be expected for the energies of activation.

---

* 'J. Chem. Soc.,' p. 3182 (1926).

† 'Phys. Rev.,' vol. 31, p. 236 (1928).

‡ 'Handbuch der Experimental Physik,' vol. 13, part 2.

This coincidence in values encourages us to advance a tentative explanation of the mechanism of these surface reactions. Oxygen molecules on adsorption enter the intrinsic field of the metallic surface, and undergo deformation, thus acquiring a definite amount of potential energy. We assume that for reaction to ensue between the oxygen molecule and the platinum atom to which it is held, an electron must be free to pass from the one to the other with no expenditure of energy; the energy required for the emission of an electron in the usual way being supplied in part by the energy acquired by the oxygen molecule on entering the intrinsic field and in part by the energy of activation, the sum of which two must equal the work function of the metal. A third case of oxidation in which the reaction products do not interfere with the rate of oxidation is to be noted in the low temperature oxidation of carbon, where the energy of activation was found by Rideal and Wright* to be 0·52 v.; carbon possessing a thermionic work function of 4·31 v. (Langmuir and Kingdon*).

These facts are summarised:—

		E.	ϕ.	$\phi - E$.
		volts.	volts.	volts.
Oxidation of	Platinum	2·74	6·35	3·61
	Tungsten	0·87	4·48	3·61
	Carbon	0·52	4·31	3·79

It is interesting to note that Blench and Garner, Garner and McKie, and McKie† obtained as the maximum heat evolution on reversible adsorption of oxygen on charcoal a maximum value of 3·10 v., higher values only being obtained when oxides of carbon were formed on the surface. Since the heat evolved may be only a part of the energy of adsorption this value is clearly a minimum of the potential energy of adsorption and is but slightly smaller than the actual potential energy obtained above.

There is, however, a further factor which may go to make up the value of $\phi - E$. We have postulated the existence of deformed and probably highly deformed oxygen molecules on the surface, and should they have an electron affinity ϕ_e it is clear that for reaction on the above view

---

* 'Phys. Rev.,' vol. 21, p. 381 (1923).

† Blench and Garner, 'J. Chem. Soc.,' vol. 125, p. 1288 (1924); Garner and McKie 'J. Chem. Soc.,' p. 2451 (1927); McKie, 'J. Chem. Soc.,' p. 2870 (1928).

$$\phi = E + \phi_a + \phi_e$$

where ϕ_a is the potential energy of adsorption. No data are available for the calculation of ϕ_e accurately.

Few other simple reactions involving the direct attack of a surface in these conditions have been investigated but the qualitative relationship between the attack of metals by halogens and their relative deformabilities supports the hypothesis. We have, therefore, considered two simple cases of heterogeneous catalytic decomposition which have been examined on a variety of metal surfaces, namely, the decomposition of ammonia and formic acid. Of these the latter is definitely not amenable to this treatment, but the investigations of Hinshelwood on the thermal decomposition of simple organic vapours indicate that they may be the results of a somewhat complicated series of changes involving possible adsorption and secondary excitation of the products of the reaction.

Some of the published data on the decomposition of ammonia on various surfaces are conflicting, the following values experimentally determined by various investigators conform closely to those anticipated on an extension of the hypothesis advanced above for surface interaction to surface catalytic reaction.

Metal.	E.	ϕ.	$\phi - E$.
Platinum	3·5	6·35	2·85
Tungsten	1·7	4·48	2·78
Molybdenum	1·39	4·36[‖]	2·97
Nickel	1·13	4·05[†] [¶]	2·87

[†] From the photo-electric threshold, since the other values are discrepant.

[‖] Schottky, *loc. cit.*

[¶] Hamer, 'J. Opt. Soc. Amer.,' vol. 9, p. 251 (1924).

The value of E for platinum is taken from the low pressure measurements of Schwab[*] which, however, does not agree with the higher pressure values of Hinshelwood and Burk.[‡] The value of E for tungsten is derived from the data of Hinshelwood and Burk which are in agreement with the mean value found by Kunsman,[§] but in disagreement with Schwab's value for this metal. The energies of nickel and molybdenum are due to Kunsman.

---

[*] 'Z. Phys. Chem.,' vol. 128, p. 161 (1927).

[‡] 'J. Chem. Soc.,' vol. 127, p. 1105 (1925).

[§] 'J. Am. Chem. Soc.,' vol. 50, p. 2100 (1928).

We may note that oxygen should react without energy of activation with any metal having a work function of less than 3·6 v. and ammonia should decompose similarly on metals of work function less than 2·8 v., thus forming reactions of the class defined by Polanyi* as elementary reactions.

On this basis the atom of platinum and oxygen will unite when the total energy required is available and electrons from the metal can pass freely in and out of the PtO_2. The platinic oxide will then, as a subsequent reaction, evaporate unchanged.

It is at first sight somewhat surprising that the platinic oxide does not decompose at once; but if it evaporates immediately, it would only decompose as a bimolecular gas reaction. Collision with a platinum atom would presumably cause decomposition but recombination would immediately ensue.

The platinum surface appears to be uniform and this may actually be the case; but it is more probable that since the platinum surface is changing continuously, this effect is really a statistical one, and reaction may occur most readily on patches of lower work function (*cf.* Richardson and Young, Butterworth†). The chance that an oxygen molecule should be activated on a low energy patch is, however, small; and in any case it is doubtful if the difference in work function is greater than 0·1 v. No evidence was obtained for the platinum evaporating in aggregates; and probably it is purely a monatomic gas.

Finally, by assuming that a metal surface may be regarded as a simple lattice structure of positive ions and electrons and that the Coulumb law of repulsion and attraction is applicable at small distances, we can make an approximate evaluation of the value of ϕ_a. If α is the polarisation constant, the dipole moment of the deformed oxygen molecule in its equilibrium position on the surface being p, then

$$\phi_a = p^2/2\alpha + p^4/n\alpha,$$

the second term referring to poles of higher order, and in this case being negligible. Assuming $\phi_a = 3 \cdot 6$ v. for platinum and $\alpha = 1 \cdot 56 \times 10^{-24}$ e.s.u., we obtain $p = 4 \cdot 26 \times 10^{-18}$ e.s.u. The undeformed molecule has an almost negligible electric moment but for complete ionisation, *i.e.*, for the formation of an oxygen molecule with a semi-polar double bond linkage $\overset{+}{0} : \overset{-}{0}$ $p = 7 \times 10^{-18}$ approximate, so that the degree of polarisation effected is somewhat less than would be required for transition into this form. Ammonia with $\alpha = 2 \cdot 21 \times 10^{-24}$ and $\phi_a = 2 \cdot 85$ v., gives $p = 4 \cdot 5 \times 10^{-18}$. Jona[*] found for the normal molecule $p = 1 \cdot 53 \times 10^{-18}$, while Smyth[†] has calculated for a possible tetrahedral model $p = 4 \cdot 77 \times 10^{-18}$ e.s.u.

---

* 'Z. Phys. Chem.,' vol. 139, p. 439 (1928).

† Richardson and Young, 'Roy. Soc. Proc.,' A, vol. 107, p. 377 (1925); Butterworth 'Phil. Mag.,' Ser. 7, vol. 6, p. 1 (1928).

Following De Boer[‡] we have attempted to evaluate the distance from the metal surface at which the oxygen is held when in the equilibrium position, *i.e.*, where $d\phi/dr = 0$. De Boer finds an expression of the form

$$\phi_a = -\,S^2\,\varepsilon^2\alpha/2r^4,$$

from which values of *ar*, the distance of the dipole centre from the charged molecule may be found, *r* being the spare lattice constant, and S being the difference between two series containing the ratio "*a*," and having a value which falls very rapidly as "*a*" increases. Reasonable values for the distance *ar* can be obtained in this way. Thus for oxygen on platinum, a face centred cube, and for tungsten, a body centred cube, we obtain respectively 1·39 and 1·36 Ångstrom units and for ammonia on the various metals (the lattice constant *r* being derived from X-ray data),

W, 1·54 ; Mo, 1·53 ; Pt, 1·25 ; Ni, 1·39 Å.U.

for the distance between the charge centre of the dipole and the point charge over which it is absorbed. The mean radius of the nitrogen molecule is 1·18 Å.U. and of the oxygen 1·45 Å.U. This implies that the nitrogen atom in the ammonia molecule is probably directly on the surface, as is also indicated by the value of the dipole moment. Oxygen must be adsorbed on an electron or the radius of the platinum positive ion must be very small.[§]

It is interesting that on all these metals there is not a wide variation in the distance *ar*. The heat of adsorption, whilst dependent to a small extent on the space lattice constants of the metal, is much more greatly affected by changes in the radius and deformability of the gas undergoing adsorption.

Summary.

The oxidation of platinum to PtO_2 at high temperatures has been shown to comprise a bulk reaction with platinum vapour and a surface action. The energy of activation of the surface action is found to be 2·75 volts in contrast with Langmuir's value of 0·87 volts on a tungsten surface. The difference between these values of 1·87 volts is identical with that of the thermionic work functions and a hypothesis of the mechanism of these surface actions is suggested. It is shown that the oxidation of carbon and the catalytic decomposition of ammonia on various metallic surfaces fall into the scheme.

---

[*] 'Phys. Z.,' vol. 20, p. 14 (1919).

[†] 'Phil. Mag.,' vol. 47, p. 530 (1923).

[‡] 'Physica,' vol. 8, p. 145 (1928).

[§] *Cf.* Davisson and Germer, 'Phys. Rev.,' vol. 30, p. 738 (1927).

Our thanks are due to Prof. T. M. Lowry, F.R.S., for communicating this paper, to Colonel Heycock, F.R.S., for the loan of a pyrometer, to the Goldsmith's Company and the Department of Scientific and Industrial Research for a grant to one of us (O.H.W.-J.) and to the Imperial Chemical Industries for assistance in purchasing the necessary apparatus.

The Forces on a Solid Body Moving through Viscous Fluid.

By Sydney Goldstein, B.A., Ph.D., St. John's College, Cambridge.

(Communicated by H. Jeffreys, F.R.S.—Received December 31, 1928.)

1. *Introduction and Summary.*

The following theorem will be proved. The drag force on a solid body of any size and shape moving with uniform velocity U through otherwise still fluid of density ρ, and of any viscosity, is ρU multiplied by the inflow along the wake, the inflow being taken at an infinite distance behind the body. The force in any direction at right angles to the velocity U can be obtained by taking a cylinder, everywhere at a great distance from the solid body, with generators at right angles to the velocity U and to the direction of the force required ; integrating, along the cylinder, the circulation around sections by planes perpendicular to the generators ; and multiplying the integral by ρU. In taking the circulation, we must cut the wake behind the solid body at right angles.

When the motion of the fluid is not steady, but oscillates within fixed limits, the theorem remains true if average values are taken over a sufficiently long time.

The proof is based on the assumption that at a great distance from the solid the disturbance it makes is small, so that squares of this disturbance may be neglected. The equations of motion then take the form first proposed by Oseen,[*] and the method of solution is that originally suggested by Lamb.[†]

Let (u, v, w) be the components of fluid velocity in three directions mutually at right angles, u being in the direction of the uniform velocity U of the body. Then, in order to prove the theorem for the drag force for non-steady motion, we must assume not only that the average values of u, v and w are sufficiently small at a great distance from the body for squares and products to be neglected, but also that the average values of u^2, uv and uw are of smaller order than r^{-2} outside the wake, and of smaller order than r^{-1} inside the wake, where r is the distance from any fixed point in the body.

Again, if the velocity components at any point in the fluid lie between fixed limits, but if the momentum of the fluid inside a surface everywhere at infinite distance from the body continually grows, then the drag is increased by the rate of growth of fluid momentum.

The corresponding formulæ for two-dimensional motion have been given by Filon.[‡] The formula for the lift force is the same as the well-known Kutta-Joukowski formula for an inviscid fluid, except that for the inviscid fluid the circulation may be taken round any circuit enclosing the cylindrical solid body, and need neither be at a great distance nor at right angles, far behind the body, to the direction of the velocity U. Similar theorems have been given by various writers for a fluid in which vorticity is confined to a boundary layer and a wake, and which is otherwise perfect.[§]

2. *The Flow at a Great Distance.*

Consider a solid body of any size and shape fixed in an unlimited sea of viscous fluid, which is moving, apart from the disturbance due to the presence of the body, with a uniform velocity U. Take an origin of co-ordinates anywhere in the body, with three axes, the axis of x being in the direction of the velocity U and the axes of y and z being at right angles to the axis of x and to each other, but otherwise unspecified. Let the fluid velocity at any point (x, y, z) have components $\mathrm{U} + u$, v, and w, so that (u, v, w) is the velocity of disturbance. Let r, θ and ϖ be spherical polar co-ordinates with the axis of x as initial line, and let the components of the velocity of disturbance along r increasing, θ increasing and ϖ increasing be u_r, u_θ and u_ϖ respectively.

---

[*] 'Arkiv. mat. astr. fysik.,' vol. 6, Nr. 29 (1910).

[†] 'Hydrodynamics,' §§ 340 and 343, or 'Phil. Mag.,' vol. 21, p. 112 (1911).

[‡] 'Roy. Soc. Proc.,' A, vol. 113, p. 7 (1926).

[§] G. I. Taylor, 'Phil. Trans.,' A, vol. 225, p. 238 (1925); Betz., 'Z. Flugtechnik Motorluftsch.,' vol. 16, p. 42 (1925); Burgers, 'Proc. R. Acad. Sci. Amsterdam,' vol. 31, p. 433 (1928).

We now assume that at a great distance from the obstacle the disturbance is small, so that, squares of small quantities being neglected, the equations of motion take the form

$$U\frac{\partial}{\partial x}(u, v, w) + \frac{1}{\rho}\left(\frac{\partial}{\partial x}, \frac{\partial}{\partial y}, \frac{\partial}{\partial z}\right)p = \nu\nabla^2(u, v, w), \tag{1}$$

where p is the pressure, ρ the density, and ν the kinematic viscosity of the fluid. The equation of continuity is

$$\frac{\partial u}{\partial x} + \frac{\partial v}{\partial y} + \frac{\partial w}{\partial z} = 0. \tag{2}$$

If we put

$$k = U/2\nu, \tag{3}$$

the equations (1) and (2) are satisfied by

$$u = \frac{\partial\phi}{\partial x} + \frac{1}{2k}\frac{\partial\chi}{\partial x} - \chi, \quad v = \frac{\partial\phi}{\partial y} + \frac{1}{2k}\frac{\partial\chi}{\partial y}, \quad w = \frac{\partial\phi}{\partial z} + \frac{1}{2k}\frac{\partial\chi}{\partial z}, \tag{4}$$

and

$$p = -\rho U\frac{\partial\phi}{\partial x}, \tag{5}$$

provided that

$$\nabla^2\phi = 0, \tag{6}$$

and

$$\left(\nabla^2 - 2k\frac{\partial}{\partial x}\right)\chi = 0. \tag{7}$$

If (ξ, η, ζ) is the vorticity, then

$$\xi = \frac{\partial w}{\partial y} - \frac{\partial v}{\partial z} = 0, \quad \eta = \frac{\partial u}{\partial z} - \frac{\partial w}{\partial x} = -\frac{\partial\chi}{\partial z}, \quad \text{and} \quad \zeta = \frac{\partial v}{\partial x} - \frac{\partial u}{\partial y} = \frac{\partial\chi}{\partial y}. \tag{8}$$

If

$$\chi = e^{kx}\chi', \tag{9}$$

then must

$$(\nabla^2 - k^2)\chi' = 0. \tag{10}$$

The general solution of (6) is

$$\phi = \sum_{n=0}^{\infty}\frac{A_n}{r^{n+1}}S_n(\theta, \varpi), \tag{11}$$

and that of (10) is

$$\chi' = \sum_{n=0}^{\infty} B_n \chi_n (kr)\, S_n(\theta, \varpi), \tag{12}$$

where

$$\chi_n (x) = (2n + 1)\, (\pi/2x)^{\frac{1}{2}}\, K_{n+\frac{1}{2}} (x), \tag{13}$$

S_n is a surface harmonic of degree n, and K_n is the modified Bessel function of the second kind. Solutions involving positive powers of r have been omitted from (11), since the velocity of disturbance must vanish at infinity. For the same reason solutions involving $I_{n+\frac{1}{2}}(kr)$ instead of $K_{n+\frac{1}{2}}(kr)$ have been omitted from (12), since $I_{n+\frac{1}{2}}(x)$ becomes exponentially large when x is large. On the other hand, when x is large

$$K_{n+\frac{1}{2}} (x) \simeq (\pi/2x)^{\frac{1}{2}}\, e^{-x}, \tag{14}$$

so that

$$\chi_n (x) \simeq (2n + 1)\, (\pi/2x)\, e^{-x}, \tag{15}$$

and

$$\chi' \simeq \frac{\pi}{2kr} e^{-kr} \sum_{n=0}^{\infty} (2n+1)\, B_n\, S_n (\theta, \varpi). \tag{16}$$

Thus the vorticity and the terms in u, v and w that depend on χ will contain the factor $e^{-k(r-x)}$ or $e^{-2kr\sin^2\frac{1}{2}\theta}$, and will therefore be insensible when r is large, unless θ is small of order $k^{-\frac{1}{2}}r^{-\frac{1}{2}}$. The vaguely defined region in which the vorticity is sensible is referred to as the wake. Then the terms in u, v and w depending on χ are insensible outside the wake. On the other hand, within the wake, the velocity of disturbance will be seen from (4), (9) and (16) to be of order $B_0 k^{-1} r^{-1}$ for large values of r, while outside it is of order $A_0 r^{-2}$ (or $B_0 k^{-2} r^{-2}$. See (27).)

Again

$$u_r = \frac{\partial \phi}{\partial r} + \frac{1}{2k}\frac{\partial \chi}{\partial r} - \chi \cos \theta = \frac{\partial \phi}{\partial r} + \frac{1}{2k} e^{kx} \frac{\partial \chi'}{\partial r} - \tfrac{1}{2} e^{kx} \chi' \cos \theta, \tag{17}$$

and the first term in ϕ gives an outward radial flow across a large sphere, equal to

$$-A_0 \int \frac{S_0 (\theta, \varpi)}{r^2}\, dS = -4\pi A_0 S_0 (0, \varpi). \tag{18}$$

This is compensated by an inward flow along the wake. In order that there should be compensation, there must be a relation between A_0 and the B, and although not strictly necessary for our present purpose, the matter is interesting enough to warrant our finding this relation.

The terms in u_r depending on χ are

$$\tfrac{1}{2} e^{kx} \sum_{n=0}^{\infty} B_n \left[\chi_n' (kr) - \chi_n (kr) \cos \theta\right] S_n (\theta, \varpi), \tag{19}$$

where $\chi_n'(x)$ is $\dfrac{d}{dx}\chi_n(x)$. For large values of r these terms are nearly equal to

$$-\frac{\pi}{4kr}e^{-k(r-x)}(1+\cos\theta)\sum_{n=0}^{\infty}(2n+1)\,\mathrm{B}_n\mathrm{S}_n(\theta,\varpi), \tag{20}$$

and if we put

$$(1+\cos\theta)\sum_{n=0}^{\infty}(2n+1)\,\mathrm{B}_n\mathrm{S}_n(\theta,\varpi)=\mathrm{F}(\theta,\varpi), \tag{21}$$

they give an *inward* radial flow equal to

$$\frac{\pi}{4kr}\int_0^{\pi}\int_0^{2\pi}e^{-kr(1-\cos\theta)}\,\mathrm{F}(\theta,\varpi)\,r^2\sin\theta\,d\theta\,d\varpi. \tag{22}$$

The integrand is sensible only when θ is small. We may, therefore, replace the limits of integration for θ by 0 and ε, where ε is small but of order larger than $k^{-\frac{1}{2}}r^{-\frac{1}{2}}$, and replace $1-\cos\theta$ by $\frac{1}{2}\theta^2$, and $\sin\theta$ by θ. This makes (22) equal to

$$\frac{\pi r}{4k}\int_0^{\epsilon}\int_0^{2\pi}e^{-\frac{1}{2}kr\theta^2}\,\mathrm{F}(\theta,\varpi)\,\theta\,d\theta\,d\varpi. \tag{23}$$

If now we put

$$\tfrac{1}{2}kr=\mathrm{R}^2\quad\text{and}\quad\mathrm{R}\theta=\eta, \tag{24}$$

(23) becomes

$$\frac{\pi}{2k^2}\int_0^{\mathrm{R}\epsilon}\int_0^{2\pi}e^{-\eta^2}\,\mathrm{F}\left(\frac{\eta}{\mathrm{R}},\varpi\right)\eta\,d\eta\,d\varpi. \tag{25}$$

The limiting value of (25), when r becomes infinite, is

$$\frac{\pi}{2k^2}\int_0^{\infty}\int_0^{2\pi}e^{-\eta^2}\,\mathrm{F}(0,\varpi)\,\eta\,d\eta\,d\varpi=\frac{\pi^2}{2k^2}\mathrm{F}(0,\varpi). \tag{26}$$

The required relation is therefore

$$-\mathrm{A}_0=\frac{\pi}{8k^2}\frac{\mathrm{F}(0,\omega)}{\mathrm{S}_0(0,\varpi)}=\frac{\pi}{4k^2}\sum_{n=0}^{\infty}(2n+1)\,\mathrm{B}_n\frac{\mathrm{S}_n(0,\varpi)}{\mathrm{S}_0(0,\varpi)}. \tag{27}$$

An alternative method of arriving at this relation, in the case of a body of revolution, will be given later.*

3. *The Formulæ for the Forces.*

Now take a surface S everywhere at a great distance from the solid. Let $(\mathrm{X}_1, \mathrm{Y}_1, \mathrm{Z}_1)$ be the force exerted by the fluid outside S on the fluid inside, and $(\mathrm{X}, \mathrm{Y}, \mathrm{Z})$ the force exerted by the fluid on the solid. Then

$\mathrm{X}_1-\mathrm{X}=$ the x — component of the rate of outflow of momentum through S

$$=\int\rho\{l(\mathrm{U}+u)+mv+nw\}(\mathrm{U}+u)\,d\mathrm{S}, \tag{28}$$

---

* See p. 232 of the following paper, "The Steady Flow of Viscous Fluid past a fixed Spherical Obstacle at small Reynolds Numbers."

where (l, m, n) are the direction-cosines of the outward drawn normal to S. With a usual notation for the stress components,

$$\begin{aligned} X_1 &= \int (l p_{xx} + m p_{yx} + n p_{zx})\, dS \\ &= \int \left\{ l\left(-p + 2\mu \frac{\partial u}{\partial x}\right) + \mu m\left(\frac{\partial v}{\partial x} + \frac{\partial u}{\partial y}\right) + \mu n\left(\frac{\partial u}{\partial z} + \frac{\partial w}{\partial x}\right)\right\} dS \\ &= \int \left\{ -lp - \mu m\zeta + \mu n\eta \right\} dS + \int 2\mu \left(l\frac{\partial u}{\partial x} + m\frac{\partial v}{\partial x} + n\frac{\partial w}{\partial x}\right) dS, \end{aligned} \tag{29}$$

where μ is the viscosity of the fluid. By using the equation of continuity we can write the second integral in the last line in the form

$$2\mu \int \left(m\frac{\partial v}{\partial x} - l\frac{\partial v}{\partial y} + n\frac{\partial w}{\partial x} - l\frac{\partial w}{\partial z}\right) dS. \tag{30}$$

To find

$$\int \left(m\frac{\partial v}{\partial x} - l\frac{\partial v}{\partial y}\right) dS, \tag{31}$$

divide the surface S into strips by planes parallel to the x, y plane. Then

$$m\frac{\partial v}{\partial x} - l\frac{\partial v}{\partial y} = -(1 - n^2)^{\frac{1}{2}} \frac{\partial v}{\partial s}, \tag{32}$$

where $\partial/\partial s$ is differentiation along a strip. Now take the surface S to be a sphere, so that n is constant along a strip. Then, since v is a single-valued function of position, the integral along a strip vanishes. Hence the integral (31) vanishes. Similarly

$$\int \left(n\frac{\partial w}{\partial x} - l\frac{\partial w}{\partial z}\right) \tag{33}$$

vanishes, so that the integral (30) vanishes.

By Green's theorem the integral (31) or (33), taken over S, is the same as the integral taken over any surface in the fluid inside S. The restriction that S is to be a sphere can therefore be removed.

Putting in the values of p, η and ζ we now find that

$$X_1 = \int \left(l\rho U \frac{\partial \phi}{\partial x} - \mu m \frac{\partial \chi}{\partial y} - \mu n \frac{\partial \chi}{\partial z}\right) dS. \tag{34}$$

Again,

$$\begin{aligned} \int \rho \{l(U + u) + mv + nw\}(U + u)\, dS = \int \rho l U^2\, dS + \int \rho U(2lu + mv + nw)\, dS \\ + \int \rho u(lu + mv + nw)\, dS. \end{aligned} \tag{35}$$

Except within the wake, u, v and w are of order r^{-2}. Within the wake, u, v and w are of order r^{-1}; but the solid angle subtended by the portion of S within the wake is also of order r^{-1}. Hence the last integral vanishes in the limit. The first integral vanishes identically. Equation (28), combined with (34), therefore gives

$$\begin{aligned} \mathrm{X} = &-\int \rho \mathrm{U}\left(l\frac{\partial\phi}{\partial x}+m\frac{\partial\phi}{\partial y}+n\frac{\partial\phi}{\partial z}\right)d\mathrm{S} \\ &-\int 2\mu\left(l\frac{\partial\chi}{\partial x}+m\frac{\partial\chi}{\partial y}+n\frac{\partial\chi}{\partial z}\right)d\mathrm{S} \\ &+\int 4k\mu\, l\chi\, d\mathrm{S}. \end{aligned} \tag{36}$$

We have here used the relation

$$2k\mu = \rho\mathrm{U}. \tag{37}$$

Hence

$$\mathrm{X} = -\rho\mathrm{U}\int\frac{\partial\phi}{\partial n}d\mathrm{S} - 2\mu\int\frac{\partial\chi}{\partial n}d\mathrm{S} + 4k\mu\int l\chi\, d\mathrm{S}, \tag{38}$$

where $\partial/\partial n$ is differentiation along the outward normal.

The condition that the total outflow through S must be zero gives

$$\int u_n\, d\mathrm{S} = 0, \tag{39}$$

or

$$\int\frac{\partial\phi}{\partial n}d\mathrm{S} + \frac{1}{2k}\int\frac{\partial\chi}{\partial n}d\mathrm{S} - \int l\chi\, d\mathrm{S} = 0. \tag{40}$$

Hence

$$4k\mu\int l\chi\, d\mathrm{S} - 2\mu\int\frac{\partial\chi}{\partial n}d\mathrm{S} = 4k\mu\int\frac{\partial\phi}{\partial n}d\mathrm{S} = 2\rho\mathrm{U}\int\frac{\partial\phi}{\partial n}d\mathrm{S}. \tag{41}$$

Thus

$$\mathrm{X} = \rho\mathrm{U}\int\frac{\partial\phi}{\partial n}d\mathrm{S}. \tag{42}$$

The contribution to the integral from the portion of S within the wake is negligible, so that the integral represents the outflow outside the wake, or the equal inflow along the wake.

Denoting this inflow by I, we have

$$\mathrm{X} = \rho\mathrm{UI}. \tag{43}$$

Similarly

$$Y_1 - Y = \int \rho \{l(U+u) + mv + nw\} v \, dS$$

$$= \int \rho U \, lv \, dS$$

$$= \rho U \int l \frac{\partial \phi}{\partial y} \, dS + \mu \int l \frac{\partial \chi}{\partial y} \, \partial S. \tag{44}$$

Also

$$Y_1 = \int (lp_{xy} + mp_{yy} + np_{zy}) \, dS$$

$$= \int \left\{ \mu l \left(\frac{\partial v}{\partial x} + \frac{\partial u}{\partial y} \right) + m \left(-p + 2\mu \frac{\partial v}{\partial y} \right) + \mu n \left(\frac{\partial w}{\partial y} + \frac{\partial v}{\partial z} \right) \right\} dS$$

$$= \int (-mp + \mu l \zeta - \mu n \xi) \, dS + \int 2\mu \left(l \frac{\partial u}{\partial y} + m \frac{\partial v}{\partial y} + n \frac{\partial w}{\partial y} \right) dS. \tag{45}$$

The last line is equal to

$$2\mu \int \left(l \frac{\partial u}{\partial y} - m \frac{\partial u}{\partial x} + n \frac{\partial w}{\partial y} - m \frac{\partial w}{\partial z} \right) dS, \tag{46}$$

which vanishes.

Hence

$$Y_1 = \rho U \int m \frac{\partial \phi}{\partial x} + \mu \int l \frac{\partial \chi}{\partial y} \, dS, \tag{47}$$

and

$$Y = -\rho U \int \left(l \frac{\partial \phi}{\partial y} - m \frac{\partial \phi}{\partial x} \right) dS. \tag{48}$$

To interpret this result, take S to be a cylinder with generators parallel to the axis of z. Let κ be the circulation taken round a section of the cylinder perpendicular to the generators. Let us assume that the terms in χ in u and v make no contribution to the circulation. Then

$$Y = -\rho U \int \kappa \, dz, \tag{49}$$

the integral being taken along the cylinder.

Since the axis of y can be taken in any direction perpendicular to the axis of x, it is unnecessary to find Z.

We must now find conditions under which the terms in χ in u and v make no contribution to the circulation; that is, the conditions that

$$\frac{1}{2k}\int\left(m\frac{\partial\chi}{\partial x}-l\frac{\partial\chi}{\partial y}\right)dS-\int m\chi\,dS \tag{50}$$

should vanish.

Now since u must be single-valued, χ must be single-valued. Since

$$m\frac{\partial\chi}{\partial x}-l\frac{\partial\chi}{\partial y}=-\frac{\partial\chi}{\partial s}, \tag{51}$$

where $\partial/\partial s$ is differentiation round a section of the cylinder,

$$\int\left(m\frac{\partial\chi}{\partial x}-l\frac{\partial\chi}{\partial y}\right)dS=0. \tag{52}$$

The expression (50) is therefore equal to

$$-\int m\chi\,dS. \tag{53}$$

The integrand is insensible except within the wake, and the solid angle subtended by the part of s within the wake is of order r^{-1}. But then χ is of order r^{-1}, and it does not need elaborate analysis to see that the integral will, in general, be finite if m tends to a finite limit as θ tends to zero. The necessary condition is therefore that m should tend to zero, so that in taking the circulation we must cut the wake behind the body at right angles.

If we impress on the whole system a velocity U in the direction opposite to that of the stream, the forces of the fluid on the solid are unaltered. We therefore have the theorem stated at the beginning of the paper.

4. *Non-steady Motion.*

We have so far considered the motion of the fluid to be steady. If the motion be not steady, then terms $\frac{\partial}{\partial t}(u, v, w)$ must be inserted in the equations of motion, and account must be taken in the equation (28) of the rate of change of momentum of the fluid inside the surface S. If the motion is periodic, and we take average values over a complete period; or if the motion oscillates between finite limits, and we take average values over a long time, these terms disappear. All our equations and expressions are linear, except the last integral in (35). The average value of this integral vanishes in the limit if the average values of u^2, uv and uw are of smaller order than r^{-2} outside the wake, and of smaller order than r^{-1} inside the wake. These conditions being satisfied, the theorem remains true when average values are taken. If the velocity components u, v and w at any point of the fluid lie between fixed limits, but if the momentum of the fluid inside the surface S continually increases, then the rate of increase must be added to the drag.

The Steady Flow of Viscous Fluid past a Fixed Spherical Obstacle at Small Reynolds Numbers.

By Sydney Goldstein, B.A., Ph.D., St. John's College, Cambridge.

(Communicated by H. Jeffreys, F.R.S.—Received December 31, 1928.)

It was proposed by Oseen* that, in considering the steady flow of a viscous fluid past a fixed obstacle, the velocity of disturbance should be considered small, and terms depending on its square neglected. This approximation is to be taken to hold not only at a great distance from the obstacle, but also right up to its surface; and involves the assumption that Ud/ν is small, where d is some representative length of the obstacle, which in the case of a sphere is taken to be its diameter, U is the undisturbed velocity of the stream, and ν the kinematic viscosity of the fluid. With this approximation, the equations of motion become linear, and can be solved; the condition of no slip at the boundary is then applied to complete the solution.

We take the obstacle to be a sphere of radius a, and take the origin of coordinates at its centre. The equations of motion are the same as equations (1) of the preceding paper; with the notation there used, we can put

$$\left.\begin{aligned} u_r &= \frac{\partial \phi}{\partial r} + \frac{1}{2k} e^{kx} \frac{\partial \chi'}{\partial r} - \tfrac{1}{2} e^{kx} \chi' \cos \theta \\ u_\theta &= \frac{1}{r}\frac{\partial \phi}{\partial \theta} + \frac{1}{2k} e^{kx} \frac{\partial \chi'}{r\,\partial \theta} + \tfrac{1}{2} e^{kx} \chi' \sin \theta \\ \text{and} \qquad u_\varpi &= 0 \end{aligned}\right\}, \tag{1}$$

where

$$\phi = \sum_{n=0}^{\infty} A_n \frac{P_n(\cos \theta)}{r^{n+1}}, \tag{2}$$

$$\chi' = \sum_{n=0}^{\infty} B_n \chi_n(kr)\, P_n(\cos \theta) \tag{3}$$

and

$$\chi_n(x) = (2n+1)(\pi/2x)^{\frac{1}{2}} K_{n+\frac{1}{2}}(x). \tag{4}$$

---

* 'Ark. Mat. Ast. Fys.,' vol. 6, No. 29 (1910).

The Legendre functions $P_n(\cos\theta)$ enter in place of the general spherical harmonics since the motion is clearly symmetrical about the axis of x.

If we put

$$\xi = kr \tag{5}$$

and

$$\mu = \cos\theta,^* \tag{6}$$

then

$$u_r = -\sum_{n=0}^{\infty} \frac{(n+1)A_n P_n(\mu)}{r^{n+2}} + \tfrac{1}{2}e^{\mu\xi}\sum_{n=0}^{\infty} B_n[\chi_n'(\xi) - \mu\chi_n(\xi)]\,P_n(\mu) \tag{7}$$

and

$$u_\theta = -\sin\theta\sum_{n=1}^{\infty}\frac{A_n P_n'(\mu)}{r^{n+2}} - \tfrac{1}{2}e^{\mu\xi}\sin\theta\sum_{n=0}^{\infty} B_n\chi_n(\xi)\left[\frac{P_n'(\mu)}{\xi} - P_n\right], \tag{8}$$

where $\chi_n'(\xi)$ is $\dfrac{d}{d\xi}\chi_n(\xi)$, and $P_n'(\mu)$ is $\dfrac{d}{d\mu}P_n(\mu)$.

The boundary conditions are

$$u_r = -U\cos\theta, \quad \text{and} \quad u_\theta = U\sin\theta \tag{9}$$

at $r = a$.

Let us write

$$e^{\mu\xi}P_m(\mu) = \sum_{n=0}^{\infty}\Psi_{n,m}(\xi)\,P_n(\mu), \tag{10}$$

$$e^{\mu\xi}P_m(\mu) = \sum_{n=1}^{\infty}\Phi_{n,m}(\xi)\,P_n'(\mu), \tag{11}$$

and

$$e^{\mu\xi}P_m'(\mu) = \sum_{n=1}^{\infty}X_{n,m}(\xi)\,P_n'(\mu). \tag{12}$$

If we differentiate (10) with respect to ξ, assuming for the moment the legitimacy of term by term differentiation, we obtain

$$\mu e^{\mu\xi}P_m(\mu) = \sum_{n=0}^{\infty}\Psi'_{m,n}(\xi)\,P_n(\mu), \tag{13}$$

where $\Psi'_{n,m}(\xi)$ is $\dfrac{d}{d\xi}\Psi_{n,m}(\xi)$.

Let us write

$$\xi_0 = ka, \tag{14}$$

P_n for $P_n(\mu)$, $\Psi_{n,m}$ for $\Psi_{n,m}(\xi_0)$, and so on. Let us then expand u_r in a

---

[*] μ is used to denote the viscosity of the fluid in this paper in equation (55) only, so that its use to denote $\cos\theta$ can cause no confusion.

series of P_n, and $u_\theta/\sin\theta$ in a series of P_n', put r equal to a, and apply the boundary conditions. This gives

$$\frac{(n+1)A_n}{a^{n+2}} - \tfrac{1}{2}\sum_{m=0}^{\infty} B_m(\chi_m'\Psi_{n,m} - \chi_m\Psi'_{n,m}) = \left.\begin{matrix} 0\ (n = 0, 2, 3, \ldots) \\ -U\ (n = 1) \end{matrix}\right\} \tag{15}$$

and

$$\frac{A_n}{a^{n+2}} + \tfrac{1}{2}\sum_{m=0}^{\infty} B_m\left(\frac{\chi_m}{\xi_0}X_{n,m} - \chi_m\Phi_{n,m}\right) = \left.\begin{matrix} U\ (n = 1) \\ 0\ (n = 2, 3, \ldots) \end{matrix}\right\}. \tag{16}$$

The first of equations (15) gives

$$\frac{A_0}{a^2} - \tfrac{1}{2}\sum_{m=0}^{\infty} B_m(\chi_m'\Psi_{0,m} - \chi_m\Psi'_{0,m}) = 0. \tag{17}$$

Eliminating A_1, A_2 … from equations (16) and the rest of equations (15) gives us

$$\tfrac{1}{2}\sum_{m=0}^{\infty}\lambda_{n,m}B = \left.\begin{matrix} -3U\ (n = 1) \\ 0\ \ (n > 1) \end{matrix}\right\}, \tag{18}$$

where

$$\lambda_{n,m} = \chi_m'\Psi_{n,m} - \chi_m\Psi'_{n,m} + \frac{(n+1)\chi_m}{\xi_0}(X_{n,m} - \xi_0\Phi_{n,m}). \tag{19}$$

According to the theorem of the preceding paper, the drag on the sphere is given by

$$D = -4\pi\rho U A_0. \tag{20}$$

Now A_0 is given in terms of the B by (17), and the B are to be found by solving (18). Theoretically, the solution of (18) is to be achieved by means of infinite determinants; practically, to find the solution numerically for any given value of ξ_0, we solve a finite number of equations. For the first approximation, we put B_1, B_2, B_3 and so on, equal to zero, and solve the first equation for B_0. For the second approximation, we put B_2, B_3, and so on, equal to zero, and solve the first two equations for B_0 and B_1. And so on. To obtain numerical solutions we must therefore be able to calculate the λ, and to calculate the λ we must be able to calculate the Ψ, Φ and X. We now return, therefore, to a consideration of the Ψ, as defined by (10).

In the first place, we have

$$\Psi_{n,m}(\xi)\int_{-1}^{1}[P_n(\mu)]^2\,d\mu = \int_{-1}^{+1} e^{\mu\xi}P_m(\mu)P_n(\mu)\,d\mu. \tag{21}$$

Since

$$\int_{-1}^{1}[P_n(\mu)]^2\,d\mu = \frac{2}{2n+1}, \tag{22}$$

it is immediately obvious that

$$(2m+1)\,\Psi_{n,m} = (2n+1)\,\Psi_{m,n}. \tag{23}$$

Next, it is a known result that

$$e^{\mu\xi} = \sum_{n=0}^{\infty} \psi_n(\xi)\, \mathrm{P}_n(\mu), \tag{24}$$

where

$$\psi_n(\xi) = (2n+1)\left(\frac{\pi}{2\xi}\right)^{\frac{1}{2}} \mathrm{I}_{n+\frac{1}{2}}(\xi). \tag{25}$$

(Compare Gegenbauer's formula, Watson's 'Bessel Functions,' p. 50. Since $e^{\mu\xi}$ is e^{kx}, and satisfies the differential equation $(\nabla^2 - k^2)\, e^{kx} = 0$, and since it remains finite at the origin, it must be developable in a series of $\mathrm{P}_n(\mu)$ with coefficients that are multiples of $\psi_n(\xi)$. It is not difficult to complete the proof of (24).)

Differentiating (24) m times with respect to ξ gives*

$$\mu^m e^{\mu\xi} = \sum_{n=0}^{\infty} \frac{d^m}{d\xi^m}\, \psi_n(\xi)\, \mathrm{P}_n(\mu). \tag{26}$$

Since

$$\mathrm{P}_m(\mu) = \frac{(2m)!}{2^m (m!)^2}\left\{\mu^m - \frac{m(m-1)}{2(2m-1)}\mu^{m-2} + \frac{m(m-1)(m-2)(m-3)}{2\,.\,4\,.\,(2m-1)(2m-3)}\mu^{m-4} + \dots\right\}, \tag{27}$$

it follows from (26) that

$$\Psi_{n,m} = \frac{(2m)!}{2^m (m!)^2}\left\{\frac{d^m}{d\xi^m} - \frac{m(m-1)}{2(2m-1)}\frac{d^{m-2}}{d\xi^{m-2}} + \dots\right\}\psi_n(\xi). \tag{28}$$

In particular

$$\Psi_{n,0} = \psi_n \tag{29}$$

and

$$\Psi_{n,1} = \psi_n' = \frac{n}{2n-1}\psi_{n-1} + \frac{n+1}{2n+3}\psi_{n+1}. \tag{30}$$

Before proceeding further, it will be useful to list certain formulæ relating to ψ_n and χ_n, as defined by (25) and (4). These are all easily obtained from formulæ containing $\mathrm{I}_{n+\frac{1}{2}}$ and $\mathrm{K}_{n+\frac{1}{2}}$. (Watson's 'Bessel Functions,' pp. 79 and 80.)

$$\psi_n' = \frac{n}{2n-1}\psi_{n-1} + \frac{n+1}{2n+3}\psi_{n+1}; \quad \frac{\psi_n}{\xi} = \frac{\psi_{n-1}}{2n-1} - \frac{\psi_{n+1}}{2n+3}. \tag{31}$$

---

* $\mathrm{P}_n(\cos\theta)$ is not numerically greater than 1, and for large values of n, $\psi_n \simeq 2^{-\frac{1}{2}}(ex/2n)^n$. These results, combined with the first equation in (31), enable us to show that the series in (26) is uniformly convergent with respect to ξ in any given interval, and therefore the term by term differentiation is justified.

$$\chi_n' = -\left(\frac{n}{2n-1}\chi_{n-1} + \frac{n+1}{2n+3}\chi_{n+1}\right); \quad \frac{\chi_n}{\xi} = \frac{\chi_{n+1}}{2n+3} - \frac{\chi_{n-1}}{2n-1}. \tag{32}$$

$$\chi_n'\,\psi_n - \chi_n\,\psi_n' = -(2n+1)^2\,\frac{\pi}{2\xi^2}. \tag{33}$$

$$\frac{d}{d\xi}\left(\frac{\psi_n}{\xi}\right) = \frac{1}{\xi}\left(\frac{n-1}{2n-1}\,\psi_{n-1} + \frac{n+2}{2n+3}\,\psi_{n+1}\right). \tag{34}$$

$$\chi_n + \chi_{-n-1} = 0. \tag{35}$$

$$\chi_n = (2n+1)\,\frac{\pi}{2\xi}\,e^{-\xi}\sum_{r=0}^{n}\frac{(n+r)\,!}{r\,!\,(n-r)\,!\,(2\xi)^r}. \tag{36}$$

$$\psi_n = \frac{2n+1}{2\xi}\left[e^{\xi}\sum_{r=0}^{n}\frac{(-)^r\,(n+r)\,!}{r\,!\,(n-r)\,!\,(2\xi)^r} + (-)^{n+1}\,e^{-\xi}\sum_{r=0}^{n}\frac{(n+r)\,!}{r\,!\,(n-r)\,!\,(2\xi)^r}\right]. \tag{37}$$

Next, since

$$m\mathrm{P}_m = (2m-1)\,\mu\mathrm{P}_{m-1} - (m-1)\,\mathrm{P}_{m-2}, \tag{38}$$

it follows that

$$m\Psi'_{n,m} = (2m-1)\,\Psi''_{n,m-1} - (m-1)\,\Psi'_{n,m-2}. \tag{39}$$

From (29), (30) and (39), and with the help of the first equation in (31), the following formula can easily be proved by induction.

$$\begin{aligned}\Psi'^{\,!}_{n,m} = \frac{\underline{|2m}\,\underline{|2n+1}}{\underline{|2n+2m+1}}\left(\frac{\underline{|n+m}}{\underline{|n}\,\underline{|m}}\right)^2 \Bigg\{ & \psi_{n+m} + \frac{n}{2n-1}\,\frac{m}{2m-1}\,\frac{2n+2m+1}{n+m}\,\psi_{n+m-2} \\ & + \frac{1\,.\,3}{2\,!}\,\frac{n\,(n-1)}{(2n-1)\,(2n-3)}\,\frac{m\,(m-1)}{(2m-1)\,(2m-3)} \\ & \qquad \frac{(2n+2m+1)\,(2n+2m-1)}{(n+m)\,(n+m-1)}\,\psi_{n+m-4} + \dots \\ & + \frac{1\,.\,3\,.\,5\,\dots\,(2r-1)}{r\,!}\,\frac{n\,(n-1)\,\dots\,(n-r+1)}{(2n-1)\,(2n-3)\,\dots\,(2n-2r+1)} \\ & \qquad \frac{m\,(m-1)\,\dots\,(m-r+1)}{(2m-1)\,(2m-3)\,\dots\,(2m-2r+1)} \\ & \qquad \frac{(2n+2m+1)\,(2n+2m-1)\,\dots\,(2n+2m-2r+3)}{(n+m)\,(n+m-1)\,\dots\,(n+m-r+1)}\,\psi_{n+m-2r} + \dots \\ & + \frac{n\,(n-1)\,\dots\,(n-m+1)}{(2n-1)\,(2n-3)\,\dots\,(2n-2m+1)} \\ & \qquad \frac{(2n+2m+1)\,(2n+2m-1)\,\dots\,(2n+3)}{(n+m)\,(n+m-1)\,\dots\,(n+1)}\,\psi_{n-m}\Bigg\}. \end{aligned} \tag{40}$$

We now turn to the $\Phi_{n,m}$ as defined by (11). First, by differentiating (24) with respect to μ, we get

$$e^{\mu\xi} = \sum_{n=1}^{\infty} \frac{\psi_n(\xi)}{\xi} \mathrm{P}'_n(\mu), \tag{41}$$

so that

$$\Phi_{n,0} = \frac{\psi_n}{\xi}. \tag{42}$$

In exactly the same way as we found (28) we find that

$$\Phi_{n,m} = \frac{(2m)!}{2^m (m!)^2} \left\{ \frac{d^m}{d\xi^m} - \frac{m(m-1)}{2(2m-1)} \frac{d^{m-1}}{d\xi^{m-1}} + \dots \right\} \frac{\psi_n(\xi)}{\xi}. \tag{43}$$

Again, differentiating (10) with respect to μ gives

$$\sum_{n=1}^{\infty} \Psi_{n,m} \mathrm{P}_n' = \xi e^{\mu\xi} \mathrm{P}_m + e^{\mu\xi} \mathrm{P}_m' = \sum_{n=1}^{\infty} (\xi \Phi_{n,m} + \mathrm{X}_{n,m}) \mathrm{P}_n', \tag{44}$$

so that

$$\Psi_{n,m} = \xi \Phi_{n,m} + \mathrm{X}_{n,m}. \tag{45}$$

Hence, from (19),

$$\lambda_{n,m} = \chi_m' \Psi_{n,m} - \chi_m \Psi'_{n,m} + \frac{(n+1)\chi_m}{\xi_0} (2\mathrm{X}_{n,m} - \Psi_{n,m}), \tag{46}$$

and it is unnecessary to calculate the $\Phi_{n,m}$ if we can calculate the $\mathrm{X}_{n,m}$.

Equation (45) gives

$$\mathrm{X}_{n,0} = 0 \quad \text{and} \quad \mathrm{X}_{n,1} = \psi_n' - \xi \frac{d}{d\xi}\left(\frac{\psi_n}{\xi}\right) = \frac{\psi_n}{\xi}. \tag{47}$$

If now we differentiate (38) with respect to μ, and use the formula

$$(2m-1)\mathrm{P}_{m-1} = \mathrm{P}_m' - \mathrm{P}'_{m-2}, \tag{48}$$

we easily find that

$$(m-1)\mathrm{P}_m' = (2m-1)\mu \mathrm{P}'_{m-1} - m\mathrm{P}'_{m-2}. \tag{49}$$

From this we derive

$$(m-1)\mathrm{X}_{n,m} = (2m-1)\mathrm{X}'_{n,m-1} - m\mathrm{X}_{n,m-2}, \tag{50}$$

just as we derived (39) from (38).

We can now easily prove the following formula by induction.

$$
\begin{aligned}
\mathrm{X}_{n,m} = {} & \frac{m\,(2n+1)}{n+1}\,\frac{\underline{|2m}\,\underline{|2n}}{\underline{|2n+2m}}\left(\frac{\underline{|n+m}}{\underline{|n}\,\underline{|m}}\right)^2 \\
& \times \left\{\frac{\psi_{n+m-1}}{\xi} + 3\,\frac{n-1}{2n-1}\,\frac{m-1}{2m-1}\,\frac{2n+2m-1}{n+m}\,\frac{\psi_{n+m-3}}{\xi}\right. \\
& \quad + \frac{1\,.\,3\,.\,5}{2\,!}\,\frac{(n-1)\,(n-2)}{(2n-1)\,(2n-3)}\,\frac{(m-1)\,(m-2)}{(2m-1)\,(2m-3)} \\
& \qquad \frac{(2n+2m-1)\,(2n+2m-3)}{(n+m)\,(n+m-1)}\,\frac{\psi_{n+m-5}}{\xi} + \dots \\
& \quad + \frac{1\,.\,3\,.\,\dots\,(2r+1)}{r\,!}\,\frac{(n-1)\dots(n-r)}{(2n-1)\dots(2n-2r+1)} \\
& \qquad \frac{(m-1)\dots(m-r)}{(2m-1)\dots(2m-2r+1)} \\
& \qquad \frac{(2n+2m-1)\dots(2n+2m-2r+1)}{(n+m)\dots(n+m-r+1)}\,\frac{\psi_{n+m-2r-1}}{\xi} + \dots \\
& \quad \left. + \frac{(n-1)\dots(n-m+1)}{(2n-1)\dots(2n-2m+3)}\,\frac{(2n+2m-1)\dots(2n+3)}{(n+m)\dots(n+2)}\,\frac{\psi_{n-m+1}}{\xi}\right\}. \qquad (51)
\end{aligned}
$$

This formula, and the formula (40), appear to be new.

Now (46) gives us $\lambda_{n,m}$ in terms of χ_m, $\Psi_{n,m}$ and $\mathrm{X}_{n,m}$; (40) and (51) give us $\Psi_{n,m}$ and $\mathrm{X}_{n,m}$ in terms of ψ_n; and (36) and (37) give χ_n and ψ_n in finite terms. Thus $\lambda_{n,m}$ can be expressed in finite terms. For our present purpose, which is to obtain numerical solutions, it would not be of much use to give a complicated general expression for $\lambda_{n,m}$. The first nine λ are therefore written out below; they are sufficient to enable us to proceed to the third approximation, which gives us the drag on the sphere with sufficient accuracy for values of ξ_0 not greater than 5, or values of the Reynolds' number, Ud/ν, not greater than 20. This is more than sufficient: the initial assumptions will have broken down before that value is reached.

Before writing down the λ and calculating out some values numerically, one thing remains to be done. We must simplify (17), and show that it leads to the same relations between A_0 and the B as we obtained in the preceding paper. (Equation (27).)

Either from (23) and (29), or direct from (40), we find that

$$\Psi_{0,m} = \psi_m/(2m+1). \qquad (52)$$

Hence

$$\chi_m'\Psi_{0,m} - \chi_m\Psi'_{0,m} = (\chi_m'\psi_m - \chi_m\psi_m')/(2m+1) = -(2m+1)\pi/2\xi_0^2, \quad (53)$$

from (33). Thus (17) becomes

$$\frac{A_0}{a^2} = -\frac{\pi}{4k^2a^2}\sum_{m=0}^{\infty}(2m+1)\,B_m \quad \text{or} \quad A_0 = -\frac{\pi}{4k^2}\sum_{m=0}^{\infty}(2m+1)\,B_m. \quad (54)$$

In order that the total flow across a large sphere should be zero, the coefficient of $P_0(\mu)$ in the expansion of u_r must vanish. But this coefficient is the right-hand side of (17) with r in place of a, and ξ in place of ξ_0. Its vanishing leads to the same relation, (54), as equation (17). This proof of (54) holds for any solid of revolution with its axis in the direction of the flow.

From (20) and (54) it follows that the drag is given by

$$D = \frac{2\pi^2\mu}{k}\sum_{m=0}^{\infty}(2m+1)\,B_m. \quad (55)$$

where μ is now the viscosity of the fluid.

It is usual to express the result in terms of a non-dimensional drag coefficient, k_D, defined by

$$D = k_D\rho U^2 S, \quad (56)$$

where S is some representative area of the obstacle, which we may conveniently take to be the maximum cross-section opposed to the flow. We therefore take S to be πa^2, so that

$$k_D = \frac{D}{\pi\rho U^2 a^2} = \frac{\pi}{\xi_0^2}\sum_{m=0}^{\infty}(2m+1)\frac{B_m}{U}. \quad (57)$$

We now write out the λ, with their expansions in powers of ξ_0 for small values of ξ_0.

$$\lambda_{1,0} = -\frac{3\pi}{4\xi_0^2}\left[2 - \frac{1}{\xi_0^2} + e^{-2\xi_0}\left(\frac{2}{\xi_0} + \frac{1}{\xi_0^2}\right)\right]$$

$$= -\frac{2\pi}{\xi_0}\left(1 - \frac{3}{4}\xi_0 + \frac{2}{5}\xi_0^2 - \frac{1}{6}\xi_0^3 + \frac{2}{35}\xi_0^4 - \frac{1}{60}\xi_0^5 + 0(\xi_0^6)\right). \quad (58)$$

$$\lambda_{1,1} = -\frac{9\pi}{4\xi_0^2}\left[2 - \frac{3}{\xi_0^2} + \frac{6}{\xi_0^4} - e^{-2\xi_0}\left(\frac{2}{\xi_0} + \frac{9}{\xi_0^2} + \frac{12}{\xi_0^3} + \frac{6}{\xi_0^4}\right)\right]$$

$$= -\frac{9\pi}{\xi_0}\left(\frac{2}{5} - \frac{1}{6}\xi_0 + \frac{4}{105}\xi_0^2 + 0(\xi_0^4)\right). \quad (59)$$

$$\lambda_{1,2} = -\frac{15\pi}{4\xi_0^2}\Big[2 - \frac{7}{\xi_0^2} + \frac{36}{\xi_0^4} - \frac{135}{\xi_0^6}$$
$$+ e^{-2\xi_0}\Big(\frac{2}{\xi_0} + \frac{25}{\xi_0^2} + \frac{108}{\xi_0^3} + \frac{234}{\xi_0^4} + \frac{270}{\xi_0^5} + \frac{135}{\xi_0^6}\Big)\Big]$$
$$= -\frac{22\pi}{7\xi_0}\,(1 + 0\,(\xi_0^2)\,). \tag{60}$$

$$\lambda_{2,0} = -\frac{5\pi}{4\xi_0^2}\Big[2 - \frac{3}{\xi_0} + \frac{3}{\xi_0^3} - e^{-2\xi_0}\Big(\frac{3}{\xi_0} + \frac{6}{\xi_0^2} + \frac{3}{\xi_0^3}\Big)\Big]$$
$$= -\pi\Big(1 - \frac{5}{6}\,\xi_0 + \frac{3}{7}\,\xi_0^2 - \frac{1}{6}\,\xi_0^3 + 0\,(\xi_0^4)\Big). \tag{61}$$

$$\lambda_{2,1} = -\frac{15\pi}{4\xi_0^2}\Big[2 - \frac{3}{\xi_0} + \frac{9}{\xi_0^3} - \frac{27}{\xi_0^5} + e^{-2\xi_0}\Big(\frac{3}{\xi_0} + \frac{18}{\xi_0^2} + \frac{45}{\xi_0^3} + \frac{54}{\xi_0^4} + \frac{27}{\xi_0^5}\Big)\Big]$$
$$= -\frac{3\pi}{\xi_0^2}\Big(1 + \frac{1}{7}\,\xi_0^2 + 0\,(\xi_0^4)\,\Big). \tag{62}$$

$$\lambda_{2,2} = -\frac{25\pi}{4\xi_0^2}\Big[2 - \frac{3}{\xi_0} + \frac{21}{\xi_0^3} - \frac{162}{\xi_0^5} + \frac{810}{\xi_0^7}$$
$$- e^{-2\xi_0}\Big(\frac{3}{\xi_0} + \frac{42}{\xi_0^2} + \frac{237}{\xi_0^3} + \frac{756}{\xi_0^4} + \frac{1458}{\xi_0^6} + \frac{1620}{\xi_0^6} + \frac{810}{\xi_0^7}\Big)\Big]$$
$$= -\frac{60\pi}{7\xi_0^2}\,(1 + 0\,(\xi_0^2)). \tag{63}$$

$$\lambda_{3,0} = -\frac{7\pi}{4\xi_0^2}\Big[2 - \frac{8}{\xi_0} + \frac{12}{\xi_0^2} - \frac{15}{\xi_0^4} + e^{-2\xi_0}\Big(\frac{4}{\xi_0} + \frac{18}{\xi_0^2} + \frac{30}{\xi_0^3} + \frac{15}{\xi_0^4}\Big)\Big]$$
$$= -\frac{4\pi}{15}\,\xi_0\Big(1 - \frac{7}{8}\,\xi_0 + 0\,(\xi_0^2)\Big). \tag{64}$$

$$\lambda_{3,1} = -\frac{21\pi}{4\xi_0^2}\Big[2 - \frac{8}{\xi_0} + \frac{16}{\xi_0^2} - \frac{51}{\xi_0^4} + \frac{180}{\xi_0^6}$$
$$- e^{-2\xi_0}\Big(\frac{4}{\xi_0} + \frac{34}{\xi_0^2} + \frac{138}{\xi_0^3} + \frac{309}{\xi_0^4} + \frac{360}{\xi_0^5} + \frac{180}{\xi_0^6}\Big)\Big]$$
$$= -\frac{8\pi}{5\xi_0}\,(1 + 0\,(\xi_0^2)\,). \tag{65}$$

$$\lambda_{3,2} = -\frac{35\pi}{4\xi_0^2}\Big[2 - \frac{8}{\xi_0} + \frac{24}{\xi_0^2} - \frac{141}{\xi_0^4} + \frac{1188}{\xi_0^6} - \frac{6750}{\xi_0^8}$$
$$+ e^{-2\xi_0}\Big(\frac{4}{\xi_0} + \frac{66}{\xi_0^2} + \frac{498}{\xi_0^3} + \frac{2265}{\xi_0^4} + \frac{6624}{\xi_0^5} + \frac{12312}{\xi_0^6} + \frac{13500}{\xi_0^7} + \frac{6750}{\xi_0^8}\Big)\Big]$$
$$= -\frac{12\pi}{\xi_0^3}\,(1 + 0\,(\xi_0^2)\,). \tag{66}$$

With these values of the λ, we have now to solve equations (18) for the B, and then the drag coefficient is given by (57). We can find the expansions of the B, and therefore also of k_D, in powers of ξ_0 from the expansions of the λ given above. Since $4\xi_0$ is equal to the Reynolds number R or Ud/ν, we can find the expansion of k_D in powers of R. The result is

$$k_D = \frac{12}{R}\left\{1 + \frac{3}{16}R - \frac{19}{1280}R^2 + \frac{71}{20480}R^3 - \frac{30179}{34406400}R^4 + \frac{122519}{560742400}R^5 - \ldots\right\}, \tag{67}$$

where, by definition, k_D is $D/\pi\rho U^2a^2$, and R is Ud/ν. The first term, $12R^{-1}$, is the value given by Stokes.[*] The second approximation, $12R^{-1} + 2\cdot25$, was given by Oseen,[†] Burgess,[‡] and others. For values of R up to and including 2, the value of k_D can be calculated from the series. For larger values it is necessary to compute the λ, and solve the equations (18) numerically. The results are shown in the following table (Table I). The second column gives the drag coefficient according to Stokes, the third according to Oseen, and the fourth according to the exact solution of Oseen's equations. The fifth column gives the correction to Oseen's second approximation, multiplied by

Table I.

$R = Ud/\nu$.	$12R^{-1}$ (Stokes).	$12R^{-1}+2\cdot25$ (Oseen).	k_D (exact solution of Oseen's equations).	$100(12R^{-1}+2\cdot25-k_D)$.	$\dfrac{100(12R^{-1}+2\cdot25-k_D)}{12R^{-1}+2\cdot25}$.
0·2	60·00	62·25	62·22	3	0·05
0·4	30·00	32·25	32·18	7	0·2
0·6	20·00	22·25	22·16	9	0·4
0·8	15·00	17·25	17·13	12	0·7
1·0	12·00	14·25	14·11	14	1·0
1·2	10·00	12·25	12·08	17	1·4
1·4	8·57	10·82	10·63	19	1·8
1·6	7·50	9·75	9·54	21	2·2
1·8	6·67	8·92	8·69	23	2·6
2·0	6·00	8·25	8·00	25	3·1
2·5	4·80	7·05	6·76	29	4·3
3·0	4·00	6·25	5·93	32	5·4
3·5	3·43	5·68	5·33	35	6·6
4·0	3·00	5·25	4·87	38	7·8
5·0	2·40	4·65	4·22	43	10
6·0	2·00	4·25	3·78	47	12
8·0	1·50	3·75	3·21	54	17
10·0	1·20	3·45	2·85	60	21
12·0	1·00	3·25	2·60	65	25
16·0	0·75	3·00	2·28	72	32
20·0	0·60	2·85	2·08	77	37

---

[*] 'Camb. Phil. Trans.,' vol. 8, p. 287 (1845).

[†] 'Ark. Mat. Ast. Fys.,' vol. 9, No. 16 (1913).

[‡] 'Amer. J. Math.,' vol. 38, p. 81 (1916).

100; and the last column gives the percentage correction. The second approximation, $12R^{-1} + 2\cdot 25$, is much better than might have been anticipated, and interpolation is most easily carried out by interpolating graphically for the difference between the exact solution and this second approximation.

When the drag coefficient is determined experimentally, the possible error is not less than 1 per cent. In addition, a certain error is introduced when approximate formulæ are used to correct for the influence of finite distance of boundaries. It is, therefore, useless to look for the influence of the correction found here for values of R less than 1·6 or so.

A fair number of experimental determinations have been carried out. The results were collected into one curve by Zahm* in 1926, and he gave the empirical formula

$$k_D = 14R^{-0\cdot 85} + 0\cdot 24 \tag{68}$$

as valid for $0\cdot 2 < R < 200000$. Since then experiments have been reported by Liebster† and Schmiedel.‡ Some values given by Zahm's empirical formula are compared below with values calculated here, with rather surprisingly good results; but it must be mentioned that the values in or near this range $(1\cdot 6 \leqslant R \leqslant 4\cdot 0)$ which were reported by Liebster and Schmiedel all lie below those given by Zahm's formula, so that the agreement with the values given here is not nearly so good.

Table II.

R.	$k_D = 14R^{-0\cdot 85} + 0\cdot 24$ (Zahm).	$k_D = 12R^{-1} + 2\cdot 25$ (Oseen).	k_D (exact solution of Oseen's equations).
1·6	9·63	9·75	9·54
1·8	8·73	8·92	8·69
2·0	8·01	8·25	8·00
2·5	6·67	7·05	6·76
3·0	5·74	6·25	5·93
3·5	5·07	5·68	5·33
4·0	4·55	5·25	4·87

Summary.

Oseen's equations for the flow of a viscous fluid at small Reynolds numbers past a fixed spherical obstacle are solved completely, and a table given of the resulting values of the drag coefficient.

---

* 'Report No. 253 of the National Advisory Committee for Aeronautics (U.S.A.),' p. 520 (1926).

† 'Ann. Physik,' vol. 82, p. 541 (1927).

‡ 'Phys. Z.,' vol. 29, p. 593 (1928).

Equilibrium in the System Methyl Alcohol-Hydrogen-Carbonic Oxide.

By D. M. NEWITT, Ph.D., B. J. BYRNE, B.Sc., and H. W. STRONG, Ph.D.,
High Pressure Gas Research Laboratories of the Imperial College of Science and Technology, London.

(Communicated by W. A. Bone, F.R.S.—Received December 21, 1928.)

About two years ago there was installed in the High Pressure Gas Research Laboratories at the Imperial College, apparatus which had been specially designed by Prof. Bone and his staff for the investigation of reaction velocities and equilibrium conditions in reversible catalytic systems ; and at his request we undertook to determine by means of it the equilibrium conditions of the system methyl alcohol-hydrogen-carbonic oxide at those temperatures at which the commercial production of pure methyl alcohol from water gas is practicable. The present paper embodies our results up to date for the temperature range 280° to 340° C. and for pressures of about 100 atmospheres.

Although the synthesis of methyl alcohol by the direct union of carbonic oxide and hydrogen has already reached a stage of development when large scale operations are being undertaken, no systematic work appears to have been carried out to determine the maximum possible yields under given temperature and pressure conditions. The value of a knowledge of equilibrium conditions in the system has not been overlooked, however, for a number of attempts have been made to calculate them from existing physical data. It may be pointed out that, whilst in the initial stages of a research the results so obtained are of undoubted value for predicting the most favourable working limits of temperature and pressure, they are not sufficiently reliable to afford guidance at a later stage, and may even be misleading. In fact our experimental results would rather indicate that a good deal of unnecessary work may have been done in striving after yields that are unattainable.

The want of concordance amongst calculated results may be illustrated by a comparison of the values of the equilibrium constant at various temperatures as deduced by two alternative methods. Thus, for example, from existing free energy data and a knowledge of the heats of combustion of carbonic oxide and methyl alcohol, K. K. Kelley obtained the following equation to express the relationship between free energy change and temperature for the reaction under consideration :—

$$\Delta F = -21{,}300 + 32{\cdot}2\,T \log T - 0{\cdot}00825\,T^2 - 42{\cdot}5\,T.$$

From the so ascertained free energy values the equilibrium constant was calculated from the relation

$$\Delta F = -RT\ ln\ K_p.$$

Audibert and Raineau, on the other hand, have used a method based upon Nernst's Heat Theorem from which they derive an equation for calculating the fraction, x, of carbonic oxide converted into methyl alcohol at any given temperature and pressure, namely,

$$\log \frac{(1-x)^3}{x(3-2x)^2} = \frac{27{,}000}{4 \cdot 571\ T} + 3 \cdot 5 \log T + 2 \cdot 99794 - 2 \log P.$$

The values of K_p calculated by means of these two equations, at three temperatures, are compared in Table I.

Table I.—Calculated Values of K_p.

Temperature ° C.	K_p.	
	Kelley.	Audibert and Raineau.
227	3·16	$5 \cdot 75 \times 10^{-2}$
327	$3 \cdot 86 \times 10^{-2}$	$3 \cdot 20 \times 10^{-4}$
427	$1 \cdot 54 \times 10^{-3}$	$7 \cdot 55 \times 10^{-6}$

More recently values for K_p have been calculated by a number of investigators from experimental figures based upon the percentage conversion of carbonic oxide to methyl alcohol under conditions favourable to the attainment of equilibrium by synthesis. Whilst these results agree fairly well amongst themselves and with the calculated K_p values based upon Nernst's theorem, they are considerably at variance with those predicted on the basis of the free energy-temperature relationship, as will be seen from an inspection of Table II.

Table II.—Experimental Values of K_p at 400° C.

Observer.	Reaction pressure atmospheres.	$K_p = \frac{P_{MeOH}}{P_{CO} \times P_{H_2}^2}$
Audibert and Raineau	150	$1 \cdot 92 \times 10^{-4}$
Lewis and Frolich	204	$1 \cdot 80 \times 10^{-5}$
Brown and Galloway	180	$1 \cdot 62 \times 10^{-5}$
,, ,,	180	$1 \cdot 98 \times 10^{-5}$

This method of determining the equilibrium constant is, however, open to the criticism that since equilibrium is approached from one side only there is no indication as to when the reaction is complete and equilibrium established.

EXPERIMENTAL.

It has been shown that the reaction

$$CO + 2H_2 \rightarrow CH_3OH$$

proceeds at a measureable rate only at temperatures of the order of 280° C. and upwards and in the presence of a suitable catalyst. It was evident therefore, from this consideration and from the calculated values of K_p, that in order to obtain adequate quantities of the three components at equilibrium, relatively high pressures must be used. This necessarily implied the use of metal apparatus specially designed to withstand large stresses, and introduced certain difficulties in regard to the measurement of pressure to which attention will be directed later. We have employed two independent methods for the determination of K_p, namely, (*a*) a static method, and (*b*) an intermittent flow method, and in each case have approached equilibrium from both sides, *i.e.*, by synthesis and by decomposition of methyl alcohol, respectively.

The Static Method and Apparatus.

The method consisted essentially in introducing a mixture of nearly the equilibrium proportions of the three components of the system into an evacuated vessel containing the catalyst and maintained at the desired temperature. The rate of increase of pressure was then followed by means of a suitable manometer until a constant pressure was reached indicative of the attainment of equilibrium. A sample of the contents of the vessel was taken and immediately thereafter sufficient either of a theoretical mixture of carbonic oxide and hydrogen ($CO + 2H_2$) or of methyl alcohol to disturb the equilibrium in the required direction was introduced into the vessel. The pressure change was again followed and a second sample taken as soon as constant conditions were reached. Analysis of the two samples then furnished the requisite information for calculating K_p at the temperature of the experiment.

The catalyst vessel, fig. 1, designed to withstand a pressure of 150 atmospheres at a temperature of 400° C., consisted of a nickel steel cylinder, flanged at one end and having an internal capacity of 500 c.cs. The flanged end was closed by means of a double end-plate A, holding the inlet valve, B, and the thermometer pocket, C. All the internal parts of the system were lined with copper. The internal cavity tapered abruptly at one end to a hole, 3/64-inch in diameter, making connection with the pressure manometer.

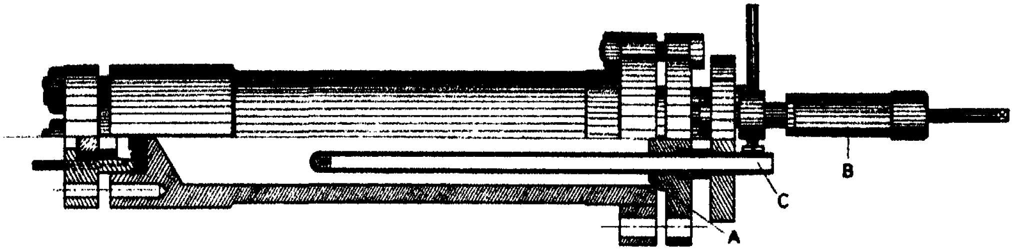

Fig. 1.

The construction of a suitable manometer for this type of work is a matter of considerable difficulty because, not only must it be sufficiently sensitive to record extremely small changes of pressure, but the design must be such that if there be any dead space it can be maintained at a temperature sufficiently high to avoid the risk of condensation of any liquid product; also any temperature effect on the pressure recording element must be reproducible.

A number of different designs of manometer were tried, the neutral disc type, illustrated in section in fig. 2, being finally adopted as fulfilling the required conditions. The pressure element of this gauge consisted of a thin corrugated metal disc, A, clamped rigidly between the end of the catalyst vessel, B, and a ⅜-inch thick steel plate, C. An unsupported area at the centre of the disc communicated with the catalyst chamber on one side and with the compensating air chamber, D, on the other side. Any movement of the disc caused by difference of pressure on the two sides was indicated and magnified by a beam of light reflected from a platinised silica mirror pivoted on the plate, C, and resting on a fine steel rod rigidly attached to the disc; the front of the compensating air chamber was fitted with a conical, transparent, quartz window, ⅝-inch thick. In practice, the unknown pressure in the catalyst vessel was balanced by a known pressure (measured on a standard Bourdon tube gauge) in the air chamber, equality of pressure on the opposite sides of the disc being indicated by the mirror resting in the zero position. By using a sufficiently thin disc it was possible to attain extreme sensitiveness and since the disc was well supported on both sides, there was little danger of permanent

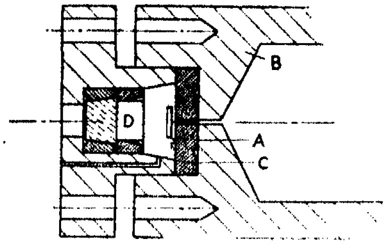

Fig. 2.

distortion or of rupture. The zero error due to permanent distortion was found not to exceed 0·1 atmosphere at the end of an experiment and no trouble was experienced through corrosion due to the gases or vapour.

The catalyst was contained in a copper gauze cage occupying the middle third of the vessel. The inlet valve, designed to give a very fine control, was provided with a long handle so that the body of the valve, including the packing could be kept within the furnace ; the valve terminated in a copper capillary tube extending into the catalyst chamber up to a point close to the catalyst holder, the object being to enable samples to be withdrawn from the immediate neighbourhood of the catalyst.

The whole apparatus was placed horizontally in an electric furnace, and was held rigidly in place by means of wedges ; the furnace was so wound as to counteract the temperature drop due to the big end heat losses and so as to give a range of constant temperature over the whole distance occupied by the catalyst chamber. The temperature of the catalyst was measured by a mercury in glass thermometer placed in the thermometer pocket which extended to the centre of the chamber. The thermometer used in our experiments was compared both before and after each series with two standard Calderara thermometers, each certified to be accurate to within 1° C., and the variation was never found to exceed this figure. The recorded temperatures are considered to be accurate to ± 1·5° C.

The Filling System and Method of Charging the Catalyst Vessel.

The general arrangement of the system is shown diagrammatically in fig. 3. The gas cylinders, A and B, contained a carbonic oxide-hydrogen mixture ($2H_2$ + CO) and nitrogen, respectively, compressed to 120 atmospheres. By means of the three valves, C, D, E, connection could be made (1) to the catalyst

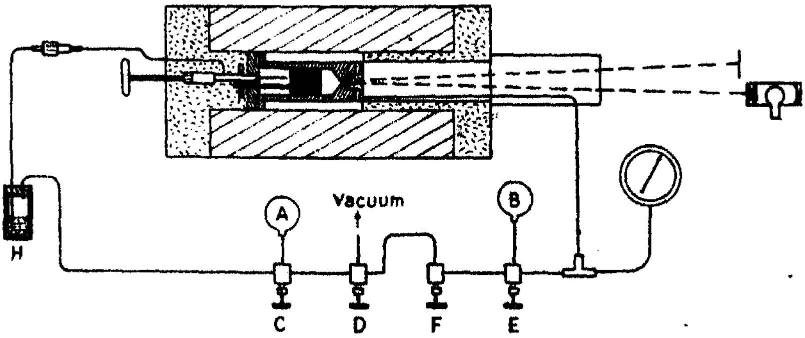

Fig. 3.

chamber by way of the steel bottle, H, containing pure methyl alcohol; (2) to a vacuum pump; and (3) to the air chamber of the neutral disc manometer and the standard Bourdon gauge. A fourth valve, F, short circuited the air chamber and the catalyst chamber and was employed when it was desired to fill the catalyst vessel rapidly, equality of pressure being automatically maintained on both sides of the neutral disc.

Immediately before carrying out any experiment the apparatus was tested for leaks by filling with nitrogen to a pressure of 100 atmospheres and maintaining it at a temperature of 300° C. for at least three hours.

Criterion of the Attainment of Equilibrium.

In order to reduce the time for attainment of equilibrium to reasonable limits it was necessary, when working at the lower temperatures, to fill into the vessel a mixture of nearly equilibrium proportions of the three components, although the exact composition of the initial mixture was unimportant. A few trial fillings were necessary in order to indicate the quantity of methyl alcohol to be placed in the bottle, H, so as to give the desired mixture. We endeavoured throughout to work with mixtures of composition such that the total pressure change in an experiment was of the order of three atmospheres or more; the time taken for the attainment of equilibrium then varied with temperature, being some four hours at 290° C. and about half this time at 320° C. It should be pointed out that as equilibrium was approached the rate of pressure change became exceedingly slow, except in the case of experiments at the higher temperatures, and if the experiment were unduly prolonged the operation of side reactions would exert a predominating influence on the pressure change. In one instance, for example, an experiment was continued for 15 hours without the pressure attaining a constant value. That side reactions were taking place was indicated by the subsequent analysis of the gaseous products which were found to contain as much as 10·5 per cent. of methane as compared with the 1 or 2 per cent. normally found.

It was necessary, therefore, to adopt an arbitrary criterion of the attainment of equilibrium, namely, when the rate of pressure rise or fall did not exceed 0·2 atmospheres per hour and this fell within the time limit mentioned above. That the system had then attained a state closely approximating to that of true equilibrium was shown by the fact that the apparent equilibrium constants at any one temperature, whether found by decomposition or by synthesis, were almost identical.

To charge the catalyst vessel the system was first evacuated; a little alcohol was then introduced into the catalyst chamber and the whole again evacuated. The remaining alcohol in the bottle was afterwards rapidly forced into the vessel together with sufficient gas to give the desired pressure, and the inlet valve closed and disconnected from the system.

Analysis of the Equilibrium Mixture.

To find the composition of the equilibrium mixture the permanent gases were first separated from the alcohol by immersing the sampling tube in a bath of petroleum ether, cooled by solid carbon dioxide to a temperature of −65° C. At this temperature the vapour pressure of hydrogen, carbonic oxide and even methane are high, that of carbon dioxide is about 1 atmosphere and that of methyl alcohol less than 0·1 mm. After cooling for 15 minutes a sample of vapour free gases was withdrawn and analysed.

The residual methyl alcohol was collected and quantitatively estimated by first converting it to nitrite and then causing the nitrite to liberate iodine from a potassium iodide solution. The free iodine was estimated by means of a standard sodium thiosulphate solution in the ordinary way.

Catalyst.

For all the experiments described herein a basic zinc chromate catalyst was used; this was prepared by running in a mixer for about an hour, a paste made up in the proportions of ZnO, 3 gram mols, Cr_2O_3, 1 gram mol, and approximately 20 gram mols of water. In addition to the above 0·5 per cent. of copper oxide in the form of copper nitrate was added to the mixture to assist in the reduction of the catalyst by means of hydrogen.

The paste was then extruded from a press through holes of ⅛-inch in diameter, dried and broken into pellets about ¼-inch long. The final reduction with hydrogen was carried out at 300° C.

Calculation of Equilibrium Constant.

Using the static method values for K_p have been determined for five temperatures between 280° C. and 338° C., this being the temperature range most suitable for the synthesis of methyl alcohol with the zinc-chromium catalyst described above. The experimental pressures were, in all cases, in the neighbourhood of 100 atmospheres and equilibrium was approached in each case by synthesis and by decomposition of the liquid component. The results are summarised in Table III. At each temperature two values for the apparent K_p are given, representing the results obtained by working with initial mixtures

Table III.

Reaction temperature °C.	Reaction pressure* atmospheres	Pressures at equilibrium (atmospheres).			K_p.	
		H_2.	CO.	CH_3OH.		
280	84·6	43·5	17·7	16·9	$5·0 \times 10^{-4}$	Decomposition.
	91·9	47·8	17·7	16·3	$4·0 \times 10^{-4}$	Syntheses.
289	99·8	53·6	20·4	18·2	$3·1 \times 10^{-4}$	Decomposition.
	100·4	54·0	19·8	16·2	$2·8 \times 10^{-4}$	Syntheses.
306	98·4	55·8	22·6	10·2	$1·4 \times 10^{-4}$	Decomposition.
	95·8	54·5	19·5	7·2	$1·2 \times 10^{-4}$	Syntheses.
320	96·4	54·5	25·2	5·0	$6·7 \times 10^{-5}$	Decomposition.
	95·8	55·7	24·0	4·8	$6·4 \times 10^{-5}$	Syntheses.
338	99·1	57·7	26·2	3·8	$4·3 \times 10^{-5}$	Decomposition.
	88·4	50·5	21·9	2·6	$4·6 \times 10^{-5}$	Syntheses.

* No attempt has been made to correct these values for deviations from Boyle's Law.

containing, in the one case a greater quantity of methyl alcohol, and in the other a less quantity than the equilibrium proportion. The closeness between the pairs of values is sufficient indication that substantially equilibrium conditions had been reached in all cases. The method of calculating K_p from the experimental observations will perhaps best be understood by giving in detail the results of one experiment. At 289° C. for example the "decomposition" experiment was carried out at an initial pressure of 93·4 atmospheres, rising to 99·8 atmospheres in 235 minutes. The actual pressure-time observations in this and the companion "syntheses" experiment are shown graphically in fig. 4. A sample of 268·1 c.cs. (temp. 20° C.) at the end of this period was analysed as already described with the following results :—

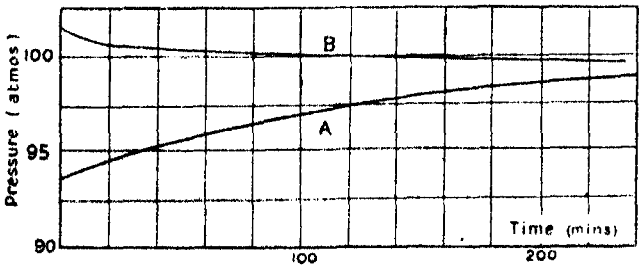

Fig. 4.—A, Decomposition. B, Synthesis.

Permanent Gases (per cent.) :—H_2, 65·8 ; CO, 25·1 ; CH_4, 1·4 ; CO_2, 5·4 ; N_2, 2·3.

Methyl Alcohol = 0·079 gm. The vapour pressure of methyl alcohol at 20° C. = 96 mm. Pressure due to permanent gases = (849 − 96) = 753 mm. Partial pressures in the reaction chamber:—

Hydrogen = $99·8 \times 65·8/122·3 = 53·6$ atmospheres.
Carbonic oxide = $99·8 \times 25·1/122·3 = 20·4$ atmospheres.
Methyl alcohol = $99·8 \times 22·3/122·3 = 18·2$ atmospheres.
$K_p = 18·2 \div (53·6)^2 \times 20·4 = 3·1 \times 10^{-4}$.

B.—*The Intermittent Flow Method.*

In the static method of approaching equilibrium the components of the system are in contact with the catalyst for comparatively long periods of time and the tendency for the occurrence of side reactions is favoured. Whilst the results of analysis indicated that such reactions had not occurred to an appreciable extent it was thought advisable to carry out a number of determinations by a dynamic method in which the time taken for the attainment of equilibrium could be considerably shortened. Briefly, the method adopted consisted in passing a mixture of methyl alcohol, carbonic oxide and hydrogen (in nearly equilibrium proportions) over a catalyst maintained at the desired temperature and determining by analysis the change in composition of the mixture.

By varying the rate of flow from fast to slow, through a series of experiments with a mixture of given composition, it was possible to determine a series of apparent equilibrium constants approaching closer and closer to the true value as the velocity diminished; and further by altering the composition of the initial mixture to approach equilibrium by synthesis or by decomposition.

The general arrangement of apparatus is shown diagrammatically in fig. 5.

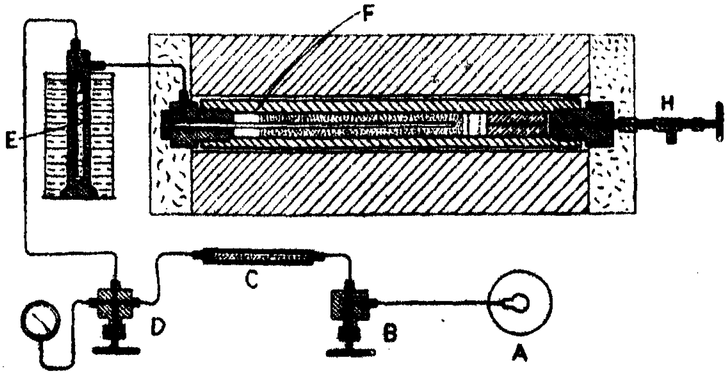

Fig. 5.

The gas cylinder, A, of 100 cubic feet capacity, contained a carbonic oxide-hydrogen mixture ($CO + 2H_2$), compressed to 150 atmospheres. The mixture passed by way of the steel control valve, B, through a calcium chloride drying tube, C, to the valve, D, where it entered the main system. Before entering the catalyst tube the gases were slowly bubbled through pure dry methyl alcohol, contained in a tall glass-lined steel bottle, E, maintained by means of an oil bath at a temperature such that the saturation quantity of alcohol was not far removed from the equilibrium quantity for the temperature and pressure conditions under investigation. By suitably altering the temperature of the oil bath it was a comparatively simple matter to adjust the composition of the initial mixture so that methyl alcohol was in defect or excess according as it was desired to proceed to equilibrium by way of synthesis or of decomposition. The figures for the saturation pressures of methyl alcohol at various temperatures were calculated from the results of Ramsay and Young* and are given in Table IV.

Table IV.—Saturation Vapour Pressure of Methyl Alcohol.

Temperature (°C.)	90	100	110	120	130	140	150	160
Pressure (atmospheres)	2·5	3·4	4·7	6·3	8·2	10·6	13·6	17·1

The saturated gases passed from the bottle, E, through a copper capillary tube directly into the catalyst tube, F. It was necessary to ensure that no condensation of methyl alcohol should occur from the time the gases left the bottle, until they had passed the catalyst and entered the train of absorption bottles which constituted the low pressure end of the system. To this end the capillary tube connecting the saturating bottle to the catalyst tube was wound with resistance wire and electrically heated to a temperature a little above the temperature of the oil bath.

The catalyst tube, F, 30 inches long by 11/2 inches internal diameter, was turned from a forging of Hadfield's ERA/HR steel, the ends being threaded to take connecting plugs made of the same metal. It was held horizontally in an electric furnace and clamped in position by means of two brackets, thus enabling the end plugs to be tightened *in situ*. The furnace was wound with two independent coils, each provided with an adjustable resistance so that a constant temperature could be maintained over the greater part of its length.

A steel pyrometer tube extended almost the full length of the catalyst chamber, the temperature being taken by means of a thermocouple at the point where the gas mixture left the catalyst; both the inside of the catalyst tube and the outside of the pyrometer tube were lined with copper. The catalyst filled the annular space between the catalyst and pyrometer tubes, the last 6 or 8 inches being in the constant temperature zone of the furnace. After leaving the catalyst the gases passed through two copper gauze screens and a small hole drilled axially through a copper plug which completely filled the rest of the tube.

---

* Ramsay and Young, 'Phil. Trans.,' A, vol. 178, p. 313 (1887).

The release valve, H, at the end of the catalyst tube, was specially designed to operate freely at high temperatures without the use of grease or oil. On leaving the high pressure side of the system the gases were first freed from condensable products by passage through glass worms immersed in a freezing mixture; then, after passing through a series of U-tubes packed with calcium chloride, they were collected in a large glass gas holder.

The liquefied products were weighed and the methyl alcohol content obtained by measuring the refractive index. The total volume of gas was measured and its composition ascertained by analysis in the ordinary way.

As it was desired to determine K_p for temperatures between 280° and 320° somewhat low pressures (70 atmospheres or thereabouts) had to be employed in order to obtain quantities of alcohol that could conveniently be handled.

At each selected temperature two series of observations, each involving a number of individual experiments, in which the rate of gas flow was changed progressively, were carried out thus furnishing the data from which the apparent values of the equilibrium constant were calculated.

The method of deriving the true equilibrium constant from the experimental results is best shown by an example. Thus at 295° C. nine experiments at pressures between 60 and 70 atmospheres were carried out, details of which are recorded in Table V. The velocity of gas flow was varied throughout the series from 56 c.cs. per minute to as much as 454 c.cs. per minute. Special interest attaches to the influence of the rate of passage of the gas mixture over the catalyst on the extent of the operation of side reactions, as indicated by the quantities of carbon dioxide and methane found in the gaseous products at the end of an experiment. Thus, for example, in experiment 1, the rate of flow was 435 c.cs. per minute and the residual gases contained 0·8 and 0·6 per cent. of carbon dioxide and methane, respectively. Comparing this result with experiment 3, in which the rate of flow was reduced to 56 c.cs. per minute, the greater time of contact with the catalyst gave rise to an increase in the carbon dioxide and methane contents to 2·1 and 1·3 per cent., respectively.

Even in this extreme case, however, the side reactions only progressed to a

Table V.—Reaction Temperature 295° C.

Experiment No.	Pressure in atmospheres.	Oil bath temperature °C.	Velocity of gas flow mins. per litre.	Weight of liquid product gms.	CH_3OH content of liquid product gms.	Volume of gaseous product c.cs.	Analyses of gaseous products.				Pressures at equilibrium atmospheres.			Apparent K_p.
							CO_2.	CO.	H_2.	CH_4.	CH_3OH.	CO.	H_2.	
1	63·0	97	2·3	0·5921	0·5890	5550	0·8	35·4	61·2	0·6	4·35	20·8	35·9	$1·63 \times 10^{-4}$
2	64·8	97	10·0	0·8068	0·7906	5548	1·6	33·5	61·0	1·2	5·87	19·7	35·9	$2·31 \times 10^{-4}$
3	64·8	97	17·9	0·8199	0·7950	5700	2·1	33·3	61·2	1·3	5·73	19·5	35·9	$2·28 \times 10^{-4}$
4	63·4	101	2·2	0·5920	0·5889	5675	0·9	34·9	61·4	0·6	4·29	20·6	36·3	$1·58 \times 10^{-4}$
5	61·2	144	7·6	1·3816	1·3715	5990	1·8	33·7	61·2	1·0	8·44	17·8	32·2	$4·54 \times 10^{-4}$
6	60·9	144	14·4	1·0978	1·0865	5565	2·2	33·3	61·7	1·1	7·42	17·8	33·0	$3·82 \times 10^{-4}$
7	69·3	114	2·4	0·9664	0·9611	6760	0·8	32·6	62·9	0·7	6·27	20·5	39·6	$2·01 \times 10^{-4}$
8	71·0	114	7·7	1·1296	1·1192	6990	1·6	31·8	62·6	1·1	7·15	20·3	39·9	$2·20 \times 10^{-4}$
9	70·3	114	14·8	1·0207	1·0090	6595	2·0	31·2	63·0	1·0	6·8	19·8	40·0	$2·15 \times 10^{-4}$

Mean true value for K_p at 295° C. = $2·20 \times 10^{-4}$ (see fig. 6).

small extent and from the point of view of equilibrium determinations were quite unimportant.

By plotting the apparent K_p values (obtained by synthesis and by decomposition) and the corresponding rates of gas flow two curves are obtained approaching one another as the rate of flow diminishes and finally meeting at the true equilibrium value. The results of the series at 295° C. are thus shown in fig. 6.

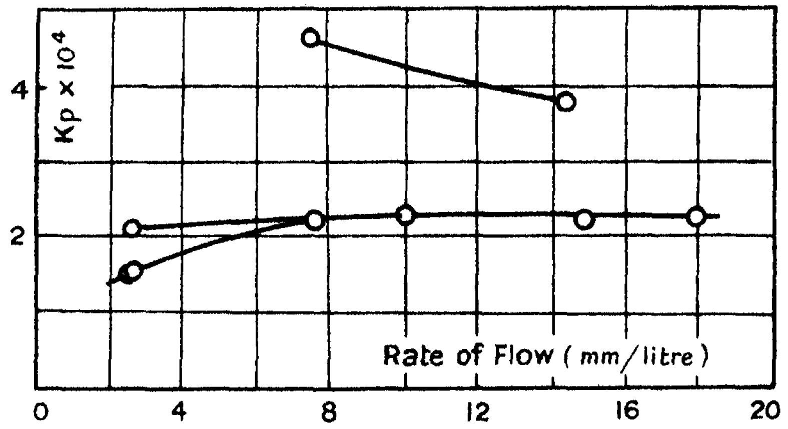

Fig. 6.

Two similar series of experiments have been carried out at 310° and 330° C., particulars of which are given in Table VI.

Table VI.—Reaction Temperature 310° C.

Experiment No.	Pressure in atmospheres.	Oil bath temperature.	Velocity of gas flow mins. per litre.	Pressures at equilibrium.			Apparent K_p.
				CH_3OH.	CO.	H_2.	
10	71·8	154	1·6	8·10	20·0	39·1	$2·66 \times 10^{-4}$
11	71·2	154	3·3	6·77	20·6	39·6	$2·10 \times 10^{-4}$
12	70·8	154	13·0	5·04	21·4	39·5	$1·51 \times 10^{-4}$
13	68·2	107	11·9	4·91	20·3	39·0	$1·60 \times 10^{-4}$
14	67·3	98	3·0	4·41	20·6	38·4	$1·45 \times 10^{-4}$
15	66·6	98	13·7	4·54	20·1	37·2	$1·63 \times 10^{-4}$

Mean true value for K_p at 310° C. = $1·60 \times 10^{-4}$.

Table VI—(continued).—Reaction Temperature 330° C.

Experiment No.	Pressure in atmospheres.	Oil bath temperature.	Velocity of gas flow mins. per litre.	Pressures at equilibrium.			Apparent K_p.
				CH_3OH.	CO.	H_2.	
16	78·0	146	3·1	4·44	20·5	45·6	$1·04 \times 10^{-4}$
17	77·9	146	7·7	3·02	21·6	47·0	$6·33 \times 10^{-4}$
18	77·4	146	12·5	2·63	21·2	46·0	$5·86 \times 10^{-4}$
19	74·4	96	2·0	2·44	22·6	45·1	$5·31 \times 10^{-5}$
20	75·9	96	9·9	2·35	21·5	45·7	$5·26 \times 10^{-5}$
21	75·3	96	18·1	1·99	19·9	45·2	$4·90 \times 10^{-5}$

Mean true value for K_p at 330° C. = $5·2 \times 10^{-5}$.

Discussion of Results.

Using the two independent methods described herein, eight determinations of the equilibrium constant for the system $CH_3OH - CO - H_2$ have been made at temperatures within the range 280–338° C. The values so obtained show fair agreement amongst themselves and, when plotted against the absolute temperature, are found to lie on a smooth curve rising very steeply in the neighbourhood of 290° C. The experimental figures are considerably lower than those obtained by calculation, the differences being best brought out by means of comparative curves as shown in fig. 7. In this connection it

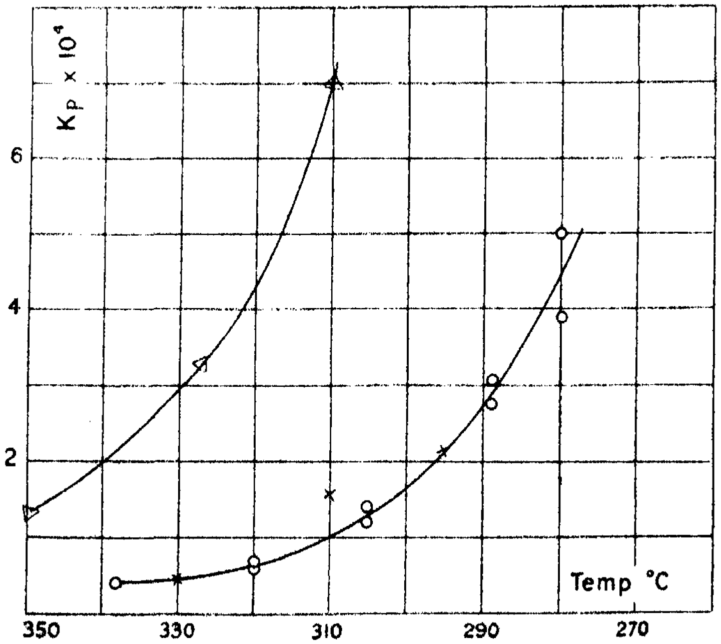

Fig. 7.—○ Static Method. × Dynamic Method. ▲ Calculated from Equation given by Audibert and Raineau.

is also of interest to calculate the yields of methyl alcohol that might be expected on the basis of the K_p values at some definite pressure. Taking 200 atmospheres as a practical working pressure and using for comparative purposes our K_p values and those calculated by Kelley and by Audibert and Raineau the figures given in Table VII are obtained for the composition of the equilibrium mixture at a temperature of 600° C. (abs.).

Table VII. Composition of Equilibrium Mixture at Temperature 600° absolute and Pressure 200 Atmospheres.

——	K_p temperature 600° absolute.	Partial pressure atmospheres.		Hydrogen.
		Methyl alcohol.	Carbonic oxide.	
Audibert and Raineau	$3 \cdot 2 \times 10^{-4}$	83·0	39·0	78·0
Kelley	$3 \cdot 86 \times 10^{-2}$	168·2	10·4	20·8
Author's	$5 \cdot 0 \times 10^{-5}$	36·4	54·6	109·0

A graphical test of the accuracy of the experimental figures is obtained by plotting values of $\ln K_p$ against the reciprocal of the absolute temperature; for since the relation between the free energy ΔF and the absolute temperature T may be taken as linear over a short temperature range, a similar relationship

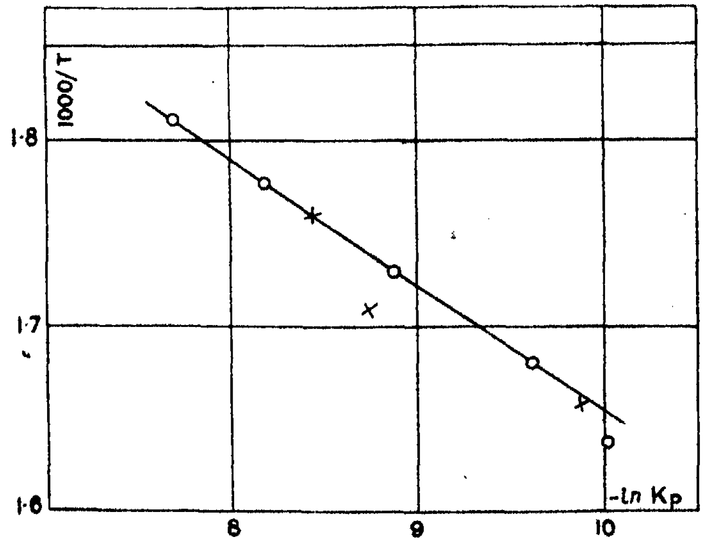

Fig. 8.—○ Static Method. × Dynamic Method.

should hold between $\ln K_p$ and temperature. That this is the case may be seen by reference to fig. 8.

Attention may be drawn to a possible source of error in the results arising from the fact that no corrections have been applied to the observed pressure values for deviations in the behaviour of the components of the system from the Gas Laws. Sufficient data are not at present available to permit of such corrections being applied but experiments are now in progress for determining the compressibility of the equilibrium mixtures at the temperatures and pressures of our experiments.

By using the experimentally obtained values of the equilibrium constant the free energy for the reaction has been calculated at the various temperatures employed, the results being recorded in Table VIII. A linear relation holds between the free energy and the absolute temperature over this range and the results may be represented very closely by the equation

$$\Delta F = 70{\cdot}5\ T - 30{,}500.$$

Table VIII.—Static Method.

°C.	Absolute.	$\frac{1000}{T}$.	$K_p = \frac{P_{CH_3OH}}{P_{CO} \times P_{H_2}^2}$	$-\ln K_p$.	RT.	Free energy ΔF.
280	553	1·81	$4{\cdot}5 \times 10^{-4}$	7·70	1100	8,480
289	562	1·78	$2{\cdot}9 \times 10^{-4}$	8·14	1118	9,100
306	579	1·73	$1{\cdot}3 \times 10^{-4}$	8·91	1150	10,250
320	593	1·68	$6{\cdot}5 \times 10^{-5}$	9·64	1179	11,350
338	611	1·64	$4{\cdot}4 \times 10^{-5}$	10·03	1218	12,230

Dynamic Method.

°C.	Absolute.	$\frac{1000}{T}$.	$K_p = \frac{P_{CH_3OH}}{P_{CO} \times P_{H_2}^2}$	$-\ln K_p$.	RT.	Free energy ΔF.
295	568	1·76	$2{\cdot}2 \times 10^{-4}$	8·42	1129	9,510
310	583	1·71	$1{\cdot}6 \times 10^{-4}$	8·74	1160	10,110
330	603	1·66	$5{\cdot}2 \times 10^{-5}$	9·85	1199	11,800

This equation enables our results to be extrapolated over the entire temperature range at which it is practicable to employ this reaction for the manufacture of methyl alcohol, and in Table IX will be found a series of K_p values for temperature intervals of 20° calculated in this way.

Table IX.—Values of K_p calculated from the Equation $\Delta F = 70 \cdot 5\ T - 30,500$.

Temperature °C.	Absolute.	Free energy ΔF.	K_p.
260	533	7,100	$1 \cdot 2 \times 10^{-3}$
280	553	8,500	$4 \cdot 5 \times 10^{-4}$
300	573	9,900	$1 \cdot 6 \times 10^{-4}$
320	593	11,300	$6 \cdot 7 \times 10^{-5}$
340	613	12,700	$2 \cdot 9 \times 10^{-5}$
360	633	14,100	$1 \cdot 3 \times 10^{-5}$
380	653	15,500	$6 \cdot 3 \times 10^{-6}$

In conclusion our thanks are due to Prof. Bone for his advice and interest throughout the work ; the investigation has been aided by grants made by the Department of Scientific and Industrial Research to the Imperial College for the work and a maintenance allowance from the Department has enabled one of us (B. J. Byrne) to participate in it.

On the Chemical Interaction of Ions and the "Clean Up" of Gases at Glass Surfaces under the Influence of the Electrical Discharge.

By JAMES TAYLOR, D.Sc., Mackinnon Student of the Royal Society.

(Communicated by Sir Joseph J. Thomson, F.R.S.—Received January 1, 1929.)

The Passage of Electrical Currents through the Walls of Electrical Discharge Tubes.

The passage of sodium through glass under the influence of an electrical discharge is well known.* With neon lamps the action is reversible.† These lamps are filled with neon (containing a little helium and hydrogen) at about 10 mms. pressure, and the electrodes are of pure iron.‡ The spectrum is that of neon, helium, and the Balmer series of hydrogen. Carbon monoxide bands are usually not present.

* Warburg, 'Ann. Physik,' vol. 40, p. 1 (1890) ; Burt, 'Phil. Mag.,' vol. 49, p. 1168 (1925) and 'J. Opt. Soc.,' vol. 11, p. 87 (1925) ; Nielsen, 'Phys. Rev.,' vol. 31, p. 304 (1928).

† Taylor, 'J. Sci. Inst.,' vol. 3, p. 400 (1926).

‡ Ryde, 'Photo. J.,' June, 1922.

Such a lamp was immersed in a bath of molten sodium nitrate which was used as negative electrode, and a potential of about 300 volts was maintained between the tube electrodes AB (see fig. 1) and the nitrate. The inside glass wall became covered with negative glow, a current of many milliamperes flowed initially through the glass, but fell off in an almost exponential manner with time to a constant smaller value (see Tables I and II). Rotation of the negative glow around the glass surface, and fatigue effects were strongly in evidence.

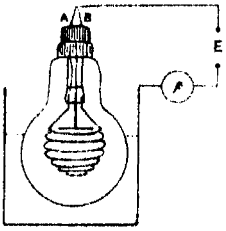

Fig. 1.

Table I.—Voltage 294. $NaNO_3$ temp. 303° C.

Time, secs.	Current, m.a.	Log, current.	Time, secs.	Current, m.a.	Log, current.
0	9	0·95	60	4·5	0·66
5	8	0·9	85	4·0	0·6
18	7	0·84	100	3·5	0·54
30	6	0·78	125	3·0	0·48
40	5	0·7	200	2·2	0·34

This set is very rough because the current fluctuated considerably. It gives the general trend, however.

Table II.—Voltage 320 at beginning and rose to 360 at end of experiment. $NaNO_3$ temp. 340° C.

Time, secs.	Current, m.a.	Log, current.	Time, secs.	Current, m.a.	Log, current.
0	50	1·7	55	11	1·04
5	28	1·45	65	9	0·95
10	25	1·4	75	8	0·9
15	23	1·36	85	8	0·9
20	21	1·32	95	8	0·9
25	19	1·28	105	7	0·84
30	16	1·2	115	7	0·84
35	11·8	1·18	125	5	0·7
40	13	1·11	135	6	0·78
45	13	1·11	145	7	0·84
50	12	1·08	155	5	0·7

Similar results were obtained with other electrolytes, such as heated phosphoric acid, copper sulphate and sodium nitrate solutions, and with conductors such as mercury.

The potential required to strike a discharge was independent of the temperature (60° C. to 400° C. investigated, see Table III) but the current decreased rapidly with decrease of temperature. The currents obtained at the lower temperatures were smaller because the resistance of the glass increased rapidly as the temperature fell. The apparent rise of the striking potential probably arises from this cause. It is obvious from the results that the types of discharges obtained are ordinary glow discharges with the glass acting as cathode, and that they require a definite sparking potential for initiation.

Table III.

Temperature,	Striking potential.	Temperature,	Striking potential.
° C.	volts.	° C	volts.
15	No visible discharge.	220	290
234	290	175	290
290	290	157	294
310	282	134	294
315	290	105	294
285	288	68	296
260	290		

Disappearance of Gas.

After a 5 minutes' run in the manner described above only a very faint trace of the hydrogen lines could be observed in the lamp spectrum. We may conclude that most of the hydrogen had disappeared. With prolonged running the hydrogen lines disappeared completely and the lamp exhibited a strong resonance radiation hood or mantle characteristic of pure neon (a little helium does not affect the conditions). Further discharge brought about an appearance of carbon monoxide bands in the spectrum. On running with reversed polarity these disappeared. The carbon oxides involved may have come from thermal decomposition of, or from some electrical action in, the glass. Experiments showed that whilst oxides of carbon could arise from a thermal decomposition (tube heated without electrical connections) the bulk arose from an electrical action. Other electrolytes and heated mercury yielded similar results.

*Relation between the Gas Disappearance and the Electrical Quantity Transference.**

A tube of the form shown in fig. 2 was constructed of "soda" glass. A was an iron spiral electrode, B a thin-walled bulb (about 0·5 mm. in thickness), and T a side tube connected via a liquid air trap and mercury-operated cut-off, to a high vacuum installation. T was also connected to a sensitive Macleod gauge and a gas-introducing apparatus, etc. The apparatus, up to the cut-off, was entirely of glass, with metal seals. It was thoroughly "baked out." B was immersed in a sodium nitrate bath S, maintained at a suitable temperature. External copper-foil electrodes E_1 and E_2 were fixed upon the tube as shown and could be connected to a Lécher wire system operating on a 7-metre wave oscillator. Fig. 3 gives a diagram of the system. As far as our present purpose is concerned it is unnecessary to go into the details of this experimental arrangement, which has been fully described elsewhere,† it is only necessary to say that by its means, brightly luminous electrodeless discharges may be maintained in the tube, at low potentials (of the order of a 100 volts and less) at a frequency of 4×10^7 cycles per second, at gas pressures from a few millimetres down to one-thousandth of a millimetre and less. Such discharges assured, over a very wide range of pressures, a copious supply of positive ions.

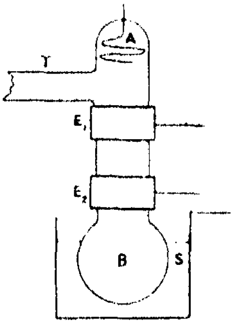

FIG 2.

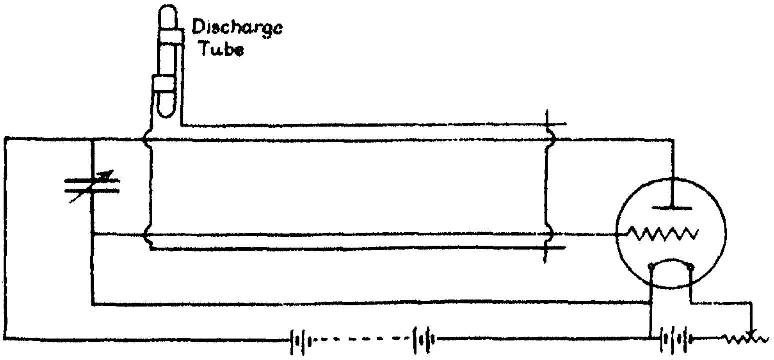

FIG. 3.

---

* 'Nature,' vol. 121, p. 708 (1928).

† 'Proc. Camb. Phil. Soc.,' vol. 24, p. 259 (1928).

The middle point of the Lécher wires system was earthed. Between A and S—S being negative—a chosen constant potential was maintained. S was connected directly to a milliamperemeter and A was earthed. With this disposition, under the action of the electric field between A and B, positive ions were pulled out of the electrodeless discharge into B, and struck the walls with a velocity depending upon the potential of S, and the gas pressure in B. Under such circumstances a current usually traversed the glass walls of B, and in most cases a progressive diminution of the pressure of the gas in the discharge tube—as measured by the sensitive Macleod gauge—took place. We were thus in a position to ascertain whether there was any relation between the quantity of gas disappeared and the quantity of electricity that had passed through the glass walls.

Theory of the Method.

Let Δ be the decrease of gas pressure in millimetres, V the volume of the apparatus in cubic centimetres, and c the number of cubic centimetres of gas at N.T.P. which has disappeared. Then

$$c = \frac{\Delta\, 273 \mathrm{V}}{760\,(273 + t_0)}, \qquad (1)$$

where t_0 is the temperature of the apparatus. Since, in the experiments to be described, part of the apparatus is at liquid air temperature, the effective temperature of the apparatus is unknown. The liquid air trap, however, usually causes a reduction of pressure of the order of 10 per cent. Now, if the whole apparatus were considered as being at air temperature, namely, from 15 to 20° C., the factor $273/(273 + t_0)$ by which the amount of gas disappeared at air temperature must be multiplied to obtain the quantity at 0° C. involves about a 10 per cent. reduction. This reduction is already effected by the liquid air trap, the factor was consequently neglected, which is equivalent to assuming that the effective temperature of the apparatus was 0° C. The cooling effect of the trap may explain partially, in addition, why the disappearances appear to be less than those calculated from the quantity of electricity that has been transferred.

Further, if Q is the total number of coulombs that have passed through the glass walls, and e is the electronic charge ($1 \cdot 59 \times 10^{-19}$ coulombs), then, assuming for the case of hydrogen that H disappears for every electronic charge transferred, we have the number of H atoms disappeared given by Q/e, and if n is the number of gas molecules per cubic centimetre at N.T.P. ($2 \cdot 7 \times 10^{19}$) this represents a volume of hydrogen gas given by

$$v = \frac{Q}{2en} \text{ c.cs. at N.T.P.} \tag{2}$$

Very similar equations would hold for other gases.

Experiments with Hydrogen.

Some preliminary experiments were carried out in hydrogen without freezing out the residual mercury vapour by liquid air. Under such circumstances, notwithstanding its low pressure, the mercury contributed the dominant characteristics to the luminous phenomena of the discharge, and at the same time only relatively small currents traversed the glass. When the mercury vapour was frozen out, the current through the glass increased about 10-fold and the electrodeless discharge exhibited the appearance characteristic of hydrogen.

The cubical contents of the apparatus were determined by measurement as 623 c.cs. Hydrogen was introduced to a pressure of $3 \cdot 67 \times 10^{-3}$ mms. A voltage of 500 was maintained between A and S (fig. 2).

A progressive diminution of the gas pressure occurred and concomitantly the current through the glass diminished. A set of results is shown in Table IV. We find from the data that assuming one hydrogen atom disappears for every electron transferred through the glass, $22 \cdot 7 \times 10^{-3}$ c.cs. of gas at N.T.P. should have disappeared, whereas actually 41×10^{-3} c.cs. disappeared. From these figures we may reasonably conclude that H_2 disappeared for every electronic charge transferred. A further experiment at $2 \cdot 5$ mms. confirmed these results. On the strength of these figures it might be assumed that H_2 invariably disappears for every electronic charge transferred. Further work showed that such was not the case. For example, at the beginning of a run

Table IV.—Temperature of $NaNO_3 = 400°$ C. 500 volts.

Pressure, $\times 10^{-3}$ mms.	Time, mins.	Current, m.a.
56·7	0	0·5
44	1	0·4
33·3	3	<0·4
26	5	0·3
18·3	7	<0·3
11	9	0·27
7·3	11, 15	0·1

Total number of coulombs passed = 0·1956.

with hydrogen, H_2 frequently disappeared for every electronic charge passed, but with continued running H disappeared for every electron transferred. The disappearance of gas appears to be dependent on the previous treatment of the glass, but the laws it follows are certainly of a nature similar if not identical with the Faraday laws of electrolysis. Summarising we may say that, within the limits of experimental error, the quantity of hydrogen disappearing is directly proportional to the quantity of electricity transferred across the glass walls.

Experiments with Oxygen.

Similar experiments were carried out in oxygen. Table V shows the result of an experiment. From this experiment we would conclude that in the case of oxygen the quantity of gas disappearing is directly proportional to the quantity of electricity transferred and that every two electron charges passed involves the disappearance of one oxygen atom. This is precisely what we might expect from a consideration of the divalent nature of oxygen, but again the results are not always the same. The disappearance depends upon the condition of the glass walls, cases were observed, for example, after prolonged runs with hydrogen, when a discharge in oxygen brought about a disappearance of more oxygen than corresponded to the rate of O per two electronic charges, in other cases when the tube had been run for a considerable time with oxygen a disappearance of only O per four electronic charges was observed. Nevertheless, it was found that the quantity of gas disappeared was directly proportional to the quantity of electricity transferred.

Table V.—Temperature of $NaNO_3$ = 330° C. 500 volts.

Pressure, $\times 10^{-3}$ mms.	Time, mins.	Current, m.a.	Pressure, $\times 10^{-3}$ mms.	Time, mins.	Current, m.a.
127·5	0	2·6	—	12	1·4
105·15	2	—	37·3	13	1·3
—	4	2·0	25	16	1·2
—	7	1·9	—	17	1·2
—	8	1·7	Current became small and variable.		
54·7	9	1·6	14·3	19	—
—	11	1·5			

Number of coulombs passed in first 16 minutes = 1·665.
Volume of gas if O^+ is carrier = 0·19 c.cs.
Actual disappearance = 0·084 c.cs.

Experiments with Nitrogen.

Table VI gives a result obtained for nitrogen. The conclusions drawn from the experiments were that in some cases N disappeared for every two electronic charges transferred, in others for every three electronic charges. The results were not, however, very satisfactory.

Table VI.—Temperature of $NaNO_3 = 325°$ C. 500 volts.

Pressure, $\times 10^{-3}$ mms.	Time, mins.	Current, m.a.	Pressure, $\times 10^{-3}$ mms.	Time, mins.	Current, m.a.
108·5	0	0·2	101	11	0·11
106	2	0·19	99·9	15	0·095
—	4	0·18	98·5	18	0·1
104	5	0·16	97	25	0·1
103	8	0·13			

Number of coulombs passed = 0·19.
Volume of gas if N^+ is carrier = 0·022 c.cs.
Actual disappearance = 0·01 c.cs.

Experiments with Helium.

A series of experiments were carried out in a similar type of apparatus to that described above, but the helium was continuously purified by means of charcoal contained in a quartz tube immersed in liquid air. No progressive disappearance of the gas was observed either in the electrodeless discharge alone or when a current was passed through the glass walls. A set of results is given in Table VII.

Table VII.—Temperature of $NaNO_3 = 330°$ C. 520–530 volts.

Pressure, $\times 10^{-3}$ mms.	Time, mins.	Current, m.a.	Pressure, $\times 10^{-3}$ mms.	Time, mins.	Current, m.a.
119	0	0·1	118–118·5	30	0·1
118·5	5	0·1	119·5	50	0·1
118	10	0·1	119·5	60	0·1
118	20	0·1			

It is to be observed that a current does flow through the glass, and that this current is of the same order of magnitude as those obtained with other gases. Thus we see that it is not necessary for there to be a disappearance of gas in order that a current may be obtained.

It should be pointed out that in the above experiments the apparatus was thoroughly "baked out" initially and run with an electrodeless discharge before the actual readings were taken.

The Conductivity of Glass and Quartz.

A thin glass bulb filled with mercury was used. The bulb was sealed on to a long glass tube so that when the mercury was heated and evaporated it refluxed back into the bulb. The bulb was immersed in a bath of sodium nitrate and the conductivity of the glass was examined, using the mercury as one electrode, the nitrate as the other. Relatively large currents traversed the glass at potentials of the order of 100 volts, when the mercury was of positive or of negative sign. Table VIII illustrates the results. When the mercury was anode the current fell off with time to small values, when it was cathode the decrease of current with time was not so marked. Whilst the current flowed, small local arcs struck between the glass and the mercury were frequently observable. The glass often cracked when such currents had flowed for a few minutes.

Table VIII.—Temperature of $NaNO_3$ = 335° C. Voltage on open circuit 450.

Time, secs.	Current, m.a.	Time, secs.	Current, m.a.
0	100	60	40
10	80	70	36
20	70	80	33
30	60	90	30
40	50	Tube broke.	

The conductivity of a small fused-silica bulb was investigated in a similar manner. It was found that a small current—teens of microamperes—could be passed in either direction through the walls.

From these experiments it is evident that the glass walls themselves conducted at the temperatures employed; the currents were much in excess of those obtained when the inner electrode was provided by a gaseous discharge.

The question of the conductivity of glass and quartz is one which has received a considerable amount of attention.* The general conclusions to be drawn from the older work are that the conduction is largely electrolytic in nature. In quartz the conductivity appears to be due to sodium in the form of Na_2SiO_3 which is present as an impurity, or, in the case of the above experiment, may be formed by the action of the nitrate upon the silica.

---

* See *e.g.*, Mellor, 'A Comprehensive Treatise on Chemistry,' vol. 6, p. 265.

In some recent work Milligan and Ferguson have investigated the conduction of soda-lime glass using mercury or carbon as anode.[*] Between 300 and 400° C. the current decreased to a small value as the electrolysis continued. This was shown to be due to a counter E.M.F. and to a high resistance layer set up. These counter E.M.Fs. were almost equal to the applied voltages.

Whilst the present work was in progress a paper has appeared by Selenyi[†] upon the electrolytic disintegration of glass. In his experiments an ordinary metal filament lamp was immersed in a bath of saltpetre at 200 to 250° C. He showed that if the nitrate was employed as cathode, then a badly conducting layer of silicic acid was formed on the inside of the bulb (anode), and oxygen was set free. Sodium was liberated at the cathode.

The Diffusion of Gases through Glass and Quartz.

In seeking an explanation of the disappearance of gas under the action of the electrical discharge an attractive possibility is that the action is a diffusion of the gas ions through the glass walls. On this hypothesis the diffusion would be increased by the high temperature of the walls and the fact that the ions are accelerated by the electric field.

Hydrogen, and to a less extent, oxygen and nitrogen are known to pass through quartz and glass at high temperatures.[‡] Furthermore, helium and the rare gases also possess the property of diffusing through silica glass. Indeed, Williams and Ferguson have shown that at 500° C. helium diffuses through at a rate 22 times that of hydrogen.[§]

In a recent publication[||] Steacie and Johnson have given reasons for supposing that the diffusion of hydrogen and helium through quartz is a simple mechanical diffusion.

We shall be compelled to reject the theory for our work, not only because, as will appear in the sequel, there is no definite evidence that the gas can be collected at the opposite side of the glass wall, but because the experiments showed conclusively that no progressive disappearance of helium took place.

---

[*] Milligan and Ferguson, 'Roy. Soc. Canada Trans.,' vol. 21, p. 263 (1927).

[†] 'Ann. Physik,' vol. 84, p. 111 (1927).

[‡] Mellor, *tom. cit.*, p. 274.

[§] 'J. Am. Chem. Soc.,' vol. 44, p. 2160 (1922), and vol. 46, p. 635 (1924).

[||] 'Roy. Soc. Proc.,' A, vol. 117, p. 662 (1928).

Experiments as to the Mechanism.

A tube with a thin glass partition G, as shown in fig. 4, was utilised. The whole apparatus was thoroughly " baked out " for many hours. There was a covering of mercury above the partition in order to make an electrical contact, and an iron-electrode wire connected to the seal-in C, dipped into it. Electric potential of the required magnitude could thus be set up across the electrodes A and C. It was determined initially by filling the bottom vessel V_1, with hydrogen at 0·3 mm. pressure, that there was no diffusion across the partition into the top vessel V_2, which was at high vacuum.

When the partition was heated by means of the small electrical furnace F there was only a very small increase of pressure with continued running—several bars—and this was certainly not greater than what occurred in the absence of hydrogen in V_1. Consequently, if there was any diffusion of hydrogen across the diaphragm it was exceedingly small in amount.

By means of the furnace F, the glass around the partition was heated to 225° C. (the mercury refluxed back) and a voltage of 600 was applied between A and G (A anode) whilst an electrodeless discharge was maintained between E_1 and E_2. Initially a current of 0·2 m.a. flowed across the glass partition; this fell off in about 10 minutes to a fairly constant value of 0·07 m.a. The hydrogen in the bottom vessel progressively disappeared and it was calculated that if it had been transferred across the partition there would have been an increase of 60×10^{-3} mms. Actually the increase was only 5×10^{-3} mms. At most 2×10^{-3} mms. of this amount could have come from the heating effect of the walls. We must conclude that the greater part of the gas had not been transferred across the partition, and that it had either been taken up in the glass walls or fixed in some other way.

The apparatus depicted in fig. 4 was found not to be entirely satisfactory and was replaced by one of the form shown in fig. 5. The figure is self explanatory. In principle the apparatus was the same as that previously used with the exception that the positive ions were projected into a thin-walled bulb B, immersed in mercury. With this disposition it was found that there was not only a hydrogen discharge in B (where the residual mercury vapour was frozen out by liquid air) but there was also a strong mercury vapour discharge in V, where the mercury was refluxing back. It was found that this latter discharge was able to clear up hydrogen itself, so that the non-appearance of gas which had disappeared from B was not a definite proof that it had not been transferred through the glass.

We can say however that, so far as the experiments go, there was no evidence that the gas which disappeared was transferred through the glass by diffusion or any other process.

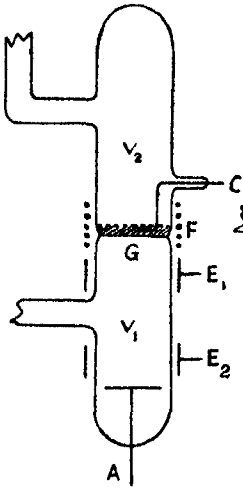

Fig. 4.

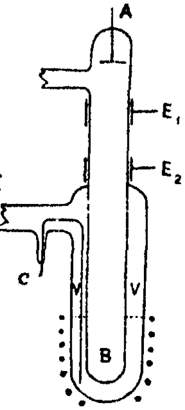

Fig. 5.

Experiments on Silica Gel.

Some experiments were carried out to see whether the "clean up" was of the nature of an occlusion of gas in the glass arising from the ions being driven with high velocity into the surface. In principle the method consisted in partly filling the bulb of the apparatus shown in fig. 2 with silica gel. The tube was "baked out" and the silica gel activated in the normal way.

The "clean up" of hydrogen was examined as before and it was found that the disappearance was not more than would have occurred in the absence of the gel. The enormous increase of surface upon which occlusion of ions was permitted was unproductive of any modification in the clean up. It is improbable then that the action is a surface occlusion. That the silica gel was suitable for occlusion purposes was proved by its large activity when cooled in liquid air.

Relative Magnitudes of the "Clean Ups" in the Electrodeless Discharge and in Glass Conduction.

We must now consider the question of the relative "clean ups" in the electrodeless discharge alone and in the combined action of the electrodeless discharge and the direct current discharge through the glass walls.

A tube of the form shown in fig. 2 was utilised. It was " baked out " and washed out several times with pure hydrogen whilst still in the furnace, and was filled when cold with 65×10^{-3} mms. of hydrogen.

A preliminary determination showed that the effect of putting liquid air on the trap was to reduce the pressure in the apparatus to about 87 per cent. of its original value. This furnishes a correction for the cooling effect.

The " clean up " due to the electrodeless discharge alone, the whole apparatus being at room temperature, was examined (with no liquid air trap so that the residual mercury vapour was not frozen out). The results are given in Table IX.

Table IX.—Clean up in Electrodeless Discharge alone. Apparatus at air temperature, no liquid air on trap.

Time, mins.	Pressure, $\times 10^{-3}$ mms.	Time, mins.	Pressure, $\times 10^{-3}$ mms.
0	65	8	66
0·5	65	11	67
1	63·5	14	68·5
3	63·5	19	70
5	65	25	71·5

Discharge cut off. Liquid air put on trap, $63 \cdot 5 \times 10^{-3}$ mms. = pressure.
Pressure change factor 88·6 per cent.
Liquid air taken off, 72×10^{-3} mms. = pressure.
Liquid air put on, $63 \cdot 5 \times 10^{-3}$ mms. = pressure.

A slow increase of pressure occurred after the first minute or two. Further, at the end of the run, putting on the liquid air brought about 11·4 per cent. reduction of the pressure. This is only about 1 per cent. in excess of the normal reduction value so that, apparently, no condensible products had been formed under the action of the discharge. It is most probable that hydrogen, which had been absorbed in the " baked out " walls, had been brought out under the action of the discharge. Indeed, it is well known that mercury vapour in a discharge has a strong tendency to bring out hydrogen from glass walls.

In immediate continuation the " clean up " was investigated with the liquid air trap functioning. The results are given in Table X. A slow but steady initial decrease of gas pressure occurred; the rate of diminution fell off with time and finally an almost constant pressure was attained. Analyzing the results we find that the " clean up " in the discharge with liquid air on the trap, had decreased the gas pressure to 89·6 per cent. of its value at the beginning of the run. Nevertheless, the pressure measured when the liquid air was

Table X.—Clean up in Electrodeless Discharge alone. Liquid air on trap. Pressure without liquid air 72 × 10^{-3} mms.

Time, mins.	Pressure, × 10^{-3} mms.	
0	63·5	Total pressure change factor with liquid air =89·6 per cent. Total do. without liquid air = 100 per cent.
1	62·5	
2·5	60·5	
4	59·5	
6	58·5	
8	57·5	
10	57·5	
13	57·5	
17	57	
26	57·5	Pressure change factor = 80·4 per cent.
	57	
Liquid air taken off	71·5	
Liquid air on	57·5	Pressure change factor = 84·6 per cent.
Liquid air off and apparatus allowed to stand for 1 hour	67·5	
Liquid air on	57	

removed from the trap was almost identical with that before the run (Table X). The inference is that, under the influence of the discharge, with liquid air on the trap, about 10 per cent. of the gas was transformed into a product that condensed out in the trap. Furthermore, this product was capable of repeated recondensations, and, as the results show, occupied exactly the same volume at air temperature as the hydrogen it had arisen from. Its time of life was long—over an hour at least, and other experiments showed it longer—and it could be absorbed gradually into the walls of the apparatus—the natural decrease of pressure of the apparatus with time showed this. These results remind us strikingly of those of Mierdel.* The natural inference is, of course, that the product was water vapour, and that a hydrogen molecule disappeared because it had united with an oxygen atom to form water, which in the unsaturated state would occupy the same volume as the hydrogen which had been "cleaned up." This is the most natural and unforced explanation of the phenomena. The oxygen comes from the glass walls by a mechanism which will be presently discussed.

In direct continuation, the "clean up" under the influence of the electrodeless discharge with the liquid air trap functioning and the bulb B immersed in molten sodium nitrate, but with no current flowing across the glass walls due to an impressed constant difference of potential between A and S, was then examined (Table XI). Apart from the initial small increase of pressure, no progressive "clean up" was obtained.

---

* 'Ann. Physik,' vol. 85, p. 612 (1928).

Table XI.—Temperature of $NaNO_3$ = 340° C. Liquid Air on Trap.

Time, mins.	Pressure, $\times 10^{-3}$ mms.	Time, mins.	Pressure, $\times 10^{-3}$ mms.
0	57	8	58·5
0·5	59	12	58
2	58·5	20	58·5
4	58·5		

A potential of about 400 volts was then put between A and S—S being negative—and the gas disappearance was investigated (Table XII). The "clean up" was great, and we may conclude without further consideration that the "clean up" in the electrodeless discharge alone is negligible relative to that brought about by the action of a constant potential across the glass walls.

Table XII.—Temperature of $NaNO_3$ = 340° C. Liquid Air on Trap. 400 volts.

Time, mins.	Pressure, $\times 10^{-3}$ mms.	Current, m.a.	Time, mins.	Pressure, $\times 10^{-3}$ mms.	Current, m.a.
0	58·5	9	6	—	2
1	51	8	7	30·5	1·7
2·5	43	6	9	27·7	0·7
4·5	36·5	2·5	11	25	0·9

Discharge cut off.
Liquid air off, 53·5 $\times 10^{-3}$ mms. = pressure.
Liquid air on, 26 $\times 10^{-3}$ mms. = pressure.
Liquid air off 0·5 hours, 45 $\times 10^{-3}$ mms. = pressure.
Liquid air on, 25 $\times 10^{-3}$ mms. = pressure.

In the results given in Table XII the condensible product is once more encountered—a product of long life which can be taken up in time by the "baked out" walls. It is, in our view, water vapour.

Further experiments showed that condensible products were formed in the case of oxygen and nitrogen. The results were similar to those for hydrogen though differing in details.

It was considered that it would be of interest to subject these condensible products to a spectroscopic examination.

Spectroscopic Examination of the Condensible Products formed under the Action of the Electric Discharge.

Initially, for purposes of comparison, spectrograms of electrodeless discharges in hydrogen, oxygen, nitrogen, carbon dioxide, water vapour and air were taken, at pressures of 2 mms. and less, both with liquid air on the traps (after a preliminary discharge had been passed through the vapour to decompose it) and without.

The spectrograms were taken photographically on a Hilger constant deviation spectrometer.

Condensible products were then formed in the way described above and for the various gases and dispositions of electrical arrangements. In order to examine the product that condensed out in an experiment, the whole apparatus was exhausted after a run, whilst the liquid air traps still functioned. After the apparatus had been thoroughly evacuated and closed, the liquid air trap was removed and the spectrogram of the condensible product was taken. The liquid air trap was again put on after this run, and the spectrum of any products formed by the action of the discharge was taken.

In the case of hydrogen it was found that after a discharge was passed for some time through the condensible product then, on again putting on the liquid air trap, part of the gas was not recondensible, but became condensible after continued discharge. In all cases the spectrogram of the condensible product was identical with the standard spectrum for water at low pressure (in both cases the carbon dioxide bands were in evidence), and the spectrogram of the part of the gas that was not recondensible after running the discharge was identical with the non-condensible product formed after running a discharge in water vapour, and further, both of these latter were almost identical with that given by hydrogen. There can be little doubt then but that the condensible product formed from hydrogen is water which partially breaks up to form hydrogen and oxygen under the influence of the discharge when there is no liquid air trap in the apparatus.

With oxygen a condensible product was formed, and this product yielded an exactly similar spectrogram to that obtained from a discharge in carbon dioxide (sometimes there were also weak hydrogen lines in the spectrum, but there was no evidence that any considerable portion of the condensible product was water).

The results on nitrogen have not yet been fully worked out.

The question now arises as to the origin of the water and carbon dioxide.

A Theory of the Clean Up. General Hypothesis of Electrolysis.

In proposing a theory of the foregoing results upon "clean up" we shall start from the experimental fact that glass must be regarded as having many of the properties of an electrolyte. Thus we must consider that at the surface of the glass walls, especially when the glass is heated, there is a certain concentration of positive and negative ions derived from the constituents of the glass and probably mainly from Na_2SiO_3. This being so, we must allow that whenever a gas ion from the discharge impinges against the glass surface there is a probability of chemical interaction occurring between the gas ion and a suitable ion of the glassy electrolyte. Chemical interaction will proceed until polarisation layers of sufficient magnitude as to repel the gas ions are set up or until the available ions in the glass surface are used up. If, however, electrical leakage across the glass takes place or if the conduction is encouraged and augmented by setting up a suitable electric field across the glass walls, as in the present experiments, then electrolytic conduction will occur and the chemical action may be sustained by the migration of ions to the inner surface and by the electrolytic decomposition products arising there. The chemical products so formed may be frozen out from the discharge by liquid air, they may be absorbed at or combined into the structure of the walls, or they may simply disintegrate.

In the simplest picture glass is to be regarded as a solution containing Na_2SiO_3 as electrolyte. For every two electronic charges transferred across the glass 2Na is liberated at the cathode. The SiO_3 radical at the anode breaks down into SiO_2 and O, which unites in the case of hydrogen discharges with one hydrogen molecule to form one molecule of water.

This simple picture may represent some of the facts, but it does not explain, for example, why under certain conditions H_2 disappears for every electronic charge, and why oxygen disappears even more readily than hydrogen. We must consider then that glass is a complex electrolytic solution probably containing peroxides (until they are reduced by continued discharge with hydrogen) and certainly containing compounds of carbon which produce chemical reactions with the gas ions impinging against the glass surface.

We could dwell for some considerable time on the possible applications of such a theory, but it seems more profitable to leave it in its present broad outline until such time as further work along similar lines has been accomplished.

Summary.

The paper describes experiments on the disappearance of gas in the electric discharge. The type of discharge tube used is shown in fig. 2, p. 255. It was of "soda glass." A was an iron electrode (spiral), B a thin-walled bulb (about 0·5 mm. in thickness) and T a sidetube connected via a liquid air trap and mercury-operated cut-off to a high vacuum installation, Macleod gauge, and gas introducing apparatus. B could be immersed in sodium nitrate baths maintained at a suitable temperature. External copper-foil electrodes E_1 and E_2 were fixed upon the tube and could be connected to a 7-metre-wave oscillator, which provided brightly luminous electrodeless discharges at low potentials (100 volts and less) at gas pressures from a few millimetres down to one-thousandth of a millimetre and less. Such discharges assured, over a wide range of pressures, a copious supply of positive ions. If a potential of suitable magnitude was maintained between A and S—S being negative—positive ions were drawn down into the bulb B and impinged on the glass walls. A current usually traversed the walls and the gas progressively disappeared. The relation between the gas disappearance and the quantity of electricity that had passed through the glass walls was investigated for hydrogen, oxygen, nitrogen and helium. For all the gases except helium it was found that the quantity of gas that disappeared was directly proportional to the quantity of electricity transferred across the glass walls. It was dependent on the previous treatment of the glass, but the laws it followed were of a nature similar if not identical with Faraday's laws of electrolysis.

In the case of hydrogen, H_2 frequently disappeared for every electronic charge passed. With continued running H disappeared for every electronic charge transferred.

With oxygen the disappearance was also dependent on the condition of the tube; usually every two electronic charges passed involved the disappearance of one oxygen atom, but in some cases O disappeared for every four electronic charges.

With nitrogen, in certain cases N disappeared for every two electronic charges, in other cases for every three charges. The results were not, however, very satisfactory.

No progressive disappearance of helium gas was observed.

There was no evidence that the disappearance of gas was due to a diffusion through the glass walls, or to occlusion arising from the ions being driven with high velocity into the surface.

Further experiments were carried out on the nature of the disappearance both in simple electrodeless discharge and in discharges with currents traversing the glass walls. It was found that concomitantly with the disappearance of gas, products were formed which were condensed out in the liquid air traps. Spectrograms of these products were taken and compared with standard spectrograms. Volumetric measurements were also made.

It was shown that the hydrogen which disappeared was changed into water, which condensed out in the liquid air trap or was absorbed in the glass walls. Oxygen was converted into carbon dioxide which is also condensible.

A tentative theory of the phenomena is given. Glass must be regarded as an electrolyte—in the simplest picture as a solution of Na_2SiO_3. On electrolysis this yields 2Na at the cathode and $SiO_2 + O$ at the anode, or inner surface of the glass. The oxygen ion unites with two of the hydrogen ions which impinge upon the glass surface, and a molecule of water is formed. This simple picture is incorrect and glass must be regarded as a complex electrolyte, probably containing peroxides and certainly containing carbon compounds. The ions of the glassy electrolyte interact with gaseous ions impinging on the glass surface to form chemical compounds.

My thanks are due to Sir Joseph J. Thomson for his continued interest in the work and for his many helpful suggestions, to the Armstrong College Research Board Committee for a grant for some of the apparatus, and to Dr. W. Taylor for his frequent discussions on the problems.

Some Experiments on Vacuum Distillation.

By C. R. Burch, B.A., Metropolitan-Vickers Company.

(Communicated by Sir Ernest Rutherford, P.R.S.—Received January 29, 1929.)

Summary.

Crude petroleum and various petroleum derivatives have been distilled under conditions practically equivalent to evaporation into a perfect vacuum. Derivatives of very high molecular weight can be fractionated in this way without detectable decomposition. Decomposition ("cracking") sets in quite suddenly, at temperatures varying from 307° to 340° C. for the oils tried.

Greases and oils can be produced having exceedingly low vapour pressures at room temperature: the former permit the free use of ground joints in high-vacuum systems (10^{-6} mm.): the latter can replace mercury in condensation pumps, and the liquid-air trap is then unnecessary in many cases, *e.g.*, the exhaustion of thermionic valves.

Introduction.

The present work represents an attempt to apply modern vacuum technique to the fractional distillation of organic substances in general, and, in particular, to the fractionation of petroleum and its derivatives.

It is not difficult to reduce the pressure in a laboratory still to a value so low that the residual gas has substantially no influence on the performance of the apparatus; this condition is reached when distillate vapour molecules collide more frequently with the walls of the still than with molecules of residual gas. In fact, little advantage can be gained by reducing the residual gas pressure in a laboratory still below the comparatively high value of 1 microbar, and a reduction in the temperature at which substances can be distilled with reasonable speed can only be effected by a modification of the shape of the still. If a cold condensing surface is placed a very short distance above the surface of the liquid to be distilled, so that a vapour molecule will in general make no collision during its passage to the condensing surface, the highest conceivable speed of distillation is reached for a given evaporating area. This arrangement was first adopted by Bronsted and Hevesy to separate the isotopes of mercury, the distillate being frozen on the condensing surface.

It was not known whether organic liquids could be evaporatively distilled in this way; distillation in conventional apparatus at reduced pressure often takes place with explosive ebullition and it is difficult to prevent froth being carried over into the condenser—indeed, some workers find it necessary to allow a small stream of air to bubble through the liquid undergoing distillation, in order to avoid frothing. When the condensing surface is placed close to the evaporating liquid this expedient cannot be adopted, as the bursting bubbles would splash on to the condensing surface. Accordingly an apparatus was set up in which the behaviour of organic substances heated *in vacuo* could be determined.

The Evaporative Still.

The still in its final form embodies some special constructional details which experience had shown to be advisable. These features are illustrated in fig. 1.

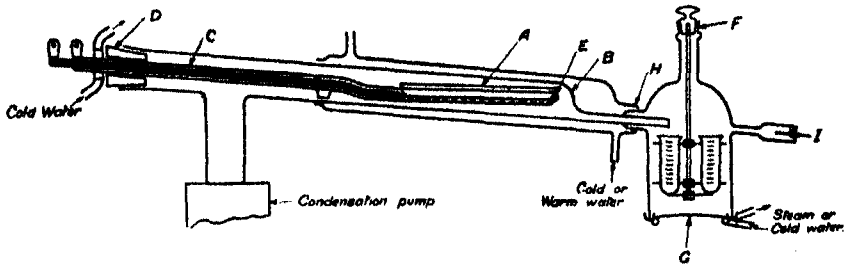

Fig. 1.

A copper evaporating tray, A, 16 cm. long, 2·5 cm. wide, and 1·1 cm. deep, provided with an electric heater in a false bottom, is supported horizontally inside a 4 cm. diameter water-jacketed glass condensing tube B, which is evacuated by a mercury condensation pump.

The false bottom, containing the heater, is silver soldered on to the tray, and is connected to the atmosphere by the pipe C, which supports the tray, so that no vapour molecule can come into contact with the heater element itself. This pipe, which contains one heater lead and is itself the other, is water-cooled immediately outside the rubber bung at D, through which leads (not shown) are brought out from a thermojunction silver soldered to the tray at E. (If a thermometer is placed in the tray trouble is experienced from bubbling, presumably due to local superheating underneath the bulb. Heater elements in the tray produce the same effect.) The lower end of the condensing tube B is sealed into a receiver chamber containing six graduated receiving tubes in a cage which can be rotated by the ground joint F. The bottom of the receiver chamber is closed by a wax joint to a metal plate, G, which can be steam heated or water cooled to break or set the joint. It was necessary to seal the condensing tube into the receiver chamber with a re-entrant seal, and to arrange the end of the water jacket in the special manner shown at H so that the spout inside the receiver chamber should assume as nearly as possible the temperature of the condensing tube. Before this was done high melting point condensates frequently set in the spout, even with the condensing tube at 100° C.

An electrode is sealed in at I; the condensation pump, the evaporating tray and the plate G are connected to earth.

The apparatus was constructed, as far as possible, with a view to fractionation. It possesses the disadvantage that the distillate from only 30 c.c. of liquid is spread over 200 cm.^2 of condensing surface, parts of which are almost horizontal; that the condensate—which is often fairly viscous—is compelled to flow through 10 cm. of "tail-pipe" and that there is a temperature difference of about 10° C. between the two ends of the tray, when this is at 300° C. It is also inconvenient to clean. The temperature gradient along the tray could be reduced by making the tray bottom thicker, though it would have been necessary to employ a larger condensing tube. But it is difficult to see how the other troubles could be removed if the essential features are maintained. The distance between evaporating liquid and condensing surface must be kept short; it must be possible to see the evaporating liquid and to keep high melting point condensates liquid as far as the receiver, and finally the apparatus must be capable of construction.

It was assumed that the condensation pump would leave no gas other than mercury vapour in the condensing tube, and that the pressure of the mercury vapour present would be the saturation pressure corresponding to the temperature of the water jacket of the pump, *i.e.*, about 1 microbar. Assuming that the effective diameter of the distillate molecule is the same as that of the mercury molecule, the mean free path of a distillate molecule in the mercury vapour present will be about 4 cm. As the average distance from the surface of the evaporating liquid to the condensing surface is 2 cm., the probability that a given distillate molecule will not collide with a mercury molecule in its passage to the condensing surface is $\epsilon^{-\frac{1}{2}}$, or about 0·6.

Of the 40 per cent. of distillate molecules which collide with mercury molecules, less than half will return towards the evaporating tray, and more than half will proceed towards the condensing surface, for assuming elastic sphere collisions, all directions with respect to the centre of gravity of the colliding molecules are equally probable after collision, and the centre of gravity is, on the average, moving towards the condensing surface.

Further collisions are more likely to prevent returning molecules reaching the evaporating tray than to prevent those which have been but slightly deflected by collisions from reaching the condensing surface; since there is persistence of velocity after collision the returning molecules must, in general, have a lower velocity, and therefore a slightly shorter free path than those which still move towards the condensing surface after collision. A precise calculation of the effect of the mercury vapour presents considerable difficulty, even if we simplify the problem by assuming that the evaporating and condensing surfaces are infinite parallel planes; moreover, we can only conjecture the effective diameter of the distillate molecule. However, it is clear that the fraction of the distillate molecules which are returned to the tray by collisions with the mercury vapour will be of the order of $\frac{1}{2}(1 - \varepsilon^{-\frac{1}{2}})$, that is, the mercury vapour reduces the speed of the still by about 20 per cent.

It is therefore quite unnecessary to place a cold trap between the condensation pump and the still, and it might even be undesirable to do so, for traces of very volatile hydrocarbons may be present in the liquid undergoing distillation, and these might be only partly condensed by the cold trap. It is thus conceivable that the presence of a cold trap could result in a higher permanent-gas pressure in the still, during the later part of a distillation, when it is especially desirable that the pressure be low.

The Removal of Gas.

All the substances distilled in this apparatus contained considerable amounts of dissolved gas, which formed bubbles and froth as the pressure was decreased. It was therefore necessary to reduce the pressure in stages, waiting until the bubbles produced by each slight reduction of pressure had burst, before a further reduction was made, and even with the less viscous oils it took many hours to evacuate the apparatus, with 30 c.c. of cold oil in the tray, without at any time producing bubbles large enough to splash the condensing surface on bursting. The outgassing process could be accelerated considerably by heating the tray (reducing the surface tension and viscosity of the oil so that the bubbles burst more readily) and in general outgassing was carried out at temperatures sufficiently high to permit its completion in 1 hour, during which time it was necessary to keep a continual watch over the bubbles in the tray, unless one was already familiar with the behaviour of the substance which was being outgassed. During the early part of the outgassing period the bubbles burst, but towards its close they grow to perhaps 1 cm. diameter and then shrink to zero without bursting. Bubbles of this type seem to be associated with the removal of gas other than air, for they do not often occur until the discharge produced by a small induction coil in the fore-vacuum of the condensation pump has changed from the rose-pink due to air, to blue or white—the pressure being from 10 to 100 microbars. In general, a mist of condensate is visible on the condensing tube towards the end of the outgassing period—outgassing at temperatures sufficiently low to prevent this proves an almost impossible task.

When the pressure has been reduced to about 50 microbars and bursting bubbles have ceased to form, the condensation pump may be safely started; in the present apparatus the tray temperature then rises about 10° C. without any change in power input to the heater.

Outgassing is not necessarily complete as soon as bubbling has ceased, and it was found that the rate of rise of temperature consequent on reduction of pressure on starting the condensation pump, formed the highest safe rate of heating for most of the oils tried. If appreciable distillation did not occur by the time the new thermal equilibrium had been reached, it was usually safe to raise the temperature two degrees per minute. In nearly all cases outgassing could be considered complete, as far as concerns risk of splashing the condensing tube, when the first few drops of distillate had run into the receiver. Regarding the degree of vacuum obtained in the still, during most distillations an induction coil giving a 1·8 cm. spark between points produced no discharge at the electrode in the receiver chamber (the point of highest permanent gas pressure in the still). When fuel oil was being distilled the discharge could not be extinguished at the still electrode until a late stage in the distillation, but this oil is known to contain some quite volatile constituents, and is not to be regarded as suitable for distilling in a vacuum-still without some preliminary reduced pressure treatment.

That the condensation pump should regularly attain the degree of vacuum necessary to prevent a visible discharge at the still electrode is perhaps not a result that could have been expected with any confidence, when one remembers that distillate vapour, at its saturation pressure at the temperature of the condensing tube, flows into the pump at the rate of several litres per second, and that this vapour may contain substances of all degrees of volatility—may contain traces, in fact, of practically any aliphatic hydrocarbon. It might be argued that there will always be present some hydrocarbon, the saturation pressure of whose vapour is considerably in excess of that of mercury at the temperature of the waterjacket of the condensation pump, but less than the residual gas pressure maintained by the fore-vacuum pumps (10–20 microbars). Such a substance might be expected to remain in the condensation pump, distil with the mercury, and be re-introduced into the low pressure side. One might argue, on these lines, that ultimately the condensation pump would be without influence on the vacuum obtained. Volatile substances of this type are certainly present, for a trap in the fore-vacuum, cooled by carbon dioxide snow in acetone, collected several cubic centimetres of a colourless mobile liquid of empyreumatic odour during a distillation of fuel oil, nevertheless, even when this trap was not used the discharge at the still electrode was extinguished at a late period during the distillation. It may be that these volatile substances combine with the P_2O_5 used as drying agent in the fore-vacuum, and indeed the P_2O_5 usually changes colour, becoming brown or red. It may be that they dissolve in the oil in the backing pumps, and are evaporated in the rough pump where the oil is constantly agitated in air. It may even be that they decompose in the condensation pump and are removed as gas, though, as will be seen later, organic bodies can operate satisfactorily in condensation pumps.

After six months' frequent use, the condensation pump shows no sign of deterioration in performance, although it generates gas internally when running, for the fore-vacuum is invariably worse when it is running, whether there is any liquid in the still or not. This effect started shortly after the apparatus was brought into use, and has not increased with time. If the pump is used continuously for many hours, gas generation decreases; possibly it is connected with oxidation of organic matter in the pump when this is left open to atmosphere.

The Process of Distillation.

The distillation process by which organic substances are normally separated, whether at atmospheric or reduced pressure, is essentially a process of equilibrant distillation; that is, the vapour immediately above the surface of the liquid in the still can exist in equilibrium with the surface layer of liquid, at the given density and temperature. The composition of the distillate depends on the temperature, but (apart from secondary effects) not on the speed of distillation, and thus temperature can be adopted as a criterion of composition in repeated fractionation. In the present process of evaporative distillation temperature is not, *per se*, a criterion of composition; it must be considered in conjunction with speed of distillation. If the evaporating liquid is a chemical individual, the rate of evaporation will be $\rho\bar{c}/4$ gm. per square centimetre per second, where ρ is the density of saturated vapour at the given temperature, and $\bar{c}$ is the mean molecular velocity. If the liquid is not an individual the rate of evaporation of the rth constituent will be $\rho_r\bar{c}_r/4$ where ρ_r is the density of the rth component in equilibrant vapour, and $\bar{c}_r$ its mean molecular velocity.

Thus, whereas the separation obtained in an equilibrant distillation depends on ρ_r, that obtained in an evaporative distillation depends on $\rho_r\bar{c}_r$. Since $\bar{c}_r$ is inversely proportional to the square root of the molecular weight, and ρ_r is in general greatest for the constituent of least molecular weight, we may generally expect an improved separation, so that the process of evaporative distillation possesses for the organic chemist a double importance. It is the only method by which substances of very high molecular weight can be distilled without any decomposition, and it is a method by which it may be possible to circumvent the stumbling block of constant boiling mixtures.

The present still has an evaporating area of 40 cm.^{2}; if then a chemical individual of molecular weight M is distilled at a temperature T° abs. corresponding to a saturation pressure P microbars, the rate of evaporation will be $0 \cdot 382\sqrt{M}\sqrt{273/T}\,.\,P$ grams per hour.

Assuming 100° C. and $M = 360$, we shall get $6 \cdot 22$ P grams per hour, and supposing a density of $0 \cdot 8$ and 30 drops per cubic centimetre, we can expect roughly 4 P drops per minute.

Calculations indicate that if the present still is run at a temperature such that the saturation pressure of distillate vapour does not exceed 2 microbars, a fraction not exceeding 20 per cent. of the distillate molecules may be returned to the tray, in a manner which favours the return of the lighter constituents, by distillate-distillate conditions, and an equal fraction may be returned by collisions with mercury molecules; these collisions are not detrimental to fractionation. Re-evaporation from the condensing surface will provide a negligible return.

This reasoning led to the choice of 10 drops per minute (say, 20 c.c. per hour) as a maximum speed desirable in fractionations. Most oils remained perfectly quiescent in the evaporating tray at this speed, and, indeed, 60 drops per minute has been achieved with quiescence with several oils, after suitable outgassing. In some cases it was necessary to use speeds lower than 10 drops per minute, otherwise small bubbles formed. These bubbles did not burst, but expanded to 3 or 4 mm. diameter and then shrank to zero. This phenomenon occurred with crude petroleum and with certain very thick oils which had been obtained as residues in an atmospheric pressure 320° C. distillation, assisted with superheated steam. The shrinking bubbles do not seem to be due to decomposition, but rather to the slowness of diffusion of the more volatile constituents from the bottom layers in the tray to the surface. Traces of quite light constituents may remain in the lower layers until the temperature is so high that they can form bubbles. These rise to the surface and expand but before they can burst the light oil vapour which they contain either dissolves in the top layers, which are *ex hypothesi* free from light oil, or else dissolves in the oil film constituting the bubble, and as quickly distills off from the outside. The phenomenon was also found with comparatively thin oils, if the outgassing operation was carried out near room temperature, and it was troublesome when a "hard asphalt" (bitumen) was being distilled. The best procedure with substances which give this trouble is to outgas with the tray so hot that an appreciable part of the total distillate comes over when the condensation pump is started, without a further increase of temperature.

The bubbles produced by decomposition behave in a quite different manner. They burst without shrinking, and they occur indiscriminately all over the tray—whereas the shrinking bubbles usually tend to arise from one or more small zones at the sides or corners of the tray—probably where there is a minute speck of dust or foreign matter. Almost as soon as the first few decomposition bubbles occur, it is found that a discharge can be produced at the electrode in the receiver chamber. It is not possible, even were it desirable, to continue the distillation after decomposition has started, as if the temperature is increased by more than a few degrees, the decomposition bubbles become sufficiently violent to splash the condensing surface—the decomposition temperature is in fact very well marked.

The Products of Evaporative Distillation.

In order to form some idea of whether the evaporative still permitted any really large reduction in the temperature at which distillation can be carried out, trials were made on a certain oil which is produced by filtration from the residue obtained when a Pennsylvanian petroleum is distilled at 320° C. at atmospheric pressure, the distillation being assisted with superheated steam. A slight cracking takes place during this distillation.

This residue-oil was outgassed at 100° C. A faint mist of condensate appeared at 112° C. and the first drop was obtained in the receiver at 165° C. Distillation proceeded at 6 drops per minute (*i.e.*, roughly 1·5 microbars saturation pressure) until 250° C. when the receiver was changed, and then at from 5 to 3 drops per minute until 314° C., when the first evidence of decomposition was seen in the form of minute bursting bubbles. Distillation was at once stopped.

I am indebted to Mr. C. H. Barton for measurements (by a cryoscopic method) of the mean molecular weights of these products, which follow together with the yields.

	Yield.	Mean molecular weight.	Appearance.
	Per cent.		
Fraction 112–350° C.	55	498	Transparent ; orange red ; evidence of wax crystals.
,, 250–314° C.	25	801	Transparent ; red with green " bloom."
Residue 314° C.	20	1550	Opaque ; green.

It was clear that the method is one of considerable power and application.

Residue oils obtained from other varieties of crude petroleum by steam-assisted distillation were also examined, and distillate yields varying from 66 per cent. to 90 per cent. were obtained with no detectable trace of decomposition. In one case, a black residue oil, produced from a Pennsylvanian crude by distillation at atmospheric pressure assisted by superheated steam, the 315° C. distillate (66 per cent.) was red paste, while the residue was practically as fluid as the original oil. A pale wax could be obtained from the distillate by pressing between filter papers. These residue oils all possess a characteristic smell ; the distillates and residues obtained in the evaporative still were odourless shortly after production, but developed a smell similar to that of the original oils on exposure to air and light.

Crude petroleum (less kerosene and petrol fractions) was examined. It was necessary to reduce the speed of distillation to about 2 drops per minute to avoid bubbling—presumably because of the great viscosity of the crude. Distillates were obtained corresponding to those got by distilling with superheated steam at 25 mm. (the partial pressure of the oil vapour being about 1 mm.) ; the evaporative distillates were, however, much lighter in colour, and did not darken appreciably on exposure to air and light for some weeks. The temperatures employed were 100°–150° lower than those used in the steam-assisted method ; it was also possible to carry the distillation further, for the 340° C. steam-assisted residue—" hard asphalt "—yielded without decomposition 30 per cent. of a very thick odourless red oil, between 223° and 307°. An exceedingly brittle pitch was left in the tray.

Attention was then devoted to fractional distillation, and temperature-yield curves were obtained for various substances. Some of the distillates were very viscous, and it was found that a layer comprising several cubic centimetres could accumulate on the surface of the condensing tube, if this was run cold, and variations in the speed of delivery of distillate into the receiver lagged many minutes behind the corresponding variations in tray temperature, consequently one could make only the vaguest estimate of the actual speed of distillation at the moment the receiver was changed. It was, therefore, necessary to run the condenser as hot as vacuum considerations permitted, and a preliminary experiment was necessary in each case, to find how hot the condenser could be run without causing a discharge at the electrode in the receiver chamber, and to find, by cooling and re-heating the condenser several times during the distillation, how cold it could be run without unduly restraining the flow of condensate. If a distilling speed of 10 drops per minute was maintained, it was not always possible to obtain a reasonably free flow of condensate, with no discharge at the still electrode. In such cases one had to be content with condensing so hot as to permit an appreciable re-evaporation. In fact, when common paraffin wax was distilled, the condensing tube being kept just hot enough to keep the condensate liquid as far as the end of the tail-pipe, a thin film of solid condensate formed over the whole of the inside of the receiver chamber. It is not easy to keep the distillate dropping at a steady rate into the receiver, and a record of temperature, distilling speed, and voltage applied to the heater during a preliminary trial is of great assistance. With this aid, the speed can be kept constant to ± 10 per cent.

Fig. 2 shows temperature-yield curves of various substances, the speed being approximately 10 drops per minute. In view of the above limitations it will be realised that these curves are essentially only rough approximations.

The oils to which fig. 2 refers are :—

A. " Lubricating oil " fraction from thick fuel oil produced by the steam-assisted method, between 300° and 360° C., at 25 mm. pressure.
B. " Cylinder oil " fraction produced from A by the steam-assisted method, at 345° C.
C. B, after treatment with absorbent earth.
D. " Heavy machine oil " fraction produced from A by the steam-assisted method at 335° C'
E. Petroleum jelly.
F. An oil used in the rotary backing pumps of the apparatus.
G. Common paraffin wax. Freezing range of first 21 per cent. of distillate, 42–37° C. ; last 16 per cent., 61–56·5° C.

In the production of the oils A–D by the steam-assisted method, slight decomposition occurs. There was no detectable decomposition in the distillations represented in fig. 2.

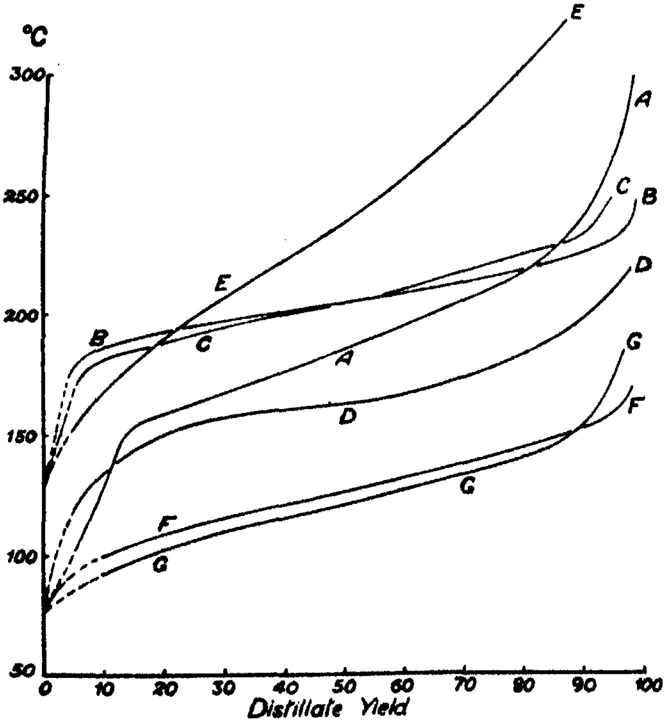

FIG. 2.

With the present evaporative still intensive repeated fractionation is almost out of the question, owing to the small capacity of the apparatus, and the high losses incidental to pouring quantities of the order of 5 c.c. from vessel to vessel, and the losses incurred in cleaning the condensing tube. But a continuously operating evaporative still could be constructed on these lines to handle larger quantities. The outgassing difficulty disappears as the liquid can be continuously outgassed in a separate vessel, and difficulties due to the slowness of diffusion diminish, as much thinner layers of liquid could be employed on the evaporating trays. With such an apparatus intensive fractionation should be a process not much more tedious than intensive fractional equilibrant distillation as practised at the present day.

If these experiments had only indicated a way in which new organic separations might be made, their performance would have been amply justified, but they have also demonstrated the existence of compounds with remarkable physical properties, two of which will now be described.

Organic Substances and High Vacua.

When petroleum jelly is distilled in the evaporative still the residue at 320° C., amounting to about 13 per cent. of the original jelly, is a substance not unlike common vacuum grease. If the tray in the still described is maintained at 320° C.—just below the decomposition temperature—the rate of distillation soon falls to about 3 drops per minute, that is, the saturation pressure of the vapour of this substance is rather less than 1 microbar at 320° C. One would naturally expect a negligible vapour pressure at room temperature. Mr. J. D. Cockcroft has had experiments carried out at the Cavendish Laboratory on the vapour pressure of this substance. An evaporation method was used, the condensing surface being cooled by liquid air. The method was not sufficiently delicate to measure the vapour pressure of this grease, but it showed that the vapour pressure was less than 10^{-3} microbars at 70° C. With the aid of this grease, then, ground joints can be employed freely in highly evacuated systems. It is probable that all the 320° evaporative still residues would have vapour pressures of this order of magnitude at room temperature.

The fact that oils exist which can be distilled without decomposition and which have vapour pressures as low as 1 microbar at 100° C. suggested that it should be possible to run a condensation pump on an oil with a vapour pressure at room temperature negligible compared with that of mercury, and thus to obtain vacua of perhaps 10^{-3} microbars without using a liquid air or carbon dioxide snow trap.

The experiment was tried with the residue obtained at 118° C., distilling speed 10 drops per minute, from the oil F. A single stage metal condensation pump was used, which had been designed for a fore-vacuum of 10–20 microbars. This was waxed on to a short length of 35 mm. glass tube, to which there was sealed a small triode such as is used in wireless reception. This triode was tested for softness by the reverse grid current method, and it soon became apparent that the ratio obtained of anode current to reverse grid current depended almost entirely on the outgassing accorded to the electrodes and the bulb. To provide a more severe test of the capabilities of the pump a low power transmitting triode (by Mullard, type 0/150) which had been open to atmosphere for two years, was sealed on to the pump, with a 1·3 cm. diameter piecing tube 30 cm. long. It was not convenient to oven the bulb of this triode; however, after the anode had been bombarded for a few hours, the following readings were obtained:—

Anode voltage.	Anode current (milliamps.).	Grid voltage.	Grid current (microamps.).	Anode dissipation.	Anode Current / Grid Current.
				watts	
3000	71·2	−20	−2·6	214	27,400
2500	48	−20	−0·5	120	96,000
1770	23·7	−20	− <0·2	32	>118,000

One end of the filament was taken as the zero of voltage; the filament was lit from a 10 volt RMS 50 cycle supply.

The electrode dimensions of the triode are approximately:—

Anode—Length 3·8 cm., diameter 3·4 cm.

Grid—Length 4·5 cm., diameter 1·0 cm., 6·3 turns/centimetre of 0·25 mm. wire.

Filament—Tungsten, 0·015 cm. diameter hairpin, 3·8 cm. long.

We can deduce a rough value for gas pressure in the triode in the following way. The ratio reverse grid current/anode current gives the expectation of ion production by an electron moving from filament to anode. This expectation is proportional to the gas pressure, and is dependent on the velocity of the electron. Lenard and Becker give a table ("Handbuch der Experimental Physik," vol. 14, p. 253, published by Wein and Harms) showing the expectation for electrons of various velocities, passing through 1 cm. of air at atmospheric pressure. The expectation falls from a maximum of 7700 (at a velocity corresponding to 148 volts) to about 2000 at a velocity corresponding to 1770 volts. When the varying speed of the electrons as they pass from filament to anode is taken into account with the aid of this table, it is found that the actual expectation of ions is about 0·465 times the expectation if the electrons all had the most favourable velocity across the whole of the inter-electrode space. Not all electrons traverse the same distance from filament to anode, since the filament is a loop, and not a single central wire. However, if we suppose that the distance traversed is the grid-anode distance (1·2 cm.), we shall obtain an upper limit to the pressure. Since the expectation of ion production was less than 1/118000, and 0·465 × 7700 ions are expected per centimetre-atmosphere, the pressure was

$$\frac{1}{[> 1{\cdot}2] \times 0{\cdot}465 \times 7700 \times [> 118000]} \text{ atmosphere,}$$

or

$$< 2 \times 10^{-3} \text{ dynes/cm.}^2.$$

It is not surprising that the pressure should increase about four times when the anode dissipation is raised to 214 watts, as this dissipation is excessive for the 0/150 triode. In fact, with 250 watts dissipation, the anode melted locally. The relatively slight increase of pressure which occurred with the more moderate dissipation of 120 watts seems to indicate that the degree of vacuum obtained was limited by gas evolution from the electrodes and bulb, but whether the limiting pressure was fixed by gas evolution from the triode or the wax joint, or by the finite vapour pressure of the oil, it was clear that the operation of a condensation pump on oil was more than an experimental *tour-de-force*, and should form a useful addition to the technique of the production of high vacua.

Messrs. J. D. Cockcroft and T. E. Allibone had confirmatory experiments carried out at the Cavendish Laboratory, in which ionisation gauges were evacuated to 10^{-3} dynes/cm.^{2} without ovening the glasswork. The speed of the pump was measured by a McLeod gauge and a calibrated leak. At 1 dyne/cm.^{2} the speed was rather greater than 2000 c.c./sec.; at higher pressures it was limited by the speed of the fore-vacuum pumps. Mr. Allibone found it possible to exhaust a discharge-tube, fitted with a metal window after the manner of Lenard, to a degree sufficient for the application of 300 kilovolts. The author attempted to measure the ultimate pressure attainable by an oil condensation pump, with an ionisation gauge. The whole of the glasswork was ovened, and after the electrodes had been bombarded, no ionisation current could be detected with the instruments available, although the ionisation current corresponding to 10^{-4} dynes/cm.^{2} could have been detected.

Conclusions.

The method of evaporative distillation can be applied to the derivatives of petroleum, and it enables distillations to be made which cannot otherwise be accomplished without decomposition. An elementary kind of fractionation is possible, and though intensive fractionation would need special apparatus, this would present no real difficulty. Petroleum derivatives of exceedingly low vapour pressure can be prepared, and some of these increase considerably the scope of the condensation pump.

In conclusion, the author wishes to express his thanks to Mr. J. D. Cockcroft, to Mr. T. E. Allibone and to Mr. C. H. Barton and Shell Mex, Ltd., who kindly supplied the petroleum products for this investigation; and to the Metropolitan-Vickers Electrical Company for permission to publish the work.

Further Experiments on the Combustion of Well-dried Carbon Monoxide and Oxygen Mixtures.—Part III.

By William A. Bone, D.Sc., F.R.S., Frank R. Weston, Ph.D., D.I.C., and Dennis A. Winter, Ph.D., D.I.C.

(Received December 21, 1928.)

[Plates 15, 16.]

In Part I of this series,* which was communicated to the Society in January, 1926, it was shown (*inter alia*) that a 6-months P_2O_5-dried $2CO_2 + O_2$ mixture, made up from highly purified ingredients, could be exploded at atmospheric pressure in a cylindrical bulb of about 100 c.c. capacity by a minimum condenser discharge spark of about 0·77 m.f. at 970 volts between platinum "balled" electrodes, although less energetic sparks had failed entirely to effect any (even local) ignition.

Since that time, the experiments have been continued with a view to determining the effect (if any) of a still more prolonged P_2O_5-drying upon the ignitibility and the "minimum spark energy" required for the ignition of such $2CO + O_2$ mixtures and the present paper summarises the results thereof.

Experimental.

Seeing that the methods and arrangements employed for (i) preparing the gases, (ii) drying and mixing them in their proper combining proportions, (iii) cleaning and drying out the explosion bulbs, (iv) introducing into them a sufficient quantity of redistilled and highly purified phosphoric anhydride and then slowly filling them at just below atmospheric pressure with the previously "well-dried" gaseous mixture, (v) sealing them up, and subsequently continuing the P_2O_5-drying *in situ*, and (vi) finally sparking and exploding the so-purified and dried mixtures, were the same as formerly (the only difference being the now greater duration of the "drying-period"), there is no need for us to recount them here, the reader being referred to our previous paper for all such details. We would, however, direct special attention to one or two points of interest in connection therewith.

(1) *Purity of the Carbonic Oxide Used.*—The carbonic oxide was prepared by dropping pure re-distilled formic acid into pure re-distilled sulphuric acid

---

* 'Roy. Soc. Proc.,' A, vol. 110, p. 615 (1926).

in a glass flask (for sketch of apparatus see Part I, p. 625, fig. 3) warmed so as to give a slow steady gas-evolution. Both of the acids used were quite arsenic-free. The gas evolved was slowly passed in succession through suitable vessels containing (i) a strong solution of potassium hydroxide, (ii) ignited calcium chloride, and (iii) re-distilled and purified phosphoric anhydride.

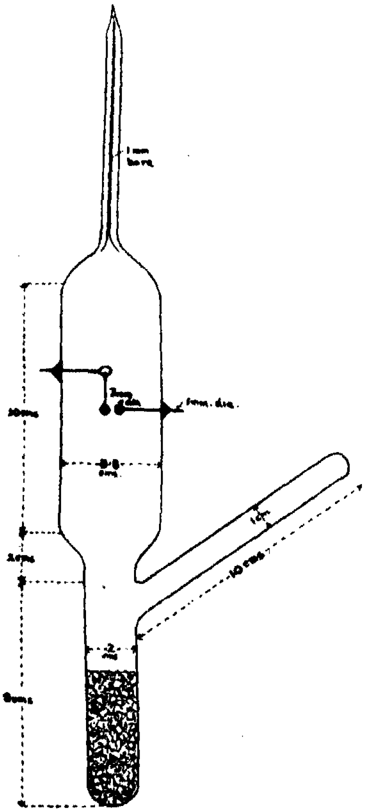

On twenty different occasions during the progress of this investigation we have tested the purity of the gas so prepared by exploding it with a measured excess of oxygen, and determining the ratio of the resulting contraction (C) to the volume of the carbon dioxide (A) formed, which theoretically should be 0·500 exactly, although in practice there is a tendency for it to come out (if anything) slightly higher. The values actually obtained all fell between 0·496 and 0·507, with a mean of 0·5013. On six occasions it came out 0·500 exactly, on six more between 0·498 and 0·502, while on only two occasions did the deviation from the theoretical ratio exceed ± 0·005, which we regard as well within the possible experimental error.

To ensure, however, that the gas so prepared and used by us was really hydrogen-free, we reduced 60 c.c. of it to 5 c.c. over an ammoniacal solution of cuprous chloride—the effect of which treatment would be to increase 12-fold the concentration of any trace of hydrogen present—but, after washing the residual gas with dilute sulphuric acid and analysing it, we obtained :—

$$C = 18 \cdot 9, \quad A = 37 \cdot 7 \quad \text{and} \quad C/A = 0 \cdot 501,$$

proving that the gas actually used in our experiments was quite free from hydrogen.

(2) *Electrical "glowing-out" of the Electrodes of the Explosion Vessels.*—The explosion vessels were cylindrical bulbs (capacity about 100 c.c.) made out of "high-resistance" glass as hard in quality as could safely be used for sealing-in

the platinium electrode. And, especially in view of certain remarks made in 'Nature' about a year ago by Prof. H. E. Armstrong, we would particularly direct attention to the fact that, during the elaborate ritual (*q.v.*) involved in preparing these bulbs for the reception of the already well-dried $2CO + O_2$ mixtures and the re-distilled and purified phosphoric anhydride for completing the drying, *the electrodes always had been glowed out repeatedly in a high vacuum for many hours (at least 20 in all), so as to remove from them any occluded hydrogen. And in the experiments now to be described the additional precaution was taken of electrically "glowing-out" the electrodes in oxygen at low pressure, as well as in a high vacuum, both of which operations were continued many hours.*

(3) *The Drying Period.*—In these further experiments, this extended over between 550 and 1000 days, instead of the 170 to 220 days as formerly. During this period the bulbs were kept in a cupboard, the lower limb of each vessel being frequently tapped so as to expose a fresh P_2O_5-surface to the gaseous mixture. Also, once a fortnight (except during long vacations) all parts of each vessel down to the side tube were thoroughly heated to at least 175° C. by means of specially designed electric heaters applied externally, in order to disperse and get rid of any possible "moisture film" adhering to the inner walls, care being taken to screen the P_2O_5 in the lower limb from the effects of the heat. In each and every case, the phosphoric anhydride maintained unimpaired its pristine "dry" powdery condition throughout the whole of the long drying period.

Explosions of the P_2O_5-*dried* $2CO + O_2$ *Mixtures.*

In order to preserve the continuity of these with the former four similar experiments of the series, they will be referred to by numbers from 5 onwards.

No. 5.—In this case the original mixture used contained $CO = 66\cdot8$, $O_2 = 32\cdot7$ and $N_2 = 0\cdot5$ per cent., and the drying period had extended over 555 days. Finally on November 10, 1927, a condenser discharge-spark of capacity 0·5 m.f. at 1000 volts was passed through the mixture without any visible result. Twenty-four hours later (*i.e.*, on November 11, 1927) in the presence of Prof. H. B. Dixon a discharge spark of capacity 1·0 m.f. at 1000 volts ($\Sigma = 0\cdot5$ Joule) was passed, resulting in an instant explosion, a brilliant flame filling the vessel, as was proved photographically, the percentage combustion being 87·8. This result, it should be noted, does not differ materially from those obtained in our previous similar experiments with 6-months P_2O_5-dried $2CO + O_2$ mixtures.

No. 6.—In this case the original mixture contained $CO = 66\cdot1$, $O_2 = 33\cdot6$

and $N_2 = 0 \cdot 3$ per cent., and the drying-period extended altogether over 758 days. Eventually on February 7, 1928 (after about 740 days)—the tube being mounted as shown in the photograph No. 1 (Plate 15)—a condenser discharge spark of 0·25 m.f. at 1000 volts was passed through the mixture without any visible results. Ten days later a similar spark—this time of 0·5 m.f. at 1000 volts—was again passed through it, but with no visible result. A photograph taken at the time (see Plate 15, No. 2) merely showed a sharp image of the spark without any " blur " or " halo " whatever around it, indicating that no combustion had occurred outside its path. Finally, another week later, *i.e.*, on February 24, 1928, in the presence of Prof. W. T. David, Dr. W. E. Garner and others, a third condenser discharge spark—this time of 1·0 m.f. at 1000 volts—was passed through the mixture, resulting in an instant explosion, a bright flame filling the whole vessel (as will be seen from the photograph No. 3 of the explosion reproduced in Plate 15), the percentage combustion being 89·25. Hence it appears that the further prolongation of the drying from 555 to 758 days had no measurable further restricting influence upon the ignitibility and combustibility of the gaseous medium.

No. 7.—The original mixture in this case contained $CO = 66 \cdot 0$, $O_2 = 33 \cdot 0$ and $N_2 = 1 \cdot 0$ per cent., and the drying period extended over 995 days. The platinum electrodes in the explosion bulb had " pointed " instead of " balled " ends as in previous cases. On October 22, 1928, after 987 days drying, a condenser discharge spark of 0·25 m.f. at 1000 volts was passed through the gaseous mixture without any visible results; but subsequently on October 30, 1928, when a condenser discharge spark of double the previous intensity (namely of 0·5 m.f. at 1000 volts) was passed through the mixture, an explosion instantly ensued, the flame filling the whole of the vessel, including its side arm, and some of the phosphoric anhydride in the bottom part being thrown up as far as the electrodes. The two photographs, Nos. 4 and 5 (Plate 16), taken of the middle part of the explosion vessel during and immediately after the explosion, respectively, show (i) how the flame had filled the vessel, and (ii) how finely divided phosphoric anhydride was thrown up on to the electrodes by the explosion. The percentage combustion during the explosion was 86·7.

No. 8.—The " dried " mixture originally filled into the bulb contained $CO = 60 \cdot 2$, $O_2 = 35 \cdot 3$, and $N_2 = 4 \cdot 5$, or rather less of the " combustible " than previously; also the filling pressure was less than usual, being only 688·6 mm. instead of the usual 735 to 745 mm. The " drying period " extended over 1005 days altogether. On the 1000th day (December 6, 1928) a condenser

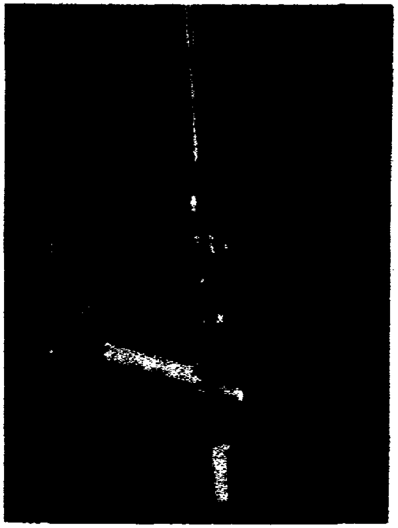

No. 1. Explosion bulb No. 6 in position for the firing trials.

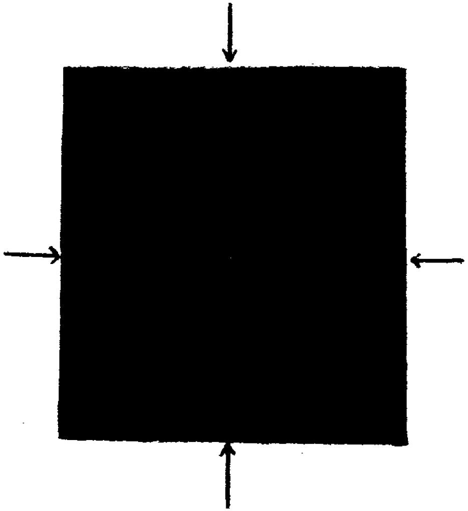

No. 2. Showing the non-effect of condenser discharge-spark 0·5 mf. at 1000 volts in No. 6 bulb. (The spark is the white dot at the centre.)

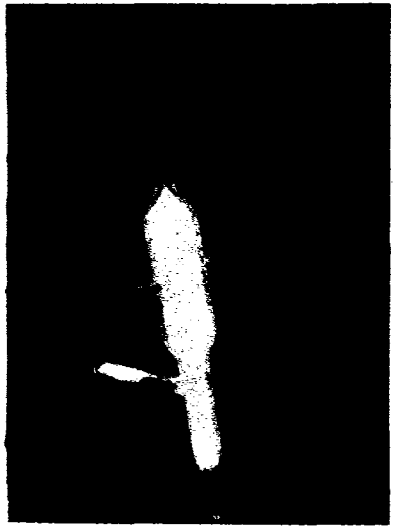

No. 3. Showing the explosion flame in No. 6 bulb when ignition had been effected with a condenser discharge-spark of 1·0 mf. at 1000 volts.

(*Facing p.* 288.)

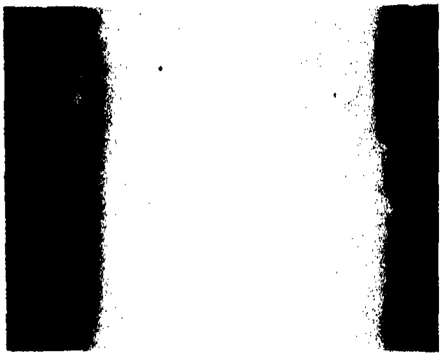

No. 4. The explosion flame. Middle part of bulb No. 7.

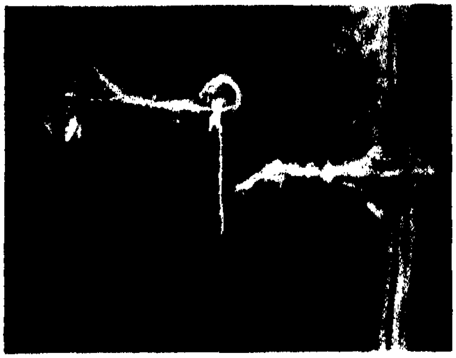

No. 5. Bulb No. 7. The phosphorus pentoxide thrown up on to the electrodes as result of the explosion.

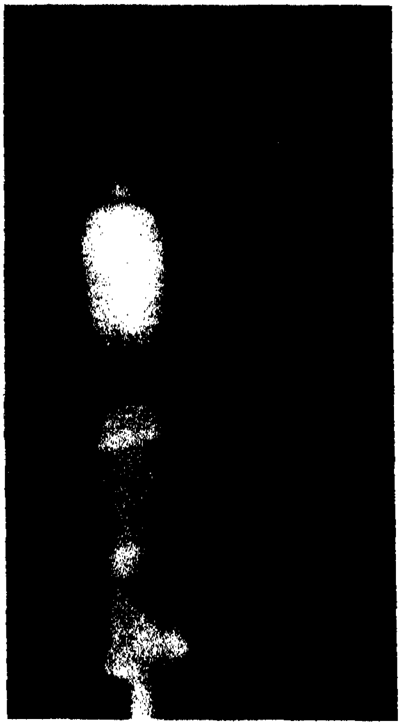

No. 6. Bulb No. 8. The explosion flame filling the bulb after ignition.

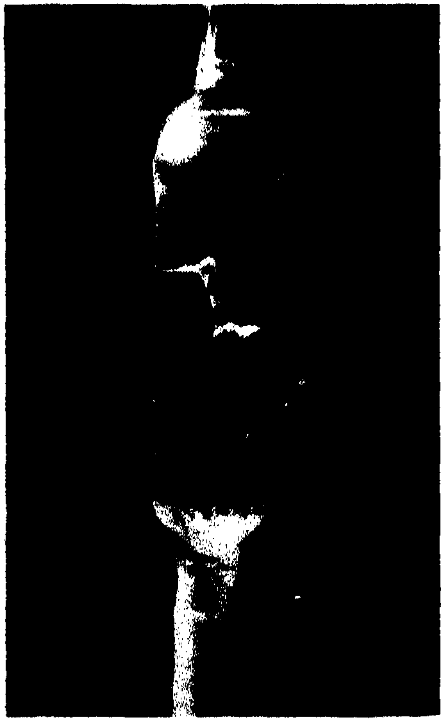

No. 7. Bulb No. 8, after the explosion.

discharge spark of 0·25 m.f. at 1000 volts was passed between the platinum "balled" electrodes of the explosion bulb but without any visible result. The next day another discharge spark—this time of 0·5 m.f. at 1000 volts—was passed through the mixture, but again without any result. On the 1005th day (December 11, 1928) a third condenser discharge spark of 1·0 m.f. at 1000 volts was passed, but once again without any visible result. On subsequently passing a fourth and still stronger discharge spark—namely of 2·0 m.f. at 1000 volts—the mixture ignited and a lambent flame slowly spread throughout it, eventually filling the body of the explosion vessel, and passing about a third way up the side arm, as shown in the photograph No. 6 (Plate 16). Phosphoric anhydride was also thrown up on to the electrodes (see photograph No. 7) much as in all the previous cases. The percentage combustion was 84·1.

In comparing the results of No. 8 with those of the preceding experiments it should be remembered that in No. 8, not only was the mixture fired decidedly weaker, but also the firing pressure was much lower, than in any previous case. Indeed in No. 8 the partial pressure of the carbonic oxide was 414 mm. only, as compared with between 485 and 495 mm. in Nos. 5, 6 and 7; and it is to this circumstance that the lesser ignitibility and milder explosion observed in No. 8 are to be attributed. It should perhaps be added that the expression "instant" used in describing the other explosions means that, so far as could be judged by the observer, the explosion started on the instant of the igniting spark being passed, rather than that the flame instantaneously filled the containing vessel.

The details of all these experiments are shown in the accompanying table, and we need only direct attention to the following points of general interest arising out of them :—

(1) In the first place, the extreme "dryness" of all the gaseous mixtures exploded is attested by the facts that (i) in all cases they had previously remained unaffected by so powerful a condenser discharge as one of 0·25 m.f. charged to 1000 volts ($\Sigma = 0\cdot125$ Joule), and in three cases by one of double such intensity, and (ii) when each was exploded by a spark of sufficient intensity, so that flame filled the vessel, the resulting combustion was always less than 90 per cent. complete.

(2) Secondly, it is abundantly clear from internal evidence that, during the long drying periods (555 to 1005 days) allowed, the extreme limit of the drying power of re-distilled and purified phosphoric anhydride had been reached. Moreover, the fact that there is practically no difference between these present results and those of similar experiments described

Table showing the Results of Experiments upon the Explosions of the P_2O_5-dried $2CO + O_2$ Mixtures.

No. of Expt.	Percentage Composition of the Gaseous Mixture.			Explosion Vessel Filled at :—		Drying Period Days.	Details of Firing Trials.	Final Pressure (corrd.) of Cold Products. mm.	Ratio P_2/P_1	Percentage Composition of the Gaseous Products.				Per-centage Com-bustion.
	CO	O_2	N_2	T° C.	& mm.					CO_2	CO	O_2	N_2	
5	66·8	32·7	0·5	15·0°	743·4	555	(i) With 0·5 microfarad at 1000 volts. $\Sigma = 0{\cdot}25$ Joule. *No ignition.* (ii) With 1·0 microfarad at 1000 volts. $\Sigma = 0{\cdot}50$ Joule. *Instant explosion.*	525·8	0·707	81·1	11·1	7·3	0·5	87·8
6	66·1	33·6	0·3	17·0°	736·2	758	(i) With 0·25 microfarad at 1000 volts. $\Sigma = 0{\cdot}125$ Joule. *No ignition.* (ii) With 0·5 microfarad at 1000 volts. $\Sigma = 0{\cdot}25$ Joule. *No ignition.* (iii) With 1·0 microfarad at 1000 volts. $\Sigma = 0{\cdot}50$ Joule. *Instant explosion.*	529·9	0·720	81·95	7·25	10·4	0·4	89·25
7	66·0	33·0	1·0	16·8°	737·3	995	(i) With 0·25 microfarad at 1000 volts. $\Sigma = 0{\cdot}125$ Joule. *No ignition.* (ii) With 0·5 microfarad at 1000 volts. $\Sigma = 0{\cdot}25$ Joule. *Instant explosion.*	526·5	0·714	80·1	12·2	6·2	1·5	86·7
8	60·2	35·3	4·5	15·0°	688·6	1005	(i) With 0·25 microfarad at 1000 volts. $\Sigma = 0{\cdot}125$ Joule. *No ignition.* (ii) With 0·5 microfarad at 1000 volts. $\Sigma = 0{\cdot}25$ Joule. *No ignition.* (iii) With 1·0 microfarad at 1000 volts. $\Sigma = 0{\cdot}50$ Joule. *No ignition.* (iv) With 2·0 microfarads at 1000 volts. $\Sigma = 1{\cdot}0$ Joule. *Instant explosion.*	506·2	0·735	68·9	12·15	12·8	6·15	84·1

in Part I hereof, but in which drying-periods of between 168 and 217 days had been allowed, shows that, in regard to gases in glass explosion vessels of dimensions such as ours, the utmost limits of phosphoric anhydride drying can be reached under all due precautions in about 6 months, a conclusion which is supported by other recent experiments in our laboratories showing that such limit lies somewhere between 120 and 240 days.

(3) Therefore, we can say further that a highly purified $2CO + O_2$ mixture which, under all necessary precautions, had been rigidly dried to the utmost limit possible with re-distilled and highly purified phosphoric anhydride will still explode and propagate flame provided that a sufficiently powerful igniting spark be used.

(4) With regard to the minimum spark energy required in any given case, obviously this will depend, not only upon the character of the discharge, but probably also upon the material and shape of the electrodes; and in an oscillatory discharge of the type employed in our experiments, where (owing to the high damping of the oscillations due to the resistance of the discharge gap) ignition is determined solely by the characteristics of the first oscillation. In this connection it may be of significance that in the one experiment (No. 7) of the whole series where *pointed* platinum electrodes were used, a discharge spark of somewhat less energy sufficed than when "*balled*" electrodes were used, a circumstance which may be attributed to greater lateral intensity of the field in the former case. Also, in comparing experiment No. 8 with the others, there is some indication that (as might be expected) the minimum spark energy depends also upon the composition of the carbonic oxide-oxygen mixture and the gaseous pressure.

In conclusion, we desire to express our best thanks to the Gas Light & Coke Company of London with the aid of whose Gas Research Fellowship at the Imperial College our work has been carried out.

The Change of Electrical Conductivity in Strong Magnetic Fields.
Part I.—*Experimental Results.*

By P. Kapitza.

(Communicated by Sir Ernest Rutherford, P.R.S.—Received February 5, 1929.)

[Plate 17.]

Introduction.

In a recent paper* the author described experiments on the change of resistance of bismuth crystals in magnetic fields up to 300,000 gauss. In agreement with previous investigators it was found that the resistance of bismuth in weak fields increases in proportion to the square of the magnetic field, and in stronger fields follows a linear law, the increase of resistance being proportional to the magnetic field up to fields of 300 kilogauss.

It was further found that this linear part of the change of resistance is, in most cases, independent of the orientation of the crystal in the magnetic field, and also of the degree of perfection of the crystal. This suggests that we are concerned with an atomic phenomenon. On studying several other substances it was found that the increase of resistance, although on a much smaller scale, is similar to that observed in bismuth, following first the square law and in fields above 60 to 100 kilogauss a linear law. This has led to a systematic study of the elements throughout the periodic table. About 35 different metals have been investigated at different temperatures, varying from room temperature to the temperature of liquid nitrogen, and the law of change of resistance mentioned above is found to be general for all.

The linear part appears to be independent of the physical (crystalline) state of the metal, and to be related to the position of the element in the periodic table. Further, it is found possible to obtain a quantitative explanation for the law of change of resistance based on some theoretical considerations which are described in detail in the second part of this paper. The hypothesis proposed for the interpretation of the experimental results throws some light on the mechanism of electrical conductivity in general, and also on the phenomenon of supra-conductivity.

The primary object of this research was not to obtain a great accuracy, but rather to carry out a survey of a large number of metals with a view to elucidating the general aspects of the phenomenon, leaving the details until some later date. The methods employed in the previous work on bismuth (*loc. cit.*) were found to be suitable, except that certain refinements, to be described later, were introduced. By this method it was possible to measure changes of resistance to one-half or one-quarter per cent. in favourable cases, and, as the change of resistance in most substances at low temperatures in a field of 300 kilogauss was more than 30 per cent., this accuracy was sufficient for the purpose in hand.

---

* 'Roy. Soc. Proc.,' A, vol. 119, p. 358 (1928).

The first part contains a description of the few improvements made on our previous methods, followed by a systematic account of the experiments on each individual metal. The second part attempts to give a theoretical generalisation of our results and a discussion of their bearing on the present theory of metallic conductivity.

(1) *The Experimental Arrangement.*

The general scheme of the experimental arrangement is shown in fig. 1, and is very similar to that used in the author's earlier experiments on bismuth crystals.*

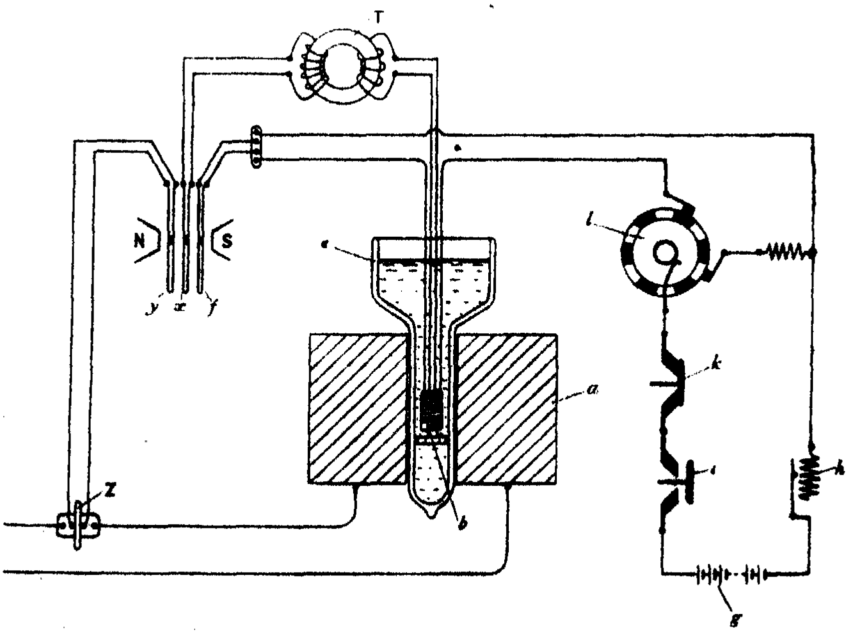

FIG. 1.

---

* *Loc. cit.*, p. 388, fig. 7.

In the coil *a* the magnetic field is produced for the short time of the experiment. In the opening of the coil is placed the Dewar flask *c* containing the conductor *b* whose behaviour is to be studied in the magnetic field. If necessary the conductor may be cooled by filling the Dewar flask with liquid nitrogen or a mixture of solid CO_2 and ether. The current is sent through the conductor from the battery *g* through the resistance *h*, and the sector interruptor *l*, and is recorded by the oscillograph *f*. The make and break of the current through the conductor is produced by the two switches, *k*, *i*, which are operated automatically and timed with the current wave through the coil in the manner described in the author's previous paper.[*] The current through the coil is recorded by the oscillograph *y* connected to the shunt *z*. The potential across the conductor is recorded by a very sensitive oscillograph *x*. The only change from the previous arrangement was that in some cases, when the resistance of the conductor was too small, it was found necessary to introduce a transformer T in the circuit. By using this transformer it was possible to obtain larger deflections with the same current passing through the conductor, as the transformer secondary, connected to the oscillograph, contained more turns than the primary and so increased the potential across the oscillograph. This transformer was specially designed, the general idea being to use a very small magnetising current of only 1 or 2 per cent. of the primary current. In this case the ratio between the current in the primary and in the secondary remained constant during the experiment to within 1 or 2 per cent. To obtain these results a ring composed of thin laminations ($d = 0 \cdot 2$ mm.) of Mumetal, which has a high permeability, ranging between 3,000 and 15,000 was used for the core of the transformer. This ring had a rectangular section 4 cm. high and 2 cm. wide, its inside diameter being 5·6 cm.

The second very important point in design was to arrange that the transformer should have as little self-induction as possible, *i.e.*, as little as possible " leakage " between the primary and the secondary of the winding. This was ensured by using the special winding shown diagrammatically in fig. 2. Two wires *a*, *b*, of the same thickness were wound together round the transformer core C, lying close to each other. One of the wires *b* is interrupted in four equally distant places and the eight ends are connected in such a way that the four equal sections of the winding are in parallel. In this way the current flowing through the wires *a* and *b* is in opposite directions, as shown by the arrows, the magnitude of the current in the wire *b* differing from that in the wire *a* by the value of the magnetising current only, which, as already stated, was very small. Evidently this gives practically a bifilar winding and very little stray magnetic field is created.

---

[*] *Loc. cit.*, p. 391, fig. 8.

The necessity for having a transformer with a small self-induction is illustrated by the two oscillograms (1 and 2, Plate 17). The curve I on these oscillograms is drawn by the oscillograph *f*, fig. 1, when a square impulse of current, produced by the sector interruptor, was sent through a conductor *b* of very small resistance. No magnetic field was produced during the experiment. Curve *p* on this oscillogram is drawn by the potential oscillograph *x*. In both cases a transformer T was introduced in the manner shown in fig. 1. The oscillogram 1 is taken with an ordinary transformer; oscillogram 2 with a transformer wound as shown and described in fig. 2. On oscillogram 1, owing to the self-induction of the transformer, the two curves I and *p*, drawn by oscillographs *f* and *x*, are not at all similar. On oscillogram 2 the shape of the curve *p* is seen to be unaffected by the self-induction of the transformer, and is practically similar to that of the curve I.

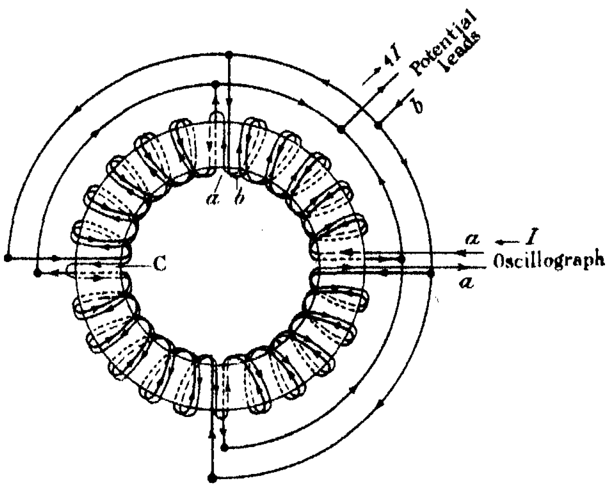

FIG. 2.

The transformer actually used did not have four sections, as in fig. 2, but eight. Its primary had 160 turns of 22 S.W.G. enamelled wire. The secondary was wound with the same wire, having eight sections with 20 turns in each. The winding was made in two layers with great care.

Special care was taken to devise a proper method for fastening the conductor in the holder. Different types of holders were used according to the material under observation, and are shown in fig. 3. In the simple cases, where the material was obtained in the form of a wire, the holder shown in fig. 3A was used. To the end of an ebonite plate *a* 1·5 mm. thick was screwed an ebonite cylinder *b*, on which was cut a double thread. The wire *c* was wound on this cylinder in a bifilar way, as shown on the figure, and the two ends of the wire *e* and *d* were soldered to two copper leaves *f* which were insulated from each other and attached to the ebonite plate *a* (only the top leaf can be seen in the drawing). These two leaves formed the potential leads. The wire was then taken to the other side of the ebonite plate, where it was again soldered to two other insulated copper leaves which formed the power leads. In a case where the wire was of a metal which could not be soldered, short platinum wires were spot-welded to it at the places where the contacts with the upper leaves had to be made, and these platinum wires were then soldered to the copper. This arrangement proved to be extremely satisfactory, only very small e.m.fs. being induced in the conductor by the changes of the magnetic field in the coil during the experiment. For liquid metals like mercury or gallium the holder shown in fig. 3B was used. The top part is similar to the holder 3A except that the cylinder *b* has a double square thread and is well fixed in a piece of glass tubing *h*. The thread is easily filled with mercury or gallium by placing a little piece of the metal at the bottom of the cylinder and screwing up the cap *g* which presses the metal into the thread. The contact between the liquid and the copper strips is made by platinum or silver

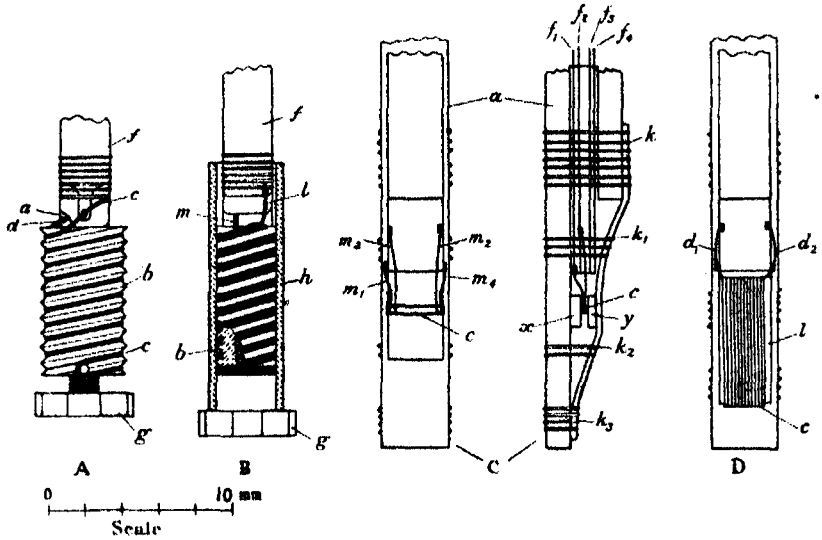

Fig. 3.

wires, *m*, *l*, which are soldered to the copper leaves *f* and immersed in the metal as shown in fig. 3B.

The greatest difficulty was found with metals such as chromium, beryllium, arsenic, etc., which could not be drawn into a flexible wire. In these cases only very small rods, about 5 to 6 mm. long, could be prepared and these had a very small resistance. The potential drop across them was also very small and sometimes smaller than the induced e.m.f. if this were not eliminated. A special holder has therefore been arranged in which, by means of adjusting the position of the rod, this induced e.m.f. can be eliminated. In fig. 3C such a holder is shown. It consisted of an ebonite plate *a* on which four insulated copper leaves, f_1, f_2, f_3 and f_4, were placed and bound by the thread *k*. To the ends of these copper leaves four platinum or silver wires, m_1, m_2, m_3, m_4, were soldered. The ends of these wires were spot welded or soldered to the ends of the rod *c* under examination, as shown on the figure. On each side of the rod *c*, distance pieces, *x*, *y*, were placed. The whole was held firmly together by means of a series of silk threads, k_1, k_2, k_3. By adjusting the thickness of the two pieces *x* and *y* a position for the rod *c* could be found such that no e.m.f. was induced in the potential circuit. This adjustment was very easily made by placing the holder in the coil and taking an oscillogram of the induced e.m.f. only, *i.e.*, by recording the deflection of the potential oscillograph when no current was passing through the crystal. By this method an initial deflection of 5 or 6 mm. could be reduced, by trial and error, to a fraction of a millimetre. All these holders (A, B and C) were used for the transverse phenomenon ($H \perp I$) in which the change of resistance is produced by the magnetic field perpendicular to the current in the conductor, this being the phenomenon in which we were chiefly interested. In a few cases where we studied the "parallel" phenomenon ($H \parallel I$) we used the holder shown in fig. 3D. This was similar to the holder C, except that instead of the rod we used a small piece of cardboard, *l*, on which the wire to be tested, *c*, was wound longitudinally, as shown on the figure, the turns being insulated by placing between them a silk thread. The ends of the wires, d_1, d_2, were soldered to the four copper leaves as shown on the drawing. The few cases in which we had to alter the shape and the design of these holders will be mentioned separately when we discuss the particular metal.

It was also found necessary to prevent shaking of the holder when it is placed in the Dewar flask. When a strong current was passing through the wires the holder shook owing to the electrodynamical forces between the current and the magnetic field, and this induced an additional e.m.f. in the wires.

To keep the holder steady we screwed to the bottom of the cylinder *b* a cross *g* which exactly filled the Dewar flask, as may be seen in fig. 1. The holder was also shaken by the large attraction of the strongly paramagnetic liquid air in the coil. To avoid this we used liquid nitrogen instead of liquid air in the later experiments. This had the further advantage that the temperature did not vary as in liquid air, where it depends upon the freshness of the liquid air. All the remaining details of the experiment were the same as in the earlier work on bismuth (*loc. cit.*).

(2) *The Metals Studied and their Purity.*

As the main object of this research was to survey the phenomenon of change of resistance over the whole of the elements of the periodic system, we had to accumulate a large number of metals. This was a difficult task as it was essential that the metals should be extremely pure.

The influence of the impurities on the phenomena studied was very marked, particularly in the lighter elements of the periodic system, and invariably reduced the change of resistance. A comparative study of the effects of different impurities in the same elements was accomplished by comparative spectroscopic analysis. By means of a small quartz Hilger spectrograph, spectra of two different samples of the element were taken close together, by illuminating the two halves of the spectrograph slit in turn with a spark produced first between electrodes of the one specimen and then of the other. Two close spectra were obtained, and simply by a comparison of the number and the intensity of the ultimate lines of the impurity it was easy to find which of the two elements was the purest. A comparison of the change of resistance of the two specimens in the magnetic field then made it possible to judge to what extent the impurities affected our results. If the quantitative analysis of the substance had not been given by the maker, a special analysis was made. We are greatly indebted to Prof. Dennis and Prof. Papish of Cornell University and to Messrs. Hilger for making a number of quantitative spectroscopical analyses for us. From all these data we find that, to ensure that the impurities shall have only a small influence on our results the substance must in no case be less than 99·9 per cent. pure, and must be even purer in the case of the lighter elements. If the substance is only 99 per cent. pure the influence of impurity is so large that the results are practically useless for our purpose.

It was found to be extremely important to take precautions to avoid contaminating the substance when it was made into a wire. This was done either by drawing or by extruding, according to the property of the metal. In the first case the wire was drawn through a set of sapphire dies. The chief precaution for keeping the wire clean was that two lots of wire were drawn through the same set of dies, one to clean the dies and the other for use in the experiment. In the second case the arrangement for extruding the wire used throughout the work was very simple. It consisted of a small steel cylinder having a cylindrical opening about 4 or 5 mm. in diameter and about 1½ cm. long, having at the bottom a wall about 2 or 3 mm. thick through which a small hole was drilled having the same diameter as the wire which we desired to extrude. A steel punch was fitted to the cylindrical opening. After placing the metal in the hole a pressure up to 1 or 2 tons was applied from a press, whilst in many cases the cylinder was heated. Before using the punch it was very carefully cleaned, and a freshly made cylinder and punch were used for each metal.

By taking comparison spectra of the original metal and of the wire it was possible to make sure that the substance was not contaminated during the drawing or extruding.

(3) *The Experiments and the Measurements.*

The experiments were performed in exactly the same way as in the earlier work on bismuth. The oscillograms, like that shown in No. 3, Plate 17, were measured as before, by magnifying them about four or five times on projection and tracing the oscillogram with a pencil. The enlargement was then measured by a rule. The change of resistance was determined by measuring the ratio of the amplitudes of the deflection of the potential oscillograph x, fig. 1. (curve p on oscillogram 3) with no field, to the amplitude when the field was on. The magnetic field was deduced from the amplitude of the curve drawn by the oscillograph y (curve H on oscillogram 3), in the way described in the previous communication.* The e.m.f. induced by the variation of the magnetic field was eliminated by the sector interruptor l, fig. 1. As the amplitudes of the curves p of the potential oscillograph x were measured only at the instant when the current in the conductor under investigation was either made or broken by the interruptor l, the e.m.f. was eliminated. The most accurate points for the curves of the change of resistance were obtained at the maximum field when the variation was least. For each metal at a given temperature, two oscillograms were taken, one in which the field varied from 0 to 125 kilogauss, and the other from 0 to 300 kilogauss. Thus the most accurate points lie in the region of 100 and 300 kilogauss. When the curves

* 'Roy. Soc. Proc.,' A, vol. 115, p. 679 (1927).

were drawn the relative accuracy of the points was taken into account. The experimental error varied with the conditions of the experiment. In a substance with a large specific resistance which was available in the form of a wire (Mo or W) the change of resistance could be measured to ¼ or ½ per cent. of the initial resistance. In the less favourable cases, like chromium or beryllium, where the substance was in the form of a rod of a few ten-thousandths of an ohm resistance, the change of resistance could be measured only to about 5 per cent. An idea of the accuracy of the experiments can be obtained from the straggling of the experimental points on each diagram.

Most of the metals were studied at three temperatures—at room temperature (about 290° K) at a temperature of 193° K, when the Dewar flask was filled with a mixture of solid CO_2 and ether, and at a temperature of 88° K, when the Dewar flask was filled with liquid nitrogen. In some earlier experiments in which liquid air was used in place of liquid nitrogen, the temperature was slightly higher, about 91° K, and varied with the freshness of the liquid air.

The results of the experimental measurements are shown in figs. 4 to 31, the relative change of the resistance, $\Delta R/R$ where ΔR is the increase of the resistance and R is the resistance at the corresponding temperature, being plotted against the corresponding magnetic field in kilogauss. As already stated, it was found that in every case in weaker magnetic fields the relative change of resistance $\Delta R/R$ is proportional to the square of the magnetic field. Afterwards, the increase of resistance follows a linear law, $\Delta R/R$ being proportional to H. If an asymptote is drawn to the linear part of the curve (asymptote BC in fig. 33), it intercepts the axis of abscissæ at a magnetic field H_k (point A, fig. 33) which we shall call the critical field. The following formulæ were found to express the change of resistance within the limits of experimental error :—

$$\frac{\Delta R}{R} = \beta \frac{H^2}{3H_k} \qquad H \leqslant H_k, \qquad \text{(A)}$$

$$\frac{\Delta R}{R} = \beta \left(H - H_k + \frac{H_k^2}{3H}\right) \qquad H \geqslant H_k. \qquad \text{(B)}$$

where β is a constant representing the tangent of the angle between the asymptote and the H axis. These two formulæ represent a continuous line, as it can easily be seen that at $H = H_k$ the curves will have the same value for the ordinate and a common tangent. The formulæ have been deduced in a strict mathematical way from certain theoretical considerations which will be discussed in Part II of this paper.

We shall find it convenient to interpret the experiments in terms of the values of H_k and β. The curves in figs. 4 to 31 are drawn by numerical valuation of the equations (A) and (B), the values of H_k and β being chosen in such a way as to fit the experimental results as closely as possible. It can be seen that the deviation of the points from this curve is always within the limits of experimental error. The values of β and H_k are given in Tables I to VIII. In these tables are given also the value of $\Delta R/R$ at a field of 300 kilogauss, and the value of R/R_r, where R is the resistance of the metal when it is cooled by solid CO_2 or liquid nitrogen, and R_r is the resistance at room temperature. This value has been determined for each substance before and after the experiment, and if nothing went wrong with the holder or the metal it remained constant. The value of R/R_r is also important as it is affected by chemical impurities and the physical state of the metal.

We shall now describe experiments on various elements in successive groups of the periodic system from 1 to 8.

(4) *Experimental Results for the Transverse Phenomenon, First Group of Elements.*

The elements in the first column of this group, Li, Na, Ka, Rb and Cs, are very difficult to handle owing to the ease with which they become oxidised and to the difficulty of providing good contacts with the potential and power leads. The change of resistance of Li and Na was small, and as it probably diminishes gradually when we come to the heavier members, we decided, owing to the experimental difficulties and the smallness of the effect, to limit our study to lithium and sodium.

The elements of the second column, Cu, Ag and Au, have been very carefully investigated as it was possible to obtain them in a high state of purity and experiment was relatively easy. The experimental results are given in Table I and on figs. 4, 5, 6 and 7.

Table I.—Transverse Effect in the First Group (H ⊥ I).
Results at the Temperature of Liquid Nitrogen.

Elements.	Source.	R/R_r.	$\Delta R/R$ at 300 k.g.	$\beta \times 10^6$.	H_k k.g.	Remarks.
Li_I	Kahlbaum …………	0·195	0·09	—	—	Liquid air temperature.
Li_{II}	The same ………………	0·137	0·15	0·7	100	Curve on fig. 4.
Na	The same ………………	0·2	0·07	—	—	Liquid air temperature.
Cu_I	Hartmann & Braun, hard.	0·17	0·47	1·95	135	Curve 3, fig. 5.
Cu_I	The same, annealed	0·141	0·35	1·90	64	Curve 1, fig. 5.
Cu_{II}	Hilger, semi-hard....	0·157	0·42	1·91	89	Curve 2, fig. 5.
Ag	Hartmann & Braun, annealed	0·181	0·38	1·47	45	Curve 1, fig. 6.
Ag	The same, hard drawn.	0·22	0·30	1·42	100	Liquid air temperature, curve 2, fig. 6.
Au_I	Heraeus, soft ………	0·216	0·28	1·16	60	Curve 1, fig. 7.
Au_{II}	Johnson & Matthey, hard.	0·32	0·16	0·93	135	Liquid air temperature, curve 2, fig. 7.

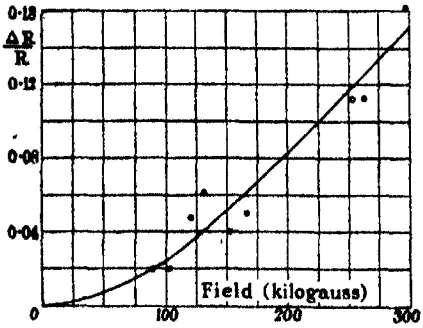

Fig. 4.—Lithium H ⊥ I.
Temperature of Liquid Nitrogen.

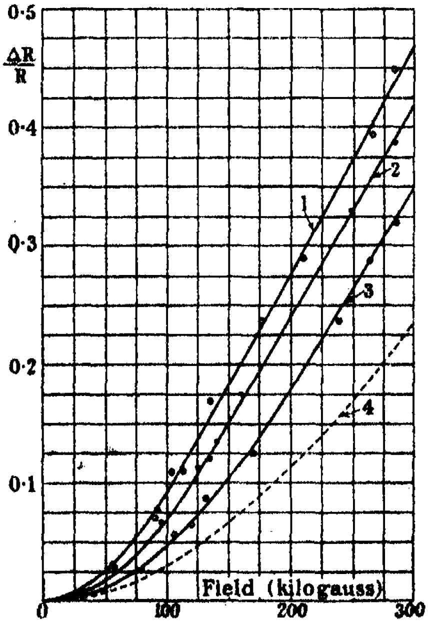

Fig. 5.—Copper. Temperature of Liquid Nitrogen.

Curve 1—H ⊥ I Cu_I annealed.
Curve 2—H ⊥ I Cu_{II} half-annealed.
Curve 3—H ⊥ I Cu_I hard drawn.
Curve 4—H ∥ I Cu_I hard drawn.

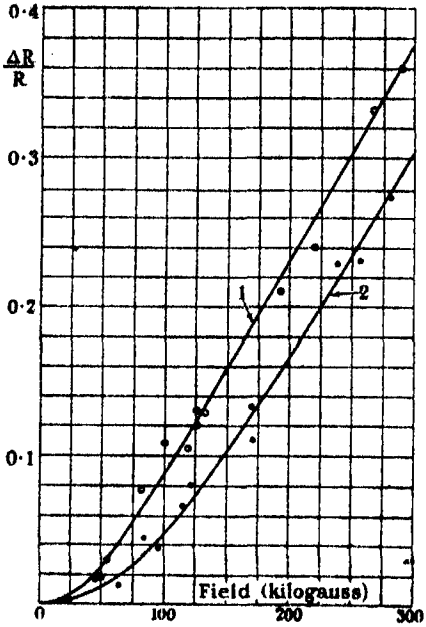

FIG. 6.—Silver $H \perp I$.

Curve I—Ag annealed. Temperature of Liquid Nitrogen.
Curve 2—Ag hard. Temperature of Liquid Air.

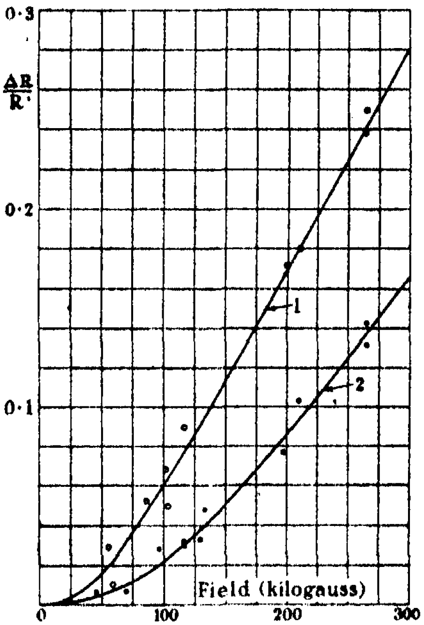

FIG. 7.—Gold $H \perp I$.

Curve 1—Au_I soft. Temperature of Liquid Nitrogen.
Curve 2—Au_{II} hard. Temperature of Liquid Air.

Lithium.—We used a lithium wire about 0·3 mm. in diameter and about 20 cm. in length which was prepared by extruding at room temperature in dried liquid paraffin. It was then fixed under paraffin to a holder similar to that shown in fig. 3A, differing only by small screws which were fitted on the ebonite plate *a*. The lithium wire was pressed by means of these to the potential and power leads, soldering not being possible with lithium. In this case, instead of using copper strips for the leads, we used silver ones as they provided better contacts. These proved to be quite satisfactory, and the lithium wire fixed in such a way did not change its resistance appreciably when kept under liquid paraffin for several days, whilst the resistance of the contacts was small. The experiment was tried on two samples of lithium, both being obtained from Kahlbaum. The first wire (Li_I) was made from lithium supplied by this firm several years ago, in the form of a lump floating in oil. The second (Li_{II}) was supplied quite recently by the same firm in the form of wires in a sealed tube. Li_{II} was found, by spectroscopic analysis, to be much purer than Li_I. Li_I contained about 1 per cent. of Mg and a "full trace" of Zn. Li_{II} was apparently of a very high purity and only very slight traces of impurity could be detected. We should estimate its purity to be well above 99·9 per cent.

At ordinary temperatures the change of resistance of both Li_I and Li_{II} in a field of 300 kilogauss was less than 2 per cent. In the same field at the temperature of liquid air the change of resistance of Li_I was 9 per cent., whilst Li_{II} changed its resistance by 15 per cent. at the temperature of liquid nitrogen, and it was possible to plot an approximate curve as shown in fig. 4. This curve was drawn by taking the value of H_k to be 100 kilogauss and β equal to 0·7. These values have indeed to be considered in this case as very approximate, but sufficient to give an idea of the order of magnitude of the phenomena of change of resistance in lithium.

Sodium.—Sodium was treated in exactly the same way as lithium, but owing to the fact that the metal was much softer and more easily oxidised, the difficulty of obtaining good contacts with the potential lead was very great, and the results obtained were even less accurate than in the case of lithium. We made only one experiment with sodium obtained from Kahlbaum, which was quite pure ("for analysis"). At room temperature the change of resistance in a field of 300 kilogauss was less than 2 per cent., and in the same field at the temperature of liquid air, 7 per cent. This shows that the change of resistance is smaller than in lithium but as the accuracy of the experiment was small, no evaluation of β and H_k could be satisfactorily made.

Copper.—This and the two following elements, silver and gold, as already stated, have been carefully studied. We found these elements very suitable for investigation not only of the influence of impurities on the phenomena of change of resistance, but also the influence of the physical state of the metal, namely, hardening and annealing. For this purpose we also found it necessary to determine the specific resistance of different wires, this data being required in the second part of this work.

For the experiments, copper wires of a diameter about 0·15 mm. and 20 to 30 cm. in length were used. This wire was obtained from Hartmann and Braun (Cu_I) already drawn, but when we used copper from Hilger (Cu_{II}) we drew the wires ourselves. The wire under investigation was fixed to the holder as shown in fig. 3A and a simple solder was used to make the contacts. The resistance of the wire at room temperature was about 0·3 ohm, and about six times smaller at a temperature of liquid nitrogen.

The analysis of the copper, Cu_{II}, from Hilger was as follows :—O = 0·04, Ni = 0·02, Fe = 0·03, As = 0·04, Pb = 0·01 and Ca = 0·001, all given in per cents. The analysis was given by the makers. The purity of the wire obtained from Hartmann and Braun, Cu_I, was compared spectroscopically with that of the copper from Hilger and was found to be about the same. We were very surprised to find that Cu_I and Cu_{II} wires gave a marked difference in the change of resistance, but the subsequent investigations showed that this was due to the state of hardening of the wire which affected the phenomenon strongly. In fig. 5 the curves 1 and 3 give the results for two pieces of the same copper wire from Hartmann and Braun (Cu_I), 3 being hard and 1 being annealed. The annealing was done in vacuum, the wire being heated to a temperature of about 700°.

It is seen from curve 3 that for the hard wire the square law holds up to a stronger field—about 142 kilogauss, but when this field is reached, the slope β of the linear part is about the same as for the annealed wire. The Hilger wire was annealed (simply by warming it in a gas flame, without special precaution), before passing it through the last few dies, and we may call it a semi-annealed wire. The curve of the change of resistance at the temperature of liquid nitrogen is shown in the same fig. 3, curve 2, and we can see from this curve that again it has the same slope β, but the critical field H_k lies between the values obtained for the two previous wires. It seemed to us a very important fact that the physical or crystalline condition of the conductor has such an immense influence on its change of resistance in a magnetic field, but it is more interesting to note that the physical state of the conductor at a given temperature only influences H_k, changing its value several times, whilst β is left practically constant. We have observed this fact with several other conductors (Ag, Au, Cd, Al) and its theoretical importance will be discussed in detail later. The data for β and H_k for the temperature of liquid nitrogen are given in Table I.

At a temperature of CO_2 the resistance of copper changes in a field of 300 kilogauss by only 5 per cent., so that at this temperature we cannot give the exact shape of the curve as the present method of measuring the change of resistance allows only an accuracy of 1 to $\frac{1}{2}$ per cent. for copper. At room temperature the increase of resistance is probably not larger than 1 or 2 per cent.

Silver.—Silver was treated in exactly the same way as copper, and wires of the same thickness and length were used. We used silver obtained from Hartmann and Braun and compared it spectroscopically with silver obtained from Hilger, which was of a very high degree of purity containing only very small traces of calcium (about 0·001 per cent.). The comparison showed that the two silvers were of the same degree of purity.

We also had a piece of very impure wire of unknown origin. This showed a change of resistance half that of the silver from Hilger or Hartmann and Braun. On fig. 6, curve 1 is for silver wire from Hartmann and Braun annealed in vacuum, the experiment being made at the temperature of liquid nitrogen. Curve 2 is for a piece of the same wire at the temperature of liquid air, but hard drawn as supplied by the firm. We see again that the curves have practically the same slope β, but a different H_k (45 and 100 kilogauss). At a temperature of solid CO_2 and ether, the change of resistance of silver is only 6 per cent. and at room temperature is less than 3 per cent. No curves are given for the reasons already given in the section on copper.

Gold.—Gold was treated in exactly the same way as copper and silver. We had two supplies of gold. One from Heraeus (Au_I), which was more than 99·99 per cent. pure, was already drawn in a wire of 0·2 mm. in diameter and was soft, whilst the other from Johnson and Matthey (Au_{II}) which was in a wire of 0·1 mm. diameter, was hard, and by spectroscopical comparison with the gold of Heraeus was found to be less pure; it also showed a smaller change of resistance.

We tried to anneal the gold of Heraeus, but it was already sufficiently soft and annealing seems to have no appreciable influence. The curve obtained at the temperature of liquid nitrogen was practically the same for the two wires and is given in fig. 7, curve 1. The hard wire of Johnson and Matthey (Au_{II}) showed a departure in the same way as observed in the case of copper and silver.

In Table I all the results for the first group of elements are given and we may notice the curious fact that β in the same column of the periodic system always diminishes from light element to heavy ones. There is practically no exception to this rule in the periodic system and we shall discuss this point in detail later.

Second Group of Elements.

This group of elements is of great interest as it shows a large change of resistance even at CO_2 temperature. We could also obtain the elements Mg, Zn, Cd and Hg in an extremely pure state and they are easy to handle, so that accurate results are possible. Be, which is the most interesting and gives the largest change, was unfortunately rather impure (only 99·8). Ca, Si and Ba we were able to obtain only in such impure states that we did not consider them worth investigation, more especially as they are more difficult to handle than the other elements of this group. The experimental results are given in Table II and figs. 8, 9, 10, 11, 12 and 13.

Table II.—Transverse Effect in the Second Group (H ⊥ I).

Element.	Source.	Room temperature.			Temperature of CO_2 and ether.				Liquid nitrogen.				Remarks.
		$\Delta R/R$ at 300 k.g.	$\beta \times 10^6$.	H_k in k.g.	R/R_r.	$\Delta R/R$ at 300 k.g.	$\beta \times 10^6$.	H_k in k.g.	R/R_r.	$\Delta R/R$ at 300 k.g.	$\beta \times 10^6$.	H_k in k.g.	
Be	Dr. Rosenhain	0·65	3·1	105	—	—	—	—	0·33	2·3	10·3	85	Curves on fig. 8.
Mg	Magnesium Co.	0·17	0·9	140	0·68	0·32	1·54	105	0·17	2·84	12·3	75	Curves on figs. 9 and 10.
Zn_I	New Jersey Zinc Co., purest.	0·06	—	—	0·680	0·12	0·56	100	0·19	0·915	4·02	68	Curves on fig. 11.
Zn_{II}	Lock Lancaster, pure	—	—	—	—	—	—	—	0·20	0·92	3·80	58	—
Zn_{III}	Kahlbaum, less pure	0·06	—	—	—	—	—	—	0·213	0·85	3·42	85	Liquid air temperature.
Cd_I	New Jersey Zinc Co.	0·08	—	—	0·680	0·19	0·73	37	0·22	0·93	3·47	35	Curves 1, 2 and 3, fig. 12.
Cd_{II}	Kahlbaum	—	—	—	—	—	—	—	0·22	1·00	3·51	12	Curve 4, fig. 12.
Hg	Kahlbaum	—	—	—	0·67	0·02	—	—	0·25	0·05	0·5	300	Liquid air temperature. The data for β and H_k are very approximate. The value of R/R_r is extrapolated for solid mercury, curve, fig. 13.

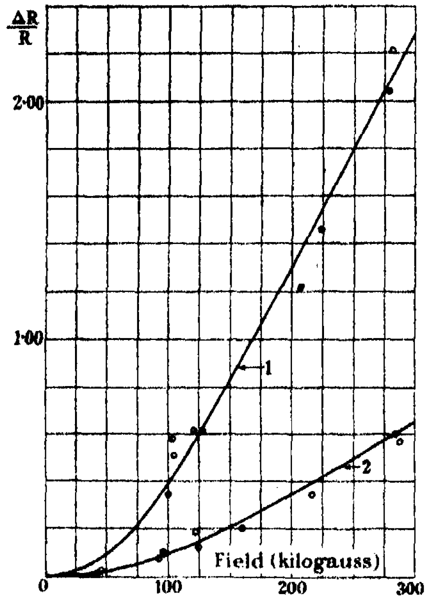

Fig. 8.—Beryllium $H \perp I$.
Curve 1—Temperature of Liquid Nitrogen.
Curve 2—Room Temperature.

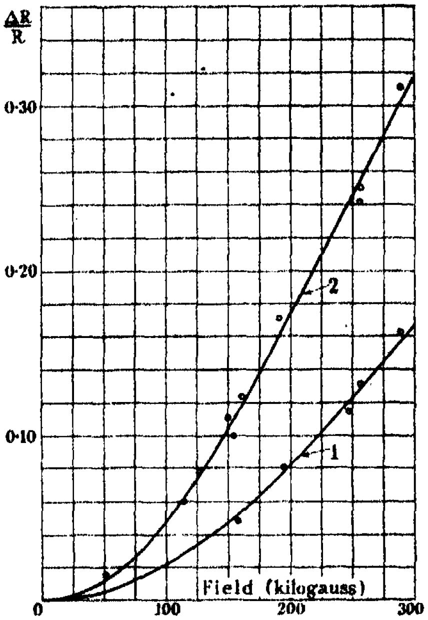

Fig. 9.—Magnesium $H \perp I$.
Curve 1—Room Temperature.
Curve 2—Temperature of Solid CO_2 and Ether.

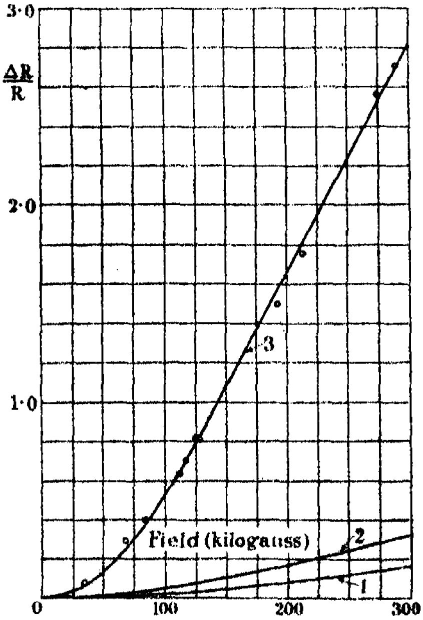

Fig. 10.—Magnesium $H \perp I$.
Curve 1—Room Temperature.

Curve 2—Temperature of Solid CO_2 and Ether.
Curve 3—Temperature of Liquid Nitrogen.

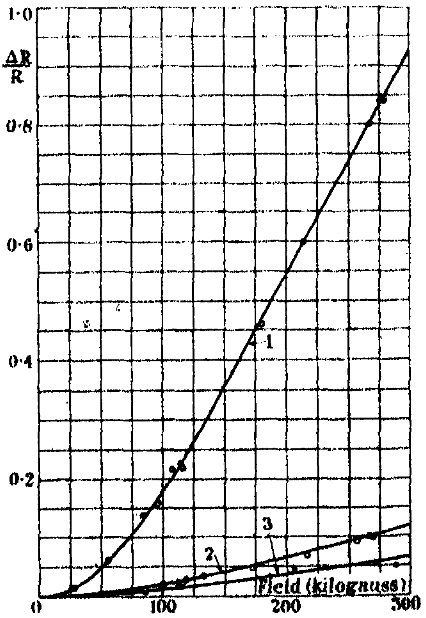

Fig. 11.—Zinc $H \perp I$.
Curve 1—Zn_I Temperature of Liquid Nitrogen.
Curve 2—Zn_I Temperature of Solid CO_2 and Ether.
Curve 3—Zn_I Room Temperature.

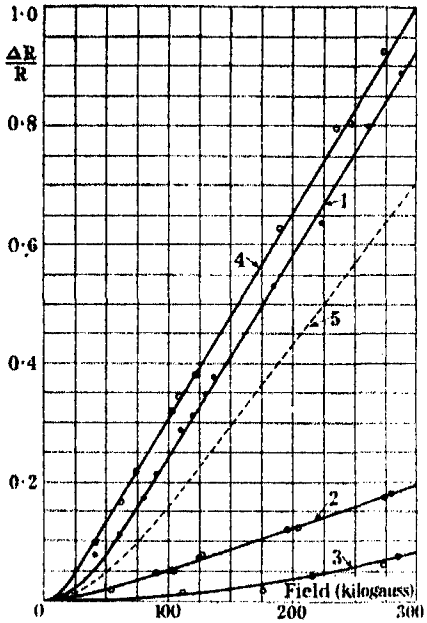

FIG. 12.—Cadmium.
Curve 1—$H \perp I$ Cd_{I} Temperature of Liquid Nitrogen.
Curve 2—$H \perp I$ Cd_{I} Temperature of Solid CO and Ether.
Curve 3—$H \perp I$ Cd_{I} Room Temperature.
Curve 4—$H \perp I$ $\mathrm{Cd}_{\mathrm{II}}$ Temperature of Liquid Nitrogen.
Curve 5—$H \parallel I$ Cd_{I} Temperature of Liquid Nitrogen.

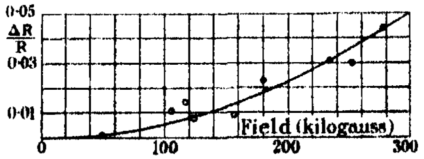

FIG. 13.—Mercury $H \perp I$. Temperature of Liquid Air.

Beryllium.—This is a difficult substance with which to experiment. It is very hard and cannot be drawn into wires. By using a thin rotating copper disc, lubricated with emery and water, on a small milling machine, we were able to cut a small rod about 0·3 mm.^{2} cross section and 6 mm. long. To this rod platinum wires of 0·2 mm. diameter were spot-welded, and the rod was fixed in the holder, fig. 3c, in the way described in Section 1. This rod had an extremely small resistance—only about 0·000275 ohm at the temperature of liquid nitrogen. In order to obtain a measurable deflection of the potential oscillograph, a current of about 8 amperes was passed through the rod, and the transformer T (fig. 1) had to be used. Fortunately Be gives a large change of resistance and reasonable curves were obtained. We had great difficulty in obtaining pure Be. We are indebted to Dr. Rosenhain of the National Physical Laboratory who provided us with the purest (99·8 per cent.) beryllium used in our experiments. This gave a change of resistance as shown on the curve in fig. 8. It can be seen that in a field of 300 kilogauss at the temperature of liquid nitrogen its resistance rises to more than three times its original value. Dr. Rosenhain gave us also some less pure specimens of beryllium which, after spectroscopic comparison with the one previously mentioned, were found not much above 99·5 pure (chief impurities were Si, Ba, Mg, Al). The change of resistance observed in this less pure beryllium was much smaller. At room temperature the pure one increased its resistance by 65 per cent. and the other by 14 per cent. At the temperature of liquid nitrogen the difference was still larger, the purest specimen showing a six times larger change of resistance.

It is evident that still purer beryllium will show an even larger change of resistance, and from certain theoretical considerations, which will be described later, we may estimate that really pure beryllium should show a change of resistance about three or four times larger than the one we observed in the purest specimen we had. Unfortunately we were unable to obtain a purer sample of beryllium. The values for H_k and β for the purest specimen are given in Table II.

Magnesium.—Magnesium was extruded into a wire of 0·2 mm. diameter. The wire was flexible and was fixed in the holder (fig. 3A) and the ends soldered to the power and potential leads by means of ordinary solder. In this way it was quite possible to provide a good contact if the magnesium was scratched under the solder. The measurements were easy and accurate. I am indebted to Dr. Aston for a piece of the magnesium which was presented to him by the Magnesium Co., Ltd. I am also indebted to Prof. Papish for making a spectroscopic examination of this substance. He found this magnesium very pure, only a trace of calcium being detected. It is practically certain that in this case the results are very little affected by any impurities, and as magnesium gave a large change of resistance we took the opportunity of investigating this metal most carefully at all temperatures. In Table II the values for β and H_k are given for three different temperatures—room temperature, temperature of solid CO_2 and temperature of liquid nitrogen—and corresponding curves are given in figs. 9 and 10. It may be observed that the β is very much affected by the change of temperature. It changes from $0 \cdot 9 . 10^{-6}$ to $12 \cdot 3 . 10^{-6}$ when the temperature falls from 19° C. to that of liquid nitrogen, whilst H_k changes less—from 140 to 75 kilogauss.

Zinc.—Zinc wires were obtained in the same way as magnesium. The wires were about 0·3 mm. in diameter. They were found to be flexible and were fixed in the holder (fig. 3A). Experiments were easy and the results accurate.

Four different specimens of zinc were investigated. The first (commercial), being very impure, gave a much smaller change of resistance than the other samples, and we shall not give any data about it.

We carefully investigated three different specimens of zinc. The purest one, Zn_I, was kindly given by the New Jersey Zinc Co., Ltd., and was of an extremely high purity. Spectroscopic analysis showed that it contained only lead to less than 0·0004 per cent. Zn_{II} (electrical zinc) was kindly given to me by the firm of Lock Lancaster. Its degree of purity was 99·98 per cent., the chief impurities being lead 0·005 per cent., iron 0·003 per cent. and cadmium 0·01 per cent. Zn_{III} was supplied by Kahlbaum (for analysis). This specimen was kindly examined by Prof. Papish spectroscopically and was found to contain a little less than 0·1 per cent. of Cd. The specific resistance of the wires made from these three brands of zinc were different, but the temperature coefficient and the change of resistance in the magnetic field were found to be about the same, as can be seen from the data given in Table II. The flexibility of the wires was also different. This is probably due to the presence of oxygen in the form of zinc oxide, which forms a non-conducting enclosure. The presence of oxygen unfortunately cannot be traced by spectral analysis. These inclusions will naturally increase the path of the current and consequently increase the specific resistance. They will also influence the flexibility of the wire.* For instance, some of the wires of Zn_{III}, which was the least flexible, cracked when immersed in liquid nitrogen. This was probably due to internal strains which were produced when the wire was cooled down, owing to the relatively smaller strength of the wire with oxide inclusions. From the data in Table II we see that β for Zn_{III} is only 12 per cent. smaller than for Zn_{II}, and Zn_{II} is about ten times purer than Zn_{III}. The difference in β between Zn_{II} and Zn_I is still smaller, only 5 per cent., whilst Zn_I is about a hundred times purer than Zn_{II}. This shows the scale of influence of impurities. To be sure of results to 10 per cent. the purity must not be less than 99·9 for zinc and for lighter elements even higher. In the case of Zn_I we may be sure that the results are independent of impurities. The change of resistance is given by curves 1, 2 and 3 of fig. 11, and in Table II for liquid nitrogen and solid CO_2 temperatures. The change of resistance at room temperature was very small—only 6 per cent.—and no accurate determinations of β and H_k were possible.

Cadmium.—Cadmium was investigated in the same way as zinc and magnesium. A wire of 3 mms. diameter was extruded and fixed in the holder, fig. 3A. Two brands of cadmium were carefully investigated. Cd_I kindly given by the New Jersey Zinc Co., Ltd., was exceptionally pure, having less than 0·0004 per cent. impurities (zinc and lead), these being only just determinable by spectroscopic analysis. Cd_{II} was from Kahlbaum ; it was spectroscopically examined by Prof. Papish, and was found also to be spectroscopically pure.

---

* The influence of oxygen was also traced by Bridgman, see 'Proc. Amer. Acad.,' vol. 60, p. 333 (1925).

In spite of equal purity, however, Cd_I and Cd_{II} were of different specific resistance. The wire of Cd_I was more flexible than that of Cd_{II} and also gave a smaller value (about 5 per cent. less) for the specific resistance. The β and the temperature coefficients of the two wires were the same. The explanation, as in the case of zinc, probably lies in the presence of oxide inclusions.

The change of resistance for Cd_I and Cd_{II} are given in fig. 12 and in Table II.

Mercury.—Mercury has been measured in a solid state only and the holder (fig. 3B) was used. Pure mercury (for analysis) was obtained from Kahlbaum. Spectroscopic investigation confirmed that the mercury was of a high degree of purity. The change of resistance of mercury is small. At the temperature of CO_2 it was only 2·5 per cent. in a field of 300 kilogauss, and at the temperature of liquid air it was 5 per cent. As the specific resistance of mercury is high and the contacts were very good, it was possible to measure the small change of resistance. The curve was rather indefinite and the separation of the constants β and H_k is only very approximate.

Third Group of Elements.

In this group we had difficulty in providing pure elements in the column Al, Ga, In and Tl, only Al and Tl being obtained in a reasonably pure state, whilst we were unable even to obtain any of the elements of the first column, Sc, Yt, La, in a metallic state. Thus this column remains uninvestigated. The results for the transverse phenomenon are given in Table III and figs. 14, 15 and 16.

Aluminium.—Aluminium was used in wires or in strips cut out from a thin sheet of aluminium. The wire, about 0·2 mm. in diameter, or the strip, was fixed in a holder, as shown in fig. 3A, and the ends of the aluminium wire were either screwed down or soldered to the copper strips by means of ordinary solder. This was done in the later experiments as it was found possible to solder aluminium and to make good contacts if the aluminium is slightly scratched with a soldering iron under the solder. The strip, about 0·5 mms. wide, was also fixed in a holder as shown in fig. 3A, but in this case the groove in

Table III.—Transverse Effect in the Third Group ($H \perp I$).

Element.	Source.	Solid CO_2 and ether.				Liquid air.				Remarks.
		R/R_r.	$\Delta R/R$ at 300 k.g.	$\beta \times 10^6$.	H_k in k.g.	R/R_r.	$\Delta R/R$ at 300 k.g.	$\beta \times 10^6$.	H_k in k.g.	
Al_I	American Aluminium Co., wire.	—	—	—	—	0·114	0·73	2·74	35	Curve 1, fig. 14, liquid nitrogen temperature.
Al_{II}	The same, strip	—	—	—	—	0·141	0·64	2·73	73	Curve 2, fig. 14.
Al_{III}	Hartmann & Braun, wire	0·58	0·09	0·4	—	0·140	0·65	2·70	65	The data are not accurate. Curve 3, fig. 14.
Ga	Hilger	0·65	0·18	0·6	8	0·21	0·87	2·90	5	Curves 1 and 2, fig. 15.
In	Dr. Francke	0·63	0·03	—	—	0·22	0·14	0·85	170	Curve 1, fig. 16.
Tl	Kahlbaum	—	—	—	—	0·23	0·16	0·73	98	Curve 2, fig. 16.

the ebonite cylinder *b* was made square instead of angular. Three specimens of aluminium were used. The purest one was made by the Aluminium Company of America. Its purity was 99·951 per cent., its impurities being as follows :—Cu 0·021, Fe 0·012, Si 0·013, Ti 0·002, Vn 0·001, in per cents. This aluminium, which we will call $\mathrm{Al_I}$, was drawn by us into wire 0·17 mm. in diameter. A second piece of aluminium, which we will call $\mathrm{Al_{II}}$, was given to us by Dr. Chadwick; this piece also came from the Aluminium Company of America. It was in sheet form, 0·1 mm. thick and a strip was cut out of it. The third sample of aluminium, $\mathrm{Al_{III}}$, was obtained from Hartmann and Braun, already in wire form of 0·15 mm. diameter. A spectroscopic comparison of these three samples showed that the $\mathrm{Al_I}$ was somewhat purer than the $\mathrm{Al_{II}}$, and $\mathrm{Al_{II}}$ than $\mathrm{Al_{III}}$. The chief impurity is copper. The specific resistances of

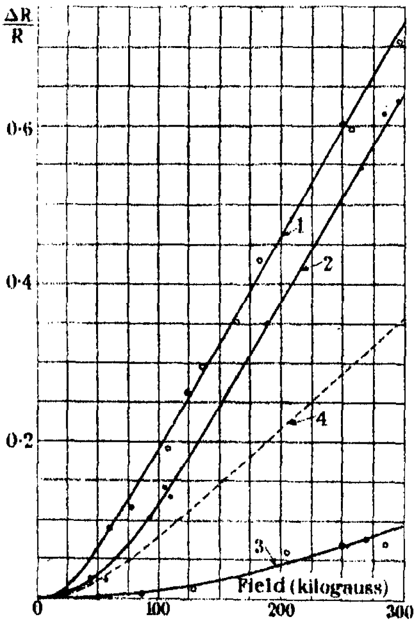

FIG. 14.—Aluminium.

Curve 1—H ⊥ I $\mathrm{Al_I}$ Temperature of Liquid Nitrogen.

Curve 2—H ⊥ I $\mathrm{Al_{II}}$ Temperature of Liquid Nitrogen.

Curve 3—H ⊥ I $\mathrm{Al_{III}}$ Temperature of Solid CO_2 and Ether.

Curve 4—H ∥ I $\mathrm{Al_{III}}$ Temperature of Liquid Nitrogen.

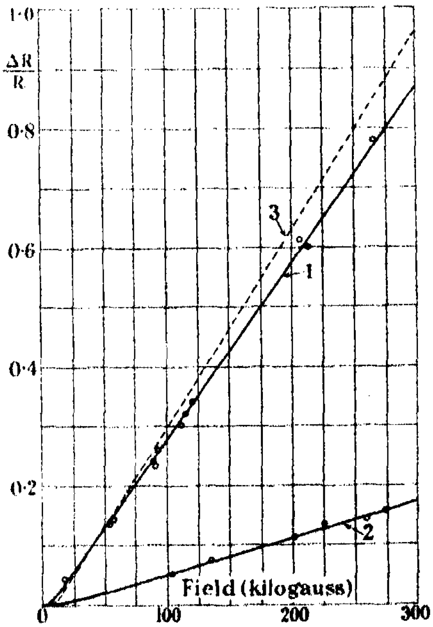

FIG. 15.—Gallium.

Curve 1—H ⊥ I Temperature of Liquid Air.

Curve 2—H ⊥ I Temperature of Solid CO_2 and Ether.

Curve 3—H ∥ I Temperature of Liquid Nitrogen.

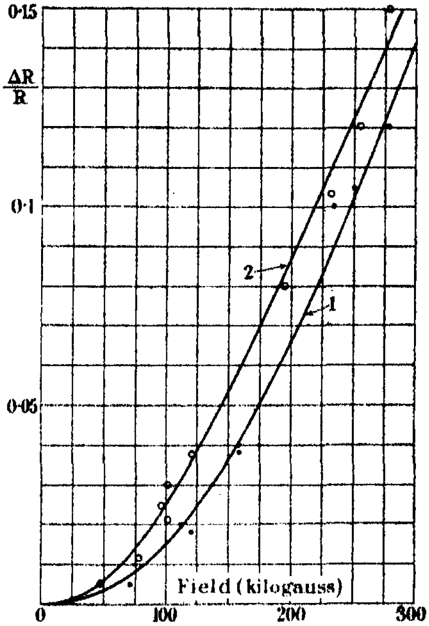

FIG. 16.—Indium and Thallium H $\perp$ I.
Curve 1—Indium. Temperature of Liquid Air.
Curve 2—Thallium. Temperature of Liquid Air.

Al_I and Al_{III} were determined at room temperature and found practically equal.

The curves for Al_I and Al_{II} are given on fig. 14 and in Table III. It appears again that only the critical field is affected by impurity, β being about the same, a phenomenon very similar to that already described in the case of Cu, Ag, Au and Cd.

Gallium.—Gallium is a metal which has a melting point at about 30°. We used the holder 3B, and, after slightly warming, filled it with liquid gallium in the same way as with mercury. The only difficulty arose from the cracking of the gallium on solidification. The screw channel of the ebonite cylinder *b* was filled with liquid gallium by turning the ebonite piston *g* to press it in. When the holder was cooled, it was found that the gallium cracked in two or three places, possibly owing to a difference in expansion between the ebonite and the gallium. This difficulty was easily overcome by simply breaking the glass tube and touching the places where the cracks were seen with a slightly warmed needle; the gallium then melted locally and the cracks disappeared. The gallium which we used was obtained from Hilger and contained the following impurities:—In 0·16, Zn 0·10, and Pb 0·011 in per cents.

We had no other sample of gallium with which to compare it. Experiments were made at three different temperatures. At room temperature the change in resistance in a field of 300 kilogauss was about 7 per cent. and no satisfactory curve could be drawn, but at the temperature of CO_2 and liquid air the change of resistance was considerable and the curves are given in fig. 15. The values of β and H_k are given in Table III. The most interesting fact about gallium is that it has the smallest critical field H_k out of all the metals which we examined. It appears to be only about 5000 gauss. In this substance it is therefore possible to reach the linear part of the curve with ordinary electromagnets.

Indium.—Indium is very easily extruded into a wire, and a wire of 0·2 mm. diameter was fixed in the holder (fig. 3A) in the ordinary way. We used two different kinds of indium, one obtained from Hilger which was supplied with the following analysis:—Pb 0·33, Na 0·025, Al 0·015, Ge 0·01, Sn 0·005, Ca 0·008, Bi 0·002 in per cents. The other was obtained from Dr. Francke of Frankfurt, and was supposed to contain no lead. We did not make a comparative spectroscopic analysis, but as the indium of Dr. Francke gave a slightly larger temperature coefficient and a slightly larger change of resistance, it was on the whole probably purer than that of Hilger. The difference is small and only the results obtained with the second sample are given in fig. 16 and in Table III. Results are only given for liquid air temperatures, since at room temperature, in a field of 300 kilogauss, the change of resistance is not more than 1 per cent., and at the temperature of solid CO_2 at the same field it is only about 3 per cent.

Thallium.—Thallium was also very easily extruded into a wire and was placed in the holder (fig. 3A). We had only one sample of thallium, this being obtained from Kahlbaum. It was spectroscopically examined by Hilger and was found to be extremely pure, only very slight traces of lead being found, so that this substance may be considered as spectroscopically pure. The results of the experiments on this substance are given in Table III and fig. 16. The β and H_k are only given for experiments at the temperature of liquid air. At room temperature the change of resistance of thallium is less than 2 per cent.

Fourth Group of Elements.

In this group of elements we were fortunate in obtaining most of the elements in a sufficiently pure state, the exceptions being titanium and graphite. Hafnium we could not obtain at all. The results for the elements of this group are given in Table IV and figs. 17, 18 and 19.

Table IV.—Transverse Effect for the Fourth Group of Elements (H ⊥ I).

Element.	Source.	Room temperature.			Solid CO_2 and ether.				Liquid air.				Remarks.
		$\Delta R/R$ at 300 k.g.	$\beta \times 10^6$.	H_k in k.g.	R/R_r.	$\Delta R/R$ at 300 k.g.	$\beta \times 10^6$.	H_k in k.g.	R/R_r.	$\Delta R/R$ at 300 k.g.	$\beta \times 10^6$.	H_k in k.g.	
G	Acheson	4·1	15	29	1·2	3·65	15	20	1·6	2·7	15	15	Curves 1, 2 and 3, fig. 17.
Ge_I	Hilger	0·5	20	45	1·02	0·45	2·4	50	—	—	—	—	Curves 2 and 3, fig. 18.
Ge_{II}	Hilger	—	—	—	—	—	—	—	1·28	0·93	3·71	55	Curve 1, fig. 18, liquid nitrogen.
Sn	Kahlbaum	0·02	—	—	—	—	—	—	0·22	0·23	1·0	75	Curve 1, fig. 19.
Pb	Kahlbaum	less 0·01	—	—	—	—	—	—	0·25	0·05	0·5	300	Curve 2, fig. 19. The values are very approximate.
Zr	Dr. de Boer	—	—	—	0·63	less 0·01	—	—	0·23	0·05	0·2	50	Very approximate.
Th	Dr. de Boer	—	—	—	0·66	above 0·03	—	—	0·266	0·155	0·78	120	Curve 3, fig. 19.

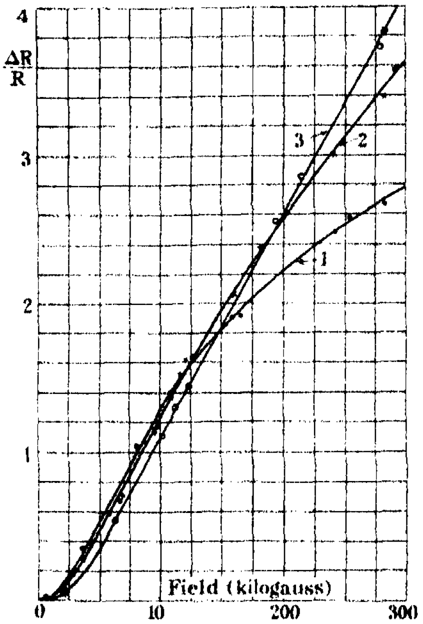

FIG. 17.—Graphite H ⊥ I.

Curve 1—Temperature of Liquid Air.
Curve 2—Temperature of Solid CO$_2$ and Ether.
Curve 3—Room Temperature.

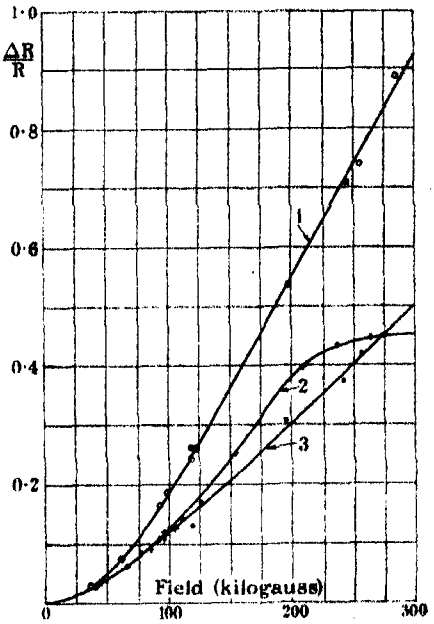

FIG. 18.—Germanium H ⊥ I.

Curve 1—Ge$_{\text{II}}$ Temperature of Liquid Nitrogen.
Curve 2—Ge$_{\text{I}}$ Temperature of Solid CO$_2$ and Ether.
Curve 3—Ge$_{\text{I}}$ Room Temperature.

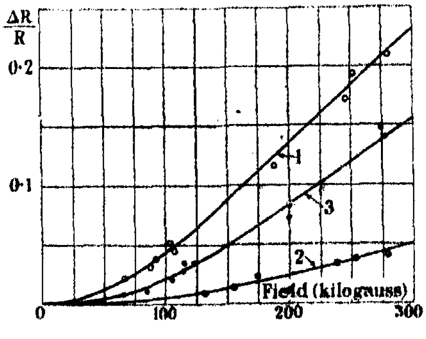

FIG. 19.—Tin, Lead, Thorium H ⊥ I.

Curve 1—Tin. Temperature of Liquid Air.
Curve 2—Lead. Temperature of Liquid Air.
Curve 3—Thorium. Temperature of Liquid Air.

Graphite.—It is not yet quite clear whether graphite has to be regarded as a metallic conductor or as a semi-conductor (conductors of the second order). However, the work of D. E. Roberts* shows that good natural crystals of Ceylon graphite behave more like a metal, having a negative temperature coefficient and a specific resistance smaller than mercury. Roberts has also shown that good Ceylon graphite crystals show a very large change of resistance, much larger than previously observed in ordinary graphite rods.† The influence of impurity and imperfection of the crystalline lattice appears to be very considerable. We had at our disposal no graphite crystals, and we only studied the change of resistance on a piece of the purest available Acheson graphite rod. A rod about 1 mm. in diameter and 6 mm. long was cut out from a lump. The contacts with this rod were made in the following way. Both ends of the rod were copper plated in such a way that a ring about 1 mm. wide was formed. This ring was scratched in two parts. The two inner parts were connected to the potential electrodes and the outer parts were connected to the power leads by means of thin silver wires soldered to the rings. The rod was placed in the holder as shown in fig. 3c. Our graphite rod was not pure enough to show the large change of resistance found in Roberts' experiment, neither did it diminish its resistance when brought to a lower temperature. The results of our experiments are given in Table IV and fig. 17. From the curves we see that in graphite the change of resistance follows, up to 100 kilogauss, exactly the same law as any other substance, *i.e.*, it changes from a square law to a linear one. Afterwards, however, there is a sharp bend in the curve. This bend is similar to that already observed by the author in bismuth (*loc. cit.*, p. 407, fig. 13) when it is impure. The analogy between the influence of impurities in bismuth and impure graphite in this case is complete, as in both cases this bending of the curve, as can be seen in fig. 17, happens at a smaller field when the temperature is lower. Thus in the case of carbon the phenomenon is also undoubtedly due to the impurities.

Germanium.—Germanium cannot be regarded as a true metal and this becomes evident if we consider its position in the periodic table. Germanium metal has a diamond like crystalline lattice. When the two elements above, germanium, carbon and silicon, are in the diamond like lattice they have no metallic conductivity. The element below germanium is tin. When it is in a diamond-like structure (grey tin) it is also non-metallic. Thus it appears that germanium also must be a non-metallic conductor (conductor of the second

---

[*] 'Phil. Mag.,' vol. 26, p. 158 (1913); 'Ann. Physik,' vol. 40, p. 453 (1913).

[†] Paterson, 'Phil. Mag.,' vol. 3, p. 643 (1902); Lows, 'Phil. Mag.,' vol. 19, p. 694 (1910).

order). It is very probable that the actual conductivity of germanium, which is observed, is entirely due to the presence of impurities, as we shall see also in the case of tellurium. We have not made a systematic study of this question, but it is suggestive when one compares the original measurement of the specific resistance of germanium given by G. Benedict,[*] of $30 . 10^{-6}$ at room temperature, with that given lately by C. C. Bidwell,[†] $89000 . 10^{-6}$, about 3000 times larger. As Bidwell used much purer germanium, it is seen that the effect of impurities is opposite to that in metallic conductors. Further purification of germanium will reduce its conductivity still more. The germanium which we used was obtained from Hilger and was fairly pure. Its spectroscopic analysis is as follows :—the total impurities were not more than 0·01 per cent., of which the main part was Ca 0·004 and Pb 0·001 per cent. Traces of potassium, carbon and silver were also found. The quantity of oxygen is unknown. Our germanium was less pure than that used by Bidwell and its specific resistance smaller than his determination. One rod, for example, gave us $2600 . 10^{-6}$. Germanium is extremely brittle and hard and it is quite impossible to cut out a rod from it. In order to prepare the rods we melted germanium in vacuum in a quartz tube having an appendix about 5 cms. long and about 1 mm. in diameter. When at about 900° the germanium melted, it was pressed into the appendix by letting in some air and the germanium then cooled and solidified. In this process it appeared that the quartz tube was not at all attacked by the germanium and probably no fresh impurities were introduced. Unfortunately, however, by this method we were unable to obtain long germanium rods. When the quartz tube was removed by dissolving it in hydrofluoric acid, the rod was found to be cracked and we obtained several small bits ranging from 1 to 5 mms. in length. The longest of these small pieces was taken for our experiments. This cracking of germanium suggests that at a higher temperature it has possibly a different modification from the diamond-like lattice and is like the modification of ordinary tin. When this modification changes to the other modification with the diamond lattice a change of volume may occur which accounts for the cracking. It is probable that this modification, if it exists, has true metallic properties as in the case of tin. When the rod was chosen it was extremely difficult to make contacts, but finally, after a number of attempts, we found it possible to solder silver leads to the end of the germanium rod by putting a drop of solder on the silver and rubbing the end of the germanium rod hard while the solder is in a liquid form. When the solder is solid the place seems to have a good contact. No potential leads were used as germanium had a very large specific resistance. The resistance in the contacts was not large, compared with the resistance of the rod. This was verified by measuring the drop of potential across the contacts by placing a sliding contact on the germanium rod. When we measured approximately the specific resistance of germanium we found that different pieces of the germanium rod had different specific resistances (differing by a factor of 2). This probably indicates that the impurities were unevenly distributed and therefore affect the conductivity of germanium in a different way. The experimental results are given in Table IV and in fig. 18. It is seen that germanium showed a rather large change of resistance. The two curves, 2 and 3, in fig. 18 are for solid CO_2 and room temperature and were taken with the same rod, Ge_I, having the highest conductivity. The experiment at liquid nitrogen temperature was performed with a different piece of germanium rod, Ge_{II}, as the first piece, Ge_I, broke owing to an accident during the experiment. This new piece had a larger specific resistance. In fig. 18 curves are given for the change of resistance of this rod. An examination of the curves in fig. 18 shows that the change of resistance in germanium follows the same law as for other conductors. First it is a square law and then there is the linear law. The curve for Ge_I at CO_2 temperature showed a characteristic bend in a field of about 250 kilogauss, this being probably due, as in the case of graphite and bismuth, to the impurities. Ge_I, which is more pure, having a larger specific resistance, did not show the bend even at the temperature of liquid nitrogen.

---

[*] 'Métallurgie,' vol. 7, p. 531 (1910).

[†] 'Phys. Rev.,' vol. 19, p. 447 (1922).

Further investigation would be of interest, but would have to be undertaken with a close examination of the crystalline and chemical state of the metal. This was outside the scope of this present research, but we are satisfied that in general germanium did not show any exceptional behaviour.

Tin.—Tin was extruded into a wire and placed in the holder (fig. 3A) in the usual way. The tin which we used was obtained from Kahlbaum and from spectroscopic analysis it was proved to be not less than 99·99 per cent. pure, this purity being probably quite sufficient to make our experimental results independent of the impurity. The results are given in Table IV and in fig. 19, curve 1, and the values of β and H_k are deduced only for the temperature of liquid air. It can be seen that even at this temperature the change of resistance is small. At room temperature the change of resistance in a field of 300 kilogauss is only about 2 per cent.

Lead.—Lead was also extruded into a wire and placed in the holder (fig. 3A). It was obtained from Kahlbaum and I am indebted to Prof. Papish who kindly made a spectroscopic examination of this metal. It was found to be spectroscopically pure except for very slight traces of copper. From a comparison with other samples of lead we found that its purity must be very high—probably about 99·999 per cent. The experimental results for lead are given in Table IV and in fig. 19, curve 2. It may be seen that lead had a very small change of resistance ; only 5 per cent. in a field of 300 kilogauss at the temperature of liquid air. We took a special interest in lead, as it is a supraconductor. The experiment was carried out very carefully, eliminating the induction phenomenon as completely as possible. In spite of the small change of resistance we were able to obtain an approximate curve, and this showed that lead follows the square law to rather higher fields. This made the separation of the β and H_k very difficult. The data which we give in the table have to be taken as very approximate, only indicating the order of the values.

Titanium.—A small lump of titanium was rolled into a small sheet and a strip ½ mm. wide was cut out. A holder (fig. 3A) with a square thread was used. To each end of the strip were spot-welded two short platinum wires and these were soldered to the copper leads of the holder. I am indebted to Dr. De Boer of the Phillips Research Laboratory for the titanium used in our experiments. Unfortunately, however, it was not very pure. The analysis of Hilger showed the presence of about 2 per cent. of silicon, the other impurities being negligible. This large content of silicon is probably sufficient to affect the results of the experiment to such an extent that they have no value. This specimen had also a very small temperature coefficient ; its resistance decreased only to 0·36 of its value at room temperature when it was dipped in liquid air. The following heavier element, Zr, has a much larger resistance change (0·23) when cooled to liquid air temperature, and with pure elements we ought to expect the opposite. The change of resistance of our titanium was only about 2 per cent. at the temperature of liquid air in a field of 300 kilogauss. Pure titanium, probably, gives a larger change of resistance. No deduction of β and H_k was made, and the results are not given in the table.

Zirconium.—Zirconium was used in a wire form and was placed in a holder similar to fig. 3A. Unfortunately we could neither solder nor spot-weld it. The contacts between the copper leads and the zirconium were made by screw contacts which were not good as zirconium is easily oxidised. This affected the results of our experiments considerably, especially as the change of resistance was small, so that the values obtained are probably subject to considerable experimental errors. The zirconium was kindly given to me, already in the form of a wire, by Dr. De Boer of the Phillips Research Laboratory, and was considered to be at least 99·9 per cent. pure. It gives a small change of resistance—only 5 per cent. in a field of 300 kilogauss at the temperature of liquid air. At room temperature no change of resistance could be determined. The values of β and H_k are very approximately given in Table IV.

Thorium.—A lump of thorium metal was rolled into a sheet and a strip was cut out. The holder (fig. 3A) with a square groove was used. Platinum wires were spot-welded in pairs to the ends of the thorium wire and were then soldered to the copper leads. I am indebted to Dr. de Boer who gave me this specimen which was considered to be 99·9 per cent. pure. It was very soft, like lead, and had good metallic properties, indicating its great purity. The change of resistance was 15·5 per cent. at liquid air temperature in a field of 300 kilogauss. At the temperature of CO_2 the change of resistance was only 3 per cent. The data for β and H_k are given in Table IV, and fig. 19, curve 3, represents the change of resistance at the temperature of liquid air.

Fifth Group of Elements.

This group of elements contains the two elements, bismuth and antimony, which are known to show a very large change of resistance in a magnetic field. Arsenic, which is above antimony in the periodic table, has the same lattice and is also strongly diamagnetic. It must, therefore, behave in the same way as the remaining two elements, although so far as I am aware this has not previously been tested.

We have carefully studied arsenic and antimony, whilst bismuth has already been studied in the form of crystals by the author, so that no special attention was paid to this substance again. Of the other metals in this group we were fortunate in obtaining vanadium and tantalum in sufficiently pure states to make the results valuable, but niobium we were unable to obtain at all. The results for this group are given in Table V and in figs. 20, 21, 22, 23, 24 and 25.

Arsenic.—For our experiments we required a rod of arsenic, 6 mm. long and ½ mm. in diameter. We found it difficult to cut out such a small rod from an arsenic crystal and we were also unable to extrude arsenic wires. We therefore made an attempt to cast it. As arsenic sublimates before melting this could not be achieved by ordinary methods, but we found it quite possible to do it in the following way. We took a thick-walled quartz tube, 3 mm. in diameter and a few centimetres long. One end of it was drawn to a thinner appendix a few centimetres long, having an inside diameter of about 0·5 mm. A few small arsenic crystals were placed in this quartz tube and it was then completely sealed up. Taking the necessary precautions to prevent poisoning by

Table V.—Transverse Effect in the Fifth Group of Elements (H ⊥ I).

Element.	Source.	Room temperature.			Solid CO_2 and ether.				Liquid air temperature.				Remarks.
		$\Delta R/R$ at 300 k.g.	$\beta \times 10^6$.	H_k in k.g.	R/R_0.	$\Delta R/R$ at 300 k.g.	$\beta \times 10^6$.	H_k in k.g.	R/R_0.	$\Delta R/R$ at 300 k.g.	$\beta \times 10^6$.	H_k in k.g.	
As	Kahlbaum, crystal	1·1	5·4	110	0·6	2·85	12·7	85	0·16	29	133	94	Curve on figs. 20, 21 and 22.
Sb	Kahlbaum	3·5	13·8	50	0·67	8·0	32·8	60	0·30	40	179	85	Curve on figs. 23, 24 and 25.
Bi	Hartmann & Braun	37	120	30	0·67	196	680	30	0·346	1360	4500	20	—
V	Dr. van Arkel	less 0·01	—	—	—	—	—	—	0·225	about 0·04	—	—	Liquid nitrogen.
Ta	Fansteel Corporation	less 0·01	—	—	—	—	—	—	0·3	about 0·01	—	—	Liquid nitrogen.

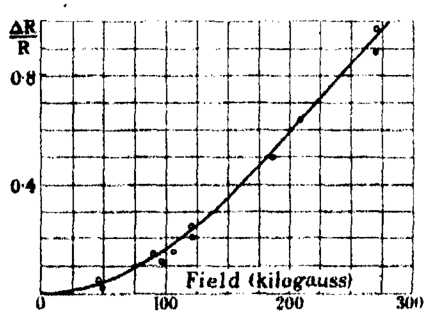

FIG. 20.—Arsenic H ⊥ I. Room Temperature.

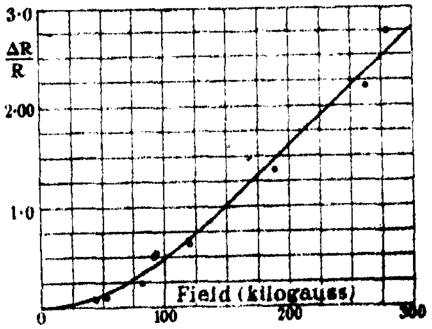

FIG. 21.—Arsenic H ⊥ I. Temperature of Solid CO_2 and Ether.

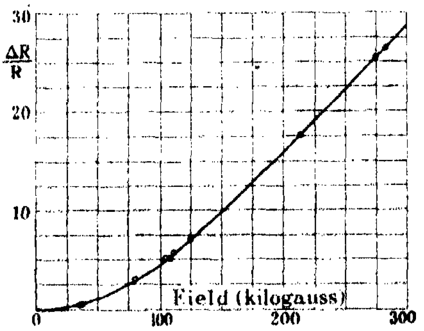

FIG. 22.—Arsenic H ⊥ I. Temperature of Liquid Nitrogen.

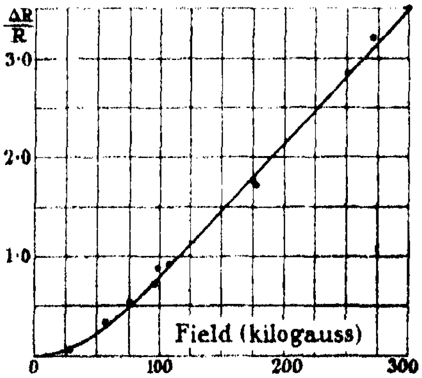

FIG. 23.—Antimony H ⊥ I. Room Temperature.

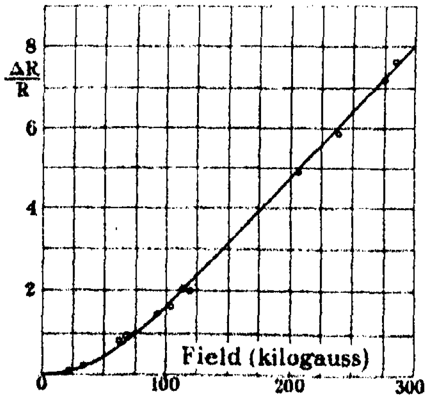

FIG. 24.—Antimony H ⊥ I. Temperature of Solid CO_2 and Ether.

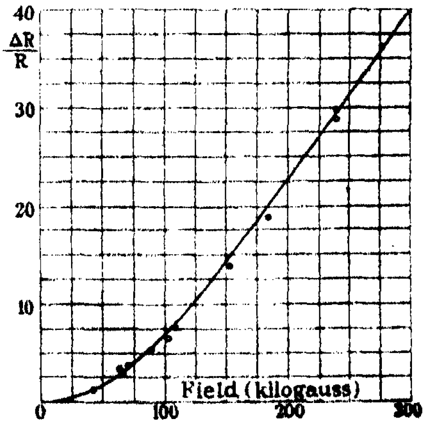

FIG. 25.—Antimony H ⊥ I. Temperature of Liquid Air.

the arsenic vapours in case the tube exploded, the tube was attached to an iron wire and placed in the flame of a Bunsen burner. Immediately it was hot the arsenic started to distil from the warm part of the tube to the cool part. By keeping the thin appendix tube cooler it was possible to arrange that it was completely filled by arsenic. Then, by further increasing the heating and still keeping the thinner tube slightly cooler so as to prevent the arsenic from leaving it, we increased the temperature to such a height that the larger part of the tube was filled with arsenic vapour which glowed in a very bright slightly reddish-yellow colour. The temperature was probably between 600 and 700° C. when it was observed that the arsenic had melted and a meniscus was formed in the tube. After heating the tube slightly more, in order to be sure that all the arsenic in the small tube had melted, the tube was taken out of the Bunsen burner flame in such a way that the outer end of the appendix tube which contained arsenic was cooled first. The tube was then broken or dissolved in hydrofluoric acid and a very good arsenic rod was obtained. It looked exactly like a metal of a bright silver colour. When breaking this rod we observed that it was a single crystal, and in all the four experiments which we made, the main cleavage plane of the crystal was always orientated parallel to the axis of the rod. This phenomenon is very similar to that observed in bismuth when the crystals are grown in glass tubes, as described in the author's previous paper (*loc. cit.*, p. 360). A small rod, 6 mm. in length and 0·6 or 0·7 mm. in diameter was used for the experiments. By means of the usual solder, silver wires could be soldered to this rod quite easily and thus form the potential and the power leads. The rod was placed in the holder (fig. 3c) in the manner previously described. It appeared that arsenic had a very high specific conductivity compared with antimony and bismuth, and the experiments were rather difficult as the rod had a very small resistance so that the transformer (fig. 1, T) in the current of the potential oscillograph had to be used. The arsenic used by us was obtained from Kahlbaum. At present we have no accurate data about its purity, but probably it is high, since its resistance diminishes considerably—to 0·16 of its value at room temperature, on being immersed in liquid air. The absence of bends in the straight part of the change of resistance curve (see figs. 20, 21 and 23) is also a strong confirmation of the purity of the material, as we know that these bends occur in bismuth when it is impure. The change of resistance in the magnetic field for arsenic follows the same law as all other substances, and as expected is large, so that the values of H_k and β as given in Table V can be easily obtained for the three temperatures at which the experiment was performed.

Antimony.—Antimony was extruded in a wire about 0·7 mm. in diameter. This wire was found to be extremely brittle and only a small piece of it in the form of a rod 6 mm. long was used. Silver wires were soldered to this rod by means of the usual solder and it was placed in the holder (fig. 3c). The antimony used was from Kahlbaum, and from a spectroscopic analysis, kindly made by Prof. Papish, was found to be very pure, containing only a trace of silicon. The experimental results for three different temperatures are given in Table V and in figs. 23, 24 and 25, and are fairly accurate. Antimony behaves in a similar way to arsenic and bismuth, showing a larger change of resistance than arsenic but a smaller one than bismuth.

Bismuth.—Bismuth has already been thoroughly examined in crystalline form in the author's previous paper (*loc. cit.*). In order to complete our results we made an experiment with an extruded wire of 1 mm. diameter, treating it in exactly the same way as antimony, holder (fig. 3c) being used. The bismuth used was the same as that used in the previous work and was obtained from Hartmann and Braun. We had it spectroscopically examined by Hilger and it was found to be of a very high purity, containing only 0·01 per cent. silver and practically no lead. It is quite possible, however, that even this impurity is sufficient to affect the results and the shape of the curve. It is possible that some of the bends previously observed* are due to the presence of these impurities. The actual value for β is probably somewhat larger for pure bismuth, particularly at lower temperatures. The results for the extruded bismuth wire are given in Table V.

Vanadium.—Vanadium was obtained in the form of a sheet out of which a strip was cut. The holder (fig. 3A) with a square thread was used. Four platinum electrodes were spot-welded to the strips and then soldered to the potential leads. I am indebted to Dr. van Arkel of the Phillips Research Laboratory who kindly supplied me with this sample. Its purity was considered to be high, but the exact purity is unknown. When immersed in liquid nitrogen it decreases its resistance to 0·225 of its original value at room temperature. This large decrease of resistance, together with the large flexibility of the strip indicated that we dealt with very pure vanadium.

In a magnetic field of 300 kilogauss at the temperature of liquid nitrogen, vanadium gave a very small change of resistance, amounting only to 3·5 per cent. At room temperature it gave no observable change of resistance. This small change of resistance made it impossible to define the values for β and H_k.

---

* *Loc. cit.*, figs. 12 and 13, p. 407, curves E'_2 and E_1.

Tantalum.—Tantalum was obtained in a wire about 0·2 mm. in diameter. Holder (fig. 3A) was used and four platinum wires were spot-welded to the tantalum wire and then soldered to the potential and power leads. The specimen of tantalum used was kindly given to me by Dr. Dushman, Research Laboratory of the General Electrical Company of America. This tantalum was made by the Fansteel Corporation of America and was fairly pure, containing less than 0·1 per cent. of impurities. When cooled down to the temperature of liquid nitrogen it diminishes its resistance to 0·3 of its original value at room temperature. In a magnetic field at room temperature tantalum gives no observable change of resistance. At liquid nitrogen temperature, in a field of 300 kilogauss, the change of resistance was about 1 per cent. The separation of β and H_k was impossible.

Sixth Group of Elements.

In this group of elements we were able to obtain all the metals except uranium in a sufficiently pure condition. We found that Cr, Mo and W show a very considerable change of resistance. This is very interesting as these metals are built from atoms belonging to the " transition group " of elements of the periodic table which, as a rule, show an apparently small change of resistance in the magnetic field. Chromium, molybdenum and tungsten form an exception. We took particular care to study these most accurately. The results are given in Table VI and in figs. 26, 27, 28 and 29.

Chromium.—Chromium could not be made into a wire and had to be used in the shape of a small rod cut out from a lump of chromium. The cutting can be performed by an ordinary high speed steel saw and a small piece cut out can be ground to the necessary shape with emery paper. A rod about 6 mm. long and about 0·5 sq. mm. cross section was used. Platinum electrodes were spot-welded to this rod, and holder (fig. 3c) was used. We had great difficulty in finding pure chromium. The first sample which we obtained from Dr. Francke of Frankfurt, Cr_I, was only 99 per cent. pure. It showed a very small change of resistance (3 per cent.) at room temperature. When cooled down by liquid air, the resistance of the rod increased by 1·15 times instead of decreasing, this being due to the considerable amount of impurity. I am indebted to Dr. van Arkel of the Phillips Research Laboratory for giving me a piece of chromium (Cr_{II}) which was purer than the previous specimen, but still far from being of the required purity to give the right order of change of resistance. On cooling by liquid nitrogen the actual resistance of Cr_{II} diminished to 0·8 of its value at room temperature. The change of resistance

Table VI.—Transverse Effect in the Sixth Group of Elements (H ⊥ I).

Element.	Source.	Room temperature.			Solid CO_2 and ether.				Liquid nitrogen.				Remarks.
		$\Delta R/R$ at 300 k.g.	$\beta \times 10^6$.	H_k in k.g.	R/R_r.	$\Delta R/R$ at 300 k.g.	$\beta \times 10^6$.	H_k in k.g.	R/R_r.	$\Delta R/R$ at 300 k.g.	$\beta \times 10^6$.	H_k in k.g.	
Cr_{III}	N.P.L.	0·3	—	—	—	—	—	—	0·083	4·40	17	44	Curve on fig. 26.
Mo	G.E.C., England	—	—	—	0·61	0·95	0·50	130	0·136	0·915	4·15	90	Curve on fig. 27.
W	G.E.C., America	—	—	—	—	—	—	—	0·195	0·938	4·10	78	Curve on fig. 28.
Te	Kahlbaum	0·36	1·4	10	1·04	0·41	2·15	10	1·15	0·33	2·95	8	Liquid air temperature. Curves on fig. 29.

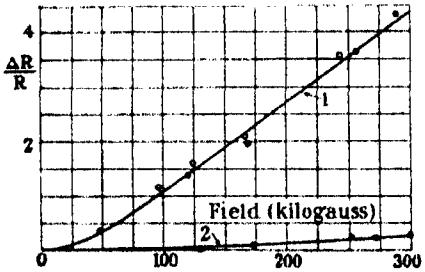

Fig. 26.—Chromium H ⊥ I.

Curve 1—Cr_{III} Temperature of Liquid Nitrogen.
Curve 2—Cr_{III} Room Temperature.

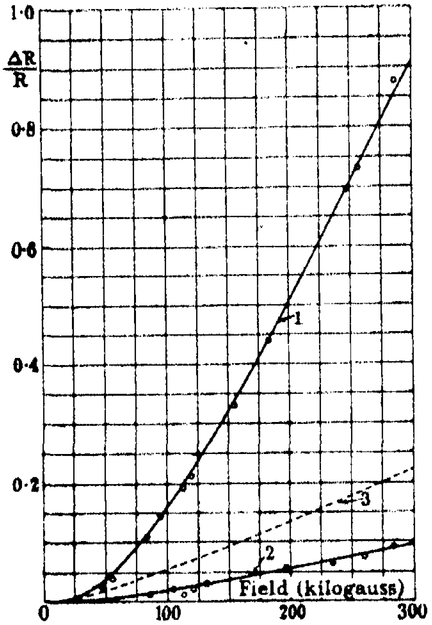

Fig. 27.—Molybdenum.

Curve 1—H ⊥ I. Temperature of Liquid Nitrogen.
Curve 2—H ⊥ I. Temperature of Solid CO_2 and Ether.
Curve 3—H ‖ I. Temperature of Liquid Nitrogen.

in a field of 300 kilogauss, at the temperature of liquid nitrogen was about 30 per cent., this being considerably more than for Cr_I. Finally Dr. Rosenhain of the National Physical Laboratory gave us a sample of chromium (Cr_{III}) which had been prepared electrolytically by Mr. Adcock. This specimen we found to be the purest. An analysis kindly given by Dr. Rosenhain showed that this chromium was spectroscopically pure, having possibly traces of nitrogen. The purity was evidently sufficient to be sure that the change of resistance in the magnetic field was not affected by impurities. The electrical properties of this chromium confirmed its great purity. When immersed in liquid nitrogen it changes its resistance to 0·083 of its value at room temperature. This is the largest change of resistance which we ever observed for a metal when cooled. The rod made of this chromium showed quite definite signs of flexibility. When tried in a magnetic field this chromium was found to be strongly paramagnetic. As chromium has several modifications a determination of the

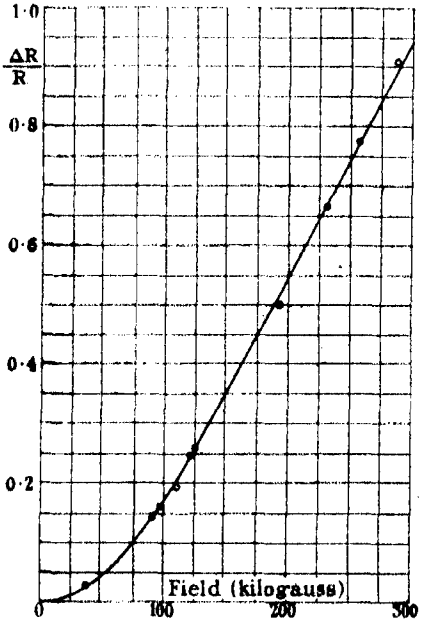

Fig. 28.—Tungsten H ⊥ I. Temperature of Liquid Nitrogen.

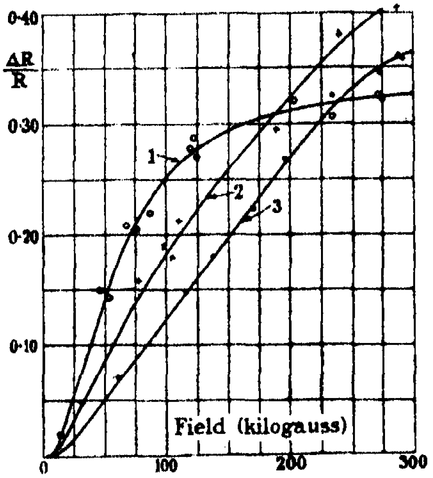

Fig. 29.—Tellurium H ⊥ I.
Curve 1—Temperature of Liquid Air.
Curve 2—Temperature of Solid CO_2 and Ether.
Curve 3—Room Temperature.

crystal structure was made. I am indebted to Dr. Bernal of the Mineralogical Laboratory for making the X-ray analysis of Cr_{II} and Cr_{III}. Both these chromiums were found to be of the α-modification. The change of resistance in a magnetic field at the temperature of liquid nitrogen was the largest which we observed for a metal, except As, Sb, Bi, C, and probably pure Be. In a magnetic field of 300 kilogauss its resistance increased 5·4 times. In spite of this large change of resistance the experiments were difficult as the small piece of chromium had an extremely small resistance—only 0·00023 ohm at the temperature of liquid nitrogen. The deflection of the potential oscillograph was very small, only a few millimetres, and even when the transformer T in fig. 1 was used very accurate readings could not be obtained. The induction effect had to be very carefully eliminated and the largest sensitivity of the apparatus had to be used. The results for Cr_{III} are given in Table VI and in fig. 26.

Molybdenum.—A molybdenum wire of 0·2 mm. diameter was used and fastened in the holder (fig. 3A) in the usual way. Four lengths of platinum wire were spot-welded to the molybdenum and soldered to the copper strips of the holder. We had some difficulty in obtaining pure molybdenum. The first sample from Messrs. Johnson & Matthey was not pure and gave rather a small change of resistance (47 per cent.) in a field of 300 kilogauss at the temperature of liquid air. A purer sample of molybdenum was kindly given by Dr. Gossling of the General Electrical Company Research Laboratory of Wembley. This was examined and found to be spectroscopically pure. It gave a larger change of resistance and the values of β and H_k obtained for it at a temperature of CO_2 and liquid nitrogen are given in Table VI and fig. 27. The experimental results are accurate owing to the high specific resistance of molybdenum.

Tungsten.—Tungsten was treated in exactly the same way as molybdenum. Two pieces of tungsten wire were tried, the first being a commercial sample. This gave a smaller resistance change than a second wire of pure tungsten, for which I am indebted to Dr. Dushman of the General Electrical Company Research Laboratory, Schenectady. It is well known that tungsten can be obtained in a very pure form. This gave a considerable change of resistance so that the experimental results are fairly accurate. The results are given in Table VI and in fig. 28.

Tellurium.—The conductivity of tellurium cannot be regarded as a metallic one. It has already been pointed out by Bridgman (*loc. cit.*, p. 369) that tellurium differs from all other conductors in that its specific conductivity diminishes with increased purity. A rise of temperature has also an opposite effect to that in ordinary metals—the electrical resistance of the substance diminishes. We have seen that germanium has the same properties so that the two substances are similar, and we shall see that in the magnetic field they also behave in a similar way. As our tellurium had a very high specific resistance, a thick rod about 3 mm. in diameter and 4 mm. long was used, this rod having a resistance of about 1 ohm. The potential and power leads were made by platinum wires melted into the tellurium. Bridgman found that good contacts can be made when a platinum wire is heated and dipped in tellurium. The rod was fixed in a holder similar to that shown in fig. 3c. The tellurium which we used was obtained from Kahlbaum and was kindly analysed by Prof. Papish, who found that it contained slightly less than 0·1 per cent. of copper and about 0·01 per cent. of silver. The change of resistance of tellurium in a magnetic field is considerable and follows a similar law to other conductors in the weaker fields, showing characteristic bends in stronger fields, which we find in impure substances (Bi, C, Ge). The bend is also shifted to weaker fields as the temperature is decreased. The values of β and H_k are given in Table VI and the change of resistance is represented by curves 1, 2 and 3 in fig. 29.

Seventh Group of Elements.

Manganese is the only element in this group which can be studied. It is not metal-like at all, but is very hard and brittle. A rod can be cut out of this substance by means of a circular diamond saw fitted to a milling-cutting machine. Silver wires can then be spot-welded to this rod. We had two samples of manganese. One was obtained from Kahlbaum and was found to be rather impure, containing, after examination by Hilger, up to 5 per cent. of aluminium. Dr. Bernal kindly examined it by the X-ray method and found it to be a mixture containing mostly α-modifications. No change of resistance was obtained at a temperature of liquid air, this being very possibly due to the large amount of impurities. I am indebted to Dr. M. Gayler of the National Physical Laboratory for giving me a piece of much purer manganese which contained only 0·01 per cent. impurity. Unfortunately this sample was filled with an immense number of cracks, which, as Dr. Gayler has explained to me, are due to the change of volume when the β-modification is transformed to the α-modification. With some difficulty a rod was cut out, but when spot-welded it broke to pieces, and no further attempts were made. We consider the study of manganese of great interest as it is the only available substance having metallic properties in this group of elements, and as soon as a convenient sample of this material is available the measurements will be undertaken.

The Eighth Group of Elements.

In this group of elements only iron, nickel, palladium and platinum are obtainable in the form of wire. The remaining elements, ruthenium, rhodium, osmium and iridium although prepared by the firm of Heraeus in an extremely pure state, cannot be prepared in flexible wire form. The change of resistance in the magnetic field of this group is very small, a few per cent. only, and can be adequately studied by the present method only if the metal is in the form of a wire having considerable resistance. This reduced our study to the Fe, Ni, Pd and Pt wires only. We will first describe the experiments with ferromagnetic metals which are known to show a considerable change of resistance in weak magnetic fields. Comparatively no large resistance change, however, is observable in strong fields.

Iron.—An iron wire about 0·2 mm. in diameter was fixed in the usual way in the holder (fig. 3A). The iron used was from Hartmann & Braun and no special study of its purity was made. At room temperature the increase of resistance in a field of 300 kilogauss was less than 2 per cent. At a temperature of liquid air, in a similar field, the increase of resistance was 5 per cent. The experimental results for this temperature are given by curve 1 in fig. 30. The points scatter a good deal, but it is quite definitely seen that at about 150 kilogauss the change of resistance practically reaches a constant value of 5 per cent. and the resistance then remains practically constant up to a field of 300 kilogauss. As the change of resistance was so small, no further attempts were made at this stage to get greater accuracy and to study the effect of the purity of iron.

Table VII.—The Transverse Effect in the Eighth Group of Elements (H ⊥ I).

Element.	Source.	Liquid nitrogen temperature.				Remarks.
		$R/R_{r.}$	$\Delta R/R$ at 300 k.g.	$\beta \times 10^6$.	H_k.	
Pd_I	Johnson & Matthey, hard.	0·22	0·06	—	—	Liquid air temperature.
Pd_{II}	Heraeus, annealed	0·17	0·10	0·43	75	Curve 1, fig. 31.
Pt	Heraeus, annealed	0·185	0·75	0·43	140	Curve 2, fig. 31.

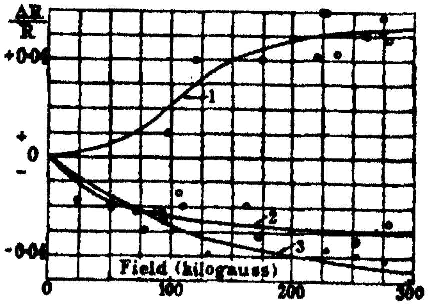

Fig. 30.—Iron and Nickel H ⊥ I.

Curve 1—Iron. Temperature of Liquid Air.

Curve 2—Nickel. Temperature of Liquid Air.

Curve 3—Nickel. Room Temperature.

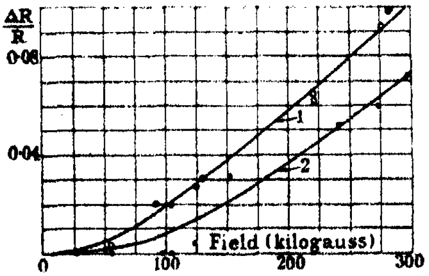

Fig. 31.—Palladium and Platinum H ⊥ I.

Curve 1—Palladium$_{II}$. Temperature of Liquid Nitrogen.

Curve 2—Platinum$_{II}$. Temperature of Liquid Nitrogen.

Nickel.—A nickel wire of 0·2 mm. in diameter was used in exactly the same way as iron wire. This was obtained from Hartmann & Braun. The change of resistance was also small and the results not very accurate. Curve

2 in fig. 30 gives the change of resistance at room temperature and curve 3 at the temperature of liquid air. It is to be observed that nickel is the only element we studied in which a decrease of resistance was found instead of an increase. This decrease was about 5 per cent. at room temperature and at a temperature of liquid air it was about 3 per cent. It can also be noted that an inverse relation between the temperature and the change of resistance exists. At lower temperatures there is a smaller change of resistance. It is probable that in ferromagnetic substances we are dealing with two phenomena of different origin which are superimposed. One is the usual increase of resistance as observed in any other metals, and which is more predominant in strong fields and at low temperatures. The other is of a ferromagnetic origin, mostly manifested in weaker fields and more or less independent of the temperature. A more detailed study, which is outside the scope of our present work, is required to clear up these points.

Palladium.—Palladium was used in wires 0·2 mm. in diameter, which were fixed in a holder of type shown in fig. 3A. The change of resistance of two specimens of palladium wire were measured. The first, Pd_I, obtained from Johnson & Matthey, of unknown purity, was hard drawn and showed at liquid air temperature in a field of 300 kilogauss an increase of resistance of 6 per cent. No separation of β and H_k was possible. The second specimen, Pd_{II}, from Heraeus, was at least 99·99 per cent. pure. It was already drawn into a wire of 0·2 mm. diameter, and we annealed it in vacuum by glowing at a very high temperature in order to get rid of included gases and to make the wire soft. It gave, at a temperature of liquid nitrogen in a field of 300 kilogauss, a change of resistance of about 10·5 per cent. The values for β and H_k could be determined and are given in Table VII and the corresponding curve in fig. 31. At room temperature no measurable change of resistance was observed.

Platinum.—Platinum wires of 0·2 mm. in diameter were fixed in the holder shown in fig. 3A. We tried three Pt wires. Before annealing we could only trace a change of resistance not exceeding 5 per cent. at liquid air temperature in a field of 300 kilogauss. After annealing in vacuum it was found possible to increase the change. We only give here the results for a platinum wire obtained from Heraeus annealed by glowing in vacuum. The purity of this platinum was not less than 99·99 per cent. The values of β and H_k have been approximately determined for the temperature of liquid nitrogen and are given in Table VII. The corresponding curve is given in fig. 31.

Alloys.—We have made no systematic investigation of alloys, but to complete our survey work we took two alloys, one being a solid solution and the other a compound. For the first we took a silver-gold alloy ; and for the other the compound of copper with arsenic known as the mineral domeykite, the chemical formula being Cu_3As.

Gold-silver Alloy.—We took 18-carat gold, which consisted of 75 per cent. gold and 25 per cent. silver. A wire about 1·5 mm. in diameter was mounted in the usual way in the holder (fig. 3A). No appreciable change of resistance was observed either at room temperature or at the temperature of liquid air. The change of resistance in a field of 300 kilogauss was less than 1 per cent. It is interesting to note that on cooling by liquid air the resistance of the wire diminished only to 0·87 of its value at room temperature.

Copper Arsenic Alloy.—A piece of domeykite was kindly given to me by Dr. Bernal of the Mineralogical Laboratory. It was an artificially prepared mineral according to the formula Cu_3As. The purity of this compound was unknown. It could be extruded into a wire, but was found to be very brittle. We therefore decided to cast a rod and put a piece of this compound in a sealed quartz tube with an appendix. The sealing of this quartz tube was necessary in order to prevent any arsenic being evaporated during the melting of the substance. The substance was cast in the appendix, the temperature of melting being about 600°. On removing the substance from the quartz tube we obtained a rod of about 1 mm. in diameter which was completely flexible. This indicated that the rod was a single crystal. A piece 6 mm. long was cut from it and placed in the holder (fig. 3C). The potential and power leads were soldered by using simple solder. This substance, at a temperature of liquid nitrogen, gave quite an appreciable increase of resistance of about 14 per cent. As we dealt here with a rod of small resistance the accuracy of the experiment was too small to determine β and H_k. The resistance of the rod on cooling down to liquid nitrogen temperature was reduced to 0·4 of its value at room temperature. Further experiments have not been undertaken, as the purity of this substance was unknown, and probably any excess of copper or arsenic over the required amount given by the formula Cu_3As will act also as an impurity. We simply regard this experiment as indicating that a metallic compound, unlike a solid solution, gives a quite definite change of resistance in a magnetic field.

(5) *The Change of the Resistance when the Current is Parallel to the Magnetic Field.*

The resistance of a metal changes also when the magnetic field is parallel to the current, this phenomenon being known as the parallel effect. In most cases the change of resistance in the parallel field is smaller than in the transverse field, although it probably obeys the same law. We did not investigate this effect as completely as we did the transverse effect, choosing only from each group of elements one which is the most easy to handle and which is considered to be the purest. The effect was studied at the temperature of liquid nitrogen using holder (fig. 3D), only substances available in the form of wires being chosen. The results are given in Table VIII and by the curves in figs. 5, 12, 14, 15 and 27 which are plotted by broken lines on the diagram, the transverse effect for the same metal being plotted by continuous lines.

Copper.—A bit of the same wire 0·15 mm. in diameter of hard drawn copper from Hartmann & Braun, as used for the transverse effect and called Cu_1, was used for these experiments. The curve obtained is given in fig. 7, curve 4, by means of a broken line. It can be seen that the curve is similar in shape to the curve obtained with the transverse field with the exception that it has a smaller slope β and a larger critical field H_k. It may be noted that the copper wire in this case when cooled to the temperature of liquid nitrogen had a resistance equal to 0·155 of that at room temperature. The same wire in the case of the transverse effect had a larger ratio $R/R_r = 0 \cdot 17$. This is probably due to the fact that, in mounting the wire on holder (fig. 3A) in the transverse effect, it was bent considerably and stretched in winding on the small ebonite cylinder *c*. In the case of the holder (fig. 3D) the wire was bent and stretched less, which accounts for this difference in the reduction of the resistance on cooling. This effect was observed in several other cases.

Table VIII.—The Parallel Effect (H || I).

Element.	Source.	Liquid nitrogen temperature.			Remarks.
		R/R_r.	$\beta \times 10^6$.	H_k.	
Cu_I	Hartmann & Braun, hard	0·155	1·3	146	Curve 4 on fig. 5.
Cd_I	New Jersey Zinc Co.	0·22	2·8	50	Curve 5 on fig. 12.
Al_{III}	Hartmann & Braun...............	0·121	1·4	43	Curve 4 on fig. 14.
Ga	Hilger	0·2	3·3	10	Curve 3 on fig. 15.
Mo	Dr. Gossling	0·135	about 1·0	—	Curve 3 on fig. 27.

Cadmium.—A bit of the same wire used in the transverse phenomenon, made of pure cadmium (New Jersey Zinc Company) and called Cd_1, was used for this experiment. The change of resistance is considerable and the curve may be considered as accurate. It is represented on fig. 12, curve 5, by means of a broken line and the date for β and H_k are given in Table VIII. We note again that β is slightly smaller and H_k is slightly larger than in the case of the transverse effect for the same wire.

Aluminium.—A bit of the wire, called Al_{III}, from Hartmann & Braun, was used. The curve for liquid nitrogen temperature is given in fig. 14 by means of a broken line and the values of β and H_k in Table VIII. Again a smaller change of resistance is observed than in the transverse field.

Gallium.—The same gallium, supplied by Hilger, which was used for the transverse effect was used in this experiment. A U-shaped wire was cast in an ebonite mould and then fixed in the holder (fig. 3D). The potential and power leads were small silver wires melted into the gallium and soldered to the copper strips of the holder. The results are accurate and are given in Table VIII and in fig. 15, curve 3. In the parallel effect also gallium has a very small value for the critical field (10 kilogauss), and it was the only element for which the parallel effect was slightly larger than the transverse. It is, however, possible that this could be partly accounted for by the difference in temperature. The parallel effect was observed at liquid nitrogen temperature and the transverse at liquid air temperature. As the constant β is very sensitive to the variations of temperature, the difference of three or four degrees may sufficiently affect its value to produce different changes in resistance.

Molybdenum.—We used a piece of the same reel of the purest molybdenum wire as was used in the transverse effect, and the results are represented in fig. 27, curve 3. The parallel effect in this case is much smaller than the transverse effect so that this curve cannot be taken as reliable since there is an experimental error due to the fact that the wire may not be set exactly parallel to the magnetic field. The small pieces of wire on the edge of the cardboard plate *i*, fig. 3D, which run perpendicular to the field, would also cause an error. This curve can only be taken as an indication of the fact that the parallel effect in molybdenum is about four times smaller than the transverse effect and accurate estimation of H_k is not possible.

(6) *Comparison with previous Investigations.*

Relatively few researches have been made on the change of resistance in magnetic fields for substances other than bismuth and the ferromagnetic elements, as the change of resistance obtainable is very small and is difficult to observe in the fields given by an ordinary electromagnet. The first successful experiments were made by Patterson[*] who studied a number of metals at room temperature in field strengths up to 30 kilogauss. He finds that the change of resistance obeys the square law, namely :—

$$\Delta R/R = \alpha H^2, \tag{C}$$

within the limits of accuracy of the experiments. This agrees in general with our result and with our formula (A) for weak fields ($H \leqslant H_k$) given in Section 3. If we compare the two formulæ we find that α is given in terms of β and H_k by

$$\alpha = \beta/3H_k. \tag{D}$$

From our experiments we know that the constant H_k is very strongly affected by the physical state of the metal; in a hard drawn copper wire for example, it may be several times greater than in an annealed one. This accounts for the discrepancy between the values given by Patterson and the later investigators. More recent investigations have been made by Grumnach[†] who worked at room temperature and noticed a departure in a few elements from the square law in stronger fields. Laws[‡] also mostly worked at room temperature, but made a determination of the constant α at the temperature of liquid air for cadmium and zinc. It is difficult to compare our results with those of previous investigators, as we can only enter the region of weak fields by extrapolation of our results, and this can be done only when the values of H_k and β are known. We have seen that these values could be accurately determined by our present method in most cases only at low temperatures. The second difficulty is that the value of α is strongly affected by the physical and chemical state of the substance, and the previous investigators give no adequate data about the state of the metals used. By extrapolating our results to low fields, however, we find that the order of agreement is as good as could be expected. For instance the value of α for zinc, at the temperature of liquid air or nitrogen, for the three different samples of zinc which we used, calculated by means of the formula (D) are: $\alpha = 1 \cdot 97 \,.\, 10^{-11}$ (Zn_{I}); $\alpha = 2 \cdot 2 \,.\, 10^{-11}$ (Zn_{II}); and $\alpha = 1 \cdot 34 \,.\, 10^{-11}$ (Zn_{III}). The value of α for zinc from Laws' experiment is equal to $1 \cdot 8 \,.\, 10^{-11}$ which lies between our values.

For cadmium we find also an agreement with our values at the same temperature, $\alpha = 3 \cdot 3 \,.\, 10^{-11}$ (Cd_{I}) and $\alpha = 9 \cdot 8 \,.\, 10^{-11}$ (Cd_{II}), Laws' value being $\alpha = 5 \cdot 1 \,.\, 10^{-11}$.

---

[*] 'Phil. Mag.,' vol. 3, p. 642 (1902).

[†] 'Ann. Physik,' vol. 22, p. 141 (1907).

[‡] 'Phil. Mag.,' vol. 19, p. 688 (1910).

De Haas* investigated very completely antimony crystals at different temperatures and in fields over 40 kilogauss. Comparing his data with ours, extrapolated to the same field strengths, we find that the increase of resistance observed by him is of the same order as ours, but larger. This is due to the difference in the physical state of the antimony. De Haas used crystals whilst in our experiment we dealt with extruded wires which have a large H_k, so that α was smaller. Heaps† studied tellurium and found $\alpha = 10{\cdot}5 . 10^{-11}$ and our experiments from the formula (D) give the value $\alpha = 5{\cdot}10^{-11}$. The difference is also such as could be expected from variations in the physical and chemical state of different specimens of tellurium, especially as we have seen that the conductivity of tellurium is probably produced by the presence of impurities.

There are also a number of investigations made by Kammerlingh Onnes‡ and his collaborators in the region of temperatures lower than liquid air where we have made no experiments and consequently no comparison is possible.

Finally it is interesting to note that it was suggested§ that the strongly diamagnetic substances give a larger change of resistance. Our experiments do not seem to confirm this suggestion. It is true that in the transition group of elements, which are strongly paramagnetic, we find a small change of resistance, but chromium, molybdenum and tungsten are exceptions which show a very large change of resistance. We specially tried our specimens of these metals and found them to be strongly paramagnetic. This paramagnetism could not be due to the presence of iron, as the elements were free of any ferromagnetic impurity. As another example, palladium, which is strongly paramagnetic, gives a larger change of resistance than diamagnetic lead and mercury.

This concludes the description of the experimental results and in the next Part we shall discuss the results and try to give a theory of the phenomena.

Summary.

(1) Some improvements on the method of measuring the change of resistance in strong magnetic fields are described.

(2) The change of resistance in a transverse field at room temperature, at temperature of solid CO_2 and ether and at the temperature of liquid nitrogen has been studied in the following metals: Li, Na, Cu, Ag, Au, Be, Mg, Zn, Cd,

---

* 'R. Acad. Amsterdam,' vol. 16, p. 1110 (1914).

† 'Phil. Mag.,' vol. 24, p. 813 (1912).

‡ See Leiden communications.

§ De Haas, *loc. cit.*

1

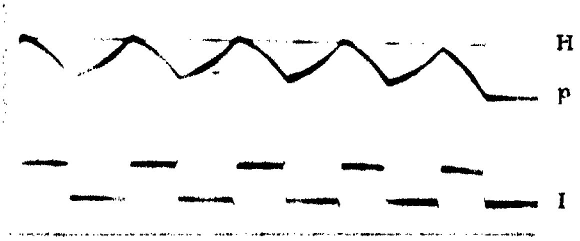

2

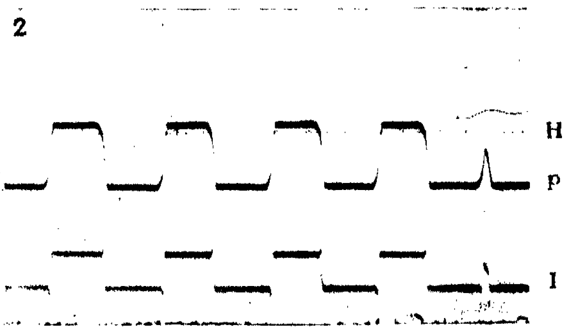

3

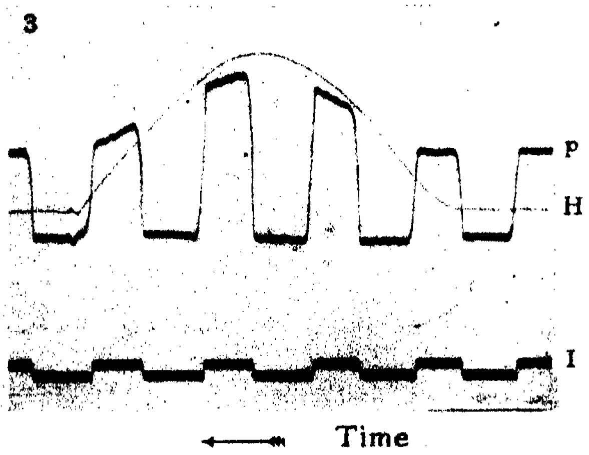

Hg, Al, Ga, In, Tl, C, Ti, Ge, Zr, Sn, Pb, Th, V, As, Sb, Bi, Ta, Cr, Mo, Te, W, Mn, Fe, Ni, Pd, Pt; in a gold-silver alloy and in Cu_3As.

(3) The change of resistance in a parallel field was measured for a few metals.

(4) It was found that in all the metals the change of resistance follows the same law which can be expressed by a formula which fits the experimental results quite well. This formula gives a square law in weak fields and a linear law in stronger fields.

(5) It has been shown that the physical change produced in a conductor by hardening and annealing has a strong influence on the phenomenon of change of resistance.

(6) The influence of the impurities is also very marked and was studied.

(7) A comparison with the results of previous experimental researches is given.

DESCRIPTION OF OSCILLOGRAMS, PLATE 17.

Oscillogram I.—An illustration of the influence of the self-induction in an ordinary transformer.

Oscillogram II.—An illustration of the influence of the self-induction in a specially wound transformer, as shown on fig. 2.

Oscillogram III.—The change of resistance in Ge at liquid nitrogen temperature. The maximum field is about 300 kilogauss.

The Change of Electrical Conductivity in Strong Magnetic Fields. Part II.—*The Analysis and the Interpretation of the Experimental Results.*

By P. Kapitza.

(Communicated by Sir Ernest Rutherford, P.R.S.—Received February 5, 1929.)

(1) *The General Theory of the Phenomenon of Change of Resistance in a Magnetic Field.*

It is seen from figs. 4 to 31 that all the curves of change of resistance, except for iron and nickel, are exactly similar in character. The increase of the resistance at the beginning is proportional to the square of the magnetic field, but later is directly proportional to the field so that the curve of change of resistance with field is practically a straight line. This change from the square to the linear law takes place gradually after a critical field H_k which for different substances ranges from 5 to 250 kilogauss. The phenomenon is so general that it would seem that it must have a general explanation. The natural explanation would be that when the field is weak, below the critical field (H_k), something hinders the appearance of the linear law which is the *True Law* of change of resistance and this law is fully established only when the field is well above the critical value. Our hypothesis to explain this is to assume an initial disturbance which already exists in the metal. Further, we assume that this disturbance is similar to that produced by the outside field and is distributed at random in the conductor. When the outside field is applied, the disturbance which causes the increase of resistance is now the vectorial sum of these two disturbances and the increase of the resistance is proportional to this sum. It is evident that in such a way the general character of the curves will be obtained. When the disturbance produced by the outside field grows larger than that of the inside field, we have the gradual approach to a linear law.

To embody these ideas in a quantitative form we assume that the already existing disturbance may be represented by a vector h, the meaning of which is that a similar disturbance can be produced by a magnetic field pointing in the same direction and having the same magnitude. For simplicity we assume the vector h to be distributed at random. If the vector h is pointing perpendicular to the current I then we assume that it will produce an increase of resistance proportional to $\beta_n h$, and if it is pointing parallel to the current it will produce an increase of resistance proportional to $\beta_p h$, where β_n and β_p are proportionally coefficients of the change of resistance for the transveres and parallel fields. If the vector h makes an angle α with the current I, the increase of resistance, as can easily be proved, will be proportional to

$$\beta_p h \cos^2 \alpha + \beta_n h \sin^2 \alpha. \tag{1}$$

It is evident that owing to the existence of this disturbance the metal will have an increased resistance which will equal

$$\frac{\Delta R_0}{R_i} = \tfrac{1}{2} \int_0^\pi (\beta_p h \cos^2 \alpha + \beta_n h \sin^2 \alpha) \sin \alpha \, d\alpha, \tag{2}$$

where R_i is the resistance of the volume of metal under consideration without the additional resistance produced by the h's. We shall call R_i the *ideal* resistance and ΔR_0 the *additional* resistance. It is evident that the resistance which we usually observe in the metal, R, is equal to the sum of R_i and ΔR_0.

After integration of (2) we obtain

$$\Delta R_0/R_i = \tfrac{1}{3}(2\beta_n + \beta_p). \tag{3}$$

Now when the outside field H is established, instead of the vector h in formula (1) we have to take the geometrical sum $H + h = \overline{H}$. To get the increase of resistance $\Delta R''$ produced by $\overline{H}$ we have to replace h in expression (1) by $\overline{H}$, and take the mean value for all orientations of h's.

We consider first the case when H is perpendicular to I, taking, as in fig. 32, I to be parallel to the Z axis and H parallel to the Y axis. We denote the angle between I and H by α, between h and H by γ, and the angle between the projection of h on the plane ZOX and I as θ, and calculate the increase of resistance $\Delta R''/R_i$ produced by the simultaneous action of H and h when h is distributed at random. We have to evaluate the following integral:—

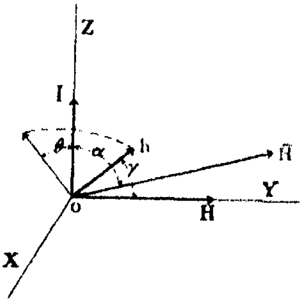

FIG. 32.

$$\frac{\Delta R''}{R_i} = \frac{1}{4\pi} \int_0^\pi \int_0^{2\pi} (\beta_n \overline{H} \cos^2 \alpha + \beta_p \overline{H} \sin^2 \alpha) \sin \gamma \, d\gamma \, d\theta. \tag{4}$$

If we express $\bar{\bar{\mathrm{H}}}$ and $\cos\alpha$ and $\sin\alpha$ in terms of the variables H, h, γ and θ, and re-arrange, we get the following integral:—

$$\frac{\Delta \mathrm{R}''}{\mathrm{R}_t} = \frac{\beta_n}{4\pi}\int_0^{\pi}\int_0^{2\pi}\sqrt{\mathrm{H}^2 + h^2 + 2\mathrm{H}h\cos\gamma}\,\sin\gamma\,d\gamma\,d\theta - \frac{\beta_n - \beta_p}{4\pi}$$
$$\int_0^{\pi}\int_0^{2\pi}\frac{h^2\sin^3\gamma\cos^2\theta}{\sqrt{\mathrm{H}^2 + h^2 + 2\mathrm{H}h\cos\gamma}}\,d\gamma\,d\theta. \qquad (5)$$

This integral, after exact evaluation gives two expressions, one of which is correct when $\mathrm{H} \leqslant h$, and the other when $\mathrm{H} \geqslant h$.

$$\frac{\Delta \mathrm{R}''}{\mathrm{R}_t} = \beta_n h\left(1 + \frac{\mathrm{H}^2}{3h^2}\right) - \frac{(\beta_n - \beta_p)}{3}h\left(1 - \frac{\mathrm{H}^2}{5h}\right) \quad \mathrm{H} \leqslant h, \qquad (6)$$

$$\frac{\Delta \mathrm{R}''}{\mathrm{R}_t} = \beta_n \mathrm{H}\left(1 + \frac{h^2}{3\mathrm{H}^2}\right) - \frac{(\beta_n - \beta_p)}{3}\frac{h^2}{\mathrm{H}}\left(1 - \frac{h^2}{5\mathrm{H}}\right) \quad \mathrm{H} \geqslant h. \qquad (7)$$

These two expressions form a continuous curve.

It is evident that the increase of resistance due to the outside field alone is equal to

$$\Delta \mathrm{R} = \Delta \mathrm{R}'' - \Delta \mathrm{R}_0. \qquad (8)$$

Inserting the values from (5), (6) and (7) in (8) we get the following two formulæ for $\mathrm{H} \leqslant h$ and $\mathrm{H} \geqslant h$:

$$\frac{\Delta \mathrm{R}}{\mathrm{R}_t} = \beta_n\frac{\mathrm{H}^2}{3h}\left(1 + \frac{1}{5}\,\frac{\beta_n - \beta_p}{\beta_n}\right) \qquad (\mathrm{H} \leqslant h). \qquad (9)$$

$$\frac{\Delta \mathrm{R}}{\mathrm{R}_t} = \beta_n\left(\mathrm{H} + \frac{h^2}{3\mathrm{H}} - h\right) + \frac{\beta_n - \beta_p}{3}\left(h - \frac{h^2}{\mathrm{H}} + \frac{h^4}{5\mathrm{H}^3}\right) \quad (\mathrm{H} \geqslant h). \qquad (10)$$

which represent the increase of resistance which should occur in a transverse magnetic field on our hypothesis. It is evident that the curve represented by this formula is of the shape required by the experiment. In the region of H varying from o to h the increase of resistance is proportional to H^2. In the region of H varying from h to ∞ we have a curve which gradually approaches a straight line and the change of resistance is proportional to H. The asymptote to this curve can be easily found from (10) to be

$$\Delta \mathrm{R}'/\mathrm{R}_t = \beta_n \mathrm{H} - \tfrac{1}{3}h\,(2\beta_n + \beta_p), \qquad (11)$$

or, if we compare (11) with (3) we find

$$\Delta \mathrm{R}'/\mathrm{R}_t = \beta_n \mathrm{H} - \Delta \mathrm{R}_0/\mathrm{R}_t. \qquad (12)$$

The following properties of this asymptote are very important for the interpretation of our results. The asymptote will intersect the axis of H's at a field H_k equal from (11) to

$$H_k = h\,(2\beta_n + \beta_p)/3\beta_n, \tag{13}$$

or from (3)

$$H_k = \frac{1}{\beta_n} \cdot \frac{\Delta R_0}{R_t}, \tag{14}$$

and the axis of $\Delta R/R_t$ at a distance

$$\Delta R/R_t = -\,\Delta R_0/R_t. \tag{15}$$

The parallel effect we treat in exactly the same way except that in this case the integration is rather simpler if we choose the axis of our polar co-ordinate system along I, when the angle θ does not come into the integral. The integration gives a very similar formula to that obtained for the transverse effect, only the second term has a plus sign and is twice as large, and if we again calculate the net increase in resistance $\Delta R/R_t$ we obtain the change of resistance in a parallel field to be

$$\frac{\Delta R}{R_t} = \beta_p \frac{H^2}{3h}\left(1 - \tfrac{2}{5}\,\frac{\beta_n - \beta_p}{\beta_p}\right) \qquad \ldots H \leqslant h, \tag{16}$$

$$\frac{\Delta R}{R_t} = \beta_p\left(H + \frac{h^2}{3H} - h\right) - \frac{2\,(\beta_n - \beta_p)}{3}\left(h - \frac{h^2}{H} + \frac{h^4}{5H^3}\right) \ldots H \geqslant h. \tag{17}$$

The curve is the same shape as in the transverse phenomena. It will follow first the square law for $H \leqslant h$ and for $H \geqslant h$ will straighten into a line. This curve will have an asymptote as before, the equation of which will be

$$\Delta R'/R_t = \beta_p H - \tfrac{1}{3}h\,(2\beta_n + \beta_p), \tag{18}$$

or if we take into account (3)

$$\Delta R'/R_t = \beta_p H - \Delta R_0/R_t \tag{19}$$

in which again we get for the critical field H_k the value

$$H_k = h\,\frac{2\beta_n + \beta_p}{3\beta_p} = \frac{1}{\beta_p}\,\frac{\Delta R_0}{R_t}. \tag{20}$$

and when $H = 0$

$$\Delta R/R_t = -\,\Delta R_0/R_t. \tag{21}$$

This expression (21) is exactly similar to (15) for the asymptote (12) in the case of the transverse field. Both asymptotes cut the axis of ordinates at a distance from the original equal to $\Delta R_0/R_t$ which only depends on the ratio of the additional resistance to the ideal resistance and is independent of the β_n, β_p, and h. It can also be shown that this property of the asymptote is not affected by any special distribution of h if it is not of constant value as is assumed in the calculations. This property of the asymptote is the most important one for our further analysis of the experimental results as it enables a determination of the ideal and the additional resistance to be made for a metal independently of the possible variations in h and β.

It is evident from expressions (9), (10), (16) and (17) that the shape of the curve for the change in resistance will be affected by the relative magnitude of the values of β_n and β_p. To investigate this point we shall first assume that $\beta_n = \beta_p = \beta_0$ when the formulæ are at once simplified. We find that the change of resistance produced by the transverse and parallel fields are similar and can be expressed by the following two equations, taking into account that from (13) and (20) $h = \mathrm{H}_k$

$$\Delta\mathrm{R}/\mathrm{R}_i = \beta_0\,\mathrm{H}^2/3\mathrm{H}_k \qquad \ldots (\mathrm{H} \leqslant \mathrm{H}_k), \quad (22)$$

$$\Delta\mathrm{R}/\mathrm{R}_i = \beta_0 \,.\, (\mathrm{H} + \mathrm{H}_k/3\mathrm{H}^2 - \mathrm{H}_k) \qquad \ldots (\mathrm{H} \geqslant \mathrm{H}_k). \quad (23)$$

The expressions for the asymptote will be also simplified, namely

$$\Delta\mathrm{R}'/\mathrm{R}_i = \beta_0\,(\mathrm{H} - \mathrm{H}_k) \quad (24)$$

or

$$\Delta\mathrm{R}'/\mathrm{R}_i = \beta_0\mathrm{H} - \Delta\mathrm{R}_0/\mathrm{R}_i. \quad (25)$$

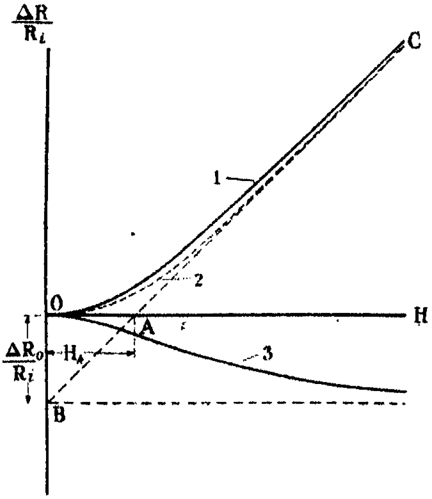

Fig. 33.

This curve is represented by a continuous line, curve 1, in fig. 33 and the asymptote by a broken line BC. From the equations (24) and (25) it is evident that the asymptote cuts the axis of abscissa at the point A such that $OA = H_k$ and the axis of ordinates at B where $OB = \Delta R_0/R_i$.

Comparing the expressions (22) and (23) with those which are given in Part I of this Paper in Section (3) and marked (A) and (B) which were used for plotting the curves in figs. 5 to 31, we see that they are identical, except that in the formulæ (A) and (B) we have in the left-hand side of the equations $\Delta R/R$ instead of $\Delta R/R_i$ and on the right-hand side β instead of β_0. This difference merely means that (22) and (23) give the change of resistance relative to the ideal resistance R_i and (A) and (B) give the change of resistance relative to the total resistance R. Formulæ (22) and (23) must be regarded as more convenient for expressing our results as we shall see later that the ideal resistance (R_i) is constant for a given element at a given temperature, and that the total resistance (R) may vary according to the physical and chemical state of the metal. It is easy to find a relation between the constants in the two formulæ, remembering that $R = R_i + \Delta R_0$ and using the equation (14) or (20), we find

$$R_i = (1 - \beta H_k)\, R \qquad (26)$$

and

$$\beta_0 = \beta\,(1 - \beta H_k) \qquad (27)$$

The change of resistance as given by the expressions (22) and (23) represent sufficiently closely the experiments described in the previous part. The difference in β_n and β_p, which has been measured in several cases, seems to have no great influence on the shape of the curve.

To see qualitatively how the change of resistance is affected by a difference in values of β_n and β_p in our hypothesis, we consider a limiting case namely, $\beta_p = 0$ when we obtain for the transverse field the following two equations. First from (13) we get $H_k = \frac{2}{3}h$ and the expressions (9) and (10) become

$$\frac{\Delta R}{R_i} = \frac{4}{5} \cdot \beta_n \frac{H^2}{3H_k} \qquad (H \leqslant \tfrac{3}{2}H_k), \quad (28)$$

$$\frac{\Delta R}{R_i} = \beta_n \left(H + \frac{H^3}{H^4{}_k}\frac{8}{81} - H_k\right) \qquad (H \geqslant \tfrac{3}{2}H_k). \quad (29)$$

The curve again follows the square law in the beginning, but the square law extends further than in the previous case (up to $1 \cdot 5\ H_k$) before it straightens out. The broken line, curve 2 on fig. 33, represents this case and is drawn to compare it with the case when $\beta_n = \beta_p$. It is seen that in the case $\beta_p = 0$ the asymptote is reached at lower fields.

Finally it is of some interest to consider roughly the case of the transverse effect when $\beta_n = 0$, but β_p is not equal to 0. Putting β_n in expressions (9) and (10) equal to zero it is seen that we obtain a decrease in the resistance instead of an increase. The change of resistance in this case is represented by the curve 3 in fig. 33. It is to be noted that this curve bears a certain resemblance to the curve obtained in the case of nickel (fig. 30), but we think that this resemblance is quite accidental and in the case of a ferromagnetic substance the phenomenon probably has a different origin from the one assumed in this case. The explanation which we give in Section (4) of Part I, where we describe the experiments with nickel and iron, is more probable.

In the case of the parallel effect, the fact that β_p is smaller than β_n will have a much stronger influence than in the transverse effect. It can easily be seen, for instance, that if $\beta_p = \frac{2}{7}\beta_n$ there will be no change of resistance observed before the critical point when the change of resistance suddenly starts.

(2) *Comparison of Experimental Curves with Theoretical.*

As has already been stated in Part I, Section (3), all the curves in the figs. 4 to 31, except in the cases of nickel and iron were drawn from the formulæ (A) and (B) which correspond to the formulæ (22) and (23) evaluated in the previous section on the assumption that $\beta_n = \beta_p$. In all these cases we saw that these formulæ represented the experimental facts within the limits of experimental error.

On the other hand the study of the parallel effect showed that in most cases β_p is smaller than β_n. If by formula (27) we transform the values of β given in the previous Part, which relate to the change of total resistance, to the values used in the previous section related to the ideal resistance, we obtain the ratio between the β_p's and the β_n's for the metals which we studied in the parallel field at the temperature of liquid nitrogen. These values are given in Table IX.

Table IX.

Element.	Cu.	Cd.	Al.	Ga.	Mo.
β_p/β_n	0·63	0·83	0·46	1·1	about 0·2

As we have already shown, a difference in β_n or β_p does not affect the general character of the curve—the square law in weak fields and the linear in strong fields—but only lowers the curve (*v.* fig. 33, curves 1 and 2). It can, however, easily be seen that this difference lies beyond the accuracy of the present research. For example, let us take one of the worst cases, aluminium wire

$\beta_p/\beta_n = 0 \cdot 46$. It can be shown that the largest difference between the assumed formulæ (22) and (23) $\beta_n = \beta_p$, and the true one, $\beta_n = 0 \cdot 46\ \beta_p$, will be at a field $H = 1 \cdot 2\ H_k$, where it amounts to 10 per cent. The increase of resistance of aluminium at $H = 1 \cdot 2\ H_k$ (42 kilogauss) is, according to our observation, 8 per cent., but ought to be $7 \cdot 2$ per cent., and the difference is just on the verge of the experimental error. Moreover, all these considerations are made on the assumption that the asymptote is already fixed, but actually there is a certain amount of latitude in the choice of the values of β and H_k which makes the difference spread over the whole curve. This example gives a sufficient justification for regarding the simple formulæ (A) and (B) or the corresponding formulæ (22) and (23) as a sufficient approximation for the present experiments. Unfortunately, other factors which are more difficult to evaluate than the difference in β_n and β_p may affect our results. In the first place we assumed that h is uniform and distributed at random. This is probably true in a non-crystalline substance, but it may not be true in the case of an orientated crystal. In order to estimate the influence of the orientation of h we made the simple assumption that all the components of h are perpendicular to I. After calculation this gave for the transverse effect a curve very similar in character to that obtained in the previous case for the transverse effect and which actually lies between curves (1) and (2) of fig. 33. On the other hand we also investigated another case where h has components only parallel to I and we again obtained a curve very similar in shape, only slightly lower than the previous one.

Finally it is also very unlikely that h has a constant value as we have assumed in our calculations. I am indebted to Mr. R. H. Fowler for performing the calculations in the case where h has a Gaussian distribution round its mean value. We will not give the mathematical analysis in this case, which is more complicated, but it has been proved that this also does not affect the general character of the curve; it merely raises the curve about the point $H = H_k$ and does not affect the square law in the beginning of the curve or the linear law at the end. h in this case will represent the mean value of the h's. In the cases when $\beta_p < \beta_n$ the influence of the Gaussian distribution of h's will tend to compensate the error made by assuming the simplifying formula $\beta_p = \beta_n$. This probably accounts for the slightly better agreement of the experimental results with the simplified formula than was at first anticipated.

Summing up all these considerations of the possible factors which influence the part of the curve of change of resistance below the critical field, we may say that it will be influenced by the ratio of β_n to β_p, and by variations in the magnitude of h and its distribution, but that the general character of the curve will be given by the simplified formula which we used. The agreement of the experimental results seems to justify our hypothesis.

The very important point which we will now discuss is how accurately we can draw the asymptotes to our curves. This question is of importance as the intersection of the asymptote with the axis of ordinates allows us to determine the additional resistance ΔR_0 and obtain the ideal resistance. Whilst this property of the asymptote is not affected by any variation in h and β, it is important to find the asymptote as accurately as possible. This depends on the influence of the simplification adopted, $\beta_n = \beta_p$, and on the values of β and H_k evaluated from the experimental curve. It can be shown for instance that if H_k is about 50 kilogauss, six times smaller than the normal field of 300 kilogauss with which we are working, the maximum error in the determination of H_k does not exceed 5 per cent., and is probably only one-half or one-third of this amount. When H_k is above 100 kilogauss, the maximum possible error rises to 10 per cent., and at 200 kilogauss it may be very large, above 30 per cent. By using the simplified formula in all cases we shall probably always slightly over-estimate the value of H_k. The β's are less affected by the simplification $\beta_p = \beta_n$.

(3) *The Additional and the Ideal Resistance.*

From our hypothesis it is evident that in a metal the observed resistance is the sum of the ideal resistance R_i and the additional resistance ΔR_0. As has been shown in Section (1), ΔR_0 can be easily obtained from the point of intersection of the asymptote with the axis of ordinates, and the value of ΔR_0 thus obtained is quite independent of the exact law which the change in resistance follows, and only depends upon the accuracy with which the asymptote is drawn to the curve.

In the first place we shall examine how ΔR_0 and R_i depend upon the physical state of the conductor. In fig. 5 curves are given for the change of resistance of copper for different stages of annealing. From a mere glance at these curves, it may be seen that the asymptote of a hard drawn wire must intersect the axis of ordinate at a point lower than that of an annealed wire. This shows that ΔR_0 is larger in a hard drawn wire. The actual values of ΔR_0 and R_i for different metals are given in Table X. To compare the values of ΔR_0 and R_i in different specimens of wire we determined their specific resistance at room temperature. We also had measured the change in the resistance (R/R_r, see Section (3) of Part I) which takes place when the substance is cooled, so that we were able to obtain the specific resistances σ at the temperature of liquid nitrogen or solid CO_2 and ether. These are given in Table X in the third column. This was divided in the ratio of R_i to ΔR_0 and thus the ideal specific resistance σ_i and the additional specific resistance $\Delta\sigma_0$ were obtained. They are given in Table X in columns four and five.

Table X.

Element.	Effect.	Specific resistance at liquid nitrogen temperature $\times 10^6$.			Remarks.
		Measured σ.	Ideal σ_i.	Additional $\Delta\sigma_0$.	
Cu_I	H ⊥ I	0·245	0·214	0·03	Annealed.
Cu_I	,,	0·300	0·223	0·077	Hard.
Cu_{II}	,,	0·258	0·214	0·044	Semi-hard.
Cu_I	H ∥ I	0·270	0·220	0·05	Hard.
Ag	H ⊥ I	0·284	0·265	0·03	Soft.
Ag	,,	0·352	0·300	0·052	Liquid air, hard.
Au_I	,,	0·487	0·452	0·035	Soft.
Au_{II}	,,	0·520	0·456	0·064	Liquid air, hard.
Al_I	,,	0·318	0·288	0·03	
Al_{II}	,,	0·394	0·315	0·08	
Al_{III}	,,	0·382	0·315	0·067	Liquid air.
Al_{III}	H ∥ I	0·342	0·321	0·021	The data are approximate.
Cd_I	H ⊥ I	1·51	1·31	0·20	
Cd_I	H ∥ I	1·51	1·30	0·21	

From the comparison of the ideal specific resistance for different specimens of Cu, Ag, Au and Al, it is seen that it has so nearly the same value for each metal that the observed variations can easily be accounted for by experimental error. On the other hand, the additional resistance is affected by the physical state of the wire, thus, for example, hard drawn copper has a value of $\Delta\sigma_0$ about 2½ times larger than the same wire when it is annealed.

This result confirms our hypothesis, for we should expect the ideal resistance to be a constant for a given temperature, whilst naturally the disturbing h's would account for the additional resistance having a higher value in a hard drawn wire where the physical disturbances are certainly more severe.

On our hypothesis also we must expect to have the same ideal resistance when the magnetic field is either transverse or parallel to the current, and this is confirmed by the experimental data, as can be seen from Table X, in the cases where we measured the parallel effect, namely, Cu, Al and Cd. The difference in $\Delta\sigma_0$ which we observe in the case of Cu and Al, for the same wire, in the transverse or parallel fields, is accounted for by the different way the wire was strained when set in the holder (figs. 3A and 3D). This point has already been discussed in the first part (Section 5, copper). The most accurate confirmation of the constancy of σ_i in both effects was obtained in cadmium, where the parallel effect was measured more accurately.

Table XI.

	$\Delta R_0/R_r$.					R_i/R_r.				
	Mg.	Zn.	Cd.	Al.	Mo.	Mg.	Zn.	Cd.	Al.	Mo.
Room temperature	0·126	—	—	—	—	0·87	—	—	—	—
CO_2	0·110	0·039	0·018	0·025	0·04	0·57	0·65	0·65	0·56	0·58
Liquid nitrogen	0·156	0·050	0·027	0·024	0·05	0·014	0·155	0·194	0·12	0·09

The next point to consider is how the additional and the ideal resistance are affected by the temperature. In Table XI are given the ratios of ΔR_0 and R_i to the room temperature resistance R_r. The values are given at room temperature, temperature of CO_2 and temperature of liquid nitrogen for those substances for which β and H_k could be evaluated at these temperatures. We see that $\Delta R_0/R_r$ has a fairly constant value at the three temperatures and there is only a slight tendency for an increase at lower temperatures. This slight increase can be accounted for either by the fact that at CO_2 and room temperatures the resistance change is small, making it impossible to separate β and H_k without a large error, and this error affects ΔR_0 considerably, since it is only a small fraction of the total resistance ; or, by the fact that we have not taken precautions to eliminate an increase in strain when the wires were cooled. It is quite probable that by winding the wire tightly on the small ebonite cylinder as in the holder (fig. 3A), extra strains due to thermal contractions are introduced which increase with decreasing temperature. This is supported by the observation which we already mentioned that all the wires mounted on holder fig. 3D, which were not curved and strained on winding, have a smaller ΔR_0 and a larger temperature coefficient. The importance of this possible strain was unfortunately realised too late. Thus we may conclude from our experiments that to a first approximation ΔR_0 is not affected by the temperature.

The ideal resistance, R_i, on the other hand, diminishes rapidly with decreasing temperature as is seen from Table XI. Since the ideal resistance appears to be independent of the irregular disturbances in a metal and is only a function of the temperature for a given element, it is of importance to know how it varies with the temperature. By assuming that the additional resistance is independent of the temperature we can determine the ideal resistance for room temperature, R_{ri}, and find its ratio to the ideal resistance at lower temperatures. The values of R_i/R_{ri} as obtained for liquid nitrogen temperatures are given for a number of elements of each group of the periodic system in Table XIII. We observe that the ideal resistance for the lighter elements is lowered much more rapidly than for the heavier ones and this is specially marked for Be, Mg and Cr.

(4) *The Residual and Additional Resistance.*

It is known that a hardened metal has a larger specific resistance and its value on cooling falls more slowly than for an annealed wire. Further it is known that when cooled down to very low temperatures approaching the absolute zero the resistance of a metal during the last 10 or 20 degrees does not alter appreciably and retains a value which was called by Kammerlingh Onnes the *residual* resistance. Experiment has shown that the residual resistance is largely affected by the physical state of the substances, exactly in the same way as our additional resistance ΔR_0, its value increasing in hard and impure metals. A closer comparison which we will now consider shows that our additional resistance and the residual resistance are identical.

Kammerlingh Onnes and Clay* were the first to separate the resistance into two parts, the first which, like ourselves, they called the ideal and the second part the residual or additive resistance. Later Nernst† adopted a very similar view and it was shown that the additive resistance varied in different specimens of wire of the same metal, increasing with the hardness and impurities but remaining approximately constant for a given metal at different temperatures, and as a rule not vanishing at absolute zero. The ideal part of the resistance for a given element was found to be a function of the temperature only. We see that there is a complete similarity between the ideal and additional resistances, derived from our hypothesis of the disturbing field. Comparing the actual values of ΔR_0 with the values of the residual resistance obtained for identical elements at low temperatures we find a further confirmation of the identity of these two quantities. In Table XII in the second row we give the ratio of the resistance of a metal at the temperature of liquid hydrogen (—253° C.) to its resistance at 0° C. These values are taken from the collection of data given by Kammerlingh Onnes and Tuyn* and we have chosen the largest and the smallest value observed. At the temperature of liquid hydrogen the resistance in most of the substances when no special precautions are taken for annealing reaches a fairly constant value equal to the residual resistance. In the first row we give the smallest and the largest value of the ratio of the additional resistance ΔR_0 to the resistance at room temperature R_r which was obtained from our measurement on the change of resistance for different specimens of the same element. Taking the room temperature instead of the temperature at 0° C., we actually obtain slightly smaller values for $\Delta R_0/R_r$, but as the difference is only on the average 5 per cent., we thought it was not worth while to introduce this correction, since only a rough comparison is possible in this case. Comparing the values of the additional and residual resistance for a given element given in Table XII we see that the identity of these values may be taken as confirmed. First, the magnitude of the two resistances is the same in all cases; secondly, the values of $\Delta R_0/R_r$ lie in most cases between the maximum and minimum values for the residual resistance, and finally if we compare more closely the data given in Kammerlingh Onnes and Tuyn's table with ours we find that wires treated approximately in the same way as in our experiments give values for the residual resistance very closely approaching the values of the additional resistance as observed by us.

---

* 'Vers. R. Ak. Wet. Amsterdam,' vol. 16, p. 169 (1908).

† 'Ann. Physik,' vol. 36, p. 395 (1911).

The only case where we have a larger value for $\Delta R_0/R_r$ than can be accounted for by experimental error is in the case of zinc. This, however, can be very easily explained by the large strains which occurred in this particular wire (Zn_I) when it was wound, these strains being manifested by the breaking of the wire on cooling as mentioned in Part I, Section (4). These large strains will account for the abnormally high value of the additional resistance in Zn_I.

The value for the residual resistances observed at low temperatures when the wire was very carefully annealed, much more carefully than in our experiments, is much smaller than the additional resistance which we observed. This would mean that these very well annealed wires should show a small additional resistance when studied in a magnetic field. The small value of ΔR_0 will cause the linear part of the change of resistance law to be reached for smaller magnetic fields, so that H_k will be smaller, and it is possible to estimate how

---

* Leiden Communication, Supplement No. 58 (1926).

Table XII.—Comparison of the Additional with the Residual Resistances.

	Li.	Cu.	Ag.	Au.	Mg.	Zn.	Cd.	Hg.*	Al.
$\Delta R_0/R_r$ (from magnetic phenomena)	0·01	0·023→0·018	0·015→0·013	0·016→0·012	0·15	0·05→0·014	0·027→0·009	0·037	0·024→0·011
R/R_0 (liquid hydrogen)	0·007	0·024→0·0015	0·023→0·0054	0·045→0·008	No data	0·016→0·007	0·024→0·02	0·049	0·06→0·04

	In.	Ga.	Tl.	Sn.	Pb.	Th.	Cr.	Mo.	W.	Pd.	Pt.
$\Delta R_0/R_r$ (from magnetic phenomena)	0·032	0·003	0·0163	0·017	0·04	0·025	0·06	0·05	0·06	0·006	0·011
R/R_0 (liquid hydrogen)	0·06→0·03	No data	0·03→0·029	0·012→0·011	0·047→0·03	No data	No data	No data	No data	0·051→0·009	0·02→0·006

* Extrapolated for solid mercury.

low the value of the critical field may drop. Tuyn and Kammerlingh Onnes* have studied the change of resistance for natural copper crystals and Meissner† single crystals of gold, cadmium and zinc. The residual resistances in these crystals are very small, ranging between 0·001 and 0·0001 of that at 0° C. We should expect from comparison with our data that the value for the critical field in such copper crystals will be about 5 kilogauss, and for gold crystals even smaller—about 3 kilogauss, so that they could be observed with an ordinary electromagnet. This indicates that most of the ΔR_0 is probably produced by the strains set up in the wire, but it is very probable that even in a mono-crystal there is some residual disturbance which is much smaller than in polycrystalline substances. It will be interesting to investigate how ΔR depends on the perfection of the crystal.

From these considerations we may give a probable explanation of the curious fact which we observed, namely, the exceptionally small value for the critical field (5 to 10 kilogauss) in gallium (Section (4), Part I). This, unlike most other metals used in our experiments, was cast in a spiral and very probably approached more than any other metal in its physical state to a mono-crystal.

(5) *The Additional Resistance and Supra-conductivity.*

Substances which are supra-conductors, mercury, thallium, tin, lead and indium were very carefully examined, but no exception to the general law in their change of resistance in magnetic fields was observed. They all had, however, a rather small increase in resistance, β being small.

If we compare the additional resistance ΔR_0 for these substances (see Table XII) with the resistance near the threshold of supra-conductivity, we find the values lie within the limits of the variation of the resistance at the threshold observed by Kammerlingh Onnes for different specimens of the same supra-conductor. This definitely indicates that the phenomenon of supra-conductivity consists in the disappearance of the additional resistance and the resistance of the conductor is then equal to its ideal resistance. If we take this point of view we must conclude that supra-conductivity is not a phenomenon confined only to the metals mentioned, but can exist in all metals, only it is masked by the additional resistance which does not disappear in most metals at low temperatures. The additional resistance from our point of view has a different origin from the ideal resistance. It is mainly, if not entirely, produced by the structural and chemical imperfections of the metal in the conductor whilst the ideal resistance depends on the temperature only and in all metallic conductors probably disappears continuously, but very rapidly, as the metal is cooled, so that at a sufficiently low temperature it has immeasurably small values. The lighter elements, as we see from Tables XI and XIII, diminish their ideal resistance with decreasing temperature much more rapidly than the heavier ones, and we should expect them to be better supra-conductors, except that nature has not provided a mechanism for annulling the additional resistance.

---

* Leiden Communication, vol. 181 (1926).

† 'Phys. Z.,' vol. 26, p. 689 (1925); 'Z. Physik,' vol. 38, p. 647 (1926).

The main cause of supra-conductivity therefore lies in the mechanism which makes the additional resistance disappear. On our hypothesis this additional resistance is very similar to the one produced by a magnetic field h distributed at random in the metal, and it is natural to expect that the disappearance of the additional resistance is more difficult when h is large. If, for instance, we increase the value of h by placing the conductor in an external magnetic field, the disappearance of the additional resistance may be hindered. This explains the influence of the magnetic field on the threshold temperature of supra-conductivity discovered by Kammerlingh Onnes,* which as expected from our views moves to lower temperatures in a magnetic field, this shift of the threshold temperature increasing as the magnetic field becomes stronger. From our experiments we also know that a strain set up in the metal is equivalent to an increase in the disturbing field h, and this ought again to move the threshold of supra-conductivity to lower temperatures. This was actually observed by Kammerlingh Onnes† in tin and indium.

At present unfortunately there is not an adequate theoretical basis to allow of speculation as to the mechanism which permits the additional resistance to be annulled. As we shall see from our next section, the theory of the increase of resistance produced by an external magnetic field is in an unsatisfactory state, and without an adequate theory it is scarcely possible to understand the true character of the disturbance produced by the h's and the origin of the additional resistance. We can only suggest a possible reason why supra-conductivity has so far been observed only in the heaviest elements. From our experiment these elements have small values of β, and this means that a magnetic distortion influences the conductivity in these elements less efficiently than in the others, although there are many other heavy elements, like platinum and gold, which have a small value of β but still are not supra-conductors.

---

* Leiden Comm., f. 139 (1914); also Tuyn and Kammerlingh Onnes, Leiden. Comm., No. 174a (1926).

† Leiden Comm., Suppl. No. 50a, 15 (1924).

Table XIII.—All Values are given for Liquid Air or Liquid Nitrogen Temperatures.

I Group.

Element.	R_i/R_{ri}.	$\beta_0 \times 10^6$.	$\Delta\sigma_a \times 10^{12}$.
Li	0·129	0·75	10†
Cu_1	0·13	2·23	3·4
Ag	0·17	1·57	4·3
Au	0·20	1·25	5·8

II Group.

Element.	R_i/R_{ri}.	$\beta_0 \times 10^6$.	$\Delta\sigma_a \times 10^{12}$.
Be*	0·06	82	—
Mg	0·016	150	120
Zn	0·15	5·1	40
Cd	0·20	3·95	68
Hg	—	0·6	47†

III Group.

Element.	R_i/R_{ri}.	$\beta_0 \times 10^6$.	$\Delta\sigma_a \times 10^{12}$.
Al	0·105	3·05	8·7
Ga	0·20	2·95	300†
In	0·20	1·00	26
Tl	0·22	0·75	44

IV Group.

Element.	R_i/R_{ri}.	$\beta_0 \times 10^6$.	$\Delta\sigma_a \times 10^{12}$.
Sn	0·21	1·08	41
Pb	0·22	0·6	51
Th	0·25	0·86	—

VI Group.

Element.	R_i/R_{ri}.	$\beta_0 \times 10^6$.	$\Delta\sigma_a \times 10^{12}$.
Cr	0·021	76	—
Mo	0·091	6·72	22
W	0·14	6·04	38

VIII Group.

Element.	R_i/R_{ri}.	$\beta_0 \times 10^6$.	$\Delta\sigma_a \times 10^{12}$.
Pd	0·165	0·45	74
Pt	0·167	0·46	86

* Beryllium was uninfluenced by impurities.

† The value for the specific resistance is taken from tables.

It is quite evident, however, that in the researches on supra-conductivity the greatest attention has to be directed to the physical and chemical state of the metal, and it is quite possible that by affecting the chemical and physical state of the metal, for example, by means of very careful crystallisation and by avoiding all possible strains, supra-conductivity may be produced in all metals.

(6) *The Significance of the Coefficients* β.

The β's which we evaluated from experimental results in the first part of this Paper and whose values are given in Tables I to VIII, determine (*v.* formulæ (A) and (B)) the increase of resistance (ΔR) relative to the normal resistance of the conductor R. On our hypothesis this resistance of the conductor R consists of two parts, the additional ΔR_0 and the ideal R_i, and only the latter, as we have seen in Section (3), is independent of the accidental disturbances produced by the *h*'s. In Section 1 we have used other β_0's which can be easily evaluated from the experimental β from equation (27). These β_0's connect the increase of resistance with the ideal resistance as can be seen from the expressions (22) and (23), and these values, being independent of the physical state of the conductor, will be discussed in this section. β_0 has, from the point of view of our hypothesis, the important significance of representing the true law of change of resistance when no disturbance exists in the metal. This can easily be seen from the two expressions for the change of resistance in transverse and parallel fields, (10) and (17), which in this case become identical with the equations (11) and (18) for the asymptotes when $h = 0$.

$$\Delta R_0/R_i = \beta_0 H. \tag{30}$$

The values of β_0 for liquid nitrogen or liquid air temperature for most elements are given in Table XIII. In most cases they differ from the experimental β's only by a few per cent.

Examining the properties of β we find first of all, as we have already described in Section 2, that β_n for a transverse field is different from β_p for a parallel field, and in most cases $\beta_n > \beta_p$. For copper, cadmium, aluminium, gallium and molybdenum we have already given the ratio of β_p to β_n in Table IX.

The β_0's are also a function of temperature and their values increase very rapidly with decreasing temperature. Thus by cooling from room temperature to liquid nitrogen, β_0 for Mg increases 100 times and for Be about 18 times. By cooling to the same temperature from the temperature of solid CO_2, β_0 increases for Zn, Cd, Ga and Mo by different values ranging from 12 to 5 times. One of the most striking properties of β_0 is that the value of β_0 for a given element is related to the position of the element in the periodic system. In Table XIII we see that in every column of each group β_0 decreases from the lighter to the heavier elements. This rule seems to have no exception, except beryllium, and in this case, as stated in Section 4, Part I, the experimental results are not final, owing to the impossibility of obtaining pure beryllium.

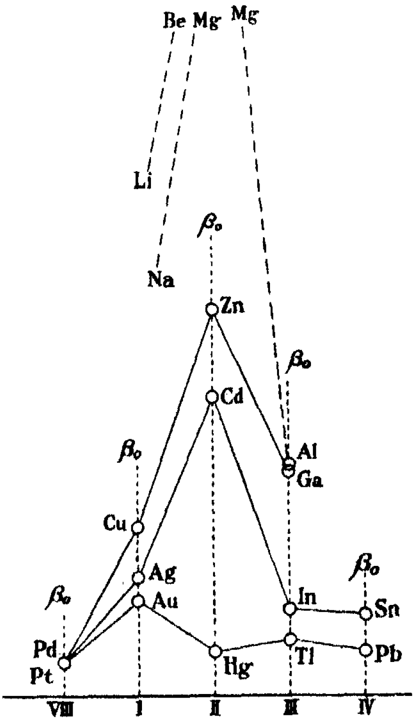

FIG. 34.

If we follow the variation of β_0 in a horizontal line we find that again there is a periodicity. To illustrate this periodicity of β_0 we plot in fig. 34 its value for each successive group of elements on one of a series of parallel lines and connect the points of neighbouring elements. From the curves so obtained it is noticeable that there is quite a definite periodicity in the value of β_0 for elements of different groups. The second group of elements apparently shows the largest β_0 and it gradually decreases when we come to the neighbouring elements in the first, third and fourth groups. The elements of the so-called "transition" group, such as titanium, vanadium, iron, nickel zirconium and tantalum have such a small value for β that we were unable to determine it by our present method. The only exceptions in this group are chromium, molybdenum and tungsten where we find a change of resistance as large as in the elements of the second group. Arsenic, antimony, and bismuth also fall out of our periodic relations. These exceptions will be discussed in one of the next paragraphs. In general it has to be admitted that since β_0 is a function of temperature a comparison of its values for different elements may not be very significant. However, the variation along the periodic table is very well marked and cannot be taken as purely accidental, and by a more detailed consideration of the periodic variation of β_0 we may find a satisfactory explanation of its meaning.

To explain it, let us consider a value which we shall call "the absolute increase of resistance per atom," $\Delta\sigma_a$. This value we take equal to

$$\Delta\sigma_a = \beta_0\sigma_i \text{A}/d, \tag{31}$$

where σ_i is the ideal specific resistance of the metal at the temperature of liquid nitrogen, A its atomic weight, d the density. It can easily be seen from (30) and (31) that $\Delta\sigma_a$ represents nothing else than the increase of resistance in a non-disturbed metal produced by a field of 1 gauss and reduced to the same numbers of atoms if calculated for different elements. The right-hand side of (31) can easily be transformed into our experimental units, namely

$$\Delta\sigma_a = \beta\text{R}/\text{R}_r \,.\, \sigma_r\text{A}/d, \tag{32}$$

where σ_r is the specific resistance at room temperature. The values of $\Delta\sigma_a$ for liquid air temperature are given in Table XIII. Most of them have been calculated by using the values of σ_r, obtained from measurements on the same wire which we used in our experiments. The others, marked by crosses, are obtained by using data taken from tables. As the specific resistance could not be measured in extruded wires (M_g, Zn, Cd, In, Tl, As and Pd) accurately, owing to the difficulty of determining the cross section of a non-circular wire, and as the possible specific resistance of our metals may differ from the values given in the table (Li, Hg, Ga) the values of $\Delta\sigma_a$ have (in general) to be regarded as approximate, with a possible error of 5 to 10 per cent. It is evident, however, that the values of $\Delta\sigma_a$ for each group have the same order of magnitude. In all the groups of elements we notice, from Table XIII, a tendency for the heavier elements to have a larger $\Delta\sigma_a$ than for the lighter ones, Mg, Cd and Ga being, however, exceptional.

Returning now to the periodic variation in β_0 we may see from (31) that

$$\beta_0 = \frac{d}{\text{A}} \cdot \frac{\Delta\sigma_a}{\sigma_i}. \tag{33}$$

and as $\Delta\sigma_a$ is more or less constant in a group of elements and even increases for the heavier elements, contrary to β_0, this means that $\sigma_i \text{A}/d$, the ideal atomic specific resistance, diminishes very rapidly as we go from the heavier to the lighter elements in each group. We have already pointed out in Section 3 that the ideal resistance R_i in the lighter elements drops much more rapidly to zero as the temperature decreases, and as R_i is proportional to σ_i this explains the variation of β_0 in each group of elements.

The $\Delta\sigma_a$'s no doubt give the most correct representation of the real magnitude of the phenomena of increase of resistance, as they represent the increase of resistance per atom, or per unit cell of the crystalline lattice for different elements. It can be seen from (31) that the β_0's become infinitely large as the ideal resistance σ_i becomes immeasurably small when at low temperatures the metal gradually reaches the supra-conductive state. The $\Delta\sigma_a$ behave in a different way at low temperatures; evidently they must keep finite and probably reach a definite value at absolute zero. This is confirmed by the way in which $\Delta\sigma_a$ depends on the temperature as can be seen from Table XIV below, where the values of $\Delta\sigma_a$ are given for temperatures of about 90° K. and 190° K.

Table XIV.

		Mg.	Zn.	Cd.	Ga.	Mo.
$\Delta\sigma_a \times 10^{13}$	190° K. (CO_2)	61	19	43	200	12
	90° K. (liquid nitrogen)	120	40	68	300	22

From this table we see that $\Delta\sigma_a$ varies more slowly with the temperature than 1/T so that it is influenced by the temperature much less than the β's or the ideal specific resistance. As the $\Delta\sigma_a$ for different elements are differently affected by the temperature it is impossible from our measurements to say what are the limiting values of $\Delta\sigma_a$ at absolute zero, but it is evident that as these values will be independent of the temperature a comparison of them will be of great value for the interpretation of the phenomena of conductivity. As, however, these limiting values can only be obtained by experiments at lower temperatures than we have available at present, we are only in a position to indicate very generally from a comparison of our data that the values of $\Delta\sigma_a$ will tend to the same order of magnitude in each group of elements and will probably have the smallest values in the first group, increasing towards a maximum in the middle of the periodic table.

(7) *The Influence of Impurities and Alloys.*

It is seen from the experimental data in Part I that impurities have a large influence on the phenomenon of change of resistance, but an exact study is very difficult since a small amount of impurity acts in a similar way to a distortion produced by hardening, stretching or bending of the conductor, and it is practically impossible to have two wires of the same physical state but with different amounts of impurity. It is also difficult to estimate the small amount of impurities with which we are concerned in a metal since this can be done only by spectroscopic analysis, and this as we have seen in the case of Zn and Cd (Section 4, Part I) misses the presence of oxygen and other gases, which no doubt influence the specific resistance of the metal.

But still from a general comparison of different data we have come to the conclusion that a small amount of impurity acts in a very similar way to a physical distortion and can be eliminated when the curve is analysed in the manner already described. This influence of small impurities can also be described as an increase in the disturbing h's which also increase H_k the critical field and thereby increase the additional resistance, but do not affect the ideal resistance (see *e.g.*, Al, Table X). There is again a similarity between the additional and residual resistances, this also being increased by impurities.*

This resemblance between the effect of impurities and physical disturbances is only true when the quantity of impurity is small, larger amounts of impurity having a different effect which is much more like a temperature effect in the sense that to the actual temperature an approximately constant temperature is added. This is manifested in the increase of R_i and decrease in β_0. A limiting case corresponds to an alloy mixture like the silver-gold which we examined, as described in Section 4, Part I. We have seen that this alloy shows no measurable change of resistance in a magnetic field, and also when cooled its resistance drops very little.

A different phenomenon was observed in a metallic compound. Of these we have studied only Cu_3As, and as described in Part I, Section 4, the experiment showed that this compound behaved much more like a pure metal, its resistance falling on cooling to liquid air temperature to 0·42 of its value at room temperature, while a considerable change of resistance was observed in a magnetic field. Thus in metallic compounds which form a crystal lattice with regularly distributed atoms of the two elements we may have probably the same undisturbed mechanism of conductivity as in a pure metal, and by more careful experimental examination we should probably find that all the properties of the additional and ideal resistance hold as observed in pure metals. The opposite happens in an alloy mixture where the atoms of the foreign substance replace the original atoms in the crystalline lattice in an irregular way. The binding between the atoms varies, the distance between them is also irregular and we have a picture similar to that produced by temperature agitation.

We have also seen that a larger amount of impurity may affect the general shape of the curve of change of resistance and cause the curve to have a sharp bend as noted, for instance, in the case of carbon and bismuth. The most probable explanation for this bend is that the impurities are not equally distributed and in the parts where the impurities are mostly concentrated the conductor is in quite a different state. The very impure parts which have an increased specific resistance are but little affected by the magnetic field, while the purer parts are very strongly affected. At the beginning the current is mostly flowing through the pure spots in the conductor, but at higher magnetic fields the distribution of the current is changed and it all passes through the impure parts of the conductor which have now the smaller specific resistance. It is evident that in smaller fields the change of resistance curve will be defined by the larger β's for the purer spots, and then gradually change to the smaller β for the impure spots. This results in a bend in the curve observed for impure carbon, bismuth and other elements.

---

* See Kammerlingh Onnes and Clay, *loc. cit.*

Thus it is seen that the influence of an addition of foreign metals in the conductor may be very complicated, and probably the present state of our knowledge of the phenomena is not adequate to understand it, so that it is sufficient to be satisfied with the fact that the influence of a small amount of impurities, which cannot be avoided, can be eliminated in determination of R_t and β_0.

(8) *The Change of Resistance in Arsenic, Antimony and Bismuth and Semi-conductors.*

Our hypothesis as given in Section 1 cannot be applied to arsenic, antimony, and bismuth without some reservation. Although the general shape of the curve can be satisfactorily expressed by formulæ (22) and (23), it can easily be shown that the meaning of the constants in the formulæ cannot be exactly the same as adopted for the other metals. The additional resistance ΔR_0 in this case, if we attempt to draw the asymptote, will be larger than R_t, which is, of course, impossible. The explanation of this exception is probably to be found in the different character of the conductivity of these three elements. We may note from the periodic table that the neighbouring elements of arsenic are germanium, selenium and phosphorus, all these being non-metallic conductors. Antimony also has two neighbouring elements, stable grey tin and tellurium, which are non-conductors. We ought to expect, therefore, that arsenic, antimony and bismuth will be non-conductors too, and actually there exists a modification of two of these metals which is non-metallic, having a cubic structure, the so-called yellow arsenic, stable below —70° C. and yellow antimony stable below —90° C. In bismuth a non-metallic modification has not yet been discovered. It is evident that the different behaviour of these three elements is closely connected with the difference of the bonds between the neighbouring atoms when they exist in the non-metallic cubic state and the usual rhombohedral lattice in the metallic state. The suggestion which we propose to make to throw some light on the mechanism of conductivity in these three metals is based on an analogy with the semi-metallic properties of the two neighbouring elements, germanium and tellurium, which we studied, and the properties of which were described in Section 4, Part I. Apparently tellurium or germanium begin to conduct if any impurities are present in the elements, and the conductivity may be increased several thousand times by increasing the amount so that the influence of impurities on these substances is exactly opposite to that observed in normal metals. The temperature also has an opposite effect, the resistance decreasing with increasing temperature. Thus in these metals in a pure state the bonds between the atoms are of such a character that an electron is not free to move under an applied electric field. The change produced in this bond either by impurities or by bringing the atoms to a closer approach by increasing their thermal agitation sets the electron free to move. We presume that in the non-metallic cubic arsenic and antimony the bonds between the atoms are of the same non-metallic character as in the pure germanium or tellurium, except that in As, Sb and Bi a different equilibrium distance between the atoms may exist and a displacement of the atoms by thermal agitation or impurities is not required for metallic conductivity to occur. It is well known that As, Sb and Bi, when in the metallic state, have a rhombohedral lattice which is very similar to the cubic and can be obtained from it by a very small elongation of one of the long diagonals of the cube. The most important difference from a cubic structure is due, however, to the distribution of the atoms. If we imagine a cubic lattice with eight atoms at the corners and displace four of them along the diagonal of deformation, we obtain the actual lattice of Bi, Sb and As. This deformation will cause some of the atoms to approach much closer to their neighbours. Thus the shortest and longest distances between neighbouring atoms differ in arsenic by 25 per cent., in antimony by 16 per cent., and least of all in bismuth by 11 per cent. The difference in distance between the atoms probably makes the binding of the closest atoms very " tight " and quite different in character from that of the atoms furthest apart which we may call " loose." It is of interest to note that the " tight " bonds probably account for the large diamagnetism of these substances as they may conceivably result in common electronic orbits between several nuclei, as was suggested by

Ehrenfest.* This point of view was adopted by the author in his previous work on bismuth crystals (*loc. cit.*), and seems to be fairly justified by experiment. The "loose" bonds probably account for the metallic conductivity in As, Sb and Bi, so that this picture can justify the assumption that the mechanism of conductivity in these elements must be similar to that observed in Te and Ge, in which "loose" bonds are produced by the separation of the atoms by heat motion or by the introduction of foreign atoms. This suggestion is confirmed if we compare the phenomena of change of resistance in these substances. We again calculate, as in Section 6, the $\Delta\sigma_a$, the absolute change of resistance per atom produced by a field of 1 gauss, as calculated from (32), only in this case it must be noted that in the Table XV we have given the value of $\Delta\sigma_a \times 10^8$ instead of $\Delta\sigma_a \times 10^{12}$, as the increase of resistance is much larger for these elements.

Table XV.

		C.	Ge.	As.	Sb.	Bi.	Te
$\Delta\sigma_a \times 10^8$	Room temperature	7	7	0·25	1	30	600
	CO_2	8	9	0·35	1·5	110	900
	Liquid air	10	20	1·0	3·8	400	1400

From this table we see that the values of $\Delta\sigma_a$ for the As, Sb, Bi group of elements lie well between the two elements of the neighbouring group, Ge and Te, and that the largest absolute increase in resistance is given not by bismuth, as is usually thought, but by tellurium, this being due to the very high specific resistance of the latter. Thus the absolute increase of resistance is of the same order for the elements of Table XV, but is about 10,000 times larger than is observed in normal metals. This fact alone is sufficient to indicate a difference of mechanism of change of resistance between the semi-conductor and the true conductor. The main difference on our picture between this group of semi-conductors, with which Bi, Sb and As have to be associated, and normal metals, is that in these semi-conductors the bonds between atoms are unsymmetrical, owing to the lack of symmetry of the crystal structure, each atom having both "tight" and "loose" bonds. In the true metals, which have a more regular lattice, each atom is more symmetrically surrounded by other atoms and all the bonds are of the loose type characteristic of the higher specific conductivity of the metal.

It is probable that in the case of semi-conductors the magnetic field has a direct influence on the equilibrium between the tight and loose bonds, thus affecting the position of the atoms in the crystal lattice. This may account for the impossibility of interpreting these results on our main hypothesis. For more definite conclusions, however, further experiments are required to find if any kind of alteration in the other magnetic properties of this group of elements occurs in a strong magnetic field. No doubt if the crystal structure is actually affected we may find magnetostriction phenomena, or a change in the diamagnetic constant in strong magnetic fields.

---

* 'Physika,' p. 388 (1925).

There is an experimental fact which supports the view that the behaviour of the semi-metallic group differs from the normal in a magnetic field. In the author's previous work (*loc. cit.*, p. 421) it was found that the parallel field produced a very small increase of resistance in bismuth crystals. This increase shows a saturation effect and is strongly affected by the perfection of the crystal, and it was even suggested that it is possible that the small residual effect observed in the best crystal rod was due to the still existing imperfection of the crystal lattice. In this way Bi differs from all the rest of the normal metals which show little difference between the parallel and transverse field.

From our point of view graphite has to be regarded also as a semi-conductor, as in the normal diamond lattice the bonds between the atoms are of a "tight" character and no conductivity is observed, but in the irregular graphite lattice there are present both "tight" and "loose" bonds and the latter account for the conductivity. As seen from Table XV graphite has a $\Delta\sigma_a$ of the same order as the other semi-conductors and is also strongly diamagnetic.

(9) *The Bearing of the Present Researches on the Theory of Metallic Conduction.*

There are two main issues from our researches which we think are of importance for the theory of metallic conductivity. The first is the phenomenon of increase of resistance in magnetic fields by itself. The second arises from the fact that the work provides a method of separating the additive and the ideal resistance from the total resistance usually measured, so that the properties of these two resistances become more evident and have to be explained by a theory of metallic conductivity.

First we will discuss the law of change of resistance. On the hypothesis which we adopted as described in the first section, and which seems to be well justified by experiment, we must admit that ***the increase of resistance of a metal in a magnetic field is directly proportional to the first power of the applied magnetic field***, both in a transverse and in a parallel field. This could not be observed previously owing to the fact that some disturbances similar to that produced by a magnetic field already exists in the metal, and to trace the linear law stronger magnetic fields have to be applied than those which account for the disturbance in the metal. Experiment shows that in most cases these magnetic fields are beyond the range covered by an electromagnet.

The theories for the change of resistance as given originally by J. J. Thomson* and Ganz† and more recently by Sommerfeld‡ are based on the assumption that the paths of the free electrons are deflected in their motion in the magnetic field. They disagree with experiment in that they predict a square law and the actual effect calculated is too small to account for the experimental results. This shows that the phenomenon has a different source than the obstruction of the paths of electrons.

Before discussing the possible explanations of the phenomena we must point out that there is an important experimental result which limits the scope of speculation, namely, that the disturbance produced by an outside magnetic field has to be similar in character to that produced by distorting the metal by strains or stresses or by introducing small quantities of foreign atoms. It must be pointed out that this inside distortion cannot conceivably be accounted for by an internal magnetic field, as this must be equal in magnitude to H_k which in some cases reaches values above 100 kilogauss, a value much larger than can be accounted for by internal fields of true magnetic origin.

Now let us take the modern view of metallic conductivity and examine one after the other the effects of the magnetic field on all the factors which determine the resistance of the metal and which are likely to be affected by a magnetic field. We take first the number of free electrons. It is easily seen that any alteration of the number is quite improbable, as in this case the transverse and the parallel fields would change the number of free electrons by the same amount and we should not have $\beta_n > \beta_p$ as observed. Secondly, in the recent works on electrical conductivity by Houston§ and Bloch‖ the resistance of a metal is accounted for by the irregularity in the crystal lattice produced by the thermal agitation of atoms. It is very difficult, however, to suppose that a uniform magnetic field may have the effect of increasing the irregularity in a crystal lattice, particularly if we consider a cubic lattice where the bonds with the neighbouring atoms are all similar and a magnetic field will affect them all equally, whereas we have seen that cubic metals like Cu, Ag, Au, Al, Cr, Mo, W change their resistance equally with the non-cubic ones.

---

* 'Rapports, Congrès Internat. Phys.,' vol. 3, p. 138 (1908).

† 'Ann. Physik,' vol. 20, p. 293 (1906).

‡ 'Z. Physik,' vol. 47, p. 43 (1928).

§ 'Z. Physik,' vol. 48, p. 449 (1928).

‖ 'Z. Physik,' vol. 52, p. 555 (1928).

Finally, we are left with the possibility that the magnetic field affects the scattering power of each individual atom. This possibility has already been discussed in our previous paper on bismuth crystals (*loc. cit.*, p. 436). The main arguments are that it is known from the Ramsauer effect that the scattering power of an atom for the electrons depends upon the symmetry of its structure, and it is conceivable that a magnetic field will somehow or other disturb the symmetry of an atom and increase its scattering power. The increased scattering power of an atom will decrease the free path of an electron and thus increase the resistance of the substance. This point of view was used as a working hypothesis in our experimental work, and the main idea of this research was to see whether the action of a magnetic field is an atomic effect. It is evident that in this case it has to be connected with the structure of the atom which is determined by the position of the element in the periodic table. First we thought to find a justification of our view in the periodic behaviour of β as given on fig. 33, but, as shown in Section 6, the reason β follows a periodic law depends mainly on the periodic variation of the ideal resistance, a very interesting fact by itself, but irrelevant for the support of our view. The values which we really have to consider to characterise the change in scattering power of an atom in a magnetic field are the $\Delta\sigma_a$, which define the absolute increase of resistance per atom, produced by a field of 1 gauss. These values were given in Table XIII and, if we exclude the metals, namely, Hg, Ga and Mg, show a definite periodic behaviour. In each group of elements the values of $\Delta\sigma_a$ have the same magnitude which increases from the lighter to the heavier elements. The exceptions of Ga and Hg can be more or less explained by the unusual crystal structure, but it is more difficult to account for Mg. The greatest difficulty in interpreting the values of $\Delta\sigma_a$ lies in the fact that they are functions of the temperature, and a fair comparison can only be made when experiments are made at such low temperatures that the $\Delta\sigma_a$'s have reached their limiting values. If we consider the influence of the temperature on $\Delta\sigma_a$ in more detail it seems to indicate that at low temperatures a periodic variation in $\Delta\sigma_a$ will be found. The results at present available seem rather in favour of our hypothesis.

Another point which supports the view that the change of resistance is connected with atomic phenomena lies in the fact that the elements of the transition group show very little change of resistance. The only exceptions are chromium, molybdenum and tungsten, which are also marked by some peculiarity in their atomic structure.*

There is no difficulty on the hypothesis under discussion in explaining the other phenomena observed in a magnetic field. The fact that the transverse phenomenon may differ in several cases from the parallel phenomenon can be accounted for by the fact that the scattering power of an atom may differ for electrons moving along and perpendicular to the axis of magnetic disturbance. The vectorial character of h which produces the additional resistance can be explained from our point of view since, owing to the asymmetry of the lattice produced by strains or the presence of foreign atoms, the individual atoms are not symmetrically bound to their neighbours, and this asymmetry in the bindings produces a distortion of the symmetry of the atom itself, which is similar to that produced by an outside magnetic field and can be added vectorially to it.

The explanation of the additional or residual resistance, ΔR_0, has also been attempted by Nordheim† on the modern theory of electric conductivity as given by Bloch (*loc. cit.*). He suggested that the residual resistance is due to the disturbance of the crystal lattice owing to the presence of foreign atoms, but it must be admitted that there are certain difficulties in this explanation, since it is difficult to suppose that a disturbance of the lattice may be vectorially added to an outside magnetic field, as we have already pointed out that at present we have no evidence that a uniform magnetic field can disturb the symmetry of a crystalline lattice.

The last point to discuss is the ideal resistance R_i, which is independent of the physical and chemical disturbances in the substance and for a given metal is a function of the temperature. This makes this value a very important one for any theory of metallic conductivity. We have not studied the exact way in which R_i varies with the temperature, but it is evident from the comparison of its value at three temperatures for which measurements were performed (290°, 190° and 88° K.), that at lower temperatures it drops very rapidly to 0 (probably exponentially). The drop in the lighter elements is specially rapid, for example, as we see from Table XI, when the temperature changes from 190° K. (CO_2) to 88° K. (liquid nitrogen), R_i diminishes in Mg by 40 times. In other substances it is less, Mo about 6, Al → 5, Zn → 4 and Cd 3 times.

In Section 5 we showed that R_i at sufficiently low temperatures probably must diminish continuously to immeasurably small values when the substance is a supra-conductor. Although there is no evidence that this is not the case for all the normal metals, the present theory of conductivity seems not to be in agreement with such a behaviour. It is therefore important to point out that there is no necessity for a sudden jump in R_i for supra-conductivity as the jump which is observed is produced by a sudden disappearance of ΔR_0. The mechanism of this can be only understood when the increase of resistance produced by a magnetic field and the origin of the disturbances receive a complete explanation.

---

* See, for instance, Hund, 'Linnenspektren.'

† 'Naturw.,' p. 1042 (1928).

(10) *Conclusion.*

In this research, as can be seen, we did not attempt to develop a very accurate method of study of the change of resistance in the magnetic field. Our main object was to make a survey of this phenomenon over the available elements of the periodic system so as to undertake at a later date a more detailed study of a few elements chosen properly with a definite working hypothesis and a clear view of the experimental requirements. It is evident from the present research that the phenomenon of the change of resistance in a magnetic field is much complicated by the irregular disturbances already existing in the metal, and the true simple phenomenon occurs only above 100,000 gauss, a region which can be attacked by our present method, but for a more accurate study it is desirable to reduce the initial disturbance to as small a value as possible. This can probably be achieved by using a very pure substance in mono-crystalline form, and as already discussed it will be possible in several cases to reach the linear part of the change of resistance curve in weak magnetic fields obtained with an ordinary electro-magnet. It is also evident that the greatest interest lies in researches at lower temperatures than have been used in the present work, in the region where $R_i = 0$ and $\Delta\ \Delta a$ reaches a constant value, and we must expect that such experiments will help us to form a more definite opinion about the mechanism of conductivity.

The hypothesis of the disturbing field seems to us in the present state fully justified by the experimental results, and offers quite a definite line for experimental researches, although there seems to be difficulty in bringing the experimental results obtained by this hypothesis into agreement with the modern theoretical views on conductivity.

It is also important to note that other magneto-electric effects, like the Hall effect and others, may be revised from the point of view that the magnetic field acting in a metal is the resultant of two disturbing fields, one external and the other internal.

The experimental work throughout all this research has been carried out

with the continuous assistance of Mr. E. Laurmann, to whom I would like to express my personal thanks.

I am indebted to Mr. J. D. Cockcroft for the correction of the MS.

My thanks are also due to Sir Ernest Rutherford for the kind interest he has shown during the progress of the work.

The work was all carried out in the Magnetic Laboratory with the support of the Department of Scientific and Industrial Research.

Summary.

(1) A theory is given for the phenomenon of change of resistance in a magnetic field which assumes that the change of resistance follows a linear law with the increasing field, and that it is masked in weak fields by disturbances existing in the metal which are equivalent to that produced by an inside magnetic field.

(2) Formulæ are obtained which agree with experimental facts and permit the separation of the ideal resistance and the additional resistance which is produced by internal disturbances.

(3) It has been shown that the additional resistance is independent of the temperature, and that the ideal resistance has a constant value for a given temperature for each metal independent of its physical and chemical state.

(4) It has been shown that the additional resistance is identical with the residual resistance which is observed close to the absolute zero.

(5) It has been suggested that supra-conductivity is a general phenomenon in all metals, but that it is masked by the additional resistance which disappears at very low temperatures in certain metals.

(6) The properties of the coefficient β of the linear law of the change of resistance is discussed, and it is shown that there is a certain connection between the value of β and the position of the element in the periodic system.

(7) The relation of the magnitude of the change of resistance with the position of the element in the periodic system is examined.

(8) The bearing of the present research on the modern theory of conductivity is discussed, and it is shown that the phenomena observed cannot be adequately explained. Some tentative suggestions are advanced in this connection.

Discussion on the Structure of Atomic Nuclei.

Opened by Sir Ernest Rutherford.

(February 7, 1929.)

Sir Ernest Rutherford: It was on March 19, 1914, that the Royal Society held its last discussion on the constitution of the atom—just fifteen years ago. I had the honour to open the discussion on that occasion, and the other speakers were Mr. Moseley, Profs. Soddy, Nicholson, Hicks, Stanley Allen, S. P. Thompson. In my opening remarks I put forward the theory of the nuclear atom and the evidence in support of it, while Mr. Moseley gave an account of his X-ray investigations, which defined the atomic numbers of the elements, and showed how many gaps were present between hydrogen number 1 and uranium number 92. Prof. Soddy drew attention to the existence of isotopes in the radioactive series, and also to a remarkable observation by Sir Joseph Thomson and Dr. Aston, who had obtained two parabolas in the positive ray spectrograph of neon, and he suggested that possibly the ordinary elements might also consist of mixture of isotopes. I think you will find that the remarks and suggestions made in this discussion fifteen years ago have a certain pertinence to-day. In particular Hicks and Stanley Allen drew attention to the importance of taking into account the magnetic fields in the nucleus, although at that time we had very little evidence on that point, and even to-day our information is very scanty.

What has been accomplished in the intervening period? On looking back we see that three new methods of attack on this problem have been developed. The first, and in some respects the most important, has been the proof of the isotopic constitution of the ordinary elements, and the accurate determination of the masses or weights of the individual isotopes, mainly due to the work of Dr. Aston. This has led in a sense to an extension of the original ideas of Moseley. The experiments of the latter fixed the number of possible nuclear charges, while Aston has shown that there are a large number of species of atoms each defined by its nuclear charge, although their masses and their nuclear constitution may be different. The essential point brought out in the earlier work of Dr. Aston was that the masses of the elements are approximately expressed by whole numbers, where oxygen is taken as 16—with the exception of hydrogen itself. But the real interest, as we now see it, is not the whole number rule itself, but rather the departures from it. That is a point I will discuss at some length later. It suffices to say at this point that the evidence from isotopes and also from the artificial disintegration of light elements shows fairly clearly that the mass units entering into the composition of the nucleus have a mass in the nucleus of about 1. This unit has been named the proton, and we believe that the proton is identical with the hydrogen nucleus when in the free state. I pointed out in the 1914 discussion that almost certainly the hydrogen nucleus corresponded to the positive electron—the counterpart of the ordinary negative electron.

The next discovery was the proof of the artificial disintegration of the elements by bombardment with alpha particles, in which I have been personally interested, as has also Dr. Chadwick, who will discuss the results obtained and their bearing on the structure of nuclei. This is the first time, I think, that definite evidence has been obtained that we can alter the actual structure of the nucleus itself by the application of external agencies. We know that in all cases where this is effected a proton is liberated at high speed. It is noteworthy that while the radioactive substances spontaneously break up always with the emission of helium nuclei or electrons, in the artificial disintegration of the lighter atoms, no helium nuclei, as far as we know, are liberated, but a proton is set free. The evidence, as a whole, indicates that while the ultimate constituents of the nucleus are protons and electrons, secondary units in the form of helium nuclei are also present in the heavier elements. I shall refer later to this important question.

The third line of attack, which has proved of great interest, has been the study of the wave-lengths of the penetrating gamma-rays which arise during the disintegration of the radioactive nucleus. As the gamma-rays have their origin in the nucleus, the frequency of these rays, first determined by Dr. Ellis, give us important evidence as to the modes of vibration, to use a general term, of the particles constituting the nucleus. I hope that Dr. Ellis later will refer among other matters to certain problems of the relation of the constituents of the nucleus with the outer electrons on which he has obtained at any rate some tentative evidence.

Dr. Chadwick and I have been especially interested in recent years in the question of the dimensions of the nucleus and the laws of force which hold in its neighbourhood. This is highly important since it is evident that we can make no calculations of quantities until we know the nature and laws of the forces near a nucleus. Information of this can be obtained by a study of the scattering of α-particles, and we have performed a large number of experiments on different elements. The methods adopted are in principle extremely simple.

An intense beam of α-particles of definite speed falls on a thin sheet of matter and the number of α-particles scattered through an angle of about 135° is counted by the scintillation method. The number of α-particles observed in this way is, in general, about 1 in 10^5 of the α-particles incident on the scattering foil. The speed of the incident α-particles is varied by placing thin sheets of mica over the source. In this way, a determination is made of the number of particles scattered by α-particles of different speeds. If the law of electrostatic action between the nucleus and the α-particle is the ordinary law of inverse square, the number scattered ought to vary as $1/E^2$, where E is the energy of the α-particle. When we examine all elements, from copper of atomic number 29 to uranium of number 92, it is found that the scattering is normal; that is to say, that the scattering agrees within experimental error with what we should expect if the law of inverse square holds in the region which is penetrated by the α-particle. Since it is to be anticipated that the law of force would change if the α-particle penetrates a nucleus, we may conclude that the radius of the copper nucleus must be less than the closest distance of approach, which in this case is about 10^{-12} cm. The corresponding distance for the uranium nucleus is about 3×10^{-12} cm., using the swiftest α-particles available. Since no change in the law of force is observed over this wide range of atomic number, we are unable to fix the dimensions of the nucleus with any certainty. All we can say is that it must be smaller than the closest distance of approach in a collision between the α-particle and the nucleus in question. If the α-particle entered into the nucleus, it is to be expected that the forces would alter, resulting in a change of the law of scattering.

Quite a different result is observed when we examine the scattering of the lighter elements. Long ago it was found that in bombarding hydrogen with α-particles the scattering is completely abnormal, and a similar result has been recently observed for helium. A detailed examination, first by Bieler and later by Chadwick and myself, has been made of the scattering of α-particles by magnesium and aluminium of atomic numbers 12 and 13 respectively. I will not go into the details of the experiments, but will merely illustrate the type of scattering curve which is observed.

Let us first suppose that the scattering is normal, that is, that the number of α-particles scattered through an angle of 135° varies as $1/E^2$ where E is the energy of the α-particle. The ratio of the observed to the theoretical scattering for different velocities of the α-particle is given by the dotted line shown in the figure. Such a straight line is found for gold and all the intermediate elements examined down to copper; but when aluminium is the scattering material, it is found that the inverse square law is nearly true for slow particles. For increasing velocity of the α-particle, the curve falls below the normal line,

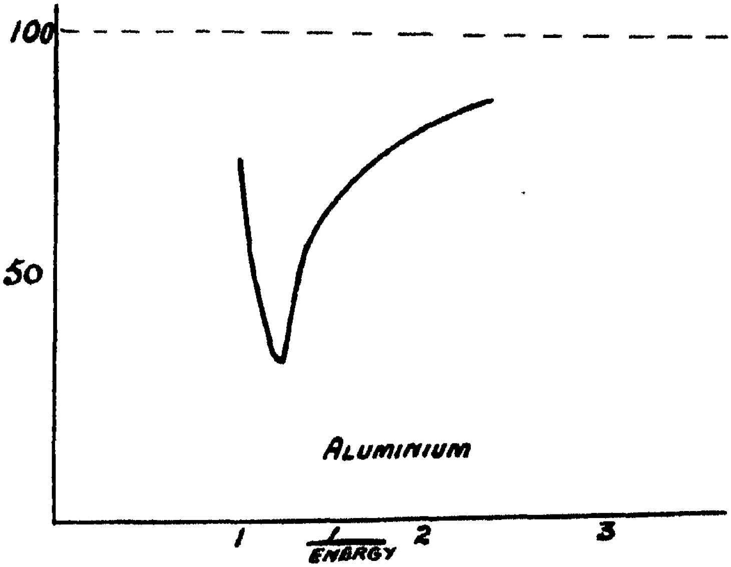

Fig. 1.

passes through a minimum and then rises again. There is some evidence that if still swifter α-particles were available, the curve would rise steeply well above the normal line. The curve shown in the figure is for the scattering of α-particles by aluminium through an average angle of 135°. A similar curve is found for magnesium. It is probable that still lighter elements would show a similar variation in the scattering curve. In some respects, the scattering of α-particles by hydrogen and helium is closely analogous.

The most natural explanation, and one which I think fits in well with the results, is to suppose that, in addition to the ordinary repulsive forces of the electric type between the nuclei, at close distances attractive forces come into play, so that the resultant force is a combination of the forces of repulsion and attraction. The scattering to be expected under these conditions was first worked out by Bieler, taking the attractive force to vary as the inverse fourth power of the distance. Later Debye and Hardmeier worked out the case for the inverse fifth power—a law of attraction that has a certain physical significance. When an α-particle approaches near to a nucleus, the intense forces must distort or polarise the charged constituents of the nucleus. This should give rise to an attractive force on the colliding α-particle, varying approximately as the fifth power of the distance from the centre of the nucleus. This point of view, it seems to me, has much to recommend it, for there must be a distortion or polarisation of the nucleus under the action of the intense forces, and this resulting attraction may become very great when the α-particle approaches near to the nucleus.

It has been shown by Hardmeier that calculations on this basis are in fair accord with the experimental observations for aluminium. It should be pointed out that the assumptions made in these calculations are somewhat artificial, for the α-particle is supposed to be a point charge and the nucleus a sphere.

Observations of the scattering of α-particles by hydrogen and helium indicate that both the hydrogen and helium nucleus appear to be surrounded by a field of force of unknown origin where the laws of force are quite abnormal. This region of abnormal forces is of about the same dimensions as the aluminium nucleus and the interpretation of the evidence suggests that in collisions this region is not spherical but rather like a plate or flat ellipsoid. It is of interest to note that the " size " of the hydrogen nucleus or proton examined in this way appears to be even larger than that of the helium nucleus.

Whatever interpretation we may place on the experimental results, it is clear that these nuclei cannot be regarded as point forces but have a certain volume or structure. It has been suggested, and it may be true, that this peculiar distribution of the forces round the α-particle and the proton may be due to magnetic forces which, on modern views, may arise from the intrinsic magnetic moment ascribed to the proton, and possibly also to the electron, quite apart from the actual motions of the constituents of the nucleus.

Now I come to an important point in the development of this argument. The observations on the scattering of α-particles by uranium metal show that within experimental error—which is unfortunately rather large in this case—the scattering is quite normal for the closest distance of approach—about $3 \cdot 5 \times 10^{-12}$ cm.—indicating that the radius of the nucleus is still smaller than this quantity. At the same time, if we examine the speed with which the slowest α-particle is spontaneously emitted from the uranium nucleus, we are driven to the conclusion that the nucleus extends to a distance about $6 \cdot 5 \times 10^{-12}$ cm.—about twice the distance found from the scattering results. We are thus faced with the difficulty that two apparently reliable methods of estimating the size of nuclei give very different values. If we try to construct a nucleus on classical ideas and to make the model self-consistent, we are driven to the conclusion that whatever system of forces is adopted, the field of force round the uranium nucleus must consist of an attractive force at small distances and a repulsive force at large distances. The variation of the potential due to these forces is shown in the diagram. The maximum of the curve represents the distance where the attractive and repulsive forces balance each other. Inside this distance the attractive forces preponderate and the potential may fall to a negative value. At large distances, the potential due to the electrostatic forces varies inversely as the distance. I think that all will agree that the potentials in the neighbourhood of the nucleus must vary somewhat in this fashion. On classical dynamics the potential may have a value of 4 or 5 million volts at a distance 4 to 5×10^{-12} cm. about. Whatever types of forces are adopted, a similar result follows. We are driven then, on these views, to the conclusion that a swift α-particle can penetrate deeply into the uranium nucleus while the scattering evidence contradicts such an assumption.

There have been attempts during the past year to avoid this impasse, and to get further information by applying the ideas of the wave mechanics. This problem has been attacked by Mr. Gamow, whom we are very glad to welcome here to-day, and also by Gurney and Condon. The variation of potential near the nucleus is supposed to be very similar in shape to that shown in fig. 2, but from the calculations of Mr. Gamow, the peak of the curve is much closer to the nucleus, at about $0{\cdot}7 \times 10^{-12}$ cm. instead of 4 or 5×10^{-12} cm. The maximum potential is correspondingly higher, about 30 million volts, and falls off exceedingly rapidly close to the nucleus. The nucleus, supposed spherical in shape, is thus surrounded by a very high potential barrier. No

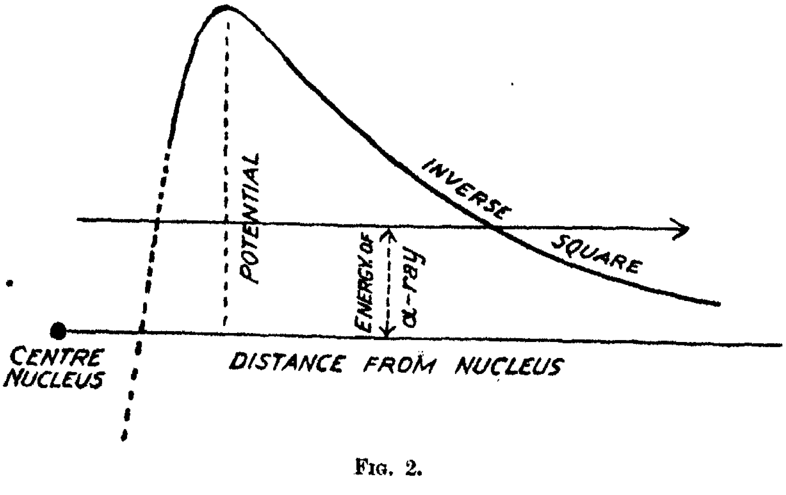

FIG. 2.

α-particle born of uranium can jump this barrier for, if it did so, it would escape with an energy much greater than is observed for any α-particle. But on the wave mechanics, particles can accomplish feats that are quite impossible on classical mechanics. Instead of the α-particle being required to jump the barrier in order to escape, the particle, or rather the wave system with which it is identified, leaks out through the barrier and finally emerges with a kinetic energy equal to the total energy it possessed inside the barrier. I will not deal further with this interesting new point of view, which will be discussed later by Mr. Fowler and Mr. Gamow. It will be seen that this theory makes the radius of the uranium nucleus very small, about 7×10^{-13} cm., and in this small nuclear volume 238 protons and 146 electrons have to be made room for. It sounds incredible but may not be impossible.

The next point I will consider is the bearing of some of the results of Dr. Aston on the structure of nuclei. You all know the essential result at which he had arrived—that the unit of mass in the structure of nuclei is the proton of mass nearly 1, while the proton (H nucleus) in the free state has a mass 1·0073 in terms of O = 16. This difference in mass between the free and nuclear proton is ascribed to this packing effect, *i.e.*, to the interaction of the electromagnetic fields of the protons and electrons in the highly condensed nucleus. On modern views, we know that there is a close relation between mass and energy and a decrease in mass means a loss of energy. The free proton has a mass 1·0073 while the proton in the nucleus has a mass very nearly 1. This apparently small loss of mass means that a large amount of energy has been emitted in the entrance of the free proton into the structure of the nucleus, an amount corresponding to about 7 million electron-volts.

Consider now the curve in fig. 3 prepared by Dr. Aston which shows on a large scale the departure of the masses of the isotopes from the whole number rule. The curve beginning at hydrogen crosses the whole number line and sinks to a minimum for an atomic weight about 120. It then rises and crosses the line again for an atomic weight about 200. Suppose now that a nucleus is built up originally from free hydrogen nuclei and electrons—I do not say I agree with such an assumption. In forming an atom of mass 120, containing 120 protons, energy has been lost corresponding to 840 million volts, and this energy has been probably radiated away into space. On such a view it is clear that the atom, instead of being as ordinarily supposed, a store of energy, is really a sink of energy; and if we took the nucleus of mercury, for example, to pieces, proton by proton, we should have to do an enormous amount of work corresponding to at least 1400 million volts.

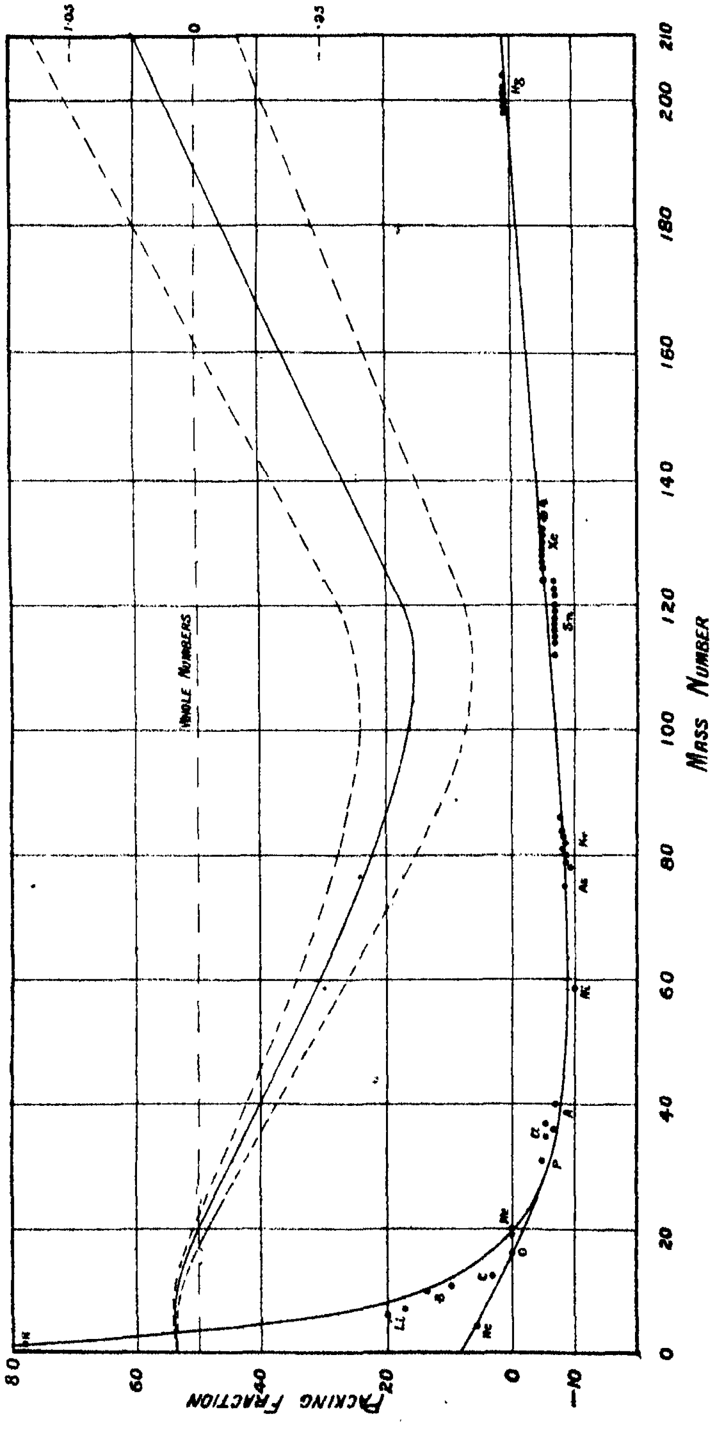

FIG. 3.—Mass Numbers and Packing Fractions.

This is certainly true if each atom is supposed to be built up of free hydrogen nuclei and electrons. You may naturally ask how such a view can be reconciled with the fact that in the transformation of uranium into lead a large amount of energy is spontaneously liberated—more than 40 million volts. If, however, we look at it from another point of view, the prospect is more encouraging. Suppose that the essential unit involved in the structure of the heavier elements is not the proton but the helium nucleus. The latter which we suppose to be made up of 4 protons and 2 electrons has already in its formation emitted a large amount of energy and its nuclear mass in the free state is 4·0018. It will be noted that the curve showing the departure from the whole number rule is a minimum for a mass of about 120 and crosses the line again for a mass of about 200. If, for simplicity, we suppose the nuclei are built up from mass 120 by successive accretions of α-particles, the mass of each added particle can be easily shown to be about 4·005 over this interval of atomic weight. It is seen that this mass is greater than that of the α-particle in the free state. No doubt also the increase of mass is not regular from atom to atom and is probably greater for a mass in the neighbourhood of 200 than for a mass about 120. If the curve given by Aston is extrapolated to include uranium, it can be shown that the addition of mass is sufficient to account at any rate approximately for the large amount of energy emitted by the radioactive bodies. It appears therefore very likely that the heavier elements are mainly composed of α-particles and that many of the α-particles have a total energy in the nucleus greater than in the free state.

We are now in a position to form a picture of the gradual building up of atomic nuclei. Probably in the lighter elements the nucleus is composed of a combination of α-particles, protons, and electrons, and that the parts of the nucleus attract one another strongly, partly it may be owing to the distortional forces and partly also to the magnetic forces. We can only speculate as to the nature of these forces. At first then a highly concentrated and firmly bound nucleus is formed accompanied by the emission of energy and for an atomic weight of about 120 a minimum mass is reached representing the closest binding. After this stage, as the atom grows in mass, the additional particles are less and less tightly bound. We may thus suppose that the nucleus consists of a tightly packed structure near its centre gradually becoming less dense towards the outside. This system is surrounded by a potential barrier which normally prevents the α-particles from escaping. This static view of the atom may not commend itself to my theoretical friends who may wish the α-particles to have complete freedom of motion within the nucleus. Such a point of view is quite legitimate and can be reconciled with the essential ideas I have put forward. In other words, if it were possible to take an instantaneous picture of the nucleus—of duration about 10^{-23} second—a dense collection of closely bound α-particles would be observed at the centre, the density fading away to the outside. No doubt all the α-particles are in motion and their waves are reflected to and fro between the potential barriers, and occasionally leak out of the system. The view I have outlined is I think reasonable, and I hope our theoretical friends will be able to define the picture more accurately; we have not only to account for a nucleus made of α-particles but have also to make room for the additional electrons, and it is not easy to confine an electron in the same cage with an α-particle. I have, however, such a strong belief in the ingenuity of our theoretical friends that I am confident that they will surmount this difficulty in some way and I hope suggestions will be made on this point to-day.

One other point. The view I have put forward explains I think why no heavier atoms than uranium can exist permanently. With increase of mass, the nuclei gain more and more energy and would become highly radioactive and disappear. Probably the higher the energy the more rapidly they would vanish, and it is probably not an accident that uranium and thorium are the sole survivors of the heavier nuclei. This is not the place to discuss the very speculative question of how the nuclei of the elements have been formed. Before attacking this question, we want much more information on the details of the structure of the nucleus itself.

Dr. F. W. ASTON: In addition to the fundamental "whole number rule" many of the results of the mass-spectrograph are suggestive in connection with the subject under discussion. Why are there no atoms of mass number 2, 3, 5, 8, etc.? Why are there never less than two protons to one electron in the nucleus? Among elements of even atomic number the number of isotopes tends to increase with atomic weight, but the difference between the masses of the extreme isotopes appears curiously limited to about 10 per cent. When we consider the elements of odd atomic number the restriction is even more remarkable. They never have more than two isotopes, and above atomic number 9 these are always two units apart and the lighter is the more abundant. This is evidence for a fundamental difference between atoms of even and those of odd atomic number. In both classes there is a tendency for the number of electrons in the nucleus to be even, in fact the only elements consisting wholly of atoms breaking this rule are beryllium and nitrogen. As Harkins pointed out long ago elements of even atomic number are vastly more abundant in nature. If we plot abundance against mass number we notice definite peaks at mass numbers of type $8n$.

One of the very few ways of obtaining direct information on the structure of nuclei is the measurement of their relative masses. Hence every effort has been made to raise the accuracy with which this can be done. The limit so far obtained with the new mass-spectrograph is, in favourable cases, as high as 1 in 10,000. The quantity measured is the percentage excess or defect from a whole number on the oxygen scale. This is called the "packing fraction" and is expressed in parts per 10,000.

In the figure the packing fractions are plotted against the mass numbers, so that the experimental error is the same at all points of the graph. The dots are actual determinations, and above mass number 20 lie roughly on a single curve with a minimum of about -10 in the region of iron and nickel. The light atoms of odd atomic number lie on a curve rising to hydrogen $+77 \cdot 8$, but those of even atomic number lie well below. This emphasises their essential class difference and suggests that the light atoms of odd atomic number have a common loosely bound, and therefore heavy, outside structure which is not present in the denser and more stable nuclei of helium, carbon and oxygen.

If we calculate the masses of the atoms from the packing fractions and then plot their arithmetical differences from whole numbers we get the curve roughly indicated in the upper part of the diagram. Here the minimum lies about midway in the range of known atomic weights. When drawing conclusions from this curve it is of great importance to remember that the experimental error is not the same at all points, but, as indicated by the broken lines, becomes very large indeed for atoms of high mass number.

Dr. J. Chadwick: When certain elements are exposed to the bombardment of α-particles, hydrogen nuclei or protons are liberated which can be detected by the scintillations they produce on a zinc sulphide screen. These protons are due to the artificial disintegration of the nuclei of the elements. The disintegration is supposed to occur when an α-particle penetrates into a nucleus and is captured by it, the result of the capture being the emission of a proton. The chance of disintegration is small; in the favourable case of nitrogen, for example, about 20 nuclei are disintegrated for every 10^6 α-particles in the incident beam. Owing to the rarity of the event, and also to various difficulties inherent in the experiments, the information so far obtained is somewhat meagre.

With the exceptions of carbon and oxygen, all elements from boron to potassium (and including these) are disintegrated under α-particle bombardment and emit a proton with considerable energy. The nuclei of all these elements therefore contain a proton. Carbon and oxygen, if they are disintegrated at all, do not emit particles with ranges greater than those of the scattered α-particles. It is possible that they break up into helium nuclei, but no proof of this has been obtained.

Some of the protons liberated in artificial disintegration have very large energies. For example, the protons liberated from aluminium by α-particles of radium C′ have a maximum energy about 40 per cent. greater than that of the incident α-particle. In some cases then there is a release of energy in the disintegration. There is a striking difference in behaviour between the elements of even atomic number and those of odd atomic number ; the protons liberated from the odd numbered elements have greater maximum energies than those from the even elements. If the disintegration consists only in the capture of an α-particle and the emission of a proton, then an element of odd number will be changed by disintegration into one of even number, and *vice versa*. The difference in behaviour of odd and even elements therefore suggests, in agreement with the evidence from relative abundance and from atomic masses, that the even elements are more stable than the odd.

A further point of interest appears from a comparison of experiments on artificial disintegration with those on the scattering of α-particles. The former experiments show that α-particles of 3 to 3·5 cm. range are effective in disintegrating aluminium, that is, are able to penetrate into the aluminium nucleus and to be captured by it. On the other hand, the scattering experiments show very clearly that the great majority of such α-particles are scattered according to the usual laws ; they indicate indeed that α-particles even of 7 cm. range should not be able to penetrate the nucleus of aluminium. The explanation of this apparent contradiction of the two sets of evidence has recently been given by Gamow, on the basis of the wave mechanics.

If we suppose that in a disintegration the α-particle is captured and that only the three bodies, the α-particle, the nucleus and the proton, are concerned in the collision, then we should expect the proton to appear at a given angle with a definite energy. Experiments with aluminium show that this is not the case, but that the protons are emitted over a wide range of energies. For example, the protons liberated at an angle of 90° to the direction of the incident α-particles of radium C′ have energies varying from about 0·3 to 1·1 of that of an α-particle of 7 cm. range. It is suggested that the most probable explanation of this observation is given by supposing that all nuclei of the same type do not have identical masses or internal energies, so that the disintegration of the initial nucleus and the formation of the new nucleus may take place with varying energy of reaction. The assumed variation in mass is small; the greatest difference in mass of the aluminium nuclei is about 0·006 mass units.

Dr. C. D. Ellis: In many radioactive disintegrations it is found that a characteristic high frequency radiation is emitted immediately after the disintegration particle has left the nucleus. These γ-rays are more frequently associated with the β-ray type of disintegration. They can be considered as the characteristic spectrum of the nucleus and their emission is due to the disturbance caused by the departure of the α- or β-particle.

The γ-rays appear to be homogeneous to at least one part in a thousand, and this fact leads to some interesting deductions about the nature of the particle that emits them. Kuhn has shown that it is probable that electrons could not emit such homogeneous high frequency radiation, and that with fair certainty this conclusion can be extended to protons. We are thus led to seek the origin of the γ-rays either in the α-particles or in the nucleus as a whole by some process such as rotation. Important evidence on this point would be provided if it were possible to deduce a system of levels to account for the γ-rays. There is indubitable evidence that some system must exist since in all the spectra many instances are found of relations of the type $\nu_1 + \nu_2 = \nu_3$. However to settle uniquely a level system by frequency differences alone demands a more accurate knowledge of the frequencies than we at present possess. There are two lines of attack which may help to surmount this difficulty. The first is a determination of the absolute intensities of the γ-rays, that is the probability that at any disintegration one quantum of the γ-ray will be emitted. It is reasonable to assume that at each disintegration there is only one excitation of the level system so that, to take a simple example, the γ-rays beginning or ending on a certain level must not have a total intensity of more than unity. More detailed criteria than this example can be obtained and will provide a valuable test of systems proposed on frequency differences relations.

The second mode of approach to this problem would appear to be furnished by some experiments which are being carried out by G. H. Aston and Ellis. They find evidence of a coupling between the nucleus and the electronic system which may be illustrated in the following way. If the γ-rays from a radioactive body fall on a sheet of lead the intensities of the photoelectric groups will depend jointly on the intensities of the γ-rays and the coefficients of absorption. Similar photoelectric groups are found to come from the radioactive atom and might be explained as a partial internal absorption of the γ-rays. If the nucleus and the electronic system were as distinct as the nucleus and the sheet of lead, then a parallelism would be expected between the intensities of the photoelectric groups from the lead and from the radioactive atom. Actually the reverse is found, and, although the experiments are not yet complete, it seems certain that remarkable oscillations occur in the ratio of the *internal to external* absorption as the scale of frequencies is ascended, and this must be taken to show a coupling. This is in itself an interesting phenomenon about the nucleus, and it is hoped may in addition provide a new method of attack on the problem of the level systems by differentiating between different γ-rays.

Dr. G. Gamow: I should like to make a few remarks with reference to the President's last words about the general constitution of the nucleus as a collection of α-particles.

A good deal of evidence exists that all the α-particles which constitute a nucleus (to the number of about 50 for the heavy elements) are in the same quantum state with quantum number unity. There is no contradiction between this and the Pauli-principle because α-particles having even charges must conform to the Bose-Einstein statistics. Such an assembly of α-particles with attractive forces between them, which vary rapidly with the distance, may be treated somewhat as a small drop of water in which the particles are held together by surface tension.

Though the exact solution of the complete problem must necessarily be very complicated, still this first rough approximation gives rise to several interesting properties of such a model. Writing down two equations as follows:—

(1) an equation connecting the energy of α-particles with the surface tension of the imaginary "water-drop," and

(2) the quantum condition of ordinary quantum mechanics,

we can obtain a relation between the "drop energy" and the number of α-particles contained in the drop—that is to say, the atomic weight of the nucleus. The general shape of the curve showing this relation agrees well with Aston's curve for the defect of mass, giving at first negative energy, and subsequently changing for larger values of N.

On the wave mechanics, the treatment of this model is to be carried out by means of Hartree's method of self-consistent field.

For a nucleus consisting of N α-particles the equation to be solved (written for one α-particle) is :—

$$\frac{\partial^2\psi}{\partial x^2} + \frac{\partial^2\psi}{\partial y^2} + \frac{\partial^2\psi}{\partial z^2} + \frac{8\pi^2 m}{h^2}\left[\mathrm{E} - (\mathrm{N} - 1)\int \psi\overline{\psi}\mathrm{U}(r)\,dv\right]\psi = 0,$$

where the second term in the bracket represents the action of the other (N — 1) α-particles, U (r) being the potential energy of two α-particles at the distance r apart.

The solution of this equation, with a much simplified assumption about the law of forces was carried out by Dr. Hartree.

Hartree takes that the second term in the bracket is simply equal to $(\mathrm{N} - 1)\,\mathrm{K}\,.\,\psi\overline{\psi}$ ($\mathrm{K} = \text{const.}$). This assumption, often used in the theory of capillarity, amounts to neglecting the Coulomb repulsive-forces between α-particles and assuming that the "radius of action" of attractive forces is small compared with nuclear dimensions.

The equation yields discrete "eigenwerte" giving energy and nuclear radius (by a suitable choice of K) of the right order of magnitude.

I hope that further calculations on such a model, based on a more exact knowledge of the forces of interaction between the α-particles, such as might be obtained from scattering experiments in helium, might give an exact fit, at any rate for lighter elements. Further difficulties arise in connection with elements heavier than argon, where the free nuclear electrons come into play, on account of our present ignorance of the behaviour of nuclear electrons.

Mr. R. H. **Fowler** : I wish to describe to you such help as the new quantum theory can give in the discussion of the structure and properties of the nucleus. The point has already been mentioned by the President in his opening remarks. I want to take it a little further. The first point to bear in mind is that the new quantum mechanics has developed in a logical way, based on the properties of electrons in atoms. It requires us to suppose that particles have many of the properties of waves. Whether we call them particles or waves is a matter of taste. It depends rather on the particular situation in which we find them. Remembering that particles are like waves, we shall expect to find that they are not, for example, always reflected from barriers of finite height. As the President said, they do not have to jump over them. They can steal through them—only rather occasionally, of course. You may say that any one of us present has a finite chance of leaving this room without opening the door, or, of course, without being thrown out through the window. [The nature of the reflection of particles at a potential hill and its close analogy with the optical phenomenon of the transmission of light through thin layers when incident at an angle greater than the critical angle was then explained in detail.]

If particles, then, can go through hills of this sort, that offers a very nice way of trying to explain the phenomena of emission of alpha-particles from heavy nuclei.

If you picture the nucleus in the way we have been talking about to-day, as something of the nature of a tiny enclosure surrounded (in three dimensions) by a potential hill (see fig. 2), we might have inside an alpha-particle, which has to be represented by a standing wave, whose energy is less than the potential energy at the top of the barrier. Classically it will stay there for ever, but in the quantum theory there is a finite chance that the wave can leak out through the thin wall and go away to infinity. When that is worked out correctly we have the quantum theory of alpha-particle emission. This idea was started independently by Dr. Gamow and by Mr. Gurney and Prof. Condon. They have worked it out, particularly Dr. Gamow, in some detail.

If the α-particle is leaking out, then, of course, it is not properly represented by a genuine standing wave. The proper picture of an alpha-particle in the nucleus is a damped oscillation. There will be a damped oscillation inside a harmonic oscillation with an ordinary damping factor--accompanied by a very weak wave outside, which represents the emission of the alpha-particle.

Actually the solution comes out very neatly, so that the damping factor appears in the solution as an imaginary part of the energy. That has been successfully done by Dr. Gamow, and he finds that it does not very much matter what precise shape you assume for the inside of the hill in doing this calculation. The main outside part of the hill is accurately known from the scattering experiments.

The chance of the alpha-particle escaping will depend very much on the energy of the alpha-particle. The greater its energy, the thinner the barrier which it has to go through and the smaller the height of the barrier it has to go through. Therefore there is obviously a very close connection between the energy of the alpha-particle, which we know as the observed energy of the alpha-particle when it comes out, and its chance of getting out, which we know as the life of the atom. That is the Geiger-Nuttall law.

[Slides comparing the observed and calculated relation between life and energy for the alpha-particle bodies of the radioactive families were then shown and discussed.]

To conclude, this is a very beautiful theory, and on its broad lines we may be absolutely confident that it is right. Its great virtue is that it gives us the Geiger-Nuttall law of alpha-ray disintegration quite independently of the details of nuclear structure.

Prof. O. W. Richardson : I would like to say a few words as to the evidence for the rotation of the nuclei.

I think *a priori* argument shows that the nuclei must be revolving in some cases. I imagine a system consisting only of one proton and one electron and I leave them to combine. They must form an atom of hydrogen in the lowest possible state, with emission of radiation. The spectroscopic evidence is overwhelming that an electron in the ground state of an atom has half a quantum of angular momentum. After the combination, then, the electron has acquired half a quantum of angular momentum ; but if nothing else has happened the principle of the conservation of momentum is violated, so I say that there is half a quantum of angular momentum in the nucleus of the unexcited hydrogen atom, opposite in sign to that of the electron. It might be urged that the emitted radiation could preserve the conservation of momentum by having a sufficiently high degree of elliptical polarisation but this alternative is highly improbable.

There is good spectroscopic evidence, of two kinds, that the nuclei are rotating. The more direct is from the hyperfine structure of certain spectral lines. Back and Goudsmit have shown that each of the " lines " of the bismuth spectrum is really a number of very fine lines. They have studied the different transitions which are possible in these lines, and they find they are governed by a new kind of inner quantum number which has the value 4½. The hyperfine separation of the lines and the general structure of the spectrum are also in agreement with this number 4½. The effect must come from the nuclear rotation because the magnetic moment of the electrons is already used up in the ordinary multiplet structure of the spectrum. Finally, in a strong magnetic field each Zeeman component breaks up into 10 equally spaced and equally intense lines corresponding to the space quantisation of a nucleus with this rotation. From the hyperfine structure in cæsium Jackson has been able to compare the nuclear spin with the electronic spin, and finds them to be of a similar magnitude.

The other spectroscopic evidence is based on the alternation of intensity which is present in the lines of the bands of symmetrical diatomic molecules, such as H_2, He_2, N_2 and O_2. It rests on a theorem due to Hund that the proper functions of a molecule must be either all symmetric or all antisymmetric in the nuclear co-ordinates. Those functions contain as factors the proper functions of the electronic motion and of the molecular rotation impulse. The latter function has the property that it is symmetrical in the nuclear co-ordinates when the rotation quantum number p is even and antisymmetrical when p is odd. Thus when p is odd the electronic functions must be symmetric in the co-ordinates of the nuclei if the whole function is to be antisymmetric, and vice versa. The converse holds when p is even. This requires that in such bands the alternate lines belong to states which do not combine with each other. If there is nothing to distinguish the nuclei, one set of functions is excluded and alternate lines of each band are missing. This is the case for He_2 from which it is concluded that the helium nucleus has no spin. In the H_2 spectrum, on the other hand, the lines have an alternating intensity corresponding to a weight ratio of 3 to 1. This is what would be expected if one set came from molecules with a nuclear moment of $\frac{1}{2}+\frac{1}{2}=1$ quantum and the other $\frac{1}{2}-\frac{1}{2}=0$. The former gives rise to three different arrangements $(+1, 0, -1)$ in space quantisation and the latter only to one. The nitrogen molecule, which also has an atom with an odd number of electrons, resembles H_2 in this respect, whilst O_2 seems to be similar to He_2.

Dr. D. R. **Hartree**: There is one point about the model of the nucleus, with the concentrated essence in the middle and then a more spread-out distribution outside. It is difficult to explain why the nuclei seem to become less radioactive as we go up the radioactive series instead of more radioactive. Is there any possibility of explaining that without some additional assumptions?

Sir Ernest **Rutherford**: Unfortunately, we do not know where the α-particle originates. It may come either from the inside or the outside of the nucleus. It is probable that in such a closely coupled system as a nucleus must be, energy is rapidly transferred from one particle to another. The growing violence of the transformations down the radiation series is certainly a striking feature of the radiation process and no obvious explanation can be offered at this stage.

I personally wish to thank each of the speakers for their contributions to the discussion, and I am sorry that time does not permit an interchange of views on many different points. Our knowledge of the nucleus is still in a very elementary state, although much greater progress has been made than I thought possible fifteen years ago.

The Total Reflexion of Electric Waves at the Interface between Two Media.

By H. M. MACDONALD, F.R.S.

(Received January 23, 1929.)

The theory of total reflexion has been treated usually by considering a train of plane waves incident on a plane surface separating two different media. It has been observed by Schuster* that there is the difficulty of seeing how the disturbance in the second medium is maintained, and he has discussed the problem of a parallel beam of waves of finite extent incident on the plane surface separating the media. It may be noticed that there is a similar difficulty in the case where there are both transmitted and reflected waves, as there is a transfer of energy in the second medium parallel to the interface at a rate which is in the ratio $\sigma' \tan \theta' / \sigma \tan \theta$ to the rate of transfer of energy in the first medium parallel to the interface.†

If the source of the electric waves in the first medium is a simple oscillator, and the velocity of propagation in the second medium is greater than the velocity of propagation in the first medium, then the rays which are bounded by the cone, whose vertex is at the oscillator, and whose semi-vertical angle is the critical angle, are transmitted into the second medium, where their boundary is the position of the plane interface outside the base of the cone, and there is no portion of the space in shadow. To obtain a shadow it is necessary that the interface is concave towards the oscillator. It is proposed in the following to discuss the problem of the transmission and reflexion of electric waves, when the surface separating the media is a sphere, and the source of the waves is a simple oscillator inside the sphere, whose axis passes through the centre of the sphere.

Using polar co-ordinates, whose origin is the centre of the sphere, and whose axis is the axis of the oscillator, if ψ denotes $H_\phi r \sin \theta$, where H_ϕ is the component of the magnetic force perpendicular to a meridian plane, ψ satisfies the differential equation

$$\frac{\partial^2 \psi}{\partial r^2} + \frac{\sin \theta}{r^2} \frac{\partial}{\partial \theta}\left(\frac{1}{\sin \theta} \frac{\partial \psi}{\partial \theta}\right) = \mathrm{K}\mu \frac{\partial^2 \psi}{\partial t^2},$$

---

* 'Roy. Soc. Proc.,' A, vol. 107, p. 15 (1925).

† This result is easily deduced from the relations given, 'Roy. Soc. Proc.,' A, vol. 108, pp. 387, 388 (1925).

inside the sphere, where K, μ are the constants of the first medium, and it satisfies the differential equation

$$\frac{\partial^2\psi}{\partial r^2}+\frac{\sin\theta}{r^2}\frac{\partial}{\partial\theta}\left(\frac{1}{\sin\theta}\frac{\partial\psi}{\partial\theta}\right)=\mathrm{K}'\mu'\frac{\partial^2\psi}{\partial t^2},$$

outside the sphere, where K′, μ' are the constants of the second medium, also at the surface of the sphere, where $r=a$, the radius of the sphere, if ψ_0 denotes the value of ψ inside the sphere, and ψ_1 denotes its value outside the sphere, since the tangential components of the magnetic and electric forces are continuous

$$\psi_0=\psi_1,\quad \frac{1}{\mathrm{K}}\frac{\partial\psi_0}{\partial r}=\frac{1}{\mathrm{K}'}\frac{\partial\psi_1}{\partial r}.$$

Hence, if b is the distance of the oscillator from the centre of the sphere,

$$\psi_0=b^{-\frac{1}{2}}r^{\frac{1}{2}}e^{\iota pt}\sum_1^\infty(2n+1)e^{\frac{1}{2}(n+\frac{1}{2})\pi\iota}\mathrm{J}_{n+\frac{1}{2}}(\kappa b)\,\mathrm{K}_{n+\frac{1}{2}}(\iota\kappa r)\sin\theta\frac{\partial\mathrm{P}_n}{\partial\theta}$$
$$+r^{\frac{1}{2}}e^{\iota pt}\sum_1^\infty\mathrm{A}_n\mathrm{J}_{n+\frac{1}{2}}(\kappa r)\sin\theta\frac{\partial\mathrm{P}_n}{\partial\theta},\qquad r>b,$$
$$\psi_1=r^{\frac{1}{2}}e^{\iota pt}\sum_1^\infty\mathrm{A}_n'\mathrm{K}_{n+\frac{1}{2}}(\iota\kappa' r)\sin\theta\frac{\partial\mathrm{P}_n}{\partial\theta};$$

where p is the frequency of the waves, $\kappa\mathrm{V}=\kappa'\mathrm{V}'=p$, $\mathrm{K}\mu\mathrm{V}^2=\mathrm{K}'\mu'\mathrm{V}'^2=1$. Therefore the constants A_n, A_n' satisfy the conditions

$$b^{-\frac{1}{2}}a^{\frac{1}{2}}(2n+1)e^{\frac{1}{2}(n+\frac{1}{2})\pi\iota}\mathrm{J}_{n+\frac{1}{2}}(\kappa b)\,\mathrm{K}_{n+\frac{1}{2}}(\iota\kappa a)+\mathrm{A}_n a^{\frac{1}{2}}\mathrm{J}_{n+\frac{1}{2}}(\kappa a)=\mathrm{A}_n'a^{\frac{1}{2}}\mathrm{K}_{n+\frac{1}{2}}(\iota\kappa' a),$$

$$\frac{1}{\mathrm{K}}\left[b^{-\frac{1}{2}}(2n+1)e^{\frac{1}{2}(n+\frac{1}{2})\pi\iota}\mathrm{J}_{n+\frac{1}{2}}(\kappa b)\frac{\partial}{\partial a}\{a^{\frac{1}{2}}\mathrm{K}_{n+\frac{1}{2}}(\iota\kappa a)\}+\mathrm{A}_n\frac{\partial}{\partial a}\{a^{\frac{1}{2}}\mathrm{J}_{n+\frac{1}{2}}(\kappa a)\}\right]$$
$$=\frac{1}{\mathrm{K}'}\mathrm{A}_n'\frac{\partial}{\partial a}\{a^{\frac{1}{2}}\mathrm{K}_{n+\frac{1}{2}}(\iota\kappa' a)\}.$$

It follows that

$$\mathrm{A}_n'\left[a^{\frac{1}{2}}\mathrm{K}_{n+\frac{1}{2}}(\iota\kappa' a)\frac{\partial}{\partial a}\{a^{\frac{1}{2}}\mathrm{J}_{n+\frac{1}{2}}(\kappa a)\}-\frac{\mathrm{K}}{\mathrm{K}'}a^{\frac{1}{2}}\mathrm{J}_{n+\frac{1}{2}}(\kappa a)\frac{\partial}{\partial a}\{a^{\frac{1}{2}}\mathrm{K}_{n+\frac{1}{2}}(\iota\kappa' a)\}\right]$$
$$=b^{-\frac{1}{2}}(2n+1)e^{\frac{1}{2}(n+\frac{1}{2})\pi\iota}\mathrm{J}_{n+\frac{1}{2}}(\kappa b)\left[a^{\frac{1}{2}}\mathrm{K}_{n+\frac{1}{2}}(\iota\kappa a)\frac{\partial}{\partial a}\{a^{\frac{1}{2}}\mathrm{J}_{n+\frac{1}{2}}(\kappa a)\}\right.$$
$$\left.-a^{\frac{1}{2}}\mathrm{J}_{n+\frac{1}{2}}(\kappa a)\frac{\partial}{\partial a}\{a^{\frac{1}{2}}\mathrm{K}_{n+\frac{1}{2}}(\iota\kappa a)\}\right],$$

$$\mathrm{A}_n\left[\frac{\mathrm{K}'}{\mathrm{K}}a^{\frac{1}{2}}\mathrm{K}_{n+\frac{1}{2}}(\iota\kappa' a)\frac{\partial}{\partial a}\{a^{\frac{1}{2}}\mathrm{J}_{n+\frac{1}{2}}(\kappa a)\}-a^{\frac{1}{2}}\mathrm{J}_{n+\frac{1}{2}}(\kappa a)\frac{\partial}{\partial a}\{a^{\frac{1}{2}}\mathrm{K}_{n+\frac{1}{2}}(\iota\kappa' a)\}\right]$$
$$=b^{-\frac{1}{2}}(2n+1)e^{\frac{1}{2}(n+\frac{1}{2})\pi\iota}\mathrm{J}_{n+\frac{1}{2}}(\kappa b)\left[a^{\frac{1}{2}}\mathrm{K}_{n+\frac{1}{2}}(\iota\kappa a)\frac{\partial}{\partial a}\{a^{\frac{1}{2}}\mathrm{K}_{n+\frac{1}{2}}(\iota\kappa' a)\}\right.$$
$$\left.-\frac{\mathrm{K}'}{\mathrm{K}}a^{\frac{1}{2}}\mathrm{K}_{n+\frac{1}{2}}(\iota\kappa' a)\frac{\partial}{\partial a}\{a^{\frac{1}{2}}\mathrm{K}_{n+\frac{1}{2}}(\iota\kappa a)\}\right].$$

Therefore

$$\psi_0 = \overline{\psi}_0 + b^{-\frac{1}{2}} e^{\iota pt} \sum_{n=1}^{\infty} (2n+1)\, e^{\frac{1}{2}(n+\frac{1}{2})\pi\iota}\, \mathrm{E}_n \mathrm{J}_{n+\frac{1}{2}}(\kappa b)\, r^{\frac{1}{2}} \mathrm{J}_{n+\frac{1}{2}}(\kappa r) \sin\theta \frac{\partial \mathrm{P}_n}{\partial\theta},$$

$$\psi_1 = b^{-\frac{1}{2}} e^{\iota pt} \sum_{n=1}^{\infty} (2n+1)\, e^{\frac{1}{2}(n+\frac{1}{2})\pi\iota}\, \mathrm{E}_n{}' \mathrm{J}_{n+\frac{1}{2}}(\kappa b)\, r^{\frac{1}{2}} \mathrm{K}_{n+\frac{1}{2}}(\iota\kappa' r) \sin\theta \frac{\partial \mathrm{P}_n}{\partial\theta},$$

where

$$\mathrm{E}_n = \frac{a^{\frac{1}{2}}\mathrm{K}_{n+\frac{1}{2}}(\iota\kappa a)\dfrac{\partial}{\partial a}\{a^{\frac{1}{2}}\mathrm{K}_{n+\frac{1}{2}}(\iota\kappa' a)\} - \dfrac{\mathrm{K}'}{\mathrm{K}}\, a^{\frac{1}{2}}\mathrm{K}_{n+\frac{1}{2}}(\iota\kappa' a)\dfrac{\partial}{\partial a}\{a^{\frac{1}{2}}\mathrm{K}_{n+\frac{1}{2}}(\iota\kappa a)\}}{\dfrac{\mathrm{K}'}{\mathrm{K}}\, a^{\frac{1}{2}}\mathrm{K}_{n+\frac{1}{2}}(\iota\kappa' a)\dfrac{\partial}{\partial a}\{a^{\frac{1}{2}}\mathrm{J}_{n+\frac{1}{2}}(\kappa a)\} - a^{\frac{1}{2}}\mathrm{J}_{n+\frac{1}{2}}(\kappa a)\dfrac{\partial}{\partial a}\{a^{\frac{1}{2}}\mathrm{K}_{n+\frac{1}{2}}(\iota\kappa' a)\}},$$

$$\mathrm{E}_n{}' = \frac{a^{\frac{1}{2}}\mathrm{K}_{n+\frac{1}{2}}(\iota\kappa a)\dfrac{\partial}{\partial a}\{a^{\frac{1}{2}}\mathrm{J}_{n+\frac{1}{2}}(\kappa a)\} - a^{\frac{1}{2}}\mathrm{J}_{n+\frac{1}{2}}(\kappa a)\dfrac{\partial}{\partial a}\{a^{\frac{1}{2}}\mathrm{K}_{n+\frac{1}{2}}(\iota\kappa a)\}}{a^{\frac{1}{2}}\mathrm{K}_{n+\frac{1}{2}}(\iota\kappa' a)\dfrac{\partial}{\partial a}\{a^{\frac{1}{2}}\mathrm{J}_{n+\frac{1}{2}}(\kappa a)\} - \dfrac{\mathrm{K}}{\mathrm{K}'}\, a^{\frac{1}{2}}\mathrm{J}_{n+\frac{1}{2}}(\kappa a)\dfrac{\partial}{\partial a}\{a^{\frac{1}{2}}\mathrm{K}_{n+\frac{1}{2}}(\iota\kappa' a)\}},$$

and $\overline{\psi}_0$ is the value of ψ when the medium is uniform throughout space, writing

$$e^{\frac{1}{2}(n+\frac{1}{2})\pi\iota}\kappa^{\frac{1}{2}} r^{\frac{1}{2}} \mathrm{K}_{n+\frac{1}{2}}(\iota\kappa r) = (\pi/2)^{\frac{1}{2}}(v - \iota u), \quad w = v - \iota u, \quad \overline{w} = v + \iota u,$$

$$e^{\frac{1}{2}(n+\frac{1}{2})\pi\iota}\kappa^{\frac{1}{2}} a^{\frac{1}{2}} \mathrm{K}_{n+\frac{1}{2}}(\iota\kappa a) = (\pi/2)^{\frac{1}{2}}(v_0 - \iota u_0).$$

$$\kappa'^{\frac{1}{2}} a^{\frac{1}{2}} \mathrm{K}_{n+\frac{1}{2}}(\iota\kappa' a) = (\pi/2)(v_1 - \iota u_1)\, e^{-\frac{1}{2}(n+\frac{1}{2})\pi\iota},$$

the value of E_n is given by

$$\mathrm{E}_n = \frac{[\kappa' w_0 w_1{}' - \kappa\mathrm{K}' w_1 w_0{}'/\mathrm{K}]\,(\pi/2)\, e^{-\frac{1}{2}(n+\frac{1}{2})\pi\iota}}{[\kappa\mathrm{K}' w_1(\overline{w}_0{}' - w_0{}')/\mathrm{K} - \kappa' w_1{}'(\overline{w}_0 - w_0)]/2\iota},$$

that is

$$\mathrm{E}_n = \pi\iota \frac{(\sigma w_0 w_1{}'/w_1 - \sigma' w_0{}')\, e^{-\frac{1}{2}(n+\frac{1}{2})\pi\iota}}{\sigma'(\overline{w}_0{}' - w_0{}') - \sigma(\overline{w}_0 - w_0) w_1{}'/w_1}.$$

or

$$\mathrm{E}_n = e^{-\frac{1}{2}(n+\frac{1}{2})\pi\iota}\pi\iota[\sigma' w_0{}' - \sigma w_0 w_1{}'/w_1]/[\sigma' w_0{}' - \sigma w_0 w_1{}'/w_1 - \{\sigma'\overline{w}_0{}' - \sigma\overline{w}_0 w_1{}'/w_1\}].$$

Similarly

$$\mathrm{E}_n{}' = \frac{\kappa^{\frac{1}{2}}\kappa'^{\frac{1}{2}}[w_0(\overline{w}_0{}' - w_0{}') - w_0{}'(\overline{w}_0 - w_0)]}{\kappa w_1(\overline{w}_0{}' - w_0{}') - \mathrm{K}\kappa' w_1{}'(\overline{w}_0 - w_0)/\mathrm{K}'},$$

that is

$$\mathrm{E}_n{}' = \kappa^{\frac{1}{2}}\kappa'^{\frac{1}{2}}(w_0\overline{w}_0{}' - \overline{w}_0 w_0{}')/[\kappa w_1\overline{w}_0{}' - \kappa'\mathrm{K}w_1{}'\overline{w}_0/\mathrm{K}' - \{\kappa w_1 w_0{}' - \kappa'\mathrm{K}w_1{}'w_0\mathrm{K}'\}],$$

or

$$\mathrm{E}_n{}' = (\kappa'/\kappa)^{\frac{1}{2}}(2\iota\sigma'/w_1)/[\{\sigma'\overline{w}_0{}' - \sigma\overline{w}_0 w_1{}'/w_1\} - \{\sigma' w_0{}' - \sigma w_0 w_1{}'/w_1\}].$$

Hence

$$\psi_0 = \overline{\psi}_0 - b^{-\frac{1}{2}} e^{\iota pt} \pi\iota \sum_{n=1}^{\infty} \sum_{k=1}^{\infty} (2n+1) \{(\sigma' w_0' - \sigma w_0 w_1'/w_1)/(\sigma' \overline{w}_0' - \sigma \overline{w}_0 w_1'/w_1)\}^k$$
$$\times\ \mathrm{J}'_{n+\frac{1}{2}}(\kappa b)\, r^{\frac{1}{2}} \mathrm{J}_{n+\frac{1}{2}}(\kappa r) \sin\theta \frac{\partial \mathrm{P}_n}{\partial\theta},$$

$$\psi_1 = 2(\kappa'/\kappa)^{\frac{1}{2}}\, \iota b^{-\frac{1}{2}} e^{\iota pt} \sum_{n=1}^{\infty} \sum_{k=0}^{\infty} (2n+1)\, e^{\frac{1}{2}(n+\frac{1}{2})\pi\iota} (\sigma'/w_1) \{(\sigma' w_0' - \sigma w_0 w_1'/w_1)^k$$
$$\times\ (\sigma' \overline{w}_0' - \sigma \overline{w}_0 w_1'/w_1)^{-k-1}\}\, \mathrm{J}_{n+\frac{1}{2}}(\kappa b)\, r^{\frac{1}{2}} \mathrm{K}_{n+\frac{1}{2}}(\iota\kappa' r) \sin\theta \frac{\partial \mathrm{P}_n}{\partial\theta},$$

that is

$$\psi_0 = \overline{\psi}_0 + \sum_{k=1}^{\infty} \psi_{0k}, \qquad \psi_1 = \sum_{k=0}^{\infty} \psi_{1k},$$

where

$$\psi_{0k} = -\pi\iota b^{-\frac{1}{2}} e^{\iota pt} \sum_{n=1}^{\infty} (2n+1) \{(\sigma' w_0' - \sigma w_0 w_1'/w_1)/(\sigma' \overline{w}_0' - \sigma \overline{w}_0 w_1'/w_1)\}^k$$
$$\times\ \mathrm{J}_{n+\frac{1}{2}}(\kappa b)\, r^{\frac{1}{2}} \mathrm{J}_{n+\frac{1}{2}}(\kappa r) \sin\theta \frac{\partial \mathrm{P}_n}{\partial\theta},$$

$$\psi_{1k} = 2(\kappa'/\kappa)^{\frac{1}{2}}\, \iota b^{-\frac{1}{2}} e^{\iota pt} \sum_{n=1}^{\infty} (2n+1)\, e^{\frac{1}{2}(n+\frac{1}{2})\pi\iota} (\sigma'/w_1)(\sigma' w_0' - \sigma w_0 w_1'/w_1)^k$$
$$\times\ (\sigma' \overline{w}_0' - \sigma \overline{w}_0 w_1'/w_1)^{-k-1}\, \mathrm{J}_{n+\frac{1}{2}}(\kappa b)\, r^{\frac{1}{2}} \mathrm{K}_{n+\frac{1}{2}}(\iota\kappa' r) \sin\theta \frac{\partial \mathrm{P}_n}{\partial\theta}.$$

In the above expressions the term ψ_{0k} represents the part of the effect at the point which is due to the waves which have been reflected k times at the surface of the sphere, and the term ψ_{1k} at a point in the second medium represents the effect there which is due to the waves which have been reflected k times at the surface and then refracted into the second medium. It will be sufficient to discuss the terms ψ_{01} and ψ_{10}, and, as will be seen there are two cases according as $\kappa' a$ is greater or less than κb, for the important part of the sum of the series for ψ_{0k} and ψ_{1k} are contributed by the terms corresponding to values of $n + \frac{1}{2}$ which are less than κb. Writing

$$\mathrm{E}_{nk} = -\pi\iota \{(\sigma' w_0' - \sigma w_0 w_1'/w_1)/(\sigma' \overline{w}_0' - \sigma \overline{w}_0 w_1'/w_1)\}^k,$$
$$\mathrm{E}'_{nk} = (2\iota\sigma'/w_1)(\sigma' w_0' - \sigma w_0 w_1'/w_1)^k/(\sigma' \overline{w}_0' - \sigma \overline{w}_0 w_1'/w_1)^{k+1},$$

then for values of $n + \frac{1}{2}$ which satisfy the condition that $\kappa b - (n + \frac{1}{2})$ is of higher order than $(\kappa b)^{\frac{1}{3}}$ and $\kappa' a > \kappa b$,

$$w_0 = (\cos\alpha_0)^{-\frac{1}{2}} e^{-\iota\phi_0}, \qquad \overline{w}_0 = (\cos\alpha_0)^{-\frac{1}{2}} e^{\iota\phi_0},$$
$$w_1 = (\cos\alpha_1)^{-\frac{1}{2}} e^{-\iota\phi_1}, \qquad \overline{w}_1 = (\cos\alpha_1)^{-\frac{1}{2}} e^{\iota\phi_1},$$
$$w_0' = -\iota(\cos\alpha_0)^{\frac{1}{2}} e^{-\iota\phi_0}, \qquad \overline{w}_0' = \iota(\cos\alpha_0)^{\frac{1}{2}} e^{\iota\phi_0},$$
$$w_1' = -\iota(\cos\alpha_1)^{\frac{1}{2}} e^{-\iota\phi_1}, \qquad \overline{w}_1' = \iota(\cos\alpha_1)^{\frac{1}{2}} e^{\iota\phi_1},$$

where

$$\phi_0 = \kappa a \cos\alpha_0 - \tfrac{1}{2}n\pi + (n+\tfrac{1}{2})\alpha_0, \qquad \kappa a \sin\alpha_0 = n + \tfrac{1}{2},$$

$$\phi_1 = \kappa' a \cos\alpha_1 - \tfrac{1}{2}n\pi + (n+\tfrac{1}{2})\alpha_1, \qquad \kappa' a \sin\alpha_1 = n + \tfrac{1}{2},$$

and therefore

$$\begin{aligned}\mathrm{E}_{nk} = -\pi\iota\,\{(-\iota\sigma'\,(\cos\alpha_0)^{\frac{1}{2}}\,e^{\iota-\iota\phi_0} + \iota\sigma\cos\alpha_1\,(\cos\alpha_0)^{-\frac{1}{2}}\,e^{-\iota\phi_0})/(\iota\sigma'\,(\cos\alpha_0)^{\frac{1}{2}}\,e^{\iota\phi_0}\\ + \iota\sigma\cos\alpha_1\,(\cos\alpha_0)^{-\frac{1}{2}}\,e^{\iota\phi_0})\}^k,\end{aligned}$$

$$\begin{aligned}\mathrm{E}'_{nk} = 2\iota\sigma'\,(\cos\alpha_1)^{\frac{1}{2}}\,e^{\iota\phi_1}\,\{-\iota\sigma'\,(\cos\alpha_0)^{\frac{1}{2}}\,e^{-\iota\phi_0} + \iota\sigma\cos\alpha_1\,(\cos\alpha_0)^{-\frac{1}{2}}\,e^{-\iota\phi_0}\}^k\\ \times\{\iota\sigma'\,(\cos\alpha_0)^{\frac{1}{2}}\,e^{\iota\phi_0} + \iota\sigma\cos\alpha_1\,(\cos\alpha_0)^{-\frac{1}{2}}\,e^{\iota\phi_0}\}^{-k-1},\end{aligned}$$

that is

$$\mathrm{E}_{nk} = -\pi\iota\,\{(\sigma\cos\alpha_1 - \sigma'\cos\alpha_0)/(\sigma\cos\alpha_1 + \sigma'\cos\alpha_0)\}^k\,e^{-2k\phi_0\iota},$$

$$\begin{aligned}\mathrm{E}'_{nk} = 2\sigma'\,(\cos\alpha_0)^{\frac{1}{2}}\,(\cos\alpha_1)^{\frac{1}{2}}\,(\sigma\cos\alpha_1 - \sigma'\cos\alpha_0)^k\\ (\sigma\cos\alpha_1 + \sigma'\cos\alpha_0)^{-k-1}\,e^{-(2k+1)\phi_0\iota + \phi_1\iota}.\end{aligned}$$

It follows that

$$\begin{aligned}\psi_{0k} = -\pi\iota b^{-\frac{1}{2}}e^{\iota pt}\sum_1^\infty (2n+1)\,\{(\sigma\cos\alpha_1 - \sigma'\cos\alpha_0)/(\sigma\cos\alpha_1 + \sigma'\cos\alpha_0)\}^k e^{-2k\phi_0\iota}\\ \times \mathrm{J}_{n+\frac{1}{2}}(\kappa b)\,r^{\frac{1}{2}}\,\mathrm{J}_{n+\frac{1}{2}}(\kappa r)\sin\theta\,\frac{\partial \mathrm{P}_n}{\partial\theta},\end{aligned}$$

that is, taking the case where $\theta < \pi/2$, and substituting the appropriate approximate value for $\sin\theta\,\dfrac{\partial \mathrm{P}_n}{\partial\theta}$,

$$\begin{aligned}\psi_{0k} = -\iota\kappa^{-1}b^{-2}e^{\iota pt}\sum_1^\infty (2/\pi)^{\frac{1}{2}}\,(n+\tfrac{1}{2})^{\frac{1}{2}}\\ \times\{(\sigma\cos\alpha_1 - \sigma'\cos\alpha_0)/(\sigma\cos\alpha_1 + \sigma'\cos\alpha_0)\}^k\,e^{-2k\phi_0\iota}\\ \times(e^{\iota\phi} - e^{-\iota\phi})\,(e^{\iota\phi_2} - e^{-\iota\phi_2})\,(\cos\alpha\cos\beta)^{-\frac{1}{2}}\,(\sin\theta)^{\frac{1}{2}}\sin\left\{(n+\tfrac{1}{2})\,\theta - \frac{\pi}{4}\right\},\end{aligned}$$

where

$$\phi = \kappa r\cos\alpha - \tfrac{1}{2}n\pi + (n+\tfrac{1}{2})\,\alpha, \quad \kappa r\sin\alpha = n + \tfrac{1}{2},$$

$$\phi_2 = \kappa b\cos\beta - \tfrac{1}{2}n\pi + (n+\tfrac{1}{2})\,\beta, \quad \kappa b\sin\beta = n + \tfrac{1}{2},$$

and therefore

$$\begin{aligned}\psi_{0k} = -(2\pi)^{-\frac{1}{2}}\kappa^{-1}b^{-2}e^{\iota pt}\sum_1^\infty (n+\tfrac{1}{2})^{\frac{1}{2}}\\ \times\{(\sigma\cos\alpha_1 - \sigma'\cos\alpha_0)/(\sigma\cos\alpha_1 + \sigma'\cos\alpha_0)\}^k\,e^{-2k\phi_0\iota}\\ \times(e^{\iota\phi} - e^{-\iota\phi})\,(e^{\iota\phi_2} - e^{-\iota\phi_2})\,\left(e^{(n+\frac{1}{2})\theta\iota - \frac{\pi\iota}{4}} - e^{-(n+\frac{1}{2})\theta\iota + \frac{\pi\iota}{4}}\right)(\cos\alpha\cos\beta)^{-\frac{1}{2}}(\sin\theta)^{\frac{1}{2}},\end{aligned}$$

since

$$\frac{\partial \phi}{\partial n} = \alpha - \tfrac{1}{2}\pi, \text{ etc.,}$$

when $k = 1$, the terms whose rate of oscillation is stationary for a real value of n within the range are the terms which have the exponential

$$e^{-(n+\frac{1}{2})\theta\iota + \frac{\pi\iota}{4} + \phi\iota + \phi_2\iota - 2\phi_0\iota}$$

as a factor, hence the principal part of ψ_{01} is given by

$$\psi_{01} = (2\pi)^{-\frac{1}{2}}\kappa^{-1}b^{-2}e^{\iota pt}\sum_1^\infty (n + \tfrac{1}{2})^{\frac{1}{2}}\{(\sigma\cos\alpha_1 - \sigma'\cos\alpha_0)/(\sigma\cos\alpha_1 + \sigma'\cos\alpha_0)\}$$
$$\times (\sin\theta)^{\frac{1}{2}}(\cos\alpha\cos\beta)^{-\frac{1}{2}}e^{-(n+\frac{1}{2})\theta\iota + \frac{\pi\iota}{4} + \phi\iota + \phi_2\iota - 2\phi_0\iota}.$$

If n_0 is the value for which the rate of oscillation is stationary

$$-\theta - 2\alpha_0 + \alpha + \beta = 0,$$

where α_0, α_1, β now have the values corresponding to the value n_0 of n, and since

$$\frac{\partial^2\phi}{\partial n^2} = \frac{1}{\kappa r\cos\alpha}, \text{ etc., if } n = n_0 + \zeta,$$

$$-(n + \tfrac{1}{2})\theta\iota + \frac{\pi\iota}{4} + \phi\iota + \phi_2\iota - 2\phi_0\iota$$
$$= \frac{\pi\iota}{4} + \iota\kappa(r\cos\alpha + b\cos\beta - 2a\cos\alpha_0)$$
$$+ \tfrac{1}{2}\iota\zeta^2\{(\kappa r\cos\alpha)^{-1} + (\kappa b\cos\beta)^{-1} - 2(\kappa a\cos\alpha_0)^{-1}\} + \ldots,$$

whence

$$\psi_{01} = (2\pi)^{-\frac{1}{2}}\kappa^{-1}b^{-2}e^{\iota pt}(n_0 + \tfrac{1}{2})^{\frac{1}{2}}\{(\sigma\cos\alpha_1 - \sigma'\cos\alpha_0)/(\sigma\cos\alpha_1 + \sigma'\cos\alpha_0)\}$$
$$\times (\cos\alpha\cos\beta)^{-\frac{1}{2}}(\sin\theta)^{\frac{1}{2}}e^{\frac{\pi\iota}{4} + \iota\kappa(r\cos\alpha + b\cos\beta - 2a\cos\alpha_0)}\int_{-\infty}^{\infty}e^{\frac{1}{2}\iota A\zeta^2}\,d\zeta,$$

where

$$A = 1/\kappa r\cos\alpha + 1/\kappa b\cos\beta - 2/\kappa a\cos\alpha_0,$$

that is, since

$$\int_{-\infty}^{\infty}e^{\frac{1}{2}\iota A\zeta^2}\,d\zeta = (2\pi/A)^{\frac{1}{2}}e^{\frac{\pi\iota}{4}},$$

$$\psi_{01} = \iota\kappa^{-1}b^{-2}e^{\iota pt}(n_0 + \tfrac{1}{2})^{\frac{1}{2}}\{(\sigma\cos\alpha_1 - \sigma'\cos\alpha_0)/(\sigma\cos\alpha_1 + \sigma'\cos\alpha_0)\}$$
$$\times (\cos\alpha\cos\beta)^{-\frac{1}{2}}(\sin\theta)^{\frac{1}{2}}\{(\kappa r\cos\alpha)^{-1} + (\kappa b\cos\beta)^{-1} - 2(\kappa a\cos\alpha_0)^{-1}\}^{-\frac{1}{2}}$$
$$\times e^{\iota\kappa(r\cos\alpha + b\cos\beta - 2a\cos\alpha_0)}.$$

If D is the distance from the oscillator O to the point where the ray is reflected first and D′ the distance of this point Q from the point P (r, θ) and C is the centre of the sphere the angle OQC $= \alpha_0$,

$$\mathrm{D} = a \cos \alpha_0 - b \cos \beta, \quad \mathrm{D}' = a \cos \alpha_0 - r \cos \alpha, \quad \sin (\alpha - a_0)/\mathrm{D}' = \sin \alpha_0 / r,$$
$$\sin (\beta - a_0)/\mathrm{D} = \sin \alpha_0 / b,$$

$$\{(r \cos \alpha)^{-1} + (b \cos \beta)^{-1} - 2 (a \cos \alpha_0)^{-1}\} \cos \alpha \cos \beta$$
$$= (br)^{-1} (\mathrm{D} + \mathrm{D}' - 2\mathrm{DD}'/a \cos \alpha_0),$$

$$\sin \theta = \sin (\alpha - a_0 + \beta - \beta_0) = (br)^{-1} \sin \alpha_0 \{a (\mathrm{D} + \mathrm{D}') - 2\mathrm{DD}' \cos \alpha_0\},$$

hence the principal part of the magnetic force at the point P due to waves after one reflexion is given by

$$\psi_{01}/r \sin \theta = \iota\kappa e^{\iota pt - \iota\kappa(\mathrm{D}+\mathrm{D}')}$$
$$\times \{(\sigma \cos \alpha_1 - \sigma' \cos \alpha_0)/(\sigma \cos \alpha_1 + \sigma' \cos \alpha_0)\}\, ab^{-1}\mathrm{D}^{-1}\mathrm{D}'^{-1}$$
$$\times \{\mathrm{D}^{-1} + \mathrm{D}'^{-1} - 2 (a \cos \alpha_0)^{-1}\}^{-\frac{1}{2}} \{\mathrm{D}^{-1} + \mathrm{D}'^{-1} - 2a^{-1} \cos \alpha_0\}^{-\frac{1}{2}} \sin \alpha_0.\text{*}$$

In the same case the value of ψ_{1k} is given by

$$\psi_{1k} = 2 (\kappa'/\kappa)^{\frac{1}{2}} \sigma' b^{-\frac{1}{2}} e^{\iota pt} \sum_1^\infty (2n + 1)\, e^{\frac{1}{2}(n+\frac{1}{2})\pi\iota} (\cos \alpha_0 \cos \alpha_1)^{\frac{1}{2}} (\sigma \cos \alpha_1 - \sigma' \cos \alpha_0)^k$$
$$\times (\sigma \cos \alpha_1 + \sigma' \cos \alpha_0)^{-k-1} e^{-(2k+1)\phi_0\iota + \phi_1\iota} \mathrm{J}_{n+\frac{1}{2}} (\kappa b)\, r^{\frac{1}{2}} \mathrm{K}_{n+\frac{1}{2}} (\iota\kappa' r) \sin \theta \frac{\partial \mathrm{P}_n}{\partial \theta},$$

that is, substituting the appropriate approximate values,

$$\psi_{1k} = (2\pi)^{-\frac{1}{2}} \sigma' \kappa^{-1} b^{-2} e^{\iota pt} \sum_1^\infty 2 \left(n + \tfrac{1}{2}\right)^{\frac{1}{2}} (\cos \alpha_0 \cos \alpha_1)^{\frac{1}{2}} (\sigma \cos \alpha_1 - \sigma' \cos \alpha_0)^k$$
$$\times (\sigma \cos \alpha_1 + \sigma' \cos \alpha_0)^{-k-1} e^{-(2k+1)\phi_0\iota + \phi_1\iota - \phi_3\iota} (e^{\iota\phi_2} - e^{-\iota\phi_2})$$
$$(\sin \theta)^{\frac{1}{2}} (\cos \alpha_3 \cos \beta)^{-\frac{1}{2}} \left(e^{(n+\frac{1}{2})\theta\iota - \frac{\pi\iota}{4}} - e^{-(n+\frac{1}{2})\theta\iota + \frac{\pi\iota}{4}}\right),$$

where

$$(\kappa' r)^{\frac{1}{2}} \mathrm{K}_{n+\frac{1}{2}} (\iota\kappa' r) = (\pi/2)^{\frac{1}{2}} e^{-\frac{1}{2}(n+\frac{1}{2})\pi\iota} w_3, \quad \phi_3 = \kappa' r \cos \alpha_3 - \tfrac{1}{2} n\pi + \left(n + \tfrac{1}{2}\right) \alpha_3,$$
$$\kappa' r \sin \alpha_3 = n + \tfrac{1}{2},$$

when $k = 0$, $\theta < \pi/2$, the terms whose rate of oscillation is stationary for a value of n within the range of the values of n are those which contain the exponential factor

$$e^{-(n+\frac{1}{2})\theta\iota + \frac{\pi\iota}{4} - \phi_0\iota + \phi_1\iota + \phi_2\iota - \phi_3\iota},$$

and if n_0 is the value of n for which the rate of oscillation is stationary

$$-\theta - \alpha_0 + \alpha_1 + \beta - \alpha_3 = 0,$$

---

* *Cf.* 'Roy. Soc. Proc.,' A, vol. 123, p. 1 (1929).

where α_0, α_1, α_3, β now have the values corresponding to the value n_0 of n, and since

$$\frac{\partial^2\phi_0}{\partial n^2} = \frac{1}{\kappa a \cos\alpha_0}, \text{ etc.,}$$

if $n = n_0 + \zeta$,

$$-(n+\tfrac{1}{2})\,\theta\iota + \frac{\pi\iota}{4} - \phi_0\iota + \phi_1\iota + \phi_2\iota - \phi_3\iota = \frac{\pi\iota}{4}$$
$$+\,\iota\,(\kappa b\cos\beta - \kappa' r\cos\alpha_3 - \kappa a\cos\alpha_0 + \kappa' a\cos\alpha_1) + \tfrac{1}{2}\iota A\zeta^2\ldots,$$

where

$$A = (\kappa b\cos\beta)^{-1} - (\kappa' r\cos\alpha_3)^{-1} - (\kappa a\cos\alpha_0)^{-1} + (\kappa' a\cos\alpha_1)^{-1},$$

and the principal part of ψ_{10} is given by

$$\psi_{10} = -(2\pi)^{-\frac{1}{2}}\sigma'\kappa^{-1}b^{-2}e^{\iota pt}2\,(n_0+\tfrac{1}{2})^{\frac{1}{2}}(\sin\theta)^{\frac{1}{2}}(\cos\alpha_0\cos\alpha_1)^{\frac{1}{2}}(\cos\alpha_3\cos\beta)^{-\frac{1}{2}}$$
$$\times\,(\sigma\cos\alpha_1 + \sigma'\cos\alpha_0)^{-1}\,e^{\frac{\pi\iota}{4}+\iota(\kappa b\cos\beta - \kappa' r\cos\alpha_3 - \kappa a\cos\alpha_0 + \kappa' a\cos\alpha_1)}\int_{-\infty}^{\infty} e^{\frac{1}{2}A\zeta^2\iota}\,d\zeta,$$

that is

$$\psi_{10} = -2\iota\sigma'\kappa^{-1}b^{-2}e^{\iota pt}(n_0+\tfrac{1}{2})^{\frac{1}{2}}(\sin\theta)^{\frac{1}{2}}(\cos\alpha_0\cos\alpha_1)^{\frac{1}{2}}(\cos\alpha_3\cos\beta)^{-\frac{1}{2}}$$
$$\times\,(\sigma\cos\alpha_1 + \sigma'\cos\alpha_0)^{-1}\{(\kappa b\cos\beta)^{-1} - (\kappa' r\cos\alpha_3)^{-1}$$
$$-\,(\kappa a\cos\alpha_0)^{-1} + (\kappa' a\cos\alpha_1)^{-1}\}^{-\frac{1}{2}}\,e^{\iota(\kappa b\cos\beta - \kappa' r\cos\alpha_3 - \kappa a\cos\alpha_0 + \kappa' a\cos\alpha_1)}.$$

If D′ now denotes the distance of the point P (r, θ) from the point Q on the surface of the sphere where the ray is refracted

$$D = a\cos\alpha_0 - b\cos\beta,\quad D' = r\cos\alpha_3 - a\cos\alpha_1,\quad \sin(\beta-\alpha_0)/D = \sin\alpha_0/b,$$
$$\sin(\alpha_1-\alpha_3)/D' = \sin\alpha_1/r,\qquad b\cos(\beta-\alpha_0) = a - D\cos\alpha_0,$$
$$r\cos(\alpha_1-\alpha_3) = a + D'\cos\alpha_1,$$

whence

$$\sin\theta = \sin(\beta - \alpha_0 + \alpha_1 - \alpha_3) = \{\kappa/D + \kappa'/D' + (\kappa'\cos a_1 - \kappa\cos\alpha_0)/a\}$$
$$\times\,\{aDD'/\kappa' br\}\sin\alpha_0,$$

also

$$\cos\alpha_3\cos\beta\,\{(\kappa b\cos\beta)^{-1} - (\kappa' r\cos\alpha_3)^{-1} - (\kappa a\cos\alpha_0)^{-1} + (\kappa' a\cos\alpha_1)^{-1}\}$$
$$= \{\kappa\cos^2\alpha_0/D + \kappa'\cos^2\alpha_1/D' + (\kappa'\cos\alpha_1 - \kappa\cos\alpha_0)\}$$
$$\times\,\{DD'/\kappa\kappa' br\cos\alpha_0\cos\alpha_1\},$$

and, substituting these expressions in the value of the principal part of ψ_{10},

$$\psi_{10}/r\sin\theta = -2\iota\kappa\kappa'\sigma'\,(a/bDD')\sin\alpha_0\cos\alpha_0\cos\alpha_1\,(\sigma\cos\alpha_1 + \sigma'\cos\alpha_0)^{-1}$$
$$\times\,\{\kappa/D + \kappa'/D' + (\kappa'\cos\alpha_1 - \kappa\cos\alpha_0/a)\}^{-\frac{1}{2}}$$
$$\times\,\{\kappa\cos^2\alpha_0/D + \kappa'\cos^2\alpha_1/D' + (\kappa'\cos\alpha_1 - \kappa\cos\alpha_0)/D\}^{-\frac{1}{2}}\,e^{\iota pt - \iota\kappa D - \iota\kappa' D'}.^{*}$$

---

[*] 'Roy. Soc. Proc.,' A, vol. 123, p. 1 (1929).

When $\kappa' a < \kappa b$, the values of the principal parts of ψ_{01} and ψ_{10} are those given above, provided that the value n_0 of n for which the terms contributing the principal parts have stationary oscillation satisfies the condition that $\kappa' a - (n_0 + \frac{1}{2})$ is of an order higher than $(\kappa' a)^{\frac{1}{3}}$, that is, if $(\sin \gamma_0 - \sin \alpha_0)/\sin \gamma$ is of higher order than $(\kappa' a)^{-\frac{2}{3}}$, where $\kappa a \sin \alpha_0 = n_0 + \frac{1}{2}$, and γ is the critical angle. It follows that these expressions give the principal part of the values of ψ_{01} and ψ_{10} if the point Q is not on nor near to that portion of the surface which is external to the right circular cone, whose vertex is the image O′ of the point O in the sphere, and whose semi-vertical angle is the critical angle.

When the point is on that portion of the surface of the sphere which is external to the cone whose vertex is O′ and semi-vertical angle the critical angle, and not near to the boundary of this portion, the appropriate approximate value of w_1'/w_1 is

$$- \{(n_0 + \tfrac{1}{2})^2 - (\kappa' a)^2\}^{\frac{1}{2}}/\kappa' a,$$

when $n_0 + \frac{1}{2} - \kappa' a$ is of higher order than $(\kappa' a)^{\frac{1}{3}}$, and the value of β_{nk} is then given by

$$\mathrm{E}_{nk} = - \pi \iota \left[\{\sigma\{(n + \tfrac{1}{2})^2 - \kappa'^2 a^2\}^{\frac{1}{2}}/\kappa' a - \iota\sigma' \cos \alpha_0\} \right.$$
$$\left. /\{\sigma\{(n + \tfrac{1}{2})^2 - (\kappa' a)^2\}/\kappa' a + \iota\sigma' \cos \alpha_0\}\right] e^{k - 2k\phi_0 \iota}.$$

Writing

$$\nu^2 = \kappa^2 (\sin^2 \alpha_0 - \sin^2 \gamma),$$

this becomes

$$\mathrm{E}_{nk} = - \pi \iota \{(\sigma\nu/\kappa' - \iota\sigma' \cos \alpha_0)/(\sigma\nu/\kappa' + \iota\sigma' \cos \alpha_0)\}^k e^{-2k\phi_0 \iota},$$

that is

$$\mathrm{E}_{nk} = - \pi \iota e^{-k\chi' \iota - 2k\phi_0 \iota},$$

where $\tan \frac{1}{2}\chi' = \kappa'\sigma' \cos \alpha_0/\sigma\nu$, and the expression for the principal part of the magnetic force at the point P $(r\theta)$ after one reflexion is now given by

$$\psi_{01}/r \sin \theta = \iota\kappa e^{\iota p t - \iota\kappa \mathrm{D} - \iota\kappa \mathrm{D}' - \chi' \iota} a b^{-1} \mathrm{D}^{-1} \mathrm{D}'^{-1} \{\mathrm{D}^{-1} + \mathrm{D}'^{-1} - 2 (a \cos \alpha_0)^{-1}\}^{-\frac{1}{2}}$$
$$\times \{\mathrm{D}^{-1} + \mathrm{D}'^{-1} - 2a^{-1} \cos \alpha_0\}^{-\frac{1}{2}}.$$

In this case the amplitude of the magnetic force in the reflected wave at Q is equal to the amplitude of the magnetic force in the incident waves at Q, and there is a change of phase $-\chi'$,* if the conjugate case of a simple magnetic oscillator at the point O is taken, the change of phase at Q in the electric force in the reflected wave is $\pi - \chi$ where $\tan \frac{1}{2}\chi = \kappa'\sigma \cos \alpha_0/\sigma'\nu$.

When the point Q is so near to either circle of intersection of the cone whose vertex is O′ and the sphere that the absolute value of $n_0 + \frac{1}{2} - \kappa' a$ is of the same order as $(\kappa' a)^{\frac{1}{3}}$ or of lower order, the appropriate approximate value of w_1'/w_1 is

---

* *Cf.* 'Roy. Soc. Proc.,' A, vol. 119, p. 525 (1928).

$$-3^{\frac{1}{3}}(\kappa' a)^{-\frac{1}{3}}\xi^{\frac{1}{3}}\mathrm{K}_{\frac{2}{3}}(\xi e^{-\pi\iota})/\mathrm{K}_{\frac{1}{3}}(\xi e^{-\pi\iota}),$$

where

$$\xi = 2\zeta^{\frac{3}{2}}, \quad 3\zeta = 6^{\frac{1}{3}}(n+\tfrac{1}{2}-\kappa' a)(\kappa' a)^{-\frac{1}{3}},\text{*}$$

and the value of E_{nk} is then

$$-\pi\iota\{3^{\frac{1}{3}}\sigma(\kappa' a)^{-\frac{1}{3}}\xi^{\frac{1}{3}}\mathrm{K}_{\frac{2}{3}}(\xi e^{-\pi\iota})/\mathrm{K}_{\frac{1}{3}}(\xi e^{-\pi\iota})-\iota\sigma'\cos\alpha_0\}^{k}$$
$$\times\{3^{\frac{1}{3}}\sigma(\kappa' a)^{-\frac{1}{3}}\xi^{\frac{1}{3}}\mathrm{K}_{\frac{2}{3}}(\xi e^{-\pi\iota})/\mathrm{K}_{\frac{1}{3}}(\xi e^{-\pi\iota})+\iota\sigma'\cos\alpha_0\}^{-k}e^{2k\phi_0\iota},$$

and therefore the principal part of the magnetic force at the point P (r, θ) is given by

$$\psi_{01}/r\sin\theta = \iota\kappa e^{\iota pt-\iota\kappa\mathrm{D}-\iota\kappa\mathrm{D}'}ab^{-1}\mathrm{D}^{-1}\mathrm{D}'^{-1}\{\mathrm{D}^{-1}+\mathrm{D}'^{-1}-2(a\cos\alpha_0)^{-1}\}^{-\frac{1}{2}}$$
$$\times\{\mathrm{D}^{-1}+\mathrm{D}'^{-1}-2a^{-1}\cos\alpha_0\}^{-\frac{1}{2}}\{3^{\frac{1}{3}}\sigma(\kappa' a)^{-\frac{1}{3}}\xi^{\frac{1}{3}}\mathrm{K}_{\frac{2}{3}}(\xi e^{-\pi\iota})/\mathrm{K}_{\frac{1}{3}}(\xi e^{-\pi\iota})-\iota\sigma'\cos\alpha_0\}$$
$$\times\{3^{\frac{1}{3}}\sigma(\kappa' a)^{-\frac{1}{3}}\xi^{\frac{1}{3}}\mathrm{K}_{\frac{2}{3}}(\xi e^{-\pi\iota})/\mathrm{K}_{\frac{1}{3}}(\xi e^{-\pi\iota})+\iota\sigma'\cos\alpha_0\}^{-1}.$$

This expression shows that the change of phase in the reflected wave begins before α_0 attains the value of the critical angle, and that the amplitude of the magnetic force in the reflected wave becomes equal to the amplitude of the magnetic force in the incident wave when the angle of incidence α_0 satisfies the condition that $(\sin\alpha_0-\sin\gamma)/\sin\gamma$ is of higher order than $(\kappa' a)^{-\frac{2}{3}}$.

When the point P is outside the sphere and the point Q is on the portion of the sphere external to the cone whose vertex is O′ there is no value of n such that $\kappa' a-(n+\frac{1}{2})$ is of higher order than $(\kappa' a)^{\frac{1}{3}}$ and for which the terms of ψ_{01} have a stationary rate of oscillation; further, when the point Q is approaching the boundary of this portion from outside it the magnetic force in the transmitted wave becomes of the order $(\kappa' a)^{-\frac{1}{6}}$ in comparison with the magnetic force in the incident wave, and there is a shadow in the space between the two cones which touch the sphere along the circles of intersection of the sphere and the cone whose vertex is O′. Again, in the shadow the magnetic force contains an exponential factor with a negative exponent due to the factor w_1^{-1} in E_{01}', when the point Q is not near the boundary of the portion of the sphere intercepted by the cone O′, and it may be inferred that the result obtained by considering the case of a train of plane waves, incident on a plane surface separating two media, gives the approximate values of the electric and magnetic forces in the two media near to the surface of separation at points which are not near to the boundary of the shadow in the second medium, and not near to the rays in the first medium incident at the critical angle when the source of the waves is at a distance from those points which is great compared with the wave-length.

---

* 'Roy. Soc. Proc.,' A, vol. 92, p. 52 (1914).

The Measurement of Flame Temperatures.

By Ezer Griffiths, D.Sc., F.R.S., and J. H. Awbery, B.A., B.Sc., Physics Department, The National Physical Laboratory, Teddington, Middlesex.

(Received January 22, 1929.)

Introduction—Meaning of Flame Temperature.

To define the "temperature" of a flame, and to be sure that the concept has a unique meaning, is no easy task.

Without entering into philosophic abstractions, it would seem that a working definition, which corresponds to the general idea of what is meant by "the temperature of a flame," would be "the temperature of a solid body which is in thermal equilibrium with the flame." Strictly, this is to argue in a circle, for "thermal equilibrium" means primarily "equality of temperature"; experimentally, it is satisfactory in that we may assume that thermal equilibrium corresponds to that thermal state which is eventually reached when the solid is left in contact with the flame for a sufficient time, provided the introduction of the solid does not alter the conditions.

The state of thermal equilibrium may also be considered to exist when there is no energy interchange between the flame and the body, but in framing an interpretation from this point of view care is required, since not only have we no direct means of examining such an interchange of energy, but also the very concept of heat energy is a derived idea, less fundamental than that of temperature.

We shall leave these matters unresolved at present and, assuming that the temperature of a flame is a notion which has a meaning to the physicist, we shall discuss methods for obtaining its numerical measure. The best justification for this point of view is the *a posteriori* one that methods which differ radically agree in assigning one unique value of the temperature associated with the flame studied, so that this temperature may justifiably be spoken of as the temperature of the particular flame.

Methods Based on Thermal Equilibrium. Electrically Heated Wire.

The method of measuring the flame temperature which was almost universally used by early workers was the insertion of a solid object, frequently a thermocouple, into the flame, and the estimation of its temperature under those conditions; it was evident from the first, however, that this method did not measure the undisturbed flame temperature but rather that of the object inserted in the flame. The inserted object cooled the flame and, to a greater extent, the larger the body. Attempts have been made to overcome this difficulty by examining a series of geometrically similar bodies—beads or wires—and extrapolating the apparent temperature to that which would be furnished by an infinitely small body, which would not disturb the flame at all.

We have devised another method, to which we shall refer in this paper as "the wire method," in which the condition of thermal equilibrium is identified by the absence of energy interchange between the body and the flame. Consider a metal wire carrying electric current and immersed in a flame. In general, when the conditions are steady, the heat generated by the current is transferred from the wire by three agencies :—(1) Part is radiated to distant cool objects; (2) part is conducted along the wire to its supports, and eventually reaches the air; (3) part is transferred to the hot gases composing the flame.

Now if the wire is at the temperature of the flame, the last action cannot take place, and all the heat generated is either radiated or conducted away. A similar condition prevails, however, if the wire is in a vacuum, since in this case also there is no convection. Thus if the point is found at which both the current and the temperature are the same for the wire in the flame and in a vacuum, this temperature will be the flame temperature; for the equality of temperature ensures that the radiation and conduction terms shall be equal in the two cases, whilst the equality of current ensures that the total heat dissipated is unaltered. Hence the remaining term (convection) is equal in both cases and, since it is zero in the vacuum, it is also zero in the flame, so that the wire is at the flame temperature.

The observations were easily carried out.* A platinum wire was arranged horizontally in the flame of a Meker burner. The wire was connected through rheostats with a large 100-volt battery, and a shunt so that currents could be measured by means of the potential drop across the latter. The apparent temperature of the wire was observed by means of a disappearing filament optical pyrometer. The same wire was next set up under a large bell jar, which was exhausted below 1/10 mm. mercury pressure, and the temperature corresponding to various values of the current was determined. Fig. 1 shows the apparatus for this observation. When the data were plotted on squared paper the two curves shown in fig. 2 were obtained: the one curve corresponding to the observations

---

* A short description of this method was published in the 'N.P.L. Annual Report for 1926,' p. 63.

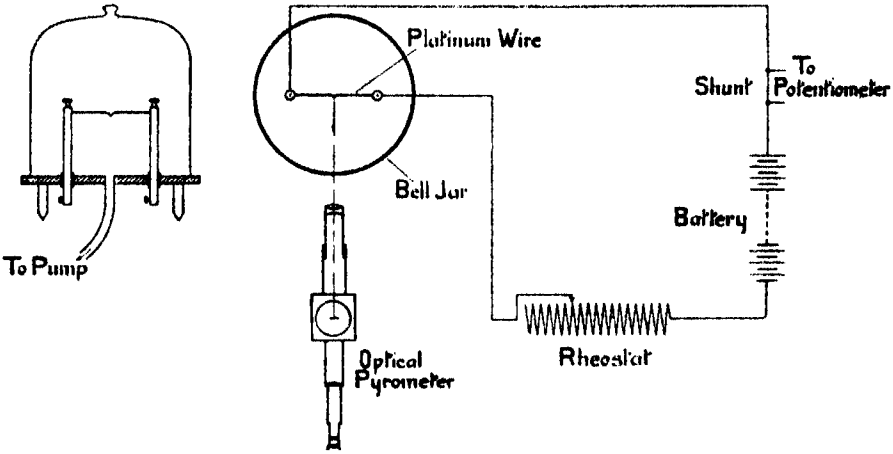

FIG. 1.

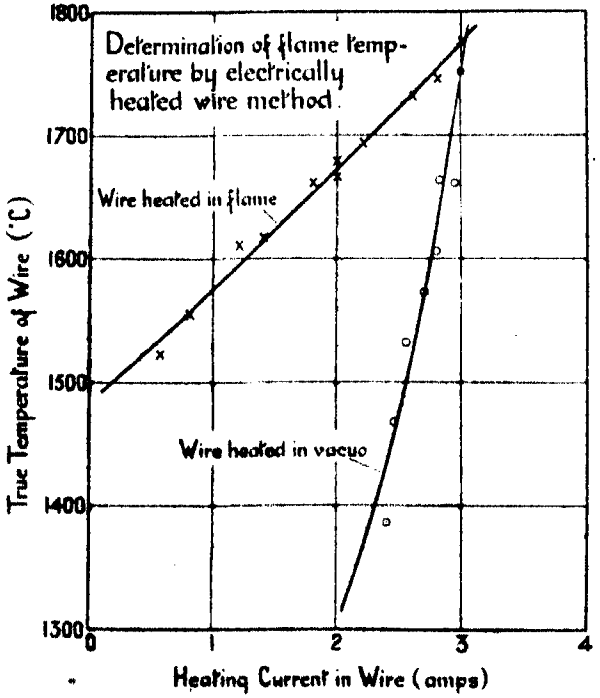

FIG. 2.

obtained when the wire was in the flame and the other when the wire was heated *in vacuo*. It will now be seen that at the point of intersection the temperature of the wire gives the temperature of the flame. For the total energy dissipation is the same for this particular temperature, whether the wire is in a flame or *in vacuo*. Further, the conduction loss and the radiation to the room are the same owing to the constancy in temperature, hence the convection loss must be so; and, as this is zero *in vacuo*, it must be zero in the flame, so that there is no energy interchange between the wire and the flame.

Before this conclusion can be considered as rigorously established, the following points require attention:—

(1) In the line of sight of the pyrometer in the one experiment there is half the thickness of the flame and in the other experiment the glass wall of the bell jar; it is evident that the error on this account must be very small, for the pyrometer operates by means of a wave-length in the red, to which both the glass and the flame are practically transparent. A direct examination of the magnitude of the error was made by sighting on a suitable incandescent object through the complete bell jar, and through the flame, thus doubling the error in each case. It appeared that apparent temperatures need increasing by 4 to 5° C. when sighting through this particular glass, and 2 to 3° C. when sighting through the flame.

(2) In the flame, but not in the vacuum, a part of the radiation is stopped before reaching distant cool objects and, in fact, takes place to an envelope of gas at a very high temperature. An exact estimate of the magnitude of the error involved here could be made by finding the absorption of a flame, but it is more easily shown to be negligible by the following experiment.

A sheet of platinum 1·2 cm. wide by 7 cm. long was supported in the vertical plane (see fig. 3). On either side burners were arranged to give two sheets of flame parallel to the plane of the strip, but not in contact with it. A constant electric current was supplied to the strip sufficient to raise it to incandescence. Observations of its temperature were then made with an optical pyrometer first with the two flames alight and secondly without the flames.

If the energy radiated to and absorbed by the strip from the flames is appreciable compared with the total energy dissipated in the strip, then the temperature of the strip should be measurably higher when the flames are alight than when they are not.

The difference observed was only of the order of 8° C. and within the limits of the errors of experiment which, of course, are of appreciable magnitude on account of stray draughts, etc.

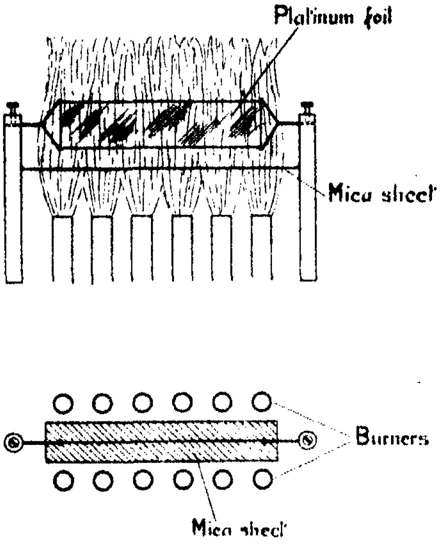

FIG. 3.

There is also the following indirect evidence to support the above conclusions :-

(1) That wires of very different diameters agree in assigning the same temperature to the flame.

(2) That this common temperature is in agreement with the flame temperature deduced by another method described later (that of spectral line reversal).

Thus with one particular flame studied we obtained the results below. For these experiments rhodium wires were employed instead of platinum because the melting point of rhodium is higher (1955° C.).

Temperature using wire 0·5 mm. diameter = 1877° C.
Temperature using wire 0·2 mm. diameter = 1886° C.
Temperature using spectral line reversal method = 1883° C.

The close agreement of the above results is fortuitous for there is considerable uncertainty in the correction to be applied to convert apparent to true temperatures.

Method of Spectral Line Reversal.

The basis of this method is the fundamental observation of Kirchhoff, that the dark lines in the solar spectrum correspond exactly to the bright lines in the spectra of various elements. In his own words: "In order to test in the most direct manner possible the frequently asserted fact of the coincidence of the sodium lines with the lines D of Frauenhofer, I obtained a tolerably bright solar spectrum, and brought a flame coloured by sodium vapour in front of the slit. I then saw the dark lines D (of the solar spectrum) change into bright ones. The flame of a Bunsen's lamp threw the bright sodium lines upon the solar spectrum with unexpected brilliance. In order to find out the extent to which the intensity of the solar spectrum could be increased without impairing the distinctness of the sodium lines, I allowed the full sunshine to shine through the sodium flame, and to my astonishment I saw that the dark lines D appeared with an extraordinary degree of clearness."

He here brings out clearly the fact that light from a hot object, if passed through a layer of some absorbing vapour, may afterwards give a spectrum in which the lines due to that material are either light or dark, according to circumstances. To verify this hypothesis, he dispensed with the sun as source and performed a purely terrestrial experiment, in which the light from an oxy-hydrogen limelight was passed through a sodium flame; as a result, instead of the usual continuous spectrum of the limelight, he obtained two dark bands in the position normally occupied by the D lines.

These experiments ultimately led him to formulate the well-known law which goes by his name: that the absorptive and emissive powers of a body are in a constant ratio. He also realised the implication of this law, that the condition which decides whether the lines shall appear bright or dark is the relative temperatures of the source and of the intervening material. If the former is hotter, the lines are dark, and conversely.

This leads immediately to the suggestion that, when the lines merge into the continuous spectrum, appearing neither dark nor bright, then the temperature of the source is equal to that of the absorbing medium.

If Kirchhoff had been in possession of appliances for the accurate control and measurement of high temperatures, he would probably have verified this theoretical deduction by laboratory experiments.

As a matter of fact, the principle was not utilised for the evaluation of flame temperatures until nearly half a century had elapsed, when Fery applied it, using his absorption pyrometer for the purpose. He points out that the method depends on the truth of the two following hypotheses:—(1) that the flames are not luminescent; (2) that the emissive power of the flames for the wave-length of the metallic lines emitted is equal to unity.

In coming independently to the subject, we recognised that these various assumptions needed justification before the method could be relied on, and we describe later experiments which provide this justification.

The experimental arrangements which we have found to be convenient in measurements by this method are illustrated in fig. 4.* The source of the continuous spectrum is the incandescent sphere of a tungsten arc known commercially as the "Pointolite lamp." An image of this sphere is sharply focussed through the flame on to the slit of a spectroscope and more than covers the aperture, so that the intensity of the light in the continuous spectrum seen in the eye-piece is independent of the geometry of the system.

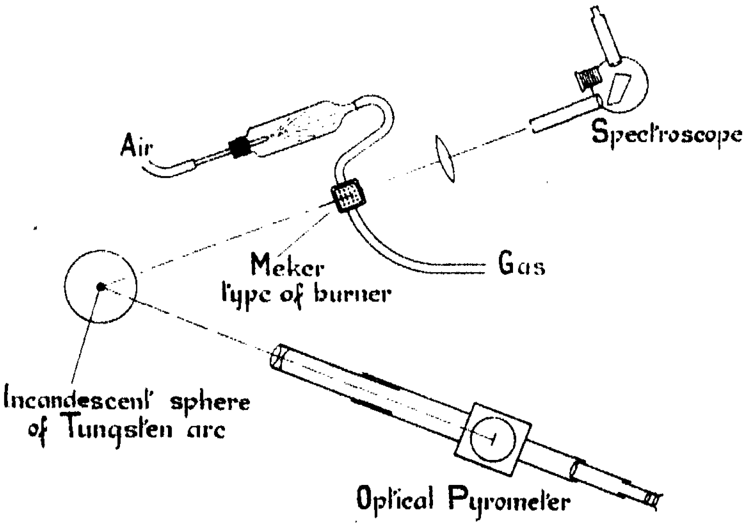

FIG. 4.

The sodium chloride† required for colouring the flame is introduced continuously and uniformly by means of the spray arrangement due to Gouy (see fig. 5).

The production of reversed lines becomes impossible if the slit of the spectroscope is opened too wide: over the permissible range we have found no variation of apparent temperature with slit width.

The current in the tungsten arc is controlled by a rheostat and adjusted until the sodium lines just merge into the continuous background. The point of disappearance can be approached from either side according to whether the sodium lines are brighter or darker than the background.

---

* This apparatus was shown at the Conversaziones of the Royal Society in May and June, 1927, and a short note on the subject published in the 'N.P.L. Annual Report for 1927.'

† It was found by experiment that the concentration of the salt solution was without influence on the result.

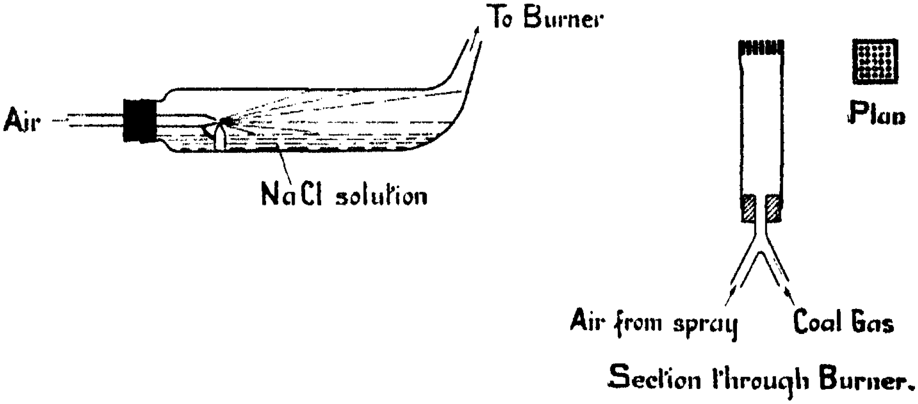

FIG. 5.

A reading of the temperature of the incandescent tungsten sphere is then taken on the pyrometer, and this gives the flame temperature directly.

The sodium lines are particularly easy to work with, but it is also possible by using a suitable design of burner to obtain the same effects with the red lithium line. The burner shown in fig. 6 was constructed to give a flame 10 inches in length by drilling some 300 holes in a slab of brass constituting the top of a rectangular enclosure supplied with gas and air. This burner was water cooled. Some experiments were made using sodium and lithium alternately and others in which both were present simultaneously. The former experiments gave the following values for the reversal of the lines :—

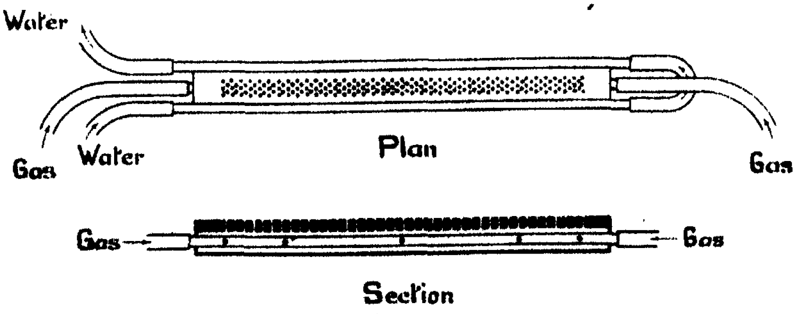

FIG. 6.

With lithium	1736° C.
With sodium	1730° C.

When the two were tested together it was easily seen that both sodium and lithium lines disappeared and reversed together. It immediately follows that the relative intensities of the sodium and lithium lines, in the same flame, are the same fractions of the intensities at the corresponding wave-lengths in the " black body " spectrum.

Whilst two cases, the red line of lithium and the yellow lines of sodium, are insufficient for founding a generalisation of this character, it is difficult to avoid the suggestion that the same may be true for all spectral lines of the type examined—first lines of a spectral series.

Determination of the Temperature of Sodium Chloride Vapour in Equilibrium with a " Black-body " Enclosure.

The experiment described below was made with the object of ascertaining whether the apparent temperature, obtained by the sodium line reversal method, of a column of sodium chloride vapour contained in an electrically heated carbon tube furnace was the same as the " black body " temperature of the furnace.

Common salt was introduced into an electrically heated carbon tube furnace, the incandescent sphere of the tungsten arc being adjusted so as to throw a beam along the axis of the furnace through the column of vapour. An optical system, shown in fig. 7, was kindly devised for us by Mr. T. Smith of the Optics Department, so that the image of the incandescent sphere on the spectroscope slit was formed by light which had traversed the furnace as a parallel beam, and by a system of stops, light from the incandescent walls of the furnace was prevented from entering the spectroscope slit. That this condition was fulfilled was verified experimentally by switching off the tungsten arc and observing in the spectrometer when the furnace was hot before the introduction

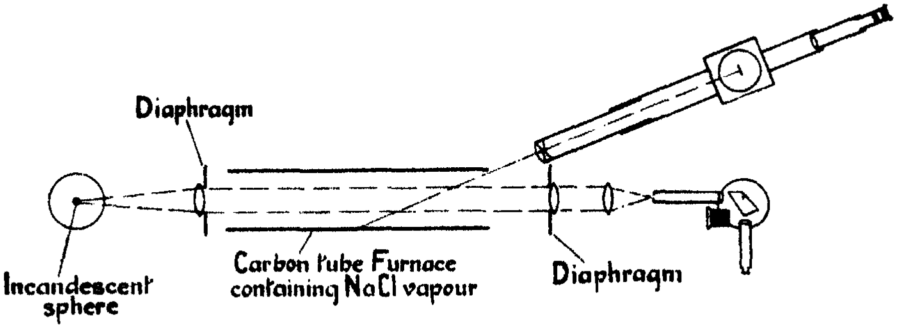

FIG. 7.

of the salt. There was practically no continuous spectrum to be observed under these conditions.

The spectroscope was arranged at the other end of the furnace, and the disappearance of the D lines examined, just as in the case of the flame.

The phenomena observed here are, however, more complicated than is the case in a flame. There is a cooler layer of vapour at the ends of the carbon tube which produces a reversal of the central region of the D lines. The line was much broadened, due presumably to the density of the vapour, but it was only the central portion that was reversed. Matching against the continuous spectrum had therefore to be made on the bright boundaries of the dark line.

The temperature of the incandescent sphere at this disappearance was 1596° C. as determined by direct observations with an optical pyrometer, whereas by sighting on the wall of the furnace with a pyrometer the actual temperature of the furnace was found to be 1600° C., which is therefore the temperature of the "black-body" in equilibrium with the vapour. The observation was difficult to carry out, owing to the complications mentioned above, and to settle the point definitely would require some means of eliminating the reversing action of the cold vapour.

Influence of Flame Thickness on Spectral Line Reversal.

It was a matter of interest to examine whether the thickness of the flame investigated had any influence on the result. Accordingly we constructed a Meker type burner which gave a flame about 2 inches by ½ inch. The temperature was taken first with the burner transverse to the direction of the beam from the incandescent sphere to the spectroscope slit, and then along it. No difference could be detected between the values for the two cases, but the limits between disappearance and appearance were greater for the thinner flame than the thicker. Since most work would be done with flames falling within these limits of thickness, it is established that the flame thickness is immaterial to the result, but to ensure sensitivity it is advisable to employ a thick flame.

The same conclusion was reached in experiments in which two separate flames were first adjusted to equality of apparent temperature and then placed in line so that the apparent temperature of the composite flame could be determined. No difference was observed in the values obtained for the composite flame and for the flames individually.

In the next section of this paper the above result is shown to be a consequence of theoretical deductions based on certain simplifying assumptions.

Apparent Temperature of a Heterogeneous Flame.

In the flames of the Meker type burners employed in the experiments so far recorded, the gas and air are thoroughly mixed, so that the flame is homogeneous throughout its thickness. In practice, however, it would frequently be desired to measure the temperatures of flames which depart markedly from this condition; thus the cones of the ordinary Bunsen burner are at different temperatures, and the question would arise whether the spectroscopic method measures any one of these or, if not, what average it takes.

To examine the matter experimentally, Meker flames at different known temperatures were set up in line, and the apparent temperature of the compound flame thus formed was measured.

Since these flames were at different distances from the spectroscope, it was desirable as a preliminary to examine the variation in apparent temperature of one of them, as its distance from the spectroscope was varied. As the distance was decreased from 30 cm. to 4 cm., the apparent temperature changed from 1835° C. to 1841° C. which, although probably real, is a negligible alteration under the circumstances contemplated.

When one flame was cooled by diluting the gas supply to it with different amounts of nitrogen, the results obtained in two sets of experiments are given below:—

1st Series.

	Apparent temperature. ° C.
Flame A	1736
Flame B	1635
Flame A in front of flame B	1728
Flame B in front of flame A	1678

2nd Series.

Flame A	1739
Flame B	1487
Flame A in front of flame B	1690
Flame B in front of flame A	1600

It appears that with the cooler flame in front of the hotter, the mean temperature measured is not far removed from the arithmetic mean temperature, although when reversed the observed value is much nearer than of the hot flame.

The matter may also be examined to some extent on theoretical grounds, but it is necessary to simplify the conditions by imagining the flame to be a slab with two plane boundaries. We shall also assume that the flame has a constant absorption coefficient for the radiation concerned, over the thicknesses considered, so that it obeys Lambert's law. This is not in agreement with some experiments due to Gouy, who finds that the radiation (and therefore presumably the absorption) is proportional to the square root of the thickness of the flame. It is difficult to believe that this law can be true over a great range, since it does not provide for a limiting radiation—in other words, it would allow a sufficiently thick flame to radiate more intensely than a black body.

At any rate as an approximation, therefore, we shall assume the usual type of absorption law as found in liquids and solids; the assumption is partially justified by the results obtained by its use.

Let the flame have thickness l, and extend indefinitely in the two directions perpendicular to its thickness. (The beam of light from the Pointolite source to the spectroscope is normal to these boundaries.) Then, if the actual production of radiation is R_1 per cubic centimetre per second, the total radiation emerging is

$$\int_0^l R_1 e^{-\rho(l-x)}\,dx = \frac{R_1}{\rho}(1 - e^{-\rho l}).$$

where ρ is the coefficient of absorption, and l the thickness. This reduces, when the flame is thick enough, to R_1/ρ. But, since the indefinitely thick flame emits with the same intensity as a black body, R_1/ρ is a constant S_1, and is proportional by Wien's law to $e^{-c_2/\lambda\theta}$ where c_2 is a known constant, and λ, θ are the wave-length and the absolute temperature respectively.

Thus we reach the result that for a flame of thickness l the radiation at a definite point of the spectrum is proportional to $Se^{-\beta/\theta}(1 - e^{-\rho l})$ where β for the sodium lines is 24,330. Next, let a beam of intensity S_0 (*e.g.*, from the Pointolite lamp) fall on the flame, so that the light emerging has intensity $S_0e^{-\rho/l} + S_1e^{-\beta/\theta}(1 - e^{-\rho l})$. Now the adjustment of S_0 that we make, to cause disappearance of the D lines, is expressed by the condition that the intensity of the original source is equal to that actually emerging from the flame. Hence, at balance, $S_0 = S_0e^{-\rho l} + S_1e^{-\beta/\theta}(1 - e^{-\rho l})$ whence

$$S_0 = e^{-\beta/\theta}.$$

This result is of fundamental importance, for it shows that the temperature measured for a single flame is its true temperature, and is independent of thickness or of absorption coefficient.

Finally, let a beam of intensity S_0 fall on two flames one behind the other, distinguished in what follows by the suffixes 1 and 2.

The light emerging from the first flame will have intensity

$$S_0' = S_0 e^{-\rho_1 l_1} + S_1 e^{-\beta/\theta_1} (1 - e^{-\rho_1 l_1}),$$

and this represents the beam which falls on the second flame. Thus the light finally emerging is

$$S_0' (e^{-\rho_2 l_2}) + S_1 e^{-\beta/\theta_2} (1 - e^{-\rho_2 l_2}).$$

As before this expression equals S_0 when the D lines match their surroundings, so that (writing x for $e^{-\rho_1 l_1}$ and y for $e^{-\rho_2 l_2}$)

$$S_0 = x [S_0 x + S_1 e^{-\beta/\theta_1} (1 - x)] + S_1 (1 - y) e^{-\beta/\theta_2}.$$

But S_0, the intensity of the source, measures the apparent temperature of the compound flame, *so that* $S_0 = S_1 e^{-\beta/\theta}$ *and the equation becomes*

$$(1 - x^2) e^{-\beta/\theta} = x (1 - x) e^{-\beta/\theta_1} + (1 - y) e^{-\beta/\theta_2},$$

where the apparent temperature of the compound flame is represented by θ.

This shows how the apparent temperature of a complex flame depends on the individual temperatures of the flames composing it. It will be noticed in particular that if the flames are exactly similar, so that $x = y$ and $\theta_1 = \theta_2$, then θ is equal to both θ_1 and θ_2. This result has been verified experimentally. If two flames are measured independently, and found to have the same temperature, then the compound flame obtained by placing them one behind the other has the same apparent temperature as either. This result is, of course, similar to that obtained from the equation for a single flame—that thickness does not affect the measurement.

To test the equation in the more general case, where the temperatures differ notably, an additional assumption, justified by the result, was made. Since the flames do not differ *greatly* in thickness or absorption coefficient, x and y may be set equal, in which case the equation reduces to

$$(1 + x) e^{-\beta/\theta} = x e^{-\beta/\theta_1} + e^{-\beta/\theta_2}.$$

This indicates that the apparent temperature of two flames is different according as they are placed in the order AB or BA. Taking $x = 0 \cdot 561$, a mean value derived from experiment, the following table exhibits the results of an experimental check of the formula.

Flame A.	Flame B.	A in front of B.		B in front of A.	
Observed.	Observed.	Calculated.	Observed.	Calculated.	Observed.
1736	1635	1706	1728	1677	1678
1739	1487	1683	1690	1622	1600

Remembering that the formula was deduced for plane flames, the agreement is satisfactory. In the second line, for example, seeing that AB, BA, might have come out anywhere between 1490 and 1740° C., even the divergence of 20° is not serious.

Distribution of Temperature from Base to Tip of Flame.

The Meker type flame appears homogeneous over its cross-section, but there is a gradient of temperature from the base to the tip.

To determine the order of magnitude of this variation a flame 14 inches in height was studied over the region for which measurements were practicable. The results obtained are summarised below :—

Distance measured upwards from base of flame..........	1	2	3	4	5	6	7 inch
Temperature	1780	1790	1755	1665	1660	1650	(1600) ° C.

The observation at 7 inches from the base was difficult, since it was approaching the limit at which reversal could be clearly seen. It will be noted that the variation from base to tip of the flame is considerable.

Absorption in the Flame of Radiation from the Wire.

In the wire method we depend on the opacity of the flame being negligible since otherwise the radiation is not the same in the flame as it is *in vacuo*. In this connection, however, it is only necessary that the energy stopped by the flame, from a wire at the flame temperature, should be negligible compared with the total radiation emission.

If the absorption bands are narrow it would be anticipated that their effect on the total radiation emission would be small, even if the absorption coefficient was nearly unity. It was, however, a matter which needed an experiment before a definite conclusion could be reached.

For this purpose the heated wire was set up in front of a thermopile connected to a sensitive galvanometer. The deflection due to the heated wire was obtained; a flame was then interposed between the wire and the thermopile, and the deflection due to the combined effect of both was observed; the current in the wire was then switched off and the deflection due to the flame alone observed. The sum of the deflections due to the heated wire and to the flame was compared with the deflection obtained when both wire and flame were acting simultaneously.

It was found that the results were in agreement within the limits of the error of experiment, showing that the absorption effect of the flame was too small to be measured by this method.

We also examined the analogous question of the absorption in one flame. of the radiation from another. Since the source and absorbing medium are now similar bodies, it is to be expected that the absorption will be very considerably increased. In a rough experiment to examine this, five flames were set up in line, in front of a thermopile, and the deflection due to each was observed. These deflections of course varied, owing to the distance being different. We then obtained the deflection for the two nearest the thermopile, and then for three, four and finally all five. Assuming that a fraction e per cent. of the radiation falling on a flame is transmitted, this gives four equations to determine e; the values were 85 per cent., 82 per cent., 85 per cent., 86 per cent.

A check on this was obtained by trying two, three and four burners, extinguishing in turn from the distant end, instead of, as previously, from the nearer end. Using the mean value 85 per cent. for e, the deflections to be expected were calculated and compared with the observed, as in the table below:—

	Observed.	Calculated.
Two burners	2·3	2·4
Three burners	3·6	3·6
Four burners	4·9	5·0

Spectroscopic Analysis of Flame Emission and Absorption.

As a matter of completeness, we also determined the intensity distribution in the emission and absorption spectra of a particular flame. As in the experiments described above, when the overall effect was under examination, the flame was set up in front of a heated platinum wire, and three sets of readings were taken: (1) flame alone; (2) wire alone; and (3) flame and wire together. The measuring instrument was a Hilger constant deviation infra red spectrometer, with a thermopile in place of the eyepiece. The computed and observed curves are set out in fig. 8.

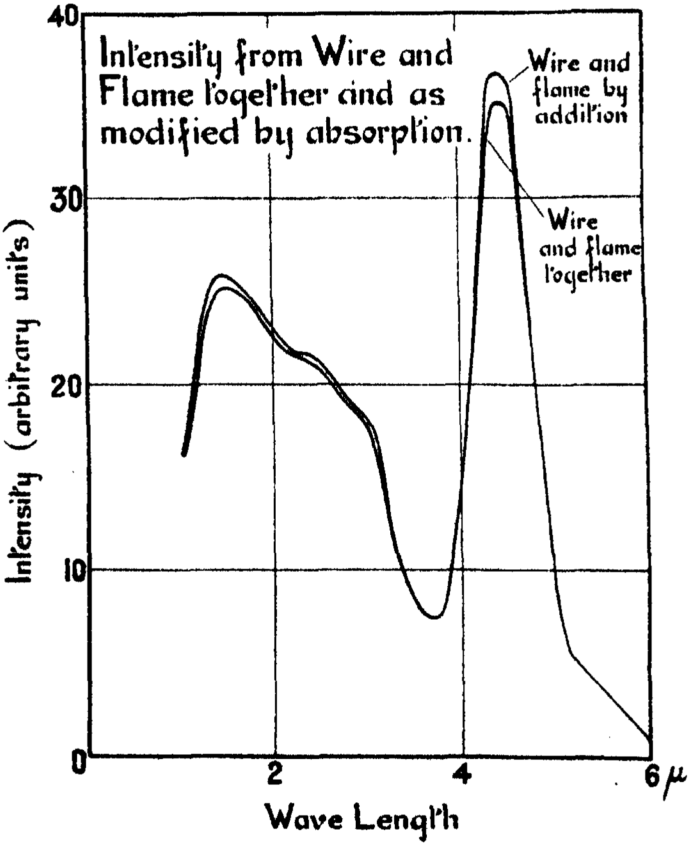

FIG. 8.

It will be seen that there is an effect due to the absorption by the flame of the radiation from the wire, but its magnitude is negligible compared with the total emission. This confirms the results obtained when the total radiation emission was directly measured by a thermopile.

Method of Measuring the Intensity of D Line Radiation from Flames of Various Thicknesses at the Same Temperature.

That the intensity of the radiation in the D lines depends upon the thickness of a flame of the dimensions commonly used was shown by the following experiment.

The image of the flame was focussed across the carbon filament of an electric lamp, the current through which could be adjusted so as to bring it to any desired temperature. The images of the filament and of the superimposed image of the flame were then focussed on to the slit of a spectroscope in the eyepiece of which could be seen the continuous spectrum due to the filament, and across it the sodium D lines from the flame. By adjustment of the current through the filament of the carbon lamp a " match" could be effected between the intensity of the D lines and the corresponding spectrum. Then the temperature of the carbon lamp filament was measured by a disappearing filament type pyrometer. From its temperature the intensity of the radiation from the carbon lamp filament could be calculated. To obtain satisfactory results with this apparatus attention has to be given to screening off of stray radiation from the various lenses constituting the optical system.

The fundamental difference between this experiment and the method previously described for obtaining flame temperatures is that in the present case the flame is not permitted to absorb light from the comparison source. Hence the variation in emission is brought into evidence, whereas in the experiments described previously absorption and emission vary together in such a way that the apparent temperature is independent of the thickness of the flame.

The Measurement of Maximum Temperatures in Gaseous Explosions.

The difficulty encountered in the use of the customary methods of measuring temperatures in the case of gaseous explosions is that the period during which the charge is at its maximum temperature is one of very short duration. Consequently any " lag " in the measuring instrument may cause serious errors. The sodium line reversal method is free from this defect.

A few preliminary tests have been made in conjunction with Mr. R. W. Fenning, of the Engineering Department, using a CO, air and N_2 mixture. A water-cooled cylindrical bomb was used as the explosion vessel. This was fitted with two windows of thick plate glass and a layer of dry powdered sodium carbonate was sprinkled inside. The light from the "Pointolite" lamp traversed the chamber so that the image of the incandescent sphere was focussed on the spectroscope slit in the usual manner, the chamber taking the place of the flame. A two-way cock connected the chamber either to a reservoir of the explosive mixture or to an exhaust pump (see fig. 9).

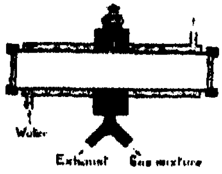

FIG 9.

The phenomena observed during the progress of an explosion were as follows: Initially in the field of the spectroscope there would be a continuous spectrum. When the mixture was fired a dark band appeared in the place of the D lines and then the bright D lines would flash up on the boundary of the field provided the temperature of the incandescent sphere was below that attained in the explosion.

By successive approximations it was found possible to adjust the temperature of the incandescent sphere until the point was reached when the D lines just appeared or did not appear at the instant following the explosion. With a little practice the observer could set the temperature of the sphere within close limits (of the order of 10° C. at 2100° C.).

Application of Method to the Study of Combustion.

In some preliminary observations we have utilised the spectral-line reversal method for temperature measurements on flames burning mixtures of carbon monoxide and air, in varying proportions.

In order that the quantity of air consumed could be measured, it was necessary to enclose the burner in a surrounding vessel which allowed no uncontrolled ingress of air. The apparatus is shown in fig. 10 where the burner

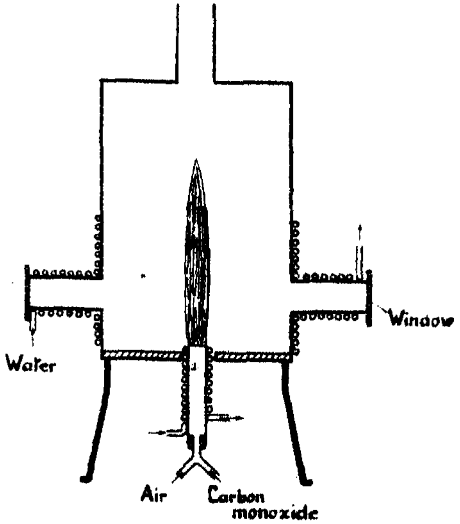

FIG. 10.

projects through the base of the vessel, which is provided with a chimney to carry off the products of combustion. The windows, necessary in the spectroscopic method, were carried on side tubes, surrounded by water-cooled piping. Without this precaution, the glass had a tendency to crack.

A typical series is shown in fig. 11, whilst the whole results obtained are shown in fig. 12, in which each curve relates to one fixed rate of air supply

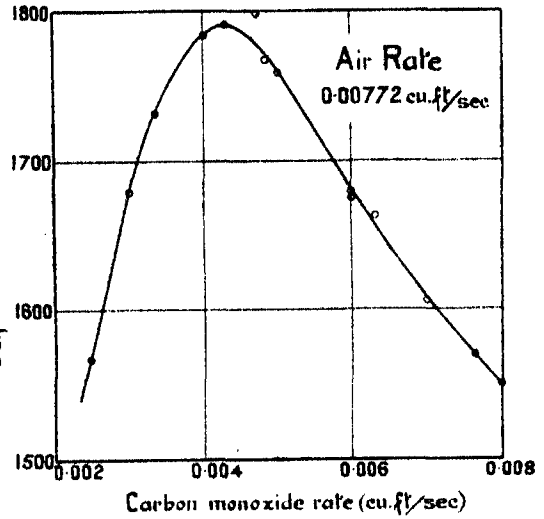

Fig. 11.

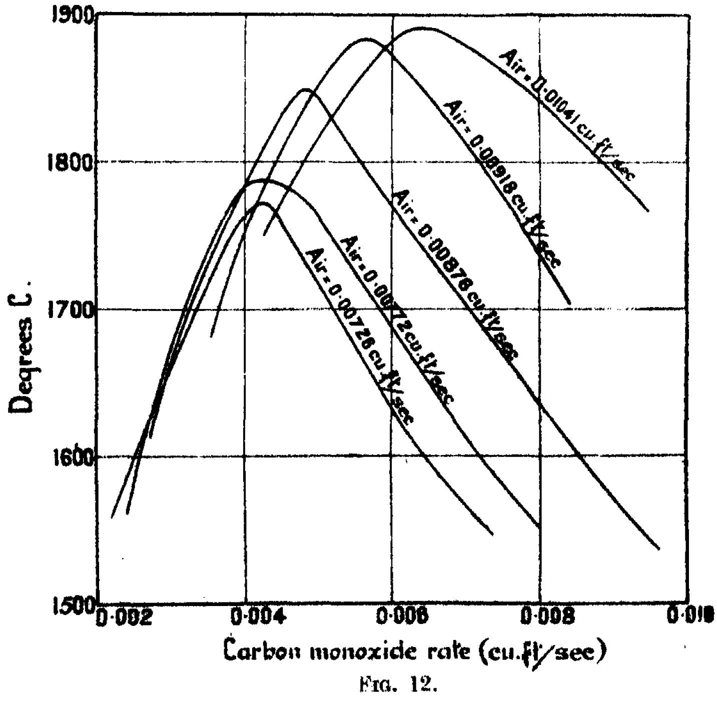

Fig. 12.

and connects temperature with rate of supply of carbon monoxide. Thus there are a number of points on the family of curves, for which the *ratio* of air to carbon monoxide is constant, and it will be noticed that these do not give the same temperature. The probable explanation for this difference is that the observations were always taken at the same height above the base of the flame; thus of two flames having the same gas-ratio, but different absolute amounts of gas and air, one will be much larger than the other, so that the temperatures do not relate to geometrically corresponding points in the two flames.

Application of Method to Measurement of Flames of Atomic Hydrogen.

At the suggestion of Dr. G. W. C. Kaye, the spectral line reversal method was applied to the measurement of the temperature of the gases between the electrodes of the atomic hydrogen blow-pipe.

In essentials, the apparatus was similar to that used for measuring ordinary Meker flames, but a few modifications were found necessary. The hot "arch" of flame above the electrodes is only about 1 cm. square, so that the beam used had to be restricted to below this size; also, the flame is hotter than the maximum attainable with the sphere of the "Pointolite" lamp, which consequently could not be used as a background. It was replaced by the positive crater of a carbon arc with an adjustable neutral glass absorption wedge in front. The apparatus is shown in fig. 13. Light from the arc, after passing the wedge, passed through the flame of the blowpipe. Immediately beyond this was a short carbon tube (internal diameter about 1 mm.) fixed in a carbon plate to restrict the light to that which had passed through the particular region of the flame it was desired to measure. The light passing through the tube was then focussed by a lens on to the slit of the spectrometer. Sodium was introduced into the blowpipe flame by pasting a mixture of sodium bromide and sodium silicate on fine asbestos string wound around the electrodes.

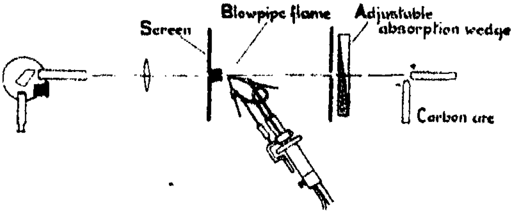

FIG. 13.

The matching of the sodium lines against the background was accomplished by adjustment of the absorption wedge until the lines could no longer be seen definitely either bright or dark, but appeared just faintly bright or dark intermittently with the fluctuations of the flame and of the arc. The spectrometer was then removed and an optical pyrometer focussed on the image of the carbon arc located in space at the position of the slit of the spectrometer. The apparent temperature of the arc was observed with this pyrometer, sighting through the carbon tube and lenses, just as for the main experiment. It was verified, by removing the wedge, and sighting on the positive crater that the calibration of the pyrometer was unaltered when used in this manner.

Observations were taken on four occasions, the apparatus having been dismantled between the first two and the last two, and the results obtained were 2525, 2490, 2540, 2510° C., of which the mean is 2515° C. This temperature is considerably below the temperature of the solid tungsten electrodes, for by direct observation with an optical pyrometer they were found to be at 3200° C.

Acknowledgments.

It is a pleasure to record our gratitude to Mr. H. T. Tizard, F.R.S., for bringing the problem of flame temperature measurements to our notice, and his kind interest during the progress of the work; to the Superintendent of the Physics Department for continued interest; and to A. R. Challoner, Observer in the Physics Department, for his skilful assistance in carrying out the experiments.

The Arc Spectrum of Silicon.

By A. Fowler, D.Sc., F.R.S., Yarrow Research Professor of the Royal Society.

(Received February 8, 1929.)

[Plate 18.]

Introductory.

In the Bakerian Lecture for 1924* it was shown that the changes in the spectrum of silicon which accompany increased energy of excitation represent successive stages of ionisation of the silicon atom. Besides the spectrum of the neutral atom (Si I), characterised by the series constant R, three other spectra were identified as Si II, Si III and Si IV, for which the series constant was 4R, 9R and 16R respectively, in accordance with Bohr's theory.

In view of the great advances in the theoretical interpretation of spectra which have since been made, it has seemed desirable to undertake a revision and extension of the earlier analyses of these spectra. The present communication gives an account of additional observational data for Si I and of the progress which has been made in the identification of the terms predicted for this spectrum by the theory of Heisenberg and Hund.

Observational Data.

The region of the arc spectrum considered in the previous paper extended from the visible spectrum to the beginning of the Schumann region about λ 1840. It was pointed out, however, that since the first triplet combinations occur in the ultra-violet, beginning at λ 2528, any additional members in sequence with them must be situated in the Schumann region. The arc spectrum in this region has accordingly been further investigated with the vacuum grating spectrograph.

In order to extend the observations as far as possible to short wave-lengths, and to minimise the introduction of lines of Si II, which appear conspicuously in the vacuum arc, the arc was passed in nitrogen at atmospheric pressure. It is known from observations in the ordinary parts of the spectrum that the substitution of nitrogen for air does not affect the spectrum of an arc, but for the present purpose nitrogen has the advantage of being transparent for short wave-lengths, whereas oxygen is strongly absorbent. Spectra obtained with an arc in nitrogen at atmospheric pressure are thus equivalent, as regards existing energy, to those given by an arc in air under ordinary conditions.

---

* 'Phil. Trans.,' A, vol. 225, p. 36 (1924).

In work with the vacuum spectrograph it is usually an advantage to place the source as near as possible to the slit, and so, instead of putting the arc in a closed vessel, it was brought within about an inch from the slit and a slow stream of nitrogen passed between the slit and the arc. The slit was covered with a fluorite plate, and a short length of water-cooled brass tube extended from the slit towards the arc. Nitrogen was admitted through a side tube. In this way, photographs of the arc spectrum extending to about λ 1600, and sometimes further, were obtained. Two pairs of lines due to Si II appeared on some of the plates, but not on all of them, and, as in the visible spectrum, it appears that such lines were practically confined to the immediate neighbourhood of the poles.

Most of the photographs were taken in the first order of a grating having 15,000 lines per inch, which was ruled at the National Physical Laboratory. The definition and resolution given by this grating are excellent, as may be gathered from the enlarged copies which are reproduced in Plate 18. At a late stage of the investigation, another grating having 30,000 lines per inch, ruled on glass, became available through the kindness of Prof. R. W. Wood. A few photographs of the silicon arc spectrum have been taken with this second grating, and in these also the definition is very good ; the additional dispersion and resolution on these plates have materially improved some of the data.

Pole pieces of elementary silicon yielded the most complete spectra, but good photographs were also obtained with potassium fluo-silicate on poles of Acheson graphite. The latter photographs were especially valuable because they included lines of carbon, most of which have been accurately measured by Bowen.* With poles of silicon, carbon was only represented by a trace of the very strong arc line at λ 1931. The photographs of the fluo-silicate spectrum were also of assistance in the classification of some of the singlets which occur in the Si I spectrum ; it was found, for example, that while the singlet DF series appeared with undiminished strength in the fluo-silicate spectrum, the singlet DD series was relatively much reduced in intensity and extent.

As the silicon used in these experiments was known to be somewhat impure, the arc spectra of numerous other elements were photographed under similar conditions for purposes of comparison. A few lines of aluminium, including some of Al II, and a line of calcium were thus identified as arising from impurities. The pair of nitrogen lines, λλ 1745·26, 1742·74, also appeared conspicuously in most of the arc spectra.

---

* 'Phys. Rev.,' vol. 29, p. 238 (1927).

Determination of Wave-lengths.

The photographs of the spectrum of potassium fluo-silicate were first carefully measured, and the wave-lengths of numerous silicon lines were obtained by interpolation with respect to the lines of carbon* and nitrogen. The most suitable lines among these were then used as standards for the reduction of the plates showing silicon lines alone. A valuable check on the values obtained for several of the silicon lines was, fortunately, provided by the analysis of the spectrum. As will be seen from Table III, a number of silicon lines which occur in the Schumann region can be calculated with great precision from the accurate values already determined for lines in the ordinary ultra-violet region. Lines on the first four rows of this table being used for the determination of the differences between the terms shown at the head, it is only necessary to add these differences to the wave numbers of some of the singlets which appear on the right in order to obtain the wave-numbers of associated lines in the Schumann region. When there could be no doubt as to the identity of calculated and observed wave-numbers the calculated values were adopted for tabulation. Such calculated wave-numbers are distinguished in Tables I and III by an asterisk; they may conveniently be collected as below, as good standards in the Schumann region are not yet very numerous.

ν.	$\lambda_{vac.}$	$\lambda_{air.}$	ν.	$\lambda_{vac.}$
47088·00	2123·683	2123·009	54090·11	1848·768
47128·14	2121·874	2121·200	54236·19	1843·788
47274·22	2115·318	2114·646	54313·25	1841·171
48014·58	2082·701	2082·035	54647·48	1829·910
48571·95	2058·801	2058·139	54793·56	1825·032
52503·29	1904·643		54870·62	1822·469
53138·25	1881·883		58578·82	1707·102
53163·53	1880·988		58724·90	1702·855
53309·61	1875·835		58801·96	1700·623
53386·67	1873·127			

An examination of the multiplets on which the above values depend, however, shows that the positions of the parent lines are not yet known with the greatest attainable accuracy, and to this extent the above values are to be considered provisional, though the errors are unlikely much to exceed one-hundredth of an angstrom.

---

* Bowen's value for the carbon line, 1931·027, was replaced by 1930·95, deduced during the present investigation.

Catalogue of Silicon Arc Lines.

A general catalogue of silicon arc lines is given in Table I. The first column gives the wave-lengths and intensities, the wave-lengths to λ 2000 being in

Table I.—Arc Lines of Silicon.

λ_{air} (Int.).	ν.	Classification.
†11231·0 (8)	8902	$4s\,^1P_1-4p\,^1S_0$
†9867·7 (5)	10131	$4s\,^3P_1-4p\,^1S_0$
†9755·8 (10)	10248	$4p\,^1D_2-3d\,^1F_3$?
§5948·552 (5)	16806·17	$4s\,^1P_1-5p\,^1S_0$
5797·869 (3)	17242·94	$4s\,^3P_2-5p\,^3D_3$?
5793·083 (2)	17257·19	$4s\,^3P_1-5p\,^3D_2$?
5780·390 (0)	17295·08	
5772·152 (1)	17319·77	$4s\,^3P_0-5p\,^3D_1$?
‡5754·240 (0)	17373·68	$4s\,^3P_2-5p\,^3P_1$
5708·408 (5)	17513·17	P_2 P_2
5701·111 (1)	17535·58	P_1 P_0
5690·435 (2)	17568·49	P_1 P_1
5684·496 (3)	17586·84	
5665·566 (1)	17645·61	P_0 P_1
5645·621 (1)	17707·94	P_1 P_2
4102·945 (5)	24365·89	$3p\,^1S_0-4s\,^3P_1$
§3905·534 (10)	25597·47	$3p\,^1S_0-4s\,^1P_1$
3020·01 (0)	33102·85	Si ?
2987·650 (5)	33461·39	$3p\,^1D_2-4s\,^3P_1$
2970·35 (2)	33656·27	$3p\,^1D_2-4s\,^3P_2$
2881·585 (10)	34692·97	$3p\,^1D_2-4s\,^1P_1$
2631·310 (5)	37992·57	$3p\,^1S_0-3d\,^1P_1$
2568·66 (2)	38919·15	$3p\,^1S_0-5s\,^3P_1$
2532·39 (2)	39476·52	$3p\,^1S_0-5s\,^1P_1$
2528·516 (10R)	39537·01	$3p\,^3P_2-4s\,^3P_1$
2524·118 (9R)	39605·89	P_1 P_0
2519·210 (8R)	39683·03	P_1 P_1
2516·123 (15R)	39731·73	P_2 P_2
2514·331 (7R)	39760·04	P_0 P_1
2506·904 (10R)	39877·83	P_1 P_2
2452·136 (3)	40768·42	$3p\,^3P_2-4s\,^1P_1$
2443·378 (3)	40914·54	P_1 P_1
2438·782 (3)	40991·64	P_0 P_1
2435·159 (8R)	41052·61	$3p\,^1D_2-3p'\,^1D_2$
2303·02 (2)	43407·86	$3p\,^1S_0-4d\,^1P_1$
‡2289·60 (1)	43662·15	
‡2278·22 (0)	43880·44	$3p\,^1S_0-6s\,^3P_1$
‡2259·57 (1)	44242·48	$3p\,^1S_0-6s\,^1P_1$
2218·917 (1)	45052·96	$3p\,^3P_2-3p'\,^3D_1$
2218·080 (2)	45069·96	P_2 D_2
2216·685 (4)	45098·32	P_2 D_3
2211·750 (2)	45198·92	P_1 D_1
2210·912 (3)	45216·07	P_1 D_2
2207·980 (2)	45276·09	P_0 D_1
2124·150 (10R)	47062·72	$3p\,^1D_2-3d\,^1F_3$
*2123·009 (2)	47088·00	$3p\,^1D_2-3d\,^1P_1$
*2121·200 (1)	47128·14	$3p\,^3P_2-3p'\,^1D_2$
*2114·646 (0)	47274·22	$3p\,^3P_1-3p'\,^1D_2$
2084·40 (2)	47960·09	$3p\,^1D_2-3d\,^1D_2$
*2082·035 (1)	48014·58	$3p\,^1D_2-5s\,^3P_1$
2065·48 (0)	48399·36	
2061·12 (1)	48501·73	
*2058·139 (5)	48571·95	$3p\,^1D_2-5s\,^1P_1$
2054·85 (1)	48652·31	
2011·05 (0)	49709·20	
2008·55 (00)	49771·05	
λ_{vac} (Int.).		
1991·94 (2)	50202·3	$3p\,^1D_2-3d\,^3P$?
1989·01 (6)	50276·4	$3p\,^3P_2-3p'\,^3P_2$
1986·39 (4)	50342·6	P_2 P_1
1984·50 (0)	50390·5	
1983·25 (4)	50422·3	P_1 P_2
1980·64 (3)	50488·7	P_1 P_1
1979·23 (3)	50524·7	P_1 P_0
1977·62 (3)	50565·8	P_0 P_1
1963·04 (00)	50941·4	
1962·13 (0)	50965·0	
1961·29 (00)	50986·8	
1960·16 (0)	51016·2	
1958·65 (0)	51055·6	
1957·92 (0)	51074·6	
1956·06 (0)	51123·2	
1955·00 (1)	51150·9	Si ?
1953·02 (0)	51202·8	
1952·53 (00)	51215·6	
1951·61 (0)	51239·7	
1950·23 (0)	51276·0	
1947·01 (1)	51360·8	
1945·03 (00)	51413·1	
1942·37 (00)	51483·5	
1940·69 (0)	51528·1	
1934·49 (00)	51693·2	

† McLennan and Shaver.
‡ Not in previous list.

§ Solar wave-lengths adopted between these limits.
* Calculated wave-lengths adopted.

Table I—(continued).

λ_{vac} (Int.).	ν.	Classification.
*1904·643 (2)	52503·29	$3p\ {}^1D_2-4d\ {}^1P_1$
1901·36 (8R)	52593·9	$3p\ {}^1D_2-4d\ {}^1F_3$
1893·25 (5)	52819·2	$3p\ {}^1D_2-4d\ {}^1D_2$
1887·74 (2)	52973·4	$3p\ {}^1D_2-6s\ {}^3P_1$
1883·80 (0)	53084·2	
*1881·883 (2)	53138·25	$3p\ {}^3P_2-3d\ {}^1F_3$
*1880·988 (0)	53163·53	$3p\ {}^3P_2-3d\ {}^1P_1$
*1875·835 (2)	53309·61	$3p\ {}^3P_1-3d\ {}^1P_1$
1874·90 (3)	53336·2	$3p\ {}^1D_2-6s\ {}^1P_1$
*1873·127 (2)	53386·67	$3p\ {}^3P_0-3d\ {}^1P_1$
1865·19 (0)	53613·8	
1861·76 (00)	53712·6	$3p\ {}^1D_2-4d\ {}^3P$?
1855·62 (00)	53890·3	
1853·17 (1)	53961·6	$3p\ {}^3P_2-3d\ {}^3D_1$
1852·49 (3)	53981·4	$3p\ {}^3P_2-3d\ {}^3D_2$
1851·82 (1)	54000·9	
1850·70 (5R)	54033·6	$3p\ {}^3P_2-3d\ {}^3D_3$
*1848·768 (2)	54090·11	$3p\ {}^3P_2-5s\ {}^3P_1$
1848·17 (3)	54107·6	$3p\ {}^3P_1-3d\ {}^3D_1$
1847·48 (4R)	54127·8	$3p\ {}^3P_1-3d\ {}^3D_2$
1846·13 (2)	54167·4	$3p\ {}^3P_1-5s\ {}^3P_0$
1845·53 (3)	54185·0	$3p\ {}^3P_0-3d\ {}^3D_1$
*1843·788 (2)	54236·19	$3p\ {}^3P_1-5s\ {}^3P_1$
1841·48 (3)	54304·2	$3p\ {}^3P_2-5s\ {}^3P_2$
*1841·171 (2)	54313·25	$3p\ {}^3P_0-5s\ {}^3P_1$
1838·00 (1)	54407·0	
1836·54 (2)	54450·2	$3p\ {}^3P_1-5s\ {}^3P_2$
*1829·910 (2)	54647·48	$3p\ {}^3P_2-5s\ {}^1P_1$
1826·45 (00)	54751·0	
*1825·032 (00)	54793·56	$3p\ {}^3P_1-5s\ {}^1P_1$
*1822·469 (2)	54870·62	$3p\ {}^3P_0-5s\ {}^1P_1$
1817·97 (0)	55006·4	$3p\ {}^1D_2-5d\ {}^1P_1$?
1814·07 (6)	55124·7	$3p\ {}^1D_2-5d\ {}^1F_3$
1809·05 (4)	55277·6	$3p\ {}^1D_2-5d\ {}^1D_2$
1799·16 (2)	55581·5	$3p\ {}^1D_2-7s\ {}^1P_1$
1797·35 (1)	55637·5	$3p\ {}^1D_2-5d\ {}^3P$?
1790·31 (2)	55856·3	
1787·78 (00)	55935·3	
1784·09 (0)	56051·0	
1783·24 (2*n*)	56077·7	
1776·86 (2)	56279·0	$3p\ {}^3P_2-3d\ {}^3P$?
1774·98 (0)	56338·7	
1774·05 (00)	56368·2	
1772·26 (0)	56425·1	$3p\ {}^3P_1-3d\ {}^3P$?
1770·89 (3R)	56468·8	$3p\ {}^1D_2-6d\ {}^1F_3$
1769·81 (3)	56503·2	$\begin{cases} 3p\ {}^3P_0-3d\ {}^3P\ ? \\ 3p\ {}^1D_2-x_1 \end{cases}$
1766·09 (4*n*)	56622·3	
1765·15 (3R)	56652·4	$3p\ {}^1D_2-6d\ {}^1D_2$
1759·63 (2)	56830·1	$3p\ {}^1D_2-8s\ {}^1P_1$
1757·34 (00)	56904·2	
1753·11 (3*n*)	57041·5	
1752·71 (0)	57054·5	
1749·78 (00)	57150·0	
1747·40 (1)	57227·9	
1743·91 (0)	57342·4	
1740·40 (2*n*)	57458·1	$3p\ {}^1D_2-7d\ {}^1D_2$
1736·58 (00)	57584·7	$3p\ {}^1D_2-9s\ {}^1P_1$
1734·78 (1*n*)	57644·2	
1727·37 (00)	57891·5	
1724·07 (00)	58002·3	
*1707·102 (0)	58578·82	$3p\ {}^3P_2-4d\ {}^1P_1$
1704·47 (3R)	58669·3	$3p\ {}^3P_2-4d\ {}^1F_3$
*1702·855 (2)	58724·90	$3p\ {}^3P_1-4d\ {}^1P_1$
*1700·623 (2)	58801·96	$3p\ {}^3P_0-4d\ {}^1P_1$
1700·43 (2)	58808·6	$3p\ {}^3P_2-4d\ {}^3D_2$
1699·73 (00)	58832·9	
1698·25 (00)	58884·1	
1697·92 (4R)	58895·6	$3p\ {}^3P_2-4d\ {}^3D_3$
1697·60 (0)	58906·7	
1696·22 (3R)	58954·6	$3p\ {}^3P_1-4d\ {}^3D_2$
1695·60 (2)	58976·2	$3p\ {}^3P_0-4d\ {}^3D_1$
1693·48 (1)	59050·0	$3p\ {}^3P_2-6s\ {}^3P_1$
1693·23 (1)	59058·7	
1690·80 (1)	59143·6	$3p\ {}^3P_1-6s\ {}^3P_0$
1689·30 (1)	59196·1	$3p\ {}^3P_1-6s\ {}^3P_1$
1687·08 (0)	59274·0	$3p\ {}^3P_0-6s\ {}^3P_1$
1686·87 (1)	59281·4	$3p\ {}^3P_2-6s\ {}^3P_2$
1682·70 (1)	59428·3	$3p\ {}^3P_1-6s\ {}^3P_2$
1676·83 (0)	59636·3	
1675·24 (3)	59692·9	
1672·62 (2)	59786·4	$3p\ {}^3P_2-4d\ {}^3P$
1670·91 (2)	59847·6	
1668·53 (1)	59933·0	$3p\ {}^3P_1-4d\ {}^3P$
1667·66 (1)	59964·3	
1666·40 (1)	60009·6	$3p\ {}^3P_0-4d\ {}^3P$
1664·51 (1)	60077·7	
1660·44 (0)	60225·0	
1653·28 (1)	60485·8	
1651·02 (0)	60568·6	
1633·95 (1*n*)	61201·4	$3p\ {}^3P_2-5d\ {}^1F_3$
1633·04 (0*n*)	61235·5	
1631·39 (0*n*)	61297·4	
1629·33 (1)	61374·9	
1627·83 (00)	61431·5	
1627·15 (00)	61457·1	
1625·68 (2*n*)	61512·7	Si ?
1622·79 (2*n*)	61622·3	Si ?
1620·39 (1)	61713·5	$3p\ {}^3P_2-5d\ {}^3P$?
1616·55 (1)	61860·1	$3p\ {}^3P_1-5d\ {}^3P$?
1615·94 (1)	61883·5	
1614·63 (1)	61933·7	$3p\ {}^3P_0-5d\ {}^3P$?
1609·02 (0)	62149·6	
1605·86 (0)	62271·9	
1597·99 (1)	62579·6	$3p\ {}^3P_2-x_1$
1595·21 (0)	62687·7	
1594·25 (1)	62725·4	$\begin{cases} 3p\ {}^3P_1-x_1 \\ 3p\ {}^3P_2-6d\ {}^1D_2 \end{cases}$
1592·27 (1)	62803·4	$3p\ {}^3P_0-x_1$
1590·60 (0)	62869·4	$3p\ {}^3P_1-6d\ {}^1D_2$

* Calculated wave-lengths adopted.

air, and those smaller than λ 2000 *in vacuo*. The second column gives the corresponding wave-numbers, reduced to vacuum throughout, while the third indicates the classification of the lines, the justification for which will appear later.

Table IA.—Other Lines which appear in the Photographs.

λ_{vac} (Int.).	Probable origin.	λ_{vac} (Int.).	Probable origin.
2073·37 (1)	Si II	1769·20 (00)	Al
2072·68 (0)		1763·93 (1)	Al II
2026·49 (1)	Mg I	1762·95 (0)	Al I ?
1936·45 (2*n*)	Al I ?	1745·26	N I
1932·25 (2*n*)		1742·74	
1862·41 (00)	Al II	1725·00 (00)	Al II
1840·09 (0)	Ca II*	1721·30 (00)	
1816·98 (2)	Si II	1670·78 (2)	Al II
1808·09 (1)			

* The other component of the Ca pair is masked by Si 1838·00.

The first three lines in Table I are the strongest of those photographed in the near infra-red by McLennan and Shaver.* Following these are 14 lines for which the new solar wave-lengths on the International scale have been adopted†; these are slightly different from the values given in the previous table, and λ 5754·240 has been added to the original list. No change has been found necessary from λ 3020 to λ 2208, except that three faint lines have been added. From the next line at λ 2124 to λ 1841, however, new wave-lengths have been substituted for those previously published, and several faint lines which are believed to be due to silicon have been included. Many of the lines of shorter wave-length than λ 1841 appear to have been observed in the vacuum arc by McLennan and Shaver, but only approximate wave-lengths were given by these observers.

Lines which appear in the photographs but have not been included in the general table are indicated in Table IA; it is possible that some of these may obscure lines of silicon. Lines for which wave-lengths have been calculated in the manner already explained are marked with an asterisk.

Predicted Terms.

The terms corresponding with the various electron configurations of Si I are indicated in Table II. The notation is similar to that adopted in previous

---

* 'Trans. Roy. Soc. Canada,' vol. 18, p. 21 (1924).

† Revision of "Rowland's Preliminary Table of Solar Spectrum Wave-lengths," by C. E. St. John and others, Carnegie Institution, 1928.

Table II.—Predicted Terms of Si I.

1_1	2_1	2_2	3_1	3_2	3_3	4_1	4_2	4_3	4_4	5_1	5_2	6_1	Effective configuration.	Term prefix.	Terms.
2	2	6	2	2									$s^2 p^2$	3*p*	**^{3}P** **^{1}D** **^{1}S**
2	2	6	2	1		1							$s^2 p . s$	4*s*	**^{3}P** **^{1}P**
2	2	6	1	3									$s p^3$	3*p′*	^{5}S **^{3}D** **^{3}P** ^{3}S **^{1}D** ^{1}P
2	2	6	2	1			1						$s^2 p . p$	*4*p*	^{3}D **^{3}P** ^{3}S **^{1}D** **^{1}P** **^{1}S**
2	2	6	2	1	1								$s^2 p . d$	3*d*	^{3}F **^{3}D** **^{3}P** **^{1}F** **^{1}D** **^{1}P**
2	2	6	2	1		1							$s^2 p . s$	5*s*	**^{3}P** **^{1}P**
2	2	6	2	1			1						$s^2 p . p$	5*p*	^{3}D **^{3}P** ^{3}S ^{1}D ^{1}P **^{1}S**
2	2	6	2	1				1					$s^2 p . d$	4*d*	^{3}F **^{3}D** **^{3}P** **^{1}F** **^{1}D** **^{1}P**
2	2	6	2	1					1				$s^2 p . f$	4*f*	^{3}G ^{3}F **^{3}D** ^{1}G ^{1}F ^{1}D

* The principal combinations of this row of terms are outside the range of the observations, in the infra-red.

papers,† terms in each row being prefixed by the n_k designation of the wandering electron; in the special case of the configuration sp^3, the adopted prefix is $3p'$. Combinations between terms on different rows, other than $3p'$, are governed by the condition $\Delta k = \pm 1$ ($k = 1, 2, 3, \ldots$ for s, p, d, …), and by the rule for inner quantum numbers associated with the term symbols, namely $\Delta j = \pm 1$ or 0, with $0 \rightarrow 0$ forbidden. Combinations of the p' terms with the others follow the rule $\Delta k = 0$, so that of the terms shown in the table only the p terms can combine with the p' terms, always subject to the inner quantum rules. These conditions are equivalent to the rule for permissible electron transitions; namely, that $\Delta k = \pm 1$ for one electron, and $\Delta k = 0$ or 2 for a second electron when two transitions occur together.

Identification of Terms.

The terms which are believed to have been identified are indicated by heavier type in Table II. They are shown, with the observed combinations, in Tables III and IIIA. There can be little doubt as to most of these, but some of the assignments presented considerable difficulty in the first instance. In particular, it should be noted that the $3p'$ and $3d$ terms yield similar combinations with the deep $3p$ terms, so that the $3p'$ terms might have been called $3d$, and subsequent d terms $4d$ and $5d$. In support of the assignments adopted, however, the first ^{3}D term does not appear to be in reasonable sequence with the second and third, and it has accordingly been identified as $3p'\,^3$D. Again, the terms designated by $3p'\,^3$P and $3p'\,^1D_2$ do not appear to be followed by other terms related to them in Rydberg sequences, as would be expected if they

---

† 'Roy. Soc. Proc.,' A, vol. 117, p. 317 (1928); vol. 118, p. 34 (1928).

Table III.—Combinations in Si I.

	Terms.	$\Delta\nu$	$3p\ ^3P_0$ 65765·00	$3p\ ^3P_1$ 65687·94	$3p\ ^3P_2$ 65541·86	$3p\ ^1D_2$ 59466·33	$3p\ ^1S_0$ 50370·90
				77·06	146·08	6075·53	9095·43
$4s\ ^3P_0$	26082·05			39605·89 (9)			
P_1	26004·91	77·14	39760·04 (7)	39683·03 (8)	39537·01 (10)	33461·39 (5)	24365·89 (5)
P_2	25810·12	194·79		39877·83 (10)	39731·73 (15)	33656·27 (2)	
$4s\ ^1P_1$	24773·40		40991·64 (3)	40914·54 (3)	40768·42 (3)	34692·97 (10)	25597·61 (10)
$3p'\ ^3D_1$	20488·94		45276·09 (2)	45198·92 (2)	45052·96 (1)		
D_2	20471·89	17·05		45216·07 (3)	45069·96 (2)		
D_3	20443·54	28·35			45098·32 (4)		
$3p'\ ^1D_2$	18413·72			*47274·22 (0)	*47128·14 (1)	41052·61 (8)	
$3p'\ ^3P_2$	15265·5			50422·3 (4)	50276·4 (6)		
P_1	15199·2	−66·3	50565·8 (3)	50488·7 (3)	50342·6 (4)		
P_0	15163·2	−36·0		50524·7 (3)			
$3d\ ^1F_3$	12403·61				*53138·3 (2)	47062·72 (10)	
$3d\ ^1P_1$	12378·33		*53386·7 (2)	*53309·6 (2)	*53163·5 (0)	*47088·00 (2)	37992·57 (5)
$3d\ ^3D_1$	11580·2		54185·0 (3)	54107·6 (3)	53961·6 (1)		
D_2	11560·3	19·9		54127·8 (4)	53981·4 (3)		
D_3	11508·3	52·0			54033·6 (5)		
$3d\ ^1D_2$	11506·2					47960·09 (2)	
$5s\ ^3P_0$	11520·5			54167·4 (2)			
P_1	11451·7	68·8	*54313·3 (2)	*54236·2 (2)	*54090·1 (2)	*48014·58 (1)	38919·15 (2)
P_2	11237·7	214·0		54450·2 (2)	54304·2 (3)		
$5s\ ^1P_1$	10894·4		*54870·6 (2)	*54793·6 (00)	54647·5 (2)	*48571·95 (5)	39476·52 (2)
? $3d\ ^3P$	9262·8		†	56425·1 (0)	56279·0 (2)	50202·3 (2)	

* Calculated values. † Masked by 56503 (3).

Table III—(continued).

	Terms.	$\Delta\nu$	$3p\,^3P_0$ 65765·00	$3p\,^3P_1$ 65687·94	$3p\,^3P_2$ 65541·86	$3p\,^1D_2$ 59466·33	$3p\,^1S_0$ 50370·90
			77·06	146·08	6075·53	9095·43	
$4d\,^1P_1$	6963·0		*58802·0 (2)	*58724·9 (2)	*58578·8 (0)	*52503·3 (2)	43407·9 (2)
$4d\,^1F_3$	6872·5				58669·3 (3)	52593·9 (8)	
$4d\,^3D_1$	6788·8		58976·2 (2)	†[58899·1]	[58753·0]		
		55·5					
D_2	6733·3			58954·6 (3)	58808·6 (2)		
		87·0					
D_3	6646·3				58895·6 (4)		
$4d\,^1D_2$	6647·1					52819·2 (5)	
$6s\,^3P_0$	6544·3			59143·6 (1)			
		52·7					
P_1	6491·6		59274·0 (0)	59196·1 (1)	59050·0 (1)	52973·4 (2)	43880·4 (0)
		231·5					
P_2	6260·1			59428·3 (1)	59281·4 (1)		
$6s\,^1P_1$	6129·3					53336·2 (3)	44242·5 (1)
$4d\,^3P$?	5755·3		60009·6 (1)	59933·0 (1)	59786·4 (2)	53712·6 (00)	
$5d\,^1P_1$?	4459·9					55006·4 (0)	
$5d\,^1F_3$	4341·6				61201·4 (1)	55124·7 (6)	
$5d\,^1D_2$	4189					55277·6 (4)	
$7s\,^1P_1$	3885					55581·5 (2)	
$5d\,^3P$?	3829		61934 (1)	61860 (1)	61714 (1)	55637 (1)	
$6d\,^1F_3$	2997					56469 (3)	
x_1	2963		62803 (1)	62725 (1)	62580 (1)	56503 (3)	
$6d\,^1D_2$	2817			62869 (0)	62725 (1)	56652 (3)	
$8s\,^1P_1$	2636					56830 (2)	
$7d\,^1D_2$	2008					57458 (2)	
$9s\,^1P_1$	1881					57585 (00)	

* Calculated values. † Masked by 58895·6 (4).

Table IIIA.—Less Refrangible Combinations in Si I.

Terms.		$\Delta\nu$	$4s\ ^3P_0$ 26082·05	77·14	$4s\ ^3P_1$ 26004·91	194·79	$4s\ ^3P_2$ 25810·12	$4s\ ^1P_1$ 24773·40	$3d\ ^1F_3$ 12403·61
$4p\ ^1D_2$?	22652								10248 (10)
$4p\ ^1S_0$	15873				10131 (5)			8902 (8)	
? $5p\ ^3D_1$	8762·28		17319·77 (1)						
		14·56							
D_2	8747·72				17257·19 (2)				
		180·54							
D_3	8567·18						17242·94 (3)		
$5p\ ^3P_0$	8469·33				17535·58 (1)				
		32·90							
P_1	8436·43		17645·61 (1)		17568·49 (2)		17373·68 (0)		
		139·47							
P_2	8296·96				17707·94 (1)		17513·17 (5)		
$5p\ ^1S_0$	7967·23							16806·17 (5)	

were $3d\ ^3P$ and $3d\ ^1D_2$. There appears also to be a definite range of higher term values associated with $3p'$ as compared with those distinguished by $3d$; with the identifications adopted, the deepest $3d$ terms range about 12000, as in many other spectra. The assignment of the $3p'$ terms is also supported by comparisons with the P II spectrum, as will appear later.

The arrangement of the deeper terms in Table III is similar to that given empirically by McLennan and Shaver,* and afterwards interpreted in relation to electronic configurations by Hund.† More precise values of the terms have now been determined, and numerous additional terms have been identified. Many of the new terms are established by confirmatory combinations, but the identification of some of them depends upon extrapolation from preceding terms. The more doubtful identifications are indicated by a ? mark.

The triplet series $3p\ ^3P - ms\ ^3P$, of which three members have been completely observed, is fully established by combinations, and may be used with confidence for the determination of term values. Of the series $3p\ ^3P - md\ ^3D$, however, only two members have been identified. The $3p\ ^3P - md\ ^3P$ is either feeble or missing, and the partial identifications shown in the table are possibly somewhat doubtful; there is evidence from P II and S III, however, that the $d\,{}^3\mathrm{P}$ separations may be so small in Si I as to be unresolvable in the present series of photographs.

---

* *Loc. cit.*

† 'Zeit. f. Phys.,' vol. 33, p. 335 (1925).

Term Values.

Several series of more than two members are available for the determination of term values. It will be of interest first to consider the series $3p\,{}^3\mathrm{P} - ms\,{}^3\mathrm{P}$. Using the Hicks' formula with the lines indicated below, and observing from Table III that $3p\,{}^3\mathrm{P}_0 - 3p\,{}^3\mathrm{P}_1 = 77{\cdot}1$, $3p\,{}^3\mathrm{P}_0 - 3p\,{}^1\mathrm{D}_2 = 6298{\cdot}7$, the term values shown are readily obtained.

$$\left.\begin{aligned} 3p\,{}^3\mathrm{P}_1 - 4s\,{}^3\mathrm{P}_0 &= 39606 \\ - 5s\,{}^3\mathrm{P}_0 &= 54167 \\ - 6s\,{}^3\mathrm{P}_0 &= 59144 \end{aligned}\right\} \begin{aligned} &\nu = 65668 - \mathrm{R}/[m + 1{\cdot}12594 - 0{\cdot}07397/m]^2 \\ &3p\,{}^3\mathrm{P}_0 = 65745;\ 3p\,{}^1\mathrm{D}_2 = 59446. \end{aligned}$$

$$\left.\begin{aligned} 3p\,{}^3\mathrm{P}_1 - 4s\,{}^3\mathrm{P}_1 &= 39683 \\ - 5s\,{}^3\mathrm{P}_1 &= 54236 \\ - 6s\,{}^3\mathrm{P}_1 &= 59196 \end{aligned}\right\} \begin{aligned} &\nu = 65702 - \mathrm{R}/[m + 1{\cdot}13359 - 0{\cdot}07991/m]^2 \\ &3p\,{}^3\mathrm{P}_0 = 65779;\ 3p\,{}^1\mathrm{D}_2 = 59480. \end{aligned}$$

$$\left.\begin{aligned} 3p\,{}^3\mathrm{P}_1 - 4s\,{}^3\mathrm{P}_2 &= 39878 \\ - 5s\,{}^3\mathrm{P}_2 &= 54450 \\ - 6s\,{}^3\mathrm{P}_2 &= 59428 \end{aligned}\right\} \begin{aligned} &\nu = 65952 - \mathrm{R}/[m + 1{\cdot}12617 - 0{\cdot}07469]^2 \\ &3p\,{}^3\mathrm{P}_0 = 66029;\ 3p\,{}^1\mathrm{D}_2 = 59730. \end{aligned}$$

Other series taken from the same multiplets necessarily give the same values for the components of $3p\,{}^3\mathrm{P}$ when corresponding components of $s\,{}^3\mathrm{P}$ are taken for calculation.

It will be seen that $s\,{}^3\mathrm{P}_0$ and $s\,{}^3\mathrm{P}_1$ give approximately the same limits, whilst $s\,{}^3\mathrm{P}_2$ leads to a considerably greater value. This was to be expected from Hund's theory, according to which, in the present spectrum, $s\,{}^3\mathrm{P}_0$ and $s\,{}^3\mathrm{P}_1$ tend towards the limit ${}^2\mathrm{P}_1$ of Si II and $s\,{}^3\mathrm{P}_2$ towards the limit ${}^2\mathrm{P}_2$. These limits differ by 287 units of wave-number,* and the mean of the above values from $s\,{}^3\mathrm{P}_0$ and $s\,{}^3\mathrm{P}_1$ is actually smaller than that from $s\,{}^3\mathrm{P}_2$ by 267 units. The agreement is as close as can be expected, in view of the inadequacy of the series formula and the possible errors of wave-numbers in the Schumann region.

If the mean value (65762) be adopted for $3p\,{}^3\mathrm{P}_0$, all other sets of corresponding terms which tend to the limit ${}^2\mathrm{P}_1$ will form Rydberg sequences. For those tending to the limit ${}^2\mathrm{P}_2$, however, the values directly determined from the combinations, as they appear in Table III, will only form Rydberg sequences when they have been increased by 287. In other words, for terms which tend to the ${}^2\mathrm{P}_2$ limit, the values determined from formulæ must be diminished by 287 units in order to refer them to the lowest level $3p\ {}^3\mathrm{P}_0$.

---

* A. Fowler, 'Phil. Trans.,' A, vol. 225, p. 24 (1925).

According to Hund, all the singlet series of Si I should tend towards the limit ${}^2\mathrm{P}_2$ of Si II. This is apparently true of the series $3p\ {}^1\mathrm{D}_2 - ms\ {}^1\mathrm{P}_1$, for which the data and a Hicks' formula are given below :—

$$
\begin{array}{ll}
3p\,{}^1\mathrm{D}_2 - 4s\,{}^1\mathrm{P}_1 = 34693\ (10) & \\
\left.\begin{array}{l}
\qquad\ \ - 5s\,{}^1\mathrm{P}_1 = 48572\ (5) \\
\qquad\ \ - 6s\,{}^1\mathrm{P}_1 = 53336\ (3) \\
\qquad\ \ - 7s\,{}^1\mathrm{P}_1 = 55581\ (2)
\end{array}\right\} &
\begin{array}{l}
\nu = 59714 - \mathrm{R}/[m + 1\cdot16731 - \\
\qquad\qquad\qquad\qquad 0\cdot05803/m]^2 \\
3p\,{}^1\mathrm{D}_2 = 59714\ ;\ 3p\,{}^3\mathrm{P}_0 = 66013.
\end{array} \\
\qquad\ \ - 8s\,{}^1\mathrm{P}_1 = 56830\ (1) & \\
\qquad\ \ - 9s\,{}^1\mathrm{P}_1 = 57585\ (00) &
\end{array}
$$

Extrapolation to the first line gives O — C = — 356, and to the last + 12 and + 13 units of wave-number respectively. If the identification of the last two lines be correct, as seems probable, the term values above deduced are rather too small, but it is sufficiently clear that the series under consideration tends to the same limit (${}^2\mathrm{P}_2$) as the $s\ {}^3\mathrm{P}_2$ terms.

The remaining singlet series present considerable difficulty. The strongest of them is $3p\ {}^1\mathrm{D}_2 - md\ {}^1\mathrm{F}_3$, for which the data are as follows :—

$$
\begin{array}{ll}
\left.\begin{array}{l}
3p\,{}^1\mathrm{D}_2 - 3d\,{}^1\mathrm{F}_3 = 47063\ (8) \\
\qquad\ \ - 4d\,{}^1\mathrm{F}_3 = 52594\ (8) \\
\qquad\ \ - 5d\,{}^1\mathrm{F}_3 = 55125\ (6)
\end{array}\right\} &
\begin{array}{l}
\nu = 59572 - \mathrm{R}/[m + 0\cdot97325 - \\
\qquad\qquad\qquad\qquad 0\cdot02281/m]^2 \\
3p\,{}^1\mathrm{D}_2 = 59572\ ;\ 3p\,{}^3\mathrm{P}_0 = 65871.
\end{array} \\
\qquad\ \ - 6d\,{}^1\mathrm{F}_3 = 56469\ (3) &
\end{array}
$$

The choice of the last line appears to be justified by the fact that the formula gives the wave-number as 56492, and by its appearance with undiminished intensity in potassium fluo-silicate, as in the case of the preceding members of this series. The inclusion of this line, however, modifies the calculated limit of the series very considerably. Thus, the last three lines give the formula

$$\nu = 59482 - \mathrm{R}/[m + 1\cdot100325 - 0\cdot326836/m]^2,$$

from which the calculated value of the first line is 46759 (O — C = + 306). If all four lines are included in a formula with a second correcting term, β/m^2, the limit becomes 59453. This is nearly the mean of the two values deduced from $3p\ {}^3\mathrm{P}_1 - ms\ {}^3\mathrm{P}_{01}$, and it seems probable that, in opposition to Hund's theory, the singlet DF series tends to the limit ${}^2\mathrm{P}_1$ of Si II. Other discordances with the theory of limits have been found by Shenstone* and by Lang and Laporte.†

The singlet $3p\,{}^1D_2 - md\,{}^1D_2$ series appears to consist of the lines shown below :—

$$3p\,{}^1D_2 - 3d\,{}^1D_2 = 47964\ (2)$$

$$\left.\begin{array}{l} - 4d\,{}^1D_2 = 52819\ (5) - \\ - 5d\,{}^1D_2 = 55278\ (4) - \\ - 6d\,{}^1D_2 = 56652\ (3) \\ - 7d\,{}^1D_2 = 57458\ (2) - \end{array}\right\} \begin{array}{l} \nu = 59737 - R/[m + 0\cdot 89538 + 0\cdot 26220/m]^2 \\ 3p\,{}^1D_2 = 59737\ ;\ 3p\,{}^3P_0 = 66036. \end{array}$$

The formula has been calculated from the second, third and fifth lines. The first line, if correctly identified, is abnormally weak as compared with succeeding members of the series, but it appears to be the only observed line available. The second and third lines, as will appear from Table III, are remarkable as giving $d\,{}^1D_2$ terms which are practically identical with $d\,{}^3D_3$ terms; they appear, however, to be too strong to be regarded as $3p\,{}^1D_2 - 3d$, $4d\,{}^3D_3$, especially as $3p\,{}^1D_2 - 3d$, $4d\,{}^3D_2$, which would be expected to be still stronger lines, are missing. The fourth line has been chosen in preference to 56622 because, like the second and third, it is much weakened in potassium fluo-silicate, while 56622 is scarcely affected, as compared with its appearance in elementary silicon. The selection of 56652 is also supported by the apparent combinations of $6d\,{}^1D_2$ with $3p\,{}^3P_{21}$. The series, however, is not very closely represented by a Hicks' formula ; by extrapolation with the formula given above, the wave-number of the first line appears as 47757 ($O - C = + 207$), while the computed value for the fourth is 56635 ($O - C = + 17$). A formula calculated from the second, third and fourth lines gives $3p\,{}^1D_2 = 59805$; and if 56622 be substituted for 56652, $3p\,{}^1D_2 = 59686$. Thus, while the series is not well represented by formulæ, it is reasonable to conclude that it leads to a value for $3p\,{}^3P_0$ similar to that deduced from $3p\,{}^3P_2 - ms\,{}^3P_2$, and that the $d\,{}^1D_2$ series tends to the limit ${}^2P_2$ of Si II, in agreement with theory.

The series $3p\,{}^1D_2 - md\,{}^1P_1$ is very feebly represented. The identification of the first two members is strongly supported by combinations, but the choice of the third depends upon extrapolation from the first two, and the order of occurrence of adjacent terms. Details of the series are as follows :—

$$\left.\begin{array}{l} 3p\,{}^1D_2 - 3d\,{}^1P_1 = 47088\ (2) \\ \qquad\quad - 4d\,{}^1P_1 = 52503\ (2) \\ \qquad\quad - 5d\,{}^1P_1 = 55006\ (0) \end{array}\right\} \begin{array}{l} \nu = 59436 - R/[m + 0\cdot 97305 + 0\cdot 01617/m]^2 \\ 3p\,{}^1D_2 = 59436\ ;\ 3p\,{}^3P_0 = 65735. \end{array}$$

---

* 'Phys. Rev.,' vol. 31, p. 317 (1928).

† 'Phys. Rev.,' vol. 31, p. 763 (1928).

The value of $3p\,{}^3P_0$ thus determined suggests that the $d\,{}^1P_1$ series tends to the ${}^2P_1$ limit of Si II, in opposition to theory, but the evidence for this is not very conclusive, in consequence of the few observed members of the series.

If the identifications of the near infra-red singlets shown in Table IIIA be correct, another series of three terms becomes available for the calculation of term values, namely,

$$\left.\begin{array}{rl} 4s\,{}^1P_1 - 3p\,{}^1S_0 = & -25598 \\ - 4p\,{}^1S_0 = & 8902 \\ - 5p\,{}^1S_0 = & 16806 \end{array}\right\} \begin{array}{l} \nu = 25022 - R/[m + 0{\cdot}74580 - 0{\cdot}27340/m]^2 \\ 3p\,{}^3P_0 = 66014\,;\ 3p\,{}^1D_2 = 59715. \end{array}$$

The close agreement of the value for $3p\,{}^3P_0$ thus determined with that derived from the series $3p\,{}^3P_1 - ms\,{}^3P_2$ not only indicates that the $p\,{}^1S_0$ series tends to the limit ${}^2P_2$ of Si II, as expected, but strongly supports the identification of the two less refrangible singlets which are involved.

As a result of the foregoing considerations, the term $3p\,{}^3P_0$, representing the lowest normal state of the Si I atom, has been assigned the value 65765. All the other terms shown in Tables III and IIIA are accordingly based upon this, and represent the energy levels as reckoned from ${}^2P_1$ of Si II. All the series of terms tending to ${}^2P_1$ may thus be represented by series formulæ without modification. Those which tend to the ${}^2P_2$ limit, however, must be increased by 287 units in order that they may form Rydberg sequences.

The general consistency of the scheme of terms will appear from Table IV (p. 436), which shows the effective quantum numbers, or Rydberg denominators, for the various terms, R being taken as 109737.

The ionisation potential of Si I represented by the adopted value of $3p\,{}^3P_0$ is 8·12 volts.

Intensities.

The intensities of some of the lines show marked irregularities. Thus, the first line of the triplet $3p\,{}^3P - 3d\,{}^1P_1$ at ν 53163 is of intensity 0, while the other two members, which would be expected to be weaker, are of intensity 2. A similar irregularity is found also in the next triplet of this series, having its first line at ν 58578. Again, in the triplet $3p\,{}^3P - 5s\,{}^1P_1$, the middle line at ν 54793 is very much fainter than the outer members of the triplet.

It is possible that the intensities of some of the lines, as observed in the arc by the method adopted for silicon, are affected by absorption due to atmospheric gases and to products of combustion. One of the photographs of potassium fluo-silicate was remarkable as showing very strong absorption bands of nitric

Table IV.—Rydberg Denominators.

	$^3P_0$.*	$^3P_1$.*	$^3P_2$.	$^1P_1$.
4*s*	2·0512	2·0542	2·0506	2·0926
5*s*	3·0863	3·0956	3·0858	3·1328
6*s*	4·0949	4·1115	4·0940	4·1356
7*s*				5·1287
8*s*				6·1272
9*s*				7·1145

	$^1F_3$.*	$^1P_1$.*	$^3D_1$.*	$^3D_2$.*	$^3D_3$.	$^1D_2$.	^3P ?.
3*d*	2·9744	2·9774	3·0784	3·0810	3·0502	3·0508	3·4421
4*d*	3·9959	3·9699	4·0204	4·0371	3·9785	3·9782	4·3667
5*d*	5·0275	4·9603 ?				4·9514	5·3542
6*d*	5·0506					5·9487	
7*d*						6·9149	

	$^3P_0$.*	$^3P_1$.*	$^3P_2$.	$^1D_2$.	$^1S_0$.
3*p*	1·2917	1·2925	1·2911	1·3552	1·4718
4*p*	—	—	—	2·1872 ?	2·6056
5*p*	3·5996	3·6066	3·5755		3·6462

* The values in these columns have been computed from the corresponding terms shown in Table III; for the remaining terms the values indicated in Table III have been increased by 287 units for the calculation of n^*.

oxide,† which totally obliterated many of the lines of silicon. This suggests that given small amounts of nitric oxide produced by the arc may be effective in reducing the intensities of some of the lines, and it is possible that the low intensity of ν 53163 may be accounted for in this way. The spectrum of nitric oxide is under investigation, in order to determine its possible effects on other lines.

Nitrogen itself produces absorption bands, but the strongest of them lie outside the range of the present observations, on the more refrangible side.

Comparison with P II.

The elements of successively higher atomic numbers than silicon are phosphorus, sulphur and chlorine, so that Si I, P II, S III and Cl IV form an isoelectronic series. The triplets of P II have been investigated in considerable detail by Bowen,‡ but no account has been given of the singlets of this spectrum. A few of the higher triplet combinations of S III have been identified by M. J. Gilles,[†] and a few of the deeper combinations of Cl IV by Bowen,[‡] but in neither case has any determination of term values yet become possible. Effective comparison can accordingly at present be made only between the triplets of Si I and P II.

---

† See Leifson, 'Astrophys. Jour.,' vol. 63, p. 82 (1926).

‡ 'Phys. Rev.,' vol. 29, p. 510 (1927); see also a note on P II and Si I in a paper on Cl IV, 'Phys. Rev.,' vol. 31, p. 36 (1928).

The terms and triplet separations in the two spectra are shown side by side in Table V, and the values of the P II terms, as given by Bowen, are also

Table V.—Terms of Si I compared with those of P II.

	Si I.		P II.			$\Delta\nu$: P II/Si I.
	ν.	$\Delta\nu$.	ν.	$\Delta\nu$.	$\nu/4$.	
$3p\ ^3P_0$	65765·00		160497·7		40124·4	
		77·06		*165·3*		
P_1	65687·94		160332·4		40083·1	2·16
		146·08		*304·6*		
P_2	65541·86		160027·8		40007·0	
$4s\ ^3P_0$	26082·05		73900·0		18475·0	
		77·14		*146·4*		
P_1	26004·91		73753·6		18438·4	1·94
		194·79		*380·7*		
P_2	25810·12		73372·9		18343·2	
$3p'\ ^3D_1$	20488·94		95246·0		23811·5	
		17·05		*20·3*		
D_2	20471·89		95225·7		23806·4	1·21
		28·35		*34·7*		
D_3	20443·54		95191·0		23797·8	
$3p'\ ^3P_2$	15265·5		83733·9		20918·7	
		—66·3		*—48·4*		
P_1	15199·2		83685·5		20921·4	0·59
		—36·0		*—11·8*		
P_0	15163·2		83674·7		20933·5	
[*]$4p\ ^3D_1$			57332·0		14333·0	
				173·5		
D_2			57158·5		14289·6	
				328·7		
D_3			56829·8		14207·5	
[*]$4p\ ^3P_0$			55273·2		13818·3	
				78·1		
P_1			55195·1		13798·8	
				247·3		
P_2			54947·8		13737·0	

[*] The principal combinations of these terms in Si I are out of range in the infra-red.

[†] 'C. R.,' vol. 188, p. 63 (1929).

[‡] 'Phys. Rev.,' vol. 31, p. 34 (1928).

Table V—(continued).

	Si I.		P II.			Δν : P II/Si I.
	ν.	Δν.	ν.	Δν.	ν/4	
$3d\ ^3D_1$	11580·2		56443·1		14110·8	
		19·9		*48·4*		
D_2	11560·3		56394·7		14098·7	1·97
		52·0		*93·4*		
D_3	11508·3		56301·3		14075·3	
$3d\ ^3P_0$	9262 ?		—		—	
				—		
P_1			50243·8		12561·0	
				38·6		
P_2			50205·2		12551·3	
$5s\ ^3P_0$	11520·5		37153·3		9288·3	
		68·8		*111·3*		
P_1	11451·7		37042·0		9260·5	1·93
		214·0		*435·5*		
P_2	11237·7		36606·5		9151·6	

shown divided by four, for readier comparison with Si I. The last column of the table indicates the ratio of the total separations ($^3P_0 - {}^3P_2$, etc.) in the two spectra. The P II terms, it should be remarked, have been deduced from $3s\ ^3P$ and $4s\ ^3P$ by an uncorrected Rydberg formula, but as this series in Si I is nearly Rydbergian, Bowen's values are probably not far from correct.

Apart from the $3p'$ terms, the terms of the two spectra exhibit the kind of relation which has been found in other comparisons of the spectrum of a neutral atom with that of the singly-ionised atom of next higher atomic number. Thus, while the reduced values of the p and s terms of P II are much smaller than those of Si I, the d terms are the greater in P II. It will be seen also that the total triplet separations are not far from twice as great in P II as in Si I.

The $3p'$ terms in the two spectra, however, show striking differences. Whereas in Si I these terms are considerably smaller than $4s\ ^3P$, in P II they are considerably greater. The ratios of the separations are also very different from those of all the other terms. The only apparent resemblance of the $3p'$ terms in the two spectra is the inversion in $3p'\ ^3P$.

Summary.

By passing an arc in nitrogen at atmospheric pressure, and using a vacuum spectrograph, the arc spectrum of silicon has been photographed to about

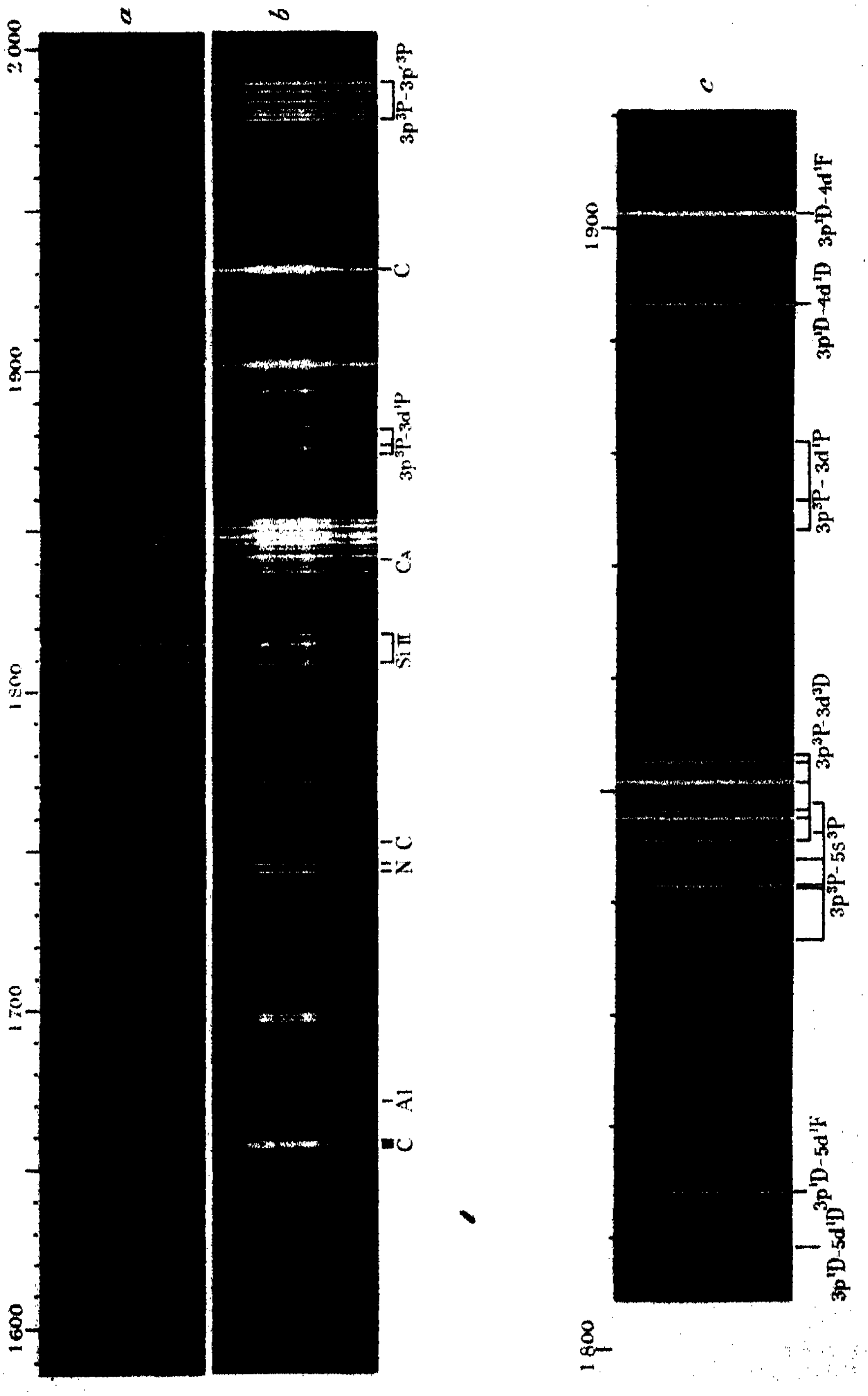

Arc Spectrum of Silicon, λ 1600 — λ 2000.

λ 1600. Many previously unrecorded lines have been observed and the analysis of the spectrum has been greatly extended. Most of the deeper terms predicted by Hund's theory have been identified, and several sequences of singlet and triplet combinations are available for the determination of term values. The deepest term, $3p\,{}^3P_0$, has been assigned the value 65765, representing an ionisation potential of 8·12 volts. Comparison with singly-ionised phosphorus, P II, shows the general similarity expected, but the terms arising from the electronic configuration sp^3 are relatively much greater in P II than in Si I.

The author's thanks are due to Mr. E. W. H. Selwyn for his suggestion of the method adopted for obtaining arcs in nitrogen, and for his skilful manipulation of the vacuum spectrograph. Mr. Selwyn was enabled to assist in the investigation by a grant from the Department of Industrial and Scientific Research.

DESCRIPTION OF PLATE 18.

(*a*) Arc spectrum of elementary silicon, λ 1600–λ 2000.

(*b*) Arc spectrum of potassium fluo-silicate, λ 1600–λ 2000.

(*c*) Arc spectrum of elementary silicon, λ 1800–λ 1900.

(*a*) and (*b*) were taken in the first order of a 1-metre metal grating, 15,000 lines per inch. The reproduction represents an enlargement of the original negatives by 7½ times.

(*c*) was taken in the first order of a 1-metre glass grating, 30,000 lines per inch. Enlarged 13 times in the reproduction.

On the Vortex Theory of Screw Propellers.

By Sydney Goldstein, M.A., Ph.D., St. John's College, Cambridge, and the Kaiser Wilhelm Institut für Strömungsforschung, Göttingen.

(Communicated by L. Prandtl, For.Mem.R.S.—Received January 21, 1929.)

1. *Introduction.*

The vortex-theory of screw propellers develops along similar lines to aerofoil theory. There is circulation of flow round each blade ; this circulation vanishes at the tip and the root. The blade may be replaced by a bound vortex system, which, for the sake of simplicity, may be taken, as a first approximation, to be a bound vortex line. The strength of the vortex at any point is equal to Γ, the circulation round the corresponding blade section. From every point of this bound vortex spring free, trailing vortices, whose strength per unit length is $-\partial\Gamma/\partial r$, where r is distance from the axis of the screw. When the interference flow of this vortex system is small compared with the velocity of the blades, the trailing vortices are approximately helices, and together build a helical or screw surface.* Part of the work supplied by the motor is lost in producing the trailing vortex system. When the distribution of Γ along the blade is such that, for a given thrust, the energy so lost per unit time is a minimum, then the flow far behind the screw is the same as if the screw surface formed by the trailing vortices was rigid, and moved backwards in the direction of its axis with a constant velocity, the flow being that of classical hydrodynamics in an inviscid fluid, continuous, irrotational, and without circulation.† The circulation round any blade section is then equal to the discontinuity in the velocity potential at the corresponding point of the screw surface. Further, for symmetrical screws, the interference flow at the blade is half that at the corresponding point of the screw surface far behind the propeller.*

---

* This system is unstable, and at a sufficient distance behind the propeller the vorticity is mainly concentrated into as many helical vortices as there are blades, with radii somewhat less than that of the original system, and into a straight line vortex along the axis. The strength of each helical vortex is nearly equal to the maximum value of the circulation round a blade section, and the strength of the straight line vortex is equal and opposite to the total strength of all the helical vortices.

† Betz, 'Göttinger Nachr.,' pp. 193–213 (1919) ; reprinted in 'Vier Abhandlungen zur Hydrodynamik und Aerodynamik,' L. Prandtl und A. Betz, Göttingen, 1927, where a selected bibliography is given. The theory takes no account of the finite size of the boss, or of the influence of compressibility of the fluid at large tip speeds. The approximation that the trailing vortices form regular helices is equivalent to neglecting the contraction of the slip stream, and is valid only for small values of the thrust coefficient. Also, in finding the most favourable distribution, the energy losses arising from the profile drag of the blade sections are not taken into account.

An approximate solution for the irrotational motion of a screw surface in an inviscid fluid was given by Prandtl.† The accuracy of the approximation increases with the number of blades and with the ratio of the tip speed to the velocity of advance, but for given values of these numbers we have no means of estimating the error, since the exact solution of the problem has not yet been found. It is the main object of this work to find the exact solution.

We consider first the important case of the two-bladed propeller; formulæ for any number of blades are given later. Finally, the application of the results is briefly considered.

2. *Formulation of the Potential Problem.*

Let R be the radius, ω the angular velocity, and v the velocity of advance of a two-bladed propeller. Let ε be the angle between 0 and $\frac{1}{2}\pi$ whose tangent is $v/r\omega$, where r is the distance from the axis of rotation. The equation to the screw surface to be considered is

$$\theta - \omega z/v = 0 \text{ or } \pi, \quad 0 \leqslant r \leqslant \mathrm{R}, \tag{1}$$

where r, θ and z are cylindrical polar co-ordinates. The axis of z is along the axis of the screw surface, with its positive direction away from the propeller.‡ If w is the velocity of the screw surface in the direction of its axis, and ϕ the potential, such that grad ϕ is the fluid velocity, the boundary conditions are that

$$w \cos \varepsilon = \frac{\partial \phi}{\partial z} \cos \varepsilon - \frac{\partial \phi}{r\,\partial \theta} \sin \varepsilon, \tag{2}$$

or

$$\omega r w = \omega r \frac{\partial \phi}{\partial z} - v \frac{\partial \phi}{r\,\partial \theta}, \tag{3}$$

for $\theta - \omega z/v = 0$ or π and $0 \leqslant r \leqslant \mathrm{R}$, and that grad ϕ should vanish for $r = \infty$.

The geometrical conditions are such that the fluid velocity is a function of r and $\theta - \omega z/v$ only. This does not by itself restrict ϕ to be a function of r and $\theta - \omega z/v$ only, since constant multiples of θ only and of z only may occur. But no term in θ or z may occur in the expression for ϕ for $r > R$, since the second would give finite velocity for infinite r, and the first would give circulation round the axis. Conditions of continuity now suffice to show that no term in θ or z may occur in the expression for ϕ for $r < R$. Hence ϕ is a function of r and ζ, where

---

* Betz, *loc. cit.*

† 'Göttinger Nachr.,' pp. 213–217 (1919); reprinted in the 'Vier Abhandlungen.'

‡ Since we are considering the motion far behind the propeller, the screw surface may be taken as extending to infinity in both directions along the axis of z.

$$\zeta = \theta - \omega z/v. \tag{4}$$

The boundary condition (3) then becomes

$$\frac{\partial\phi}{\partial\zeta} = -\frac{\omega^2 r^2}{v^2 + \omega^2 r^2}\,\frac{wv}{\omega} \tag{5}$$

for $\zeta = 0$ or π and $0 \leqslant r \leqslant R$.

It is convenient to take wv/ω temporarily equal to 1. Also, let

$$\mu = \omega r/v. \tag{6}$$

Then (5) becomes

$$\frac{\partial\phi}{\partial\zeta} = -\frac{\mu^2}{1+\mu^2} \tag{7}$$

for $\zeta = 0$ or π, and $0 \leqslant r \leqslant R$.

The differential equation satisfied by ϕ, namely $\nabla^2\phi = 0$, can then be written

$$\left(\mu\frac{\partial}{\partial\mu}\right)^2\phi + (1+\mu^2)\frac{\partial^2\phi}{\partial\zeta^2} = 0. \tag{8}$$

In addition to satisfying (7), ϕ must be a single-valued function of position, and its derivatives must vanish when r is infinite. It must also be continuous everywhere except at the screw surface.

3. *Solution of the Potential Problem.*

3.1. *The Form of the Solution.**—It is not difficult to see that the conditions of the problem are such that ϕ is an odd function of ζ and of $\frac{1}{2}\pi - \zeta$, and since it is a single-valued function of position, continuous for $r > R$, it can be expanded, for $r > R$, in a series of sines of even multiples of ζ. Assuming such an expansion, differentiating term by term, and substituting in 2 (8), we find that the coefficient of $\sin 2n\zeta$ must be a linear function of $I_{2n}(2n\mu)$ and $K_{2n}(2n\mu)$, where I_n and K_n are the modified Bessel functions. But

---

* The reasons for adopting the form and method of solution to be described will be clear to anyone who reads Appendices 1 and 2.

$I_{2n}(2n\mu)$ cannot occur, since grad ϕ must vanish when r, or μ, is infinite. Hence we may assume

$$\phi = \sum_{n=1}^{\infty} c_n \frac{K_{2n}(2n\mu)}{K_{2n}(2n\mu_0)} \sin 2n\zeta, \text{ for } r > R, \tag{1}$$

where the c_n are constants to be determined,

$$\mu_0 = \omega R/v, \tag{2}$$

and $K_{2n}(2n\mu_0)$ has been inserted in the denominator for future convenience. We shall assume that the expansion holds also for $r = R$.

For $0 \leqslant r \leqslant R$, we put

$$\phi = -\frac{\mu^2}{1+\mu^2}\zeta + \phi_1, \tag{3}$$

so that

$$\left(\mu\frac{\partial}{\partial\mu}\right)^2 \phi_1 + (1+\mu^2)\frac{\partial^2\phi_1}{\partial\zeta^2} = \left(\mu\frac{d}{d\mu}\right)^2\left(\frac{\mu^2}{1+\mu^2}\right)\zeta, \tag{4}$$

and

$$\frac{\partial\phi_1}{\partial\zeta} = 0 \tag{5}$$

at $\zeta = 0$ and π.

Consider first the region for which $0 \leqslant \zeta \leqslant \pi$. For this region

$$\zeta = \frac{\pi}{2} - \frac{4}{\pi}\sum_{m=0}^{\infty}\frac{\cos(2m+1)\zeta}{(2m+1)^2}. \tag{6}$$

If we assume

$$\phi_1 = f_0(\mu) + \sum_{m=0}^{\infty} f_m(\mu)\cos(2m+1)\zeta, \tag{7}$$

differentiate term by term, and substitute in (4), we find that

$$\left(\mu\frac{d}{d\mu}\right)^2 f_0(\mu) = \tfrac{1}{2}\pi\left(\mu\frac{d}{d\mu}\right)^2\left(\frac{\mu^2}{1+\mu^2}\right), \tag{8}$$

and

$$\left(\mu\frac{d}{d\mu}\right)^2 f_m(\mu) - (2m+1)^2(1+\mu^2)f_m(\mu) = -\frac{4}{\pi}\frac{1}{(2m+1)^2}\left(\mu\frac{d}{d\mu}\right)^2\left(\frac{\mu^2}{1+\mu^2}\right). \tag{9}$$

ϕ must be finite at $r = 0$, and so contains no term in $\log\mu$. Hence

$$f_0(\mu) = \tfrac{1}{2}\pi\,\mu^2/(1+\mu^2). \tag{10}$$

If we put

$$f_m(\mu) = -\frac{4}{\pi}\frac{1}{(2m+1)^2}\left\{\frac{\mu^2}{1+\mu^2} - g_m(\mu)\right\}, \tag{11}$$

then

$$\left(\mu\frac{d}{d\mu}\right)^2 g_m(\mu) - (2m+1)^2(1+\mu^2)\,g_m(\mu) = -(2m+1)^2\mu^2, \tag{12}$$

a particular solution of which is $S_{1,2m+1}(\overline{2m+1}\,i\mu)$, where $S_{1,\nu}(z)$ is a Lomme function as defined in Watson's 'Bessel Functions,' § 10.71, p. 347. The general solution contains, in addition, terms in $I_{2m+1}(\overline{2m+1}\,\mu)$ and $K_{2m+1}(\overline{2m+1}\,\mu)$.

Corresponding to equation 10.71 (3) of Watson's 'Bessel Functions' we have

$$S_{1,\nu}(iz) = \frac{\nu\pi}{2\sin\frac{1}{2}\nu\pi} I_\nu(z) + \nu e^{\frac{1}{2}\nu\pi i} K_\nu(z) - t_{1,\nu}(z), \tag{13}$$

where

$$t_{1,\nu}(z) = \frac{z^2}{2-\nu^2} + \frac{z^4}{(2^2-\nu^2)(4^2-\nu^2)} + \frac{z^6}{(2^2-\nu^2)(4^2-\nu^2)(6^2-\nu^2)} + \dots$$
$$+ \frac{z^{2m}}{(2^2-\nu^2)(4^2-\nu^2)\dots(4m^2-\nu^2)} + \dots \tag{14}$$

In order to have a function which is real when z is real, and which (for positive ν) has no singularity at $z = 0$, we define the function $T_{1,\nu}(z)$ as being equal to the expression on the right of (13) without the term in $K_\nu(z)$. Thus

$$T_{1,\nu}(z) = \frac{\nu\pi}{2\sin\frac{1}{2}\nu\pi} I_\nu(z) - t_{1,\nu}(z) \tag{15}$$

where $t_{1,\nu}(z)$ is given by (14).* Then $T_{1,2m+1}(\overline{2m+1}\,\mu)$ is also a particular solution of (12). Its value is found by putting $(2m+1)$ for ν and $(2m+1)\mu$ for z in (14) and (15). As the general solution of (12) which remains finite on the axis, when μ is zero, we find then

$$g_m(\mu) = T_{1,2m+1}(\overline{2m+1}\,\mu) + b_m I_{2m+1}(\overline{2m+1}\,\mu), \tag{16}$$

where the b_m are constants to be determined.

If now in (3) we substitute for ζ from (6), for ϕ_1 from (7), for f_0 from (10) and for f_m from (11), we find

$$\phi = \frac{4}{\pi}\sum_{m=0}^{\infty}\frac{g_m(\mu)}{(2m+1)^2}\cos(2m+1)\zeta$$
$$= \sum_{m=0}^{\infty}\left[\frac{4}{\pi}\frac{T_{1,2m+1}(\overline{2m+1}\,\mu)}{(2m+1)^2} + a_m\frac{I_{2m+1}(\overline{2m+1}\,\mu)}{I_{2m+1}(\overline{2m+1}\,\mu_0)}\right]\cos(2m+1)\zeta, \tag{17}$$

where the a_m are new constants to be determined, and μ_0 is $\omega R/v$, as before. This expression holds for $0 \leqslant r \leqslant R$, and for $0 \leqslant \zeta \leqslant \pi$. Also ϕ is an odd function of ζ, and for $-\pi \leqslant \zeta \leqslant 0$, we have the same expression with the opposite sign. The discontinuity in ϕ at $\zeta = 0$ or π is thus

---

* The expression given in (15) for $T_{1,\nu}(z)$ is indeterminate when ν is an even integer. This happens in the case of the four-bladed propeller, and will be discussed later.

$$[\phi] = \frac{8}{\pi} \sum_{m=0}^{\infty} \frac{T_{1,\,2m+1}(\overline{2m+1}\,\mu)}{(2m+1)^2} + 2 \sum_{m=0}^{\infty} a_m \frac{I_{2m+1}(\overline{2m+1}\,\mu)}{I_{2m+1}(\overline{2m+1}\,\mu_0)}. \tag{18}$$

It remains to determine the constants a_m in (17) and c_m in (1) from the conditions of continuity at $r = R$. But to do this we shall require to have the numerical values of the T functions and their derivatives. These are not tabulated, and so we must find formulæ for computing them. It will be convenient to discuss at the same time the numerical evaluation of the first term of (18), which is independent of μ_0. This term gives the result for infinite μ_0, that is, infinite R; the second term gives the influence of the edge.

3.2. *Discussion of the T Functions.*—The formulæ defining T, given in 3.1 (14) and (15) (p. 444), are suitable for computation for small μ. Again, $T_{1,\,\nu}(z)$ and $S_{1,\,\nu}(iz)$ differ only by a multiple of $K_\nu(z)$, which is exponentially small for large values of the real part of z. Hence for $|\arg z| < \frac{1}{2}\pi$, $T_{1,\,\nu}(z)$ has the same asymptotic expansion as $S_{1,\,\nu}(iz)$, namely

$$T_{1,\,\nu}(z) \sim 1 - \nu^2/z^2 + \nu^2(\nu^2 - 2^2)/z^4 - \nu^2(\nu^2 - 2^2)(\nu^2 - 4^2)/z^6 + \dots \tag{1}$$

(Watson's 'Bessel Functions,' § 10.75, p. 351).

Another formula for $T_{1,\,2m+1}(\overline{2m+1}\,\mu)$ can be found by substituting

$$T_{1,\,2m+1}(\overline{2m+1}\,\mu) = \tau_0(\mu) + \tau_2(\mu)/(2m+1)^2 + \tau_4(\mu)/(2m+1)^4 + \dots \tag{2}$$

in the equation 3.1 (12) and equating to zero the coefficients of powers of $(2m + 1)$. This gives

$$\tau_0 = \mu^2/(1 + \mu^2), \tag{3}$$

and

$$\tau_{r+2} = \frac{1}{1+\mu^2}\left(\mu \frac{d}{d\mu}\right)^2 \tau_r, \tag{4}$$

so that

$$\tau_2 = 4\mu^2(1 - \mu^2)/(1 + \mu^2)^4, \tag{5}$$

$$\tau_4 = 16\mu^2\{1 - 14\mu^2 + 21\mu^4 - 4\mu^6\}/(1 + \mu^2)^7, \tag{6}$$

and

$$\tau_6 = 64\mu^2\{1 - 75\mu^2 + 603\mu^4 - 1065\mu^6 + 460\mu^8 - 36\mu^{10}\}/(1 + \mu^2)^{10}. \tag{7}$$

(The expansion is probably convergent for some values of μ_0 and asymptotic for others.) It is not immediately obvious that the formal solution of 3.1 (12) so obtained represents $T_{1,2m+1}\,(\overline{2m+1\,\mu})$; that this is so becomes clear on comparing numerical values calculated from 3.1 (14) and (15), or from (1) above, with those calculated from (2).

By using the formulæ 3.1 (14), (15), 3.2 (1), (2) to (7) we can now tabulate $T_{1,2m+1}\,(\overline{2m+1\,\mu})$. We find that it is always very near to $\mu^2/(1+\mu^2)$, and for any given value of μ approaches nearer and nearer this value as m increases. If we put

$$\frac{\mu^2}{1+\mu^2} - T_{1,2m+1}\,(\overline{2m+1\,\mu}) = F_{2m+1}(\mu), \tag{8}$$

the values of $F_{2m+1}(\mu)$ for various values of m and μ are given in the table below.

Table I.

μ.	$F_1(\mu)$.	$F_3(\mu)$.	$F_5(\mu)$.	$G(\mu)$.
0·2	−0·1060	−0·0156	−0·0055	0·1260
0·4	−0·1287	−0·0271	−0·0110	0·2450
0·6	−0·1052	−0·0231	−0·0096	0·3524
0·8	−0·0656	−0·0125	−0·0049	0·4447
1·0	−0·0316	−0·0026	−0·0005	0·5259
1·2	−0·0039	+0·0040	+0·0021	0·5930
1·4	+0·0140	+0·0075	0·0034	0·6501
1·6	+0·0251	0·0087	0·0036	0·6979
1·8	0·0311	0·0085	0·0034	0·7381
2·0	0·0336	0·0080	0·0030	0·7720
2·5	0·0316	0·0048	0·0020	0·8360
3·0	0·0254	0·0035	0·0011	0·8791
3·5	0·0192	0·0021	0·0007	0·9087
4·0	0·0141	0·0014	0·0005	0·9296
4·5	0·0102	0·0009	0·0003	0·9446
5·0	0·0073	0·0006	0·0002	0·9555
6·0	0·0039	0·0003	0·0001	0·9698
7·0	0·0021	0·0002	0·0001	0·9783
8·0	0·0012	0·0001	—	0·9836
9·0	0·0007	0·0001	—	0·9872

The last figure in the entries in this table may be incorrect.

Then

$$\frac{8}{\pi}\sum_{m=0}^{\infty}\frac{T_{1,2m+1}\,(\overline{2m+1\,\mu})}{(2m+1)^2} = \frac{8}{\pi}\,\frac{\mu^2}{1+\mu^2}\sum_{m=0}^{\infty}\frac{1}{(2m+1)^2} - \frac{8}{\pi}\sum_{m=0}^{\infty}\frac{F_{2m+1}(\mu)}{(2m+1)^2}$$

$$= \pi\left\{\frac{\mu^2}{1+\mu^2} - \frac{8}{\pi^2}\sum_{m=0}^{\infty}\frac{F_{2m+1}(\mu)}{(2m+1)^2}\right\}. \tag{9}$$

The expression in curly brackets is also tabulated in Table I, where it is denoted by $G(\mu)$. Since the F are small, and decrease with m, the tabulation is rapid.

The values of $G(\mu)$ for $\mu = 2{\cdot}8, 3{\cdot}8, 4{\cdot}8, 5{\cdot}5, 5{\cdot}8, 6{\cdot}5, 6{\cdot}8, 7{\cdot}5, 7{\cdot}8, 8{\cdot}5, 8{\cdot}8, 9{\cdot}5$ and $9{\cdot}8$ will be required later. They were found by interpolating in tables of $\mu^2/(1+\mu^2) - G(\mu)$, etc.

This completes the discussion of the first term of 3.1 (18) (p. 445). To evaluate the second term we shall require the values of the derivatives of the T functions, formulæ for which are obtained by differentiating the formulæ for the T functions themselves. The approach of $(2m+1)\,T'_{1,2m+1}(\overline{2m+1}\,\mu)$ is to $2\mu/(1+\mu^2)^2$.

A few values are given below for exhibition purposes. (The dash denotes differentiation, so that $T'_{1,\nu}(z)$ is $dT_{1,\nu}(z)/dz$).

$T'_{1,1}(5) = 0{\cdot}0185,\quad 3T'_{1,3}(15) = 0{\cdot}0152,\quad 2\,.\,5/(1+25)^2 = 0{\cdot}0148.$

$T'_{1,1}(3) = 0{\cdot}0723,\quad 3T'_{1,3}(9) = 0{\cdot}0630,\quad 2\,.\,3/(1+9)^2 = 0{\cdot}0600.$

$T'_{1,1}(2) = 0{\cdot}1543,\quad 3T'_{1,3}(6) = 0{\cdot}1649,\quad 2\,.\,2/(1+4)^2 = 0{\cdot}1600.$

3.3. *The Determination of the Constants a_m.*—We must now turn to the determination of the constants a_m in 3.1 (17) and (18) (pp. 444–5) from the conditions of continuity at $r = R$. The conditions are the continuity of ϕ and of $\partial\phi/\partial r$. At $r = R$, and $\zeta = 0$ or π, singularities are to be expected, and so we cannot obtain analytical conditions for continuity there. Also ϕ is an odd function of ζ. Hence it is sufficient to ensure continuity for $0 < \zeta < \pi$, and continuity for $-\pi < \zeta < 0$ will automatically follow. But in the range $0 < \zeta < \pi$,

$$\cos(2m+1)\,\zeta = \frac{8}{\pi}\sum_{n=1}^{\infty}\frac{n}{4n^2-(2m+1)^2}\sin 2n\zeta. \tag{1}$$

We substitute this into 3.1 (17), re-arrange the resulting double series, and equate the coefficient of $\sin 2n\zeta$ so obtained to the coefficient of $\sin 2n\zeta$ in 3.1 (1) (p. 443), for $\mu = \mu_0$. We then differentiate both 3.1 (1) and 3.1 (17) term by term with respect to μ and repeat the process. This gives us the equations

$$\sum_{m=0}^{\infty}\left\{\frac{4}{\pi}\,\frac{T_{1,2m+1}}{(2m+1)^2} + a_m\right\}\frac{8n}{4n^2-(2m+1)^2} = \pi c_n, \tag{2}$$

and

$$\sum_{m=0}^{\infty}\left\{\frac{4}{\pi}\,\frac{T'_{1,2m+1}}{(2m+1)^2} + a_m\frac{I'_{2m+1}}{I_{2m+1}}\right\}\frac{4(2m+1)}{4n^2-(2m+1)^2} = \pi c_n\,\frac{K'_{2n}}{K_{2n}}. \tag{3}$$

The argument of the functions $T_{1,2m+1}$, $T'_{1,2m+1}$, I_{2m+1}, and I'_{2m+1} is $(2m+1)\,\mu_0$; that of K_{2n} and K'_{2n} is $2n\mu_0$. Dashes denote differentiations, as before. Both equations hold for all integral values of n. Eliminating c_n gives us the equation

$$\frac{\pi}{4}\sum_{m=0}^{\infty}\frac{a_m\left\{(2m+1)\dfrac{\mathrm{I}'_{2m+1}}{\mathrm{I}_{2m+1}}-2n\dfrac{\mathrm{K}'_{2n}}{\mathrm{K}_{2n}}\right\}}{4n^2-(2m+1)^2}=$$

$$2n\frac{\mathrm{K}'_{2n}}{\mathrm{K}_{2n}}\sum_{m=0}^{\infty}\frac{\mathrm{T}_{1,2m+1}}{(2m+1)^2[4n^2-(2m+1)^2]}-\sum_{m=0}^{\infty}\frac{(2m+1)\,\mathrm{T}'_{1,2m+1}}{(2m+1)^2[4n^2-(2m+1)^2]}. \tag{4}$$

We have then an infinite number of linear equations with an infinite number of unknowns. The standard method of solving is to find successive approximations—to solve the first equation with $a_1 = a_2 = a_3 = \ldots = 0$, then the first two equations with $a_2 = a_3 = \ldots = 0$, and so on. But we may anticipate from the singularity in ϕ at the edges ($r = \mathrm{R}$, $\zeta = 0$ or π) that the convergence will be very slow. We have to solve for a whole set of values of μ_0, and the work would be prohibitive and the results inaccurate. Fortunately we can escape this difficulty.

We have seen that, so long as μ_0 is not too small, $\mathrm{T}_{1,2m+1}(\overline{2m+1}\,\mu_0)$ is nearly equal to $\mu_0^2/(1+\mu_0^2)$, and that $(2m+1)\mathrm{T}'_{1,2m+1}$ is small compared with $\mathrm{T}_{1,2m+1}$; also $(2m+1)\mathrm{I}'_{2m+1}/\mathrm{I}_{2m+1} - 2n\mathrm{K}'_{2n}/\mathrm{K}_{2n}$ is nearly equal to $(1+\mu_0^2)^{\frac{1}{2}}(2m+1+2n)$, and $\mathrm{K}'_{2n}/\mathrm{K}_{2n}$ is nearly equal to $-(1+\mu_0^2)^{\frac{1}{2}}$.* Thus approximately our equations may be written

$$\frac{\pi}{4}\sum_{m=0}^{\infty}\frac{a_m}{2n-2m-1}=-2n\frac{\mu_0^2}{1+\mu_0^2}\sum_{m=0}^{\infty}\frac{1}{(2m+1)^2[4n^2-(2m+1)^2]}$$

$$=-\frac{\mu_0^2}{1+\mu_0^2}\frac{\pi^2}{16n}, \tag{5}$$

or

$$\sum_{m=0}^{\infty}\frac{a_m}{2n-2m-1}=-\frac{\mu_0^2}{1+\mu_0^2}\frac{\pi}{4n}. \tag{6}$$

These equations may be solved exactly (Appendix 3), the solution being $a_m = -\dfrac{\mu_0^2}{1+\mu_0^2}\mathrm{A}_m$, where

$$\mathrm{A}_0 = 1,\quad 3\mathrm{A}_1 = \tfrac{1}{2},\quad 5\mathrm{A}_2 = \frac{1\,.\,3}{2\,.\,4},\quad 7\mathrm{A}_3 = \frac{1\,.\,3\,.\,5}{2\,.\,4\,.\,6},\ldots \tag{7}$$

We then put†

$$a_m = -\frac{\mu_0^2}{1+\mu_0^2}\mathrm{A}_m + \epsilon_m, \tag{8}$$

---

* See the asymptotic approximations to $\mathrm{I}_n(nx)$ and $\mathrm{K}_n(nx)$ given by Nicholson, 'Phil. Mag.,' vol. 20, p. 938 (1910). But the approximations are much better than might be expected, especially for $(2m+1)\,\mathrm{I}'_{2m+1}/\mathrm{I}_{2m+1} - 2n\mathrm{K}'_{2n}/\mathrm{K}_{2n}$.

† The symbol ϵ is differently used in section 2.

substitute in (4), and solve numerically for ε_0, ε_1, ... in the manner described above. The ε are small; even for the lowest value of μ_0 to be considered, namely 2, the degree of accuracy we shall finally aim at is attained if ε_0 is found correct to two significant figures, with a possible error of 1 or 2 in the second figure, if ε_1 is found to one significant figure, and if the other ε are ignored. The convergence is slow, but not so slow that we cannot manage this with a reasonable amount of labour. The equations were solved numerically for $\mu_0 = 2$, 3 and 5, with the following results:—

$$\mu_0 = 2; \quad \varepsilon_0 = -0{\cdot}061, \ \varepsilon_1 = 0{\cdot}013. \tag{9}$$

$$\mu_0 = 3; \quad \varepsilon_0 = -0{\cdot}047, \ \varepsilon_1 = 0{\cdot}007. \tag{10}$$

$$\mu_0 = 5; \quad \varepsilon_0 = -0{\cdot}033, \ \varepsilon_1 = 0{\cdot}004. \tag{11}$$

It will be seen that, to one significant figure, $-\varepsilon_0$ is 0·06 when μ_0 is 2; it is 0·05 when μ_0 is 3, and 0·03 when μ_0 is 5. It was therefore taken, without any further ado, to be 0·04 when μ_0 is 4; to be 0·02 when μ_0 is 6, and 0·01 when μ_0 is 7; and the other ε were neglected for these values of μ_0.* For higher values of μ_0 all the ε may be neglected.

Thus we find the a_m to a sufficient approximation. The I functions can be found in tables, and the second term in 3.1 (18) easily calculated. Unless μ is very near indeed to μ_0, the terms decrease rapidly, and we require only the first few terms.

3.4. *The Distribution of Circulation.*—From 3.1 (18), 3.2 (9) and 3.3 (8)

$$[\phi]/\pi = G(\mu) - \frac{2}{\pi}\sum_{m=0}^{\infty}\left(\frac{\mu_0^2}{1+\mu_0^2}A_m - \varepsilon_m\right)\frac{I_{2m+1}(\overline{2m+1}\,\mu)}{I_{2m+1}(\overline{2m+1}\,\mu_0)}, \tag{1}$$

where $G(\mu)$ is the expression in curly brackets in 3.2 (9) and is tabulated in Table I, A_m is given in 3.3 (7) and ε_m in 3.3 (9), (10), (11) and the paragraph following.

As mentioned in the introduction, $[\phi]$ is equal to the circulation round the corresponding blade section. If now we restore the factor wv/ω, temporarily taken as 1 from the end of section 2 onwards, we have

$$\frac{\Gamma\omega}{\pi w v} = G(\mu) - \frac{2}{\pi}\sum_{m=0}^{\infty}\left(\frac{\mu_0^2}{1+\mu_0^2}A_m - \varepsilon_m\right)\frac{I_{2m+1}(\overline{2m+1}\,\mu)}{I_{2m+1}(\overline{2m+1}\,\mu_0)}. \tag{2}$$

---

* This will increase the possible error in the calculated value of $\Gamma\omega/\pi w v$ at $\mu = 3{\cdot}8$ when μ_0 is 4 to about 7 or 8 in the last figure. Consequently, the corresponding point in the graph may be displaced this amount if the curve can thereby be smoothed. The actual displacement was from 0·334 to 0·330.

There is no further difficulty in computing the expression on the right. The values for $\mu_0 = 2, 3, 4, \ldots 9, 10$ are given in Table II below. These are the calculated points from which the full line curves in fig. 1 were drawn. It may be mentioned that in terms of the usual parameter J, equal to $v/n\mathrm{D}$, where n is the number of revolutions per unit time and D is the diameter, we have

Table II.—The Values of $\Gamma\omega/\pi wv$.

μ_0 μ	2.	3.	4.	5.	6.	7.	8.	9.	10.
0·0	0	0	0	0	0	0	0	0	0
0·2	0·092	0·111	0·120	0·124	0·125	0·126	0·126	0·126	0·126
0·4	0·175	0·213	0·232	0·240	0·243	0·245	0·245	0·245	0·245
0·6	0·243	0·303	0·331	0·344	0·349	0·351	0·352	0·352	0·352
0·8	0·295	0·379	0·418	0·434	0·441	0·443	0·445	0·445	0·445
1·0	0·329	0·440	0·489	0·511	0·520	0·523	0·525	0·526	0·526
1·2	0·341	0·485	0·548	0·575	0·585	0·590	0·592	0·593	0·593
1·4	0·331	0·514	0·592	0·626	0·640	0·646	0·649	0·650	0·650
1·6	0·295	0·533	0·628	0·669	0·687	0·694	0·696	0·698	0·698
1·8	0·220	0·537	0·654	0·704	0·724	0·732	0·736	0·737	0·738
2·0	0	0·525	0·670	0·731	0·755	0·766	0·769	0·771	0·772
2·5		0·427	0·676	0·770	0·810	0·826	0·832	0·835	0·836
2·8		0·303	*	*	*	*	*	*	*
3·0		0	0·621	0·775	0·838	0·863	0·873	0·877	0·878
3·5			0·486	0·747	0·846	0·884	0·899	0·905	0·908
3·8			0·334	*	*	*	*	*	*
4·0			0	0·671	0·830	0·890	0·915	0·924	0·927
4·5				0·519	0·786	0·882	0·920	0·935	0·940
4·8				0·351	*	*	*	*	*
5·0				0	0·701	0·858	0·918	0·941	0·950
5·5					0·543	*	*	*	*
5·8					0·368	*	*	*	*
6·0					0	0·717	0·874	0·932	0·955
6·5						0·554	*	*	*
6·8						0·376	*	*	*
7·0						0	0·728	0·883	0·941
7·5							0·560	*	*
7·8							0·382	*	*
8·0							0	0·734	0·890
8·5								0·566	*
8·8								0·386	*
9·0								0	0·738
9·5									0·569
9·8									0·388
10·0									0

* Not calculated.

$$\mu_0 = \pi/\mathrm{J}. \tag{3}$$

In view of recent and possible future developments, values of μ_0 as low as 2 were considered.

In general, the error in any entry in Table II should not exceed 2 or 3 in the last figure.

In the notation here used, Prandtl's approximate solution is

$$\frac{\Gamma\omega}{\pi w v} = \frac{2}{\pi}\,\frac{\mu^2}{1+\mu^2}\cos^{-1} e^{-f}, \tag{4}$$

where

$$f = (1-\mu/\mu_0)\,(1+\mu_0{}^2)^{\frac{1}{2}}. \tag{5}$$

This is shown by the broken lines in fig. 1.

3.5. *The Determination of the Flow.*—The potential for the flow for $r \leqslant \mathrm{R}$, $0 \leqslant \zeta \leqslant \pi$, is given by 3.1 (17), where the a_m have been determined to a sufficient approximation. Restoring the factor wv/ω, we may write, using 3.2 (8)

$$\begin{aligned}\frac{\omega\phi}{wv} &= \frac{4}{\pi}\,\frac{\mu^2}{1+\mu^2}\sum_{m=0}^{\infty}\frac{\cos(2m+1)\,\zeta}{(2m+1)^2} - \frac{4}{\pi}\sum_{m=0}^{\infty}\frac{\mathrm{F}_{2m+1}(\mu)}{(2m+1)^2}\cos(2m+1)\,\zeta \\ &\qquad - \sum_{m=0}^{\infty}\left(\frac{\mu_0{}^2}{1+\mu_0{}^2}\mathrm{A}_m - \varepsilon_m\right)\frac{\mathrm{I}_{2m+1}(\overline{2m+1}\,\mu)}{\mathrm{I}_{2m+1}(\overline{2m+1}\,\mu_0)}\cos(2m+1)\,\zeta \\ &= \frac{\mu^2}{1+\mu^2}(\tfrac{1}{2}\pi-\zeta) - \frac{4}{\pi}\sum_{m=0}^{\infty}\frac{\mathrm{F}_{2m+1}(\mu)}{(2m+1)^2}\cos(2m+1)\,\zeta \\ &\qquad - \sum_{m=0}^{\infty}\left(\frac{\mu_0{}^2}{1+\mu_0{}^2}\mathrm{A}_m - \varepsilon_m\right)\frac{\mathrm{I}_{2m+1}(\overline{2m+1}\,\mu)}{\mathrm{I}_{2m+1}(\overline{2m+1}\,\mu_0)}\cos(2m+1)\,\zeta. \end{aligned} \tag{1}$$

Hence

$$\begin{aligned}\frac{\omega}{wv}\frac{\partial\phi}{\partial\zeta} &= -\frac{\mu^2}{1+\mu^2} + \frac{4}{\pi}\sum_{m=0}^{\infty}\frac{\mathrm{F}_{2m+1}(\mu)}{2m+1}\sin(2m+1)\,\zeta \\ &\qquad + \sum_{m=0}^{\infty}\left(\frac{\mu_0{}^2}{1+\mu_0{}^2}\mathrm{A}_m - \varepsilon_m\right)\frac{\mathrm{I}_{2m+1}(\overline{2m+1}\,\mu)}{\mathrm{I}_{2m+1}(\overline{2m+1}\,\mu_0)}(2m+1)\sin(2m+1)\,\zeta. \end{aligned} \tag{2}$$

Since $\mathrm{F}_{2m+1}(\mu)$ is given in Table I, this is easily calculated. We notice that the first series in the last term of 3.1 (17) cannot be differentiated term by term with respect to ζ, since the resulting series does not converge.

Also

$$\begin{aligned}\frac{\omega}{wv}\frac{\partial\phi}{\partial\mu} &= \frac{4}{\pi}\sum_{m=0}^{\infty}\frac{\mathrm{T}'_{1,\,2m+1}(\overline{2m+1}\,\mu)}{2m+1}\cos(2m+1)\,\zeta \\ &\qquad - \sum_{m=0}^{\infty}\left(\frac{\mu_0{}^2}{1+\mu_0{}^2}\mathrm{A}_m - \varepsilon_m\right)\frac{\mathrm{I}'_{2m+1}(\overline{2m+1}\,\mu)}{\mathrm{I}_{2m+1}(\overline{2m+1}\,\mu_0)}(2m+1)\cos(2m+1)\,\zeta. \end{aligned} \tag{3}$$

The first term approaches $\dfrac{2\mu}{(1+\mu^2)^2}(\tfrac{1}{2}\pi-\zeta)$. Since

$$\mathrm{I}'_{2m+1}(\overline{2m+1}\,\mu_0)/\mathrm{I}_{2m+1}(\overline{2m+1}\,\mu_0)$$

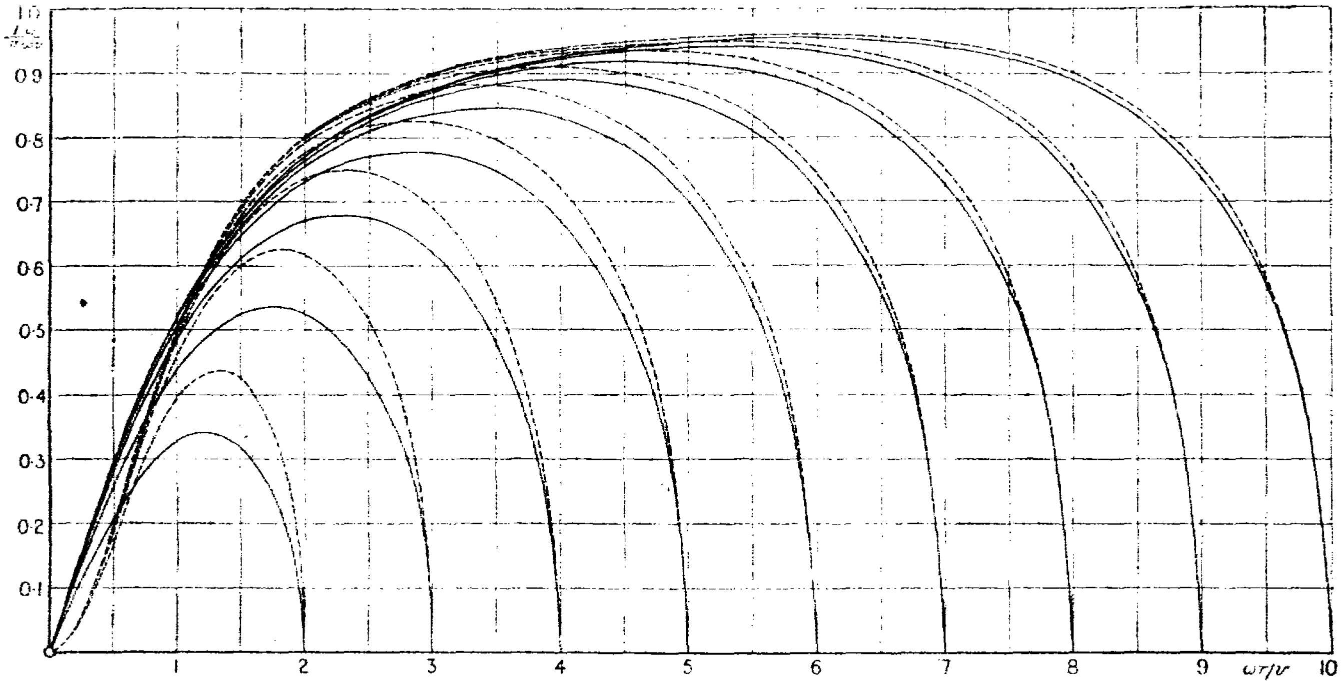

FIG. 1.—THE DISTRIBUTION OF CIRCULATION ALONG A PROPELLER BLADE, FOR A TWO-BLADED PROPELLER, WHEN THE ENERGY LOST IN THE SLIP STREAM IS A MINIMUM FOR A GIVEN THRUST.

The ordinates are $\Gamma\omega/\pi w v$, the abscissæ $\omega r/v$. Here Γ is the circulation at a distance r from the axis, ω the angular velocity and v the velocity of advance of the propeller. The flow far behind the propeller is the same as if the screw surface formed by the trailing vortices was rigid and moved backwards along its axis with velocity w. Also π is 3·14 .... The curves are drawn for a series of values of $\omega R/v$, where R is the radius of the propeller. The value of $\omega R/v$ corresponding to any curve is the abscissa of the point, other than the origin, where the ordinate vanishes. The full line curves give the exact solution, the dotted curves Prandtl's approximate solution, drawn for the same value of w (that is, when the thrust coefficient is small, for the same efficiency).

tends, with increasing m, to become independent of m, we can easily see from 3.3 (7) (p. 448) that the second term becomes infinite at $\mu = \mu_0$, like a multiple of $(1 - \mu^2/\mu_0^2)^{-\frac{1}{2}}$.

If u_r, u_θ and u_z are the fluid velocities in the directions of r, θ and z increasing respectively, then

$$u_\theta = \frac{1}{r}\frac{\partial\phi}{\partial\zeta} = \frac{\omega}{v}\frac{1}{\mu}\frac{\partial\phi}{\partial\zeta}, \tag{4}$$

$$u_z = -\frac{\omega}{v}\frac{\partial\phi}{\partial\zeta} \tag{5}$$

and

$$u_r = \frac{\omega}{v}\frac{\partial\phi}{\partial\mu}. \tag{6}$$

Hence the fluid velocities at any point are easily found from (2) and (3).

At the surface, u_θ and u_z are determined by the boundary condition alone, and are

$$u_\theta = -w\,\mu/(1+\mu^2), \quad u_z = w\,\mu^2/(1+\mu^2). \tag{7}$$

At the propeller the velocities are half as much, if the contraction of the slipstream be neglected.

The potential for the flow for $r > \mathrm{R}$ is given by 3.1 (1) (p. 443), from which we see that the flow dies away rapidly as r increases. It is of some interest to find approximations for the constants c_n. This is done in Appendix 3, and the result is

$$c_m = \frac{\mu_0^2}{1+\mu_0^2}\frac{\mathrm{C}_m}{2m}, \tag{8}$$

where

$$\mathrm{C}_1 = \tfrac{1}{2}, \quad \mathrm{C}_2 = \frac{1\,.\,3}{2\,.\,4}, \quad \mathrm{C}_3 = \frac{1\,.\,3\,.\,5}{2\,.\,4\,.\,6}, \ldots \tag{9}$$

Expressions for the fluid velocity can be written down at once. Thus

$$u_z = -w\frac{\mu_0^2}{1+\mu_0^2}\left[\frac{1}{2}\frac{\mathrm{K}_2(2\mu)}{\mathrm{K}_2(2\mu_0)}\cos 2\zeta + \frac{1\,.\,3}{2\,.\,4}\frac{\mathrm{K}_4(4\mu)}{\mathrm{K}_4(4\mu_0)}\cos 4\zeta + \ldots\right], \tag{10}$$

and so on.

4. *The Solution for any Number of Blades.*

4.1. Let us suppose there are p blades. Then

$$\left(\mu\frac{\partial}{\partial\mu}\right)^2\phi + (1+\mu^2)\frac{\partial^2\phi}{\partial\zeta^2} = 0, \tag{1}$$

$$\frac{\partial\phi}{\partial\zeta} = -\frac{\mu^2}{1+\mu^2}\frac{wv}{\omega} \text{ for } r \leqslant \mathrm{R}, \text{ at } \zeta = 0, \frac{2\pi}{p}, \frac{4\pi}{p}, \ldots \frac{2(p-1)\pi}{p}, \tag{2}$$

and grad ϕ vanishes for $r = \infty$.

The solution for $r \leqslant R$, $0 \leqslant \zeta \leqslant 2\pi/p$ is

$$\frac{\omega\phi}{wv} = \frac{8}{p\pi} \sum_{m=0}^{\infty} \frac{T_{1,p(m+\frac{1}{2})}\overline{(m+\frac{1}{2}p\mu)}}{(2m+1)^2} \cos(2m+1)\frac{p\zeta}{2}$$

$$- \frac{2}{p} \frac{\mu_0^2}{1+\mu_0^2} \sum_{m=0}^{\infty} A_m \frac{I_{p(m+\frac{1}{2})}\overline{(m+\frac{1}{2}p\mu)}}{I_{p(m+\frac{1}{2})}\overline{(m+\frac{1}{2}p\mu_0)}} \cos(2m+1)\frac{p\zeta}{2}, \qquad (3)$$

where, approximately, the A_m have the same values as before, namely,

$$A_0 = 1, \quad 3A = \tfrac{1}{2}, \quad 5A_2 = \frac{1 \,.\, 3}{2 \,.\, 4}, \ldots \qquad (4)$$

The exact values can be calculated in the same way as for two blades. The approximation becomes better and better the greater μ_0 and the greater the number of blades.

For $r > R$,

$$\frac{\omega\phi}{wv} = \frac{2}{p} \frac{\mu_0^2}{1+\mu_0^2} \sum_{n=1}^{\infty} \frac{C_n}{2n} \frac{K_{pn}(pn\mu)}{K_{pn}(pn\mu_0)} \sin pn\zeta, \qquad (5)$$

where, approximately,

$$C_1 = \tfrac{1}{2}, \quad C_2 = \frac{1 \,.\, 3}{2 \,.\, 4}, \quad C_3 = \frac{1 \,.\, 3 \,.\, 5}{2 \,.\, 4 \,.\, 6}, \ldots \qquad (6)$$

As before, $T_{1,p(m+\frac{1}{2})}\overline{(m+\frac{1}{2}p\mu)}$ is near to $\mu^2/(1+\mu^2)$. We put

$$\frac{\mu^2}{1+\mu^2} - T_{1,p(m+\frac{1}{2})}\overline{(m+\frac{1}{2}p\mu)} = F_{p,2m+1}(\mu), \qquad (7)$$

so that

$$\sum_{m=0}^{\infty} \frac{T_{1,p(m+\frac{1}{2})}\overline{(m+\frac{1}{2}p\mu)}}{(2m+1)^2} = \frac{\pi^2}{8} \frac{\mu^2}{1+\mu^2} - \sum_{m=0}^{\infty} \frac{F_{p,2m+1}(\mu)}{(2m+1)^2}, \qquad (8)$$

and we find for the distribution of circulation

$$\frac{p\Gamma\omega}{2\pi wv} = \frac{\mu^2}{1+\mu^2} - \frac{8}{\pi^2} \sum_{m=0}^{\infty} \frac{F_{p,2m+1}(\mu)}{(2m+1)^2}$$

$$- \frac{2}{\pi} \frac{\mu_0^2}{1+\mu_0^2} \sum_{m=0}^{\infty} A_m \frac{I_{p(m+\frac{1}{2})}\overline{(m+\frac{1}{2}p\mu)}}{I_{p(m+\frac{1}{2})}\overline{(m+\frac{1}{2}p\mu_0)}}. \qquad (9)$$

The A_m are given in (4); the I functions are the modified Bessel functions, defined as in Watson's 'Bessel Functions.' The F are related to the T functions by (7); to calculate the T functions we have formulæ 3.1 (14) and (15) (p. 444), and formula 3.2 (1) (p. 445). Also

$$T_{1,p(m+\frac{1}{2})}(\overline{m+\tfrac{1}{2}}\,p\mu) = \tau_0(\mu) + \frac{4\tau_2(\mu)}{p^2(2m+1)^2} + \frac{16\tau_4(\mu)}{p^4(2m+1)^4} + \dots, \qquad (10)$$

where

$$\tau_0 = \mu^2/(1+\mu^2), \qquad (11)$$

and

$$\tau_{r+2} = \frac{1}{1+\mu^2}\left(\mu\frac{d}{d\mu}\right)^2 \tau_r, \qquad (12)$$

so that the τ are the same as in 3.2 (3) to (7) (p. 445).

The only new point that arises for a three-bladed propeller is that the Bessel functions $I_{3/2}$, $I_{9/2}$, ... are not tabulated.* There are simple finite expressions for these functions, and to calculate the value for any one value of the argument is not difficult. But to make even a rough table involves a not inconsiderable amount of work. The numerical work for the three-bladed propeller is therefore left over for the present.

4.2. *The Four-bladed Propeller.*—For a four-bladed propeller we have to calculate $T_{1,\nu}(z)$, where ν is an even integer. The analytical peculiarity mentioned in the footnote on p. 444 enters, the expression 3.1 (15) for $T_{1,\nu}(z)$ becoming indeterminate. However, the asymptotic expansion 3.2 (1) (p. 445) terminates, and is equal to† $S_{1,\nu}(iz)$ or $T_{1,\nu}(z) + (-1)^{\frac{1}{2}\nu}\nu K_\nu(z)$, so that $T_{1,\nu}(z)$ can be calculated from the formula

$$T_{1,\nu}(z) = 1 - \nu^2/z^2 + \nu^2(\nu^2-2^2)/z^4 - \nu^2(\nu^2-2^2)(\nu^2-4^2)z^6 + \dots$$
$$- (-1)^{\frac{1}{2}\nu}\nu K_\nu(z). \qquad (1)$$

The numerical calculations were carried through for $\mu_0 = 5$, the approximate values of the A_m being taken as in 4.1 (4) (p. 454). The values of $2\Gamma\omega/\pi wv$, as given by 4.1 (9) with p equal to 4, are shown in the table below (Table III) and by the full line graph in fig. 2. The values of $F_{2,1}(\mu)$ or $\mu^2/(1+\mu^2) - T_{1,2}(2\mu)$, are also exhibited. It was not necessary to calculate $F_{2,5}(\mu)$, and the term in $F_{2,3}(\mu)$ never contributed more than 1 to the third figure.‡

---

* No tables are recorded in Watson's 'Bessel Functions' or in Mises, 'Verzeichnis berechneter Funktionentafeln,' Berlin, 1928.

† Watson, 'Bessel Functions,' § 10.71, p. 347.

‡ If the F are neglected, and we put $\mu^2/(1+\mu^2)$ for T in (1) with ν equal to $(4m+2)$ and z equal to $(4m+2)\mu$, we have an approximate formula to calculate K. This method, for example, gives $K_6(1\cdot 2)$ equal to 1197·4221 instead of 1197·4227, as given by Watson.

Table III.—Values of $F_{2,1}$ (μ) and $2\Gamma\omega/\pi wv$ for a Four-bladed Propeller for $\mu_0 = 5$.

μ.	$F_{2,1}(\mu)$.	$2\Gamma\omega/\pi wv$.	μ.	$F_{2,1}(\mu)$.	$2\Gamma\omega/\pi wv$.
0·1	−0·0150	0·022	1·8	0·0157	0·750
0·2	−0·0341	0·066	2·0	0·0152	0·785
0·4	−0·0517	0·180	2·5	0·0115	0·848
0·6	−0·0432	0·300	3·0	0·0077	0·881
0·8	−0·0248	0·411	3·5	0·0050	0·887
1·0	−0·0075	0·506	4·0	0·0033	0·851
1·2	+0·0047	0·586	4·5	0·0021	0·714
1·4	+0·0117	0·652	4·8	0·0017	0·505
1·6	0·0149	0·706	5·0	0·0015	0

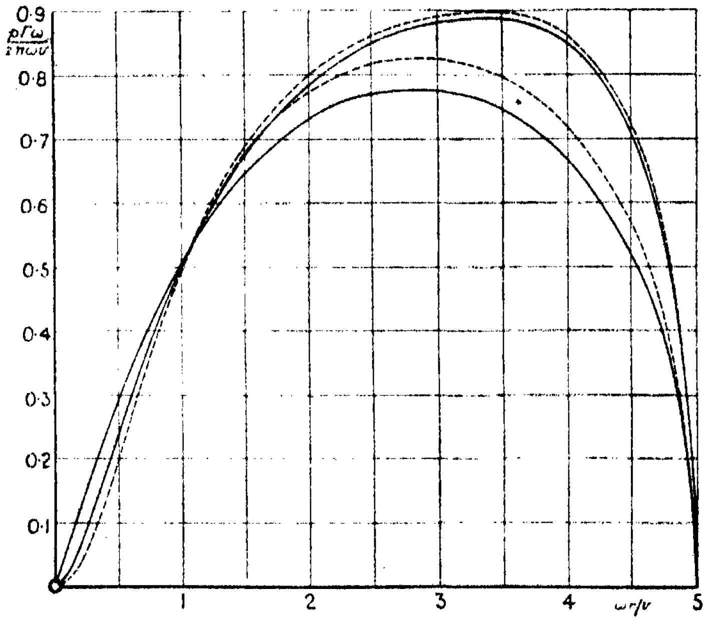

Fig. 2.—The Distribution of Circulation along a Propeller Blade for a Four-bladed and for a Two-bladed Propeller, when the Energy lost in the Slip Stream is a Minimum for a given Thrust.

The full line curves give the exact solution, the dotted curves the Prandtl approximation. In each case the curve with the greater maximum ordinate refers to a four-bladed propeller, the one with the less to a two-bladed propeller. The ordinates are $p\Gamma\omega/2\pi wv$, and the abscissæ $\omega r/v$, where p is the number of blades and the other symbols have the same meaning as before (fig. 1). The curves are drawn for $\omega R/v$ equal to 5. As before, each full line curve and the corresponding dotted curve are drawn for the same value of w.

The Prandtl approximation for a four-bladed propeller is

$$\frac{2\Gamma\omega}{\pi w v} = \frac{2}{\pi}\frac{\mu^2}{1+\mu^2}\cos^{-1} e^{-2f}, \tag{2}$$

where

$$f = (1+\mu_0^2)^{\frac{1}{2}}(1-\mu/\mu_0). \tag{3}$$

This is given by the broken line curve of fig. 2.

5. *The Application of the Solution.*

Let

$$\mathrm{K} = \frac{p}{2\pi}\frac{\Gamma\omega}{wv}, \tag{1}$$

where p is the number of blades. We shall assume the distribution found in the previous sections, so that K is a given function of r/R for any given value of μ_0, or $\omega\mathrm{R}/v$.

Let T be the thrust and Q the torque of the propeller, ρ the density of the fluid in which it is operating, and c_T and c_Q the non-dimensional coefficients defined by

$$c_\mathrm{T} = \mathrm{T}/\pi\rho\mathrm{R}^2v^2, \tag{2}$$

and

$$c_\mathrm{Q} = \omega\mathrm{Q}/\pi\rho\mathrm{R}^2v^3. \tag{3}$$

If η is the efficiency,

$$\eta = v\mathrm{T}/\omega\mathrm{Q} = c_\mathrm{T}/c_\mathrm{Q}. \tag{4}$$

Let u_θ and u_z be the circumferential and axial components of velocity far behind the propeller, as given by 3.5 (7), so that $u_\theta = -w\mu/(1+\mu^2)$, and $u_z = w\mu^2/(1+\mu^2)$. The velocities at the blade are half as much, if the contraction be neglected.

Let

$$r/\mathrm{R} = x \quad \text{and} \quad w/v = \lambda. \tag{5, 6}$$

Then

$$\mu = \omega r/v = \mu_0 x. \tag{7}$$

Let us first neglect the profile drag of the blade sections. Then

$$\frac{d\mathrm{T}}{dr} = p\rho\Gamma(rw + \tfrac{1}{2}u_\theta) = p\rho\Gamma\left(rw - \tfrac{1}{2}w\frac{\mu}{1+\mu^2}\right), \tag{8}$$

from which we find

$$\frac{dc_\mathrm{T}}{dx} = 2\lambda\mathrm{K}x - \frac{\lambda^2\mathrm{K}x}{1+\mu_0^2x^2}, \tag{9}$$

so that

$$c_\mathrm{T} = 2\lambda\mathrm{I}_1 - \lambda^2\mathrm{I}_2, \tag{10}$$

where

$$\mathrm{I}_1 = \int_0^1 \mathrm{K}x\,dx, \quad \text{and} \quad \mathrm{I}_2 = \int_0^1 \frac{\mathrm{K}x\,dx}{1+\mu_0^2x^2}. \tag{11, 12}$$

I_1 and I_2 are functions of μ_0, most easily found by plotting the integrand and using a planimeter. They can be plotted against μ_0 once and for all.

Further

$$\frac{dQ}{dr} = p\rho\Gamma r\left(v + \tfrac{1}{2}u_x\right) = p\rho\Gamma r\left(v + \tfrac{1}{2}w\,\frac{\mu^2}{1+\mu^2}\right), \tag{13}$$

from which we find

$$\frac{dc_Q}{dx} = 2\lambda K x + \frac{\lambda^2\mu_0^2 K x^3}{1+\mu_0^2 x^2}, \tag{14}$$

so that

$$c_Q = 2\lambda I_1 + \lambda^2\mu_0^2 I_3, \tag{15}$$

where

$$\mu_0^2 I_3 = \mu_0^2\int_0^1 \frac{K x^3\,dx}{1+\mu_0^2 x^2} = I_1 - I_2. \tag{16}$$

Hence

$$\eta = \frac{I_1 - \tfrac{1}{2}\lambda I_2}{I_1 + \tfrac{1}{2}\mu_0^2\lambda I_3}. \tag{17}$$

Thus, working at any given value of μ_0, we find λ in terms of c_T from (10), and then η from (17). We thus get a series of curves of η against c_T for different values of μ_0, or of η against μ_0 for different values of c_T. The thrust and torque grading curves are given by (9) and (14).

The theory holds only for small values of λ, for which we have approximately

$$\eta = \frac{1}{1 + \tfrac{1}{2}\mu_0^2\lambda\, I_3/I_1 + \tfrac{1}{2}\lambda\, I_2/I_1} = \frac{1}{1+\tfrac{1}{2}\lambda},^{*} \tag{18}$$

and

$$\lambda = c_Q/2I_1. \tag{19}$$

We easily find that the energy lost per unit time is $\pi\rho v^3 R^2\lambda^2 I_1$.

If θ is the blade angle, the incidence of any section is $\theta - \phi$, where†

$$\tan\phi = \frac{v + \tfrac{1}{2}u_x}{r\omega + \tfrac{1}{2}u_\theta} = \frac{1}{\mu_0 x}\,\frac{1 + \tfrac{1}{2}\lambda\,\mu_0^2x^2/(1+\mu_0^2x^2)}{1 - \tfrac{1}{2}\lambda/(1+\mu_0^2x^2)} = \frac{1}{\mu_0 x}\left(1 + \tfrac{1}{2}\lambda\right)\text{ approx.} \tag{20}$$

We pass on to consider the effect of profile drag. Let ε be the ratio of drag to lift for a wing of infinite aspect ratio with the same section as the blade element at a distance r from the axis.† The contribution of the drag to the element of thrust is then $-\varepsilon\, dQ_0/r$, where dQ_0 is the element of torque in the absence of profile drag. The contribution to the element of torque is similarly $\varepsilon r\, dT_0$, where dT_0 is the element of thrust in the absence of profile drag. Hence

---

* This form is preferable to $1 - \tfrac{1}{2}\lambda_1$, since $\mu_0^2 I_3$ is greater than I_2.

† The symbol ϕ is differently used in sections 2, 3 and 4. The symbol ϵ is differently used in sections 2 and 3.

$$\frac{dc_T}{dx} = \frac{dc_{T_0}}{dx} - \frac{\varepsilon}{\mu_0 x}\frac{dc_{Q_0}}{dx}, \tag{21}$$

and

$$\frac{dc_Q}{dx} = \frac{dc_{Q_0}}{dx} + \varepsilon\mu_0 x\frac{dc_{T_0}}{dx}. \tag{22}$$

dc_{T_0}/dx and dc_{Q_0}/dx are given by (9) and (14). Hence

$$\frac{dc_T}{dx} = 2\lambda Kx - \lambda^2\frac{Kx}{1+\mu_0^2x^2} - \frac{2\lambda}{\mu_0}\varepsilon K - \lambda^2\mu_0\frac{\varepsilon Kx^2}{1+\mu_0^2x^2}, \tag{23}$$

and

$$\frac{dc_Q}{dx} = 2\lambda Kx + \lambda^2\mu_0^2\frac{Kx^3}{1+\mu_0^2x^2} + 2\lambda\mu_0\varepsilon Kx^2 - \lambda^2\mu_0\frac{\varepsilon Kx^2}{1+\mu_0^2x^2}. \tag{24}$$

Consequently

$$c_T = 2\lambda I_1 - \lambda^2 I_2 - \frac{2\lambda}{\mu_0}I_4 - \lambda^2\mu_0 I_5, \tag{25}$$

and

$$c_Q = 2\lambda I_1 + \lambda^2\mu_0^2 I_3 + 2\lambda\mu_0 I_6 - \lambda^2\mu_0 I_5, \tag{26}$$

where

$$I_4 = \int_0^1 \varepsilon K\, dx, \tag{27}$$

$$I_5 = \int_0^1 \frac{\varepsilon Kx^2\, dx}{1+\mu_0^2x^2}, \tag{28}$$

and

$$I_6 = \int_0^1 \varepsilon Kx^2\, dx. \tag{29}$$

Then

$$\eta = \frac{c_T}{c_Q} = \frac{I_1 - \frac{1}{2}\lambda I_2 - I_4/\mu_0 - \frac{1}{2}\lambda\mu_0 I_5}{I_1 + \frac{1}{2}\lambda\mu_0^2 I_3 + \mu_0 I_6 - \frac{1}{2}\lambda\mu_0 I_5}. \tag{30}$$

For small values of λ and ε,

$$\eta = \frac{1}{1+\frac{1}{2}\lambda + I_7/I_1},$$

where

$$I_7 = I_4/\mu_0 + \mu_0 I_6 = \frac{1}{\mu_0}\int_0^1 \varepsilon K\,(1+\mu_0^2x^2)\, dx. \tag{32}$$

Thus the influence of friction is of order $\varepsilon\mu_0$, and friction has more influence on propellers the greater the ratio of tip speed to forward velocity. The determination of ε depends upon the incidence, and therefore on the angle ϕ. For some purposes it is advantageous to take a rough average of ε, and write

$$I_7 = \frac{\bar{\varepsilon}}{\mu_0} \int_0^1 K (1 + \mu_0^2 x^2)\, dx. \tag{33}$$

The integral is then a pure function of μ_0. Any losses dependent on the variation of the distribution of Γ from that taken here can be thrown into the ε term.

For accurate work we take a set of values of λ, calculate ϕ from (20), find ε and determine I_4, I_5 and I_6 graphically. The corresponding values of c_T are given by (25), and of η by (30). Hence we get the curve of η against c_T for the given blade and the value of μ_0 considered. We can get a set of curves for different values of μ_0, which can be turned into a set of curves of η against μ_0 for different values of c_T.

The above considerations are valid only if λ, or $c_T/2I_1$, is small. For moderate loads we get a better approximation if, following Prandtl, we replace v by $v + \frac{1}{2}w$. Again, according to Betz, 'Handbuch der Physik,' vol. 7, pp. 256–259 (1927), the contraction in the slip stream can be allowed for by considering a screw surface for which μ_0 is $\omega R/(v + w)$, so that the solution of the potential problem given here will still retain its usefulness. But there are still difficulties to be overcome in applying it, and a closer discussion must remain over.

My thanks are due to Prof. Betz, who suggested the problem to me.

Summary.

The distribution of circulation along a propeller blade when, for a given thrust, the energy lost in the slip-stream is a minimum, is calculated exactly and compared with the approximate Prandtl formula. Numerical values are given, for a two-bladed propeller, for various values of $\omega R/v$, where ω is the angular velocity, R the radius, and v the velocity of advance of the propeller. From these values the curves in fig. 1 were drawn. An example ($\omega R/v = 5$) was also computed numerically for a four-bladed propeller, and the result is shown in fig. 2. The distribution for any number of blades and any value of $\omega R/v$ can be worked out numerically by the method used, the work being easier the greater the number of blades and the greater $\omega R/v$. Formulæ for the fluid velocities far behind the propeller were found, from which numerical values can be worked out by the help of methods and numerical tables given.

Formulæ are set out for the distribution of thrust and torque, and for the efficiency, when the distribution of circulation is that calculated.

APPENDIX 1.

The Solution in Trigonometrical Series for a Rotating Lamina.

If the screw surface moves along its axis with velocity w and rotates with angular velocity $\omega w/v$ about its axis, its displacement is merely along its own surface. The fluid motion is therefore the same whether the surface moves along its axis with velocity w, or rotates about its axis with angular velocity ω_1, equal to $-\omega w/v$. If ω/v becomes zero while ω_1 remains finite, we fall back on the case of the rotating lamina, whose solution* is

$$\phi + i\psi = -\tfrac{1}{4} i \mathrm{R}^2 \omega_1 e^{-2t}, \tag{1}$$

where $t = \xi + i\eta$, and ξ, η are elliptical co-ordinates given by

$$\tau = re^{i\zeta} = \mathrm{R} \cosh t. \tag{2}$$

The solution is easily put into the form of trigonometrical series. For

$$\mathrm{R}e^{-t} = \tau - (\tau^2 - \mathrm{R}^2)^{\frac{1}{2}}. \tag{3}$$

Hence

$$\begin{aligned} \mathrm{R}^2 e^{-2t} &= 2\tau^2 - \mathrm{R}^2 - 2\tau(\tau^2 - \mathrm{R}^2)^{\frac{1}{2}} \\ &= 2\tau^2 - \mathrm{R}^2 \mp 2\tau \mathrm{R} i \left\{1 - \tfrac{1}{2}\frac{\tau^2}{\mathrm{R}^2} - \frac{1\,.\,1}{2\,.\,4}\frac{\tau^4}{\mathrm{R}^4} - \frac{1\,.\,1\,.\,3}{2\,.\,4\,.\,6}\frac{\tau^6}{\mathrm{R}^6} \right. \\ &\qquad \left. - \frac{1\,.\,1\,.\,3\,.\,5}{2\,.\,4\,.\,6\,.\,8}\frac{\tau^8}{\mathrm{R}^8} - \ldots\right\} \text{ for } |\tau| < \mathrm{R} \\ &= 2\tau^2 - \mathrm{R}^2 - 2\tau^2 \left\{1 - \tfrac{1}{2}\frac{\mathrm{R}^2}{\tau^2} - \frac{1\,.\,1}{2\,.\,4}\frac{\mathrm{R}^4}{\tau^4} - \frac{1\,.\,1\,.\,3}{2\,.\,4\,.\,6}\frac{\mathrm{R}^6}{\tau^6} - \ldots\right\} \\ &\qquad \text{for } |\tau| > \mathrm{R}. \end{aligned} \tag{4}$$

Hence

$$\begin{aligned} \phi &= \tfrac{1}{2}\omega_1 r^2 \sin 2\zeta \mp \tfrac{1}{2}\mathrm{R}^2\omega_1 \left\{\frac{r}{\mathrm{R}}\cos\zeta - \tfrac{1}{2}\left(\frac{r}{\mathrm{R}}\right)^3 \cos 3\zeta - \frac{1\,.\,1}{2\,.\,4}\left(\frac{r}{\mathrm{R}}\right)^5 \cos 5\zeta \right. \\ &\qquad \left. - \frac{1\,.\,1\,.\,3}{2\,.\,4\,.\,6}\left(\frac{r}{\mathrm{R}}\right)^7 \cos 7\zeta - \ldots\right\} \text{ for } r \leqslant \mathrm{R} \\ &= -\tfrac{1}{2}\mathrm{R}\omega_1 \left\{\frac{1\,.\,1}{2\,.\,4}\left(\frac{\mathrm{R}}{r}\right)^2 \sin 2\zeta + \frac{1\,.\,1\,.\,3}{2\,.\,4\,.\,6}\left(\frac{\mathrm{R}}{r}\right)^4 \sin 4\zeta + \ldots\right\} \text{ for } r \geqslant \mathrm{R}. \end{aligned} \tag{5}$$

The discontinuity in ϕ is $\omega_1 r(\mathrm{R}^2 - r^2)^{\frac{1}{2}}$.

---

* Lamb, 'Hydrodynamics,' chap. iv, § 72.

APPENDIX 2.

The Solution of the Potential Problem for $\omega R/v$ small.

We return to the potential problem formulated in section 2, namely,

$$\left(\mu\frac{\partial}{\partial\mu}\right)^2\phi + (1+\mu^2)\frac{\partial^2\phi}{\partial\zeta^2} = 0, \tag{1}$$

$$\frac{\partial\phi}{\partial\zeta} = -\frac{\mu^2}{1+\mu^2} \text{ at } \zeta = 0 \text{ or } \pi \text{ for } 0 \leqslant r \leqslant R, \tag{2}$$

grad $\phi = 0$ at $r = \infty$, and ϕ is a single-valued function.

We assume

$$\phi = \sum_{n=1}^{\infty} a_n I_{2n}(2n\mu)\sin 2n\zeta + \sum_{m=0}^{\infty} b_m \frac{I_{2m+1}(\overline{2m+1}\,\mu)}{I_{2m+1}(\overline{2m+1}\,\mu_0)}\cos(2m+1)\zeta$$

$$\text{for } r \leqslant R,\ 0 \leqslant \zeta \leqslant \pi, \tag{3}$$

and

$$\phi = \sum_{n=1}^{\infty} c_n \frac{K_{2n}(2n\mu)}{K_{2n}(2n\mu_0)}\sin 2n\zeta \text{ for } r \geqslant R. \tag{4}$$

Then

$$\left(\frac{\partial\phi}{\partial\zeta}\right)_{\zeta=0 \text{ or } \pi} = \sum_{n=1}^{\infty} 2na_n I_{2n}(2n\mu). \tag{5}$$

Now

$$\frac{\mu^2}{1+\mu^2} = 2\sum_{n=1}^{\infty}(-1)^{n-1} I_{2n}(2n\mu), \tag{6}$$

if μ is less than $0\cdot66$ ... (Watson's 'Bessel Functions,' Chap. 17).

Hence, if $\mu_0 < 0\cdot66$ ..., we can take

$$a_n = (-1)^n/n. \tag{7}$$

The constants b_m and c_n are then to be found from the conditions of continuity at $\mu = \mu_0$, namely, the continuity of ϕ and of $\partial\phi/\partial r$. This can be done numerically as in 3.3, by expanding $\cos(2m+1)\zeta$ in a sine-series; or by assuming all but a finite number of the b_m and c_n to be zero, and equating the expressions for ϕ, and also for $\partial\phi/\partial r$, at a finite number of selected values of ζ between 0 and π. The convergence will be slow.

APPENDIX 3.

The Approximate Determination of the Constants a_m and c_n.

1. Let

$$\phi = \sum_{n=1}^{\infty} \frac{1}{2n}\left(\frac{r}{a}\right)^{2n} \sin 2n\theta - \sum_{m=0}^{\infty} \mathrm{A}_m \left(\frac{r}{a}\right)^{2m+1} \cos(2m+1)\theta \qquad \text{for } r \leqslant a,\ 0 \leqslant \theta \leqslant \pi,$$

$$= \sum_{n=1}^{\infty} \mathrm{B}_r \left(\frac{a}{r}\right)^{2n} \sin 2n\theta \qquad \text{for } r \geqslant a. \tag{1}$$

For $r \leqslant a$, $-\pi \leqslant \theta \leqslant 0$, let ϕ be as in the first line with the sign of the second term changed.

Expand $\cos(2m+1)\theta$ in a sine-series for $0 \leqslant \theta \leqslant \pi$, and equate coefficients of $\sin 2n\theta$. We obtain

$$\mathrm{B}_n = \frac{1}{2n} - \frac{4}{\pi} \sum_{m=0}^{\infty} \frac{2n}{4n^2 - (2m+1)^2} \mathrm{A}_m. \tag{2}$$

Differentiate the two expressions for ϕ with respect to r and repeat the process. This gives

$$-\mathrm{B}_n = \frac{1}{2n} - \frac{4}{\pi} \sum_{m=0}^{\infty} \frac{2m+1}{4n^2 - (2m+1)^2} \mathrm{A}_m. \tag{3}$$

Eliminate B_n. Then

$$\sum_{m=0}^{\infty} \frac{\mathrm{A}_m}{2n - 2m - 1} - \frac{\pi}{4n} = 0. \tag{4}$$

The equations (2), (3) and (4) hold for all positive integral values of n.

The value of ϕ so found is the solution of the problem defined by

$$\frac{\partial^2\phi}{\partial x^2} + \frac{\partial^2\phi}{\partial y^2} = 0, \tag{5}$$

$$\left(\frac{1}{r}\frac{\partial\phi}{\partial\theta}\right)_{\theta = 0 \text{ or } \pi} = \frac{1}{r} \sum_{n=1}^{\infty} \left(\frac{r}{a}\right)^{2n} = \frac{r}{a^2 - r^2}, \tag{6}$$

grad $\phi = 0$ at $r = \infty$, ϕ is a single-valued function.

This problem can be solved in finite terms by means of elliptic co-ordinates ξ, η for which

$$t = \xi + i\eta, \tag{7}$$

$$z = re^{i\theta} = a \cosh t. \tag{8}$$

The boundary condition becomes

$$\frac{\partial \phi}{\partial \xi} = \cot \eta \quad \text{at} \quad \xi = 0, \tag{9}$$

and the solution is

$$\phi + i\psi = i \log (1 - e^{-2t}). \tag{10}$$

Now

$$e^{-2t} = 2z^2/a^2 - 1 - 2(z/a)(z^2/a^2 - 1)^{\frac{1}{2}}, \tag{11}$$

so that

$$\begin{aligned}\phi + i\psi &= i \log 2 + i \log [1 - z^2/a^2 + (z/a)(z^2/a^2 - 1)^{\frac{1}{2}}] \\ &= i \log 2 + \tfrac{1}{2}i \log (1 - z^2/a^2) - \sin^{-1} z/a \\ &= i \log 2 - \tfrac{1}{2}i\,(z^2/a^2 + z^4/2a^4 + z^6/3a^6 + \ldots) \\ &\quad - \left(\frac{z}{a} + \frac{1.1}{2.3}\frac{z^3}{a^3} + \frac{1.3}{2.4}\frac{1}{5}\frac{z^5}{a^5} + \frac{1.3.5}{2.4.6}\frac{1}{7}\frac{z^7}{a^7} + \ldots\right).\end{aligned} \tag{12}$$

Thus

$$\begin{aligned}\phi &= \tfrac{1}{2}\left(\frac{r^2}{a^2}\sin 2\theta + \tfrac{1}{2}\frac{r^4}{a^4}\sin 4\theta + \ldots\right) \\ &\quad - \left(\frac{r}{a}\cos \theta + \frac{1.1}{2.3}\frac{r^3}{a^3}\cos 3\theta + \frac{1.3}{2.4}\frac{1}{5}\frac{r^5}{a^5}\cos 5\theta + \ldots\right),\end{aligned} \tag{13}$$

and the solution of the equation (4) is

$$A_0 = 1, \quad 3A_1 = \tfrac{1}{2}, \quad 5A_2 = \frac{1.3}{2.4}, \quad 7A_3 = \frac{1.3.5}{2.4.6}, \ \ldots \tag{14}$$

The solution of the equations 3.3 (6) is then

$$a_m = -\frac{{\mu_0}^2}{1 + {\mu_0}^2} A_m, \tag{15}$$

where the A_m are given by (14).

2. With the approximations described in 3.3, the equations 3.3 (3), p. 447, become

$$\frac{4}{\pi}\sum_{m=0}^{\infty} \frac{(2m+1)\,a_m}{4n^2 - (2m+1)^2} = -c_n. \tag{16}$$

This is the condition that

$$\sum_{m=0}^{\infty} (2m+1)\,a_m \cos (2m+1)\,\theta = -\sum_{n=1}^{\infty} 2n\,c_n \sin 2n\theta \tag{17}$$

for $0 \leqslant \theta \leqslant \pi$.*

---

* This comes directly if we differentiate 3.1 (1) and 3.1 (17) term by term with respect to μ, equate the results for μ equal to μ_0, and make the approximations described in 3.3.

Omit temporarily the factor $-\mu_0^2/(1+\mu_0^2)$, and take

$$(2m+1)\,a_m = \frac{1\,.\,3\,.\,5\,\ldots\,(2m-1)}{2\,.\,4\,.\,6\,\ldots\,2m}. \tag{18}$$

Let

$$C = \sum_{m=0}^{\infty} (2m+1)\,a_m \cos(2m+1)\,\theta, \tag{19}$$

and

$$S = \sum_{m=0}^{\infty} (2m+1)\,a_m \sin(2m+1)\,\theta, \tag{20}$$

so that

$$C + iS = \frac{e^{i\theta}}{(1-e^{2i\theta})^{\frac{1}{2}}} = \pm i\,\frac{1}{(1-e^{-2i\theta})^{\frac{1}{2}}}$$

$$= \pm i\left(1 + \tfrac{1}{2}e^{-2i\theta} + \frac{1\,.\,3}{2\,.\,4}e^{-4i\theta} + \ldots\right). \tag{21}$$

Then

$$C = \pm\left(\tfrac{1}{2}\sin 2\theta + \frac{1\,.\,3}{2\,.\,4}\sin 4\theta + \ldots\right), \tag{22}$$

and

$$S = \pm\left(1 + \tfrac{1}{2}\cos 2\theta + \frac{1\,.\,3}{2\,.\,4}\cos 4\theta + \ldots\right). \tag{23}$$

Putting $\lambda = \frac{1}{2}\pi$ in S, we see that the upper sign must be taken. Restoring the factor $-\mu_0^2/(1+\mu_0^2)$, we have finally

$$c_n = \frac{\mu_0^2}{1+\mu_0^2}\,\frac{C_n}{2n} \tag{24}$$

where

$$C_1 = \tfrac{1}{2},\quad C_2 = \frac{1\,.\,3}{2\,.\,4},\quad C_3 = \frac{1\,.\,3\,.\,5}{2\,.\,4\,.\,6}\ldots, \tag{25}$$

The Spectrum of H_2. The Bands analogous to the Parhelium Line Spectrum.—*Part* II.

By O. W. Richardson, F.R.S., Yarrow Research Professor of the Royal Society, and P. M. Davidson, B.A., King's College, London.

(Received January 28, 1929.)

Errata in Part I.—On p. 70, line 22, the three values of 2α should read 1·935, 1·635 and 1·465. These give an "average α" $= 0{\cdot}839$ which is identical with the value $0{\cdot}85_0$ got in the other way. We now learn from a letter from Prof. Birge that this "constant" (the α in $B_n = B_0 - \alpha n$) has the same value for the initial states of Dieke and Hopfield's AB bands as for the final states of our systems.

In Tables I and IX the intensity measures attributed to Kapuscinski and Eymers are not in many cases the values finally published by them. Their paper should be consulted if accurate values are required. The final values show an even better agreement with our classification than the preliminary ones.

Synopsis.—§ 6. The system with P strong R weak, now called $3\,^1A \rightarrow 2\,^1S$. § 7. Comparison of $3\,^1A \rightarrow 2\,^1S$ (P > R), $3\,^1B \rightarrow 2\,^1S$ (Q) and $3\,^1C \rightarrow 2\,^1S$ (R > P). § 8. Five systems coming from electronic levels with principal quantum number 4. These are denoted by $4\,^1A \rightarrow 2\,^1S$, $4\,^1B \rightarrow 2\,^1S$, $4\,^1C \rightarrow 2\,^1S$, $4\,^1\chi \rightarrow 2\,^1S$ and $4\,^1E \rightarrow 2\,^1S$. § 9. The Electronic Terms and the New Quantum Mechanics. Determination of Ionisation Potential (15·381 volts) and Heat of Dissociation ($4{\cdot}465 \pm 0{\cdot}04$ volts) of H_2 and of Heat of Dissociation (2·50 volts) Vibration Frequency at Zero Amplitude ($\omega_0 = 2280$ wave numbers) and $x\omega_0$ ($= 60$) of the Hydrogen Molecule Ion H_{2+}. These values agree with Burrau's computations based on the wave mechanics.

§ 6. *System with* P *strong,* R *weak.*

This system has no Q branches and the P are stronger than the R branches. It resembles the strong Q system in that the lines do not show the Zeeman effect. These are set out in Table XI* in the same form as in Table I. The same type of alternation of intensity is met with as in the other systems and

---

[*] In these and similar tables the data are the wave-numbers given by Gale, Monk and Lee ('Astrophysical Journal,' vol. 67, p. 89 (1928)), followed by their eye estimates of intensity in brackets and preceded by the intensity measures of Kapuscinski and Eymers ('Roy. Soc. Proc.,' A, vol. 122, p. 58 (1929). In some cases the wave-numbers have been recalculated from Gale, Monk and Lee's wave-lengths data.

Table XI.

n' ↓	m ↓	n'' →	0.	1.	2.	3.	4.	5.	6.	7.	8.
0	1	R	25·4 21931·77 (4)	9·8 20613·46 (1)		2·2 18085·38 (1)					
		P									
	2	R	11·4 22040·15 (2h)	20723·48 (0)					14661·75 (*oh*)		
		P									
	3	R				9·9 18320·06 (6)	17111·01 (2)		14790·72 (00)		
		P	123 21815·61 (10)	34·0 20503·04 (6)	12·7 19226·51 (4)	2·9 17984·12 (2)	16774·97 (4)				
	4	R									
		P	73 21847·63 (8)	16·7 20540·69 (8)	7·5 19268·84 (2)	18030·83 (0)					
	5	R				8·8 18582·32 (1)			15077·91 (0)		
		P	188 21884·68 (10)	60·5 20585·01 (9)	14·5 19319·42 (6)	6·1 18086·52 (3)					
	6	R									
		P	31·4 21930·40 (4)	8·7 20639·38 (1)	19381·36 (0b)		16961·69 (0)				
	7	R									
		P	22·7 21972·38 (3)	8·5 20691·47 (3)		2·4 18224·10 (2)					
1	1	R	41·2 24020·51 (5)	3·7 22702·20 (1)	13·4 21420·70 (3)	20174·02 (1)	18960·97 (0)	17780·91 (0)	16633·48 (0)		
		P									
	2	R	11·9 24111·46 (2)	22794·99 (00a)	2·8 21515·19 (1)		19058·30 (1)	2·4 17879·60 (4)			
		P									
	3	R	25·3 24182·88 (3)		6·0 21593·77 (2)	3·7 20351·33 (1)	19142·24 (1)	17·3 17966·06 (4)			
		P	115 23904·31 (8)	13·3 22591·78 (2)	50·6 21315·17 (7)	24·5 20072·80 (6)	6·7 18863·74 (2)	6·0 17687·41 (3)			
	4	R	8·5 24242·95 (1)								
		P	53·5 23919·08 (4)	8·7 22612·15 (2)	27·5 21340·34 (4)		4·2 18897·03 (0)	2·9 17724·28 (2)			
	5	R									
		P	124 23916·10 (5)	32·9 22616·55 (4)	71·5 21350·86 (6)	26 20118·28 (5)	13·7 18918·02 (9)	7·5 17750·16 (2a)	16614·02 (0)		
	6	R									
		P	115 23904·31 (8)	7·4 22613·42 (1)	10·6 21355·38 (2)		18935·50 (0)	17773·21 (0a)			
	7	R									
		P									

Table XI—(continued).

n′ ↓	m ↓	n″ →	0.		1.		2.		3.		4.		5.		6.		7.		8.	
2	1	R	12·2	26030·59 (1)?		24711·93 (0)														
		P													2·4	18643·27 (1)				
	2	R			3·1	24790·49 (0)										18728·43 (0)				
		P		25922·59 (00)		24605·98 (1)				22081·00 (0)		20869·20 (1)	7·8	19690·44 (1)						
	3	R		26175·68 (1*dh*)	10·8	24862·88 (1)			24·4	22343·81 (6)					5·3	18814·43 (1)		17702·34 (0)		
		P	20·8	25914·34 (2)	64·1	24601·62 (4)	3·3	23325·04 (0)	15·1	22082·61 (3*ah*)	39·5	20873·55 (5)	23·3	19697·24 (4)			19·6	17441·32 (8)		16360·00 (00)
	4	R		26240·18 (1)?	12·7	24933·37 (2)														
		P	20·8	25914·34 (2)				23335·70 (*rd*)	27·1	22097·47 (7)		20892·33 (1)		19719·71 (1)		18578·84 (0)		17470·40 (1)?		
	5	R		26297·15 (*ah*)	4·9	24997·57 (1)														
		P				?				22110·79 (3)		20910·65 (5)		19742·75 (1)		18995·00 (1)				
	6	R																		
		P							3·9	22126·88 (0)	18·7	20932·78 (*ah*)								
	7	R																		
		P			$\overline{193}$	24608·70 ($\overline{8a}$)			7·6	22141·31 (2)	0·2	20954·51 (2)		19798·96 (1*h*)						
3	1	R				26418·48 (1)	7·7	25136·92 (1*h*)												
		P																		
	2	R			15·6	26468·69 (1)	7·2	25188·73 (1)					6·4	21552·84 (1*h*)?						
		P																		
	3	R		27819·78 (1)	30	26507·15 (3)	27·9	25230·57 (3)	10·1	23988·08 (2)				?			5·9	19346·69 (1)	5·1	18265·45 (1)
		P			10·3	26308·04 (1)	14·6	25031·45 (3)		23789·02 (1)		22579·93 (0*a*)		21403·60 (0)	5·0	20259·51 (1)	6·4	19147·64 (1*dh*)		
	4	R			11·8	26516·07 (1)	9·5	25244·08 (1)	3·0	24006·09 (00*a*)				21628·20 (0*a*)						
		P		27592·52 (*r*)D	14·3	26285·73 (0)	11·5	25013·86 (2)			4·4	22570·63 (0)	6·7	21397·77 (1)	17·2	20256·59 (3)				
	5	R																		
		P		27552·92 (*r*)T		26253·29 (1*a*)	27·9	24987·70 (3)	5·3	23755·16 (1)	6·7	22555·02 (1*h*)		21386·97 (0)	11·4	20250·78 (2)	8·3	19146·47 (1)		
	6	R																		
		P						24935·25 (0*a*)						21353·26 (00)	3·8	20222·49 (00)				
	7	R																		
		P																		

Note.—A bar over an intensity figure in these tables means that the value is for a blend of which the line forms part.

to about the same degree. In the $n' = 0$ and 1 progressions the maximum intensity is at about R (1) in the R branches and about P (5) in the P branches, in $n' = 2$ and $n' = 3$ the maximum of intensity is near R (3) and P (3) in the respective branches. It thus appears that for low initial vibrational energy the probability of a transition is dominated by the initial state and for high initial vibrational energy the final state has most influence. The first lines are R (1) and P (3) in the $n' = 0$, 1 and 3 progressions but $n' = 2$ P (2) seems to be present. It should, however, be remembered that the identity of P (1) and P (2) lines is not so secure as that of R lines and P lines with $m > 2$ as they only satisfy the vibration difference rule and they might be Q (1) or Q (2) lines or R (1), R (2) lines in a band with P weak. However, we have not been able to find a satisfactory alternative allocation of this set of lines.

The line 23904·31 (8) has to do duty in $1' \rightarrow 0''$ as both P (3) and P (6). Its frequency is correct and its intensity too high in both positions. The same applies to 25914·34 (2) which is both P (3) and P (4) in $2' \rightarrow 0''$.

There are several clashes with the α, β, γ, etc., systems. Thus 18320·06 (6) = 9·9 $0' \rightarrow 3''$ R (3) is the same as ${}_2\alpha_1$ P (2) which no doubt accounts for most of the strength, 15077·91 (0) = $0' \rightarrow 6''$ R (5) is the same as $0' \rightarrow 0''$ P (5) in $2\,{}^3S - 3\,{}^3S$, 17966·06 (4) = 17·3 $1' \rightarrow 5''$ R (3) is the same as ${}_3\alpha_2$ Q (4) which accounts for most of the strength here, 24111·46 (2) = 11·9 and 24182·88 (3) = 25·3 R (2) and R (3) of $1' \rightarrow 0''$ coincide respectively with ${}_2\gamma_2$ Q (4) and ${}_2\gamma_2$ Q (2). Most of the strength indicated here may belong to the present system. 18935·50 (0) = P (6) of $1' \rightarrow 4''$ is the same as ${}_6\alpha_4$ Q (2). 22126·88 (0) = 3·9 P (6) of $2' \rightarrow 3''$ is the same as ${}_1\gamma_2$ Q (1) and 19742·75 (1) = P (5) of $2' \rightarrow 5''$ is the same as ${}_0\beta_1$ Q (1). 20259·51 (1) = P (3) of $3' \rightarrow 6''$ is the same as ${}_3\alpha_1$ Q (1) and 26468·69 (1) = 15·6 R (2) of $3' \rightarrow 1''$ is the same as ${}_2\gamma_1$ Q (4) (?). In every case except the last the line is in the correct position for both bands to within the accuracy of the measurements. In the case of ${}_2\gamma_1$ Q (4) there is a small defect so that this line should be given to the present bands. Most of the strength of $2' \rightarrow 1''$ P (7) is required as $2' \rightarrow 1''$ Q (5) of the strong Q system of Part I.

This system contains a number of lines for which the Zeeman effect is known to be absent and none for which it is known to occur, with the exception of 21420·70 (3) = R (1) $1' \rightarrow 2''$. This line has the correct intensity so far as we can judge; so that this looks like a genuine abnormality. The line 21930·40 (4) P (6) of $0' \rightarrow 0''$ is marked Z in Merton and Barratt's tables, but that refers to an unresolved line of which 21930·40 is one of three components so that the Zeeman response may belong to one of the other lines.

The initial rotational term differences and some other properties of this band system are set out in the form previously adopted in Table XII.* These rotational terms are very peculiar and present a curious oscillation in the second term difference both with m and with n'. Such peculiarities might arise if lines of other bands were mixed with the correct ones but we believe them to be real. The only alteration in the lines which seems possible is the replacement of the P (7) lines in the $0' \rightarrow n''$ progression in Table XI by 23·8 22002·39 (5), 6·5 20721·47 (4), 5·2 19472·12 (1) and 18254·15 (0). This would change F (6) — F (5) in the 0′ levels from 262·81 to 292·74 and the next difference would become 60·15 instead of 30·22. This, however, does not seem very helpful. With terms of this sort it is impossible to say much about the values of B and of I but the four values given should be within 20 per cent. of the correct value. The P (2) lines of $3' \rightarrow n''$ would be practically coincident with the Q (2) lines of the corresponding band in the strong Q system of Part I if they existed.

The intensity diagram using the P (3) lines is shown in fig. 4. It is essentially the same as that for the two preceding systems except that corresponding lines are weaker throughout. Its resemblance to the R strong P weak system is, however, closer than to the strong Q system. Some of the intensities entered in fig. 4 differ from Kapuscinski and Eymers' final values. In $1' \rightarrow 5''$ 17·3

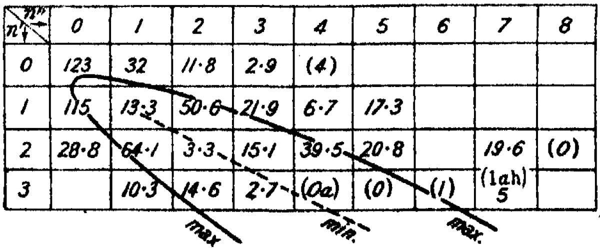

n' \ n''	0	1	2	3	4	5	6	7	8
0	123	32	11·8	2·9	(4)				
1	115	13·3	50·6	21·9	6·7	17·3			
2	28·8	64·1	3·3	15·1	39·5	20·8		19·6	(0)
3		10·3	14·6	2·7	(0a)	(0)	(1)	(1ah) 5	

FIG. 4.

---

* The data in this and similar tables are got from the data for the final state given in Part I and the wave-number differences of consecutive lines. For example, $R(m) = \nu_0 + F'(m+1) - F''(m)$, therefore $R(m) - R(m-1) = F'(m+1) - F'(m) - [F''(m) - F''(m-1)]$. The values of $F''(m) - F''(m-1)$ are given on p. 69 of Part I, the m values being got by adding $\frac{1}{2}$ to the j values in that table. The data are usually the averages of a number of determinations. The meaning of the quantity F (5) — F (4), for instance, is that it is the difference of the energy of the initial states of the two P lines whose final states are given by $m = 5$ and $m = 4$ (or two R lines given by $m = 3$ and $m = 2$).

Table XII.

Initial vibration state→	0′.		1′.		2′.		3′.	
F (8) − F (7) for P lines								
1st difference								
F (7) − F (6)	262·81				208·62			
,,		30·22				28·61		
F (6) − F (5)	232·59		175·09		180·01		118·27	
,,		43·77		26·26		33·96		6·16
F (5) − F (4)	188·82		148·83		146·05		112·11	
,,		41·75		19·09		30·85		25·12
F (4) − F (3)	147·07		129·74		115·20		86·99	
,,						46·34		
F (3) − F (2)					68·86			
2B, for m small, about	40				50			
I, for m small, about	$1 \cdot 4 \times 10^{-40}$				$1 \cdot 1 \times 10^{-40}$			
ν_e	21818·98		23921·64		25943·64		27672·12	
$\Delta\nu_e$		2102·66		2022·00		1728·48		
Next $\Delta = 2x\omega_e$			80·66		293·52			
ϵ about	$-\frac{1}{2}$		$-\frac{1}{2}$		$-\frac{1}{2}$		$-\frac{1}{2}$	

is a mistake. It should be 6·0. This improves the regularity a little. Correcting the others would make no serious difference.

The lines are accounted for on the exclusion principles which were found operative in the other band systems, viz., $\Delta j = 0$ or ± 1 and $\begin{array}{l} s \rightarrow a \\ a \rightarrow s \end{array}$. This will be clear from fig. 5. In the $n' = 0$ and 1 progressions the first lines to appear are R (1) and P (3); so that the lowest initial rotational level is that for $j = 1\frac{1}{2}$. In the $n' = 2$ progression P (2) appears to be present and it may also be in the $n' = 3$ progression where it appears to coincide with the corresponding lines of the strong Q system. In these vibrational levels a lower rotational level $j = \frac{1}{2}$ therefore is, or at least may be, present. On comparing fig. 5 with fig. 3 (Part I) it will be seen that the a levels have the same j values as a levels for R strong, P weak and as s levels for strong Q. The term values in Table XII for small values of m are approximately of the form $F(m) = B(j - \varepsilon)^2$ if $\varepsilon = -\frac{1}{2}$.

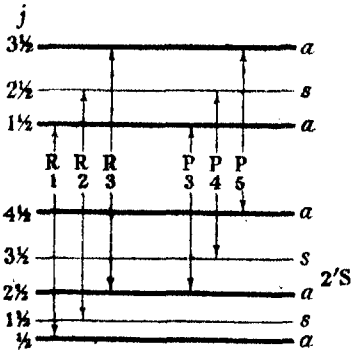

Fig. 5.

The values of ν_0 in Table XII have been got from the R (1) lines by putting $R(1) = \nu_0 + F'(1\frac{1}{2}) - F''(\frac{1}{2})$ and assuming the formula $F(m) = B(j - \varepsilon)^2$ with $\varepsilon = -\frac{1}{2}$ holds up to and including the lowest ΔF in the table. It seems likely that the result will be correct to within one or two wave-numbers. There is evidently a big drop in the vibration differences of the ν_0s at the third interval. Assuming the quadratic formula in n' to apply to the two first intervals we have $x\omega_0 = 40 \cdot 33$ and $\omega_0 = 2143$.

§ 7. *Comparison of the Three Preceding Systems.*

Some of the more characteristic features of these systems are collected in Table XIII. At the top are placed the rotational energy level differences for the vibrationless states separated by lines marked with the j values of the levels. These are set out so that levels with similar or corresponding energy differences lie in the same row of the table. The thick lines denote the levels with the greater weights. The ratio of the weights keeps in the neighbourhood of 3 to 1 but there is evidence that it is a function of the degree of vibrational excitation. It is evident from the table that there is a close resemblance between all three systems; but Q is closer to the P strong than to the R strong

Table XIII.

	R > P.			Q.			P > R.		
j values of levels and 1st and 2nd energy differences at $n' = 0$ vibrational level.				6½			5½		
					282·09			262·81	
	6½			5½		$52 \cdot 10_5$	4½		30·22
		217·45			$229 \cdot 98_5$			232·59	
	5½		53·07	4½		52·97	3½		43·77
		164·38			$177 \cdot 01_5$			188·82	
	4½		51·90	3½		$52 \cdot 51_5$	2½		41·75
		112·48			124·50			147·07	
	3½		47·24	2½		49·77	1½		
		65·24			74·73				
	2½		42·54	1½					
		22·70							
	1½		30·23						
		−7·53							
	½								
ε about		+1½			+½			−½	
Zeeman response		strong			weak			weak	
ν_0^0	21606·49			21849·36			21818·98		
Δ_1		2225·75			2097·23			2102·66	
ν_1^0 Δ_2	23832·24		229·70	23946·59		155·67	23921·64		80·66
Δ_1		1996·05			1941·56			2022·00	
ν_2^0 Δ_2	25828·29		180·39	25888·15		167·23	25943·64		293·52
Δ_1		1815·66			1774·33			1728·48	
ν_3^0	27643·95			27662·48			27672·12		
$x\omega_0$		114·85			77·835			40·33	
ω_0		2340·60			2175·06			2143·00	
$2B_0$ for m large, about		56·6			56·6				
$2B_0$ for m small, about		40			50			40	

system. The values of ν_0, ω_0, $x\omega_0$ and ε are nearer and they agree in not giving the Zeeman effect. Also for any particular value of j we get an s level in the Q system and an a level in the strong P or *vice versa*. These properties suggest the combination of the strong P and Q systems into one system having an upper 3P level. However, these P and Q systems show nothing like the degree of similarity present in the corresponding portions of $3\,^3P \rightarrow 2\,^3S$.* The difference in the character of the rotational terms shown by Tables XII and II (Part I), particularly for the higher vibrational numbers, seems too great for them to be classed together in this way. It appears also that $j = \frac{1}{2}$ is present in one, and possibly in two, vibrational levels of the strong P system, though not in $n' = 0$. Other features which contradict the usual classifications have been mentioned in Part I, § 5. It may, however, possibly be significant that the initial rotational levels of the P strong system show the curious irregularity already referred to, whilst there is a definite abnormality in the structure of the $n' = 1$ vibrational level of the R′P′ branches of $3\,^3P \rightarrow 2\,^3S$.

The $\nu_0 s$ and the quantities derived from them in Table XIII do not in all cases have the same values as have been assigned to them in previous tables. This is because they have been obtained in a different way. Looking broadly at the rotational terms for the R strong, Q and P strong systems it seems certain that they are of a type with ε about $1\frac{1}{2}$, $\frac{1}{2}$ and $-\frac{1}{2}$ respectively. The values of ν_0 have been calculated from the lowest numbered lines present (R (1) or Q (2)) assuming the expression $F(m) = B(j - \varepsilon)^2$ to apply at the levels $j = 1\frac{1}{2}$ and $2\frac{1}{2}$ and any lower levels which may be required. On this view the result should be exact for the R > P system where the initial level of R (1) has no rotational energy, it involves the extrapolation of one level for the Q system and two levels for P > R. The error should, therefore, be greatest for P > R, but even here it is not likely to be very serious. The fact that the resulting values of $x\omega_0$ are as 3 : 2 : 1, that is to say, proportional to $1\frac{1}{2} + \varepsilon$ is very interesting.

§ 8. *Some related Systems with a Higher Initial Electronic Level.*

There are several progressions starting in the region between $\lambda = 3620$ and $\lambda = 3700$ which include practically all the lines of any strength in that neighbourhood. There can be no doubt that these are $0' \rightarrow n''$ progressions of $4 \rightarrow 2$ electron transitions. In the strong systems already described the $0' \rightarrow n''$ progressions are characterised by having the maximum strength in the $0' \rightarrow 0''$ band, the strength gradually falling off as n'' increases. On the other hand the progressions with $n' > 0$ each have two intensity maxima and a minimum in between which lies at a lower value of n'' the smaller the value of n'. All the progressions referred to have the former type of intensity distribution. On account of the high energy of the initial states of these bands even at the 0′ vibration level it is not to be anticipated that the higher initial vibration levels will be well developed. However, one of the $1' \rightarrow n''$ progressions has been found; in fact it was discovered in the earlier work.* This progression has its 0″, 2″ and 3″ bands strong and the 1″ band very weak like the $1' \rightarrow n''$ progressions already described. We propose to indicate these progressions provisionally by the symbols 4′A, 4′B, 4′C, $4'\chi$, $4'\psi$, 4′E. The lines and intensities are set out in Table XIV.

---

* Richardson and Das, 'Roy. Soc. Proc.,' A, vol. 122, p. 688 (1929).

Some of these systems are really very strong and they include some of the really strong lines of the spectrum. Thus in 4′E the lines 27134·40 (5), 27151·72 (5), 25832·96 (3), 25821·86 (5), 25826·42 (2), 25852·00 (2) and 24545·26 (3) would all be marked (10) on the usual scale of eye estimation if they were lines with the same intrinsic energy in the red part of the spectrum. There are also some very strong lines in 4′C. There are a few doubtful elements in this table and some lines are included which have larger defects than we should usually consider admissible. As a rule we reject or query all lines which have a defect of 0·10 wave number,† but we cannot expect to maintain this accuracy with faint lines in this part of the spectrum. This is due not only to the fact that there are nearly 10 wave-numbers per Ångström but also to the intensity of the continuous background which is always present in this region. In Finkelnburg's tables, for example, he frequently catalogues as the same line, lines for which his measurements differ from those of Gale, Monk and Lee by about 0·5 wave-number although claiming an accuracy of about 0·01 Å for both sets of measurements. In 4′B the lines for $m = 2$ are only given by Finkelnburg. This makes the propriety of their inclusion doubtful since, as a rule, his method of excitation tends to bring up the lines of high, rather than of low, rotational quantum number. 4′C is the least satisfactory of these progressions. The absence of $0' \rightarrow 2''$ R (1) is anomalous, but this would be the case however these R (1) lines might be interpreted. The weakness of $0' \rightarrow 1''$ R (2) suggests that the R (2) lines might belong to some other $1' \rightarrow n''$ progression. The lines attributed to P (2) and R (3) are all quite doubtful and show large defects. The absence of

---

[*] Richardson, 'Roy. Soc. Proc.,' A, vol. 115, p. 543 (1927).

[†] There are a small number with defects a little larger than this which inadvertently have not been queried.

Table XIV.

4′ A.

n′ ↓	m ↓	n″→		0.		1.		2.		3.	4.	5.
0	1	R		27487·25 (1)				24887·49 (0) F	2·4	23640·67 (1)		
		P										
	2	R										
		P	12·4	27347·00 (0)	12·2	26030·59 (1)	3·6	24750·65 (1)			? 22293·62 (00)	? 21114·89 (*oh*)
	3	R										
		P	19·5	27371·04 (2)	22·3	26058·46 (2)		24781·84 (0)	2·8	23539·49 (0)		
	4	R										
		P		27401·95 (0) F		26094·79 (1)	16·7	24823·07 (3)				
	5	R										
		P		27458·54 (0) F		26158·88 (1) F						

4′ B.

n′ ↓	m ↓	n″→		0.		1.		2.		3.	4.	5.
0	1	R				26081·47 (0) F		24800·16 (0) F ?		23553·21 (0) F		
		P										
	2	R		27468·37 (1) F ?				? 24871·12 (00) F				
		P		27330·03 (2) F		26013·70 (1) F		24733·82 (0) F		23488·33 (0) F		
	3	R			19·0	26246·05 (1)		24969·36 (0)				
		P	45·6	27283·85 (3)	52·1	25971·40 (2)	23·4	24694·77 (1*a*)	5·4	452·30 (1)		
	4	R										
		P	12·3	27275·60 (1)	15·3	25968·71 (0)	8·0	24696·90 (1)				
	5	R										
		P	16·5	27291·87 (1*a*)	19·4	25992·16 (1)		24726·47 (0*a*)	2·4	493·95 (0)		

4′ C.

0	1	R	109	27207·60 (7)	86·7	25889·38 (4)		(24607·88)	12·6	23361·12 (2)	9·3	22147·95 (3)	? 20967·65 (0)
		P											
	2	R	46·5	27213·38 (3)		25896·97 (00)	6·4	24617·06 (1)	5·5	23371·69 (1) ?	4·3	22160·21 (1)	
		P	?	27143·38 (*r*) D			?	24547·79 (0)					
	3	R	?	27248·84 (0*a*)	?	25936·44 (1)†	7·6	24660·11 (2) ?	?				
		P	16·8	27091·55 (1)			4·6	24502·37 (0)	2·4	23259·97 (0)			
	4	R		27324·60 (0*a*)		26017·70 (00*b*)		24745·69 (00)			3·1	22302·72 (00)	
		P	17·8	27020·93 (1)	32·6	25713·98 (2)		24442·38 (0) F		23204·17 (0) F			
	5	R											
		P											
	6	R											
		P		26986·01 (0)	13·3	25695·06 (1)	<3·4	24437·03 (0) F					

Note.—There is a line 18880·40 (00) at the place for R (4) of $n'' = 7$.

4′ χ.

0	2	R		27561·03 (0/1) F		26244·32 (0) F or				23719·99 (00) F			
	or 3			27510·53 (00) F ?		26194·74 (00*a*) ?			or	23669·34 (00) F			
	4	R		27515·16 (1)	13·3	26202·65 (1)	6·3	24926·04 (0)		23683·94 (0) F ?			21298·60 (1) F ?
	5	R		27501·79 (1*a*)		26194·74 (00*a*)		24922·93 (0)					
	7	R		27520·06 (1)	23·4	26220·42 (2)		24954·84 (1)	6·8	23722·19 (0)			21354·07 (00)
		P		27112·40 (0*a*)		25831·43 (0)							

Table XIV—(continued).

4′ Ψ.

n′ ↓	m ↓ n″→	0.	1.	2.	3.	4.	5.
1	2	29489·05 (0) M. & B.		26893·50 (0)	25648·06 (0) F	24436·62 (00a)	23257·56 (00) F
	3	29448·03 (2)	28135·41 (r) T	27·9 26859·00 (2h)	29·2 25616·58 (3)	24407·51 (1)	$\boxed{23230 \cdot 80\ (4)}$
	4	29436·17 (0) M. & B.	?	27·9 ? 26859·00 (2h)	25619·83 (0a)	24414·65 (0)	23241·59 (00) F
	5	29447·27 (3) F		26882·53 (0/1) F	25650·11 (1)	24449·75 (0) F	

4′ E.

0	1 R	27181·08 (00b)	27·6 25862·73 (2)				? 20941·20 (00) F	1R
	2 R	19·0 27149·30 (1)	42·5 25832·96 (3)	11·8 24553·10 (1)	2·4 23307·83 (0)		20917·32 (0) F	2R
	2 P							
	3 R	119 27134·40 (5)	154 25821·86 (5)	51·0 24545·26 (3)	13·6 23302·87 (2)	4·1 22093·84 (1)	20917·32 (0) F	3R
	3 P		16·7 25752·38 (1)	5·4 24475·79 (1)	23233·45 (00) F		20847·87 (0) F	3P
	4 R	27133·28 (1)	44·3 25826·42 (2)	24554·67 (0)	3·0 23316·46 (0)			
	4 P		25650·11 (1)				20762·33 (00) F	4P
	5 R	32 27151·72 (2)	51·2 25852·00 (2)	21·1 24586·49 (1)	6·8 23353·90 (1h)			
	5 P		8·2 25567·97 (1)	? 24302·60 (0) F			20701·83 (00)F	5P
	6 R	27189·85 (0a)	25899·02 (1)	3·4 24640·91 (0a)				
	6 P			24245·80 (0a)	23019·86 (00) F		20663·60 (0a)	6P
	7 R	27247·65 (0a)	8·6 25966·76 (0)					
	7 P	? 26743·98 (00)					20653·46 (00) F	7P

P (5) is not accounted for. Two alternatives are given for the $m = 2$ lines of 4′χ. The upper ones are the more probable but neither is to be regarded as certain as there are large defects in each case. It is quite possible that this progression has no $m = 2$ lines. The interpretation of 4′χ as R and P lines rests mainly on the existence of the two P (7) lines having the same initial states as the two R (5) lines which are the strongest lines in the system. In 4′ψ there are large defects in all except the $m = 3$ lines which are the strongest. This, however, is probably inevitable from the part of the spectrum in which these bands lie. It is thought that the lines are the band lines except 23238·80 (4) and 26859·00 (2*h*) (as $m = 4$) which possibly conceal the true lines. Apart from the lines mentioned, all the others in Table XIV are believed to be accurate to about 0·10 wave-number.

The rotational energy level differences and some other properties of the bands are set out in Table XV. In this and similar tables F (*m*) means that term of the initial states which belongs to a line ending on the *m*th final state. The corresponding initial states depend on whether the line is a P, Q or R line. The evidence about this is not as certain as might be desired. In 4′A there are only three R lines, in 4′C the R (1), R (2), R (3) and P (3) lines may not really belong to the same bands as the others and in 4′χ there are only two P lines. In 4′ψ no rotational combinations have been found, and in 4′B they are doubtful, so that the branches could be either P, Q or R. In the very intense progression 4′E the P branches fail in the 0″ band but are present in the others.

It is clear from the values of ΔF in Table XV that the ABCχ $0' \rightarrow n''$ progressions all belong to the same type and that the $1' \rightarrow n''$ progression ψ belongs to one of them, whereas the ΔF values for the strong progression 4′E are of a quite different character. The five similar progressions are also of the same type as the three strong systems already described in these papers in which ϵ is semi-integral (using semi-integral j values). This similarity tends to support the reality of the small number of R lines associated with 4′A and of P lines associated with 4′χ since the $3' \rightarrow 2'$S systems had either R strong and P weak or vice versa.

If we take these combinations as genuine this completely determines the j values for the initial levels of the A and χ systems. This can be most easily explained by drawing a diagram as in fig. 6 in which the levels of the successive systems are set out so that successive initial levels having similar values are set out in the same horizontal row; but this statement does not apply to the E system where the levels are not of similar type. Below are set out lines to indicate the levels of the final state $2\,^1$S, the levels of greater weight being marked

Table XV.

Progression.	A.		B.		C.		χ.		ψ.		E.	
F (7) — F (6)											$278 \cdot 55_5$	$53 \cdot 4_5$
F (6) — F (5)											$225 \cdot 08_5$	$54 \cdot 96$
F (5) — F (4)	$208 \cdot 27_5$	$62 \cdot 30_5$	167·93	61·12			169·98	68·93	157·26	54·58	$170 \cdot 12_5$	$56 \cdot 18_5$
F (4) — F (3)	145·97	44·63	106·81	75·69	190·82	78·06	101·05	68·62	102·68	67·04	113·94	51·54
F (3) — F (2)	101·34		31·12		112·76	68·13	32·43		35·64		62·40	55·37
F (2) — F (1)					44·63						7·07	
ν_e	27356·93		27373·74		27212·46		27603·74		29533·45		27178	
2B											60	
I_e											$0 \cdot 92 \times 10^{-40}$	
ϵ for m small, about	$-\frac{1}{2}$		$+\frac{1}{2}$?		$+1\frac{1}{2}$		$+2\frac{1}{2}$?		$+\frac{1}{2}$?		+2	

a and the weaker levels *s*, on the right, and the j values for these levels being given on the left. The first line of 4′A being an R (1) line it must go from $j = 1\frac{1}{2}$ to $j = \frac{1}{2}$ and it comes from a strong level, the P (3) lines, which come from this level, being the strongest lines of this system. Similarly with χ; if the P (7) lines are right the first line is R (2) and the corresponding j value for the initial level is $2\frac{1}{2}$. This is a weak level, the R (3) and R (5) lines being the strong lines of this system. It has been pointed out that there is an element of uncertainty about the reality of the R (2) lines of this system. However, that makes no difference to the j values. If R (2) is missing, the first is R (3) and that fixes the next higher level as that of $j = 3\frac{1}{2}$ and as an *a* level. The only difference is that the lower level at $j = 2\frac{1}{2}$ would be absent.

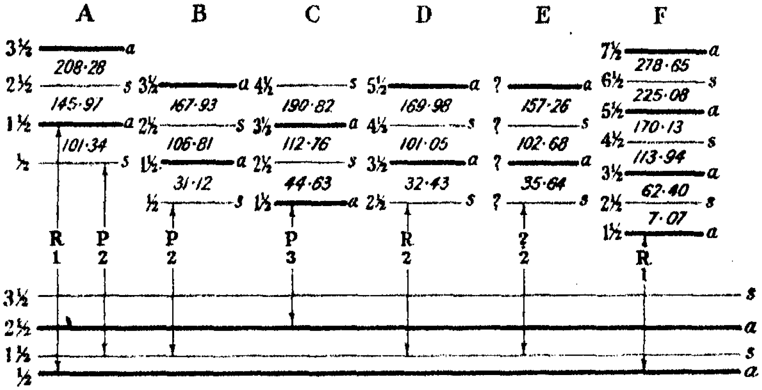

FIG. 6. (In this figure χ is marked D, ψ is marked E and E is marked F.)

Similarly the R and P combinations determine the j values for 4′C in the manner shown. This, however, is not as satisfactory as the arrangement for A and χ. It is true that the strongest lines come from the strong level at $j = 1\frac{1}{2}$, but the next strongest lines come from $j = 2\frac{1}{2}$ which should be a weak level. However, the facts would be accounted for if the $3\frac{1}{2}$ level, instead of being strong, were absent or very abnormally weak. This hypothesis is not so unreasonable because there is a definite abnormality in the intensity of the strong R (1) lines at $n'' = 2$, whatever these lines are, and another in the R (2) lines at $n'' = 1$ if they belong to these bands. It is possible that the $j = 3\frac{1}{2}$ level is not at the place indicated by the R (3) lines in Table XIV as there are some other $m = 3$ lines in this neighbourhood which would do for it, but at present they are thought to belong to another band system. In any event the $j = 3\frac{1}{2}$ level of 4′C would appear to be abnormal, in intensity in the one case and in magnitude in the other.

With the j values thus settled the initial rotational terms are approximately of the form $F(m) = B(j - \epsilon)^2$ where $\epsilon = -\frac{1}{2}$ for 4′A, $\epsilon = +1\frac{1}{2}$ for 4′C, and $\epsilon = +2\frac{1}{2}$ for 4′ χ. With these values of ϵ occurring there seems no reason why the intermediate value $\epsilon = +\frac{1}{2}$ should be excluded. This value of ϵ was, therefore, given to the remaining system 4′ B. This requires the strong lines to be P branches not Q. Some support for this has been found in a search for the corresponding R lines with Finkelnburg's new tables. Five lines were found at the expected places although three of them have rather large defects. These are queried in the table. Two others are given by Gale, Monk and Lee. The fact that the lines are not found in every case in the 0″ and 1″ bands where they should be strongest and are found in the weaker 2″ and 3″ bands is not unreasonable as they are probably all rather weak and may easily be lost in the dense continuous background in which the 0″ and 1″ bands lie. Further support for this arrangement is derived from the fact that it makes all the level values go smoothly from A through B and C to χ as ϵ increases by steps of 1 from $-\frac{1}{2}$ to $+2\frac{1}{2}$. The alternative treatment of 4′ B would be to regard it as the Q′ branches of 4′ C. This would give it $\epsilon = +1\frac{1}{2}$ and would raise all the j values given to its levels in fig. 6 by unity. The system with $\epsilon = +\frac{1}{2}$ would still be missing and the R fragments in 4′ B in Table XIV would be fortuitous. This now seems unlikely.

The progression 4′ Ψ is not an $0' \rightarrow n''$ progression but it has the correct intensity distribution for a $1' \rightarrow n''$ progression. We have no rotational combinations for it and it might possibly belong to either B or χ. We think, however, that it should be given to B as it seems too strong for an upper vibrational level of 4′ χ. If it belongs to 4′ χ the value of $\omega_0(1 - x)$ for the initial levels of this system is 1929·71, and if it belongs to 4′ B the value of $\omega_0(1 - x)$ for that system is 2159·71. Either of these values would be reasonable. Provisionally, at any rate, we propose to make Ψ the $1' \rightarrow n''$ set of progressions of the 4′ B system. This makes the branches P branches, the value of $\epsilon = +\frac{1}{2}$ and the successive upper levels starting from the lowest have the j values $\frac{1}{2}$, $1\frac{1}{2}$, $2\frac{1}{2}$ and $3\frac{1}{2}$.

The very strong system 4′ E is evidently in a different class from the others. We do not wish to say anything further about it at present except that it appears to be a $4' \rightarrow 2\,{}^1S$ system corresponding to some $3' \rightarrow 2\,{}^1S$ systems of a type different from those we have described already and which we propose to describe in our next paper.

Apart from some perturbations, which have been referred to, these bands which come from 4′ electronic levels all show the alternation in intensity which is so well marked a feature of all the other bands of this spectrum. When allowance is made for the temperature effect on the distribution of intensity among the lines of a band the weight ratio of alternate states is found to be 3 to 1 as was the case with the other systems. This is particularly well shown by the figures for the very strong system 4′ E where the data are more complete than for the others. The transitions are also governed by the same rules as in the other bands, namely $\Delta j = 0$ or ± 1, and only $s \rightarrow s$ or $a \rightarrow a$ allowed.

§ 9. *The Electronic Terms and the New Quantum Mechanics.*

To evaluate the electronic terms it is necessary to decide which of the five $4' \rightarrow 2\,{}^1S$ systems should be assigned to the same electronic series as each of the three $3' \rightarrow 2\,{}^1S$ systems. This is a matter of some delicacy since, owing to the peculiar character of the upper levels, the usual rules are not very helpful. We have decided to class together those systems which have the same ε values as this quantity determines the main outlines of the term structure and there are other points which indicate that this arrangement is right. Thus the system we have previously called P strong R weak should be $3\,{}^1A \rightarrow 2\,{}^1S$ ($\varepsilon = -\frac{1}{2}$) the system called strong Q should be $3\,{}^1B \rightarrow 2\,{}^1S$ ($\varepsilon = +\frac{1}{2}$) and the system called R strong P weak should be $3\,{}^1C \rightarrow 2\,{}^1S$ ($\varepsilon = +1\frac{1}{2}$). The order of intensity of the systems is the same for both sets of electronic levels, thus $3'\,A < 3'\,B < 3'\,C$ and $4'\,A < 4'\,B < 4'\,C$. It is satisfactory that 4′ A and 3′ A are both PR systems with R weak and that 4′ C and 3′ C are both PR systems with P weak. The fact that $4'\,B \rightarrow 2\,{}^1S$ is classed as a PR system with R weak and $3'\,B \rightarrow 2\,{}^1S$ as a Q system does not seem to us to be an argument against connecting them together in this way. All this implies is that the a and s character of the terms for a given j value is inverted in the 4′ B as compared with the 3′ B level. This type of inversion in successive electronic levels is well established for $1\,{}^1S$ and $2\,{}^1S$,* for $2\,{}^3S$ and $3\,{}^3S$† and for $3\,{}^3P$ and $4\,{}^3P$.†

If these systems are really connected in this way their ν_0 lines should be approximately connected by a Rydberg formula of the type $\nu_0 = A - \dfrac{109678 \cdot 3}{(m-x)^2}$ where A is the electronic term of $2\,{}^1S$, x is a small constant and $m = 3$ for 3′ A, 3′ B, 3′ C and $m = 4$ for 4′ A, 4′ B and 4′ C. Here and in the wave-mechanics calculation energies are taken as measured relative to the unexcited ionic state. On making these computations we find from ${}^1A \rightarrow 2\,{}^1S$, $A = 34361$, $x = 0 \cdot 0428$ from ${}^1B \rightarrow 2\,{}^1S$, $A = 34369$, $x = 0 \cdot 0402$ and from

---

* Hori, 'Z. Physik,' vol. 44, p. 834 (1927).

† Richardson and Das, 'Roy. Soc. Proc.,' A, vol. 122, p. 688 (1929).

$^1C \rightarrow 2\,^1S$, $A = 34265 \cdot 5$, $x = 0 \cdot 0566$. The variation in the values of A is presumably due to x not being constant. The closeness of the first two values and the divergence of the third suggests that for the last system the variation of x may be considerable. We have accordingly discarded the last value of A. The mean of the other two is $A = 34365$. If we adopt this we obtain from the ν_0's the current term values $R/(m-x)^2$ and the values of x given in Table XVI. These data are thought to be reliable to something near the last figure given.

Table XVI.

System.	$4'A \rightarrow 2\,^1S$.	$3'A \rightarrow 2\,^1S$.	$4'B \rightarrow 2\,^1S$.	$3'B \rightarrow 2\,^1S$.	$4'C \rightarrow 2^1\,S$.	$3'C \rightarrow 2\,^1S$.
ν_c	27356·93	21818·98	27373·78	21849·36	27212·46	21606·49
$R/(m-x)^2$	7008·07	12546·02	6991·22	12515·64	7152·54	12758·51
Denominator	3·9561	2·9567	3·9608	2·9603	3·9146	2·9320
x	0·0439	0·0433	0·0392	0·0397	0·0854	0·0680

From the value of A we can calculate a value of the spectroscopic ionisation potential I_{H_2} of the hydrogen molecule. Hori's value of ν for his R (0) line of the Lyman band $3' \rightarrow 0''$ $2\,^1S \rightarrow 1\,^1S$ is 94075. Subtracting from this the sum of the first three vibration differences of the $j = 1\frac{1}{2}$ rotational states of $2\,^1S$, viz., $1316 \cdot 41 + 1279 \cdot 84 + 1245 \cdot 25 = 3841 \cdot 50$ we get for the $0' \rightarrow 0''$ R (1) (in our notation R (1) = R (0) of Hori) of $2\,^1S \rightarrow 1\,^1S$ $\nu = 90233 \cdot 5$ $= \nu_0 + F'(1\frac{1}{2}) - F''(\frac{1}{2})$. This gives $\nu_0 = 90204 \cdot 2$. If we add this to the $2\,^1S$ term 34365 we get $124569 \cdot 2$ wave-numbers $= 15 \cdot 381$ volts as the spectroscopic value of the ionisation potential of H_2. The calculated value of this quantity for H_2 on the basis of the old quantum mechanics was $23 \cdot 7$ volts* whereas the experimental electrical value is $15 \cdot 9$ volts. The electrical value should be a little higher than the spectroscopic value owing to some vibrational energy being given to the hydrogen molecule ion when H_2 is ionised.

It is possible to check this value against other known or calculable quantities. We can suppose the hydrogen molecule to be broken up into its ultimate constituent parts, namely two protons and two electrons in either of two ways. In the first way we first ionise the molecule obtaining one electron and one hydrogen molecule ion (H_2+) and then we break up the molecule ion. These two successive processes involve an expenditure of work $= I_{H_2} + I_{H_2+}$ where

---

* Pauli, 'Ann. Physik,' vol. 68, p. 177 (1922).

I_{H_2} is the ionisation potential of neutral H_2 and I_{H_2+} is the lost energy of the molecule ion. In the second way we first dissociate the molecule into two atoms and then ionise the atoms separately. This involves an amount of work $I_D + 2I_H$ where D is the heat of dissociation of H_2 and I_H is the ionisation potential of the hydrogen atom. As the initial and final states are the same for both ways, we must have $I_{H_2} + I_{H_2+} = I_D + 2I$. The value of I which is the equivalent of Rydberg's constant in volts is known very accurately and 2I is 27·085 volts. The value of I_{H_2+} has been calculated by Burrau* on the wave mechanics as $16 \cdot 16 \pm 0 \cdot 03$ volts using a correction pointed out by Condon.† If this value is combined with the spectroscopic value of I_{H_2} just obtained we get $I_D = 4 \cdot 476 \pm 0 \cdot 03$. The best value of this quantity is the value deduced by Witmer‡ by extrapolation of the vibrational levels of the $1\,^1S$ state. This is $I_D = 4 \cdot 34$ volts. It is stated by Dieke and Hopfield|| that this may be wrong by 0·1 volt; but it seems improbable that the error can be greater than this. Niessen¶ has recently revised the old quantum mechanics model of H_2 by assigning half quantum numbers to it. By assigning the quantum numbers $(0, \frac{1}{2}, 1)$ to the ellipsoidal co-ordinates of unexcited H_2 he finds $I_{H_2+} = 16 \cdot 47$ volts. This would lead to $I_D = 4 \cdot 78$ which is quite excluded by our results.

The spectroscopic value of I_{H_2} just used has been got by the application of the formulæ of the old quantum mechanics and the assumption of the applicability of a Rydberg formula to the ν_es so obtained. We shall now calculate the ionisation potential by applying the formulæ of the wave-mechanics to the elucidation of the spectroscopic data and assuming that the resulting electronic frequencies will still obey a Rydberg formula. If we indicate by bars the values of corresponding quantities in terms of the results of the wave-mechanics we have $\bar{\nu}_e = \nu_e + s'' - s'$, $s = \frac{1}{2}\omega_0 + \frac{1}{4}x\omega_0$, $\bar{\omega}_0 = \omega_0 + x\omega_0$, $\overline{x\omega_0} = x\omega_0$ and in the rotational terms we have to replace the half integral j^2 values by $j(j+1)$; here s is the displacement of the level caused by the vibrational zero point energy.

We have only one pair of systems $3'\,B \rightarrow 2\,^1S$ and $4'\,B \rightarrow 2\,^1S$ for which we have more than one upper vibrational level so that we have confined this calculation to them. For $3'\,B \rightarrow 2\,^1S$ we have $s'' = 673 \cdot 76$, $s' = 1106 \cdot 99$, $\bar{\nu}_e = 21416 \cdot 13$. For $4'\,B \rightarrow 2\,^1S$ we have assumed $x\omega_0$, which is

---

* 'K. Danske Vid. Selsk., Math-fys.,' vol. 7, No. 14 (1927).

† Quoted by Birge, 'Proc. Nat. Acad. of Sciences,' vol. 14, p. 12 (1928).

‡ 'Phys. Rev.,' vol. 28, p. 1223 (1926).

|| 'Phys. Rev.,' vol. 30, p. 400 (1927).

¶ 'Z. Physik,' vol. 43, p. 699 (1927).

unknown, to have the same value as for $3'\,B \rightarrow 2\,{}^1S$. The effect of this is small so that if it were wrong it would make little difference. With this assumption we have for $4\,'B \rightarrow 2\,{}^1S$, $s' = 1137\cdot24$, $s'' = 673\cdot76$, $\bar{\nu}_e = 26910\cdot30$. Assuming these $\bar{\nu}_e s$ to be given by a Rydberg formula

$$\bar{\nu}_e = \overline{2\,{}^1S} - 109678\cdot3/(m-x)^2, \quad m = 3,\ 4,$$

we get $x = 0\cdot0339$, $\overline{2\,{}^1S} = 33883$.

If the electronic terms are of this form, then replacing $2\,{}^1S$ in general by the symbol A instead of $\bar{\nu}_e = \nu_e + s'' - s$ we have $\bar{A} - \bar{f}(m) = A - f(m) + s'' - s'$, where m is the principal electronic quantum number, *i.e.*,

$$f(m) + s' - \bar{f}(m) = A + s'' - \bar{A}.$$

As Birge* has pointed out, if we extrapolate the left-hand side to $m = \infty$, $f(m) = \overline{f(m)} = 0$ and we are left with an s' which is the s for the hydrogen molecule ion. If we apply this to the appropriate values of A, $\bar{A}$ and s'' we find $s\infty = 1155\cdot7$, and the same value would be found if, instead, we used the constants for $3'\,B$ or $4'\,B$. From these we select a mean value $s\infty = s = 1155 = 0\cdot14$ volt. This enables us to find the value of ω_0 and $x\omega_0$ for the hydrogen molecule ion because we have another relation between these quantities, namely, the heat of dissociation of the molecule ion $= I_D + I_H - I_{H_2} = \omega_0{}^2/4x\omega_0$ if we make the further assumption, probably not strictly true, that x is constant. Using $I_D = 4\cdot34$, $I_H = 13\cdot543$ and $I_{H_2} = 15\cdot381$ in this together with $1155 = s = \frac{1}{2}\omega_0 + \frac{1}{4}x\omega_0$ we get $\omega_0 = 2280$ and $x\omega_0 = 60$ for the hydrogen molecule ion and for its heat of dissociation the equivalent of $2\cdot502$ volts.

The value of $\bar{\omega}_0 = \omega_0 + x\omega_0$ can be calculated by Burrau's method for H_{2+} on the wave-mechanics. It is given in his notation by $(2\pi\bar{\omega}_0)^2 = \dfrac{2}{M}\dfrac{d^2E}{d\varepsilon^2}$ where M is the mass of the hydrogen atom, E is the total energy and ε the inter-nuclear distance. From his graph of E as a function of ε he finds the value of $\frac{1}{4}\bar{\omega}_0$ to be equivalent in volts to $0\cdot07$. The value of $\bar{\omega}_0$ from our spectroscopic data is equivalent to $0\cdot28$ volts and there is complete agreement to the degree of accuracy of the methods.

We now return to the calculation of the ionisation potential of H_2 on the wave-mechanics. We have as before R (0) of $0' \rightarrow 0''$, $2\,{}^1S \rightarrow 1\,{}^1S = 90233\cdot5 = \bar{\nu}_e - s'' + s' + F'(1) - F''(0)$. The rotational terms are S terms, so that $\sigma = 0$ and $\varepsilon = 0$, $F''(0) = 0$ and $F'(1) = 2B'_0 = 38\cdot89$. Since $S'' = 2159\cdot4$ and $S' = 673\cdot7$ $\bar{\nu}_e = \overline{1\,{}^1S} - \overline{2\,{}^1S} = 91680\cdot2$, so that with the value $\overline{2\,{}^1S} = 33883\cdot0$ already calculated we get $\overline{1\,{}^1S} = 125563\cdot2$. To get the interval between the $\bar{\nu}_e$ of the ion and the ground level of 1 ^1S we have to subtract the vibrational zero point energy which is present on the wave-mechanics from this. Its value for the 1 ^1S state is 2159·4 from which the above interval is found to be 123403·8 wave-numbers = 15·235 volts. If we add this to Burrau's value 16·30 ± 0·03 for the $\bar{\nu}_0$ of the molecule ion and subtract twice the Rydberg constant in volts (27·085) as before we find for the computed value of the heat of dissociation of H_2 $I_D = 4 \cdot 450 \pm 0 \cdot 03$ volts. This agrees with Witmer's value (4·34) to the accuracy attributed to it by Dieke and Hopfield (0·1 volt) so that we may claim to have a very good confirmation of the wave-mechanics.

---

* 'Proc. Nat. Acad. Sci.,' vol. 14, p. 12 (1928).

There is no possibility of an uncertainty of the order of 0·1 volt in the value 15·235 volts we have determined for the spectroscopic ionisation potential such as might arise for example if the $4' \rightarrow 2\,^1S$ and $3' \rightarrow 2\,^1S$ systems had been wrongly coupled together. This would require an alteration in 2 ^1S of about 800 wave-number. We have made computations of this using a number of different combinations of the various $4' \rightarrow 2\,^1S$ and $3' \rightarrow 2\,^1S$ systems and none of them, even the most improbable ones, causes a change which approaches such an amount. If there is such a misfit, it must be either in the theory or in the other data.

There is still one small matter left to be cleared up. We seem to have calculated two discrepant values of the spectroscopic ionisation potential 15·381 volts by treating the spectroscopic data by the formulæ of the old quantum mechanics and 15·235 volts by the formulæ of the wave-mechanics. These values, however, have led to the same value of the heat of dissociation of H_2 to the accuracy of the wave-mechanics computations. There is no discrepancy here, because only one of the two is actually the ionisation potential; it is the higher value 15·381. The lower value is the work to remove an electron from unexcited H_2 in such a way as to leave H_{2+} without vibrational energy. On the wave-mechanics this is not the condition of normal unexcited H_{2+} which has an additional half quantum of vibrational energy. The difference of these quantities should therefore be equal to this zero point energy. Actually it is 0·146 volts which is the value we found for this zero point energy on p. 486.

The method of calculating the zero point energy of the molecule ion on p. 486 rests, in general, on a broader basis than that there given. Strictly it does not require to rest on the assumption that both the ν_es got by the old quantum formulæ and by those of the wave-mechanics follow a *Rydberg* formula but it requires that they both follow some formula of the type

$\nu_e = f(m'') - f(m')$ where $f(m')$ tends to zero as the current electronic quantum number $m' \to \infty$. In the present case where we have only two electronic upper levels no doubt consistent results would not have been obtained unless the Rydberg formula were rather close to the correct form.

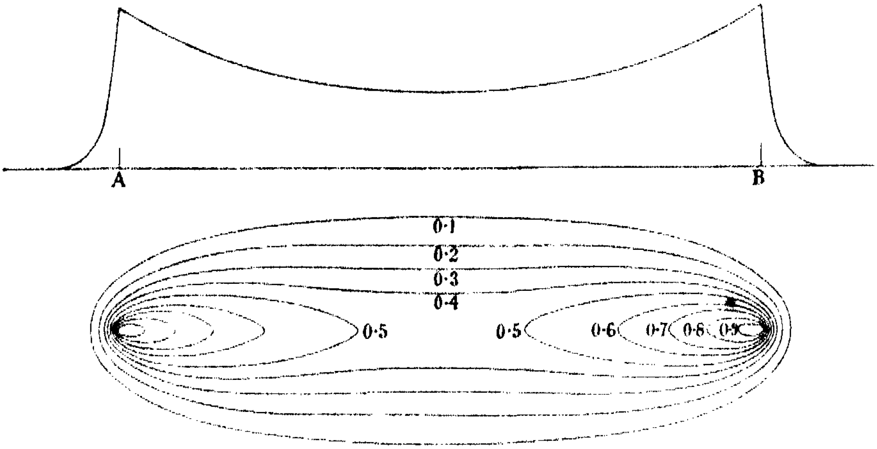

FIG. 6A.

We have taken the liberty of appending (fig. 6A) a copy of Burrau's diagram of the configuration of mean electric density (or the statistical distribution of electrons) in the neighbourhood of the nuclei of the hydrogen molecule ion which is strongly supported by the results of the present paper. The maximum electric density, which occurs at the nuclei, is given the arbitrary value 1 and the curves of equal density for densities equal to 0·9, 0·8, etc., down to 0·1 for any plane through the internuclear axis are shown in the lower part of the figure. In the upper part the positions of the nuclei are indicated by A, B and the ordinates of this curve give the density at various points on the nuclear axis taken as abscissæ.

[*Added in proof.*—In view of the excellent agreement with Burrau's calculated results for the hydrogen molecule ion it seems appropriate to combine them with the spectroscopic value of the ionisation potential here found, so as to obtain an improved determination of the heat of dissociation of H_2. This yields the value $4 \cdot 46_5 \pm 0 \cdot 04$ volts given in the synopsis.]

The Wave Equation in Five Dimensions.

By J. W. Fisher, Ph.D., Wheatstone Laboratory, King's College, London.

(Communicated by O. W. Richardson, F.R.S.—Received January 21, 1929.)

It is well known that the primary object of introducing a 5-dimensional relativity scheme is to enable the paths of all particles, charged or uncharged, to be represented by the geodesics of the space. Having selected suitable forms for the coefficients of the fundamental tensor $\gamma_{\mu\nu}$ to satisfy this requirement, we proceed to write down, in the appropriate tensor form, the well-known wave equation for a changed particle. Now the 4-dimensional form of this equation is certainly not a simple one, and, if the physical world is really based on a 5-dimensional scheme, we should naturally expect that such a fundamental equation would have a particularly simple mathematical form, and the form which is naturally suggested is

$$\text{div grad } \psi = 0. \tag{1}$$

The components of the fundamental tensor can be written*

$$\left.\begin{array}{c} \gamma_{ik} = g_{ik} + \gamma_{55}\,\alpha^2\phi_i\,\phi_k\,; \qquad \gamma_{5i} = \alpha\gamma_{55}\phi_i \\ \gamma^{ik} = g^{ik}; \quad \gamma^{5i} = -\alpha\phi^i; \quad \gamma^{55} = \alpha^2\phi^i\phi_i + \dfrac{1}{\gamma_{55}} \end{array}\right\}, \tag{2}$$

with γ_{55} and α both constant (independent of x) and

$$|\gamma_{\mu\nu}| = \gamma_{55}\,|g_{ik}|,$$

ϕ_i denotes the electromagnetic 4-vector potential. If now we suppose that all quantities, except ψ, are independent of x^5 and, moreover, that the dependence of ψ on x^5 is expressed by

$$\frac{\partial\psi}{\partial x^5} = \frac{2\pi i}{h}\,p_5\psi, \tag{3}$$

we easily deduce that

$$\pentagon\psi = \text{div grad } \psi = \Box\psi - \frac{4\pi i}{h}\,\alpha p_5\phi^i\,\frac{\partial\psi}{\partial x_i} - \frac{4\pi^2}{h^2}\left(p_5{}^2\alpha^2\phi^i\phi_i + \frac{p_5{}^2}{\gamma_{55}}\right)\psi,$$

remembering that

$$\frac{1}{\sqrt{g}}\,\frac{\partial}{\partial x_i}\,(\sqrt{g}\phi^i) = 0. \tag{4}$$

---

* O. Klein, 'Z. Physik,' vol. 46, p. 188 (1927).

Now the conventional wave equation for a charged particle in 4-dimensions is

$$\Box\,\psi - \frac{4\pi i}{h} e\phi^i \frac{\partial\psi}{\partial x_i} - \frac{4\pi^2}{h^2}(e^2\phi^i\phi_i - m_0^2c^2)\,\psi = 0. \tag{5}$$

We have written e instead of the usual e/c since we take the unit of e $1/\sqrt{4\pi}$ times the ordinary electromagnetic unit. Thus it is clear that we must choose

$$p_5 = e/\alpha\,; \quad p_5^2/\gamma_{55} = -\,m^2c^2 \quad \text{or} \quad p_5 = imc\sqrt{\gamma_{55}}. \tag{6}$$

This leads to a value of α which includes e, m, viz. :—

$$\alpha = e/imc\sqrt{\gamma_{55}}. \tag{7}$$

The constant γ_{55} remains arbitrary. This interpretation differs of course from that hitherto assumed and will require further consideration. It does, however, have the great advantage that we have now done away with the right-hand side of our wave equation, which is thus reduced to the simple form div grad $\psi = 0$, with the ordinary interpretation of the operation div in a 5-space. An important consequence of (7) is that the components of the fundamental tensor are not only functions of the co-ordinates, but depend also on the nature of the particle used to explore the field. This idea differs from that inherent in the classical field theories, in which the field at any point is regarded as being uninfluenced by the nature of the test particle. Since, however, all our experimental verifications of geometrical principles necessarily involves the employment of particles (electrons, protons or quanta) this can hardly be regarded as an objection ; in fact it is really the most natural kind of thing to assume, since the mutual interaction is the only thing that really concerns us and this depends quite as much on the nature of the test particle as on those particles considered already present. By taking this step then we have definitely linked the geometry to the particles used to demonstrate the theorems. In Klein's theory the x^5 component of the momentum is $p_5 = e/\alpha$, but, since he regards α as a world constant, he arrives at the geodesic principle by giving different charges different momenta p_5. In our case the geodesic is different for different charges. It is only in the case of neutral particles that we revert to the old theory. The charge e in fact can be interpreted in terms of the interaction of charged particles. Ordinary space time conceptions would then have a statistical origin. Other simplifications appear if we follow out this idea. The projection $d\theta$ of the 5-dimensional world line element $d\sigma$ in the x^5 direction is given by

$$d\theta = \sqrt{\gamma_{55}}\,dx^5 + \frac{\gamma_{5i}}{\sqrt{\gamma_{55}}}\,dx^i = \sqrt{\gamma_{55}}\,(dx^5 + \alpha\phi_i\,dx^i). \tag{8}$$

Now a simple calculation shows that in order to make the 4-dimensional path agree with the 5-dimensional geodesics we must take

$$\frac{d\theta}{ds} = \frac{e}{\alpha\sqrt{\gamma_{55}}\,mc}, \tag{9}$$

where ds is the 4-dimensional line element. This, combined with (7), gives

$$d\theta = i\,ds. \tag{10}$$

Now it is easy to see that

$$d\sigma^2 = \gamma_{\mu\nu}\,dx^\mu\,dx^\nu = d\theta^2 + ds^2, \tag{11}$$

and so we arrive at the significant result

$$d\sigma = 0, \tag{12}$$

in other words, the world lines of all particles, charged or uncharged, are null geodesics in the 5-space, just as those of light are null geodesics in the 4-space time. Moreover, it is essential that we should choose $\frac{d\sigma}{ds} = \text{const.} = \frac{\mathrm{I}}{m}$, say, and it is the invariant I which, in 5 dimensions, plays an analogous rôle to that of m in space time. We see from (11) and (9) that

$$\mathrm{I}^2 = m^2 + e^2/\alpha^2\gamma_{55}c^2 = 0, \tag{13}$$

again a striking result. The 5-vector momentum is defined by $\mathrm{P}_\mu = \mathrm{I}\gamma_{\mu\nu}\frac{dx^\nu}{d\sigma}$, and the components are all finite since both I and $d\sigma$ are zero ; we find at once

$$\mathrm{P}_k = mg_{ki}\frac{dx^i}{ds} + \frac{e}{c}\phi_i \text{ as in 4-dimensions,}$$

$$\mathrm{P}_5 = imc\sqrt{\gamma_{55}}. \tag{14}$$

In short we may say that in the 5-space everything has become a radiation problem, for the wave equation has the same form as that of light in space-time, and in both cases the line elements vanish. A third point of resemblance is to be found in the fact that I vanishes, for we derive the wave equation $\Box\,\psi = 0$ for light if we make m (and, of course, e) zero in the Schrödinger equation (5). Consequently the vanishing of I constitutes a third point of resemblance between the ψ equation in 5 dimensions and the equation for radiation in 4 dimensions. The light quantum must be regarded as having zero mass but, of course, a finite momentum $h\nu/c$. We must now return to an important consequence of (7) and (2). The contravariant components of the 5-dimensional curvature tensor are* :

$$\left.\begin{aligned} P^{ik} &= R^{ik} - \tfrac{1}{2}\gamma_{55}\alpha^2 F^{\alpha i}F_\alpha{}^k = R^{ik} + \tfrac{1}{2}\frac{e^2}{m^2c^2}F^{\alpha i}F_\alpha{}^k \\ P^{5i} &= \tfrac{1}{2}\alpha F^i - \alpha\phi_k P^{ik} = \frac{ic}{mc\sqrt{\gamma_{55}}}(\phi_k P^{ik} - \tfrac{1}{2}F^i) \\ P_i{}^k &= R_i{}^k - \tfrac{1}{2}\frac{e^2}{m^2c^2}F_i{}^a F_a{}^k - \tfrac{1}{2}\frac{e^2}{m^2c^2}\phi_i F^k \\ P_5{}^i &= \frac{e}{2imc}\sqrt{\gamma_{55}}\,F^i \\ P\ &= R + \tfrac{1}{4}\frac{e^2}{m^2c^2}F \end{aligned}\right\}, \tag{15}$$

where $F = \text{rot}\,\phi$ and $F^i = \text{div}^i F^{ik}$. The R's refer to the 4-dimensional components. Now it will be seen that for a neutral particle, or for a charged one in no electric field, the P^{ik} are the only non-vanishing components, and they are equal to the R^{ik} so that, under these conditions, we can adopt the usual Einstein equations, viz.,

$$R^{ik} - \tfrac{1}{2}g^{ik}R = \kappa(T^{ik} + S^{ik}).$$

Now, in order to obtain neutral matter, we are compelled to consider macroscopic processes and, since an atom behaves macroscopically as a neutral mass particle, we are at liberty to use it as a whole to define the 4-dimensional geometry as required by the general theory of relativity. Although the fifth dimension does not in this case complicate the curvature tensor there is still a motion in the fifth dimension since $p_5 \neq 0$. In Klein's theory there is no resultant momentum in the x_5 direction for a neutral mass owing to the zero total charge, but in that case the components of a neutral atom would have x_5 momentum components of opposite signs and the atom would not remain within finite limits in the 5-dimensional world. This consequence is avoided by the present scheme. The fifth co-ordinate seems to be of especial importance when charges are present in electric fields. It is difficult to conceive of any geometrical scheme of this kind within the atom itself; in order to define the curvature at a certain point (or rather small region) it is necessary to imagine some cyclic displacement of a vector in that region and, consequently, a corresponding displacement of the particle with which the vector is associated. If the particle is to be neutral, in order to fit in with the old relativity scheme, the dimensions of the displacement must be large compared with those of the particle, *i.e.*, the atom. We can no longer, following Rosenfeld and Klein, identify $-\gamma_{55}\alpha^2$, which in our case becomes e^2/m^2c^2, with $16\pi G/c^2$, G being the gravitation constant, since e^2/m^2c^2 is no longer a world constant for all particles ; in fact it seems unlikely that the 5-dimensional curvature can be expected to introduce the value of G. By analogy with the case of the electromagnetic energy tensor of radiation in 4-dimensional relativity, which contributes nothing to the curvature tensor when no charges are present, we might be tempted to set $P^{\mu\nu} = P = 0$, which for a charged particle would lead to $R = -\frac{1}{4}\, e^2/m^2c^2\, F$, so that for such a particle the 4-dimensional curvature scalar would be slightly different from zero.

---

* Rosenfeld, 'Bull. Acad. R. Belg.,' vol. 13, p. 304 (1927).

We have seen that there is a striking analogy between the equations for radiation in ordinary space time and the wave equation for a single particle in the 5-space. We know, however, that the equation for light is not a scalar one ; it can be regarded as an equation for the 4-vector ϕ_i, or as that satisfied by the antisymmetric tensor F_{ik}. The tensor forms are not quite the same, however, for, in an infinite world, we have*

$$\Box\, F_{ik} = 2R_{ikmn}F^{mn},$$

while ϕ_i satisfies the equation $\Box\, \phi_i = 0$. As Eddington points out, the latter is not physically important, since it involves the arbitrary convention $(\phi^k)_k = 0$, a relation already used in the deduction of the wave equation (4). Without entering any further into this question we may note that the correspondence between the radiation equation and the single particle wave equation strongly suggests the possibility of introducing a 5-dimensional (tensor) analogue of the more fundamental Maxwell equations. Such first order equations might be capable of expressing the quantum behaviour of several electrons, including the "spin," the successful treatment of which depends, in all probability, on the choice of a suitable notation, such as that introduced by Eddington. The five perpendicular matrices occurring in his equation are, however, of four rows and columns since they arise as products of 4-point matrices. This, together with the fact that rotations in the associated 5-space correspond to a rotation of half as much in the original 4-space, forms the basis of the numerical success of his theory. It is not easy to see how this can be arranged for in a purely 5-dimensional theory.†

---

* Eddington, 'Mathematical Theory of Relativity," p. 176.

† I wish to acknowledge my indebtedness to Dr. Flint for many helpful discussions on this subject.

The Structure of the Benzene Ring in $C_6(CH_3)_6$.

By KATHLEEN LONSDALE, D.Sc. (London), Amy Lady Tate Scholar.

(Communicated by R. Whiddington, F.R.S.—Received January 25, 1929.)

Since benzene itself is not crystalline at ordinary temperatures the study of the benzene nucleus or ring has had to be referred to certain of its derivatives. The most hopeful line of attack appeared to be in the direction of the fully substituted derivatives, such as C_6Cl_6, or else by way of compounds such as naphthalene and anthracene which contain more than one ring. The results so far obtained, however, have only shown that the ring is centro-symmetrical,* a fact confirmed by the recent examination of crystalline benzene itself,† that its approximate width (given by the difference in lengths of the naphthalene and anthracene molecules) is 2·49 Å.,‡ and that there exist in the nucleus two periodicities of about 1·28 and 2·66 Å.§

If the ring be supposed to consist of six carbon atoms of diameter 1·54 arranged as in the diamond pattern,|| then periodicities of 1·26 and 2·52 would exist, the width of the ring itself being 2·52. If, on the other hand, the benzene nucleus is a plane ring of six carbon atoms of diameter 1·42, such as occurs in the graphite structure,¶ then the periodicities would be 1·23 and 2·46, the width of the ring being 2·46 (fig. 1). The experimental observations (*loc. cit.*) could not definitely decide between these alternative structures, and no other criterion was found which would distinguish with certainty between a puckered and a plane ring. One of the chief difficulties encountered in the study of these various benzene derivatives was that the unit cell invariably contained more than one

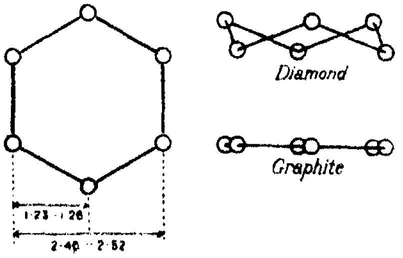

FIG. 1.

---

* Mark, 'Ber. Deut. Chem. Ges.,' vol. 57, p. 1820 (1924); Plummer, 'Phil. Mag.,' vol. 50, p. 1214 (1925).

† Cox, 'Nature,' vol. 122, p. 401 (1928).

‡ W. H. Bragg, 'Proc. Phys. Soc.,' vol. 34, p. 33 (1921).

§ W. H. Bragg, 'Z. Krist.,' vol. 66, p. 22 (1927).

|| W. H. and W. L. Bragg, 'X-rays and Crystal Structure,' p. 99 (4th edition, 1924).

¶ Hassel and Mark, 'Zeit. Phys.,' vol. 25, p. 317 (1924); Bernal, 'Roy. Soc. Proc.,' A, vol. 106, p. 749 (1924).

molecule, a fact which necessarily complicated any structure determination by introducing the question of relative orientations.

Hexamethylbenzene, $C_6(CH_3)_6$, proved to be free from this difficulty. The unit cell was found to be triclinic and contained one molecule only.

Experimental Investigation.

After purification the crystals melted at 164° C. Flat prisms were obtained on recrystallisation from benzene, and the measured density of these was 1·042 grs./c.c. at 18·5° C. The prisms as a rule showed only three pairs of faces (fig. 2), there being a good cleavage parallel to one of these pairs. No previous crystallographic data were available, so that all measurements were made directly on the ionisation spectrometer using a Coolidge tube with a Mo anticathode. All three crystal faces gave excellent reflections on the ionisation spectrometer; they were therefore provisionally adopted as axial planes. The tabular face of the prism was called (100), the cleavage plane (001) and the remaining side plane (010). It was found that the unit cell thus defined contained one molecule of $C_6(CH_3)_6$, and that in every case the spacings calculated agreed with the observed spacings. Well over 100 reflections were observed in five different zones, and no plane was found to have a spacing which was a multiple of that calculated. Nor were any sub-multiple spacings found, except of course in the case of higher order reflections from planes whose first orders had actually been observed. The unit cell chosen is therefore one of the infinite number of possible minimum cells, and subsequent calculations have shown that structurally the cell is a reasonable one. Mean values of the axial spacings can be calculated by using all the observed spacings and angles. These are given below and compared with those directly measured.

(*h k l*).	Mean observed spacing.	Direct measurement.	Measured angles between axial planes.
	Å		
100	7·736	7·733	010 : 001 = 129° 18′
010	6·008	6·012	001 : 100 = 80° 48′
001	3·694	3·695	100 : 010 = 74° 0′

The measured angles between planes generally agreed with those calculated from the above data to within 5′. The observed data lead to a value of

1·035 grs./c.c. for the density. The lengths of axes and the axial angles calculated from the mean observed data are (fig. 2):—

$a = 9{\cdot}010$ Å.	$\alpha = 44° 27'$
$b = 8{\cdot}926$	$\beta = 116° 43'$
$c = 5{\cdot}344$	$\gamma = 119° 34'$

$$a : b : c = 1{\cdot}0095 : 1 : 0{\cdot}5987.$$

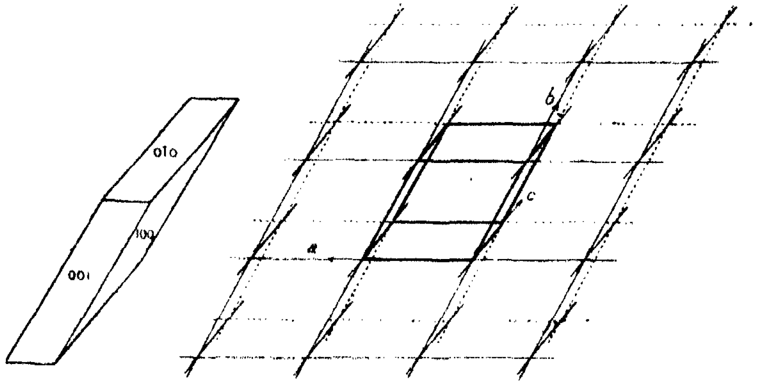

Habit. Lattice.

Fig. 2.

The space-group is either C_1^1 or C_i^1, the molecule being either asymmetrical or centro-symmetrical. As far as external symmetry is concerned, the crystals appear to possess centro-symmetry, and this fact, combined with the knowledge that C_6H_6, C_6Cl_6 and C_6Br_6 are all centro-symmetrical, would make it appear probable that $C_6(CH_3)_6$ is also centro-symmetrical. The crystals are easily deformed by slipping about any of the crystallographic axes. In this respect also they are similar to other fully-substituted benzene derivatives.

Structure Investigation.

It appears from the observations that *a* and *b* are equal to within 1 per cent. and that the angle between them is nearly $2\pi/3$. This fact at once suggested that it would be worth while to examine the [001] zone for any evidence of hexagonal structure. The planes observed in that zone were divided into three groups:—

(1) Planes ($h\,k\,0$) lying in the acute angle between (100) and (010), *e.g.*, (310) (130).

(2) Planes $(k\,\overline{h+k}\,0)$ lying in the acute angle between $(0\bar{1}0)$ and $(1\bar{1}0)$, *e.g.*, $(1\bar{4}0)$ $(3\bar{4}0)$.

(3) Planes $(\overline{h+k}\,h\,0)$ lying in the acute angle between $(\bar{1}10)$ and $(\bar{1}00)$, *e.g.*, $(\bar{4}30)$ $(\bar{4}10)$.

In spite of the equality of *a* and *b*, corresponding planes obtained by successive rotations through (approximately) $\pi/3$, such as (310) $(1\bar{4}0)$ $(\bar{4}30)$, show considerable divergence of spacing, because of the obliquity of the *c* axis to the (001) plane. It was necessary, therefore, to compare not intensities but structure factors for each of these series of planes. The structure factors S were obtained from the observed intensities I by means of the formula

$$S \propto \sqrt{I} \div \left(\Sigma F e^{-M} \times \sqrt{\frac{0 \cdot 15 + \cos^2 2\theta}{\sin 2\theta}}\right)$$

where $(0 \cdot 15 + \cos^2 2\theta)$ is a measure of the polarisation factor for MoKα radiation under the conditions of the experiment.*

F is the scattering power of the atom,

e^{-M} is the temperature factor.

Now to a first approximation the effect of the hydrogen atoms must be neglected and therefore the value of Fe^{-M} taken applies to carbon atoms only. Miss Knaggs, of the Davy Faraday Laboratory, very kindly supplied me with some unpublished data concerning the temperature factors for graphite and diamond. She found that for diamond no change either of spacing or of intensity could be observed after a decrease in temperature from 15° C. to − 183° C. This result agrees with previous high temperature observations by Backhurst† and low temperature observations by Ehrenburg, Ewald and Mark‡ on various planes of diamond. Similar measurements made by Backhurst on the (0001) cleavage plane of graphite showed a decrease of intensity of about 10 per cent. over a range of 900° upwards from room temperature. Miss Knaggs, however, found that not only were the absolute measurements of intensity for that plane identical, within the limits of experimental error, at 15° C. and at −183° C., but that the relative intensities of all orders up to the fourth were also the same at the two temperatures. She agreed with Backhurst in finding an abnormally large coefficient of expansion perpendicular to the (0001) plane of graphite. These observations show that the temperature factor for carbon can safely be neglected.

---

* Bishop, 'Phys. Rev.,' vol. 28, p. 625 (1926); Kirkpatrick, 'Phys. Rev.,' vol. 29, p. 632 (1927).

† 'Roy. Soc. Proc.,' A, vol. 102, p. 340 (1922).

‡ 'Z. Krist.,' vol. 66, p. 547 (1928).

A difficulty arose in the evaluation of F. It was found that when the structure factors were calculated using Ponte's* F curve, derived from measurements on diamond, the results so obtained were still slightly dependent upon the angle of deviation. This is also true of the observations on graphite recorded by Bernal (*loc. cit.*). Although other considerations have shown rigorously† that the carbon atoms in graphite all lie in the (0001) planes, yet the structure factors deduced for the various orders of reflection from that plane are *not* equal, if Ponte's F curve is adopted, but exhibit a regular falling off with increased angle of diffraction. Moreover, Ponte himself mentions that his one observation on graphite leads to a value of F_c not on his curve, and suggests that F_c may decrease more rapidly with sin θ for graphite than for diamond. An attempt to obtain an F curve more applicable to this compound was therefore made as follows: the observations of the relative intensities of five orders of graphite (0001) are recorded by Bernal as

$$100 : 12\cdot4 : 2\cdot0 : 0\cdot4 : 0\cdot08 : 0.$$

Now according to Ponte the absolute value of F_c corresponding to the first of these is 3·4, and the structure of graphite is such that the structure factors calculated from each of the orders should be the same. Hence since

$$S_{0001} \propto \sqrt{I} \div \left(F_c \times \sqrt{\frac{1 + \cos^2 2\theta}{\sin 2\theta}}\right), \text{ approx.,}$$

we see that

$$\frac{F_c^{000n}}{F_c^{0002}} = \sqrt{\frac{I_n}{I_2} \times \frac{1 + \cos^2 2\theta_2}{1 + \cos^2 2\theta_n} \cdot \frac{\sin 2\theta_n}{\sin 2\theta_2}},$$

$$F_c^{000n} = \frac{3\cdot4}{10} \sqrt{I_n \times \frac{1 + \cos^2 2\theta_2}{1 + \cos^2 2\theta_n} \cdot \frac{\sin 2\theta_n}{\sin 2\theta_2}}.$$

Thus the lower curve shown in fig. 3 was obtained. It is not claimed that this is necessarily a true F curve for graphitic carbon, but only that under the given experimental conditions it represents the falling off of scattering power with sin θ.

Since we do not know whether the carbon atoms in $C_6(CH_3)_6$ behave like those in diamond or in graphite, two sets of structure factors have been calculated using each of the above curves. These may be regarded as limiting values of the structure factors for the given planes. However, the use of the "graphite" F values practically removed the dependency on angle previously

---

* 'Phil. Mag.,' vol. 3, p. 195 (1927).

† Ott, 'Ann. Physik,' vol. 85, p. 81 (1928).

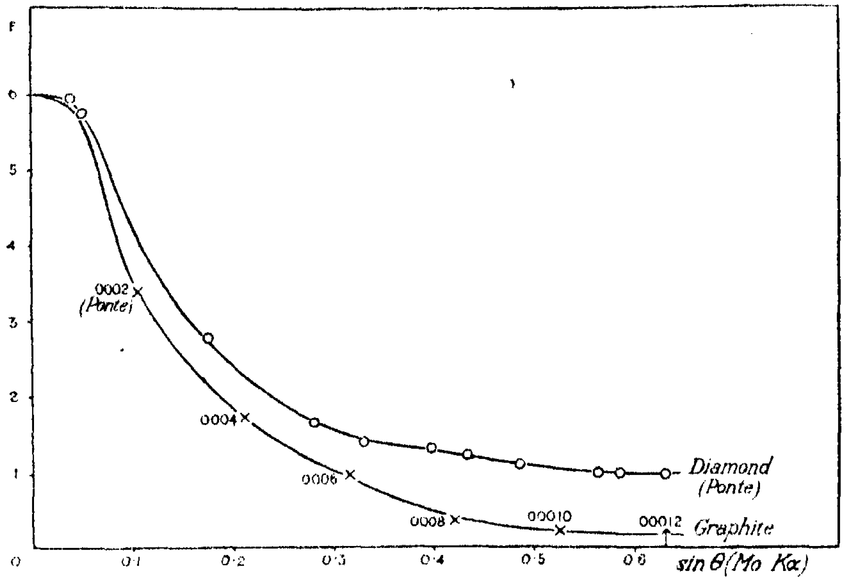

FIG. 3.—F : sin θ (MoKα).

remarked, and therefore it is likely that they represent the variation in scattering power most closely. The series of "observed" structure factors thus obtained for each of the three groups of planes are shown graphically in fig. 4.

The curves given are based on the behaviour of graphite. The crosses show the structure factors calculated on the behaviour of diamond. The difference is not great except in the case of small-spacing planes. When no reflection was found from the plane in question an arrow is drawn, the height of which represents the structure factor corresponding to the minimum observable intensity. The actual structure factor for the given plane must then lie somewhere along the arrow and cannot be greater than the height of the arrow. For the sake of comparison, similar arrows are shown for planes whose reflections were more intense than this minimum value. The height of the arrow is obviously an inverse measure of the spacing of the plane, and the ratio of the observed structure factor to the height of the arrow is a measure of the probable accuracy of the factor. The intensities used are not absolute values, but are merely the "peak" value of the intensity for each reflection, relative to that of (001). Owing to the extreme softness of the crystals it was not possible to obtain any required section, and the shape of the crystal has undoubtedly influenced the relative intensities to a certain extent. In spite of this, a remarkable similarity is at once observable between the three groups

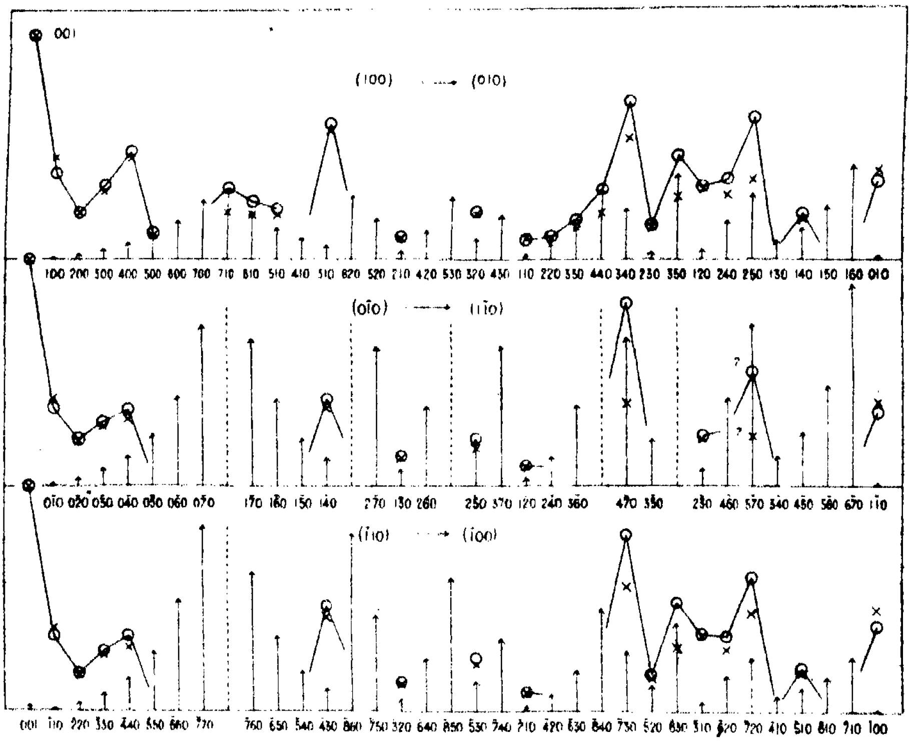

Fig. 4.

of structure factors. This indicates most clearly a hexagonal arrangement of atoms in the [001] zone.

The reflections from the (001) cleavage plane were also of great interest. It was found that the intensities fell off regularly in the first four orders, no further orders being observable. The relative values were

$$100 : 9 \cdot 51 : 1 \cdot 87 : 0 \cdot 29 : < 0 \cdot 08 : < 0 \cdot 08.$$

Using the "diamond" and "graphite" F values respectively, the corresponding structure factors are proportional to

$$\begin{array}{ccccccccccc} 2 \cdot 21 & : & 1 \cdot 93 & : & 1 \cdot 71 & : & 1 \cdot 10 & : & < 0 \cdot 89 & : & < 1 \cdot 35 \\ \downarrow & & \downarrow & & \downarrow & & \downarrow & & \downarrow & & \downarrow \\ 2 \cdot 64 & : & 2 \cdot 45 & : & 2 \cdot 65 & : & 2 \cdot 52 & : & < 3 \cdot 28 & : & < 7 \cdot 01 \end{array}$$

It is clear that there is a marked similarity between the reflection from this plane and those from the corresponding cleavage plane of graphite. Moreover, the structure factor obtained from the observations is larger than that for any other plane in the crystal. These two facts combine to prove that the carbon atoms, at least, all lie in or near the (001) planes. The question now arises : How near do they lie ? An answer to this question is best attempted after the approximate positions of the atoms have been found.

Location of the Carbon Atoms.

It has been mentioned above that the structure factor for (001) was the largest observed. The factors for the planes (340) $(\bar{4}70)$ and $(\bar{7}30)$ are, however, almost as large. This is very important, because these are small-spacing planes, and therefore any deviation of the atoms away from these planes will cause a more rapid falling off of structure factor than would a similar movement away from a plane of larger spacing. In other words, the exceptionally large factors observed for these planes prove that the carbon atoms must lie at or very near their intersections with one another. There are 36 such intersections in the unit cell (fig. 5) and only 12 carbon atoms for which to find places. The problem is considerably simplified by the fact, already demonstrated, that there is a hexagonal arrangement of atoms in the [001] zone. If it can be shown which two of the positions 1—6 in one sector are occupied by carbon atoms, then the positions of the remaining ten carbon atoms automatically follow. Fifteen possibilities present themselves if only two out of six positions are to be filled. It is a simple matter to calculate structure factors for, say, the first six orders of the (100) plane for each of these possibilities. These calculations are shown graphically in fig. 6.

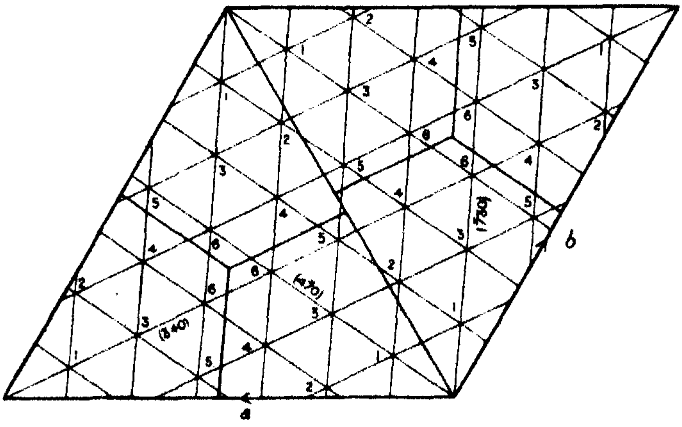

FIG. 5.

It will be seen that only one arrangement fulfils the necessary conditions, namely, that the second, fifth and sixth orders should all be smaller than the first, third and fourth (compare observed factors in fig. 4). This arrangement involves the placing of carbon atoms in the positions 1 and 3, and the ten corresponding positions obtained by rotation through $2\pi/6$ in the (001) plane, about the c axis (fig. 7).

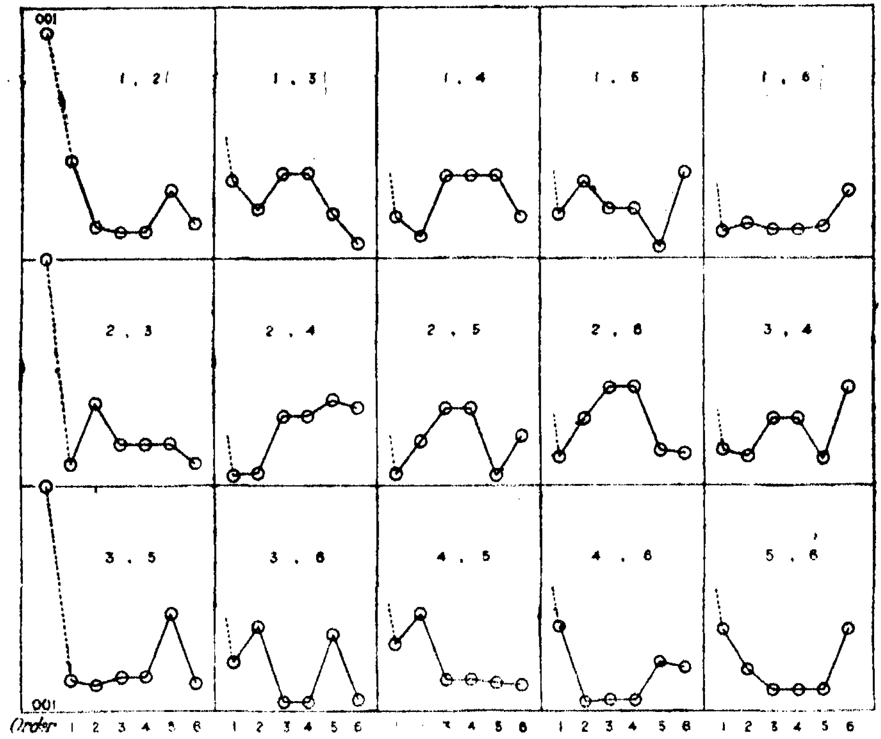

FIG. 6.

A number of important deductions can be made even from this approximate result:—

(1) *The molecule exists in the crystal as a separate entity.*

(2) *The benzene carbon atoms are arranged in ring formation.*

(3) *The ring is hexagonal or pseudo-hexagonal in shape.*

These facts have been believed by chemists for a long time and nearly all the models which have been suggested have conformed to these rules; but so far no aromatic substance except the one under investigation has had a simple enough structure for the positions of the separate atoms to be found *without* any previous hypotheses as to the shape or size of the molecule. The above reasoning, in fact, supplies a definite proof, from an X-ray point of view, that the chemist's conception of the benzene ring is a true representation of the facts.

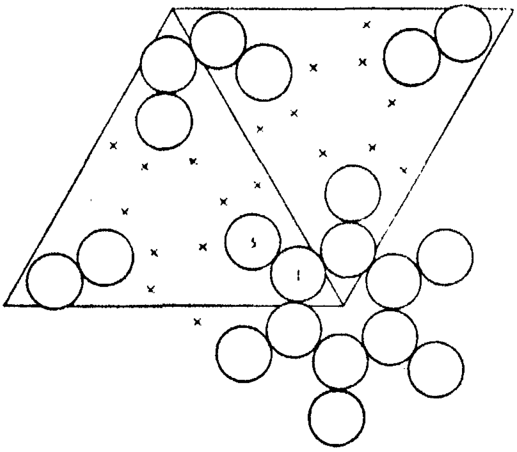

FIG. 7.

The mean distance from centre to centre of adjacent carbon atoms in the molecule is 1·48 Å. (The slight difference between *a* and *b* and the deviation of γ from 120° of course involves a slight variation in the distances from one intersection to another.) This distance is a mean of the carbon diameters in diamond (1·54) and in graphite (1·42). We must now see whether the carbon atom positions and the consequent diameters can be found more exactly.

The carbon atoms have been placed at such of the intersections of (340) $(4\bar{7}0)$ $(\bar{7}30)$ and (001) that they actually lie along the lines

$$\left.\begin{aligned} 3x/a + 4y/b &= 0 \\ 4x/a - 7y/b &= 0 \\ -7x/a + 3y/b &= 0 \end{aligned}\right\} \qquad \text{(A)}$$

at distances of about 1·48 and 2·96 from the origin. Three kinds of variation from these positions are now to be investigated :—

(1) A motion away from or towards the origin along the lines A, *i.e.*, a variation in the atomic diameters and consequently in the size of the ring.

(2) A variation in the directions along which the atoms lie, *i.e.*, a rotation of the ring as a whole in the (001) plane.

(3) Shifts of the atoms perpendicular to the (001) plane, *i.e.*, a puckering of the benzene ring and side-chain carbon atoms.

The effect of each kind of variation upon the structure factors is best shown graphically.

Result of Variation in Atomic Diameters.

The co-ordinates of the points of intersection at which the carbon atoms lie are :—

Aromatic : $(\mp \tfrac{7}{37}a \pm \tfrac{4}{37}b\ 0)$ $(\pm \tfrac{3}{37}a \pm \tfrac{7}{37}b\ 0)$ $(\mp \tfrac{4}{37}a \pm \tfrac{3}{37}b\ 0)$

Aliphatic or side-chain : $(\pm \tfrac{14}{37}a \pm \tfrac{8}{37}b\ 0)$ $(\pm \tfrac{6}{37}a \pm \tfrac{14}{37}b\ 0)$ $(\mp \tfrac{8}{37}a\ \tfrac{6}{37} \pm b\ 0)$

Their exact distances from the origin are 1·488, 1·472, 1·472, 2·976, 2·944, 2·944. For purposes of calculation it is much easier to leave the distances in these proportions than to make them exactly equal. The effect of this approximation upon the structure factors is negligible at the present stage. Fig. 8 (*a*) is a composite curve showing the "observed" structure factors obtained by taking the mean of the three curves given in fig. 4. Where no reflection was observed, the arrow given is that corresponding to the smallest of the three arrows, and the structure factor must be understood to be less than that amount. The structure factors for the planes (100) → (010) [or $(0\bar{1}0) \rightarrow (1\bar{1}0)$, or $(\bar{1}10) \rightarrow (\bar{1}00)$] have been calculated on the assumption that the atoms lie in the above initial positions and the resulting curve is shown in fig. 8 (*b*). The (001) values are also shown in each case, and for the sake of comparison the calculated and observed structure factors have been made to correspond for this one plane, since the observations are entirely relative. The following curves (*c*)–(*h*) show typical results of variation in the distance of the atoms from the origin. Actually a considerably larger parameter range was tested in order to obtain definite limits for the possible values of the radii. The agreement is clearly much better when the diameter of the aromatic carbon atom is less than 1·48 (*e*) (*f*) than when it is greater (*c*) (*d*). If, however, the diameter is decreased too much obvious discrepancies begin to appear. As suggestions have recently been made* that the diameter of carbon in organic compounds may be as small as 1·30, curves (*g*) and (*h*) have been given, in the first of which the aromatic carbon diameter is 1·42 and the aliphatic 1·30, and in the second the diameters of both aromatic and aliphatic carbon atoms are 1·30. The agreement in the first case is distinctly poor, and the second is quite out of the question. The best agreement is obtained when the diameter of aromatic carbon is 1·42 ± 0·03 Å. and that of the side-chain (aliphatic) carbon 1·54 ± 0·12 Å. Thus *the aromatic carbon atom is of the same*

---

* **Hendricks, 'Z. Krist.,' vol. 68, p. 189 (1928).**

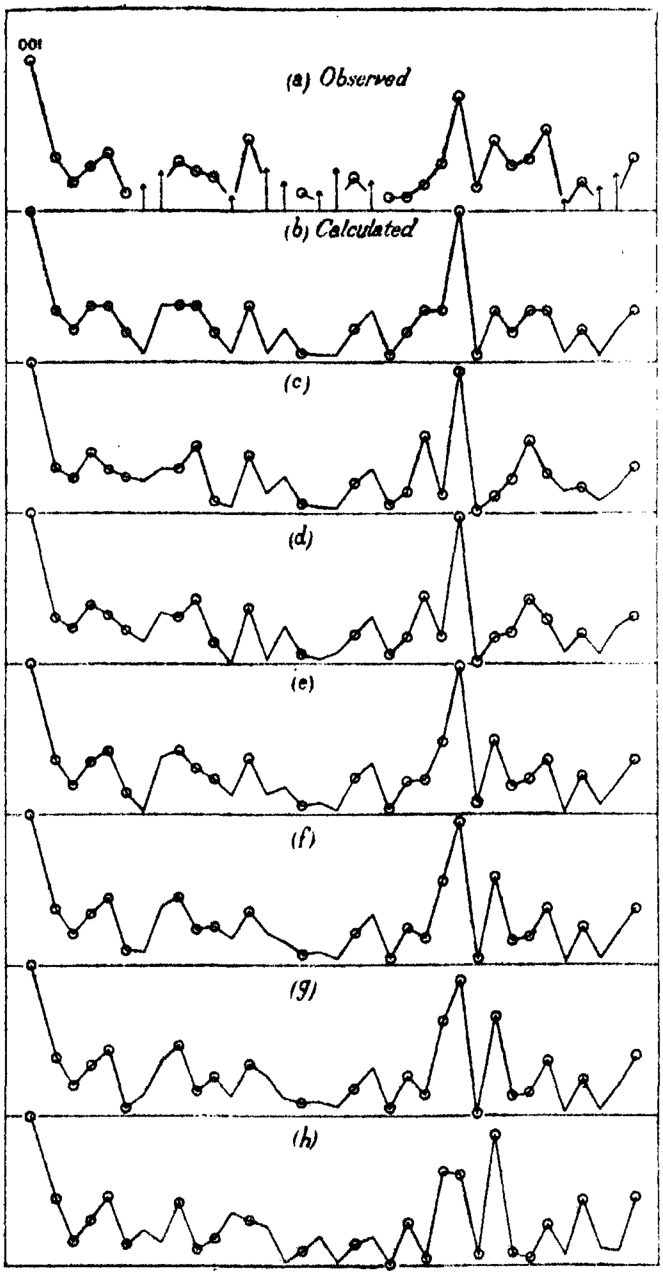

(a) Calculated from observed intensities using graphite F values.

Mean of $\begin{cases} 100 \to 010 \\ 0\bar{1}0 \to \bar{1}10 \\ \bar{1}10 \to \bar{1}00 \end{cases}$

(b) C atoms along lines $(3/a)\,x + (4/b)\,y = 0$, etc., at distances 1·48, 2·96, from origin.
(Aromatic C) $d_1 = 1{\cdot}48$
(Aliphatic C) $d_2 = 1{\cdot}48$

(c) Distances from origin 1·54, 3·08
$d_1 = 1{\cdot}54$
$d_2 = 1{\cdot}54$

(d) Distances from origin 1·54, 3·02
$d_1 = 1{\cdot}54$
$d_2 = 1{\cdot}42$

(e) Distances from origin 1·42, 2·90
$d_1 = 1{\cdot}42$
$d_2 = 1{\cdot}54$

(f) Distances from origin 1·42, 2·84
$d_1 = 1{\cdot}42$
$d_2 = 1{\cdot}42$

(g) Distances from origin 1·42, 2·78
$d_1 = 1{\cdot}42$
$d_2 = 1{\cdot}30$

(h) Distances from origin 1·30, 2·60
$d_1 = 1{\cdot}30$
$d_2 = 1{\cdot}30$

FIG. 8.

size as that in graphite. The carbon atom in the methyl group will be considered more fully at a later stage.

Result of Rotation of Ring in the (001) *Plane.*

The angle between the a axis and the line $\frac{7}{a}x - \frac{3}{b}y = 0$ is 94°. The line $\frac{2}{a}x - \frac{1}{b}y = 0$ makes an angle of 89° 46′ with a. Thus by turning the whole system of atoms in an anti-clockwise direction through 4° 14′, the molecule is brought into a " symmetrical " position, in which the a, b and [1$\bar{1}$0] directions bisect the sides of the benzene ring. As fig. 9 (a) shows, this has a disastrous effect upon the calculated structure factors. Thus the factors for (430) (340) become equal, as do also those for (310) (130); whereas observation has shown that the structure factor of (430) is small and that of (340) very large, and similarly that of (310) is fairly large and that of (130) very small. The calculated curve has been given on a basis of 1·42, 1·54 as the aromatic and aliphatic carbon diameters respectively. but the same result would apply for any other

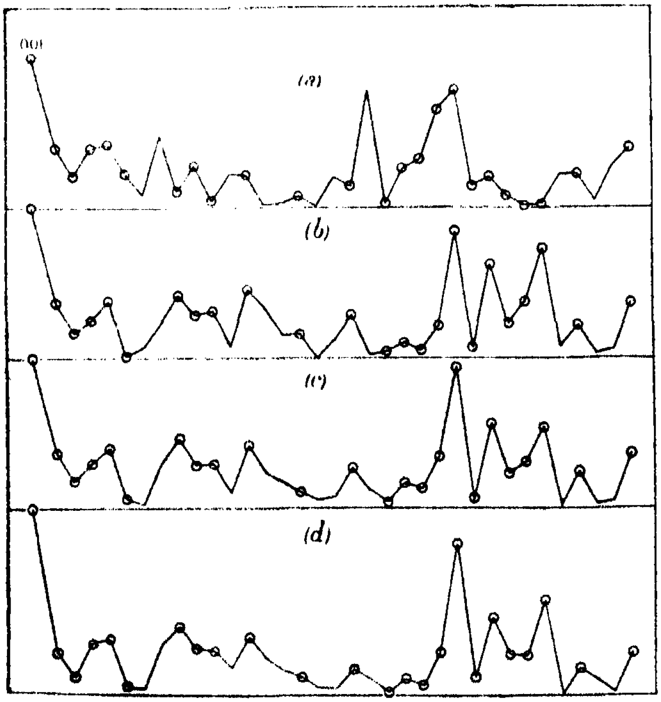

C atoms lie along line making angle θ_1 with a, θ_2 with b, and symmetrical positions, at distances 1·42, 2·90 from origin.

(a) $\theta_1 = 89° 46'$
$\theta_2 = 29° 48'$

(b) $\theta_1 = 98° 27'$
$\theta_2 = 21° 7'$

(c) $\theta_1 = 96° 30'$
$\theta_2 = 23° 4'$

(d) Same as (c) but with addition of H atoms in arbitrary positions.

Fig. 9.

figures; it is simply the effect of placing the ring symmetrically with respect to the *a* and *b* axes.

An almost equal rotation (of 4° 27′) in a clockwise direction from its initial situation will bring the ring into such a position that one of its sides is perpendicularly bisected by the *projection* of the *c* axis upon the (001) plane. It will be seen from fig. 9 (*b*) that in some respects the agreement with observation is improved by this movement, the factors for (310) and (250), for example, being increased. In other respects, however, the agreement is not so good. Fig. 9 (*c*) shows the result of a clockwise rotation of only 2° 30′, the atoms being still left at distances of 1·42, 2·90 from the origin, and this curve combines the best features of both 8 (*e*) and 9 (*b*). At this stage it was thought advisable to consider the possible effect of the neglected H atoms upon the structure factor calculations. There are 18 H atoms in the unit cell. Since their scattering power is small compared with that of the carbon atoms, the arguments used above in limiting the positions of the latter cannot be held to apply to the H atoms. They are not necessarily in or even near the (001) plane and they may not be arranged trigonally or hexagonally about the centre of the ring. In fact it does not seem feasible to attempt their exact location. An estimate of their importance may, however, be gained by placing them arbitrarily in any reasonable positions (say, by distributing them evenly about the unoccupied space in the cell) and then calculating the effect upon the structure factor curve. For example, fig. 9 (*d*) shows the result of placing all the atoms in the (001) plane and one-third of the way between nearest C atoms in neighbouring molecules (see small crosses in fig. 7). It is clear that no great errors are introduced by the neglect of the H atoms, since their arbitrary insertion in reasonable positions in the structure causes scarcely any disturbance of the agreement previously attained. Naturally, it would be possible to find positions for the H atoms which would materially upset the agreement, but such positions are special cases and the very closeness of the agreement shows that they are unlikely. Thus in fig. 9 (*d*) the factor for (001) is relatively too large, but that is because (for convenience' sake) the H atoms were given a very special position with regard to that one plane.

Result of Puckering the Ring.

That the carbon atoms must lie very near, if not in, the (001) plane, is proved not only by the large structure factor and " normal " intensity decrease for the various orders of that plane, but also by the fact that the observed structure factors for planes in general are almost independent of their last index " *l*."

Thus fig. 10 (*a*) shows the observed structure factors for the set of planes (*h l l*) and in fig. 10 (*b*) are given the observed factors for the corresponding planes (*h l* 0). The similarity is most marked.

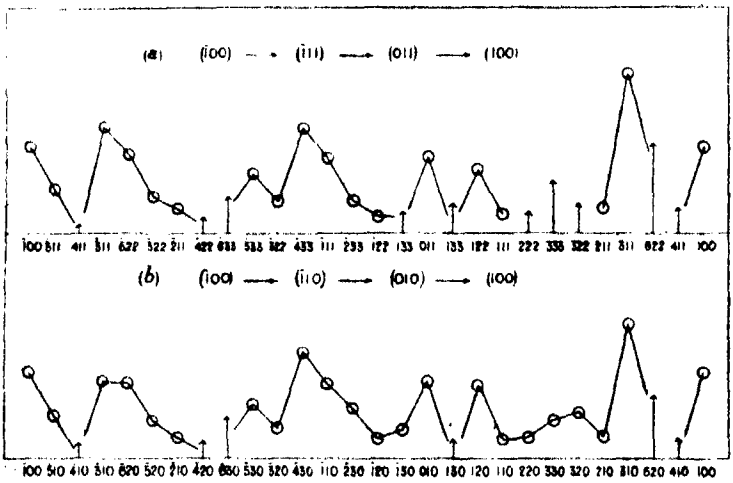

FIG. 10.

The structure factors are calculated from the assumed positions (x, y, z) of the atoms of scattering power A according to the formula

$$S = \Sigma A \cos 2\pi \left(\frac{h}{a}x + \frac{k}{b}y + \frac{l}{c}z\right).$$

Since this expression has to be very nearly independent of l, z must be zero or very near zero for all the atoms. Any puckering of the ring is bound to be shown up most clearly in the smaller spacing planes having high values of l. It will also, however, disturb the hexagonal structure in the [001] zone, as can be seen from fig. 11.

This shows the projections *along the c axis* on to the (001) plane of various

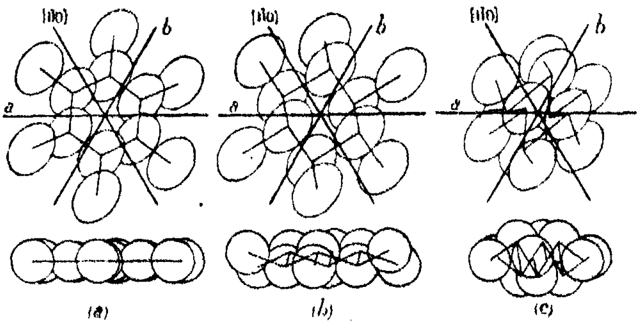

FIG. 11.

types of molecule. The spherical atoms of course project into ellipses, the ratio of the minor to the major axis being equal to the ratio of the (001) spacing to the length of the c axis. In each case the length of the minor axis is the same as the diameter of the actual atom. Only this oblique projection can show the effect on the [001] zone of movements of the atoms perpendicular to the (001) plane. The plane molecule of course retains its hexagonal configuration after projection (fig. 11 (*a*)). The greater the puckering, the greater the departure from hexagonal symmetry in the projection. Fig. 11 (*b*) shows the appearance of the "diamond" type of benzene ring after projection. Fig. 11 (*d*) represents the projection of the model suggested by Morse* in which the aromatic carbon atoms would lie at distances of ± 0·611 and the side-chain carbon atoms at ∓ 0·06 Å. from the (001) plane.

In order to introduce both effects, *i.e.*, the effect on the hexagonal symmetry in the [001] zone and the effect on planes having high values of l, a selection of the observed structure factors has been given in fig. 12 (*a*). In fig. 12 (*b*) the corresponding calculated structure factors are shown for the arrangement of carbon atoms (neglecting the hydrogens) which was found to give the best agreement for all planes in the [001] zone (see fig. 9 (*c*)). The co-ordinates of these atoms are shown in Table I. They lie along lines making angles of θ_1 with $+a$ and θ_2 with $+b$, at distances of 1·42 and 2·90 Å. from the origin.

Table I.

θ_1.	θ_2.	Aromatic carbons.	Side-chain carbons.
° ′	° ′		
+ 96 30	− 23 4	A (+ 0·64 + 1·62 0)	G (+ 1·31 + 3·31 0)
+156 30	+ 36 56	B (− 0·98 + 0·65 0)	H (− 2·00 + 1·33 0)
−143 30	+ 96 56	C (− 1·62 − 0·97 0)	J (− 3·31 − 1·98 0)
− 83 30	+156 56	D (− 0·64 − 1·62 0)	K (− 1·31 − 3·31 0)
− 23 30	−143 4	E (+ 0·98 − 0·65 0)	L (+ 2·00 − 1·33 0)
+ 36 30	− 83 4	F (+ 1·62 + 0·97 0)	M (+ 3·31 + 1·98 0)

Fig. 12 (*c*) shows the result of leaving atoms G–M in the (001) plane, but of shifting A, C, E through 0·255 Å. perpendicular to (001) on the $+c$ side and B, D, F by the same amount in the negative direction. This has the effect of puckering the ring to just the extent required for the "diamond" structure. The projection of the c axis on the (001) plane makes an angle of only about 9° with the b axis, and therefore atoms lying outside the (001) plane are in projecting moved nearly parallel to (100). Hence the structure factors for the

---

* Morse, 'Proc. Nat. Acad. Sci.,' vol. 13, p. 789 (1927).

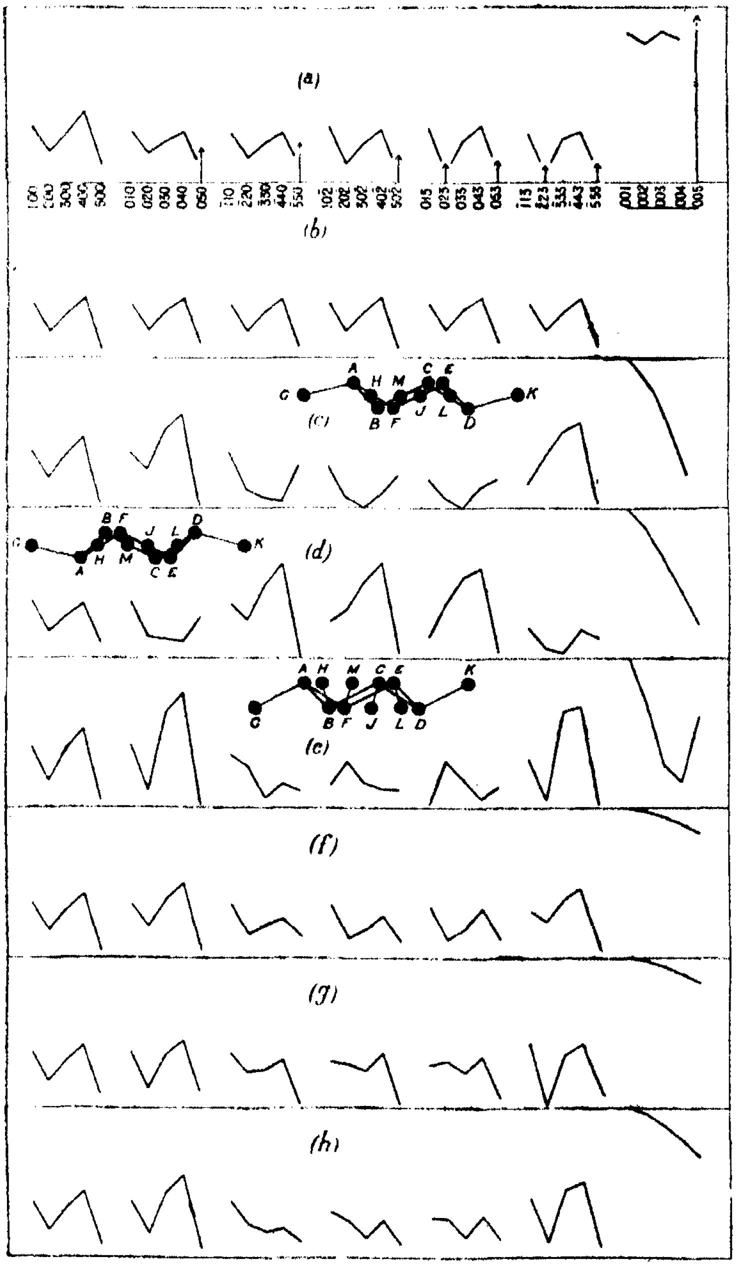

Observed.

Calculated for *plane ring.*
All C atoms in (001) plane.

Puckered ring.
A, C, E at + 0·255 Å.
B, D, F at − 0·255
G–M in plane.

A, C, E at − 0·255
B, D, E at + 0·255
G–M in plane.

A, C, E, H, K, M at
+ 0·255 from (001).
B, D, F, G, J, L at
− 0·255 from (001).

A, C, E at + 0·10 Å.
B, D, F at − 0·10
G–M in plane.

A–F in plane.
H, K, M at + 0·10.
G, J, L at − 0·10

A, C, E, H, K, M at + 0·1
B, D, F, G, J, L at −0·1
from (001) plane.

Fig. 12.

various orders of (100) are not much affected by puckering. Those of (010) and ($1\bar{1}0$) are affected almost equally by movements in opposite directions. This is seen by comparing (*c*) and (*d*), the latter being obtained by an inversion of the ring, so that A, C, E are at a perpendicular distance of —0·255 Å. from (001), and B, D, F at +0·255. In both cases the agreement is completely spoilt. The hexagonal structure in the [001] zone is lost and the structure factors are now markedly dependent upon the value of *l*. The effect of shifting the side-chain C atoms, G–M, perpendicular to the (001) plane is to accentuate the disagreement even further (fig. 12 (*e*)). The calculations illustrated in (*f*) (*g*) and (*h*) show, in fact, that neither the nuclear nor the side-chain carbon atoms can be as much as 0·1 Å. from the (001) plane. Variations of the first two co-ordinates of the atomic positions do not alter this result, in fact small movements of the atoms *parallel* to the (001) plane do not appreciably affect curves (*c*)–(*h*).

Thus the "diamond" type of benzene ring is shown to be wholly inadmissible.

Other models, such as that of Morse, in which the carbon atoms are even further from the (001) plane, can be dismissed simply by a consideration of the structure factors for that plane only, irrespective of their position relative to the [001] zone. The relative values of the structure factors are shown in Table II.

Table II.

	001	002	003	004	005	006	100	010	$1\bar{1}0$
Observed using Diamond F values	100	87·5	77·5	49·9	<40·4	<61·2	45·3	39·0	37·2
Observed using Graphite F values	100	92·8	100·3	95·3	<124	<268	38·2	34·3	32·8
Calculated for carbons only— Plane ring (Table I)	100	100	100	100	100	100	35·2	34·5	34·2
Diamond type ring A, C, E ±0·255 B, D, F ∓0·255: G–M in (001)	100	86·4	66·5	44·1	23·1	7·5	36·4 36·6	34·6 35·7	35·3 34·1
Diamond type ring A, C, E ±0·255 B, D, F ∓0·255: G–M at ∓ 0·255	100	71·3	28·4	−17·8	−61·8	−94·5	40·4 39·5	41·3 35·8	34·9 41·3
Diamond type ring A, C, E ±0·255 B, D, F ∓0·255: G–M at ± 0·765	100	−17·9	−39·3	26·2	35·5	−68·5	58·8 64·8	44·1 75·1	76·8 40·7
Morse ring: Aromatic carbons at 0·865 from origin, ±0·611 from (001), aliphatics at 1·90, and ∓ 0·06 Å	100	32·8	− 3·1	25·7	88·8	120·9	91·9 91·9	86·6 86·6	84·5 84·5

The very compactness of the Morse model is also a drawback, since that is bound to lead to a structure factor for (100) which is much too large compared with that for (001). The figures in the last three columns of Table II are obtained on the assumption that the atoms lie along the directions given in Table I (first and second columns), but the result is not changed much by a rotation of the ring into any other position.

The conclusions are that :—

(1) *Only a plane ring can account both qualitatively and quantitatively for the hexagonal structure of the* [001] *zone, for the lack of dependence upon* l *and for the relative values of the structure factors observed for* (001) *and a large number of other planes.*

(2) *The diameter of the aromatic carbon atom is* 1·42 ± 0·03 Å., *that is, the ring is similar to that occurring in graphite, not only in structure but also in dimensions.*

Structure and Position of the Methyl Groups.

It has already been shown in fig. 12 (g) that the side-chain carbon atoms cannot even be as much as 0·10 Å. away from the (001) plane, and that they are therefore co-planar with the ring itself. In order to complete the structure determination it is necessary to consider whether the methyl group scatters as a whole or not. Fig. 13 (a) shows the result of placing the atoms as in Table I, but of taking the scattering power of the side-chain group as 9, as compared with 6 for that of the aromatic carbon. The agreement is not quite as good as before ; nor is it materially improved by slight variations in the positions of the atoms. If the hydrogen atoms had actually given up their electrons to the carbon of the methyl group, this arrangement should have given a better agreement with experiment, since the whole of the scattering material in the

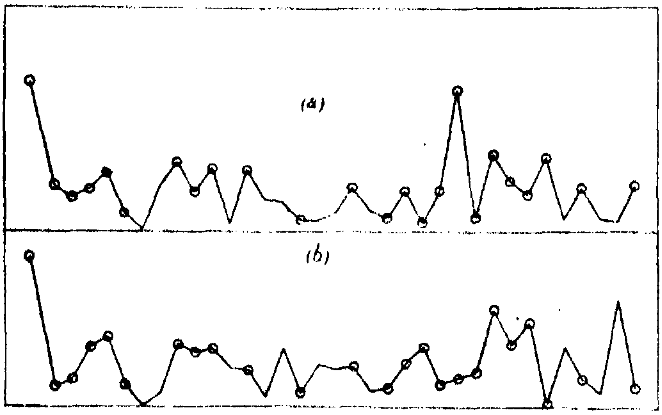

Atoms lie along same directions as in fig. 9 (c).

(a) C (6) at distance 1·42 from origin. CH_3 (9) at distance 2·90 from origin.

(b) C (6) at distance 1·42 from origin. CH_3 (9) at distance 3·62 from origin.

FIG. 13.

cell would be accounted for. Fig. 13 (*b*) shows the result of placing a group of scattering power 9 along the line joining the origin to each aromatic carbon atom but at a distance of 3·62 from the origin (fig. 14). In such positions methyl groups of neighbouring molecules would touch one another in the (001) plane.

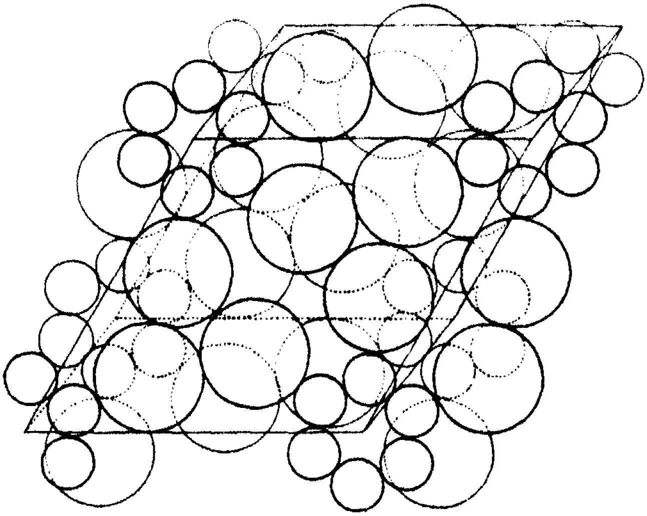

Fig. 14.—Orthogonal projection of unit cell on to (001) plane.

This arrangement, in which the methyl group, of diameter 3·0 Å., is considered to scatter spherically as a whole, is even more out of the question. It is quite clear that there cannot be anything like a spherical distribution of electrons in the methyl group. The group as a whole extends over such a volume that its " diameter " may be said to be about 3·0 Å., but it does not scatter like a single atom of the same diameter, such as Br or I. In scattering power it is heavily weighted at the end nearer to the benzene ring by its carbon atom, which appears to retain its own electronic system more or less unchanged. The hydrogen atoms do not appear to give up their single electrons to the carbon atom, but these probably form a kind of atmosphere enveloping the H nuclei. In fact the methyl group acts towards X-rays like an electronic shuttlecock, whereas single atoms behave rather like tennis balls. The carbon atom of the methyl group lies in the plane of the benzene ring so that, as in graphite, *three of the valencies of the aromatic carbon atom are co-planar.* The X-ray results can offer no direct evidence as to the behaviour of the fourth valency, except that it must be so disposed as to give the ring as a whole a centre of symmetry. This last condition quite eliminates the Kekulé static model, with its three double bonds. The radius of the side-chain (aliphatic) carbon atom in the structure giving the best agreement with experiment (Table I, fig. 9 (*c*)) is 1·54 ± 0·12 Å. It appears, therefore, to resemble the carbon atom in diamond rather than that in graphite. The evidence in favour of this suggestion, however, is incomplete, since in this compound we cannot trace the directions of the three remaining valencies.

Concluding Remarks.

It is difficult to see exactly why this crystal should have been triclinic instead of, say, monoclinic like C_6Cl_6 or orthorhombic like benzene itself. The slight asymmetry *in* the (001) plane must be due to a certain lack of symmetry of the benzene ring together with a possible variation in the orientation of the attached methyl groups. This lack of symmetry, other than centro-symmetry, falls into line with previous observations (Mark, Cox, Bragg, *loc. cit.*) upon benzene and its fully-substituted derivatives. The displacement of successive (001) planes with respect to one another, illustrated in figs. 2 and 14, is, however, rather unexpected. A displacement certainly occurs in graphite also, but it is a symmetrical displacement. The centre of each hexagon of atoms lies vertically above an atom in the neighbouring (0001) plane. The displacement in the case of $C_6(CH_3)_6$ seems quite arbitrary. Two facts emerge from fig. 14, however, which may help to elucidate the problem. One is that the orthogonal projection of the *c* axis upon the (001) plane is almost perpendicular to one pair of sides of the benzene ring; and the other that the methyl groups (considered now as a whole, since it is only their volume that is in question) in one (001) plane lie more or less beneath the gaps in the plane above. Possibly if the exact shape and orientation of the methyl groups could be determined the problem of the crystal system would resolve itself into a question of the most convenient "packing." The (001) cleavage is readily explained since the cleavage planes are merely layers of flat molecules. Although very good, the cleavage is not, of course, as remarkable as the graphite cleavage, since the connection between the (001) planes is not between carbon and carbon, but between methyl and methyl, or carbon and methyl. The easy distortion of the crystals by slipping about the crystallographic axes may be caused by the rolling of methyl groups upon one another.

The writer had no available photographic apparatus when this investigation was undertaken, but Sir William Bragg was kind enough to allow photographs to be taken at the Davy Faraday Laboratory. Laue photographs taken by sending the X-ray pencil along the c axis, like the ionisation spectrometer measurements, did not show the hexagonal structure directly. Only when the variation in spacing caused by the obliquity of the c axis to the (001) plane is allowed for, by calculation of the structure factors, does this hexagonal structure become revealed. A rotation photograph taken with the c axis as axis of rotation helped to confirm the size of the unit cell and the relative importance of some of the small-spacing planes. I am indebted to Dr. A. Müller for taking these photographs.

My thanks are also due to Prof. Ingold, F.R.S., who kindly supplied me with the material used in this investigation, to the Council of Bedford College, London, for a scholarship enabling me to work in the Physics Laboratories of the University of Leeds, and to the Royal Society for a grant covering the cost of some of the apparatus employed.

Summary.

The selected minimum cell of $C_6(CH_3)_6$ has dimensions

$a = 9\cdot010$ Å. $\quad \alpha = 44° \ 27'$
$b = 8\cdot926 \quad \beta = 116° \ 43'$
$c = 5\cdot344 \quad \gamma = 119° \ 34'$

and contains one molecule, which is probably centro-symmetrical. The structure factors for a large number of planes have been calculated from the observed intensities and are found to obey the following rules :—

1. The factors in the [001] zone repeat themselves closely throughout the series of planes $(100)\rightarrow(010)$, $(010)\rightarrow(1\bar{1}0)$ and $(\bar{1}10)\rightarrow(\bar{1}00)$. They, therefore, indicate a hexagonal structure in the zone.

2. The factors are almost independent of the last index l, which shows that the carbon atoms at least must all lie within $0\cdot1$ Å. of the (001) cleavage plane.

It is shown from the relative values of the factors that a unique structure can be assigned to the molecule, which exists as a separate entity and has a ring form.

The benzene ring is similar in shape and size to the six-carbon ring in graphite, the aromatic carbon atoms having a diameter of $1\cdot42$ Å. Three of the valencies of aromatic carbon are co-planar, the ring itself and all the side-chain carbon atoms lying in one plane.

The methyl group does not scatter like a single atom but is heavily weighted in scattering power at the end nearer to the benzene ring.

The puckered or "diamond" type of benzene ring and the more compact model suggested by J. K. Morse are shown to be wholly inadmissible.

The Ionisation of Potassium Vapour.

By R. W. Ditchburn, Ph.D., Trinity College, Cambridge, Isaac Newton Student, and F. L. Arnot, B.Sc., Trinity College, Cambridge, John Coutts Scholar of The University of Sydney.

(Communicated by Sir Joseph Thomson, F.R.S.—Received January 11, 1929.)

Introduction.

The experiments described here differ from previous experiments on ionisation in alkali-metal vapours in that it is possible to measure the *m*/*e* ratio for the ions produced.

Three methods of producing ions have been employed: photo-ionisation, ionisation by electron impact, and "ionisation" by the attachment of K^+ ions to neutral potassium atoms. In the following we shall first describe the experimental methods, next give the results obtained by each method of ionisation with a brief discussion on each, and then proceed to a general discussion of the whole of the results.

Experimental.

The apparatus, which is shown diagrammatically in fig. 1, is somewhat similar to that used by Smyth.* A jet of potassium vapour streams up in the direction MN. Ions formed in the region round N are pulled out of the vapour stream by an electric field between E_1 and E_2 and further accelerated by a stronger field between E_2 and E_3. They then pass through two slits S_1 and S_2 and are bent by a magnetic field into an arc of a circle of approximately 10 cm. radius. When the field is adjusted to the right value they pass through the slit S_3 and falling on the plate P are measured by the electrometer. Fig. 4 shows a typical arrangement of potentials for experiments on ions formed by

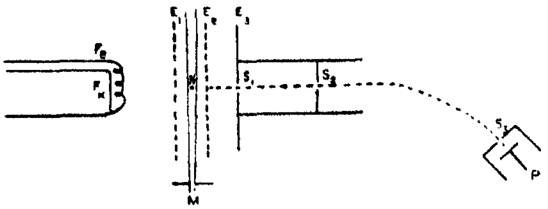

Fig. 1.

---

* 'Roy. Soc. Proc.,' A, vol. 102, p. 283 (1922); vol. 104, p. 121 (1923).

attachment of K^+ from the Kunsman filament F_k; fig. 6 for experiments on ions produced by electron impact; and fig. 5 for experiments on ions formed by photo-ionisation. In the photo-ionisation experiments the beam of light travels in a direction at right angles to the plane of the paper and is focussed at N.

The apparatus is shown in more detail in fig. 2.

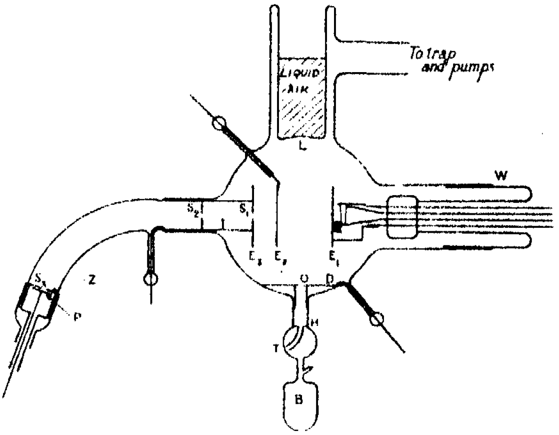

FIG. 2.

The four wire pinch carries the electrode E_1, and two filaments having one common connection. One of these is a Kunsman* filament emitting K^+ ions and the other an oxide coated platinum strip emitting electrons.

The wax joint W enables the filaments to be removed for recoating and also makes it possible to alter the distance between E_1 and E_2. The electrodes E_1 and E_2 are pieces of copper gauze stiffened at the edges by rings of copper. The electrode I is a soft iron cylinder in which two copper discs have been mounted. Two slits S_1 and S_2 in these discs collimate the beam of ions, while the iron cylinder shields them from the stray field of the magnet. The beam of potassium is defined by the opening O in the copper diaphragm D and by the hole H and is condensed on the liquid air cooled surface L. The trap T was used to prevent liquid potassium being shot up into the apparatus if the potassium boiled violently—as happened occasionally.

The light, which was produced by an iron arc taking a current of 20 amperes, entered through a quartz window in a direction perpendicular to the section of the apparatus shown in the figure. The beam of light was focussed on to the beam of vapour, and after passing through the bulb entered the usual form of light trap. The metal diaphragm D used to become rather hot with the result that a number of molecules were reflected off it so that it failed to produce a sharply defined beam. This disadvantage did not occur in an earlier form of apparatus employing an internally sealed glass diaphragm. Owing, however, to stray charges collecting on the glass diaphragm, the electrostatic conditions were very unsteady. The ions, which have only very low speeds in the region between E_1 and E_2, are easily deflected out of the line of slits. For this reason a metal diaphragm which could be kept at a constant potential was employed. It was then found by using the Kunsman filament (with the furnace cold) that the ratio of the ion-currents to the electrode E_3 and to the plate P was perfectly constant, the value being about 5000 to 1.

---

* 'Phys. Rev.,' vol. 27, p. 739 (1926).

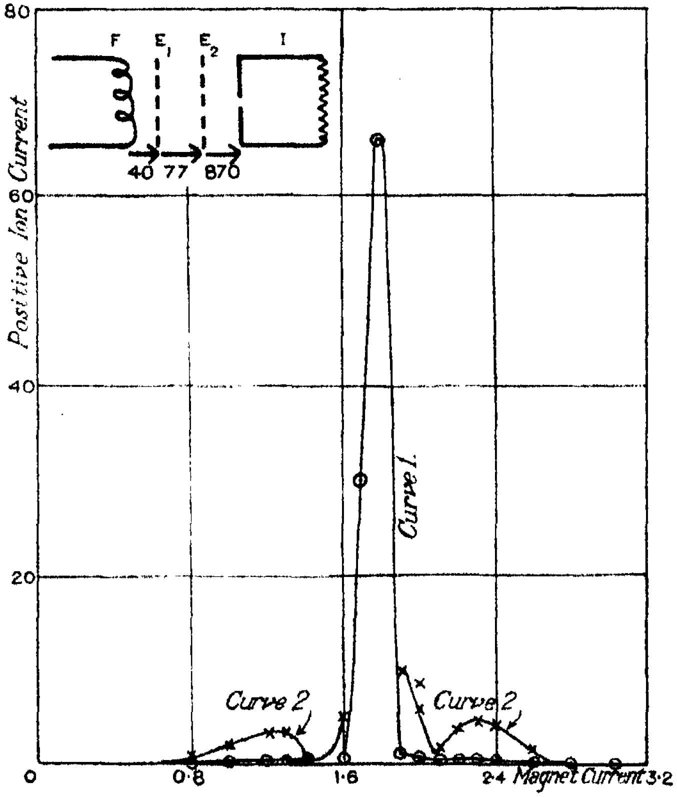

FIG. 3.

The resolving power of the apparatus is shown by curve 1 of fig. 3 in which the ordinates represent the ion current for different magnetic fields, the furnace being cold, and the ions being produced by the Kunsman filament. It may be noted that the only ion present is K^+. The absence of Na^+ ions is due to the purity of the potassium salt used in preparing the Kunsman mixture[*] and also to the low temperature at which the filament was run. The current taken from the Kunsman filament was generally less than 10^{-7} amp. Curve 2 is a magnification of curve 1, the ordinates being multiplied by 10. It will be seen that there are two very small and rather flat maxima, one on each side of the main maxima. These appear to be due to reflection of particles from the glass walls of the apparatus. Their size is very small, at most 1½ per cent. of the main peak, and usually much less so that in the main experiments they are nearly always masked by much stronger effects.

Various accelerating potentials ranging from 300 to 1000 volts were applied to the ions, the field required for a 1000-volt K^+ ion being about 2900 gauss. In any one experiment the potentials were kept constant and the magnetic field was varied. Fields up to 6000 gauss were used. The value of the stray magnetic field between E_2 and E_3 was less than 30 gauss. Although this was too small to affect seriously the paths of the positive ions, it should prevent any electrons passing through the slit S_1.

The vacuum system consisted of a mercury diffusion pump backed by a Gaede rotary pump. The pressure at the back of the diffusion pump read on a McLeod gauge was kept below 0·003 mm. A liquid air trap was inserted between the diffusion pump and the apparatus. Tests with the diffusion pump off showed that the only effect of a rise of pressure to about 0·005 mm. was to reduce slightly the resolving power of the apparatus. The actual pressure in the apparatus during an experiment was probably considerably less than 10^{-5} mm. of Hg. The potassium was purified in the way described by Clarke.[†]

When it became necessary to recoat a filament it was found that the vacuum could be safely let down with nitrogen without in any way affecting the potassium. On re-evacuating it was only necessary to heat the potassium fairly strongly for a few minutes when the occluded nitrogen would be given off. The temperature to which the potassium was heated varied between 280° and 380° C., though for any one run the temperature was kept constant to within about 2° C.

Owing to the heating up of the diaphragm D the vapour pressure cannot be accurately measured. A rough calculation shows that it is almost certainly between 5×10^{-4} and 5×10^{-5} mm. and probably near to 10^{-4} mm.

---

[*] We are indebted to Mr. E. T. S. Appleyard for the Kunsman mixture used.

[†] 'Proc. Camb. Phil. Soc.,' vol. 23, p. 953 (1927).

Results.

(1) *The Attachment of Ions.*

Fig. 4 shows the type of curve obtained when a beam of K^+ ions is accelerated into the vapour. Comparison with fig. 3 shows that in addition to the main peak at mass-number 39 (corresponding to ions from the Kunsman filament which have passed through the vapour without suffering collision) there are two well-marked subsidiary maxima at 76 and 19. The former shows the existence of a molecule K_2^+. It will be shown below that the latter is almost certainly due to the formation of an unstable K_2^+ ion which dissociates on entering the magnetic field into K^+ and K. The K^+ ion so formed has only half the energy of the K^+ ion from the Kunsman filament and therefore appears at mass-number 19.

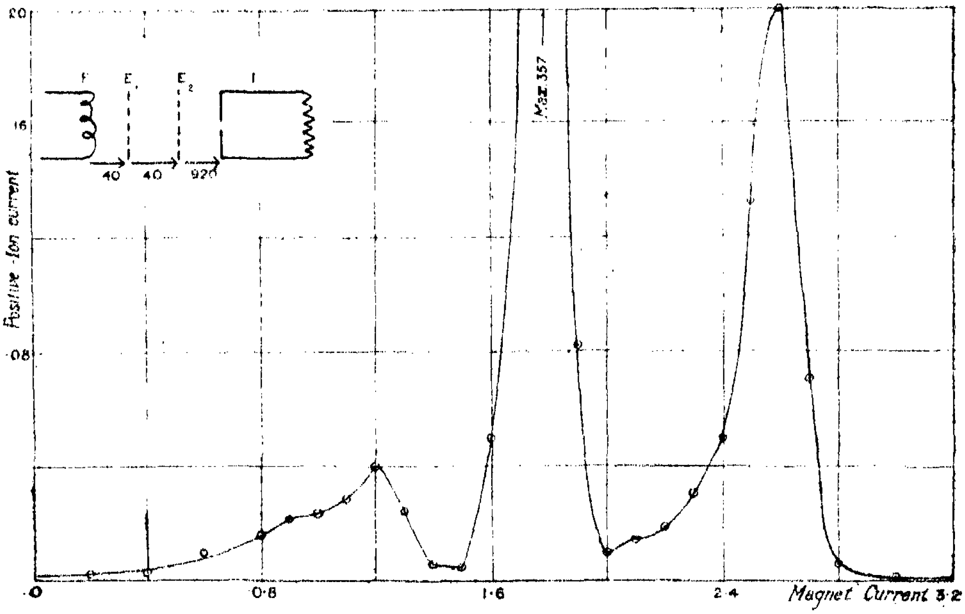

FIG. 4.

With this general outline in mind we shall now proceed to discuss the collision and dissociation processes in more detail.

The Collision Process.—There are at least two ways in which K_2^+ ions may be formed (*a*) by the attachment of K^+ ions to neutral K atoms and (*b*) by the impact ionisation of K_2 by K^+ ions. It seems probable that the first is the effective process for the following reasons: (1) Harnwell* has shown for a number of permanent gases that a positive ion cannot ionise an atom or molecule with a higher ionisation potential than its own even though it has sufficient kinetic energy to do so. Since the ionisation potential of K_2 is higher than that of K it is unlikely that K^+ should ionise K_2 by collision. (2) If K_2^+ ions are formed by collision of K^+ with K_2 we should expect that in the majority of cases the collision would not be a head-on collision. Thus the two particles would in general be thrown out of the line of the slits and would not reach the electrometer. So we should expect that for every K_2^+ ion which reached the electrometer there would be a large number thrown out of the line of the slits and we should expect these ions to disappear from the K^+ peak. As nearly as can be measured, one K_2^+ ion is found for every K^+ lost. These and other more detailed considerations suggest very strongly that the K_2^+ ion is formed by attachment and not by impact ionisation.

The number of K_2^+ ions formed, including those which dissociate, is about 10 per cent. of the number of incident K^+ ions. This represents the chance of attachment in a path of 4 cm. in potassium vapour at a pressure of 10^{-4} mm. Interpreted as a collision-radius this probability gives a value of 4×10^{-8} cm. This value is subject to the uncertainty of vapour pressure estimate and is only correct to within a factor of about 3. We have not made any special study of the variation of the probability of attachment with the speed of the initial ion but a comparison of different curves suggests that there is no rapid change of probability for speeds between 20 and 200 volts.

It is interesting to consider the momentum relations involved in this type of collision. The linear momentum relation requires that the velocity of the K_2^+ ion immediately after it is formed must be one-half that of the K^+ ion from which it was formed (neglecting the very small thermal velocity of the K atom). This means that one-half of the kinetic energy of the impacting particle must be radiated or transformed into potential or rotational energy. It is scarcely possible that more than a fraction of a volt can be permanently retained as potential or rotational energy. The excess of energy is probably radiated during the collision or during the electronic rearrangement which takes place immediately after collision. It probably appears as continuous radiation. The angular momentum relation requires that the emitted radiation shall carry away a considerable amount of angular momentum.

We have tested very carefully for the existence of a peak at mass number 120

---

* 'Phys. Rev.,' vol. 29, p. 683 (1927); see also Dempster, 'Phys. Rev.,' vol. 27, p. 108 (1926).

(corresponding to K_3^+) but have never been able to detect one. There are, however, two very small peaks at mass numbers 13 and 54. Inspection of a number of curves shows that these are not due to experimental error although they are very small. In view of the results obtained with electron-formed ions it seems probable that these are due to K_3^+ ions which have dissociated partly according to the process.

$$K_3^+ \longrightarrow K_2^+ + K \text{ (giving a peak at 55)}$$

and partly according to the process:

$$K_3^+ \longrightarrow K^+ + K_2 \text{ (giving a peak at 13).}$$

It is probable that these are due to attachment of K_2^+ molecules to K atoms rather than to direct attachment of K^+ to K_2. This matter will be discussed more fully in connection with the ions formed by electron impact.

The Dissociation Process.—The proportion of K_2^+ ions which dissociate is affected by two conditions, the temperature of the furnace and the total potential V_3. The effect of these two factors is shown in the following table :—

Set.	1. Temperature.	2. V_3.	3. Undissociated molecules.	4. Dissociated molecules.	5. Ratio.	6. Times $\times 10^{-6}$ sec.	
						T_1.	T_2.
	° C.	Volts.					
1	323	1000	5·2	1·04	5·0	6·0	2·3
2	275	980	6·6	0·96	6·9	7·6	2·3
3	275	590	5·1	1·5	3·4	7·3	3·0
4	380	205	3·53	7·4	0·5	9·3	5·3

Neglecting column (6) for the present we see from sets 1 and 2 that when V_3 is kept constant the proportion of undissociated molecules is increased by lowering the temperature. From sets 2 and 3 we see that when the temperature is kept constant increasing V_3 increases the proportion of undissociated molecules. Thus we see that a high temperature and a low voltage favour the dissociation process and set 4 shows the effect of using both these factors together.

It is to be noted that whatever the variation of temperature and voltage the maximum number of dissociated molecules appear to have dissociated exactly on entering the magnetic field. This is shown by the fact that the lowest peak always appears at the same mass number. If a molecule breaks up before it has fallen through the whole voltage it will receive part of its acceleration as K^+ and appear at a mass number between 19·5 and 39. If it breaks up after passing through part of the magnetic field it may appear at any mass number between 19·5 and 78. Both the peak at 78·0 and that at 19·5 show a slight broadening indicating that a small proportion of molecules may break up in this way. The majority, however, appear to follow one of two courses. Either they dissociate on entering the magnetic field or they go right through the magnetic field without breaking up. It has long been known from the positive ray experiments of J. J. Thomson that unstable molecular ions exist in discharge tubes and that some break up on their way through the positive ray apparatus, but the dissociation was not attributed to the magnetic field. Franck and Grotian* have explained some experiments on mercury vapour on the assumption that a quasi-stable mercury molecule can be dissociated by a magnetic field. Hogness and Lunn† have interpreted their own results and also those of Smyth‡ on nitrogen on the assumption that the $N_2{}^+$ ion has two states : (*a*) (produced from N_2 by impact of electrons with greater than 24 volts energy) which can be dissociated by a magnetic field, and (*b*) (produced by electrons with energy between 21 and 24 volts) which cannot be dissociated by the magnetic field. The $O_2{}^+$ ion also possesses two similar states, and behaves in an exactly similar manner. It appears that the present experiments can best be interpreted by assuming that the $K_2{}^+$ ion (formed by attachment) has two such states. The effect of the temperature and voltage change is to alter the proportion of molecules in the two states. Presumably the increase of temperature transfers molecules from state (*b*) to state (*a*) by a collision of the second kind. The way in which the voltage change acts is more obscure. The following hypothesis is very attractive : all the molecules are formed initially in state (*b*) which is an excited state. These pass from state (*b*) to state (*a*) (probably by radiation) in a time of about 10^{-5} sec. Decreasing the voltage merely increases the time which the molecules take to reach the magnetic field and thus increases the number which enter the field in state (*a*) and are dissociated. This hypothesis cannot be definitely proved or disproved with the present apparatus because ions formed in different parts of the space between E_1 and E_2 take very different times to reach the magnetic field. This is because they move very slowly between E_1 and E_2. The times T_1 (for a molecule formed at E_1) and T_2 (for a molecule formed at E_2) are shown in the table. It will be seen that if this is the mechanism of transfer the life of the excited state is of the order 3×10^{-6} sec.

---

* 'Z. Physik,' vol. 6, p. 35 (1921).

† 'Phys. Rev.,' vol. 26, p. 786 (1925) ; vol. 27, p. 732 (1926).

‡ 'Roy. Soc. Proc.,' A, vol. 104, p. 121 (1923).

While the above hypothesis is very attractive it is possible that voltage change acts in some more indirect way. For example, an increase of speed will probably decrease the chance of collision with a stray gas molecule.* The pressure is too low for this to be a likely mechanism unless the K_2^+ ion has a very large collision radius. It is also possible that the electric field has some electrostatic effect on the ion. But calculation shows that the polarisation forces set up by the electric fields used are exceedingly small. It is not easy to see in what way the magnetic field effects the dissociation. It is worth noting that the K_2^+ ion is initially in the stray field of the magnet (about 30 gauss) and does not dissociate there. Thus 30 gauss is not sufficient to dissociate it. On the other hand fields ranging from 1000 to 3000 gauss seem to be equally effective. If the magnetic field merely acted by splitting up a metastable into a non-metastable state we should rather expect a very small field to be sufficient. It can be shown quite simply that unless the ion is spinning so rapidly as to have an enormous magnetic moment no appreciable amount of energy can be transferred to it even by a field of 3500 gauss. There are so many difficulties involved if we assume a rapid spin that we are almost forced to accept the view that the ion does not receive any appreciable amount of energy from the field. From the energy point of view the ion is probably near a state of neutral stability.

(2) *The Photo-ionisation Experiments.*

Fig. 5 shows a typical curve obtained with light-formed ions. The arrangement o potentials is shown in the top right-hand corner of the graph. The curve is identical with that obtained from the Kunsman filament (fig. 3) except that it is slightly broader. The increase of breadth is entirely accounted for by the 40 volts inhomogeneity in the velocities owing to the fact that ions are formed in different parts of the space between E_1 and E_2. Thus the only ion present is K^+.

It is necessary to make careful tests to be sure that the ions are due to direct photo-ionisation of the vapour and not to ionisation by the impact of photo-electrons from the electrodes and from the potassium which has been condensed in the bulb. The most decisive test is made by inserting a sheet of glass in the path of the beam of light. When the light is badly focussed so as to throw a good deal of light on to the electrodes and sides of the bulb the positive ion current is reduced by only about 10 per cent. on inserting the glass. This shows that about 90 per cent. of the radiation effective in releasing photo-electrons is able to pass through the glass. When the light is well focussed so that nearly all of it passes through the beam of vapour to the light trap the positive-ion current is reduced by about 85 per cent. on inserting the glass. We know that the glass cuts out all the photo-ionisation effect and only 10 per cent. of the impact ionisation effect, and hence we conclude that about 80 per cent. of the ions are due to photo-ionisation in this case. In the earlier apparatus, when we had a sharp beam of vapour it was possible to make another test. If the beam of light was sharply focussed on to the beam of vapour a considerable ion-current was obtained, but on shifting the light very slightly so as to focus just beside the beam of vapour practically no positive ions could be measured. Another proof that the ions are not due to impact ionisation is given by the fact that the curves obtained are not at all like those obtained with impact ionisation by a beam of electrons from a heated filament (see below fig. 6).

---

* See the results of Durbin, 'Phys. Rev.,' vol. 30, p. 848 (1927).

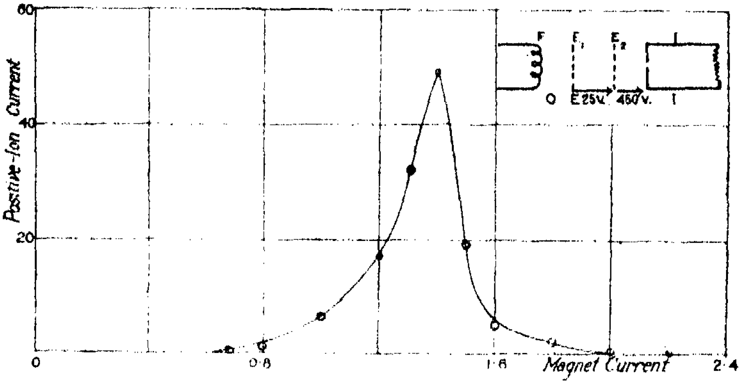

FIG. 5.

As has been stated above the only ion found is K^+. Since the ion has to start from zero velocity it takes 10^{-6} sec. to reach the electrode E_2 and if a K_2^+ ion was formed and dissociated in this time we should not be able to detect its existence since it would receive practically all its acceleration as K^+. At present we can only say certainly that if such an ion exists its " life " is less than 2×10^{-6} sec., *i.e.*, less than the life of the K_2^+ ions formed by attachment. One other result of these photo-ionisation experiments should be mentioned. If the probability of attachment of K^+ to K were very large we should expect to find a considerable number of K_2^+ ions due to attachment of

K^+ photo-ions. No such ions are found and hence we conclude that the probability of attachment of very slow K^+ ions is no greater than the probability of attachment of K^+ ions of about 50 volts energy.

Before we can discuss the meaning of this result it is necessary to decide whether the K^+ ion is produced by the direct ionisation of K atoms or by the ionisation and dissociation of K_2 molecules. At first sight it might appear that since only about one part in a thousand of the vapour is in the molecular state* it is much more likely that the K^+ ion comes directly from atoms and not from molecules. The following reasons appear to outweigh this consideration :—

(1) Lawrence† has shown that the photo-electric threshold for potassium vapour is near λ 2600 and that the efficiency of ionisation increases with the frequency of the light. If the ionisation were atomic we should expect the threshold to be at λ 2860 (the series limit) and the efficiency of ionisation to decrease with frequency.

(2) The work of Harrison on sodium, of Foote, Molher and Chenault on caesium and of one of us‡ on potassium has shown that there is a continuous absorption at the series limit of the alkali-metals and that it decreases in intensity with increasing frequency. A similar result for the Balmer series-limit is obtained from stellar spectrograms and the well-known λ^3 law holds approximately for X-ray limits. The experiments on potassium indicate that the absorption at the series-limit is only one-thousandth part of the absorption in the region 2600–2200 A.U. Thus we conclude that the series-limit photo-ionisation of the atom exists but that it accounts for only a very small fraction of the total ionisation produced by an iron arc.

(3) It has been suggested§ that the ionisation at λ 2600 may correspond to ionisation of the atom with excitation of the K^+ ion formed. But the difference in energy between the threshold at λ 2600 and the series limit is only a fraction of a volt, and is too small to correspond to the difference in energy states of spark spectra. Moreover it has been shown

---

* See Ditchburn, 'Roy. Soc. Proc.,' vol. 117, p. 486 (1928); Carrelli and Pringsheim, 'Z. Physik,' vol. 44, p. 643 (1927); Walter and Barratt, 'Roy. Soc. Proc.,' vol. 119, p. 257 (1928).

† 'Phil. Mag.,' vol. 50, p. 345 (1925).

‡ Harrison, 'Phys. Rev.,' vol. 24, p. 466 (1923); Foote and others, 'Phys. Rev.,' vol. 26, p. 195 (1925); Ditchburn, *loc. cit.*

§ Lawrence, 'Phys. Rev.,' vol. 28, p. 947 (1926).

by one of us* that a value of the heat of dissociation obtained from this limit agrees very well with the values obtained from entirely different methods. From these and other more detailed considerations it seems that the K^+ ions are formed from the dissociation of K_2^+ molecules and not by direct ionisation of the atom. The reason why the photo-ionisation of K_2 cannot produce a stable K_2^+ molecule will be brought out in the course of the general discussion.

(3) *Electron Formed Ions.*

Fig. 6 is a typical curve for ionisation by electrons of about 100 volts energy. There are seven maxima at mass numbers 1, 2, 13, 26, 38·5, 52, 76. The first two of these represent H_2^+ and H^+ due to hydrogen occluded in the alkali metal. It is very difficult to remove the last traces of hydrogen and they appear to have no effect on the rest of the results. The type of curve obtained with electrons of lower energy (36 volts) differs from fig. 6 in several ways. This curve we shall refer to as " curve α."

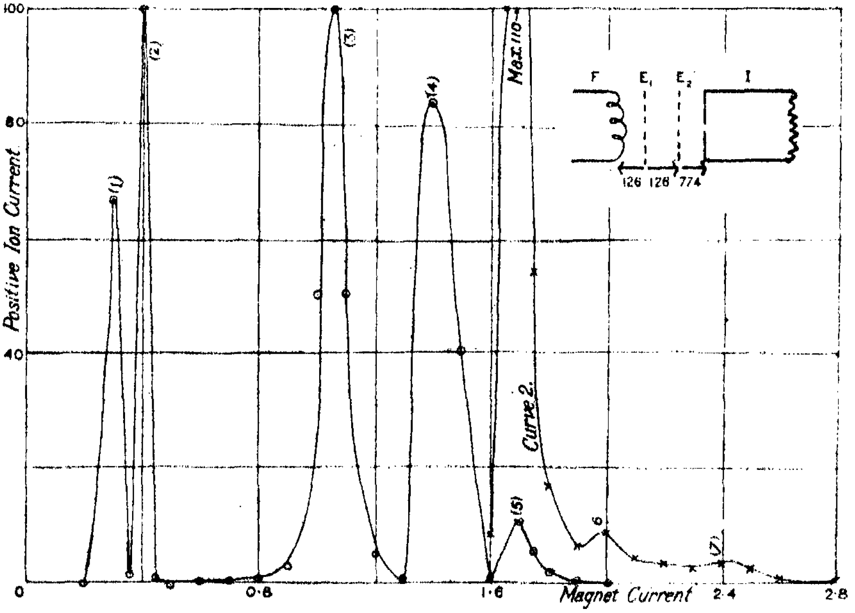

FIG. 6.—In Curve 2 the ordinates are multiplied by a factor of ten.

(1) Maxima 3 and 4 (mass numbers 13 and 26) are much stronger in fig. 6 than in " curve α."

---

* Ditchburn, 'Proc. Camb. Phil. Soc.,' vol. 24, p. 320 (1928).

(2) Maximum 5 is much stronger in "curve α" than in fig. 6. In fig. 6 it appears at mass number 38·5, in "curve α" at mass number 37. This difference is quite outside the experimental errors.

(3) In fig. 6 maximum 6 is much stronger than maximum 7; in "curve α" maximum 7 is much stronger than maximum 6.

It will be seen that the phenomenon is more complicated than with the ions formed by attachment or by photo-ionisation. The following appears to be the most probable explanation of maxima 3, 5, 6, 7:—

(1) The primary process of ionisation is

$$K_2 + \varepsilon \rightarrow K_2^+ + \varepsilon + \varepsilon. \qquad (1)$$

This K_2^+ ion is in an excited state.

(2) The K_2^+ ion so formed breaks up either spontaneously or as the result of a distant collision in a time of order 10^{-6} sec. *if it is not previously involved in process* (3).

$$K_2^+ \rightarrow K^+ + K. \qquad (2)$$

The product of this process goes to form peak 5.

(3) When an intimate collision between a K_2^+ ion formed by process (1) and a potassium atom takes place

$$K_2^+ + K \rightarrow K_3^+ \qquad (3)$$

This process (3) is analogous to the mechanism of the formation of H_3^+. This compound was initially discovered in discharge tubes by Sir J. J. Thomson* and the mechanism of its formation has been fully investigated by Dempster,† Smyth and Hogness and Lunn.

(4) The K_3^+ formed by process (3) breaks up on entering the magnetic field in one or other of the following ways.

(Peak 3) $$K_3^+ \longrightarrow K^+ + K_2 \qquad (4A)$$

or

(Peak 6) $$K_3^+ \longrightarrow K_2^+ + K. \qquad (4B)$$

Hogness and Lunn did not find any unstable H_3^+ ions but Sir Joseph Thomson (*loc. cit.*) had earlier obtained a parabola corresponding in mass to an H_3^+ ion which had dissociated to H_2^+.

It will be seen that peak 3 is very much stronger than peak 6 indicating that process (4A) is at least 50 times as probable as process (4B). The explanation of this is very interesting. Harnwell* has shown that when an ionised atom or molecule A collides with a neutral atom or molecule B an electron is transferred from B to A if, and only if, the ionisation potential of A is greater than that of B (*i.e.*, the "electron-affinity" of A greater than that of B). Harnwell further showed that if the ionisation potential of A is greater than that of B the probability of electron transfer is greatest when the difference of the two ionisation potentials is least. Now the ionisation potential of K_2 is 4·8 volts and that of the atom is 4·3 volts, *i.e.*, the ionisation potential of K_2 is higher than but very near to the ionisation potential of K. Thus conditions are very favourable for the electron transfer and in general the K_3^+ molecule formed by process (3) consists of a neutral K_2 molecule with a K^+ ion loosely attached. On entering the magnetic field the K^+ ion breaks away giving process (4A). Peak 7 is due to the attachment of a few K^+ ions formed by process (2) to K atoms in a way exactly analogous to the processes described in a previous section (see p. 521 above).

---

* 'Rays of Positive Electricity,' pp. 86, 196.

† Dempster, 'Phil. Mag.,' vol. 31, p. 438 (1916); Smyth, 'Phys. Rev.,' vol. 25, p. 452 (1925); Hogness and Lunn, 'Phys. Rev.,' vol. 26, p. 44 (1925).

We shall now discuss the difference between the results for slow and fast electrons. It appears that the difference is due to the fact that the K_2^+ ion formed by the impact of 120 volt electrons is more highly excited than the K_2^+ ion formed by the impact of 35 volt electrons. This is analogous to the behaviour of N_2 and O_2 [see results quoted above (p. 523) from the papers of Smyth, Hogness and Lunn].

The more highly excited ion has a greater probability of collision and this affects the curves in the following way: (1) Peaks 3 and 6 are increased relative to peak 5 in fig. 6 because the process (3) is favoured by the increased probability of collision. (2) Peak 5 is larger in "curve α" because then there are fewer collisions leading to process (3). It is shifted to a lower mass number because the K_2^+ ions formed by process (1) are allowed to travel a considerable distance down the electric field before process (2) takes place and they are dissociated into K^+ ions. They thus have an appreciably lower velocity than a K_2^+ ion which has fallen down the whole field and so appear to have a lower mass number. In the curve shown in fig. 6, the K_2^+ ions make collisions soon after formation and the majority of them go to process (3) but those that do follow process (2) form K^+ ions which have nearly the full velocity and appear at mass number 39. (3) Peak 7 which is due to a tertiary process dependent on peak 5 follows the latter both as regards its size and the shift to lower mass number.

---

* 'Phys. Rev.,' vol. 29, p. 830 (1927).

The origin of peak 4 is, perhaps, the most difficult problem of this part of the work. It appeared at one time that it was due to N_2^+ impurity, but its mass number is definitely too low, and in a number of curves, taken under different conditions, it seems to increase and decrease with peak 3. Since we have assessed the latter to a secondary process of potassium ionisation it seems reasonable to assess peak 4 to another secondary process. Its mass number exactly agrees with that of a K_3^{++} ion which has broken up in the magnetic field according to the process.

$$\text{(Peak 4)} \qquad K_3^{++} \longrightarrow K^+ + K^+ + K. \qquad (6)$$

The experiment does not give any information as to how these K_3^{++} ions are formed. It is possible that they are produced by the ionisation of K or K_2 to K^{++} or K_2^{++} and subsequent attachment.*

The size of the electron currents is about 100 micro amps and allowing for the fact that only 1 in 10^4 of the positive ions reach the electrometer we find that about one in 10^{-3} to 10^{-4} of the electrons makes an ionising collision. This is equivalent to a target radius of 10^{-7} for the potassium molecule.

This explanation is self-consistent and is consistent with the results obtained with the Kunsman filament and light formed ions; it is exactly analogous with the explanation of the ionisation of H_2 (except† that there is no H_3^{++}); and it is in line with the results of Hogness and Lunn, etc., on both nitrogen and oxygen.

The chief difficulty is that it involves the assumption that the probability of ionisation of the K_2 molecule is very high (equivalent to a target radius of about 10^{-7}) and is much higher than the probability of ionisation of the atom. As we have seen above, however, the absorption of *quanta* by the molecule is much greater than by the atom. It is possible to escape from this difficulty by assuming that the initial ionisation process consists in ionising the atom and forming an excited K^+ ion which has an extraordinarily high probability of attachment. The high probability of attachment would have to be due to the ion being in an excited state since the photo-ionisation experiments show that very slow K^+ ions have no specially high probability of attachment. In this way an excited K_2^+ ion is formed which follows the processes described above. Or, it is possible to assume that K_3^+ ions are formed by direct attachment of K^+ to K_2. It is not possible to enter into a detailed discussion of these theories. It cannot be claimed that the present results are sufficiently comprehensive to disprove them but on the whole the view we have given above seems to be favoured by a considerable weight of evidence.

---

* Foote and Mohler have shown that the second ionisation potential of potassium is about 32 volts ('Phys. Rev.,' vol. 28, p. 46, 1926).

† If the K_3^{++} is formed in the way we have suggested the absence of H_3^{++} is not surprising because H^{++} and H_2^{++} are both physically impossible.

Negative Ions.—A test was made for the existence of negative ions. It was necessary to raise the electron current by a factor of about 10 before any could be detected. Very little work was done with these ions but two peaks were found. One corresponds to K^- ions. The other may be due to unstable K_2^- ions or to some impurity. It was not investigated carefully. The probability of electron attachment is of the order 10^{-5} (for 100 volt electrons), *i.e.*, 10^4 times less than the probability of attachment of K^+ ions.

It is perhaps worth noting that Sir Joseph Thomson* found O_2^- and O^- in discharge tubes but practically no N_2^- in positive ray spectra. Smyth found N_2^- and Hogness and Lunn found O_2^- and O^-. Both Smyth and Hogness and Lunn state that the number of negative ions was so low that they could not do any detailed work on them. In the present work the negative currents could be made quite strong enough to be investigated.

General Discussion.

We shall now consider our results in connection with the band spectra of the alkali-metal molecules and other optical data. All the known bands of the alkali-metals are degraded to the red and according to the theory of molecules developed by Franck† and others this indicates that the electronic transitions giving rise to these bands are such that the binding energy of the molecule is less in the higher electronic state than in the lower. It has also been shown‡ that for this type of transition the moment of inertia is greater in the higher than in the lower state. No bands of the K_2^+ molecule have been observed but for the purposes of this discussion we shall assume that all the transitions of the K_2 and K_2^+ molecules are such that the moment of inertia increases and the heat of dissociation decreases on excitation. Thus we may represent different states of the molecules by the series of curves shown in fig. 7.

By a series of experiments on the excitation of molecules by light and by electron impact Franck showed that the initial action of the light or electron on a molecule is to change solely its electronic configuration. The nuclei being very heavy are not disturbed in the initial process. Thus if the state of the system before excitation is represented by A_1 (fig. 7) its state immediately after excitation will be represented by some point (such as P, R or S) vertically above A_1. He also showed that if as a result of such a transition the molecule is brought into a state represented by R (potential energy greater than the work of dissociation) it dissociates, *i.e.*, it does not radiate energy and go to the state A_3.

---

* 'Rays of Positive Electricity,' p. 71; Smyth, 'Roy. Soc. Proc.,' A, vol. 104, p. 121 (1923); Hogness and Lunn, 'Phys. Rev.,' vol. 27, p. 732 (1926).

† 'Trans. Faraday Soc.,' vol. 21, p. 536 (1925).

‡ 'Report on Molecular Spectra of the National Research Council of America.'

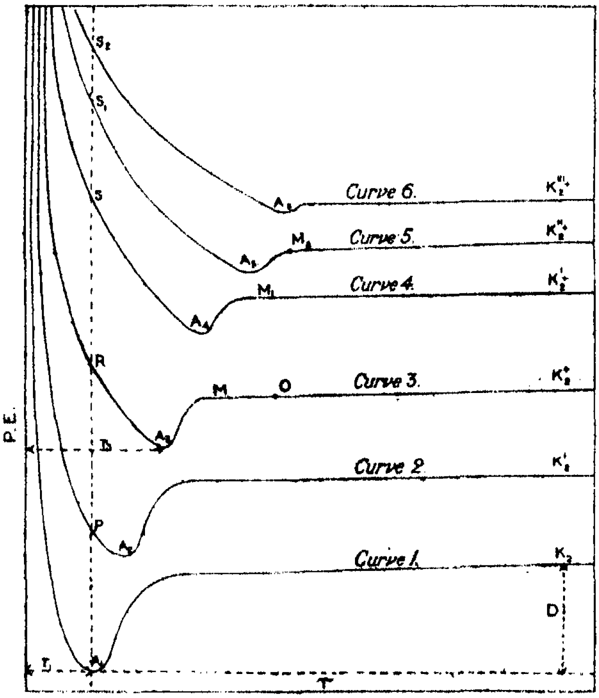

FIG. 7.*

We shall use these two results of the Franck theory but in considering transient states of the molecule we shall need to take into account the kinetic as well as the potential energy of the nuclei. Probably kinetic energy considerations are not of much importance in connection with the tightly-bound molecules (energies of dissociation of several volts) to which Franck and his colleagues have given their chief attention. In considering the interaction between a quantum or electron with 10 or 100 volts energy and a loosely-bound molecule, whose energy of dissociation is only a few tenths of a volt, the possibility of a small fraction of the available energy being transformed into nuclear kinetic energy may be very important.*

---

* To economise space the figure is out of proportion in two ways: (1) The curves ought to be much more separated in the vertical direction (*i.e.*, $A_1R = 4 \cdot 5$ volts, $A_1S_2 = 50$ volts). (2) The difference in the depths of the hollows ought to be much greater than shown, *i.e.*, that of curve 1 is $0 \cdot 5$ volt, and that of curve 3 is of the order $0 \cdot 005$ volt.

From the study of the ions formed by attachment two important and definite results stand out: (1) the K_2^+ molecule possesses a state of sufficient stability to enable it to pass through our apparatus and be measured at mass number 78. To do this it must exist for at least 10^{-5} sec. and must survive the magnetic field of 3000 gauss. Call this stable state, state (1). It is important in this connection that 10^{-5} sec. is a very long time compared with a period of molecular vibration† (10^{-12} sec.). (2) The K_2^+ molecule has also a state in which it is energetically unstable and can be dissociated by the magnetic field, state (2). It is in state (1) a short time after it has been formed by attachment and passes over to state (2) by a transition which involves emission of energy.

We can now picture the process of capture and dissociation as follows: When the K atom and the K^+ ion are widely separated they are both in their lowest electronic states and the system is represented by the point $r = \infty$ on curve (3). The ion approaches the atom along a hyperbolic orbit and the representative point moves in along curve (3) until the nearest distance of approach is reached. Four processes may occur as the atom and ion approach each other.

(1) If the nearest distance of approach is too large for attachment (*e.g.*, if the representative point only reaches 0) the atom and ion may separate after an elastic collision, *i.e.*, the representative point moves out along curve (3).

(2) If, however, an inelastic collision occurs, either the atom or the ion becomes excited; the representative point is thus transferred to curve (4) and moves out along it as the atom and ion separate.

(3) If the collision is more intimate, *e.g.*, suppose the representative point reaches M, then if the collision is elastic attachment will not occur. But if the atom and ion make an inelastic collision, as in process (2), the representative point is transferred to A_4 on curve (4). The ion is then under strong polarising

---

* *Note added in Proof.*—Since the above was written a paper has been published by Condon ('Phys. Rev.,' vol. 32, p. 858, 1928) in which it has been shown by the use of the new quantum mechanics that the momenta (and hence the energy) of the nuclei may alter slightly under certain conditions.

† This is also of interest in connection with the "unstable" molecules (*e.g.*, CH_3^+) found in positive ray parabolas. The fact that they register shows that they exist for a much longer time than 10^{-12} sec. They thus possess a considerable degree of stability.

forces; it radiates kinetic energy and is captured in the same manner as an electron is bound by an ionised atom on the old quantum theory.

(4) If the collision is still more intimate, so that the representative point is carried into the hollow at A_3, attachment may occur without excitation. Molecular ions formed by this last process will be perfectly stable.

Consider now the molecules formed by process (3). After the attachment the state of the molecular ion is represented by A_4 (or by a small vibration in the hollow round A_4). This is the stable state (1) in which the molecular ion does not dissociate. The excited molecular ion, after an interval of about 10^{-8} sec., makes an electronic transition on to the curve (3). Since the nuclei do not move till after the electronic transition, the state immediately after the transition will be represented by M (vertically below A_4). This is the state (2). The nuclei have a little kinetic or vibrational energy and this energy may either dissociate them along curve (3) or they may move inwards, radiate a little energy and take up a stable position at A_3 (or vibrating in the hollow round A_3). It will be seen that when the nuclei are at M (or during the transition from A_4 to M) very slight forces may decide whether they are to be dissociated or not. It is only necessary to alter the distribution of their energy slightly to make the difference. In the absence of any controlling force, the distribution may be regarded as a "probability" one—a certain portion go to A_3 and the remainder dissociate.

The magnetic field may affect the proportion of atoms which dissociate in one or both of the following ways: (1) It may slightly affect the distribution of energy during or immediately after the transition from A_4 to M so as to favour dissociation. (2) It may merely shorten the life of the state represented by A_4 (or by M). It must be remembered that all molecules which travel through the apparatus in states A_4 and M as well as those in state A_3 are counted as stable. Thus any agency which shortens the life of the states A_4 or M is going to decrease the proportion of "stable molecules" even though it does not affect the distribution of energy. Our experiments could possibly be explained on the view that the second of these effects is the only one. It appears probable however that both effects exist—especially in view of the experiment of Franck and Grotrian.*

It is not possible from our present results to determine the ratio of the number of molecules attached directly to state A_3 (*i.e.*, by process (4)) to those attached initially in higher states such as A_4 (*i.e.*, by process (3)). But in view of the fact that under certain conditions 50 per cent. dissociate it appears that at least half are initially attached in the higher states (by process (3)).

---

* 'Z. Physik,' vol. 6, p. 35 (1921).

If the above explanation of the process of attachment is correct we should expect the maximum distance of approach required for capture to be slightly greater than r_3, *i.e.*, of the same order but rather greater than r_1, the radius of gyration of the normal potassium molecule. Since r_1 is 3×10^{-8}, the value of r_3 should be about 4×10^{-8} to 6×10^{-8}. This value is in good agreement with the experimentally determined value (4×10^{-8} cm.) of the collision radius for the formation of $K_2{}^+$ ions by attachment (see p. 521).

Let us now consider the results of the photo-ionisation experiment. The present experiment shows definitely that no stable $K_2{}^+$ molecule is formed by photo-ionisation. This is at once explained on Franck's theory. The photo-ionisation process is represented by a transition from the point A_1 on curve (1) to the point R on curve (3), the ordinate of R being greater than that of M. Thus the molecule at R is unstable and dissociates in a time of the order of one molecular vibration. The photo-ionisation has previously been discussed in more detail by one of us.* It is there shown that in order to explain the frequency of the photo-electric threshold it is necessary to assume that the molecule at R has only a little more than sufficient energy to dissociate it. This assumption fits in well with our explanation of the present work.

The results of the experiments on ions formed by electron impact are explained as follows. Even the slowest electrons employed in our experiments had much more than sufficient energy to ionise the molecule. Thus the primary result of the impact of a 36-volt electron on a K_2 molecule is to remove the system from A_1 on curve (1) to S_1 on curve (5) representing a high state of excitation of the $K_2{}^+$ molecule, *i.e.*, one electron is removed from the molecule and another electron is removed from its normal orbit to an excited state. The system in the state represented by S_1 is very unstable. It moves down the curve to A_5 and then makes a transition on to curve (4) at M_1 with the emission of vibrational and electronic energy. At M_1 the molecule is quasi-stable and has a much larger collision radius than the normal molecule. The impact of a 100-volt electron moves the system from A_1 to S_2 on curve (6), *i.e.*, to a state of still higher excitation than that produced by the 36-volt electron. The resulting quasi-stable molecular ion is represented by M_2, *i.e.*, it possesses a larger collision radius and a greater degree of instability than the molecular ion produced by the 36-volt electron. Thus the $K_2{}^+$ ion formed by the 100-volt electron is easily dissociated by a distant collision

---

* Ditchburn, 'Proc. Cam. Phil. Soc.,' vol. 24, p. 320 (1928).

(process 2, p. 528). The K_2^+ ion represented by M_1 is unaffected by very distant collisions and makes a more intimate collision which leads to the formation of a K_3^+ ion (process 3, p. 528). Thus no stable K_2^+ ions can be formed by a primary process.

In view of the incompleteness of the data on alkali-metal molecules any theory must of necessity be somewhat tentative. It may be claimed, however, that the above view does agree with and explain in a qualitative way all that is at present known concerning these molecules. It appears that in a general way the work of Hogness and Lunn and of Smyth, etc., on Hg_2, N_2, O_2, H_2 can be explained along similar lines—but this does not fall within the scope of the present paper. Before any serious quantitative work can be done it will be necessary to have a more complete knowledge of the band spectra and a more detailed investigation by the methods described in this paper.

Summary.

1. Experiments are described in which ions are formed in a beam of potassium vapour and analysed in an apparatus similar to that used by Smyth and others.

2. The ions are produced in three ways: (1) by photo-ionisation; (2) by electron impact; and (3) by the attachment of K^+ ions from a Kunsman filament to K atoms. The only stable ion formed by photo-ionisation is K^+. With electron impact we obtain K^+ and K^- and evidence of the existence of unstable K_2^+, K_3^+ and K_3^{++}. The results obtained with 100-volt electrons show important differences from those obtained with 36-volt electrons. With ions formed by attachment we find definitely stable and unstable K_2^+ ions. Some information has been obtained concerning the conditions affecting the formation and dissociation of these K_2^+ ions.

Estimates are given of the probabilities of ionisation by electron impact, of the formation of K^- and of the attachment of K^+ to K. It is shown that the "lives" of the unstable compounds are of the order 10^{-6} sec.

3. A qualitative explanation of the results is given. The processes discussed are somewhat similar to those involved in the ionisation of hydrogen and other molecules. It is necessary to assume that the moment of inertia of the K_2 molecule and the K_2^+ molecular ion always increases on excitation. This agrees with results obtained from the band spectra.

It is a great pleasure for us to record our appreciation of the helpful interest and advice of Sir J. J. Thomson and Sir Ernest Rutherford in this work.

The Determination of Parameters in Crystal Structures by means of Fourier Series.

By W. LAWRENCE BRAGG, M.A., F.R.S., Langworthy Professor of Physics, Manchester University.

(Received February 9, 1929.)

1. *Introduction.*

The Fourier representation of the results of X-ray analysis was first suggested by W. H. Bragg.* It was developed independently by Duane, and used by Havighurst and Compton† to give striking representations of the distribution of scattering matter in crystals. Duane and Havighurst were first in applying the method to the much more accurate X-ray measurements available in 1925, and in showing how useful it could be.

Duane used a formula derived by Epstein and Ehrenfest.‡ They showed that the intensity of an X-ray reflexion from a plane (*h k l*) of a crystal is proportional to the square of the coefficient of a term in the Fourier series, representing the density $\rho\ (x, y, z)$ of the diffracting material in the crystal as a function of x, y, z. The general term may be written

$$A\,(h\ k\ l)\,\sin\,(2\pi hx/a - \delta_h)\,\sin\,(2\pi k/b - \delta_k)\,\sin\,(2\pi lz/c - \delta_l)$$

Duane reversed the line of thought, and showed that it is possible to deduce the density in the crystal from the measured intensities of X-ray reflexion. The X-ray measurements give the values of $(A\ (h\ k\ l)\ )^2$ but not the phase angles δ_h, δ_k, δ_l. This difficulty, Duane showed, could be surmounted in certain simple cases.

Havighurst§ used this triple Fourier series to determine the density of scattering matter in such crystals as rock-salt, NaCl. The calculations are lengthy, and Havighurst confined himself to evaluating the series along certain lines (cube edges or face-diagonals). Later, he used the same series for the determination of crystal parameters and analysed by its aid the mercurous halides which have structures with two parameters.

Compton made the further step of correlating the coefficients A (*h k l*) with the absolute value F $(h\,k\,l)$ of the structure factor. F $(h\,k\,l)$ is the ratio of the wave amplitude scattered in a given direction by all atoms in the unit cell, to that which would be scattered according to the classical formula by a single electron under the same conditions. Using the values of F, and adding to the series a suitable constant term, Compton showed that the series represents the "electron density" at any point in the crystal. He used a simple Fourier series to express the distribution of scattering matter in sheets parallel to a given plane; for this the values of F for the different orders of reflexion by parallel planes are alone required. He also developed a formula for the radial distribution of scattering matter in an atom; for this a knowledge of the atomic scattering curve (F curve) is necessary.

---

* 'Phil. Trans.,' A, vol. 215, p. 253 (1915).

† Duane, 'Proc. Nat. Acad. Washington,' vol. 11, p. 489 (1925); Havighurst, *ibid.*, vol. 11, p. 502 (1925); Compton, "X-rays and Electrons," p. 151.

‡ 'Proc. Nat. Acad. Sci.,' vol. 10, p. 133 (1924).

§ 'J. Amer. Chem. Soc.,' vol. 48, p. 2113 (1926).

The first Fourier representations of distribution of scattering matter by Havighurst and Compton were based on measurements of the quantity F $(h\,k\,l)$ by Bragg, James and Bosanquet.* Compton's formula for the sheet distribution of scattering matter has been used to check the results of crystal analysis (beryl, topaz and alum)† and to measure the thermal agitation of atoms.‡

It is interesting to note that the formula of Duane is implicitly developed in a paper by Ewald in 1921 on the reciprocal lattice, referred to more fully below. It was formulated by A. B. Porter for a corresponding optical problem in 1905, and W. H. Bragg's treatment in 1915 is based on Porter's equations. Porter based his work on Abbe's diffraction theory of microscopic vision. The correlation of the intensities of spectra with coefficients in the terms of a Fourier series is indeed a well-known optical principle due originally to Abbe fifty years ago, and used by him to discuss the resolving power of microscopes; it is now becoming clear that it has its most far-reaching and perfect expression in the interpretation of X-ray diffraction.

2. *The Double Fourier Series.*

In Havighurst's calculations, although a triple Fourier series in x, y, z is used, the density is only calculated for a series of points along a chosen line in the crystal. In Compton's calculations the density in sheets parallel to a plane, or the radial density distribution, is measured. In both cases the density is in effect expressed as a function of one variable (distance along a line, perpendicular to a plane, or along an atomic radius), though theoretically the formula may be used for a complete expression of the density throughout the crystal. The difficulty of dealing with all three variables is one of calculation, as, in order to get a passably accurate expression for the density, hundreds of terms must be evaluated and summed for every point x, y, z.

---

* 'Phil. Mag.,' vol. 41, p. 304 (1921), and vol. 42, p. 1 (1921).

† Beryl—Bragg and West, 'Roy. Soc. Proc.,' vol. 111, p. 691 (1926); Topaz—Alston and West, 'Z. Kryst.,' vol. 69, p. 149 (1928); Alum—Cork, 'Phil. Mag.,' vol. 4, p. 688 (1927).

‡ James and Firth, 'Roy. Soc. Proc.,' A, vol. 117, p. 62 (1927).

The present paper describes evaluations of the series which are more extensive than those previously carried out, in that the density is *calculated for values of two variables*. The values of F $(h\,k\,l)$ are measured for all crystal reflexions around a given zone; for instance, if the zone is the a axis of the crystal, the values of F $(0\,k\,l)$ are used. A Fourier series is formed in which these values appear as coefficients, the variables being the co-ordinates y and z. Values of y and z are taken at convenient intervals, and the Fourier series is summed for every pair of co-ordinates. The result is a series of figures in rows and columns which indicate the distribution of scattering matter in the unit cell, as projected on the face (100). The direction of projection is parallel to the a axis.

The calculations can be made quite rapidly. In the cases described below, the required range of each co-ordinate is divided into 24 intervals in one direction and 12 in the other, and the Fourier series of about 40 terms is summed for 288 points.* This is done for the a, b and c axes as zone axes in turn, leading to projections of the unit cell upon its faces (100), (010) and (001). The projections (shown as contoured diagrams in figs. 1*a*, 2*a* and 3*a*) indicate clearly the spatial distribution of scattering matter throughout the unit cell when they are considered in combination. They enable the atomic parameters to be measured, and the number of electrons in each atom to be counted. It is the object of the present paper to describe this analysis, and to compare its results with those obtained by other ways of analysing a crystal.

In order to form the Fourier series which represents the density distribution, it is necessary to know both the amplitudes and the phase constants of all the terms. X-ray measurement determines the former, but not the latter, for it is concerned with intensities which depend on the square of the amplitude coefficients alone. If, however, the crystal has centres of symmetry, and the origin of co-ordinates is taken to be at one of these centres, the equations assume a much more simple form.

---

* A comparison shows that the amount of calculation required for projection on a plane is much less than that required for a complete survey of density throughout the unit cell. Suppose that F $(h\,k\,l)$ values for the general planes were used, which represented reflexion up to as high an angle as those taken into account in the present calculations for planes around each zone. The number of terms in the Fourier series representing the density at a point then proves to be between 200 and 300 instead of 40, and the series would have to be summed for 48 times as many points.

It will be assumed that the crystal has a centre of symmetry at the origin, and that the formula for the projection on the face (100) is required. The axes of the unit cell are of lengths a, b, c, and make angles α, β, γ with each other, so that $bc \sin \alpha$ is the total area of the face on which projection is made. Let $\rho(y, z)$ be the density of scattering matter per unit area of the projection at the point y, z. It may then be shown that

$$\rho(y, z) = (1/bc \sin \alpha) \, . \sum_{-\infty}^{+\infty} \sum_{-\infty}^{+\infty} \mathrm{F}(0\,k\,l) \cos 2\pi (k\,y/b + lz/c). \qquad (1)$$

In this formula, there are no phase-constants, but $\mathrm{F}(0\,k\,l)$ must be given the correct sign. It is positive or negative, according to whether the scattering matter in the unit cell diffracts a wave in the same or the opposite phase to that scattered by an electron at the origin. All positive and negative values of k and l are taken into account (*i.e.*, although $\mathrm{F}(0\,k\,l)$ is identical with $\mathrm{F}(0\,\bar{k}\,\bar{l})$ the corresponding terms are counted as separate contributions to the series).

In the special case where $k = 0$, $l = 0$, the value of $\mathrm{F}(0\,0\,0)$ must be taken to be Z, the total number of electrons in the unit cell. The corresponding member of the Fourier series is a constant. When integrating $\rho(y, z)$ over the face (100), all terms vanish, except the term involving $\mathrm{F}(0\,0\,0)$. Thus

$$\int_{-b/2}^{+b/2} \int_{-c/2}^{+c/2} \rho(y, z)\, dy\, dz \sin \alpha = \mathrm{F}(0\,0\,0) = \mathrm{Z}. \qquad (2)$$

Formula (1) is an extension, to two dimensions, of the formula derived by Compton for the distribution of scattering matter in sheets, and holds for a cell of any shape provided that it has a symmetry centre. It may be proved by forming the expression for $\mathrm{F}(0\,k\,l)$

$$\mathrm{F}(0\,k\,l) = \int_{-b/2}^{+b/2} \int_{-c/2}^{+c/2} \rho(y, z)\, dy\, dz \sin \alpha \cos 2\pi (ky/b + lz/c). \qquad (3)$$

When a series $\Sigma\Sigma\, \mathrm{A}(q, r) \cos 2\pi (qy/b + rz/c)$ is substituted for $\rho(y, z)$ all terms vanish on integration except those for which $q = k$, $r = l$ and $q = -k$, $r = -l$. Remembering that $\mathrm{F}(0\,k\,l) = \mathrm{F}(0\,\bar{k}\,\bar{l})$, this shows that the coefficient $\mathrm{A}(k, l)$ of the series is equal to $\mathrm{F}(0\,k\,l)/bc \sin \alpha$.

It will readily be seen that formula (1) gives the projection of scattering matter in the unit cell, in a direction parallel to any zone axis, on any crystal plane. The zone axis is taken as one axis of reference, and two other axes of reference are chosen in the plane. A set of indices $(h\,k\,l)$ becomes a set such as $(0\,\mathrm{K}\,\mathrm{L})$ referred to the new axes, and $\mathrm{F}(h\,k\,l)$ must now be labelled $\mathrm{F}(0\,\mathrm{K}\,\mathrm{L})$. Formula (1) then applies.

The formula quoted above is a special case of the general formula for the density at the point x, y, z in a crystal cell of any shape and symmetry. The reflexion from the plane $(h\,k\,l)$ must now be characterised by both an amplitude and a phase constant. Following Ewald (*loc. cit.*) $\mathrm{F}(h\,k\,l)$ may be expressed as a complex quantity

$$\mathrm{F}(h\,k\,l) = |\,\mathrm{F}(h\,k\,l)\,|\,e^{i\theta(h\,k\,l)},$$
$$= \frac{\mathrm{V}}{abc}\int_{-a/2}^{+a/2}\int_{-b/2}^{+b/2}\int_{-c/2}^{+c/2} \rho(x, y, z)\, e^{2\pi i(hx/a+ky/b+lz/c)}\,dx\,dy\,dz. \qquad (4)$$

V is the volume of the unit cell, and a, b, c are the lengths of its edges.

If we assume a series for (x, y, z) of the form

$$\rho(x, y, z) = \sum_{-\infty}^{+\infty}\sum_{-\infty}^{+\infty}\sum_{-\infty}^{+\infty} \mathrm{A}(pqr)\cos\left(2\pi(px/a + qy/b + rz/c) + \alpha(pqr)\right),$$

a formal solution is given by

$$\mathrm{A}(h\,k\,l) = |\,\mathrm{F}(h\,k\,l)\,|\,.\,\frac{1}{\mathrm{V}}.$$
$$\alpha(h\,k\,l) = -\,\theta(h\,k\,l).$$

The series for (x, y, z) is thus

$$\rho(x, y, z) = \frac{1}{\mathrm{V}}\sum_{-\infty}^{+\infty}\sum_{-\infty}^{+\infty}\sum_{-\infty}^{+\infty} |\,\mathrm{F}(h\,k\,l)\,|\cos\left(2\pi(hx/a+ky/b+lz/c) - \theta(h\,k\,l)\right). \qquad (5)$$

As before, $\mathrm{F}(0\,0\,0)$ is equal to Z, the total number of electrons in the unit cell. In this general case $|\,\mathrm{F}(h\,k\,l)\,| = |\,\mathrm{F}(\bar{h}\,\bar{k}\,\bar{l})\,|$ and $\theta(h\,k\,l) = -\,\theta(\bar{h}\,\bar{k}\,\bar{l})$. All terms except the constant term in the series occur in identical pairs, but it is convenient to keep the series in this form for the sake of symmetry of expression.

3. *Application of the Double Fourier Series.*

The Fourier series is applied in this paper to a crystal which has already been analysed by other methods.* The crystal is diopside, $\mathrm{CaMg(SiO_3)_2}$, the structure of which depends on 14 parameters. Extensive measurements of $\mathrm{F}(0\,k\,l)$, $\mathrm{F}(h\,0\,l)$, $\mathrm{F}(h\,k\,0)$ are available and are quoted in the paper referred to above. All 14 parameters had been determined by Warren and Bragg, and it is therefore of interest to see how closely the former values agree with the parameters deduced from the projections of density on the cell faces. The average difference, in this quite complex crystal, proves to be only 0·5 per cent. Other interesting points arise from a consideration of the projections, which are dealt with below.

---

* Warren and Bragg, 'Z. Krist.,' vol. 69, p. 167 (1928).

The main point which it is desired to emphasise, is one discussed by West and the author* in a recent paper on the analysis of complex crystals. If absolute measurements of X-ray diffraction are available, the analysis of complex crystals is far more simple and certain than it is when merely comparative or qualitative estimates of diffraction are made. The paper on the structure of diopside was intended to be an illustration of the use of these measurements. The 14 parameters of the crystal can be deduced by using the absolute measurements without making any assumptions as to the probable arrangement of the atoms. In the present paper, the values of the parameters are derived in a quite different way, and the agreement in the results shows that the crystal has been analysed correctly.

The two methods of analysis are not independent, for the former analysis was used to give the correct sign to each coefficient $F(h\,k\,l)$. If the sign could be determined otherwise, the complete analysis could be made by the Fourier series. This point is briefly discussed in section 9 of the paper by Bragg and West. In the previous analysis of diopside, atomic scattering curves (F curves) for the atoms were used, and values of the parameters were found which made the observed and calculated values of $F(h\,k\,l)$ agree, signs being of course disregarded. For convenience, we may denote by $|F(h\,k\,l)|$ the quantity we can deduce from X-ray measurements of intensity, and by $F(h\,k\,l)$ the coefficient of the Fourier series. When the analysis of the structure was completed it was possible to give the right sign to each coefficient, *i.e.*, to determine $F(h\,k\,l)$. In the present analysis, therefore, the magnitudes of the Fourier coefficients depend only on X-ray measurement, but their signs are found by a previous analysis. It will be realised, however, that there is in general very little doubt about the sign of each coefficient, once an approximate analysis of the crystal has been made. It is determined in most cases by the positions of the heavier atoms of calcium, magnesium, and silicon, and quite approximate estimates of their parameters will suffice. The sign is only doubtful when F is very small, and in that case it does not matter.

As was emphasised by Duane, any given set of X-ray results may be explained even in the case of a centrosymmetrical crystal by as many different arrangements of scattering matter as there are permutations of signs in the Fourier

---

[*] Bragg and West, 'Z. Krist.,' vol. 69, p. 118 (1928).

coefficients. The test for the correct solution is that it is reasonable, or that it indicates a distribution of scattering matter which outlines atoms such as we know to exist in the crystal. In the former analysis, the existence of four molecules of $CaMg(SiO_3)_2$ in the unit cell was assumed from the start, and these atoms were moved about until the experimental results were explained. In the present analysis we show in effect that a certain set of signs given to the measured values of $|F(h\,k\,l)|$ leads to a distribution of density which (*a*) gives consistent projections on all three cell faces; (*b*) gives the correct number of atoms in the unit cell; (*c*) gives the correct number of electrons to each atom. The evidence for the correctness of the solution is set forth, using the Fourier series, in a new form which is perhaps more attractive and easy to grasp.

It must be realised, however, that the analysis by assigning parameters to atoms which make observed and calculated results agree, and the analysis by finding a suitable set of signs for Fourier terms, fundamentally depend upon precisely the same criteria for their success. We assume as one criterion, for instance, that the calcium atom contains about 18 electrons with a spatial distribution which we have been able to estimate. In the first type of analysis this yields an F curve for the scattering by calcium, and such F curves are used in comparing calculated and observed results. In an analysis entirely conducted by the Fourier method, signs would be adjusted till the series outlined a recognisable calcium atom, again with the number of electrons and spatial distribution which we expect. Every step in the one type of analysis may be paralleled by a similar step in the other.

4. *Tabulation of Experimental Results for Diopside.*

The crystal diopside is monoclinic, with $a = 9 \cdot 71$ Å, $b = 8 \cdot 89$ Å, $c = 5 \cdot 24$ Å, $\beta = 74° \, 10'$. The unit cell contains four molecules of $CaMg(SiO_3)_2$, hence the total number Z of electrons in the unit cell is 432. The space group is C_{2h}^6 (2C*i* — 6).

The projections dealt with in this paper are upon the three faces (100), (010) and (001) of the unit cell. Sets of values of $F(0\,k\,l)$, $F(h\,0\,l)$, $F(h\,k\,0)$ are required which are as extensive as possible. These values, taken from the paper on diopside, may be put in the form of tables such as those below.

In Table I, for example, l varies along the rows and k along the columns. Owing to the conditions imposed by the space group, only even values of k appear, and also $F(0\,0\,l)$ is zero when l is odd. The complete table would show negative values of k as well as of l. This is unnecessary because $F(0\,k\,l) = F(0\,\bar{k}\,\bar{l})$; we may say that every table has a centre of symmetry at the value

432 corresponding to F (0 0 0). Negative values of F are denoted by a bar above the figure. As mentioned above, the magnitudes of F are in every case determined by experimental measurement. The sign of each coefficient is determined by a previous analysis of the crystal, which need only be assumed to be approximately correct.

Table I.—Values of F (0 k l).

When $k = 0$, l is even. k is always even. When l is odd, F (0 k l) $= -$ F (0 k $\bar{l}$).

Index l →	$\bar{8}$	$\bar{7}$	$\bar{6}$	$\bar{5}$	$\bar{4}$	$\bar{3}$	$\bar{2}$	$\bar{1}$	0	1	2	3	4	5	6	7	8
Index k ↓ 0	38	—	29	—	136	—	$\overline{175}$	—	432	—	$\overline{175}$	—	136	—	$\overline{29}$	—	38
2	0	0	0	0	0	0	75	$\overline{44}$	19	44	75	0	0	0	0	0	0
4		26	33	$\overline{26}$	0	50	72	$\overline{82}$	0	82	72	$\overline{50}$	0	26	33	$\overline{26}$	
6			0	29	0	$\overline{44}$	88	50	94	$\overline{50}$	88	44	0	$\overline{29}$	0		
8				0	0	0	28	25	0	$\overline{25}$	28	0	0	0			
10								66									
12								29									

Table II.—Values of F (h 0 l).

For all reflexions, h and l are even.

Index l →	$\bar{8}$	$\bar{6}$	$\bar{4}$	$\bar{2}$	0	2	4	6	8
Index h ↓ 0	38	$\overline{29}$	136	$\overline{175}$	432	$\overline{175}$	136	$\overline{29}$	38
2	0	0	19	$\overline{88}$	0	46	0	$\overline{36}$	0
4	0	$\overline{72}$	90	$\overline{128}$	15	$\overline{80}$	77	$\overline{49}$	0
6		0	0	0	100	$\overline{82}$	59	$\overline{30}$	
8			33	$\overline{51}$	76	$\overline{32}$	0		
10				$\overline{63}$	56	$\overline{44}$			
12					0				

Table III.—Values of F $(h\,k\,0)$.

For all reflexions, $h + k$ is even. F $(h\,k\,0)$ = F $(h\,\bar{k}\,0)$.

		Index h→ 0	1	2	3	4	5	6	7	8
Index k ↓	0	432		0		15		100		76
	1		0		76		$\bar{63}$		41	
	2	19		$\bar{51}$		$\bar{23}$		$\bar{19}$		$\bar{32}$
	3		13		50		37		0	
	4	0		16		$\bar{50}$		0		
	5		$\bar{84}$		$\bar{55}$		0		$\bar{96}$	
	6	$\bar{94}$		31		29		0		
	7		0		0		40			
	8	0		$\bar{17}$						

In order to get a perfect representation of the scattering power in the crystal, it would be necessary to measure all values of F up to indices so high that the values become vanishingly small. It will be clear from the tables that the experimental results fall far short of the ideal. All values of F have been measured up to a glancing angle represented by $\sin\theta = 0\cdot45$ for planes $(0\,k\,l)$ and $(h\,0\,l)$, and $\sin\theta = 0\cdot30$ for the planes $(h\,k\,0)$, using rhodium Kα radiation for which $\lambda = 0\cdot615$ Å. Hence the Fourier representation will be in all cases imperfect, and particularly so for the projection on the c face where values of F $(h\,k\,0)$ are used.

5. *Ewald's Reciprocal Lattice.*

The figures in these tables may be given an interesting interpretation by the elegant method of the "Reciprocal Lattice*" which we owe to Ewald.† Every set of parallel planes of a crystal is represented by a point in the reciprocal lattice. The line joining this point to the origin of the reciprocal lattice is at right angles to the crystal planes, and its distance from the origin is inversely proportional to their spacing. Since there is a definite structure-factor for each set of planes, a corresponding figure or "weight" can be attached to the point of the reciprocal lattice. The structure factors for first, second and high orders of X-ray reflexion become a set of figures attached to points in a row at equal intervals, the first order being nearest the origin. The assemblage of points corresponding to reflexion by all planes of the crystal builds up a space lattice, the reciprocal lattice.

---

* It will be realised that each point in the reciprocal lattice corresponds to a simple sinusoidal distribution of density in the crystal, and that the complete representation of a given set of parallel crystal planes is an extended row of points.

† 'Z. Krist.,' vol. 56, p. 129 (1921).

We may consider the " weights " attached to the points of reciprocal lattice as being, in our notation, the values $F(h\,k\,l)$. In general $F(h\,k\,l)$ is a complex quantity, according to Ewald, representing both the amplitude and phase of the scattered wave. In the particular case considered here, it is real but positive or negative. The indices h, k, l give the co-ordinates of the point with reference to the axes of the reciprocal lattice. We attach a weight $F(0\,0\,0)$ to the origin equal to Z, the number of electrons in the unit cell of the crystal.

If this convention be adopted, it will be seen that the figures in Tables I, II and III represent *plane sections, through the origin, of Ewald's reciprocal lattice.* The origin of the lattice is always at the figure 432. The Fourier representation may therefore be summed up as follows. Any plane of the reciprocal lattice passing through the origin has a two-dimensional array of figures. These are the coefficients of a Fourier series, which gives the projection of the scattering matter in the crystalline cell on a plane. The direction of projection is that of the zone axis corresponding to the plane section of the reciprocal lattice. The orientation of the crystal plane on which projection takes place is obviously immaterial. Any convenient plane inclined to the zone axis, and any axes of reference in that plane, can be chosen. The indices $(h\,k\,l)$ must, of course, be transformed into indices $(h'\,k'\,l')$ to correspond to the new axes which have been chosen. This merely means that having chosen our axes of reference in the crystal plane, we must choose a corresponding frame of reference for the network of points in the central section of the reciprocal lattice.

It is interesting to note that the whole development of the Fourier representation is implicitly contained in the paper by Ewald referred to above. He develops it, however, only in respect to a set of scattering points in the crystal, and not to a continuous distribution of scattering matter.

6. *Summation of the Fourier Series.*

The Fourier series for projections on (100), (010) and (001) faces of the unit cell are summed in Tables IV, V and VI. The figures in these tables correspond to series

$$S(y, z) = \Sigma\,\Sigma\,F(0\,k\,l)\cos 2\pi(ky/b + lz/c)$$
$$S(x, z) = \Sigma\,\Sigma\,F(h\,0\,l)\cos 2\pi(hx/a + lz/c)$$
$$S(x, y) = \Sigma\,\Sigma\,F(h\,k\,0)\cos 2\pi(hx/a + ky/b).$$

To make the tables more compact, the actual sums of the series are divided by 10. The density per unit area at any point in a projection is given by

$$S(y, z)/bc \sin \alpha, \qquad S(x, z)/ac \sin \beta, \qquad S(x, y)/ab \sin \gamma.$$

(Since the crystal in the present example is monoclinic, $\sin \alpha = \sin \gamma = 1$.) Thus in order to derive the density per unit area from the figures in the tables, they must be multiplied by 10 and divided by the area of the face on which projection is being made.

The origin is taken to be at the centre of the unit cell. This origin is marked in each table, and the range of the figures in the *a*, *b* or *c* direction is indicated. It is not necessary to calculate the density all over the cell face as it repeats by symmetry. Since an atom in the general position becomes eight atoms in the unit cell, owing to the symmetry elements, it follows that it is only necessary to plot the density distribution over one-eighth of the surface of each face. The continuation of these sets of figures over the whole of each face will be clear if they are considered in conjunction with the contoured diagrams of figs. 1A, 2A, 3A.

Table IV.—Projection on Face (100).

$S(y, z) \times 10^{-1}$.

↑	163	122	58	29	2	$\bar{6}$	3	$\bar{6}$	2	29	58	122	163
	129	83	40	24	6	$\bar{4}$	33	$\bar{4}$	6	24	40	83	129
	65	30	17	25	30	42	76	42	30	25	17	30	65
	28	9	24	52	75	134	191	134	75	52	24	9	28
	22	22	48	83	112	214	285	214	112	83	48	22	22
	17	29	51	69	91	212	289	212	91	69	51	29	17
	2	13	21	24	33	143	210	143	33	24	21	13	2
	0	4	0	$\bar{5}$	$\bar{6}$	67	111	67	$\bar{6}$	$\bar{5}$	0	4	0
	12	11	0	1	6	29	49	29	6	1	0	11	12
	24	16	4	22	35	25	25	25	35	22	4	16	24
	29	16	3	37	68	44	36	44	68	37	3	16	29
$\frac{b}{2}$	31	13	0	42	78	76	79	76	78	42	0	13	31
	33	8	$\bar{6}$	31	70	112	137	112	70	31	$\bar{6}$	8	33
	31	5	$\bar{8}$	20	54	142	193	142	54	20	$\bar{8}$	5	31
	29	4	$\bar{5}$	15	40	156	224	156	40	15	$\bar{5}$	4	29
	24	4	2	12	27	139	213	139	27	12	2	4	24
	12	$\bar{1}$	2	7	12	93	159	93	12	7	2	$\bar{1}$	12
	$\bar{1}$	$\overline{12}$	$\bar{2}$	$\bar{1}$	$\bar{2}$	45	97	45	$\bar{2}$	$\bar{1}$	$\bar{2}$	$\overline{12}$	$\bar{1}$
	2	$\bar{5}$	7	12	15	37	74	37	15	12	7	$\bar{5}$	2
	17	13	21	33	45	66	95	66	45	33	21	13	17
	22	18	16	31	50	86	111	86	50	31	16	18	22
	28	21	$\bar{2}$	6	23	68	91	68	23	6	$\bar{2}$	21	28
	65	50	3	$\bar{5}$	$\bar{4}$	34	52	34	$\bar{4}$	$\bar{5}$	3	50	65
	129	99	38	12	$\bar{6}$	10	19	10	$\bar{6}$	12	38	99	129
↓	(163)	122	58	29	2	$\bar{6}$	3	$\bar{6}$	2	29	58	122	163

Origin ← $\frac{c}{2}$ →

Table V.—Projection on Face (010).

$S(x, z) \times 10^{-1}$.

$\frac{c}{4}$

364	291	138	33	20	48	55	48	76	127	162	159	150	159	162	127	76	48	55	48	20	33	138	291	364
330	242	121	25	14	39	36	34	71	131	167	160	136	128	125	101	70	63	74	64	23	21	117	264	330
249	206	76	8	8	19	24	20	54	115	146	128	91	78	74	68	72	77	94	78	29	9	82	192	249
150	106	24	$\bar{13}$	3	27	17	9	40	95	109	82	52	28	32	45	57	87	109	97	34	$\bar{3}$	31	114	150
73	36	$\bar{14}$	$\bar{24}$	16	26	20	5	18	59	67	40	7	0	14	36	63	98	127	87	50	$\bar{5}$	1	52	73
32	5	$\bar{30}$	$\bar{26}$	8	30	20	19	17	38	40	15	$\bar{10}$	$\bar{7}$	14	40	66	104	130	117	59	8	$\bar{2}$	24	32
17	$\bar{4}$	$\bar{25}$	$\bar{21}$	6	18	14	8	13	25	13	1	$\bar{13}$	$\bar{4}$	18	41	65	94	110	100	57	10	3	20	17
18	4	$\bar{14}$	$\bar{16}$	$\bar{5}$	1	4	8	16	16	4	$\bar{7}$	$\bar{12}$	2	16	34	53	71	82	70	46	16	14	23	18
21	10	$\bar{3}$	$\bar{11}$	$\bar{16}$	$\bar{16}$	$\bar{8}$	11	25	14	2	$\bar{8}$	$\bar{7}$	2	21	21	36	51	56	46	27	16	18	24	21
18	14	3	$\bar{5}$	$\bar{12}$	$\bar{7}$	11	33	35	34	6	2	2	4	5	13	28	43	35	32	17	13	14	20	18
21	16	14	0	2	14	34	61	56	36	10	12	12	12	6	19	30	56	54	37	22	26	14	14	21
12	14	17	21	19	33	50	78	68	43	21	18	22	18	15	27	55	74	66	40	28	33	17	10	12
(2)	8	19	25	29	45	73	87	71	39	21	24	28	24	21	39	71	87	73	45	29	25	19	8	2

Origin ← $\frac{a}{2}$ →

Table VI.—Projection on Face (001).

$S(x, y) \times 10^{-1}$.

$\frac{b}{4}$

122	87	22	$\bar{15}$	5	50	80	80	67	47	30	11	6	11	6	47	67	80	80	50	5	$\bar{15}$	22	67	122
54	31	0	$\bar{3}$	31	68	79	65	49	43	37	22	10	8	27	51	81	95	85	40	$\bar{5}$	$\bar{7}$	68	157	216
17	5	$\bar{4}$	12	48	76	70	44	34	35	39	26	11	4	19	45	78	94	82	38	$\bar{5}$	8	100	217	273
14	1	$\bar{12}$	$\bar{11}$	32	57	47	20	10	14	24	14	2	$\bar{6}$	2	20	46	58	55	25	$\bar{4}$	15	102	207	258
40	21	$\bar{8}$	$\bar{16}$	6	25	21	1	$\bar{6}$	$\bar{5}$	6	5	3	5	6	9	10	15	19	12	$\bar{12}$	$\bar{2}$	58	137	174
85	56	3	$\bar{25}$	$\bar{11}$	18	29	15	0	$\bar{11}$	$\bar{6}$	5	28	47	55	31	4	$\bar{11}$	$\bar{5}$	2	$\bar{1}$	$\bar{3}$	21	60	83
151	116	46	4	15	52	74	62	31	6	1	25	75	121	135	96	37	$\bar{2}$	$\bar{4}$	12	17	6	6	14	23
189	154	78	36	51	91	115	101	56	19	7	36	103	170	197	155	80	23	13	29	37	22	5	4	5
171	140	78	44	60	102	119	97	54	9	$\bar{9}$	17	87	163	203	173	102	39	21	30	32	16	0	$\bar{4}$	$\bar{1}$
118	96	50	30	46	75	82	61	28	$\bar{4}$	$\bar{18}$	$\bar{7}$	44	111	156	150	104	57	36	31	18	0	$\bar{8}$	0	$\bar{10}$
66	51	23	13	28	46	42	27	18	7	$\bar{6}$	$\bar{11}$	5	47	94	113	104	85	66	44	14	$\bar{9}$	$\bar{11}$	5	20
37	26	12	11	21	26	16	10	21	30	26	2	$\bar{8}$	14	58	98	117	122	108	78	33	1	0	26	43
(25)	20	12	13	20	22	11	9	28	47	45	16	$\bar{8}$	7	44	93	126	139	129	94	42	7	10	40	59

Origin ← $\frac{a}{2}$ →

The positions of the atoms are revealed by the figures. A heavy atom makes the figures rise to an obvious maximum. A light atom (oxygen) is sometimes so close to a heavier neighbour in a projection that its position is not shown by a separate maximum value.

Some of the figures are negative, indicated by a bar above them. In a case of X-ray diffraction such as this, where anomalous scattering does not occur, negative scattering matter has no significance. The density should be positive everywhere, approaching a zero value in the regions between the atoms. The appearance of negative values may be partly due to errors in measurements of F. but even if these were perfect, negative values are to be expected because the Fourier series is not complete. Additional values of F for higher indices would make the figures correspond more closely to the ideal values.

The diagrams in figs. 1A, 2A and 3A were made by plotting the figures giving the density distribution in their positions on each face of the unit cell, and then drawing contour lines through points of equal density. The contours are drawn at intervals of 40, corresponding to intervals of 400 in the actual values of

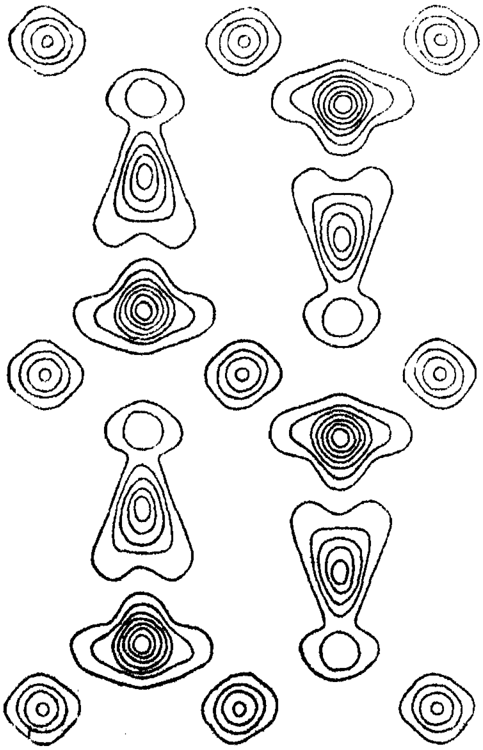

Fig. 1A.

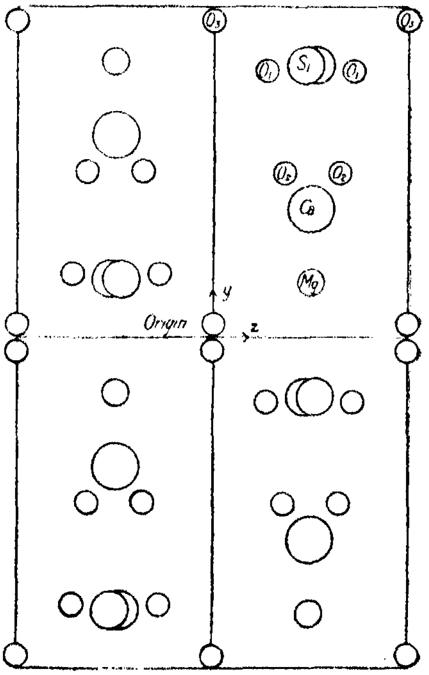

Fig. 1B.

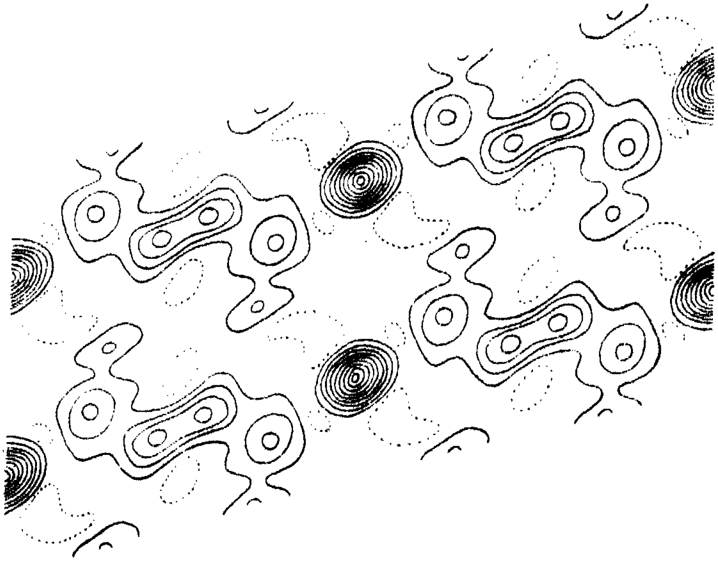

FIG. 2A.

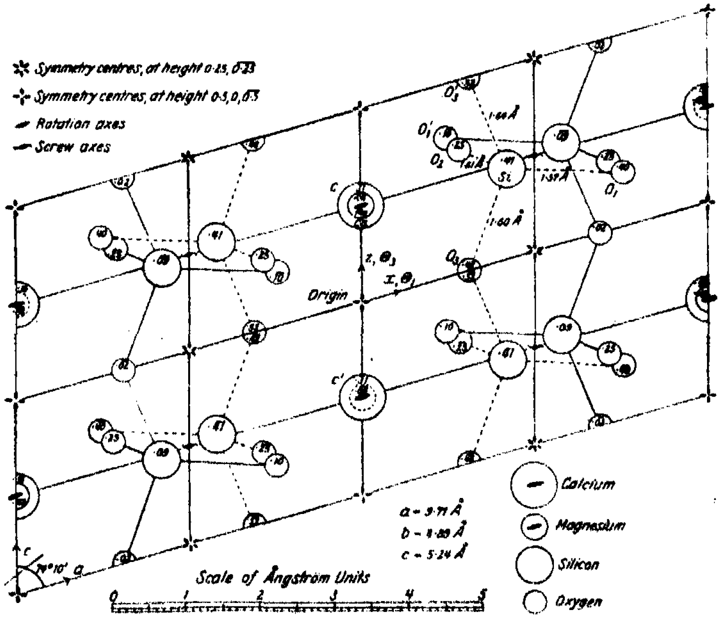

FIG. 2B.

S (*y*, *z*), etc. The positions of the atoms as found in the previous paper on diopside are shown in figs. 1B, 2B, 3B, and the two sets of figures are seen to correspond very closely. In the projection on (010) the areas enclosing

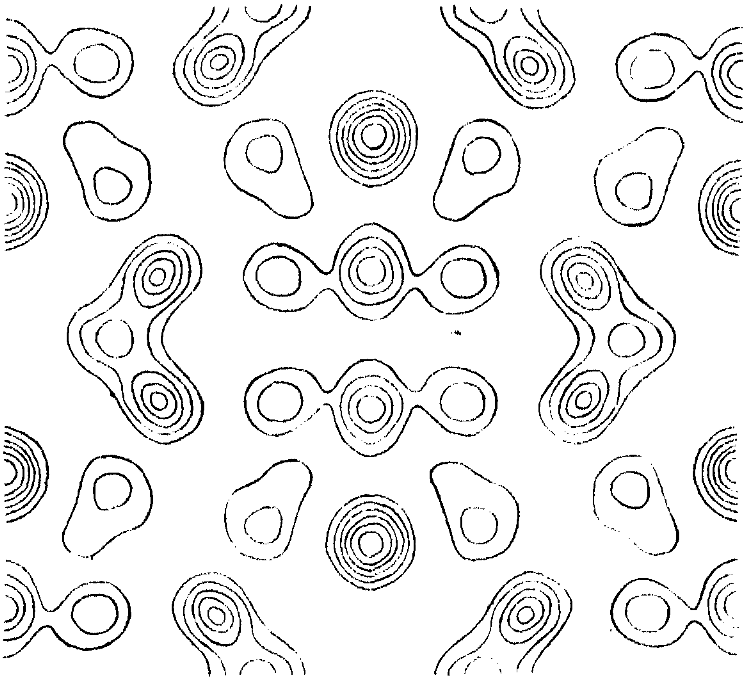

Fig. 3a.

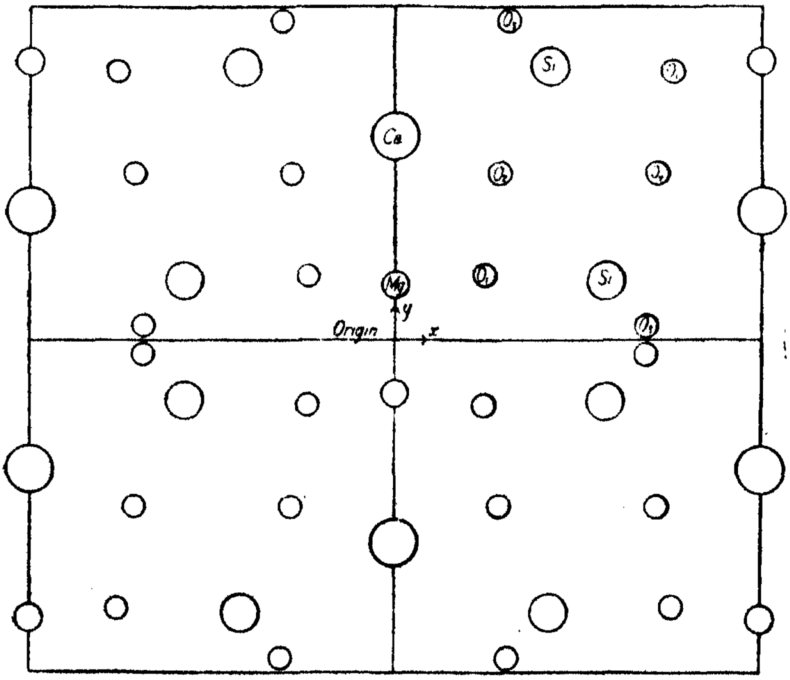

Fig. 3b.

negative values are marked by dotted lines, these lines being the contours of zero level where $S(x, z) = 0$. The zero contours are not marked in the other projections. The first continuous contour line around each atom or group passes through all points where S is 400, the next through points where it is 800, and so forth.

7. *The Number of Electrons in the Atoms, and their Identification.*

The density in the space between the atoms is in general quite small. Since this is the case, it is possible to draw an approximate boundary around each atom or group of atoms in a projection and to calculate the total number of electrons in that area. We may take, as an instance, the projection on (010), and count the number of electrons in the most obvious rounded mass shown in that projection, where the contour lines rise to a peak of 364 (3640). The figures S are plotted at intervals $a/24$, $c/24$. The density per unit area is equal to

$$S(x, z)/ac \sin \beta$$

and this density may be taken to be the average density over a cell with sides $a/24$, $c/24$. This little cell of area $ac \sin \beta/24^2$ contributes an amount

$$(S(x, z)/ac \sin \beta) \, . \, (ac \sin \beta/24^2) = S(x, z)/2304.$$

Thus the total number of electrons in the whole mass of scattering matter is given by

$$\Sigma \, S(x, z)/2304,$$

where $\Sigma \, S(x, z)$ is 10 times the sum of all the numbers in Table V which outline the atom or group in question. Although the boundary enclosing these numbers is somewhat indefinite, trial shows that it does not matter much where it is drawn because the density between the atoms is so small. In the case considered, the number of electrons proves to be 28·3, corresponding to a superimposed calcium atom and magnesium atom (18 + 10). The remaining atoms in the projection (010) are so superimposed that it is difficult to disentangle them, but all atoms stand out clearly in one projection or another. The following table shows the electron-count in all cases where it is possible. There are three kinds of oxygen atom, O_1, O_2 and O_3.

Projection on (100).

Atoms.		No. of electrons.
Ca + $2O_2$	......	35·3
Si + O_1	......	20·1
Mg	......	13·3
O_3	......	8·0

Projection on (010).

Atoms.		No. of electrons.
Ca + Mg	......	28·3
O_3	......	7·7 approx.

Projection on (001).

Atoms.		No. of electrons.
Ca	......	16·6
Mg	......	12·6
Si + O_3	......	19·8
O_2	......	9·6
O_1	......	8·0

Two points of interest may be noted. The average number of electrons in the oxygen atoms is distinctly less than 10, being in fact 8·3. It is thus much nearer to the value 8 for a non-ionised atom than to the value 10 for O^{-2}. The average number for Si + O is equal to 20, so that according to these figures the number of electrons in the silicon atom is 11·7, and in the oxygen atom is 8·3. The estimate of 9·6 electrons for O_2 in the (001) projection is at variance with these estimates, and the discrepancy shows that too much reliance must not be placed upon them. Nevertheless it is interesting to see that the figures do not correspond to ions Si^{+4}, O^{-2} each with 10 electrons. They suggest, on the other hand, that both the oxygen atoms and the silicon atoms are only partially ionised. As against this, if the estimates given above for the numbers of electrons in all the atoms of the projection on (001) are added, the sum for the molecule $CaMg(SiO_3)_2$ is 104 which does not check with the correct number 108. Some electrons have been missed in the count, and the missing electrons may belong to the diffuse oxygen atoms. It is indeed difficult to make estimates for the oxygen atoms, since their boundaries are not precise and the incomplete Fourier series leads to irregular variations of the density between the atoms. For instance, it is possible to see in the figures of Table VI at the point $a/2$, 0, a small mass of scattering matter which cannot be associated with any atom, and is a kind of optical "ghost."

The other point of interest is the division of electrons between calcium and magnesium. The total number is found to be 28, corresponding to the figures 18 + 10 which we would expect. The magnesium atom, however, appears to have more than its due share of these electrons. The material is reported to contain 1·12 per cent. of FeO, and if this iron replaces magnesium it would raise the average number of electrons in the Mg position from 10 to 10·5. The number of magnesium in the projections is, however, between 12 and 13 whereas calcium appears to have about 16 electrons instead of 18. The possibility that calcium and magnesium interchange their positions to a certain extent is suggested. In view of the complexity of the crystal, and the difficulty of allowing for extinction in correcting some of the observed intensities, it would be misleading to stress any of these figures unduly.

It is quite clear that the atoms can be successfully identified by counting the electrons in them.

8. *The Parameters of the Structure.*

The position of an atom as shown in a projection may either be taken to be the point where the density shows a maximum, or to be the centre of gravity of the whole mass of scattering matter. For the oxygen atoms the latter has been determined, but this can only be done when the atom stands out clearly separated from its neighbours. In some cases overlapping is so extensive that no precise co-ordinates can be found. An interesting special case is shown in the projection on (100) fig. 1*a*. Two oxygen atoms overlap at the centre of the figure, forming a single rounded mass. These oxygen atoms are derived from each other by inversion at the centre. It is clear that their co-ordinates in both *b* and *c* directions are very nearly equal to zero, but it is impossible to find their precise values. The information derived from the various projections is tabulated below.

Table VII.

Projection.	(100).			(010).			(001).		
	θ_1.	θ_2.	θ_3.	θ_1.	θ_2.	θ_3.	θ_1.	θ_2.	θ_3.
		°	°	°		°	°	°	
Ca	—	−107	90	0	—	90	0	−108	—
Mg	—	30	90	0	—	90	0	34	—
Si	—	146	(90)	78	—	85	74	147	—
O_1	—	(148)	(50)	137	—	55	135	151	—
O_2	—	(100)	(115)	43	—	125	51	91	—
O_3	—	(180)	(0)	52	—	0	52	(180)	—

The figures in brackets are approximate because of overlapping of atoms. The values for O_1 and O_2 in the (010) projection are bracketed because the position of the centre of gravity of the pair can be placed at the co-ordinates given in the table although these two atoms cannot be resolved.

The parameters deduced from all three projections are combined below, and are compared with the parameters deduced by the analysis in a previous paper.

Table VIII.

	Parameters determined by Fourier analysis.			Values given in previous paper on diopside.		
	θ_1.	θ_2.	θ_3.	θ_1.	θ_2.	θ_3.
	°	°	°	°	°	°
Ca	0	−107·5	90	0	−110	90
Mg	0	32	90	0	30	90
Si	76	146·5	85	76	148	85
O_1	135	151	(50)	136	145	50
O_2	51	91	(115)	51	90	115
O_3	52	(180)	0	56	173	0

Even when the results of the three projections are combined, certain co-ordinates of the oxygen atoms remain doubtful. They might be obtained by taking, for instance, the calcium atom as outlined in the (001) projection and subtracting it from the group Ca + 2O in the (100) projection, so as to leave the oxygen atoms clearly defined, but the figures are perhaps not sufficiently accurate to make such a process sure. It seems better to give in the table definite values only in those cases where they can be read directly from the projections.

The parameters are given in degrees, in accordance with the notation in the previous paper. The average difference between the two sets of values, for all figures except those in brackets, is 1·6°. If the parameters are expressed as fractions u, v, w of the axial lengths a, b, c, this corresponds to an average difference of 0·005 in these fractions. For a crystal with 14 parameters this is a small difference, and the agreement is evidence of the effectiveness of quantitative measurements in analysing complex structures.

Table IX.

	Parameters determined by Fourier analysis.			Values given in previous paper on diopside.		
	u.	*v*.	*w*.	*u*.	*v*.	*w*.
Ca	0	−0·299	0·25	0	−0·306	0·25
Mg	0	0·089	0·25	0	0·083	0·25
Si	0·211	0·407	0·236	0·211	0·411	0·236
O_1	0·375	0·419	(0·14)	0·378	0·402	0·139
O_2	0·142	0·253	(0·32)	0·142	0·250	0·320
O_3	0·145	(0·50)	0·00	0·155	0·480	0·00

9. *Analysis by Fourier Series.*

The diopside crystal was first analysed by making calculated and observed values of $|F(hkl)|$ agree. This determined the sign of $F(hkl)$ and it was possible to form the Fourier representation of the distribution of scattering matter. It is interesting to see whether any of the labour of finding suitable parameters could have been shortened by employing the Fourier analysis at an earlier stage.

This appears to be the case. Consider the projection on (010) where calcium and magnesium atoms are superimposed, fig. 2A. In Table II it will be seen that $F(h0l)$ is positive when $\pm l$ is 0, 4, 8 and negative when $\pm l$ is 2, 6. This means that the sign of $F(h0l)$ is determined by the position of the calcium and magnesium atoms, so that all terms in the Fourier series

$$\Sigma\Sigma\, F(h0l) \cos 2\pi (hx/a + lz/c)$$

are positive at the point $x = 0$, $z = c/4$, where these atoms are situated. The sole exception is F (202). It so happens that for this spectrum alone oxygen and silicon contributions to F (202) more than neutralise those of calcium and magnesium.

If therefore some hint had been obtained at an early stage of the analysis that the calcium and magnesium atoms were superimposed in this projection, and that they determined the sign of $F(h0l)$, it would then have been possible to use the Fourier series to find the projection on (001) and so the x and z co-ordinates of all the atoms. This would have been done without the labour of trying different values for the parameters, and seeing which gave the best agreement between calculated and observed values of $F(h0l)$.

There is no such simple rule for the signs of $F(0kl)$ and $F(hk0)$, and it is necessary to analyse the crystal in order to determine these signs. However a study of the contribution of the various atoms to these F values shows that, in every case except F (022), the sign is determined by the calcium, magnesium, and silicon atoms. Therefore a knowledge of the positions of these heavy atoms would make it possible to form the Fourier series, and so to fix the oxygen atoms. This would be of great advantage in analysis, because the determination of the oxygen parameters is a troublesome matter owing to their small scattering power.

To sum up, a preliminary analysis of the crystal which gives approximate positions of the heavy atoms, suffices to fix the signs of the coefficients F. The Fourier series may thus be formed, and the positions of all the atoms accurately read off on the projections.

It is interesting to re-interpret the ordinary process of analysis by the conceptions of the Fourier series. In particular, a study of the effect of extinction is very illuminating. Extinction affects the most powerful reflexions, and allowance for it is an uncertain matter. When comparing calculated and observed values of F, the discrepancies for the powerful reflexions are very obvious, and might seem to cast doubt on the success of the analysis. In our analyses of complex crystals by quantitative measurements we have always held, however, that this doubt is not justified, and that the agreement for a large number of reflexions of high order is ample evidence for the correctness of the solution. When now the Fourier series is formed, it is clear that the effect of allowance for extinction on the calculated distribution of scattering matter is very small. For instance, in the (010) projection of diopside, the position of the superimposed calcium and magnesium atoms is shown by a peak rising to 3640. The strongest reflexion is (002) and F (002) is taken to have a value of 175. It may be in error by 30 units owing to incorrect allowance for extinction, but clearly this will hardly affect the peak of 3640. The density is determined by a large number of F values not affected by extinction, and the few reflexions at low angles which are so affected are relatively unimportant.

If the form of the Fourier series

$$\Sigma\,\Sigma\,\mathrm{F}\,(0\,k\,l)\cos 2\pi\,(hx/a + lz/c)$$

be considered, it will be seen that each term represents a series of periodic undulations of density, parallel to a line whose slope is determined by the indices k, l. The higher the indices k and l, the shorter is the wave-length. We may thus distinguish the effect on the projection of the different terms. Those with low indices group the density into certain masses which begin to outline the atoms. The terms with high indices trim the outlines, and give precision to the atoms. The number of electrons in each atom is determined by the terms with low indices. Since these are affected by allowance for extinction, the numbers of electrons counted in section 7 must be accepted with reserve. On the other hand, the precise positions of the atoms are almost entirely determined by the terms with high indices. Hence the values of the parameters may be relied on to be correct.

This is merely another way of regarding the familiar consideration that reflexions with low indices must be measured accurately if we are to tell whether the atoms are ionised or not, and that reflexions with high indices serve to fix the positions of the atoms with precision.

Summary.

The representation of the scattering matter in a crystal by Fourier series, first used by W. H. Bragg and later developed by Duane, Havighurst and Compton, is applied here to the determination of the parameters in a complex crystal.

A series is used which gives the projection of the scattering matter in the unit cell on each of its faces in turn. For instance, when projection is made on the face (100) of the cell, the formula for the density $\rho(y, z)$ of the scattering matter at a point y, z is as follows :—

$$\rho(y, z) = (1/bc \sin \alpha) \sum_{-\infty}^{+\infty} \sum_{-\infty}^{+\infty} \mathrm{F}(0\,k\,l) \cos 2\pi (ky/b + lz/c).$$

In this formula, $\mathrm{F}(0\,k\,l)$ is the value of the structure factor for the reflexion $(0\,k\,l)$ measured in absolute units. The formula applies to a cell of any shape, provided that it has a centre of symmetry. F (0 0 0) is taken to be the number of electrons in the unit cell.

This series is evaluated for the crystal diopside $\mathrm{CaMg(SiO_3)_2}$. The signs of the coefficients $\mathrm{F}(0\,k\,l)$ had been fixed by a previous analysis of the crystal. The projections are shown as contoured diagrams in figs. 1A, 2A and 3A. The positions of the atoms agree very closely with those given by the previous analysis, figs. 1B, 2B and 3B, made by finding values for the parameters which gave agreement between calculated and observed values of F. A comparison of the two sets of 14 parameters is shown in Table IX.

It is possible to count the numbers of atomic electrons in the projections. They are approximately as follows :—Ca 16·5, Mg 12·5, Si 11·5, O 8·5–9. It is interesting to note that the oxygen does not appear to be an ion O^{-2} with 10 electrons.

The groups of F values used for any projection may be conveniently described as the weights attached to a network of points on a central section of Ewald's reciprocal lattice.

The employment of Fourier series in analysing complex crystals is discussed, and it is concluded that it may be used in conjunction with an analysis of the usual type made by assigning parameters to the atoms, and may considerably shorten the labour of analysis. The series is particularly of value in discovering the positions of the lighter atoms and in leading directly to precise values of the parameters.

In a recent paper by Mr. West and the author in the 'Zeitschrift für Krystallographie,' entitled "A Technique for the X-ray Examination of Crystal Structures with many Parameters," examples were given to show that the use of absolute measurements of X-ray diffraction enabled these complex crystal structures to be solved with directness and accuracy. The use of the same measurements in the method of Fourier series affords further evidence in support of the effectiveness of such absolute measurements.

It is with great pleasure that I acknowledge my indebtedness to my father, Sir William Bragg, for suggestions which materially contributed to the work described in this paper. At the time when I was following up the connection between our usual methods of analysis and the analysis by Fourier series, a connection briefly treated in the paper by Mr. West and myself, my father showed me some results which he had obtained by using relative values of the first few terms of two- and three-dimensional Fourier series to indicate the general distribution of scattering matter in certain organic compounds. It was largely as a result of his suggestions that I was encouraged to make all the computations for these two-dimensional series, using the extensive absolute measurements which we had made on certain crystals.

A New Band System of Carbon Monoxide ($3\,^1S \rightarrow 2\,^1P$), *with remarks on the Ångström Band System.*

By R. C. Johnson, M.A., D.Sc., Lecturer in Physics in the University of London, King's College, and R. K. Asundi, B.A., M.Sc., Bombay University Research Scholar.

(Communicated by O. W. Richardson, F.R.S.—Received January 29, 1929.)

Introduction.

A large number of band spectra have now been discovered and correlated, which are definitely attributable to the CO molecule. It is not proposed to enter in this communication into a general discussion of these, but a summary of the recognised energy levels is given in Table I. Column (1) gives a purely arbitrary designation employed by Birge in referring to them in his papers. Column (3) gives the nature of the electronic levels as at present accepted.

Table I.

Name.	Energy (ν).	Nature.	Name.	Energy (ν).	Nature.
X	0	$1\,^1S$	B*	86929	$2\,^1S$
	48438		C*	91923	$3\,^1S$
*a**	to	$2\,^5P$?	*c*	92093	
	48534		E*	92923	
a′	58927		F	99730	
A*	64765	$2\,^1P$	G	105266	
*b**	83825	$2\,^5S$?	X′	114966	Ionisation

The following band systems arising from these levels are well known:—

$a \rightarrow X$	Cameron bands.
$A \rightarrow X$	4th positive carbon bands.
$b \rightarrow a$	3rd positive carbon bands.
$B \rightarrow A$	Ångström bands.
$c \rightarrow a$	" 3A " bands of Duffendack and Fox.

In point of fact, all the levels which are starred (*) give rise to emission spectra by transitions down to the normal level X, and these have been observed by Hopfield and Birge.† Excepting the Cameron bands they are all, however, in the Schumann region, and being less familiar have not been given special names. The four levels a', E, F, and G, were found first in absorption by Birge and Hopfield and they have only been announced comparatively recently. The level C has been located hitherto as the initial level of a system C $\rightleftarrows$ X found in both emission and absorption in the Schumann region, and its nature has not been known with any certainty. The purpose of the present communication is to give details of a new band system* from this initial level C to the final level A. This has its final state in common with the Ångström system. Four bands have been observed, (0, 0), (0, 1), (0, 2) and (0, 3), and a fine structure analysis has been made of three of these. From this it is clear that the nature of the initial level is $3\,^1\mathrm{S}$, and it has been labelled as such in Table I.

---

† 'Phys. Rev.,' vol. 29, p. 922 (1927).

Vibrational Quantum Analysis and Correlation with the Ångström System.

The Ångström bands are due to an electronic transition $2\,^1\mathrm{S} \rightarrow 2\,^1\mathrm{P}$, and consist of two n'' progressions ($n' = 0$ and 1). Some doubtful bands which have been supposed to constitute a third progression $n' = 2$ are probably part of a different system. The vibrational quantum analysis of the Ångström system is recorded in Table II in the case of those bands for which accurate data are available. Higher members of the two progressions are known but have not been accurately measured under high dispersion. The bands (0, 1), (0, 2), (0, 3) and (1, 1) have been analysed in detail by Hulthén† in work which furnished one of the earliest verifications of the combination principle. The correct assignment of j-values (and here $j = m$), to these bands, is obtained by reducing Hulthén's m-values by half on the old quantum theory, or by 1 on the new quantum theory. The constants of Table II have been re-evaluated by us from Hulthén's data. The fine structure of the (0, 0) and (1, 0) bands was first given by Jassé,‡ but as the data on these bands appeared to be much less extensive than Hulthén's, and as moreover these bands have been alleged to have an abnormal structure, we have obtained new plates in the first order of a 21-foot grating, and the constants of Table II have been evaluated from these. The data for the (0, 4) and (0, 5) bands have also been obtained from a fine structure analysis which we have made from our own plates.

We have obtained four bands of the new CO system, the data of which are given in Table III. Only approximate measurements of the (0, 0) band were

---

* Asundi, 'Nature,' vol. 123, p. 47 (1929).

† 'Ann. Physik,' vol. 71, p. 41 (1923).

‡ 'C. R.,' vol. 182, p. 692 (1926).

Table II.—Ångström Bands. ($2\,^1S \rightarrow 2\,^1P$.) [$\nu_0$ (vac.) ν_H (vac.) λ_H (air).]

n' \ n"	0.		1.		2.		3.		4.		5.
0	22171·2 22162·3 4510·90	(1489·1) (1487·0)	20682·1 20675·3 4835·34	(1441·8) (1443·3)	19240·3 19232·0 5198·22	(1413·1) (1412·1)	17827·2 17819·9 5610·15	(1377·4) (1376·9)	16449·8 16443·0 6079·94	(1342·6) (1342·6)	15107·2 15100·8 6620·34
1	24253·7 24243·8 4123·61	(1489·8) (1487·4)	22763·9 22756·4 4393·14								

Table III.—New System. ($3\,^1S \rightarrow 2\,^1P$.) [$\nu_0$ (vac.) ν_H (vac.) λ_H (air).]

n' \ n"	0.	1.		2.		3.
0	[27174·7 27165·8 3680·05]	25686·1 25678·6 3893·19	(1442·9) (1443·1)	24243·2 24235·5 4125·02	(1412·7) (1411·8)	22830·5 22823·7 4380·18

possible owing to confusion with one of the so-called spurious bands associated with the third positive carbon system. The constants of the (0, 0) band are therefore values calculated from the (0, 0) Ångström band by addition of ν 5003·5, which is the interval between the $3\,^1S$ and $2\,^1S$ levels as deduced from the other bands. The fine structure analysis of the (0, 1), (0, 2) and (0, 3) bands has been effected, and details are presented later. It will be found that the combination data obtained from this analysis fully support the evidence of Tables II and III that this new system and the Ångström system have a common final state $2\,^1P$. The fact that the new system has only one progression corresponding to $n' = 0$ is to be expected; it is similar in this respect to the third positive carbon bands, the 3A bands, etc., and this feature appears to be generally true for the higher electronic levels of molecules.

Three of the bands recorded in Table III were observed by Duffendack and Fox* when investigating the excitation of the spectra of CO by electronic impacts. Their wave-lengths (under low dispersion) were λλ 3679·5, 3894·8 and 4380·1. On the basis of their general similarity in appearance and behaviour to the Ångström system, these writers criticise the validity of the vibrational quantum analysis of the latter system, which they considered should be modified in some way to include these new bands. There is, however, no doubt of the correctness of the present vibrational analysis of the Ångström system (due originally to Birge).* The above three bands are seen to be the (0, 0), (0, 1) and (0, 3) bands of a distinct system arising from an electronic level 5003·5 ν (= 0·62 volts) above the initial level of the Ångström bands. Fine structure analysis shows this level to be $3\,^1S$. Deslandres' band at λ 3893 which Wolter† could not obtain, is undoubtedly the (0, 1) band of this system.

---

* 'Phys. Rev.,' vol. 65, p. 220 (1927).

Fine Structure Analysis.

Fine structure data for the (0, 1), (0, 2) and (0, 3) bands have been obtained from two independent sets of plates taken in the first order of a 21-foot grating. These are analysed and recorded in Tables IV, V and VI. The wave-length data are believed to be accurate to within 0·01 A.U. for the stronger lines.

Table IV.—Fine Structure of (0, 1) Band.

Old Q.T. j.	New Q.T. j.	P branch.		Q branch.		R branch.	
		λ_{air}.	ν_{vac}.	λ_{air}.	ν_{vac}.	λ_{air}.	ν_{vac}.
1½	1	3892·495	*c* 25683·2	—	—	—	—
2½	2	92·843	*b* 680·9	—	—	3890·10	25699·0
3½	3	93·083	*a* 679·3	3891·34	25690·8	88·96	706·5
4½	4	93·186	678·7	90·85	694·1	—	(713·2)
5½	5	93·083	*a* 679·3	90·25	698·1	86·748	*d* 721·2
6½	6	92·843	*b* 680·9	89·52	702·8	85·431	729·9
7½	7	92·495	*c* 683·2	88·717	708·2	84·013	739·3
8½	8	92·084	685·9	87·806	714·2	82·514	749·3
9½	9	91·503	689·8	86·748	*d* 721·2	80·91	759·9
10½	10	—	—	85·63	728·6	79·19	771·3
11½	11	—	—	84·394	736·7	77·377	783·4
12½	12	89·252	704·6	83·06	745·6	75·46	796·1
13½	13	88·264	711·2	81·605	755·3	73·30	810·5
14½	14	87·190	718·3	80·058	765·5	71·33	823·6
15½	15	86·007	726·1	78·413	776·5	69·096	838·5
16½	16	84·730	734·6	76·648	788·2	—	—
17½	17	83·28	744·1	74·78	800·7	—	—
18½	18	—	—	72·819	813·7	—	—
19½	19	—	—	70·736	827·6	—	—
20½	20	—	—	68·59	841·9	—	—

a, b, c, d, are blends of 2 lines.

---

* 'Nature,' vol. 117, p. 230 (1926).

† 'Z. Wiss. Photogr.,' vol. 9, p. 361 (1911).

Table V.—Fine Structure of (0, 2) Band.

Old Q.T. j.	New Q.T. j.	P branch.		Q branch.		R branch.	
		$\lambda_{air.}$	$\nu_{vac.}$	$\lambda_{air.}$	$\nu_{vac.}$	$\lambda_{air.}$	$\nu_{vac.}$
1½	1	4124·30	*a* 24240·1	4123·44	*24244·8	4122·11	*24252·6
2½	2	24·61	*b* 237·9	23·25	* 246·5	21·29	**f* 257·4
3½	3	24·885	*c* 236·3	22·87	* 248·1	20·26	* 263·5
4½	4	24·997	*d* 235·6	22·33	*e* 251·3	19·09	270·4
5½	5	24·997	*d* 235·6	21·69	255·1	17·75	278·3
6½	6	24·885	*c* 236·3	20·89	259·8	16·33	* 286·6
7½	7	24·61	*b* 237·9	19·94	265·3	14·75	296·0
8½	8	24·30	*a* 240·1	18·983	271·0	13·04	306·1
9½	9	23·695	243·3	17·75	278·3	11·19	317·0
10½	10	23·059	247·0	16·45	285·9	09·26	328·4
11½	11	22·33	*e* 251·4	15·04	* 294·2	07·17	340·8
12½	12	21·29	*f** 257·4	13·46	* 303·6	04·95	354·0
13½	13	20·26	* 263·5	11·78	313·5	02·61	367·9
14½	14	19·09	270·4	09·93	324·4	—	—
15½	15	17·82	277·9	07·97	336·1	—	—
16½	16	16·33	* 286·6	05·896	348·4	—	—
17½	17	14·77	295·9	03·66	361·6	—	—

* Confused with fine structure lines of Ångström band λ 4123.
a, *b*, *c*, *d*, *e*, *f*, are blends of 2 lines.

Table VI.—Fine Structure of (0, 3) Band.

Old Q.T. j.	New Q.T. j.	P branch.		Q branch.		R branch.	
		$\lambda_{air.}$	$\nu_{vac.}$	$\lambda_{air.}$	$\nu_{vac.}$	$\lambda_{air.}$	$\nu_{vac.}$
1½	1	4379·42	22827·7	4378·71	22831·3	4377·273	*c* 22838·8
2½	2	79·84	825·3	78·44	832·8	76·19	844·5
3½	3	80·08	*a* 824·3	77·925	* 835·5	75·02	850·6
4½	4	80·25	*b* 823·4	77·273	*c* 838·8	73·59	858·1
5½	5	80·25	*b* 823·4	76·54	842·6	72·06	866·1
6½	6	80·08	*a* 824·3	75·57	847·8	70·23	*d* 875·7
7½	7	79·68	* 826·3	74·485	853·4	68·534	*e* 884·6
8½	8	79·19	828·9	73·22	860·0	66·60	*f* 894·7
9½	9	78·50	832·5	71·82	867·6	—	—
10½	10	77·68	836·8	70·23	*d* 875·7	—	—
11½	11	76·69	841·9	68·534	*e* 884·6	—	—
12½	12	75·57	847·8	66·60	*f* 894·7	—	—
13½	13	74·29	854·5	64·61	905·1	—....	—
14½	14	72·86	861·9	—	—	—	—

* Confused with lines of the Ångström band λ 4393.
a, *b*, *c*, *d*, *e*, *f*, denote blends of 2 lines.

The bands each have three branches of the P, Q and R type, and are precisely similar to the Ångström bands in structure. The lines R (½) and Q (½) were not observed, and this is consistent with a ${}^1S \rightarrow {}^1P$ transition for which $\sigma'' = 1$

and hence for which $j''_{\text{min.}} = 1\frac{1}{2}$. (Using the numbering of the new quantum theory R (0) and Q (0) would be the missing lines. Unless otherwise stated we shall employ the numbering of the old quantum theory in the present paper.)

The three branches which theory predicts for a transition of this type are :—

$$\left.\begin{aligned} \mathrm{R}(j) &= \mathrm{F_B}'(j+1) - \mathrm{F_B}''(j) \\ \mathrm{Q}(j) &= \mathrm{F_B}'(j) - \mathrm{F_A}''(j) \\ \mathrm{P}(j) &= \mathrm{F_B}'(j-1) - \mathrm{F_B}''(j) \end{aligned}\right\} \qquad (1)$$

and the combination principle provides the following relationships :—

$$\left.\begin{aligned} &(a)\ \ \mathrm{R}(j) - \mathrm{Q}(j) = \Delta_1\mathrm{F_B}'(j) + [\mathrm{F_A}''(j) - \mathrm{F_B}''(j)] \\ &(b)\ \ \mathrm{Q}(j+1) - \mathrm{P}(j+1) = \Delta_1\mathrm{F_B}'(j) - [\mathrm{F_A}''(j+1) - \mathrm{F_B}''(j+1)] \\ &(c)\ \ \mathrm{R}(j) - \mathrm{P}(j) = \Delta_2\mathrm{F_B}'(j) \\ &(d)\ \ \mathrm{R}(j) - \mathrm{Q}(j+1) = \mathrm{F_A}''(j+1) - \mathrm{F_B}''(j) \\ &(e)\ \ \mathrm{Q}(j) - \mathrm{P}(j+1) = \mathrm{F_B}''(j+1) - \mathrm{F_A}''(j) \\ &(f)\ \ \mathrm{R}(j-1) - \mathrm{P}(j+1) = \Delta_2\mathrm{F_B}''(j) \\ &(g)\ \ \mathrm{R}(j) - \mathrm{Q}(j+1) + \mathrm{Q}(j-1) - \mathrm{P}(j) = \Delta_2\mathrm{F_A}''(j) \end{aligned}\right\} \qquad (2)$$

In general, the quantities (*a*) and (*b*) will not be exactly equal, but will exhibit so-called combination defects. The same is true of (*d*) and (*e*). In Table VII

Table VII.—Combination Data for the State $3\,^1\mathrm{S}$ ($n = 0$).

Old Q.T. *j*.	λ 3893·19 (0, 1).		λ 4125·02 (0, 2).		λ 4380·18 (0, 3).		Weighted mean value.
	R(*j*) − Q(*j*).	Q(*j*+1) −P(*j*+1).	R(*j*) −Q(*j*).	Q(*j*+1) −P(*j*+1).	R(*j*) − Q(*j*).	Q(*j*+1) −P(*j*+1).	
½	—	—	—	4·7*	—	3·6	3·6
1½	—	—	7·8*	8·7*	7·5	7·5	7·5
2½	—	11·5	10·9*	11·8*	11·7	11·2*	11·6
3½	15·7	15·4	15·4*	15·7	15·1	15·4	15·5
4½	19·1	19·4	19·1	19·5	19·3	19·2	19·3
5½	23·1	23·5	23·2	23·5	23·5	23·5	23·5
6½	27·1	27·3	26·8	27·4	27·9*	27·1	27·2
7½	31·1	31·0	30·7	30·9	31·2	31·1	31·1
8½	35·1	35·3	35·1	35·0	34·7*	35·1	35·1
9½	38·7	38·8	38·7	38·9	—	38·9	38·8
10½	42·7	—	42·5	42·8	—	42·7	42·7
11½	46·7	—	46·6	46·2*	—	46·9	46·7
12½	50·5	50·7	50·4	50·0*	—	50·6	50·6
13½	(55·2)*	54·3	54·4	54·0	—	—	54·3
14½	58·1	58·2	—	58·2	—	—	58·2
15½	62·0	62·1	—	61·8*	—	—	62·1
16½	—	66·1	—	65·7	—	—	65·9
17½	—	69·6	—	—	—	—	69·6

* Unreliable ; arising from lines which are blends.

are given the values of (*a*) and (*b*) the combination data for the initial state of the system. It will be noted that no appreciable combination defect appears up to the limit of observations ($j = 17\frac{1}{2}$). This is a feature characteristic of the highly stable CO molecule ; the A and B sub-states of the P levels do not become appreciably separate till quite high values of the rotational quantum number are attained. While this statement is true for the vibrational levels $n = 1$, 2, 3, 4 and 5 of the 2P state, it would appear to need qualification for the state $n = 0$, for which combination defects seem to arise from almost the lowest j-values. This curious result is evident from the data of the (0, 0) Ångström band, as we shall see later.

The procedure adopted to evaluate the molecular constants of the electronic levels from combination data has been as follows. The combination data were expressed by a cubic formula thus :—

$$\Delta_1 F(j) = \alpha + \beta j + \gamma j^2 + \delta j^3, \tag{3}$$

the coefficients α, β, γ, and δ being evaluated by the method of least squares. From this the value of $F(j)$ can at once be written down :—

$$F(j) = \text{constant} + \left(\alpha - \frac{\beta}{2} + \frac{\gamma}{6}\right) j + \tfrac{1}{2}\left(\beta - \gamma + \frac{\delta}{2}\right) j^2 + \tfrac{1}{3}\left(\gamma - \tfrac{3}{2}\delta\right) j^3 + \delta j^4. \tag{4}$$

In the case of the initial state (of a ^1S type) we know $F(j)$ should have the form

$$\begin{aligned} F'(j) &= B'(j - \rho)^2 + D'(j - \rho)^4 \\ &= \text{const.} - 2\rho(B' + 2\rho^2 D')j + (B' + 6\rho^2 D')j^2 - 4\rho D' j^3 + D' j^4, \end{aligned} \tag{5}$$

where ρ is a " secondary ρ " representing a very small departure from exact half-integral j-values. Comparison of the coefficients of j, j^2 and j^3, in equations (4) and (5), gives the molecular constants B', ρ and D'. The value of D' obtained thus is not usually in agreement with the coefficient of j^4 in (4), but the former value is considered more reliable as being less subject to errors arising from the existence of still higher terms in j. Subsequent to the evaluation of the constants on this basis, a linear form for $\Delta_1 F$ was found to express the combination data to an accuracy well within the limits of error. The constants B' and ρ derived in this way differed slightly from those already obtained on the basis of a cubic equation for $\Delta_1 F$. A linear form was also found to be quite adequate to express the combination data of the initial Ångström level ($2\,^1S$, $n' = 0$) and also that of the four common final levels (2P, $n'' = 0, 1, 2, 3$). The constants B and ρ as deduced on these alternative bases are given in Table X. It will be observed that the values of D obtained on the assumption of a cubic form for $\Delta_1 F$ are positive in all but one case, an indication that no physical value can be attached to this coefficient. We consider that the values of B and ρ obtained by use of a linear form for $\Delta_1 F$ are the more reliable. On this basis the probable errors of representation of the data are about 0·05 ν for the $2\,{}^1P$ state and 0·1 ν for the ${}^1S$ states. The linear representation of the data of Table VII is

$$\Delta_1 F'(j) = 1{\cdot}8837 + 3{\cdot}88638j$$

giving for the rotational function of the state ($3\,{}^1S$, $n' = 0$)

$$1{\cdot}94319\,(j - 0{\cdot}01530)^2, \qquad j = \tfrac{1}{2}, 1\tfrac{1}{2}, 2\tfrac{1}{2}, \ldots.$$

It is interesting to compare these constants with those of the initial state of the Ångström bands ($2\,{}^1S$, $n = 0$). For the constant B_0' Hulthén gives 1·943. The slight departure from exact half-integral quantum numbers is, however, not discussed by Hulthén and we have therefore re-evaluated B_0' (and ρ) using his data for the Ångström bands (0, 1), (0, 2) and (0, 3). Here again the combination defect is not apparent up to the limit of observations (near $j = 25\tfrac{1}{2}$), so that $\Delta_1 F'(j) = R(j) - Q(j) = Q(j+1) - P(j+1)$. The mean of the six values of $\Delta_1 F'(j)$ thus obtained for each value of j are given in Table VIII. These are expressed by :—

$$\Delta_1 F'(j) = 2{\cdot}0388 + 3{\cdot}88083j,$$

giving for the rotational function

$$1{\cdot}94041\,(j + 0{\cdot}02535)^2.$$

Table VIII.—$\Delta_1 F'(j)$ Values for State $2\,{}^1S$, ($n = 0$).

j.	$\Delta_1 F'(j)$.	j.	$\Delta_1 F'(j)$.	j.	$\Delta_1 F'(j)$.	j.	$\Delta_1 F'(j)$.
$\tfrac{1}{2}$	3·80	$7\tfrac{1}{2}$	31·10	$14\tfrac{1}{2}$	58·40	$20\tfrac{1}{2}$	81·60
$1\tfrac{1}{2}$	7·80	$8\tfrac{1}{2}$	35·05	$15\tfrac{1}{2}$	62·23	$21\tfrac{1}{2}$	85·40
$2\tfrac{1}{2}$	11·65	$9\tfrac{1}{2}$	38·90	$16\tfrac{1}{2}$	66·13	$22\tfrac{1}{2}$	89·30
$3\tfrac{1}{2}$	15·60	$10\tfrac{1}{2}$	42·80	$17\tfrac{1}{2}$	70·00	$23\tfrac{1}{2}$	93·15
$4\tfrac{1}{2}$	19·54	$11\tfrac{1}{2}$	46·75	$18\tfrac{1}{2}$	73·85	$24\tfrac{1}{2}$	97·05
$5\tfrac{1}{2}$	23·43	$12\tfrac{1}{2}$	50·65	$19\tfrac{1}{2}$	77·80	$25\tfrac{1}{2}$	100·90
$6\tfrac{1}{2}$	27·35	$13\tfrac{1}{2}$	54·50				

One would have expected the value of B_0 for the $2\,{}^1S$ state to be somewhat greater than for $3\,{}^1S$, arising out of a smaller moment of inertia which is consequent upon a closer binding for the former electron. The slight change the other way clearly arises from the change of sign of the small secondary ρ involved in the two cases. The closeness of the values of B_0, and hence of I_0, for the two ^1S states is remarkable—and is indicative of the high stability of the CO molecule. This stability shows itself in several ways, *e.g.*, in the high value of the heat of dissociation, in the large number of vibration quanta which may be associated with the molecule in its normal ($1\,^1S$) state, and in the existence of several band spectra of the ionised molecule. We turn now to the common final electronic state ($2\,^1P$) of both these band systems. The combination data are furnished by Table IX. The two columns for each band give respectively $R(j) - Q(j+1)$ and $Q(j) - P(j+1)$. Excepting the state $n = 0$ it will be observed here also that

$$R(j) - Q(j+1) = Q(j) - P(j+1)$$

up to about $j = 22\frac{1}{2}$, say. Beyond this point slight combination defects appear giving $Q(j) - P(j+1) < R(j) - Q(j+1)$. (See (*d*) and (*e*) of equation (2).) In the case of the (0, 0) and (1, 0) bands such defects appear with the lowest j-values, and for purposes of evaluating $\Delta_1F''(j)$, and hence the constants of the level $n = 0$, the arithmetic mean has been used. The

Table IX.—Combination Data for the $2\,^1P$ State.

$(Q(j) - P(j+1))$ $(R(j) - Q(j+1))$.

j.	$n'' = 0$.				$n'' = 1$.						$n'' = 2$.				$n'' = 3$.			
	λ 4511.		λ 4123.		λ 3893*.		λ 4835.		λ 4303.		λ 4125*.		λ 5108.		λ 4380.*		λ 5610.	
$1\frac{1}{2}$	6·25	6·36	6·12	—	5·0	5·6	5·8	—	6·1	—	6·9	6·1	6·2	6·5	6·0	6·0	6·0	6·2
$2\frac{1}{2}$	9·48	9·57	9·57	9·86	9·2	8·2	9·0	9·1	9·2	9·2	10·2	9·3	9·3	9·6	8·5	9·0	9·2	9·2
$3\frac{1}{2}$	12·75	12·91	12·93	13·24	12·1	12·4	11·9	12·2	12·3	12·1	12·5	12·2	12·4	12·6	12·1	11·8	12·2	12·3
$4\frac{1}{2}$	—	16·0	(15·3)	15·96	15·4	15·1	15·7	15·5	15·4	15·3	15·7	15·3	15·6	15·7	15·4	15·5	15·3	15·4
$5\frac{1}{2}$	19·09	19·3	—	19·4	18·8	18·4	18·5	18·6	18·5	19·0	18·8	18·5	18·7	18·8	18·3	18·3	18·4	18·4
$6\frac{1}{2}$	21·5	22·5	—	22·2	21·9	21·7	21·9	21·7	21·8	21·7	21·9	21·3	21·8	21·6	21·5	—	21·5	21·5
$7\frac{1}{2}$	24·85	25·89	26·0	25·7	25·0	25·1	25·1	24·9	25·1	24·9	25·2	25·0	25·1	25·0	24·5	—	24·5	24·6
$8\frac{1}{2}$	28·9	29·6	29·56	29·64	28·3	28·1	28·2	28·2	28·1	28·0	27·7	27·8	28·0	28·0	27·5	—	27·5	27·6
$9\frac{1}{2}$	—	31·8	32·4	32·1	31·4	31·3	31·3	31·3	31·4	31·3	31·3	31·1	31·1	31·1	30·8	—	30·7	30·7
$10\frac{1}{2}$	—	34·6	—	34·6	—	34·9	34·5	34·5	34·5	34·6	34·5	34·2	34·2	34·2	33·8	—	33·7	33·6
$11\frac{1}{2}$	—	—	—	—	—	37·8	37·7	37·7	37·6	37·8	36·8	37·2	37·4	37·3	36·8	—	36·8	36·8
$12\frac{1}{2}$	—	—	—	—	41·0	40·8	40·9	40·9	40·8	40·7	40·1	40·5	40·6	40·4	40·2	—	39·9	39·9
$13\frac{1}{2}$	—	—	—	—	44·1	—	44·0	44·1	44·5	44·2	43·1	43·5	43·6	43·5	34·2	—	42·9	43·0
$14\frac{1}{2}$	—	—	—	—	47·2	47·1	47·2	47·3	47·3	47·2	46·5	—	46·7	46·7	—	—	45·9	46·0
$15\frac{1}{2}$	—	—	—	—	50·4	50·3	50·4	50·5	—	50·6	49·5	—	49·7	49·9	—	—	49·0	49·0
$16\frac{1}{2}$	—	—	—	—	53·6	—	53·5	53·6	—	53·7	52·5	—	52·6	52·9	—	—	52·0	52·1
$17\frac{1}{2}$	—	—	—	—	56·6	—	56·7	56·7	—	—	—	—	55·8	55·9	—	—	55·1	55·1
$18\frac{1}{2}$	—	—	—	—	—	—	59·9	59·8	—	—	—	—	59·0	59·5	—	—	58·1	58·2
$19\frac{1}{2}$	—	—	—	—	—	—	63·0	62·9	—	—	—	—	61·8	62·1	—	—	61·1	61·2
$20\frac{1}{2}$	—	—	—	—	—	—	66·1	66·0	—	—	—	—	65·1	65·0	—	—	64·1	64·3
$21\frac{1}{2}$	—	—	—	—	—	—	69·2	69·0	—	—	—	—	68·2	68·3	—	—	67·2	67·3
$22\frac{1}{2}$	—	—	—	—	—	—	—	—	—	—	—	—	71·0	71·5	—	—	70·2	70·4
$23\frac{1}{2}$	—	—	—	—	—	—	—	—	—	—	—	—	73·9	74·5	—	—	73·1	73·5
$24\frac{1}{2}$	—	—	—	—	—	—	—	—	—	—	—	—	—	77·9	—	—	76·2	76·5
$25\frac{1}{2}$	—	—	—	—	—	—	—	—	—	—	—	—	—	—	—	—	79·1	79·6

combination data relating to the Ångström bands (0, 1), (1, 1), (0, 2) and (0, 3) are taken from Hulthén's paper. The data for the (0, 0) and (1, 0) bands have been taken from our own plates. We have used these data in preference to those of Jassé for reasons previously given—and incidentally, Jassé's assignment of quantum numbers has been found to be subject to a slight error. Details of this are presented later. Data of the $n'' = 0$ state are not available from the (0, 0) band of the new $3\,^1S \rightarrow 2\,^1P$ system, this band being confused with other fine structure work and at present impossible of analysis. The best values of the $\Delta_1 F''(j)$ data have been taken for each of the four vibrational levels $n'' = 0, 1, 2$ and 3, and these have been subject to the procedure already outlined in the case of data of the $(3\,^1S, n = 0)$ and $(2\,^1S, n = 0)$ levels. Equation (5) is, however, replaced in the case of the $2\,^1P$ level by

$$\begin{aligned} F''(j) &= B[(j-\rho)^2 - 1 + \rho/j]^2 + D[(j-\rho)^2 - 1 + \rho/j]^4 \\ &= Dj^4 - 4\rho Dj^3 + (B - 2D + 6\rho^2 D)j^2 - 2\rho(B - 3D + 2\rho^2 D)j \\ &\qquad + \text{constant} + \text{small terms in negative powers of } j, \end{aligned}$$

and by comparison of terms in j, j^2 and j^3, the values of B, ρ and D can be evaluated. The data thus obtained are collected in Table X. As in the case of the other levels, the assumption of a linear form for $\Delta_1 F''(j)$, corresponding to the simpler rotational function $B''(j-\rho)^2$ was found to express the data adequately. For the four vibrational levels of the $2\,^1P$ state the equations obtained were :—

$$\begin{aligned} \Delta_1 F''(j) &= 1\cdot6918 + 3\cdot18970j \quad (n'' = 0) \\ \Delta_1 F''(j) &= 1\cdot2191 + 3\cdot16778j \quad (n'' = 1) \\ \Delta_1 F''(j) &= 1\cdot7481 + 3\cdot09076j \quad (n'' = 2) \\ \Delta_1 F''(j) &= 1\cdot6239 + 3\cdot05319j \quad (n'' = 3) \end{aligned}$$

and these represent the data in each case with a probable error of about 0·05 v.

Table X.—Molecular Constants.

Electron level.	Vibrational level. (n.)	(Cubic form for Δ_1F.) D.	(Cubic form for Δ_1F.) B.	(Cubic form for Δ_1F.) ρ.	(Linear form for Δ_1F.) B.	(Linear form for Δ_1F.) ρ.	$I \times 10^{40}$ gm. cm^2.	r (A.U.).
$2\,^1P$	0	—	—	—	1·59485	−0·03040	17·343	1·2384
	1	+0·000278	1·60410	+0·18536	1·58389	+0·11515	17·463	1·2427
	2	+0·003253	1·55883	−0·02480	1·54538	−0·06559	17·898	1·2589
	3	+0·005035	1·54892	+0·01821	1·52660	−0·03187	18·119	1·2658
	4	—	—	—	1·51060	+0·01940	18·310	1·2724
	5	—	—	—	1·48592	−0·00433	18·615	1·2832
$2\,^1S$	0	+0·008532	1·95978	+0·01737	1·94041	−0·02536	14·2547	1·1228
$3\,^1S$	0	−0·004583	1·94214	+0·01820	1·94319	+0·01530	14·234	1·1220

The values of B″ and ρ thus derived are believed to be the more accurate and from these the corresponding values of I_n'' and r_n'' have been calculated.

The constants of the $n'' = 0$ state call for several detailed remarks. The first of the above equations was obtained from the values which we summarise below :—

j	1½	2½	3½	4½	5½	6½	7½	8½	9½	10½
$\Delta_1 F''(j)$	6·36	9·6	12·9	15·98	19·2	22·36	25·8	29·62	31·9	34·58

From the data of the λ 4511 and λ 4123 bands of Table IX it will be observed that combination defects are present. The $Q(j) - P(j+1)$ data are, however, less reliable than those of $R(j) - Q(j+1)$ owing to the somewhat imperfect resolution of P branch lines round the head. For the latter reason the combination relations (2*f*) and (2*g*) have not been used. The actual data used and recorded above are the weighted means of the $R(j) - Q(j+1)$ values obtained from the bands λλ 4511 and 4123 in Table IX. An analysis of Jassé's data using equations (2*f*) and (2*g*) gave $B'' = 1{\cdot}5661$, $\rho = -0{\cdot}0587$. The constants for the levels $n = 4$ and 5 have been deduced from a fine structure analysis which we have made, for the first time, of the (0, 4) and (0, 5) Ångström bands at λλ 6080 and 6620. These are preliminary values only, and it is not proposed to enter into fuller details of these in the present paper. Before discussing the molecular constants of Table X it will be convenient to present the new experimental data, and corrected analysis of the (0, 0) and (1, 0) Ångström bands.

The Ångström Bands λλ 4511 *and* 4123.

New measurements of these bands have been made with the aid of a 21-foot grating, and the data are recorded and analysed in Table XI. The line P (½) is, of course, the null line, while Q (½) and R (½) should be absent by reason of the ¹P character of the final state. This we have verified. Referring to Jassé's analysis of the λ 4511 band, the line ν 22172·3 is believed to be extraneous to the band, and ν 22171·8 should be labelled Q (1½). In addition ν 22175·7 is considered to be extraneous in origin. It has also been alleged that these bands λλ 4511, 4123 differed in their structure from the remaining bands of the Ångström system, each having an additional P′ and R′ branch. Three or four lines purporting to belong to each of such branches are given by Jassé, and from these Birge[*] has calculated a moment of inertia of about ¾ the normal value. We incline to the opinion, from a study of our experimental data, that these " branches " are spurious. There is a considerable amount of fine

[*] 'Phys. Rev.,' vol. 28, p. 1170 (1926).

Table XI.—Fine Structure of the Ångström Bands λλ 4511, 4123.

Old Q.T. *j*.	P branch.		Q branch.		R branch.	
	λ_{air}.	ν_{vac}.	λ_{air}.	ν_{vac}.	λ_{air}.	ν_{vac}.
1½	4509·714	*a* 22168·16	4508·96	22171·87	4507·35	22179·78
2½	10·236	165·62	08·64	173·42	06·246	185·12
3½	10·576	163·94	08·21	175·55	05·03	*c* 191·22
4½	10·80	*b* 162·8	07·65	178·31	03·67	197·89
5½	(10·90)	(162·3)	06·92	181·89	02·13	205·5
6½	10·80	*b* 162·8	06·046	186·20	00·455	213·76
7½	10·43	164·66	05·03	*c* 191·22	4498·59	222·95
8½	10·079	166·37	03·84	197·06	96·48	233·40
9½	09·714	*a* 168·16	02·476	203·80	94·46	243·29
10½	—	—	00·91	211·52	92·06	255·13
11½	—	—	4499·08	220·56	—	—
12½	—	—	96·795	231·84	—	—
13½	—	—	93·926	246·03	—	—
14½	—	—	90·427	263·37	—	—
1½	4122·35	*a* 24251·20	4121·85	24254·13	—	—
2½	22·89	*b* 248·01	21·607	255·56	4119·596	*e* 24267·40
3½	23·235	*c* 245·99	21·27	257·54	18·62	273·15
4½	23·47	*d* 244·61	20·868	259·91	17·564	279·38
5½			20·272	263·42	16·35	286·54
6½			19·596	*e* 267·40	15·05	294·21
7½			18·81	272·03	13·52	303·25
8½	23·235	*c* 245·99	17·87	277·57	11·82	313·29
9½	22·89	*b* 248·01	16·84	283·65	10·18	323·00
10½	22·35	*a* 251·20	15·62	290·85	08·34	333·89
11½	—	—	14·19	299·29	—	—
12½	—	—	12·40	309·86	—	—

a, b, c, d, e, indicate blends of 2 lines.

structure work in these regions arising from the triplet system* of carbon, and possibly from another system at present unrecorded. This, we consider, may account for the above additional " branches."

The Vibrational Levels of the $2\,{}^1\mathrm{P}$ *State.*

With regard to the molecular constants of the ${}^1\mathrm{S}$ states of the CO molecule (see Table X), we have already remarked on their exceptionally small variation. The constants of the various vibrational levels of the $2\,{}^1\mathrm{P}$ state require further examination. The value of B_n falls with increasing vibrational quantum number roughly according to the expected relation $\mathrm{B}_n = \mathrm{B}_0 - \alpha n$ where α is approximately 0·022. The value of B_1 appears to be somewhat high however (this was very pronounced when the cubic form was used). In addition, the unusually large positive value of ρ at once marks out the state $n = 1$ as unusual. The constants for the $n = 0$ state appear to be normal. Numerous calculations were made on the data of the $n = 1$ state, and all confirmed its exceptional nature. For example, the intervals between head and origin for the (0, 0), (0, 1), (0, 2), (0, 3), (0, 4) and (0, 5) bands are respectively 8·9, *6·8*, 8·3, 7·3, 6·8 and 6·4 ν. If such unusual features had occurred in B_0 and ρ_0 they would have occasioned less surprise in view of the fact that the $n = 0$ level has hitherto been regarded as subject to a perturbation of some 6 ν from the expected position. This was announced and discussed by Birge (*loc. cit.*). We have therefore been led to make a re-examination of the vibrational data of the Ångström system with a view to determining the reality of this supposed perturbation of the $n'' = 0$ level, and if possible to find a clue to the unusual nature of the $n'' = 1$ level. The data for this purpose are given in Table II. The band heads of the two progressions ($n' = 0$ and 1) of the Ångström system are according to Birge given by

---

* 'Roy. Soc. Proc.,' A, vol. 103, p. 383 (1923).

$$\nu = \left\{\begin{matrix} 22156\cdot6 \\ 24238\cdot0 \end{matrix}\right\} - (1497\cdot28n'' - 17\cdot2n''^2).$$

This expresses the Ångström heads with the following residual errors $(o - c)$ ν :

n'' / n'	0	1	2	3	4	5
0	+5·7	−1·3	+1·1	0	+0·3	+0·6
1	+5·8	−1·5				

It has been found, however, that if the following expression is used, the residuals are, on the whole, smaller, and *the perturbed level is* $n'' = 1$ *and not* $n'' = 0$ (*as given by Birge*).

$$\nu_H = \left\{\begin{matrix} 22162\cdot3 \\ 24243\cdot8 \end{matrix}\right\} - (1500\cdot52n'' - 17\cdot68n''^2).$$

The corresponding residuals are :—

n'' / n'	0	1	2	3	4	5
0	0	−4·2	0	0	−0·1	−0·9
1	0	−4·6				

The level $n'' = 1$ appears to be perturbed by about 4·2 ν (probably the more reliable figure). The final state of the Ångström system being identical with the initial state of the 4th positive carbon system, we have tested the above vibrational function ($1500 \cdot 52n' - 17 \cdot 68n'^2$) on a number of n' progressions of the latter system, using the data available (see Birge's paper, p. 1164). The available data are admittedly so poor (most of the bands are in the Schumann region) that it is impossible to verify a displacement of the $n = 1$ level. The above vibrational function appears however to give at least as good a representation of the available data as that proposed by Birge. More accurate data are very desirable, and in the light of such data a slight readjustment of the above vibrational function may be necessary, but of the perturbation of the $n = 1$ level we think that little doubt can be entertained. If the data for ν_0 (see Table II) are used, the $n' = 0$ progression can be expressed by

$$\nu_0 = 22172 \cdot 7 - (1501 \cdot 6n'' - 17 \cdot 7n''^2)$$

with residuals

$n'' \backslash n'$	0	1	2	3	4	5
0	−1·5	−6·7	0	0	+0·3	0

We have been unable to satisfy ourselves how far −1·5 ν represents a small but genuine perturbation of the $n'' = 0$ level. It would appear to be an amount well outside the limits of experimental error. Such a small perturbation of a level adjacent to a strongly disturbed one is by no means unprecedented in band spectra. We hope to make a fuller critical survey of this and other matters with still better data.[*]

We have examined our grating plates on which the $3\,^1S \rightarrow 2\,^1P$ system was photographed, for a possible system arising from the E → A transition (see Table I). The first four members of the $n' = 0$ progression should be at about λλ 3550·4, 3747·2, 3961·6 and 4196·4. There is some evidence of the presence of these bands, although they are faint, and much confused with "spurious" third positive, and other band structure.[*]

---

[*] *Note added in Proof.*—A paper has just appeared by G. Herzberg ('Z. Physik,' vol. 52, p. 815 (1929)), in which eight bands of the new CO system are recorded. The initial state is there described as D^1. There can however be no doubt, in the author's opinion, that the initial state is $3\,^1S$.

Summary.

(1) Details are given of a new band system of CO corresponding to the electronic transition $3\,{}^1S \rightarrow 2\,{}^1P$. Four bands of the $n' = 0$ progression have been observed, the heads of which are at λλ 3680·05, 3893·15, 4125·02 and 4380·18.

(2) Fine structure analysis of the (0, 1), (0, 2) and (0, 3) bands has been made. The missing lines R (½) and Q (½) confirm the nature of the electronic transition. The structure of these bands is in every respect similar to the Ångström system with which they share the final state in common. Combination defects are not apparent until high j-values are attained.

(3) The correct assignment of (half-integral) j-values has been applied to the Ångström system. New experimental data are provided in the case of the (0, 0), (1, 0), (0, 4) and (0, 5) bands, and the combination data derived from these, and from the new system, along with Hulthén's data, have been used to evaluate the constants of the $3\,{}^1S$, $2\,{}^1S$ and $2\,{}^1P$ levels of the CO molecule.

(4) Minor corrections have been made to Jassé's analysis of the (0, 0) Ångström band. This, with the (1, 0) band, is believed to be normal in type, differing from the other bands only in the earlier onset of combination defects

(5) The state $n = 1$ of the $2\,{}^1P$ level is believed to suffer a vibrational perturbation. The level $n = 0$, which has been hitherto regarded as perturbed, is believed to be normal, or, alternately, to suffer from perturbation of a secondary character.

A New Integrating Photometer for X-Ray Crystal Reflections, etc.

By W. T. Astbury, Davy Faraday Research Laboratory, Royal Institution.

(Communicated by Sir William Bragg, F.R.S.—Received January 30 (1929),

[Plate 19.]

In a previous communication* it was shown how a new principle in photometry could be applied to the construction of a simple "α-ray photometer" with possible integrating properties. It will be the object of the present paper to describe how the theoretical and practical development of this principle has now led to the design of an integrating photometer which has been found experimentally to give correct measurements of the total intensity in X-ray crystal reflections, and which also seems capable of adaptation to the measurement of the integrated intensity of other types of radiation.

Briefly, the new method uses a carbon print of a negative instead of the negative itself, and α-rays instead of light. In ordinary photometric procedure the density of the photographic image is found by transmitting through it a beam of light which then falls on some light-sensitive receiver such as a photo-electric cell. In the procedure about to be described, the density of the negative is not measured, but, by using the "stopping power" for α-rays of a carbon tissue positive, ionisation in an α-ray electroscope is produced in direct proportion to the original X-ray intensity which formed the negative. Carbon printing-paper or "tissue" consists of paper supporting a uniform† gelatine film, impregnated with an insoluble colloidal pigment, and sensitised by immersion in dilute aqueous potassium dichromate. The gelatine then possesses the property of becoming insoluble on exposure to light, so that after printing in the usual manner, development involves only the washing away in warm water of the still soluble portions of the film. It is a comparatively simple matter to obtain the insoluble film stripped from all support and free to be placed as an absorbing layer in the path of the α-particles from a small deposit of polonium. The stronger the original X-rays, the blacker the photographic image and the weaker the light which falls on the tissue during printing. This means that the stripped tissue is a film of varying thickness—during development, in fact, the relief is easily seen. It is thinnest where the original X-rays were the most intense, so that when it is used as an absorbing layer for α-rays, the ionisation in the α-ray electroscope increases with increasing X-ray intensity, and, in fact, can be made directly proportional to it. The total ionisation can thus be made a measure of the total X-ray intensity whatever its distribution over the photographic image.

---

* 'Roy. Soc. Proc.,' A, vol. 115, p. 640 (1927).

† *Cf.* previous communication.

It is this *integrating* property which gives the photometer here described its peculiar value as a practical instrument. The measurement of integrated intensities, particularly in X-ray crystallography, is a problem of great importance and difficulty; and it is the purpose of the present paper to show that this measurement is now possible, with quite simple apparatus, and with an accuracy sometimes already exceeding that warranted by our theoretical knowledge of the subject.

In this paper the following order will be adopted; first, the theory of the method will be outlined, indicating how we are in practice able to control the shape of the X-ray intensity—α-ray ionisation curves; next, the construction of the photometer and the technique of its use will be described. Then an account will be given of the experimental tests which have already been made of the integrating properties of the instrument; and finally the applicability of the photometer to the integrated measurement of radiation in general other than X-rays, will be discussed.

Theory of the Method.

The problem to be solved is how to make the α-ray ionisation increase in direct proportion to the X-ray intensity. There are obviously three main factors involved: (1) the action of the X-rays on the photographic plate; (2) the action of the light in the printing process; and (3) the action of the insoluble film when placed in the path of the α-particles. If employed in an arbitrary manner, these various processes will, of course, not combine to produce the desired result, but by reasoned control they can be made to interact so that a linear relation between X-ray intensity and α-ray ionisation is obtained over a considerable range. The theory of this interaction will now be sketched.

The blackening or density D of a photographic image is defined as $\log_{10} I_0/I$, if it transmits a light intensity I when the incident light intensity is I_0. The blackening of photographic plates by X-rays has been investigated by Bouwers* and others. Bouwers has shown that it is accurately described by Busé's formula†

$$D = C \log_{10} (X/a + 1) \tag{1}$$

---

* 'Z. Physik,' vol. 14, p. 374 (1923).

† 'Physica,' vol. 2, p. 84 (1922).

so long as there is little or no potassium bromide in the developer. In this equation X is the X-ray intensity, while C and a are constants. C increases exponentially to a limiting value as the time of development is increased, but its most important property is that *it is independent of the wave-length of the incident X-rays.* For this reason it is permissible to calibrate an X-ray photograph with rays of different wave-length from that of the crystal reflections. In fact, it is simplest to calibrate with the main X-ray beam, as in the experiments described below. Fig. 1 shows one of Bouwers' graphs.

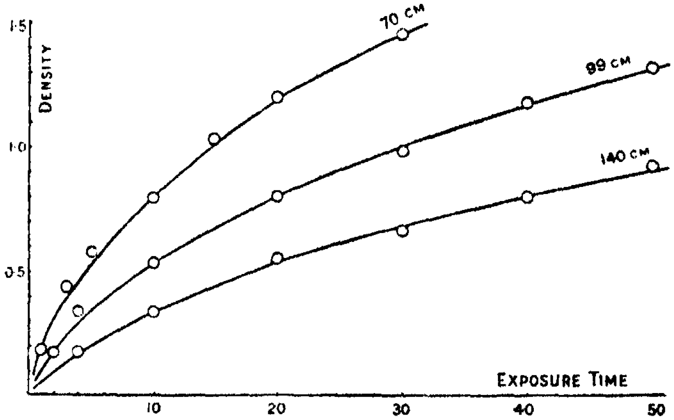

FIG. 1.—Curves (from Bouwers); $D = 1\cdot2 \log (T/2\cdot8 + 1)$; $D = 1\cdot2 \log (T/5\cdot6 + 1)$; $D = 1\cdot2 \log (T/11\cdot2 + 1)$.

The curves pass through the origin, that is, there is no induction period (Schwellenwert), and up to densities of about 1 they agree very well with the exponential form, $D = D_0 (1 - e^{-aX})$, a characteristic which plays an important part in the action of the α-ray photometer. The Schwarzschild constant for X-rays is practically unity (Bouwers found $0\cdot99 \pm 0\cdot02$), and calibration can be carried out by time exposures. Doubling the time of exposure for a given intensity is photographically equivalent to doubling the intensity and keeping the time constant, a simplification which does not hold in the case of ordinary light.

During printing, a minimum exposure will be required to bring about insolubility in the carbon tissue, but the important feature is that *the surface of development is a surface of constant exposure.* This means that the combined density of the negative and finished print is a constant, being merely the density of the print at places corresponding to zero X-ray intensity. If the thickness of the tissue at such places be T and μ be the absorption coefficient of the tissue for the printing light, then, by the definition of density,

$$(T - t) = kD/\mu, \tag{2}$$

where t is the thickness of tissue corresponding to a density D and k converts Naperian to natural logarithms. This equation is an expression of the linear relation which experiment has shown to hold between the optical density of a carbon tissue and the logarithm of its exposure to the printing light.*

$(T - t)$ represents the difference between the maximum tissue thickness and the thickness at any given point. It thus represents the depths of the *hollows* left after development with warm water. From (2) it is directly proportional to the photographic density, and therefore, since for weak X-ray intensities the density is almost proportional to the intensity, the contour of a carbon print of a weak X-ray photograph is a direct reproduction of the intensity distribution in the photograph. *The contour of the depressions in the developed tissue is the counterpart of the peaks recorded by the ionisation spectrometer.*

From (1) and (2),

$$(T - t) = \frac{kC}{\mu} \log_{10}\left(\frac{X}{a} + 1\right). \tag{3}$$

Turning now to consider the parts played by the α-rays and the electroscope, we recall at once† that when a radioactive deposit is covered by successive thicknesses of matter the α-ray ionisation produced decreases approximately according to an exponential law with the thickness of matter traversed by the rays. Fig. 2 shows curves obtained on gradually decreasing the distance between a polonium deposit and the electroscope. The α-rays from polonium have a range in air of about 3·8 cm., and it is at about this distance that what

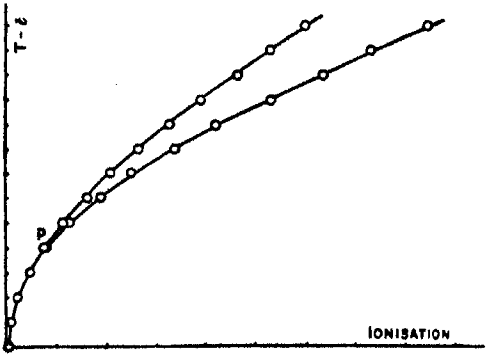

Fig. 2.

---

* See, for instance, Hardy and Perrin, 'J. Franklin Inst.,' vol. 205, p. 197 (1928).

† Rutherford, 'Radioactive Substances and their Radiations,' p. 146. The theoretical form of the "electroscope curve" has been worked out by W. H. Bragg ('Phil. Mag.,' June, 1906, p. 754).

we shall call the "electroscope curve" commences. In fig. 2 the ordinates represent the distance in millimetres the α-rays have penetrated the electroscope. It will be seen that the electroscope curves are of a form similar to that of the photographic curves shown in fig. 1. In fact, both types of curve are sufficiently near exponential to be treated, in the argument which follows, as curves of the same form. The upper curve in fig. 2 was obtained after inserting a "stop" or diaphragm in the bottom of the electroscope. This has the effect of limiting the divergence of the α-ray beam and thereby giving rise to a steeper curve of the same type (see fig. 3).

It is clear that the α-ray property of having a short and definite range allows us to make zero X-ray intensity correspond with zero α-ray ionisation (in what follows we shall call this α-ray intensity). It is necessary merely to cover the polonium with the maximum thickness of carbon tissue ($X = 0$, $D = 0$, $t = T$) in the print, and then raise or lower the electroscope until the α-rays just begin to penetrate its base. If now we cover the polonium with some other part of the print where the X-ray intensity is not zero, the rays enter the electroscope to a distance corresponding to the decrease in thickness of the tissue, that is, to $(T - t)$. Thus the curves in fig. 2 can be taken to represent the increase of α-ray intensity with increasing $(T - t)$. This statement is not strictly correct, since fig. 2 was obtained by simply increasing the air space between the polonium and the electroscope; but the resemblance is sufficiently close to make the point in question, which is that the curves $(T - t)/\alpha$-ray intensity are also practically exponential—at least, as will be seen below, parts of them may be selected to conform to the required conditions.

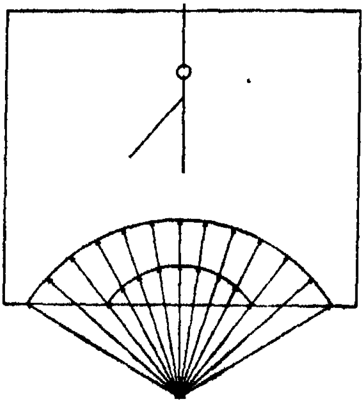

Fig. 3.

Equation (3) shows the relation between $(T - t)$ and the X-ray intensity X. We are aiming at a direct proportionality between X and the α-ray intensity α. If this proportionality is to hold, then the electroscope curve must be of the form

$$(T - t) = \frac{kC}{\mu} \log_{10}\left(\frac{\alpha}{b} + 1\right). \tag{4}$$

Experiment shows that this condition must be satisfied, and so if we can make the necessary adjustments in the constants we shall have obtained the required result. Comparing (3) and (4), the general equation connecting X and α is

$$A \log_{10}(X/a + 1) = B \log_{10}(\alpha/b + 1) \tag{5}$$

where A and B are constants.

Thus

$$X = a\left[(\alpha/b + 1)^{B/A} - 1\right],$$

and

$$\frac{dX}{d\alpha} = \frac{aB}{Ab}\left(\frac{\alpha}{b} + 1\right)^{B/A-1}. \tag{6}$$

We require $dX/d\alpha$ to be constant, and this is possible only if $(B/A - 1) = 0$, *i.e.*, if $A = B$, as was clear above. But if $B > A$, $dX/d\alpha$ increases with α, and the curve gradually turns up, while if $B < A$, $dX/d\alpha$ decreases with α, and the curve gradually turns down.

From (3), $A = kC/\mu$ and can therefore be increased or diminished by (*a*) increasing or diminishing C, the "contrast factor" of the negative, by suitable modification of the developer or type of photographic plate; and/or by (*b*) decreasing or increasing μ by variation of the type of carbon tissue or the strength of the dichromate solution used for sensitising it.

With regard to the factor B, it is clear that this too is capable of being modified in a manner suitable to the end in view. While the factor A ($= kC/\mu$) is a measure of the steepness of the photographic curve shown in fig. 1, B is a measure of the steepness of the electroscope curve shown in fig. 2. It may be modified by (1) selecting a certain range of the electroscope curve (which is not a true exponential curve throughout); and/or by (2) increasing the steepness by use of a diaphragm in the base of the electroscope to limit the divergence of the α-ray beam, after the manner exemplified by the upper curve of fig. 2. And now one point must be emphasised without further delay, and that is, that *it is necessary to reject the first few millimetres of the electroscope curve owing to the "straggling" of the α-particles.* As was pointed out in the previous Paper, if we use that electroscope position for which the α-rays are just beginning to enter when the polonium is covered by the maximum thickness of tissue ($X = 0$), there is a distinct discontinuity in the curve X/α. Near the origin the curve turns sharply downwards towards the α-axis. Owing to the straggling of the α-particles at the end of their range, the ionisation increases at first only slowly (see fig. 2). The region of slow increase lying in advance of the main stream of α-particles amounts to some 4 mm. Its effect may be eliminated in a very simple fashion, namely, by arithmetical subtraction. As before, the polonium must be covered by the maximum thickness of tissue ($X = 0$)

and the electroscope then lowered till the α-rays have penetrated to about 4 mm. The ionisation due to these last 4 mm. must then be subtracted from every subsequent reading. By this means we use a section of the electroscope curve commencing somewhere near the point P in fig. 2, and yet still retain for X/α a curve which passes through the origin. The experimental procedure will be explained more fully below.

The factor A, since it contains both C and μ, is beyond further control when once the print has been made, and therefore successful manipulation of it depends upon the reliability of photographic materials. On the other hand, the factor B is a property of the α-rays and the electroscope. It can be modified after the photographic processes are complete and unalterable. It thus offers us a powerful means of arriving at the required linear law in spite of photographic irregularities, and enables us to treat every photograph on its own merits, according to the fundamental principle of all photometry.

Fig. 4 (lower curve) shows how a linear law may be obtained by altering A, and fig. 5 by altering B. For fig. 4 the negative was an Agfa duplitised X-ray film. Five minutes development at 18° C. with Agfa Rodinal, 1 in 20, gave a curve slightly concave upwards (*i.e.*, C, and therefore A, was too small), but increasing this time to 7 minutes increased the contrast factor C just sufficiently to give a straight line. In a similar manner, by the use of more powerful developer or films with greater contrast other curves were obtained showing varying degrees of *downward* concavity. As an example we may quote the Schleussner Donio duplitised X-ray film, which when developed as above for 5 minutes gave the curve 1 of fig. 5. It is thus more "contrasty" than the Agfa film developed under similar conditions. The upper curve of fig. 4 is an

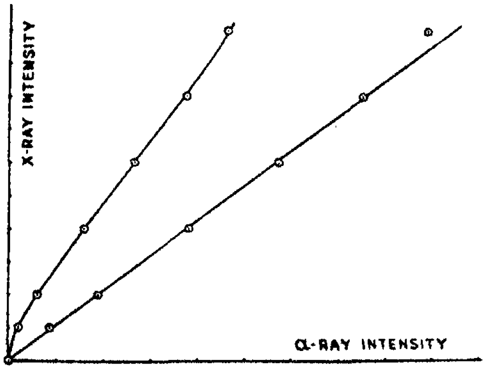

FIG. 4.

example of the type obtained if the ionisation due to the " tail " of the electroscope curve is not eliminated. This curve was plotted with the electroscope in such a position that the α-rays were just beginning to penetrate the base when the polonium was covered with the maximum thickness of tissue. It will be seen that near the origin the α-ray intensity increases more slowly than is required. However, on lowering the electroscope through 4 mm. and repeating the observations, but afterwards subtracting the ionisation due to this 4 mm. " tail " from every reading, the lower curve is obtained. The *observed* ionisation for zero X-ray intensity is zero in the upper curve, while in the lower it is that due to the first 4 mm. of the α-ray beam which penetrate the electroscope. Subtracting this now from *every* observed value of the ionisation, we once more obtain a curve through the origin—the curve, in fact, which represents the *increase* in ionisation with X-ray intensity when we make zero X-ray intensity correspond with the point P in the electroscope curve (fig. 2).

The four curves of fig. 5 show the effect of inserting a diaphragm in the base

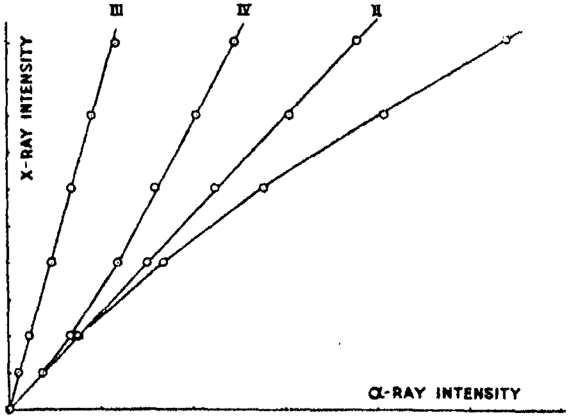

Fig. 5.

of the electroscope. The less the divergence of the α-ray beam the greater the factor B, and, as shown above, increasing B tends to make the curve (X-ray intensity)/(α-ray intensity) concave upwards. Curve 1 was obtained without a diaphragm from a Schleussner Donio duplitised X-ray film developed for 5 minutes at 18° C. with Agfa Rodinal, 1 in 20. Owing to the strong contrast obtained in this make of film, it is convex upwards. (It should be stated here that in all the curves shown in this paper, with the exception of the upper curve of fig. 4, the ionisation " tail " has been eliminated.) On inserting a diaphragm which limited the divergence of the α-ray beam to about 67½°, curve 2 was obtained. It is linear and is the one required for integration purposes. A smaller diaphragm (38½°) gave curve 3, still practically linear; but with the same diaphragm as for curve 2, with the addition of a small tube 1 cm. long projecting inside the electroscope, a curve (4) was obtained which was *concave* upwards. These curves of fig. 5 demonstrate in a striking manner what a powerful method is afforded by modification of the divergence of the α-ray beam. We need only to take the precaution of using such a film or development as will always give rise to a curve which is slightly convex upwards, and then it is only a matter of choosing the correct diaphragm to obtain the required linear relation between X-ray intensity and α-ray intensity. In fact, it can be shown theoretically, as follows, that it is always possible to obtain a curve which is concave upwards, thus ensuring that, if we start with a convex curve, such as the Donio above, we can always pass through a curve which is linear over a considerable range.

The limiting case arrived at by cutting down the divergence of the α-ray beam is a single α-particle. For a single α-particle it is known that the cube of the velocity at any point of its range is proportional to the length of range still remaining to be traversed (Rutherford, *op. cit.*, p. 157). Thus, if V be the velocity of the particle on entering the electroscope,

$$V^3 \propto (T - t).$$

And therefore, since the ionisation produced is proportional to the lost energy of the particle,

$$\alpha \propto (T - t)^{2/3},$$

i.e.,

$$\alpha = K\,[\log (X/a + 1)]^{2/3},$$

from (4) and

$$d\alpha/dX = 2K/3a\,[\log (X/a + 1)]^{1/3}\,(X/a + 1),$$

which always decreases as X increases, that is, the curve X/α is concave upwards.

Construction and Technique of the Photometer.

In its essentials the construction of the α-ray photometer is of the simplest. The rays from a uniform or effectively uniform deposit of polonium pass via a hole in a thin strip of mica through the carbon tissue into an α-ray electroscope. We shall defer for the moment the question of the uniformity of the radioactive deposit and pass at once to the slit. This is a hole in a cleavage flake of mica a little over 1/50 mm. thick. Mica is chosen for two reasons:

(1) it is necessary, for integration purposes, to have the carbon tissue and the polonium as close to each other as can possibly be effected without actual contact; (2) a transparent slit is necessary in order to facilitate the adjustment of any required photographic spot within its perimeter. The integrating properties of the photometer require only that the spot shall lie somewhere within the confines of the slit, and mica offers obvious advantages over glass from the point of view of thinness, durability, and the ease with which holes of various shapes and sizes can be cut in it. The polonium deposit lies immediately under the slit—again as close as possible without actual contact—and is carried by a slider which can be withdrawn and, after adjustment of the spot over the hole, pushed back always into a position defined by a metal stop.

The constituent parts of the photometer may be conveniently considered under three heads: the photometer table, the electroscope, and the supporting framework. The fundamental arrangement described in the paragraph above is incorporated into the photometer table, which consists essentially of a metal table in the centre of which is cut a rectangular hole sufficiently large to allow room for the movement of the polonium deposit on its slider. The slider runs in grooves under the table, and the whole is so arranged that the radioactive deposit is almost flush with the upper surface of the table. The hole in the table is then covered with the mica strip so that the slit lies immediately over the polonium in its normal position. The mica is held down flat against the table by a pair of pressure bars, while a second pair of pressure bars serve to hold the carbon tissue flat against the mica slit. This arrangement ensures that the tissue and radioactive deposit, when readings are being taken, shall lie parallel and as close together as possible—in fact, separated by only the thickness of the mica slit.

Fig. 6 is a plan of the photometer table, a metal plate some 15 cm. square and 3 mm. thick. The slider S, running in grooves underneath, carries a smooth and accurate bearing through which passes the shaft supporting the disc D, which in turn supports the polonium R. The function of this arrangement, whereby the polonium can be continuously rotated while the observations are in progress, will be explained below. For the present, it should be noticed that the polonium lies very close under the mica strip M_1, which covers the central rectangular cavity H. O_1 is the slit in M_1, which is held flat against the table by the pressure bars P_1, held firm in their turn by the screws E. During the observations the tissue lies on the top of M_1, and it is held down flat by the pressure bars P_2 and a second mica strip M_2 which is cemented to the under surface of these bars. A hole O_2, slightly larger than O_1, permits the passage of the α-particles through this second mica strip. It should be emphasised that this arrangement is *not* a double slit. O_1 is the true slit;

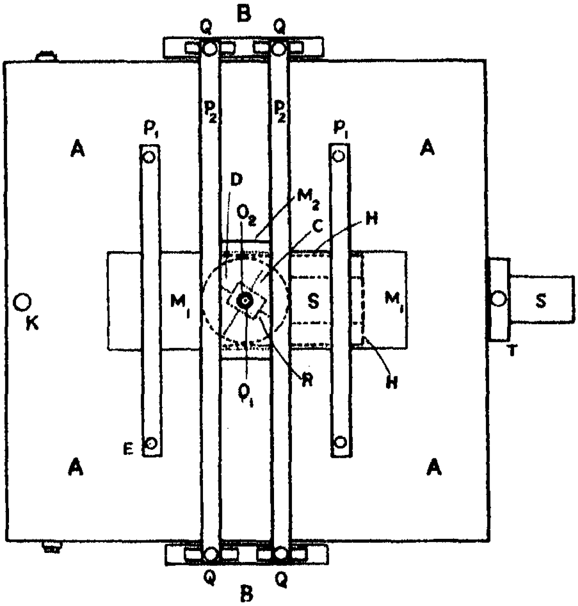

Fig. 6.—A, Table. S, slider for polonium. R, polonium. D, disc on which polonium is mounted. C, axes inscribed on disc. M_1, mica strip for slit. O_1, slit in same. M_2, mica strip for holding tissue. O_2, hole in same. P_1, pressure bars for mica strip. E, screws for same. P_2, pressure bars for tissue. B, pivots for same. Q, adjustment screws for same. K, elevating knob for same. T, metal stop for slider. H, central hole in table.

O_2 is merely an aperture in the pressure strip M_2. The tissue under examination is inserted between M_1 and M_2 and moved with forceps until the photographic spot is enclosed by the slit O_1.

For this purpose, the table is fitted with a contrivance for raising P_2 and M_2 through a few millimetres when necessary. The ends of P_2 are held by adjustment screws Q working in slots in a bar B which is part of a rectangular metal frame F (see now the elevation of the table shown in fig. 7). This frame is connected at G to a lever N pivoted at L which can be depressed by applying the thumb to a loose knob K passing through the table. Actually, there are two such systems BFNL, one at either end of the pressure bars P_2, and they are connected by a cross bar at the centre of which acts the knob K (see plan, fig. 6). By this means it is easy to raise the pressure bars by the left hand, while using the right hand to insert and adjust the tissue. On releasing the knob K, a phosphor-bronze strip V, acting as a spring, brings down the pressure bars again on to the tissue. The under sides of the pressure bars are padded with rubber strips to avoid injury to the tissue.

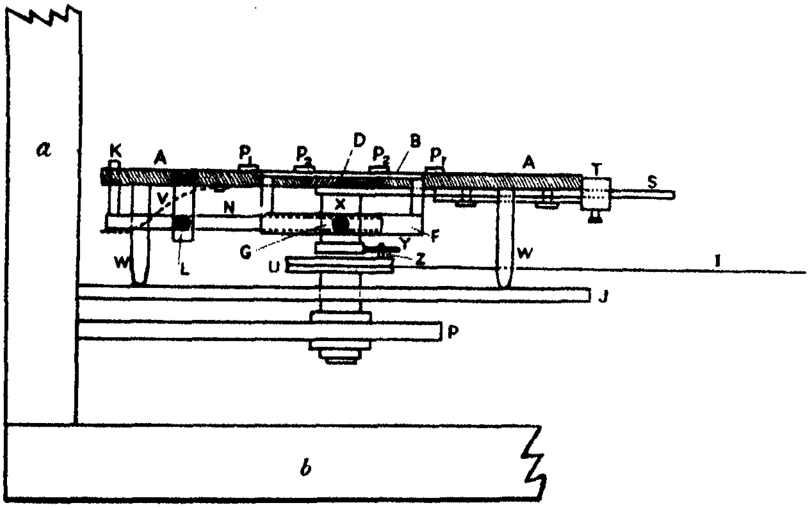

Fig. 7.—BFGNLK, system for elevating pressure bars on depressing K. V, spring for restoring pressure bars on releasing K. W, table legs. J, frame on which legs slide. X, shaft for polonium disc D. Y and Z, engaging pins. V, driving pulley. I, driving belt. P, support and bearing for driving pulley. *a*, main pillar of photometer. *b*, base.

Fig. 7 shows further a side view of the disc D for rotating the polonium and its shaft X. At right angles to the end of this shaft is a horizontal pin Y, which engages a vertical pin Z in a pulley U working in a separate bearing and support P mounted on the main pillar *a* of the photometer. The object of this combination is that, on stopping the rotation of the pulley U, the whole of the photometer table with its attachments may be slid out from under the electroscope which is mounted higher up on the main pillar *a*. The legs W of the table slide along the supports J, and after adjustment of the tissue the table is slipped back under the electroscope until it meets a position stop, which may conveniently be the pillar *a* itself.

Fig. A (Plate 19) is a photograph of the photometer table viewed from above, while fig. B shows the view from below and also the slides, the driving pulley and the main pillar of the electroscope. The slotted disc shown in this photograph connects with the vertical pin of the driving pulley. It is an unnecessary complication; the horizontal pin Y shown in fig. 7 is, of course, all that is necessary.

We may now turn again to the consideration of the question of the radioactive deposit. It is clear that, for integration purposes, the α-ray activity of the polonium deposit must be uniform over the area of the slit. Unfortunately, the attainment of such an ideal presents a problem of serious practical difficulties, which do not appear to have been yet overcome in the commonly used methods of deposition.[*] It has recently been shown[†] that the atoms in radioactive deposits tend to cluster in colonies, but this seems to be too small scale a phenomenon to have serious consequences for an integrating photometer such as is described here. In any case, the method described below of surmounting the major difficulty of getting a uniform deposit in the macroscopic sense, automatically minimises these microscopic variations.

The procedure adopted was as follows. Glass tubes that had contained radium emanation were ground up, and the deposit of Ra D, E and F on the walls dissolved off with dilute sulphuric or hydrochloric acid. After the fragments of broken glass had settled, a piece of polished silver foil was suspended in the solution for a time sufficient for a strong deposit of polonium (Ra F) to form on it. This initial deposit appears always to be slightly contaminated with Ra D and E, and so for further purification the washed silver foil was then dissolved in a minimum of nitric acid and the silver reprecipitated as silver chloride by the addition of hydrochloric acid. The solution of polonium salts was then separated by decantation and further washing of the precipitate with dilute hydrochloric acid. (The presence of a moderate amount of HCl prevents the precipitated AgCl from carrying the polonium down with it.[‡]) This solution was then evaporated several times to dryness with hydrochloric acid in order to drive off all remaining nitric acid, and finally the invisible deposit on the walls of the vessel was dissolved in dilute hydrochloric acid. This final solvent should be very dilute in order to obtain a good deposit later. All the above operations were carried out in small vessels made from Pyrex glass tubing.

The actual deposition was carried out in the small vessel sketched in fig. 8. It was made from two pieces of glass tubing connected by a ground glass joint. A silver disc, ground plane and very highly polished, was attached to the "stopper," while the small bulb which comprised the "body" of the vessel held the concentrated polonium solution. When the stopper was in position the bulb was full of solution except for a bubble of air about as broad as the silver disc. The whole was mounted in a cork and fixed to a revolving shaft at right angles to the length of the vessel. The bubble then acted as a stirrer and also served, once in each revolution, to sweep the silver surface clear of air bubbles. Periodically, the vessel was also turned in the cork about its main axis. By this means it was found possible to deposit the polonium with a uniformity of perhaps 5 per cent. One deposit gave the following results (time of fall of electroscope leaf) when a small exploring hole was moved across it and readings taken every millimetre: 153½, 152½, 155, 147½, 147, 150½, 148 seconds. Mean, 150½; average variation, 2½ seconds, or about 2 per cent.

---

[*] Lattès and Lacassagne, 'C. R.,' vol. 178, p. 630 (1924); Escher-Desrivières, 'C. R., vol. 179, p. 158 (1924); Curie 'J. Chim. Phys.,' vol. 22, p. 471 (1925); Rona and Schmidt, 'Z. Physik,' vol. 48, p. 784 (1928).

[†] Chamié, 'C. R.,' vol. 184, p. 1243 (1927), and vol. 185, p. 770 (1927).

[‡] Escher-Desrivières, *loc. cit.*

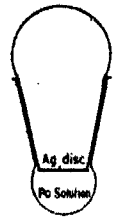

Fig. 8.

The method used to minimise such irregularities as these was as follows. The metal foil on which the polonium was deposited was cemented to a piece of graph paper slightly larger than itself, and the whole mounted on a piece of the adhesive insulating tape used by electricians. (This tape is adhesive on both sides, and has also the advantage that it can be removed from a metal surface and afterwards, by the application of a slight pressure, made to adhere again any number of times.) The system (fig. 9) metal foil, graph paper, and adhesive tape, was then mounted on a rotating disc on the surface of which were drawn two rectangular axes of co-ordinates intersecting at the centre of the disc. By this means the polonium, in a preliminary exploration of its surface, could be rotated about any known point and afterwards transferred to the disc in the photometer table. This latter disc D (figs. 6 and 7), it will be remembered, has also engraved on it two rectangular axes of co-ordinates.

While the polonium was being rotated on the testing disc about any given point, a small exploring hole was moved across it and electroscope readings taken. The rotation automatically reduces the labour of such an exploration, since moving along a radius r gives the distribution of activity in an area πr^2. Very few trials serve to indicate the point in the deposit rotation about which produces the greatest reduction in the errors of the non-rotated deposit. Actually, for the curves described in this paper quite a crude deposit was used, made by allowing a drop of concentrated polonium solution to evaporate on a piece of silver foil. Exploration of its surface by the rotating disc method gave the results shown in Table I for an area of 4 mm. diameter, which in general is sufficiently large to cover the spots on good rotation photographs. The point (1½, 0) was obviously the most satisfactory centre of rotation. This

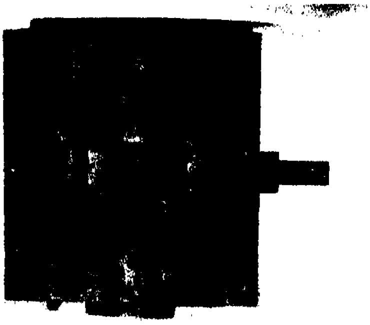

Fig. A.

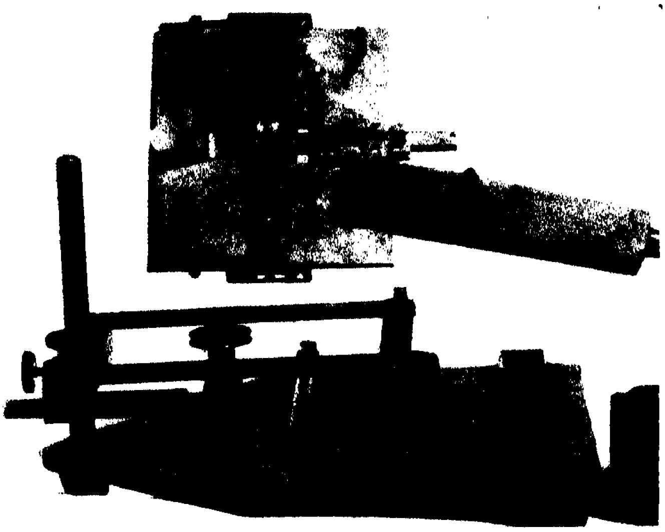

Fig. B.

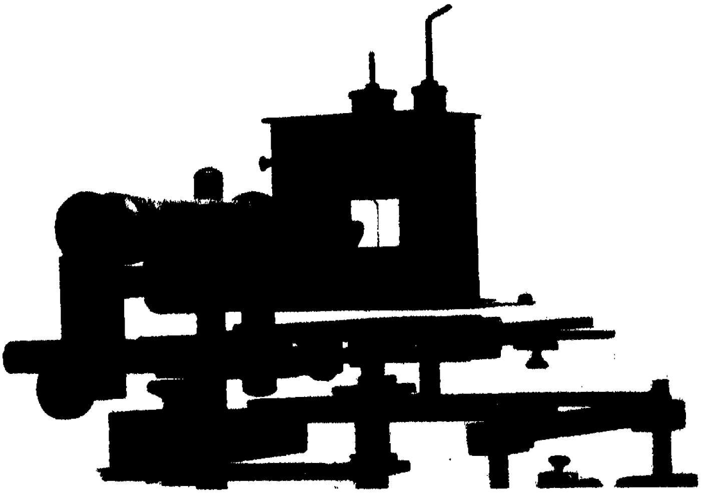

Fig. C.

(*Facing p.* 588.)

Table I.

Co-ordinates.	Electroscope readings (seconds) at ½-mm. intervals.					Mean error.	Percentage error.
0, 0	65·1	65·7	64·6	64·2	61·5	1·1	1·7
−1, 0	64·4	62·7	64·1	63·4	60·5	1·1	1·7
+1, 0	63·4	63·5	63·2	62·1	60·6	1·0	1·6
0, −1	68·8	67·7	66·3	64·1	62·6	2·0	3·0
+1, −1	63·6	65·4	64·2	62·4	60·6	1·4	2·2
+2, 0	62·0	63·2	62·5	63·1	62·5	0·4	0·6
+1½, 0	65·8	65·2	66·2	65·9	65·7	0·2	0·3

fact having been ascertained, the polonium was transferred to the corresponding setting on the disc D of the photometer table. It should be mentioned that it is not essential for the centre of rotation to lie exactly under the centre of the slit O_1. The preliminary exploration may have shown that rotation about a certain point produces a *ring* of uniformity, say, between radii r_1 and r_2. It may then be convenient to use this ring in conjunction with a slit of diameter $(r_1 - r_2)$. In such a case, the stop T on the slider S must be moved to a corresponding position.

The α-ray electroscope (base about 7 × 4, height 7 cm.) used in these experiments was of the simple Wilson type. Its leaf was charged to 200 volts by momentary connection with the "live" side of the electricity mains. The base (fig. 10) could be slid off and consisted of a double metal frame held together by four small screws. Various thicknesses of aluminium leaf (outline dotted in the figure), each of stopping power equivalent to about 2 mm. of air, could thus be clamped between the two frames and the whole then re-attached to the bottom of the electroscope. Further, after the aluminium leaf had been gripped between the metal frames, there remained a shallow cavity ABCD which could be used as a receptacle for the diaphragm required to limit the divergence of the α-ray beam. The diaphragms actually used were simply rectangles of aluminium foil equal to ABCD in the centres of which were punched out holes with cork borers of various sizes.

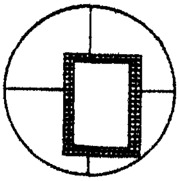

Fig. 9.

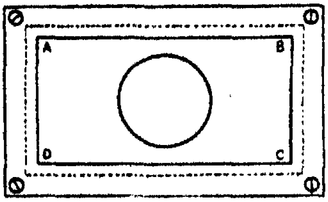

Fig. 10.

The tele-microscope (about 1 inch focus in these experiments) was carried by an arm with the usual degrees of freedom, but this arm was connected rigidly to the electroscope, so that, once the leaf had been brought to focus, the complete electroscope-microscope system could be moved up or down the main pillar *a* without disturbing this adjustment. The pillar *a* was graduated in $\frac{1}{2}$ mm., and the electroscope could be clamped at any height (within the range of the α-particles) above the photometer table. The pillar *a* carried also the bearing P of the driving pulley U. It also partly supported the slides J along which ran the feet W of the photometer table. These slides were further supported by screw-legs resting on the main base of the instrument (see fig. B, Plate 19). Fig. C (Plate 19) is a photograph of the photometer as a whole with the table slid into position under the electroscope. The driving pulley U was driven by a small motor placed on the bench to the right of the photometer. This motor was, of course, run continuously while readings were being taken. When it was necessary to move the tissue to a new position over the slit, the motor was stopped and the photometer table slid from under the electroscope and placed on the opal glass lid of an illuminated viewing box.

We may now briefly outline the procedure to be followed when actually measuring the X-ray intensities recorded on the carbon tissue. As an example, we may consider the results shown graphically in fig. 4. The method of making the test negatives and prints is described below, and so, for the moment, we shall assume that a stripped print is at hand of a uniform set of spots of known X-ray intensities. The complete photometer would presumably be supplied with a set of mica strips such as M_1, each punched with a hole O_1 of definite size and shape. (These holes are easily cut in a mica flake by aid of a fragment of a broken safety-razor blade.) That slit which is slightly larger than the spots to be tested is chosen and screwed down in its place on the photometer table, after which the tissue is inserted so that the slit is covered by a region of zero X-ray intensity. The polonium is then slipped back, the table replaced under the electroscope, the driving motor started, and the electroscope lowered until the α-rays are just beginning to enter. For the region of zero X-ray intensity and subsequently for all the spots in turn, the α-ray ionisation is then measured by taking the time for the leaf to fall across the whole of the eyepiece scale. In general, owing to the probability variations of the α-ray emission, it is necessary to take the mean of two or three readings. Table II shows readings (upper curve of fig. 4) obtained in this manner.

The last column of this table requires now a little further explanation. It has been stated above that to get rid of the discontinuity near the origin which

Table II.

X-ray intensity.	Times of fall of leaf (seconds).	Mean time of fall.	Reciprocal ($\times 10^3$).	Reciprocal ($\times 10^3$), after subtraction of " tail."
0	1304	1304	0·77	0
10	609	609	1·64	0·87
20	314	314	3·19	2·42
40	138·6, 141·8	140·2	7·13	6·36
60	87·8, 88·2	88·0	11·36	10·59
80	63·4, 63·6	63·5	15·75	14·98
100	51·8, 52·0	51·9	19·27	18·50

is due to the " straggling " at the end of the range of the α-particles, it is necessary to lower the electroscope until some 4 mm. of the range is included within it. As a matter of fact, it is impossible to define clearly this adjustment in such terms, since the " straggling " prevents one from saying exactly when the ionisation is beginning. In Table II, for instance, there is still a very small *observed* ionisation for zero X-ray intensity, which means that the upper curve of fig. 4 is in reality only a very close approximation to the ideal curve in which zero X-ray intensity would correspond to *observed* zero α-ray ionisation. But, as explained above, the ionisation associated with the tip of the range may always be subtracted from every observed ionisation, thus making zero X-ray intensity and zero α-ray intensity always correspond. This had been done as a matter of course in Table II. The " tail " there is indeed very small, but it has to be subtracted to make the curve pass strictly through the origin. The point now that must be made quite clear is that if the " tail " is expressed, not in millimetres of range, but as a definite quantity of ionisation, it is precisely defined and is a constant for a given slit and source of α-particles. In other words, we must lower the electroscope, not through a vague 4 mm., but until the leaf registers a certain definite ionisation. (With the slit and source used in these experiments, this quantity corresponded to a time of fall of about 2 minutes.) With any slit and source, this quantity of ionisation, the " optimum tail " which must be subtracted in order to obtain the closest approximation to a linear law, must be first determined once and for all. It is a constant of the instrument—or rather it is a " constant " which is slowly decreasing at a known rate owing to the decay of the polonium (" half period " about 136 days).

Table III.

X-ray intensity.	Times of fall of leaf (seconds).	Mean time of fall.	Reciprocal ($\times 10^3$).	Reciprocal ($\times 10^3$) after subtraction of " tail."
0	123, 123	123	8·13	0
10	86·2, 85·8	86·0	11·63	3·50
20	63·4, 63·6	63·5	15·75	7·62
40	42·6, 42·6	42·6	23·47	15·34
60	32·2, 32·4	32·3	30·96	22·83
80	26·6, 26·2 26·0, 26·2	26·2	38·17	30·04
100	22·8, 23·2 22·6, 23·2	23·0	43·48	35·35

Table III shows the observed results for the lower curve of fig. 4. The "optimum tail" has been subtracted and a close approximation to a linear law obtained.

While fig. 4 is an example of a linear law obtained through suitable development only, fig. 5 illustrates how the same end may be attained by limiting the divergence of the α-ray beam. The observations are taken in a similar manner to the above, with a slight modification. A very small diaphragm may have the effect of limiting the known optimum tail itself, and to allow for this the electroscope must first be lowered to its optimum position without diaphragm. Afterwards the tail subtracted must be the tail *with* diaphragm.

In the previous communication introducing the α-ray photometer, it was pointed out that a source of error is found in the fact that the range of α-particles in air depends, of course, on the temperature of the air. It was also shown how the error may be eliminated by making the base of the electroscope of a suitable thickness of aluminium leaf, which ensures that the α-rays, while outside the electroscope, describe practically the whole length of their paths not through air but through a metal. Unfortunately, though this procedure may and should be adopted in all ordinary cases of photometry and when using the linear calibration by development only, it is impracticable when using the diaphragm as a linear calibrator. The reason for this is that the diaphragm method assumes that the spot to be integrated is a point source of α-radiation—a sound enough assumption in the case of ordinary crystal reflections when the diaphragm in the electroscope base is at least 2 cm. above the slit. But this, of course, involves introducing the *maximum* air path between the slit and the electroscope, and, in fact, it is obvious that no other course is permissible. The only solution with the outfit described here is to avoid draughts and to see that, while a set of readings is being taken, the temperature of the air in the neighbourhood of the electroscope is practically constant. Happily, the trouble is not so serious as it would at first sight appear. Experiments are now being carried out in the Davy Faraday Research Laboratory of the Royal Institution in which the electroscope is replaced by an ionisation chamber and a constant reading (leaking) electrometer. With such an arrangement the time required for a complete set of readings is so small compared with that involved by the electroscope method that the variations of room temperature can be ignored.

Experimental Tests of the Integrating Property of the Photometer.

The basic experiment of the photometric procedure described in the present paper is simply this: that when we cover a *uniform* radioactive deposit with successive thicknesses of *uniform* carbon tissue, then, provided that the angle of emergence of the α-rays from the tissue be not allowed to exceed a certain limiting value defined by the "stop" in the base of the electroscope, the increase in ionisation recorded by the electroscope is directly proportional to the increase in X-ray intensity as represented by the thickness of the tissue. In this system, the depth of which is very small compared to its width, one and the same proportionality holds for every point on its surface. Every such point is the apex of a cone of rays the base of which is restricted to a small area of the active deposit lying immediately below it. If now we replace the uniform tissue by a *non-uniform* tissue, yet keeping every other part of the system quite unchanged, it is clear that the total recorded ionisation still bears the same proportionality to the total X-ray intensity, *provided that the tangent to the surface of the tissue never falls within the angle of emergence of the α-rays.* Thus when we consider that an average X-ray spot in a carbon print will be about 1 mm. in diameter and something of the order of 1/100 mm. in depth, we see that the instrument under discussion should be capable of integrating intensities over a very considerable range. The required angle which the generator of the α-ray cone makes with the surface of the tissue appears to be about 60°, which means that, neglecting the small error associated with the edges of the slit, only very sudden changes in intensity, such as absorption edges, will present any difficulty. Presumably, the tendency will be for the instrument to round off such discontinuities slightly.

For reasons explained in the paper already several times referred to, a valid test of the photometer must be carried out by aid of some device which does not involve actual crystal reflection. Such a device is described below, but nevertheless, it should be mentioned that preliminary tests were made on the relative intensities of the Cu Kα and Cu Kβ spots reflected by a given crystal plane (third order of (100) of tartaric acid). These tests were made on the old Kodak films which have now been withdrawn from the market, hence there is no point in reporting here the conditions of development, etc. Later research showed that the only really safe method of linear calibration is the diaphragm method, but the photographs in question were examined before the details of this method had been worked out. They were examined by a composite method in which the calibration was partly by development and partly by diaphragm. A preliminary film and print were prepared of a step-wedge of known X-ray intensities of Cu Kα rays. The print was tested by the electroscope and diaphragms, and the divergence of the α-ray beam required to give a linear law was noted. A negative and prints of the α and β spots were then prepared under the same conditions of development and printing, and finally these prints were examined under the electroscope using the same divergence of the α-ray beam as had been found necessary in the case of the step-wedge print. The weakness of this method lies in the assumption that photographic material from one and the same batch is sufficiently uniform always to give the same results. We know this assumption to be frequently unsound, but, as a matter of fact, in the case in question very satisfactory agreement was found. The spots (reflected from a minute crystal of tartaric acid) had an irregular shape of maximum width about 2 mm., and they were examined with a circular slit of 3 mm. diameter. The respective intensities of the backgrounds of each were deduced from a measurement of three backgrounds, one between the spots, one immediately to the left of the α spot, and one immediately to the right of the β spot. Four prints of the same negative gave, for the intensity ratio Cu Kα/Kβ, 5·5, 5·8, 5·3, 5·7; mean, 5·58. Correcting for the absorption of the window of the X-ray tube (1/1000 inch of aluminium) this gives $\alpha/\beta = 6\cdot 1 \pm 0\cdot 1$, a result which compares very favourably with that (6·0) obtained by Siegbahn and Záček from *line* spectra examined by the more familiar and non-integrating photometric methods.

A stricter test of the integrating powers of the photometer was carried out by aid of a set of artificial X-ray spots the intensities of which were known without any ambiguity. The method of photographing these spots was as follows.* A drill of suitable shape having been prepared after repeated trials, six identical cup-shaped hollows, equally spaced in a line, were drilled in a zinc plate about 3 mm. thick, the faces of which had previously been machined to parallelism. These depressions had a maximum diameter of 2 mm. and their depth, also about 2 mm., were tested in each case by means of a spherometer. After it had been ascertained by the spherometer and a careful scrutiny through a lens that the six hollows had indeed been made as identical as the method permitted, they were filled with sealing-wax and the lower face of the zinc plate machined down until some tenth of a millimetre was left to form the base of the cups. The sealing-wax was then dissolved out and the plate, tested once more for parallelism, was ready for use.

---

* I am greatly indebted to Mr. C. H. Jenkinson of the Davy Faraday Laboratory for the trouble and care which he took in preparing for me the metal plate for these spots. He also constructed the photometer shown in the Plate.

It had been pointed out above that the constant C in the X-ray photographic blackening curve is independent of wave-length, and also that the Schwarzschild index is practically unity. For these reasons it is permissible to calibrate X-ray photographs by time exposures with heterogeneous rays. To this end a brass disc was cut into sectors of such relative dimensions that, when the disc was rotated rapidly in front of the test plate described above, the relative intensities of the spots registered on a film placed immediately behind the plate were 100, 80, 60, 40, 20, and 10. (The films used were Schleussner "Donio" duplitised X-ray films, and they were developed for 5 minutes at 18° C. with Agfa Rodinal, 1 in 20.) The X-rays were supplied by a Coolidge tube of molybdenum anticathode distant about 6 feet away, and placed so that the common normal to the X-ray film, the test plate and the rotating disc passed approximately through its focal spot. On the same film were photographed also a set of six *uniform* spots, 2 mm. diameter, of the same relative intensities, and made by substituting for the test plate a metal plate through which had been drilled six identical holes; and finally another set of the non-uniform spots, but this time without the rotating sectors. The film after development thus showed three rows of spots: (1) six uniform circular spots of 2 mm. diameter and of relative intensities 100, 80, 60, 40, 20 and 10; (2) a slightly weaker set of six non-uniform circular (artificial X-ray) spots of 2 mm. diameter and of the same relative intensities; (3) another set of the same six non-uniform spots but all apparently of the same intensity. Carbon tissues of this negative were then prepared as described below.

The three sets of spots on the tissues were tested as follows: (*a*) with the known "optimum tail" the diaphragm was determined which gave a linear relation between X-ray intensity and α-ray intensity for the six uniform (calibration) spots; (*b*) under the same conditions were measured the integrated intensities of the six apparently identical non-uniform spots; (*c*) still with the conditions unaltered the integrated intensities of the six graded non-uniform spots were measured. The procedure (*b*) was introduced in order to correct as far as possible for the slight mechanical inaccuracies which were to be expected in the manufacture of the test plate. It demonstrated that there were indeed small discrepancies between the supposed identical cup-shaped hollows, for the observed integrated intensities of the six "equal" non-uniform spots were in the ratio, 1·04 : 1·02 : 1·02 : 1·00 : 0·97 : 0·96 (mean of seven prints of three negatives). This correction was subsequently applied to the observed integrated intensities of the six graded non-uniform spots. It is not a strictly logical correction, since it assumes what we are trying to prove, namely, the integrating property of the photometer; but its introduction undoubtedly gives us a fairer estimate of the true intensities of the spots which we have taken to be 100, 80, 60, 40, 20 and 10.

Four tissues gave the following results (Table IV) for the integrated intensities of the six non-uniform test spots.

Table IV.

(1)	8	16	40	59	79	102
(2)	12	21	42	57	80	99
(3)	9	17	40	60	79	102
(4)	9	19	42	59	78	98
Uncorrected mean	9½	18	41	59	79	100
Corrected mean	9	17½	40½	59	81½	104
Probable error of mean	±½	1	⅓	½	⅓	1
Theoretical intensities	10	20	40	60	80	100

As (so far as the author is aware) the first single-reading integrations by photographic means of non-uniform patches of radiation, these results may be regarded as very satisfactory, especially in view of the fact that the spot of strength 10 corresponded in intensity to what would be considered a very weak crystal reflection. There is now no doubt that the α-ray photometer is an integrating photometer, and that, even in its present stage of development, it is fully capable of giving results of at least the order of accuracy usually required in crystal analysis.

A series of negatives and prints were also taken with a view to testing the reliability of the method of calibration by development, using similar conditions to those which yielded the results shown graphically in fig. 4. The mean intensity values were surprisingly good—in fact, not very inferior to those shown in Table IV—but the variations were greater. Where great accuracy is not required, the method may be recommended on account of speed, since the prints may be measured off directly without a preliminary examination of a set of uniform spots. But if it is a question of making really certain, it is, of course, not advisable to trust to the uniformity of photographic materials, and calibration by diaphragm should be resorted to always.

Preparation of the Carbon Tissues.

An account of the preparation of the carbon tissues for the α-ray photometer has already been given (*loc. cit.*), and it may be said that the main points there emphasised still hold. But a more reliable, yet probably simpler, technique has since been evolved, and it is desirable that the new modifications should be described.

The Autotype Company's photogravure tissues G 12 were used throughout, for the simple reason that they have a greater sale and are therefore more likely to be fresh when bought. The sensitising solution was a 2½ per cent. aqueous solution of *pure* potassium dichromate, without the addition of ammonia. The sensitising was always carried out in a glass dish and wooden float floating in a large bath of water at 16° C., the tissue being held (to prevent the initial curling) in a framework of glass rods such as that sketched in fig. 11. The sensitising occupied 3 minutes, with a continuous rocking motion on the surface of the water-trough, the tissue being turned over every half-minute. After the first minute or so it is generally sufficiently soaked to slip from the glass framework. This may then be removed and the sensitising completed without its aid. Each tissue, immediately after withdrawal from the sensitising bath, was squeegeed with a flat rubber squeegee face downward on to a sheet of plate glass which had previously been cleaned very carefully first with soap and water and then with methylated spirit and French chalk. After squeegeeing, all adhering liquid was wiped away with a damp wash-leather until the paper backing of the tissue appeared almost dry. It is advisable, in order to eliminate all air bubbles, to drop a small pool of the dichromate solution on to the plate glass before each squeegeeing operation.

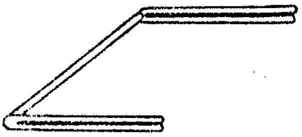

FIG. 11.

The drying of the tissue on the plate glass was carried out in a dark cupboard containing a fan. The drying was usually complete in about 2 hours, after which the tissues were stored in a light-tight box in a desiccator. When dry there is no difficulty in removing them from the plate glass. They either jump off spontaneously, or they may be easily stripped off after inserting a knife blade under one corner. It is strongly recommended that tissues for accurate work should be sensitised, printed and developed all on the same day.

English sunlight being uncertain for a large part of the year, the printing was always done about 60 cm. in front of a 15-20 amp. arc (without lenses), the exposure being judged by a simple actinometer. The heat rays were cut off by means of a sheet of plate glass placed between the arc and the printing frame.

An easier but more effective method of developing has been adopted. The tissue after printing was first soaked till limp (that is, 2 or 3 minutes) in a 50 per cent. mixture of methylated spirit and water, after which it was squeegeed face downward on to the polished side of a piece of sheet aluminium slightly larger than itself. (The Autotype Company supplies these aluminium sheets.) It was then carefully wiped with a damp wash-leather and allowed to stand for some 20 minutes between blotting paper. The stripping and developing was carried out in a tank of hot water (42° C.), the aluminium and the film adhering to it being held vertically in a clamp operated by a small water motor. This motor moved the metal sheet vertically up and down in the water of the developing tank two or three times per second. The temperature of the large mass of water in the tank varied very little during the development, but in any case it could be very easily kept constant by occasionally allowing a bunsen flame to play against the side of the tank. Ten minutes was allowed for development, after which the photograph was withdrawn from its clamp, immersed in cold water for a few seconds, and then set aside to dry. On the following day the tissue was stripped from the aluminium by aid of tweezers, after first inserting a knife edge under one corner. It should be specially noted that these aluminium sheets used as described above require *no* waxing solution. This circumstance eliminates a possible source of error in the technique described previously. The sheets should be cleaned occasionally with cotton wool moistened with dilute acetic acid.

When once a tissue has been stripped from its aluminium support, it should never be handled with the bare fingers, but should always be manipulated by aid of tweezers.

Applicability of the Photometer to the Measurement of the Integrated Intensity of other Radiations.

It has been shown above how the integrating action of the α-ray photometer depends upon the balancing of two exponential curves, the electroscope curve and the photographic density curve. It follows then that it can be applied in an analogous manner to that employed in the X-ray problem, to the measurement of the integrated intensity of any radiation the photographic density curve of which is exponential or approximately so. Fortunately, theory suggests,* and experiment has actually demonstrated, that the blackening law given by Busé's formula (1) above is not confined to X-rays alone. It holds for α- and β-rays and also, with a certain modification, for visible light. These cases will now be briefly discussed.

α-rays.—Kinoshita† and Briggs‡ have both shown that the Schwarzschild factor is approximately unity, and that the photographic density curve is of the form $D = D_0 (1 - e^{-cN})$, where c is a constant and N is the number of α-particles incident per unit area. Such a law suggests that the rate of increase of the density is proportional both to the number of α-particles striking the plate at any moment and to the number of halide grains that remain unacted upon at that moment.

β-rays.—The photographic action of these rays has been examined by Bothe,§ Salbach‖ and, most thoroughly, by Ellis and Wooster.¶ There seems little doubt that β-rays are photographically quite analogous to X-rays. The Schwarzschild factor is again unity, and the blackening curve can always be expressed by Busé's formula, whatever the velocity of the particles. Exactly as was shown for X-rays of different wave-lengths, the constant C (see equation (1) above) is a purely photographic constant, since all the blackening curves can be superimposed by adjusting the scales of the abscissæ.

γ-rays.—Bouwers has shown (*loc. cit.*) that the photographic density curve for X-rays has a form which is independent of wave-length, so presumably γ-rays would also conform to the X-ray blackening laws.

It is to be noticed that in the case of the radiations discussed above the respective photographic actions differ only in the time required to produce a given density. The form of the density curve is always the same, when the purely photographic factors remain unchanged. As a consequence, calibration can be carried out in every case by time exposures with heterogeneous rays. Any such set of calibration spots will serve directly for the measurement of homogeneous radiation, but with heterogeneous rays an appropriate multiplying factor for each wave-length or velocity must also be determined in order to make allowance for the variation in the *speed* of photographic action with varying wave-length or velocity. Bouwers* has done this in a photographic investigation of the intensity distribution in the continuous X-ray spectrum.

---

* Silberstein, 'Phil. Mag.,' vol. 45, p. 1062 (1923).

† 'Roy. Soc. Proc.,' A, vol. 83, p. 432 (1909).

‡ 'Roy. Soc. Proc.,' A, vol. 114, p. 313 (1927).

§ 'Z. Physik,' vol. 8, p. 243 (1922).

‖ 'Z. Physik,' vol. 11, p. 107 (1922).

¶ 'Roy. Soc. Proc.,' A, vol. 114, p. 266 (1927).

These considerations suggest a method of making a fuller use of Laue photographs than has hitherto been possible. By aid of the technique described in this paper we may first measure the apparent total intensity in each Laue spot, and then apply a composite correcting factor to allow (1) for the energy distribution in the continuous spectrum of the X-ray tube used for taking the photograph, and (2) for the respective photographic actions of the various wave-lengths (including the absorption edges caused by the silver and bromine in the emulsion). The correcting factor may be obtained by taking, simultaneously with the Laue photograph, a spectrum photograph of the X-rays emerging from the same or another window of the X-ray tube. (N.B.—Variations in the hardness of a gas tube, if such exist, are also automatically corrected for by this procedure.) As crystal reflector for this spectrum photograph a cleavage flake of graphite mounted on glass appears to offer considerable advantages, since from such a flake all reflections but the first order of the basal plane are of negligible intensity. Both Laue and spectrum photographs must be taken on pieces of the same film or plate and must be subjected to the same photographic treatment right up to the completion of the carbon prints.

Light.—It is interesting to note that Busé's formula, which has been found to characterise so admirably the X-ray and β-ray photographic density curves, was deduced from an examination of intensity photographs taken with visible light. Busé used "Imperial" plates and a developer *free from potassium bromide.* That his observations agreed with equation (1) above means, of course, that his plates showed no "induction period," a result which is apparently at variance with what is usually found in the case of visible light. As the elimination of the induction period is so important for the purpose of an integrating photometer, it was thought desirable to try to reproduce this result.

Dr. Toy and other workers at the British Photographic Research Association kindly carried out this investigation for me. Twelve exposures, of increasing intensity but each of 1 minute duration, were made on an "Imperial Special Rapid" (backed) plate, which was then developed for 5 minutes at 18° C. with a plain pyro-soda developer, free from potassium bromide. (Composition: A, 16 gm. pyrogallic acid and 80 gm. sodium sulphite crystals made up to 1 litre with water; B: 75 gm. sodium carbonate crystals made up to 1 litre with water; 50 c.c. of A + 50 c.c. of B + 33 c.c. of water.) The light used for the exposures was confined to a narrow region in the blue-green, though this was merely to cut down the intensity of the available source to a convenient range. The densities (opal contact densities) of the negative were measured with a Toy photometer.* The results are plotted in fig. 12. They recall at once the X-ray curves shown in fig. 1, but, unfortunately, there is still a small induction period. A carbon print, prepared as above, gave, without any limiting diaphragm, an approximate linear relation between light intensity and α-ray intensity, but, of course, the line did not quite pass through the origin.

---

* 'Acta Radiol.,' vol. 4, p. 368 (1925).

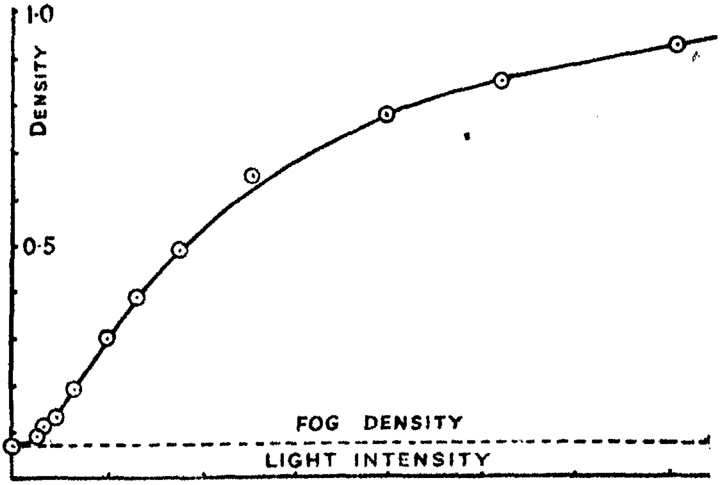

Fig. 12.

The author was obliged to abandon these researches at this point, but there is no doubt that there yet remains a promising field of investigation with regard to visible light. Whether the induction period can always be eliminated by direct means seems to be still questionable, but in any case there is always the indirect method to fall back upon. If a small but uniform preliminary exposure is given to the whole of the plate before the actual photograph is taken, the general background so produced may be considered as the region of *zero* light intensity and the measurements carried out exactly as described above for X-rays. There should then be no difficulty in obtaining direct proportionality between the α-ray intensity and the additional light intensity of the photograph itself.

---

* On this photometer the density of the most intense point in fig. 4 was about 0·6. It would be distinctly higher on the Moll photometer. Incidently, it should be noted that *the α-ray photometer can also be used as a densitometer, if a standard wedge is printed simultaneously with the negative under examination.*

The arguments briefly outlined in the present section have been brought forward with the purpose of making the following point. The α-ray photometer has demonstrated its usefulness in the very important problem of the intensity measurements in X-ray crystal analysis, but there appears to be no great difficulties in the way of its application to the measurement of the integrated intensity of most other types of radiation; in other words, instead of remaining merely an integrating micro-photometer for X-rays, there seems to be no reason why it should not be developed into a *universal* integrating micro-photometer. It is hoped that other workers may be in a position to put the points discussed in this section to the test of experiment.

Summary.

(1) The theory and constructional details are given of an integrating micro-photometer in which the photographic negative is replaced by a carbon print and light by α-rays.

(2) Direct proportionality is obtained between the X-ray intensities used to make the negative and the α-ray ionisations observed in the electroscope.

(3) Successful experimental tests on both real and artificial X-ray spots are described.

(4) It is shown how the use of such an integrating microphotometer may be extended to the measurement of α-, β- and γ-rays, and also of visible light.

The author is greatly indebted to the Managers of the Royal Institution for affording him all the facilities of the Davy Faraday Research Laboratory, and especially to the Director, Sir William Bragg, for his constant interest and encouragement. He also wishes to acknowledge his indebtedness to Dr. Russ, of the Middlesex Hospital, for emanation tubes; to Dr. Helen S. Gilchrist for co-operation in various attempts to obtain a uniform polonium deposit by chemical and electro-chemical means; to Mr. H. Smith for continuous help in the preparation of the carbon tissues; to Mr. F. J. Tritton, of the Autotype Company, for expert advice on the same; to Mr. C. H. Jenkinson for the great trouble he took in the construction of the photometer and test-plates; and to Dr. Toy and the British Photographic Research Association for the measurement of photographic densities and the preparation and photometering of the light test-negative.

The Adsorption of Hydrogen on the Surface of an Electrodeless Discharge Tube.

By M. C. JOHNSON, M.A., M.Sc., Lecturer in Physics, University of Birmingham.

(Communicated by S. W. J. Smith, F.R.S.—Received February 9, 1929.)

1. *Introduction.*

It is well known that the pressure of hydrogen in a perfectly sealed vessel can be permanently decreased under the action of electric discharges; this is most marked when the vessel is in liquid air, but we shall here be concerned with its occurence at ordinary temperatures. Since considerable dissociation of hydrogen accompanies any discharge, this loss of pressure is intelligible by analogy with Langmuir's experiments on hot tungsten filaments. In these he shows that hydrogen atoms dissociated at the high temperature cease to contribute to gas pressure if they reach the walls of the vessel, since they are strongly adsorbed on glass, whose adsorption of ordinary diatomic hydrogen is negligible. Langmuir* states that data are of the order of magnitude for the adsorbed layer to be of monomolecular thickness.

The concept of a monomolecular adsorbed layer has been much used since, sometimes with the further assumption that it constitutes a closely packed sheet of atoms, but for the permanent gases the evidence for its existence is not conclusive. It is opposed to Freundlich's view of adsorption, and Evans and George† and others have given direct evidence of multimolecular layers of several gases on glass.

For decision on this matter it is necessary to investigate the progressive decrease in the rate at which hydrogen disappears from a discharge, which we shall refer to as fatigue. We must have reason to believe that the glass is initially in the optimum state for adsorbing, and that the fatigue is due to the exhausting of that state and not to lack of gas or to any reaction traceable to other surfaces such as hot metals.

Accordingly in the present work the hydrogen is dissociated by electrodeless discharge instead of by hot wires, and the fatigue is followed by means of a continuous reading micromanometer, under differing conditions of the surface but the same conditions of gas and of discharge. From the resulting graphs we are able to place some confidence in the estimation of the maximum covering which the surface can acquire. This will be referred to as a saturation layer, without prejudice to the possibility of there remaining still vacant places on which atoms could have been crowded if in contact with each other. Using the term in this sense, it is found that the glass is saturated when the layer is monomolecular but not closely packed. The heat of adsorption is calculated by means of a theorem due to Frenkel.

---

* 'J. Am. Chem. Soc.,' vol. 38, p. 2270 (1916).

† 'Roy. Soc. Proc.,' A, vol. 103, p. 190 (1923).

2. *Experimental.*

Most experiments on the disappearance of gas from discharge tubes are complicated by loss and gain at metal surfaces. That this may be considerable, even in the optimum case of hydrogen and aluminium, was shown in a previous paper.* For the present problem the action of hydrogen on glass alone had to be isolated by eliminating metal electrodes and also the usual external electrodes of the "ozoniser" type, which may be open to the objection of allowing slight electrolytic liberation of gases from the glass.† Accordingly we excite and dissociate the hydrogen by inducing from outside the ring discharge recently investigated by Sir J. J. Thomson.‡ Mierdel§ has recently studied the loss of gas in this type of discharge, without, however, dealing with the questions of the present paper.

A cylindrical glass bulb of about 150 c.c. capacity was arranged so that it could be surrounded alternately by (*a*) an oven consisting of a mica-covered brass tube wound with a heating coil and lagged with asbestos, and (*b*) a solenoid of seven turns of guttapercha-covered wire of negligible resistance, coupled through an oil condenser of 0·008 microfarad to a spark gap excited by a 16-inch coil, and thus forming part of an oscillating circuit.

The bulb could be evacuated to the cathode ray stage indicated by an attached discharge tube, and baked during evacuation up to 300° C. Pure hydrogen could then be admitted through a hot palladium tube and the bulb finally shut off from pumps and left in connection only with a micromanometer. Experiments then consisted in taking micromanometer readings at 15-second intervals, before, during, and after excitation of the hydrogen by the high frequency currents induced from the surrounding solenoid.

---

* 'Roy. Soc. Proc.,' A, vol. 118, p. 706 (1928).

† Taylor, 'Nature,' vol. 122, p. 347 (1928).

‡ 'Proc. Phys. Soc.,' vol. 40, p. 79 (1928).

§ 'Ann. Physik,' vol. 85, p. 612 (1928).

3. *Temperature Limits.*

The temperature at which the glass bulbs were baked out was deliberately kept below 300° C. for the following reason. The work of Sherwood[*] and others has made it appear probable that when glass is gassed out at increasing temperatures, most of the surface layers (mainly H_2O and CO_2) are removed at little over 200° C. and a minimum in the yield of gas reached soon after. At higher temperatures of, say, 350–500° the outgassing consists more of a diffusion from the interior, and ultimately marks the beginning of a change in constitution of the glass. In the present experiments it is not desirable to complicate adsorption with diffusion and absorption; as far as possible the interior of solids is left undisturbed and changes confined to the removal and replacement of superficial layers.

Mierdel showed that the cooling of the electrodeless tube by liquid air increased the loss of hydrogen; this was also avoided and the present experiments conducted at approximately 20° C. in order to isolate the "activated" hydrogen shown by Langmuir to be monatomic. It is known from the work of Wendt and Landauer,[†] Elliott,[‡] and others, that another "activated" hydrogen, probably H_3, is formed in discharges, and does not adsorb on glass but condenses at liquid air temperatures. This probably masks the true adsorption in the experiments of Mierdel.

4. *Pressure Measurement.*

Langmuir showed that the fatigue characterising the rate of loss of hydrogen was not due to any cessation of the action of his tungsten, and some observations on the existence of this fatigue in the presence of metals were also made by Campbell.[§] But to enable the fatigue to supply evidence as to the saturation of an adsorbing surface, a gauge was required which could follow continuously changes of between 10^{-1} and 10^{-3} mm. pressure. The McLeod gauge usually needs a minute or two between each reading and further involves the movement of a large mass of mercury over large surfaces; for the present work it was desirable to avoid having to assume that isolated readings represented true initial and final conditions. The quartz fibre and other oscillatory gauges are even less suited to continuous reading. Ionisation gauges are under suspicion in any study which could be vitiated by gas reactions at incandescent surfaces. In the end the simple optical lever method of magnifying small changes in the level of a mercury U-tube was chosen. Shrader and Ryder* and Carver† have described gauges depending on this principle. We find a suspension overcomes some of the difficulties which may be traced to pivoted supports in their types of gauge.

---

[*] 'J. Am. Chem. Soc.,' vol. 40, p. 1645 (1918).

[†] 'J. Am. Chem. Soc.,' vol. 42, p. 930 (1920).

[‡] 'Trans. Faraday Soc.,' vol. 23, p. 60 (1927).

[§] 'Phil. Mag.,' vol. 48, p. 569 (1924).

The micromanometer designed in conjunction with Mr. G. O. Harrison, Curator of the Physics Workshop, and constructed by him in several forms, is shown in fig. 1 as finally adopted. A glass float rests on the mercury surface, hung by platinum strips which are wound round a glass rod of about 1 mm. diameter, which carries a mirror for lamp and scale observation. Small

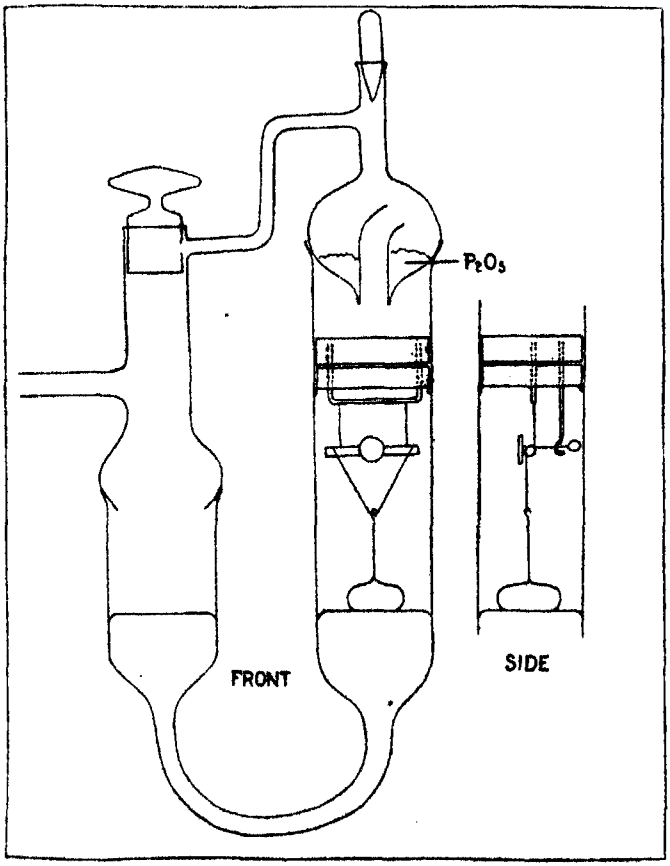

Fig. 1.—Micromanometer.

---

* 'Phys. Rev.,' vol. 13, p. 321 (1919).

† 'J. Am. Chem. Soc.,' vol. 45, p. 59 (1923).

changes of pressure in the opposite limb cause the suspension of the float to wrap or unwrap round the glass rod. Rotation free from lift is secured for the rod by a glass counterweight. The rod is suspended from a brass ring by two platinum wires rolled flat. The ring rests on projections in the glass walls. The whole is readily removable for cleaning, and when placed on a slate slab cemented to a wall, is remarkably constant in zero, dead beat, and free from external disturbance. Calibration showed that with scale at 1 metre, one division reading corresponded to 9×10^{-4} mm. change of pressure. Hence a range of about 0·5 mm. with a detectable sensitivity of 10^{-4} mm. was available. Since the movement of the spot of light can be followed without the intermission or adjustment required in other gauges, it should prove useful for fine analysis of reaction velocity in gaseous systems. If adapted for photographic recording, its speed need only be limited by the inertia of the mercury.

5. *Fatigue Diagrams.*

The graph relating pressure of hydrogen in the closed system to time (fig. 2) shows a typical series of measurements of the disappearance of hydrogen, the arrow indicating the instant of switching on the excitation current. In order not to confuse the several lines on the single graph the actual points are only inserted in one curve to indicate the order of accuracy of the reading. Notes as to conditions of the separate experiments are as follows :—

Curves I and II.—Indefinite liberation of gas when tube unbaked, probably the emission of water vapour and carbon dioxide from the glass walls, and corresponding to common experience with all new vacuum apparatus.

Curve III.—Loss of hydrogen in discharge after thorough baking of tube.

Curves IV and V.—Repetitions of III after re-baking, re-evacuating, and re-admitting hydrogen each time to same initial pressure.

Hence we find the fatigue mentioned by Langmuir and Campbell is a two-fold phenomenon ; estimation of density in the gas layer adsorbed on to the walls from the discharge is indefinite unless account is taken of both kinds of fatigue. We have (*a*) a saturation—in the sense defined above—observable in any one curve and almost completed in about 4 minutes, and (*b*) a decrease in the depth which this saturation curve can reach on second, third, etc., repetitions of the experiment after re-baking, although care is taken that gas and discharge conditions are the same at the beginning of each experiment. This second kind of fatigue, or dependence on past history of surface, is clearly connected with a further observation, that when the system is kept closed during a rebaking, the recovery of initial pressure is only partial, a fact already noted by Langmuir with hot filaments.

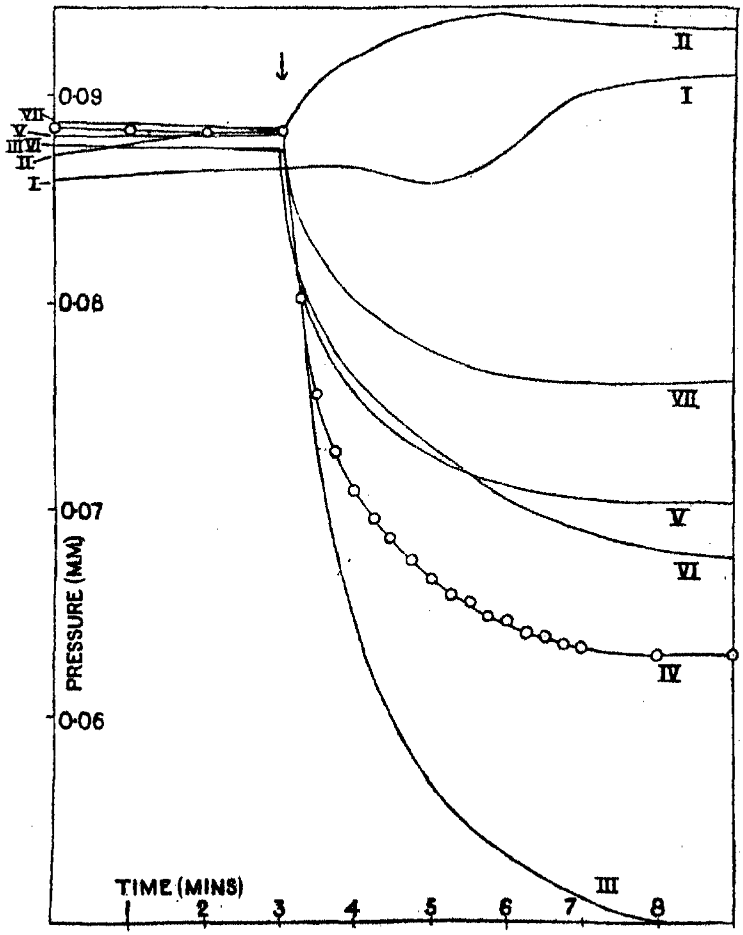

FIG. 2.—Fatigue diagrams.

If, after a series of the above type, air is admitted at atmospheric pressure for a few days and the experiments repeated, a partial recovery of adsorptive capacity is found, followed by a second fatigue sequence. In this way the above series is supplemented by curves VI and VII.

It being apparently impossible to recover completely the initial adsorbing power of a tube, experiments were repeated with a second apparatus, neither specimen of glass being allowed to be "fatigued" by any adsorption between its original emergence from the blow-pipe and its participation in its first curve. Again, the deepest curve was the first after baking, and inaugurated a similar sequence, but with the second tube the whole set of phenomena were on a smaller scale, the initial curve not being as deep as the initial curve of the first tube. Both tubes were of soda glass of approximately the same hardness and melting point; the second appeared noticeably greener than the first. Through the kindness of Dr. H. B. Keene and Mr. F. T. Richards I am informed that the two glasses are spectroscopically very similar, differences in intensities of certain lines being not greater than differences in successive spectrograms of the same glass.

6. *Density of Adsorbed Layer.*

The sequence of fatigue diagrams for identical gas and discharge conditions leaves no doubt of the existence of saturation in the sense in which we have used the term. The capacity of the surface is never greater than when newly made and first gassed out before any adsorption has taken place. Since the temperature range chosen eliminates the complication of condensible H_3, we assume, on Langmuir's theory, that if we measured the total pressure loss on the deepest curve, twice the number of H_2 molecules disappearing would represent the maximum number of H_1 atoms adhering to the glass walls. In some of the experiments the induced current was shut off before complete saturation could be guaranteed, in others it was maintained until the apparatus began to warm up sufficiently to complicate pressure measurement at strictly constant volume. For calculation of saturation where there was any chance of recognisable difference between an actual curve and extrapolation thereof to parallelism with the axis, both are separately made use of and the result taken from their mean.

In this way from initial and final pressures on the deepest curve for each tube, and from a careful measurement of the volume of gas between the cut-off tap and the mercury of the micromanometer, we calculate by means of the known number of molecules per unit volume at N.T.P. the maximum number of atoms adsorbed, (i). The area on which adsorption takes place, (ii), is then measured from the region of the discharge tube covered by the glow when the current is on. Sir J. J. Thomson has shown in his studies of this type of discharge* how very localised are its effects, and that the region of excitation is confined to the length of the brightly visible ring. Now it is well known that in estimating the area of a solid on which gas adsorption is taking place, this mere geometrical measurement is apt to be an underestimate, especially in crystalline metals.* Accordingly the density of adsorbed hydrogen layer obtained by dividing (i) by (ii) is strictly an upper limit. But fused glass probably presents the nearest approach to a smooth amorphous surface that is known, and this reservation is of little importance compared with the corresponding uncertainty in the "true" area of a metal surface.

---

* 'Proc. Phys. Soc.,' vol. 40, p. 86 (1928).

We find that the two tubes are saturated with the following density of atomic layer.

—	Tube 1.	Tube 2.
Volume of region of loss of pressure (in cm.^{3})	198	164
Area for adsorption (in cm.^{2})	85	52
Initial pressure (in mm. Hg)	0·087	0·090
Final pressure (in mm. Hg)	0·0485	0·075
Mean surface density of adsorbed H_1 (atoms per cm.^{2})	$5 \cdot 9 \times 10^{15}$	$3 \cdot 2 \times 10^{15}$
Mean atomic spacing in layer (in cm.)	$1 \cdot 3 \times 10^{-8}$	$1 \cdot 8 \times 10^{-8}$

The last figures give the mean distance between centres of adsorbed atoms, thus shown to constitute a monomolecular layer. The various estimates of the "diameter" of hydrogen—*e.g.*, from viscosity—all concern the molecule, and for the atomic diameter we can only use Bohr's normal orbit

$$d = 2h^2/4\pi^2me^2 = 1 \cdot 06 \times 10^{-8} \text{ cm.}$$

This value predicts the correct ionisation potential of the hydrogen atom and is reliable as a "structural diameter," which may be slightly smaller than a "collision diameter."

By comparing d with the above mean separations we see that not even on the glass with the greater capacity for adsorption is the monomolecular layer closely packed, although this experiment probably offers a stricter guarantee of what we have termed saturation than is otherwise obtainable. Taking the maximum possible density which the layer could attain if Bohr orbits were in contact, namely, $8 \cdot 9 \times 10^{15}$ per square centimetre, we find the ratio of actual to maximum possible packing of the atoms is 0·66 and 0·36 for the two tubes. Langmuir (*loc. cit.*) has made similar calculations, but not with hydrogen, for gases on glass, and his corresponding ratios are :—

CO.	A.	O_2.	CH_4.	N_2.
0·13 0·32	0·20	0·14	0·04 0·36	0·26

---

* Bowden and Rideal, 'Roy. Soc. Proc.,' A, vol. 120, p. 59 (1928); Constable, 'Roy. Soc. Proc.,' A, vol. 119, p. 197 (1928).

7. *Structure in the Adsorbed Layer.*

The state of aggregation of the layer adsorbed at a gas-solid interface is sometimes considered to approximate to that of a solid, and sometimes to that of a gas. In the former case it should possess bonds connecting together the gas atoms which would then constitute the " packed sheet " sometimes referred to in the literature. In the latter case it should possess bonds only between gas atoms and solid. The present experiments are only consistent with the latter view, as saturation is reached without close contact between the gas atoms. The loose packing is then due to one of two causes : (*a*) we may postulate a freedom of movement of the gas atoms parallel to the surface, in which case the adsorbed layer is held by the average field of the whole surface rather than by individual bonds between each gas atom and each atom in the solid lattice ; (*b*) alternatively we may regard the gas atoms as bound, each to one atom of the solid. The average separation of the latter is not calculable in a glass, but is not likely to be less than the mean separation between silicon and oxygen atoms in a silica lattice. This is 1·6 A.U. and 2·2 A.U.* according as we consider atoms in the same or adjacent molecules. The mean of these measurements is greater than the separations in either of our adsorbed layers. Hence adoption of this view of the adsorption bond would imply that some proportion of the solid atoms do not possess attached gas atoms even at saturation. From our experiments this proportion is seen to vary in different glass specimens. The well known but unexplained irregularity in the distribution of more and less active areas on catalysts indicates that such a variation is to be expected.

8. *Heat of Adsorption.*

Frenkel's theory of adsorption† provides a relation between density of layer, temperature, gas pressure, and the strength of the bond between gas and solid, *i.e.*, the heat of adsorption. Frenkel himself applied his equation to Langmuir's experiments on the adhesion of oxygen to tungsten and obtained a rather high heat of adsorption ; but he admits this is a case in which diffusion of gas into the solid is a probable complication not reckoned with. The other recent case to which Frenkel's theory has been applied is Cockcroft's experiments‡ on the condensation of metallic vapours on cold solids. The case of the present paper seems particularly suited to treatment by this equation because of the freedom from complication by solution, absorption, diffusion, or condensation at the temperature of the experiment, and because of the possibility of estimating a saturation density of the monomolecular layer.

---

* McKeehan, ' Phys. Rev.,' vol. 21, p. 507 (1923).

† ' Z. Physik,' vol. 26, p. 117 (1924).

‡ ' Roy. Soc. Proc.,' A, vol. 119, p. 293 (1928).

In Frenkel's formula

$$\frac{S}{n} = \sigma\left(1 + \frac{\sqrt{2\pi m\kappa T}}{p\sigma\tau}\right)e^{-\frac{u}{\kappa T}}.$$

S/n = ratio of surface area to total number of atoms adsorbed.
= $1/5{\cdot}9 \times 10^{15}$ (tube 1).
= $1/3{\cdot}2 \times 10^{15}$ (tube 2).
p = gas pressure in dynes/cm.^{2} at saturation.
= $0{\cdot}0485$ mm. = 65 dynes/cm.^{2} (tube 1).
= $0{\cdot}075$ mm. = 100 dynes/cm.^{2} (tube 2).
σ = cross section of adsorbed atom, $0{\cdot}88 \times 10^{-16}$ cm.^{2}.
m = mass of adsorbed atom, $1{\cdot}64 \times 10^{-24}$ gram.
κ = Boltzmann's constant, $1{\cdot}3 \times 10^{-16}$.
T = absolute temperature, 293°.
u = heat of adsorption.
τ = period of vibration of surface atoms. Frenkel considers that this does not vary greatly from the value 10^{-13} in different substances.

Calculating the heat of adsorption and reducing from ergs per atom to calories per gram-molecule, we find—

Tube 1. Heat of adsorption = $1{\cdot}115 \times 10^4$ calories per gram-molecule.
Tube 2. Heat of adsorption = $1{\cdot}06 \times 10^4$ calories per gram-molecule.

No other determination of heat of adsorption of H_1 on glass can be found for comparison, but the following estimations have been published for H_2 on metal catalysts, and are of interest as being of the same order of magnitude, since the glass is undoubtedly a catalyst in this case :—

H_2 on Pd	18000 cal./gm. mol.
,, Pt	13760 ,,
,, Ni	11000–13000,,
,, Cu	9500 ,,

9. *Conclusion.*

(i) Sequences of curves are constructed showing the decrease of pressure in hydrogen excited by the electrodeless discharge. Fatigue is separable into two effects: (*a*) the curvature of each pressure-time graph; (*b*) a decrease in depth of successive curves with the same electrical and gas conditions.

(ii) The average separation of atomic centres in the adsorbed layer on two specimens at saturation is $1 \cdot 3 \times 10^{-8}$ cm. and $1 \cdot 8 \times 10^{-8}$ cm. Closest packing of Bohr orbits would give $1 \cdot 06 \times 10^{-8}$ cm., while attachment to the solid atom by atom, assuming all spaces occupied, would give a probable minimum value of $1 \cdot 9 \times 10^{-8}$ cm.

(iii) The layer never reaches greater than monomolecular thickness.

(iv) The heat of adsorption of H_1 on glass is $1 \cdot 115 \times 10^4$ cal./gm. mol. and $1 \cdot 06 \times 10^4$ cal./gm. mol. for the two specimens.

It is a pleasant duty to thank Prof. S. W. J. Smith, F.R.S., for making this work possible, and for the kindness of discussion and criticism, and also Mr. G. O. Harrison, without whose skill in design and construction the measuring apparatus would not have been evolved.

On the Design and Use of a Double Camera for Photographing Artificial Disintegrations.

By P. M. S. Blackett, Cavendish Laboratory, Cambridge.

(Communicated by Sir Ernest Rutherford, P.R.S.—Received February 21, 1929.)

[Plates 20, 21.]

1. *Discussion of Various Types of Camera.*

In a recent paper* a small automatic Wilson Chamber has been described in detail. This was used to photograph the artificial disintegration of nitrogen.† It was shown from a study of the conditions in the chamber itself, that it is not possible to increase the number of expansions above about four a minute without detriment to the tracks. An increase in the speed of photographing tracks is therefore to be sought in the increase in the number of tracks in a photograph. It is shown in the following investigation that this number is limited by considerations concerning the size of the chamber, the width of the

* Blackett, 'J. Sci. Instr.,' vol. 4, p. 433 (1927).

† Blackett, 'Roy. Soc. Proc.,' A, vol. 107, p. 349 (1925).

tracks, the design of the camera and the demand that each track shall have a reasonable chance of not being obscured by its neighbours.

The importance of obtaining the best possible conditions needs no emphasis when it is remembered that it is generally necessary to photograph at least half-a-million tracks to obtain a few disintegration collisions with any one element.

A camera of the type used by Shimizu,* and used also by the writer,† is by no means the most suitable. It consists effectively of two separate cameras placed at right angles, fig. 1A. As the two focal planes *aa*, *bb* are at right angles to each other and at 45° to the plane of the chamber, there is only a very limited region of the object space, near the line of intersection of the two focal planes, which is in sharp focus. The beam of alpha rays, which must be directed along this line, must therefore be of small angle and so can only contain a few tracks.

An ordinary stereoscopic camera is also unsuitable owing to the small angle between the two directions of photographing. For the accuracy of the determination of the angles in space, from the two photographs, increases as the angle between the axes of the two cameras increases. If the highest accuracy is required the two photographs must be taken from directions nearly at right angles. Now the trigonometrical computations required to give the actual angles in the object space are laborious. They become very laborious unless the photographic plates are either parallel or at right angles to each other. There are therefore two possible arrangements. In the first, fig. 1B, the two plates P, P′, are both in the same plane, which is both parallel to the plane of the chamber, and to the plane containing the principal planes of both lenses. There are two disadvantages to this arrangement. To get a large angle of intersection of the directions, of say about 60°, it is necessary to photograph at an angle of 30° off the axes of the lenses. With ordinary photographic

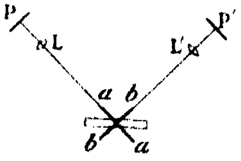

FIG. 1A.

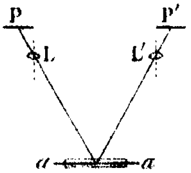

FIG. 1B.

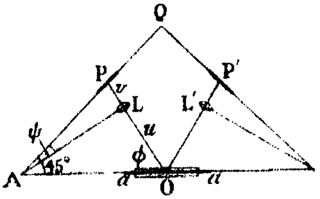

FIG. 1C.

---

* 'Roy. Soc. Proc.,' A, vol. 99, p. 425 (1921).

† 'Roy. Soc. Proc.,' A, vol. 102, p. 294 (1922).

lenses of fairly large aperture the definition so far off the axis is insufficient for the highest resolution. The second disadvantage concerns the accuracy of the trigonometrical reduction. The theory of the calculation* shows that the errors in the calculated angles increase with the distance of a track image from the origin, that is with the distance from the track image to the foot of the perpendicular from the lens centre on to the plate. In this arrangement this distance is large and the accuracy consequently small.

The second possible arrangement is with the plates at right angles, as in fig. 1c, but with the lenses tilted so that the plane of the chamber is conjugate with both plates. This is attained by arranging that the principal plane of each lens passes through the line of intersection of the plane of the chamber and the plane of the photographic plate.† In this method the lenses are used axially and yet sharp photographs are obtained of the whole of the chamber on two plates mutually at right angles. I am indebted to Mr. T. Smith, of the National Physical Laboratory, for the advice to adopt this method. Since in this arrangement the direction of the lens axis passes through the centre of the chamber and makes only a small angle (8½° in the camera described below) with the normal to the plate, the *average* distance of the track images from the origins is much smaller than in the arrangement shown in fig. 1B, and only a little greater than in the arrangement in fig. 1A, which from this point of view is the best.

It may be mentioned that the theory of the trigonometrical calculations given by the writer‡ for the type of camera shown in fig. 1A, is applicable without modification to this new type of tilted lens camera.

The camera was designed for use with a standard pattern Wilson chamber supplied by the Cambridge Scientific Instrument Company (Plate 20). This has a diameter of about 17 cm., but the actual effective diameter of the space in which good tracks can be photographed is about 12·5 cm. The effective part of the chamber then appears, if viewed from the direction of the cameras, as roughly elliptical in shape, of length 12·5 cm., and breadth about 9 cm. In order to be able to use standard cinematograph films and cameras, the size of the photograph is fixed at that of the standard gate, which measures 2·5 × 1·8 cm. Thus the image of the effective part of the chamber, of length 12·5 cm., will just cover the photograph if the camera has a magnification of 1/5. This magnification, given so immediately by the demands of convenience, was adopted for the camera. The general question of the choice of the best magnification will be discussed in the next section.

---

* Blackett, 'Roy. Soc. Proc.,' A, vol. 103, p. 62 (1923).

† See for instance 'Dict. Appl. Phys.,' vol. 4, p. 400.

‡ 'Roy. Soc. Proc.,' A, vol. 103, p. 71 (1923).

A photograph of a beam of alpha rays is reproduced on Plate 21, No. 4. This, and some of the others reproduced, were taken by Mr. D. S. Lees.

Having settled the magnification it remains to make the focal length of the lenses as large as possible, in order that the angular field of the lenses should be small, which is the requisite condition for accurate calculations.* The lenses used are a pair of Taylor Hobson Cooke Anastigmats, of 9·55 cm. focus and $f/4 \cdot 5$ aperture. Longer focal length lenses would have been used but for the expense and bulk of the resulting camera. The lenses were usually used at $f/11$ when photographing alpha rays† (see section 2). It is useful, however, to fit these large aperture lenses so as to have the extra light power available if occasion arises—for instance, when good definition or a large depth of focus is not required.

2. *The Choice of the Best Magnification.*

Apart from the practical limitation due to the size of the film and the size of the standard chamber, the choice of magnification must depend on the demand for the greatest light power consistent with a certain depth of focus.

A beam of alpha rays has always a considerable depth. The number of tracks within a given horizontal angle in the chamber is proportional to the strength of the source and to the angular depth of the beam—the stronger the source the shallower the beam for a given number of tracks. But strong sources are difficult to obtain, and, when used, produce a heavy background of cloud due to the beta and gamma rays. The actual beam used has a maximum depth of 2 cm. at a distance of 14 cm. from the source, so that some of the tracks near their ends will be as much as 1 cm. out of focus. Since near the source the tracks are all in focus, we will take as an average track one that is 0·5 cm. out of focus. It is necessary to choose the optical system so that the definition of such a track is sensibly perfect.

---

* *Loc. cit.*

† The definition of the lenses was tested by visual observation under a high magnification of the image of a slit. It was found that for apertures of $f/11$ and below the resolving power on the axis was certainly up to the theoretical, and no decrease was noticed up to angles of 10° off the axis. (The extreme rays from the object utilised in the camera only make angles of 6° with the axis.) At the full aperture of $f/4 \cdot 5$ the effect of the aberrations was to strengthen the intensity of the lateral images, rather than to broaden the central one.

If u be the object and v the image distance, and f the focal length, a change of δu in u will result in a change δv in v given by

$$\delta v = m^2 \delta u \tag{1}$$

where $m = v/u =$ the magnification of the camera.

The Rayleigh* condition for sensibly perfect definition demands that the difference of path between the axial and extreme rays should be not greater than $\lambda/4$. Now a change of δv introduces a change of path difference of

$$a^2 \delta v/8v^2$$

where a is the diameter of the lens, so that Rayleigh's condition gives

$$\delta v = 2v^2\lambda/a^2. \tag{2}$$

Using (1) and the relation $v = f(1+m)$, we get

$$\delta u = 2\lambda(1+m)^2 f^2/m^2a^2. \tag{3}$$

If we introduce the relative aperture A given by

$$\mathrm{A} = a/f,$$

we find from (3) for the critical aperture A_c, that is the largest aperture consistent with the required depth of focus,

$$\mathrm{A}_c = \frac{1+m}{m}\sqrt{\frac{2\lambda}{\delta u}}. \tag{4}$$

Taking $m = 1/5$, $\delta u = 0 \cdot 5$ cm., $\lambda = 4 \cdot 4 \times 10^{-5}$ cm., we find $\mathrm{A}_c = 1/12 \cdot 6$, so that the lens must not be worked at a larger aperture than $f/12 \cdot 6$.

Since whatever magnification we choose it is always possible to choose the aperture, as shown above, so as to give any required depth of focus, it is necessary to choose that magnification which gives the greatest intensity of image. Suppose that a source of light emits energy σ per unit area and unit solid angle. The photographic intensity of the image, that is the energy per unit area, is given by

$$\mathrm{I} = \sigma\pi\mathrm{A}^2/4(1+m)^2,$$

provided that the geometrical image of the source is large compared with the diffraction disc of the lens. Substituting the value of A_c from (4), we get for the intensity of the image, when the aperture has its critical value,

$$\mathrm{I} = \sigma\pi\lambda/2m^2\delta u. \tag{5}$$

---

* Rayleigh, 'Coll. Papers,' vol. 1, p. 415, also 'Dict. Appl. Phys.,' vol. 4, p. 221.

This shows that under these conditions the intensity of the image varies inversely as the depth of focus multiplied by the square of the magnification. It is therefore desirable to make the magnification as small as possible. A limit, however, is set to the useful reduction in m by the limited resolving power of the photographic emulsion. The finest lines reproducible on Kodak normal ciné film* are of the order of 20 μ. The lowest useful value of m is that which gives the image of a track a breadth of about this amount. Now the breadth of a track image can be taken as equal to the sum of the width ϵ of the diffraction pattern due to a line source, and the width D of the geometrical image of the track. For the former we have

$$\epsilon = 2v\lambda/a = 2\lambda(1 + m)/\mathrm{A}, \tag{6}$$

and for the latter $m\mathrm{D}_0$, where D_0 is the width of the track itself.† The total breadth Δ is therefore

$$\Delta = m\mathrm{D}_0 + 2\lambda(1 + m)/\mathrm{A}, \tag{7}$$

and this becomes, on substituting for the critical aperture A_c from (4),

$$\Delta = m(\mathrm{D}_0 + \sqrt{2\lambda\delta u}). \tag{8}$$

Taking $\mathrm{D}_0 = 0 \cdot 09$ mm. (see section 3), $\lambda = 4 \cdot 4 \times 10^{-5}$ cm., $\delta u = 0 \cdot 5$ cm. we find that (8) gives $\Delta = 156 \times m$ microns. A magnification of $1/7 \cdot 8$ would therefore give an image of the minimum reproducible breadth of 20 μ. If the camera had been given this magnification instead of 1/5, the advantage would have been, either, an increased intensity for a given depth of focus, or an increased depth of focus for a given intensity. If this had been done a

---

[*] The resolving power of various emulsions are given by Sandwik ('J. Opt. Soc. Am.,' vol. 14, p. 169 (1927)). See also 'Photography as a Scientific Implement,' 1924. The resolving power, that is the number of lines to the millimetre resolvable, of Kodak normal film is probably about 30, though a somewhat higher value might be obtained with special care in the control of exposure, development and quality of light. (See Huse, 'J. Opt. Soc. Am.,' vol. 1, p. 119 (1917).) The breadth of a single line can be taken as roughly half the spacing, that is about 15 μ. The writer has, however, found that in practice the narrowest line reproducible *with the desired blackness* is somewhat greater than this, in fact about 20 μ. Many workers with a Wilson chamber have used process plates, and with these a considerably higher resolution can be obtained. No suitable process ciné film appears to be made. Kodak positive film is much too slow. The relation of size of the grains of Kodak normal film to the track breadth can be seen in Plate 21, No. 5.

[†] The ratio of the diffraction breadth to the geometrical breadth, for the case of critical aperture, is $\sqrt{2\lambda/\delta u}/\mathrm{D}_0$. This is independent of m and has the value of $0 \cdot 74$ for the case considered above. The assumption made above that this ratio is small is therefore not correct, but since the ratio does not depend on m, equation (5) will still give the right variation with m though not with δu.

narrower and cheaper film might have been used. Or alternatively, the pressure in the chamber might have been reduced so as to increase the length of the tracks and yet give an image still utilising the full width of the normal film. The advantage to be gained by the latter procedure will be discussed in detail in section 6.

It is instructive to discuss the behaviour of the image breadth when the aperture is varied from its critical value. For *any* aperture the image breadth of a track *in focus* is given by (7), and is shown in curve 1, fig. 2, for the values of the constants.

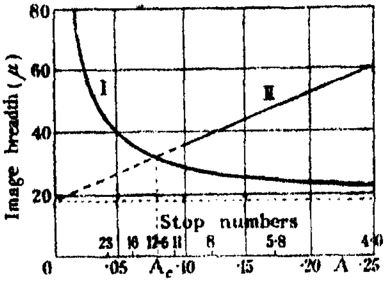

FIG. 2.

The curve gives the image breadth in microns plotted against the aperture A. The stop numbers $s = 1/A$ are also given, as they are of familiar import. For apertures smaller than the critical aperture, the tracks in the beam, supposing them to be all within the assigned distance δu of the focal plane, are all in sensibly perfect focus. Thus for $A < A_c$, curve 1 gives the breadth of *all* the tracks.

When A is somewhat larger than A_c the breadth of the image of an average track, that is one out of focus by an amount δu, cannot be calculated simply. An investigation such as Rayleigh's (*loc. cit.*) applied to the special problem would be required. But for apertures considerably larger than the critical the image breadth of an average track can be calculated by means of geometrical optics. A point source placed a distance δu from the true focal plane will give, from purely geometrical considerations,* an image of diameter ε_1, given by

$$\varepsilon_1 = m^2 A\, \delta u/(m + 1).$$

The total breadth can therefore be taken as

$$\Delta = mD_0 + m^2 A\, \delta u/(m + 1). \tag{9}$$

This is valid only for A considerably larger than A_c.

The values of Δ from (9) are plotted as curve 2, fig. 2. The curve is shown full, over the region for which the expression is approximately valid. Thus for large apertures the breadth of the *average* track increases with the aperture, due to the lack of perfect focus; while for small apertures the breadth of *all* tracks increases as the aperture decreases, due to the increase in the diffraction disc. The two curves cut when $A = A_c$. This follows from the fact that the right-hand sides of (7) and (9) are equal when the aperture has its critical value given by (4). Although the actual breadth of the image in the undetermined region where A is somewhat larger than A_c cannot be determined exactly, and although it is therefore not possible to say exactly for what stop the *minimum* occurs it cannot be far from the value $A_c = 1/12 \cdot 6$. Usually $f/11$ has been used, though on some occasions $f/16$.

---

* It may be noted that the photographic intensity of the image of a *point source out of focus* is independent of the aperture. For the area of the image and the light collected by the lens both vary as A^2. For a *line source out of focus* the photographic intensity increases as A.

3. *The Observed Breadths of the Tracks.*

To design the optical system of the camera one must know roughly the breadth D_0 of the tracks one is photographing. In order to decide on the best number of tracks in the beam, it is necessary to know not only the breadth D_0, but how it varies with the pressure and constitution of the gas; in particular how it varies when the gas is reduced in pressure or is diluted with hydrogen or helium (see section 6).

No measurements of track breadths can have much significance unless carried out with careful attention to photometric technique, owing to the spreading of the photographic images with increasing exposure. Needless to say the expansion ratio, vapour pressure, electric field and timing would also require accurate control. Such systematic measurements are lacking. The track breadth also varies along the range of the alpha ray track, increasing with the ionisation. The photograph of a collision shown in 6, Plate 21, shows how the image breadth varies with the ionisation along the tracks.

Rough measurements made on photographs taken without special precautions with the new camera at $f/11$ give values of about 30 μ for the breadth of the images. Since the diffraction breadth is 12 μ, this gives a real breadth of about $5 \times (30 - 12) = 90\ \mu$, in rough agreement with the value of 0·1 mm. given by Wilson.

It might be expected that the breadth of a track would increase, as the pressure was reduced or as the gas was diluted with hydrogen or helium, proportionately with the reciprocal of the stopping power. This is however far from being true. The range of the delta rays, at least of those that are long enough to emerge from the core of the track, certainly varies inversely as the stopping power, but the breadth of the core itself appears to vary far more slowly as the pressure or composition is changed. For instance track images have been obtained with a mixture of 80 per cent. hydrogen and 20

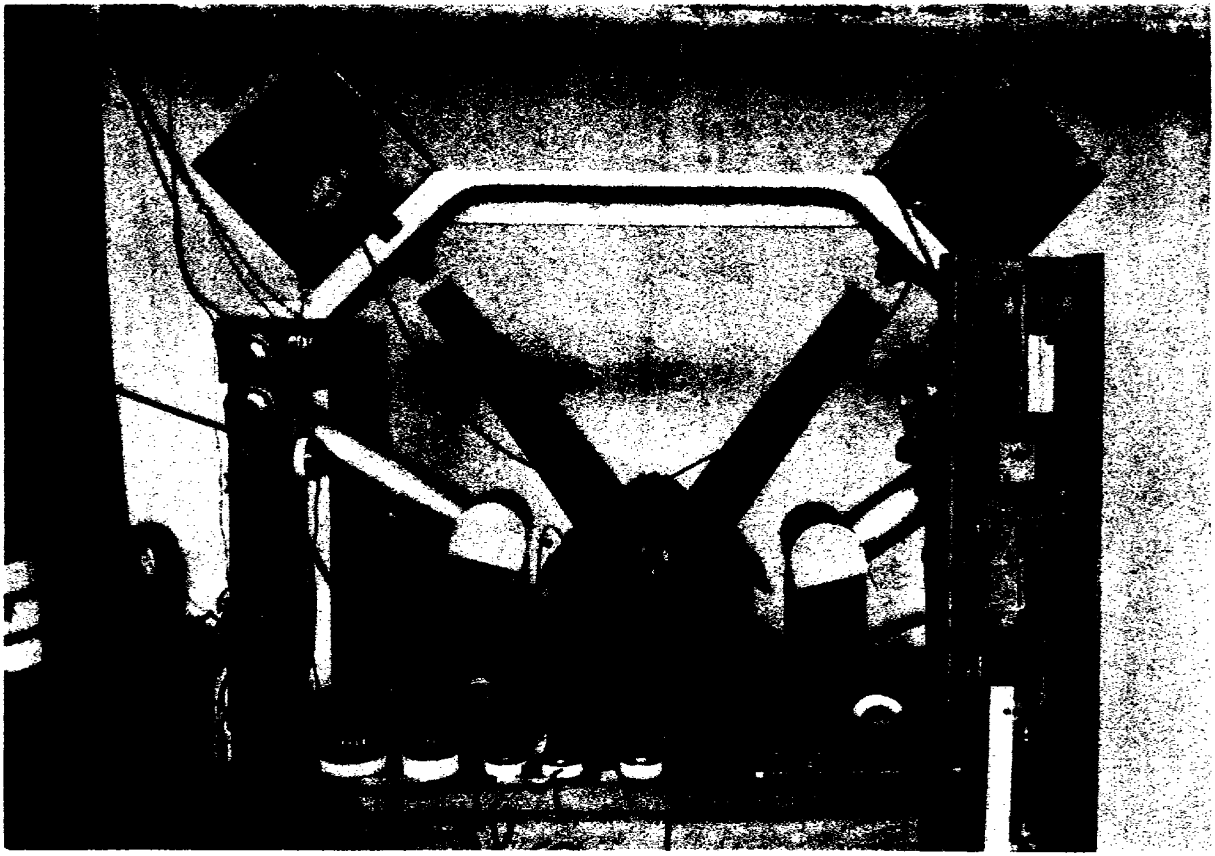

THE CAMERA IN USE WITH A WILSON CHAMBER.

The chamber is enclosed in a wooden box, with tubular light screens, so that the apparatus does not require to be used in a completely darkened room. The two mercury lamps stand to the right and left of the chamber.

(*Facing p.* 620.)

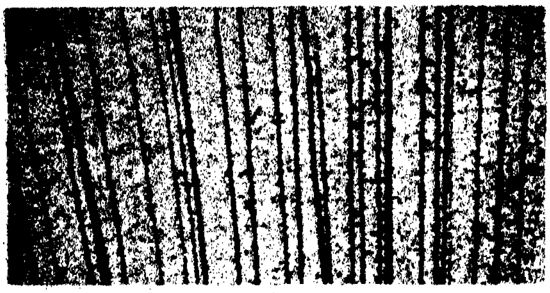

1

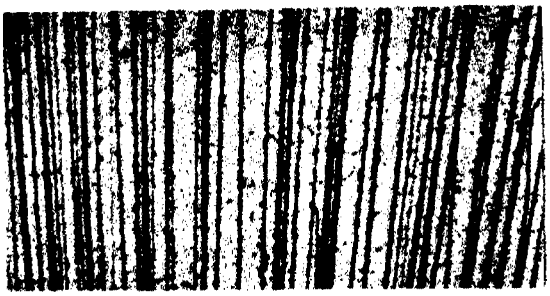

2

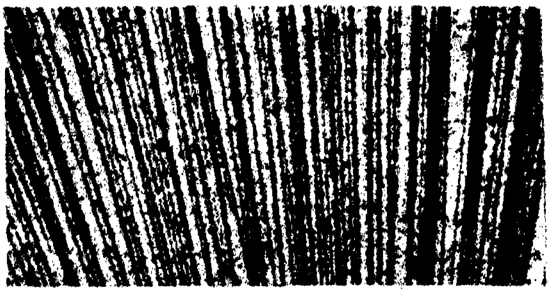

3

4

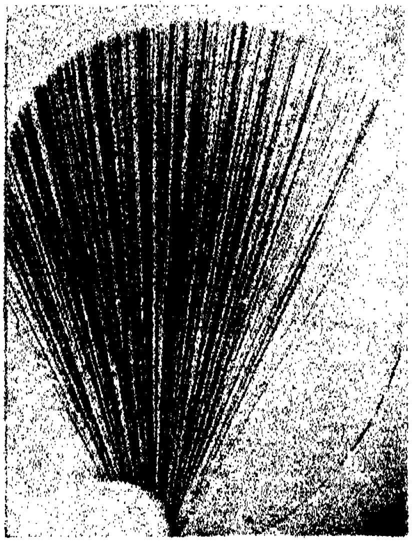

5

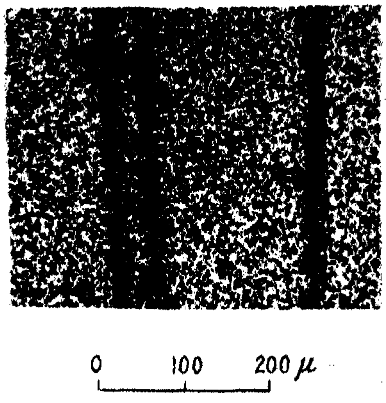

6

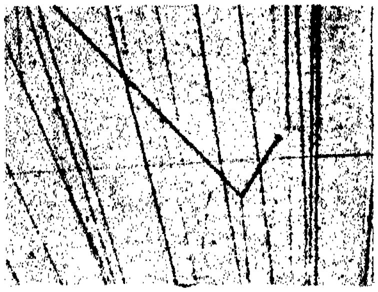

Figs. 1, 2, 3, 6, enlarged 13 times; fig. 4, × 3; fig. 5, × 110.

per cent. oxygen at half an atmosphere total pressure, which had a breadth of 33 μ, whereas the range of the particles in this gas is about five times the range in air at normal pressure. The variation of D_0 with the changes in pressure and composition, which will be considered in section 6, is thus so small that it will be sufficient when discussing the optimum conditions of working, to assume it to be constant and equal to 30 μ.

The finest track images obtained with this camera are about 25 μ broad. Some of these, enlarged 110 times, are shown on Plate 21, photograph No. 5, and some enlarged 13 times in No. 6.

4. *The Theory of the Camera.*

The arrangement of the chamber, lenses and plates is shown diagrammatically in fig. 1c. Let AO represent the plane of the chamber and O its centre. Let AQ be the plane of one of the two photographic plates. Since these are to be at right angles to each other and symmetrical with the chamber, the angle PAO = 45°. Let L be the centre of one of the lenses. Since we wish to use the lens axially OL must be its axis. And since the planes AP and AO are to be conjugate, its principal plane must pass through A.* Hence ALO = 90°. Hence L lies on the semicircle of which AO is the diameter. Join OL to cut AQ at P. Then P is the image on the plate of the point O in the object space. Let OL = u, and PL = v. Then the magnification m of the camera is given by

$$m = v/u.$$

The position of L on the circle ALO can be found when m is given. If we denote $\angle$ POA by ϕ, and $\angle$ PAL by ψ, we have

$$\psi = \phi - 45^\circ.$$

From the figure we have

$$m = v/u = \tan\psi \tan\phi = \tan(\phi - 45^\circ)\tan\phi,$$

or

$$m = (1 + \tan\phi)\tan\phi/(1 - \tan\phi).$$

Solving for tan ϕ we get

$$\tan\phi = \tfrac{1}{2}\left(1 + m \pm \sqrt{(1 + m)^2 + 4m}\right).$$

Taking the positive sign and putting $m = 1/5$, we get

$$\phi = 53^\circ\,27' \quad \text{and} \quad \psi = 8^\circ\,27'.$$

---

* 'Dict. App. Phys.,' *loc. cit.*

Thus for this magnification, by tilting the lenses through 8° 27′, relative to their plates, we can arrange that the whole plane of the chamber is in focus at once on two plates at right angles to each other.

For $f = 9{\cdot}55$ cm., $m = 1/5$, we find $u = 57{\cdot}3$ cm., $v = 11{\cdot}4$ cm. The distance apart of the two lenses is about 66 cm., and the overall length of the camera about 120 cm. The method of construction of the camera is clear from the photograph, Plate 20. An aluminium casting has two faces at its ends making angles of 45° with the top. To these two faces are attached standard Ensign ciné-cameras.* Each lens is carried on a brass bush, the two faces of which are inclined at an angle of $8\frac{1}{2}°$. The casting was machined true to about 1/4°. Final adjustment to the plate holder was made with an engineer's level. The origin on the plates of each camera, that is the foot of the perpendicular drawn from the lens centre on to the plate, was determined by replacing the film by a mirror and by using the coincidence of a pin point with its reflected image, as a criterion for the line joining lens centre and pin point to be at right angles to the plate (*loc. cit.*, p. 74). The accuracy of adjustment of the inclination of the plates is probably about 1/4° and the accuracy of determination of the origin about $0{\cdot}2$ mm.

5. *The Optimum Number of Tracks.*

In a photograph of an alpha ray beam, containing approximately parallel tracks, some of the tracks will lie so close to others that they cannot be distinguished. If Δ is the breadth of the image of a track, we will say that its *image* is *resolved* if no other track image lies within a distance 2Δ on either side of it. Two tracks just resolved are shown on Plate 21, No. 5. Let us suppose that all the tracks in the beam are parallel and that there are n of them. If l is the width of the image of the beam, the average distance apart of the track images is $d = l/n$. Then taking the distribution of the parallel track images to be a random one, the probability that there is *no other* track image within a distance 2Δ on either side of any given track image is

$$e^{-4\Delta/d}.$$

We will call a *track resolved* if both its images are resolved, that is, if there is no other track image within a distance 2Δ on either side of either image. The probability of this, assuming that the distributions in the two photographs are independent,[*] is

---

* A much better construction would be to attach the film holders directly to the casting, making the system of two lenses and two film holders one rigid metal structure. The method described of using the ready-made wooden cameras with film holders complete is definitely inferior but was adopted in order to save time and expense.

$$e^{-8\Delta/d},$$

and so the number N of resolved tracks is

$$\mathrm{N} = ne^{-8\Delta/d} = ne^{-8\Delta n/l}. \tag{10}$$

The value of n which gives N its maximum value N_m will be called the optimum number of tracks n_0, and is given by

$$n_0 = l/8\Delta. \tag{11}$$

The average distance apart is then

$$d = l/n_0 = 8\Delta,$$

and the number of resolved tracks is

$$\mathrm{N}_m = n_0/e = 0 \cdot 37\ l/8\Delta.$$

This result shows that the number of resolved tracks has its maximum value, when the average distance apart of the tracks is eight times their width ; and that then 37 per cent. of all the tracks are resolved.

Taking $\Delta = 30\ \mu$ and $l = 1 \cdot 8$ cm., we find $n_0 = 75$ and so the number of resolved tracks is about 28.

---

[*] The assumption that the distribution of tracks in the two photos are independent can be given the following justification. Consider n points distributed at random in a rectangle (representing the cross section of the actual alpha ray beam) of length a and height b, so that the superficial density of points is n/ab. Then the fraction of points which are not resolved, that is the fraction of them which have other points within a distance δ of them, is

$$p_1 = 1 - e^{-\pi n \delta^2/ab}.$$

If now the points are projected on to a line making an angle ϕ with a, the linear density of the projected points, assuming $a > b$, is $n/a \cos \phi$, and the fraction of these which are not resolved is

$$p_2 = 1 - e^{-2\delta n/a \cos \phi}.$$

Applying this to an alpha ray beam and its photograph, p_1 is the fraction of *tracks* which are not resolved, and p_2 the fraction of *images* which are not resolved. Then taking as a typical case[†] $n = 100$, $\delta = 1/10$ mm., $a = 5$ cm., $b = 1$ cm. and $\cos \phi = 0 \cdot 7$, we find that

$$p_1 = 1/160 \qquad p_2 = 0 \cdot 44.$$

Thus only a small fraction of the unresolved track images are due to unresolved tracks. This refers to the conditions near the middle of the chamber. Very near the source, where a and b are small, p_1 will be larger relatively to p_2 than farther along the beam. But for the beam as a whole we conclude that the chance that a track is not resolved in a photograph because it is not resolved in space is quite small.

[†] All these distances refer to the object space and not image space.

The optimum number of tracks for a parallel beam 1 cm. wide is 42. The photographs on Plate 21, Nos. 1, 2 and 3, show beams having about 50, 100 and 180 tracks per centimetre. The fraction of the tracks resolved in these three cases is theoretically 0·56, 0·29 and 0·11. The photographs show somewhat higher fractions than these, probably because the desire to choose a photograph, which will reproduce well, leads unwittingly to the choice of a photograph in which the tracks are exceptionally evenly spaced. The centre part of No. 3 certainly represents such an exceptional distribution.

In practice however an alpha ray beam is not parallel but consists of a divergent cone, giving a fan-shaped beam. (Plate 21, No. 4.) At a distance R on the photograph from the image of the source (effectively a point) the width of the beam* can be taken as an arc of length $R\phi$, where ϕ is the angular width of the image of the beam. The number of tracks resolved at a distance R from the source is from (10) putting $l = R\phi$,

$$N = ne^{-8\Delta n/R\phi}.$$

It is convenient to introduce the length

$$R_n = 8\Delta n/\phi, \tag{12}$$

which represents the distance from the source along the image of the beam to that region where the tracks are at their optimum distance apart. Then we have

$$N = ne^{-R_n/R} = \phi\, R_n e^{-R_n/R}/8\Delta$$

so that the number of tracks which are resolved at a distance R from the source increases along the beam from zero at the source to the value n/e when $R = R_n$ and tends to n as $R \to \infty$. Thus close to the source, where the probability that an alpha particle will cause a disintegration is large, the probability that the track will be resolved is small. It is clear that a too large number of tracks in a photo may result in all the disintegration collisions that do occur being marred because they are not resolved.

Let us denote by $f(R)dR$ the chance that there will be a disintegration collision on an image of a track between distances R and $R + dR$ from the image of the source. The total number of resolved collisions is

$$Y = \int_0^R N f(R)\, dR = \frac{\phi}{8\Delta} R_n \int_0^R e^{-R_n/R} f(R)\, dR. \tag{13}$$

---

* In many cases in practice the photograph is cut off at some distance from the source. This case is intermediate between that of a parallel beam and a complete fan, but can be worked out numerically if required.

Supposing that $f(\mathrm{R})$ is known from other experiments (*e.g.*, by the scintillation method) we require to find the value of R_n which makes Y a maximum. Then from (12) the optimum number of tracks is calculated. As an approximate representation of $f(\mathrm{R})$, which, though crude, is adequate for our purpose,[*] we will take

$$f(\mathrm{R}) = \text{const.} = \mathrm{K}, \quad \text{for } 0 < \mathrm{R} < \mathrm{R_L},$$
$$f(\mathrm{R}) = 0, \quad \text{for } \mathrm{R} > \mathrm{R_L};$$

that is that the chance of a disintegration collision is constant along the first part of the image of a track up to a distance $\mathrm{R_L}$ from the image of the source, and then zero for the rest of the range. Then (13) becomes

$$\mathrm{Y} = \frac{\phi \mathrm{R}_n}{8\Delta} \mathrm{K} \int_0^{\mathrm{R_L}} e^{-\mathrm{R}_n/\mathrm{R}}\, d\mathrm{R},$$

which on introducing the new variable

$$x = \mathrm{R}/\mathrm{R}_n$$

gives

$$\mathrm{Y} = \frac{\phi}{8\Delta} \mathrm{K}\mathrm{R_L}^2 \frac{\phi(a)}{a^2}, \tag{14}$$

where

$$\phi(a) = \int_0^a e^{-1/x}\, dx = a e^{-\frac{1}{a}} + \mathrm{E}i\left(-\frac{1}{a}\right),$$

and

$$a = \mathrm{R_L}/\mathrm{R}_n. \tag{14A}$$

The maximum of $\phi(a)/a^2$ occurs for

$$\frac{a}{2} e^{-\frac{1}{a}} + \mathrm{E}i\left(-\frac{1}{a}\right) = 0,$$

which, using the tabulated values[†] of $\mathrm{E}i(x)$ gives $a = 1{\cdot}67$, and so from (14A)

$$\mathrm{R}_n = 0{\cdot}6\mathrm{R_L}.$$

From (12) the optimum number of tracks, which will again be denoted by n_0, is given by

$$n_0 = 0{\cdot}6\mathrm{R_L}\phi/8\Delta. \tag{15}$$ [‡]

The maximum value of $\phi(a)/a^2$ is $0{\cdot}165$, so that the maximum value of Y is

$$\mathrm{Y}_m = 0{\cdot}021\phi\mathrm{K}\mathrm{R_L}^2/\Delta. \tag{16}$$

---

[*] Actually $f(\mathrm{R})$ increases fairly rapidly towards the source (Rutherford and Chadwick, 'Phil. Mag.,' vol. 42, p. 809 (1921), also Gamov, 'Z. Physik,' vol. 52, p. 510 (1928)), but the simple assumption made above is convenient and will serve our purpose sufficiently well.

[†] Jahnke and Emde, 'Funktionentafeln,' p. 19.

[‡] Equation (15) expresses the simple result, for a divergent beam of particles with a constant probability of disintegration up to a distance $\mathrm{R_L}$, that the greatest number of resolved collisions is obtained when the number of particles is chosen so that the average distance apart of the tracks at a distance $\mathrm{R_L}$ from the source is about *thirteen* times this width.

Curve 1, fig. 3, gives $\phi(a)/a^2$, which is proportional to Y, as a function of n/n_0. It therefore represents the relative number of resolved collisions as a function of the number of tracks in the beam, expressed as a fraction of the optimum number. The decrease of Y to the left of its maximum is due to the reduction in the number of tracks; the decrease to the right to the reduction in the fraction resolved. This fraction, which is

$$F = Y/KR_L n = \phi(a)/a,$$

is given in curve 2, as a function of n/n_0. For the optimum number of tracks ($n = n_0$), F has the value 0·28; that is, if the number of tracks is chosen so as to be that given by (15), then the number Y of resolved collisions is a maximum, and the fraction of those collisions that do occur that are resolved is 0·28.

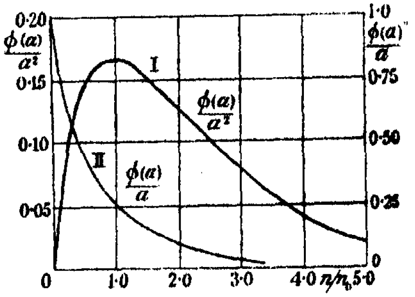

FIG. 3.

As an example, suppose that the first 5·0 cm. of the range at N.T.P. of an 8·6 cm. alpha particle is effective in producing disintegrations. To get R_L, we must multiply by the magnification of the camera, which is 1/5, and by the expansion ratio, say 1·33, so that $R_L = 1{\cdot}33$ cm. Then taking the angular breadth ϕ of the beam as one radian, and the breadth of the track images as 30 μ, we find from (15) that the optimum number of tracks is 33. And even with this small number only 28 per cent. of collisions that do occur are resolved.

The limitation of the number of tracks in a photograph, imposed by the demand that the greatest possible number of collisions should be resolved is very drastic. It cannot, however, be denied that on some occasions the number may with advantage be made larger than the optimum. If one is content that one image only be resolved the permissible number of tracks is doubled; and it is possible that even this concession to quantity rather than quality may not always satisfy the impatience of the experimenter. With very rare types of collision the choice lies not so much between many unresolved and a few resolved, as between a very few unresolved and none at all. From curve 1, fig. 3, it may be seen that the total number of collisions may be increased by a factor three ($n = 3n_0$), at the cost of reducing the number of resolved collisions by one-half. Photographs Nos. 1, 2 and 3, Plate 21, show the appearance of photographs for which $n/n_0 = 1{\cdot}2$, $2{\cdot}4$, $4{\cdot}3$ respectively.

6. *The Effect of the Reduction of the Pressure, and the Dilution of the Gas.*

The yield can, however, often be increased, and without any concession to quality, by a suitable choice of the pressure and composition. It is convenient to transform (16) so as to contain quantities referring to the alpha rays themselves instead of to their images.

Let $K'\nu$ be the chance that an alpha particle makes a disintegration collision in going a distance of 1 cm. in a gas in which there are ν atoms in 1 c.c. The chance K that a collision will occur in 1 cm. of the image is $K'\nu/m$, where m is the magnification. Hence $K = K'\nu/m$. Substituting this in (16) and putting $\Delta = mD_0$*, and $R_L = m\rho_L$, so that ρ_L is the length of the part of the actual track in the chamber along which disintegration occurs, we get

$$Y_m \propto K'\nu\rho_L{}^2/D_0. \tag{17}$$

We will take D_0 to be constant, as was decided in section 3. If it is found to vary either with the pressure or composition, this variation can easily be taken into account.

Consider first the effect of a change of pressure of the gas. We have then $\rho_L n$ = constant, so that

$$Y_m \propto 1/\nu.$$

Thus the yield of collisions is inversely proportional to the pressure. The lower the pressure, the longer the tracks, and the more that can be accommodated in a given angle without interference. The limit to the reduction in pressure is clearly set by the condition that the effective length of the track should just fill the chamber. For instance, for the case considered in section 4, ρ_L has a value of 6·7 cm. when the initial pressure is atmospheric, and so would just fill the chamber when the pressure was reduced to half an atmosphere. By this simple means the yield of disintegration collisions is doubled. In this connection the possibility must be remembered of increasing still further the size of the chamber; combining this either with an increase in the size of the film or a decrease in the magnification.

Consider now the effect of dilution with a gas of lower stopping power, such as hydrogen or helium, while keeping the total pressure constant. Let the gas A under investigation be diluted with a gas B, so as to form a mixture containing f atoms of A and $(1-f)$ of B. If α is the ratio of the stopping power of B to that of A, the range of the particles, and so the value of ρ_L, will be increased, compared with the case of all A, ($f = 1$), in the ratio

---

* Strictly equation (8) should be used. But the neglect here of the diffraction width will not matter.

$$1 : [f + \alpha(1 - f)].$$

Then since the number ν of atoms of A in unit volume is proportional to f we have from (17)

$$Y_m \propto f[f + (1 - f)\alpha]^{-2} = P.$$

This has a maximum value of

$$[4\alpha(1 - \alpha)]^{-1},$$

which occurs for

$$f = \alpha(1 - \alpha)^{-1}.$$

For instance, if $\alpha = \frac{1}{4}$, which corresponds to the dilution of nitrogen with helium, we find $f = 1/3$ and $P = 4/3$. Thus, if nitrogen be diluted with twice its volume of helium, the yield of resolved nitrogen disintegration collisions is increased by 33 per cent.

Apart from the increased yield there is an additional advantage to be gained by a reduction of pressure and dilution. The range of any recoil atom or product of disintegration will be increased and so the details of the collision process will be the more easily observed. The dilution method has the advantage, and with the usual Wilson chamber the very great advantage, of enabling the total initial pressure to be kept at atmospheric. There is also the advantage of obtaining many collisions with the helium or hydrogen used for the dilution.

In practice the cases which arise are often more complicated than those considered here; for instance, when the probability of a disintegration varies rapidly along the range; or when the part of the beam photographed does not include the source from which the rays diverge. These cases can be dealt with in the same general way, but will in general require numerical evaluation.

Summary.

1. A double camera is described for use with a Wilson chamber when photographing the artificial disintegration of elements. The camera takes two sharp photographs of the plane of the chamber on two films at right angles to each other.

2. The interrelation of the depth of focus, the intensity of the images and the magnification of the camera is discussed. It is shown that it is desirable to reduce the last as far as possible, but that a limit is set by the finite resolving power of the photographic emulsion.

3. It is shown that there exists an optimum number of tracks in a beam, at which the number of *resolved* collisions is a maximum. If there are more than this the tracks obscure each other.

4. The gain in yield of resolved collisions to be obtained by the reduction of pressure or the dilution of the gas with hydrogen or helium is discussed.

I wish to thank Mr. D. S. Lees, of Emmanuel College, for the photographs reproduced and for carrying out the adjustment and testing of the camera.

The cost of the camera was borne by a grant from the Government Grant Committee of the Royal Society.

The Absorption Band Spectrum of Chlorine.

By A. Elliott, B.Sc., Armstrong College Fellow.

(Communicated by T. H. Havelock, F.R.S.—Received February 13, 1929.)

[Plate 22.]

Introduction.

The familiar yellow-green colour of chlorine is due to a broad region of absorption in the violet and blue regions of the spectrum. This absorption is continuous, *i.e.*, it shows no sign of structure under high resolving power, and extends from about 2300 A.U. towards the direction of lower frequency, becoming exceedingly feeble in the neighbourhood of 5000 A.U. The maximum of absorption lies at 3300 A.U.[*] In addition to this continuous absorption, a feeble band absorption exists in the region 4785–6220 A.U. approximately, part of which is overlapped by the continuous absorption.

The absorption band spectrum of chlorine has been studied by several workers, the first accurate measurements having been made by Laird,[†] who measured the wave-lengths of some thousands of lines, but did not make any analysis. More recently Kuhn and Nakamura[‡] have measured the wave-lengths and frequencies of the heads of the bands, and have arranged them into five pro-

[*] Halban and Siedentopf, 'Z. Phys. Chem.,' vol. 103, p. 80 (1922).

[†] 'Astrophys. J.,' vol. 14, p. 85 (1901); Kuhn, 'Z. Physik,' vol. 39, p. 77 (1926).

[‡] Nakamura, 'Kyoto Coll. Sc. Mem.,' A, vol. 9, p. 315 (1926).

gressions, each having a common vibrational quantum number in the lower state (the initial state in absorption).

We will follow the usual practice in denoting the vibration quantum numbers in the upper and lower electronic states by n' and n'' respectively. Kuhn has assigned vibrational quantum numbers to the various bands in the progressions, the values for n' being, however, arbitrary. Each progression having a common value of n'' converges to a limit as n' increases, and the absorption of a quantum of energy greater than that represented by the convergence limit results in the dissociation of the molecule. The excess of this energy over that required for dissociation appears as kinetic energy of the resultant atoms, one of which according to the idea of Franck[*] is in the normal state, the other being in a metastable excited ${}^2P_1$ state. Since the kinetic energy of the atoms is not quantised, it follows that the absorption beyond the limit of convergence is continuous. Each progression of bands may therefore be expected to have a continuous absorption extending from its convergence point towards the direction of greater frequencies. From observations on the change in intensity of the bands with temperature, Kuhn has concluded that the progression nearest the violet is due to molecules in which n'' is 1 (see later section on assignment of vibrational quantum numbers).

The halogen molecules appear to be so constituted that a large vibration is set up when the molecule suffers a change in electronic energy from a lower to a higher state. This has been commented on and Franck (*loc. cit.*) has proposed a simple mechanical model to account for the phenomenon. Kuhn suggests that the vibration produced on activation of a normal chlorine molecule possessing no vibrational energy (*i.e.*, one in which $n'' = 0$) is so great that dissociation of the molecule occurs, and a continuous spectrum results. This remarkable result tends to the view that the molecules responsible for the first band observed in any progression (*i.e.*, the bands having the lowest n') undergo such an increase in vibrational energy that the lowest value of n' in the progression may be rather high, and this result is confirmed by the assignment of vibrational quantum numbers made in this paper from the vibrational isotope effect.

The isotope effect has been briefly described in a letter communicated to 'Nature' (December 29, 1928) and will be dealt with separately in the second portion of this paper. The absolute vibration quantum numbers will be used throughout in designating the bands measured.

---

[*] 'Trans. Faraday Soc.,' vol. 21, p. 536 (1925).

Part I.—*Rotation Constants of the* $Cl_{35}Cl_{35}$ *Molecule.*

Experimental.—The band absorption in chlorine is very weak, so that it is necessary to use a considerable thickness of chlorine in order to observe it. Absorption tubes up to 12·6 m. have been employed by previous workers. In the present investigation, two tubes of approximately 1·6 m., filled with chlorine at 1 and 2 atmospheres respectively, have been used. These tubes were of Pyrex glass, 3 cm. in diameter, with plane ends fused on, by the use of a method which has been described by Fairchild.* This method presents no special difficulties, and does not appear to be so well known as it deserves to be. The tubes were cleaned with chromic and nitric acids and afterwards well washed, dried, and baked out under vacuum. Chlorine from a cylinder, after having been washed through a tower of water and dried by sulphuric acid and a long column of phosphorus pentoxide, was admitted to the tubes, the pressure being read by a mercury manometer protected from the action of the chlorine by a layer of sulphuric acid. When the desired pressure was attained, the chlorine supply was cut off and the pressure reduced by cooling part of the tubes with solid carbon dioxide and ether so that the tubes could be sealed off.

As a source of illumination, a 500-watt tungsten filament lamp was employed at first, but as the exposures with the grating were very long (about 15 hours in some cases), it was found preferable to use a carbon arc, an image of the crater being thrown on the slit through the tube. The exposures with this arrangement were never longer than 1 hour, though there was the disadvantage that there was a faint Swan band, extending from 5165 A.U. towards the blue end of the spectrum, superposed on the continuous spectrum of the pole. The presence of this band was not, however, of much consequence, since lines appearing on the chlorine spectrum which were due to the arc itself could be identified by comparison with a photograph of the carbon arc alone.

The spectrum was photographed in the second order of a 21-foot grating, with which the dispersion was about 1·25 A.U. per millimetre. At first, the tube containing chlorine at 2 atmospheres was employed, but it was found that the band lines developed under these conditions were broad and diffuse and difficult to measure. Photographs with the tube at 1 atmosphere were then taken, and a great increase in sharpness and in resolution was obtained. It appears likely that the best results would be obtained by using a much longer tube at a smaller pressure, but the situation of the grating forbade this

---

* 'J. Opt. Soc. Amer.,' vol. 4, p. 496 (1926).

Table I.—Wave-lengths, etc., of Band Lines in $Cl_{35}Cl_{35}$.

Under the heading "Int." are given the absorption coefficients α for the centre of the band lines calculated from the expression

$$I = I_0 e^{-\alpha\rho x},$$

where I_0 and I are the initial and transmitted light intensities respectively, x is the thickness of the chlorine in centimetres and ρ is the chlorine concentration in gram-molecules per litre.

Band 2 → 17.

j.	P branch.			R branch.		
	λ in I. A.U.	ν in cm.⁻¹.	Int.	λ in I. A.U.	ν in cm.⁻¹.	Int.
13½	5197·79	19233·60	0·020			
15½	5199·74	19226·37	0·030	5197·62	19234·23	0·027
16½	5200·82	19222·40	0·024			
17½	5201·93	19218·31	0·031	5199·55	19227·10	0·034
18½	5203·12	19213·92	0·024	5200·63	19223·11	0·020
19½	5204·37	19209·29	0·027	5201·73	19219·04	0·027
20½	5205·72	19204·30	0·031	5202·90	19214·70	0·034
21½	5207·10	19199·21	0·031	5204·15	19210·08	0·044
22½	5208·54	19193·92	0·024	5205·50	19205·10	0·048
23½	5210·07	19188·27	0·027	5206·87	19200·06	0·034
24½	5211·64	19182·49	0·014	5208·31	19194·75	0·024
25½	5213·29	19176·43	0·027	5209·82	19180·18	0·030
26½	5214·99	19170·17	0·024	5211·41	19183·34	0·020
27½	5216·78	19163·61	0·037	5213·05	19177·32	0·027
28½	5218·61	19156·89	0·027	5214·74	19171·08	0·024
29½	5220·53	19149·82	0·044	5216·53	19164·51	0·034
30½	5222·54	19142·44	0·024	5218·36	19157·79	0·024
31½	5224·56	19135·07	0·031	5220·25	19150·87	0·034
32½				5222·23	19143·57	0·017
33½				5224·27	19136·12	0·030

Band 2 → 18.

j_P.	j_R.	P and R branches.		
		λ in I. A.U.	ν in cm.⁻¹.	Int.
5½	7½	5157·41	19384·18	0·034
6½	8½	5157·87	19382·47	0·020
7½	9½	5158·37	19380·60	0·044
8½	10½	5158·97	19378·31	0·034
9½	11½	5159·58	19376·03	0·037
10½	12½	5160·30	19373·35	0·027
11½	13½	5161·06	19370·48	0·054
12½	14½	5161·88	19367·38	0·020
13½	15½	5162·79	19364·00	0·051

Table I—(continued).

Band 2 → 18—(continued).

j_P.	j_R.	P and R branches.		
		λ in I. A.U.	ν in cm.$^{-1}$.	Int.
14½	16½	5163·70	19360·58	0·041
15½	17½	5164·77	19356·57	0·048
16½	18½	5165·86	19352·47	0·034
17½	19½	5167·03	19348·11	0·061
18½	20½	5168·26	19343·50	0·061
19½	21½	5169·53	19338·74	0·075
20½	22½	5170·88	19333·69	0·037
21½	23½	5172·29	19328·42	0·054
22½	24½	5173·76	19322·93	0·041
23½	25½	5175·33	19317·06	0·054
24½	26½	5176·92	19311·13	0·044
25½	27½	5178·62	19304·80	0·058
26½	28½	5180·39	19298·22	0·041
27½	29½	5182·19	19291·49	0·051
28½	30½	5184·08	19284·46	0·048
29½	31½	5186·03	19277·22	0·054
30½	32½	5188·04	19269·76	0·034
31½	33½	5190·14	19261·97	
32½	34½			
33½	35½			

Band 2 → 19.

j.	P branch.			R branch.		
	λ in I. A.U.	ν in cm.$^{-1}$.	Int.	λ in I. A.U.	ν in cm.$^{-1}$.	Int.
13½	5131·10	19483·59	0·075			
14½						
15½	5133·14	19475·85	0·054	5131·22	19483·13	0·048
16½	5134·26	19471·58	0·037			
17½	5135·43	19467·15	0·048	5133·27	19475·36	0·048
18½	5136·70	19462·35	0·051	5134·39	19471·09	0·044
19½	5138·00	19457·44	0·041	5135·61	19466·46	0·061
20½	5139·37	19452·22	0·031	5136·87	19461·61	0·054
21½	5140·82	19446·73	0·044	5138·17	19456·77	0·041
22½	5142·33	19441·05	0·031	5139·63	19451·24	0·024
23½	5143·91	19435·07	0·044	5141·01	19446·04	0·034
24½	5145·57	19428·81	0·031	5142·55	19440·19	0·024
25½	5147·28	19422·33	0·048	5144·16	19434·11	0·054
26½	5149·06	19415·65	0·034	5145·82	19427·85	0·048
27½	5150·91	19408·64	0·054	5147·53	19421·39	0·051
28½	5152·83	19401·43	0·037	5149·31	19414·70	0·048
29½	5154·82	19393·92	0·037	5151·16	19407·70	0·058
30½				5153·12	19400·32	0·017
31½				5155·15	19392·71	0·051

in the present instance. All the measurements were made from plates taken with 1 atmosphere of chlorine. Iron arc lines superposed on the chlorine photographs were used as standards, and the frequencies of the chlorine lines were derived in the usual manner from measurements made with a Hilger measuring micrometer (type L 13). The accuracy of measurement varies considerably throughout the spectrum, on account of the large number of lines which are overlaid by neighbouring lines, due to the overlapping of bands in the various progressions, and also to the overlapping of adjacent bands in the same progression. It is not likely that the measurement of the centre of density of a line is anywhere more in error than 0·05 cm.$^{-1}$.

Analysis.—The notation used here will be that adopted in the "Report on Molecular Spectra in Gases." For the sake of convenience, half quantum numbers will be used in the rotation term $F(j) = Bj^2 + Dj^4$, rather than the form derived from the new quantum mechanics ($F(j) = Bj(j+1)$, with integral values of j), especially as for the present calculation of rotation constants there is no esential difference between the two forms.

The general appearance and structure of the bands may be seen from Plate 22.

A feature of these bands is the close similarity of the P and R branches, and the remarkable way in which they run side by side. This is particularly noticeable in the case of the 2 → 18 band, in which the P and R branches actually are superposed throughout. Only P and R branches have been found, and it is certain that no Q branch of any appreciable strength exists, a fact which is in harmony with Mulliken's suggestion* that these bands are of the type $^1S \rightarrow {}^1S$. Combination differences (Table II) have been found for the three bands. Since the phenomenon of alternating intensities is present in these bands, the differences in Table II are derived from strong and weak lines alternately. The differences in which the corresponding j value is even are derived from strong lines. It has not been possible to resolve lines near the heads of the bands.

There is very good agreement between the corresponding members of the three sets of differences, and this affords decisive evidence in favour of the view that these three bands have a common lower vibrational state.

---

[*] 'Phys. Rev.,' vol. 28, p. 1202 (1926).

Table II.—Combination Differences for the Normal State.
$[R(j-1) - P(j+1) = 2\Delta F''(j).]$

2 → 17.	2 → 18.	2 → 19.	Average.	*j*.
	8·15			8½
	9·12			9½
	10·12			10½
	10·93			11½
	12·03			12½
	12·77			13½
	13·91			14½
	14·91			15½
15·92	15·89	15·98	15·93	16½
	17·08			17½
17·81	17·83	17·92	17·85	18½
18·81	18·78	18·87	18·82	19½
19·83	19·69	19·73	19·75	20½
20·78	20·57	20·66	20·67	21½
21·81	21·68	21·70	21·73	22½
22·61	22·56	22·43	22·53	23½
23·63	23·62	23·71	23·65	24½
24·58	24·71	24·54	24·61	25½
25·57	25·57	25·47	25·54	26½
26·45	26·67	26·42	26·51	27½
27·50	27·58	27·47	27·52	28½
28·64	28·46		28·55	29½
29·44	29·52		29·48	30½

The average value of the combination differences have been plotted against j, j being half-integral and chosen so that the resultant curve passes as close to the origin as possible. This curve is reproduced in the figure (p. 636).

From the way in which the combination differences derived from the weak lines fall into line with those from the strong lines, there can be no doubt that both sets of lines belong to one band. The curve is approximately linear, and can consequently be extrapolated to the origin in order to decide the correct numbering.

Since the normal term differences are $R(j-1) - P(j+1) = 2\Delta F''(j)$ it is possible, the value of j for each value of $2\Delta F''(j)$ being known from the curve, to assign appropriate j values to the lines. The numbering is set out in Table I above, each line being indicated as usual by the j value in the lower electronic level (the initial level in absorption). The numeration cannot be in doubt by 1 unit as the extrapolation of the $2\Delta F''(j)$—(j) curve is certain. It now follows that the excited term differences for each band can be evaluated, and these are given in Table III.

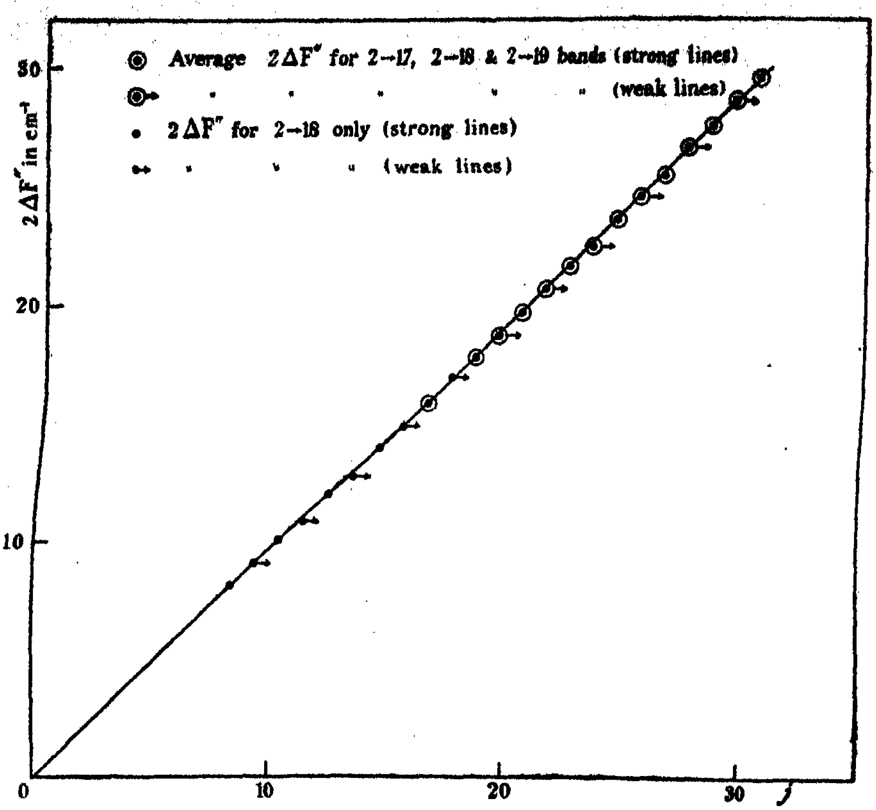

These term differences were plotted against j and extrapolate fairly closely to the origin. As in the case of the normal state, the curves are approximately linear, and the differences derived from the weak lines agree with those from the strong lines. In this case, the differences corresponding to odd values of j are derived from strong lines.

Calculation of Rotation Constants.—Taking for the rotation term the form

$$F(j) = Bj^2 + Dj^4 \tag{1}$$

it is seen that

$$\Delta F(j) = 2Bj + 4Dj^3,$$

and

$$\Delta F(j)/j = 2B + 4Dj^2. \tag{2}$$

The values of $\Delta F(j)/j$ are given in Table IV, in which the values derived from strong and weak lines are given separately. There is no indication of a progressive change in $\Delta F(j)/j$ in any one band, and consequently D must

Table III.—Combination Differences for the Excited State.

$[(\mathrm{R}j) - \mathrm{P}(j) = 2\Delta \mathrm{F}'(j).]$

2 → 17.	2 → 18.	2 → 19.	*j*.
	3·58		7½
	4·16		8½
	4·57		9½
	4·96		10½
	5·55		11½
	5·97		12½
	6·48		13½
	6·80		14½
7·86	7·43	7·28	15½
	8·11		16½
8·79	8·46	8·21	17½
9·19	8·97	8·74	18½
9·75	9·37	9·02	19½
10·40	9·81	9·49	20½
10·87	10·32	10·04	21½
11·18	10·76	10·19	22½
11·79	11·36	10·97	23½
12·26	11·80	11·38	24½
12·75	12·26	11·78	25½
13·17	12·91	12·20	26½
13·71	13·31	12·75	27½
14·19	13·76	13·27	28½
14·69	14·27	13·78	29½
15·35	14·70		30½
15·80	15·25		31½

be negligible. The values of B are found by averaging $\Delta \mathrm{F}(j)/j$ and making use of equation (2). Since the positions of the weaker lines are not so well determined as those of the stronger lines, the B values appearing at the end of this paper are those derived from strong lines only. The values of $\Delta \mathrm{F}(j)/j$ are slightly smaller for the weak than for the strong lines, but a greater accuracy of measurement is necessary before any conclusion can be drawn from this difference, which may be accidental.

The value of j at the turning point may be calculated when B′ and B″ are known, since at this point

$$j = -\mathrm{B}'/(\mathrm{B}' - \mathrm{B}'').$$

The values for j for the turning point for the 2 → 17, 2 → 18, and 2 → 19 bands are 1·08, 1·005 and 0·935 respectively. For the R branch of the 2 → 18 band, the parabola will therefore be symmetrical about the point at which $j = 1$ approximately, and consequently R and P lines which are situated at equal intervals from this point will be superposed.

Table IV.—$\Delta F(j)/j$ for Normal and Excited States.

j.	$\Delta F(j)/j$.							
	Normal state.		Excited state.					
			2 → 17.		2 → 18.		2 → 19.	
	Strong.	Weak.	Strong.	Weak.	Strong.	Weak.	Strong.	Weak.
7½					0·2387			
8½						0·2447		
9½					0·2405			
10½						0·2362		
11½					0·2413			
12½						0·2389		
13½					0·2400			
14½						0·2345		
15½			0·2535		0·2397		0·2348	
16½	0·4827					0·2458		
17½			0·2511		0·2437		0·2346	
18½	0·4824			0·2484		0·2424		0·2362
19½		0·4826	0·2500		0·2403		0·2313	
20½	0·4817			0·2536		0·2393		0·2315
21½		0·4807	0·2528		0·2400		0·2335	
22½	0·4828			0·2484		0·2391		0·2264
23½		0·4793	0·2509		0·2417		0·2334	
24½	0·4827			0·2502		0·2405		0·2323
25½		0·4825	0·2500		0·2404		0·2310	
26½	0·4818			0·2485		0·2435		0·2302
27½		0·4819	0·2493		0·2420		0·2318	
28½	0·4828			0·2489		0·2414		0·2328
29½			0·2490		0·2419		0·2336	
30½				0·2517		0·2410		
31½			0·2508		0·2421			
Average	0·4824	0·4814	0·2508	0·2500	0·2418	0·2406	0·2331	0·2316

Part II.—*Isotope Effect in the Band Spectrum of Chlorine.*

Rotation Constants of $Cl_{35}Cl_{37}$.—Chlorine is an isotopic element, in which the nuclear masses of the two isotopes are 35 and 37, present in the proportions 3·35 : 1. Three molecules $Cl_{35}Cl_{35}$, $Cl_{35}Cl_{37}$ and $Cl_{37}Cl_{37}$ must therefore be present in the proportions 11·3 : 6·7 : 1 respectively. These molecules differ only in respect of nuclear mass, and in all other respects are identical. The vibrational isotope effect in this case will therefore take the form of a tripling of all the band heads in the system. The isotopic separation of band origins is according to Mulliken*

$$\nu_1 - \nu_2 = (1 - \rho_{1,2})(\omega_1'n' - \omega_1''n'') - (1 - \rho_{1,2}^2)(b_1'n'^2 - b_1''n''^2), \quad (3)$$

---

* 'Phys. Rev.,' vol. 25, p. 119 (1925).

where $\rho_{1,2} = \sqrt{\mu_1/\mu_2}$, μ being the "reduced mass."[*] Denoting the molecules $Cl_{35}Cl_{35}$, $Cl_{35}Cl_{37}$ and $Cl_{37}Cl_{37}$ by the suffixes 1, 2 and 3 respectively,

$$\rho_{1.2} = \rho_{2.3} = 0 \cdot 9863.$$

Since for the higher members of the progression which are now under consideration, the multiplicand of $(1 - \rho_{1,2})$ in equation (3) above is positive, it follows that $\nu_1 > \nu_2 > \nu_3$. Consequently in the isotope pattern there will be three bands for each vibration transition, the strongest having the greatest, and the weakest having the least frequency. The intensity of each band should be proportional to the abundance of the molecules responsible for its production.

In the case of the (2 → 18) band, the expected weaker band has been found on the low frequency side, and the measurement and analysis have been carried out in this case. The very weak band due to $Cl_{37}Cl_{37}$ has not been observed. The (2 → 17) and (2 → 19) bands are more confused than (2 → 18) by other band lines, and here the companion bands have not yet been measured. The wave-lengths, wave-numbers and intensities of the $(2 \rightarrow 18)_{35-37}$ band are given in Table V below. In this band, as we should expect from the theory of the

Table V.—Wave-lengths, etc., of Band Lines in $Cl_{35}Cl_{37}$.
Band (2 → 18).

j_P.	j_R.	P and R branches.		
		λ in I. A.U.	ν in cm.$^{-1}$.	Int.
14½	16½	5166·25	19351·03	0·034
15½	17½	5167·25	19347·29	0·048
16½	18½	5168·27	19343·47	0·065
17½	19½	5169·40	19339·24	0·054
18½	20½	5170·58	19334·83	0·034
19½	21½	5171·86	19330·03	0·044
20½	22½	5173·14	19325·23	0·031
21½	23½	5174·53	19320·04	0·034
22½	24½	5175·94	19314·82	0·041
23½	25½	5177·44	19309·20	0·034
24½	26½	5179·02	19303·33	0·031
25½	27½	5180·64	19297·26	0·024
26½	28½	5182·38	19290·81	0·034
27½	29½	5184·09	19284·44	0·044
28½	30½	5185·92	19277·62	0·048
29½	31½	5187·78	19270·73	0·034
30½	32½	5189·77	19263·34	0·034
31½	33½			
32½	34½			

---

[*] If the two point masses of a rigid dipole be m_a and m_b and are situated at a distance d from each other, then the moment of inertia about an axis through the centre of gravity perpendicular to the axis of figure is $d^2 m_a m_b/(m_a + m_b)$. The quantity $m_a m_b/(m_a + m_b)$ is called the "reduced mass" of the dipole. ω' and ω'' are the vibration frequencies of the nuclei in the upper and lower electronic states respectively.

rotational isotope effect, the structure is identical with that of the $(2 \rightarrow 18)_{35-35}$ band and P and R branches are superposed.

The j values for the $(2 \rightarrow 18)_{35-37}$ band have been arrived at in the way described in Part I. Term differences for the normal and excited states, along with the values of $\Delta F(j)/j$, are given in Table VI.

Table VI.—Combination Differences for Normal and Excited States in $(2 \rightarrow 18)_{35-37}$.

j.	$2\Delta F''(j)$ (normal).	$\Delta F''(j)/j$.	$2\Delta F'(j)$ (excited).	$\Delta F'(j)/j$.
$16\frac{1}{2}$			7·56	0·2291
$17\frac{1}{2}$	16·20	0·4629	8·05	0·2300
$18\frac{1}{2}$	17·26	0·4664	8·64	0·2335
$19\frac{1}{2}$	18·24	0·4678	9·21	0·2362
$20\frac{1}{2}$	19·20	0·4683	9·60	0·2342
$21\frac{1}{2}$	20·01	0·4654	9·99	0·2323
$22\frac{1}{2}$	20·83	0·4629	10·41	0·2313
$23\frac{1}{2}$	21·90	0·4658	10·84	0·2307
$24\frac{1}{2}$	22·78	0·4756	11·49	0·2345
$25\frac{1}{2}$	24·01	0·4709	11·94	0·2341
$26\frac{1}{2}$	24·76	0·4673	12·52	0·2362
$27\frac{1}{2}$	25·71	0·4675	12·82	0·2331
$28\frac{1}{2}$	26·53	0·4654	13·19	0·2315
$29\frac{1}{2}$	27·47	0·4657	13·71	0·2324
$30\frac{1}{2}$			14·28	0·2340
	Average	0·4671		0·2328

The rotation constants B, moments of inertia and internuclear distances are calculated as before, and appear in the table of constants (Table VII) at the end of the paper. It should be noted that, although the B values are appreciably different, the internuclear distances calculated from the analysis of the $(2 \rightarrow 18)_{35-35}$ and $(2 \rightarrow 18)_{35-37}$ bands are in very good agreement, and this affords sufficient justification for ascribing the latter band to the molecule $Cl_{35}Cl_{37}$.

Assignment of Vibrational Quantum Numbers.—Kuhn (*loc. cit.*) has described some experiments in which the change in intensity with temperature of the various progressions in bromine and chlorine was observed, and it was found that the convergence progression was weakened with increase of temperature in the case of the first gas, but became stronger in the case of chlorine. A result similar to that found in bromine has been found in iodine by Pringsheim.* All the other progressions in the three gases increased in intensity with increase of temperature. Kuhn concluded that the values of n'' in the convergence progression were 0, 0 and 1 for iodine, bromine and chlorine respectively, and that the non-vibrating chlorine molecule gave rise to a continuous absorption. The new quantum mechanics (Fuess*) requires the vibration quantum numbers to be of the form $n + \frac{1}{2}$ (n being integral), and an experimental confirmation of this in the case of boron monoxide has been made by Jenkins.† The above quantum numbers for the convergence progression (and consequently those for the other progressions) should therefore on this basis be increased by $\frac{1}{2}$. A more accurate investigation of the dependence of absorption in chlorine on temperature is, however, desirable, in order to confirm the absence of the progression in which the initial vibration quantum number is $\frac{1}{2}$.

---

* 'Z. Physik,' vol. 5, p. 130 (1921).

Taking Kuhn's assignment of quantum numbers for the initial state (in absorption) with the addition of one-half unit, the quantum numbers for the excited state may be calculated from the magnitude of the isotopic separation of the band origins. The origins of the chlorine bands cannot be observed by inspection of the spectrum, but may be calculated from the frequency of any of the lines comprising them whose j values are known when B′ and B″ have been determined for the band in question, since $\nu = B'j'^2 - B''j''^2$.

The origins of the $(2 \rightarrow 18)_{35-35}$ and $(2 \rightarrow 18)_{35-37}$ bands have been determined in this way from four lines in each band and the following mean values arrived at :—

$$\nu_1 = \text{origin of } (2 \rightarrow 18)_{35-35} = 19389 \cdot 0 \pm 0 \cdot 1 \text{ cm.}^{-1},$$

$$\nu_2 = \text{origin of } (2 \rightarrow 18)_{35-37} = 19379 \cdot 4 \pm 0 \cdot 1 \text{ cm.}^{-1}.$$

The separation of the two isotopic bands is therefore $9 \cdot 6 \pm 0 \cdot 2$ cm.$^{-1}$. If in equation (3) we replace n by $n + \frac{1}{2}$ and also write $\rho + 1 = 2$ since ρ is nearly unity, we have for the vibrational effect

$$\nu_1 - \nu_2 = (1 - \rho) [\omega_1' (n' + \tfrac{1}{2}) - \omega_1'' (n'' + \tfrac{1}{2}) - 2b_1' (n' + \tfrac{1}{2})^2 + 2b_1'' (n'' + \tfrac{1}{2})^2]. \quad (4)$$

It is to be noted that the simple approximation‡

$$\nu_1 - \nu_2 = (1 - \rho) \nu_1,$$

which may be used in many band spectra cannot be used here. This is due to the fact that the vibration frequency ω in the excited state is much less than in the normal state,§ and also to the large value assumed by n', making the term $b' (n' + \frac{1}{2})^2$ of considerable importance.

---

* 'Ann. Physik,' vol. 80, p. 367 (1926).

† 'Phys. Rev.,' vol. 29, p. 921 (1927).

‡ Mulliken, *loc. cit.*

§ Kuhn, *loc. cit.*

Equation (4) may be used to determine n' when the values of the constants are known. The value of b_1 may be found from a curve in which the vibration frequency ω is plotted against n, since the slope of this curve is $-2b$. The fact that arbitrary values of n' must be used in drawing the curve is of no importance, since except for very large values of n the curves are linear. The fundamental vibration frequency ω in the normal state is given by Kuhn as 565 cm.$^{-1}$. In the excited state this frequency is not known, but may be expressed as

$$\omega_1' = \bar{\omega}_1' + 2b_1'n'$$

where $\bar{\omega}_1'$ is the frequency of vibration of the molecule responsible for the band in question. The data of Nakamura (*loc. cit.*), which are more complete in respect of band head measurements, have been used in determining ω_1' and b_1'. All vibration data for chlorine are derived from measurements of band heads, but no appreciable error can be introduced by this since the origins and heads are so near to one another. The following are the values of the constants adopted in calculating n':

$$n'' = 2. \quad \omega_1'' = 565 \text{ cm.}^{-1}. \quad \omega_1' = 120 + 10\cdot9\, n' \text{ cm.}^{-1}.$$
$$2b_1'' = 10\cdot0 \text{ cm.}^{-1}. \quad 2b_1' = 10\cdot9 \text{ cm.}^{-1}.$$

The value of n' calculated from equation (4) is 17·6. The nearest whole number to this is 18, but the values of the above constants are not sufficiently accurate to test whether the hypothesis of half-quantum numbers, used in equation (4), is justified or not. The above absolute value of n' shows that Kuhn's arbitrary values must be increased by 12, since the $(2 \rightarrow 18)$ band is in his numeration called $(2 \rightarrow 6)$. The value of ω_1' is also altered by the change in numeration, and is now 316 cm.$^{-1}$.

Intensity Measurements.—The spectrum photographs of the chlorine bands have been photometered with a Moll self-registering microphotometer, and the absorption coefficients for the centres of the band lines calculated. The measurement of intensities in absorption band spectra is difficult and the results subject to large errors, and this is especially so in the case of the chlorine bands, where the number of lines which are overlaid by neighbouring lines is considerable. Density marks were photographed on a plate taken from the same packet and developed with that used for photographing the chlorine spectrum, in order that the light intensity corresponding to the various values of the plate density (which is measured by the microphotometer) might be calculated. The technique of such intensity measurements has been worked out in the Utrecht Institute* and is described by Baly.† In calculating absorption coefficients it was assumed that the light absorbed was proportional to the difference between the intensity of the continuous background and the centre of the absorption line. Since the bands measured only cover a small range of wave-lengths (less than 100 A.U.), it was unnecessary to make any correction for the change in the intensity-density curve with change of wave-length. The absorption coefficients for the lines are given in Tables I and V. An inspection of these tables shows clearly that in the bands due to the molecule $Cl_{35}Cl_{35}$, the lines comprising them alternate in intensity. In the case of the band due to $Cl_{35}Cl_{37}$ there are some irregularities on account of lines which are overlaid by lines of the stronger isotope, but no regular alternation can be observed throughout the band. This is in accordance with the theory of Hund,‡ according to which alternation in intensity of band lines is only to be expected when the nuclear masses are equal. The ratio of the mean intensity (of strong and weak lines) in the band $(2 \rightarrow 18)_{35-35}$ to that in the band $(2 \rightarrow 18)_{35-37}$ has been determined in the following way.

A well separated line of $(2 \rightarrow 18)_{35-37}$ (the line $P(25\frac{1}{2}) + R(27\frac{1}{2})$, every line in the two bands being doubled on account of the superposition of the P and R branches) was taken and compared with the mean intensity in $(2 \rightarrow 18)_{35-35}$ of $P(24\frac{1}{2}) + R(26\frac{1}{2})$, $P(25\frac{1}{2}) + R(27\frac{1}{2})$ and $P(26\frac{1}{2}) + R(28\frac{1}{2})$. The portion of the photometer curve on which these lines appear was enlarged and from it a curve was drawn in which the ordinates were proportional to light intensity. The curve was then analysed in so far as the uncertain shape of the chlorine band lines permitted, and the lines above appear to be fairly free from overlying lines. From these measurements the ratio of intensities of the two bands was found to be 1·75 : 1. If this ratio depends only on the numbers of the two kinds of molecules present, then from the abundance of the isotopes the ratio should be 1·67 : 1, and this value agrees fairly well with the experimental value from the intensity measurements.

From the same three lines in the $(2 \rightarrow 18)_{35-35}$ band the ratio of strong to weak lines in that band has been determined, and is found to be 1·42 : 1. More accurate intensity measurements are, however, desirable in view of the theoretical interest attaching to the problem of alternating intensities in band spectra, and further work is now in progress.

---

* 'Proc. Phys. Soc.,' vol. 37, p. 334 (1925).

† "Spectroscopy," vol. 3, p. 156.

‡ 'Z. Physik,' vol. 42, p. 93 (1927).

Table VII.—Rotation Constants.*

Band.	B″.	B′.	I″.	I′.	r″.	r′.
	cm.$^{-1}$.	cm.$^{-1}$.	gm. cm.^{2}.	gm. cm.^{2}.	cm.	cm.
$(2 \rightarrow 17)_{35-35}$	0·2412	0·1254	114×10^{-40}	220×10^{-40}	$0 \cdot 991 \times 10^{-8}$	$1 \cdot 376 \times 10^{-8}$
$(2 \rightarrow 18($$_{35-35}$	0·2412	0·1209	114	228	0·991	1·401
$(2 \rightarrow 18)_{35-37}$	0·2337	0·1164	118	237	0·993	1·409
$(2 \rightarrow 19)_{35-35}$	0·2412	0·1166	114	237	0·991	1·429

Summary.

The analysis of the rotation structure of three chlorine bands shows that only P and R branches exist. From the values obtained for the molecular constants, it is found that the normal chlorine molecule expands considerably on the absorption of a quantum of radiation, as is to be expected from the corresponding decrease in the vibration frequency.

The discovery and measurement of the isotope effect has made it possible to assign vibration quantum numbers for the excited state, and these numbers are found to be rather high, as the first band observed in the progression in which $n'' = 1$ has the value $n' = 12$.

It is found that in the bands which are due to the molecule $Cl_{35}Cl_{35}$, in which the nuclear masses are equal, the band lines show an alternation in intensity, the ratio being approximately 1·4 : 1. This effect is not, however, present in the non-symmetrical molecule $Cl_{35}Cl_{37}$. The molecules $Cl_{35}Cl_{35}$ and $Cl_{35}Cl_{37}$ are found to have different moments of inertia, but equal internuclear distances, and must be identical except in respect of nuclear mass. Approximately, the mean intensity of the lines in each band is proportional to the number of molecules present of the kind required for the production of the band.

In conclusion, the author wishes to express his thanks to Prof. W. E. Curtis for much valuable help during the progress of the research, to Mr. Wilfred Hall of Tynemouth for the use of his large grating spectrograph, and to Prof. L. S. Ornstein, in whose Institute at Utrecht the intensity measurements have been made, for the facilities and assistance necessary for that part of the work.

---

* In Table VII, $B'' = \frac{h}{8\pi^2 c I''}$, where h is Planck's constant, c is the velocity of light *in vacuo*, and I″, r″ are respectively the moment of inertia and half-internuclear distance of the molecule in the lower electronic state. The same quantities in the upper electronic state are denoted by ′.

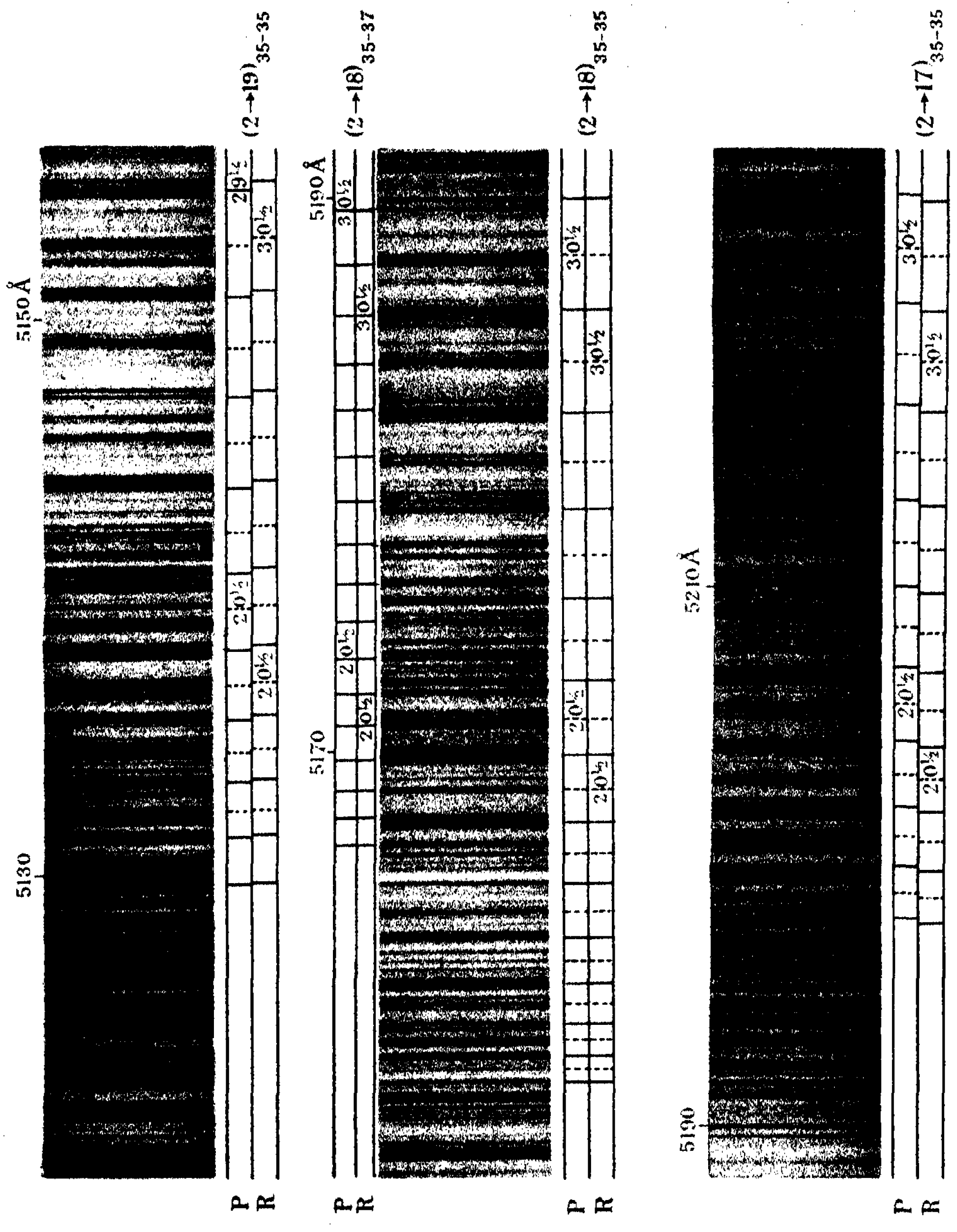

Chlorine Absorption Bands.

(*Facing p.* 644.)

Streamline Flow through Curved Pipes.

By C. M. White, King's College, London.

(Communicated by E. V. Appleton, F.R.S.—Received, February 1, 1929.)

NOTATION.

C, a numerical coefficient, defined as $Fd/8\mu v$, representing the increase of resistance due to curvature. d, diameter of pipe. D, mean diameter of coil. d/D, curvature ratio. F, intensity of frictional drag on wall of pipe, *i.e.*, shear stress at boundary. g, gravitational acceleration. m, hydraulic mean depth, = area/perimeter. v, mean velocity of flow, = volume flowing per unit time/cross sectional area of pipe. ρ, density of fluid. μ, viscosity of fluid.

All the values given in the paper are dimensionless, except in those cases in which some dimension is specifically stated.

Note.—All curves are plotted logarithmically.

The problem of the determination of the law of resistance for flow through smooth straight pipes has been the subject of many exhaustive investigation The result is conclusive. It may be said that the law of resistance is clearly defined over an extremely wide range of those variables which influence flow through such smooth straight pipes. Expressing the coefficient of resistance in the form $F/\rho v^2$, and the flow as $\rho vd/\mu$, it has been shown that $F/\rho v^2$ is a function of $\rho vd/\mu$. The general form of this function* is given graphically in fig. 1, which is based primarily on the experiments of Saph and Schoder, Stanton and Pannell, and Schiller.† It will be seen that there is a very definite

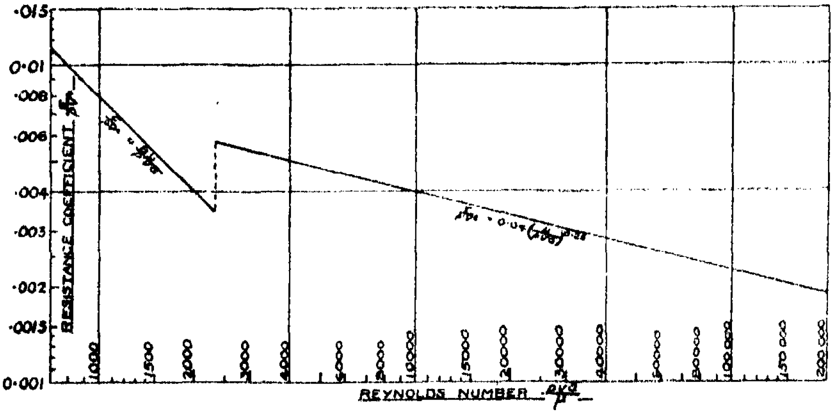

Fig. 1.—Resistance to Flow through smooth straight pipes.

---

* Davies and White, 'Engineering' (*in the press*).

† 'Trans. Am. Soc. C. E.,' vol. 51, p. 253 (1903); 'Phil. Trans.,' A, vol. 94, p. 199 (1914); 'Z. angew. Math.,' vol. 3, p. 2 (1923).

discontinuity in the curve when the Reynolds number reaches 2300, indicating the change from streamline to turbulent motion. Below 2300 the tests agree very closely with the law $F/\rho v^2 = 8(\rho vd/\mu)^{-1}$. This equation, apart from its corresponding forms for non-circular pipes, appears to be the only solution of the hydrodynamic equations which has as yet been obtained for flow through pipes. This solution represents streamline flow. The second line in fig. 1, for flows greater than $\rho vd/\mu = 2300$, indicates, of course, the existence of a second solution representing turbulent flow. Above 2300, and up to at least 100,000, the equation $F/\rho v^2 = 0\cdot04\,(\rho vd/\mu)^{-\frac{1}{4}}$—which no doubt is an approximation to this second solution—represents the observed results within the accuracy of the experimental errors.

With regard to the influence of curvature, however, comparatively few records are available. In the present paper, the author describes some tests recently carried out in the Engineering Department at King's College, London. These tests, when considered in relation to the results of other workers, appear to define the influence of curvature upon the law of resistance with satisfactory accuracy for a range of $\rho vd/\mu$ up to about 9000.

While this range relates to flows far below those of chief interest to the water engineer, it has, nevertheless, considerable practical application. Coils of tube are largely used in connection with heating and refrigeration in order to transfer heat from one fluid to another. Under such conditions, both the pressure required to obtain the necessary circulation and the rate of heat transfer for a given circulation will depend upon the magnitude of the resistance. The range is of particular interest also from the theoretical point of view, since it includes the change from streamline to turbulent flow, the cause of which still remains unexplained, although the tests of Schiller* go far, in that they show that the initial state of the fluid is a governing factor.

The present investigation had its origin in a re-examination, by the author, of some earlier experimental work on curved pipes, which it was hoped might provide information concerning the circumstances determining the limits within which flow must be streamline in character. It was seen, however, that additional experimental data were necessary; the investigation actually developed into a more general study of flow through curved pipes. The experimental part of the work consisted of tests of three pipes, Nos. I, II and III, whose curvature ratios, d/D, were respectively 1/15, 1/50 and 1/2050. The pipes are numbered in the order of their curvatures, but the order in which they were tested was II, I and III. In each case, irregularities in the passage leading to the pipe were provided, in order to produce a turbulent state of flow at the entrance to the pipe. This turbulence, however, would not influence the motion within the testing length of the pipe, unless the conditions within the pipe were such that the turbulence was self-sustaining, because, in every case, a length of curved pipe at least equal to 180 diameters was interposed as an entrant or stilling length between the entrance and the first gauge point. It will be seen later that the particular dimensions of each of the individual pipes were selected in order to obtain information on some specific point which was in doubt at the time.

---

* 'Z. angew. Math.,' vol. 1, p. 436 (1921).

When the investigation was undertaken there appeared to be only two sets of relevant experiments on record: those of Grindley and Gibson,[*] which were made to determine the viscosity of air; and those of Eustice[†] who was directly interested in the effect of curvature. The former tests, while they extended over a wide range of Reynolds number, from 25 to 1400, were unfortunately confined to one radius of curvature, namely, 112 times the pipe radius. On the other hand, the experiments of Eustice—although they covered a wide range of curvature, and provided much valuable information of a qualitative nature—were open to certain criticisms. The pipes themselves were oval in cross section, and, moreover, no provision was made to enable a uniform state of flow to become established throughout the length of pipe under test. Taking this into account, it was reasonable to question whether these results would be found to be truly representative of flow through coiled pipes of circular section, and further experimental evidence appeared to be necessary before the point could be decided. The only coiled pipe for which he gave the results in full was that with a cross sectional area of 0·0735 sq. cm. and a coil diameter of 2·59 cm. If the section had been of circular form the curvature ratio would have been 1/8·5, but, in view of the actual form, it appeared reasonable to assume the curvature ratio to be 1/14·6. The tests of this pipe covered a remarkably wide range of flows, the Reynolds numbers varying from 21 to 6000.

An investigation of the problem had been made by Dean,[‡] who showed mathematically that the product $\mathrm{F}/\rho v^2 \,.\, \rho v d/\mu$, *i.e.*, $\mathrm{F}d/\mu v$ is a function of the criterion $\rho v d/\mu \,.\, (d/\mathrm{D})^{\frac{1}{2}}$.[§] It should be emphasized that, in obtaining this result,

---

[*] 'Roy. Soc. Proc.,' A, vol. 80, p. 114 (1908).

[†] 'Roy. Soc. Proc.,' A, vol. 84, p. 107 (1910).

[‡] 'Phil. Mag.,' vol. 5, p. 673 (1928), also vol. 4, p. 208 (1927).

[§] The actual notation used by Dean was somewhat different. His result is

$$\mathrm{F}_c/\mathrm{F}_s = f[\mathrm{G}^2 a^7/\mu^2 \nu^2 \mathrm{R}],$$

where F_c = flux in curved pipe, F_s = flux in straight pipe, G = pressure gradient, a = radius of pipe, R = radius of coil, μ = coefficient of viscosity, ν = kinematic viscosity.

Dean assumed an essentially streamline type of motion. Unfortunately the series he obtained in his solution was such that a numerical result could be obtained for only extremely small values of the criterion; nevertheless, the work was of the utmost value in that it pointed to a basis of correlation for the existing data.

It appeared to the author that, if it could be shown that the conditions of flow assumed by Dean did in fact represent the actual motion of the fluid, then a single but extended series of tests, with one pipe only, would provide all the information that was necessary to determine the function

$$Fd/\mu v = f[\rho v d/\mu \, . \, (d/D)^{\frac{1}{2}}].$$

As neither Grindley and Gibson's nor Eustice's experiments provided sufficient data for the purpose, the author arranged for the pipe No. II to be tested. It was evident that the tests would have to extend over a range of flows at least twice as great as that investigated by Eustice, and this consideration led to the selection of a diameter of 0·63 cm. A larger pipe would not give measurable pressure gradients with very small flows, since, for reasons of manufacture, the length without joints is limited to 20 metres, while a smaller pipe is undesirable on account of irregularities in diameter. The curvature ratio, 1/50, intermediate between those of Grindley and Gibson and that of Eustice, was selected in the hope that a comparison would show that Dean's assumptions were justified. This hope was not realised, since the test results with this pipe, when considered on the basis of Dean's theory, definitely differed from those of Eustice, and were only in rough agreement with those of Grindley and Gibson.

Tests with a pipe of greater curvature were clearly necessary, and pipe No. I with a curvature ratio of 1/15 was accordingly made and tested. It should be noted that both pipe No. II and the pipe used by Grindley and Gibson were very long, and there were possibilities in both cases of small inaccuracies in the determination of their diameters, while Eustice's pipe was not circular in cross section. It was thus desirable that the cross section of this pipe, No. I, should be as nearly circular as possible, and that its dimensions should be known to a high degree of accuracy. In view of this and the greater curvature to which this pipe had to be coiled, it was necessary, from a purely constructional point of view, to adopt a larger diameter than that used for pipe No. II. This led to the use of lubricating oil in the place of water for those tests with the smallest flows, since the pressure gradients, using water, would have been too small for accurate measurement with the available manometers.

The results of these tests were particularly satisfactory. The agreement with pipe No. II was so good that it was reasonably certain that the motion closely followed the type investigated by Dean. And since by using oil, in addition to water, a range of Reynolds numbers from 0·06 to 40,000 was explored, it could be said that the results covered the whole practical range of $\rho vd/\mu \,.\, (d/D)^{\frac{1}{2}}$, the criterion found by Dean. This pipe, then, gave all the data necessary to express the relationship $Fd/\mu v = f[\rho vd/\mu \,.\, (d/D)^{\frac{1}{2}}]$ in the form of a curve. It was felt, however, that unless Dean's criterion could be shown to apply to a pipe of very different curvature ratio, the results could not be accepted with complete confidence. A wide range of the criterion $\rho vd/\mu \,.\, (d/D)^{\frac{1}{2}}$ had certainly been explored, but only by varying $\rho vd/\mu$. The range of $(d/D)^{\frac{1}{2}}$ throughout had not exceeded 0·1 to 0·26, and, since on the one hand the resistance is not at all sensitive to changes of d/D, while on the other hand a small error in pipe diameter causes considerable effect, it was just possible that the agreement between pipes Nos. I and II might be accidental. In order to examine this point, it was desirable to extend the range of curvature as distinct from the range of Reynolds number, the quantity $\rho vd/\mu \,.\, (d/D)^{\frac{1}{2}}$ of course still coming within the range previously covered. It is impossible to extend the range of curvature much in an upward direction, because certain difficulties of manufacture arise; but even could these be overcome, there still remains the ultimate limit, in that the curvature ratio of a pipe cannot exceed unity. No such definite limitation, however, exists in the other direction, although, as explained later, in an almost straight pipe the effect of curvature upon streamline flow may not be sufficient to be measurable before it is masked by turbulence. A curvature ratio approximately 1/135th of that of pipe No. I was selected for pipe No. III in the hope that, on the one hand, before turbulence set in, the resistance would show a sufficiently marked deviation from that of a straight pipe to enable Dean's theory to be established beyond question, and that, on the other hand, the increase due to curvature would be less than that usually observed due to the beginning of turbulence in a straight pipe. It was hoped that as a result this curved pipe would show the characteristic sudden increase of resistance at the critical point—a point which was by no means well defined in the curves obtained from the other pipes. The small internal diameter of 0·3 cm. was adopted in order that the exact value of the diameter might be determined by the most precise method, namely, by observation of the resistance to flow through the pipe before it was bent. This method was permissible in the particular case of pipe No. III, since the slight curvature desired could be obtained by elastic bending, and without appreciable distortion of the bore. The tests of this pipe provided the desired data, and so completed the experimental part of the investigation. There were then five sets of results available, and their scope is indicated in the table below.

Diameter of pipe, cm.	Diameter of coil, cm.	Curvature ratio.	Range of flow, Reynolds Numbers.	Fluid.	Remarks.
—	2·59	—	20 to 5000	Water	Oval pipe, area 0·0735 cm.^{2}. Tested by Eustice.
0·317	36·6	1/112	25 to 1400	Air	Tested by Grindley and Gibson
0·630	31·7	1/50	16 to 13000	Water	Author's pipe No. II.
1·032	15·62	1/15·15	0·058 to 41000	Oil water	Author's pipe No. I.
0·2980	610·5	1/2050	220 to 4000	Water	Author's pipe No. III.

Pipe No. II, a thick walled lead pipe, 18 metres long and 0·630 cm. bore, was coiled on a drum 30·5 cm. in diameter, giving a mean coil diameter of 31·7 cm. A length of some 400 pipe diameters was allowed for stilling, and there were 300 diameters between the last gauge point and the outlet. The measuring length was thus 2000 diameters. Alternative gauge points were provided, in order that any possible periodic effect might be checked, but they were found to be unnecessary. No attempt was made to jacket the apparatus against temperature changes; but the temperature of the water was measured both at the inlet and at the outlet of the pipe, and the supply was maintained at room temperature.

The great length of this pipe, 18 metres, and the smallness of its diameter rendered impossible a precise determination of its diameter by direct means. Pieces cut from the ends before it was coiled had an internal diameter of 0·630 cm. determined by plugs. The coiling would, however, modify this by an unknown amount; but in view of the thickness of the walls, it was hoped that the alteration would be small. That this was so is shown by the test points for the smallest flows, which do not show any marked tendency to lie away from the line $F/\rho v^2 = 8\mu/\rho v d$. In all, some 170 tests were made (see fig. 2). It will be seen that a range of flows of about 1000 to 1, with a correspondingly greater range of pressure gradients, was covered by these tests of a single pipe. Such a wide range necessitated frequent changes in the measuring devices. Considerable overlapping was adopted as a practice, whenever a change was made; and, under these conditions, some scattering of test points is inevitable. Bearing this in mind the results are satisfactorily consistent.

Fig. 2 shows that for flows less than $\rho v d/\mu = 80$, there is no measurable deviation from the line representing streamline flow in straight pipes. It is not until the Reynolds number exceeds 100, that this curved pipe begins to show a greater resistance than that of a straight pipe of the same diameter and length. It is convenient to think of the curvature as causing an increase of resistance such as that indicated by C in fig. 2. From 100 up to 6000 the effect of the curvature becomes progressively more marked, until at 6000 the resistance is 2·9 times that of a straight pipe in which the flow is assumed to be streamline. It will be seen that the curve definitely touches the line which represents turbulent flow in smooth straight pipes, and that there appears to be a change of law at this point. The conclusion is later drawn that the flow becomes turbulent at a Reynolds number of 6000. The investigation was not intended to extend to turbulent flows, neither was the apparatus suitable. The work was not therefore pursued further in this direction.

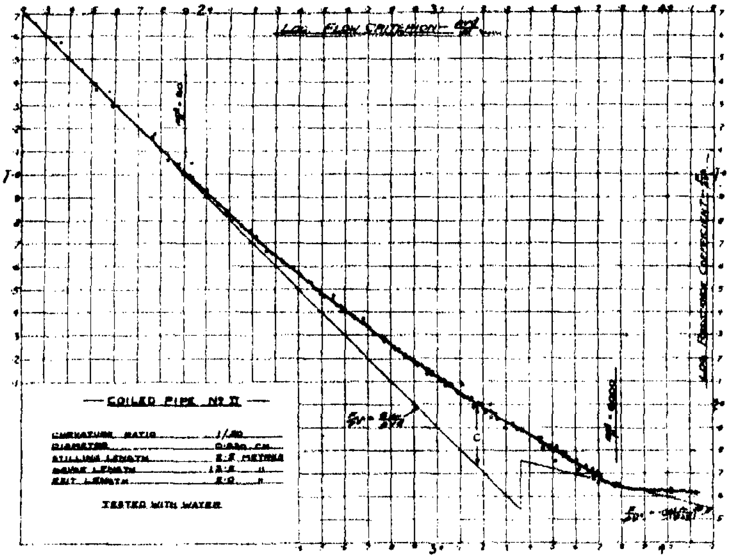

FIG. 2.

Before considering the tests with pipe No. I, which had the greatest curvature ratio 1/15·15, it is desirable to emphasise that accuracy of measurement of the size of the pipe was the foremost consideration in the selection of the pipe for these tests. The earlier work had thrown doubt either upon the strict accuracy of certain assumptions which had to be made in order to compare

Eustice's results with the present experiments, or, alternatively, upon the truth of the assumptions upon which Dean based his theory. The conditions of the problem were such that even a small error in the size of the pipe would, it seemed, leave the question of the effect of curvature in almost as doubtful a position as before. It was felt that, from the point of view of accuracy, a pipe diameter less than 1 cm. could not be used. After several attempts at coiling, a curvature ratio of 1/15 was found to be the greatest which would give reasonable freedom from distortion. The following were the leading dimensions of this pipe :—

Coiled pipe No. I.

Number of turns	$9\frac{1}{2}$.
Mean diameter of turn	15·62 cm.
Total length of tube	485·1 cm.
Coiled length of tube	466·1 cm.
Internal volume	406·0 c.c.
Diameter (from volume)	1·032 cm.
Entrant length (diameters)	178 coiled ; 188·5 total.
Gauge length (diameters)	190·1.
Exit length (diameters)	83·5.

The coiling naturally caused the section to become somewhat oval, but an estimate, based on external measurements, showed that the amount was unimportant. The largest diameter was approximately 5·6 per cent. greater than the smallest. Such a distortion, however, is negligible in its effect upon the relative value of the hydraulic mean depth, which is only 0·04 per cent. less than that of a circle of the same area. On the other hand, the coiling did have considerable effect upon the cross sectional area, and the coiled tube had an area which was roughly 4 per cent. less than that of the pipe in its original straight state.

As stated earlier, some of the tests of this pipe, No. 1, were carried out with oils having a greater viscosity than water. The oil supply was maintained by gravity ; and, as the available height was only 10 feet, it became necessary to use oils with different viscosities in order to cover the desired range of Reynolds number. This procedure has the peculiar advantage that the pressure gradients in the pipe can always, even with the widest range of Reynolds number, be measured accurately with a simple manometer. Additional complications are, of course, involved—the most troublesome is the determination of the viscosity of the oil simultaneously with the tests of the curved pipe—but the resulting gain, both in accuracy and in ease of control more than compensates for the disadvantages.

In its original state, the mineral lubricating oil used had a viscosity which was roughly 500 times that of water. With this particular oil it was possible to explore a range of Reynolds number from 0·45 downwards, but from 0·45 upwards it was necessary to use a fluid with a somewhat lower viscosity. Actually the lubricating oil was diluted with lamp oil to reduce its viscosity, and the range 0·06 to 500 was explored by stages, each necessitating a progressively greater dilution. From 500 upwards, water could be used.

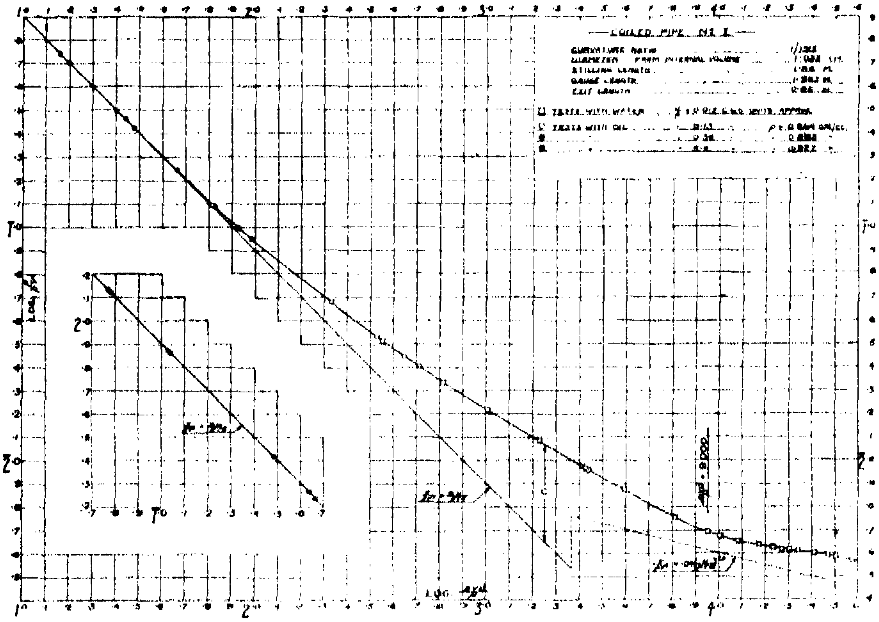

FIG. 3.

The results obtained with this pipe are shown in fig. 3 in which log $(F/\rho v^2)$ is plotted in the usual way on a base of log $(\rho vd/\mu)$. It will be seen that the general character of the curve is similar to that for pipe No. II (fig. 2) although the departure from the line $F/\rho v^2 = 8\mu/\rho vd$ is more marked. The individual test points lie with remarkable consistency on a smooth curve. In this connection it may be mentioned that all the observations were read to at least one-tenth of 1 per cent., though a claim for an accuracy of this order in the result could not, of course, be sustained. The agreement between the tests with oil and those with water at the point where they overlap is particularly satisfactory, since it is an answer to the possible criticism that the use of oil might have introduced errors of a systematic nature. A further check against such errors is also provided by the test points with the smallest flows. These lie accurately on the line $F/\rho v^2 = 8\mu/\rho vd$.

The leading dimensions of pipe No. III were :—

Radius of curvature	3·05 metres.
Total length of pipe	4·25 metres.
Diameter (from flow when straight)	0·298 cm.
Entrant length	650 diameters.
Gauge length	671 diameters.
Exit length	106 diameters.

The test results from this pipe are particularly interesting in connection with the change from laminar to turbulent motion. The pipe was tested both in its original straight state, and also when elastically bent to a curvature of 1/2050. Both sets of results are shown in fig. 4. It will be seen that the increased resistance due to curvature does not become apparent until $\rho vd/\mu = 550$, and that the increase at 2250 is only about half the vertical displacement between the two laws of resistance $F/\rho v^2 = 8\mu/\rho vd$ and $F/\rho v^2 = 0 \cdot 04\,(\mu/\rho vd)^{\frac{1}{4}}$. One of the factors which led to the selection of the particular curvature of this pipe was the desire to know whether the value of the lower critical velocity would

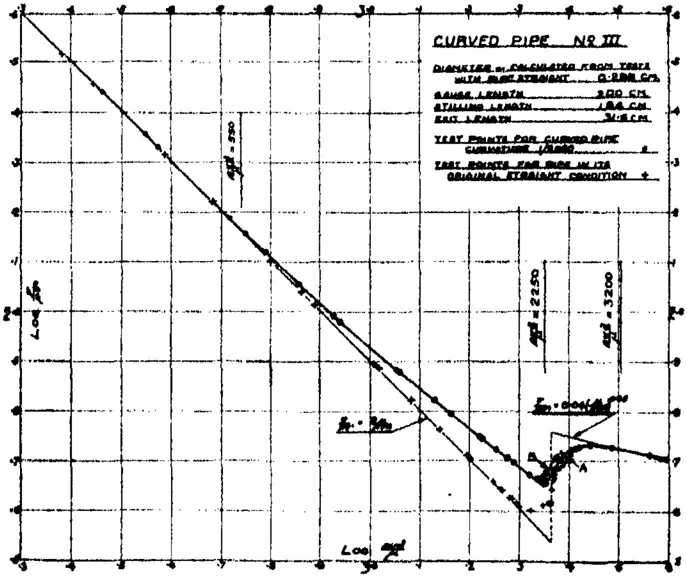

FIG. 4.

be altered appreciably by slight curvature of the pipe. Fig. 4 shows that there is a discontinuity at $\rho vd/\mu = 2250$, and the form of the rising curve leaves but little doubt that, in this pipe, turbulent flow is established in the region 2250 to 3200. It would be unwise, however, to draw any definite conclusion concerning the exact value of $\rho vd/\mu$ at which the rise takes place, for the reason that the conditions of the test of this pipe departed considerably from the ideal. The pipe was only 0·298 cm. in diameter, and, as such a small pipe would be manufactured by drawing down from a larger size, it is more than likely that its interior was not of uniform diameter. Further, the holes for the gauge connections were relatively large, about 0·15 cm. in diameter. Yet another defect became apparent when the calculations were completed. Sufficient damping had not been provided between the manometer and the gauge holes. The effect of this is noticeable in the two curves shown in fig. 4 and marked A and B. The curve A was obtained with a mercury and water manometer, while B was obtained with a simple water manometer. In the latter case there was greater surging of water to and fro between the manometer and the pipe, and this would tend to cause an earlier rise of the curve. In spite of these defects, the tests of this pipe do show definitely that there is not any marked change in the lower critical velocity due to a curvature ratio of 1/2050. At the same time, the effect of this curvature is by no means negligible in its influence upon the resistance, since at $\rho vd/\mu = 2250$ the curved pipe offers roughly 25 per cent. greater resistance.

In order to compare the results given in figs. 2, 3 and 4 with those of Eustice and of Grindley and Gibson, it is necessary to express all in the same manner. As originally published, Grindley and Gibson's results were not reduced to a dimensionless form. Fortunately the test readings were given in detail, and it has been possible to recalculate the results and to express them in the conventional manner—fig. 5. One small adjustment has been made to the original data given by Grindley and Gibson. Their determination of the diameter of the pipe gave the value 0·317 cm. If this value be used then the points relating to flows less than $\rho vd/\mu = 200$ lie below the laminar line for straight pipes. The most probable explanation appears to be that actually the diameter of the pipe was slightly more than 0·317 cm. A matter of 1½ per cent. in the diameter is sufficient to account for the discrepancy. An adjustment of this magnitude has been made, and, accordingly, fig. 5 is based on an assumed diameter of 0·322 cm. The heavy line passing among the test points has been selected by inspection to represent a fair mean of the results.

Eustice tested a relatively short length of flexible hose constructed of rubber reinforced with canvas. The total length of the pipe was 97·8 cm. and the diameter when straight 0·358 cm. This pipe was coiled to various radii in order to study the progressive effect of curvature; but for the purpose of the present comparison it is only necessary to consider one set of tests, namely, that with the greatest curvature. In this case the coil had a mean diameter of 2·59 cm. The coiling caused the pipe to become oval in cross section to a considerable degree (see fig. 6), and resulted in a reduction in the area of 31·2 per cent. Eustice rather ingeniously compensated for this effect by comparing the resistance of the pipe in its coiled state with that when compressed to an oval form between straight boards. He made the comparison when both the cross sectional areas and the velocities were the same in the two cases. This comparison, however, may be open to the objection that, although the areas may be the same in the two cases, it does not follow that the geometrical form of the cross section is also the same. The method used here in comparing this oval pipe with the other circular pipes requires some explanation. The form

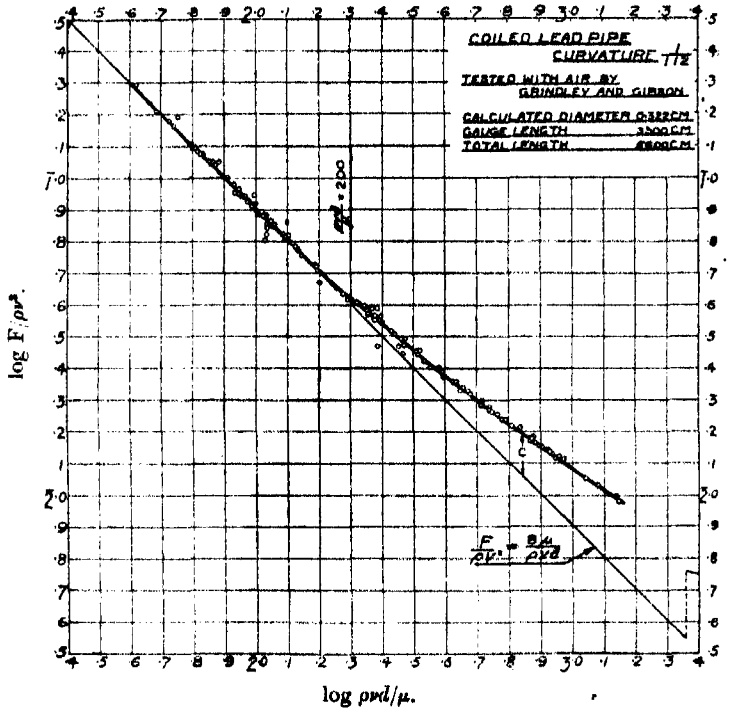

Fig. 5.

of the cross section is assumed to be an ellipse with the ratio of the axes = 2·94.[*] It is customary, when comparing the resistance of non-circular pipes, to make the comparison under conditions giving the same value of the flow criterion $4\rho vm/\mu$. But this comparison is satisfactory only in the case of turbulent flow. For streamline flow in a circular pipe $F/\rho v^2 \times 4\rho vm/\mu = 8$, but in an elliptical pipe of the form mentioned $F/\rho v^2 \times 4\rho vm/\mu = 9$ very closely, a discrepancy of 12½ per cent. In order that the law of resistance may in both cases be expressed as $F/\rho v^2 \times$ flow criterion $= 8$, it is necessary to define the flow criterion, for the elliptical pipe, not as $4\rho vm/\mu$ but as $3{\cdot}56\rho vm/\mu$. In comparing the oval pipe with round pipes, it is here assumed that $3{\cdot}56\, \rho vm/\mu$ is equivalent to the Reynolds number $\rho vd/\mu$ for round pipes. This assumption may be open to criticism, but it does at least provide a practical basis for comparison, and one which is not without the virtue of simplicity. It may give rise to a small discrepancy for turbulent flow, but the amount is not likely to exceed 3 per cent. of $F/\rho v^2$ for the particular section under consideration.

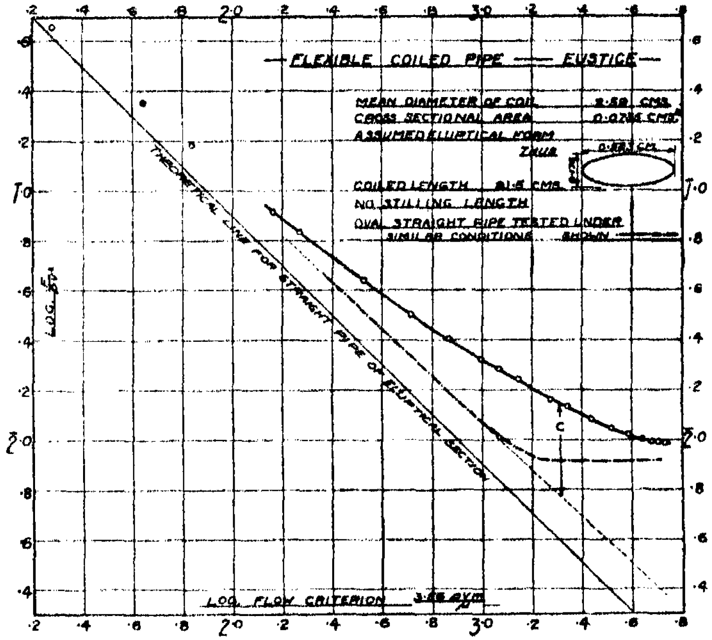

FIG. 6.

---

[*] This ratio is obtained by taking the perimeter to be the same as that of the original unstrained pipe and the area to be 31·5 per cent. less.

In fig. 6 two curves are seen, of which the upper relates to the coiled state, while the lower shows the result obtained when the pipe was squeezed between straight boards. It will be seen that the lower curve lies above the theoretical line. This is probably due to the fact that the pipe was not provided with an adequate stilling length, although it might be due partly to a lack of uniformity in the cross sectional area. It may be mentioned that, while the curved pipe would be less influenced by the lack of stilling length, yet, on the other hand, it would be somewhat more sensitive to irregularity of cross sectional area. It is not unreasonable, therefore, to regard the curvature in this case as causing displacements such as that marked C in fig. 6.

The five sets of results shown in figs. 2 to 6 are more easily compared when they are replotted in a modified form. In fig. 7, instead of the resistance coefficient $F/\rho v^2$, curves are given showing the increase of this coefficient of resistance caused by the curvature, plotted on the usual base $\rho v d/\mu$. The observed coefficient for the curved pipe is divided by the theoretical value of the coefficient for laminar flow through a straight pipe in which the Reynolds number has the same value, and the resulting quotient is then plotted logarithmically on a base of the flow expressed as a Reynolds number. The ordinates of fig. 6 are equal, therefore, to the vertical displacements such as C in figs. 2 to 6—an advantage of logarithmic plotting.

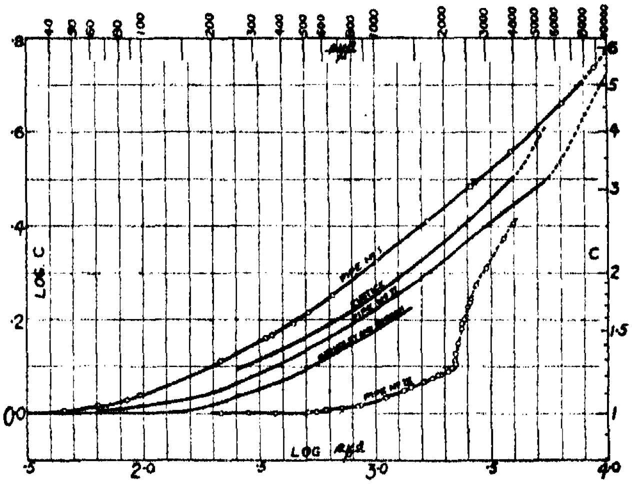

FIG. 7.

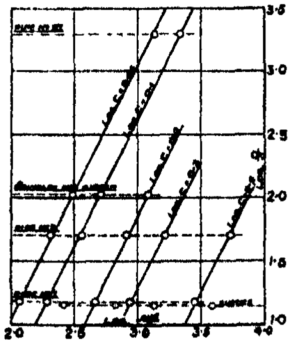

FIG. 8.

The results are now in a form which enables them to be considered in relation to Dean's theory. But, before doing so, it is well to point out that the theory involves certain assumptions which may or may not be in accordance with the actual conditions of flow. In this respect, of course, it is like all other theories, in that it demands experimental confirmation before it can be accepted at all, and a clear definition of the range over which it applies before it can be used with confidence. Fig. 7 provides considerable information on both these points. Dean showed mathematically that, for a given pressure gradient, the ratio of the mass flows through two pipes of different curvatures is determined by the value of the criterion $\rho vd/\mu\,(d/D)^{\frac{1}{2}}$. It is more convenient to express this result in an alternative form, by stating that the ratio C of the resistance coefficient of a curved pipe to that of a straight pipe (in which the flow number $\rho vd/\mu$ is the same) is a function of the criterion $\rho vd/\mu\,(d/D)^{\frac{1}{2}}$.

If C is actually a single valued function of $\rho vd/\mu\,(d/D)^{\frac{1}{2}}$ then, owing to logarithmic plotting, the various curves of fig. 7 should all be of identical form, and the influence of the different curvature ratios should be represented by a horizontal displacement of each curve in relation to its neighbours. This displacement should be equal to half the difference of the logarithms of the curvature ratios of any two pipes under consideration. Fig. 7 shows that, on the whole, the experimental results do conform to these requirements. The shape of those parts of the curves indicated by full lines is approximately the same, and the spacing appears to be approximately proportional to $\log (d/D)^{\frac{1}{2}}$. The spacing, however, varies somewhat for different values of C, and reference to fig. 8 is necessary in order to obtain conclusive evidence. In fig. 8, which shows the Reynolds number for a given value of C plotted logarithmically against the appropriate value of D/d, the uniform slope of 2–1 of the lines, confirms Dean's deduction conclusively. The only set of points which systematically disagree are those relating to Eustice's pipe. The discrepancy was not unexpected however, and does not weaken the general conclusion. On the contrary, bearing in mind the different entry conditions of these tests, the form of this curve in fig. 7 is sufficiently like those of the round pipes to lend support to the view that the function $c = f[\rho vd/\mu \,.\, (d/D)^{\frac{1}{2}}]$, determined by experiments with round pipes, may be found to apply also to other cases of flow in curved paths. In plotting the points marked Eustice in fig. 8, the curvature ratio of this pipe was taken as $0{\cdot}178/2{\cdot}59$ or $1/14{\cdot}6$. It is to be expected that a pipe having a wide cross section would show less curvature effect than a circular pipe—and this is confirmed. The oval pipe gives approximately the same resistance as a circular pipe of curvature

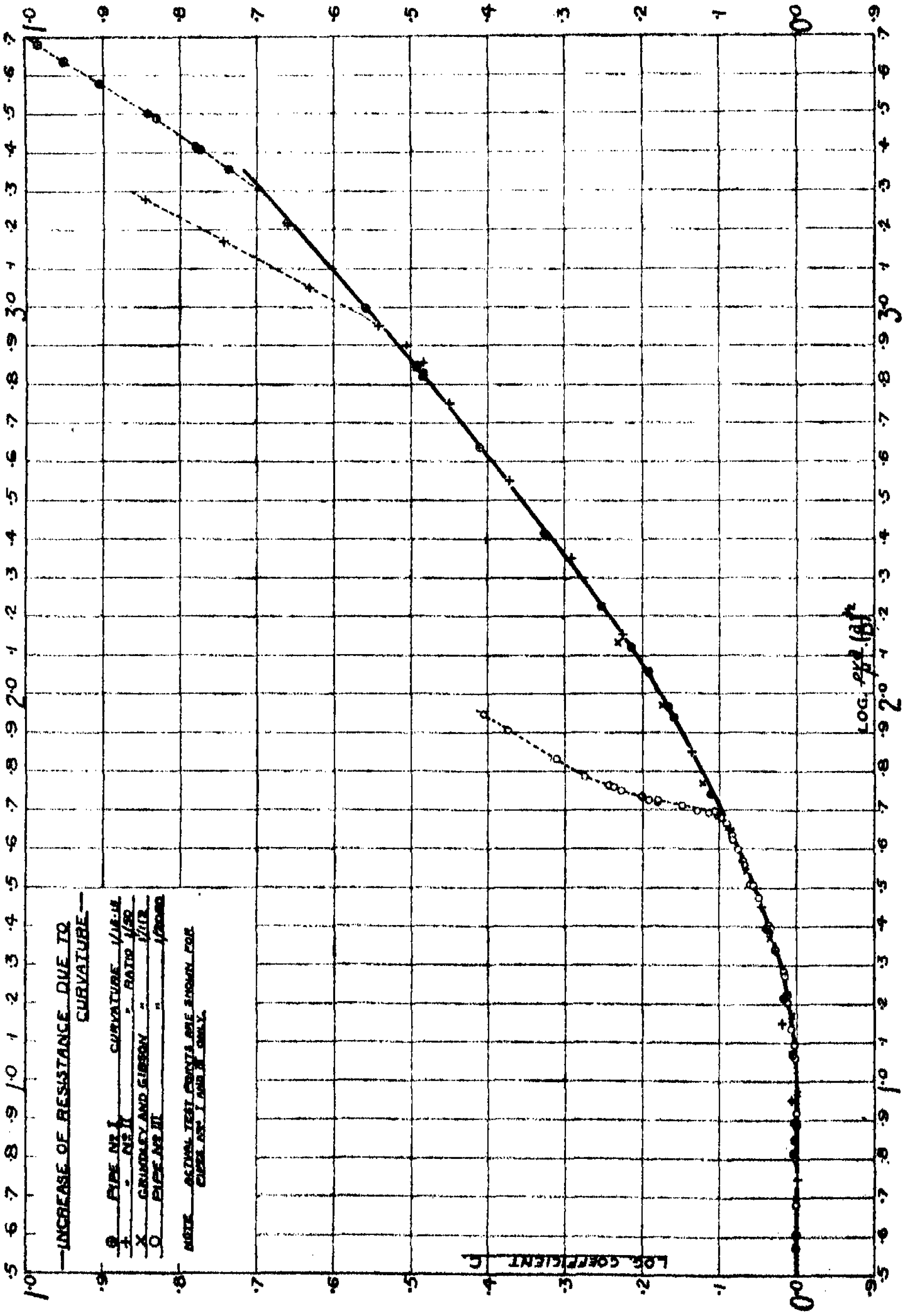
—INCREASE OF RESISTANCE DUE TO CURVATURE—
● PIPE No I CURVATURE 1/15·15
+ " No II " RATIO 1/50
X GRINDLEY AND GIBSON " 1/112
○ PIPE No III " 1/2050
NOTE ACTUAL TEST POINTS ARE SHOWN FOR PIPES No I AND III ONLY.
LOG. COEFFICIENT C
LOG. ρvd/μ (a/R)^½
1·0
·9
·8
·7
·6
·5
·4
·3
·2
·1
0·0
·9
1·0
2·0
3·0
·5
·6
·7
·8
·1
·2
·3
·4

FIG. 9.

ratio = 1/32. The ratio Effective Curvature/Nominal Curvature for the oval pipe is roughly the same therefore as the Breadth/Width ratio of its cross section.

The results given in fig. 7 are replotted in fig. 9 in a more general form. Here, the ordinates are identical with those of fig. 7, but Dean's criterion, $\rho v d/\mu \,.\, (d/\mathrm{D})^{\frac{1}{2}}$, is used for the abscissæ. All the experiments—with the exception of those of Eustice, which are omitted from this figure—conform satisfactorily to a single curve for values of the criterion up to 50. Above this value the various curves progressively leave the main curve, and the points of successive departure appear to depend upon the curvature ratios of the particular pipes concerned. It seems clear that these points, at which the individual curves leave the main curve, coincide with a change in the type of motion, and it is perhaps permissible to suggest that the change is from the kind of double helical streamline motion described by Dean, to something very closely akin to the ordinary turbulent motion associated with flow through straight pipes. Dean, in his theory of the manner in which curvature causes an increase in the resistance, shows that it is due, in effect, to an internal circulation in the plane of the cross section of the pipe, superimposed upon the normal streamline velocity distribution. Fig. 10, a reproduction of one of Dean's explanatory diagrams, shows the circulation effect produced by the pressure gradients which arise owing to centrifugal action. If complete slipping at the boundary were to occur, and as a result the fluid were to move through the tube much as a rubber cord might be drawn through it, then the whole effect would cease. In a straight pipe, the velocity distribution curve for turbulent flow is considerably flatter than that for streamline flow. In the former case the maximum velocity is only about 1·25 times the mean velocity, as compared with twice the mean velocity in the latter. The effective radial pressure gradients for turbulent flow in a curved pipe may thus be expected to be considerably less, at a given Reynolds number, than if the flow were streamline. Since the pressure gradients are less, and since, apart from this, eddy motion itself would tend to restrict an ordered circulation, it follows that the effect of curvature is likely to become less marked. A closing up of the

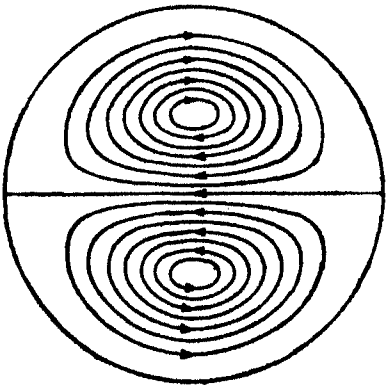

FIG. 10.

horizontal spacing of the various curves in fig. 7 is to be expected, therefore, when the flow becomes turbulent. This closing up, which it will be seen is well defined, corresponds to the dispersion in fig. 9. This marks the limit of the range over which Dean's theory applies. Bearing in mind that the motion assumed in deriving the theory is essentially streamline, it is reasonable to suggest that the points at which the respective curves leave the main curve, are those at which turbulent motion begins.

It may be said, therefore, that the points at which the individual curves leave the main curve in fig. 9, in providing a rough indication of the upper limit of Dean's theory, also provide an indication of the beginning of turbulence. The information is little more than qualitative, but nevertheless it is sufficient to show that this limit does not depend upon the value of the Reynolds number alone—neither does it depend upon Dean's criterion. On the contrary, it appears that turbulence begins—under the conditions of the tests—when the resistance coefficient $F/\rho v^2$ decreases to $0 \cdot 0045$, more or less irrespective of the curvature of the pipe. Dean's theory applies only when the value of $F/\rho v^2$ is greater than $0 \cdot 0045$.

It should be noted that, although the state of the fluid before it entered the pipe may have differed somewhat in the various tests, yet in every case there were irregularities in the passages just before the curved pipes. These irregularities—a thermometer pocket, stop cock, and sharp bend—would presumably tend to augment any disturbance originally present in the fluid and would thus tend to build up complete turbulence. It is not unreasonable, therefore, to expect a considerable degree of turbulence in the fluid as it was fed to the pipe, particularly in the case of those tests in which the Reynolds number exceeded 2000. In spite of this, it appears that a Reynolds number not less than 9000 is necessary in order that the turbulence shall persist throughout the length of the pipe when the curvature is 1/15. Even with the relatively small curvature of 1/50, streamline flow is maintained up to 6000, a figure more than twice that which would be obtained were the pipe straight. There is an indication, therefore, that for large disturbances, flow in curved pipes is more stable than flow in straight pipes. This is directly opposed to the opinion sometimes expressed that curvature tends to cause instability.

In conclusion, the foregoing results show that the loss of head h in a length l of coiled pipe of diameter d, in which the mean velocity of flow is v, may be expressed by the equation

$$h = C \,.\, 8\mu/\rho v d \,.\, 4lv^2/gd,$$

where μ/ρ is the kinematic viscosity of the fluid, and where the numerical coefficient C depends upon both the flow and the curvature.

The value of C is given by the empirical equation

$$C^{-1} = 1 - [1 - (11{\cdot}6/\kappa)^{x}]^{1/x},$$

where $\kappa = \rho v d/\mu \,.\, (d/D)^{\frac{1}{2}}$ and $x = 0{\cdot}45$.

This equation represents the experimental results for values of κ greater than 11·6 and up to at least 2000. Below $\kappa = 11{\cdot}6$, $C = 1$. Typical values of C, taken from the curve in fig. 9, are given in the table.

$\rho v d/\mu \,.\, (d/D)^{\frac{1}{2}}$ κ.	$Fd/8\mu v$ C.	$\rho v d/\mu \,.\, (d/D)^{\frac{1}{2}}$. κ.	$Fd/8\mu v$ C.
0	1	60	$1{\cdot}30_9$
11·6	1	100	1.50_3
13	$1{\cdot}01_4$	200	$1{\cdot}89_7$
17	$1{\cdot}02_8$	400	2·48
20	$1{\cdot}04_5$	600	2·85
25	$1{\cdot}07_9$	1000	3·61
40	$1{\cdot}18_9$	2000	4·93

These values are probably true for a wide range of fluids and pipes, but there is the definite limitation that they do not apply under conditions in which the product $C \,.\, 8\mu/\rho v d$ is less than 0·0045.

The author expresses his indebtedness to Mr. W. A. de Silva, a research student, both for the entire experimental work in connection with pipe No. II and for the calculations necessary to reduce Grindley and Gibson's results to dimensionless form. He would also like to thank Profs. Gilbert Cook and Alex. H. Jameson, of King's College, for their support.

On the Measurement of the Dielectric Constants of Liquids, with a Determination of the Dielectric Constant of Benzene.

By L. Hartshorn, A.R.C.S., B.Sc., D.I.C., and D. A. Oliver, B.Sc., National
Physical Laboratory.

(Communicated by D. W. Dye, F.R.S.—Received January 4, 1929.)

Introduction.

It has long been recognised that the dielectric constant of a substance gives an important indication of its constitution, and the classical papers of Nernst and Drude giving methods for the determination of dielectric constants, have been followed by a long series of papers giving the dielectric constants of several hundreds of pure liquids and solutions. Since the publication of Debye's dipole theory in 1912, the literature of the subject has become even more voluminous than before.

In surveying the mass of data one is struck by the very large discrepancies which exist in the values obtained by different observers for any one substance, and it is very difficult to decide whether they are due to the difficulty of preparing and purifying the substance, differences in experimental conditions such as frequency of the applied E.M.F., or errors in the methods of measurement. In order to make it possible to compare the results of different observers, and to provide a fundamental basis for new measurements, it is important that the value of at least one standard liquid should be known with unquestionable accuracy. The object of the present investigation was to provide such a value. Benzene was chosen as the standard liquid since it has been very widely used in the past, and it is used as a standard in the measurement of other physical properties.

At least twenty determinations of the dielectric constant of benzene are on record, the values given ranging from 2·24 to 3·8. The high values are only obtained when the measurements are made with alternating E.M.Fs. of very high frequency (of the order 10^{10} cycles per second), and since measurements at these frequencies are very difficult the values must be viewed with a certain amount of suspicion. If we restrict ourselves to frequencies below 5×10^8 cycles per second, we find that there are a number of values in the region 2·28, and from a survey of all the available data in 1925 it was concluded that the most probable value for the dielectric constant of benzene at 20° C. was $2{\cdot}283 \pm 0{\cdot}002$. Over the range 10° to 30° C. the variation of dielectric constant with temperature appeared to be linear, the actual change in the value being $-0\cdot0019$ per 1° C. In the year 1925 two new determinations were made, each giving a value of 2·24. This discrepancy was regarded as very serious, as in one case it was claimed that the accuracy obtained was greater than had hitherto been reached. In the preparation of data for International Critical Tables, by one of us, the older value 2·283 had been used throughout, and thus it was of the utmost importance that one or other of the values should be checked. A study of the various methods of measurement revealed the fact that all of them involved errors which had not been satisfactorily avoided. In the method to be described it is shown that these errors are eliminated, so that a determination of the dielectric constant of a given liquid can be made with a probable error of only one part in ten thousand.

Principle of the Method.

Most methods for the determination of dielectric constants consist of two measurements of the capacity of a condenser, the first measurement being made when the dielectric medium of the condenser is air (or a vacuum), and the second when the dielectric medium is the substance under investigation. The ratio of these two capacities gives the required value of the dielectric constant. The capacity to be measured is usually small—less than 0·001 microfarad—and, in general, the capacity when the dielectric medium is air (which will be referred to as the " air capacity ") is considerably smaller than that when the dielectric medium is the substance under examination (in our case referred to as the " liquid capacity ").

The dielectric constant of the substance is only accurately given by this ratio if certain conditions are satisfied in making the measurements, and these conditions can only be fulfilled by using a test condenser of special design. The essential conditions are :—

(*a*) The " air capacity " must be located entirely in air, *i.e.*, none of the lines of force representing it must pass through solid insulating material, such as, for example, a glass container, or supporting pillars or washers for the plate systems of the condenser.

(*b*) The " liquid capacity " must be located entirely in the liquid under test, and must be geometrically identical with the " air capacity."

Effects of Connecting Leads.—Whatever the method of measurement used, it will be necessary to connect the condenser to the measuring circuit by a pair of connecting wires, and these will possess a certain capacity (the " leads capacity "). The above conditions can only be satisfied if the " leads capacity " can be eliminated from the measurements, since the leads can never be entirely immersed in the liquid in determining the " liquid capacity." The elimination of the leads capacity is one of the most important parts of the measurements, so that it must be considered in some detail. Let AB, fig. 1, represent the two plate systems of a condenser, which can be connected to a measuring circuit by the leads L_1, L_2. Suppose it is desired to measure the capacity C_{AB} between A and B. In addition to C_{AB} it is important to recognise that the system comprises several other capacities, viz., the capacity c_2 between the two leads L_1 and L_2, and the " cross capacities " c_3 and c_4 between the two plate systems and the opposite leads. In addition, when A and B are disconnected from L_1 and L_2 respectively, there will also be the capacities c_5 between L_1 and A, and c_6 between L_2 and B. Now a little consideration will show that when L_1 and L_2 are connected to A and B respectively, the total capacity of the system is $C_{AB} + c_2 + c_3 + c_4$. If now the lead L_1 is disconnected at A, the capacity becomes $c_5 (C_{AB} + c_3)/(c_5 + C_{AB} + c_3) + c_2 + c_4$. If both L_1 and L_2 are disconnected at A and B the capacity becomes a still more complicated function of the various component capacities. If again the condenser AB is removed, we are left with a single leads capacity c_2', which is slightly different from c_2. The important point is that it is not possible to determine the capacity C_{AB} by taking the difference of the readings obtained when the condenser is firstly connected to the leads, and secondly disconnected, either at one or both plate systems. Almost all previous observers have assumed that satisfactory measurements can be made in this way, and many of the existing discrepancies are probably due to this. The authors have used a special method whereby the capacities c_2, c_3, c_4, c_5 and c_6 are almost completely eliminated and the single capacity C_{AB} can be determined.

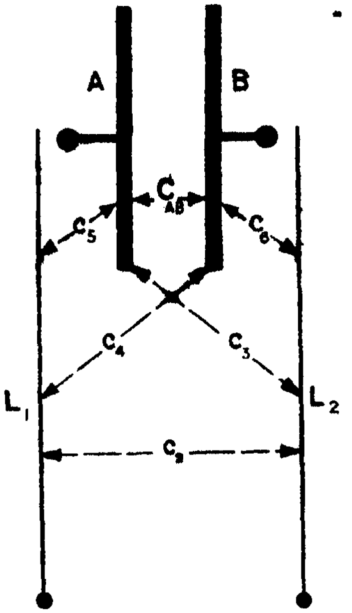

Fig. 1.—Component Capacities of Condenser and Leads.

Although enormous sensitivities can now be obtained in capacity measurements, especially at radio frequencies, so that changes in capacity can be measured to an accuracy of 0·001 μμF., we came to the conclusion, as a result of some preliminary measurements, that in measuring a single capacity such as C_{AB}, the probable error would be at least 0·01 μμF. owing to the difficulties associated with these leads capacities. Thus the larger the capacity to be measured, the smaller is the probable percentage error due to leads capacities. The accuracy obtainable in a dielectric constant determination will therefore depend almost entirely on the accuracy with which the "air capacity" can be measured, this being the smaller of the two capacities required. It is important therefore, to make the test condenser of as large a capacity as possible. As the authors were aiming at an accuracy of one part in ten thousand, it was concluded that the condenser should have a capacity of at least 100 μμF., and should preferably be larger than this, as the error in the elimination of the leads capacities may be greater than 0·01 μμF. The "air capacity" actually used varied from 117 μμF. to 334 μμF.

Effects of Solid Insulation.—It is obvious that some form of solid insulating material must be used to separate the two plate systems of the test condenser, and a certain amount of capacity must be located in this material. In order to satisfy conditions (*a*) and (*b*) this capacity must be eliminated from the measurements. For this purpose the test condenser was given the form shown diagrammatically in fig. 2. Here A and B represent the plate systems of the condenser, which are attached by small insulators *pp* to a third conductor S, which forms an electrostatic shield for A and B. The whole system may be regarded as consisting of three capacities, the mutual capacity C_{AB} of the plate systems A and B, and the capacities C_{AS} and C_{BS} between the plate systems and the screen. Now although there is a solid insulator in the electrostatic field represented by each of the capacities C_{AS} and C_{BS}, the mutual capacity C_{AB} is located entirely in air, since all the lines of force which pass through the insulator *p* from A must terminate on the screen S; they cannot possibly

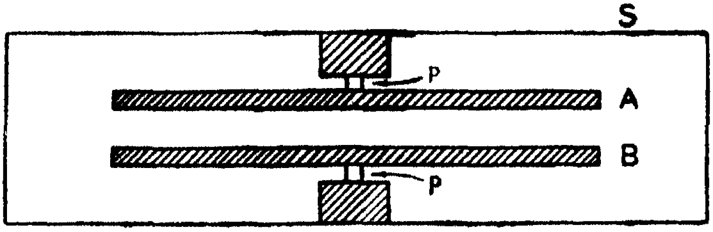

FIG. 2.—Condenser with perfect mutual Capacity C_{AB}.

reach the plate B. Also since none of the lines of force of the system can pass out of the screen S, the condenser can be placed in any surrounding without affecting the three component capacities. Thus if the condenser is given the form shown in fig. 2 and the mutual capacity C_{AB} only is measured, the two conditions essential for accuracy can be satisfied.

The Measuring Circuit.—It will be noticed that in order to satisfy the conditions for high precision, the measuring circuit used must permit of the separation of the component capacities of the electrostatic system formed by the test condenser and its connecting leads. It must be possible to measure the mutual capacity C_{AB}, and to eliminate the capacities not required, viz., the capacities to shield C_{AS}, C_{BS}, the leads capacities c_2, c_3, c_4, c_5 and c_6 (fig. 1), and also the capacities to earth of the whole system. The simple four-arm Wheatstone network is unrivalled for this class of work, and was therefore used by the authors. The arrangement is shown in fig. 3. The bridge network GDEF consists of two capacity arms C_1 and C_2, and two resistance arms R_3 and R_4. Alternating voltage of telephonic frequency is applied between the points G and E, and a telephone T connected to the points F and D serves as a detector of balance. If the bridge is balanced by varying one or more of the quantities C_1, C_2, R_3, R_4, a condition of balance is $C_1R_4 = C_2R_3$. If the resistance arms R_3 and R_4 are shunted by capacities C_3 and C_4, and one or both of these is adjusted so as to preserve the balance of the bridge the above equation still holds.

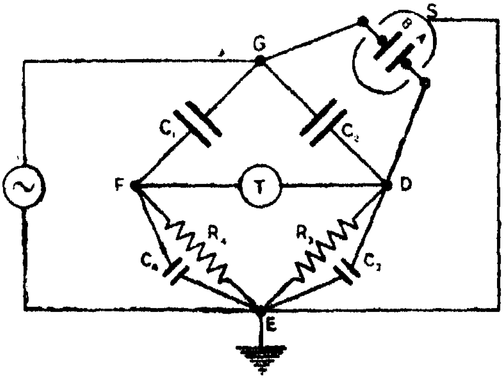

Fig. 3.—The Bridge Network.

This bridge may be conveniently used for the measurement of small capacities in the following way. C_1, C_2, R_3 and R_4 are given suitable values and the bridge is balanced by varying one of these quantities, say C_1. The capacity to be measured is then connected to the points G and D, *i.e.*, it is placed in parallel with C_2, and balance again obtained. From the change in the bridge reading the capacity added to C_2 may easily be calculated. In taking the difference of two readings in this way greater accuracy is obtained than is possible when only one reading is taken, since errors common to the two readings cancel out.

The capacity thus measured is the total capacity added to the points G and D. We have now to show how the bridge will eliminate component capacities not required, and how this property can be used to eliminate the capacities associated with the leads. Let the test condenser be connected to the bridge as in fig. 3, the plate systems A and B being connected to the points D and G respectively, and the screen S being connected to the point E which is earthed. The capacity C_{BS} is now connected across the points G and E. It therefore merely shunts the source of alternating current and does not affect the bridge reading. The capacity C_{AS} is connected across the points D and E, and is therefore in parallel with the condenser C_3. This will affect the readings of C_3 or C_4 at balance, but the equation $C_1R_4 = C_2'R_3$, where C_2' represents the total capacity between the points G and D, still holds. It is evident that $C_2' = C_2 + C_{AB} + c$, where c represents the resultant leads capacity, and thus the bridge reading, C_1, is independent of the screen capacities C_{AS} and C_{BS}, but is a linear function of the mutual capacity C_{AB}. Since the test condenser is perfectly shielded by the screen S, which is earth connected, there are no additional earth capacities to consider.

In order to consider the elimination of the leads capacity, let the test condenser and leads be represented by the network of fig. 1, the leads L_1 and L_2 representing the wires joining the plates A and B to the points D and G respectively. For a complete representation the screen S and its associated capacities should be included in fig. 1, but as we have shown that these capacities are eliminated in the bridge measurements, they will not be considered further. The leads L_1 and L_2 must, however, be supposed to enter the screen through small holes. Provision must also be made for breaking the connection between L_1 and A, and L_2 and B, by displacing the leads L_1 and L_2 the slightest possible amount, so that the capacities c_2, c_3, c_4, etc., may be considered entirely unaltered by the disconnection. Now let the connections be made as follows, the screen S being earthed the whole time and the bridge being balanced after each change of connection:—

(α) Connect L_1 to A and L_2 to B. The total capacity added to condenser C_2 is evidently $C_{AB} + c_2 + c_3 + c_4$.

(β) Break the connections L_1A and L_2B and connect A and B to the screen S. Capacities to A and B, viz., c_5 and c_3, c_4 and c_6, have now become capacities to screen and are eliminated from the measurements as previously explained, while C_{AB} is short-circuited and disappears. The capacity added to C_2 is now c_2.

(γ) Make the connection L_2B and disconnect B from the screen. The capacity added to C_2 is now $c_2 + c_4$.

(δ) Connect A to L_1; disconnect A from the screen; disconnect L_2B; connect B to the screen S. The capacity finally added to C_2 is $c_2 + c_3$.

Since each of the bridge readings, (α), (β), (γ), (δ), is a linear function of the corresponding capacity added to C_2 between the points G and D, the mutual capacity C_{AB} is given by the reading $(\alpha + \beta) - (\gamma + \delta)$. Thus by taking these four readings the various lead capacities are completely eliminated. The capacities to screen are also eliminated, and the quantity measured is the true mutual capacity of the two plate systems A and B, which is purely an " air capacity." If now the test condenser is immersed in the liquid to be investigated so that it completely fills the screen, and the mutual capacity of A and B is again measured, we get a pure " liquid capacity," and the ratio of the two capacities gives the dielectric constant of the liquid with reference to that of air, no corrections being necessary.

Mechanical Design of Test Condenser.—It will now be apparent that the design of the test condenser must satisfy a number of important requirements :—

(1) It must possess a capacity of at least 100 μμF.

(2) It should be as rigid as possible, so that the geometrical configuration is the same for the " air capacity " and " liquid capacity " measurements.

(3) The air gap between the plates must be sufficiently large to ensure that unavoidable minute displacements of the plates will cause no appreciable changes in capacity. 1 mm. was taken as the minimum permissible air gap.

(4) It must be completely enclosed in a conducting screen.

(5) The plate systems should be insulated from the screen, the solid insulating material being so arranged that none of it lies in the electrostatic flux connecting the two plate systems A and B directly.

(6) It must be possible to disconnect the plate systems A and B from the leads at points inside the screen, and this disconnection must cause the smallest possible change in the position of the leads.

(7) Any tendency to form air bubbles inside the condenser when filling with the liquid must be avoided.

Details of the design of a condenser fulfilling these requirements will be given in the following section. Meanwhile it should be noticed that the condenser will necessarily need a considerable quantity of liquid to fill it, say, 500 c.c. This is a disadvantage when it is desired to investigate liquids of the highest possible purity, since such large quantities are seldom available. In this investigation it was therefore decided to make measurements of the highest accuracy on a commercial liquid (benzene, A.R. grade), and then to compare this standardised benzene with the more highly purified samples by a comparison method requiring a smaller quantity of liquid. In the comparison measurements the capacities associated with the leads and the solid insulating material were included in the measurements, *i.e.*, the method used was essentially the same as that employed by Nernst, Turner,[*] and many later investigators. Measurements of the capacity of the test condenser are made : (*a*) when filled with dry air, (*b*) when filled with the standard liquid, (*c*) when filled with the liquid under examination. Measurements (*a*) and (*b*) allow the stray capacities to be calculated, and assuming that they are the same for measurement (*c*) the dielectric constant of the liquid under test is obtained. In the particular case in which the two liquids have very nearly the same dielectric constant, the assumptions are sensibly true, and high accuracy is obtainable. Since the same accuracy of capacity measurement is necessary in both the standard and the comparison measurements, the test condenser for the comparison measurements should also have a large capacity. The comparison condenser was designed to satisfy conditions (1), (2), (3), (4) and (7) enumerated above. Conditions (5) and (6) were ignored in this case and the condenser designed to require as small a quantity of liquid as possible, subject to the other conditions being fulfilled.

Detailed Description of Apparatus.

(*a*) *The Standard Test Condenser.*—This condenser is shown in fig. 4. The electrodes consist of circular brass plates, 5 mm. thick. Each plate system is insulated by three small pieces of quartz, about 1 mm. cube, placed centrally on three brass pillars, rigidly attached to the base of the instrument. The holes in the bottom plate were chamfered in order to prevent the formation of air bubbles at this point when filling the condenser with liquid. The various connections and disconnections were made by means of two pairs of wire plungers which pass through the top of the shield and make contact with the plates. One plunger of each pair is insulated by a short length of thick-walled glass tubing, held in position by a contracting brass collar, which is made a push fit in a hole through the top of the shield (A, fig. 4). The other plungers pass through small brass bushes (B, fig. 4). These uninsulated plungers were permanently connected by a fine wire to the screen terminal. The insulated plungers were connected to fine wires passing to the measuring apparatus and formed the leads L_1 and L_2 of fig. 1. Thus, either plate system was connected

---

[*] Nernst, 'Z. Phys. Chem.,' vol. 14, p. 622 (1894); Turner, 'Z. Phys. Chem.,' vol. 35, p. 385 (1900).

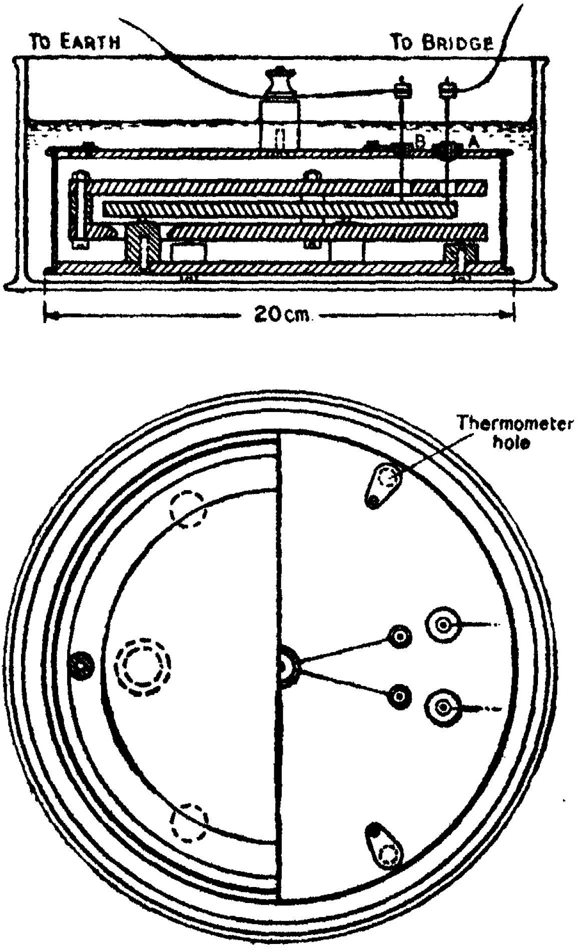

Fig. 4.—Standard Test Condenser (not to scale).

to the bridge, by depressing the appropriate plungers. To disconnect a plate system from the bridge and to connect it to earth, the insulated plunger was raised a fraction of a millimetre and the corresponding uninsulated plunger pressed into contact. In this way all the connections and disconnections could be made without moving the leads sufficiently to cause any detectable changes in the component capacities of the system.

Three sets of supporting pillars for the central plate, and separating cylinders for the two outer plates were made, with the heights necessary to give air gaps of 1, 2 and 3 mm. between the plate systems, as desired. The mutual capacities of the plate systems corresponding to these air gaps are 334, 172 and 117 $\mu\mu$F. respectively.

(*b*) *The Comparison Test Condenser.*—This is shown in detail in fig. 5. It consists essentially of a flat plate condenser, contained in a stoppered glass tube, into which the liquid can be distilled through the inlet D. The displaced air escapes through the outlet E to which a drying tube is attached. The bottom outlet F allows the liquid to run out with the minimum disturbance of the apparatus, and is also necessary for drawing dry air through the condenser, as a preliminary to an "air capacity" measurement. The internal diameter of the glass tube was 4·6 cm. and a length of 8 cm. was allowed for

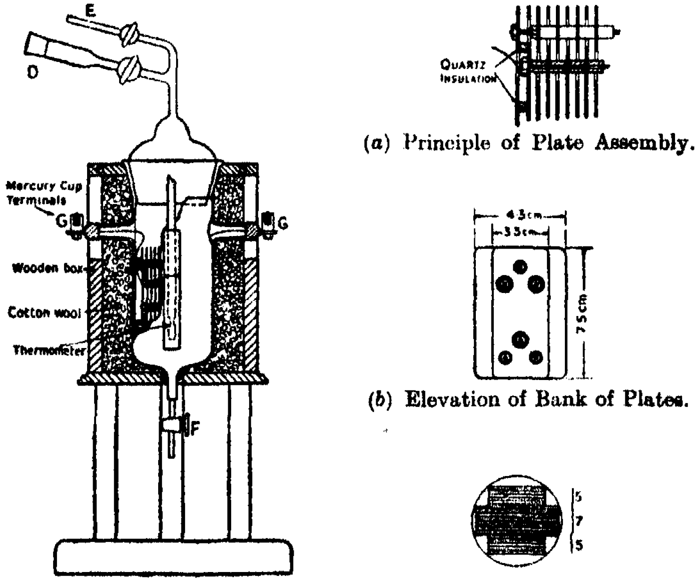

(*a*) Principle of Plate Assembly.

(*b*) Elevation of Bank of Plates.

General Arrangement.

(*c*) Plan of Bank of Plates.

FIG. 5.—Comparison Test Condenser.

the condenser plates, which were arranged to fill this space as completely as possible.

The general arrangement of the details is shown in fig. 5 (*a*), (*b*) and (*c*).

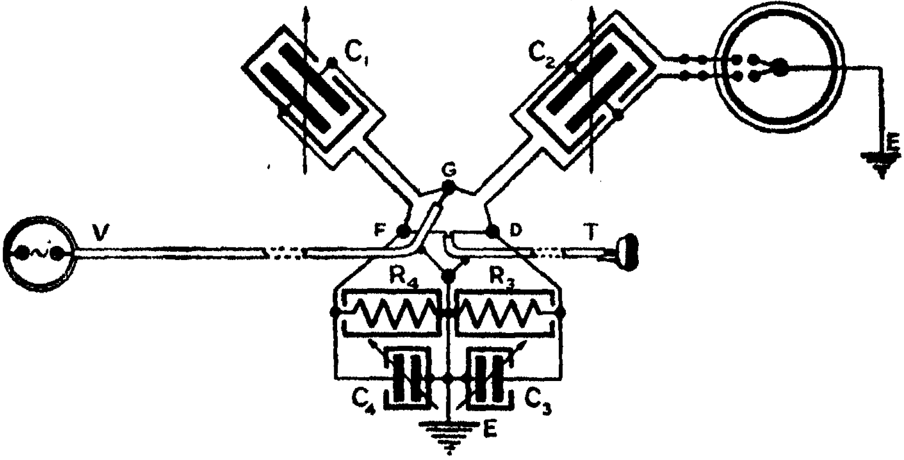

FIG. 6.—The Bridge showing Shielding Arrangements.

Each set of plates is clamped up separately, and the two sets are insulated from one another, by small slips of quartz, inserted between the end plates of each bank. These were gripped in position by tightening the outer clamping nuts. Brass springs held by these nuts were arranged to press against the sides of the glass tube, thereby making the whole rigid. A clearance of a few millimetres was left between the plates and the bottom of the tube to avoid undue contact with the glass.

This condenser was shielded as completely as possible by clamping a flexible cylinder of thin brass sheet round the glass tube. Parts not covered by this shield were wrapped with tin foil, care being taken to secure good contact between all parts of the shield. The temperature was read by means of a thermometer which stood in a brass tube brazed on to the shield. Sufficient mercury was poured into this tube to cover the bulb of the thermometer and so make good thermal contact with the condenser.

The capacity of the condenser was of the order of 440 $\mu\mu$F., and 120 c.c. of the liquid were required for satisfactory comparisons.

(*c*) *The Alternating Current Bridge.*—The general arrangement of the bridge has already been described (fig. 3). The components actually used were all shielded as completely as possible by having them enclosed in metal cases. The electrical connections, including those of these shields, are shown in detail in fig. 6. C_1 was a variable standard air condenser of maximum value 3000 μμF., which was accurately calibrated, C_2 was an adjustable condenser of the same range of great constancy, but not necessarily accurately calibrated, R_3 and R_4 were non-reactive resistance coils of values ranging from 1000 to 5000 ohms. C_3 and C_4 were variable air condensers with a maximum value of about 2000 μμF. The detector T was a 1000-ohm Brown earpiece. The leads connecting it to the bridge were enclosed by a flexible metal sheath which was connected to earth. The metal case of the telephone was also connected to this sheath. The lead from E to the source of current V consisted of a brass tube, through which the lead from G to V passed. In this way, the lead to G which was at high potential, was enclosed by an earthed shield.

Since all the components of the bridge were carefully shielded we may legitimately assume that silence of the telephone detector indicated a true balance of the bridge network, quite independent of undesirable capacity effects between the bridge, the detector and the oscillator. Also as previously explained, stray capacities in the test condenser and its connecting leads were completely eliminated, the probable error due to these being certainly less than 0·03 μμF. The bridge, however, necessarily departs slightly from the ideal case shown in fig. 3, since the resistance coils will never be perfectly non-reactive, and the condensers C_1 and C_2 will never be "perfect," *i.e.*, they will possess conductances, which, although very small, are at least measurable. It remains to consider the effect of these instrumental defects upon the measurements. If G_1 is the conductance of the condenser C_1, it is convenient to consider the "loss angle" δ_1, defined by the equation $\tan \delta_1 = G_1/C_1\omega$, where $\omega = 2\pi \times$ frequency. If the total conductance in the arm GD (fig. 6) of the bridge is G_2, and the total capacity is C_2, its loss angle is

$$\tan^{-1} G_2/C_2\omega = \delta_2.$$

The resistance ratio arms of the bridge will possess a certain residual inductance, and a certain self capacity, but at any given frequency they may be regarded as consisting of a certain "equivalent shunt resistance" which may be slightly different from the direct current resistance, in parallel with a certain small capacity. Let R_3 and R_4 in fig. 6 represent these equivalent shunt resistances. The corresponding small shunt capacities will be included in C_3 and C_4. Taking these effects into account it may readily be shown that a condition for balance of the bridge is

$$C_1 = R_3C_2/R_4 + R_3 \{C_2C_4\omega \tan \delta_2 - C_1C_3\omega \tan \delta_1\}.$$

In measuring the "liquid capacity" the loss angle δ_2 is chiefly caused by the conductance of the benzene, and when measuring the air capacity the value of δ_2 will be different, and unless the second term in the above equation can be shown to be negligible, this must be allowed for. In the case of our measurements on benzene, the value of $\tan \delta_2$ was measured and found to be less than 0·001. Assuming that $\tan \delta_1 = 0$ and giving C_2 and C_4 their maximum values, the second term in the above equation was found to cause a correction of less than 5 parts in 100,000. Since this represents the most unfavourable case, this term was neglected and the bridge equation became simply

$$C_2 = R_4 C_1/R_3.$$

In the practical case, C_2 was first given a convenient value and the bridge balanced, the reading of C_1 being noted. The capacity C to be measured was then thrown in parallel with C_2, a second balance obtained and the new reading of C_1 (say C_1') noted. For this second balance we have $(C_2 + C) = R_4C_1'/R_3$, and taking differences $C = R_4 (C_1' - C_1)/R_3$.

In our measurements the ratio coils R_3 and R_4 were chosen so that the difference in reading of the standard condenser $(C_1' - C_1)$, in the case of the "air capacity" measurement was about 1000 $\mu\mu$F. The same ratio arms were used for the corresponding "liquid capacity," so that a difference in reading of about 2300 $\mu\mu$F. was obtained for this. The ratio of these two differences gives the ratio of the liquid and air capacities, whatever the values of the resistances R_3 and R_4. For accurate determinations with the standard test condenser, the 1 and 2 mm. air gaps were employed exclusively, for which ratio arms of 1000 : 3000 ohms, and 1000 : 5000 ohms respectively were used. To obtain at least two independent measurements of a given capacity, using different parts of the range of the standard measuring condenser, C_1 (fig. 6), the condenser C_2 was varied some convenient amount after a series of four readings, and the observations repeated.

Except in the special case when the effect of frequency was being investigated, a frequency of 1000 cycles per second was used throughout, the source of current V being a valve oscillator. A sensitivity of about 1 part in 20,000 in the capacity adjustment of C_1 was obtained when the P.D. applied to the bridge was of the order of 100 volts. Since the bridge absorbs very little power this voltage is easily obtained by the use of a small step-up transformer, in conjunction with a valve oscillator of the usual type.

(*d*) *The Standard Measuring Condenser.*—This condenser was designed by Dr. Dye, F.R.S.,* and constructed at the National Physical Laboratory in

---

* 'Nat. Phys. Lab. Ann. Rep.,' p. 84 (1924).

1924. Its range is from about 200 to 2900 μμF., and the capacity can be read to about 0·1 μμF. at all parts of its scale. A worm gear controls the rotation of the moving system. Drums on both worm and worm wheel shafts are graduated to read directly in micro-microfarads. The openness of scale on the worm or "vernier" drum is about 3 mm. for 1 μμF.; and hence in the most precise work readings to the nearest 0·05 μμF. can be taken. The scale of this condenser was calibrated using the capacity bridge described above, and the calibration was checked from time to time by making measurements on condensers of 500 μμF. and 1000 μμF. capacity using various portions of the scale. Backlash in the adjustment of the condenser was very slight, but error due to this was minimised by always setting the condenser by a rotation in the same direction. Individual measurements on a given capacity did not usually differ by as much as 0·2 μμF. and by taking a few independent measurements values differing by only 0·05 μμF. were frequently obtained. In general, the probable error on a capacity of 1000 μμF. was considered to be 1 part in 10,000.

Experimental Procedure.

(*a*) *Absolute Determination with the Standard Test Condenser.*—The brass plates having been cleaned with benzene and dried, the "air capacity" was measured by taking the four capacity readings α, β, γ and δ, previously described. The shield was then removed, taking care not to disturb the plates, and the containing vessel was filled with benzene. To avoid the formation of bubbles, the condenser was supported at a slight tilt, and filled by pouring down the side of the containing vessel at the lower end. The shield was then lowered into the liquid obliquely, entrapped air escaping through small countersunk holes in its top. Readings of capacity and temperature were taken until both were constant. The four readings necessary to determine the "liquid capacity" were then made. Immediately before and after taking the chief capacity reading, α, the temperature of the benzene was measured at three equally spaced points in the liquid, using a standard thermometer, the bulb of which passed through holes in the top of the screen. The differences between the readings were not usually greater than 0·02° C.

(*b*) *Determination with the Comparison Condenser.*—The bridge was essentially the same as before, but in this case the ratio arms R_3 and R_4 were 2000 and 1000 ohms respectively. The comparison condenser was connected in parallel with the condenser C_2 by means of fine wires (No. 30), the ends of which dipped into the mercury cups G (fig. 5). Undesirable movement of these leads were prevented by clamping them to terminals rigidly fixed a few centimetres away from the mercury cups. The shield of the comparison condenser was permanently connected to the earthed point E of the circuit.

The capacity of the comparison condenser was measured by the difference of two readings, obtained as follows:—

(1) With the condenser connected to the bridge as described above.

(2) With the condenser disconnected at one of the mercury cups G, viz., the one connected to the point D.

The disconnection was always made in the same way, the end of the lead being moved away by a definite amount. When the test condenser is connected to the bridge, the total capacity in the arm GD may be written $C_2 + c_l + C_m$, where c_l represents the capacity of the leads joining the test condenser to C_2, and C_m represents the mutual capacity of the plate systems of the test condenser. When the disconnection is made, let c_t be the capacity between the disconnected lead and the terminal from which it has just been disconnected. Then the capacity in the bridge arm GD is now $C_2 + c_l + c_tC_m/(C_m + c_t)$, which, if C_m is very large compared with c_t, becomes $C_2 + c_l + c_t$. Thus the change in capacity on making the single disconnection is $C_m - c_t$. Measurements made by the authors showed that c_t was of the order $0 \cdot 1$ $\mu\mu$F. It is therefore not negligible, but by making the disconnection always in the same way, c_t is made sensibly constant in which case it can be eliminated from comparison measurements. The use of thin wires helps to keep c_t small.

Dry air having previously been drawn slowly through the condenser for several hours, a measurement of the "air capacity" was made. The condenser was then connected up to an all-glass distillation apparatus by means of the ground glass joint in the side tube D (fig. 5), and the sample distilled directly into it. It was found that by running the liquid slowly down the side of the glass tube the formation of air bubbles could be avoided, successive fillings giving capacity values of great consistency. A volume of 150 c.c. of liquid was adopted as the standard amount and used throughout, as this ensured complete immersion of the plates and connections to the mercury cup terminals. Thermostatic control of the temperature of the condenser during the measurements was found to be unnecessary, if the apparatus was left in a constant temperature room overnight. Having completed the measurements of temperature and capacity, the procedure was repeated, using the benzene standardised by the absolute method, the liquid in this case being poured slowly into the test condenser.

The calculation of the dielectric constant was made as follows: it has been shown above that the difference between a pair of bridge readings gives $(C_m - c_t)$ for the particular filling of the test condenser, air or liquid. For convenience this quantity will be referred to as the capacity reading. Let C_0 be the "air capacity," and C_1 the corresponding "liquid capacity" reading when the condenser is filled with the liquid of unknown dielectric constant. Let C_2 be the "liquid capacity" reading in the case of the standardised liquid, and C_0' the corresponding value for the "air capacity" reading. This may be slightly different from C_0, due to small changes in the test condenser. In each case this "air capacity" includes a component which is not subsequently increased by the introduction of the liquid. This capacity is located in the solid dielectric used in the construction. Denote it by c_x, and denote the true air capacity by C_a. It follows that the capacity reading C_0 is given by $C_0 = C_a + c_x - c_t$. Both c_x and c_t are unaffected by filling the condenser with liquid and it is convenient to represent $c_x - c_t$ by c_s (the effective stray capacity) which is regarded as a constant of the comparison condenser. Thus we have for the liquid of known dielectric constant, ε_2

$$C_0' = c_s + C_a',$$
$$C_2 = c_s + \varepsilon_2 C_a',$$

from which the value of c_s may be calculated. Then for the liquid of unknown dielectric constant, ε_1, we have

$$C_0 = c_s + C_a,$$
$$C_1 = c_s + \varepsilon_1 C_a,$$

from which, knowing c_s, the value of the dielectric constant may be determined. The values of ε_1 and ε_2 are, of course, the values of the dielectric constants at the temperatures at which the observations were made. The values were reduced to a common temperature basis, using data on the temperature variation of the dielectric constant, obtained by us from measurements made with the comparison condenser.

The dielectric constant of a liquid as initially determined is referred to air, and hence to obtain the absolute value or the value referred to a vacuum, we must multiply the apparent value by the dielectric constant of air. The dielectric constant of *dry* air at normal pressure from 12° C. to 17° C. is 1·00055 and an effective value for air of normal humidity (about 60 per cent. at 16° C.) was found to be $1\cdot0006_5$, which value was used in the final reduction of the results for the standard test condenser. It is considered to be accurate to 1 part in 20,000.

Results—Determination of the Dielectric Constant of Benzene.

Absolute Measurements with the Standard Test Condenser.—A typical set of data for an absolute determination of the dielectric constant of a sample of benzene (A.R. grade) is given in Table I. Two such samples were used. Sample I was supplied by Messrs. Hopkin & Williams, Ltd., London, and Sample II by Messrs. British Drug Houses, Ltd., London.

Table I.—Absolute Determination of Dielectric Constant—Typical Results.
Sample I. A.R. grade benzene.

Air gap, 1 mm. Ratio arms, $R_3 = 3000$ ohms, $R_4 = 1000$ ohms.

Dielectric.	Connection.	Temperature, C.	C_1 $\mu\mu$F.	C_m $\mu\mu$F.	Dielectric constant $\epsilon^{I}_{16 \cdot 4_7 \,{}^{\circ}\mathrm{C.}}$ (air = 1).
Air (normal humidity)	α	° $16 \cdot 5$	$2005 \cdot 2_5$	$1001 \cdot 9_0$	$2 \cdot 2929$
	β		$1001 \cdot 8_0$		
	γ		$1003 \cdot 3_5$		
	δ		$1001 \cdot 8_0$		
Benzene, Sample I	α	$16 \cdot 4_7$	$2802 \cdot 4_0$	$2297 \cdot 2$	
	β		$502 \cdot 7_0$		
	γ		$505 \cdot 2_0$		
	δ		$502 \cdot 7_0$		

As $\partial\epsilon/\partial t = -0 \cdot 0020_5$. $\epsilon^{I}_{15^{\circ}\mathrm{C.}} = 2 \cdot 2959$ (damp air = 1).
$= 2 \cdot 2961$ (dry air = 1).

Dielectric Constant (*vacuum* = 1) *of Sample I at* 15° C.

$$2 \cdot 2959 \times 1 \cdot 0006_5 = 2 \cdot 2974.$$

Throughout the course of this work such measurements as the above were carried out at intervals on both samples of benzene. In Table II is given a summary of these determinations and it will be noted that air gaps of both 1 and 2 mm. were employed. The maximum discrepancy between the results obtained with the different air gaps is less than 2 parts in 10,000 and the average divergence is one-half of that amount. The determinations involving the larger capacity are almost certainly the better, and there is no doubt that the method will give an accuracy of 1 part in 10,000. This agreement obtained when using "air capacities" so widely different as 334 and 172 $\mu\mu$F. is considered to be of the greatest importance, since it is only by measurements of this kind that the elimination of stray capacities can be convincingly demonstrated.

Table II.—Summary of Determinations of Dielectric Constant in the Standard Test Condenser of Samples of A.R. Grade Benzene.

Sample of benzene.	Date.	Air gap.	Dielectric constant (vacuum = 1) at 15° C.	
		mm.	Observed.	Mean.
Sample I (Hopkin & Williams, A.R. grade).	8.6.26	1	2·3000	2·3000
	10.6.26	2	2·2999	
	30.11.26	1	2·2977	2·2977
	2.12.26	1	2·2977	
	4.5.27	1	2·2974	2·2975
	6.5.27	2	2·2976	
Sample II (British Drug Houses A.R. grade).	21.9.26	1	2·3002	2·3002
	24.1.27	1	2·2966	2·2968
	28.1.27	2	2·2970	

Each sample of benzene exhibited a marked decrease in value with time. No drying agents were used, and we are unable to put forward a satisfactory explanation of this effect. The absorption of water on exposure to the air during a determination would raise the dielectric constant.

Comparison Measurements.—A number of careful measurements were carried out to demonstrate that if one liquid is standardised absolutely and comparisons are made between it and a second liquid, the value so obtained for the second liquid is identical with that obtained by the direct employment of the absolute method. These tests were made with the two samples of A.R. grade benzene, and details of the comparison are set out in Table III.

Now $\varepsilon^{I}_{15\cdot0^\circ\,\mathrm{C.}}$ (dry air = 1) = 2·2961 (Table I). By calculation from the above measurements, we find—

$\varepsilon^{II}_{15\cdot0^\circ\,\mathrm{C.}}$ (dry air = 1) .... = 2·2953

or

$\varepsilon^{II}_{15\cdot0^\circ\,\mathrm{C.}}$ (vacuum = 1) .... = 2·2966

The value obtained by the absolute method was 2·2968 (see Table II).

These values, derived in two ways, are seen to agree to less than 1 part in 10,000, which shows that all the measurements involved are on a satisfactory basis.

Table III.—Comparison Measurements of Dielectric Constants—Typical Results.

Samples I and II. A.R. Grade Benzene.

Determination of ε^{II} in terms of ε^{I}. Ratio arms, $R_3 = 2000$ ohms, $R_4 = 1000$ ohms.

Dielectric.	Condenser.	Temperature, C.	C_t $\mu\mu$F.	$(C_m - c_t)$ $\mu\mu$F.
Air (dry)	Connected Disconnected	15·7°	$1\ 775 \cdot 2_0$ $900 \cdot 4_0$	$C_0 = 874 \cdot 8_0$
Benzene, sample II	Connected Disconnected	$15 \cdot 6_5$	$2\ 698 \cdot 9_0$ $699 \cdot 5_0$	$C_1 = 1\ 999 \cdot 4$
Air (dry)	Connected Disconnected	16·5	$1\ 701 \cdot 0_0$ $826 \cdot 1_0$	$C_0' = 874 \cdot 9_0$
Benzene, sample I...........	Connected Disconnected	$16 \cdot 3_3$	$2\ 803 \cdot 8_5$ $804 \cdot 8_5$	$C_2 = 1\ 999 \cdot 0$

Results for Pure Benzene.—A sample of pure benzene was prepared starting with the liquid of A.R. grade and using the process described by Richards and Shipley.* Briefly, the procedure involves treatment with sulphuric acid, caustic soda, distilled water, and mercury, the liquid finally being dried with calcium chloride and sodium wire. Measurements were also made on another pure sample obtained from the firm of Kahlbaum.

Our early observations showed that as far as dielectric constant measurements are concerned, water is by far the most troublesome impurity, and when measuring with an accuracy of 1 part in 10,000 it is difficult to obtain a degree of dryness which is reproducible. In our final determinations, every precaution was taken to avoid moisture absorption from the atmosphere, the test condenser and the still. The benzene was distilled directly into the comparison condenser from an all-glass distillation apparatus. Before charging the still, a few cubic centimetres of pure benzene were distilled over, after which the sample was introduced with freshly cut pieces of sodium, and the one open end of the apparatus closed by a drying tube. At least two weeks were allowed to elapse before distillation. The first few cubic centimetres were, of course, rejected.

---

* 'J. Am. Chem. Soc.,' vol. 36, p. 1825 (1914).

A selection of the more important of our results is given in Table IV. Generally speaking, samples which had been purified in the ordinary way, finishing with a drying for one day over sodium, followed by a distillation from sodium gave a value of ε at 15° C. of 2·294. A further drying with sodium for several months reduced this value to 2·292. The prolonged drying of an A.R. grade sample of benzene over phosphorus pentoxide also gave a value of 2·292 from which we conclude that moisture is the only impurity of importance in dielectric constant measurements.

Table IV.—Summary of the Dielectric Constants of Various Samples of Benzene.

Sample of benzene.	Drying agent.	Period of drying.	Dielectric constant (vacuum = 1) at 15·0° C.
N.P.L.	Sodium wire	4 months	2·2928
Kahlbaum	,,	6 hours	2·2942
,,	,,	6 months	2·2920
Hopkin & Williams (A.R. grade)	None (as received)	—	2·3000
	Phosphorus pentoxide	8 months	2·2920

The frequency of the alternating current used in these standardisations was 1000 cycles per second, but the dielectric constant was found to be invariable to the limit of observation over the audio frequency range.

The temperature coefficients of the dielectric constants of the various samples of benzene were determined in the comparison condenser, as only small volumes of the liquids were available. The relation between dielectric constant and temperature in all cases was linear for our range of 12° C. to 22° C. For convenience in reducing results to a common temperature basis, the data obtained were expressed in the form $\varepsilon_t = \varepsilon_{15} + \frac{\partial \varepsilon}{\partial t}(t - 15)$. The values of $\frac{\partial \varepsilon}{\partial t}$ for all samples are given in Table V, from which we deduce

$$\partial\varepsilon/\partial t = -\,0{\cdot}0019_{8\,\pm\,3} \text{ for pure benzene.}$$

$$\partial\varepsilon/\partial t = -\,0{\cdot}0020_5 \text{ for A.R. grade benzene.}$$

Table V.—Temperature Coefficients of Dielectric Constant for Pure and A.R. Grade Samples of Benzene.

Sample of benzene.	$\partial\epsilon/\partial t$.
N.P.L.	$-0{\cdot}0019_5$
Kahlbaum	$-0{\cdot}0020_1$
Hopkin & Williams (A.R. grade)	$-0{\cdot}0020_8$
British Drug Houses (A.R. grade)	$-0{\cdot}0020_3$

The power factor of the comparison condenser filled with liquid was also measured in a number of cases. It was found that the mean values of the power factors of the condenser when filled with A.R. grade benzene were 0·0005 and with pure dry benzene $0{\cdot}0000_5$ at a frequency 1000 cycles per second. If we neglect the conductance of the condenser itself, we obtain from these power factor values the following upper limits for the specific conductivity for the samples of benzene; A.R. grade, 6×10^{-13}, pure benzene 6×10^{-14} ohm^{-1} cm.^{-1}.

For the purpose of comparison, determinations of some of the other physical constants of some of our samples of benzene were made. The freezing point and refractive index were determined in the Physics Department of the National Physical Laboratory. The boiling points were determined by us during the final distillation. The fraction actually tested distilled over within a temperature range of 0·02° C. in each case. These subsidiary data are recorded in Table VI.

Table VI.—Various Physical Constants for Different Samples of Benzene.

Sample of benzene.	Boiling point, Centigrade (760 mm.).	Freezing point, Centigrade (H scale).	Refractive index at 15° C. for sodium D_1 line.
	°	°	
N.P.L.	80·1	5·32	1·5038
Kahlbaum	—	5·22	1·5040
A.R. grade	—	5·16	—
A.R. grade (dried 8 months with P_2O_5).	80·0	—	—

The "best" value for the boiling point given by International Critical Tables is 79·6° C., but the published values range from 79·6° C. to 80·6° C. Richards and Shipley in their research on the freezing point of benzene as a fixed point in thermometry give a value of 5·48° C., but this was obtained after many fractional crystallisations which were not carried out in our case. A value for the refractive index of pure benzene as interpolated from Landolt and Bornstein's tables was found to be 1·5039, which is practically identical with the values for our pure samples. In the light of these data it is considered that the sample which was purified by the authors (marked N.P.L.) is representative of the "pure benzene" used for other standard determinations of physical constants.

Our final conclusion is that the most probable value of the dielectric constant of benzene is $2{\cdot}292_{5\pm5}$ at 15° C. Therefore

The dielectric constant of benzene at 20° C. = $2{\cdot}282_{5\pm5}$ (vacuum = 1).

---

* Richards and Shipley, *loc. cit.*

The probable error is given as ± 2 parts in 10,000, but this is considered to be determined mainly by the difficulty of getting the test condenser filled with benzene which can be considered perfectly pure. The method of measurement used will give a value for any given liquid, with a probable error not greater than ± 1 part in 10,000 as is shown by the results already quoted.

In Table VII we have collected together the results of the most accurate previous determinations, reducing them to a temperature basis of 20° C., using our own value for the temperature coefficient when necessary. It is to be noted that the discrepancies in the values of the temperature coefficient are even greater than those in the values of the dielectric constant itself. Our own experiments show that different samples of benzene give practically the same temperature coefficient, and we can only ascribe the discrepancies to experimental error.

Table VII.—Previous Determinations of the Dielectric Constant and Temperature Coefficient of Benzene.

Temperature, Centigrade. (t°).	ϵ_{t° (air = 1).	$\partial\epsilon/\partial t$.	ϵ_{20° (vacuum = 1).	Frequency cycles/sec.	Authority.*	Date.
° 18	2·235	−0·0020	2·231	1500	Nernst	1894
—	—	$-0{\cdot}0015_7$	—	Audio	Ratz	1896
19	2·26	—	2·26	4×10^8	Drude	1897
18	2·288	−0·0016	2·285	5000	Turner	1900
—	—	$-0{\cdot}0019_2$	—	Audio	Tangl	1903
17	2·287	—	2·282	4×10^8	Colley	1910
15	2·283	−0·0015	2·276	6×10^5	Isnardi	1922
30	2·260					
14·8	2·291	—	2·282	800	Waibel	1923
20	2·276	−0·0019	2·277	10^6	Graffunder	1923
21·8	$2{\cdot}23_9$	$-0{\cdot}0015_3$	$2{\cdot}24_8$	10^6	Meyer	1924
20	$2{\cdot}28_5$	$-0{\cdot}0015_2$	$2{\cdot}28_6$	10^6	Grutsmacher	1924
20	2·270	$-0{\cdot}0018_5$	2·271	Audio	Lange	1925
25	$2{\cdot}24_7$	—	$2{\cdot}25_8$	1000	Harris, H.	1925
15	$2{\cdot}291_{5\pm5}$	$-0{\cdot}0019_{8\pm8}$	$2{\cdot}282_{5\pm5}$	1000	Author's	1928

---

[*] Nernst, 'Z. Phys. Chem.,' vol. 14, p. 622 (1894); Ratz, 'Z. Phys. Chem.,' vol. 19, p. 94, (1896); Drude, 'Z. Phys. Chem.,' vol. 23, p. 269 (1897); Turner, 'Z. Phys. Chem.,' vol. 35, p. 385 (1900); Tangl, 'Ann. Physik,' vol. 10, p. 748 (1903); Colley, 'Phys. Z.,' vol. 11, p. 324 (1910); Isnardi, 'Z. Physik,' vol. 9, p. 153 (1922); Waibel, 'Ann. Physik,' vol. 72, p. 161 (1923); Graffunder, 'Ann. Physik,' vol. 70, p. 225 (1923); Meyer, 'Ann. Physik,' vol. 75, p. 801 (1924); Grutsmacher, 'Z. Physik,' vol. 28, p. 342 (1924); Lange, 'Z. Physik,' vol. 33, p. 169 (1925); Harris, 'J. Chem. Soc.,' vol. 127, p. 1049 (1925).

In conclusion, we wish to thank Dr. Holmes, late of the Chemical Research Laboratory, Teddington, and the many of our colleagues in various departments of the National Physical Laboratory who have helped us in the various aspects of the problem of which they have special knowledge.

The Molecular Dimensions of Organic Compounds. Part I.—*General Considerations.*

By Prof. T. M. Lowry, F.R.S., and Dr. A. G. Nasini.

(Received November 7, 1928.)

The investigation now described had for its object the examination of the physical properties of compounds, such as benzene and thiophen, which have long been known as examples of "mimicry" in organic chemistry, in order to find out whether the persistent similarity of boiling-point, which Victor Meyer observed* in corresponding compounds of the two series, extends also to their other properties. In particular it was of interest to know whether these compounds exhibited the remarkable similarity of properties which Langmuir found in the case of "isosteric" substances, such as CO_2 and N_2O, or CO and N_2, in which the electronic configuration is similar although the distribution of mass and charge in the nuclei is different.

The substances selected for the investigation were :—

(1) Benzene and thiophen.
(2) Toluene and methylthiophen.
(3) Benzene and cyclohexane.
(4) Benzene, pyridine and thiazole.

The first two pairs differ as a result of the replacement of two CH-groups by S, and are typical examples selected from Victor Meyer's series. The third pair was introduced because the boiling-points and freezing-points of the two compounds, C_6H_6 and C_6H_{12}, differ by less than 1°, in spite of the profound change effected by adding six atoms of hydrogen to the aromatic hydrocarbon. The fourth comparison involves the effect of replacing a single CH-group by an atom of *nitrogen* in the aromatic ring ; the further effect of replacing two more CH-groups by an atom of *sulphur* could not be determined on account of the difficulty of obtaining a supply of pure thiazole.

Collision-areas.

The most interesting comparison is in reference to the collision-areas of the molecules, as deduced from the viscosities of the vapours, since this property is specially dependent on molecular configuration, and provided some of the most striking coincidences in Langmuir's tables of data. The experimental papers which follow are therefore devoted mainly to this question. It is also here that some of the most striking regularities are observed. Thus the *decrease* in the collision-area $\bar{A}$ on passing from benzene to thiophen is almost the same as that observed on passing from toluene to α-methylthiophen.

---

* See, for instance, the table in Richter's 'Organic Chemistry,' vol. 2, p. 489 (1898).

Benzene .. $\bar{A}$	$= 19{\cdot}0\ \text{Å}^2$	Toluene .... $\bar{A}$	$= 21{\cdot}8\ \text{Å}^2$
Thiophen ..	$= 16{\cdot}7$	Methylthiophen..	$= 19{\cdot}9$
	2·3		1·9

A similar comparison of the same data shows that an *increase* of collision area of about the same amount is produced on replacing H by CH_3 :—

Toluene ...... $\bar{A}$	$= 21{\cdot}8\ \text{Å}^2$	Methylthiophen.. $\bar{A}$	$= 19{\cdot}9\ \text{Å}^2$
Benzene	$= 19{\cdot}0$	Thiophen	$= 16{\cdot}7$
	2·8		3·2

If we assume that the experimental errors are of the order of 2 per cent., these numbers could all be rounded off to integral values, showing a decrease of 2 units on replacing C_2H_2 by S and an increase of 3 units on replacing H by CH_3. These two opposite changes are so nearly equal in magnitude that when they are superposed they produce an agreement between the collision areas of α-methylthiophen and benzene, which is much closer than that which is observed between benzene and thiophen or between toluene and methylthiophen, where a close concordance might perhaps have been anticipated.

The collision area of pyridine ($\bar{A} = 20{\cdot}0\ \text{Å}^2$) can only be compared with that of benzene ($\bar{A} = 19{\cdot}0$), since only preliminary data are available for thiazole. From these data, the replacement of one CH-group by an atom of nitrogen is seen to produce an *increase* of collision area of 1 unit, whereas the replacement of two CH-groups by an atom of sulphur produced a *decrease* of 2 units. An interesting result of these small successive changes of collision area is to produce an almost complete identity in the collision area of pyridine (20·0) and of α-methylthiophen (19·9).

The general character of the viscosity-measurements is brought out clearly in figs. 2 and 3 (Parts II and III) in which the viscosities of the vapours are plotted against temperature. Thus the close analogy of benzene and toluene with toluene and methylthiophen is shown by the analogous increases of slope on replacing C_2H_2 by S or CH_3 by H in the two cases. The line representing the viscosity of pyridine agrees so closely with that for methylthiophen that the difference could not be shown in a diagram.

Other Properties.

In addition to measuring the viscosity of the vapours, measurements were made of other physical properties of the six compounds now under consideration, whenever this was required in order to provide comparative data. The results are set out in Table I, where new results are printed in heavy type. The principal deductions from this table are set out below.

Table I.

Substance.	Molecular weight.	Density 20°/4° C.	Boiling-point.	Freezing-point.	Critical temperature.	Viscosity of liquids C.G.S.	Viscosity of vapours C.G.S. × 10^4.
			°	°	°		
Benzene	78·05	0·878	80·5	5·48	288	0·0064 (20°)	**0·94** (100°)
Thiophen	84·11	1·063	84·3	−29·8	317	0·0066 (20°)	**1·03** (96·2°)
Cyclohexane	84·13	0·778	80·8	6·15	280	0·0097 (20°)	**0·88** (104°)
Toluene	92·1	0·866	110·3	−94·5	321	0·0054 (25°)	**0·88** (96°)
α-Methylthiophen	98·1	**1·016**	112·1	**−51**	**321**	**0·00667** (25°)	**0·965** (100°)
Pyridine	79·08	0·981	115·5	−42	344	0·00877 (25°)	**0·958** (98·2°)

Substance.	Mean collision area in Å^2.	Sutherland's constant.	Surface tension dynes per cm.^{2}.	Specific cohesion a^2.	Eötvos constant.
Benzene	**19·0**	**380**	27·7 (25·1°)	6·47 (25·1°)	2·20 $^{25^\circ}_{55^\circ}$
Thiophen	**16·7**	**407**	31·5 (25·4°)	6·10 (25·4°)	2·03 $^{25^\circ}_{47^\circ}$
Cyclohexane	**22·3**	**330**	25·7 (24·6°)	6·78 (24·6°)	3·22 $^{24^\circ}_{58^\circ}$
Toluene	**21·8**	**370**	28·4 (26°)	6·73 (26·0°)	2·12 $^{21^\circ}_{104^\circ}$
α-Methylthiophen	**19·9**	**400**	**30·8** (24·5°)	**6·09** (24·5°)	2·35 $^{24^\circ}_{46^\circ}$
Pyridine	**20·0**	**320**	34·9 (25°)	7·30 (25·0°)	2·14 $^{17^\circ}_{56^\circ}$

(*a*) *Replacement of* —CH : CH— *by* —S—.—In view of the very close relationship between benzene and toluene, it might have been expected that the replacement of two methenyl groups by an atom of sulphur would have been accompanied by equal changes in the properties of the two compounds, even if the "mimicry" of the hydrocarbon by its sulphur-containing analogue were too incomplete to keep the properties substantially unchanged. This expectation is very largely fulfilled in the case of the vapours, where the viscosity is increased by 0·09 and 0·085, and the collision-area is decreased by about 2 units, as a result of this replacement in the two hydrocarbons. In the case of the liquids also, this analogy is still very largely maintained. Thus the small rise in the boiling-points of the liquids under atmospheric pressure, 3·8° in benzene and of 1·8° in toluene, which accompanies this substitution, is shown by the measurements of vapour-pressure (see Part III) to persist over a wide range of pressures, although the vapour-pressure curves naturally approach one another as the temperature is reduced. There is also a similar increase, of 0·185 and 0·150, in the densities of the liquids, and of 3·8 and 2·4 in their surface tensions, although the Eötvos constants change in opposite directions. On the other hand the increments of liquid viscosity are quite different, since toluene is much less viscous than methylthiophen, whereas the viscosity of benzene and thiophen are nearly equal to each other as well as to that of α-methylthiophen.

Finally, in the case of the solids all evidence of analogy disappears, since there is a *fall* of melting-point of 35° on passing from benzene to thiophen, but a *rise* of 43° on passing from toluene to methylthiophen. A similar inequality was observed by Langmuir in the freezing-points of isosteric compounds, which provided almost the only exceptions to their general uniformity of properties. It was attributed by him to the dependence of the freezing-points on the stray field of force round the molecule, since this would be quite different for isosteric compounds in view of the different distribution of their nuclear charges. A similar explanation may be given of the irregularity of freezing-points in the present series, and this explanation may perhaps also serve to account for the irregularity in the viscosities of the liquids, since these must obviously depend on the fields of force between the molecules. In any case it is clear that the close similarity of compounds of the benzene and thiophen series extends only over a restricted range of properties and has no application to the solid state.

(*b*) *Replacement of* H *by* CH_3.—A comparison of benzene with toluene and of thiophen with methylthiophen shows that when hydrogen is replaced by methyl the viscosity of the vapour is decreased by almost the same amount in the two cases, namely, $0{\cdot}94 - 0{\cdot}88 = 0{\cdot}06$ and $1{\cdot}03 - 0{\cdot}965 = 0{\cdot}065$, and this results, as we have seen, in an almost identical increase in the collision area. The surface-tension of the homologues is, however, practically identical both for benzene and toluene, and for thiophen and methylthiophen. This replacement results in a *rise* of 29·8 and 27·8° in the boiling-point, but produces a *fall* of 100° and 81° in the freezing-point.

(*c*) *Cyclohexane*, of which the freezing-point and boiling-point agree very closely with those of benzene, differs widely from it both in the vapour and in the liquid state. In particular, the viscosity of the vapour is substantially lower than that of benzene, but agrees exactly with that of toluene ; and the mean collision area, which is much greater than that of benzene, is again almost identical with that of toluene. The specific cohesion of the liquid is also practically the same for cyclohexane and toluene, but differs from that of benzene ; and the high viscosity of the liquid is without a parallel in this series of compounds. The surface-tension and Eötvos constants of cyclohexane also differ widely from the almost identical values recorded for benzene and toluene.

(*d*) *Pyridine and α-methylthiophen.*—The similarity in collision area of these two compounds, to which attention has already been directed, finds a counterpart in some other properties, *e.g.*, in the densities, which differ only by 0·035, in the boiling-points, which differ only by 3·40°, and even in the freezing-points, which differ only by 9° ; nevertheless the viscosities of the liquids and their surface tensions differ widely from one another.

To sum up, the data collected in Table I show that concordance in physical properties in these closely-related compounds is always very partial and incomplete. In particular, the obvious division into two groups, boiling at about 80° and 110° respectively, cuts across an equally obvious classification into three liquids of similar density to that of water, and three of much lower density ; in the same way, the coincidence of boiling-point and freezing-point of benzene and cyclohexane, which suggests a far-reaching resemblance in the cohesive forces of liquid and solid, is not followed up by any close concordance in the other properties of the compounds. We therefore conclude that the similarity exhibited by isosteric compounds is probably unique, and cannot be reproduced in compounds which are related less closely to one another in atomic and electronic structure. In these latter compounds similarity of properties and regular differences are therefore generally confined, in an even more marked degree than in isosteric compounds, to properties which depend on the configuration of the molecules, rather than on the intramolecular forces, which play so important a part in the solid state, and in some of the properties of liquids.

Summary.

(1) The resemblance which V. Meyer observed in the boiling-points of benzene and thiophen and of their derivatives has been made the basis of a

comparative study of the physical properties of benzene with thiophen and of toluene with α-methylthiophen. A comparison has also been made of the physical properties of benzene and cyclohexane, since the boiling-points and freezing-points of these two hydrocarbons are almost identical.

(2) Measurements have been made of the viscosities of the vapours of benzene, toluene, cyclohexane, thiophen, methylthiophen and pyridine. From these results the mean collision areas, and the values of Sutherland's constant have been deduced.

(3) In spite of the close resemblance of benzene to thiophen and of toluene to methylthiophen, the collision areas are altered by about 10 per cent. when two CH-groups are replaced by an atom of sulphur; in each case, however, the change is accompanied by an almost constant decrement of 2 $Å^2$. On the other hand, the replacement of H by CH_3 is accompanied by a constant increment of 3 $Å^2$. The collision area of the molecule is also increased by about 1 $Å^2$ when one CH-group is replaced by an atom of nitrogen on passing from benzene to pyridine.

(4) As a result of these increments and decrements, the collision area of methylthiophen, which differs substantially from that of toluene, is practically identical with that of pyridine. A marked similarity, which has not been recorded hitherto, is also observed between other physical properties (*e.g.*, the boiling-point and freezing-point) of these two compounds.

(5) In none of the cases now investigated is the similarity of properties as close as in Langmuir's isosteric compounds. Thus the vapours exhibit regular increments rather than identity of properties; and the physical properties of the liquids and solids, which depend on the force-fields of the molecules as well as on their dimensions, show still wider differences.

The Molecular Dimensions of Organic Compounds.—Part II. The Viscosity of Vapours: Benzene, Toluene and Cyclohexane.

By Dr. A. G. Nasini.

(Communicated by T. M. Lowry, F.R.S.—Received November 7, 1928.)

The measurements of gaseous viscosities, which are described below, formed a part of an extensive investigation of the physical properties of some closely-related aromatic compounds; but measurements such as these have an independent value, since they provide a means of calculating the atomic diameter of a monatomic molecule* or the mean collision area of a polyatomic molecule.

In the case of benzene, the data recorded hitherto,† for the viscosity of the vapour differ so widely as to be quite untrustworthy; and the measurements either cover so narrow a range of temperature or are of so low an order of accuracy that it is impossible to calculate even an approximate value for Sutherland's constant. For the viscosities of the vapours of toluene and of cyclohexane no earlier data of any kind appear to have been determined.

Experimental Methods.

The early measurements of Meyer and Schumann (*loc. cit.*) were made by transpiration through a capillary at the boiling-point, and have been criticised by Brillouin. The dissertation of Rappenecker describes a simple apparatus for driving out a known volume of vapour through a capillary heated to a known temperature by means of a vapour jacket; but this simple process does not appear to lend itself to exact measurements. The experiments now described were therefore made with a modified form of Rankine's apparatus as used by Smith‡ to measure the viscosity of water-vapour.

In Rankine's method, the substance is distilled from one receptacle to another through a capillary tube, in a sealed apparatus containing only the liquid and its vapour. The *quantity* of vapour that has "transpired" through the capillary is generally determined by measuring the volume of liquid distilled or condensed; for this purpose, the receptacles at either end of the capillary usually take the form of narrow calibrated quill tubes. The *pressure* under which transpiration takes place depends on the vapour-pressure of the liquid in the two receptacles; but this pressure is not necessarily given by the difference of vapour-pressure of the liquid at the temperatures of the two surrounding thermostats, since the latent heat of vaporisation tends to lower the temperature of the evaporating liquid and to raise the temperature of condensation. It is therefore safer to make direct measurements of the driving-pressure, rather than to rely upon the tabulated values of the vapour-pressure. If the substance has no action on mercury this can be done with the help of mercury manometers at either end of the capillary. In the case of corrosive liquids, the use of a mercury-manometer can be avoided by distilling the liquid to and from a U-tube, the closed limb of which is under the normal vapour-pressure of the liquid. The difference of level in the two limbs then shows the pressure under which the liquid is evaporating or condensing.*

---

* Experiments on the monatomic gases will be described in a later paper.

† Meyer and Schumann, 'Wied. Ann.,' vol. 7, p. 497 (1879); Rappenecker, 'Z. Phys. Chem.,' vol. 72, p. 695 (1910).

‡ Rankine, 'Roy. Soc. Proc.,' A, vol. 88, p. 575 (1913); Smith, *ibid.*, vol. 106, p. 83 (1924).

The apparatus used is shown in fig. 1. The evaporation-bulb *e* takes the form of a graduated tube with a bore of about 1·8 mm., attached to a bulb of about 4 cm. diameter. This provides a reservoir of vapour at a definite driving-pressure, which can be measured by mercury manometer *d*, attached to the evaporation-bulb by means of a T-tube. The other arm of the T-tube leads through a spiral *g* to the capillary *h*. The vapour which has passed through the capillary is condensed in a bulb *m* of about 2 cm. diameter. The condensation bulb in this apparatus was not provided with a manometer (although one was introduced later), since the vapour-pressure of benzene is accurately known over a large range of temperatures, and the dimensions of the receptacle were

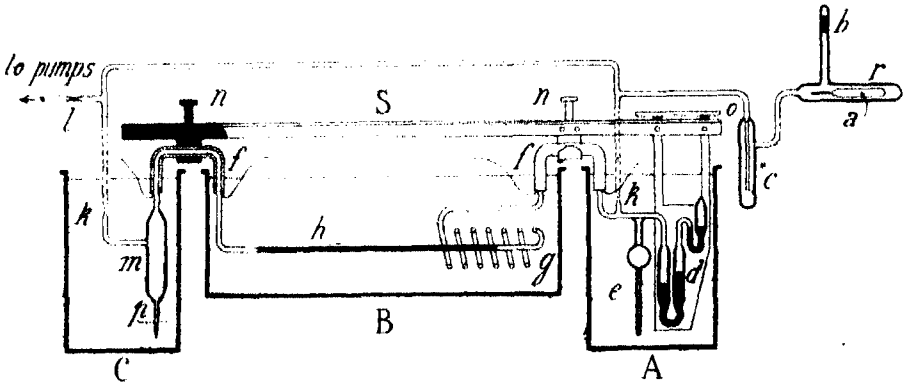

FIG. 1.—Apparatus for Measurement of Viscosity of Vapour.

---

* Rankine, *loc. cit.*

such that a uniform vapour-pressure was easily established. In order to prevent condensation from occurring elsewhere, the exposed parts of the apparatus were wound with chromel wire at *ff* and heated electrically. The asbestos twine in which the chromel wire was wrapped was partially coated with sealing-wax in order to prevent the absorption of water by capillarity and consequent cooling by evaporation.

The manometer and evaporation-bulb were immersed in a thermostat A, the spiral and capillary in a bath B (which contained water for measurements up to 100°, or oil for measurements at higher temperatures) and the condensation-bulb in the thermostat C. The thermostats A and C were of large capacity (about 30 litres) and were fitted with glass windows, so that the pressure and level of the evaporating liquid could be read. The temperature was kept constant within 0·1° by means of Lowry's spiral thermo-regulator. The liquid in the bath B was kept at a uniform temperature by means of three stirrers connected in series; it was heated by gas, and the temperature was kept constant within 0·5° by hand regulation. The baths were shielded from one another by means of iron or asbestos sheets, and their temperatures were measured by means of standard or standardised thermometers, the readings being corrected for the emergence of the mercury-thread from the bath.

The manometer was immersed in the same thermostat as the evaporation-bulb, since there was always a gradient of temperature during evaporation, which prevented the condensation of liquid on the surface of the mercury. Conversely it was found that the liquid in the measuring-tube *e* did not begin to evaporate until any liquid that had distilled on to the surface of the mercury had evaporated. The use of a supplementary thermostat at a higher temperature to contain the manometer was therefore unnecessary.

The manometer was fitted with Waran's device* for maintaining the vacuum by means of an auxiliary U-tube, as shown in fig. 1. It was evacuated by connecting the two open ends to a high-vacuum pump and boiling the mercury until all air had been expelled; one side of the manometer was then sealed and air was carefully admitted on the other side. A glass mirror, the back of which was covered with paraffin wax, was immersed in the thermostat in order to avoid errors from parallax. A table cathetometer was used to read the manometer, and a travelling microscope with a magnification of 12 was used to read the level of the evaporating liquid.

The transpiration apparatus was made entirely of "duroglass." Before being put together all the parts were cleaned with a mixture of nitric and chromic acids, and rinsed with distilled water; and the glass-blowing was done with cotton wool filters in order to avoid contamination of the capillary. The apparatus was secured to a metallic bar, which could be clamped firmly in position at *nn*. A small plate of metal *o*, attached to the bar, was used as a stand for a spirit level, by means of which the manometer and the graduated tube of the evaporation-bulb could be adjusted to a vertical position. The apparatus was thus rendered transportable, and could be immersed in baths which had already been regulated to the desired temperature.

---

* 'Proc. Phys. Soc.,' vol. 35, p. 199 (1923).

The capillaries were calibrated by means of short threads of mercury. The dimensions of the capillaries were, for the experiments with benzene, cyclohexane, and toluene $\Sigma l/r^4 = 1 \cdot 18 \times 10^9$ cm.$^{-3}$, for pyridine $0 \cdot 972 \times 10^9$ cm.$^{-3}$, for thiazole $4 \cdot 995 \times 10^9$ cm.$^{-3}$.

Filling the Viscometer.

Special care was needed to exclude all traces of air when filling the viscometer, since the presence of foreign gases might alter the pressure on the condensation side, which is assumed to be equal to the tabulated vapour-pressure of the liquid. In the case of benzene, Smith's method (*loc. cit.*) could be used with some modification, but a different method was adopted for liquids which could only be obtained in small quantities. This method also served to eliminate the use of greased stop-cocks.

Two methods were used for freeing the liquid from dissolved air: (1) The liquid was boiled repeatedly, and then introduced by the usual method into a small tube *a* ending in a long and fine capillary; this tube, which contained from 3 to 7 c.c., was sealed off when filled completely with liquid. (2) The liquid was distilled from a bulb connected to a liquid air trap to which the tube *a* was sealed. The apparatus was evacuated by means of a diffusion pump, and the distillation was effected while the pumps were still working. After two or three distillations the apparatus was sealed off from the pumps, and then contained only the solidified substance. This was allowed to melt, and the liquid was distilled into the tube *a*, which was finally sealed off. It is advisable to connect the apparatus with the pumps by means of a stop-cock lubricated with metaphosphoric acid or other suitable lubricant in case of obstructions of the liquid-air trap. Both methods are equally good, but when the second method is used care has to be taken to distil two or three times with ample free space, because at these low temperatures occlusion of gas by some organic compounds takes place to a remarkable extent.

The tube *a* containing the air-free liquid, was introduced into the tube *r*, carrying a side tube in which a small iron bar encased in glass (and operated by an external electromagnet) was provided in order to break the capillary of the bulb; the tube *r* was then sealed and the apparatus was ready to be evacuated. In some of the later experiments, however, the capillary was inserted in the bore of a mercury stop-cock and broken by turning the tap. The stop-cock was hand-ground until it held a vacuum without lubricant, but a trace of metaphosphoric acid was put at the ends of the tap to prevent it from sticking.

On account of the well-known difficulty of evacuating an apparatus through a capillary tube, the viscometer was evacuated on both sides. A rotary oil-pump, which reduced the pressure to 0·01 mm., was used in series with two Waran's diffusion pumps, and the apparatus was heated with a flame in order to expel all humidity and occluded gases. The vacuum was tested by a McLeod gauge and by a discharge tube; the discharge tube was also used in order to test for leakage. When evacuated, the apparatus was sealed off at *l*. The capillary of *a* was then broken and the liquid was distilled into the viscometer at *l* and *m*. The viscometer was then sealed off at *k* and was ready for use. The trap *c* was used to prevent glass fragments from the broken capillary going inside the viscometer. The tube *p* on the condensation bulb *m* was used in order to empty the apparatus when a series of experiments had been completed.

Each experiment occupied 1 or 2 hours, or more. Readings were taken every 10 minutes of the manometer, of the level of the evaporating liquid, and of the various thermometers. The temperature of the oil bath, which was hand regulated, was checked continuously. Times were controlled by means of a precision stop-watch.

Purification of Materials.

(*a*) *Benzene.*—Two litres of benzene were shaken for a day with concentrated sulphuric acid to eliminate traces of thiophen, then with aqueous soda and with water; the liquid was dried by prolonged boiling with calcium chloride, under a reflux condenser, and fractionally distilled; the middle fraction was fractionally crystallised and centrifuged. The product melted at 5·43° C.

(*b*) *Toluene.*—Pure toluene, from Messrs. British Drug Houses, was accurately fractionated; the middle fraction was collected and boiled over melted sodium for 6 hours. The toluene was then distilled fractionally over sodium, and the portion boiling between 110·2° and 110·3° C. under 760 mm. pressure was collected.

(*c*) *Cyclohexane.*—One litre of cyclohexane was shaken for a day with fuming sulphuric acid, and then with water for 6 hours : it was then dried by boiling it with calcium chloride under a reflux condenser. The product was fractionally crystallised and the crystals centrifuged ; the purification was followed by observing the progressive increase of the melting-point. The final product melted at 6·45° C. The density of the sample was found to be 0·7830 at 13·7°, 0·7688 at 30·6°, and 0·7575 at 41·6° relatively to water at 4°.

Calculation of Results.

The absolute viscosity of the vapour was calculated by means of Meyer's formula

$$pv = \frac{\pi r^4}{16\eta} \frac{(p_1^2 - p_2^2)}{l}.$$

When expressed in terms of the transpired mass this formula takes the form :—

$$\eta = \frac{\pi r^4}{16 l} \frac{(p_1^2 - p_2^2)t}{p_0 m} \rho \frac{T_0}{T_1},$$

where r = radius of the capillary ; l = length of the capillary ; p_1 and p_2 = pressures at the ends of the capillary ; p_0 = normal pressure (760 mm.) ; t = time in seconds ; m = mass transpired in the time t ; ρ = density of vapour at N.T.P. ; T_1 = absolute temperature of the capillary ;[*] $T_0 = 273°$ absolute.

Account has to be taken of the coefficient of slipping of the molecules, depending on their mean free path, the pressure, and the distance of the walls of the apparatus. When the mean free path is of the same order of magnitude as the diameter of the capillary, this correction is of considerable importance. From the classical experiments of Kundt and Warburg, the coefficient of slipping ζ was estimated to be 0·71 times the mean free path, whilst Knudsen gave 0·85. From the kinetic theory of gases the formula should be

$$\zeta = 1{\cdot}70\eta\sqrt{3\mathrm{RT}}/(p_1 + p_2),$$

where R is the gas constant. In the calculations this coefficient is introduced as a factor, $\eta_{\text{corr.}} = \eta\,(1 + 4\zeta/r)$, where r is the radius of the capillary.

Another precaution to be observed in choosing the diameters of the capillary and the pressures to be used is concerned with the velocity of transpiration of vapour through the capillary. Reynold's criterion for liquids has been shown to apply also to gases in the form

$$r\,d\,v/\eta < 1000,$$

where v is the velocity of efflux, r the radius of the capillary and d the density of the gas; but in the present experiments we are far from reaching the maximum velocity allowed.

The correction for the expansion of the glass with rise of temperature is very small, and amounts only to about 0·5 per cent. at the highest temperatures reached.

Tabulated Measurements of Viscosities of Vapours.

The experimental data for benzene are collected in Table II, where the value Δ represents the difference of the squares of the pressure, which is the function that is effective in viscosity experiments. The mean values of the viscosity at different temperatures are tabulated in Table III and are plotted in fig. 2. The corresponding data for toluene are shown in Tables IV and V, and the data for cyclohexane in Tables VI and VII.

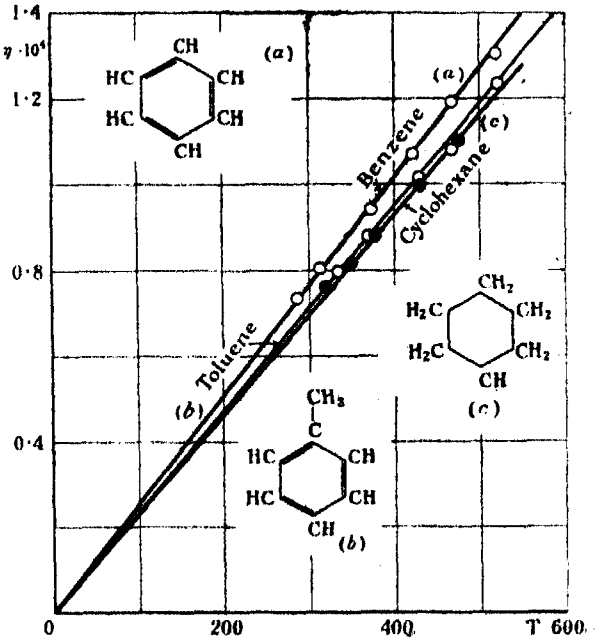

FIG. 2.—Viscosity of Benzene, Toluene and Cyclohexane.

From Table II it is seen that the viscosity is independent of the pressure over a fairly wide range; this constancy serves incidentally as a check against the presence of foreign gases in the viscometer. Moreover, the present results, obtained from determinations made at relatively low pressures, do not differ sensibly from those made at normal pressures, by a method giving relative values, and with an entirely different apparatus. In experiment 1 of the benzene series, and in most of the experiments on cyclohexane, the pressure on the condensation side was reduced to zero by cooling with solid carbon dioxide or liquid air (see Part III below). In the case of toluene, of which the vapour pressure is accurately known, the pressure was generally reduced to 0·686 mm. by surrounding the condensation bulb with melting ice.

Table II.—Viscosity of Vapour of Benzene.

No.	Temperature °C.	p_1 cm.	p_2 cm.	Δ.	Mass transpired gr./hour.	$\eta \times 10^4$ C.G.S.	η (corr.) $\times 10^4$ C.G.S.
1	15·5	4·37	—	19·1	0·0928	0·721	0·736
2	41	8·2	5·75	34·15	0·1353	0·796	0·802
3	94·5	11·97	6·83	96·5	0·2815	0·938	0·944
4	96·7	12·03	6·83	98	0·2846	0·936	0·943
5	101	13·02	10·42	60·8	0·1773	0·922	0·927
6	104·9	13·25	10·42	67·1	0·1891	0·944	0·952
7	105·2	13·29	10·93	58·6	0·1663	0·936	0·941
8	146·5	12·5	6·83	109·4	0·2492	1·052	1·061
9	151·5	12·92	10·2	63·1	0·1391	1·074	1·082
10	151·6	12·9	10·2	62·4	0·1382	1·070	1·078
11	197·1	13·48	10·42	73·1	0·1332	1·173	1·182
12	196·98	13·54	10·42	74·7	0·1375	1·161	1·170
13	197·4	13·86	10·42	83·5	0·1533	1·169	1·178
14	251·1	14·14	10·42	91·2	0·1343	1·303	1·313
15	246·0	14·29	10·93	84·7	0·1268	1·294	1·305

Table III.—Mean Values.

Temperature.	Viscosity.	Temperature.	Viscosity.
°C.		°C.	
15·5	$0·736 \times 10^{-4}$	149·9	$1·074 \times 10^{-4}$
41·0	$0·802 \times 10^{-4}$	197·2	$1·176 \times 10^{-4}$
100·5	$0·941 \times 10^{-4}$	248·5	$1·309 \times 10^{-4}$

Table IV.—Viscosity of Vapour of Toluene.

No.	Temperature °C.	p_1.	p_2.	Δ.	Mass transpired gr./hour.	$\eta \times 10^4$ C.G.S.	η corr. $\times 10^4$ C.G.S.
1	60·76	5·28	0·686	27·40	0·1253	0·7725	0·7848
2	60·8	5·275	0·686	27·35	0·124	0·7807	0·7936
3	95·0	5·064	Zero	25·18	0·0935	0·8635	0·882
4	96·8	5·153	0·686	26·00	0·0982	0·863	0·880
5	149·0	5·45	0·686	29·23	0·0828	0·986	1·008
6	154·6	5·45	0·686	29·23	0·0811	0·994	1·017
7	195·0	5·686	0·686	31·87	0·076	1·057	1·083
8	194·1	5·696	0·686	31·98	0·0763	1·058	1·084
9	249·2	5·69	0·686	31·93	0·0608	1·185	1·220
10	252·0	5·58	0·686	31·1	0·0589	1·185	1·240

Table V.—Mean Values.

Temperature.	Viscosity.	Temperature.	Viscosity.
° C.		° C.	
60·8	$0{\cdot}789 \times 10^{-4}$	194·5	$1{\cdot}083 \times 10^{-4}$
95·9	$0{\cdot}881 \times 10^{-4}$	250·6	$1{\cdot}232 \times 10^{-4}$
151·8	$1{\cdot}012 \times 10^{-4}$		

Table VI.—Viscosity of Vapour of Cyclohexane.

No.	Temperature ° C.	p_1.	p_2.	Δ.	Mass transpired gr./hour.	$\eta \times 10^4$ C.G.S.	η corr. $\times 10^4$ C.G.S.
1	46	7·07	Zero	50	0·2214	0·7554	0·7658
2	46·4	7·16	Zero	51·3	0·2283	0·751	0·7612
3	77·6	6·113	Zero	37·36	0·1412	0·806	0·820
4	78·5	6·82	Zero	46·53	0·1742	0·8115	0·8246
5	76·06	6·08	Zero	36·97	0·141	0·802	0·806
6	103·7	6·23	Zero	38·82	0·1266	0·869	0·886
7	104·9	6·16	Zero	37·95	0·1233	0·870	0·887
8	156·1	6·37	Zero	40·54	0·1007	0·982	1·005
9	156·9	6·396	Zero	40·9	0·104	0·977	0·990
10	204·8	6·534	Zero	42·6	0·0882	1·079	1·109
11	199·7	10·95	7·07	69·96	0·145	1·09	1·100

Table VII.—Mean Values.

Temperature.	Viscosity.	Temperature.	Viscosity.
° C.		° C.	
46·2	$0{\cdot}763 \times 10^{-4}$	156·5	$0{\cdot}997 \times 10^{-4}$
77·4	$0{\cdot}820 \times 10^{-4}$	202·2	$1{\cdot}104 \times 10^{-4}$
104·3	$0{\cdot}886 \times 10^{-4}$		

In Table VIII the values of the viscosity of benzene vapour at 0° C. and 100° C. as found by other observers are compared with those now recorded.

Table VIII.—Viscosity of Vapour of Benzene at 0° and 100° C.

$\eta_0 \times 10^4$ C.G.S.		$\eta_{100} \times 10^4$ C.G.S.	
0·709	**Puluj**	1·176	**Schumann**
0·689	**Schumann**	0·93	**Rappenecker**
0·694	**Nasini**	0·94	**Nasini**

One of the features of this table is that the value at 0°, slightly extrapolated from the present data, corresponds very nearly with Schumann's value. On the other hand, the number found for 100° C. is identical with Rappenecker's value, but differs widely from that of Schumann, thus confirming Rappenecker's criticism of the data of Meyer and Schumann, which (as Brillouin* pointed out) lead to molecular volumes of about half the value of those found by Kopp. Rappenecker's own method, however, is not free from criticism, since, besides the difficulties encountered in obtaining a reproducible contact surface, no account was taken of the variation of surface-tension of mercury, even at so high a temperature as 212° C. It is therefore not surprising that his value for the viscosity of benzene-vapour at this temperature is higher than that calculated from my results.

Relationship between Viscosity and Temperature—Sutherland's Constant.

As may be seen from fig. 2, the viscosities of the three hydrocarbons, when plotted against the temperature, fall upon straight lines passing through the origin. The values for benzene at 15·5° and 41° C. fall upon the appropriate line, although this could scarcely have been expected in the case of observations made at so low a temperature and with such slight superheating.

Several formulæ, based upon the use of different molecular models, have been proposed for the relationship between gaseous viscosity and temperature.† In a large number of cases the best model has been found to be that of Sutherland, namely, an elastic spherical molecule with a weak field of attraction; but it has been shown theoretically that accurate results cannot be obtained by this method in the case of vapours. A more accurate model of Sutherland's type has been worked out by Hassé and Cook‡; for some cases already tested, it gives different values for the force-constants in the formula, but an equally good agreement is obtained in the calculation of the experimental curves when using a formula of the old type. A mixed field of attraction and repulsion has been postulated by Lennard Jones,§ but in his formula it appears that a particular molecular field has to be attributed to every different type of molecule; Sutherland's model then appears as a particular case of the general formula, in which the index of the repulsive field is $\eta = \infty$. Since the force-field cannot be determined from viscosity data alone, but must be combined with data for gaseous compressibility and crystal dimensions, which are not available in the cases now under consideration, no attempt has been made to deduce the force-fields for the present series of compounds. On the other hand it has been thought useful to calculate the unambiguous value of the Sutherland constant S in the well-known equation

---

* Brillouin, 'Leçons sur la Viscosité des Liquides et des Gaz,' Paris, Gauthier-Villars, p. 82 (1907).

† Kuenen, "Die Eigenschaffen der Gase," 'Ak. Verlagsgesel., Leipzig' (1919).

‡ 'Phil. Mag.,' vol. 3, p. 977 (1927).

§ 'Roy. Soc. Proc.,' A, *passim* (1924–1926).

$$\eta = \mathrm{KT}^{3/2}/(\mathrm{S} + \mathrm{T}),$$

where η is the viscosity, T is the absolute temperature, and K is another arbitrary constant. For this purpose $\mathrm{T}^{3/2}/\eta$ was plotted against T and the value of S was deduced by extrapolation from the straight line which expresses the relationship between these two quantities. The values deduced in this way were as follows :—

Benzene, S = 380. Toluene, S = 370. Cyclohexane, S = 330.

The value for benzene differs very widely from the value S = 700, previously given by Rappenecker ; but this is not surprising in view of the fact that his observations were made at two temperatures only, and under conditions which might easily give rise to an error of 100 per cent. in the value of this constant. Moreover, the value given by Rappenecker is inherently improbable, since it is one of the highest in the literature, whereas the figure now given is of a much more normal character in that it is about three-quarters of the critical temperature (583° A) of the substance, and is in good general concordance with the values for the two closely-related hydrocarbons, toluene and cyclohexane. Its validity is also confirmed by the well-established character of the linear relation on which it is based. Although therefore the values of this constant are always rather uncertain, especially in the case of vapours, it is believed that the numbers now given are substantially correct.

Molecular Area.

Chapman's formula giving the mean molecular area presented by molecules in thermal collision is

$$\overline{\mathrm{A}} = \pi\sigma^2 = \frac{0{\cdot}491\,(1 + \varepsilon_a)\,\rho\overline{\mathrm{V}}}{4{\cdot}2^{\frac{1}{2}}\nu\eta\,(1 + \mathrm{S}/\mathrm{T})},$$

where σ is the radius of the molecule, ρ the density of the gas at N.T.P., $\overline{\mathrm{V}}$ the mean molecular velocity, ν the number of molecules per cubic centimetre, η the coefficient of viscosity, S Sutherland's constant, T the absolute temperature, whilst $(1 + \varepsilon_a)$ is a factor depending on T and S, which in the present case differs but little from unity.

The mean collision areas of the three hydrocarbons deduced by means of Chapman's formula from the data now recorded are :—

Benzene, $\bar{A}$ = 19·0 Å^2. Toluene, $\bar{A}$ = 21·8 Å^2. Cyclohexane, $\bar{A}$ = 22·3 Å^2.

The mean collision areas of benzene and toluene, as deduced from the viscosities of the vapours, may be compared with the areas deduced from Bragg's crystal models. For this purpose E. Mack* constructed solid models to represent the structures deduced from crystallographic data and from X-ray analysis ; the area of the shadow cast by the model in a series of fortuitous positions was then measured with a planimeter and a constant average was obtained, even in an extreme case, after about 60 measurements. A comparison of Mack's values with those now recorded shows the following results :—

	From model.		From viscosity.	
Benzene	28·9	2·6 A^2	19·0	2·85 A^2.
Toluene	31·5		21·85	

The absolute values differ by about 50 per cent., but the differences are of similar magnitude. Other values for the mean area of the benzene molecule are as follows :—

A. From Huggins' model with hydrogen atoms of diameter 1·35 A.	$\bar{A}$ = 24·0
B. From N. K. Adam's measurements of the benzene radical in an oriented film	$\bar{A}$ = 23·8
C. From diffusion of vapours by Le Blanc and Wuppermann	$\bar{A}$ = 25·3
D. Ditto by Winkelmann	$\bar{A}$ = 26·1

Summary.

(1) An apparatus, based on Rankine's method, has been constructed for measuring the viscosity of vapours.

(2) With this apparatus the viscosity of benzene has been measured from 15° to 251°, that of toluene from 61° to 252°, and that of cyclohexane from 46° to 205°.

---

* 'J. Amer. Chem. Soc.,' vol. 47, p. 2468 (1925).

(3) From these measurements, Sutherland's constants and the mean collision areas for the three hydrocarbons have been deduced as follows:—

	S.		$\bar{A}$.
Benzene	380	....	19·0
Toluene	370	....	21·8
Cyclohexane	330	....	22·3

(4) The values for benzene have been compared with those deduced by other workers, but no earlier data are available for toluene or for cyclohexane.

The Molecular Dimensions of Organic Compounds. Part III.—*The Viscosity of Vapours: Thiophen and α-Methylthiophen, Pyridine and Thiazole.*

By Dr. A. G. Nasini.

(Communicated by Prof. T. M. Lowry, F.R.S.—Received November 7, 1928.)

The measurements described below were made with the purpose of determining the effect of replacing two methenyl-groups in the benzene ring by an atom of sulphur. This investigation differed from those described in Part II, in that the substances were no longer available in indefinitely large quantities, and that in consequence of this difficulty of supply a large number of their physical properties were still undetermined. Thus, in addition to the viscosities of the vapours, which were the only measurements that it was necessary to make in the case of benzene, toluene and cyclohexane, the experiments on thiophen included measurements of density and of vapour-pressure, and those on methylthiophen included measurements of the melting point of the solid, and of the boiling point, critical temperature, vapour pressure, viscosity and surface tension of the liquid. Moreover, even in the measurements of vapour viscosity, certain modifications were introduced as a result of the altered conditions of working. In particular, trials were made to find out how the transpiration-apparatus would work when the "condensation pressure" was reduced to zero, since this method of working would make it possible to determine the viscosity of a vapour without determining also the vapour-pressure curve, a point of special importance when the substance can only be obtained in small quantities.

Purification of Materials.

(*a*) *Thiophen.*—The thiophen was fractionally distilled over sodium, and a middle fraction was used which boiled within one-tenth of a degree at 84·3° under 760 mm. pressure at 30·3°.

(*b*) *Methylthiophen.*—The specimen was kindly supplied by Dr. Challenger, who had obtained it from Kimmeridge shale.* The product was regenerated through mercuric acetate and was finally purified through the mercuric chloride compound. The purified product boiled at 112·1°, and was believed to be substantially pure, although the quantity available was not sufficient for fractional distillation through a still-head.

(*c*) *Pyridine.*—A sample which had already been purified by fractional distillation was regenerated from its mercuric chloride compound. The product boiled within one-tenth of a degree at 115·4° C. (corr.).

(*d*) *Thiazole.*—The sample used in the present experiments was lent by the Chemical Laboratory of Pisa, to which I desire to express my thanks. It had been prepared by the Wissenschaftliches Chemisch Institut of Berlin, by the method of Traumann and Popp.† Its boiling-point, 116·8° C., corresponded exactly to that given by other observers‡; but its density, 1·104 at 21·3° C., differed greatly from the only datum existing in the literature, namely, Popp's value, 1·198 at 17° C. This sample was fractionated by means of a micro-dephlegmator. The product boiled within one-tenth of a degree, and gave a mercury chloride compound similar to that previously described by other authors. The smell was practically indistinguishable from that of pyridine, a characteristic quality already observed by Popp. A preliminary analysis showed a percentage of sulphur rather lower than the theoretical value, but no further analyses were made since the whole of the sample was required for the physical measurements; as no more of the costly material was available, the physical measurements are only of a preliminary character.

Measurements of Viscosity.

Prof. Rankine§ has suggested that Meyer's formula for the velocity of effusion might not hold when the pressure in the transpiration apparatus is zero on one side of the capillary; but it can be shown both theoretically and experimentally that trustworthy results may be obtained under these conditions when using the apparatus and methods described below.

---

* Challenger, Kinks and Haslam, 'J. Chem. Soc.,' vol. 127, p. 162 (1925), *et seq.*

† 'Ann. Chem.,' vol. 250, p. 273 (1889).

‡ Willstätter and Wirth, 'Ber. d. Chem. Ges.,' vol. 42, p. 1909 (1909); Popp, *loc. cit.*

§ 'Roy. Soc. Proc.,' A, vol. 91, p. 201 (1915).

It is well known that at very low pressures the law of efflux changes, and that the formula of Poiseuille must be replaced by that of Knudsen[*] and Smoluchowski[*]

$$v_{(p=1)} = \tfrac{4}{3}\sqrt{2}\pi \,.\, r^3/\mathrm{L} \,.\, (p_1 - p_2)/\sqrt{d}$$

for $f = 1$, where v is the volume of gas transpired in unit time, p_1 and p_2 are the pressures of transpiration, d is the density of the gas, r is the radius of the molecules, and f is the proportion of molecules not regularly reflected from the walls; L is the length of the capillary. The experiments of Kundt and Warburg[†] indicate that, when allowance is made for the coefficient of slipping, the coefficient of gaseous viscosity may be considered correct until the pressure is as low as 1 mm. of mercury. We may therefore assume that the limit at which the law of efflux changes is at 1 mm., and proceed to calculate the position in the capillary at which this pressure is reached. Given that the velocity of flow is determined by the difference of the squares of the pressures at the two ends of the capillary, and by the reciprocal of its length, we have

$$x/l = p_2^2/p_1^2$$

where l is the total length of the capillary and x is the distance from the end of the capillary at which the pressure p_1 on the evaporation side is reduced to p_2. For the capillaries used in the present experiments, the values of x, when $p_1 =$ 8 cm., and $p_2 = 0 \cdot 1$ cm. can be shown to be about 0·06 mm. The law of efflux would therefore only be changed for a distance along the capillary which is negligible compared with other sources of error in the apparatus; and this theoretical conclusion was confirmed by experimental observations, which showed that no difference could be detected between the data obtained by the usual method and by the method of zero pressure.

The apparatus used in order to test the two methods of working was constructed entirely of Jena glass 59^{III}, and was connected by a ground joint to the Thuringen glass leads of the pump-system. The new apparatus was provided with a manometer on the condensation side, in order to avoid errors arising from the possible presence of foreign gases in the viscometer. The higher pressures of condensation were obtained by means of thermostats, or

---

[*] Knudsen, 'Ann. Physik,' vol. 28, pp. 75, 999 (1909), vol. 31, pp. 205, 633 (1910), vol. 33, p. 1435 (1910), and vol. 34, p. 283 (1911); Smoluchowski, 'Ann. Physik,' vol. 33, p. 1559 (1920).

[†] See Brillouin, 'Leçons sur la Viscosité des Liquides et des Gaz,' Paris, p. 30 (1907); 'Pogg. Ann.,' vol. 155, p. 337, 525 (1875); vol. 156, p. 177 (1875).

Dewar flasks filled with ice water. The zero pressures were produced by immersing the bulb in a Dewar flask filled with liquid air or with solid carbon dioxide and ether, whilst the manometer was kept in a large transparent Dewar flask filled with water at room-temperature. The pressures at the two manometers were read by means of a table cathetometer and one of the more usual type. The apparatus had a capillary 40 cm. long, of radius about 0·009 cm., and its resistance was $\Sigma \frac{l}{r_4} = 4{\cdot}995 \times 10^9$ cm.$^{-3}$.

Tabulated Results.

The observations on the viscosity of thiophen-vapour are given in Table IX, and the mean values for different temperatures are shown in Table X. The corresponding data for α-methylthiophen are given in Tables XI and XII. The values for pyridine are given in Tables XIII and XIV, and those for thiazole in Table XIV.

Table IX.—Viscosity of Thiophen.

No.	Temperature °C.	p_1 cm.	p_2 cm.	Δ.	Mass transpired gr./hour.	$\eta \times 10^4$ C.G.S.	η (corr.) $\times 10^4$ C.G.S.
1	19·9	3·6	Zero	12·96	0·0699	0·680	0·696
2	54	7·06	Zero	49·87	0·1804	0·909	0·924
3	54·86	7·054	Zero	49·75	0·1804	0·905	0·920
4*	55·7	8·25	2·36	62·49	0·0539	0·897	0·909
5	73·8	7·407	Zero	54·85	0·1774	0·959	0·975
6	73·3	7·22	Zero	52·15	0·1690	0·959	0·975
7*	96·5	8·19	2·36	62·09	0·0419	1·01	1·027
8*	96·4	8·30	Zero	68·94	0·0466	1·017	1·039
9	95·7	8·03	5·81	30·63	0·0872	1·017	1·027
10	150·1	7·98	Zero	63·7	0·1393	1·163	1·188
11	150·1	7·96	Zero	63·3	0·1377	1·168	1·193
12*	193·6	8·44	Zero	71·25	0·0304	1·277	1·315
13	198·6	7·89	Zero	62·26	0·1100	1·294	1·324
14	199·5	7·94	Zero	63·16	0·1110	1·298	1·330
15*	199·6	8·39	2·28	65·18	0·0270	1·290	1·320
16	245·4	6·97	Zero	48·65	0·0713	1·416	1·463
17	245·5	7·00	Zero	49·00	0·0721	1·410	1·457

Table X.—Mean Values.

Temperature.	Viscosity.	Temperature.	Viscosity.
°C.		°C.	
19·9	$0{\cdot}696 \times 10^{-4}$	150·1	$1{\cdot}190 \times 10^{-4}$
54·8	$0{\cdot}918 \times 10^{-4}$	197·8	$1{\cdot}322 \times 10^{-4}$
96·2	$1{\cdot}031 \times 10^{-4}$	245·4	$1{\cdot}460 \times 10^{-4}$

Table XI.—Viscosity of Vapour of Methylthiophen.

No.	Temperature ° C.	Δ.	Mass transpired gr./hour.	$\eta \times 10^4$ C.G.S.	η (corr.) $\times 10^4$ C.G.S.
1	50·0	24·66	0·1160	0·822	0·839
2	50·0	23·00	0·109	0·818	0·835
3	99·5	25·2	0·0902	0·943	0·966
4	100·0	25·8	0·0923	0·941	0·964
5	150·0	27·73	0·0798	1·032	1·060
6	150·3	28·88	0·0822	1·043	1·061
7	199·7	30·7	0·0700	1·165	1·201
8	200·2	30·4	0·0693	1·164	1·200
9	249·6	29·6	0·0544	1·308	1·356
10	249·7	28·4	0·0535	1·300	1·348

Table XII.—Mean Values.

Temperature.	Viscosity.	Temperature.	Viscosity.
° C.		° C.	
50·5	$0·837 \times 10^{-4}$	200·0	$1·200 \times 10^{-4}$
100·0	$0·965 \times 10^{-4}$	249·6	$1·352 \times 10^{-4}$
150·0	$1·060 \times 10^{-4}$		

Table XIII.—Viscosity of Vapour of Pyridine.

No.	Temperature ° C.	p_1 cm.	p_2 cm.	Δ.	Mass transpired gr./hour.	$\eta \times 10^4$ C.G.S.	η (corr.) $\times 10^4$ C.G.S.
1	95·9	4·546	0·71	20·16	0·0720	0·934	0·954
2	100·6	4·55	0·71	20·21	0·0706	0·941	0·961
3	147·9	4·596	0·69	20·67	0·0565	1·044	1·071
4	149·5	4·97	0·685	24·26	0·0663	1·064	1·094
5	199	5·06	0·685	25·16	0·05526	1·186	1·220
6	199·3	5·06	0·71	25·13	0·0417	1·192	1·226
7	267·7	5·33	0·72	27·9	0·0481	1·318	1·361
8	262·2	5·35	0·72	28·11	0·04997	1·292	1·332

Table XIV.—Mean Values.

Pyridine.		Thiazole (provisional values).	
Temperature.	Viscosity.	Temperature.	Viscosity.
° C.		° C.	
98·2	$0·958 \times 10^{-4}$	99·4	$1·161 \times 10^{-4}$
148·7	$1·083 \times 10^{-4}$	152·9	$1·299 \times 10^{-4}$
199·1	$1·223 \times 10^{-4}$	200·3	$1·412 \times 10^{-4}$
265	$1·346 \times 10^{-4}$	252·5	$1·537 \times 10^{-4}$

In these tables, values obtained with the new apparatus are marked with an asterisk (these experiments lasted from 3 to 4 hours), and are seen to be in good agreement with those obtained with the old apparatus, for which $\Sigma l/r^4 = 1 \cdot 179 \, . \, 10^9$ cm.$^{-3}$. From these data the limit of error can be estimated at less than 2 per cent. A similar concordance is seen between the observations made at different pressures. We therefore conclude that Meyer's efflux formula is valid throughout the range of conditions used in these experiments. When plotted against the temperature as in figs. 1 and 2, the viscosity data fall on a straight line, which (with the exception of the preliminary data for thiazole) passes through the origin; but the values for thiophen at low temperature show a slight deviation from the others.

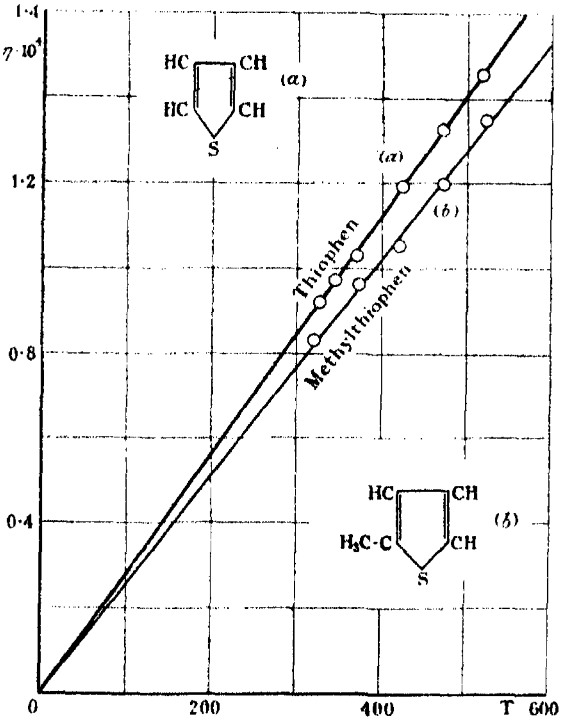

FIG. 1.

The values of Sutherland's constant and the mean collision areas of the vapours were calculated by the methods described in Part II as follows:—

Thiophen	S = 407	$\bar{A} = 16 \cdot 7$ Å^2
Methylthiophen	S = 400	$\bar{A} = 19 \cdot 9$ Å^2
Pyridine	S = 320	$\bar{A} = 20 \cdot 0$ Å^2

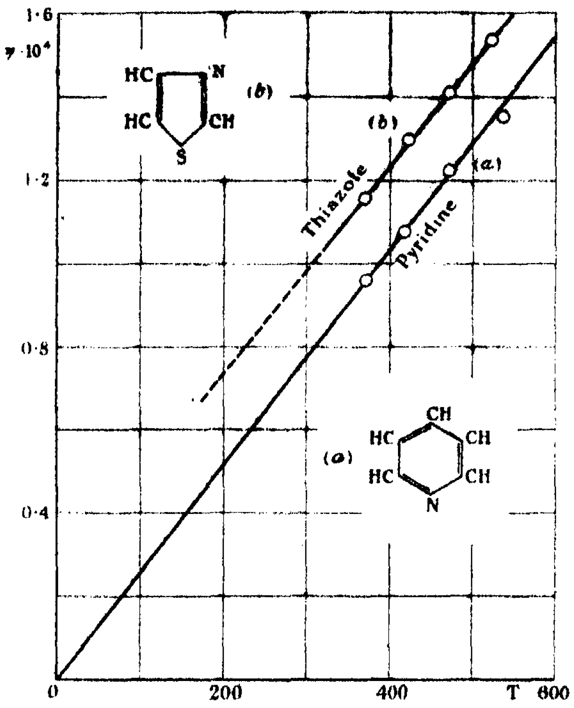

FIG. 2.

Other Properties.

Density.—The following observations were made, using an Ostwald pyknometer of about 5 c.c. capacity with ground glass caps.

Table XV.—Densities.

(*a*) Thiophen.	(*b*) Methylthiophen.
1·0711 at 13·7° 1·0518 at 30·3°	1·0134 at 23·9° 1·0084 at 30·6° 0·9960 at 41·6°

Vapour-pressure.—The vapour-pressures of thiophen and of methylthiophen were determined with Smith and Menzies' isoteniscope.* Apart from the small quantity of liquid required, the method has the advantage of a complete expulsion of the air from the measurement-chamber, and a very sensitive adjustment of the pressure through the differential manometer formed by the liquid itself. The thermostat was hand-regulated by means of an electrical resistance, the stirring being almost riotous, as an essential condition for accurate results; the temperatures were given by standardised thermometers completely immersed in the bath. The pressures were read by another observer by means of a cathetometer, the pressure readings being corrected for the expansion of the scale and for capillarity, and finally reduced to 0° C.

---

* 'J. Amer. Chem. Soc.,' vol. 103, p. 959 (1913).

Table XVI.—Vapour-pressures.

(*a*) Thiophene.		(*b*) Methylthiophen.		(*c*) Thiazole (provisional values).	
Temperature ° C.	Pressure cm. Hg.	Temperature ° C.	Pressure cm. Hg.	Temperature ° C.	Pressure cm. Hg.
20·2	6·32	33·3	38·16	23·5	1·70
25·05	7·98	34·2	39·85	34·05	2·98
29·2	9·66	39·55	51·7	43·2	4·73
41·35	16·47	51·30	83·3	53·92	7·82
50·6	24·34	63·6	147·9	61·3	10·78
60·1	34·1	75·0	226·65	71·87	16·44
70·5	49·0	84·8	318·3	82·4	24·90
79·9	64·15	94·8	443·6	84·75	27·18
84·2	75·81			92·0	36·03

The data for thiophen and for methylthiophen should be compared with Kahlbaum's values for benzene* and with the values for toluene given by Drucker and Jiméno.†

Viscosity of Liquid.—This was determined by means of a small Ostwald viscometer, with an upper bulb of about 1 c.c. capacity constructed according to the design of Bingham.‡ The viscometer was immersed in a large thermostat with transparent glass windows, special care being taken to maintain the instrument in a vertical position. The time of efflux, determined by a standardised stop-watch, was 280·8 seconds for water and 206·4 seconds for methylthiophen, giving for the viscosity of α-methylthiophen the value 0·00667 C.G.S. units at 25·1°.

Surface-tension.—Sugden's method was adopted, since it is very convenient for determinations with small quantities of liquid. The readings were made in a large electrically-controlled thermostat, fitted on one side with a specially-selected piece of plate-glass. The stand on which the apparatus was mounted could be adjusted by means of levels. The readings were made by means of a table-cathetometer reading to 0·01 mm. over a length of 4 cm. The capillaries were cleaned with nitric acid and chromic acid mixture, and rinsed with water distilled *in vitro*. The radii of the capillaries were $r_1 = 0{\cdot}0489$ cm., $r_2 = 0{\cdot}1324$ cm. The surface-tension is given by the formulæ $a^2 = \mathrm{H}/(1/b_1 - 1/b_2)$ and $\gamma = \frac{1}{2}g(\mathrm{D} - d)\,a^2$, where a is the specific cohesion, D the density of the liquid, d the density of the vapour (or of air and vapour if the measurement has been made in air), H the vertical distance between the two menisci, and b_1 and b_2 their radii of curvature. The following results were obtained.

---

* 'Z. phys. Chem.,' vol. 26, p. 603 (1898).

† 'Z. phys. Chem.,' vol. 90, p. 513 (1915).

‡ 'J. Chem. Soc.,' vol. 103, p. 959 (1913).

Table XVII.—Surface Tension of Methylthiophen.

Height H in cm.	Temperature.	a^2.	γ.	K.
0·826	24·5	6·22	30·79	2·74 (1°–2°)
0·810	29·8	6·09	30·03	2·27 (1°–3°)
0·771	46·1	5·79	28·21	2·055 (2°–3°)

Melting-point.—The melting-point of α-methylthiophen, —51° C., was determined in a Dewar flask, containing a mixture of solid carbon dioxide and ether, in which were arranged two concentric test-tubes. The inner tube containing the substances was fitted with a small glass stirrer, and the temperature was determined by means of a standardised pentane thermometer.

Critical Temperature.—This was determined by visual observation in small sealed tubes. These were filled by means of an apparatus similar to that described in Part II. The substance was distilled over liquid air, and when only the air-free liquid and its vapour were present the liquid was distilled into the sample tubes sealed to the apparatus. A part of the liquid was allowed to boil under the saturation pressure, and the tube was sealed off whilst the liquid was boiling. Four tubes were prepared, but one burst, and the determinations were made with the three remaining tubes. These were heated in a Magnus stove, gas-heated and hand-regulated, in which a fall of temperature of 1° in 5 minutes could be obtained.

The thermometer was standardised by means of the melting-point of purified lead under the same condition as those used for the sample tubes. The three determinations varied within one degree. The critical temperature recorded for α-methylthiophen was 231°, in close agreement with the accepted value for toluene.

Summary.

(1) A further modification of the apparatus used for measuring the viscosity of vapours is described, in which a zero pressure is used on the condensation side of the capillary. The validity of this method has been shown both by theoretical considerations and by comparative measurements.

(2) The viscosities of thiophen, methylthiophen and pyridine have been determined, but only a preliminary series of measurements was made with thiazole.

(3) The values of Sutherland's constant and of the mean collision areas were deduced as follows:—

	S.		$\bar{A}$.
Thiophen	407	....	16·7
Methylthiophen........	400	....	19·9
Pyridine	320	....	20·0

(4) Measurements were made of the freezing-point, boiling-point, critical temperature, vapour-pressure, surface-tension and viscosity of α-methylthiophen. The boiling-point recorded for thiazole was also confirmed.

My thanks are due to Prof. T. M. Lowry for suggesting this problem for research and for providing the necessary apparatus, as well as for his advice and sympathetic interest. My thanks are also due to Prof. L. Rolla for the hospitality in his laboratory and for placing at my disposal the apparatus necessary for the continuation of the work. I am indebted also to the Società Boracifera di Larderello and to the Chairman, Prince Ginori Conti, for a generous maintenance grant in Florence, and to Mr. Robert Mond who presented me with a complete set of Hyvac pumps.

Quantum Mechanics of Many-Electron Systems.

By P. A. M. Dirac, St. John's College, Cambridge.

(Communicated by R. H. Fowler, F.R.S.—Received March 12, 1929.)

§ 1. *Introduction.*

The general theory of quantum mechanics is now almost complete, the imperfections that still remain being in connection with the exact fitting in of the theory with relativity ideas. These give rise to difficulties only when high-speed particles are involved, and are therefore of no importance in the consideration of atomic and molecular structure and ordinary chemical reactions, in which it is, indeed, usually sufficiently accurate if one neglects relativity variation of mass with velocity and assumes only Coulomb forces between the various electrons and atomic nuclei. The underlying physical laws necessary for the mathematical theory of a large part of physics and the whole of chemistry are thus completely known, and the difficulty is only that the exact application of these laws leads to equations much too complicated to be soluble. It therefore becomes desirable that approximate practical methods of applying quantum mechanics should be developed, which can lead to an explanation of the main features of complex atomic systems without too much computation.

Already before the arrival of quantum mechanics there existed a theory of atomic structure, based on Bohr's ideas of quantised orbits, which was fairly successful in a wide field. To get agreement with experiment it was found necessary to introduce the spin of the electron, giving a doubling in the number of orbits of an electron in an atom. With the help of this spin and Pauli's exclusion principle, a satisfactory theory of multiplet terms was obtained when one made the additional assumption that the electrons in an atom all set themselves with their spins parallel or antiparallel. If s denoted the magnitude of the resultant spin angular momentum, this s was combined vectorially with the resultant orbital angular momentum l to give a multiplet of multiplicity $2s+1$. The fact that one had to make this additional assumption was, however, a serious disadvantage, as no theoretical reasons to support it could be given. It seemed to show that there were large forces coupling the spin vectors of the electrons in an atom, much larger forces than could be accounted for as due to the interaction of the magnetic moments of the electrons. The position was thus that there was empirical evidence in favour of these large forces, but that their theoretical nature was quite unknown.

The old orbit theory is now replaced by Hartree's method of the self-consistent field,* based on quantum mechanics. The simplifying feature of the old theory, according to which each electron has its own individual orbit, is retained, but the " orbit " is now a quantum-mechanical state of the single electron, represented by a wave function in three dimensions. The only action of one orbit on another is assumed to be that of a static distribution of electricity, causing a partial screening of the nucleus. A theoretical justification for Hartree's method, showing that its results must be in approximate agreement with those of the exact Schrödinger equation for the whole system, has been given by Gaunt.† The method, however, suffers from the same limitation as the old orbit theory. It cannot give an explanation of multiplet structure without an extraneous assumption of large forces coupling the spins.

The solution of this difficulty in the explanation of multiplet structure is provided by the *exchange* (austausch) interaction of the electrons, which arises owing to the electrons being indistinguishable one from another. Two electrons may change places without our knowing it, and the proper allowance for the possibility of quantum jumps of this nature, which can be made in a treatment of the problem by quantum mechanics, gives rise to the new kind of interaction. The energies involved, the so-called exchange energies, are quite large. In fact it is these exchange energies between electrons in different atoms that give rise to homopolar valency bonds, as shown by Heitler and London.‡

The application of the new exchange ideas to the problem of multiplet structure has been made by Wigner§ and Hund.‖ The new theory provides no justification for the assumption that the electrons all set themselves with their spins parallel or antiparallel. In fact it does not allow any meaning to be given to this assumption, since in quantum mechanics the component of the spin angular momentum of an electron in any direction is a q-number with the two eigen-values $\pm \frac{1}{2}h$, so that one cannot *in general* give a meaning to the direction of the spin of an electron in a given stationary state. What the new theory shows instead is that *for each stationary state of the atom there is one definite numerical value for s, the magnitude of the total spin vector.* If it were not for this theorem, a measurement of s for the atom in a given stationary state would lead to one or other of a number of possible results, according to a definite probability law. This theorem forms the basis of the theory of multiplets. It is quite sufficient to replace the previous idea of the electrons all setting themselves parallel or antiparallel, since it shows that we can take s to be a quantum number describing the states of the atom, while s combined vectorially with l gives a multiplet of multiplicity $2s + 1$.

---

* D. R. Hartree, 'Proc. Camb. Phil. Soc.,' vol. 24, p. 89 (1928).

† J. A. Gaunt, 'Proc. Camb. Phil. Soc.,' vol. 24, p. 328 (1928). It is pointed out by Gaunt that there does not seem to be any theoretical justification for Hartree's method of calculating energies and that its extremely good agreement with observation is probably accidental. The somewhat different method proposed by Gaunt is the one that should be used in connection with the present paper.

‡ W. Heitler and F. London, 'Z. Physik,' vol. 44, p. 455 (1927).

§ E. Wigner, 'Z. Physik,' vol. 43, p. 624 (1927).

‖ F. Hund, 'Z. Physik,' vol. 43, p. 788 (1927).

Further developments of the theory of exchange have been made by Heitler, London and Heisenberg,* containing applications to molecules held together by homopolar valency bonds and to ferromagnetism. The treatment given by these authors makes an extensive use of group theory and requires the reader to be well acquainted with this branch of pure mathematics. Now group theory is just a theory of certain quantities that do not satisfy the commutative law of multiplication, and should thus form a part of quantum mechanics, which is the general theory of all quantities that do not satisfy the commutative law of multiplication. It should therefore be possible to translate the methods and results of group theory into the language of quantum mechanics and so obtain a treatment of the exchange phenomena which does not presuppose any knowledge of groups on the part of the reader. This is the object of the present paper. The treatment of groups on the lines of quantum mechanics has the advantage that it often gives a simple physical meaning to an abstract theorem in the theory of groups, enabling one to remember the theorem more easily and perhaps suggesting a simpler way of proving it. A further advantage of the treatment of the exchange phenomena on these lines is that one can avoid doing more work in the theory of groups than is strictly necessary for the physical applications, which results in a considerable shortening in the method.

In §§ 2 and 3 the general theory is given of systems containing a number of similar particles, showing the existence of exclusive sets of states (*i.e.*, sets such that a transition can never take place from a state in one set to a state in another), and giving their main properties. In § 4 an application is made to electrons, a proof being obtained of the fundamental theorem in italics above. The subsequent work is concerned with an approximate calculation of the energy levels of the states, the result of this being expressible by the single simple formula (26). This formula shows that in the first approximation the exchange interaction between the electrons may be replaced by a coupling between their spins, the energy of this coupling for each pair of electrons being equal to the scalar product of their spin vectors multiplied by a numerical coefficient given by the exchange energy. This form of coupling energy is, however, just what was required in the old orbit theory. We obtain in this way a justification for the assumptions of this old theory, in so far as they can be formulated without contradicting the quantum-mechanical description of the spin. The formula (26), combined with Hartree's method for determining approximate wave functions for the different electrons, should provide a powerful way of dealing with complicated atomic systems.

---

* See various papers in the 'Z. Physik,' vols. 46–51. An excellent account of the whole theory is also contained in Weyl's book, 'Gruppentheorie und Quantummechanik.'

§ 2. *Permutations as Dynamical Variables.*

We consider a dynamical system composed of n similar particles, the rth particle being describable by certain generalised co-ordinates denoted by the single symbol q_r. Thus a wave function representing a state of the system will be a function of the variables $q_1, q_2, \ldots, q_n$, which may be written

$$\psi(q_1, q_2 \cdots q_n) = \psi(q)$$

for brevity. Suppose now that P is any permutation of $q_1, q_2, \ldots, q_n$. This P is an operator which can be applied to any wave function $\psi(q)$ to give as result another definite function of the q's, namely

$$\mathrm{P}\psi(q) = \psi(\mathrm{P}q),$$

where $\mathrm{P}q$ denotes the set of q's obtained by applying the permutation P to $q_1, q_2, \ldots, q_n$. Further P is a linear operator. Now in quantum mechanics any dynamical variable is a linear operator which can operate on any wave function, and conversely any linear operator that can operate on every wave function may be considered as a dynamical variable. Thus *any permutation* P *may be considered to be a dynamical variable.*

The present paper consists in a study of these permutations P as dynamical variables. There are no classical analogues to these variables and hence they give rise to phenomena, *e.g.*, the existence of exclusive sets of states and other exchange phenomena, which have no classical analogue. There are $n!$ of these variables, one of them, P_1 say, being the identity, which must thus be equal to unity. One can add and multiply these variables and form algebraic functions of them, in exactly the same way in which one can add and multiply and form algebraic functions of the ordinary co-ordinates and momenta. The product of any two permutations is a third permutation, and hence any function of the permutations is reducible to a linear function of them. Any permutation P has a reciprocal P^{-1} satisfying $PP^{-1} = P^{-1}P = P_1 = 1$.

A permutation P, like any other dynamical variable, can be represented by a matrix. If we take the representation in which the q's are diagonal, P will be represented by a matrix, whose general element may be written

$$(q_1' q_2' \ldots q_n' \mid P \mid q_1'' q_2'' \ldots q_n'') = (q' \mid P \mid q'')$$

for brevity. This matrix must satisfy

$$\int (q' \mid P \mid q'')\, dq''\, \psi(q'') = P\psi(q') = \psi(Pq'),$$

and hence

$$(q' \mid P \mid q'') = \delta(Pq' - q''). \tag{1}$$

We are using the notation $\delta(x)$, where x is short for a set of variables x_1, x_2, x_3, ..., to denote

$$\delta(x) = \delta(x_1)\,\delta(x_2)\,\delta(x_3)\ldots$$

which vanishes except when each of the x's vanishes. With this notation we have

$$\delta(Pq' - q'') = \delta(q' - P^{-1}q''),$$

since the condition that the left-hand side shall not vanish, which is that the q'''s shall be given by applying the permutation P to the q''s, is the same as the condition that the right-hand side shall not vanish, which is that the q''s shall be given by applying the permutation P^{-1} to the q'''s. Thus we have an alternative expression for the matrix representing P.

$$(q' \mid P \mid q'') = \delta(q' - P^{-1}q''). \tag{2}$$

The conjugate complex of any dynamical variable is given when one writes $-i$ for i in the matrix representing that variable and also interchanges the rows with the columns. Thus we find for the conjugate complex of a permutation P, with the help of (2) and (1)

$$\begin{aligned}(q' \mid \bar{P} \mid q'') = \overline{(q'' \mid P \mid q')} &= \delta(q'' - P^{-1}q') \\ &= (q' \mid P^{-1} \mid q'')\end{aligned}$$

or

$$\bar{P} = P^{-1}.$$

Thus a permutation is not in general a real variable, its conjugate complex being equal to its reciprocal.

Any permutation of the numbers 1, 2, 3, ..., n may be expressed in the cyclic notation, *e.g.*, for $n = 8$

$$P_a = (143)(27)(58)(6), \tag{3}$$

in which each number is to be replaced by the succeeding number in a bracket, unless it is the last in a bracket, when it is to be replaced by the first in that bracket. Thus P_a changes the numbers 12345678 into 47138625. The type of any permutation is specified by the partition of the number n which is provided by the number of numbers in each of the brackets. Thus the type of P_a is specified by the partition $8 = 3 + 2 + 2 + 1$. Permutations of the same type, *i.e.*, corresponding to the same partition, we shall call *similar*. (The usual language of group theory is to call them conjugate.) Thus, for example, P_a in (3) is similar to

$$P_b = (871)\,(35)\,(46)\,(2). \tag{4}$$

The whole of the $n!$ possible permutations may be divided into sets of similar permutations, each such set being called a *class*. The permutation $P_1 = 1$ forms a class by itself. Any permutation is similar to its reciprocal.

When two permutations P_a and P_b are similar, either of them P_b may be obtained by making a certain permutation P in the other P_a. Thus, in our example (3), (4) we can take P to be the permutation that changes 14327586 into 87135462, *i.e.*, the permutation

$$P = (18623)\,(475).$$

We then have the algebraic relation between P_b and P_a

$$P_b = PP_aP^{-1}. \tag{5}$$

To verify this, we observe that the product $P_a\psi$ of P_a with any wave function ψ is changed into $P_b\psi$ if one applies the permutation P to the P_a in the product but not to the ψ. If we multiply the product by P on the left we are applying this permutation to both the P_a and the ψ, so that we must insert another factor P^{-1} between the P_a and the ψ, giving us $PP_aP^{-1}\psi$ to equate to $P_b\psi$.

Equation (5) is the general formula showing when two permutations P_a and P_b are similar. Of course P is not uniquely determined when P_a and P_b are given, but the existence of any P satisfying (5) is sufficient to show that P_a and P_b are similar.

§ 3. *Permutations as Constants of the Motion.*

We now introduce a Hamiltonian H to describe the motion of the system, so that any stationary state of energy H′ is represented by a wave function ψ satisfying

$$H\psi = H'\psi,$$

in which H is regarded as an operator. This Hamiltonian can be an arbitrary function of the dynamical variables provided it is symmetrical between all the particles. This symmetry condition requires that an element $(q' \mid H \mid q'')$ of the matrix representing H shall be unaltered when one applies any permutation to the q''s and the same permutation to the q'''s, *i.e.*,

$$(q' \mid H \mid q'') = (Pq' \mid H \mid Pq'') \tag{6}$$

for arbitrary P.

The fact that H is symmetrical leads at once to the equation

$$PH = HP. \tag{7}$$

This equation may be verified by a similar argument to that used for equation (5), or alternatively by a direct application of the matrix representatives. Thus from (1)

$$(q' \mid PH \mid q'') = \int \delta (Pq' - q''') \, dq''' \, (q''' \mid H \mid q'') = (Pq' \mid H \mid q'')$$

and from (2)

$$(q' \mid HP \mid q'') = \int (q' \mid H \mid q''') \, dq''' \, \delta (q''' - P^{-1}q'') = (q' \mid H \mid P^{-1}q''),$$

and the two right-hand sides are now equal from (6). Equation (7) shows that *each permutation variable is a constant of the motion.* The P's are still constants when arbitrary perturbations are applied to the system, provided the perturbation energy to be added to the Hamiltonian is symmetrical. Thus the constancy of the P's is absolute.

In dealing with any system in quantum mechanics, when we have found a constant of the motion α, we know that if for any state α initially has the numerical value α' then it always has this value, so that we can assign different numbers α' to the different states and so obtain a classification of the states. This procedure is not so straightforward, however, when we have several constants of the motion α which do not commute (as is the case with our permutations P), since we cannot assign numerical values for all the α's simultaneously to any state. The existence of constants of the motion α which do not commute is a sign that the system is degenerate. We must now look for a function β of the α's which has one and the same numerical value β' for all those states belonging to one energy level H′, so that we can use β for classifying the energy levels of the system. We can express the condition for β by saying that it must be a function of H (a single-valued function is implied) according to the general definition of a function of a variable in quantum mechanics, or that β must commute with every variable that commutes with H, *i.e.* every constant of the motion. If the α's are the only constants of the motion, or if they are a set that commute with all other independent constants of the motion, our problem reduces to finding a function β of the α's which commutes with all the α's. We can then assign a numerical value β' for β to each energy level of the system. If we can find several such functions β, they must all commute with each other, so that we can give them all numerical values simultaneously and obtain a complete classification of the energy levels.

An example of this procedure is provided by the study of the angular momentum of an isolated system. This angular momentum has three components m_x, m_y, m_z, each a constant of the motion, which do not commute. We look for a function of m_x, m_y, m_z which commutes with them all three. We can conveniently take for this function the variable k defined by

$$k(k+h) = m_x^2 + m_y^2 + m_z^2. \tag{8}$$

For each energy level of the system there will now be one definite numerical value k' for k. This constant of the motion k is the only significant one for purposes of classifying the states, as the others merely describe the degeneracy.

We follow this method in dealing with our permutations P. We must find a function χ of the P's such that $P\chi P^{-1} = \chi$ for every P. It is evident that a possible χ is ΣP_c, the sum of all the permutations P_c in a certain class c, *i.e.* the sum of a set of similar permutations, since $\Sigma P P_c P^{-1}$ must consist of the same permutations summed in a different order. There will be one such χ for each class. Further, there can be no other independent χ, since an arbitrary function of the P's can be expressed as a linear function of them with numerical coefficients and it will not then commute with every P unless the coefficients of similar P's are always the same. We thus obtain all the χ's that can be used for classifying the states. It is convenient to define each χ as an average instead of a sum, thus

$$\chi_c = \Sigma P_c / n_c,$$

where n_c is the number of P's in the class c. An alternative expression for χ_c is

$$\chi_c = \Sigma_r P_r P_c P_r^{-1} / n\,!, \tag{9}$$

the summation being extended over all the $n!$ permutations P_r. For each permutation P there is one χ, $\chi(P)$ say, equal to the average of all permutations similar to P. One of the χ's is $\chi(P_1) = 1$.

The dynamical variables $\chi_1, \chi_2 \dots \chi_m$ obtained in this way will each have a definite numerical value for every stationary state of the system. Thus for every permissible set of numerical values $\chi_1', \chi_2' \dots \chi_m'$ for the χ's there will be a set of states of the system. Since the χ's are absolute constants of the motion these sets of states will be exclusive, *i.e.* transitions will never take place from a state in one set to a state in another.

The permissible sets of values χ' that one can give to the χ's are limited by the fact that there exist algebraic relations between the χ's. The product of any two χ's, $\chi_p\chi_q$, is of course expressible as a linear function of the P's, and since it commutes with every P it must be expressible as a linear function of the χ's, thus

$$\chi_p\chi_q = a_1\chi_1 + a_2\chi_2 + \dots + a_m\chi_m \tag{10}$$

where the a's are numbers. Any numerical values χ' that one gives to the χ's must be eigen-values of the χ's and must satisfy these same algebraic equations. For every solution χ' of these equations there is one exclusive set of states. One solution is evidently $\chi_p' = 1$ for every χ_p, and this gives the set of states with symmetrical wave functions. A second obvious solution is $\chi_p' = \pm 1$, the + or − sign being taken according to whether the permutations in the class p are even or odd, and this gives the set of states with antisymmetrical wave functions. The other solutions may be worked out in any special case by ordinary algebraic methods, as the coefficients a in (10) may be obtained directly by a consideration of the types of permutation to which the χ's concerned refer. Any solution is, apart from a certain factor, what is called in group theory a character of the group of permutations. The χ's are all real variables, since each P and its conjugate complex P^{-1} are similar and will occur added together in the definition of any χ, so that the χ''s must be all real numbers.

The number of possible solutions of the equations (10) may easily be determined, since it must equal the number of different eigen-values of an arbitrary function B of the χ's. We can express B as a linear function of the χ's with the help of equations (10); thus

$$B = b_1\chi_1 + b_2\chi_2 + \dots + b_m\chi_m. \tag{11}$$

Similarly we can express each of the quantities $B^2, B^3 \dots B^m$ as a linear function of the χ's. From these m equations, together with the equation $\chi(P_1) = 1$, we can eliminate the m unknowns $\chi_1, \chi_2 \dots \chi_m$, obtaining as result an algebraic equation of degree m for B,

$$B^m + c_1B^{m-1} + c_2B^{m-2} + \dots + c_m = 0.$$

The m solutions of this equation give the m possible eigen-values for B, each of which will, according to (11), be a linear function of $b_1, b_2 \dots b_m$ whose coefficients are a permissible set of values $\chi_1', \chi_2' \dots \chi_m'$. These m sets of values χ' thus obtained must be all different, since if there were fewer than m different permissible sets of values χ' for the χ's there would exist a linear function of the χ's every one of whose eigen-values vanishes, which would mean that the linear function itself vanishes and the χ's are not independent. Thus the number of permissible sets of numerical values for the χ's is just equal to m, which is the number of classes of permutations or the number of partitions of n. This number is therefore the number of exclusive sets of states.

The properties of the P's which are not properties of the χ's will only describe the degeneracy of the states. If we obtain a matrix representation of all the P's consistent with each of the χ's being a certain number χ', then the number of rows and columns of the matrices will be the degree of degeneracy of the states in the exclusive set χ', *i.e.*, the number of independent states belonging to each energy level. This degeneracy is an *essential* one and cannot be removed by any perturbation that is symmetrical between all the similar particles.

§ 4. *Multiplet Structure.*

The preceding theory of systems composed of similar particles will now be applied to the case when the particles are electrons. The new features which this requires us to take into consideration are the spin of the electrons and Pauli's exclusion principle.

The three Cartesian co-ordinates x, y, z of the rth electron we denote by the single symbol x_r. The spin angular momentum and magnetic moment of this electron will be of the form $\frac{1}{2}h\,\boldsymbol{\sigma}_r$ and $\frac{1}{2}eh/mc\,.\,\boldsymbol{\sigma}_r$, where $\boldsymbol{\sigma}_r$ is a vector whose components σ_{rx}, σ_{ry}, σ_{rz} satisfy

$$\sigma_{rx}^2 = 1, \qquad \sigma_{rx}\sigma_{ry} = i\sigma_{rz} = -\sigma_{ry}\sigma_{rx}, \tag{12}$$

with similar relations obtained by cyclic permutation of the suffixes x, y and z. We take x_r and σ_{rz} to be the variables describing the rth electron that appear in the wave function. It is convenient to write the wave function

$$\psi\,(x_1\sigma_1x_2\sigma_2 \ldots x_n\sigma_n) = \psi\,(x\sigma)$$

without the suffixes z attached to the σ's, these suffixes being understood whenever one is dealing with the variables in wave functions.

The exclusion principle now requires that ψ shall be antisymmetrical in the x's and σ's together, *i.e.*, that if any permutation is applied to the x's and also to the σ's, ψ must remain unchanged or change sign according to whether the permutation is an even or an odd one. Thus permutations applied to the x's and σ's together, produce only trivial effects and no useful results would be obtained by considering them as dynamical variables. We can, however, consider permutations P applied to the x's alone and apply our preceding theory to these. Any of these permutations is a constant of the motion when we neglect the forces due to the spins, so that the Hamiltonian does not involve the spin variables $\boldsymbol{\sigma}$. We can now introduce our χ's as functions of these P's and assert that for any permissible set of numerical values χ' for the χ's there will be one exclusive set of states. Thus there exist these exclusive sets of states for systems containing many electrons even when we restrict ourselves to a consideration only of those states that satisfy the exclusion principle. The exclusiveness of the sets of states is now, of course, only approximate, since the χ's are constants only when we neglect the spin forces. There will actually be a small probability for a transition taking place from a state in one set to a state in another.

Since ψ is antisymmetrical, the result of any permutation P applied to the x's must equal $\pm$ times the result when the same permutation is applied to the σ's. Thus if we denote by P^{σ} a permutation applied to the σ's considered as a dynamical variable, we shall have

$$\mathrm{P}_r = \pm\, \mathrm{P}^{\sigma}{}_r, \tag{13}$$

for each of the $n\,!$ permutations P_r. Thus instead of studying the dynamical variables P we can get all the results we want, *e.g.*, the characters χ', by studying the variables P^{σ}. The P^{σ}'s are much easier to study on account of the fact that the variables σ in the wave function have domains consisting each of only the two points 1 and -1, which are the two eigen-values of each σ_z. This fact results in there being fewer characters χ' for the group of permutations of the σ variables than for the group of general permutations, since it prevents a function of the variables σ_1, σ_2, ..., from being antisymmetrical in more than two of them.

The study of the dynamical variables P^{σ} is made specially easy by the fact that we can express them as algebraic functions of the dynamical variables $\boldsymbol{\sigma}$. Consider the quantity

$$\mathrm{O}_{12} = \tfrac{1}{2}\{1 + (\boldsymbol{\sigma}_1,\ \boldsymbol{\sigma}_2)\}.$$

With the help of (12) we find readily that

$$(\boldsymbol{\sigma}_1,\ \boldsymbol{\sigma}_2)^2 = (\sigma_{1x}\sigma_{2x} + \sigma_{1y}\,\sigma_{2y} + \sigma_{1z}\sigma_{2z})^2 = 3 - 2\,(\boldsymbol{\sigma}_1,\ \boldsymbol{\sigma}_2), \tag{14}$$

and hence that

$$\mathrm{O}_{12}{}^2 = \tfrac{1}{4}\{1 + 2\,(\boldsymbol{\sigma}_1,\ \boldsymbol{\sigma}_2) + (\boldsymbol{\sigma}_1,\ \boldsymbol{\sigma}_2)^2\} = 1. \tag{15}$$

Again, we find

$$\mathrm{O}_{12}\sigma_{1x} = \tfrac{1}{2}\{\sigma_{2x} - i\sigma_{1z}\sigma_{2y} + i\sigma_{1y}\sigma_{2z} + \sigma_{1x}\}$$
$$\sigma_{2x}\mathrm{O}_{12} = \tfrac{1}{2}\{\sigma_{1x} + i\sigma_{1y}\sigma_{2z} - i\sigma_{1z}\sigma_{2y} + \sigma_{2x}\}$$

and hence

$$\mathrm{O}_{12}\sigma_{1x} = \sigma_{2x}\mathrm{O}_{12}.$$

Similar relations hold for σ_{1y} and σ_{1z}, so that we have

$$\mathrm{O}_{12}\boldsymbol{\sigma}_1 = \boldsymbol{\sigma}_2\mathrm{O}_{12}$$

or

$$\mathrm{O}_{12}\boldsymbol{\sigma}_1\mathrm{O}_{12}^{-1} = \boldsymbol{\sigma}_2.$$

From this we can obtain with the help of (15)

$$\mathrm{O}_{12}\boldsymbol{\sigma}_2\mathrm{O}_{12}^{-1} = \boldsymbol{\sigma}_1.$$

These " Vertauschungs " relations for O_{12} with $\boldsymbol{\sigma}_1$ and $\boldsymbol{\sigma}_2$ are precisely the same as those for P^σ_{12}, the permutation consisting of the interchange of the spin variables of electrons 1 and 2. Thus we can put

$$\mathrm{O}_{12} = c\mathrm{P}^\sigma_{12}$$

where c is a number. Equation (15) shows that $c = \pm 1$. To determine which of these values for c is the correct one, we observe that the eigen-values of P^σ_{12} are 1, 1, 1, -1, corresponding to the fact that there exist three independent symmetrical and one antisymmetrical function $\mathrm{F}(\sigma_{1z}, \sigma_{2z})$ of the two variables σ_{1z}, σ_{2z}, whose domains contain only two points each. Thus the mean of the eigen-values of P^σ_{12} is $\frac{1}{2}$. Now the mean of the eigen-values of $(\boldsymbol{\sigma}_1, \boldsymbol{\sigma}_2)$ is evidently zero and hence the mean of the eigen-values of O_{12} is $\frac{1}{2}$. Thus we must have $c = +1$, and so we can put

$$\mathrm{P}^\sigma_{12} = \tfrac{1}{2}\{1 + (\boldsymbol{\sigma}_1, \boldsymbol{\sigma}_2)\}.$$

In this way any permutation P^σ consisting simply of an interchange can be expressed as an algebraic function of the $\boldsymbol{\sigma}$'s. Any other permutation P^σ can be expressed as a product of interchanges and can therefore also be expressed as a function of the $\boldsymbol{\sigma}$'s. With the help of (13) we can now express the P's as algebraic functions of the $\boldsymbol{\sigma}$'s and eliminate the P^σ's from the discussion. We have, since the $-$ sign must be taken in (13) when the permutations are interchanges,

$$\mathrm{P}_{12} = -\tfrac{1}{2}\{1 + (\boldsymbol{\sigma}_1, \boldsymbol{\sigma}_2)\}. \tag{16}$$

The formula (16) may conveniently be used for the evaluation of the characters χ' which define the exclusive sets of states. We have, for example, for the permutations consisting of interchanges

$$\chi_{12} = \chi(\mathrm{P}_{12}) = -\tfrac{1}{2}\left\{1 + \frac{2}{n(n-1)}\Sigma_{r<t}(\boldsymbol{\sigma}_r, \boldsymbol{\sigma}_t)\right\}.$$

If we introduce the variable s to describe the magnitude of the total spin angular momentum, $\frac{1}{2}\Sigma_r\boldsymbol{\sigma}_r$ in units of h, through the formula

$$s(s+1) = (\tfrac{1}{2}\Sigma_r\boldsymbol{\sigma}_r, \tfrac{1}{2}\Sigma_t\boldsymbol{\sigma}_t),$$

analogous to (8), we have

$$2\Sigma_{r<t}(\sigma_r, \sigma_t) = (\Sigma_r \sigma_r, \Sigma_t \sigma_t) - \Sigma_r(\sigma_r, \sigma_r).$$
$$= 4s(s+1) - 3n.$$

Hence

$$\chi_{12} = -\tfrac{1}{2}\left\{1 + \frac{4s(s+1) - 3n}{n(n-1)}\right\} = -\frac{n(n-4) + 4s(s+1)}{2n(n-1)}. \qquad (17)$$

Thus χ_{12} is expressible as a function of the variable s and of n the number of electrons. Any of the other χ's could be evaluated on similar lines and would be found to be a function of s and n only, since there are no other symmetrical functions of all the σ variables which could be involved. There is therefore one set of numerical values χ' for the χ's, and thus one exclusive set of states, for each eigen-value s' of s. The eigen-values of s are

$$\tfrac{1}{2}n, \qquad \tfrac{1}{2}n - 1, \qquad \tfrac{1}{2}n - 2, \ldots$$

the series terminating with $\frac{1}{2}$ or 0.

We obtain in this way a proof of the fundamental theorem of multiplet structure, that for each stationary state of the atom there is one definite numerical value s' for s. We obtain further that the probability of transitions occurring in which s changes is small, of the order of magnitude of the spin forces.

The degree of degeneracy of the states in any exclusive set $s = s'$ must equal the number of independent eigen-functions $F(\sigma_1, \sigma_2)$ that the variable s has, belonging to the eigen-value s'. This is just $2s' + 1$, as can be seen without detailed calculation from the fact that any of the Cartesian components of the total spin angular momentum, $\frac{1}{2}\Sigma\sigma_{rx}$ say, has the $2s' + 1$ eigen-values

$$s', \qquad s' - 1, \qquad s' - 2, \ldots \qquad -s'.$$

When the spin forces are not neglected, each $(2s' + 1)$-fold degenerate energy level will in general be split up into $2s' + 1$ non-degenerate energy levels, differing slightly one from another. Thus the exclusive set of states $s = s'$ becomes a system of multiplets of multiplicity $2s' + 1$.

§ 5. *Determination of Energy Levels.*

We must now consider the application of perturbation theory for an approximate calculation of the energy levels. We shall take first the general case of a system with n similar particles, discussed in §§ 2 and 3. We shall follow the usual method in the theory of the perturbations of the stationary states of a degenerate system, according to which, if we label the states of the unperturbed system α', α'', ..., we obtain the matrix $(\alpha' \mid V \mid \alpha'')$ representing the perturbation energy V and neglect all those matrix elements α', α'' for which the unperturbed states α' and α'' have two different energies. The remaining matrix elements will form a number of small matrices, one referring to each energy level of the unperturbed system, and having as the number of its rows and columns the number of independent states belonging to this energy level. The eigen-values of these matrices will then be, in the first approximation, the changes in the energy levels caused by the perturbation.

We suppose that for our unperturbed states each of the similar particles has its own "orbit," represented by a wave function $(q_r|\alpha)$ involving only the co-ordinates q_r of this one particle. We shall have altogether n orbits, one for each particle, which we assume for the present to be all different, and label α_1, α_2, ..., α_n. The wave function representing an unperturbed state of the whole system will then be the product.

$$(q_1 \mid \alpha_1)(q_2 \mid \alpha_2) \ldots (q_n \mid \alpha_n) = (q \mid \alpha) \tag{18}$$

say, for brevity. If we apply an arbitrary permutation P_a to the α's, we shall obtain another wave function

$$(q_1 \mid \alpha_r)(q_2 \mid \alpha_s) \ldots (q_n \mid \alpha_t) = (q \mid P_a\alpha) \tag{19}$$

representing another unperturbed state with the same energy. There are thus altogether n ! unperturbed states with this energy, if we assume there are no other causes of degeneracy. The matrix elements of V that we must take into consideration are therefore of the type $(P_a\alpha \mid V \mid P_b\alpha)$, where P_a and P_b are two permutations of the α's, and form a matrix with n ! rows and columns. The eigen-values of this matrix are what we must calculate.

It is necessary in the present discussion to distinguish between the two kinds of permutations, those of the q's and those of the α's. The essential difference between them can perhaps be seen most clearly in the following way. Let us consider a permutation in the general case, say that consisting of the interchange of 2 and 3. This may be interpreted either as the interchange of the objects 2 and 3 or as the interchange of the objects in the places 2 and 3, these two operations producing in general quite different results. The first of these interpretations is the one we have been using throughout §§ 2 and 3, the objects concerned being the q's. A permutation with this interpretation can be applied to an arbitrary function of the q's. A permutation with the second interpretation has a meaning, however, when applied to a function of the q's only if each of the q's has a definite specifiable place in the function. This is not the case for a general function of the q's, but it is the case for any of the $n\,!$ functions of the type (19), the place of each q being specified by the α with which it is bracketed. Any permutation applied to the q's in given places now produces the same result as the reciprocal permutation applied to the α's. A permutation *of* the q's (*i.e.*, one with the first interpretation) since it can be applied to any function of the q's, may be regarded as an ordinary dynamical variable. On the other hand a permutation of places or of the α's can be considered as a dynamical variable only in a very restricted sense, since it has a meaning only when multiplied into one of the $n\,!$ wave functions (19) or into some linear combination of them. We denote such a permutation of the α's, considered as a dynamical variable in this restricted sense, by a symbol P^a.

We can form algebraic functions of the variables P^a, which will be other variables in the same restricted sense. In particular we can form $\chi(P^a{}_a)$, the average of all P^a's similar to $P^a{}_a$. This must equal $\chi(P_a)$, the average of the similar permutations of the q's, since the total set of all permutations of a given type must evidently be the same whether the permutations are applied to the objects q or to the places α.

If we set up arbitrarily a one-one correspondence between the q's and the α's, as is done automatically when we label both the q's and the α's by the numbers 1, 2, 3, ..., n, as in (18), then, if we have any permutation of the q's, we can give a meaning to this same permutation of the α's. This meaning is such that

$$(q \mid \alpha) = (\mathrm{P}q \mid \mathrm{P}\alpha).$$

In this equation we can apply a permutation P_a to the α's on both sides, which will give us

$$(q \mid \mathrm{P}_a\alpha) = (\mathrm{P}q \mid \mathrm{P}_a\mathrm{P}\alpha) \tag{20}$$

an equation which shows us the connection between permutations of the q's and those of the α's when applied to the wave function (19).

The matrix $(\mathrm{P}_a\alpha \mid \mathrm{V} \mid \mathrm{P}_b\alpha)$, which we must now study, may be obtained from the matrix $(q' \mid \mathrm{V} \mid q'')$ representing the same dynamical variable V by a canonical transformation, in which the transformation functions are just $(q \mid \mathrm{P}_a\alpha)$, the wave function (19), and its conjugate complex $(\mathrm{P}_a\alpha \mid q)$, provided these functions are properly normalised. Thus

$$(\mathrm{P}_a\alpha \mid \mathrm{V} \mid \mathrm{P}_b\alpha) = \iint (\mathrm{P}_a\alpha \mid q')\, dq'\, (q' \mid \mathrm{V} \mid q'')\, dq''\, (q'' \mid \mathrm{P}_b\alpha). \tag{21}$$

Again, for arbitrary P,

$$\begin{aligned}(\mathrm{P}_a\mathrm{P}\alpha \mid \mathrm{V} \mid \mathrm{P}_b\mathrm{P}\alpha) &= \iint (\mathrm{P}_a\mathrm{P}\alpha \mid q')\, dq'\, (q' \mid \mathrm{V} \mid q'')\, dq''\, (q'' \mid \mathrm{P}_b\mathrm{P}\alpha)\\ &= \iint (\mathrm{P}_a\mathrm{P}\alpha \mid \mathrm{P}q')\, dq'\, (\mathrm{P}q' \mid \mathrm{V} \mid \mathrm{P}q'')\, dq''\, (\mathrm{P}q'' \mid \mathrm{P}_b\mathrm{P}\alpha)\end{aligned}$$

when we apply the permutation P to the variables of integration q' and q''. With the help of (20), this reduces to

$$(\mathrm{P}_a\mathrm{P}\alpha \mid \mathrm{V} \mid \mathrm{P}_b\mathrm{P}\alpha) = \iint (\mathrm{P}_a\alpha \mid q')\, dq'\, (\mathrm{P}q' \mid \mathrm{V} \mid \mathrm{P}q'')\, dq''\, (q'' \mid \mathrm{P}_b\alpha). \qquad (22)$$

Now since V is symmetrical between all the particles, we must have

$$(q' \mid \mathrm{V} \mid q'') = (\mathrm{P}q' \mid \mathrm{V} \mid \mathrm{P}q''),$$

like (6), and hence, comparing (21) and (22), we obtain

$$(\mathrm{P}_a\alpha \mid \mathrm{V} \mid \mathrm{P}_b\alpha) = (\mathrm{P}_a\mathrm{P}\alpha \mid \mathrm{V} \mid \mathrm{P}_b\mathrm{P}\alpha) \qquad (23)$$

Let $(\mathrm{P}\alpha \mid \mathrm{V} \mid \alpha) = \mathrm{V}_\mathrm{P}$ for brevity. Then, taking $\mathrm{P} = \mathrm{P}_b{}^{-1}$ in (23), we obtain

$$(\mathrm{P}_a\alpha \mid \mathrm{V} \mid \mathrm{P}_b\alpha) = (\mathrm{P}_a\mathrm{P}_b{}^{-1}\alpha \mid \mathrm{V} \mid \alpha) = \mathrm{V}_{\mathrm{P}_a\mathrm{P}_b{}^{-1}}.$$

Thus the general matrix element $(\mathrm{P}_a\alpha \mid \mathrm{V} \mid \mathrm{P}_b\alpha)$ depends only on the ratio $\mathrm{P}_a\mathrm{P}_b{}^{-1}$, and of the total of $(n\,!)^2$ matrix elements there are only $n\,!$ different ones. The coefficient of any V_P in this matrix will be a matrix, each of whose elements is 0 or 1, the 1 occurring when

$$(\mathrm{P}_a\alpha \mid \mathrm{V} \mid \mathrm{P}_b\alpha) = \mathrm{V}_\mathrm{P},$$

i.e., when $\mathrm{P}_a\mathrm{P}_b{}^{-1} = \mathrm{P}$. But this matrix, multiplied into any wave function $(q \mid \mathrm{P}_b\alpha)$, gives the result $(q \mid \mathrm{P}_a\alpha)$ with $\mathrm{P}_a\mathrm{P}_b{}^{-1} = \mathrm{P}$, *i.e.*, it gives the result $(q \mid \mathrm{P}\mathrm{P}_b\alpha)$, so that it is precisely the matrix representing the variable P^a, or the permutation P applied to the α's. Thus the whole matrix $(\mathrm{P}_a\alpha \mid \mathrm{V} \mid \mathrm{P}_b\alpha)$ is equal to the matrix representing $\Sigma\, \mathrm{V}_\mathrm{P}\mathrm{P}^a$, where the summation is over all the $n\,!$ permutations P, and we can put

$$\mathrm{V} = \Sigma\, \mathrm{V}_\mathrm{P}\mathrm{P}^a. \qquad (24)$$

This formula shows that the perturbation energy V is equal to a linear function of the permutation variables P^a, with numerical coefficients V_P, which are the exchange energies. It is, of course, only an approximate formula, as it holds only with neglect of those matrix elements of V that refer to two different energy levels of the unperturbed system. It can, however, be used for the calculation of the energy levels in the first approximation, and is very convenient for this purpose as the expression $\Sigma\, \mathrm{V}_\mathrm{P}\mathrm{P}^a$ is easily handled. This expression, it should be remembered, is a dynamical variable only in the restricted sense mentioned above, but this sense is just sufficiently general for equation (24) to be valid with neglect of those matrix elements of V referring to two different energy levels of the unperturbed system.

As an example of an application of (24) we shall determine the average energy of all those states arising from a given state of the unperturbed system that belong to one exclusive set. This requires us to calculate the average eigen-value of V when the χ's have specified numerical values χ'. Now the average eigen-value of P^a equals that of $P^a{}_a P^a (P^a{}_a)^{-1}$ for arbitrary $P^a{}_a$ and thus equals that of $(n\,!)^{-1}\,\Sigma_a P^a{}_a P^a (P^a{}_a)^{-1}$, which is $\chi'(P^a)$ or $\chi'(P)$. Hence the average eigen-value of V is $\Sigma V_P \chi'(P)$. A similar method could be used for calculating the average eigen-value of any function of V, it being only necessary to replace each P^a by $\chi(P)$ to perform the averaging.

The modifications required in the theory when the orbits $\alpha_1, \alpha_2, \alpha_3, \ldots$, or the undisturbed system are not all different may easily be made. Suppose, for example, that α_1 and α_2 are the same. Then the permutation $P^a{}_{12}$ that causes an interchange of α_1 and α_2 must equal unity. Only functions of the P^a's that commute with $P^a{}_{12}$ now have a meaning. This, however, is sufficient for us to be able to follow out the same sort of argument as before, and obtain a result of the same form (24). The term in the summation in (24) that involves the permutation $P^a{}_{12}$ now does not occur, since it could be added on to the term involving the identical permutation $P^a{}_1$. For the remaining terms, any two terms $P^a{}_a$ and $P^a{}_b$ must have the same coefficient if the permutations $P^a{}_a$ and $P^a{}_b$ can be obtained from one another by the interchange of α_1 and α_2. This results in $\Sigma V_P P^a$ commuting with $P^a{}_{12}$ and thus having a meaning. The condition $P^a{}_{12} = 1$ will impose restrictions on the possible numerical values χ' that the χ's can have and will reduce the number of characters.

§ 6. *The Energy Levels in the Case of Electrons.*

We shall now consider the application of the formula (24) to the case of electrons. If we assume only Coulomb forces between the electrons, then the perturbation will consist of a number of terms, each involving the co-ordinates of one or at most two electrons, so that all the exchange energies V_P will vanish except those referring to the identical permutation P_1 and to simple interchanges of two orbits, $P^a{}_{rs}$. Thus (24) reduces to

$$V = V_1 + \Sigma_{r<s} V_{rs} P^a{}_{rs},$$

V_{rs} being the exchange energy of orbits r and s. Since the P^a's have exactly the same properties as the P's, we can replace the P^a's in this expression for V by P's without changing its eigen-values. This gives us

$$V = V_1 + \Sigma_{r<s} V_{rs} P_{rs}, \tag{25}$$

where the = sign is now to be interpreted as denoting the equality of the eigen-values of the two sides and not the complete equality of the two sides as dynamical variables or operators.

With the help of (16), the result (25) may be put in the more expressive form

$$V = V_1 - \tfrac{1}{2}\Sigma_{r<s} V_{rs}\{1 + (\boldsymbol{\sigma}_r, \boldsymbol{\sigma}_s)\}. \tag{26}$$

This shows that, for the purpose of calculating energies, the exchange interaction due to the equivalence of the electrons may be replaced by a constant perturbation energy $-\tfrac{1}{2}\Sigma_{r<s}V_{rs}$, together with a coupling between the spin vectors with energy $-\tfrac{1}{2}V_{rs}(\boldsymbol{\sigma}_r, \boldsymbol{\sigma}_s)$ for each pair of electrons r, s. It is this coupling which may be considered as giving rise, for instance, to the large differences in energy between the singlet and triplet terms of helium. The total number of eigen-values of the right-hand side of (26) is 2^n, a factor 2 occurring for the representation of the spin vector of each of the n electrons. These 2^n eigen-values will not, in general, all be different, as each one will occur repeated a number of times to give the correct multiplicity of the corresponding term.

When two of the orbits of the unperturbed system are the same, say the orbits 1 and 2 are the same, the only eigen-values of the right-hand side of (25) or (26) that will be eigen-values of V are those consistent with the equation $P_{12} = 1$ or $P^\sigma{}_{12} = -1$. In this case we have $V_{12} = 0$ and

$$V_{1r} = V_{2r} \quad (r = 3, 4, 5, \ldots),$$

which results in the right-hand side of (26) being symmetrical between $\boldsymbol{\sigma}_1$ and $\boldsymbol{\sigma}_2$. It follows from this that any eigen-function $F(\sigma_{1z}, \sigma_{2z}, \sigma_{3z}, \ldots)$ of this right-hand side, considered as an operator, must be either symmetrical or antisymmetrical between σ_{1z} and σ_{2z}. The condition $P^\sigma{}_{12} = -1$ now shows that only the antisymmetrical ones, representing states for which the spins $\boldsymbol{\sigma}_1$ and $\boldsymbol{\sigma}_2$ are antiparallel, must be taken into account. The number of eigen values of (26) that must be used is thus reduced by a factor 4, on account of there being only one antisymmetrical eigen-function for every three symmetrical ones. The case of more than two orbits the same cannot occur with electrons.

In our theory of the energies we have nowhere had to assume that the wave functions $(q \mid \alpha_1)$, $(q \mid \alpha_2)$, ..., representing the various orbits in the unperturbed system, are orthogonal, or that they are eigen-functions of any unperturbed Hamiltonian H_0. This enables an important generalisation to be made in the application of our results. It is not necessary that we should be able to split up our Hamiltonian for the whole system H into a Hamiltonian for the unperturbed system H_0 and a perturbation energy V, and then use the eigen-functions of H_0 to give our $(q \mid \alpha_1)$, $(q \mid \alpha_2)$, ... We can take our $(q \mid \alpha_1)$,

$(q \mid \alpha_2)$ to be *any* functions giving a good approximation to the actual distribution of electrons in the system, and must then throughout the analysis replace V, which now no longer exists, by the whole Hamiltonian H. The wave functions supplied by Hartree's theory can thus very conveniently be used. The only mathematical conditions which the $(q \mid \alpha_1)$, $(q \mid \alpha_2)$, ..., need satisfy is that in the matrix $(\alpha' \mid H \mid \alpha'')$ representing H, those matrix elements for which the α'''s are not simply a permutation of the α''s must be small.

As an example of the application of (25), Heitler's formula* for the interaction of two atoms A and B, each with n valency electrons, will be deduced. The fundamental theorem of multiplet structure shows that there will be a quantum number s describing the magnitude of the resultant spin of the electrons in both atoms. This same theorem shows that, provided the interaction between the atoms is small compared with the exchange energies within either of them, the whole energy of the system will depend very largely on the magnitudes s_A and s_B of the resultant spins for the two atoms separately, so that for each energy level of the whole system there must be definite numerical values for s_A and s_B, which will thus be two more quantum numbers describing states of the whole system. For valency electrons the resultant spin vector has its maximum possible value (we can if we like in this case speak of the electron spins all being parallel) and hence

$$s_A = s_B = \tfrac{1}{2}n. \tag{27}$$

Again, if ζ is the valency of the homopolar bond uniting the two atoms (*i.e.*, $\zeta = 1, 2, \ldots$, for a single, double, ... bond)

$$s = n - \zeta. \tag{28}$$

We now apply our formula (25), taking the summation only over pairs of orbits r, s of which one is in each atom, since we want the interaction energy between the two atoms. This gives

$$V = V_1 + \Sigma_{AB}\, V_{rs}\, P_{rs}.$$

As a rough approximation we may take all the exchange energies V_{rs} between two orbits one in each atom to be equal. Calling these exchange energies V_Q, we get

$$V = V_1 + V_Q\, \Sigma_{AB}\, P_{rs}.$$

We must now evaluate $\Sigma_{AB}\, P_{rs}$, summed over all pairs one in each atom, which we can best do by first summing over all possible pairs and then subtracting the two sums for pairs both in atom A and both in atom B respectively. Thus

---

* W. Heitler, 'Z. Physik,' vol. 47, p. 835 (1928), equation (33).

$$\begin{aligned}\Sigma_{AB}\,P_{rs} &= \Sigma\,P_{rs} - \Sigma_{AA}\,P_{rs} - \Sigma_{BB}\,P_{rs} \\ &= -\tfrac{1}{4}\{2n(2n-4) + 4s(s+1)\} + \tfrac{1}{4}\{n(n-4) + 4s_A(s_A+1)\} \\ &\qquad + \tfrac{1}{4}\{n(n-4) + 4s_B(s_B+1)\}\end{aligned}$$

by a three-fold application of (17), in the first case to a system of $2n$ electrons. This reduces to

$$\begin{aligned}\Sigma_{AB}\,P_{rs} &= -\tfrac{1}{4}\{2n^2 + 4s(s+1) - 4s_A(s_A+1) - 4s_B(s_B+1)\} \\ &= \zeta - (n-\zeta)^2.\end{aligned}$$

Thus

$$V = V_1 + V_Q\{\zeta - (n-\zeta)^2\},$$

which is Heitler's result.

INDEX TO VOL. CXXIII. (A)

Acharya (D. P.) *See* Kichlu and Acharya.

Adsorption of hydrogen on discharge tube (Johnson), 603.

Arnot (F. L.) *See* Ditchburn and Arnot.

Astbury (W. T.) A New Integrating Photometer for X-Ray Crystal Reflexions, etc., 575.

Asundi (R. K.) *See* Johnson and Asundi.

Atomic nuclei, discussion (Rutherford and others), 373.

Awbery (J. H.) *See* Griffiths and Awbery.

Baldwin (O. R.) The Relativity Theory of Divergent Waves, 119.

Benzene, dielectric constant (Hartshorn and Oliver), 664.

Benzene ring, structure (Lonsdale), 494.

Blackett (P. M. S.) On the Design and Use of a Double Camera for Photographing Artificial Disintegrations, 613.

Bone (W. A.), Weston (F. R.) and Winter (D. A.) Further Experiments on the Combustion of Well-dried Carbon Monoxide and Oxygen Mixtures, III, 285.

Bragg (W. L.) The Determination of Parameters in Crystal Structures by means of Fourier Series, 537.

Burch (C. R.) Some Experiments on Vacuum Distillation, 271.

Byrne (B. J.) *See* Newitt and others.

Camera for photographing artificial disintegrations (Blackett), 613.

Carbon monoxide, band system (Johnson and Asundi), 560.

Chalk (L.) *See* Foster and Chalk.

Chapman (S.) and Stagg (J. M.) On the Variability of the Quiet-Day Magnetic Variation at Eskdalemuir and Greenwich, 27.

Chlorine, absorption band spectrum (Elliott), 629.

Clean-up of gases at glass surfaces (Taylor), 252.

Combustion of carbon monoxide oxygen mixtures (Bone and others), 285.

Conductivity, thermal, of gas mixtures (Ibbs and Hirst), 134.

Cox (H. L.) *See* Gough and Cox.

Crystal of zinc, alternating torsional stresses (Gough and Cox), 143.

Crystal reflexions, integrating photometer (Astbury), 575.

Crystal structure, parameters by Fourier series (Bragg), 537.

Davidson (P. M.) *See* Richardson and Davidson.

Dielectric constants of liquors (Hartshorn and Oliver), 664.

Dirac (P. A. M.) Quantum Mechanics of Many-Electron Systems, 714.

Discussion on the structure of atomic nuclei (Rutherford and others), 373.

Ditchburn (R. W.) and Arnot (F. L.) The Ionisation of Potassium Vapour, 516.

Electric waves, reflexion at interface (Macdonald), 1, 391.

Elliott (A.) The Absorption Band Spectrum of Chlorine, 629.

Equilibrium in methyl alcohol-hydrogen-carbonic oxide (Newitt and others), 236.

Fisher (J. W.) The Wave Equation in Five Dimensions, 489.

Flame temperatures (Griffiths and Awbery), 401.

Foster (J. S.) and Chalk (L.) Relative Intensities of Stark Components in Hydrogen, 106.

Foster (J. S.) and Rowles (W.) Patterns and Paschen-Back Analogue in the Stark Effect for Neon, 80.

Fowler (A.) The Arc Spectrum of Silicon, 422.

Goldstein (S.) The Forces on a Solid Body moving through Viscous Fluid, 216. The Steady Flow of Viscous Fluid past a Fixed Spherical Obstacle at Small Reynolds Numbers, 225. On the Vortex Theory of Screw Propellers, 440.

Gough (H. J.) and Cox (H. L.) The Behaviour of a Single Crystal of Zinc subjected to alternating Torsional Stresses, 143.

Griffiths (E.) and Awbery (J. H.) The Measurement of Flame Temperatures, 401.

Hartshorn (L.) and Oliver (D. A.) On the Measurement of the Dielectric Constants of Liquors with a Determination of the Dielectic Constant of Benzene, 664.

Hirst (A. A.) *See* Ibbs and Hirst.

Hydrogen spectrum, parhelium bands (Richardson and Davidson), 54, 466.

Ibbs (T. L.) and Hirst (A. A.) The Thermal Conductivity of Gas Mixtures, 134.

Ions, chemical interaction at glass surfaces (Taylor), 252.

Johnson (M. C.) The Adsorption of Hydrogen on the Surface of an Electrodeless Discharge Tube, 603.

Johnson (R. C.) and Asundi (R. K.) A New Band System of Carbon Monoxide ($3\,^1S \rightarrow 2\,^1P$), with remarks on the Angstrom Band System, 560.

Kapitza (P.) The Change of Electrical Conductivity in Strong Magnetic Fields. I.—Experimental Results, 292. II.—The Analysis and the Interpretation of the Experimental Results, 342.

Kichlu (P. K.) and Acharya (D. P.) Infra-red Radiations of Active Nitrogen, 168.

Lea (F. C.) The Penetration of Hydrogen into Metal Cathodes and its effect upon the Tensile Properties of Metals and their Resistance to Repeated Stresses; with a Note on the Effect of Non-Electrolytic Baths and Nickel Plating on these properties, 171.

Lonsdale (K.) The Structure of the Benzene Ring in $C_6(CH_3)_6$, 494.

Lowry (T. M.) and Nasini (A. G.) The Molecular Dimensions of Organic Compounds. I.—General Considerations, 686.

Macdonald (H. M.) The Reflexion and Transmission of Electric Waves at the Interface between Two Transparent Media, 1. The Total Reflexion of Electric Waves at the Interface between Two Media, 391.

MacDonald (J. K. L.) Stark Effect in a Violet Region of the Secondary Spectrum of Hydrogen, 103.

Magnetic fields, strong, change of electrical conductivity (Kapitza), 292, 342.

Magnetic variation, quiet-day variability (Chapman and Stagg), 27.

Menon (A. S.) *See* Watson and Menon.

Molecular dimensions of organic compounds (Lowry and Nasini), 686, 692, 704.

Nasini (A. G.) The Molecular Dimensions of Organic Compounds. II.—The Viscosity of Vapours: Benzene, Toluene and Cyclohexane, 692. III.—The Viscosity of Vapours: Thiophen and α-Methylthiophen, Pyridine and Thiazole, 704.

Nasini (A. G.) *See also* Lowry and Nasini.

Newitt (D. M.), Byrne (B. J.) and Strong (H. W.) Equilibrium in the System Methyl Alcohol—Hydrogen—Carbonic Oxide, 236.

Nitrogen, active, infra-red radiations (Kichlu and Acharya), 168.

Oil Films, thin, electrical conductivity (Watson and Menon), 185.
Oliver (D. A.) *See* Hartshorn and Oliver.

Penetration of hydrogen into metal cathodes (Lea), 171.
Photometer for X-ray crystal reflexions (Astbury), 575.
Platinum, combustion of (Rideal and Wansbrough-Jones), 202.
Potassium vapour ionisation (Ditchburn and Arnot), 516.

Quantum mechanics of many-electron systems (Dirac), 714.

Relativity theory of divergent waves (Baldwin), 119.
Richardson (O. W.) and Davidson (P. M.) The Spectrum of H_2—The Bands analogous to the Parhelium Line Spectrum, 54, 466.
Rideal (E. K.) and Wansbrough-Jones (O. H.) An Investigation of the Combustion of Platinum, 202.
Rowles (W.) *See* Foster and Rowles.
Rutherford (Sir Ernest) and others. Discussion on the Structure of Atomic Nuclei, 373.

Silicon arc spectrum (Fowler), 422.
Spectrum, absorption, of chlorine (Elliott), 629.
Spectrum, arc, of silicon (Fowler), 422.
Spectrum, infra-red, of active nitrogen (Kichlu and Acharya), 168.
Spectrum of carbon monoxide, new band system (Johnson and Asundi). 560.
Spectrum of H_2, parhelium bands (Richardson and Davidson), 54, 466.
Spectrum. *See* also Stark effect.
Stagg (J. M.) *See* Chapman and Stagg.
Stark components in hydrogen, intensity (Foster and Chalk), 108.
Stark effect, neon (Foster and Rowles), 80.
Stark effect, violet region of hydrogen (MacDonald), 103.
Stream line flow through curved pipes (White), 645.
Strong (H. W.) *See* Newitt and others.

Taylor (J.) On the Chemical Interaction of Ions and the "Clean-up" of Gases at Glass Surfaces under the Influence of the Electrical Discharge, 252.

Vacuum distillation experiments (Burch), 271.
Viscosity of vapours (Nasini), 692, 704.
Viscous fluid, flow past spherical obstacle (Goldstein), 225.
Viscous fluid, forces on solid body (Goldstein), 216.
Vortex theory of screw propellers (Goldstein), 440.

Wansbrough-Jones (O. H.) *See* Rideal and Wansbrough-Jones.
Watson (H. E.) and Menon (A. S.) The Electrical Conductivity of Thin Oil Films. I.—General Nature of the Phenomenon, 185.
Wave equation in five dimensions (Fisher), 489.
Weston (F. R.) *See* Bone and others.
White (C. M.) Streamline Flow through Curved Pipes, 645.
Winter (D. A.) *See* Bone and others.

Zinc crystal under alternating torsional stresses (Gough and Cox), 143.

END OF THE ONE HUNDRED AND TWENTY-THIRD VOLUME (SERIES A).

I. A. R. I. 75.

IMPERIAL AGRICULTURAL RESEARCH
INSTITUTE LIBRARY
NEW DELHI.

Date of issue.	Date of issue.	Date of issue.
18.11.57		
10 JUL 1986		